CLINICAL RADIOLOGY OF THE HORSE

Fourth Edition

JANET A. BUTLER, CHRISTOPHER M. COLLES, SUE J. DYSON,
SVEND E. KOLD AND PAUL W. POULOS



with website

WILEY Blackwell

Downloaded From Vet-eBooks.com

Clinical Radiology of the Horse

Fourth Edition

JANET A. BUTLER
B&W Equine Group, Berkeley, UK

CHRISTOPHER M. COLLES
BVetMed, PhD, MRCVS, Hon FWCF
Avonvale Veterinary Practice Ltd., Banbury, UK

SUE J. DYSON
MA, VetMB, PhD, DEO, FRCVS
Centre for Equine Studies, Animal Health Trust, Newmarket, UK

SVEND E. KOLD
DVM, Dr Med Vet, CUEW, RFP, MRCVS
Svend Kold Ltd., Tetbury, UK

PAUL W. POULOS
JR, DVM, PhD, DipACVR
California, USA

With contributions from SARAH PUCHALSKI
DVM, DipACVR
California, USA

WILEY Blackwell

Downloaded From Vet-eBooks.com

This edition first published 2017 © 2017 by John Wiley & Sons, Ltd.
Third edition © 2008 by Janet Butler, Christopher Colles, Sue Dyson, Svend Kold and Paul Poulos
Second edition © 2000 by Blackwell Science Ltd, a Blackwell Publishing Company
First edition © 1993 by Blackwell Science Ltd, a Blackwell Publishing Company

Registered Office
John Wiley & Sons, Ltd, The Atrium, Southern Gate, Chichester, West Sussex, PO19 8SQ, UK

Editorial Offices
9600 Garsington Road, Oxford, OX4 2DQ, UK
The Atrium, Southern Gate, Chichester, West Sussex, PO19 8SQ, UK
1606 Golden Aspen Drive, Suites 103 and 104, Ames, Iowa 50010, USA

For details of our global editorial offices, for customer services and for information about how to apply for permission to reuse the copyright material in this book please see our website at
www.wiley.com/wiley-blackwell

The right of the author to be identified as the author of this work has been asserted in accordance with the UK Copyright, Designs and Patents Act 1988.

All rights reserved. No part of this publication may be reproduced, stored in a retrieval system, or transmitted, in any form or by any means, electronic, mechanical, photocopying, recording or otherwise, except as permitted by the UK Copyright, Designs and Patents Act 1988, without the prior permission of the publisher.

Designations used by companies to distinguish their products are often claimed as trademarks. All brand names and product names used in this book are trade names, service marks, trademarks or registered trademarks of their respective owners. The publisher is not associated with any product or vendor mentioned in this book. It is sold on the understanding that the publisher is not engaged in rendering professional services. If professional advice or other expert assistance is required, the services of a competent professional should be sought.

The contents of this work are intended to further general scientific research, understanding, and discussion only and are not intended and should not be relied upon as recommending or promoting a specific method, diagnosis, or treatment by health science practitioners for any particular patient. The publisher and the author make no representations or warranties with respect to the accuracy or completeness of the contents of this work and specifically disclaim all warranties, including without limitation any implied warranties of fitness for a particular purpose. In view of ongoing research, equipment modifications, changes in governmental regulations, and the constant flow of information relating to the use of medicines, equipment, and devices, the reader is urged to review and evaluate the information provided in the package insert or instructions for each medicine, equipment, or device for, among other things, any changes in the instructions or indication of usage and for added warnings and precautions. Readers should consult with a specialist where appropriate. The fact that an organisation or Website is referred to in this work as a citation and/or a potential source of further information does not mean that the author or the publisher endorses the information the organisation or Website may provide or recommendations it may make. Further, readers should be aware that Internet Websites listed in this work may have changed or disappeared between when this work was written and when it is read. No warranty may be created or extended by any promotional statements for this work. Neither the publisher nor the author shall be liable for any damages arising herefrom.

Library of Congress Cataloging-in-Publication Data

Names: Butler, Janet A., author. | Colles, Christopher M., author. | Dyson, Sue J., author. | Kold, Svend E., author. | Poulos, Paul W., author.
Title: Clinical radiology of the horse / Janet A. Butler, Christopher M. Colles, Sue J. Dyson, Svend E. Kold, Paul W. Poulos.
Description: Fourth edition. | Chichester, West Sussex, UK ; Ames, Iowa : John Wiley & Sons Ltd., 2016. | Preceded by Clinical radiology of the horse / Janet A. Butler … [et al.]. 3rd ed. 2008. | Includes bibliographical references and index.
Identifiers: LCCN 2016026160| ISBN 9781118912287 (cloth) | ISBN 9781118912263 (Adobe PDF) | ISBN 9781118912270 (ePub)
Subjects: LCSH: Horses–Anatomy–Atlases. | Veterinary radiography–Atlases. | MESH: Horse Diseases–radiography | Horses–anatomy & histology
Classification: LCC SF765 .C56 2016 | NLM SF 951 | DDC 636.1/0891–dc23
LC record available at https://lccn.loc.gov/2016026160

A catalogue record for this book is available from the British Library.

Wiley also publishes its books in a variety of electronic formats. Some content that appears in print may not be available in electronic books.

Front cover images reproduced from figures within the book: *Top row, from left to right:* See figure 7.30's caption; see figure 10.32b's caption; see 12.15a's caption; see figure 8.40's caption. *Bottom row, from left to right:* See figure 1w.11g's caption; see figure 9.3b's caption; see figure 9.34b's caption; see figure 7.28b's caption.

Set in 10.5/13pt Times Ten by SPi Global, Pondicherry, India

1 2017

Downloaded From Vet-eBooks.com

Contents

ABOUT THE AUTHORS v
PREFACE TO THE FOURTH EDITION vii
ABOUT THE COMPANION WEBSITE ix

1 GENERAL PRINCIPLES 1
Introduction, 1; Principles of radiography, 3; Principles of radiographic interpretation: radiology, 15; Radiological appearance of physiological changes and some common pathological lesions, 20

2 COMPUTED AND DIGITAL RADIOGRAPHY 41

3 THE FOOT 55
Distal phalanx (pedal bone), 55; Hoof, 97; Navicular bone, 113

4 THE PROXIMAL AND MIDDLE PHALANGES AND THE PROXIMAL INTERPHALANGEAL JOINT 149

5 METACARPOPHALANGEAL AND METATARSOPHALANGEAL (FETLOCK) JOINTS 175

6 THE METACARPAL AND METATARSAL REGIONS 215

7 THE CARPUS AND ANTEBRACHIUM 259

8 THE SHOULDER, HUMERUS, ELBOW AND RADIUS 301
Scapulohumeral (shoulder) joint and humerus, 301; Humeroradial, humeroulnar and radioulnar (elbow or cubital) joints and radius, 330

9 THE TARSUS 349

10 THE STIFLE AND TIBIA 399
Stifle, 399; Tibia, 440

11 THE HEAD 449
Cranium, 451; Paranasal sinuses (frontal, maxillary, conchal) and maxilla, 466; Teeth and mandible, 480; Pharynx, larynx and Eustachian tube diverticulum, 512

12 THE VERTEBRAL COLUMN 531
Cervical vertebrae, 531; Thoracolumbar vertebrae, 569; Sacrum and coccygeal vertebrae, 602

Downloaded From Vet-eBooks.com

13 THE PELVIS AND FEMUR 609
Pelvis, 609; Femur, 632

14 THE THORAX 639

15 THE ALIMENTARY AND URINARY SYSTEMS 687
Oesophagus, 694; Abdomen and gastrointestinal tract, 705; Urinary system, 715

16 MISCELLANEOUS TECHNIQUES 723
Arthrography and bursography, 723; Tendonography, 724; Angiography, 725; Venography, 730; Myelography, 733; Pneumocystography, 743; Intravenous Pyelography, 744; Other techniques, 744

APPENDIX A: FUSION TIMES OF PHYSES AND SUTURE LINES 749

APPENDIX B: EXPOSURE GUIDE, IMAGE QUALITY AND FILM PROCESSING FAULTS 753

APPENDIX C: GLOSSARY 761

INDEX 767

Downloaded From Vet-eBooks.com

About the authors

Janet A. Butler
Jan has specialised in equine radiography and has 40 years' experience in this field. She joined the Animal Health Trust in Newmarket in 1975 where she gained considerable experience working with many internationally renowned veterinary surgeons. Since 1997 she has been working in private practice, initially at the Willesley Equine Clinic in Gloucestershire, which since 2009 has been part of the B&W Equine Group.

Christopher M. Colles
Chris qualified from the Royal Veterinary College, London in 1971. After three years in mixed practice (where he obtained a Part I Diploma in Radiology) he joined the Animal Health Trust as a clinician in 1975. He was awarded a PhD for work on Navicular Disease in 1981, and has carried out research in many areas of equine orthopaedics and radiology, having a particular interest in the horse's foot. In 1988 he returned to practice, where he became a senior partner in Avonvale Veterinary Practice, specialising in equine orthopaedics, until his recent retirement from practice. Chris still carries out some second opinion veterinary work, and teaching. He is recognised by the Royal College of Veterinary Surgeons as a Specialist in Equine Orthopaedic Surgery. Chris was awarded an Honorary Fellowship of the Worshipful Company of Farriers in 2000 in recognition of his research into conditions of the foot, and involvement with farriery education.

Sue J. Dyson
After qualifying from the University of Cambridge in 1980, Sue worked for a year at New Bolton Center, University of Pennsylvania, and then spent a year in private practice in Pennsylvania. Sue then joined the Centre for Equine Studies of the Animal Health Trust, Newmarket, where she has specialised in lameness diagnosis and diagnostic imaging. Sue is recognised as a Specialist in Equine Orthopaedics by the Royal College of Veterinary Surgeons and holds the RCVS Diploma in Equine Orthopaedics. She is an Associate of the European College of Veterinary Diagnostic Imaging. She has published widely on lameness, radiography, ultrasonography, nuclear scintigraphy and magnetic resonance imaging.

Svend E. Kold
Svend qualified from The Royal Veterinary and Agricultural University in Copenhagen in 1979. He then spent over 10 years at the Animal Health Trust in Newmarket, where he completed his Dr.Med.Vet Thesis on femorotibial subchondral bone cysts. After a sabbatical year at Colorado State University, he joined the Willesley Equine Clinic, Gloucestershire in 1991, where he was a partner until 2009. He is now a private consultant. He specialises in lameness

Downloaded From Vet-eBooks.com

Downloaded From Vet-eBooks.com

Preface to the fourth edition

When we wrote the first edition of *Clinical Radiology of the Horse*, it was with the intention of providing a comprehensive book dedicated to equine radiography and radiology which would be of practical help to the practitioner, as well as providing specialist information. We have now evolved to the fourth edition, but our aims remain the same. The authors have all practised radiography and radiology and have pooled our collective knowledge and experiences to write a book by consensus, rather than a multi-author text. This has tested the patience and endurance of us all, but we hope that it continues to enhance the value of the book to the reader. We thank Paul Poulos who contributed extensively to the first three editions of the book, but having now retired has opted out of involvement with the fourth edition. We wish him well for the future. We welcome Sarah Puchalski who has contributed to three of the chapters in the fourth edition, and whose additional expertise we hugely appreciate. Once again Geoff Lane has cast his knowledgeable eye over the chapter on the head, and we are grateful for his assistance in this area, while acknowledging that any errors remain our own.

We have continued to update the text of the book, reflecting advances in our own knowledge and collective experiences and incorporating relevant new published material. We are aware that there are some readers who would prefer this to be a referenced text, but that does not fit with our original aims. We have however endeavoured to include in the Further Reading lists comprehensive references not only to radiography and radiology, but also to complementary imaging techniques including ultrasonography, scintigraphy, computed tomography and magnetic resonance imaging. In some chapters these references have been collected together to refer to specific anatomical regions and conditions. In the text, which continues to focus on radiography and radiology, we make reference to other imaging techniques where they may provide valuable additional information.

We realise that in many parts of the world digital imaging has superseded conventional film-screen radiography; however, we hope that this text will continue to be used worldwide, and so we have maintained references to conventional radiography. Whatever method of radiography is used, we believe that attention to the basic details of patient preparation, positioning, exposure values and appropriate collimation are crucial for optimal image quality.

We have replaced the majority of figures with digital images, but there are a few examples of relatively unusual conditions illustrated using conventional film-screen images. We have greatly expanded the number of images by providing additional figures online. This has enabled us to provide many more examples both of normal variants and a variety of abnormal conditions. We hope that the detailed figure legends will encourage readers to evaluate

Downloaded From Vet-eBooks.com

Downloaded From Vet-eBooks.com

About the companion website

This book is accompanied by a companion website:

www.clinical-radiology-horse.com

The website includes:

- Over 200 additional figures
- All the figures from the book
- A full list of further reading references from the book, with CrossRef hyperlinks

All the figures, including those available on the companion website, are cited in the printed book. Those that are prefixed with the letter 'w', e.g. Figures 1w.4c–f, appear online only. They are not in the printed book or e-book formats.

How to access the website

Carefully scratch away the top coating of the label within the box, below, to reveal your unique PIN access code. Then visit www.clinical-radiology-horse.com to register your PIN and access the site.

Scratch off the sticker, below:



If you have purchased this title as an e-book, Wiley Customer Care will provide your unique PIN access code for the companion website. Visit http://support.wiley.com to request via the 'Live Chat' or 'Ask a Question' tabs, within 90 days of purchase, and please have your receipt for verification.

Downloaded From Vet-eBooks.com

Downloaded From Vet-eBooks.com

Chapter 1
General principles

INTRODUCTION

There are many books that describe the principles of radiography. This book does not attempt to provide detailed information in this area, and readers who do not have a working knowledge of radiography are advised to consult one of the standard texts in order to obtain the necessary understanding of radiographic physics. This book does aim to provide up-to-date information specific to the horse. As various forms of competitive and pleasure riding have become more popular, the demand on veterinary surgeons to provide the highest quality of treatment has increased. Similarly radiography of the horse in sickness as well as in health, for insurance and purchase examinations, has increased. The book is intended for all who radiograph horses and read radiographs, be they equine specialist, general practitioner or student. It gives information on equipment required, radiographic techniques, positioning, and the views required to examine the various areas of the horse adequately. It also provides information on the normal radiographic anatomy of the immature and skeletally mature horse, variations, and incidental findings. Finally it gives information on the types of lesion that may be detected, with examples of as many of the more common problems as practical, as well as brief clinical remarks where appropriate. The 'Further reading' lists at the end of each chapter are not intended to be complete lists of every paper written on the subject of the chapter. They list references that the authors consider of particular interest, and that are complementary to the text. Many of these references give more detailed information in specific areas than can be justified in a textbook of this type.

Interpreting the clinical significance of radiological changes is always difficult. We set out to indicate certain lesions that may always be regarded as clinically significant, and some that are known to have no clinical significance. The section in each chapter on 'Normal variation and incidental findings' attempts to differentiate between variations that have no clinical significance at any time (e.g. radiolucent lines in the fibula, that represent remnants of separate centres of ossification) and those that may be clinically significant for a specific but limited period of time, and therefore require further clinical investigation to determine their significance (e.g. entheseophyte formation). The radiograph is only a reflection of the state of the tissues at the fraction of a second when they were radiographed. There are many findings which indicate a past event that has 'left its mark', but which

Clinical Radiology of the Horse, Fourth Edition. Janet A. Butler, Christopher M. Colles, Sue J. Dyson, Svend E. Kold and Paul W. Poulos.
© 2017 John Wiley & Sons, Ltd. Published 2017 by John Wiley & Sons, Ltd.
Companion website: www.clinical-radiology-horse.com

Downloaded From Vet-eBooks.com

is no longer clinically significant. For example, entheseophyte formation at the insertion of a ligament may indicate a sprain to that ligament at some time in the past. As entheseophytes take time to form, once they are visible on radiographs they no longer represent an acute injury, but are the result of an incident that occurred at least several weeks previously; on the other hand, their radiographic appearance might be used to approximate their age.

Radiography is a continually developing science, and as more powerful and sophisticated equipment becomes generally available, the diagnostic possibilities for veterinary practitioners become ever greater. It is hoped that this book will enable veterinarians to get the best out of their equipment, to obtain diagnostic radiographs, and to give a correct and meaningful diagnosis from the radiographs. The information in the text has been collated from the literature where possible, and complemented by the authors' experience. In some areas, however, there is no published work, or published information is contradictory. In these circumstances the authors have relied on their own collective experience, but have only presented information if all the authors are in agreement. (For example, reported physeal closure times for some physes vary widely between texts. The times given are based on the authors' experience of radiographic closure, in some cases backed up by radiographic examinations of animals specifically to aid completion of this text.) The authors are experienced clinicians who routinely obtain and read equine radiographs, and it is hoped that the broad range of experience that they offer to the reader will prove to be of practical value. It is important to remember that, as radiography is a developing science, 'new' lesions and radiographic views are continually being found and described, and no text can hope to be complete when published, let alone as time progresses.

This text has made use of current terminology. *Nomina Anatomica Veterinaria* (5th edition, 2005) was consulted for anatomical terms and names. In some instances we refer first to the correct nomenclature, but make subsequent reference to the more commonly used colloquial name (e.g. distal sesamoid bone and navicular bone). It should be noted that long bones have cortices and a myeloid cavity (the medulla), sesamoid bones and short bones (e.g. the central and third tarsal bones) have compact bone and spongiosa. Radiographic views are described using the method advocated by the American College of Veterinary Radiologists, which first describes where the x-ray beam originates relative to the horse (e.g. dorsolateral), then where the beam is directed to (e.g. palmaromedial) (i.e. dorsolateral-palmaromedial oblique). Reference to Figure 1.1 may help to elucidate the current terminology used. While at first sight this may appear cumbersome, it does provide a specific description of the views, which allows them to be reproduced accurately. Terminology in common usage is included in parentheses and serves only to maintain continuity with other texts and references. A glossary (Appendix C) is also included and lists former and current scientific terminology as well as common lay terms.

We have not set out to provide radiographs of every variation of all lesions. Rather we have given typical examples of lesions, and in the text have indicated how these may vary. We also hope that the reader will use this text as a basis to understand why certain types of radiographic lesions form, and the processes that are likely to cause them, so that an inexhaustible supply of radiographic variations would be superfluous. Although we have done our utmost to find radiographs that reproduce well, we ask the reader to

Downloaded From Vet-eBooks.com

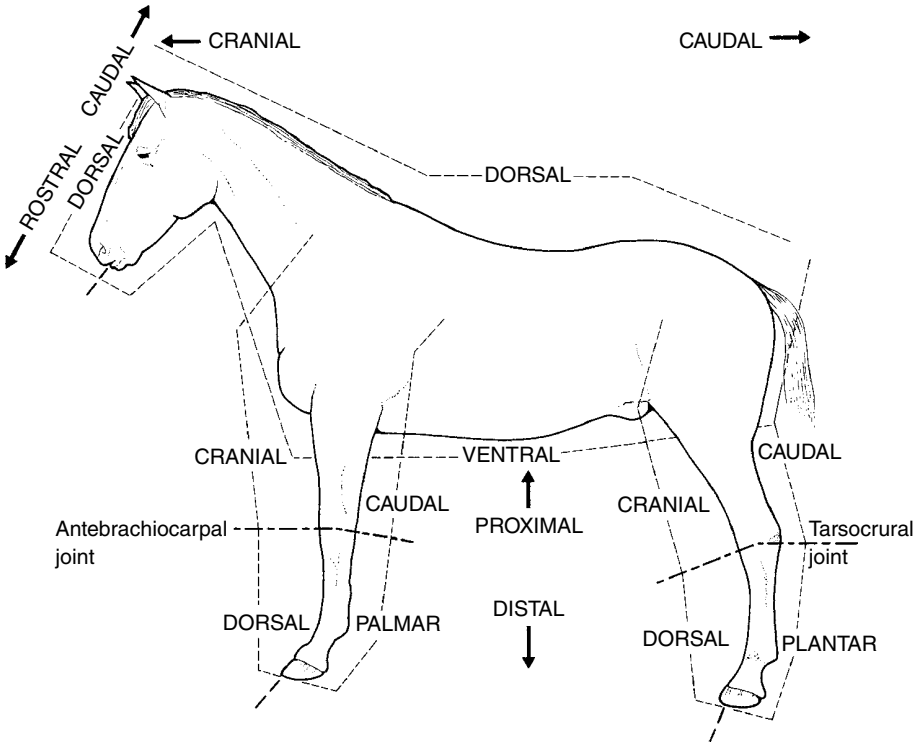


Figure 1.1 Correct nomenclature to describe various aspects of the horse.

remember that inevitably some detail is lost in the process of transferring radiographs to print, however all images can be viewed on the website, and this also provides additional images that are not present in the printed version.

PRINCIPLES OF RADIOGRAPHY

The following paragraphs serve only as a reintroduction to the subjects of image production and differentiation. For more detailed information the reader is referred to the standard radiography texts. It is important that any radiograph is of maximum quality and yields sufficient detail to allow subtle radiographic lesions to be detected.

Production of x-rays

An x-ray beam consists of high-energy electromagnetic radiation. It is produced by accelerating a beam of electrons into a tungsten target. This results in the production of a beam of x-rays, and the liberation of considerable energy as heat. A small target area produces a narrower beam of x-rays, and better definition on the resultant radiograph than a larger target area. The area of the target struck by electrons is called the 'focal spot'. Ninety-nine percent of the energy from the electron beam is given off as heat, not x-rays, and so there is a risk of the target being melted. Dissipating this heat and keeping the target as small as possible are major factors in design of x-ray tubes. For generators with a large output, the target in the tube is the edge of a disc. By rotating the disc at very high speeds during x-ray production, the area being heated is continually being changed, allowing a small focal spot in spite of high output. This is standard in large static x-ray generators.

Downloaded From Vet-eBooks.com

Smaller mobile or portable generators generally have fixed targets, which does limit the output possible. Any x-ray beam is made up of photons of mixed wavelengths. The older half- and full-wave rectification in small x-ray generators resulted in very marked variations in the energy of the individual photons of the x-ray beam. The high-frequency generators currently available have greatly improved the consistency of the x-ray beam produced, causing less scatter and a better resultant image.

Production of a radiographic image

An image is created by detecting the differential absorption of x-rays that pass through an object placed in the path of the primary x-ray beam. The x-rays that pass right through the object are either detected using conventional x-ray film, or digital images are created (see Chapter 2). The number of x-rays that are absorbed by a given thickness of a specific tissue varies between tissues, and thus affects the number of x-rays passing through to form the image. For example it is more difficult to penetrate bone than air, and therefore less x-rays reach the film if they have to penetrate bone rather than air. The areas of the image relating to relatively unobstructed x-rays are black, whereas the areas protected by bone, which absorbs or deflects a proportion of the x-rays, are paler or white. Intermediate densities of tissues produce variable shades of grey. Fat is the least dense tissue, and gives relatively black tones, with muscle and bone giving increasingly light tones. It is the juxtaposition of these tissues of varying densities that allows differentiation of form and structure.

Exposure factors

Exposure factors affect the *opacity* and *contrast* of the radiographic image. The quantity of photons (x-rays) reaching the film (or digital sensor) affects opacity (blackness). This is primarily controlled by the milliampere (mA), higher mA resulting in a greater number of photons being produced in the x-ray beam. By lengthening the time for which the beam is produced, the total number of photons is increased in proportion, i.e. doubling the time, doubles the number of photons reaching the film. This is normally recorded for any exposure as mAs, i.e. mA times time (milliampere seconds).

A major factor influencing the number of photons reaching the film is the distance of the film from the focal spot. This is known as the focus–film distance (FFD), or the source–image distance (SID). Because the x-ray beam spreads out to cover a two-dimensional area, the number of photons reaching the film falls as a square of the distance. This means that changing the distance by a relatively small amount can have a marked effect on image opacity, although it has only a minor effect on contrast, because all areas experience a similar percentage drop in numbers of photons reaching the film.

The kilovoltage (kV) governs the energy of the x-rays and their ability to penetrate through tissue. The higher the kV, the greater the energy of the x-rays, and the greater their ability to penetrate tissues. This has some effect on opacity, but more importantly affects contrast. Soft tissues such as fat and muscle absorb limited numbers of x-rays, even of low kV. Bone however absorbs far more x-rays of low kV than high kV, so there is a relatively large difference in numbers of x-rays passing through the soft tissues compared to

Downloaded From Vet-eBooks.com

the bone using low kV, giving relatively high contrast. Increasing the kV allows relatively more x-rays to penetrate through the bone, and so affects both opacity and contrast. A low kV produces a high-contrast image but has low exposure latitude; therefore the exposure values are critical for a diagnostic image. A high kV results in low contrast, but has wider exposure latitude and the exact exposure levels are less critical. With digital radiography this can be more difficult to appreciate as the algorithms applied to the image during processing can override adjustments to kV and mA.

To obtain a radiograph with the same opacity as an original but with reduced contrast, halve the mAs and increase the kV by 15% (approximately 10 kV). Conversely, to increase contrast levels, double the mAs and reduce the kV by 15% to achieve the same opacity. Normally for good bone detail the kilovoltage should be less than 70 kV. Attenuation of the x-ray beam is heavily dependent on the atomic number of the tissues, and it is desirable that photoelectric absorption predominates. Increasing the kV also results in more forward scatter (see Grid below).

X-ray film and image intensifying screens

Although in many countries conventional x-ray film has been largely replaced by imaging plates, x-ray film is still in use and therefore merits discussion. Details of the structure of film, image intensifying screens and chemistry cannot be covered here, but are readily available in other radiographic textbooks. The principle however is important to an understanding of radiography. In simple terms a film consists of a cellulose acetate sheet coated with a light- (or x-ray) sensitive emulsion (a layer of complex silver halide crystals). When these crystals are subjected to x-rays (or light), they undergo partial chemical reduction, creating a latent image. Submersion in developer completes the chemical reduction. Subsequently when immersed in fixer, the reduced crystals are insoluble and remain on the film, but the unexposed crystals are dissolved, leaving the visible image. To make the system more sensitive, it is usual for the film to be placed in a cassette, which places an image intensifying screen on either side of the film. The screens fluoresce when stimulated by x-rays, and because the film is much more sensitive to light than x-rays, an image can be produced with a reduced x-ray exposure.

Important variables include the type of film being used and the compatibility of the screens, which intensify the image. It is important to match the spectral output of the screen with the spectral sensitivity of the film (see Appendix B). The large number of film and screen combinations available is beyond the scope of this book. The clinician should rely on a veterinary radiologist or knowledgeable sales person to help decide which film–screen combination is best suited to the x-ray machine and the practice, although Appendix B gives some guidelines. With a high-output x-ray machine (100 kV, 100 mAs), it is worthwhile investing in high-definition screens for use with single emulsion, relatively slow film, for distal extremity work. This gives excellent detail, but is unsuitable for low-output machines, because long exposure times result in loss of definition through movement blur. Rare earth screens are essential for obtaining high-quality images proximal to the carpus and tarsus. Old screens are like old horses, they collect scars and lose performance as they age, and therefore should be replaced on a regular basis in order to maintain the optimum level of performance. It is also important

Downloaded From Vet-eBooks.com

that screens are cleaned regularly, to prevent the build-up of dust and extraneous materials within the cassette, which can result in white spots and lines on processed films.

Film processing

Good darkroom practice is an important consideration in the final quality of the radiograph but is often overlooked. Correct processing, whether manual or automatic, plays a major role. Standard darkroom procedures are available in any standard radiology text and are not covered here. There are however some processing errors that often cause film artefacts (see Appendix B) and thus affect interpretation. The following is a brief review of some of the basics principles that most often affect film quality and interpretation, especially when hand processing.

Film fogging

The most common darkroom problem whether using hand or automatic processing is fogging of the film either by light leaking into the darkroom, or improper darkroom lighting. Regardless of whether blue- or green-sensitive films are used, never rely on red or ruby bulbs as the source of darkroom lighting. For blue-sensitive film use a Wratten Series 6B filter with a 7–10 Watt bulb and for green-sensitive film use a Kodak GS1 filter with a 7–10 Watt bulb. In general the Kodak GS1 works with both blue- and green-sensitive film. The safelight should be a least 1 metre from the working area. There are two methods to check film for possible fogging:

1 In the darkroom place a sheet of film on the counter, then place an object on the film. Turn on the darkroom safelight and wait for approximately 30 seconds. This is the time it normally takes to place a film in a processor or on a hanger. Process the film as normal. If the darkroom is adequately dark and the safelight is suitable for the film, the film will be perfectly clear after developing. If the filter is incorrect or there is light leakage in the room, there will be fogging of the film around the object and the area covered by the object will be clear.

2 Expose a film in the cassette to an x-ray beam of 1–2 mAs and 40–50 kVp. This increases the sensitivity of the film. In the dark room place the exposed film on the counter and cover two thirds of the film with cardboard. Turn on the safelight for 30 seconds then move the cardboard over another third and continue the exposure for an additional 30 seconds. Process the film normally and compare the areas for fogging as described above.

Processing

There are three stages in the processing cycle that affect the final quality of the radiograph:

- Developer – converts exposed silver halide grains to metallic silver
- Fixer – converts unexposed, undeveloped silver halides into a form that can be removed from the emulsion and clear the film
- Washing – removes residual chemicals from film emulsion.

Important factors are the temperature and dilution of the chemicals and the time the film is in the developer and fixer.

[6]

Downloaded From Vet-eBooks.com

1 Prepare the chemicals to the correct working dilution and agitate to ensure even mixing. Temperature is absolutely correlated with processing time. Deviation from time and temperature guidelines results in under- or over-development and loss of detail. At the optimal temperature of 20°C (68°F) developing time should be 5 minutes. A variation in time should be calculated for other temperatures. The temperature of the solutions should be checked after the rinse water has been on for at least 15 minutes. The darkroom should be kept at a constant temperature to assist in maintaining the solutions at the ideal temperature.
2 During development, fixing and washing, agitate the film several times to remove any air bubbles that cling to the emulsion. Air bubbles cause light or dark spots, or circular artefacts on the film, depending upon which solution the bubbles occurred in. Care must be taken to prevent films touching or being scraped by the hangers during agitation in order to prevent scratches of the wet (swollen) emulsion, or the development of kissing defects. A kissing defect occurs when two films cling to each other during any phase of the developing process, resulting in an area of incorrect processing. This can also occur when two films overlap each other in an automatic processor. When processing several films, all films should be loaded into hangers prior to being processed in order to maintain optimal timing.
3 Chemical levels must be high enough to cover the film in the hanger. Low chemical levels result in portions of the films being undeveloped which can result in loss of important information. To avoid chemical carry-over, in order to maintain developer and fixer strengths, fluid should drain from the film and hanger prior to placement in each solution, including the rinse tank. Loss of strength of developer results in underexposed film, while loss of fixer strength results in yellowing with age. Developer should be replenished after every session of processing to maintain it at correct working strength.
4 Developer deteriorates when not in use, therefore it must be changed regularly. If not kept covered the developer oxidizes. In either case this results in underdevelopment.
5 If it is essential to examine a wet film, wait until fixing is complete then quickly rinse the film and view it. Remember that wet films have swollen emulsion and detail is lost until the film is dry, when the halide crystals will have coalesced into a more definitive image!
6 The final wash is an important part of the processing cycle to remove residual chemicals from the emulsion. This prevents discolouration and fading of the image.

AUTOMATIC PROCESSING

The advantages of an automatic processor over manual processing are considerable. There is absolute consistency of processing, which enables a consistent estimate of exposure values, and results in marked improvement in film quality. There are also benefits of economy and speed. With automatic processing a dry film is available to read within 60–90 seconds compared with approximately 1 hour for manually processed film. Both manual and automatic processing require proper upkeep and maintenance of equipment to ensure diagnostic quality films. Regular maintenance of the processor is important as is making sure that processing fluids are fresh and in adequate

Downloaded From Vet-eBooks.com

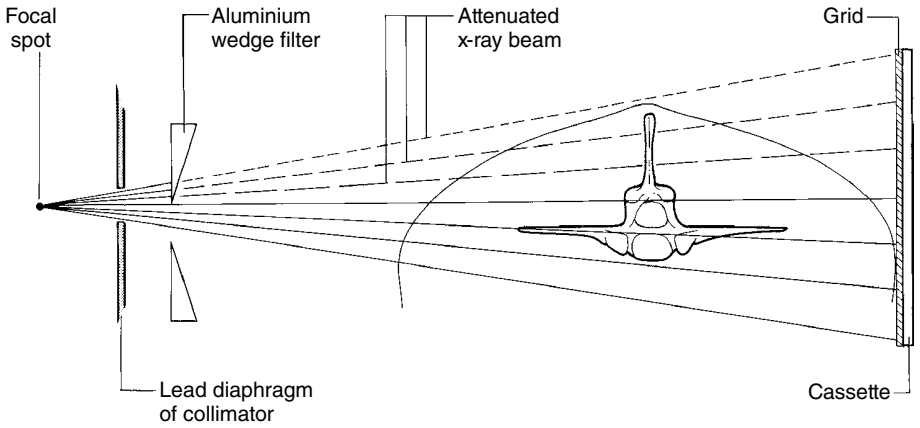


Figure 1.2 Use of an aluminium wedge filter placed between the x-ray machine collimator and the object to be radiographed. The upper leaves of the filter placed in the x-ray beam reduce the exposure of the upper part of the beam.

supply. The most common problems with an automatic processor occur when upkeep is not maintained.

Radiographic practice

In several parts of the following text, reference is made to an aluminium wedge filter (Figure 1.2). This is placed immediately in front of the x-ray tube, and absorbs a proportion of the x-rays. It allows the intensity of the beam to be reduced in specific areas. It is of particular value when radiographing parts of the horse that show a marked change in soft-tissue thickness from one side of the film to the other, e.g. the thoracolumbar spine or stifle, but is of less value when used with digital systems.

Exposure chart

It is advantageous to record the exposure settings used for each image, and gradually build an exposure chart. This should include a record of the size and age of the horse, the area radiographed, and the exposures and the film–screen combination or imaging plate used. This allows better and more consistent radiographs to be obtained, and also provides a basis for estimating the required exposures for animals of different sizes and ages. When creating this chart, it is important to maintain a constant FFD. A reduction in FFD increases the radiation reaching the screen by a square of the change in distance (necessitating a reduction in the exposure factors). An increase in distance has the opposite effect. Generally in equine radiography a FFD of 75–100 cm is used. Note that single emulsion film is particularly sensitive to changes in radiation dose; a slight change in FFD can therefore have a relatively big effect on exposure.

Grids

Most of the radiation during an exposure passes through the subject and exposes the film, or is absorbed by the tissues. Some radiation however is deflected (termed 'scatter') and this results in a low background exposure over the entire film, causing reduced film contrast. Good collimation of the primary beam reduces the amount of scatter at acquisition (Figures 2w.1a–c). The effect of scatter can be reduced by placing a grid in front of the cassette to absorb the scattered radiation. As a rough guide, grids are generally only needed if the area being radiographed exceeds 11 cm in thickness. Thus equine extremities below

Downloaded From Vet-eBooks.com

the carpus and tarsus usually do not require the use of a grid. Grids are generally not required for soft-tissue evaluation, and may be contraindicated in this situation. There are numerous types of grid, and advice on the best one for any specific situation is beyond the scope of this text. The disadvantages of a grid are that they increase the exposure required and produce lines on the films, which are sometimes found objectionable when reading the radiograph. If a focused grid is used, the x-ray beam must be perpendicular to the grid, centred on it, and at the correct FFD. When grids are of value, this is noted in the discussion of the projections described in the following text. Grids used with digital radiography have particular problems, and can cause serious image artefacts. The reader is advised to obtain specialist advice before acquiring grids for use with digital systems.

An alternative strategy is to use an air gap between the horse and the imaging plate rather than a grid. This can be helpful in areas surrounded by large muscle masses, for example the back or the pelvis, but will result in increased magnification of the area being radiographed.

Preparation and positioning

Preparation of the patient is essential to good radiography. Quiet and careful handling reduces movement, and sedation is often beneficial. Blinkers, blocking the horse's line of vision, may make it less apprehensive. Cotton wool earplugs or background music may make the horse less aware of the noise of the x-ray machine. Areas to be radiographed should be brushed to remove mud from the coat, which can produce confusing artefacts. For radiographs of the feet, the shoes normally need to be removed and the feet trimmed to remove loose horn and dirt.

It is important to ensure correct positioning of the horse before acquiring the radiograph. A small deviation in limb position can result in poor quality images with misleading information, making accurate interpretation difficult (Figure 1.3). In a well-positioned radiograph, the x-ray beam is perpendicular to the cassette to minimise image distortion.

Acquisition of additional images

It is important, if possible, to assess all the acquired images before terminating the examination. The images should be scrutinised for correct positioning and exposure, the presence of artefacts, and the identification of one or more potential lesions. Incorrect positioning may create an image which appears to have a lesion, but which disappears with correct positioning (Figures 1.4a and 1.4b, Figures 1w.4c–f; Figures 3.68b and 3.68c). The interpretation of the closeness of spinous processes is a good example. When on the margin of an image two spinous processes may appear separated because of a divergent x-ray beam, but if in the centre of the image clearly impinge (Figures 1w.5a and 1w.5b). Alternatively a lesion can be missed with inappropriate positioning, but become apparent on an image acquired with the limb correctly positioned (Figures 1.6a and 1.6b). Artefacts due to superimposition of normal structures, or the result of an opacity due to mud on the skin, can be confirmed by examination of the horse and an additional image can be acquired if necessary (Figure 1.7a, Figures 1w.7b–e). A lesion may be suspected from conventional images, but acquisition of additional images using additional projections may verify its presence and/or determine its

Downloaded From Vet-eBooks.com



Figure 1.3(a) Lateromedial radiographic image of a hock of a 7-year-old riding horse with distension of the tarsocrural joint. This radiograph is not of diagnostic quality. The horse was standing base wide during image acquisition and as a result this is not a true lateromedial view. There is considerable overlap of the joint spaces of the talocalcaneal-centroquartal, centrodistal and tarsometatarsal joints. The trochleas of the talus are not superimposed.



Figure 1.3(b) Lateromedial radiographic image of a hock of a 7-year-old riding horse, the same hock as in Figure 1.3(a). This is a well-positioned image and the joint spaces of the talocalcaneal-centroquartal, centrodistal and tarsometatarsal joints are clearly defined. The trochleas of the talus are superimposed.

position more accurately (Figures 1w.8a–e). Ideally the presence of a lesion should be verified in more than one plane.

Progression of lesions

Images acquired at the time of onset of lameness may show advanced radiological abnormality despite the short duration of clinical signs (e.g. advanced degenerative joint disease of the centrodistal joint) (Figure 1w.9). Clearly the development of radiological changes preceded the onset of recognisable pain. Alternatively images acquired immediately after acute onset of lameness may show no detectable abnormality, but sequential examinations may reveal progression of the underlying disease process (Figure 1.10a–c). In some instances there will be resolution of a lesion over time (Figures 1w.11a–i), but some lesions remain radiographically evident after they cease to be of clinical significance (Figure 1w.12).

Downloaded From Vet-eBooks.com



Figure 1.4(a) Caudocranial radiographic image of a stifle. Medial is to the left. The medial femorotibial joint space appears to be markedly narrowed. This was the result of inappropriate positioning during image acquisition. The limb to be examined should be positioned caudal to the contralateral limb. Compare with Figure 1.4(b).



Figure 1.6(a) Dorsopalmar radiographic image of a right metacarpophalangeal joint of a 4-year-old pony. Medial is to the left. The proximal sesamoid bones are superimposed over the metacarpophalangeal joint space.



Figure 1.4(b) Caudocranial radiographic image of the same stifle as Figure 1.4(a). Medial is to the left. The medial femorotibial joint space is normal.



Figure 1.6(b) Dorsal 10° proximal-palmarodistal oblique image of the same metacarpophalangeal joint as in Figure 1.6(a). Medial is to the left. The proximal sesamoid bones are now projected proximal to the metacarpophalangeal joint space which appears narrower medially, consistent with degenerative joint disease. Narrowing of a joint space should ideally be confirmed by being seen on more than one image.

Downloaded From Vet-eBooks.com



Figure 1.7(a) Dorsoproximal-palmarodistal oblique image of a right front foot. Lateral is to the right. There is a radiolucent line in the lateral palmar process of the distal phalanx. This could potentially be misdiagnosed as a fracture but note that the line extends just proximal to the proximal margin of the bone and is the result of inadequate packing during image acquisition.



Figure 1.10(a) Dorsolateral-palmaromedial oblique (flexed) image of the right front foot of a 9-year-old pleasure horse with sudden-onset severe right forelimb lameness the previous day while misbehaving when loading to travel. There is a narrow radiolucent line through the lateral palmar process of the distal phalanx (arrows) representing a fracture.

Radiation safety

Radiation safety, i.e. ensuring that personnel around the horse do not receive doses of radiation, is extremely important. There are codes of practice available in different countries, but the basic principles can be summarised as follows:

1 Keep the number of people present when radiographing a horse to the absolute minimum required for its safe handling.

2 Use appropriate restraint of the horse to keep it still during exposures (so that repeat exposure to radiation is not necessary). Sedation may be required.

3 Use cassette holders whenever possible. Because radiation intensity follows the inverse square law, increasing distance from the source is an important safety factor. Certain views, where 'patient tolerance' is low, may prompt the hand holding of cassettes. This may be justified if it reduces the repetition of radiographs or prevents the horse panicking. If it is essential to hand hold a cassette, then large cassettes should be used, with the x-ray beam well collimated, and the holder's gloved hands as far from the primary x-ray beam as possible.

4 The primary x-ray beam should be well collimated, and a light beam diaphragm used to enable maximum collimation. *No part of any attending person, even if covered with protective clothing, should be placed in the primary beam.* Protective lead clothing protects from scattered radiation only, not the primary beam. Remember that the primary beam continues through the patient and cassette, and personnel standing on the opposite side of the patient are at risk.

Downloaded From Vet-eBooks.com



Figure 1.10(b) Dorsolateral-palmaromedial oblique (flexed) image of the same right front foot as Figure 1.10(a), 8 days later, i.e. 9 days after the onset of lameness. The margins of the fracture line are less distinct (arrows).



Figure 1.10(c) Dorsolateral-palmaromedial oblique (flexed) image of the same right front foot as Figures 1.10(a) and (b), 17 days after the onset of lameness. The fracture line has become wider, especially distally (arrows). This is typical progression of a fracture.

5 All personnel who must remain present during radiography must wear protective gowns, and if near the primary beam should also wear gloves or similar hand and arm protection, and a thyroid protector.
6 All personnel working with and around x-ray machines should be monitored using a film badge or dosimeter system.
7 Walls of a room or stable provide a primary barrier but be aware that although dense breeze block will stop the primary beam, a wooden partition will not.
N.B. Digital processing of images will marginally reduce the radiation dose, but this is not a reason to ignore normal radiation safety precautions. In practice the use of digital imaging often increases the number of images acquired, and increases the need for vigilance regarding radiation safety.

Examination for purchase

Because of the general acceptance of this text world-wide, it is impossible to write a comprehensive section that covers all areas of the radiographic examination included as part of a pre-purchase examination in all countries. When making such an examination, it is necessary to take into account many variable factors such as the breed and intended use, as well as considering both the country of origin and the country to which an animal is being sold. This carries many different legal implications and is therefore well beyond a text that is limited to radiology. Guidelines regarding this have been published, and the reader is referred to 'Further reading'.

As a general guide, the radiographic portion of a pre-purchase examination must first take into account the general health, age and condition of the

Downloaded From Vet-eBooks.com

horse. It is important that the previous and intended use(s) of the horse are considered, with special emphasis on conditions prevalent in the relevant breed or use of the horse. The radiographic evaluation should follow the physical examination, to include areas that might be expected to face the greatest stress in the performance of the expected use, and to investigate potentially significant findings discovered during the physical examination. It is essential that if adequate interpretation is to be made, film quality must be good, and an adequate number of views obtained to evaluate the specific area(s) of concern. No simple guide can be given for this, except to say that as a general rule there must be at least two views of a suspected lesion, and it is clinically better to have too many views than too few, bearing in mind the overriding importance of radiation safety. When imaging apparently normal joints (such as fetlock or hock) it is generally necessary to obtain dorsopalmar (dorsoplantar), lateromedial and two oblique views of each joint. If the horse is to be insured, the insurance company may have specific minimum requirements for views to be obtained. Sales companies for Thoroughbred yearlings and racehorses in training frequently specify what views of which joints are required. Some countries have a designated set of radiographs that should be obtained as part of a pre-purchase examination. If a client is purchasing a horse abroad they should be advised that the radiographs obtained may not be the same as in their own country, where additional views may be considered necessary to provide a comprehensive examination.

A report on pre-purchase radiographs should begin with a clear identification of the animal examined. This must be followed by sections on each area examined, stating the views obtained and giving a clear and concise description of the radiological findings, starting with the most significant finding. Finally an opinion on the potential significance of any abnormalities should be provided, relative to the intended use of the horse. If for any reason the radiographic study is limited, this should be clearly stated in a disclaimer. For example, 'The owner refused to allow sedation and therefore the examination of the foot is incomplete'; or, 'The study is compromised by the presence of shoes which could not be removed due to permission being refused'. In extensive reports it is useful to finish with a clear summary of significant findings relevant to the potential use of the horse if purchased.

Records and labelling

Radiographic images and reports are part of medical records, and should be stored carefully with patient records. In the United States both radiographs and radiographic reports must be kept for legal reasons for a minimum of 7 years, and this is a good principle to apply. The quality of the films/images will reflect on the quality of the practice, and this becomes particularly important when films may be viewed by other practitioners, for example in a pre-purchase examination. All films and digital images should be clearly identified with permanent labels at the time of acquisition.

With the increasing use of radiography, and the rise in litigation involving veterinarians worldwide, it is essential that radiographs are carefully labelled. This should be done digitally or photographically on the film, either by the use of one of the special tapes produced for this purpose, attached to

Downloaded From Vet-eBooks.com

the cassette when the film is exposed, or by a labelling light-box system in the darkroom. Labels should include as a minimum:

1 The identity of the horse and owner.
2 The limb radiographed.
3 The date.
4 Lateral or medial markers where relevant should be placed on the cassette.
5 The identity of the veterinary practice.
6 The view employed (assuming this cannot be determined from the radiograph).

Digital systems may produce such labelling automatically, and the technician acquiring the images should ensure that correct information is recorded.

It is essential that a complete examination is carried out, with an adequate number of views of each area involved. The exposures must be correct to demonstrate any lesions present, the radiographs must be of diagnostic quality, and images should include all of the area being examined (e.g. images of hock joints frequently miss the proximal aspect of the calcaneus, or the tarsometatarsal joint). An inadequate examination may be at best inconclusive and at worst totally misleading. Such examinations in the hands of the legal profession may prove devastating!

PRINCIPLES OF RADIOGRAPHIC INTERPRETATION: RADIOLOGY

It is important to read radiographic films when they are dry. The emulsion swells when wet and detail cannot be appreciated on wet films.

It is helpful if radiographs are always viewed using the same orientation, i.e. with the horse facing to the viewer's left, medial on the left, and when appropriate the left side on the right. This aids interpretation, as only one image need be remembered for each area radiographed. (This varies slightly from the convention that any film should be viewed as if the examiner was looking at the patient face on, e.g. the left forelimb is viewed with medial to the left, and the right forelimb with medial to the right.) The number of views required for any area varies, and is mentioned in the text. It is important to obtain an adequate number of views to ensure that no lesion is missed, and an attempt to compromise with fewer views is a false economy. The use of 'special' views, e.g. oblique and 'skyline' views, of suspected lesions can be very rewarding.

Adequate radiological interpretation is dependent on complete and systematic evaluation of all of the information that is found on the image. Films should be viewed on a viewing box, in a room with subdued light. This optimises the ability of the reader to differentiate structures and to obtain the maximum information from a film. The darker the film, the more important it becomes that the conditions under which it is read are ideal.

Initially the film should be evaluated from a distance of several feet before viewing closely, in order to get an overall impression before concentrating on details. Areas of diffuse, subtle change in radiopacity are usually more readily identified from a distance than close up. Masking the light around the edge of the radiograph also improves the ability to read a film, as do high-intensity illumination devices.

Downloaded From Vet-eBooks.com

Digital images should be viewed on high-definition flat screens, again in a room with subdued light. As with film, it is helpful to mask the image to remove light areas around the point of interest. In many systems it is then possible to select the area of most relevance, and to adjust contrast and brightness of the region concerned to aid evaluation of a wide range of tissue densities. Most systems also allow for enlargement of the whole image, or of specific regions of interest (see Chapter 2).

With film or digital images, start by assessing the image itself:

- Is the quality of the image adequate for interpretation?
- Is the view correctly positioned to allow correct interpretation?
- Are there any processing or other artefacts (e.g. mud on the horse) that will influence interpretation?

Then move on to assess the area radiographed:

- Is there any soft-tissue swelling?
- Is there any alteration of opacity of the soft tissues?
- What is the approximate age of the patient?

Finally look at the outline of the bones and their detailed internal structure:

- If an 'abnormality' is identified, ensure that it is real – can it be seen on another view? Can it be explained by positioning or overlap of other bones or soft-tissue structures? Is it a variation rather than an abnormality, e.g. the position and shape of a nutrient foramen can vary considerably. Could a radiolucent zone be explained by introduction of air during a previously performed local analgesic technique (Figure 1.13a and b). Intra-articular gas appears as a semicircular or more diffuse radiolucent area, often in the proximal



Figure 1.13(a) Dorsolateral-palmaromedial oblique image of the distal metacarpal region and metacarpophalangeal joint of a mature horse. There are radiolucent areas superimposed over the third metacarpal bone. These gas shadows are the result of inadvertent introduction of air into the metacarpophalangeal joint while performing intra-articular analgesia. Such lucent areas may persist for up to 48 hours. Note also the periarticular osteophyte formation on the dorsoproximal medial aspect of the proximal phalanx consistent with degenerative joint disease. There are also multiple radiolucent lines in the lateral proximal sesamoid bone.

Downloaded From Vet-eBooks.com



Figure 1.13(b) Dorsomedial-palmarolateral oblique image of the same limb as Figure 1.13(a). There are discrete radiolucent areas (arrows) in the soft tissues distal to the distal aspect of the second metacarpal bone representing air in the palmar recess of the metacarpophalangeal joint.

part of a joint, whereas extra-articular gas appears as a linear radiolucency. These lucencies may persist for up to 48 hours after injection

- Would additional views aid or complete adequate evaluation?
- If it is a true radiographic lesion, describe it in radiological terms.

In this process of description it is often possible to determine if it is an active or inactive process. In general, terms like smooth, regular and well marginated (defined) lead towards a conclusion of normal, benign or long-standing lesions. Terms such as roughened, irregular, sharp, poorly demarcated or destructive, lead to a conclusion of active disease. If the process is considered to be pathological, then think what pathological process could cause this change and then consider what diseases could cause this type of pathology.

If images are obtained to confirm the presence of a specific disease or disease process and are not completely evaluated, the severity of the condition, complications of the process or other concurrent lesions may be overlooked. Thus to read radiographs successfully, it is important to relate the changes seen to known behaviour of the tissues under consideration, rather than relating the radiographic appearance to a clinical condition seen before. The latter method relies heavily on experience and does not allow interpretation of changes that have not been previously encountered. It is important to remember that each radiograph can only represent a fraction of a second in the life of the patient, and the development of a disease process. It is a static image of a dynamic process. When a radiograph is read, all the changes from the normal should be considered and used to build up an impression that can then be related to disease processes known to occur in the region.

Downloaded From Vet-eBooks.com

For accurate interpretation it is important to take into account factors such as the period of time for which the clinical signs have been present, the age, sex and breed of the patient, and the validity of the history and possible complicating factors. A working diagnosis can then be formed, which will complement any laboratory findings and other imaging techniques, and help to confirm a clinical diagnosis. There is no substitute for a good clinical history and examination, and radiographs should only be used as an aid to the clinical diagnosis.

It is beneficial to have bone specimens available when reading radiographs, particularly oblique images. An anatomy book and a library of normal radiographs of each anatomical area at different ages are invaluable. If problems are encountered in evaluating an area, it is often helpful to obtain a similar radiograph of the contralateral limb for comparison, thus providing a perfect age-, sex- and breed-matched radiograph. Remember that, in the neonate, some structures are not ossified and therefore cannot be seen. More confusing is the appearance of partially ossified structures (e.g. incompletely ossified subchondral tissues have an irregular opacity, which may seem similar to the radiographic appearance of infection). The normal radiographic appearance of the structures of immature animals is therefore described in each chapter. Digital images are easily transferred electronically, therefore it is always easy to get the advice of an expert if there are queries concerning interpretation.

Radiographs are only one part of a jigsaw puzzle and may be used for several purposes:

- To confirm, refute or suggest a diagnosis
- To give information on progression and severity of a condition, and aid formation of a prognosis
- To add information regarding size, shape, position, alignment and possibly duration of a lesion.

When reading a radiograph the result must be fitted into the general picture presented to the clinician. It is one aid to diagnosis that the clinician has available. In some cases special views or contrast studies may provide valuable additional information. There are many other complementary imaging techniques (e.g. ultrasonography, nuclear scintigraphy, computed tomography and magnetic resonance imaging) and other sources of clinical information that are available. The radiograph is an aid to diagnosis and not the ultimate diagnosis in itself.

One of the most difficult questions to answer is how long a lesion has been present. This is often of importance, but can seldom be answered with any degree of certainty. Minimum times for certain lesions to develop can be estimated, but the time for which a lesion has been present often remains uncertain. The following pointers may be of value:

- Osteophyte formation of any type is not normally visible, even under optimum conditions, in less than 3 weeks
- Treatment after injury may delay osteophyte formation
- Incomplete or fissure fractures may take up to 2 weeks to become visible
- Active bone changes are characterised by lesions with irregular or fuzzy margins, which may be less opaque than the parent bone
- Inactive bone changes are generally smooth, regular and uniformly opaque

Downloaded From Vet-eBooks.com



Figure 1.14(a) Dorsolateral-palmaromedial oblique image of the left carpus of a 7-year-old National Hunt racehorse with acute-onset lameness after a fall. There is a non-displaced fracture of the proximal palmar aspect of the intermediate carpal bone (arrows). There is a radiolucent area distal to the accessory carpal bone partially superimposed over the ulnar carpal bone. This is air in the palmar recess of the middle carpal joint after intra-articular analgesia.



Figure 1.14(b) Dorsolateral-palmaromedial oblique image of the left carpus of the same horse as Figure 1.14(a), acquired 13 months later. The horse had been managed conservatively at the owner's request and had raced successfully, but recently lameness had deteriorated. The fracture fragment is now displaced (arrows). There is extensive periarticular osteophyte formation on the distal dorsomedial aspect of the radius, the proximodorsal aspect of the radial carpal bone, and the proximomedial aspect of the third carpal bone consistent with degenerative joint disease. There are several mineralised opacities on the proximodorsal aspect of the third metacarpal bone.

- Large productive changes may take months to form and become smooth in outline
- An old inactive bone lesion may not indicate current disease, although it may be present in the same region as a current problem
- Bone models according to the stress applied to it (Wolff's law). Non-stressed bone does not model
- Scars in bone, as in any other tissue, do not model.

It can be difficult to predict the progression of an injury accurately based purely on one set of radiographs. Sequential radiographs acquired at weekly intervals may demonstrate dramatic changes which may have a major influence on prognosis (Figures 1.14a and 1.14b). Do not be tempted to over interpret radiographs acquired at the time of an acute injury (Figures 1w.14c and 1w.14d).

It should be noted that the terms remodel and model are frequently used incorrectly in radiology (see Appendix C: Glossary). In this text, the term remodel is frequently employed because of its common usage. Modelling is, however, a more correct term, compatible with changes detectable radiographically (and histologically).

Downloaded From Vet-eBooks.com

RADIOLOGICAL APPEARANCE OF PHYSIOLOGICAL CHANGES AND SOME COMMON PATHOLOGICAL LESIONS

Bone changes

The basic ability of bone to respond to stimuli is affected by various factors, such as diet, disease and the physiological state of other organs such as the lungs, kidneys and gastrointestinal tract.

It is important to remember that the normal bone status varies throughout life. During the period of skeletal growth, there is increased bone formation relative to resorption. The skeleton of the young individual lacks density and is more pliable (35% mineral to 65% matrix and cells). As the individual matures, the density gradually increases (approaching 65% mineral and 35% matrix and cells). With advancing age the bone–mineral balance changes towards decreased formation and increased resorption.

Although it is common to think of bone as being largely calcium, the mineral content of bone is roughly 35% calcium, 17% phosphorus and 12% copper and other minerals. Radiologically it is not possible to detect a decrease in mineralisation of less than approximately 30% of the total mineral content, and therefore changes in bone mineralisation may be undetectable radiographically early in a disease process. Diagnostic ultrasonography may be helpful in early detection of some bony changes affecting surfaces of bones, e.g. periosteal new bone formation.

It is important to remember that some changes reflect past history, rather than the response to current stimuli; thus some radiographic lesions may no longer have clinical significance, but persist as incidental findings.

Wolff's law states that bone models according to the stresses placed on it, and modelling is dependent upon bone function and the distribution of the load. Forces are applied to bone at the sites of attachment of ligaments and tendons or through the joints. Application of a load may deform the part concerned. Deformity is dependent upon the degree of the stress and the number of loading cycles.

When evaluating radiographs it should be remembered that bone is a living dynamic tissue that can only respond in a finite predictable way to an infinite number of outside stimuli or insults.

Demineralisation of bone

GENERALISED DEMINERALISATION

Generalised demineralisation or osteoporosis may be recognised by: thinning of the cortices; coarser, more obvious trabecular pattern; apparent radiographic overexposure due to reduced bone density (check the FFD, exposure values and processing technique). With digital imaging, exposure differences are more difficult to detect, and evaluation of the cortices and the trabecular pattern becomes more important. Generalised demineralisation (Figure 1.15) may result from a mobilisation of minerals because of a need elsewhere in the body, e.g. in pregnancy, dietary inadequacy or metabolic imbalance (e.g. secondary nutritional hyperparathyroidism), or renal disease. Alternatively the lack of mineral may indicate that the patient is very young or very old.

Downloaded From Vet-eBooks.com



Figure 1.15 Slightly oblique lateromedial image of the distal aspect of a limb of a mature pony, showing generalised demineralisation due to secondary nutritional hyperparathyroidism. Note the thin poorly defined cortices and the very prominent trabecular pattern (compare with Figure 5.8a, of a normal metacarpophalangeal joint).



Figure 1.16(a) Dorsolateral-plantaromedial oblique image of the metatarsophalangeal joint a 15-year-old sports horse with severe lameness of 2 months' duration, associated with disruption of the medial collateral ligament and bone trauma. There is a generalised loss of opacity of the lateral proximal sesamoid bone, the third metatarsal bone and the proximal phalanx reflecting disuse osteopenia.

LOCALISED DEMINERALISATION

Loss of mineral in a single limb indicates a process limited to that area, e.g. the loss of mineral in one limb may relate to disuse osteopenia (Figures 1.16a and 1w.16b). Mineral is lost due to muscular inactivity and/or reduction in weight bearing. It should be compared with the contralateral limb if a generalised disease might be implicated.

FOCAL DEMINERALISATION

Focal loss of bone (Figure 1.17) may indicate the presence of infection, neoplastic invasion, or replacement of bone by fibrous tissue as a result of a previous disease process (this may be considered to be equivalent to a scar in bone).

Downloaded From Vet-eBooks.com



Figure 1.17 Lateral-lateral image of the summits of the spinous processes in the mid-thoracic region. There is extensive demineralisation of the spinous process of the ninth thoracic vertebra. The cortex is also irregular in outline.

It is also seen:

- As an osteochondral defect in osteochondrosis (although this may actually represent delayed mineralisation rather than demineralisation)
- In osseous cyst-like lesions
- As subchondral bone loss in degenerative joint disease
- In association with vascular abnormalities
- Along fracture lines.

It may also result from continuous pressure on bone, as in chronic proliferative synovitis or other space-occupying masses.

Increased bone production

Increased bone production may result in increased bone density and thus radiopacity.

A generalised increase in bone density may be due to fluorine poisoning or a hereditary disease such as osteopetrosis. In some species, but as far as is known not the horse, mineral deposition could indicate hypervitaminosis A.

CORTICAL THICKENING

Wolff's law states that bone models according to the stresses placed on it, and is dependent on its function and the distribution of the load. Cortical thickness, particularly of the third metacarpal and metatarsal bones,

Downloaded From Vet-eBooks.com

changes from a young, skeletally immature, untrained horse to a mature trained horse. The dorsal cortex becomes significantly thicker than the palmar cortex. If a horse has a marked conformational abnormality, such as 'off set knees', the distal limb bones will model accordingly, resulting in increased thickness of the cortices of the regions of the bones carrying increased load.

FOCAL NEW BONE FORMATION

Osteophytes are spurs of bone at the margin of a joint. Osteophyte formation occurs in response to various stimuli. The time taken for an osteophyte to develop after a stimulus varies between individuals and depends upon the inciting cause. It may take as little as 2 weeks, or may take several weeks. Osteophyte formation with uniform opacity and a smooth outline is likely to be longstanding and inactive. More lucent osteophyte formation, or a formation with a more lucent tip, is likely to be actively developing. *Periarticular osteophytes* may be associated with intra-articular pathology, and develop at the margins of articular cartilage and periarticular bone (Figure 1.18). They also develop as a consequence of joint instability.

Entheseophytes are spurs of bone that develop where tendons, ligaments or joint capsules attach to bone. They represent the response of bone to stress applied through these structures, whether it is tearing of a portion of a ligament, chronic stress applied by a tendon, capsular traction, or chronic capsular distension. It may be difficult to differentiate between osteophytes and entheseophytes in some areas.

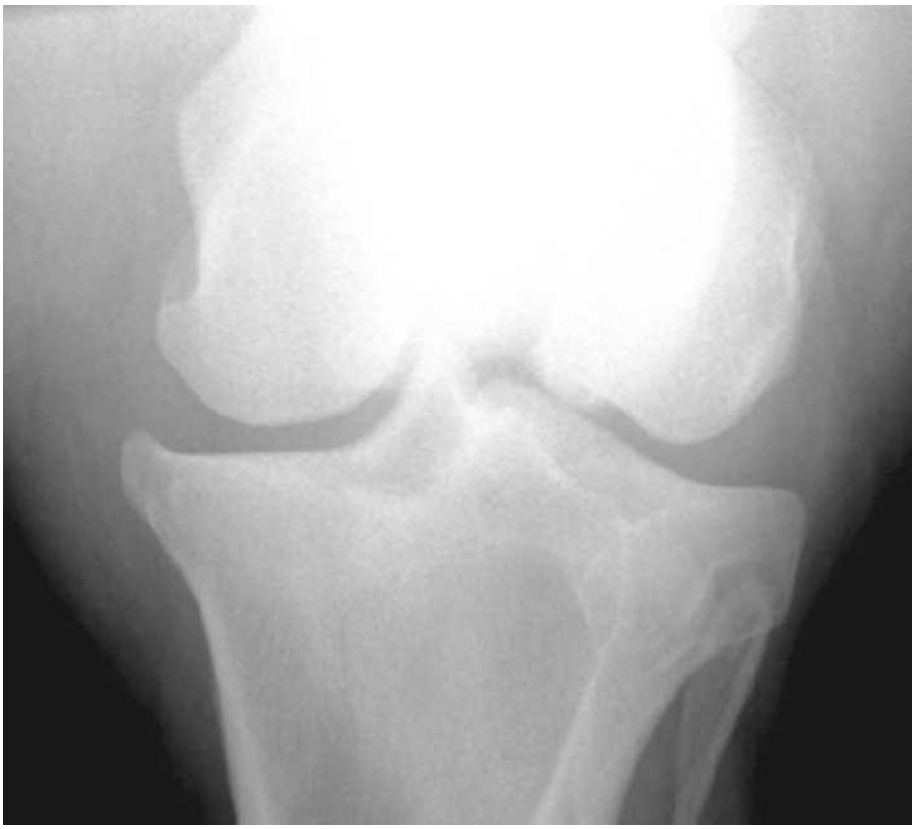


Figure 1.18 Caudocranial radiographic image of a stifle of a 14-year-old Welsh Section D Cob. Medial is to the left. There is a moderately sized osteophyte on the proximomedial aspect of the tibia, reflecting osteoarthritis. Lameness was improved by intra-articular analgesia of the femorotibial and femoropatellar joints. Arthroscopic evaluation revealed a tear of the medial meniscus, severe fibrillation of the cranial ligament of the medial meniscus and abnormalities of the articular cartilage.

Downloaded From Vet-eBooks.com

PERIOSTEAL AND ENDOSTEAL NEW BONE

Periosteal and endosteal new bone formation result from inflammation of the periosteum or endosteum. This may result from a fracture (the callus forming endosteal and periosteal new bone), trauma, infection, abnormal stress at a soft tissue attachment, or tumour formation.

SCLEROSIS

Sclerosis is a potentially misleading term. Its true pathological definition is increased hardness of a tissue, a phenomenon that cannot be determined radiologically. It is a term adopted by radiologists to describe localised increased opacity of the bone due to increased bone mass within existing bone. It is most readily recognized in trabecular bone, and occurs in response to several stimuli including:

- Stress (e.g. increased thickness and/or opacity of the subchondral bone in degenerative joint disease)
- An attempt to wall off infection (e.g. in the medullary cavity adjacent to an area of osteomyelitis; in response to osteitis of cortical bone adjacent to the site of infection; adjacent to sequestration)
- To support or protect a weakened area (e.g. a rim of increased opacity surrounding an osseous cyst-like lesion).

Bone lesions

Physitis (epiphysitis)

Physitis (or physeal dysplasia) is the term that should be used to describe abnormal widening and bony irregularity at the epiphyseal and metaphyseal margins of the growth plate in skeletally immature horses. The metaphysis of the bone is broadened and asymmetrical. There is increased opacity of the metaphysis adjacent to the physis, which may be more irregular in appearance than normal, with parallel radiolucent lines reflecting retained cartilage cones. The cortices of the metaphysis may be abnormally thick. Soft-tissue swelling over the area of involvement is usually present, and there may be an associated angular limb deformity. These changes are secondary either to rapid cartilage production or to defects in mineralisation and/or ossification to produce the primary spongiosa.

Although any physis may be involved in this process, physitis is most commonly associated with the distal radial (see Figure 7.23) and distal metacarpal/metatarsal physes. Focal osteochondral defects have been noted histologically and result from repeated haemorrhage and/or microfractures that interfere with the blood supply to the mineralising cartilage. Osteochondrosis-like defects have also been described.

Widened metaphyseal and physeal bone that is produced during the acute stage of the disease may persist throughout life, resulting in an irregular or flared appearance at the location of the physeal scar, although in many cases, considerable modelling towards normality occurs.

Neoplasia

Primary tumours and metastatic malignancy of the long bones of horses are rare. The majority of tumours that involve bone occur in the skull (see Chapter 11, 'Significant findings – Other causes of opacity of the maxillary

Downloaded From Vet-eBooks.com

sinus' and 'Significant findings – Tumours') or occasionally the spine (see Chapter 12, 'Cervical vertebrae – Neoplasia' and 'Thoracolumbar vertebrae – Neoplasia'). Tumours result in space-occupying lesions that may be radiopaque or radiolucent. Adjacent bone may be distorted in outline, and there may be associated new bone production. It is frequently not possible to differentiate specific tumour types by their radiological appearance. A malignant tumour may be similar radiographically to the result of infection, and differentiation is based on history, clinical signs, laboratory tests and biopsy.

Osteitis and osteomyelitis

Osteitis is inflammation of bone, and osteomyelitis is inflammation of cortical bone and its myeloid cavity. In bones that do not have a myeloid cavity (e.g. the distal phalanx), it is not appropriate to use the term osteomyelitis. Osteitis is usually the result of trauma or inflammation in adjacent soft tissues. It is characterised by new bone formation and sometimes bone resorption. Differentiation should be made between aseptic osteitis and infectious osteitis (see below).

Infectious osteitis and infectious osteomyelitis

Infectious osteitis (inflammation of bone due to infection) and infectious osteomyelitis (inflammation of the bone involving the myeloid cavity) are common in the horse. In an adult, infectious osteitis is more common and is usually seen at a single site, often related to trauma such as wire cuts or puncture wounds. The hallmarks of infection are:

- Soft-tissue swelling with bone destruction and new bone formation
- An attempt to wall off infection resulting in radiopaque bone forming adjacent to the area of bone infection and destruction
- Infection of bone may result in the formation of a sequestrum (a piece of dead, initially radiopaque bone) surrounded by an involucrum (an area of lucent granulation tissue) (see Figures 6.23b and 6.23c). A radiolucent tract may be visible extending from the infected area (a sinus)
- The distal phalanx, distal sesamoid (navicular) bone and skull show a slightly different reaction to infection. In these bones, infection tends to cause destruction of bone with little evidence of new bone formation
- In the foal, osteomyelitis is more common and may occur simultaneously at several sites, often extending into adjacent joints. The converse is also true, and septic arthritis commonly extends into adjacent bone causing an osteomyelitis. Osteomyelitis in the foal tends to be very destructive and there is usually very little response by the bone to wall off the infection.

A useful classification of infection of bone and joints has been devised by Firth (see below, 'Infectious arthritis').

Hypertrophic osteopathy

Hypertrophic osteopathy was formerly known as Marie's disease, hypertrophic pulmonary osteoarthropathy or hypertrophic osteoarthropathy. It is now termed hypertrophic osteopathy because it has been shown that pulmonary involvement is not a prerequisite for the development of the disease, as was once thought, although pulmonary lesions may be present. Hypertrophic osteopathy principally affects the metaphyses and diaphyses of the long bones, while sparing the joints. The disease is typified by periosteal new bone that often appears to be forming perpendicular to the cortices of the bone

Downloaded From Vet-eBooks.com



Figure 1.19(a) Dorsolateral-palmaromedial oblique image of the left metacarpophalangeal joint of a 10-year-old Thoroughbred mare. There is palisading new bone on the distal dorsal aspect of the third metacarpal bone and the dorsal and palmar aspects of the proximal phalanx, with overlying soft tissue swelling. The metacarpophalangeal and proximal interphalangeal joints are not involved. The areas of new bone formation were painful on palpation and the mare moved stiffly. All four limbs were involved. Diagnosis: hypertrophic osteopathy.

and is irregular in outline in the acute stage (Figures 1.19a and 1w.19b). In the early stages, soft exposures must be used to avoid overexposure of this relatively lucent new bone. Later the margins of the new bone become more opaque and smoother, and the appearance of the original cortex of the bone becomes less clear. The bony lesions develop secondarily to a primary lesion, usually in the thorax or occasionally the abdomen, such as a tumour, an abscess or diffuse granulomatous disease. The cause and distribution of the bony lesions are not understood, however, the bone changes may regress and remodel if the primary disease can be identified and successfully treated.

Enostosis-like lesions and other circumscribed opacities

An enostosis is defined as bone developing within the medullary cavity or on the endosteum, resulting in a region of increased radiopacity. In the horse enostosis-like lesions have been described as focal or multifocal, intramedullary sclerosis. They are usually in the diaphyseal region of long bones, near the nutrient foramen, often developing on the endosteal surface of the bone. The most common sites are the tibia, radius, humerus and third metacarpal and metatarsal bones (Figures 1.20, 6w.24a and b, and 10w.40). The aetiology and clinical significance of the lesions are unknown. However, they may be associated with lameness, which usually resolves with rest. Enostosis-like lesions are frequently associated with focal increased radiopharmaceutical

Downloaded From Vet-eBooks.com

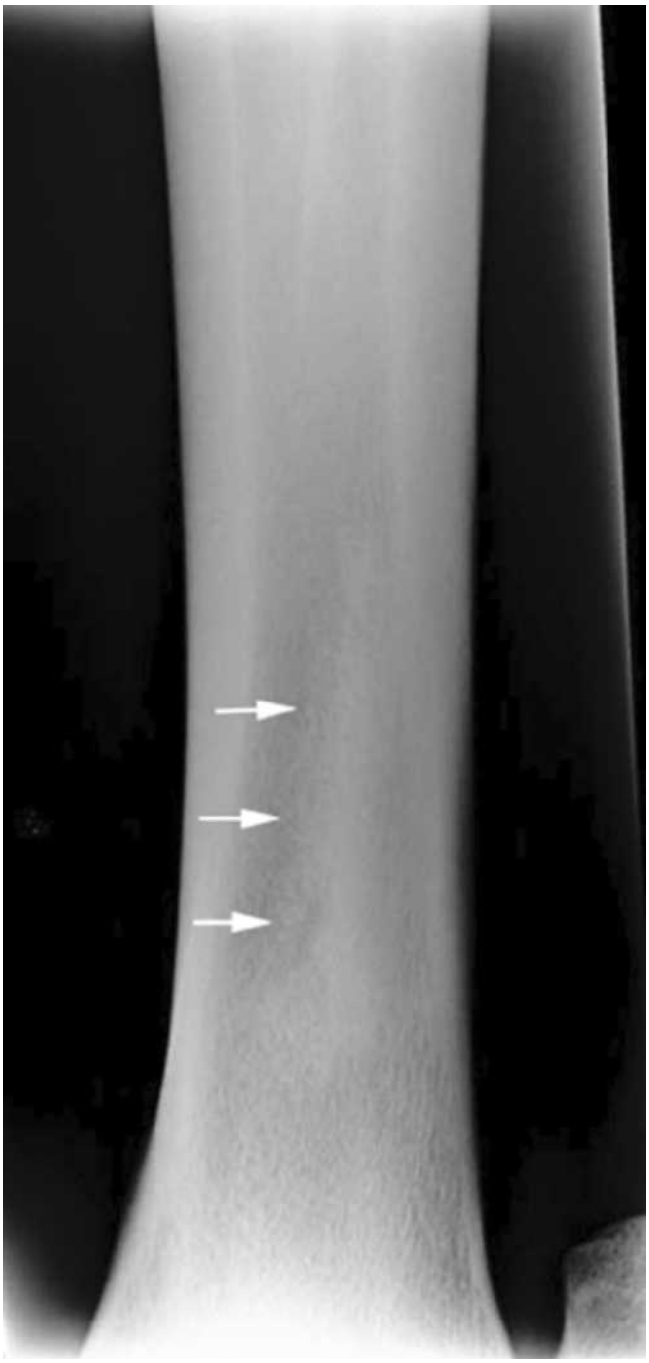


Figure 1.20 Craniolateral-caudomedial oblique image of a tibia. There is a vertical linear band of increased opacity in the middle of the distal aspect of the tibial diaphysis (arrows). This is an enostosis-like lesion.

uptake, whether or not they are causing lameness. Such focal radiopacities should be differentiated from endosteal callus secondary to a fatigue or stress fracture. Small focal opacities in the proximal metaphyseal (Figure 10w.41) or diaphyseal region of the tibia have been recognised. Their aetiology and clinical significance are unknown.

Heterotopic ossification

Heterotopic ossification, also known as myositis ossificans, is a well-recognised condition in humans, typified by the development of bone at sites where bone does not normally exist. The aetiology is unknown. It may occur

Downloaded From Vet-eBooks.com

after muscle trauma, but can also develop after brain or spinal cord injury, burns and surgery. It is generally associated with regional pain. It occurs rarely in the horse (Figure 8w.20a and b).

Fractures

A fracture is a discontinuity of the bone seen radiologically as a lucent line or lines. Radiography is performed to establish the type, severity and degree of displacement of the fracture, and to assess the damage to adjacent joints and surrounding soft tissues. Later radiographs may be obtained to assess the degree of reduction achieved and to monitor healing. In order to establish the presence of a fracture, at least two projections, preferably obtained at right angles to each other, are essential. Many more views may be necessary to establish the exact configuration of the fracture.

Fatigue (stress) fractures and other non-displaced and/or incomplete fractures can be extremely difficult to detect in the acute stage. Mach lines due to edge enhancement should not be confused with fractures. These are particularly evident with certain digital imaging software. For best detection of a fracture, the x-ray beam must be parallel to the plane of the fracture, and thus detection may necessitate obtaining many views at 5° angles to each other. Two radiolucent lines often represent a single complete fracture, which traverses through two cortices, e.g. dorsal and palmar, and should not be confused with two fractures. During the normal healing process there is osteoclasis along the fracture line within 5–10 days, resulting in apparent broadening of the lucent fracture line (see Figures 1.10a–c, 6.29a and 6.29b). Thus a fracture line that was not readily apparent in the initial radiographs may be detected on follow-up films obtained 5–10 days later. In the acute stage, nuclear scintigraphy may be a better method of detecting the presence of an incomplete fracture or a fatigue fracture. Some fractures are never visible radiographically, despite there being strong evidence of a fracture from nuclear scintigraphic evaluation. Some radiographically detectable stress (fatigue) fractures may be preceded by the development of increased opacity before the fracture becomes apparent.

A fracture should be evaluated to establish whether it is unicortical or bicortical, simple, multiple or comminuted, whether there is articular involvement, the degree of displacement of the fracture fragments and to identify any concurrent pathology which may adversely influence the prognosis.

Fractures involving the physis of a bone may be classified according to Salter-Harris, based upon the configuration and relationship of the fracture plane to the metaphyseal growth plate. Salter-Harris classifies the fractures as follows (Figure 1.21):

Type I Fracture through the zone of hypertrophied cells without involvement of the adjacent epiphysis or metaphysis

Type II Fracture through the physis across part of the width of the bone and through the metaphysis, leaving a segment of the metaphysis attached to the epiphysis

Type III Fracture through the physis across part of the width of the bone and through the epiphysis, entering the joint

Type IV Fracture across the epiphysis, physis and a portion of the metaphysis, perpendicular to the plane of the physis

Type V Compression fracture of the physis with minimal displacement

Downloaded From Vet-eBooks.com

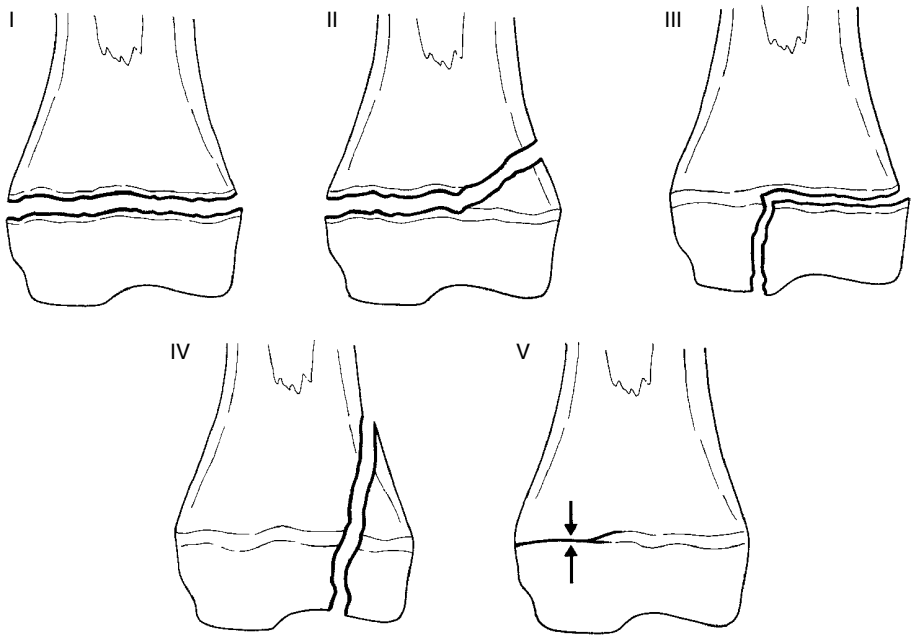


Figure 1.21 Salter-Harris classification of physeal fractures. See text for descriptions.

Although this classification has now been further extended, we feel that the above classification is adequate for practical clinical purposes.

Fracture healing should be monitored radiographically to determine the progression of healing. The time interval between re-examinations depends on the severity of the fracture, the type of repair and the clinical reassessment of the patient. Following initial mineral resorption along the fracture line, and formation of a fibrous callus, calcified periosteal and endosteal callus develops. The amount and quality of callus that develops depends upon the degree of stability at the fracture site (Figure 1.22) and the presence or absence of concurrent infection. Endosteal callus is more difficult to see radiographically, but ultimately results in disappearance of the fracture line. Stability of the fracture may develop long before the fracture line disappears radiographically. Some bones (e.g. the proximal and distal sesamoid bones and the accessory carpal bone) tend to heal by fibrous union, resulting in a persistent lucent line. The rate of healing varies and is dependent on many factors, including the age of the horse, its nutritional and metabolic status, the degree of stability of the fracture, the site of the fracture, the presence or absence of periosteum, the blood supply to the bone, and the presence or absence of infection. Infection is likely to be progressive and impair osseous union unless there is stability at the fracture site.

If a fracture is repaired by internal fixation, and there is adequate stability at the fracture site, healing should be predominantly by primary union, with minimal periosteal callus. Instability at a fracture site results in secondary union by the production of periosteal callus (Figure 1.23), or may result in fibrous union or malunion of the fracture.

If a fracture has been repaired by internal fixation, the implants and surrounding bone should be examined carefully on follow-up radiographs. The development of localised lucent zones around the implants indicates loosening of the implant, or infection, and it may be necessary to remove one or more selected portions of the implant. Diagnostic ultrasonography may be helpful in early detection of osteomyelitis in some cases, e.g. detection of fluid around a screw head.

Downloaded From Vet-eBooks.com

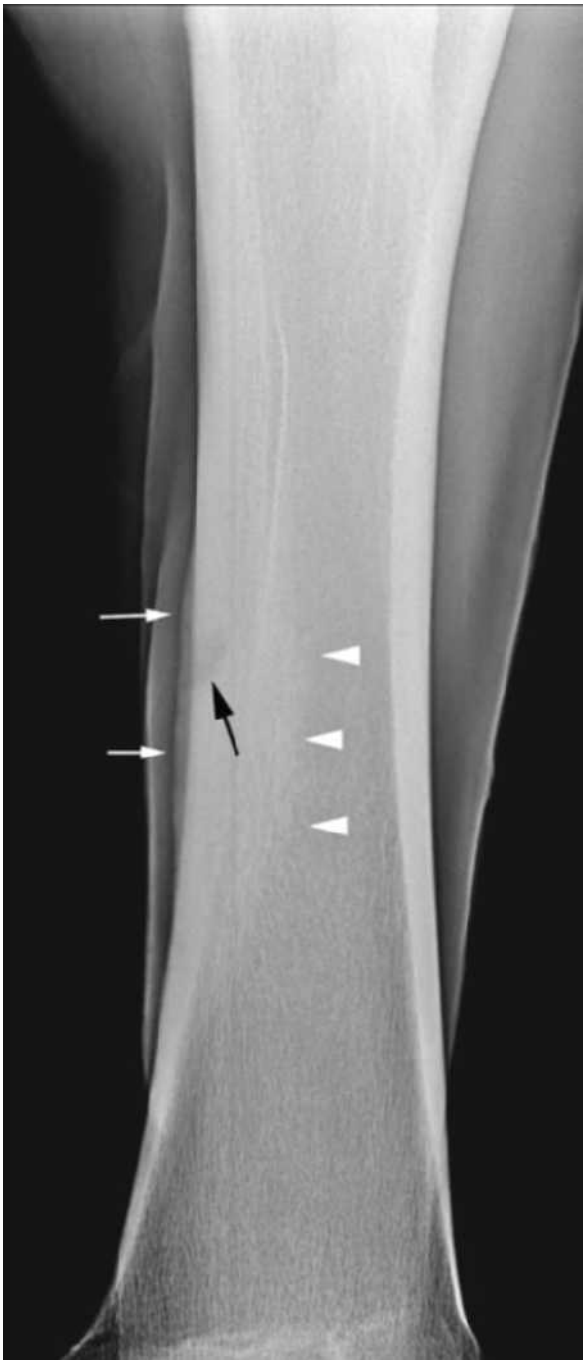


Figure 1.22 Craniocaudal image of a radius of a 6-year-old Irish Sports Horse obtained 4.5 weeks after a kick injury. Lameness was not apparent until 3 days after the injury and progressively deteriorated over the following week. Medial is to the left. There is marked endosteal reaction of the medial cortex of the mid-diaphyseal region (arrowheads), extending proximal and distal to an ill-defined radiolucent line through the cortex, an incomplete fracture (black arrow). There is smoothly marginated periosteal new bone, callus, extending proximal and distal to the radiolucent line (white arrows) and mild overlying soft tissue swelling.



Figure 1.23 Dorsopalmar image of the distal metacarpal region of a 3-year-old Thoroughbred racehorse with sudden onset of left forelimb lameness 6 weeks previously. Medial is to the left. There is an approximately horizontal radiolucent line traversing the distal metaphyseal region, representing a complete fracture and very extensive irregularly marginated periosteal callus extending along the medial and lateral cortices, reflecting a secondary healing response to an unstable fracture.

Downloaded From Vet-eBooks.com



Figure 1.24 Lateromedial image of a stifle. Cranial is to the left. There is a complete transverse, articular, non-union fracture of the patella. The fracture margins are rounded and have increased radiopacity. There are also some small mineralised opacities overlying the caudal aspect of the fracture. The distal half of the distal part of the patella has generalised loss of opacity.

If implants are removed when there is stability at the fracture site, radiolucent tracts will persist for 8–12 weeks where the implants passed though the bone. These tracts may act as stress points until adequate remineralisation has occurred, and are potential sites for fracture to recur. Such stress points, of course, are also present with the implants in place.

Whether a fracture is treated conservatively or surgically, once initial mineral resorption along the fracture line has occurred, there should be progressive narrowing of the fracture line or lines, and they should gradually disappear. Healing may be complete within 6–12 weeks, but some fractures take considerably longer. A horse may be sound and be able to withstand work, despite the persistence of a radiolucent fracture line and some fractures heal more completely once careful controlled walking exercise is initiated. In some locations (e.g. third metacarpal condylar fractures) the long-term persistence of a lucent line is commonly associated with recurrent lameness. If a fracture line persists beyond 6 months it can be considered to be a delayed union. There may be increased opacity of the bone adjacent to the fracture line, and the ends of the bone may become slightly flared (Figure 1.24).

Downloaded From Vet-eBooks.com

Although delayed union is not uncommon in the horse, non-union (complete failure of osseous union after 12 months) is rare, except in the areas previously mentioned where healing is frequently by fibrous union. If there is apparent healing by fibrous union, it is usually impossible to state when the original fracture occurred. Fractures of the distal sesamoid (navicular) bone usually heal by fibrous union, and frequently lucent zones develop adjacent to the fracture line. These lucent zones are indicative of a fracture of at least 6–8 weeks' duration.

Joint lesions

Swelling

Soft-tissue swelling in and around joints may be classified as shown below.

INTRA-ARTICULAR SWELLING

With intra-articular swelling the joint capsule is distended and in a non-weight-bearing patient there may be a widened joint space. In some locations (e.g. the carpus) the normal dorsal lucent fat pad may disappear due to compression. Joint distension is usually associated with inflammation and may be septic or aseptic. Softly exposed radiographs may demonstrate distended joints away from weight bearing parts of the joint. If several joints are involved in a neonatal animal, septic arthritis should be considered. If several joints are involved in older animals, immune-mediated disease should be considered, especially if the occurrence is cyclical in nature.

PERIARTICULAR SWELLING

Periarticular swelling does not involve the joint space, but may involve the joint capsule as is seen in sprains. Periarticular swelling may also be caused by conditions that are more obvious on examination of the patient than on the radiograph, such as wire cuts, puncture wounds and external trauma. With cuts and wounds, gas may be evident within the soft-tissue swelling. Generalised periarticular swelling may result in the inability to differentiate between intra-articular and extra-articular fluid accumulation. The inability to differentiate may result from massive swelling or the loss of soft-tissue fat which is normally found in the pericapsular, peritendonous and periligamentous areas.

Trauma

Joint trauma may be classified as follows:

SPRAIN

Joint sprain is the wrenching of a joint with partial rupture or other injury of its attachments, but without luxation of bones. There is usually rapid swelling, heat and pain. Sprains must be differentiated from fissure fractures and other causes of acute joint swelling. Sprains may be classified as shown in Table 1.1.

Downloaded From Vet-eBooks.com

Table 1.1 Classification of sprains.

Type of tissue damage	Radiographic finding
Ligament strain or partial rupture	Soft-tissue swelling
Ligament rupture	Soft-tissue swelling
Ligament avulsion	Soft-tissue swelling and the presence of a bone fragment



Figure 1.25(a) Dorsal 15°proximal-palmarodistal oblique image of a metacarpophalangeal joint of an event horse with acute onset severe lameness 3 days previously. The horse was bearing full weight on the limb without discomfort. Lateral is to the right. The bones are in normal alignment. There is a small osseous opacity just proximal to the lateral epicondyle of the third metacarpal bone (arrow).



Figure 1.25(b) Stressed dorsopalmar image of the same horse as in Figure 1.25(a). Lateral is to the right. There is luxation of the metacarpophalangeal joint, and an avulsion fracture from the lateral epicondyle of the third metacarpal bone (arrow).

If ligament rupture or avulsion is suspected, stressed radiographs (Figures 1.25a and 1.25b; see 'Subluxation and luxation', below) should be obtained to assess the integrity of the joint and the possibility of subluxation. Ultrasonography may yield additional information.

Downloaded From Vet-eBooks.com

SUBLUXATION AND LUXATION (DISLOCATION)

Luxation is the complete loss of contact between the articular surfaces of a joint. Subluxation of a joint is partial loss of contact between joint surfaces, and may be intermittent. Luxation and subluxation in the horse are usually the result of trauma, although congenital luxation of the patella occurs rarely. Subluxation of the proximal interphalangeal joint (Figure 4.9) may develop without an obvious cause, but may also occur secondary to injury of the oblique or straight sesamoidean ligaments. Luxation is usually easily identified radiographically (Figure 8.23), but multiple radiographic views are required in order to assess whether or not there is a concurrent fracture that may adversely influence the prognosis. If luxation is incomplete (i.e., subluxation), radiological assessment is more difficult. Radiographs should be obtained in the weight-bearing position and compared carefully with the normal anatomy. When luxation or subluxation is suspected clinically, so-called 'stress radiographs' may be helpful to determine the integrity of the periarticular soft tissues such as the collateral ligaments. Stress radiographs are obtained with the limb not weight bearing, with force applied to the joint in either a mediolateral or dorsopalmar direction to determine whether the bones may be moved abnormally in relation to each other (Figures 1.25a and 1.25b). Ultrasonography may yield additional information.

INTRA-ARTICULAR FRACTURES

Intra-articular fractures exist when there is a break in the articular surface. Unless there is some degree of displacement, damage to the articular cartilage may not be seen, but should be assumed to exist. A small degree of displacement is indicated by the presence of a slight 'step' in the two sides of the articular portion of the fracture line. Fissure fractures are not displaced and many views may be required in order to identify the fracture, as the x-ray beam must be exactly aligned in the plane of the fissure. Such a fracture may only involve one cortex of the bone.

Fractures of the articular margin are termed chip fractures. Radiographs should be carefully inspected for evidence of additional chips, pre-existing degenerative joint disease, or other concurrent pathology, which may adversely affect the prognosis. Differentiation between chip fractures, ectopic mineralisation and separate centres of ossification may not be possible. The position of the mineralised body relative to the articular margin, the size and shape of the body, and the contour of the articular margin should all be assessed carefully. A recent chip fracture may have a sharp edge, and a fracture 'bed' may be discernible. Separate centres of ossification, or old chip fractures, may be very well rounded uniformly opaque bodies, and a fracture bed is usually not detectable. Ectopic mineralisation may be present within the joint capsule following embedding of a displaced mineralised fragment.

A slab fracture is a fracture extending from one joint surface to another, e.g. from the proximal to distal articular surface of the third carpal or tarsal bones. These fractures may be extremely difficult to detect radiographically in the acute stage if not displaced. Oblique views, including skyline views, are invaluable in the carpus. In the tarsus it may be necessary to re-radiograph the joint after 7–10 days when some demineralisation has occurred along the fracture line.

Downloaded From Vet-eBooks.com

Infectious arthritis

Infectious arthritis is most commonly seen in young foals, and frequently involves several joints. It may occur in an adult, usually associated with trauma, but may be iatrogenic. Radiographic features of joint infection include:

- Periarticular soft-tissue swelling
- Joint capsule distension, with or without apparent widening of the joint space
- Irregularity of outline of the subchondral bone
- Lucent zones in the subchondral bone, with or without areas of increased opacity
- Periarticular osteophyte formation, due to secondary degenerative joint disease
- Partial collapse of the subchondral bone.

The presence of bony abnormalities indicates that the disease is advanced and warrants a guarded prognosis. The absence of detectable radiological abnormalities does not preclude a diagnosis of infection. The speed of development and degree of cartilage and bone destruction depend on the causative organism.

In a neonate, care should be taken to differentiate the radiographic appearance of incompletely ossified bones, which may have an irregular outline and granular opacity, similar to that seen in infection. Reference should be made to the text in the subsequent chapters, which describes the appearance of incomplete ossification where it is a normal feature at birth. In a foal, joint infection may develop secondarily to infection of an adjacent physis, or may spread from a joint to an adjacent epiphysis.

Firth (1983) classified infectious polyarthritis of foals into several syndromes as follows:

1 Physeal type P osteomyelitis. There are areas of irregularity and focal widening in the physis. At this point the term physitis may appear more appropriate than physeal osteomyelitis; however, once the changes have advanced sufficiently far to be seen radiographically, there is usually also involvement of the metaphyseal or epiphyseal bone adjacent to the site of origin. Infection may continue to extend into the epiphysis or metaphysis, where the infection is characterised by relatively opaque areas of bone surrounded by lucent areas. These are frequently triangular in shape. As the condition progresses, soft-tissue swelling associated with the joints may be seen, and this may develop into infectious arthritis secondary to underlying osteomyelitis.

2 Type E osteomyelitis begins in the epiphysis and progression is similar. The classification is only used to denote where the nidus of infection was established.

3 Type S osteomyelitis actually begins in the synovium, and extends from there, rapidly becoming septic arthritis, or extends into the physis and possibly also the metaphysis and epiphysis.

4 Type T osteomyelitis is limited to the tarsus and must be differentiated from aseptic necrosis of the central and third tarsal bones. Type T cases usually present because of generalised tarsal enlargement or tarsocrural joint capsule distension. Although the central and third tarsal bones are occasionally involved, the majority of pathology is noted in the distal tibial physis and/or tarsocrural joint. The main radiographic findings include soft-tissue

Downloaded From Vet-eBooks.com

swelling, distension of the tarsocrural joint and irregularity of the distal tibial physis (type P osteomyelitis). When the central and third tarsal bones are involved, they are normal in shape but have a mottled lucent appearance.

5 Type C osteomyelitis. Recently osteomyelitis of the carpal bones has been described, and appears similar in many respects to tarsal osteomyelitis. It may therefore be appropriate to include a fifth category in Firth's classification – osteomyelitis identical to type T, but localized to a single carpal bone (Figure 7.21a,b).

Synovial osteochondromatosis

Synovial osteochondromatosis represents a very unusual synovial response in the horse and can be primary or secondary. The condition describes metaplastic and focal formation of cartilage within the intimal layer of the synovial membrane. The condition is also uncommon in other domestic animals, although it occurs more frequently in humans. Cartilage may undergo mineralisation and become evident radiographically. Treatment usually involves arthroscopic removal of osteochondral bodies and resection of abnormal synovium. Recurrence is quite common and malignant transformation rarely occurs, although, to date, this has not been reported in the horse.

Subchondral bone cysts and osseous cyst-like lesions

The terms subchondral bone cyst (SBC) and osseous cyst-like lesion (OCLL) are sometimes used loosely to describe the same lesions. They are usually solitary, circular lucent areas in a bone, which may be surrounded by a narrow rim of increased opacity. They are usually unicameral (single chambered) but may be multicameral. They are often close to the articular surface of the bone and sometimes a 'neck' connecting the cyst-like lesion with the joint surface can be identified.

Differentiation between an SBC and an OCLL cannot be made based on their radiographic appearance, but is based on the gross structure.

An SBC is a structure with a fibrous lining and filled with fluid or semisolid tissue. Cysts in some locations in some joints fulfil these criteria (e.g. medial femoral condyle), but there is limited information available about the infrastructure of cysts in many locations so these are described as OCLLs. Some OCLLs ultimately fill in radiologically, but others persist virtually unchanged. Osseous cyst-like lesions and SBCs occurring near the articular surface in young horses may appear to migrate progressively away from the joint surface, as normal endochondral ossification occurs.

An SBC and some OCLLs may first be identified as a small lucent depression in the articular surface (see Chapter 10, 'Osseous cyst-like lesions' and Figure 10.21). This progressively enlarges and a rim of increased opacity may develop around the cyst-like lesion. They are often close to the articular surface of the bone and sometimes there is a 'neck' visible connecting the cyst with the joint surface. The radiographs should be carefully examined for evidence of concurrent secondary degenerative joint disease.

The exact cause of SBCs and OCLLs is uncertain. It has been suggested that they are part of the osteochondrosis syndrome, but the evidence for this is limited. There is evidence that some SBCs and OCLLs are traumatic in origin. An OCLL may develop in association with degenerative joint disease and there are probably other aetiologies which have not been identified.

Downloaded From Vet-eBooks.com

Osseous cyst-like lesions which occur deep within bone, such as in the carpal bones, are rarely associated with lameness, whereas SBCs and OCLLs close to an articular surface, such as in the medial femoral condyle, are frequently associated with lameness. Small OCLLs in the phalanges have been identified close to articular margins as incidental findings of no clinical significance; some of these have been seen to disappear radiographically with conservative management.

Osteochondrosis

Osteochondrosis is considered to be a disturbance of endochondral ossification, but there is increasing evidence to show that there may also be primary subchondral bone lesions. The disease may be generalised, although only evident radiographically in certain joints. The femoropatellar, tarsocrural, metacarpophalangeal or metatarsophalangeal (fetlock) and scapulohumeral joints are the most commonly affected in the horse (see Chapters 10, 9, 5 and 8, respectively). The radiological appearance of osteochondritic lesions is variable among individuals, and the joints involved, but the changes normally include:

- Discrete osteochondral fragments
- Alterations in the contour of the articular surface, e.g. flattening or a depression of the subchondral bone plate
- Irregularly shaped lucent zones in the subchondral bone
- Increased opacity surrounding the lucent zones
- Secondary modelling of joint margins.

Lesions are not always of clinical significance but must be interpreted in the light of the clinical signs. Some lesions remodel gradually and become increasingly opaque and may eventually "heal" radiographically. Clinical signs are generally recognised in horses less than 3 years of age, but occasionally horses remain asymptomatic until later in life, especially if the horse does not work until a later age.

Degenerative joint disease

Degenerative joint disease (DJD), osteoarthrosis, osteoarthritis and secondary joint disease are often used synonymously in veterinary medicine, yet distinctions can be made in some cases.

Arthritis simply means inflammation of a joint, and if recognized radiographically is seen as joint capsule distension without evidence of new bone involvement. There is inflammation of the synovial lining and changes in the quantity and quality of synovial fluid. Osteoarthritis or osteoarthrosis indicate that bone has become involved and that an inflammatory soft-tissue component may (itis) or may not (osis) be present. The term secondary joint disease is used when the primary cause is known, such as in osteochondrosis or intra-articular fracture. Degenerative joint disease is used to refer to any number of causes that affect the joint and its supporting structures. In the horse, the degenerative process, which results in DJD, may be associated with poor conformation and/or hard use. Advanced DJD, however, is sometimes seen in immature horses, less than 3 years of age, with no identifiable predisposing cause. Any condition that damages cartilage directly, causes joint instability, or subjects the joint to abnormal directional forces, can

Downloaded From Vet-eBooks.com

cause DJD. Immune-mediated joint disease should be considered whenever there is polyarthritis and sepsis can be ruled out.

Radiographic abnormalities (so-called cardinal signs) associated with DJD include:

- Periarticular osteophyte formation
- Increased opacity of subchondral bone, and loss of trabecular pattern
- Ill-defined small lucent zones in the subchondral bone
- Small well-defined osseous cyst-like lesions
- Narrowing of the joint space
- Joint capsule distension
- Periarticular soft-tissue swelling.

One or more of the above may be seen in association with DJD in any joint. If possible, periarticular osteophyte formation should be differentiated from entheseophyte formation. Small periarticular osteophytes are not necessarily synonymous with clinically significant DJD. It must also be borne in mind that the absence of detectable radiological abnormalities does not preclude the presence of cartilage degeneration. As DJD progresses, radiological abnormalities become more obvious. Ultrasonography may give useful information about the integrity of the articular cartilage.

Dystrophic and metastatic mineralisation (calcification)

Calcium is seldom deposited alone. Even in bone the opacity seen on radiographs is due to a mixture of calcium, phosphorus, zinc, manganese and magnesium, and therefore dystrophic and metastatic calcification is more correctly termed mineralisation. Mineralisation in soft tissue can occur in association with inflammation, neoplasia, trauma or metabolic disease. The most reliable indication of the cause of the mineralisation is the location in which it occurs, combined with knowledge regarding the organs or structures located in the area. Knowledge of what diseases result in mineralisation of a particular organ provides valuable information, and occasionally a definitive diagnosis. The size, shape and pattern of mineralisation may vary, and therefore are poor indications of a specific aetiology.

Soft-tissue mineralisation has been classified as being metastatic or dystrophic. Metastatic mineralisation is the deposition of minerals in tissues that have not previously been damaged. It is associated with hypercalcaemia, hypercalciurea and hyperphosphataemia.

Dystrophic mineralisation is the process whereby mineral is deposited in injured, degenerating or necrotic tissue, and is commonly seen in the horse. It can occur secondary to any injury to soft tissue, e.g. in tumours that have become necrotic, at the site of fat necrosis, subsequent to infarction, and in association with inflammation or haemorrhage. Either type of mineralisation may eventually result in the formation of mature bone.

Additional figures

The book companion website at www.clinical-radiology-horse.com includes additional figures that are not included in the printed book or e-book formats. Please see '**About the Companion Website**' at the start of the book for details on how to access the website. These figures are prefixed with the letter 'w' in the printed book, e.g. Figures 1w.4c–f.

Downloaded From Vet-eBooks.com

FURTHER READING

Ahern B., Boston, R., Ross, M. (2014) Enostosis-like lesions in equids: 79 cases (1997–2009). *J. Am. Vet. Med. Assoc.* **245**, 1042–1047

Bassage, L., Ross, M. (1998) Enostosis-like lesions in the long bones of 10 horses: scintigraphic and radiographic features. *Equine Vet. J.* **30**, 35–42

Bushberg, J., Seibert, J., Leidholt, E., Boone, J. (2002) *The essential physics of medical imaging*, 2nd edn., Lippincott William & Wilkins

Firth, E. (1983) Current concepts of infectious polyarthritis in foals. *Equine Vet. J.* **15**, 5–9

Bushong, S. (2001) *Radiologic science for technologists: Physics, biology and protection*, 7th edn., Mosby, St. Louis

Garret, K., Berk, J. (2006) How to properly position Thoroughbred repository radiographs. *Proc. Am. Assoc. Equine Pract.* **52**, 600–608

Greet, G., Greet, T. (1996) The use of specific radiographic projections to demonstrate three intra-articular fractures. *Equine Vet. Educ.* **8**, 208–211

Harrison, L., Edwards, G. (1996) Radiographic investigation of osteochondrosis. *Equine Vet. Educ.* **8**, 172–176

Holmes, M., Pilsworth, R. (2007) *Radiation safety in equine practice*. DVD British Equine Veterinary Association, Newmarket

Kirberger, R., Gottschalk, R., Guthrie, A. (1996) Radiological appearance of air introduced during regional limb anaesthesia. *Equine Vet. J.* **28**, 298–305

Lavin, L. (2006) *Radiography in veterinary technology*, 4th edn., W.B. Saunders

Mair, T., Dyson, S., Fraser, J., et al. (1996) Hypertrophic osteopathy (Marie's disease) in Equidae: a review of twenty-four cases. *Equine Vet. J.* **28**, 256–262

May, S. (1996) Radiological aspects of degenerative joint disease. *Equine Vet. Educ.* **8**, 114–120

O'Neill, H., Bladon, B. (2011) Retrospective study of scintigraphic and radiological findings in 21 cases of enostosis-like lesions in horses. *Vet. Rec.* **168**, 326

Phillips, T. (1998) The use of radiography in the pre-purchase examination. In: *British Equine Veterinary Association Manual: The Pre-Purchase Examination*, Ed. Mair, T. pp154–160. *Equine Vet. J.*, Newmarket

Smallwood, J., Shiveley, M., Rendano, V., Habel, R. (1985) A standard nomenclature for radiographic projections used in veterinary medicine. *Vet. Radiol.* **26**, 2–9

Smith, M. (2014) Synovial osteochondromatosis. *Equine Vet. Educ.* doi: 10.1111/eve/12205

Thrall, D. (2013) *Textbook of Veterinary Diagnostic Radiography*, 6th edn., Elsevier, St. Louis

Downloaded From Vet-eBooks.com

Downloaded From Vet-eBooks.com

Chapter 2
Computed and digital radiography

Digital radiography is a generic term that has been widely used to describe both computerised (computed) radiography and direct capture digital radiography. Both techniques result in a radiographic image captured electronically and displayed as a digital image on a computer monitor. The image can be archived digitally and/or transferred into a 'hard copy' using a laser printer. The generation of the x-ray beam remains unchanged and, just as with conventional film–screen radiography, the quality of the digital image is greatly affected by the quality of the x-ray generator, the radiographer's technique and the ability of the radiographer to choose correct exposure factors.

New terms have come into common usage. DICOM is an acronym for Digital Imaging and Communication in Medicine and is a standardisation of image format to facilitate exchange of images. A DICOM file contains a header, which gives the patient information and image data relevant to the image. The term PACS, Picture Archiving and Communication System, applies to the combined hardware and software used for digital imaging, allowing communication between computers. As with any computer-based system, training in the use of both hardware and software and in information technology, and maintenance support for the system are invaluable.

Digital processing of radiographic images is a very rapidly developing field. The earliest systems were the computerised radiography systems, and while still widely used at the time of writing, the current research and development trends are primarily with direct digital systems. The current trends in equine radiography are towards wireless direct digital systems for use both in the field and in hospitals as the cost of direct systems becomes less prohibitive. However, computerised radiography in a hospital situation provides more flexibility because two horses can be examined simultaneously. The cost of several large digital radiography imaging plates remains high.

COMPUTERISED RADIOGRAPHY

Computerised or computed radiography (CR) has similarities to conventional film–screen radiography, despite the absence of film and chemical processing. The phosphor plate, otherwise known as an imaging plate, is stored in a cassette, allowing existing x-ray equipment to be used, but replacing a traditional film cassette with a computed radiography imaging plate.

Clinical Radiology of the Horse, Fourth Edition. Janet A. Butler, Christopher M. Colles, Sue J. Dyson, Svend E. Kold and Paul W. Poulos.
© 2017 John Wiley & Sons, Ltd. Published 2017 by John Wiley & Sons, Ltd.
Companion website: www.clinical-radiology-horse.com

Downloaded From Vet-eBooks.com

Computed radiography uses photostimulable phosphors (storage phosphors) to capture the image. The storage phosphors are coated on to either a flexible or rigid plate (dependent on the system), much like screens used in conventional radiography. The storage phosphors come from the barium fluorohalide family, with trace amounts of impurities added to their crystalline structure to alter their physical properties. These are deposited on to the backing plate in powder form, the size of the phosphor grain used influencing the resolution of the system. Low-resolution imaging plates use a larger phosphor grain than high-resolution plates. Most systems are designed to be around 10–20 phosphor grains thick.

Computed radiography storage phosphors differ from traditional screen phosphors because instead of emitting light in response to the incident radiation, they store the energy as a latent image. This is subsequently stimulated using a laser beam, and released in an image plate reader. The amount of energy released is directly proportional to the intensity of radiation reaching the imaging plate during exposure.

Imaging plate reading

In most commercially available systems a flying spot readout system is used. In this system a laser spot scans the exposed plate using a mirror in a point to point raster pattern. This causes the phosphor to release the stored energy as a violet blue glow. The intensity of the phosphor glow is directly proportional to the amount of energy stored from the exposure made. The glow is captured by the system and enhanced using photomultiplier tubes. The resultant optical signal is converted into a digital signal using an analogue-to-digital converter. The digital signal is processed within the control computer using algorithms predetermined for different body parts. The total processing time is currently between 40 and 90 seconds, depending on the system, and only one imaging plate can be read at a time. The systems are developing rapidly, and readers are advised to seek up-to-date information if considering purchase of any digital system.

The resultant image should be transmitted to a high-resolution monitor for image reading. With the larger stationary readers the image is displayed on an adjacent workstation monitor on which the image can be checked for appropriate positioning and exposure. However, the image is usually displayed at a much lower resolution than the information captured and this image should not be used for diagnostic purposes.

The laser scan does not release all the energy stored in the phosphor. After scanning, the plate requires an erase cycle, in which the phosphor plate is exposed to a bright fluorescent light. This removes any remaining residual energy, enabling the plate to be reused. This process takes up to 30 seconds.

The latent image can be stored for up to 24 hours, but generally it is best to 'read the plate' as soon as possible after exposure. Just as with conventional film–screen radiography, it is possible for dust and other foreign bodies to get into the cassette holding the imaging plate, therefore regular cleaning using the manufacturer's recommended procedure (e.g. pure alcohol and lint-free wipes) is essential. The imaging plate must be allowed to dry before it can be reused, so this is a procedure to be carried out at the end of a day. There should be a regular system of cleaning and a log maintained.

Downloaded From Vet-eBooks.com

The plates can be subject to physical damage, either during exposure or in the plate reader, both of which can result in artefacts. Correct handling of the plates is therefore important.

DIRECT DIGITAL RADIOGRAPHY

Direct digital, direct digital capture, direct radiography (DR) and digital radiography are synonymous terms used to describe a system which converts the x-ray photons to a digital signal without the use of a phosphor plate. This saves considerable time and energy. As with computed radiography, direct digital radiography is used in conjunction with conventional x-ray machines. There are two types of sensors (panels) currently in use. In both types the image is captured by an electronic array, and transmitted directly to a computer to generate the required image. The image is initiated by a thin layer of scintillation material made of caesium iodide, which emits light when stimulated by x-rays. Under this layer of scintillant is the recording layer. In a charge-coupled device (CCD plate) under the scintillation layer are myriad chips, electronically coupled together. The more reliable but more expensive panels use a layer of amorphous silicon as a detector (like one huge computer chip), converting the light into digital data. In direct digital systems the digital data is transmitted either directly via a cable attaching the panel to the processing computer, or via a radio link to the computer. In either case the image appears on the monitor in a few seconds.

The purchase price of a direct digital radiography system is currently becoming comparable to computed radiography. Large (26×32 cm) panels are becoming affordable, allowing the use of direct digital radiography for areas other than the distal aspect of the limbs. The cable connection to the computer which processes the image may be of some concern when dealing with a horse that is difficult to restrain, with an inherent risk of damage to the equipment. Since images can be read within a few seconds however, there are potential time savings compared with either conventional radiography or computed radiography. Wireless systems are now replacing cables, and while they have been slower to transfer data than the cable systems, as development proceeds this is becoming less of a problem, and it is likely that cable systems will become uncommon as time progresses. At the time of writing, the most sensitive panels in production are for wireless DR systems.

Development of these systems progresses rapidly, and as the processing systems are becoming lighter and more sensitive, the development of battery-powered x-ray generators is also progressing. Fully portable battery-powered x-ray systems are now available, with the generator and processing systems linked, and exposure values fully automated, controlled by feedback from the sensor to the generator. Such systems currently only have enough power for distal limb radiography, but in the foreseeable future this may also change.

IMAGE RESOLUTION

Images are comprised of pixels and the pixel size determines spatial resolution, the ability to define two objects close together. To increase resolution the number of pixels is increased without changing the field of view (the physical area being examined), thus decreasing the matrix size. A 2048×2048

Downloaded From Vet-eBooks.com

(2-K) matrix or higher is recommended for digital radiography. Dynamic range refers to the number of shades of grey that can be represented. Each pixel has a bit depth which determines the number of shades of grey that can be represented. Eight bits represents a greyscale range of 256 (2^8), ranging from 0 (white) to 255 (black). The human eye can only resolve a limited number of shades of grey, therefore excessive bit depth results in large file sizes without providing additional useful information. The dynamic range of most digital x-ray systems is determined by the computer and software. Most use an 8-, 10- or 12-bit dynamic range (i.e. 2^8, 2^{10} or 2^{12}). The American College of Radiologists recommends a minimum of 10-bit depth.

EXPOSURE FACTORS

When choosing exposure factors for digital radiography it is important to recognise the change in technology from conventional film–screen radiography and how to optimise exposure factors, which are different for digital systems. In film–screen radiography mAs controls the opacity of the image. This is because the same medium is used for detection of the photons and for the display of the resulting image, making them intimately linked. In digital radiography the image display and image detection are separated. The mAs still determines the number of photons absorbed into the imaging plate, which affects the density and the noise in the stored image, but this data is also subjected to image processing in the form of algorithms. These algorithms control the display of the signal and hence the image opacity seen on screen.

kVp controls contrast in both film–screen and computed radiography, higher kV penetrating denser tissues better. With conventional film–screen radiography the response is non-linear, which means that matching of subject contrast to kVp and film–screen combination is important. With digital radiography the response is linear and it can therefore compensate for loss of subject contrast through image processing and algorithms. Thus digital radiography offers higher contrast resolution and exposure latitude compared with conventional film–screen radiography.

When choosing an exposure it is still important to adjust kVp and mAs to body part and size of the individual, but it is equally important to choose the correct algorithm which controls how the image is displayed. It is not necessarily straightforward to determine whether the imaging plate has been under- or overexposed, because the displayed image is further processed.

Overexposure

With conventional film–screen radiography an overexposed image appears relatively black throughout and an underexposed image appears relatively white (assuming there are no development problems). With digital radiography the digital image is selected from a portion of the black–white spectrum. Overexposure may take the image out of the part of the spectrum being read by the computer, thus it does not result in overall blackening of the image, but the image appears light, white, or pale (Figure 2w.1a). A region of the image may be overexposed compared with the rest of the image, and this can mimic a lesion or create a region that cannot be accurately interpreted.

Downloaded From Vet-eBooks.com

Underexposure

With conventional film–screen radiography an underexposed image appears relatively white (assuming there are no development problems). With digital images an underexposed image may appear dark. It will usually however have a grainy, mottled appearance. This is caused by image noise, created because there is inadequate data for the computer to assign a grey shade to the underexposed region of the image. Graininess may obscure detail, for example trabecular architecture.

Each manufacturer's system produces a figure which gives an estimation of whether or not the exposure was appropriate. Different manufacturers use different terminology for this figure and have a different range they consider appropriate. Terminology includes exposure index, S value, DDI and REX. To determine whether an image needs to be repeated the exposure index (or equivalent) should be consulted. If this figure is within reasonable limits (set by the manufacturer's guidelines), an image acquired using computed radiography can be manipulated on the display rather than repeated.

Algorithms

Algorithms process the image stored on the system, and determine how it is displayed. They can give different weight to different areas of the black–white spectrum, and therefore play an integral part in how the image is displayed. In some instances they can be modified by the user, however it is vital that appropriate training by the manufacturer has been given. If images of certain specific body areas are not being adequately displayed, then assistance with modifying algorithms should be sought from the service provider.

Imaging an area within which there are tissues of widely differing densities potentially poses some difficulties, and it may result in the more dense area appearing completely white and without detail and less dense areas being black and 'burnt out'. Most systems can display a histogram of pixel density across different areas, and/or have other features to indicate areas that are outside the readable densities. It is important to recognise these areas, and if they contain potentially important information, then additional images, with exposure factors adjusted accordingly, are required in order to obtain the missing information.

Grids can be used with both computed and digital radiography, but may cause problems, and the manufacturer of the system should be consulted for advice. With a CR system grid lines that have a similar frequency (lines/cm) as the laser reader cause a wavy (moiré) pattern of lines (Figure 2.2) that may destroy image quality. Other combinations can also be a problem. Generally grids should have at least 60 lines/cm and grid lines should preferably run perpendicular to the plate reader's laser scan lines. However some systems have grid line removal software that may eliminate this problem. In the authors' experience, while grids remain important for radiography of thick areas such as the thoracolumbar region, they can often be dispensed with for imaging the distal aspects of the limbs. It may be necessary to borrow several grids from the manufacturer to determine which is most appropriate. In some instances the use of an air gap between the patient and the imaging plate may be more appropriate than a grid, but this does lead to magnification of the image.

Downloaded From Vet-eBooks.com



Figure 2.2 Lateral-lateral image of the mid-cervical vertebrae obtained using a grid and a computed radiography system. There are repetitive light and dark bands extending from the top of the image to the bottom. These are moiré lines.

Appropriate collimation of the x-ray beam and standard focus–image plate distances (source–image distances) are particularly important with digital imaging in order to achieve optimal image quality. Lack of collimation can affect the algorithm and the appearance of an image because the system processes the whole of the image as one exposure. This can be improved in some systems by selecting the area to be processed. The better the initial image however, the better will be the end result, despite all processing applied to the image. Collimation is particularly important in areas with large changes in density of tissues within the exposed area (Figures 2w.1a,b and c). The system looks for unexposed black and grey areas and tries to subtract white areas so that only useful information is processed. The system effectively looks for collimation lines. Good collimation also eliminates scattered radiation at acquisition; collimation of an image in the software will not remove scatter (Figures 2w.3a and 2w.3b).

MONITORS

When reviewing digital images it is important to choose the highest-resolution monitor that is affordable. Cathode ray tubes (CRTs) are seldom used nowadays, images usually being produced on active-matrix liquid crystal displays (AMLCDs).

Downloaded From Vet-eBooks.com

The resolution of monitors is measured by the number of pixels displayed on the screen at any one time. This is displayed as two numbers multiplied together, which is often abbreviated, e.g. a 1028 × 768 pixel monitor and a 1600 × 1200 pixel monitor are referred to as 1 Meg (megapixel) and 2 Meg monitors respectively. With 3 Meg and 5 Meg monitors widely available, the limiting factor is cost. Monitor specification also includes spatial resolution and contrast resolution. Spatial resolution is described as either pixels/mm or line pairs/mm. Three millimetres per pixel is equivalent to 6 mm/line pair. Contrast or depth resolution is described as grey values or bits. An 8 bit image has 256 grey levels; a 12 bit image has 4096 grey levels. However, the human eye can only resolve approximately 100 scales of grey. The American College of Radiologists has recommended that computed radiography image capture should be digitised to at least 2.5 line pairs/mm and that the image should be digitised to 10 bits per pixel or more.

The monitor ideally should be a true DICOM monitor and not just a DICOM-compatible monitor. The DICOM-compatible monitor only shows a representation of a DICOM image; the grey scale is reduced, and greatly affects the image quality. The high-resolution DICOM-compatible monitors on the market should be able to display digital images in varying degrees of luminance with various background colour settings that are similar to film choices. This should aid user preference being accommodated when viewing radiographs, and allow adjustment for the lack of grey scale.

COMPUTED RADIOGRAPHY ARTEFACTS

Imaging plate artefacts

Flexible imaging plates are found in many tabletop/compact computed radiography systems and are very susceptible to cracking. This generally starts around the edges, and will then begin to spread into the more central areas of the plate, overlying the image being examined. These artefacts may appear on radiographs as linear radiopacities or radiolucencies. If this occurs it is imperative that the plate is replaced.

Backscatter from dense objects behind the imaging plate can cause the plate to be exposed from behind, creating a 'ghost-like' image over the radiograph. This is more likely with large exposures. It can be prevented by placing a piece of rubberised lead or equivalent behind the cassette to absorb the scattered radiation.

Hair stuck on the imaging plate results in a linear curved white artefact, because anything blocking the imaging plate's emission of light will be blocked when scanned by the laser in the reader. Other debris causes a white artefact of variable shape. A linear black line on one side of the image can be the result of backscatter transmitted through the cassette hinge.

Plate reader artefacts

Imaging plates are automatically erased after they are read, to prepare them for the next exposure. If imaging plates have not been used for a period of time, they should be manually erased before use. Imaging plates are sensitive not only to x-rays but also to other electromagnetic radiation

Downloaded From Vet-eBooks.com

(ultraviolet and gamma rays) and particulate radiation (alpha and beta radiation). These are present as natural background radiation. Thus imaging plates are susceptible to background noise creating black dots (Figure 2.4a), unless manually erased shortly before use (Figure 2.4b). Most computed radiography readers have a dedicated erase cycle and manufacturers will provide guidelines on the maximum recommended period of time between erasure and usage.

Some manufacturers provide more than one erasure setting; if an incorrect exposure is made it is vital to choose the correct setting to ensure the plate is fully erased. If this does not happen it could result in a 'ghost' image from the previous exposure appearing on the next radiograph.

Dirt and dust in the plate reader can attach to the reader optics, which can cause horizontal or vertical white lines on images depending on the orientation of the plate. If lines are seen it is important to have the plate reader serviced to clean the particles from the optics or mirror. To maintain cleanliness



Figure 2.4(a) A poor-quality caudocranial radiographic image of an immature stifle obtained using a computed radiography system. Superimposed over the denser tissues of the femur and surrounding musculature is a dark speckled pattern, an artefact created by the digital system. This can occur when there are tissues of greatly varying opacity within the area being examined.

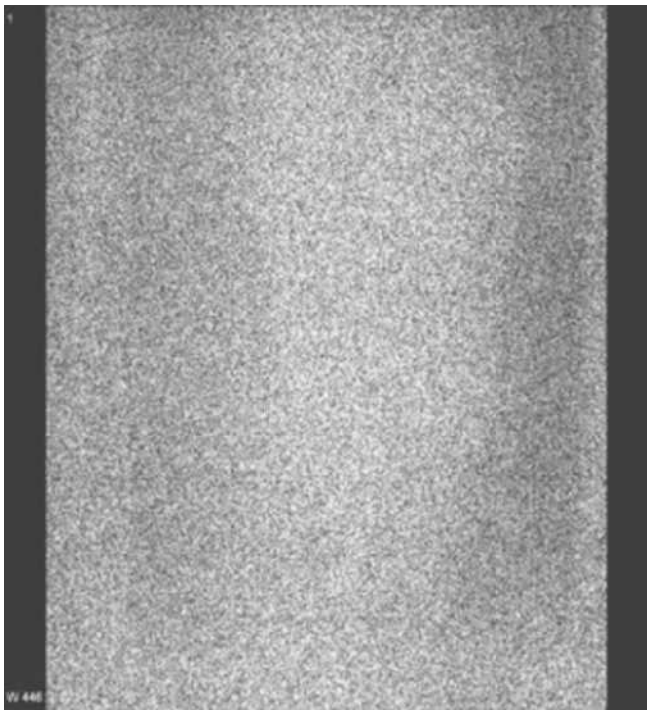


Figure 2.4(b) Background noise, the result of processing a computed radiography imaging plate that had not been cleared for several days.

Downloaded From Vet-eBooks.com

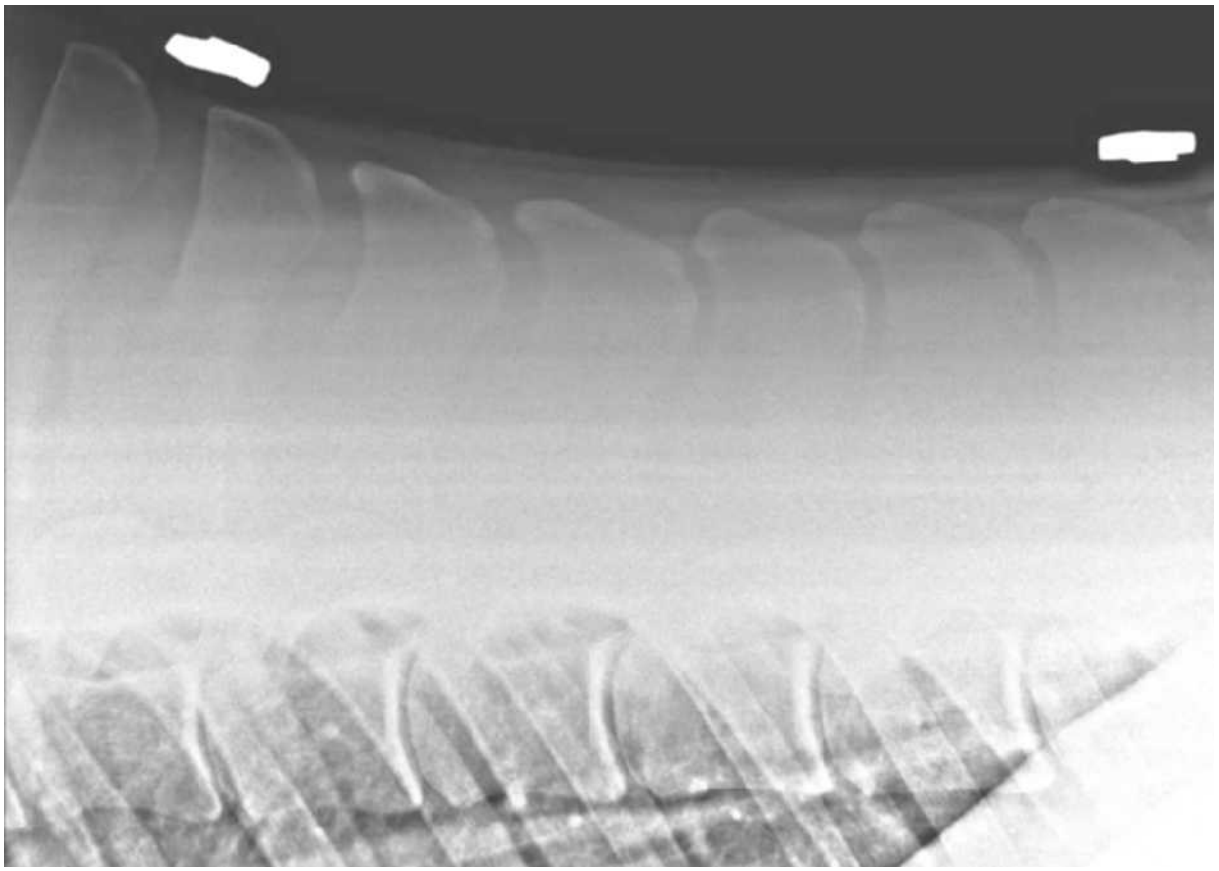


Figure 2.5 Lateral-lateral image of the 12th to 18th thoracic vertebrae of a 620kg Warmblood horse, obtained using a computed radiography system. The image is not ideally collimated; both the spinous processes and vertebral bodies have been exposed. There are multiple horizontal lines across the image, which are artefacts.

the reader should be in a dust-free environment. Imaging plates should be cleaned on a regular basis (as directed by the manufacturer), and the plate housing should be cleaned before submitting plates to be read. Multiple lines may appear across an image, which represent an artefact during image acquisition or processing (Figure 2.5).

Operator-induced artefacts

Operator errors may be more frequent in instances where a new computed radiography machine has been installed as a replacement for conventional screen–film combinations. It is important to store the imaging plates correctly. They must be protected from direct heat and extremes of humidity to prevent environmental damage to the imaging plate, and should also be stored where they will not be subjected to inadvertent exposure either from a direct exposure or from scatter. They are much more sensitive to scattered radiation than a conventional film–screen cassette.

As with film–screen systems, it is also important to identify the correct side of the cassette for exposure. This should be easily recognisable, and is often marked with a sticker stating 'tube side'. If an exposure is made on the wrong side, there will be a distinctive pattern across the image, resulting in the need for a repeat.

Downloaded From Vet-eBooks.com

IMAGE READING

The angle of the monitor can influence the information that can be obtained from the image. The image should be viewed from perpendicular to the monitor because contrast ratios can change rapidly (10: 1) for a change in viewing angle from 90° to 85°. Ambient light is also critical to minimise reflections on the monitor. If using a laptop computer it should have an antireflective or antiglare screen. The monitor should be viewed in dim light; ideally the reading room should be illuminated at 2–25 lux (sunlight is 105 lux). A room fitted with blinds to obscure direct sunlight is ideal. When acquiring x-rays in the field, they should be reviewed once back at the practice under optimum viewing conditions.

Image manipulation

The image can be manipulated in a variety of ways, including alteration of brightness and contrast, magnification, and by edge enhancement. Alteration of brightness and contrast should enable thorough examination of the internal architecture of bone, the bone margins and the surrounding soft tissues on a single image, if these were not evident on the original image (Figures 2.6a and 2.6b). Thus potentially more information can be gained with appropriate



Figure 2.6(a) Lateromedial image of an immature stifle obtained using a computed radiography system. Cranial is to the left. The image has been windowed for optimal evaluation of the internal osseous architecture.



Figure 2.6(b) Lateromedial image of an immature stifle obtained using a computed radiography system. This is the same as Figure 2.6(a), obtained at the same exposure (i.e. identical exposure factors and algorithm), but the image has been windowed to permit better evaluation of both the soft tissues and some of the bone margins cranially.

Downloaded From Vet-eBooks.com



Figure 2.7(a) Lateromedial image of the left metatarsophalangeal joint of a 4-year-old Thoroughbred flat racehorse with bilateral hindlimb lameness associated with fetlock region pain. The image was acquired using computed radiography. There is increased opacity of the plantar aspect of the condyles of the third metatarsal bone.



Figure 2.7(b) The same image as Figure 2.7(a) windowed, thus changing the appearance of the trabecular architecture. The relatively greater opacity of the condyles of the third metatarsal bone compared with the metaphyseal region of the proximal phalanx is clearly apparent, and increased opacity of the plantar aspect of the condyles is more obvious than in Figure 2.7(a).

manipulation. Maximal information will always be obtained from a well-positioned, appropriately exposed image, and digital imaging and image manipulation are not a substitute for poor technique. Digital imaging provides the opportunity to enhance good radiographic technique.

It is necessary to learn how to examine a digital image. With both a conventional film–screen image and a digitally acquired image it is important to view the image both from a distance and close up. With a conventional film–screen image it is important to use high-intensity illumination to examine bone margins more closely. With a digital image the reader should examine the entire image making use of the windowing facility to alter brightness and contrast as necessary (Figures 2.7a and 2.7b), to evaluate all the structures in the image. Use of the inverted window can help to identify more subtle changes, e.g. periosteal new bone (Figures 2w.8a and 2w.8b). However, with optimal exposure factors and algorithms, little image manipulation should be necessary. The use of edge enhancement may or may not help image interpretation, by increasing the contrast between areas of different densities. Incorrect use of edge enhancement may produce confusing artefacts. For example, it may create the impression of increased bronchial wall opacity in a thoracic image. Enlarging the image is often useful, but excessive enlargement results in the image becoming more pixelated (grainy) and potentially more difficult to interpret. It is also important to recognise that when examining large bones, such as the distal aspect of the femur, windowing the image by alteration of the brightness and contrast may result in the apparent development of radiolucent areas (Figure 2.9) which should not be misinterpreted as pathological lesions. Because the brightness and contrast of images can be manipulated easily, detection of conditions such as osteoporosis or increased lung density becomes more difficult.

Downloaded From Vet-eBooks.com



Figure 2.9 Coned caudocranial image of the right stifle of a 12-year-old Welsh Cob mare with left hindlimb lameness associated with the femorotibial joint. The image was acquired using computed radiography. Medial is to the left. The potentially superior image quality of a digital radiograph can lead to over-interpretation. There is a relatively radiolucent, oval-shaped area in the medial femoral condyle. This should not be misinterpreted as a subchondral bone cyst.

The size of the displayed image is scaled according to the screen size, so real size may be more difficult to determine. Many images have a scale at the side of the image, and if this is present then very accurate measurements can be made much more easily than on conventional radiographs. Some software allows 'true' size measurement calibration. Angle measurements can also be obtained. A ratio measurement facility is useful for sagittal ratio measurements of the cervical spine.

It should be possible to show more than one image on the monitor simultaneously in order to compare different views of the same area, or to compare images obtained on two different occasions. This facility is a feature of the software provided with the system. The ease with which previous images can be recalled for viewing depends on the system and method of archiving.

IMAGE ARCHIVING AND TRANSMISSION

Digital radiography removes the necessity for hard copy. It can also make image retrieval much easier. All images can be stored electronically and the method used depends on the number of images acquired daily. The retrieval systems vary considerably and it is important to establish how images can be searched, e.g. patient name, owner, case number, area examined. Whatever system is used for image storage, it is vital that it is backed up as for any computer system, to ensure data is not irretrievably lost. Some systems have an automatic back-up system (e.g. CD burn and autorun), but others require a regular back-up protocol to be instituted. (Images can be stored on magnetic disk (hard disk), DVDs (digital versatile disks), optical disks or magneto optical discs.)

Downloaded From Vet-eBooks.com

A DICOM server can be used for data storage in a multisite practice that can be accessed via a telemedicine network, allowing any authorised user connected to the system to view and handle files from many sites. Additional software may be required to function fully with some management systems.

Teleradiology is the electronic transmission of radiographic images from one location to another for the purposes of interpretation and/or consultation. Although in theory digital images can be readily e-mailed, they do create large data files, which may not be suitable for transmission, unless specialised software is used. The reader should refer to their system advisers for up-to-date details of this rapidly changing field. Images can readily be saved to CDs, allowing transfer of information between users. It is necessary however to ensure that, if DICOM files are used, the recipient of the disk has the necessary software to read the information. Many manufacturers now provide a software viewing package that is loaded on to the disk with the digital images. There are many companies that facilitate transfer of large data files.

Conversion to a compressed format allows more efficient storage and transmission. The original DICOM image can be compressed with patient data attached, or files may be compressed by conversion to other formats. This may open the opportunity for fraudulent manipulation of images, and so should only be used with due consideration. Developments in software and hardware are progressing so rapidly that it is not sensible for a book such as this to offer further detailed advice on storage and manipulation of files, as it will inevitably be out of date before the book is published!

A potential problem with digital radiography is the different file formats in which images may be saved, which can lead to difficulties when being opened by a remote user. Although some systems load viewer software with the images on to a CD or DVD, this is not universal. The files may not open with standard Windows applications and the header information (patient details) may be inaccessible. Some systems open automatically in their own format, but for others special software and a DICOM viewer are required. Many modern veterinary computer systems running with Windows already have a DICOM viewer installed, but this is not universal.

Software and software tools for viewing DICOM images are not standardised. Some are more intuitive to understand than others. As with most Windows software, placing the mouse arrow over the tool symbol will usually produce a short text describing the function of the tool, but if images have been sent from another country, this is likely to be in the language of the country of origin of the images. It may be necessary to resort to trial and error, in the knowledge that with true DICOM files if the result is not what was wanted, the operation can be cancelled and the image returned to the original stored image.

ADVANTAGES OF DIGITAL RADIOGRAPHY COMPARED WITH CONVENTIONAL FILM–SCREEN RADIOGRAPHY

The capital costs of digital equipment can be weighed against the absence of costs of conventional film and the chemicals required for processing. Digital systems eliminate the potential health and safety and environmental issues of darkroom processing, and eliminate the need for a darkroom. They also eliminate the environmental hazard of disposal of processing chemicals. Digital imaging should also reduce the number of images

Downloaded From Vet-eBooks.com

acquired, because fewer repeat x-rays are needed due to inappropriate exposures, and fewer repeat images are needed with different exposures to detect specific lesions. There is reduced storage area needed for both processing chemicals and archiving of x-rays. The risk of processing artefacts is reduced. The time taken to obtain images is also reduced, especially with direct digital radiography. For a practitioner in the field, acquisition of images with digital radiography is no longer limited by the number of available cassettes. Images can be viewed on a laptop computer in the field, and although this may not have the same resolution as a better monitor, the images can be assessed for suitability of positioning and a preliminary diagnosis made. The development of battery-powered x-ray generators for use with more sensitive DR imaging plates, and smaller computers to process the images is making portable x-ray systems truly available in almost any circumstances. Whether radiography should be attempted in all these circumstances is open to debate. It is crucial that appropriate radiation safety measures are employed.

Images are readily archived, and retrieval should be easier and more reliable than with conventional radiographs. Images are less likely to be lost (assuming that files are backed up), or misfiled. Image quality should also be stable over time. Images can easily be transmitted electronically making it much easier to obtain a second opinion on interpretation. Images acquired on behalf of a prospective purchaser can easily and rapidly be sent to their own veterinary surgeon or insurance underwriter's veterinary surgeon for independent review.

Although theoretically film–screen radiographs contain more detailed information than computed or digital radiographs, given equivalent standards of radiography, in practice we have found that image quality and diagnostic capabilities have actually increased using digital systems. For example, the recognition of osseous fragments distal to the medial and lateral angles of the distal border of the navicular bone has increased. The potential for increased detail means relearning what is normal, and not over-interpreting normal findings as pathological lesions. Over-interpretation is a common problem when first using a digital system (Figure 2.9).

Additional figures

The book companion website at www.clinical-radiology-horse.com includes additional figures that are not included in the printed book or e-book formats. Please see '**About the Companion Website**' at the start of the book for details on how to access the website. These figures are prefixed with the letter 'w' in the printed book, e.g. Figures 1w.4c–f.

FURTHER READING

American College of Radiology (2005) *ACR Technical Standard for Teleradiology*, American College of Radiology

Cesar, L., Scheler, B., Zink, F., et al. (2001) Artefacts found in computed radiography. *Brit. J. Radiol.* **74**, 195–202. www.idoimaging.com

Robertson, I., Thrall, D. (2013) Digital radiographic imaging. In: *Textbook of Veterinary Diagnostic Radiology*, 6th edn., Ed. Thrall, D., pp 22–37, Elsevier, St. Louis

Downloaded From Vet-eBooks.com

Chapter 3
The foot

The foot is a complex area, involving several bones and important soft tissue structures as well as the hoof wall. This chapter has therefore been subdivided into anatomical areas in order to make description easier. Although several of these areas may be obtained on a single radiograph, radiographs centred on the area of interest are required for accurate appraisal.

Except where stated otherwise, the text refers to both front and hind feet.

Distal phalanx (pedal bone)

RADIOGRAPHIC TECHNIQUE

Equipment

Radiographs of the distal phalanx (third phalanx, pedal bone) can be obtained with low-output (minimum 15 mA) portable x-ray machines. Digital imaging or slow, high-detail screens with compatible film are recommended to obtain maximum definition.

Prior to obtaining radiographs, the shoe should be removed and the sole and hoof wall cleaned of mud and dirt. Loose flakes of horn from the sole, bulbs of the heel and frog should be trimmed. Particular care should be taken if the frog clefts are deep. A sharp pointed instrument, such as a searching knife, a hoof pick or rat tail file, is helpful for removal of packed debris. The clefts should finally be cleaned using a stiff brush. Radiographs of the distal phalanx do not normally require the foot to be packed, although packing around the point of the frog will eliminate air shadows from the foot and may avoid confusion in some cases, especially if a fracture is suspected. Care must be taken to ensure that the sole is packed evenly, because the low exposures required to assess the solear margin of the distal phalanx can also result in images of uneven packing. Loose packing may mimic, or mask, fractures; excessive packing may create radiopaque artefacts (Figure 3.1). These packing artefacts are particularly evident on digital radiographs. Previous paring of the foot in search of a sub-solear abscess may result in confusing radiolucent areas superimposed over osseous structures.

Lateromedial and dorsopalmar or plantarodorsal views of the distal phalanx may be obtained using a grid (see relevant view for details), although this is not essential. Oblique views, particularly palmaroproximal-palmarodistal

Clinical Radiology of the Horse, Fourth Edition. Janet A. Butler, Christopher M. Colles, Sue J. Dyson, Svend E. Kold and Paul W. Poulos.
© 2017 John Wiley & Sons, Ltd. Published 2017 by John Wiley & Sons, Ltd.
Companion website: www.clinical-radiology-horse.com

Downloaded From Vet-eBooks.com

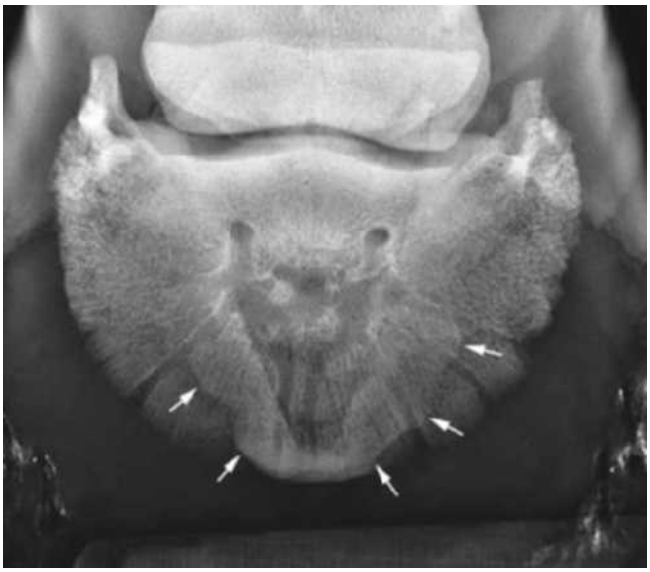


Figure 3.1 Dorsoproximal-palmarodistal oblique image of a foot. There is a region of diffuse increased opacity (arrows) which outlines the position of the frog. This is the result of excessive packing material placed in the frog clefts.

oblique and dorsoproximal-palmarodistal oblique views of the palmar processes, and soft exposures (e.g. radiographs to assess separation of the hoof wall from the distal phalanx, lucent lines in the dorsal hoof wall, or subtle modelling of the extensor process), are best obtained without a grid. When using digital systems, grids may cause moiré lines on the image, and so radiographs of areas such as the distal phalanx are better obtained without a grid.

Positioning

Any examination of the distal phalanx should always include lateromedial and dorsoproximal-palmarodistal oblique views. Mediolateral views have a similar appearance to lateromedial views and may be used if preferred. For hind feet it may be easier to obtain plantarodorsal rather than dorsoplantar views.

Lateromedial view

Lateromedial views of the distal phalanx normally require the foot to be raised on a block of sufficient height to bring the solear surface of the foot level with the centre of the x-ray beam. This also allows the bottom of the cassette to be placed lower than the solear surface of the foot, so that it is included on the image. Ideally both feet should be on a block so that the horse is weight bearing evenly on the foot to be radiographed. The cassette can be supported on the floor, or on a second block, to minimise the risk of movement blur. The x-ray beam should be horizontal, and centered on the distal phalanx, aligned parallel with a line drawn tangential to the bulbs of the heel. Care must be taken when assessing the hoof–pastern axis with this technique, since this will be altered if the horse is not fully weight bearing on a level surface. An 8:1 ratio grid will give the best results for this view when using film, but acceptable results can be obtained without the use of a grid. Digital images are best obtained without a grid.

A survey lateromedial view of the entire foot and pastern may be obtained. In this case the maximum information will be obtained if the x-ray beam is centered on the navicular bone – the beam should be centered approximately

Downloaded From Vet-eBooks.com

1 cm below the coronary band, and midway between the most dorsal and most palmar aspects of the foot at the level of the coronary band. The x-ray beam should be aligned parallel with a line drawn tangential to the bulbs of the heel. The importance of a true lateromedial view for accurate interpretation cannot be overemphasised. This may be difficult to obtain in horses with marked distortion of the hoof capsule, obvious toe-in or toe-out conformation, or if there is a poor medial–lateral hoof balance. If specific lesions of the distal phalanx are anticipated, the x-ray beam should be centered on the lesion, or on the distal phalanx, at approximately the region of insertion of the deep flexor tendon – a point approximately midway between the coronary band and the ground surface at the junction of the dorsal and middle thirds of the hoof. The beam should be aligned parallel with a line drawn tangential to the bulbs of the heel.

Dorsoproximal-palmarodistal oblique view

A dorsoproximal-palmarodistal oblique view gives good visualisation of the body, solear margin and palmar processes (wings) of the distal phalanx, and is suitable for use as a routine view. It may be obtained in one of two ways. The technique giving least distortion is the 'upright pedal' view. The toe of the foot is placed on a wooden block with a groove cut along its top surface (referred to as a 'navicular block', see Figure 3.63c), and the limb is manipulated until the sole of the foot is vertical. A horizontal x-ray beam is centered on the coronary band and aligned perpendicular to the sole of the foot (Figure 3.2a). The imaging plate is positioned vertically against the sole of the foot. A low-ratio grid (6:1) is ideal for this view when using film, but acceptable results can be obtained without the use of a grid (Figure 3.2b). For digital images, better results may be obtained without a grid.

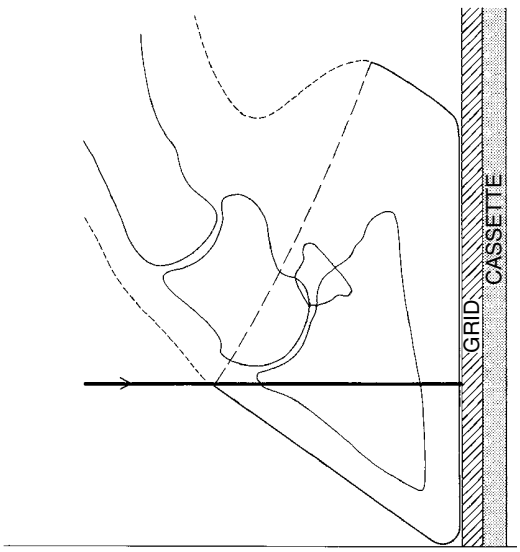


Figure 3.2(a) Positioning to obtain a dorsoproximal-palmarodistal oblique ('upright pedal') image of the distal phalanx. The x-ray beam (arrow) is centered on the coronary band.



Figure 3.2(b) Dorsoproximal-palmarodistal oblique radiographic image of the distal phalanx of a normal adult horse, obtained using the 'upright pedal' technique. The image was acquired with the toe of the foot in a v-shaped block; the horizontal line across the image is created by the block.

Downloaded From Vet-eBooks.com

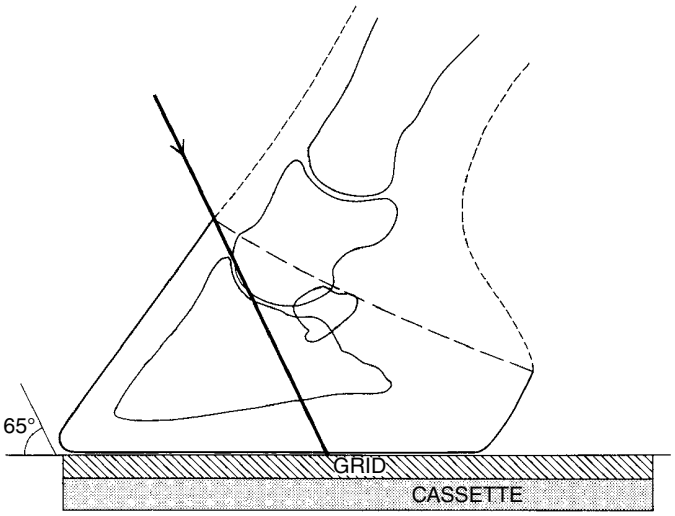


Figure 3.3(a) Positioning to obtain a dorsoproximal-palmarodistal oblique ('high coronary') image of the distal phalanx. The x-ray beam (arrow) is centered on the coronary band.



Figure 3.3(b) Dorsoproximal-palmarodistal oblique radiographic image of the distal phalanx of a normal adult horse (the same horse as Figure 3.2b), obtained using the 'high coronary' technique. Note the apparent elongation of the bone (compare with Figure 3.2b).

For hind feet it is often preferable to obtain a plantarodorsal view rather than a dorsoplantar projection of the foot. This allows good assessment of the structures within the foot and makes little difference to interpretation of radiographs of the distal phalanx. The foot is positioned in a similar manner to that for a dorsoproximal-palmarodistal oblique view. Often the toe may simply be rested on a plane block, and supported by an assistant with the sole vertical. The x-ray beam is centered on the middle of the frog, perpendicular to the sole of the foot. The imaging plate is positioned vertically, dorsal to the foot, and as close to the foot as possible.

A similar view, a dorsoproximal-palmarodistal (high coronary) oblique, may be obtained with the horse standing on a tunnel containing the cassette. The x-ray beam is angled in a dorsoproximal-palmarodistal oblique direction, at approximately 65° to the horizontal, centered on the coronary band (Figure 3.3a). This technique has the disadvantage that the beam is oblique to the cassette, and therefore results in some distortion. It may be useful for assessing fractures, and is helpful in some horses that resent placing the foot in a 'navicular block'. A parallel 6:1 ratio grid is used if the x-ray beam can be aligned with the grid lines; otherwise a better result is obtained without a grid (Figure 3.3b). This technique may be more practical when there is limited assistance or with difficult horses.

Dorsopalmar (weight-bearing) view

A dorsopalmar weight-bearing view is useful for identification and assessment of a sagittal fracture of the distal phalanx, assessment of the width of the distal interphalangeal joint space and lateromedial foot imbalance,

Downloaded From Vet-eBooks.com

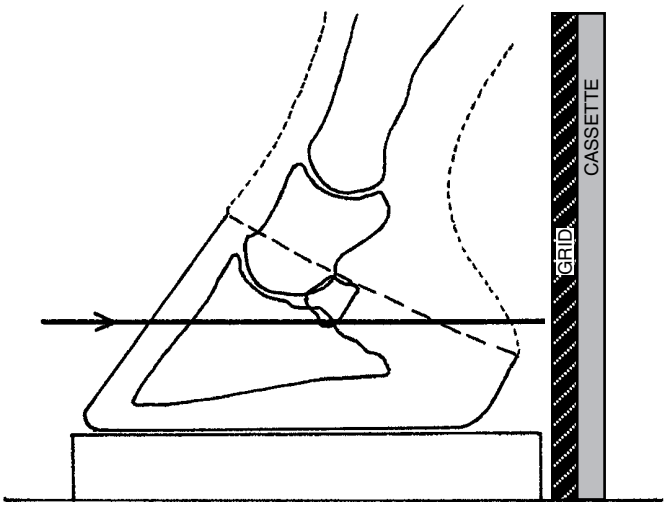


Figure 3.4 Positioning to obtain a dorsopalmar (weight-bearing) image of the distal phalanx and navicular bone (see Figure 3.12). The x-ray beam (arrow) is centered midway between the coronary band and the ground surface of the hoof.

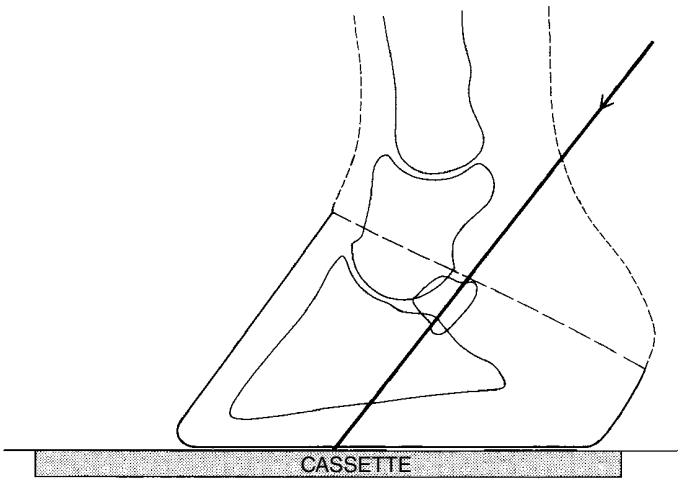


Figure 3.5 Positioning to obtain a palmaroproximal-palmarodistal image of the distal phalanx (see Figure 3.13). The x-ray beam is centered between the bulbs of the heel.

assessment of ossification of the ungular cartilages and identification of changes in opacity of the submural soft tissues. The horse stands weight bearing on the limb, on a flat block, so that the cassette may be placed lower than the solear surface of the foot. For assessment of foot imbalance and the width of the distal interphalangeal joint, both front feet should be on blocks of similar height with the horse weight bearing evenly. A horizontal x-ray beam is centered midway between the coronary band and the ground surface, at the midline of the hoof (Figure 3.4). It should be aligned at right angles to a line drawn across the bulbs of the heel. This ensures a straight dorsopalmar image of the foot. If it is desired to record medial or lateral deviation of the limb distal to the fetlock, the beam should be aligned parallel to the metacarpal region. A 6:1 ratio grid is preferred, but is unnecessary with digital imaging.

Palmaroproximal-palmarodistal oblique view

This view is used to give good visualisation of the palmar processes of the distal phalanx, particularly for identification of separation of the laminae of the heel of the foot, or a frontal plane fracture of a palmar process that may not be detectable in any other view.

The horse stands on a cassette tunnel, flat on the floor. The foot to be radiographed is positioned as far caudally under the horse as is consistent with the horse standing flat on the foot. The x-ray machine is placed ventral to the thorax of the horse and the x-ray beam centered between the bulbs of the heel (Figure 3.5). The angle of incidence of the x-ray beam to the cassette is 45–70°, dependent upon the slope of the pastern and the positioning of the foot. The beam is angled so that the image of the fetlock is not superimposed over the palmar processes of the distal phalanx. If the foot is positioned too far forward, it is impossible to avoid superimposition of the image of the fetlock over the foot, especially if the ergot is prominent. This view is obtained without a grid. An alternative technique to obtain this view is described below (see 'Navicular bone – Palmaroproximal-palmarodistal oblique view' and Figure 3.64b).

Downloaded From Vet-eBooks.com

Other oblique views

Oblique views of the distal phalanx and hoof wall are often required to assess the hoof wall, lamellar tissue and the distal phalanx. These are particularly valuable if fractures involving the body or palmar processes of the distal phalanx are suspected, and to identify new bone on the dorsal aspect of the distal phalanx, or mineralisation in the dermal laminae. They also help to identify periarticular modelling on the dorsomedial and dorsolateral aspects of the distal interphalangeal joint (Figure 3.40b), or entheseophytes on the middle or distal phalanges, irregularity of the solear aspect of the distal phalanx, fracture of the articular margin of the distal interphalangeal joint, and entheseophyte formation on the navicular bone. Obliquity is determined by one of two factors:

1 An attempt to align the x-ray beam parallel with the line of a fracture.

2 Positioning the x-ray beam so that new bone will be 'skylined' (i.e. the beam will form a tangent to the surface of the distal phalanx at the region of the new bone). For this purpose, reduced exposures should be used, and a grid is unnecessary.

Osteophyte or entheseophyte formation on the dorsolateral or dorsomedial aspects of the distal phalanx are often best seen on flexed oblique views, which open the distal interphalangeal joint. The toe of the foot is placed in a navicular block with the sole of the foot approximately vertical, or on a flat block balanced on the toe. Dorsal 60° lateral-palmaromedial oblique (flexed) and dorsal 60° medial-palmarolateral oblique (flexed) views are obtained. A horizontal x-ray beam is used, centered on the coronary band (Figure 3.6). To highlight the lateral and medial palmar processes using the above technique, dorsal 45° lateral-palmaromedial oblique (flexed) and dorsal 45° medial-palmarolateral oblique (flexed) views respectively should be obtained.

Alternatively, dorsal 45° lateral-palmaromedial (weight-bearing) (Figure 3.7) and dorsal 45° medial-palmarolateral (weight-bearing) oblique images can be used. The horse stands weight bearing on the limb, on a flat block, so that the cassette may be placed lower than the solear surface of the foot. A horizontal x-ray beam is centered 1 cm below the coronary band, midway between the dorsal and palmar margins of the foot. The x-ray beam may also be aligned tangential to a visible defect on the hoof wall. However, the articular margins of the proximal and distal interphalangeal joints are less easy to assess than in the corresponding oblique images acquired with the limb flexed.

Alternatively, to image the palmar processes, the horse should stand on a tunnel containing the cassette. The beam should be angled 45° proximally and centered on the coronary band just behind the midpoint between the dorsal midline and bulb of the heel on the lateral or medial aspect of the foot (Figure 3.8). A lateral 45° proximal-mediodistal oblique image highlights the lateral palmar process, a medial 45° proximal-laterodistal oblique image highlights the medial side. This technique may be preferable in foals; it can be difficult to support a sedated foal with the foot in an upright position. It also permits more consistent angulation of the x-ray beam in foals in order to obtain comparable follow-up radiographs.

The frog clefts should be carefully cleaned and packed to avoid radiolucent artefacts mimicking a fracture.

Downloaded From Vet-eBooks.com

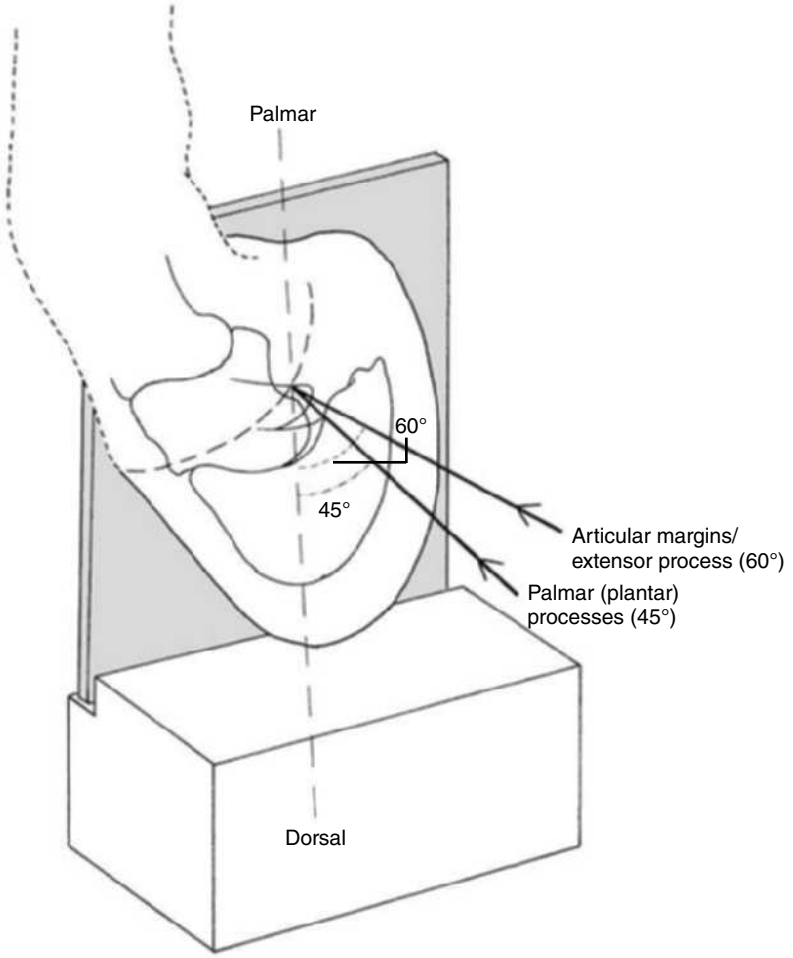


Figure 3.6 Positioning to obtain a dorsolateral-palmaromedial oblique (flexed) image of the distal phalanx and interphalangeal joints. The use of a 'Hickman or navicular block' rather than a flat block may help to stabilise the toe. The x-ray beam (arrow) is centered on the coronary band. An angle of 45° from dorsal highlights the lateral or medial palmar process of the distal phalanx (see Figure 3.15). The dorsal margins of the interphalangeal joints are best imaged with an angle of 60° from the dorsal plane (see Figure 3.14).

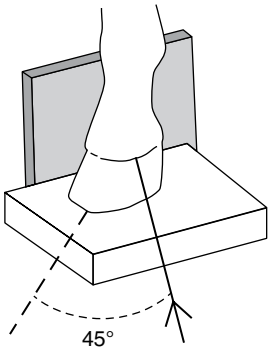


Figure 3.7(a) Positioning to acquire a dorsal 45° lateral-palmaromedial oblique (weight-bearing) image of a foot.

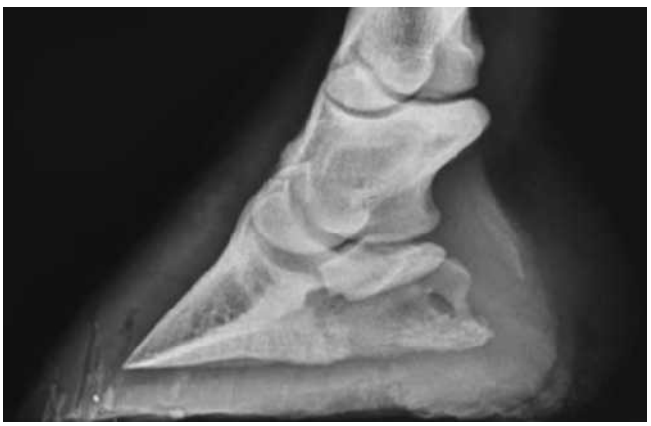


Figure 3.7(b) Dorsal 45° lateral-palmaromedial oblique (weight-bearing) image of a normal adult horse.

Downloaded From Vet-eBooks.com

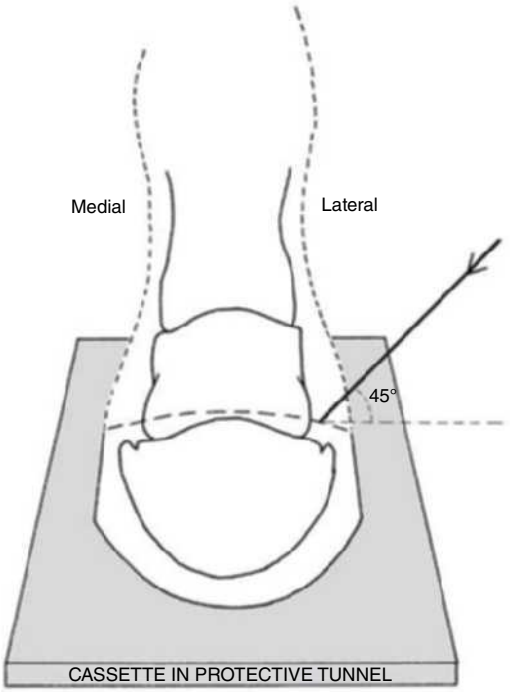


Figure 3.8 Technique to obtain a lateral 45° proximal-mediodistal oblique image of the distal phalanx to skyline the lateral palmar process. The x-ray beam is centered on the coronary band. See also Figure 3.16.

NORMAL ANATOMY

The front and hind distal phalanges have a similar appearance, but the distal phalanx of the hind feet are slightly narrower mediolaterally than those of the front feet.

Immature horse

The distal phalanx develops from a single centre of ossification, which is present at birth (Figures 3.9a and 3.9b). It continues to enlarge and model until at least 18 months of age. The palmar processes are not evident at birth, and gradually ossify over 12 months, but may not obtain their full length until about 18 months.

Skeletally mature horse

Lateromedial view

The dorsal surface of the distal phalanx is smooth and opaque (Figure 3.10a). The dorsal compact bone is of variable thickness. It may be slightly dorsally convex from the solear margin to the base of the extensor (pyramidal) process, especially in the hindlimbs, and should meet the solear margin at a sharp angle. In horses with a large crena marginis solearis (Figure 3.17a), a radiolucent indentation or a double line may be seen at the junction of these margins (Figure 3.17b). There are considerable variations in the shape of the extensor process, but they are usually bilaterally symmetrical (see Figure 3.18). It is generally accepted that the dorsal hoof wall and the dorsal aspect of the distal

Downloaded From Vet-eBooks.com

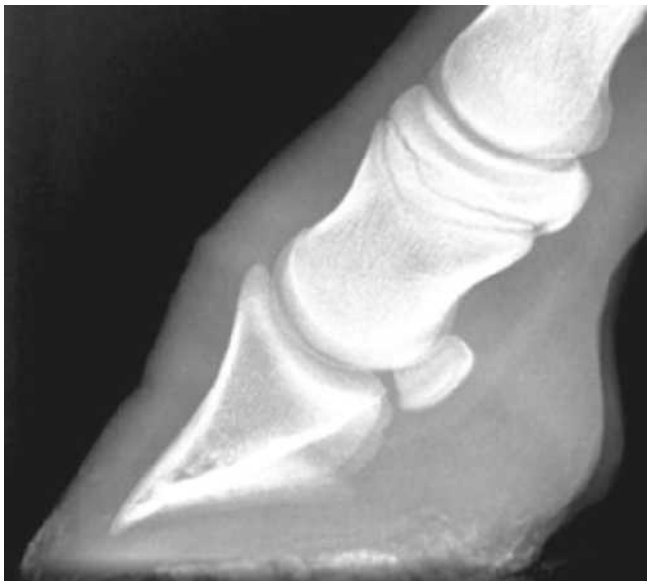


Figure 3.9(a) Slightly oblique lateromedial radiographic image of the foot of a normal foal of approximately 2 months of age. Note the rounded extensor process of the distal phalanx and the rounded shape of the navicular bone. The proximal physis of the middle phalanx is open. The foot shape is more upright than in an adult.



Figure 3.9(b) Dorsoproximal-palmarodistal oblique radiographic image of a foot of a normal foal of approximately 2 months of age. The medial and lateral borders of the distal phalanx are rather poorly defined.

phalanx should be parallel; however, there are a number of studies in both Thoroughbreds and Warmbloods which have demonstrated that the angle of the dorsal aspect of the distal phalanx to the horizontal is often less than the angle of the dorsal hoof wall to the horizontal. The orientation of the hoof wall may be distorted due to poor hoof care, for example an excessively long toe. There is a radiolucent 'halo' between both the hoof wall and sole and the dorsal and distal aspects of the distal phalanx respectively, representing the lamellae and sublamellar dermis (Figure 3w.10b). Narrowing of this halo or increase in its opacity may reflect abnormal lamellar epidermis.

The solear surface of the distal phalanx is smooth in outline and is said to be normal if at a 3–10° angle to the sole, sloping proximally toward its palmar aspect. There are significant breed differences, with Thoroughbreds generally having a smaller angle than Warmbloods. The solear canal of the distal phalanx (through which runs the terminal arch of the digital arteries) is seen between the solear surface of the bone and the distal interphalangeal joint. It is seen with a variable degree of clarity, depending on the exposure factors used and the direction of the x-ray beam. It may appear as a very distinct radiolucent zone in the middle of the bone, proximal to the solear surface, but in some bones it is barely evident. Palmar to the solear canal is a sharply defined, smoothly outlined relatively opaque band of bone, the facia flexoria. The deep digital flexor tendon inserts on the palmar aspect (Figure 3.10a).

The articular surfaces of the middle and distal phalanges are reasonably congruous. There is sometimes a smoothly outlined V-shaped notch in the articular margin of the distal phalanx (Figure 3.17c). The middle of the articular

Downloaded From Vet-eBooks.com



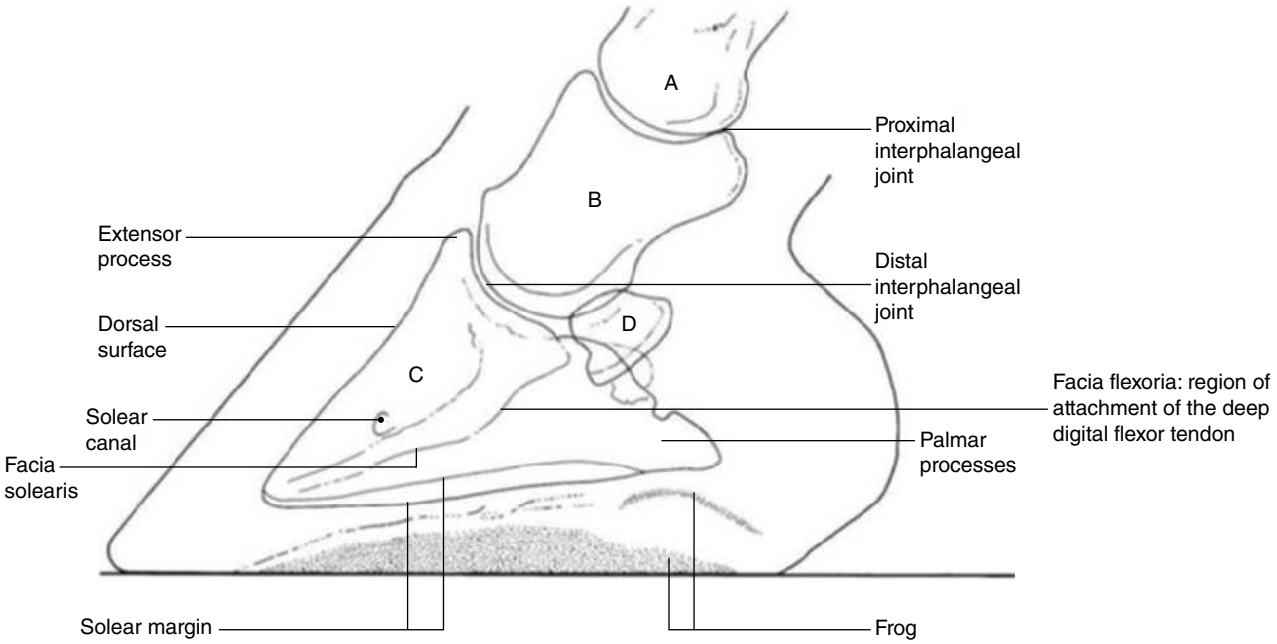


Figure 3.10(a) Well-positioned lateromedial radiographic image and diagram of a normal adult foot. A = proximal phalanx, B = middle phalanx, C = distal phalanx, D = navicular bone. The toe of the foot has been cut off.

margin of the middle phalanx may be slightly flattened. The width of the joint space is affected by the amount of weight being borne on the foot, and the presence of any effusion within the joint.

Dorsoproximal-palmarodistal oblique view

The appearance of the distal phalanx on dorsoproximal-palmarodistal oblique upright pedal and high coronary views is essentially the same (Figure 3.11), although the high coronary image (with the foot stood on a

Downloaded From Vet-eBooks.com

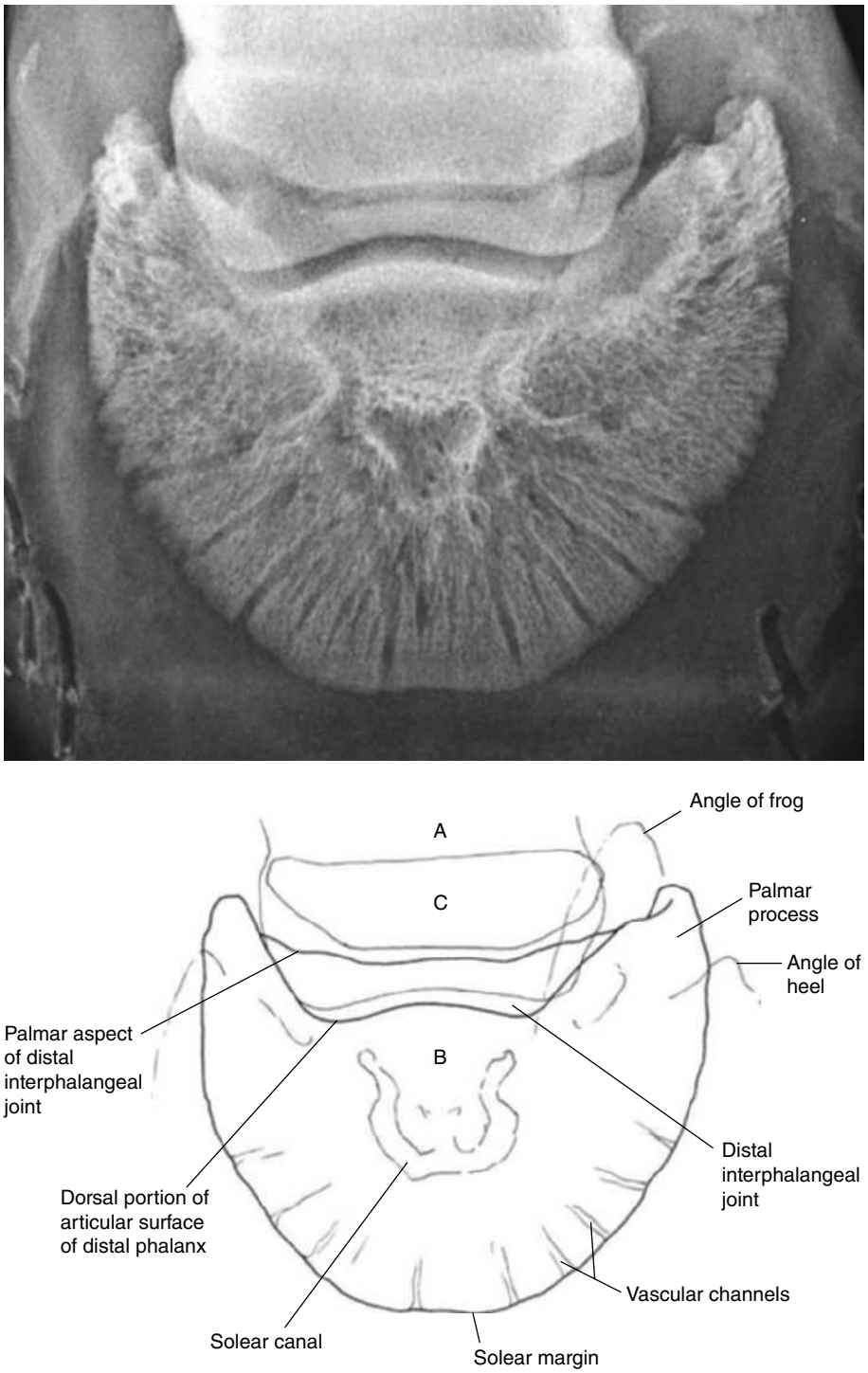


Figure 3.11 Dorsoproximal-palmarodistal oblique (upright pedal) radiographic image and diagram of a normal adult distal phalanx. Lateral is to the right. A = middle phalanx, B = distal phalanx, C = navicular bone. There is an ill-defined oblique radiolucent line crossing the distal interphalangeal joint laterally, which represents a packing defect.

Downloaded From Vet-eBooks.com

cassette tunnel) does result in some distortion and elongation of the image. The solear margin is well defined, describing a regular curved outline. Some irregularity may be present, especially at the periphery of the vascular channels. The distal phalanges of the hind feet are narrower and have a slightly more pointed outline at the toe than those of the front feet.

A distinct, somewhat blunted V-shaped notch (crena marginis solearis) may be present in the midline in the dorsal aspect of the solear margin of the bone. This is usually present bilaterally, and is variable in size (up to 1.5 cm in depth) (Figure 3.17a and b).

Vascular channels are evident as radiolucent lines, radiating between the solear canal and the solear margin. They are variable in number and width, and may appear to narrow or widen slightly close to the solear margin (Figure 3w.19).

The solear canal is extremely variable in its appearance. It is usually an irregular, roughly U-shaped radiolucent canal seen in the centre of the distal phalanx, extending from the level of the distal interphalangeal joint to approximately midway between the joint and the solear margin of the bone. However, variations in shape are common (Figure 3w.20a–f).

The distal interphalangeal joint is evident as two distinct lines, the uppermost representing the palmar aspect of the articulation of the distal phalanx with the middle phalanx, close to its articulation with the distal sesamoid (navicular) bone. The lower of the two lines represents a more dorsal portion of the articular surface of the distal phalanx, its exact position depending on the angulation of the bone when radiographed.

Approximately oval-shaped radiolucent areas in the proximolateral and proximomedial aspects of the distal phalanx are seen with variable clarity at the insertions of the collateral ligaments of the distal interphalangeal joint (Figure 3.21). These should not be confused with osseous cyst-like lesions.

Dorsopalmar (weight-bearing) view

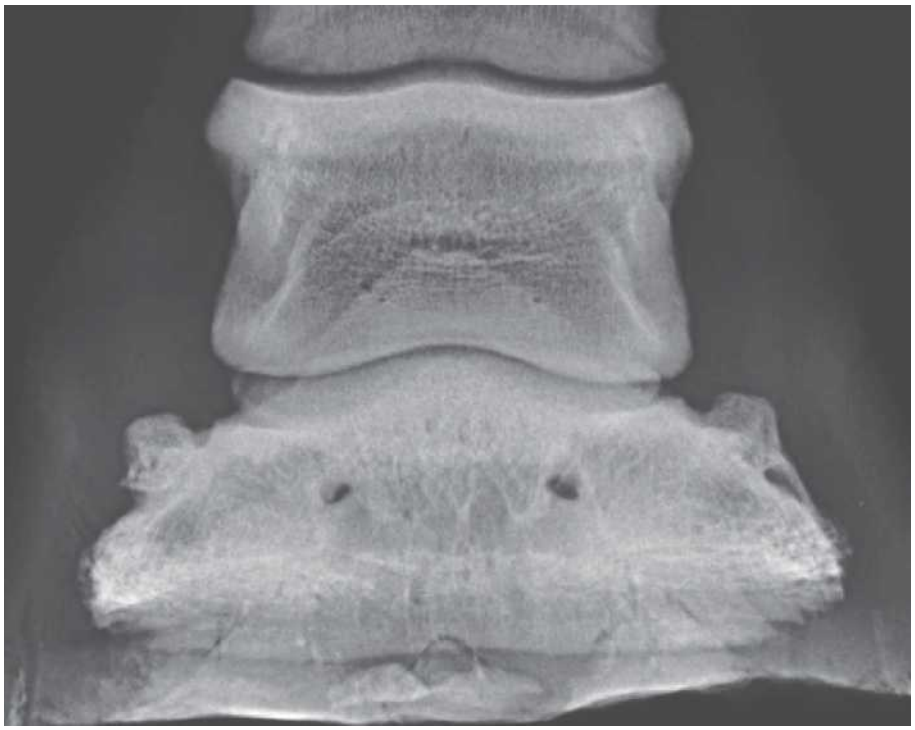
In a dorsopalmar (weight-bearing) image (Figure 3.12), the openings of the solear canal are seen as two distinct circular foramina distal to the articular surface of the distal phalanx. The extensor process may be difficult to examine, as it is superimposed over the distal end of the middle phalanx and the navicular bone. The parietal sulci (dorsal grooves) of the distal phalanx are seen as notches on the lateral and medial aspects of the bone. Occasionally these appear as a complete foramen rather than a notch. The solear margin of the bone should be an equal distance from the ground surface of the foot laterally and medially.

This is the best view to assess mediolateral foot balance (see, below, 'Hoof – Hoof balance' and Figures 3.12, 3.22 and 3.49). The degree and symmetry of ossification of the ungular cartilages (sidebone) are also best evaluated in this projection, although the extent of dorsal and palmar ossification cannot be assessed.

Palmaroproximal-palmarodistal oblique view

The palmar aspects of the palmar processes of the distal phalanx are seen on either side of the navicular bone (Figure 3.13). The axial and abaxial surfaces have a relatively smooth appearance, although some irregular radiolucencies

Downloaded From Vet-eBooks.com



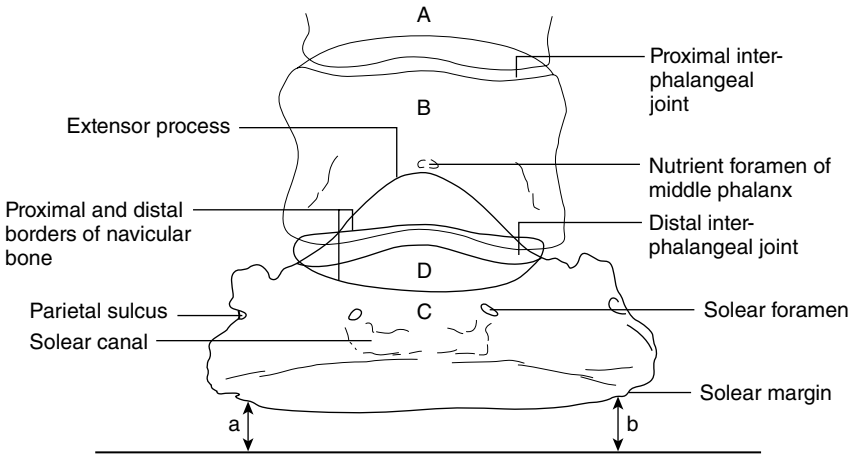


Figure 3.12 Dorsopalmar radiographic image and diagram of a normal adult foot. The radiographic image has been collimated so that the medial and lateral extremities of the hoof wall cannot be seen. Medial is to the left. The sole is thicker medially than laterally. Arrows a and b indicate the height between the distal border of the distal phalanx and the ground surface. A = proximal phalanx, B = middle phalanx, C = distal phalanx, D = navicular bone.

Downloaded From Vet-eBooks.com

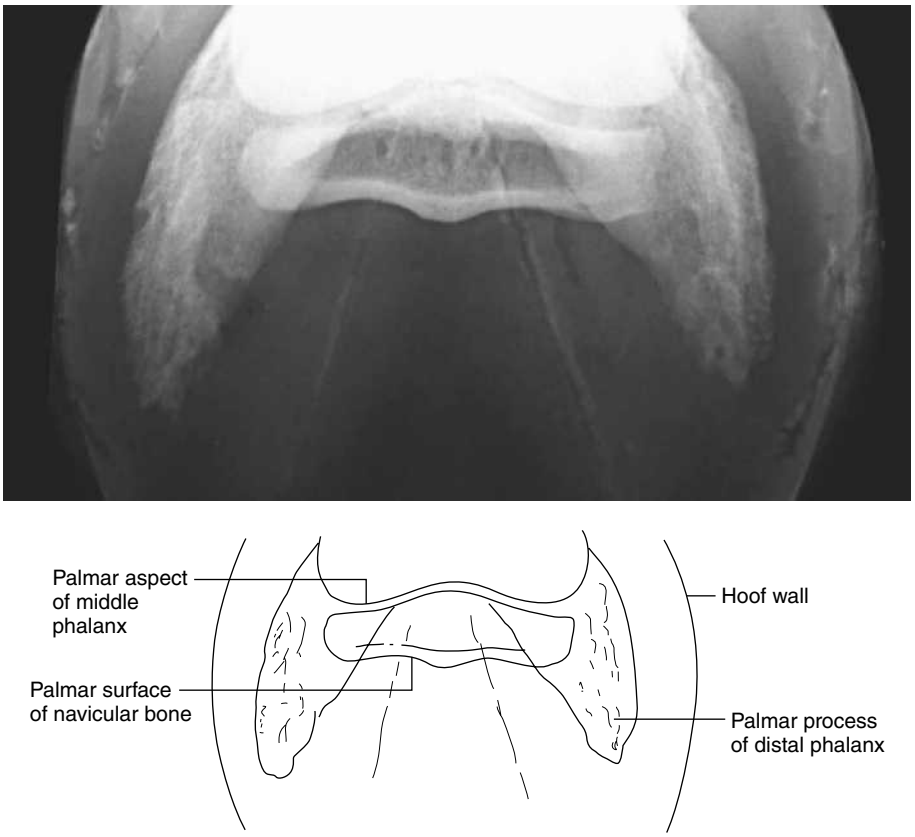


Figure 3.13 Palmaroproximal-palmarodistal oblique radiographic image and diagram of a normal adult foot. Medial is to the left. The slightly irregular margins of the palmar processes of the distal phalanx are normal. The horse had very deep frog clefts, so these were difficult to pack completely. Note also the radiolucent areas in the hoof wall medially and laterally, representing nail holes and the circumferential radiolucent area in the palmar lateral aspect of the hoof wall, representing an area of hoof wall separation.

within the body of each palmar process are often present. An oval opaque ring may be present in the palmar processes, representing mineralisation in the base of the ungular cartilage (see also 'Ossification of the ungular cartilages', below). A lucent 'halo' is evident between the hoof wall and the distal phalanx, representing the lamellae and sublamellar dermis (Figure 3w.10b).

Dorsal 60° lateral-palmaromedial oblique and dorsal 60° medial-palmarolateral oblique (flexed) views

The contour of the extensor process of the distal phalanx is smoothly curved. Depending on the degree of flexion, one of the condyles of the middle phalanx may be partially superimposed over the extensor process. The eminence for the origin of a collateral ligament on the dorsal aspect of the middle phalanx on the opposite side is also seen (Figure 3.14). These eminences tend to be more prominent in heavier breeds of horses and cob types compared with Thoroughbred types. A lucent line courses obliquely across the distal phalanx. This may be either an edge effect created by the superimposition

Downloaded From Vet-eBooks.com



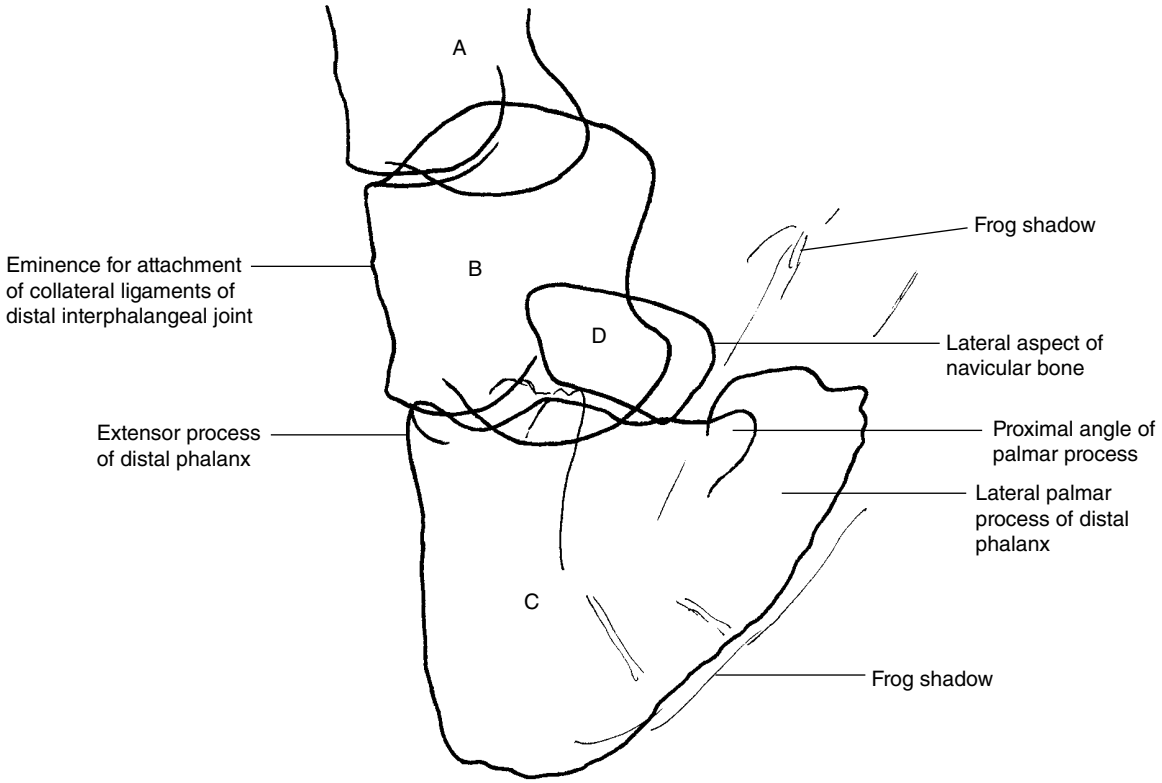


Figure 3.14 A dorsal 60° lateral-palmaromedial oblique (flexed) image and diagram of the pastern and foot of a normal adult horse. A = proximal phalanx, B = middle phalanx, C = distal phalanx, D = navicular bone.

Downloaded From Vet-eBooks.com



Figure 3.15 Dorsal 45° lateral-palmaromedial oblique (flexed) image of a foot of a normal adult horse.

of the contralateral palmar process, or a frog shadow, depending on the projection angle. It should not be confused with a fracture. There is a variably sized notch or foramen on the palmar aspect of the palmar process, the parietal incisure or foramen of the palmar process, leading to the parietal sulcus (dorsal groove).

The dorsal 60° lateral-palmaromedial oblique (flexed) view (Figure 3.14) allows better evaluation of the proximal and distal interphalangeal joint margins than the dorsal 45° lateral-palmaromedial oblique (flexed) view (Figure 3.15). The lateral 45° proximal-medial distal oblique (flexed) view permits more assessment of the lateral palmar process (Figure 3.16).

NORMAL VARIATIONS AND INCIDENTAL FINDINGS

On lateromedial projections there are variations in the shape of the distal phalanx, largely due to differences in the degree of concavity of the solear border, and the angle the solear border makes to the horizontal. Variations

Downloaded From Vet-eBooks.com

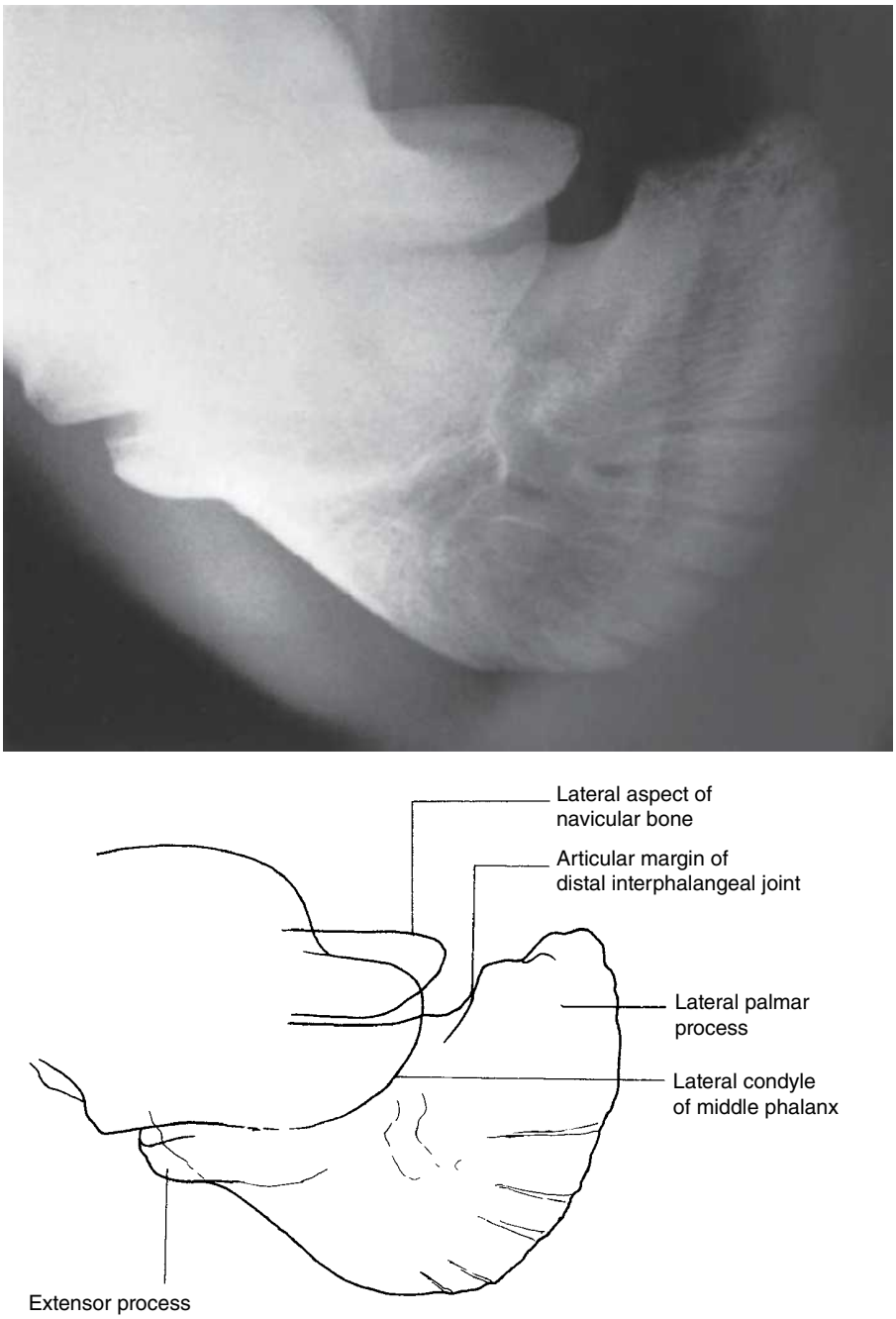


Figure 3.16 Lateral 45° proximal-medial distal oblique view to highlight the lateral palmar process of the distal phalanx.

in shape of the distal phalanx seen in a lateromedial image are not necessarily correlated with external characteristics of the hoof capsule.

Some horses have one or more asymmetrical feet, so that when viewed from dorsally a line which bisects the metacarpus/metatarsus does not bisect the foot. The foot usually extends further laterally than medially. In such feet the shape of the distal phalanx often mirrors that of the hoof capsule in a

Downloaded From Vet-eBooks.com

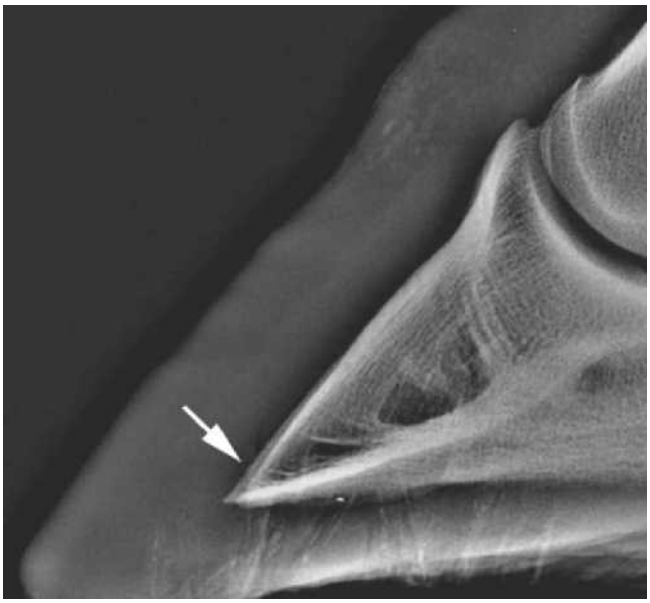


Figure 3.17(a) Lateromedial image of a normal adult horse, the same foot as Figure 3.17(b). Note the duplicated appearance of the dorsal margin of the bone at the toe (arrow). This is created by the moderately-sized crena solearis.



Figure 3.17(b) Dorsoproximal-palmarodistal oblique image of a distal phalanx of a normal adult horse, the same horse as Figure 3.17(a). There is a moderately-sized notch at the toe of the distal phalanx, the crena solearis. Note also the concave shape of the proximal border of the navicular bone.



Figure 3.17(c) Lateromedial image of a distal interphalangeal joint of an adult horse. There is a V-shaped notch in the middle of the articular surface of the distal phalanx, of questionable clinical significance. Note also the smoothly outlined depression in the sagittal ridge of the navicular bone.

Downloaded From Vet-eBooks.com

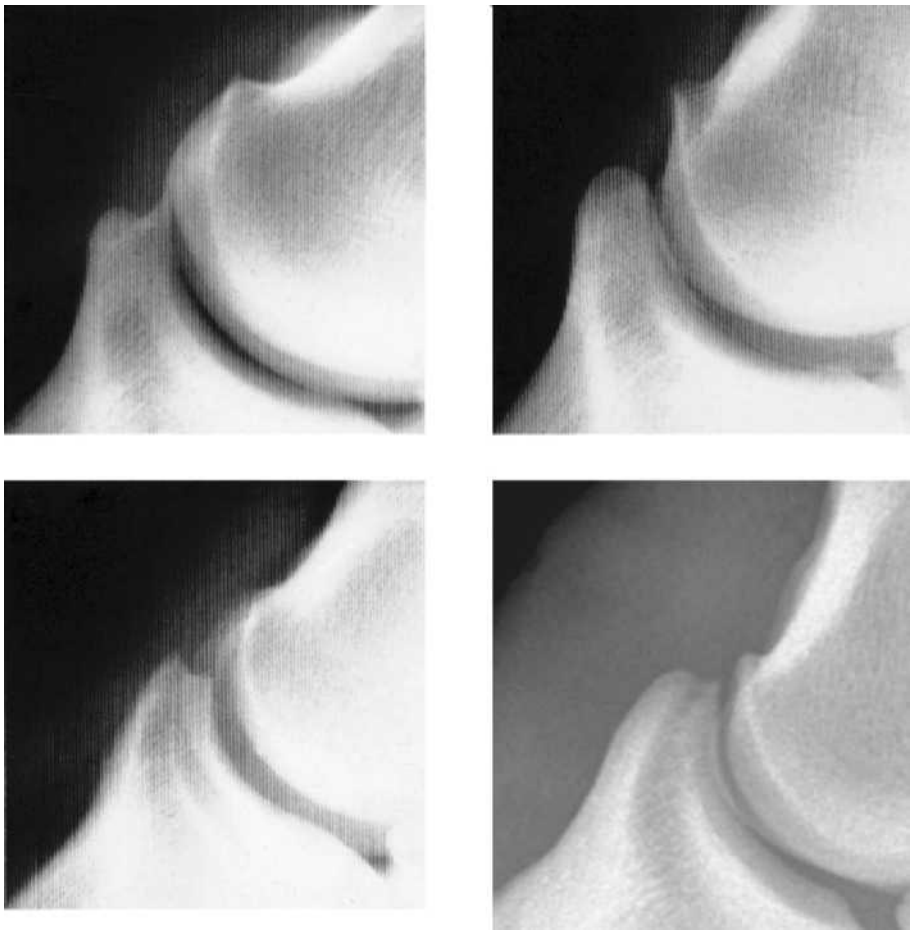


Figure 3.18 Lateromedial radiographs of the extensor process of normal distal phalanges, showing the variation in shape that may occur.



Figure 3.21 Dorsoproximal-palmarodistal oblique radiographic image of a normal distal phalanx. Medial is to the left. There are quite clearly demarcated smoothly outlined radiolucent areas medially and laterally (arrows) at the insertion sites of the collateral ligaments of the distal interphalangeal joint. These are normal and are seen with variable clarity, depending on the shape of the foot and its position during image acquisition. There are some irregularities of the solear margin of the distal phalanx at the quarters, medially and laterally, and a smoothly outlined depression, a crena, at the toe of the distal phalanx. These are normal variants. There is a moderately sized entheseophyte on the proximolateral aspect of the navicular bone.

Downloaded From Vet-eBooks.com



Figure 3.22 Dorsopalmar image of a foot. Lateral is to the right. The hoof capsule is asymmetrical and this is mirrored by the shape of the distal phalanx. An imaginary perpendicular line which bisected the middle phalanx would have a wider portion of the hoof capsule and the distal phalanx lateral to the line compared with medial to the line. The medial aspect of the hoof capsule is much more upright compared with the lateral aspect. Note also that the distal medial aspect of the distal phalanx is lower than the lateral aspect.

dorsopalmar image (Figure 3.22). In most cases with good farriery this should not cause a problem, but with severe asymmetry, or with feet where adequate care is not given to maintaining hoof balance, this should be regarded as a potential cause of clinical problems.

A small circumscribed bony 'fragment' palmar to the palmar processes of the distal phalanx may represent a separate ossification centre or possibly a fracture sustained early in life. When present they are usually evident palmar to both palmar processes of both feet, although they may only occur in one foot or only at one palmar process (Figures 3.23 and 3w.25b). Their diameter may vary between approximately 1 and 10 mm. These 'fragments' are best seen in lateromedial or dorsal 60° lateral-palmaromedial oblique or dorsal 60° medial-palmarolateral oblique (flexed) views, but may also be seen in a dorsoproximal-palmarodistal oblique view. There may be slight increased opacity at the palmar aspect of the palmar process and at the dorsal aspect of the separate centre of ossification (Figure 3.23). These fragments should not be confused with clinically significant fractures of the palmar process, which are usually larger, and tend to have a sharper division from the body of the bone (see below, Distal phalanx – Fractures and Figures 1w.8c–e, 3.45b).

A small radiopaque 'fragment' (usually less than 6 mm in diameter) is sometimes present proximal to the extensor process (Figure 3.24). This is usually present in the midline, and may represent a separate centre of ossification, a fracture, or dystrophic mineralisation within the common digital extensor tendon. A fragment may be present bilaterally. Many of these fragments have a smooth outline, but trabecular architecture within the fragment may be seen. These fragments may be of no clinical significance, although some usually larger fragments may cause lameness (see 'Significant findings', below). In surveys of allegedly sound horses, no fragments were identified in 392 foals of 4–7 months of age; fragments were identified in 2.2% of 676 Warmblood stallions undergoing routine assessment, and in 4.5% of 3,749 Warmbloods undergoing pre-sales radiography.

Downloaded From Vet-eBooks.com

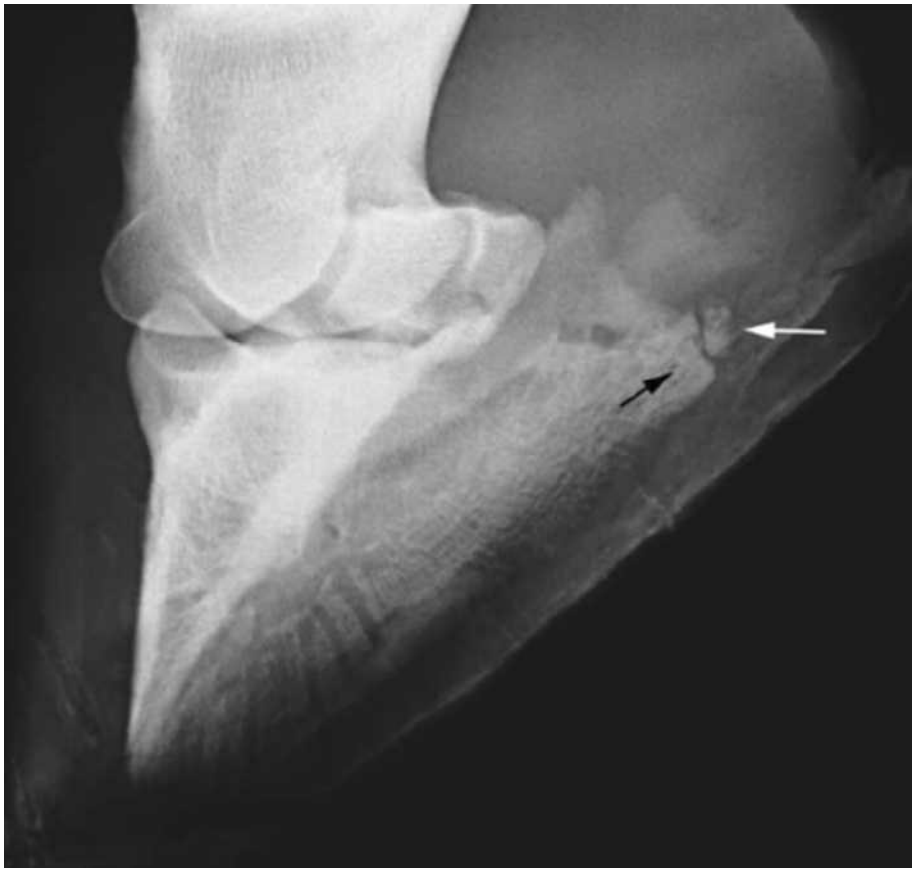


Figure 3.23 Dorsolateral-palmaromedial oblique image of a foot, highlighting the lateral palmar process of the distal phalanx, which has a separate centre of ossification palmarly (white arrow). The palmar aspect of the main part of the palmar process has increased opacity (black arrow). These are normal variants.

Some degree of ossification of the ungular cartilages may be regarded as normal; the degree of ossification is breed and type dependent, being more common in heavier horses. Fusion between the ossified cartilage and the distal phalanx may not be present, or it may be partial or complete. One or several ossification centres may be present, proximally, midway or distally in the cartilage. In most horses the ungular cartilages are approximately symmetrically ossified medially and laterally, and there is symmetry between the front feet. Ossification may extend slightly more proximally in one cartilage, usually the lateral one; this is usually not of clinical significance (see 'Ossification of the ungular cartilages [sidebone]', below). Normally, ossified ungular cartilages have a smooth surface to their compact bone, and a clear trabecular architecture within the spongiosa. They are usually of similar width medially and laterally. In a dorsopalmar image the ungular cartilages are orientated vertically. Occasionally in a lateromedial image of the palmar processes of the distal phalanx there is proximal extension of bone on the most palmar aspect (Figure 3w.25).

Occasionally, on the dorsoproximal-palmarodistal oblique view, there may be a smoothly marginated, concave defect in the solear margin of the distal phalanx. These may extend 10–20 mm around the border, and be up to 5–6 mm in depth. They probably represent areas of resorption of bone resulting from pressure on the bone, secondary to infection or severe bruising (but see also 'Keratoma', below). As long as there is a well-defined margin to the bone, and no associated hoof wall distortion, these defects usually have no clinical significance. Once formed, they do not progress or regress over time.



Figure 3.24 Lateromedial radiograph of the dorsal aspect of a distal interphalangeal joint. There is a radiopaque body proximal to the extensor process of the distal phalanx, which was an incidental finding in this horse (these fragments are of variable clinical significance).

Downloaded From Vet-eBooks.com

In some horses one or both of the parietal sulci of the distal phalanx appear as a foramen rather than a notch. Occasionally a well demarcated osseous cyst-like lesion is identified axially, distal to the articular surface of the distal phalanx; the overlying proximal cortex may have a smoothly demarcated indentation, but is clearly intact. Small cyst-like lesions may also be present at the medial or lateral margins of the joint within the distal phalanx and be of no clinical significance. Magnetic resonance imaging also suggests that the prevalence of asymptomatic osseous cyst-like lesions is probably much higher than previously recognised. Their significance must be assessed for each individual case, as they may be asymptomatic but can be associated with lameness.

SIGNIFICANT FINDINGS

Pedal osteitis

The term *pedal osteitis* strictly means inflammation of the distal phalanx, and has been widely used to describe a broad spectrum of radiographic abnormalities of the distal phalanx. It is likely that there are both septic and aseptic forms of what has become known as 'pedal osteitis', but there is currently a dearth of information concerning the aetiology of some of the radiological changes described. The authors acknowledge that there is a wide variation in the radiological appearance of the distal phalanx in apparently normal horses, and that any radiological changes that develop in the distal phalanx tend to persist. The term osteitis, which implies active inflammation, is therefore not always appropriate. Because of the present lack of knowledge, the authors have elected to describe several discrete radiological findings and their associated clinical signs under the general heading of 'pedal osteitis complex', without ascribing a specific name or aetiology to them. Other conditions with a known aetiology are then discussed under separate subheadings.

Pedal osteitis complex

The most common change referred to as part of the pedal osteitis complex is modelling of the solear margin of the bone. Changes are most obvious on dorsoproximal-palmarodistal oblique images (Figures 3.26a and 3w.26b). The solear margin of the bone loses its relatively smooth, opaque outline due to demineralisation. In some cases the bone near the solear margin may have some increased radiolucency, making its visualisation difficult (see Figure 1w.12). In more severe or long- standing cases, larger areas of bone may be resorbed from the solear margin of the bone, resulting in apparent widening of the vascular channels primarily at the solear margin. If the margins of the bone have a clearly defined (if irregular) border, then they are less likely to be of clinical significance.

On lateromedial images these changes may be evident as modelling of the tip of the bone, the solear margin no longer having a straight outline but curving proximally towards the dorsal aspect of the bone. This change appears to be exaggerated if the radiograph is not a true lateromedial projection (due to the curved outline of the solear margin). In more advanced cases new bone may be laid down on the dorsal surface of the bone at the toe. This change is frequently seen in animals that, over a period of time,

Downloaded From Vet-eBooks.com

have taken increased pressure on the sole, e.g. after laminitis, or in horses with either flat soles or a 'club' foot. New bone formation along the distal portion of the dorsal compact bone is nearly always considered abnormal. Slight new bone formation seen in oblique views along the middle portion of the dorsal compact bone is sometimes seen in horses not displaying lameness and may or may not be of clinical significance. However, it probably reflects abnormal stress on the suspensory apparatus of the distal phalanx.

A second change associated with the pedal osteitis complex is seen in the palmar processes of the distal phalanx. It is best assessed on dorsoproximal-palmarodistal oblique or palmaroproximal-palmarodistal oblique radiographs. Discrete circular radiolucent areas, 2 mm or 3 mm in diameter, are present in the palmar processes of the bone, and these may be associated with new bone, particularly on the axial surfaces of the palmar processes (Figures 3.26a and 3w.26b). Modelling changes of the palmar processes may also be seen in a lateromedial image. The solear aspect of the palmar processes may have an irregular outline (Figure 3.26c). There may be a change in shape with elongation of the palmar processes, seen also in a dorsolateral-palmaromedial (or dorsomedial-palmarolateral) (flexed) oblique view (Figure 3.26d). These changes are sometimes seen in association with an abnormally thin sole and/or abnormal orientation of the solear surface of the distal phalanx seen in a lateromedial image (the solear surface of the distal phalanx may be horizontal, or the palmar processes may be lower than the toe) (see also 'Long-toe, low-heel syndrome', below).

In a lateromedial image there may be an irregular outline of the distal aspect of the palmar processes of the distal phalanx (Figure 3w.27a) or a convex contour of the distal palmar aspect of the palmar processes (Figure 3w.27b).

These changes, and those described above, are probably associated with concussion of the bone and may be related to poor foot conformation and shoeing imbalances. They may be associated with lameness that is most marked on hard surfaces. Treatment is by corrective trimming and shoeing. Although the condition may resolve clinically, the radiological changes usually remain throughout life. Nuclear scintigraphy may help to determine the significance of these radiographic changes within the distal phalanx. Focal intense or moderately increased radiopharmaceutical uptake in one (most commonly the medial) or both palmar processes may occur with or without

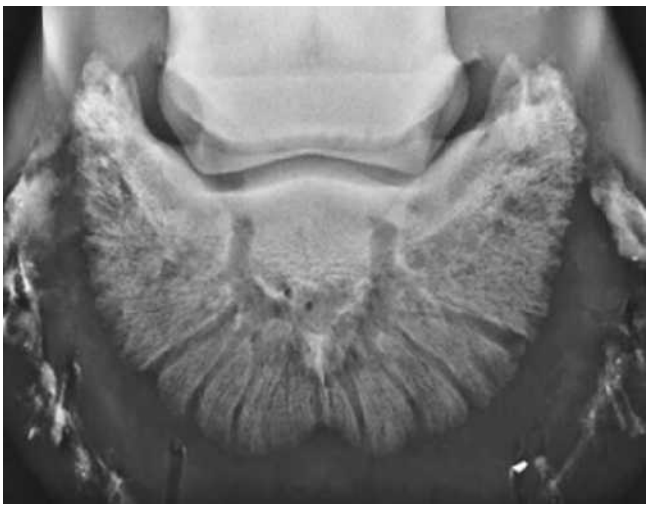


Figure 3.26(a) Pedal osteitis complex. Dorsoproximal-palmarodistal oblique ('upright pedal') image of a distal phalanx; lateral is to the right. There is demineralisation of the solear margin of the distal phalanx towards the palmar aspect of the bone and diffuse patchy lucent areas in the palmar processes. There are broad vascular channels. Note also the large notch at the toe of the distal phalanx, the crena solearis, and the entheseophyte on the proximolateral aspect of the navicular bone.

Downloaded From Vet-eBooks.com



Figure 3.26(c) Lateromedial image of a distal phalanx of a 12-year-old Selle Francais with low, collapsed heels and foot pain. There is modelling and irregularity in outline of the solear margin of the distal phalanx. Nuclear scintigraphic examination confirmed increased bone activity in this area. Note also the small radiolucent zone immediately distal to the extensor process.



Figure 3.26(d) Dorsal 60° medial-palmarolateral (flexed) oblique image of a distal phalanx of a 10-year-old Dutch Warmblood with low, collapsed heels and foot pain. There is modelling and elongation of the medial palmar process of the distal phalanx. Nuclear scintigraphic examination confirmed increased bone activity in this region.

Downloaded From Vet-eBooks.com

detectable radiographic abnormality, although generally in association with altered signal intensity on magnetic resonance images. This may indicate acute or chronic bone trauma.

Mineralised lesions on the dorsal aspect of the distal phalanx may be seen (Figures 3.27c and 3w.27d). These are usually approximately midway between the proximal border and solear margins of the bone on its dorsal surface, either in the midline, or slightly dorsomedially and/or dorsolaterally. These lesions are best seen on a lateromedial and/or oblique images. Slight irregularities associated with the parietal sulci may be normal. The aetiology of this lesion is uncertain, although it may be a reflection of abnormal stress on the suspensory apparatus of the distal phalanx. It can be seen in any type of horse, but is most commonly seen in heavier types. It may represent new bone on the dorsal surface of the distal phalanx, or mineralisation within the dermal tissue or dermal laminae. Although slight roughening of the dorsal compact bone may be an incidental finding, mineralisation in the laminae is usually associated with lameness.

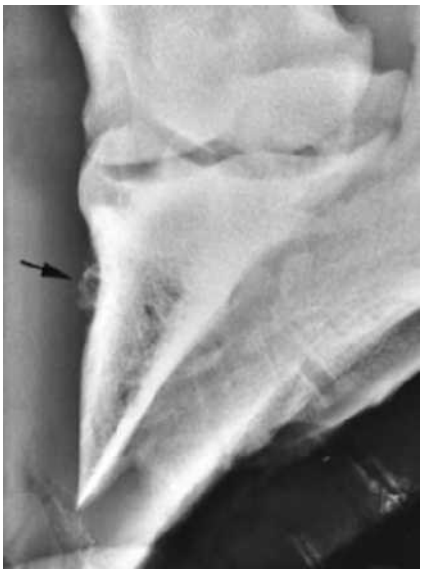


Figure 3.27(c) Pedal osteitis complex. Dorsomedial-palmarolateral oblique (flexed) image of a foot. There is new bone formation on the dorsolateral aspect of the distal phalanx (arrow) at a typical location approximately midway between the proximal and distal aspects of the bone. This reflects abnormal stress on the suspensory apparatus of the distal phalanx.

Infectious osteitis

The distal phalanx has no medullary cavity and therefore infection of this bone is, strictly speaking, an infectious osteitis, not osteomyelitis. It has only a single layer of fibrous periosteum, which thins distally, therefore new bone formation associated with infection is less obvious than at other locations. Infections of the foot are common, but only infrequently do they involve the distal phalanx, with a resultant infectious osteitis. In foals infectious osteitis of the distal phalanx may occur secondary to haematogenous spread of infection, but also occurs as the result of the close vicinity of the solear laminar tissue to the distal phalanx in foals. When present, infection most commonly involves the dorsal or solear surfaces of the distal phalanx, where it may cause focal demineralisation (this may appear on a dorsoproximal-palmarodistal oblique image as a defect in the solear margin of the bone; Figures 3.28a and 3w.28b–d). The lucent lesion usually has an irregular margin and there is seldom surrounding increased opacity, although new bone may be present at its margins (most easily seen on tangential views). There may be signs of chronic bone inflammation including a focal or generalised loss of radiopacity and widening of the vascular channels. Early lesions are more difficult to detect and are seen as an irregular margin or ill-defined lucent area in the solear margin of the distal phalanx. High-quality radiographs are essential. In more advanced cases a radiopaque sequestrum is sometimes seen, surrounded by a lucent border.

Infectious osteitis is extremely painful and usually requires surgical treatment. The prognosis following surgery is fair to good, depending on the extent of tissue that has been involved. Supportive shoeing may be required until complete solear integrity and strength has eventually been regained (see also 'Hoof – Infection', below).

Penetrating wounds through the sole of the foot may result in infectious osteitis of the solear surface of the distal phalanx. Initially this appears as a lucent area of bone on a dorsoproximal-palmarodistal oblique image. Occasionally antibiotic treatment of these lesions will result in a pocket of inspissated pus being walled off within the distal phalanx. This may result in a well-defined radiolucent zone appearing as an osseous cyst-like lesion

Downloaded From Vet-eBooks.com

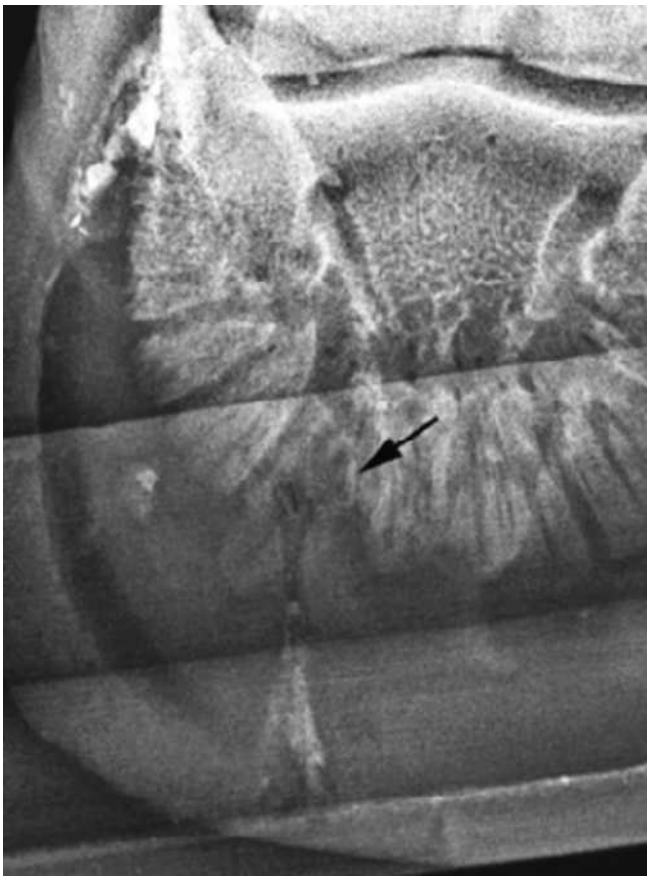


Figure 3.28(a) Infection of the distal phalanx; infectious osteitis. Collimated dorsoproximal-palmarodistal oblique radiographic image of a distal phalanx of a yearling Thoroughbred cross with a draining sinus just medial to the toe of 3 months' duration. Medial is to the left. Medial to the toe there is a large radiolucent defect in the distal phalanx, the result of infection (arrow). There is radiodense material within the draining tract. There is a broad curved radiolucent line within the hoof medially representing separation. There is radiopaque material on the medial aspect of the hoof, the result of inadequate preparation of the foot prior to radiography.

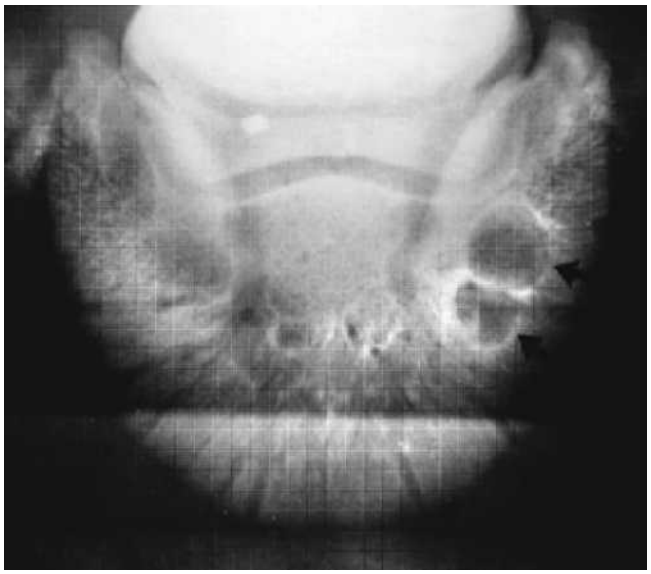


Figure 3.28(e) Infection of the distal phalanx. Dorsoproximal-palmarodistal oblique image of a distal phalanx, showing lucent areas (arrowed) surrounded by increased opacity. These represent inspissated pus within the distal phalanx. (The increased opacity at the toe of the bone is due to superimposition of the block supporting the foot.) The image was acquired using conventional film and screen and a cross-hatch grid, which caused the lines on the reproduction of the image.

(Figure 3.28e). These lesions may cause intermittent lameness when the horse is worked on a hard surface. Close examination of these lesions reveal no connection with the distal interphalangeal joint, which may help to differentiate them from other osseous cyst-like lesions.

Osseous cyst-like lesions

Osseous cyst-like lesions not connected to the distal interphalangeal joint may be associated with infectious osteitis (see above).

Solitary subchondral bone cysts or osseous cyst-like lesions (see 'Subchondral bone cysts and osseous cyst-like lesions' in Chapter 1.) close to or associated with the distal interphalangeal joint are occasionally seen. Care should be taken not to confuse this with a lucency created by a cavity

Downloaded From Vet-eBooks.com

frequently seen in the centre of the frog. They are generally most easily seen on the dorsopalmar or dorsoproximal-palmarodistal oblique images (Figure 3.29a). There may be a depression in the subchondral bone overlying the cyst and sometimes a communicating canal to the joint can be identified. When cysts are present, the distal interphalangeal joint should be carefully inspected for evidence of secondary degenerative joint disease. Lameness associated with subchondral bone cysts in the midline rarely resolves with conservative treatment. Surgical treatment of the cyst has proved successful in some cases, especially in horses less than 3 years of age. Although subchondral bone cysts in the distal phalanx are usually single round discrete structures, occasionally a multiloculated osseous cyst-like lesion of variable shape occurs (Figures 3w.29b and 3w.29c). Small osseous cyst-like lesions (1–3 mm diameter) may occur at the lateral or medial border of the distal interphalangeal joint as an incidental finding, and if associated with lameness a better prognosis may be given for conservative treatment in these cases. Osseous cyst-like lesions may occasionally be seen at a pre-purchase examination in a clinically sound horse. Their significance is unpredictable. A poorly or well-defined osseous cyst-like lesion may be seen in the axial aspect of a palmar process of the distal phalanx at or palmar to the insertion of one of the collateral ligaments of the distal interphalangeal joint (Figure 3.29d). These vary in size and occur more commonly medially than laterally. These osseous cyst-like lesions reflect bone necrosis at the ligament's insertion and may or may not be associated with desmitis of the body of the ligament. The prognosis is poor.

Occasionally on a lateromedial image of the distal phalanx, an ill-defined radiolucent line is seen within the extensor process, approximately 1–2 cm palmar to the apex (Figure 3.29e). The presence of an osseous cyst-like lesion has been confirmed at arthroscopic evaluation of the joint, and generally the surrounding bone and cartilage are also abnormal. Response to surgical debridement has been poor.

Keratoma

The most common space-occupying mass to involve the distal phalanx is a keratoma. Typically it is seen on a dorsoproximal-palmarodistal oblique view. Additional oblique views may be required for better visualisation. Pressure from the mass on the dorsal aspect of the distal phalanx causes resorption of bone. This is most easily seen at the solear margin of the bone, where a distinct semicircular notch is evident on a dorsoproximal-palmarodistal oblique image. This has a smooth outline, the bone underlying the keratoma frequently having increased opacity, which helps to differentiate this lesion from infection. There is usually no new bone associated with the lesion (Figure 3.30a).

A keratoma may occur at any point in the hoof wall. Although initially causing little distortion of adjacent tissues, it causes deformation of the wall, sole and white line as it progresses. A keratoma in the hoof wall is most commonly seen in the dorsal half of the foot, but have also occasionally been recorded in the solear horn and frog. A keratoma may cause lameness as it enlarges, and may be associated with secondary infection. Treatment is by surgical removal of the keratoma and carries a reasonable prognosis,

Downloaded From Vet-eBooks.com



Figure 3.29(a) Osseous cyst-like lesion. Dorsoproximal-palmarodistal oblique image of a distal phalanx. There is a central osseous cyst-like lesion in the distal phalanx (white arrows), surrounded by a narrow rim of increased opacity. There is a small, smoothly outlined depression in the subchondral bone of the distal phalanx proximal to the lesion, but no communication with the distal interphalangeal joint could be identified. The osseous cyst-like lesion was not believed to be contributing to lameness. The radiolucent zones in the distal phalanx medially and laterally represent the depressions in which the collateral ligaments of the distal interphalangeal joint insert.



Figure 3.29(d) Osseous cyst-like lesion at the insertion of a collateral ligament of the distal interphalangeal joint. Dorsoproximal-palmarodistal oblique image of a foot. Medial is to the left. There is a broad rim of increased opacity around a relatively radiolucent area medially (arrows), which represents a lesion at the insertion of the medial collateral ligament of the distal interphalangeal joint, which was confirmed using magnetic resonance imaging.

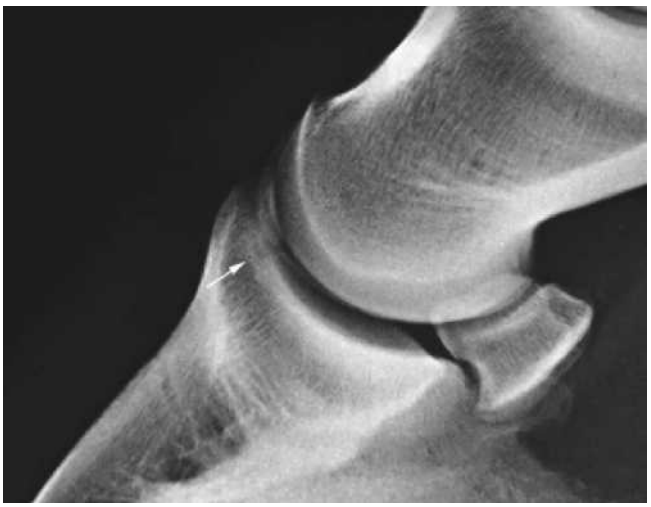


Figure 3.29(e) Collimated lateromedial image of the right front foot of a Warmblood showjumper, with lameness improved by intra-articular analgesia of the distal interphalangeal joint. There is an ill-defined osseous cyst-like lesion in the dorsoproximal aspect of the distal phalanx (arrow), which communicated with the distal interphalangeal joint. The lesion was treated by surgical debridement; however, lameness persisted.

although the mass may recur up to several years later, especially if removal was incomplete. A more accurate determination of the extent of a keratoma may be acquired using magnetic resonance imaging or computed tomography. A small keratoma-like lesion may be detectable using magnetic resonance imaging which is not detectable radiologically and may be an incidental finding.

Downloaded From Vet-eBooks.com

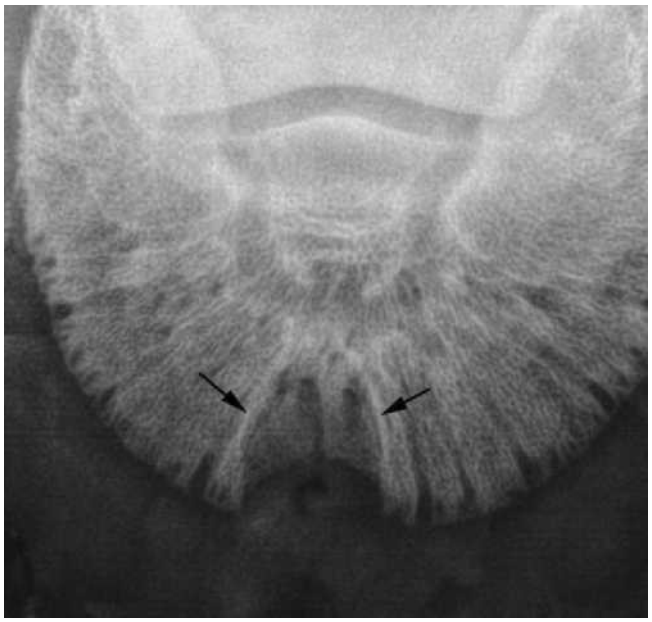


Figure 3.30(a) Keratoma. Dorsoproximal-palmarodistal oblique image of a distal phalanx. There is a large, smoothly outlined defect in the toe of the distal phalanx (arrows) resulting from resorption of bone due to pressure caused by a keratoma. The margins of the defect have slightly increased opacity.

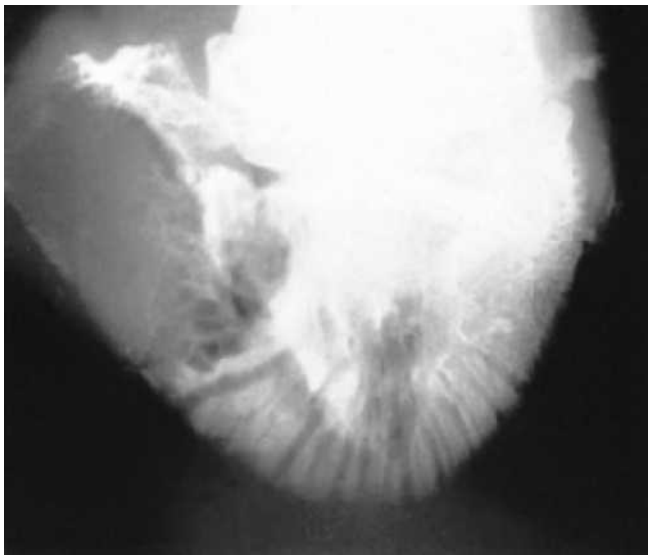


Figure 3.30(b) Fibrosarcoma. Dorsolateral proximal-palmaromedial distal oblique image of the distal phalanx, showing modelling of the bone resulting from a fibrosarcoma.

Tumours

Tumours have been recorded infrequently (e.g. fibrosarcoma, neurofibroma, haemangioma, squamous cell carcinoma, glomus tumour, metastatic renal adenocarcinoma and malignant melanoma). They tend to be associated with modelling of adjacent bone (Figure 3.30b). Non-neoplastic focal fibroplasia may also occur, resulting in a smoothly marginated defect anywhere in the margin of the distal phalanx.

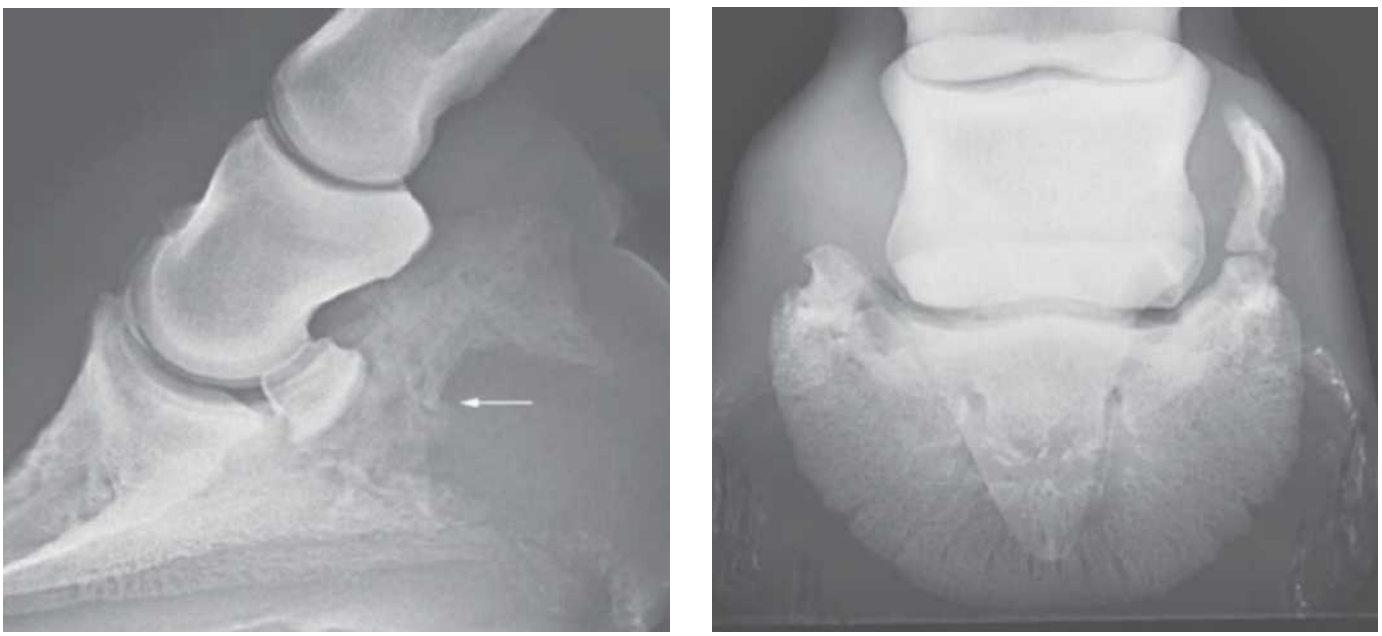
Ossification of the ungular cartilages (sidebone)

The ungular cartilages of the equine foot are attached distally to the palmar processes of the distal phalanx and extend both proximally and in dorsal and palmar (plantar) directions. Some ossification of the ungular cartilages is a common finding, particularly in heavy breeds, cob-types and large British native ponies. Ossification usually occurs from the base of the cartilage at its attachment to the distal phalanx and extends a variable distance proximally. Mild ossification is generally of no clinical significance. The degree of ossification is usually approximately bilaterally symmetrical within a foot and between front feet. If there is asymmetry within a foot, the lateral cartilage is usually more extensively ossified. Marked asymmetry of ossification is unusual (Figure 3.31) and may be associated with lameness. There may be one or more additional separate centres of ossification, which may be completely isolated, or may fuse with the area of ossification at the base of the cartilage. In some cases a radiolucent line remains at the junction between the two areas of ossification. In these cases, radiological differentiation between two separate centres of ossification, and a fracture of the ossified cartilage (see below) may be difficult (Figure 3.32). In a normal horse the

Downloaded From Vet-eBooks.com



Figure 3.31 Dorsopalmar radiographic image of a foot of a 7-year-old Irish Sports horse. Medial is to the left. There is mild ossification of the medial ungular cartilage and extensive ossification of the lateral ungular cartilage. The lateral ossified ungular cartilage has rather heterogeneous opacity. Such marked asymmetry of ossification may be a risk factor for lameness. This horse was unilaterally lame in association with evidence of bone trauma of the distal phalanx distal to the lateral ossified cartilage and desmitis of the ipsilateral collateral ligament of the distal interphalangeal joint.



(a) (b)

Figure 3.32 Ossification of the lateral ungular cartilage. Separate centres of ossification in the proximal and distal aspects of the cartilage have met to give almost complete ossification of the cartilage. (a) Lateromedial view. There is a radiolucent line (arrow) between the two ossification centres. Note also modelling of the dorsal articular margins of the distal interphalangeal joint. (b) Dorsoproximal-palmarodistal oblique image of a different horse. Lateral is to the right. There is a separate ossification centre of the lateral ossified ungular cartilage.

Downloaded From Vet-eBooks.com

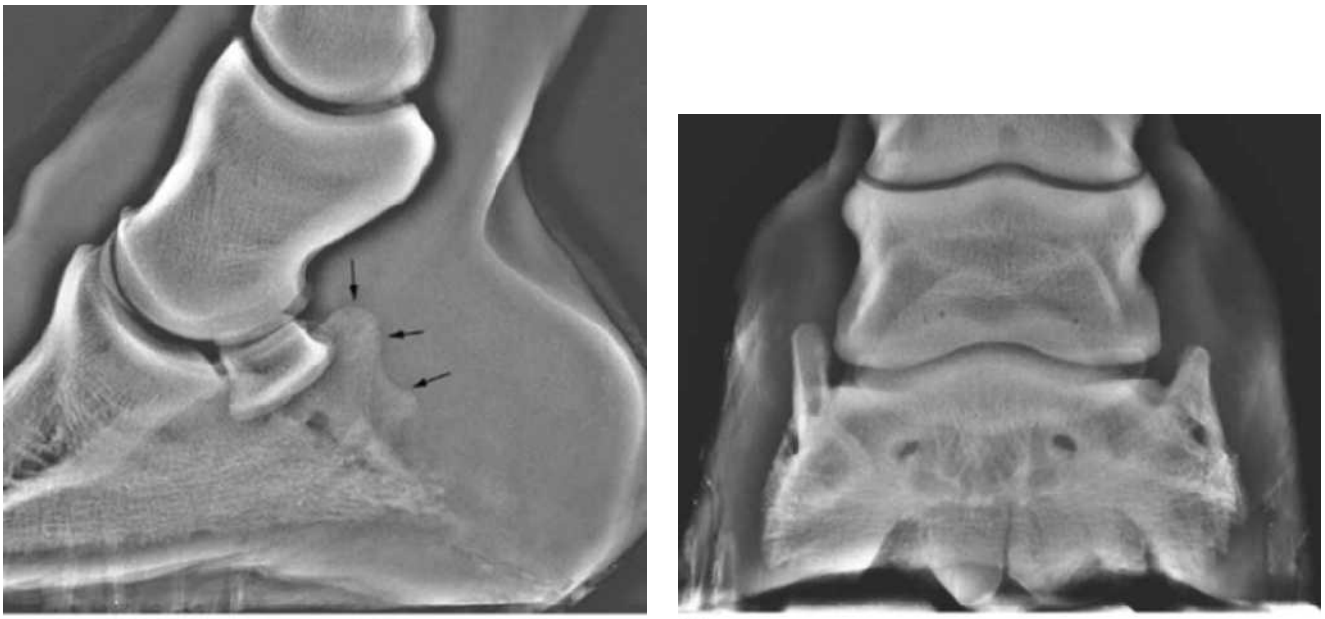


Figure 3.34 Ossification of the ungular cartilages. Ossification from the distal aspect (arrows) of the ungular cartilages: (a) lateromedial image; (b) dorsopalmar image; medial is to the left. There is slightly greater ossification of the medial ungular cartilage than the lateral. Note the clear demarcation between the compact bone of the ossified cartilages and the spongiosa in the dorsopalmar image.

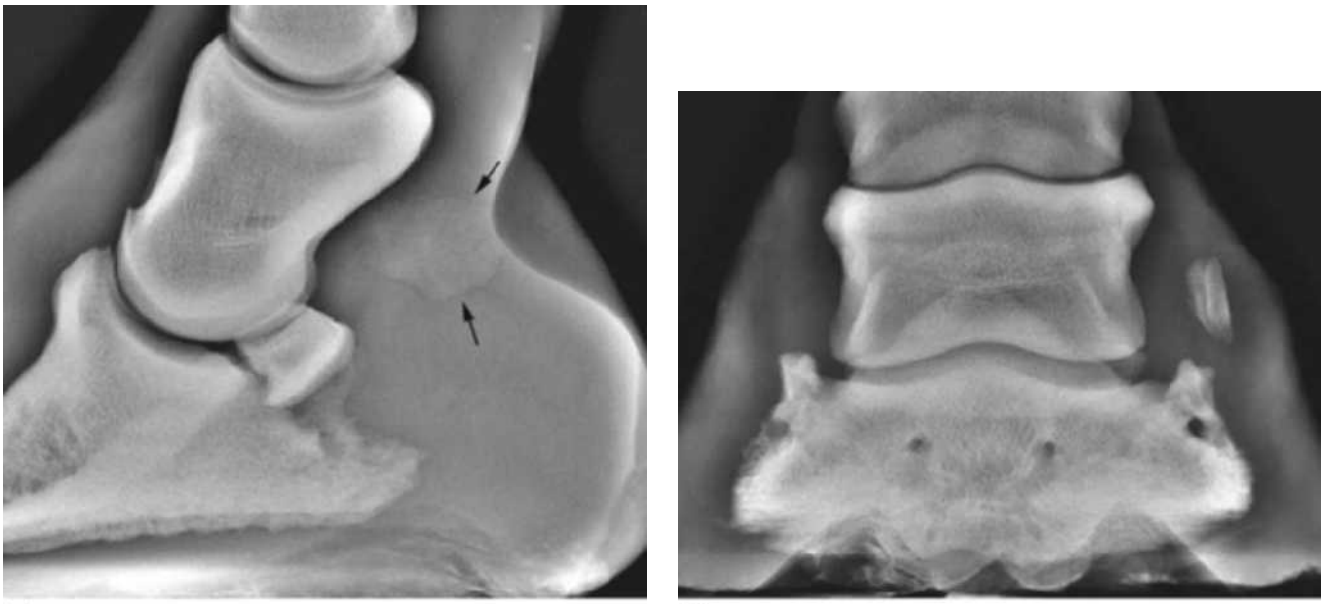
margins of the compact bone of ossified cartilages are smooth and the compact bone is clearly demarcated from the trabecular bone of the spongiosa. The medial and lateral ungular cartilages are of similar width.

In a dorsopalmar image ossified ungular cartilages are usually orientated vertically, with the proximal portion directed slightly axially (Figure 3w.33a). In some horses with extensive ossification the ungular cartilages bend away from the phalanges (Figure 3w.33b). A grading system to describe the proximodistal extent of ossification seen on a weight bearing dorsopalmar image has been described (Figures 3.34, 3.35 and 3.36):

- Grade 0 = No ossification
- Grade 1 = Ossification up to the level of the medial or lateral margins of the distal interphalangeal joint
- Grade 2 = Ossification up to the level of the mid sagittal aspect of the distal interphalangeal joint
- Grade 3 = Ossification up to the most proximal aspect of the distal sesamoid (navicular) bone (excluding proximal entheseophytes)
- Grade 4 = Ossification up to the midpoint of the middle phalanx (based on the most proximal aspect of the joint surface)
- Grade 5 = Ossification proximal to the midpoint of the middle phalanx.

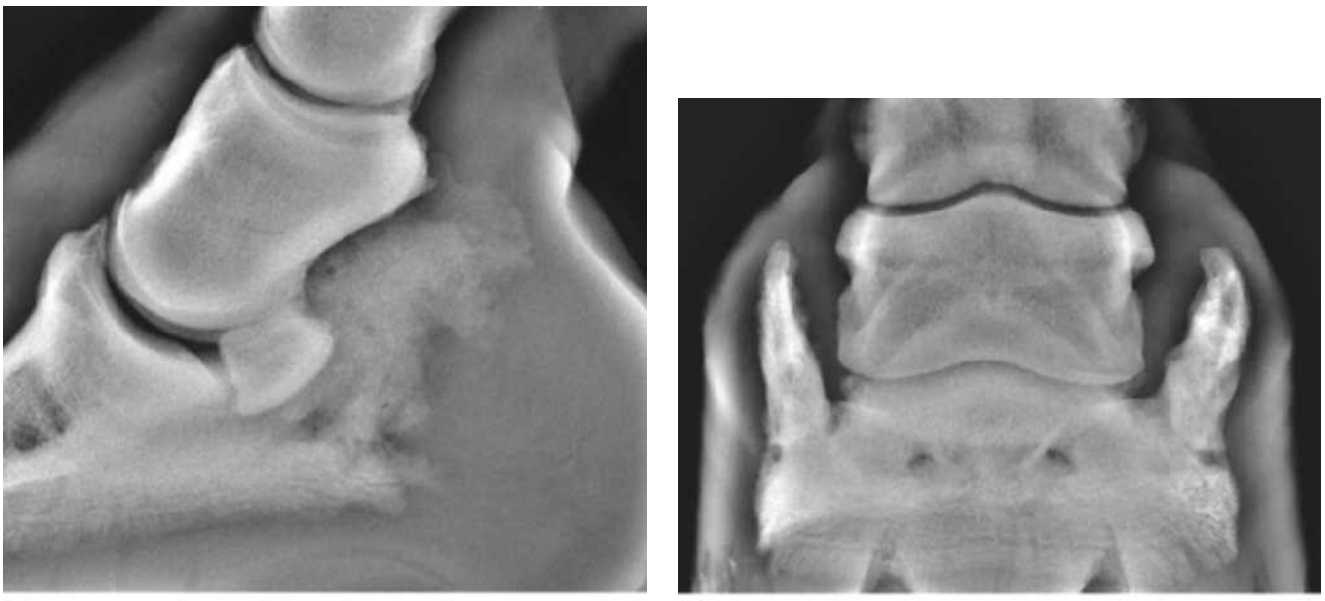
The dorsopalmar extent of ossification can only be reliably determined from dorsolateral-palmaromedial (flexed) and dorsomedial-palmarolateral (flexed) oblique images (Figure 3.37a). Extensive ossification is often accompanied by increased opacity of the trabecular bone, modelling of the compact bone, reduced compactospongiosa demarcation, sometimes also associated with increased opacity of the ipsilateral aspect of the distal phalanx (Figure 3.37b). Such changes may alter the biomechanical function of the ossified cartilages and

Downloaded From Vet-eBooks.com



(a) (b)

Figure 3.35 Ossification of the ungular cartilages. A separate centre of ossification in the proximal half of the lateral ungular cartilage: (a) lateromedial image – note that the proximal area of ossification is seen as a poorly defined radiopaque area (arrows) proximal to the navicular bone; (b) dorsopalmar image; lateral is to the right. There is mild ossification at the base of both the medial and lateral ungular cartilages. There is a separate centre of ossification in the proximal aspect of the lateral ungular cartilage.



(a) (b)

Figure 3.36 Complete ossification of the ungular cartilages: (a) lateromedial image; (b) dorsopalmar image; medial is to the left. In the lateromedial image (a) the superimposition of the ossified ungular cartilages over the navicular bone gives the appearance of increased opacity of the spongiosa of the navicular bone. There is diffuse increased opacity of the palmar processes of the distal phalanx. Note also modelling of the extensor process of the distal phalanx and the small osseous spur on the proximopalmar aspect of the middle phalanx. In the dorsopalmar image (b) the lateral ungular cartilage is thicker than the medial ungular cartilage; both ungular cartilages have smoothly irregular inside margins. There is diffuse increased opacity of the spongiosa of the distal half of each ossified ungular cartilage with complete loss of demarcation between the spongiosa and the compact bone.

Downloaded From Vet-eBooks.com

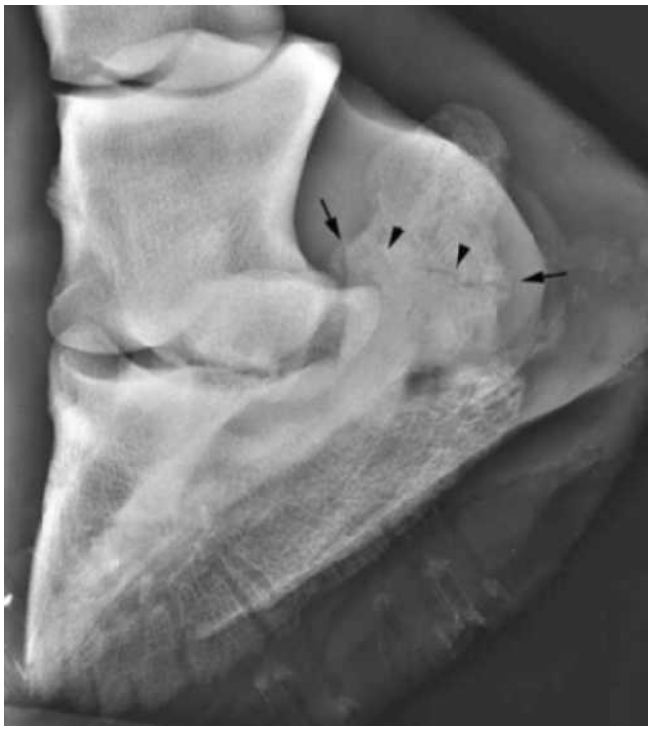


Figure 3.37(a) Dorsolateral-palmaromedial oblique (flexed) image of a foot. There is extensive ossification of the lateral ungular cartilage. There is an ill-defined transverse radiolucent line through the ossified cartilage (black arrowheads), on the dorsal and palmar aspects of which is smoothly marginated callus (black arrows). There is diffuse increased opacity of the spongiosa of the distal half of the ossified ungular cartilage.

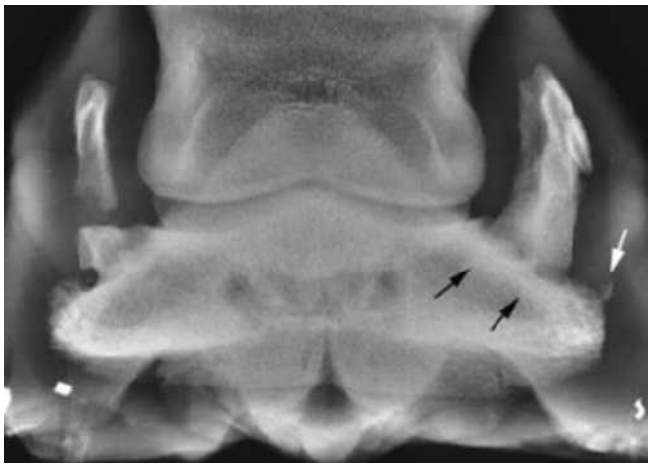


Figure 3.37(b) Dorsopalmar image of a foot; medial is to the left. There is a separate ossification centre of the medial ungular cartilage. There is extensive ossification of the lateral ungular cartilage which is diffusely thickened. There is diffuse increased opacity in spongiosa of the distal half of the lateral ungular cartilage with loss of definition between the compact bone and the spongiosa. Distal to the lateral ungular cartilage the band of radiopaque bone in the distal phalanx is thicker (black arrows) compared with medially. There is new bone formation on the lateral aspect of the distal phalanx (white arrow).

predispose to fracture or bone trauma of either the ossified cartilage or the ipsilateral aspect of the distal phalanx. These injuries are associated with lameness.

Extensive ossification of the ungular cartilages is commonly associated with entheseous new bone formation on the distal lateral and palmarolateral and palmaromedial aspects of the proximal phalanx. This is thought to reflect abnormal stress at the attachment sites of the ligaments between the ungular cartilages and the proximal phalanx (Figures 3w.37c–e).

The clinical significance of ossification of the ungular cartilages of the foot (colloquially known as sidebone) is controversial. Although sidebone was considered a potential problem in working draught horses, in riding horses it was previously thought to be of no clinical significance. However, there is increasing evidence suggesting that extensive ossification and mediolateral asymmetry of ossification may be predisposing factors for and contribute to foot-related pain.

In normal horses there is greatest radiopharmaceutical uptake at the junction between the base of an ungular cartilage and the distal phalanx, probably reflecting that this is a stress point. Horses with moderate to extensive ossification of the ungular cartilages of the foot are at higher risk than horses with mild or no ossification of both fracture of the ossified cartilage and bone trauma at the junction of the ungular cartilage with the distal phalanx. Fractures can also occur in the body of an ossified ungular cartilage, or proximally (Figure 3w.37f; see also Figures 1w.11d–f). Fracture of an ossified cartilage is rare, but causes acute onset of lameness which normally

Downloaded From Vet-eBooks.com



Figure 3.38 Lateromedial image of a foot. There is a large entheseophyte distal to the extensor process of the distal phalanx, an entheseophyte at the insertion of the common digital extensor tendon.

resolves with rest. Differentiation between a fracture and trauma to the junction between separate centres of ossification can be challenging. A fracture may have a sharp irregular contour, with associated modelling of the adjacent ends of the disrupted bone and/or adjacent increased opacity. The presence of increased radiopharmaceutical uptake and/or increased signal intensity in fat-suppressed magnetic resonance images can help to determine the clinical significance of radiological abnormalities.

Extensive ossification of the ungular cartilages has also been associated with bone trauma of the ossified ungular cartilage, a fracture of the ipsilateral aspect of the distal phalanx, injuries of the closely related collateral ligaments of the distal interphalangeal joint and the chondrocoronal and chondrosesamoidean ligaments. Magnetic resonance imaging is required to diagnose these soft-tissue injuries.

Entheseophytes adjacent to the extensor process of the distal phalanx

The common digital extensor tendon inserts immediately distal to the extensor process of the distal phalanx. Tearing of the insertion may result in lameness and entheseophyte formation on the proximodorsal aspect of the distal phalanx immediately distal to the extensor process (Figure 3.38). This change must be distinguished from the normal variation in shape of the extensor process (see Figure 3.18). The outline caused by formation of entheseophytes is irregular, and there may be alteration in the opacity and trabecular structure of the underlying bone. Its significance must be interpreted in the light of clinical signs, since the radiographic changes persist despite resolution of lameness. Entheseous new bone formation may also reflect chronic instability of the distal interphalangeal joint. It can be seen as an isolated finding, or in association with radiological evidence of degenerative joint disease of the distal interphalangeal joint, or large fractures of the extensor process of the distal phalanx (Figure 3.47a).

Osseous changes at the insertion of the deep digital flexor tendon and distal sesamoidean impar ligament

The deep digital flexor tendon and distal sesamoidean impar ligament insert on the facia flexoria of the distal phalanx, in a smoothly outlined concavity (Figure 3.10a). The compact bone at this site should be smooth and regular. Insertional injury of the deep digital flexor tendon or, less commonly, the distal sesamoidean impar ligament may result in irregular new bone formation, or an ill-defined lucent area in the normally uniformly opaque bone (Figure 3.39). This is usually associated with lameness. Transcuneal ultrasonography, magnetic resonance imaging or contrast-enhanced computed tomography may provide additional information.

Degenerative joint disease of the distal interphalangeal joint

Degenerative joint disease of the distal interphalangeal joint is a common cause of lameness, although frequently associated with little, if any, radiographic change. Radiographic abnormalities are seen most easily on lateromedial (Figure 3.40a) and flexed oblique views (Figure 3.40b). Modelling of

Downloaded From Vet-eBooks.com

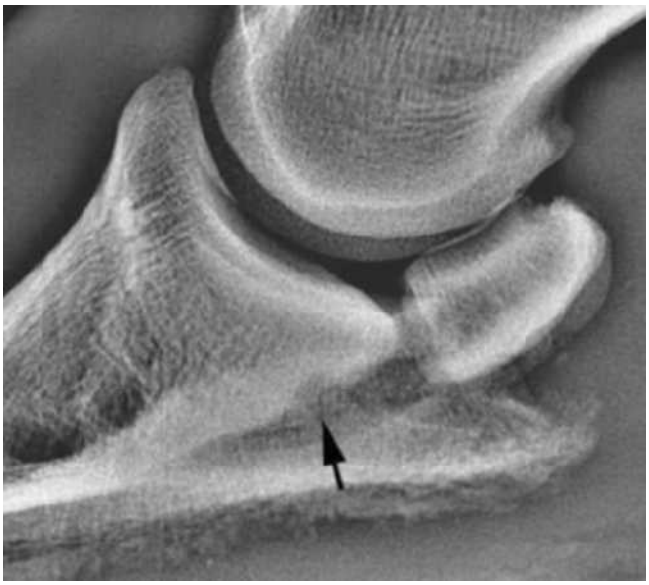


Figure 3.39 Lateromedial image of a foot of a horse with severe bilateral forelimb lameness. There is an ill-defined radiolucent area in the proximopalmar aspect of the distal phalanx (arrow) in the region of insertion of the distal sesamoidean impar ligament and deep digital flexor tendon. The palmar compact bone of the navicular bone is thickened and has an ill-defined dorsal border. There is diffuse increased opacity of the spongiosa of the proximal half of the bone. The horse had an erosion in the palmar compact bone of the navicular bone with extensive adhesions to the deep digital flexor tendon.

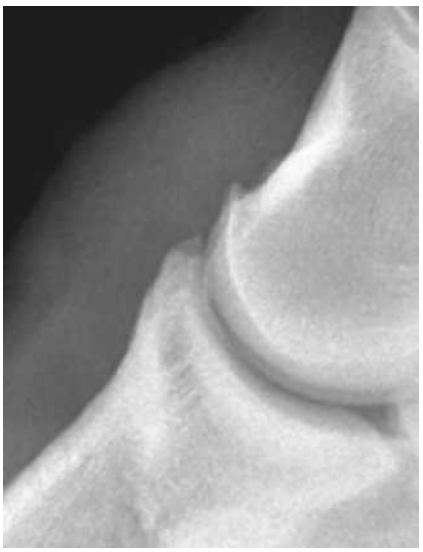


Figure 3.40(a) Lateromedial radiographic image of the distal phalanges of a 7-year-old showjumper with lameness substantially improved by intra-articular analgesia of the distal interphalangeal joint. There is modelling of the extensor process of the distal phalanx and the distal dorsal aspect of the middle phalanx, consistent with degenerative joint disease. Note that the spur on the apex of the extensor process of the distal phalanx is less opaque than the parent bone.



Figure 3.40(b) Dorsomedial-palmarolateral oblique (flexed) image of a pastern and foot of a 6-year-old Warmblood with degenerative joint disease of the distal interphalangeal joint. There is modelling of the distal dorsolateral aspect of the middle phalanx (white arrow) and the proximal dorsolateral aspect of the distal phalanx (black arrow).

Downloaded From Vet-eBooks.com

the extensor process of the distal phalanx is commonly, but not invariably, associated with degenerative joint disease (see also 'Entheseophytes on the extensor process of the distal phalanx', above), and its presence should alert the clinician to examine the joint carefully. It is important to distinguish between modelling, modelling with loss of trabecular architecture and modelling with fragmentation. Arthroscopic assessment of the extensor process often reveals poor quality bone despite relatively normal radiographs. Radiographic changes of degenerative joint disease include periarticular osteophytes on the proximal articular margin of the distal phalanx, on the distodorsal and/or distal palmar aspects of the middle phalanx, and slight irregularity and incongruity of the joint surfaces, particularly the articular surface of the extensor process. The navicular bone is an integral part of the distal interphalangeal joint. Periarticular osteophytes on the dorsoproximal articular margin of the navicular bone may also be an indicator of osteoarthritis, but should not be confused with entheseophyte formation, which occurs more palmad. An increased number of abnormally shaped and sized radiolucent zones (synovial invaginations of the distal interphalangeal joint) on the distal border of the navicular bone may be seen in association with degenerative joint disease of the distal interphalangeal joint. New bone on the dorsal diaphysis of the middle phalanx may also be associated with degenerative joint disease (capsulitis) (Figure 3.41). In more advanced cases some subchondral bone lucency may be visible at the dorsal aspect of the joint, or there may be altered trabecular architecture. There may also be narrowing or unevenness of the joint space visible on a dorsopalmar (weight-bearing) view (Figure 3.42). Genuine narrowing of the joint space reflects advanced degenerative joint disease, but should not be confused with the distal interphalangeal joint space being widened on one side due to a hoof imbalance or incorrect positioning during imaging. A mediolateral hoof imbalance may result in this appearance on dorsopalmar images, despite the horse bearing full weight on the limb, and this is not synonymous with degenerative joint disease. A mediolateral hoof imbalance may also make it difficult to obtain true lateromedial images.

Degenerative joint disease carries a poor prognosis once radiographic changes are present, although modelling of the extensor process alone need not be associated with current lameness. Some cases will respond to careful

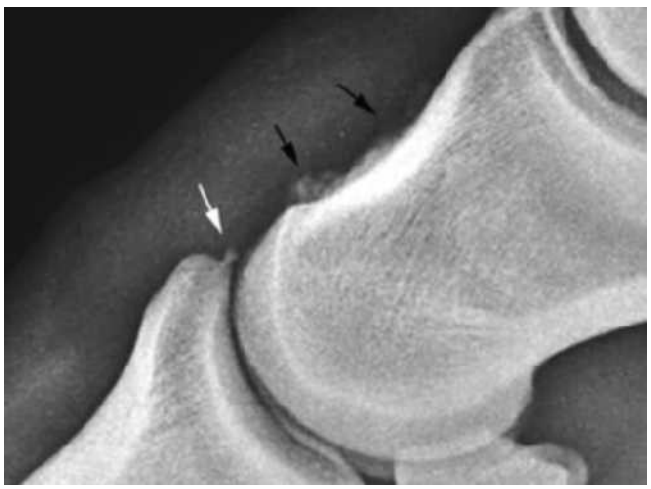


Figure 3.41 Lateromedial image of the left forelimb of a 2-year-old Thoroughbred racehorse with recent onset of lameness which was abolished by intra-articular analgesia of the distal interphalangeal joint. There is modelling of the extensor process of the distal phalanx (white arrow) and new bone on the dorsal aspect of the distal half of the middle phalanx (black arrows), consistent with degenerative joint disease. The horse had similar lesions bilaterally.

Downloaded From Vet-eBooks.com

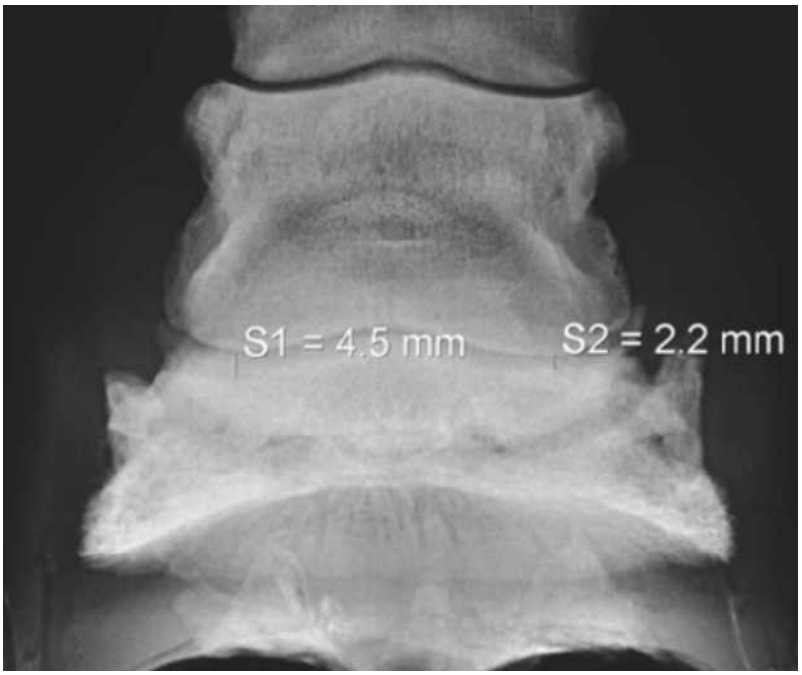


Figure 3.42 Dorsopalmar radiographic image of a foot of a 5-year-old Warmblood gelding with severe lameness. Medial is to the left. The lateral aspect of the distal interphalangeal joint (S2 = 2.2 mm) is considerably narrower than the medial aspect (S1 = 4.5 mm). This is consistent with advanced degenerative joint disease. Compare with the much more consistent joint space width of the proximal interphalangeal joint. There is also a large entheseophyte on the proximal lateral aspect of the navicular bone.

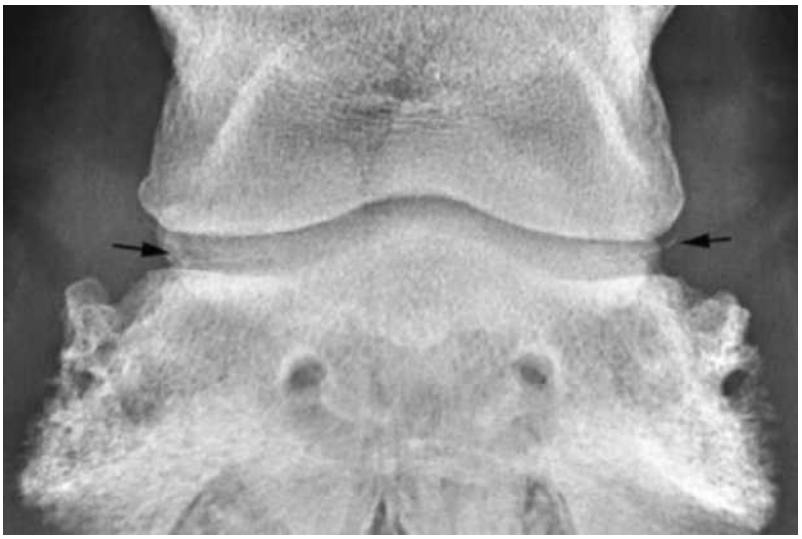


Figure 3.43 Dorsopalmar image of the left front foot of an 8-year-old Warmblood with accentuation of lameness after arthroscopic removal of a small extensor process fragment. There is linear increased opacity within the distal interphalangeal joint consistent with intra-articular mineralisation (arrows). Lameness was substantially improved by intra-articular analgesia of the distal interphalangeal joint.

balancing of the feet, the use of anti-inflammatory drugs and/or intra-articular medication. Modelling changes of the distal interphalangeal joint are sometimes seen in association with navicular disease.

In rare cases, linear mineralisation has been seen within the distal interphalangeal joint parallel with the articular surface (Figure 3.43), associated with pain localised to the joint. The aetiology of this is unknown.

Subluxation of the distal interphalangeal joint

Dorsopalmar subluxation of the distal interphalangeal joint is usually the result of partial or complete disruption of the deep digital flexor tendon. It is best identified on a lateromedial projection. There is widening of the joint

Downloaded From Vet-eBooks.com

space and the middle phalanx is displaced in a palmar direction. Mediolateral subluxation of the joint occasionally occurs as a result of disruption of a collateral ligament of the distal interphalangeal joint. This can be difficult to recognise in radiographs obtained with the foot bearing weight evenly. 'Stressed' dorsopalmar radiographs obtained with the horse standing on a wedge-shaped block may reveal abnormal widening of the joint space. The prognosis is very guarded.

Agenesis or hypoplasia of the distal phalanx

Agenesis (congenital absence of) or hypoplasia of the distal phalanx is a rare radiographic finding in foals, usually associated with malformation of the hoof capsule. It may occur alone or in association with dysgenesis of the navicular bone.

A bipartite distal phalanx and navicular bone have been described.

Fractures

Common fracture sites of the distal phalanx in foals and adult horses are shown in Figure 3.44. A fracture classification has been proposed, although not all fractures fit into this model:

- Type 1 – non-articular fractures of a palmar or plantar process
- Type 2 – articular fractures that are not mid-sagittal and extend from the distal interphalangeal joint to the medial or lateral aspect of the solear margin
- Type 3 – articular mid-sagittal fractures of the distal phalanx
- Type 4 – extensor process fractures
- Type 5 – multi-fragment fractures
- Type 6 –non-articular fractures involving the solear margin, and extending from one point of the solear margin to another
- Type 7 – non-articular fractures of the palmar or plantar process of the distal phalanx in foals.

A fracture through the body or a palmar process of the distal phalanx may initially be difficult to see on radiographs, but after 7–10 days some rarefaction adjacent to the fracture occurs making identification easier (see Figures 1.10a–c). An acute fracture appears as a well-defined narrow radiolucent line (or lines) with normal adjacent trabecular architecture. Sagittal, parasagittal and marginal fractures are normally best seen on a

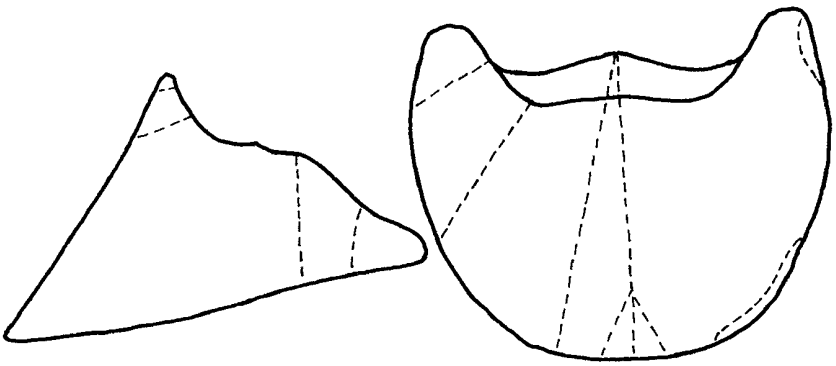


Figure 3.44 The common fracture sites of the distal phalanx.

Downloaded From Vet-eBooks.com

dorsoproximal-palmarodistal oblique image (Figure 3.45a), although some fractures of a palmar process may first be suspected on a lateromedial image (see Figure 1w.8c). When a fracture is suspected it may be necessary to obtain a number of slightly different oblique views in order to assess it clearly and to ascertain if it is articular or non-articular. A significant proportion of fractures are not detectable in a standard dorsoproximal-palmarodistal oblique projection, especially in the acute stage. If a fracture is suspected (either on clinical grounds or as the result of nuclear scintigraphic examination), but it is not detectable on the standard radiographic images, alternative views should be obtained. These should include a palmaroproximal-palmarodistal oblique view, and weight-bearing and flexed lateral 45° proximal-medial distal oblique, or medial 45° proximal-lateral distal oblique views with additional oblique views at 5° intervals.

A fracture is best seen as a lucent line when the x-ray beam is in line with the plane of the fracture (Figure 3.45b). Frequently it appears as two lines, representing the exit points through dorsal and palmar surfaces of the bone. By careful comparison of a number of slightly different oblique views, it is possible to establish whether a fracture is simple or comminuted. It should also be remembered that more than one fracture may be present. Some palmar process fractures of the distal phalanx occur as the result of repetitive stress-related bone trauma, rather than a single event traumatically-induced fracture. In these



Figure 3.45(a) Sagittal fracture of the distal phalanx (dorsoproximal-palmarodistal oblique image). Note the separate lucent lines which represent the fracture through the dorsal and solear cortices. The shoe was left in place to give support to the foot until the injury was fully assessed.

Downloaded From Vet-eBooks.com



Figure 3.45(b) Palmar process fracture of the distal phalanx (dorsoproximal lateral-palmarodistal medial oblique image).

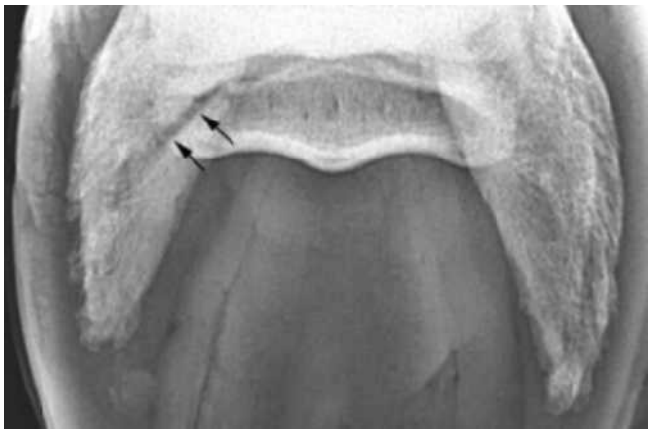


Figure 3.45(c) Palmaroproximal-palmarodistal oblique image of a 7-year-old Thoroughbred event horse with acute onset of lameness 3 weeks previously. Medial is to the left. There is an incomplete fracture of the medial palmar process of the distal phalanx (arrows). This fracture was not detectable in any other radiographic projection.

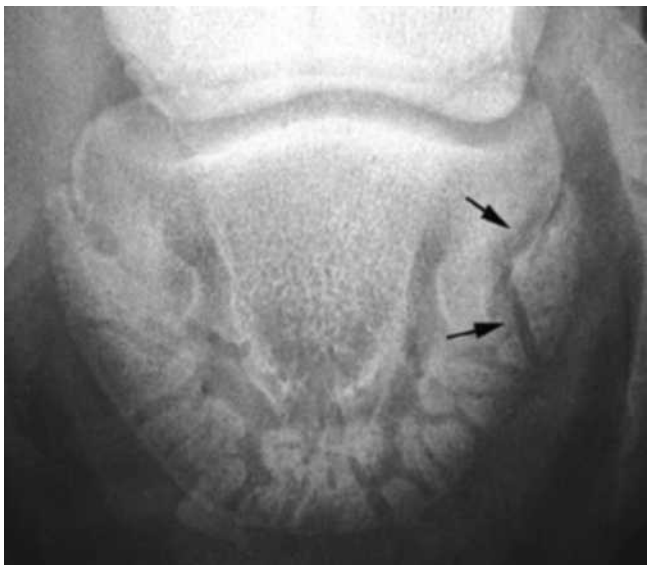


Figure 3.45(d) Dorsoproximal-palmarodistal oblique image of a forelimb of a Thoroughbred foal, 5 months of age, first examined for lameness 6 days previously. Lateral is to the right. There is a complete non-articular simple fracture of the lateral palmar process of the distal phalanx (arrows).

cases the surrounding trabecular architecture is disrupted and there may be pre-existing increased opacity. Precise ageing of such a fracture is difficult.

Sagittal and parasagittal fractures of the body of the distal phalanx normally occur as the result of direct trauma to the foot, and are associated with sudden-onset lameness, and pain to pressure and concussion of the foot. Fractures of the distal phalanx which enter the distal interphalangeal joint, occurring in animals more than 18 months old, may respond best to internal fixation. Fractures which do not enter the distal interphalangeal joint, and fractures in animals of less than 18 months of age, have a good prognosis simply

Downloaded From Vet-eBooks.com

with conservative treatment. Traditionally the feet are shod with a broad-webbed straight bar shoe, and most importantly correct mediolateral balance.

Palmar process fractures are also generally related to acute trauma, with sudden-onset severe lameness; however, there are notable exceptions. In some horses with a palmar process fracture, in a very short time (24 hours) there is no reaction to hoof testers and lameness is mild. Some palmar process fractures occur as the result of repetitive stress-related bone trauma, rather than a single traumatic event. Again, such cases may show minimal pain. In racehorses in Australia and the United States of America, palmar process fractures occur most commonly on the lateral aspect of the left front foot and the medial aspect of the right front foot, associated with counter-clockwise racing. In sports horses, however, medial palmar process fractures are more prevalent. Frontal plane fractures of a palmar process are usually only detectable in lateromedial or palmaroproximal-palmarodistal oblique (Figure 3.45c) views of the distal phalanx.

Fractures of the body of the distal phalanx and its palmar processes heal from the solear margin of the bone proximally. Some horses never develop complete bony union radiographically, even though clinically sound. Partial or non-union palmar process fractures can be seen as an incidental finding.

Non-articular osseous fragments on the abaxial margin of one or both palmar processes may occur in foals from a few weeks to 1 year of age (Figure 3.45d and Figures 3w.45e and 3w.45f). Although palmar process fractures may be associated with a club foot appearance and lameness, they are frequently seen without associated clinical signs. Fractures may occur in both front feet and occasionally involve both palmar processes in a single foot. They appear as a triangular-shaped bone fragment of the distal angle of the palmar process, or an oblong bone fragment extending from the incisure of the palmar process to the solear margin. These fractures heal by osseous union, with rapid resolution of lameness (if present).

A fracture of the solear margin of the distal phalanx (running parallel and adjacent to the margin of the bone) is best seen on the dorsoproximal-palmarodistal oblique view (Figure 3.46). These fractures frequently occur in animals that are flat-footed and suffer repeated bruising of the sole, or in foals. These horses are frequently footsore and several sources of pain may contribute to the lameness. There is seldom a history of acute onset of lameness, with the possible exception of foals. Many of these fracture fragments persist radiographically, although some may heal and others appear to be resorbed. These fractures may also be seen in association with chronic laminitis where there has been increased solear pressure. Treatment is usually by shoeing with a broad-webbed seated-out shoe, to give increased protection to the sole, while correcting any problems of foot balance and conformation. Occasionally these fractures may become infected and may require surgical removal of the fragment. A reasonable outcome can be given for these fractures, but their presence usually indicates that the foot is prone to concussion and this must be taken into account when considering a prognosis.

A fracture of the extensor process of the distal phalanx is best seen on a lateromedial radiograph. A small radiopaque fragment proximal to the extensor process may represent a recent fracture, a fracture sustained early in life, or a separate ossification centre (see Figure 3.24). A fragment may be homogeneously radiopaque, with a smooth outline, or have peripheral compact

Downloaded From Vet-eBooks.com

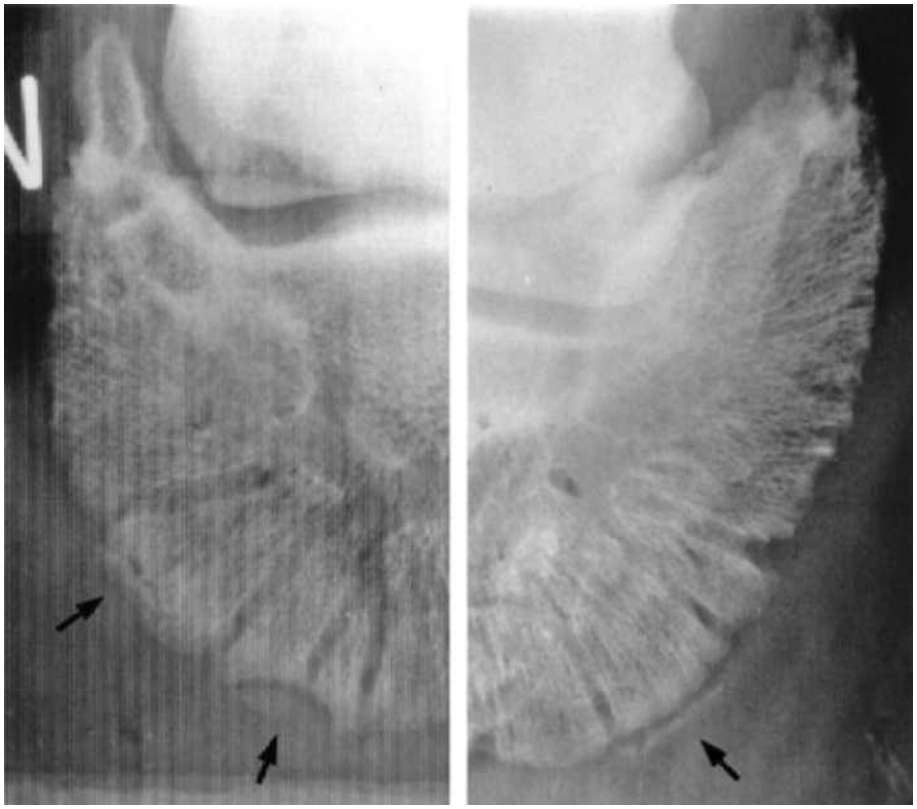


Figure 3.46 Fracture of the solear margin of the distal phalanx (arrows) of two horses (dorsoproximal-palmarodistal oblique image). The radiographs were acquired using conventional film-screen technique, and with a grid, which causes the vertical moiré lines on the images.

bone surrounding bone with trabecular architecture. It is often not possible to determine the significance of such fragments radiographically. Local analgesic techniques may help to determine their clinical significance. Lameness associated with a fragment less than approximately 5 mm in diameter, or not involving the joint surface, frequently resolves with conservative treatment, although the fragment may persist radiographically. Lesions approximately 5–10 mm in diameter, which are shown clinically to be causing lameness, may require surgical removal. The radiographs should be inspected carefully for evidence of osteoarthritis of the distal interphalangeal joint, which may adversely influence the prognosis (Figure 3.47a). A fracture of the extensor process more than 10 mm from its proximal border carries a poor prognosis. A discrete osseous fragment proximal to the extensor process, often occurring bilaterally, may be seen as an incidental finding.

Large extensor process fragments involving up to one-quarter to one-third of the articular surface of the distal phalanx are sometimes seen either unilaterally or bilaterally in young horses starting work and are associated with acute onset of lameness. There is usually extensive increased opacity of the distal phalanx palmar to the fragment, indicating chronicity, despite a recent onset of clinical signs (Figure 3w.47b). There may be entheseous new bone at the insertion of the common digital extensor tendon reflecting chronic instability of the distal interphalangeal joint. It has been suggested that such fragments could be secondary to an osseous cyst-like lesion in the

Downloaded From Vet-eBooks.com



Figure 3.47(a) Slightly oblique lateromedial radiographic image of the left front foot of a 10-year-old Thoroughbred with left forelimb lameness. There is a large, articular, displaced fracture of the extensor process of the distal phalanx, with extensive periarticular new bone on the dorsal aspect of the middle phalanx, entheseophyte formation at the insertion of the common digital extensor tendon on the distal phalanx, and mineralisation in the soft tissues on the dorsal aspect of the diaphysis of the middle phalanx. There is also periarticular modelling of the dorsoproximal aspect of the middle phalanx and a small periarticular osteophyte on the dorsoproximal aspect of the navicular bone. The horse had been examined radiographically 2 years previously, and no abnormality had been detectable.

extensor process and associated abnormal ossification. The prognosis for long-term full athletic function is guarded with conservative or surgical management.

Occasionally fractures of the dorsomedial or dorsolateral aspect of the articular margin of the distal phalanx occur. These may respond well to surgical removal of the fragment.

An avulsion fracture at the insertion of a collateral ligament of the distal interphalangeal joint is a rare injury.

Hoof

RADIOGRAPHIC TECHNIQUE

The radiographic views for examination of the hoof wall are similar to those for the distal phalanx (see 'Distal phalanx [pedal bone] – Radiographic technique', above); however, the exposures should be considerably reduced in order to see the hoof wall when using conventional film and screens, and it is preferable not to use a grid. The wide latitude available using digital radiography may allow the distal phalanx and hoof wall to be examined simultaneously, but for thorough examination of the hoof wall further radiographs may be required. With conventional film images, it may be useful to place a radiodense marker on the hoof wall in order to mark its outer surface; however, this should not be necessary with digital images correctly exposed. Marking can be achieved using tape and a piece of wire, but this is difficult to contour to follow the precise contours of the hoof wall. The use of a thin line of barium paste outlines the dorsal hoof wall more precisely and can also be used to outline the ventral aspect of the sole and frog. However, barium is difficult to remove completely, so if plain radiographs are required they should be obtained first. In cases where separation of the distal phalanx from the hoof wall is suspected, the use of a small screw or thumb tack to mark a precise location on the hoof wall may be beneficial.

Downloaded From Vet-eBooks.com

Technique to assess hoof balance

For assessment of hoof conformation and hoof balance on radiographs, extra care must be taken to ensure that exact lateromedial and dorsopalmar radiographic images of the feet are obtained, and that the horse is correctly positioned.

For forelimbs, the horse must stand taking weight evenly on both front feet, with the metacarpal bones vertical. If the distal aspect of the limb is abducted by 5° rather than perpendicular to the ground, the medial aspect of the distal and proximal interphalangeal joints will appear narrowed. Ideally the feet would be on the ground, but in order to obtain images of the distal aspect of the foot, it is usually necessary for the front feet to be on a block or blocks, to allow the bottom edge of the cassette to be below the distal aspect of the feet. This block should be as thin as possible (usually 2.5 to 5 cm is adequate – any greater thickness will affect the evaluation of dorsopalmar balance). Whether the radiographs are obtained with the shoes in place or removed depends on individual circumstances, but in either case the feet should be carefully cleaned and the frog clefts trimmed. All images should include the ground surface of the hoof, the entire foot, and should extend proximally to include at least the fetlock joint.

Dorsopalmar views

The x-ray beam should be kept horizontal, and centred on the midline of the hoof wall, midway between the coronary band and the ground surface. The beam should be parallel to the long axis of the horse (i.e. parallel to the spine). In practical terms this is probably most easily achieved by having the hind foot, front foot and X-ray generator in line (assuming the hindlimb is not abducted).

Lateromedial views

The beam is kept horizontal, centred just below the coronary band, midway between the dorsal and palmar extremes of the coronary band. It should be aligned parallel to a line drawn across the bulbs of the heel. This will probably not be at right angles to the long axis of the horse.

Hind feet

Assessment of hind foot balance is more difficult. Positioning the hindlimbs of the horse on low blocks with the metatarsal bones vertical is more difficult than for forelimbs, but is essential. The hindlimbs will usually be slightly rotated with the toes outward. The lateromedial views can be obtained with the same guidelines as for the front feet. For dorsoplantar views however the x-ray beam should again be parallel with the ground, but to allow for the rotation of the hindlimb, it is positioned at right angles to a line drawn across the bulbs of the heel, NOT parallel with the long axis of the horse.

NORMAL ANATOMY

By anatomical definition, the hoof is all of the integument of the horse's foot, i.e. it includes epidermis, dermis and subcutaneous tissue. The keratinised portion of the hoof (formed by the stratum corneum of the limbus, corona, wall,

Downloaded From Vet-eBooks.com

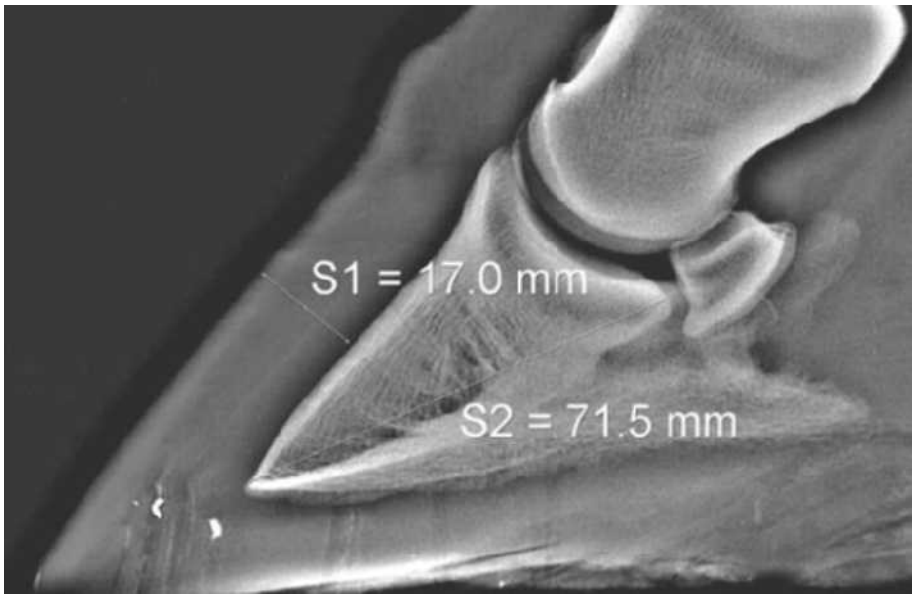


Figure 3.48 Lateromedial image of a foot of a normal horse, but with a long toe. The hoof distal phalanx distance (S1, 17.0 mm) and dorso palmar length of the distal phalanx length (S2, 71.5 mm) ratio (23.8%) is within the normal range (≤25%). There is moderate ossification of one or both ungular cartilages.

sole, frog and heel bulbs) is termed the hoof capsule. The horny wall (comprising stratum internum, stratum medium and stratum externum) is termed the hoof wall. The majority of the hoof wall is formed by the stratum medium and is approximately 50–65% of the width of the dorsal aspect of the hoof wall. The tissues of the dermal laminae are slightly less dense than the horn of the hoof wall. For this reason a radiolucent halo effect is seen immediately around the distal phalanx on correctly exposed radiographs. The normal hoof distal phalanx distance varies, with a mean of 16 mm in Thoroughbreds and 18 mm in Warmbloods. In heavy horses (draught horses) this may be greater still. Single measurements are potentially unreliable due to both variable size of horses and variable magnification and the use of ratios is preferable. The normal ratio between the hoof distal phalanx distance and the dorso palmar length of the distal phalanx is approximately ≤25% ±3% (Figure 3.48). There is also considerable individual variation in the thickness of the sole. For consistency sole depth is best measured as the distance between the tip of the toe of the distal phalanx and the ground surface. Although theoretically the angle of the dorsal hoof wall to the ground surface and the angle of the heel to the ground surface should be the same (the angle dependent on the horse's conformation), usually the heel is at a more acute angle. Published values for these angles vary considerably. The vertical distance between the distal aspect of the coronary band and the most proximal aspect of the extensor process of the distal phalanx is the coronary extensor process distance, and published values vary considerably.

NORMAL VARIATIONS AND INCIDENTAL FINDINGS

Slight variation in hoof conformation is acceptable, and to a large extent is dictated by the shape of the distal phalanx. However, a recent study indicated that the shape and orientation of the distal phalanx cannot be accurately predicted from assessment of the shape of the hoof capsule. Hoof shape and conformation can be altered by hoof trimming, sometimes resulting in distortion of the hoof capsule. Feet which are incorrectly trimmed (out

Downloaded From Vet-eBooks.com

of balance) may have altered limb flight and may cause intermittent lameness, due to foot pain or pain elsewhere in the limb, resulting from uneven weight bearing.

No other normal variations have been recognised.

DIGITAL ANGIOGRAPHY AND VENOGRAPHY

Techniques to obtain digital angiograms and venograms are described under 'Angiography' and 'Venography' in Chapter 16.

SIGNIFICANT FINDINGS

Hoof balance

Assessment of hoof conformation on lateromedial and dorsopalmar (weight-bearing) radiographs is possible, and can be helpful, but great care in interpretation is needed, and images must be correctly positioned if correct conclusions are to be drawn. More information is usually obtained from clinical evaluation of the horse by an experienced clinician.

Dorsopalmar views

On dorsopalmar (weight-bearing) images, the distal margin of the distal phalanx should be the same height from the ground on the lateral and medial aspects of the foot (Figure 3.12). Although a recent study demonstrated that in 63% of feet the medial distance was significantly smaller than the lateral, this conformation is incorrect, and probably reflects a common trimming error, and the horse's ability to compensate for minor imbalances. It may also reflect a faster growth rate at the lateral heel in comparison with the medial heel.

The centre of the extensor process of the distal phalanx should be seen overlying the axis of the middle phalanx, and the proximal sesamoid bones should appear symmetrically placed relative to the third metacarpal/metatarsal bone. There may be rotation of the limb, or rotation between the fetlock and foot, in which case the extensor process or the proximal sesamoid bones will not appear as described, and this may indicate that alterations in shoeing will be required to compensate for conformational variations.

The third metacarpal/metatarsal bone should be vertical, and a line bisecting the long axis of the bone should extend distally to bisect the distal interphalangeal joint, and the ground surface of the foot. The distal limb joints should be symmetrically placed about this line, and the hoof walls and coronary band should also be bilaterally symmetrical (Figure 3.49). While this conformation is ideal, it is seldom seen in practice. Correct trimming and shoeing should attempt to compensate, ensuring the ground surface of the foot (or shoe) is placed symmetrically below the fetlock joint. In some horses gross examination reveals that there is more foot and pastern lateral (or occasionally medial) to the central limb axis of the more proximal aspects of the limb; this is mirrored by the shape of the distal phalanx (Figure 3.22). This can be compensated for to some extent by trimming and shoeing, but this can only support poor conformation, not correct it. A collapsed heel can be supported and a flared wall trimmed.

Downloaded From Vet-eBooks.com



Figure 3.49 Dorsopalmar image of the front foot of a normal mature horse. Medial is to the left. The proximal, middle and distal phalanges have mediolateral symmetry.

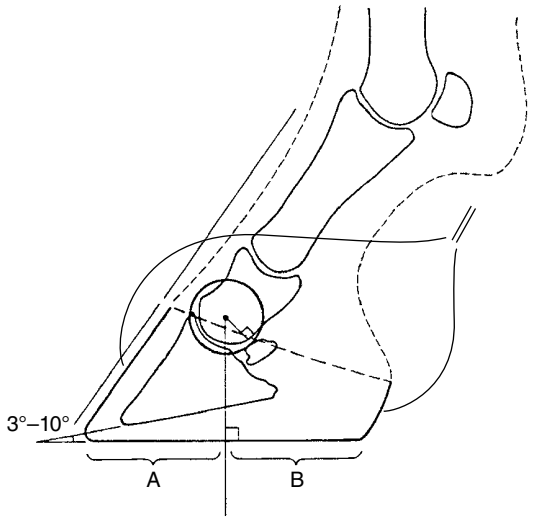


Figure 3.50 Correct hoof conformation. Lateromedial image. Note that A = B.

Lateromedial views

On lateromedial (weight-bearing) views, the distal margin of the distal phalanx should be closer to the ground at the toe of the foot than at the heel, traditionally sloping between 3° and 10° (Figure 3.50). If the distal margin of the distal phalanx is parallel with the ground, this may predispose to trauma of the distal phalanx, solear bruising and associated lameness. If the palmar processes are lower than the toe (sometimes referred to as 'reverse inclination') (Figure 3.58a) this predisposes to lameness. Such conformation results

Downloaded From Vet-eBooks.com

in increased stress on the podotrochlear apparatus and deep digital flexor tendon. Secondary changes in the palmar processes may occur; see 'Pedal osteitis complex', above. The thickness of the sole should also be assessed from the lateromedial image; the ventral aspect of the sole can be highlighted by barium paste for accurate evaluation. It has been suggested that a small solear depth, in combination with abnormal orientation of the distal aspect of the distal phalanx to the horizontal (0° or with the palmar processes lower than the toe) can cause chronic foot pain associated with compression of the solear papillae and abnormal orientation of the terminal papillae, demonstrated using venography.

The centre of the radius of curvature of the distal interphalangeal joint should be vertically above the middle of the bearing surface of the foot (Figure 3.50). If this lies over the dorsal or palmar (plantar) third of the bearing surface of the foot, this may predispose to lameness.

The angle of the dorsal aspect of the distal phalanx should be parallel with the dorsal hoof wall; however, this can be altered by poor trimming. Moreover, in many normal horses there is slight divergence from proximal to distal (Figure 3w.51a) (i.e. the angle of the distal phalanx to the horizontal is greater than that of the hoof wall), or in some horses the dorsal aspect of the distal phalanx is at a smaller angle to the horizontal than the dorsal hoof wall (Figure 3w.51b). In these cases the hoof balance and trimming should be carefully assessed because it may not be ideal.

The angle the horn of the heel subscribes with the ground surface should be virtually the same as that of the dorsal hoof wall. This is often easier to assess clinically than on X-rays. However, it is usually slightly smaller. If the angle of the horn of the heel is substantially smaller than that of the dorsal hoof wall, there will be distortion of the heel, which will predispose to bruising, corns and pain in the palmar aspect of the foot.

SIGNIFICANT FINDINGS

Laminitis

Conventionally, lateromedial radiographs have been used to assess the hoof and distal phalanx in horses with laminitis, but important additional information may be acquired from weight-bearing dorsopalmar and dorsoproximal-palmarodistal oblique ('upright pedal') images. The primary radiographic changes detected in laminitis (other than in angiographic examinations) relate to changes in the dorsal hoof wall and lamellar tissues. These include inflammation, stretching or separation of the lamellae, and separation of the distal phalanx from the hoof wall resulting in rotation and/or sinking of the distal phalanx. The hoof distal phalanx distance may be increased. In a normal foot there is a radiolucent 'halo' between the distal phalanx and both the hoof wall and sole. This is the lamellae and sublamellar dermis (Figure 3w.10b). Narrowing of this halo or increase in its opacity may reflect abnormal lamellar epidermis, with the formation of a lamellar wedge of amorphous horn (Figure 3.52a). Increase in the hoof distal phalanx distance and increase in the ratio of the hoof distal phalanx distance to the palmar length of the distal phalanx may be indicators of chronic laminitis (Figure 3.52b), despite the absence of rotation of the distal phalanx. Measurements above 20 mm and 27% respectively are rarely

Downloaded From Vet-eBooks.com



Figure 3.52(a) Chronic laminitis. Lateromedial image of the left front foot of a 17-year-old pony. The toe of the foot is very long. There is rotation of the distal phalanx. There is loss of the normal radiolucent halo around the distal phalanx and an extensive lamellar wedge.

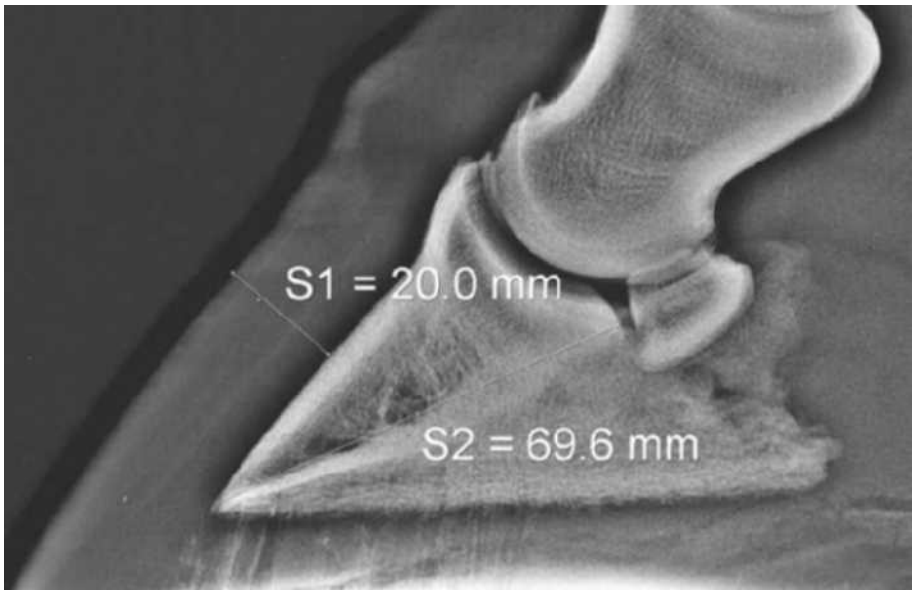


Figure 3.52(b) Chronic atypical laminitis. Lateromedial image of the right front foot of a 7-year-old Warmblood. The hoof distal phalanx distance (S1, 20.0 mm) to palmar length of the distal phalanx (S2, 69.6 mm) ratio is 28.7%. The distal border of the distal phalanx has a horizontal orientation. The toe of the foot is long. There is moderate ossification of one or both ungular cartilages.

recognised in normal horses. With rotation or sinking of the distal phalanx, sole depth may be reduced (Figures 3w.52c and 3w.52d).

Rotation of the distal phalanx reflects loss of function of the suspensory apparatus of the distal phalanx due to lamellar stretching and separation, with the toe moving distally and away from the hoof wall. This results in the dorsal wall of the hoof ceasing to be parallel to the dorsal wall of the distal phalanx. If the limb is loaded, this rotation around the distal interphalangeal joint results in loss of parallel alignment of the dorsal aspects of the middle and distal phalanges. As the condition progresses, on very high-quality radiographs, a faint radiolucent line may appear between the distal phalanx and the sole or hoof wall. This initially represents serum collected between the dermal and epidermal laminae and is visible because of the slight difference between fluid and horn densities. Subsequently this radiolucent line may become more apparent indicating necrotic laminar tissue. With growth of the hoof wall, the lucent lines may move distally relative to the coronary

Downloaded From Vet-eBooks.com

band (Figure 3.53a). Increasing width of this lucent line however is indicative of progressive rotation or laminar necrosis. With extension of the lucent line to the sole, a portal for infection may be established (see also 'Infectious osteitis', above). This is also a common site for haematogenous spread of infection. With chronic laminitis there may be tissue of uniform opacity between the hoof wall and the distal phalanx, reflecting the development of a lamellar wedge.

The degree of rotation may be important in assessing prognosis, but this is subject to dispute. Measurement of rotation is subjective, and recent trimming of the dorsal hoof wall can make the degree of rotation appear less, while overgrowth of the wall can make the degree of rotation appear greater. It may be helpful to place a radiodense marker (e.g. barium paste) on the dorsal aspect of the hoof wall in order to delineate its position in relation to the distal phalanx, and in particular to mark the position of the coronary band. Since laminitis may affect all four feet, lateromedial radiographs of all feet may be required. If progressive rotation is suspected, radiographs obtained at regular intervals may be valuable to monitor progress. Generally, the more marked the rotation and the more rapidly it progresses, the worse the prognosis. Laminitis is a notoriously difficult and inconsistent condition to treat. The appearance of the toe of the distal phalanx is an important indicator for prognosis. On dorsoproximal-palmarodistal oblique views increased radiolucency or resorption of the solear margin at the toe may be seen. On lateromedial images modelling, with reduced mineralisation of the solear surface, and/or new bone laid down on the dorsal surface of the toe (so-called ski-jump; Figure 3.53b) all justify a more guarded prognosis for return to full athletic function. Occasionally there is new bone along most of the dorsal aspect of the distal phalanx. Extensive demineralisation of the solear margin and solear margin fragmentation may occur following laminitis with rotation of the distal phalanx. These abnormalities are best detected on softly exposed dorsoproximal-palmarodistal oblique views. Faint parallel narrow radiolucent lines in the horn tissue at the toe on



Figure 3.53(a) Lateromedial radiographic image of the left front foot of a 6-year-old Arab gelding with chronic laminitis. The radiograph was obtained with a shoe on, a linear radiodense marker on the dorsal hoof wall and a drawing pin at the apex of the frog. The toe of the foot is excessively long. There is rotation of the distal phalanx. There are linear radiolucent areas in the dorsal hoof wall.

Downloaded From Vet-eBooks.com

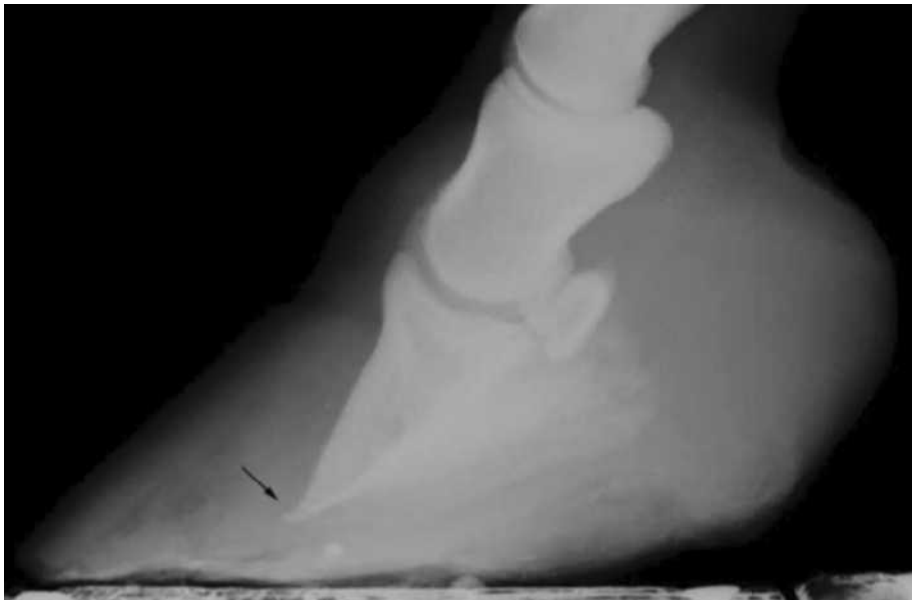


Figure 3.53(b) Laminitis. Lateromedial image of a case of chronic laminitis, showing rotation of the distal phalanx. Note the mottled lucent areas in the separated laminae at the toe of the foot and new bone formation on the dorsal aspect of the toe of the distal phalanx (arrow). There is new horn growth below the coronary band with divergence of the horn distally.

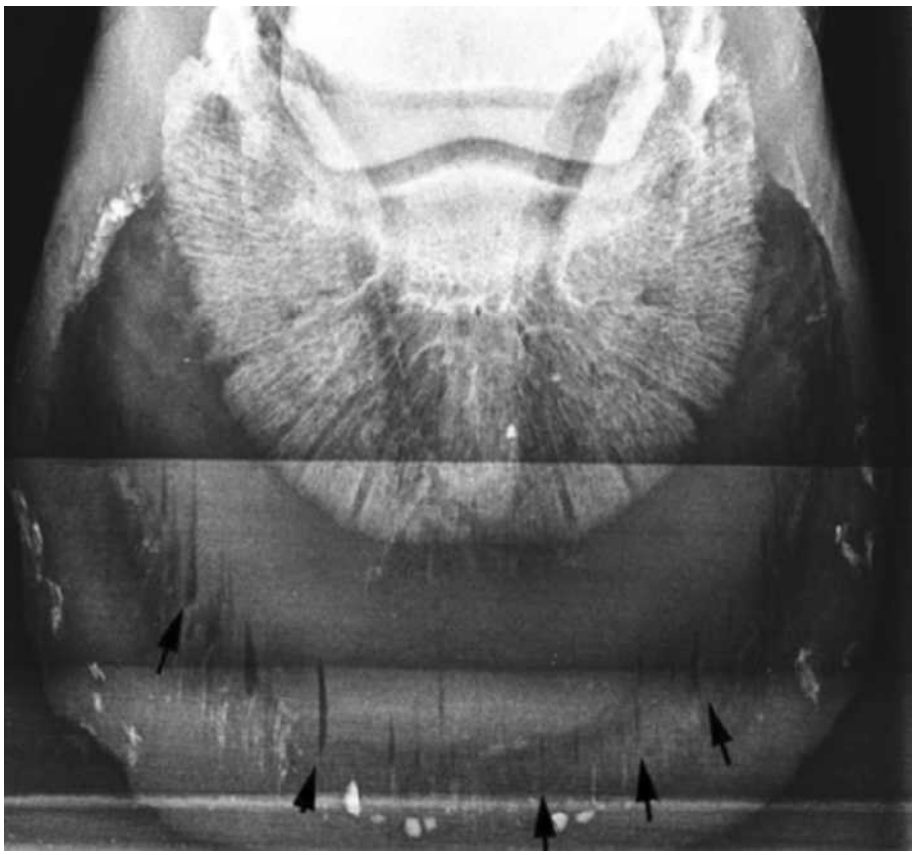


Figure 3.53(c) Laminitis. Dorsoproximal-palmarodistal oblique image of a right front foot. There are multiple vertical radiolucent lines representing laminar separation (arrows).

dorsoproximal-palmarodistal oblique views reflects damage to the horn tissues and is characteristic for chronic laminitis (Figure 3.53c).

With rotation and/or sinking of the distal phalanx the sole of the foot may become convex ('dropped'). This may be most marked below the toe of the distal phalanx, immediately in front of the point of the frog.

Downloaded From Vet-eBooks.com

Infection of the laminar tissues may be a complication of laminitis. This may result in gas shadows, evident as areas of increased radiolucency between the distal phalanx and hoof wall, or the distal phalanx and the sole. Infection of the distal phalanx may also occur in chronic cases.

In 'sinker syndrome' (a very severe form of laminitis, sometimes referred to as founder), the entire distal phalanx sinks within the hoof capsule. This may be difficult to assess on a single radiographic examination, in the early stages, because the dorsal wall of the hoof and distal phalanx may remain parallel. Assessment of the vertical distance between the coronary band and the extensor process of the distal phalanx compared with the contralateral limb, or previous radiographs, may allow a more objective assessment to be made (Figure 3.54a) but it should be remembered that with rotation there will also be some increase in this distance. Initially there may be soft-tissue swelling at the coronary band, which appears more opaque at its dorsal aspect. This is rapidly followed by the development of a distinct depression immediately above the coronary band (Figure 3.54b). A small screw placed in the dorsal hoof wall in these cases will help in the comparison of repeat radiographs obtained on successive days, measuring from the marker to a set point on the distal phalanx (usually the proximal border of the extensor process). Care must be taken to reproduce positioning and magnification factors accurately when repeat images are acquired. There may be compression and distortion of the coronary dermis between the hoof wall and the extensor process of the distal phalanx. The presence of sinking can be assessed from a lateromedial image, however a weight-bearing dorsopalmar image may reveal that the distal phalanx is tilted because of asymmetrical loss of support (usually dropping more medially). There is reduced distance between the solear margin of the distal phalanx and the ground surface on the side to which the distal phalanx is tilted (Figure 3.55). This results in apparent widening of the distal interphalangeal joint space on the ipsilateral side. The presence of parallel vertically-orientated radiolucent lines in the hoof in a dorsopalmar image represents failure of the suspensory apparatus of the distal phalanx because of physical separation of the dermal and epidermal lamellae (Figure 3.55).

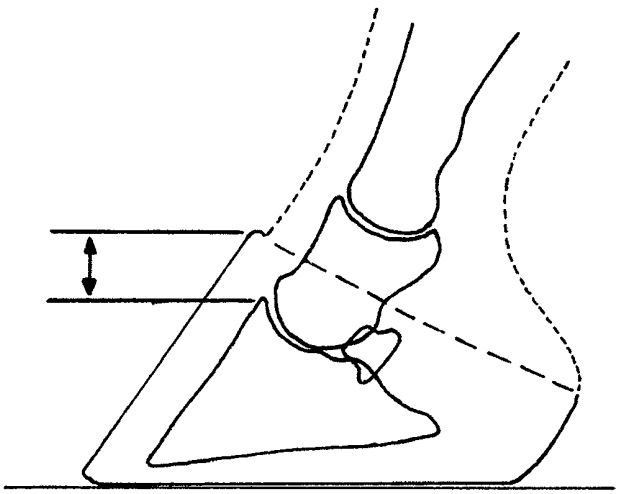


Figure 3.54(a) Diagram to show a method to evaluate 'sinking' of the distal phalanx. Monitor the distance between horizontal lines drawn at the levels of the coronary band and the proximodorsal aspect of the extensor process of the distal phalanx.

Downloaded From Vet-eBooks.com



Figure 3.54(b) Slightly oblique lateromedial radiographic image of a foot of a 14-year-old Warmblood with severe laminitis. There is marked sinking of the distal phalanx. The distance between the coronary band (arrow), above which is a depression, and the extensor process of the distal phalanx is B, 22.9 mm. The dorsal hoof wall is abnormally thick, A, 33.0 mm. The toe of the distal phalanx is obscured by the shoe.

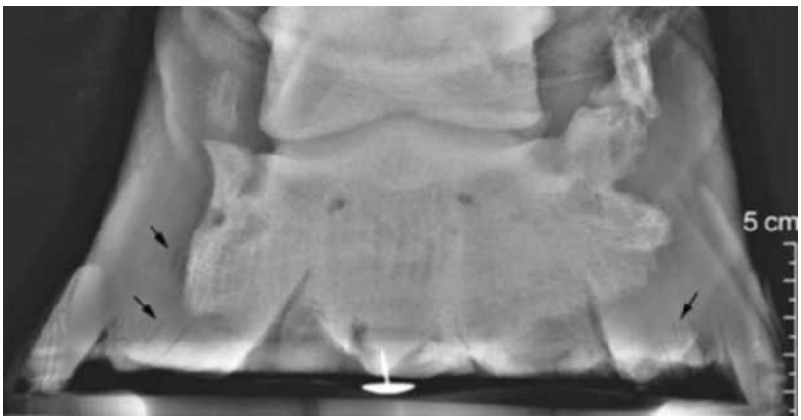


Figure 3.55 Dorsopalmar image of a foot of an Irish Draught cross gelding with chronic laminitis. Medial is to the left. There are multiple approximately vertical radiolucent lines representing laminar separation (arrows). The distal phalanx is tilted medially, with widening of the distal interphalangeal joint space medially. There is a drawing pin representing the position of the apex of the frog. There is a moderate sized separate centre of ossification of the medial ungular cartilage. There is moderate ossification of the lateral ungular cartilage with a large proximal separate centre of ossification.

Radiographic evidence of previous laminitis is sometimes seen in an apparently clinically normal horse. This includes increase of the hoof distal phalanx distance (Figure 3.56), with or without a radiolucent line, and modelling of the toe of the distal phalanx. Variable magnification may make linear measurements inaccurate, so use of the ratio between the hoof distal phalanx distance and the palmar length of the distal phalanx is preferred. Uncorrected rotation of the distal phalanx may also be evident. Despite apparent soundness, such horses may have reduced performance. Determination of the duration of laminitis based upon radiographs is challenging. However there is evidence to support that formation of the wedge-shaped opacity on a lateromedial radiograph, consistent with a lamellar wedge forming, takes 4 weeks to develop.

Treatment of laminitis must include systemic treatment followed by corrective farriery. Lateromedial radiographs are helpful to the farrier when

Downloaded From Vet-eBooks.com

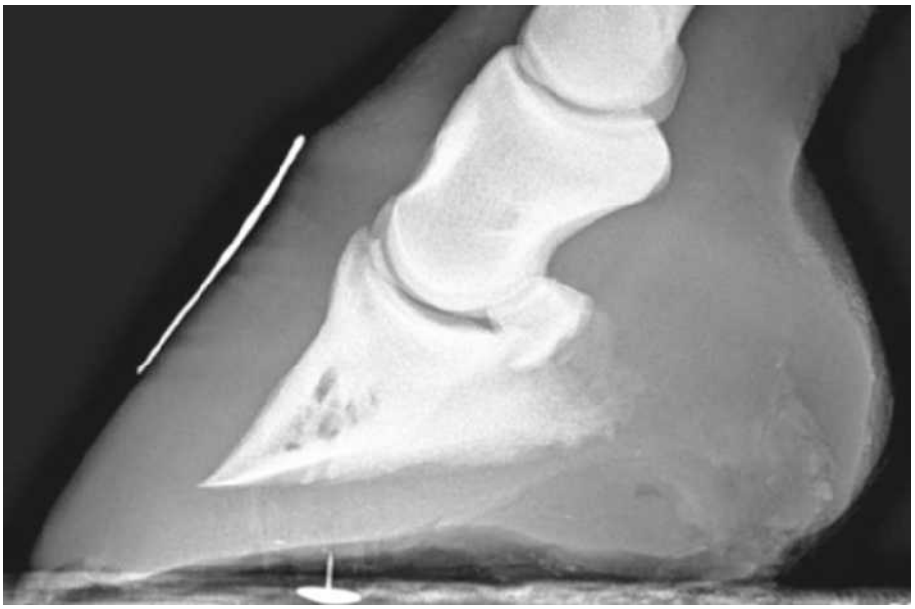


Figure 3.56 Lateromedial radiographic image of a foot of a 7-year-old pony with chronic foot soreness associated with chronic laminitis. There is a linear radiopaque marker on the dorsal aspect of the hoof wall, extending from the coronary band distally. There is a drawing pin at the apex of the frog. The dorsal hoof wall is abnormally thick and there is modelling of the toe of the distal phalanx.

dressing the dorsal wall of the hoof parallel with the dorsal surface of the distal phalanx and to assist correct placement of corrective shoes.

Venography and laminitis

The technique of venography is described under 'Venography' in Chapter 16. Its value in laminitis remains equivocal. Sequential lateromedial and dorsopalmar images should be acquired rapidly. In a normal horse the lateral and medial digital veins, capillaries and arteries are filled in a retrograde manner, permitting visualisation of the terminal arch, coronary plexus, sublamellar vessels, circumflex veins, and veins in the solear and terminal papillae (Figure 3.57a). The contrast medium stays within the vessels and the distal phalanx is proximal to the circumflex vein.

In laminitis there may be alteration of the vasculature, notably compression of vessels in the coronary plexus, sublamellar plexus, terminal and solear papillae and the circumflex vein (Figure 3.57b). The position of the distal dorsal aspect (toe) of the distal phalanx relative to the circumflex vein may be altered. There may be distribution of the contrast medium into the abnormal sublamellar tissues (Figure 3w.57c and 3w.57d). There may be distortion of the circumflex vessels dorsally because of inward growth of solear horn. Venography permits evaluation of the severity of vascular changes and can predict osseous pathology (e.g. distal displacement of the distal phalanx) before it happens. It can be used to develop treatment protocols to mechanically and therapeutically address forces that restrict perfusion of the digit and to monitor the response to treatment.

Long-toe low-heel syndrome

On lateromedial radiographs of a normal foot, the centre of the radius of curvature of the distal interphalangeal joint should be vertically above the centre of the bearing surface of the foot (see Figure 3.50). If the joint is over the palmar third of the bearing surface, this indicates poor dorsopalmar

Downloaded From Vet-eBooks.com

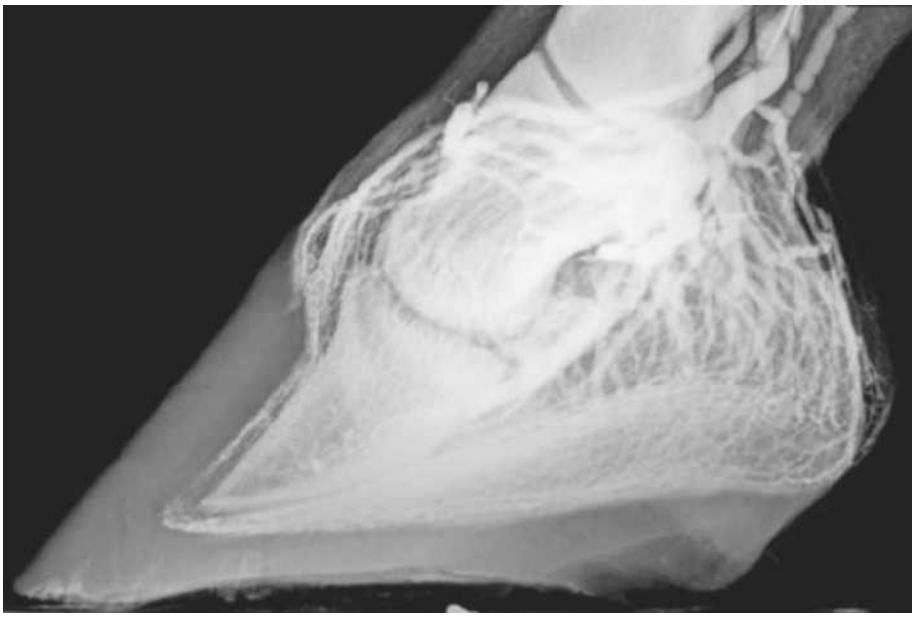


Figure 3.57(a) A normal lateral venogram. Note that the circumflex vasculature is several millimetres distal to the toe of the distal phalanx. The anastomosis of the circumflex vasculature and the dorsal lamellar vasculature has a normal triangular appearance. The coronary plexus is filled normally.

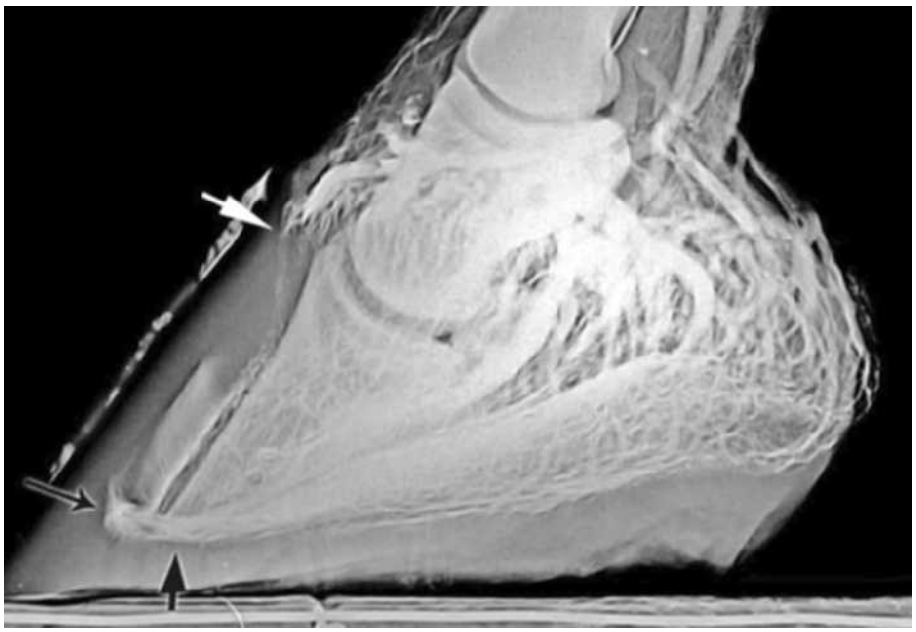


Figure 3.57(b) An abnormal lateral venogram (compare with Figure 3.57a) of an 18-year-old American Saddlebred with laminitis of 7 days' duration. Plain radiographs revealed no evidence of rotation of the distal phalanx. Note the lack of filling of the vessels at the dorsal aspect of the coronary band (white arrow); perfusion of the coronary plexus is truncated at the proximal aspect of the extensor process of the distal phalanx. There is rectangular pooling of radiographic contrast medium in the dorsal lamellar vasculature extending 12 mm proximally on the dorsal aspect of the distal phalanx. The apex of the distal phalanx is ventral to the circumflex vasculature (large grey arrow), causing distortion of both the circumflex lamellar anastomosis (small grey arrow) at the toe and the terminal solear papillae. These vascular changes are secondary to distal displacement or sinking of the distal phalanx.

Downloaded From Vet-eBooks.com

hoof balance which may contribute to lameness. On a weight-bearing lateromedial radiograph it is also important to assess the position of the solear margin of the distal phalanx relative to the ground. If the palmar processes of the distal phalanx are closer to the ground than the toe, this indicates extremely poor hoof balance and is usually associated with lameness (Figure 3.58a). Palmaroproximal-palmarodistal oblique views of the distal phalanx should be obtained in these cases, to look for abnormal radiolucent areas within the palmar processes, irregularities of the margins of the palmar processes and for increased lucency around the palmar processes indicative of separation of the laminae at the heel (Figure 3.58b). New bone formed on the axial or abaxial surfaces of the palmar processes of the distal phalanx is suggestive of repeated trauma to this area. The solear margin of the distal phalanx should also be examined for indications of increased radiolucency, and solear margin fractures (see 'Pedal osteitis complex', above, and 'Fractures', above).



Figure 3.58(a) Lateromedial image of a foot of a horse with chronic foot pain. The palmar processes of the distal phalanx are lower (more distal) than the toe. The toe of the foot is rather long (compare with Figure 3.10a).



Figure 3.58(b) Low heel conformation. Palmaroproximal-palmarodistal image of a distal phalanx, showing separation of the laminae around the medial (M) palmar process seen as an area of increased lucency (arrows). Compare with the uniform opacity surrounding the lateral palmar process.

Downloaded From Vet-eBooks.com



Figure 3.59 Dorsopalmar radiographic image of a front foot of a 3-year-old French Thoroughbred. Medial is to the left. There is marked mediolateral hoof imbalance. The distance between the distal medial aspect of the distal phalanx and the ground (17.8 mm) is considerably less than laterally (24.2 mm).

Mediolateral foot imbalance

Mediolateral foot balance can be assessed on weight-bearing dorsopalmar radiographs of the feet, provided that the horse is loading both front feet squarely with the limbs vertical. The relative distance of the medial and lateral solear margins of the distal phalanx from the ground can be assessed (Figure 3.59). In addition, the alignment and congruity of the distal and proximal interphalangeal joints should be noted. This assessment is most accurately made with the horse standing with both feet on a relatively low (5 cm) wooden block. Uneven load bearing makes interpretation difficult. The authors believe that careful clinical assessment of the distal aspect of the limb is also essential for assessment of mediolateral imbalance, because other aspects of conformation must also be taken into account.

Infection

Sub-solear infection of the foot is usually diagnosed clinically, but the extent of the area involved can be difficult to assess. Radiographically lucent zones may be seen within the hoof (Figure 3w.60). These vary in shape and size, but with the careful use of oblique views the extent of hoof separation can be determined. They must be distinguished from the lucent lines seen with separation of the hoof wall in laminitis (see 'Laminitis', above). The margin of the distal phalanx should be inspected carefully for evidence of infectious osteitis of the distal phalanx (see 'Distal phalanx [pedal bone] – Infectious osteitis', above), particularly if infection is recurrent.

In some cases, clinical signs may indicate the presence of infection, but a discharging sinus may be slow to occur. This is most common if the sole is hard or unusually thick, and in cases of haematogenous spread of infection rather than foreign body penetration. In these cases high-quality digital radiographs may reveal a lucent zone beneath or adjacent to the distal phalanx, indicating infection (Figure 3w.60), but radiographs in this situation are frequently unrewarding.

Downloaded From Vet-eBooks.com

Infection is occasionally seen in conjunction with the presence of a radiopaque foreign body. See also 'Distal phalanx (pedal bone) – Infectious osteitis', above.

Penetrating injuries

Penetrating injuries of the foot are common and can have catastrophic consequences if not recognised early and treated appropriately. If a radiodense foreign body has penetrated the sole and is still *in situ* then lateromedial and dorsopalmar radiographs should be obtained in order to determine the depth and direction of penetration. It is important to establish whether it is likely that a synovial cavity (distal interphalangeal joint or navicular bursa) has been punctured, or if either a bone or the deep digital flexor tendon has been traumatised or contaminated. If the foreign body is absent or has been removed a metal probe carefully inserted into the tract can help to determine the extent of the penetration. Fistulography or sinography (see Chapter 16), as well as ultrasonography, can also be helpful. Penetration of synovial cavities or the deep digital flexor tendon warrant rapid intervention with extensive flushing and antimicrobial treatment of the penetrated structures before infection can become established. If infection does become established, a poor prognosis is warranted.

Hoof wall separation

Separation of the hoof wall may occur for a number of reasons other than laminitis (see 'Laminitis', above) and infection (see 'Hoof – Infection', above). Excessive length of horn at the toe may result in the dorsal aspect of the hoof wall lifting away from the distal phalanx. A radiolucent area will be evident under the hoof wall (Figure 3.61a), although it frequently becomes packed with radiodense material (mud). Separation can also occur as a result of an acute traumatic incident, e.g. jumping on hard uneven ground.

The term 'seedy toe' is used to describe a condition in which there appears to be separation of the dermal and epidermal laminae, or there is poor horn formation from the dermal laminae. The aetiology of this condition is uncertain. It may reflect mechanical stretching of the white line from unbalanced feet. It may initially be detected proximally and, as the horn grows down, the separated area moves distally. Seedy toe can be seen radiographically as a lucent area in the laminar portion of the hoof wall (Figure 3.61b). It may have no apparent opening through the hoof wall or white line when first detected. When the distal margin of the separated area reaches the bearing surface, trimming the foot will open into the separated area, which may then act as a portal for infection. If the lesion is extensive, the increased loading on the adjacent laminae may result in lameness, particularly on hard ground. The extent of the lesion may be determined by the careful use of oblique views. (The term 'seedy toe' is sometimes used to refer to the separated laminae seen in the hoof after rotation of the distal phalanx in laminitis. These two conditions should be distinguished from each other, because they have different aetiologies and require different treatments.)

Downloaded From Vet-eBooks.com



Figure 3.61(a) Laminar separation at the toe. Lateromedial image of the right front foot of a Thoroughbred with mild right forelimb lameness. The toe of the foot is excessively long and distorted in shape, with apparent divergence of the dorsal hoof wall and the dorsal aspect of the distal phalanx. There is separation of the hoof wall at the toe of the foot. This extends up the dorsal wall and laterally around the toe. The granular opaque material is dirt packed into the separated area.

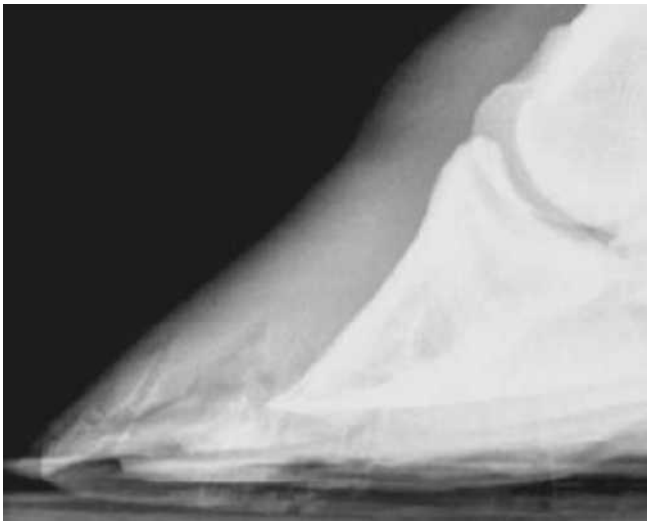


Figure 3.61(b) Slightly oblique lateromedial view of a right front foot with an excessively long toe, resulting in apparent rotation of the distal phalanx. There is a radiolucent defect extending from the toe of the foot, reflecting necrotic material in the white line, so called seedy toe. There is also a radiolucent line distal to the distal phalanx, parallel with the sole.

Navicular bone

RADIOGRAPHIC TECHNIQUE

In this chapter the distal sesamoid bone is referred to as the navicular bone. Being a sesamoid bone the navicular bone is surrounded by compact bone (often incorrectly referred to as cortices) with a central spongiosa; there is no medulla.

Equipment

Adequate radiographs of the navicular bone can be obtained using portable x-ray equipment, but a minimum output of 15 mA at 80 kV is required. With machines of low output (less than 40 mA at 80 kV), digital systems or rare earth screens and appropriate films are essential to avoid movement blur. Machines with a high mA output allow short exposure times, and therefore fine-grain high-definition screens and compatible films can be used to obtain more detail. Dorsoproximal-palmarodistal oblique radiographs of the navicular bone obtained using traditional x-ray technique should be acquired with a grid (8:1 or 6:1 ratio). However, with digital systems a grid may not be necessary and if used should be appropriate for the individual digital system, to avoid moiré lines. Ideally separate images, appropriately centred, exposed and collimated, should be acquired for assessment of the navicular bone and

Downloaded From Vet-eBooks.com

distal phalanx, rather than relying on windowing an image of the entire foot. Careful collimation of the x-ray beam will also enhance the quality of the radiographs.

It is essential that the shoes are removed and the feet carefully cleaned prior to radiography (including for pre-purchase examinations). Loose horn in the sole and irregular growth of the frog should be removed. Scrubbing the feet with water can result in artefacts due to loose packing in the frog clefts (see below).

The frog clefts need to be packed to eliminate air shadows being cast over the navicular bone for at least one dorsoproximal-palmarodistal view, and for the palmaroproximal-palmarodistal oblique view. This can be achieved using Playdoh or equivalent, Vaseline or soft soap. The latter two may trap air bubbles creating artefacts which may mimic pathology. Packing should be kept to a minimum, and restricted to the frog clefts, not filling the whole sole of the foot, to avoid creating artefacts. The use of a water bath is not recommended because this increases scatter, resulting in reduced contrast on the final radiograph.

Positioning

For complete evaluation of the navicular bone it is recommended that lateromedial, dorsoproximal-palmarodistal oblique and palmaroproximal-palmarodistal oblique views should be obtained. Two dorsoproximal-palmarodistal oblique images may be required to rule out artefacts, and to identify or verify the presence of a distal border fragment. In some cases a dorsopalmar (weight-bearing) view should also be obtained.

Lateromedial view

A lateromedial radiograph is obtained with the foot to be examined placed on a flat block. It is preferable, but not essential, for the foot to be bearing weight. The x-ray beam should be horizontal and centered on the end of the navicular bone (approximately 1 cm below the coronary band at a point midway between the most dorsal and most palmar aspects of the coronary band). The beam is aligned parallel to a line drawn across the bulbs of the heel, so that it traverses the navicular bone through its long axis. A true lateromedial view is essential to evaluate the thickness of the palmar compact bone, the junction between the compact bone and the trabecular bone of the spongiosa and the trabecular architecture, and to identify periarticular osteophytes and modelling of the proximal and distal aspects of the bone. These may indicate entheseous new bone at the attachments of the collateral sesamoidean ligament and the distal sesamoidean impar ligament. Despite standardised positioning and centering of the x-ray beam, it is not always possible to obtain true lateromedial images of the navicular bone, and middle and distal phalanges on one radiograph in all horses. This depends on hoof capsule shape, mediolateral imbalance and variation in shape of the bones. Several different images at slightly different angles (e.g. lateral 3° dorsal-medial palmar oblique, lateral 3° palmar-medial dorsal oblique, or lateral 3° proximal-mediodistal oblique) may be required in order to obtain truer lateromedial images of all structures (Figures 3.62a–c). In some horses although the palmar compact bone and sagittal ridge of the navicular bone are clearly defined

Downloaded From Vet-eBooks.com



Figure 3.62(a) Dorsopalmar image of a right front foot with mediolateral imbalance of the distal phalanx. Lateral is to the right. The medial aspect of the distal phalanx is lower than laterally. This may influence the position of the distal phalanx and navicular bone in a lateromedial view, as in Figure 3.62b.

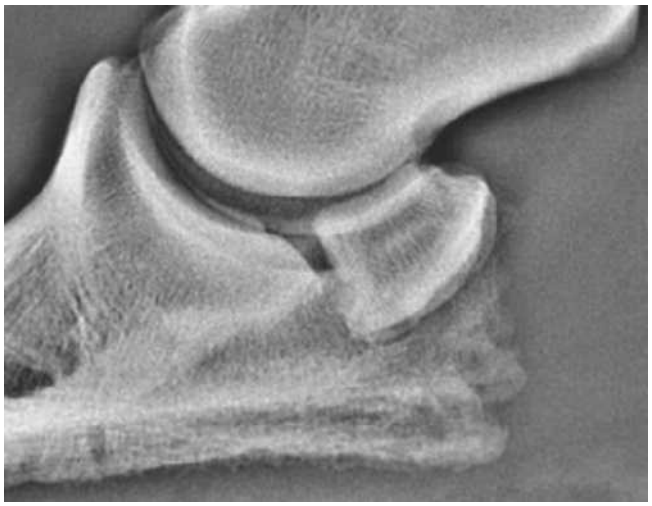


Figure 3.62(b) Lateromedial image of the same foot as in Figure 3.62(a). The medial and lateral palmar processes of the distal phalanx are not superimposed because of the mediolateral imbalance of the distal phalanx. Compare the position of the palmar processes of the distal phalanx and the definition of the palmar compact bone of the navicular bone with Figure 3.62(c).

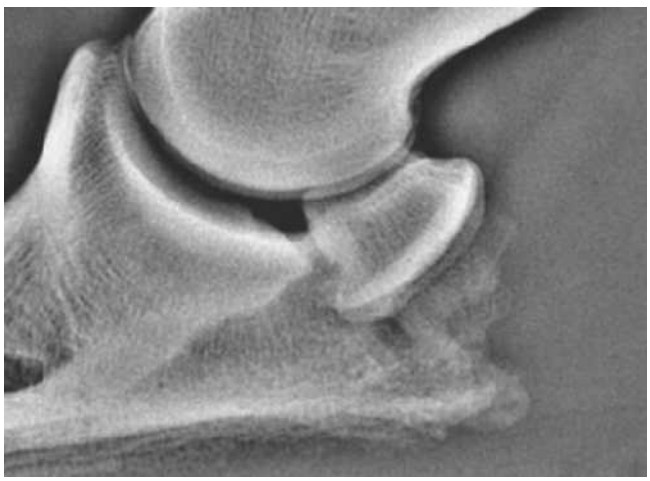


Figure 3.62(c) Lateral 3°proximal-medial distal oblique image of the same foot as Figures 3.62(a) and (b). The medial and lateral palmar processes of the distal phalanx are now superimposed and a more true lateromedial image of the navicular bone has been acquired. The dorsal margin of the palmar compact bone of the navicular bone is much more clearly defined compared with Figure 3.62(b). Note the rather irregular appearance of the distal aspect of the palmar processes of the distal phalanx.

there may be slight obliquity of the more dorsal aspects of the bone, which is difficult to eradicate completely, despite further alteration of the x-ray beam angle (dorsopalmarly and/or proximodistally).

Dorsoproximal-palmarodistal oblique views

Two dorsoproximal-palmarodistal oblique views are helpful to aid recognition of artefacts and to determine the presence of one or more distal border fragments. These views can be obtained using either of two techniques, the 'upright pedal' view or the 'high coronary' view. The former results in less distortion and is recommended by the authors, although it may be more practical to use the 'high coronary' technique when out in the field.

Downloaded From Vet-eBooks.com

DORSOPROXIMAL-PALMARODISTAL OBLIQUE ('UPRIGHT PEDAL') VIEW

The toe of the foot is placed on a navicular block (see below), and the dorsal wall of the foot and the pastern angled forwards at approximately 85° to the horizontal (Figure 3.63a). The x-ray beam is kept horizontal and centered 2–3 cm proximal to the coronary band at the midline of the foot. The beam should be well collimated. The cassette is placed behind and as close as possible to the foot. The dorsal wall of the foot and pastern should be in a straight line. If the navicular block is placed too close to the horse, the fetlock and pastern joints will flex too much and the x-ray beam will traverse too great a distance through the middle phalanx, with resultant loss of quality of the radiograph. If positioned too far in front of the horse, the dorsal wall of the hoof and the pastern become too upright and the distal border of the navicular bone is superimposed over the distal interphalangeal joint. This image highlights the body of the bone, and the dorsal articular margin of the distal aspect of the bone.

A second dorsoproximal-palmarodistal (upright pedal) oblique view may be helpful to identify the presence of distal border fragments and to aid interpretation and to differentiate artefacts. This view is obtained in a similar manner to the first, but with the dorsal wall of the hoof and the pastern vertical and the x-ray beam centered on the coronary band (Figure 3.63b). This image highlights the palmar margin of the distal aspect of the bone. Superimposition of the distal border of the navicular bone over the distal interphalangeal joint increases contrast and facilitates distal border fragment detection.

A 'navicular block' can take a number of forms, but is basically a solid block of wood with a groove cut in the top in which the toe of the foot can be rested (Figure 3.63c) while the limb is held by an assistant. By moving the block forward or backward relative to the horse, the dorsal wall of the hoof can be positioned at different angles. A horse will normally stand quietly if the limb is raised on a block about 25 cm high. With a smaller block the horse

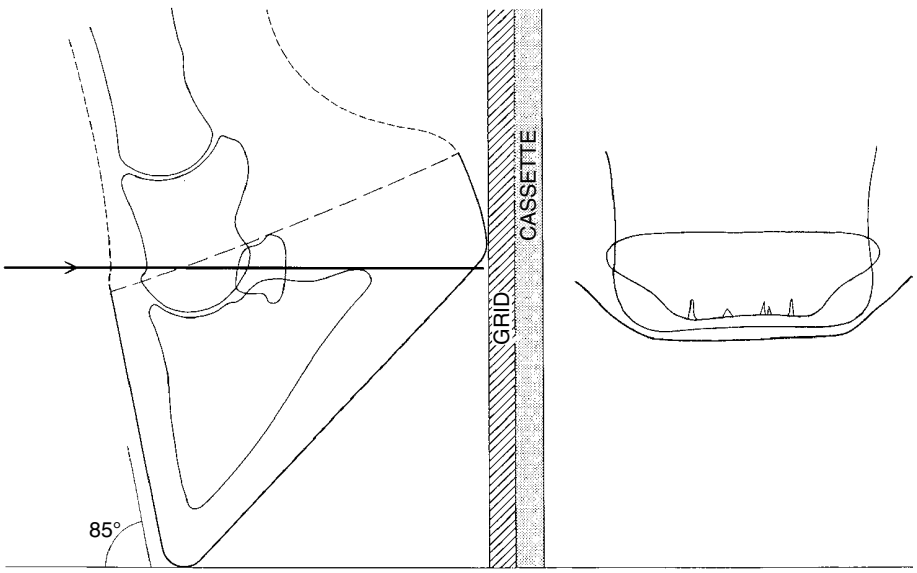


Figure 3.63(a) Positioning to obtain a dorsoproximal-palmarodistal oblique image of the navicular bone (85° upright pedal view). Inset diagram shows resultant radiographic positioning of the distal border of the navicular bone proximal to the distal interphalangeal joint.

Downloaded From Vet-eBooks.com

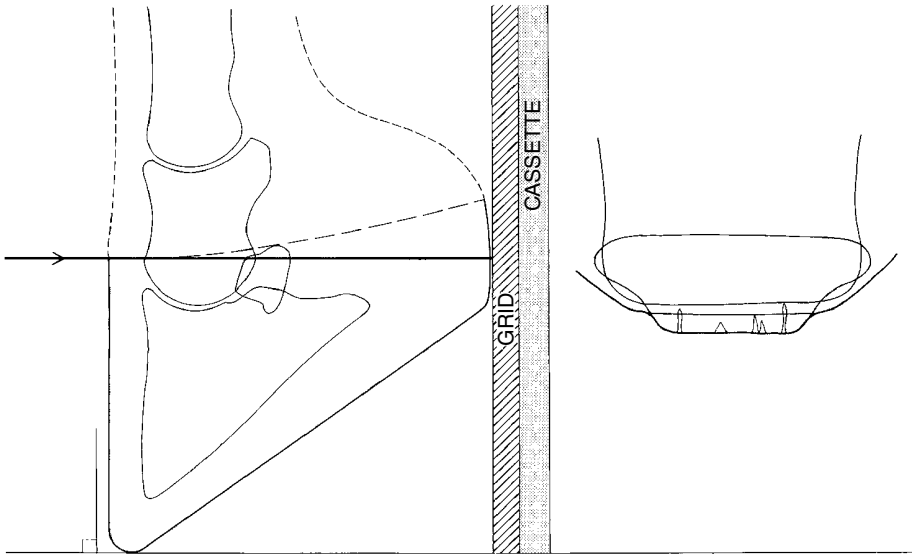


Figure 3.63(b) Positioning to obtain a dorsoproximal-palmarodistal oblique image of the navicular bone (90° upright pedal image). Inset diagram shows resultant radiographic positioning of the distal border of the navicular bone superimposed over the distal interphalangeal joint.

will continually try to straighten the limb and stand on it. It is also important to have a block that feels solid, to give the horse confidence.

DORSOPROXIMAL-PALMARODISTAL OBLIQUE ('HIGH CORONARY') VIEW

To obtain images using the 'high coronary' technique the imaging plate cassette is placed in a suitable tunnel on the floor, and the horse stands on it. The x-ray beam is centered 2 cm above the coronary band in the midline, and angled distally, at an angle of 65° to the horizontal (i.e. a dorsal 65° proximal-palmarodistal oblique view). It is recommended that two views should be obtained with 10–15° difference in angle of the beam.

If using conventional film–screen radiography the image may be improved by the use of a parallel grid. A grid ratio of 6:1 is preferable to 8:1 because of the difficulty of aligning the foot, grid lines and x-ray beam. If using digital systems a grid is not required. Alignment of the grid with the x-ray beam and the foot is more difficult than with the upright pedal view.

The 'high coronary' technique has the disadvantage that the x-ray beam is not at right angles to the film or grid, nor is the film parallel to the palmar surface of the navicular bone (see Figure 3.3a). This results in distortion of the image. Nonetheless, in some horses ease of handling the animal may outweigh other considerations, and some people prefer to use this technique routinely. The authors normally prefer to use the 'upright pedal' view.

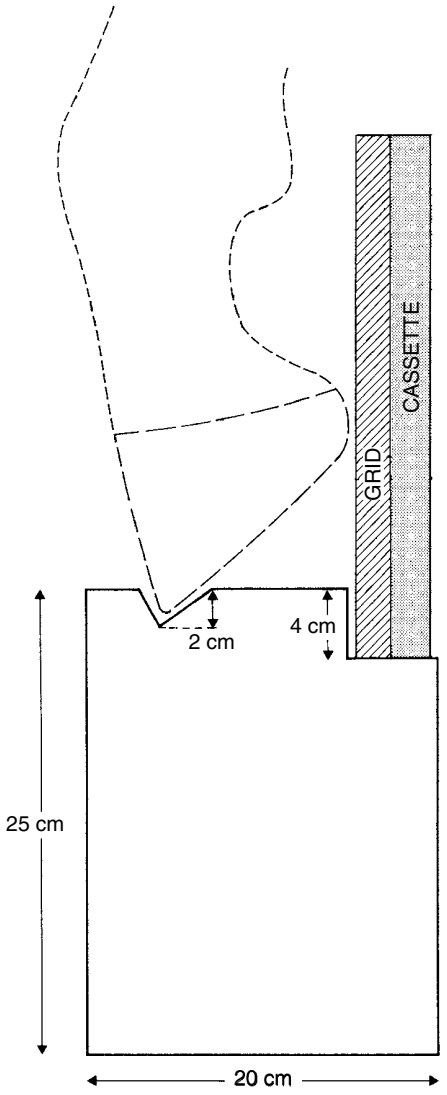


Figure 3.63(c) A 'navicular block' (used to position the foot for radiographs of the navicular bone and distal phalanx in the 'upright pedal' position).

Palmaroproximal-palmarodistal oblique view

The palmaroproximal-palmarodistal oblique view provides good visualisation of the spongiosa and palmar compact bone of the navicular bone.

The foot to be radiographed is positioned palmar to the contralateral forelimb, on a cassette tunnel containing the cassette. The heel should be flat on the

Downloaded From Vet-eBooks.com

ground, but the weight of the horse should be forward on the contralateral limb. The x-ray machine is placed ventral to the thorax of the horse. The x-ray beam is centered between the bulbs of the heel at the base of the pastern at an angle of approximately 45° to the horizontal (Figure 3.64a), getting the x-ray beam as near to parallel to the palmar surface of the navicular bone as possible.

Alternatively, the horse stands on a cassette tunnel which is placed on a wedge-shaped block, which has a slope raising the toe of the foot approximately 10–15°. The contralateral limb can be lifted to restrict movement. The x-ray beam is angled at approximately 30° from the horizontal, centering as above (Figure 3.64b). In both techniques it is important to avoid superimposition of the palmar aspect of the fetlock over the navicular bone, and the limb should be positioned appropriately. The angle of the x-ray beam should be parallel to the palmar surface of the navicular bone, and both foot conformation and limb placement will have an effect on the optimal angle of the x-ray beam (Figures 3w.64c–e). An upright foot conformation will require a larger (more upright) angle, whereas if the heel is low the angle should be reduced. The distal limb conformation of some horses occasionally makes this extremely difficult to achieve. Poor technique can create artefacts and mimic pathology, in particular resulting in poor definition of the margin between compact and trabecular bone and loss of trabecular architecture (Figures 3.68b and 3.68c).

This view can be difficult to acquire in a small pony, especially if fat, because the x-ray machine cannot physically be placed in the optimum position. It can also be difficult to acquire in a horse with severe palmar foot pain, which results in unwillingness to extend the distal interphalangeal joint as it increases the load on the podotrochlear apparatus and deep digital flexor

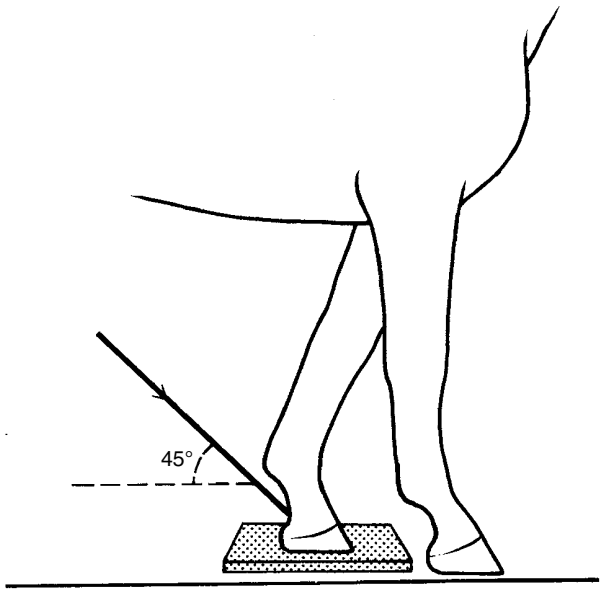


Figure 3.64(a) Positioning to obtain a palmar 45° proximal-palmarodistal oblique view of the navicular bone. The heel of the foot to be examined should be on the ground, caudal to the contralateral foot, with the weight of the horse forward on the opposite limb. The x-ray beam (arrow) is centered on the midline between the bulbs of the heel, at the distal aspect of the pastern.

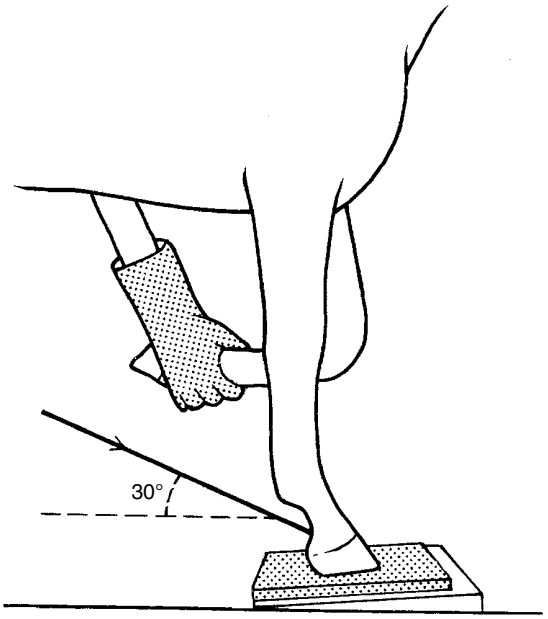


Figure 3.64(b) Positioning to obtain a palmar 30° proximal-palmarodistal oblique view of the navicular bone, with the foot on a wedge-shaped block, with the toe elevated. The x-ray beam (arrow) is centered on the midline, between the bulbs of the heel.

Downloaded From Vet-eBooks.com

tendon. Use of sedation and analgesia may facilitate positioning. Obtaining this view in hindlimbs may also be more difficult than in forelimbs.

Dorsopalmar (weight-bearing) view

A true dorsopalmar radiograph is obtained with the horse bearing weight on the limb (see Figure 3.4). The x-ray beam is kept horizontal, and centered approximately 2 cm below the coronary band at the dorsal aspect of the foot. It is aligned perpendicular to a line tangential to the bulbs of the heel. The cassette is placed vertically behind the foot, at a right angle to the x-ray beam.

This is not a standard view for examining the navicular bone, but can give valuable additional information about both a fracture of the navicular bone and proximal border entheseophytes.

Dorsoplantar views of the hind feet

It is normally easier to obtain plantarodorsal rather than dorsoplantar views of the hind feet. The positioning of the limb for these views is the same as for the dorsoproximal-palmarodistal oblique view of the forefeet, except that a low flat block (5 cm) is recommended for supporting the toe. The cassette is placed in front of the foot and the x-ray beam is centered in the midline of the bulbs of the heel, level with the dorsal aspect of the coronary band. It does result in relatively greater magnification of the navicular bone than a dorsoplantar view.

NORMAL ANATOMY

Immature horse

The navicular bone usually ossifies from a single centre, and at birth has an oval outline on dorsopalmar views. It continues to ossify until about 18 months of age, at which time it has acquired its adult shape. If the feet are slightly different shapes in early life, then the navicular bones may not be a perfect pair.

Skeletally mature horse

Lateromedial view

Lateromedial radiographs of the navicular bone show the joint surfaces which articulate with the middle and distal phalanges (Figures 3.65a–d). The palmar aspect of the bone is seen as two lines, the more palmar representing the sagittal ridge of the bone, and the more dorsal representing the main palmar aspect of the compact bone. A smoothly demarcated depression is frequently seen in the central part of the sagittal ridge (Figure 3.65c). The palmar compact bone is either of similar thickness proximally to distally (Figure 3.65b) or is thicker proximally than distally (Figure 3.65d). The dorsal third of the distal border of the bone articulates with the distal phalanx. At the distal palmar aspect of the navicular bone is a smoothly defined ridge which is the region of origin of the distal sesamoidean impar ligament. There is usually a notch of variable depth between the articular surface and the ridge on the distal border of the bone, called the fossa. Lucent zones (also

Downloaded From Vet-eBooks.com



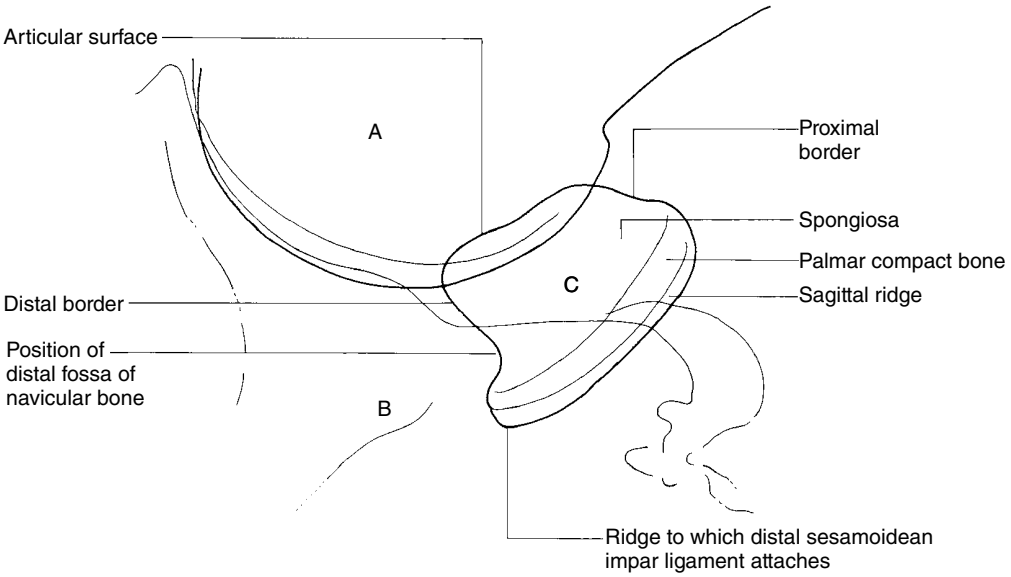


Figure 3.65(a) Lateromedial radiographic image and diagram of a normal adult navicular bone. Note that the palmar compact bone of the navicular bone is thickest proximally. A = middle phalanx, B = distal phalanx, C = navicular bone. The margins of joint space between the distal aspect of the navicular bone and the distal phalanx are convergent towards the palmar aspect.

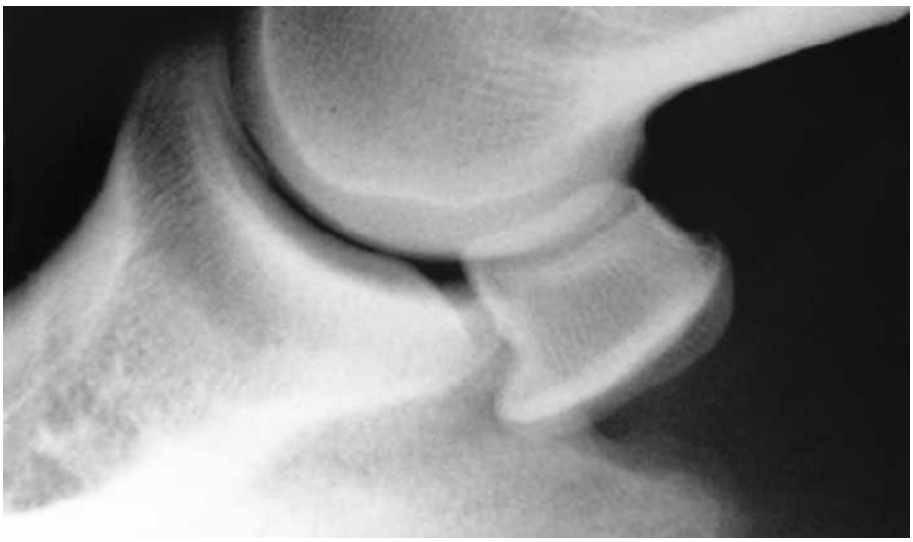


Figure 3.65(b) Lateromedial image of a normal adult navicular bone. The margins of the joint space between the navicular bone and the distal phalanx are parallel (compare with Figure 3.65a). There is mild proximal and distal extension of the palmar compact bone of the navicular bone.

Downloaded From Vet-eBooks.com



Figure 3.65(c) Lateromedial image of an adult navicular bone, showing a smooth concave depression in the palmar aspect of the sagittal ridge (arrow), a normal finding. The palmar compact bone of the navicular bone is thicker proximally than distally, also a normal finding.

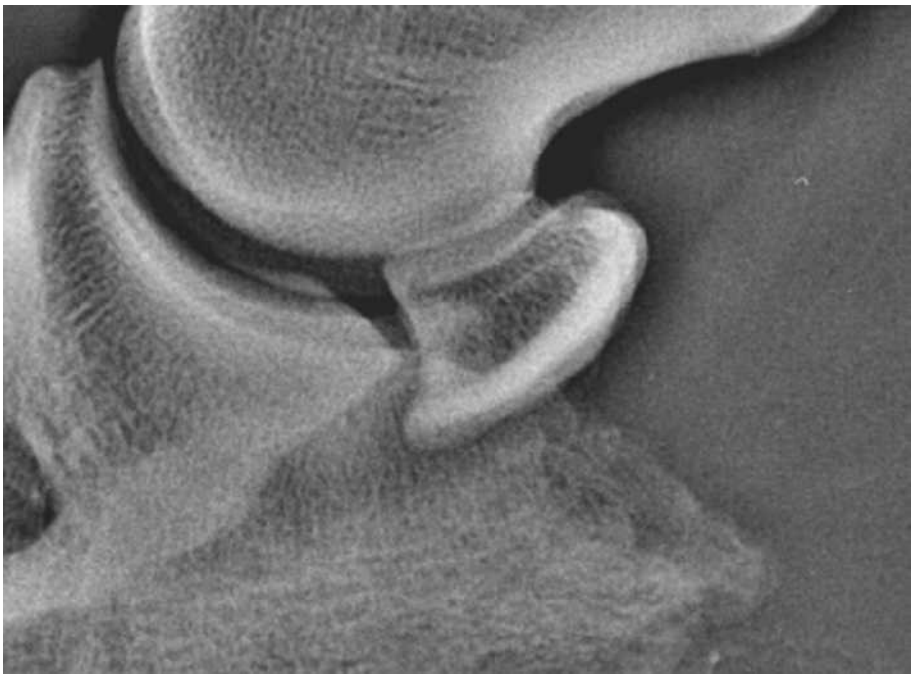


Figure 3.65(d) Lateromedial image of an adult navicular bone. There is distal extension of the palmar compact bone. The palmar compact bone is slightly thicker proximally than distally.

referred to as nutrient foramina and synovial invaginations of the distal interphalangeal joint) extending proximally from this fossa are generally not evident in a normal horse on a lateromedial view. A clear linear trabecular pattern is seen within the spongiosa. The spongiosa and the compact bone around the periphery have a distinct interface. In the majority of horses the outline of the deep digital flexor tendon is seen as a faint opacity palmar to the navicular bone.

Downloaded From Vet-eBooks.com

Dorsoproximal-palmarodistal oblique views

DORSOPROXIMAL-PALMARODISTAL OBLIQUE ('UPRIGHT PEDAL') VIEW

The outline of the navicular bone varies considerably among animals, but is normally a mirror image of that of the contralateral limb (Figure 3.66). Several triangular-shaped lucent zones are often visible along the distal horizontal border of the bone (see 'Normal variations and incidental findings – Dorsopalmar ['upright pedal'] view'). The distal border is seen as two lines: one (the more prominent and more proximal) represents the articulation of the bone with the distal phalanx; the other represents the distal border of the ridge from which the distal sesamoidean impar ligament originates. On poorly positioned images the proximal border of the bone may also be evident as two lines representing the palmar and dorsal margins. Four different shapes of the proximal border have been described in Warmblood horses, straight, undulating, concave and convex, and it is suggested that shape may be heritable and possibly related to risk of disease.

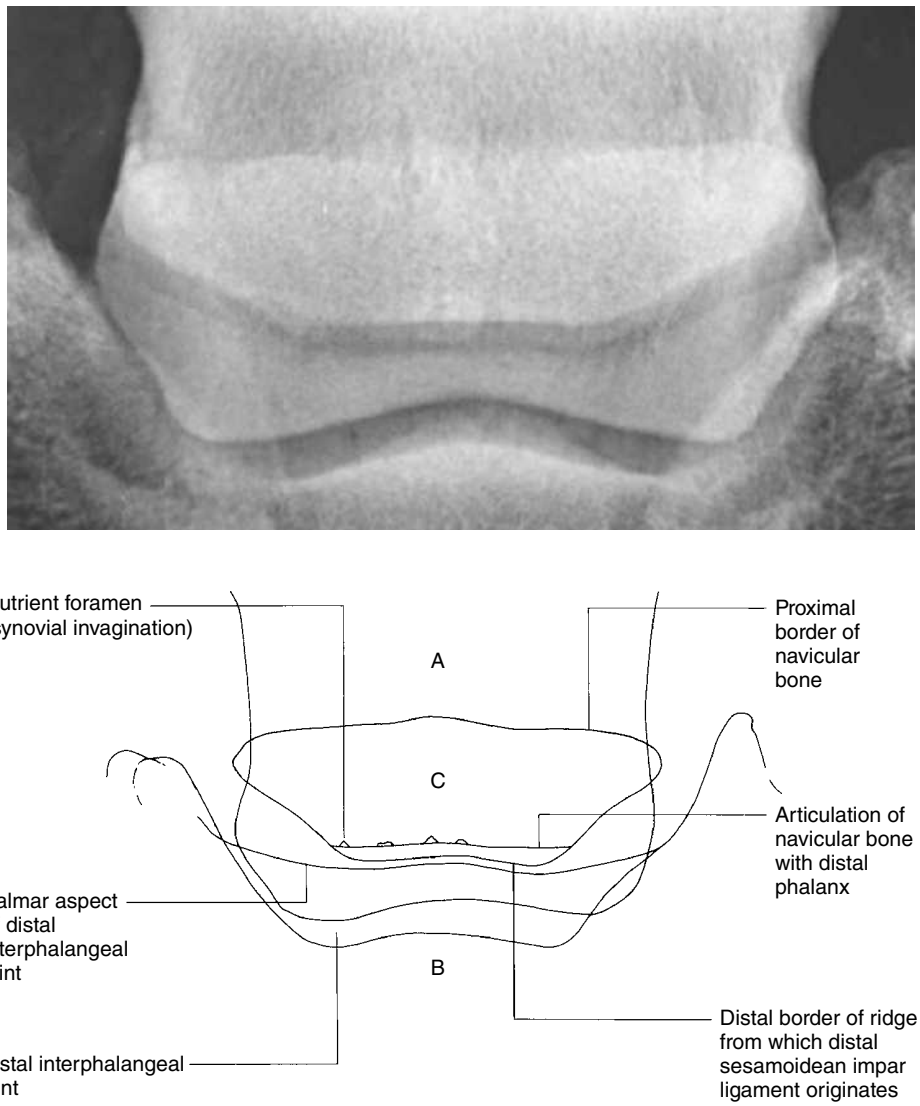


Figure 3.66 Dorsoproximal-palmarodistal oblique radiographic image and diagram of a normal adult navicular bone (upright pedal view). A = middle phalanx, B = distal phalanx, C = navicular bone.

Downloaded From Vet-eBooks.com

The image seen using this technique (Figure 3.67a) is distorted when compared with the upright view (Figure 3.67b), the navicular bone appearing longer in a proximodistal direction.



Figure 3.67(a) Dorsoproximal-palmarodistal oblique image of a normal navicular bone obtained using the 'high coronary' technique. Note the slight elongation of the navicular bone in a proximodistal plane compared with Figure 3.67(b) and loss of definition of its margins.



Figure 3.67(b) Dorsoproximal-palmarodistal oblique image of the same foot as Figure 3.67(a), obtained using the 'upright pedal' technique.

Downloaded From Vet-eBooks.com

Palmaroproximal-palmarodistal oblique view

In a well-positioned and exposed palmaroproximal-palmarodistal oblique image the dorsal articulation of the navicular bone with the middle phalanx should be clearly seen and the palmar aspect of the palmar compact bone should be seen as a distinct single line. If these cannot be seen then an additional radiograph should be obtained. The navicular bone has distinct dorsal and palmar compact bone of uniform opacity, separated by the spongiosa, which has a distinct trabecular pattern (Figures 3.68a and c, 3w.64e). The lucent zones seen on the distal border of the bone in dorsoproximal-palmarodistal views are visible within the spongiosa as circular or oval lucencies. The palmar compact bone has an even thickness, but a small, crescent-shaped or oval lucency may be evident in the sagittal ridge. The thickness of the compact bone may vary among breeds and among individuals, but a distinct margin between the compact bone and the spongiosa should always be present. In horses with upright foot conformation the palmar compact bone is usually thinner than in horses with more normal foot conformation (compare Figures

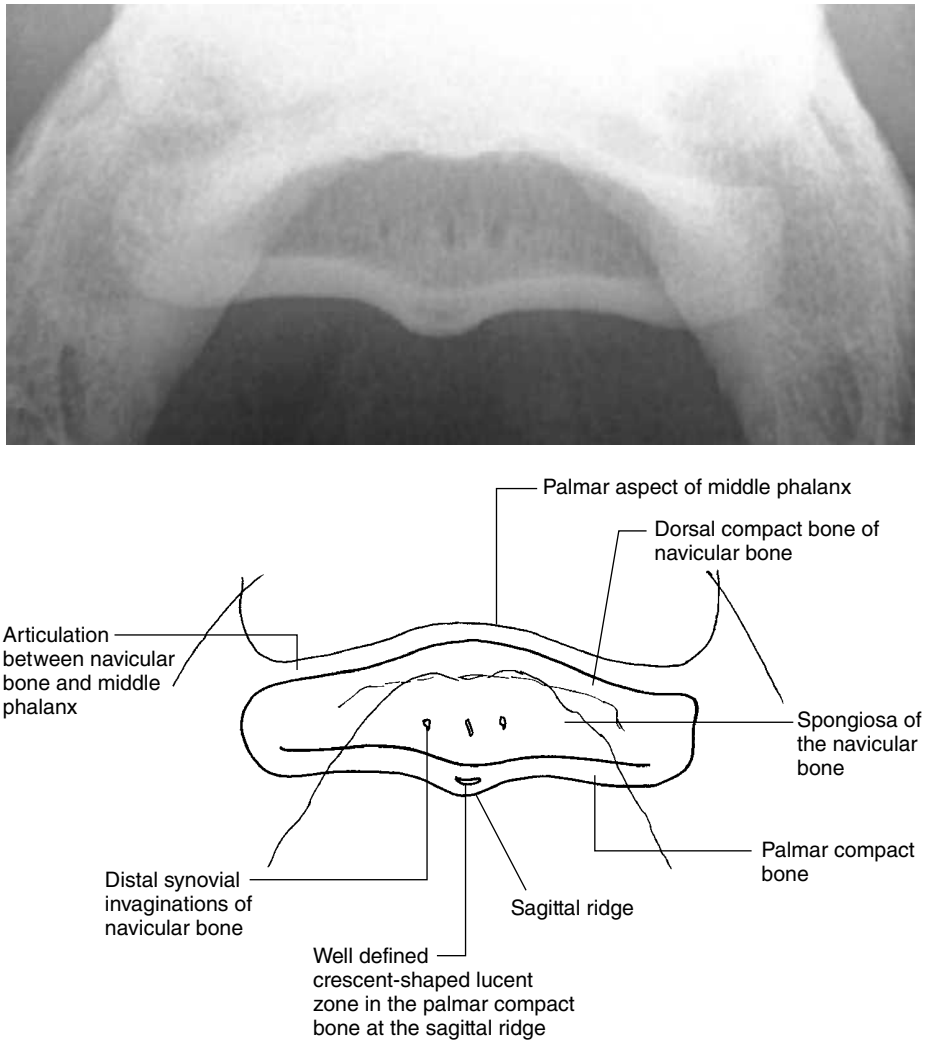


Figure 3.68(a) Palmaroproximal-palmarodistal oblique image and diagram of a normal adult navicular bone. Note the well-defined lucency in the palmar compact bone in the sagittal ridge, which may or may not be present.

Downloaded From Vet-eBooks.com

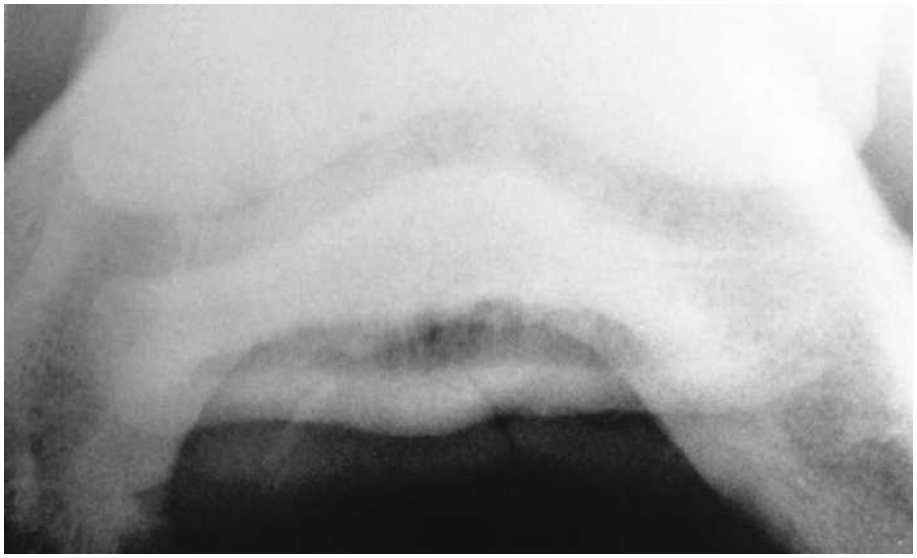


Figure 3.68(b) Palmar 45° proximal-palmarodistal oblique image of the navicular bone of a normal horse with an upright foot conformation. The spongiosa of the navicular bone is partially obliterated by the distal phalanx. The dorsal compact bone of the navicular bone cannot be assessed. There is apparent increased opacity of the spongiosa and poor compactospongiosa demarcation. The x-ray beam was not parallel to the palmar aspect of the navicular bone and the foot had been positioned too far forward. Compare with Figure 3.68(c).

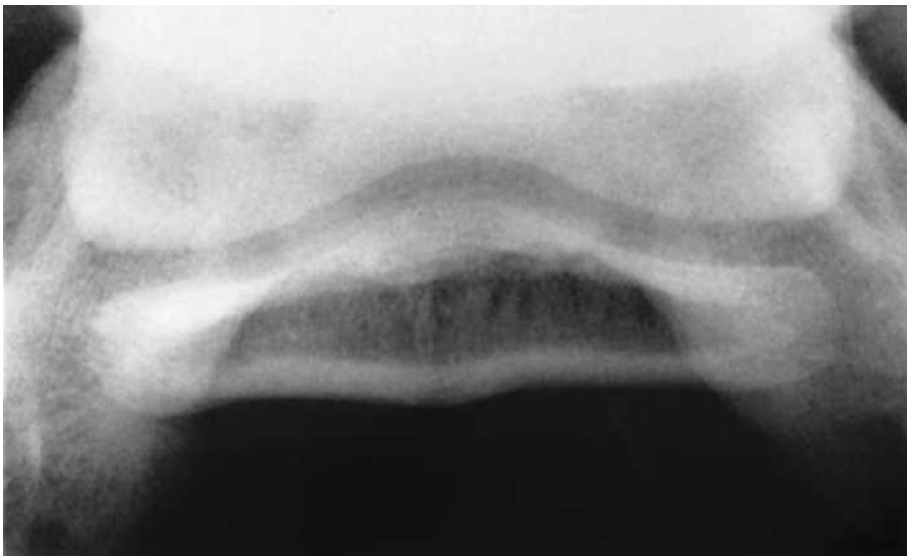


Figure 3.68(c) Palmar 50° proximal-palmarodistal oblique image of the navicular bone of the same horse as in Figure 3.68(b). There is a clear trabecular pattern within the spongiosa and excellent demarcation between the spongiosa and the compact bone. Note also that the palmar compact bone appears narrower than in Figure 3.68(b). The sagittal ridge is relatively flat, a normal variation.

3.68a and 3w.64e). In a horse with asymmetrical front feet, one being more upright than the other, the palmar compact bone of the navicular bone of the more upright foot is usually narrower than the contralateral limb. This reflects differential loading and the bone responding according to Wolff's law.

The crescent-shaped lucent zone in the sagittal ridge of the navicular bone is rarely seen in very young horses. It represents early navicular bone modelling in response to stress and is of unknown clinical significance. A relatively opaque reinforcement line develops in the subchondral bone parallel with the palmar compact bone in the region of the sagittal ridge. The intervening bone is relatively radiolucent and is projected in the palmaroproximal-palmarodistal oblique view as the crescent-shaped lucent zone in the sagittal ridge. If the bone between the reinforcement line and the palmar compact bone becomes compacted, then the lucent zone becomes less clear and may be obliterated.

Downloaded From Vet-eBooks.com

Dorsopalmar (weight-bearing) view

The navicular bone is largely obscured by the extensor process of the distal phalanx. The medial and lateral margins of the bone are seen clearly, as is its proximal border (see Figure 3.12).

NORMAL VARIATIONS AND INCIDENTAL FINDINGS

The outline of the navicular bone is extremely variable.

Lateromedial view

The navicular bone may be trapezoid in shape (Figure 3.10a), but frequently the palmar compact bone has proximal and/or distal elongations (Figure 3.65b and d). Such proximal and distal elongation should be differentiated from entheseophyte formation at the insertion of the collateral sesamoidean ligament or the origin of the distal sesamoidean impar ligament respectively. On a lateromedial image entheseophytes are less radiopaque compared with extension of the palmar compact bone, because they are thinner (Figures 3w.69a and 3w.69b). Entheseophytes are readily confirmed in a dorsoproximal-palmarodistal oblique and/or dorsopalmar images (see below and also 'Navicular disease', below). In addition an elongation of the bone usually shows as a smooth continuation of the palmar surface of the bone. An entheseophyte does not usually appear continuous with the sagittal ridge.

In a well-positioned lateromedial view there is an opaque line in the spongiosa palmar and parallel to the dorsal compact bone. This represents part of the medial and lateral aspects of the dorsal compact bone. If there are two radiopaque lines this indicates slight obliquity of the image.

The margins of the joint space between the navicular bone and the distal phalanx may be parallel (Figure 3.65b) or convergent (Figure 3.65a). The thickness of the palmar compact bone of the navicular bone is variable, tending to be thinner in horses with an upright foot conformation. It is usually bilaterally symmetrical unless there is disparity in foot shape, when the more upright foot usually has thinner palmar compact bone and the trabecular architecture may be more distinct (Figure 3w.70a). Marked increase in thickness of the palmar compact bone may reflect disease (Figure 3.76a). A small, shallow smooth-edged depression is present in the centre of the sagittal ridge of many normal horses (Figure 3.65c).

Dorsopalmar ('upright pedal') view

The number and size of the lucent zones along the distal border of the navicular bone vary among individuals and among breeds. It is probably normal to have up to seven lucent zones in the bone, and these are normally conical, and taller than they are wide. It has been demonstrated that compared with computed tomography, radiography underestimates the number and size of distal border synovial invaginations. The hind feet generally have two or three fewer than the front. There may be a double contour along the proximal border of the navicular bone. This may be due either to elongation of the palmar compact bone proximally, or entheseophyte formation.

Downloaded From Vet-eBooks.com

New bone on the proximal border of the navicular bone may be present in clinically normal horses. This is entheseophyte formation in the insertion of the collateral sesamoidean ligaments. It is normally most prominent at the medial and lateral aspects of the proximal border. Entheseous new bone is more common on the lateral aspect of the navicular bone than the medial. Its clinical significance is equivocal, but indicates previous stress to the ligament insertions. It may reflect a foot imbalance. Entheseous new bone along the proximal border may accompany other changes in the navicular bone, and be associated with 'navicular disease', especially if extensive. (On plantarodorsal views the navicular bone appears slightly larger relative to the middle phalanx.)

A double contour along the distal border of the bone represents the distal articular margin proximally and the distal aspect of the palmar compact bone distally. Discrete mineralised fragments are sometimes detectable distal to the navicular bone (see 'Navicular disease – Dorsoproximal-palmarodistal oblique ['upright pedal'] view', below and Figures 3.74 and 3.80). Although these occur more commonly in association with navicular disease, they are sometimes present as an incidental finding at the time of examination, particularly if there are no other detectable abnormalities of the navicular bone, but could potentially be associated with lameness in the future. These opacities may represent an avulsion fracture, separate centres of ossification or dystrophic mineralisation within the distal sesamoidean impar ligament.

Palmaroproximal-palmarodistal oblique view

Large nutrient foramina or synovial invaginations along the distal border of the navicular bone appear as large oval-shaped lucencies within the spongiosa. The thickness of the palmar compact bone varies considerably among horses. It is usually bilaterally symmetrical unless there is disparity in foot shape, when the more upright foot usually has a thinner palmar compact bone (Figure 3w.70b). The prominence of the sagittal ridge varies between horses, and sometimes appears flattened (Figure 3.68c).

A small, well-defined crescent-shaped or oval lucency may be evident in the sagittal ridge (Figure 3.68a).

SIGNIFICANT FINDINGS

Common artefacts

Structures overlying the navicular bone on radiographs are easily misinterpreted as radiographic lesions. The following should be borne in mind:

1 There is a variably-sized depression in the palmar aspect of the middle phalanx, proximal to the articular surface, which may appear relatively lucent, and is easily superimposed over the navicular bone.

2 The clefts and central sulcus of the frog are superimposed over the navicular bone on the dorsoproximal-palmarodistal oblique ('upright pedal') view. They can mimic radiolucencies or fractures, especially if poorly filled with packing or if the packing becomes loose.

3 Excess and poorly distributed packing in the frog clefts can appear as an opacity proximal to the navicular bone, mimicking entheseophyte formation.

Downloaded From Vet-eBooks.com

If there is difficulty in differentiating lesions from artefacts, it is recommended that the foot be re-packed and the view repeated using a slight change in angle. Packing should be limited to the frog clefts, and not spread across the sole or heel, unless there are significant 'holes' in the sole which may need to be filled individually with packing.

4 The marrow cavity in the middle phalanx, when present, is variable in size. It is easily superimposed over the navicular bone and care should be taken, when assessing radiographs, not to confuse it with a lucent lesion in the navicular bone.

5 There is a row of nutrient foramina in the proximal end of the middle phalanx running across the shaft of the bone, immediately distal to the transverse prominence or tuberosity. These foramina are seen to varying degrees on the dorsoproximal-palmarodistal oblique ('upright pedal') view, depending on the angle of the projection. If the pastern is angled too far forward during radiography, these foramina may be superimposed over the navicular bone, giving the appearance of abnormal proximal nutrient foramina.

6 A radiolucent lesion in the middle phalanx may be superimposed over the navicular bone and mimic an osseous cyst-like lesion in the navicular bone.

Congenital abnormalities of the navicular bone

Occasionally the navicular bone is absent. This abnormality can occur alone or in association with dysgenesis of the distal phalanx.

A navicular bone may be bipartite (Figures 3w.71a and 3w.71b) or occasionally tripartite. This may occur in a single limb of a horse or in more than one limb. In contrast to a fracture, the radiolucent line between the separate bone sections is broad with or without lucent areas adjacent to it, and the bone margins tend to be smooth and rounded. A bipartite navicular bone may be associated with lameness. A bipartite navicular bone has been described in association with a bipartite distal phalanx.

Navicular disease

The term 'Navicular disease syndrome' has unfortunately been coined by some clinicians to refer to almost any condition causing pain in the palmar aspect of the foot, whether the navicular bone is involved or not. We strongly urge readers not to use this terminology. There is however a degenerative condition of the navicular bone that has traditionally been referred to as navicular disease, which is the subject of this section.

For the purposes of this book, the term 'navicular disease' is used to describe a clinical condition, causing a unilateral or bilateral progressive forelimb lameness which is not permanently alleviated by rest or corrective shoeing alone. It is acknowledged that there are horses which show clinical signs typical of navicular disease which may have pain arising from the navicular bone or its associated soft-tissue structures, but the condition can be alleviated by rest or shoeing. The term 'navicular syndrome' may be used to encompass these horses since they may at a later stage progress towards a less responsive disease. They must be differentiated from horses which have pain in the palmar aspect of the foot due to other causes (see 'Long-toe low-heel syndrome', above).

Recent advances in knowledge with the advent of magnetic resonance imaging and pathological investigation of less chronic cases of navicular

Downloaded From Vet-eBooks.com

disease indicate that there is a variety of different pathological changes that may affect the navicular bone, and thus confirm that the term navicular disease may be oversimplistic. There are a variety of different conditions that can affect the bone which do not necessarily have a unifying pathogenesis.

Considerable controversy exists over the significance of radiographic changes in the navicular bone. To relate them to the clinical situation, it is probably best to use the description given above (see 'Navicular bone – Normal anatomy' and 'Normal variations and incidental findings') as being indicative of a normal bone, and accept that a number of apparently normal horses do have radiographic changes in the navicular bones. When these changes are present in sound horses, their significance is equivocal. Some clinicians consider that they may predispose the horse to developing navicular disease at a later date, but this is by no means certain. Repeat radiographs are sometimes obtained after a period of 4–6 months, to assess the progression of such lesions. Progression, however, can occur in animals which remain clinically normal, and those that become lame may show no such progression. Bilateral radiographic abnormalities are frequently seen in horses with unilateral lameness, and unilateral changes may be seen in horses that are bilaterally lame.

It is probably best, therefore, to accept that the more changes present, and the greater the degree of change, the more likely the horse is to have navicular disease. In the absence of radiographic abnormality, navicular disease should only be diagnosed with extreme caution unless supported by magnetic resonance imaging findings. Significant abnormalities of the navicular bone have been detected using magnetic resonance imaging in horses in which the navicular bone has been radiographically normal. These abnormalities have been verified histologically. Radiographic abnormalities of the navicular bone are frequently accompanied by lesions of the collateral sesamoidean ligament and/or the distal sesamoidean impar ligament and/or the deep digital flexor tendon which may adversely influence prognosis.

Although navicular disease is generally assumed to be a disease of the front feet, it can occur in hind feet, either unilaterally or bilaterally.

Lateromedial view

There are contradictory reports about changes in the shape of the navicular bone in navicular disease. It is however known that the bone models because of chronic stress on the collateral sesamoidean ligaments and distal sesamoidean impar ligament, resulting in entheseophyte formation, and proximal or distal elongation of the palmar compact bone may develop.

There may be alteration in thickness of the palmar compact bone, which may result in the palmar compact bone becoming thicker distally than proximally. In some cases the distal fossa may become more prominent. In advanced cases some lucency of the bone proximal to the fossa may be seen. The trabecular bone may appear more opaque with increase in thickness of the palmar and/or dorsal compact bone, and reduction of the cross-sectional area of the spongiosa. There is also reduced definition between the areas of compact and trabecular bone. Irregular endosteal new bone may be seen dorsal to the palmar compact bone of the navicular bone (Figure 3.76a).

When a radiolucent lesion is present in the body of the bone, it may be seen on a lateromedial image, but often is not identifiable (Figure 3.72a). It is generally accepted as confirming some form of pathological process in the

Downloaded From Vet-eBooks.com

navicular bone (Figure 3.72b). If it penetrates the palmar surface of the bone, it may be evident as a sharp-edged lesion in the palmar compact bone (see Figure 3.72c). This lesion must be differentiated from the previously described depression in the sagittal ridge (see Figure 3.65c).

Entheseophytes can be seen on a lateromedial image on the proximal and distal borders of the bone (Figure 3.76a). These are described in more detail under 'New bone formation'. Irregularity of the bone at the origin of the distal sesamoidean impar ligament (Figure 3.39) is an indication that the dorsoproximal-palmarodistal oblique view should be carefully examined. This irregularity may be due to either entheseophyte formation in the distal sesamoidean impar ligament or to a mineralised opacity distal to the bone. Osteophytes on the dorsoproximal margin of the navicular bone may be an indicator of degenerative joint disease of the distal interphalangeal joint. They do not indicate navicular disease, although they may be seen in association with it.



Figure 3.72(a) Oblique lateromedial image of the left hind navicular bone of a 5-year-old general-purpose Thoroughbred cross horse with lameness improved by perineural analgesia of the plantar digital nerves or intrathecal analgesia of the navicular bursa. There is distal extension of the plantar compact bone of the navicular bone. Compare with Figure 3.72(b).



Figure 3.72(b) Dorsoproximal-plantarodistal oblique image of the left hind navicular bone seen in Figure 3.72(a). There are two large radiolucent areas abaxial to the sagittal midline in the distal half of the spongiosa of the navicular bone.

Downloaded From Vet-eBooks.com



Figure 3.72(c) Lateromedial image of the right front navicular bone of an 8-year-old Quarterhorse cross gelding with lameness of 5 months' duration. There is an ill-defined radiolucent area in the sagittal ridge of the palmar compact bone (arrow). This lesion was the result of a penetrating injury.

Dorsoproximal-palmarodistal oblique ('upright pedal') view

The lucent zones on the distal border of the navicular bone, representing synovial invaginations, frequently have a change in shape from the normal described above (compare Figure 3.66 with Figures 3.73a–d). It has been suggested that lucent zones of certain shapes have a greater significance than others. There is evidence that the greater the number of abnormally shaped lucent zones, the more likely are clinical signs of navicular disease to be present. Similarly an increased number of lucent zones (more than seven), and the radiographic appearance of lucent zones on the lateral, medial or proximal borders of the bone (Figure 3.73d), are all indicators of abnormality. An irregular appearance of lucent zones, i.e. of many different shapes and sizes, and lucent zones surrounded by a halo of increased opacity should also be viewed with suspicion. However, it is important to recognise that the navicular bone is an intimate part of the distal interphalangeal joint and an increase in number, size and shape of these radiolucent zones may reflect distal interphalangeal joint disease. The distal border of the navicular bone provides the origin of the distal sesamoidean impar ligament, therefore injury to this ligament may also be associated with changes to the architecture of the distal aspect of the navicular bone, including entheseophyte formation, avulsion fragments and possibly alterations of the radiolucent zones.

If there is a lucent area at the medial or lateral angle of the distal border of the navicular bone (at the junction between the horizontal and medial and lateral sloping borders), it is likely that there is an associated distal border fragment (Figure 3.74). The frequency of recognition of such fragments has increased with better-quality radiographs obtained with digital or computerised radiography. Fragments may occur laterally and/or medially, lateral fragments being more common. Fragments occur more commonly in lame horses with other radiological abnormalities of the navicular bone than in sound horses undergoing a pre-purchase examination. Comparison between radiographs and high-field magnetic resonance images indicates that large distal border fragments can reliably be detected with good radiographic technique, but small fragments may be overlooked. A distal border fragment seen in association with a radiolucent area at the ipsilateral angle of the distal aspect of the navicular bone is likely to be of clinical significance. Distal border fragments are often seen in association with other

Downloaded From Vet-eBooks.com

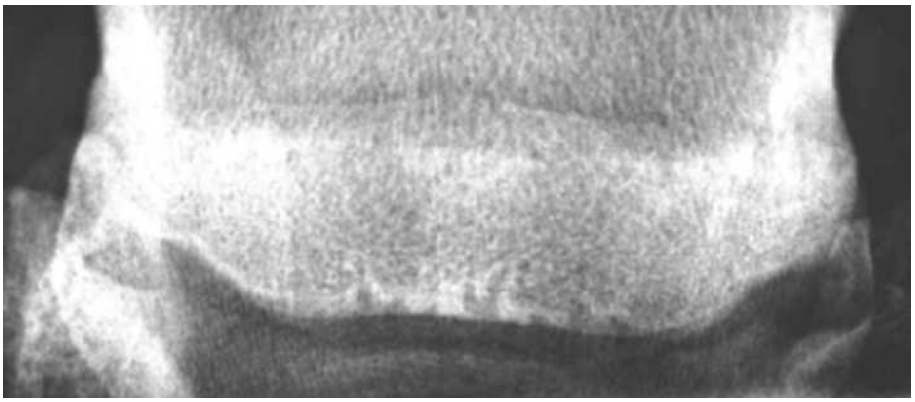


Figure 3.73(a) Dorsoproximal-palmarodistal oblique image of a navicular bone of a 5-year-old Quarterhorse gelding. There are multiple variably shaped and sized radiolucent zones along the horizontal distal border of the navicular bone.

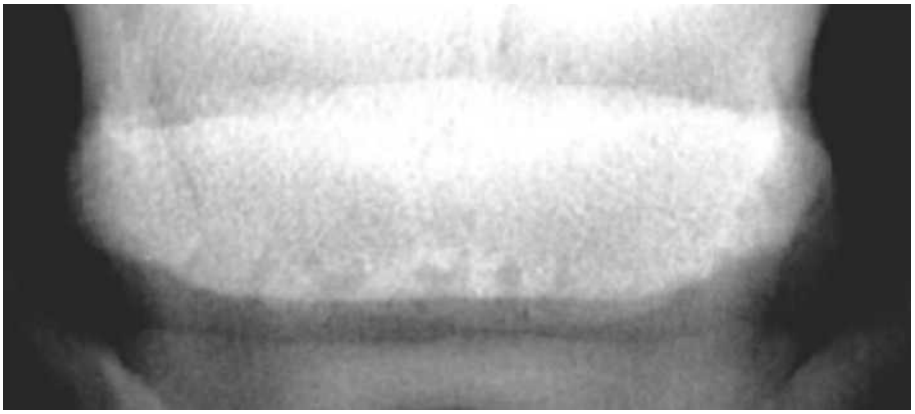


Figure 3.73(b) Dorsoproximal-palmarodistal oblique image of a navicular bone of a 7-year-old crossbred gelding. Medial is to the left. There are multiple large variably shaped lucent zones along the distal horizontal and medial sloping borders of the navicular bone.

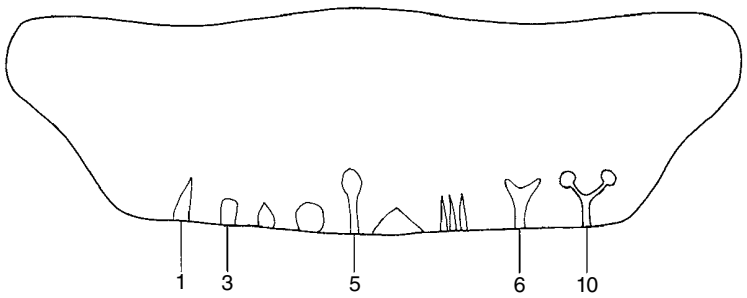


Figure 3.73(c) Diagram of a dorsoproximal-palmarodistal oblique image of a navicular bone showing distal nutrient foramina (synovial invaginations) of different shapes (after Colles, 1982). The numbers refer to the scoring system of MacGregor (1986). Larger numbers may indicate foramina of greater clinical significance.

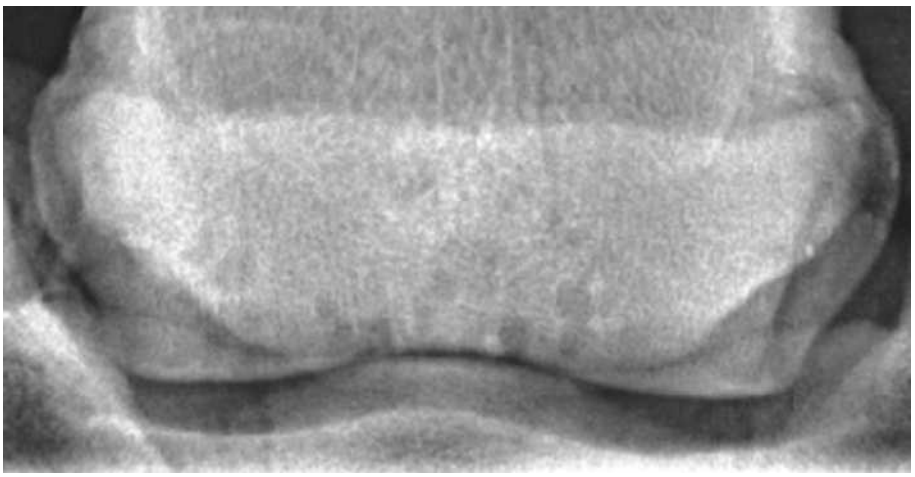


Figure 3.73(d) Dorsoproximal-palmarodistal oblique image of a navicular bone of a 7-year-old Warmblood gelding. Medial is to the left. There are multiple large lucent zones along the distal medial sloping and distal horizontal borders of the navicular bone and ill-defined lucent zones in the spongiosa of the bone. The lateral proximal border of the bone is modelled.

Downloaded From Vet-eBooks.com

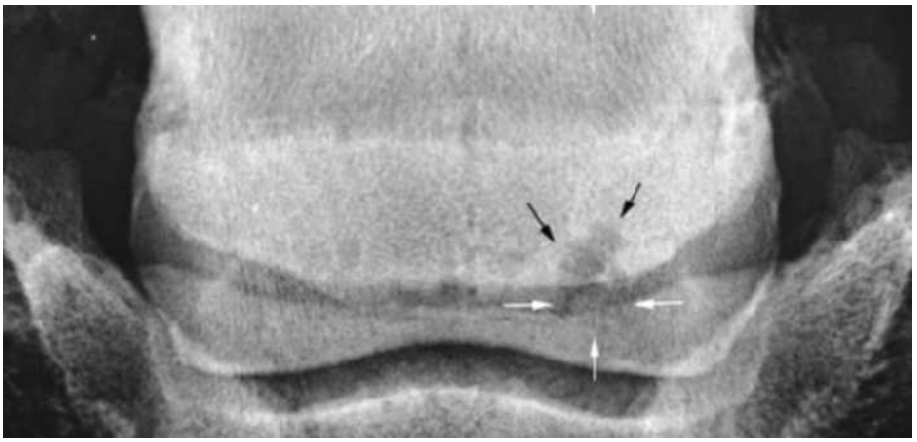


Figure 3.74 Dorsoproximal-palmarodistal oblique radiographic image of the navicular bone of an 8-year-old Thoroughbred cross gelding. Medial is to the left. There are several variably shaped and sized lucent zones along the distal border of the navicular bone. There is a large radiolucent zone at the lateral angle of the navicular bone (black arrows), distal to which is an osseous fragment (white arrows).

radiological abnormalities of the navicular bone suggestive of navicular disease. However, occasionally a fragment is identified together with a radiolucent area in the adjacent parent bone, which has been verified using magnetic resonance imaging as the likely cause of lameness in the absence of any other detectable abnormality. The presence of such fragments may be associated with fibrosis, chondroid metaplasia, tears in the adjacent distal sesamoidean ligament, and bone necrosis in the adjacent navicular bone. Mineralised fragments in isolation with no other abnormality of the navicular bone may be seen unassociated with current clinical signs. These lesions may be associated with 'navicular disease', or may be unrelated lesions. Their clinical significance remains equivocal, and should be assessed on an individual case basis.

Distinct areas of radiolucency within the navicular bone (Figure 3.75a) which are not associated with the distal border of the bone should always be regarded with extreme caution. Although clinical signs may not be present at the time of examination, lameness is likely to develop. The majority of these lucent lesions occur in the central one-third of the bone, but the entire bone should be inspected carefully. If these lesions are detected on dorsoproximal-palmarodistal oblique views, it is important to inspect lateromedial and palmaroproximal-palmarodistal oblique views carefully to ascertain whether they are contained within the body of the bone or penetrate the palmar surface (Figure 3.75b). If the lesion progresses to penetrate through the palmar surface of the bone, adhesion of the deep digital flexor tendon will result. Adhesions may also occur in the absence of other radiological changes in the navicular bone. Once adhesions are present, a very poor prognosis must be given.

In advanced stages of the disease there may be an appreciable increase in opacity of the bone, with or without thickening of the palmar compact bone and loss of definition between the palmar compact bone and the spongiosa. This is best assessed on the lateromedial or palmaroproximal-palmarodistal oblique views. This warrants a very poor prognosis for treatment.

Downloaded From Vet-eBooks.com

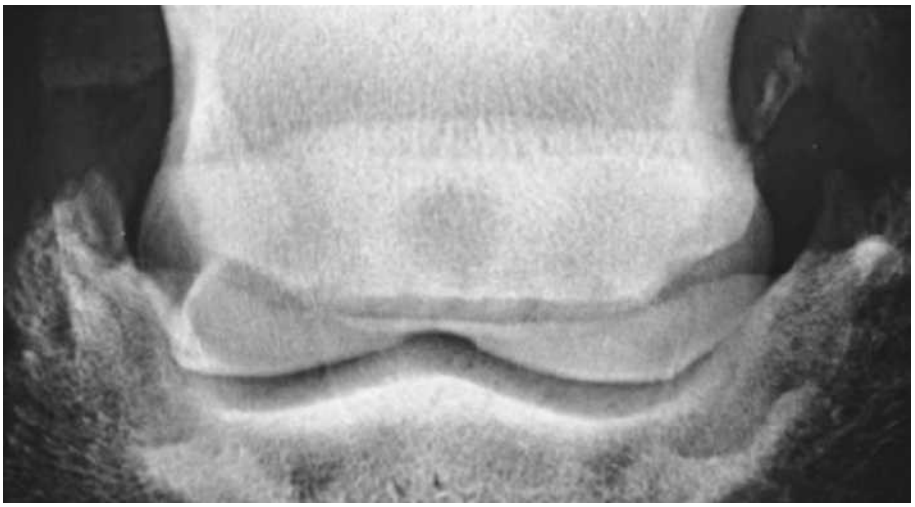


Figure 3.75(a) Dorsoproximal-palmarodistal oblique radiographic image of a navicular bone of a 6-year-old Warmblood gelding. There is a large circular radiolucent zone in the centre of the bone, which penetrated the palmar compact bone. See Figure 3.75(b).

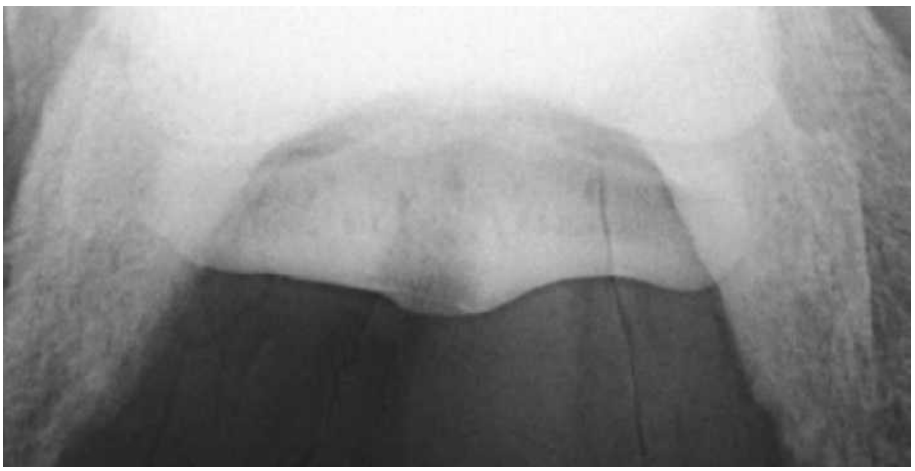


Figure 3.75(b) Palmaroproximal-palmarodistal oblique radiographic image of the same navicular bone as in Figure 3.75(a). There is a large radiolucent defect in the palmar compact bone at the sagittal ridge. The palmar compact bone is markedly thickened and there is extensive increased opacity of the spongiosa of the navicular bone. There was an adhesion of the deep digital flexor tendon to the palmar compact bone defect.

Occasionally an avulsion fracture can be identified at the insertion of the distal sesamoidean impar ligament on the distal phalanx.

Palmaroproximal-palmarodistal oblique view

On a palmaroproximal-palmarodistal oblique view, alterations in the shape of the lucent zones on the distal border of the bone cannot be identified, but increased size and numbers are sometimes evident early in the course of navicular disease.

This view may help to determine whether lucent lesions are present in the spongiosa or palmar compact bone, or both (Figure 3.75b). A palmaroproximal-palmarodistal oblique view cannot highlight the entire palmar compact bone from its proximal to distal border, and a focal defect which does penetrate the palmar aspect may not be detectable radiographically, either because the x-ray beam is not tangential to that portion of the bone, or as a result of summation of surrounding normal dense bone. In some horses, however, significant radiolucent zones in the palmar compact bone are only seen in a palmaroproximal-palmarodistal oblique image, in all other views the navicular bone appearing normal (Figure 3.75c).

Downloaded From Vet-eBooks.com

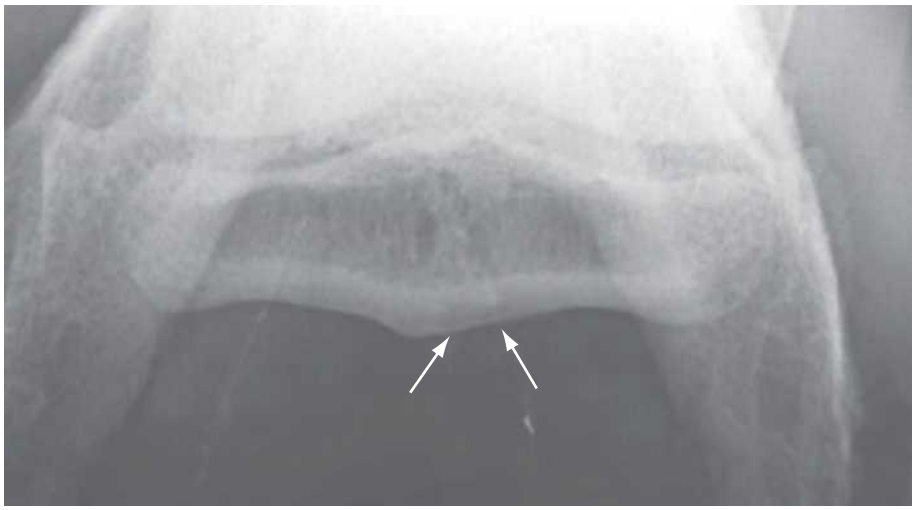


Figure 3.75(c) Palmaroproximal-palmarodistal oblique radiographic image of a navicular bone of a 6-year-old Warmblood cross gelding. Medial is to the left. There is a large radiolucent defect in the palmar compact bone of the navicular bone lateral to the sagittal ridge (arrows). There are also two large oval-shaped radiolucent zones in the spongiosa. No significant abnormalities were detected in other radiographic projections.

Localised thinning or reduced radiopacity of the palmar compact bone is associated with fibrocartilage degeneration, which may ultimately be associated with tendon adhesions.

The palmar compact bone may become uniformly thicker, encroaching into the spongiosa (Figure 3.76a), or endosteal new bone may develop (Figure 3.76b). The trabecular pattern of the spongiosa may become less obvious due to generalised increased radiopacity and/or thickening of trabeculae, resulting in loss of compact and spongious bone definition (Figure 3.75b). This may be artefactual (Figure 3.68b) due to inappropriate radiographic technique, and so it is important to compare the lateromedial and palmaroproximal-palmarodistal oblique images. It is important to be critical of the positioning of both the lateromedial and the palmaroproximal-palmarodistal oblique images. If positioning is inadequate an additional image should be acquired.

Occasionally new bone is seen on the palmar aspect of the palmar compact bone (Figure 3.77). This may be seen in the absence of other radiographic abnormalities, emphasising the importance of this radiographic view in horses with suspected navicular pathology. Such new bone warrants a poor prognosis for future soundness.

A distal border fragment may be seen superimposed over the spongiosa in some horses, resulting in an area of relatively increased opacity. This is usually apparent when there is an extensive radiolucent region in the distal aspect of the navicular bone seen in a dorsoproximal-palmarodistal oblique view, which highlights the potential presence of a fragment.

The zoom facility of digital and computed images or a magnifying glass for conventional images may be useful to study the palmar compact bone in fine detail.

Positive contrast studies of the navicular bursa may enhance the interpretation of palmar fibrocartilage changes, but care must be taken not to cause iatrogenic lesions. Defects may also be identified using transcuneal ultrasonography.

New bone formation

The clinical significance of new bone along the margins of the navicular bone is questionable. Large amounts of new bone accompanied by other changes however may be significant.

Downloaded From Vet-eBooks.com

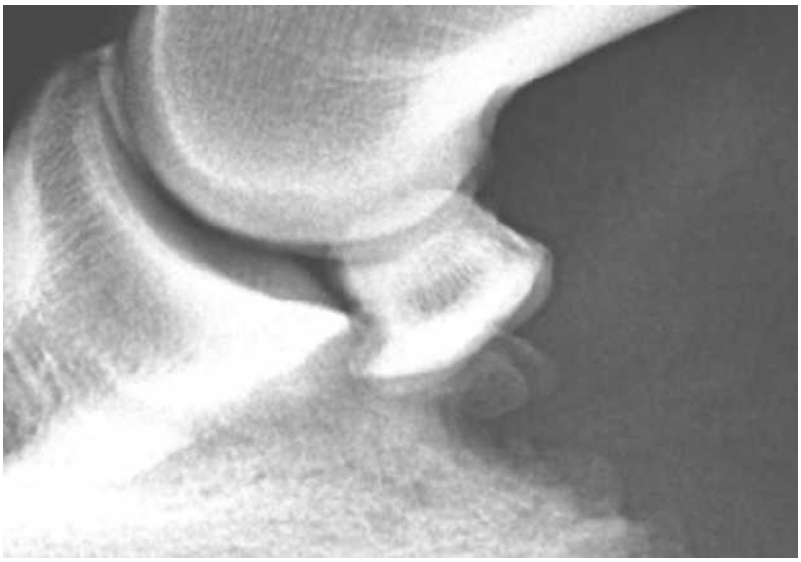


Figure 3.76(a) Lateromedial radiographic view of the navicular bone of a 4-year-old Warmblood mare with bilateral forelimb lameness. The palmar compact bone of the navicular bone is abnormally thick and there is distal extension of the palmar compact bone.

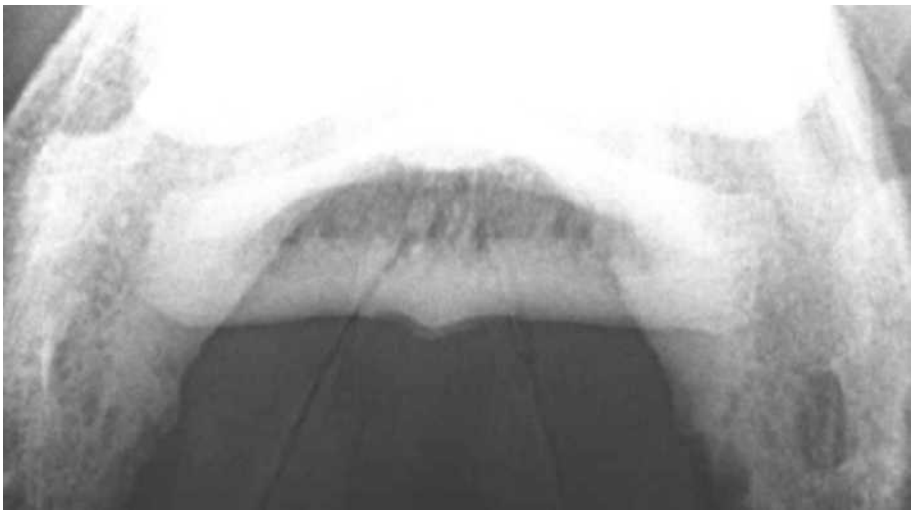


Figure 3.76(b) Palmaroproximal-palmarodistal oblique radiographic image of a navicular bone of a 7-year-old general-purpose riding horse. The palmar compact bone of the navicular bone is thick and there is considerable endosteal new bone.

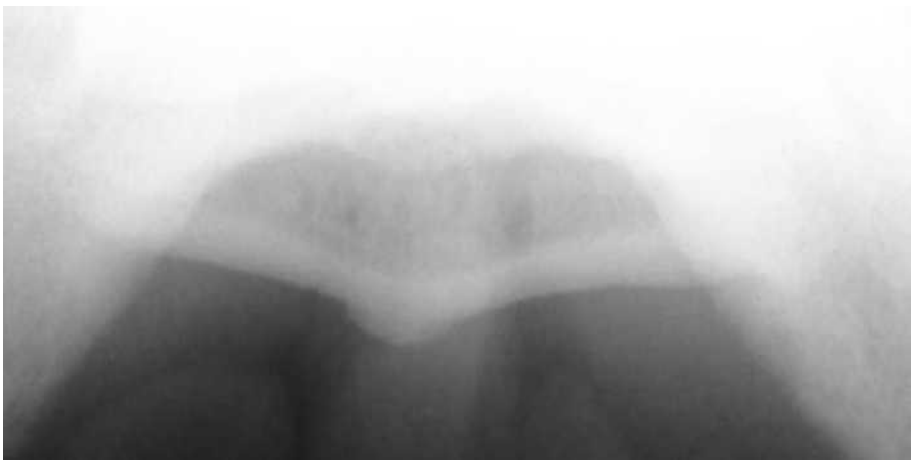
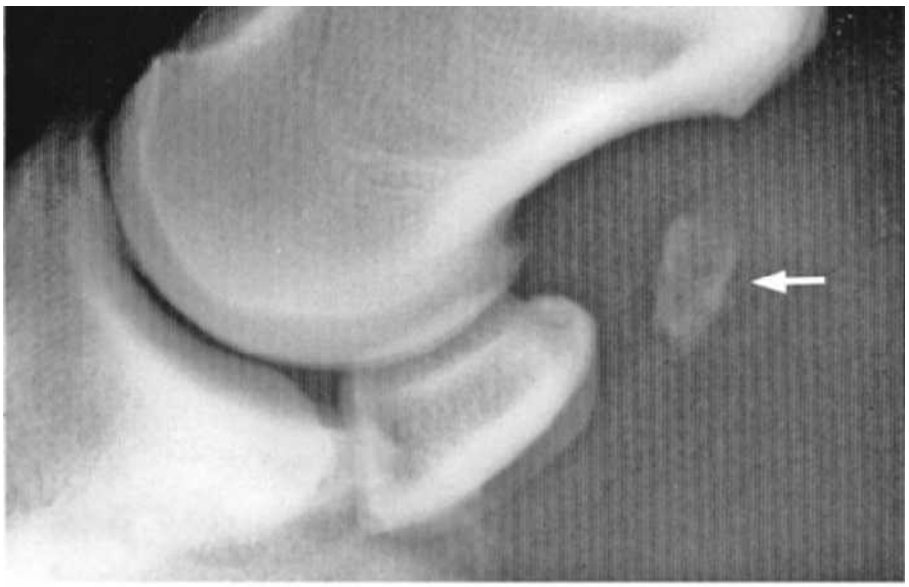


Figure 3.77 Palmaroproximal-palmarodistal oblique radiograph of a navicular bone. Note the irregular outline of the sagittal ridge due to new bone formation.

Downloaded From Vet-eBooks.com

Entheseophyte formation is frequently seen in the collateral sesamoidean ligaments. This is seen on the proximal border of the bone on dorsopalmar and dorsoproximal-palmarodistal oblique views, and on the palmar aspect of the proximal border of the bone on lateromedial views (see 'Navicular bone – Normal variations and incidental findings', above). Entheseophytes are believed to reflect abnormal tension in the collateral sesamoidean ligaments of the navicular bone, and should be differentiated from osteophytes (see below). There is a significantly higher incidence on the lateral side of the foot. Larger entheseophytes are more likely to be of clinical significance than small entheseophytes.

Dystrophic mineralisation or ossification, or an avulsion fracture can occasionally occur at the insertion of the collateral sesamoidean ligaments, seen as a discrete opacity proximal to the lateral or medial border of the bone. It is often, but not always, associated with lameness (Figures 3.78a and 3.78b).



(a)



(b)

Figure 3.78 Radiographs of a navicular bone, showing dystrophic mineralisation in the lateral collateral sesamoidean ligament (arrow): (a) lateromedial image; (b) dorsoproximal-palmarodistal oblique ('upright pedal') image (lateral is to the right). Note that there is some dirt in the frog clefts and modelling of the proximal border of the navicular bone. There are a number of enlarged lucent zones along the distal border of the bone, some of which also show a change in shape. The images were acquired using conventional film, screen and a grid. The vertical moiré lines on these reproductions of the images are the result of the grid.

Downloaded From Vet-eBooks.com

Periarticular osteophytes are occasionally seen along the dorsal margin of the proximal border on lateromedial views (Figure 3.79). They are frequently seen in association with degenerative joint disease of the distal interphalangeal joint and warrant a poor prognosis.

Entheseophytes on the distal margin of the navicular bone at the origin of the distal sesamoidean impar ligament tend to be smaller than on the proximal border, and are thought to be more significant.

Discrete radiopaque fragments may be seen along the distal border of the bone (Figures 3.74 and 3.80). These are of variable aetiology, but cannot be differentiated radiographically. They may be located within a depression in the distal border of the bone and are more common at the medial and lateral borders of the bone. They may result from avulsion fractures, fractures of

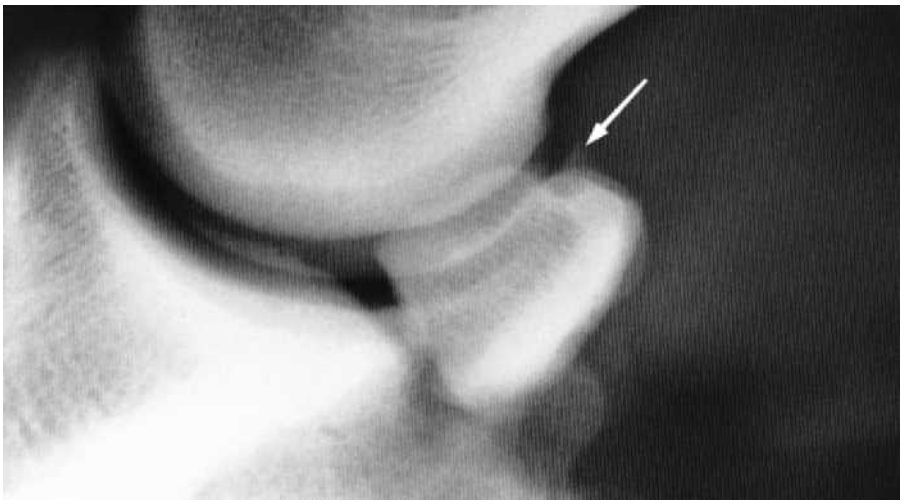


Figure 3.79 Lateromedial image of a navicular bone, showing periarticular osteophytes (arrow) on the dorsoproximal border.

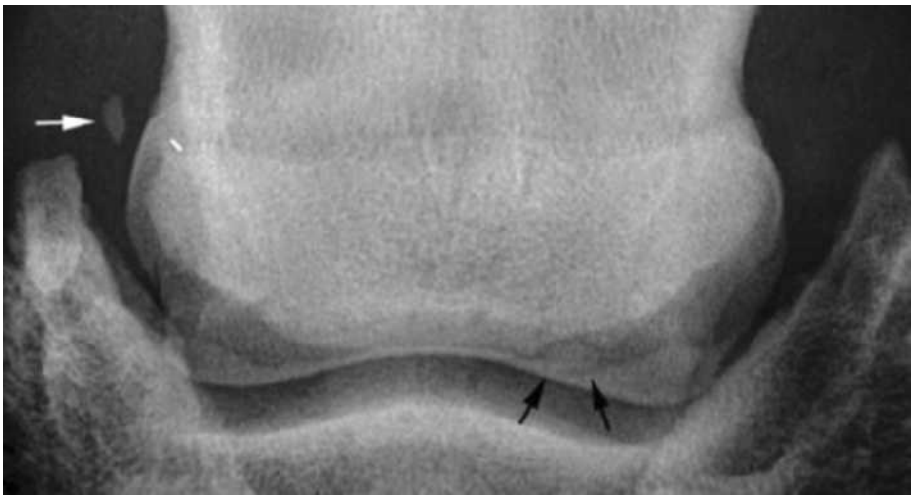


Figure 3.80 Dorsoproximal-palmarodistal oblique radiographic image of a navicular bone. Medial is to the left. There is a well-defined osseous opacity distal to the navicular bone at the lateral angle (black arrows). The opacity of the navicular bone is relatively normal, however there is a concave defect in the navicular bone proximal to the fragment. Note also the discrete mineralised opacity proximomedial to the navicular bone (white arrow), probably dystrophic mineralisation within the collateral sesamoidean ligament.

Downloaded From Vet-eBooks.com

entheseophytes, or dystrophic mineralisation in the distal sesamoidean impar ligament. Their significance is discussed above, 'Dorsoproximal-palmarodistal oblique ('upright pedal') view'.

Mineralisation in the deep digital flexor tendon

Focal mineralisation occasionally occurs in the deep digital flexor tendon palmar to the middle phalanx or the navicular bone (Figure 3.81). The cause of this is unknown, but probably reflects chronic tendon injury (see Chapter 1). It carries a poor prognosis. It is most easily seen on a lateromedial view, but should not be confused with ossification of the ungular cartilages, which can be differentiated on a dorsopalmar (weight-bearing) view. Dystrophic mineralisation, in or close to the navicular bursa, or palmar to the deep digital flexor tendon, has also been seen as a sequel to repetitive medication of the navicular bursa (region) with corticosteroids although this is not a common complication.

Infection

Infection of the navicular bursa or bone usually occurs subsequent to a penetrating wound or after an injection into the navicular bursa. Plain radiographs obtained at the time of injury may reveal no abnormality, but if a draining sinus is present, contrast radiography may be of value (see 'Fistulography'). The use of a radiodense probe can also be useful to determine the depth and orientation of a penetrating injury. Lateromedial and palmaroproximal-palmarodistal oblique views should be obtained. Follow-up radiographs may be helpful if lameness persists. Extensive ill-defined lucent lesions, and occasionally increased opacity of the palmar compact bone of the navicular bone, warrant a very poor prognosis. If a penetrating



Figure 3.81 Lateromedial radiographic image of a foot of a 9-year-old Warmblood pleasure horse. There is mineralisation in the deep digital flexor tendon (arrow). There is modelling of the proximal border of the navicular bone and periarticular osteophyte formation, together with periarticular osteophyte formation involving both the proximal and distal interphalangeal joints. The distal solear margin of the distal phalanx slopes downwards from dorsal to palmar.

Downloaded From Vet-eBooks.com

wound has occurred, immediate and extensive flushing of the navicular bursa and antimicrobial treatment are required.

Fractures

Small radiopaque bodies in the distal sesamoidean impar ligament, adjacent to the distal border of the bone, are discussed previously (see above, and Figures 3.74 and 3.80). They are very difficult to demonstrate clearly on any radiographic view, but are most easily detected on the dorsoproximal-palmarodistal oblique view. Occasionally a fracture occurs at the insertion of the collateral sesamoidean ligament.

Fractures through the body of the navicular bone normally occur parallel to the sagittal ridge of the bone, or slightly obliquely to it, and at varying distance from it (Figure 3.82a). There is normally little or no displacement, and the fracture may be very difficult to see, particularly in the acute stage. After 2–4 weeks the fracture line becomes more obvious due to bone demineralisation. Subsequently lucent zones develop along the fracture line (Figure 3.82b) and an increased number of lucent zones along the distal border of the bone may be seen, especially in the bone immediately adjacent to the fracture. Several dorsopalmar views of slightly varying obliquity as well as palmaroproximal-palmarodistal views may be required to confirm the presence of a fracture, and to differentiate it from overlying artefacts (such as lucent lines caused by the frog). A parasagittal fracture viewed on several radiographs should remain in the same position relative to the margins of the bone, should not extend beyond the bone margins and should be seen in both dorsoproximal-palmarodistal oblique and palmaroproximal-palmarodistal oblique views. It may be necessary to adjust the packing in the frog clefts. Damage to the adjacent deep digital flexor tendon may also occur. Occasionally fractures are comminuted; in some horses this may only be detectable in a palmaroproximal-palmarodistal oblique image (Figure 3w.82c).

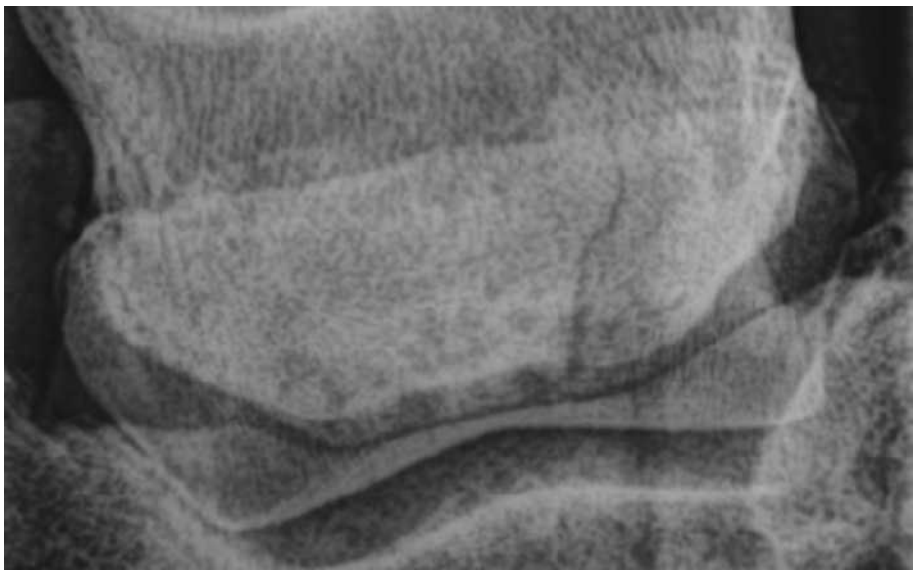


Figure 3.82(a) Dorsoproximal-palmarodistal oblique image of a navicular bone. Medial is to the left. There is a parasagittal fracture of the body of the bone (the fracture is of 2 weeks' duration).

Downloaded From Vet-eBooks.com



Figure 3.82(b) Dorsoproximal-palmarodistal oblique radiographic image of the navicular bone of a 9-year-old general-purpose riding horse with recent onset lameness improved by perineural analgesia of the palmar digital nerves. Medial is to the left. There is a chronic parasagittal fracture of the navicular bone laterally. The fracture line is quite wide and there are lucent areas adjacent to it. There is modelling of the lateral aspect of the navicular bone. This radiological appearance could also be consistent with a bipartite navicular bone. Radiopharmaceutical uptake in the bone was normal and lameness was due to a core lesion of the deep digital flexor tendon.

Surgical fixation of an acute fracture (less than 10 weeks' duration) should be considered. More longstanding fractures may respond to surgery, but the success rate becomes poorer the longer the fracture has been present. Radiolucencies along the length of the fracture line and adjacent to it generally start to develop 6–8 weeks after the fracture occurs. Fractures usually cause acute lameness for 1 or 2 days, with rapid improvement at the walk within a week, although if trotted lameness persists. There is usually only limited response to pressure or concussion of the hoof.

Fractures carry a poor prognosis for return to work without internal fixation. Prognosis is favourable for breeding purposes. In very small ponies a slightly better prognosis for return to work can be given with conservative management. If a fracture appears chronic radiographically at the time of onset of lameness (i.e. a broad radiolucent line with multiple lucent zones along the fracture line), the fracture may not be the cause of lameness, as fractures normally heal by fibrous rather than osseous union. Nuclear scintigraphy may be helpful to determine if it is an active lesion.

Fractures occasionally occur horizontally across the bone, close to and parallel with its distal border (Figure 3w.82d). There may be one large fracture or two or three smaller pieces. Occasionally comminuted fractures occur. Horizontal fractures are more common in hindlimbs than forelimbs. Rupture of the distal sesamoidean ligament with proximal displacement of the navicular bone has been reported in hindlimbs, with or without concurrent avulsion fractures.

Occasionally an avulsion fracture occurs at the insertion of the distal sesamoidean impar ligament on the distal phalanx (Figure 3.83).

Proximal displacement of the navicular bone

Complete disruption of the distal sesamoidean impar ligament results in proximal displacement of the navicular bone. There may or may not be associated avulsion fragments of the distal aspect of the bone. This unusual injury

Downloaded From Vet-eBooks.com



Figure 3.83 Dorsoproximal-palmarodistal oblique radiographic image of the right front foot of a 6-year-old Thoroughbred event horse. Lateral is to the right. There is an ill-defined radiolucent area in the proximolateral aspect of the distal phalanx (arrows) with ill-defined opacities superimposed. These represented avulsion fractures at the insertion of the distal sesamoidean impar ligament. There are also several variably shaped and sized lucent zones along the distal border of the navicular bone.

occurs more in hindlimbs than in forelimbs. Some horses have returned to full work (steeplechasing) following prolonged rest. Proximal displacement of the navicular bone occasionally occurs subsequent to ligament disruption by a deeply penetrating foreign body.

Osseous lesions of the foot which may be missed using radiography

Since the advent of magnetic resonance imaging we have recognised that some osseous pathology can be detected with no associated radiological abnormalities. Magnetic resonance imaging has higher sensitivity for identification of osseous cyst-like lesions in the middle and distal phalanges close to the articular margins of the distal phalanx. Focal defects in the proximopalmar aspect of the distal phalanx with extensive surrounding osseous reaction are associated with severe lameness improved by intra-articular analgesia of the distal interphalangeal joint. Focal or more diffuse areas of increased signal intensity in fat-suppressed images in the distal dorsal aspect of the middle phalanx or anywhere in the distal phalanx may represent bone trauma. There is a form of navicular disease characterised by diffuse increased signal intensity in the spongiosa in fat-suppressed images. Focal erosions of the palmar compact bone of the navicular bone may not be apparent radiologically in the early stages of development. Occasionally a palmar process fracture of the distal phalanx has been detected which was not evident on radiographs.

Additional figures

The book companion website at www.clinical-radiology-horse.com includes additional figures that are not included in the printed book or e-book formats. Please see '**About the Companion Website**' at the start of the book for details on how to access the website. These figures are prefixed with the letter 'w' in the printed book, e.g. Figures 1w.4c–f.

Downloaded From Vet-eBooks.com

FURTHER READING

CONGENITAL ABNORMALITIES

Aanes, W.A. (1984) Congenital phalangeal hypoplasia in Equidae. *J. Am. Vet. Med. Ass.* **185**, 554–556

Benninger, M., Deiss, E., Ueltschi, G. (2005) Bipartite distal phalanx and navicular bone in an Andalusian stallion. *Vet. Radiol. Ultrasound* **46**, 69–71

Bertone, A., Aanes, W. (1984) Congenital phalangeal hypoplasia in Equidae. *J. Am. Vet. Med. Ass.* **185**, 554–556

DISTAL PHALANX, UNGULAR CARTILAGES AND DISTAL INTERPHALANGEAL JOINT

Baird, A., Seahorn, T., Morris, E. (1990) Equine digital sequestration *Vet. Radiol.* **31**, 210–213

Bertone, A., Aanes, W. (1984) Congenital phalangeal hypoplasia in Equidae. *J. Am. Vet. Med. Ass.* **185**, 554–556

Bhatagnar, A., Pleasant, R., Dascanio, J., et al. (2010) Hoof conformation and palmar process fractures of the distal phalanx in Warmblood foals. *J. Equine Vet. Sci.*, **30**, 349–355.

Boado, A., Kristoffersen, M., Dyson, S., Murray, R. (2005) Use of nuclear scintigraphy and magnetic resonance imaging to diagnose chronic penetrating wounds in the equine foot. *Equine Vet. Educ.* **17**, 62–68

Boys-Smith, S., Clegg, P., Hughes, I., Singer, E. (2006) Complete and partial hoof wall resection for keratoma removal: postoperative complications and final outcome in 26 horses (1994–2004) *Equine Vet. J.* **38**, 127–133

Cauvin, E., Munroe, G. (1998) Septic osteitis of the distal phalanx: findings and surgical treatment in 18 cases. *Equine Vet. J.* **30**, 512–519

Contino, E., Barrett, M., Werpy, N. (2014) Effect of limb positioning on the radiographic appearance of the distal and proximal interphalangeal joint spaces of the forelimbs of horses during evaluation of dorsopalmar radiographs. *J. Am. Vet. Med. Ass.* **244**, 1186–1190

Crowe, O., Hepburn R., Kold, S., Smith, R. (2010) Long-term outcome after arthroscopic debridement of distal phalanx extensor process fragmentation in 13 horses. *Vet. Surg.* **39**, 107–114

Dakin, S., Robson, K., Dyson, S. (2006) Fracture of the ossified cartilage of the foot: 10 cases. *Equine Vet. Educ.* **18**, 130–136

Dechant, J., Trotter, G., Stashak, T., Hendrickson, D. (2000) Removal of large extensor process fractures of the distal phalanx via arthrotomy in horses: 14 cases (1992–1998). *J. Am. Vet. Med. Ass.* **217**, 1351–1355

Denoix, J.-M., Jacquet, S., Lepeule, J. et al. (2013) Radiographic findings of juvenile osteochondral conditions detected in 392 foals using a field radiographic protocol. *Vet. J.* **197**, 44–51

Down, S., Dyson, S., Murray, R. (2007) Ossification of the cartilages of the foot. *Equine Vet. Educ.* **19**, 51–56

Dyson, S. (1991) Lameness due to pain associated with the distal interphalangeal joint: 45 cases. *Equine Vet. J.* **23**, 128–135

Dyson, S. (1998) The puzzle of distal interphalangeal joint pain. *Equine Vet. Educ.* **10**, 119–125

Dyson, S., Murray, R. (2004) Collateral desmitis of the distal interphalangeal joint in 62 horses (January 2001–December 2003). *Proc. Am. Ass. Equine Pract.* **50**, 248–256

Dyson, S., Murray, R. (2007) Magnetic resonance imaging of the equine foot. *Clin. Techniques in Equine Pract.* **6**, 46–61

Dyson, S., Murray, R., Schramme, M., Branch, M. (2003) Lameness in 46 horses associated with deep digital flexor tendonitis in the horse: diagnosis confirmed with magnetic resonance imaging. *Equine Vet. J.* **35**, 681–690

Dyson, S., Murray, R., Schramme, M., Branch, M. (2004) Collateral desmitis of the distal interphalangeal joint in 18 horses (2001–2002). *Equine Vet. J.* **36**, 160–166

Dyson, S., Murray, R., Schramme, M. (2005) Lameness associated with foot pain and results of magnetic resonance imaging in 199 horses (January 2001–December 2003). *Equine Vet. J.* **37**, 113–121

Dyson, S. (2011) Nonseptic osteitis of the distal phalanx and its palmar processes. *Equine Vet. Educ.* **23**, 472–485

Dyson, S., Bronw, V., Collins, S., Murray, R. (2010) Is there an association between ossification of the cartilages of the foot and collateral desmopathy of the distal interphalangeal joint or distal phalanx injury? *Equine Vet. J.* **42**, 504–511

Dyson, S., Tranquille, C., Collins, S. et al. (2011) An investigation of the relationships between angles and shapes of the hoof capsule and the distal phalanx. *Equine Vet. J.* **43**, 295–301

Dyson, S., Nagy, A. (2011) Injuries associated with the cartilages of the foot. *Equine Vet. Educ.* **23**, 581–593

Dyson, S., Tranquille, C., Collins, S. et al. (2011) External characteristics of the lateral aspect of the hoof differ between non-lame and lame horses. *Vet. J.* **190**, 364–371

Faramarzi, B., McMicking, H., Halland, S., Kaneps, A., Dobson, H. (2014) Prevalence of palmar process fractures of the distal phalanx and association with front hoof conformation in foals. *Equine Vet. J. doi*: 10.1111/evj.12375

Floyd, A. (2010) Use of a grading system to facilitate treatment and prognosis in horses with negative palmar angle syndrome (heel collapse): 107 cases. *J. Equine Vet. Sci.* **30**, 666–675

Fraser, B., Else, R., Jones, E. (2006) Intraosseous epidermoid cyst of the third phalanx in a Thoroughbred gelding. *Vet. Rec.* **159**, 360–362

Giraldo, L., Redding, R. (2005) Radiographic diagnosis: Foreign body in the distal interphalangeal joint. *Vet. Radiol. Ultrasound* **46**, 304–305

Honnas, C., O'Brien, T., Linford, R. (1988) Distal phalanx fractures in horses: a survey of 274 horses with radiographic assessment of healing in 36 horses. *Vet. Radiol.* **29**, 98–107

Downloaded From Vet-eBooks.com

Jones, L., Dyson, S. (2015) Radiological characterisation of ossification of the ungular cartilages in horses: 271 cases (2005–2012). *J. Am. Vet. Med. Assoc.* **247**, 801–811

Kaneps, A.J., O'Brien, T.R., Redden, R.F., Stover, S.M., Pool, R.R. (1993) Characterisation of osseous bodies of the distal phalanx of foals. *Equine Vet. J.* **25**, 285–292

Keegan, K., Twardock, R., Losonsky, J., Baker, G. (1993) Scintigraphic evaluation of fractures of the distal phalanx in 27 cases (1979–1988). *J. Am. Vet. Med. Assoc.* **202**, 1993–1997

Kidd, J. (2011) Pedal bone fractures. *Equine Vet. Educ.* **23**, 324–323

Kristiansen, K., Kold, S. (2007) Multivariable analysis of factors influencing outcome of 2 treatment protocols in 128 cases of horses responding positively to intra-articular analgesia of the distal interphalangeal joint. *Equine Vet. J.* **39**, 150–156

Kummer, M., Geyer, H., Imboden, I., Lischer, C. (2006) The effect of hoof trimming on radiographic measurements of the front feet of normal Warmblood horses. *Vet. J.* **172**, 58–66

Linford, R.L., O'Brien, T.R., Trout, D.R. (1993) Qualitative and morphometric radiographic findings in the distal phalanx and distal soft tissues of sound Thoroughbred racehorses. *Am. J. Vet. Res.* **54**, 38–51

Mair, T.,Linnenkohl, W. (2012) Low-field magnetic resonance imaging of keratomas of the hoof wall. *Equine Vet. Educ.* **24**, 459–468

Mair, T., Sherlock, C. (2008) Collateral desmitis of the distal interphalangeal joint in conjunction with concurrent ossification of the cartilages of the foot in nine horses. *Equine Vet. Educ.* **20**, 485–492

McDiarmid, A.M. (1998) Distal interphalangeal joint lameness in a horse associated with damage to the insertion of the lateral collateral ligament. *Equine Vet. Educ.* **10**, 114–118

Nagy, A., Dyson, S., Murray, R. (2007) Scintigraphic examination of the cartilages of the foot. *Equine Vet. J.* **39**, 250–256

Nagy, A., Dyson, S., Murray, R. (2008) Radiographic, scintigraphic and magnetic resonance imaging findings in the palmar processes of the distal phalanx. *Equine Vet. J.* **40**, 57–63

Neil, K., Axon, J., Todhunter, P. et al. (2007) Septic osteitis of the distal phalanx in foals: 22 cases (1995–2002) *J. Am. Vet. Med. Ass*. **230**, 1683–1690

Ohlsson, J., Jansson, N. (2005) Conservative treatment of intra-articular distal phalanx fractures in horses not used for racing. *Aust. Vet. J.* **83**, 221–223

O'Sullivan, C.B., Dart, A.J., Malikides, N., et al. (1999) Nonsurgical management of type II fractures of the distal phalanx in 48 Standardbred horses. *Aust. Vet. J.* **77**, 501–503

Petterson, H. (1976) Fractures of the pedal bone in the horse. *Equine Vet. J.* **8**, 104–109

Rabuffo, T., Ross, M. (2002) Fractures of the distal phalanx in 72 racehorses: 1990–2001. *Proc. Am. Assoc. Equine Pract.* **48**, 375–377

Rendano, V., Grant, B. (1978) The equine third phalanx: its radiographic appearance. *Vet. Radiol.* **19**, 125–135

Rijkenhuizen, A., de Graaf, K., Hak, A., et al. (2012) Management and outcome of fractures of the distal phalanx: a retrospective study of 285 horses with a long term outcome in 223 cases. *Vet. J.* **192**, 176–182

Robson, K., Kristoffersen, M., Dyson, S. (2007) Palmar or plantar process fractures of the distal phalanx in riding horses: 22 cases (1994–2003). *Equine Vet. Educ.* **20**, 40–46

Ruohoniemi, M., Tulamo, R-M., Hackzell, M. (1993) Radiographic evaluation of ossification of the collateral cartilages of the third phalanx in Finnhorses. *Equine Vet. J.* **25**, 453–455

Ruohoniemi, M., Karkkainen, M., Tervahartiala, P. (1997) Evaluation of the variably ossified collateral cartilages of the distal phalanx and adjacent anatomic structures in the Finnhorse with computed tomography and magnetic resonance imaging. *Vet. Radiol. Ultrasound* **38**, 344–351

Ruohoniemi, M., Tervahartiala, P. (1999) Computed tomographic evaluation of Finnhorse cadaver forefeet with radiographically problematic findings on the flexor aspect of the navicular bone. *Vet. Radiol. Ultrasound* **40**, 275–281

Ruohoniemi, M., Makela, M., Eskonen, T. (2004) Clinical significance of ossification of the cartilages of the front feet based on nuclear scintigraphy, radiography and lameness examinations in 21 Finnhorses. *Equine Vet. J.* **36**, 143–148

Scott, E., McDole, M., Shires, M. (1979) A review of third phalanx fractures in the horse: sixty-five cases. *J. Am. Vet. Med. Assoc.* **174**, 1337–1343

Scott, E., Snyder, S., Schmotzer, W., Pool, R. (1991) Subchondral bone cysts with fractures of the extensor processes in a horse. *J. Am. Vet. Med. Ass.* **199**, 595–597

Schades, S., Arnoczky, S., Bowker, R. (2014) The microvasculature in the equine distal phalanx: implications for fracture healing. *Vet. Comp. Orthop. Traumatol.* **27**, 102–106

Selberg, K., Werpy, N. (2011) Fractures of the distal phalanx and associated soft tissue and osseous abnormalities in 22 horses with ossified sclerotic ungual cartilages diagnosed with magnetic resonance imaging. *Vet. Radiol. Ultrasound* **52**, 394–401

Sherlock, C., Mair, T. (2011) Osseous cyst-like lesions/subchondral bone cysts of the phalanges. *Equine Vet. Educ.* **23**, 191–204

Sherlock, C., Eggleston, R., Howerth, E. (2012) Conservative management of a transverse fracture of the distal phalanx in a Quarter Horse. *J. Am. Vet. Med. Ass.* **240**, 82–86

Silva, S., Vulcano, L. (2002) Collateral cartilage ossification of the distal phalanx in the Brazilian jumper horse. *Vet. Radiol. Ultrasound* **43**, 461–463

Smallwood, J.E., Albright, S.M., Metcalf, M.R., Thrall, D.E., Harrington, B.D. (1989) A xeroradiographic study of the developing equine foredigit and metacarpophalangeal region from birth to six months of age. *Vet. Radiol.* **30**, 98–110

Downloaded From Vet-eBooks.com

Smith, M., Crowe, O., Ellson, C., et al. (2005) Surgical treatment of osseous cyst-like lesions in the distal phalanx arising from collateral ligament insertion injury. *Equine Vet. Educ.* **17**, 195–200

Smith, S., Dyson, S., Murray, R. (2004) Is there an association between distal phalanx angles and deep digital flexor tendon lesions? *Proc. Am. Assoc. Equine Pract.* **50**, 328–331

Stock, K., Hamann, H., Distl, O. (2005) Prevalence of osseous fragments in distal and proximal interphalangeal, metacarpo- and metatarsophalangeal and tarsocrural joints of Hanoverian Warmblood horses. *J. Vet. Med. A* **52**, 388–394

Story, M., Bramlage, L. (2004) Arthroscopic debridement of subchondral bone cysts in the distal phalanx of 11 horses (1994–2000). *Equine Vet. J.* **36**, 356–361

Ter Braake, F. (2005) Arthroscopic removal of large fragments of the extensor process of the distal phalanx in 4 horses. *Equine Vet. Educ.* **17**, 101–104

Van Hoogmoed, L., Snyder, J., Thomas, H., Harmon, F. (2003) Retrospective evaluation of equine prepurchase examinations performed between 1991–2000. *Equine Vet. J.* **35**, 375–381

Verschooten, F., deMoor, A. (1982) Subchondral cystic and related lesions affecting the equine pedal bone and stifle. *Equine Vet. J.* **14**, 47–54

Verschooten, F., Van Wearable, B., Verbeeck, J. (1996) The ossification of cartilages of the distal phalanx in the horse – an anatomical, experimental, radiographic and clinical study. *J. Equine Vet. Sci.* **16**, 291–305

Verwilghen, D., Serteyn, D., Pille, F., et al. (2009) Prevalence of radiographic findings in candidate sires (2001–2008). *Vlaams Dergeneeskundig Tirjdschrift* **78**, 419–428

Wagner, P., Balch-Burnett, O. (1982) Surgical management of subchondral bone cysts of the third phalanx. *Equine Pract.* **4**, 8–14

Yovich, J., Stashak, T., DeBowes, R., Ducharme, N. (1986) Fractures of the distal phalanx of the forelimb in eight foals. *J. Am. Vet. Med. Ass.* **189**, 550–554

Young, A., Dimock, A., Puchalski, S. et al. (2012) Magnetic resonance and radiographic diagnosis of osseous resorption of the flexor surface of the distal phalanx in the horse. *Equine Vet. J.* **44** (Suppl 43) 213–217

HOOF WALL, FOOT BALANCE AND CORRECTIVE FARRIERY

Colles, C.M., Ware, R. (2010) *The principles of farriery*. J Allen, London

LAMINITIS AND VENOGRAPHY

Collins, S.N., van Eps, A.W., Pollitt, C.C., Kuwano, A. (2010) The lamellar wedge. *Vet. Clin. N. Am.: Equine Pract*. **26**, 179–195.

Cripps, P., Eustace, R. (1999a) Radiological measurements from the feet of normal horses with relevance to laminitis. *Equine Vet. J.* **31**, 427–432

Cripps, P., Eustace, R. (1999b) Factors involved in the prognosis of equine laminitis in the UK. *Equine Vet. J.* **31**, 433–442

D'Arpe, L., Bernardini, D. (2010) Digital venography in horses and its clinical application in Europe. *Vet. Clin. N. Am.: Equine Pract* **26**, 339–359

Eustace, R. (2010) Clinical presentation, diagnosis and prognosis of chronic laminitis in Europe. *Vet. Clin. N. Am.: Equine Pract* **26**, 391–403

Hunt, R. (1993) A retrospective evaluation of laminitis in horses. *Equine Vet. J.* **25**, 61–64

Koblik, P., O'Brien, T., Coyne, C. (1988) Effect of dorsopalmar projection in obliquity on radiographic measurement of distal phalangeal rotation angle in horses with laminitis. *J. Am. Vet. Med.Ass*. **192**, 346–349

Kuwano, A., Katayama, Y., Kasashima, Y., Okada, K., Reilly, J.D. (2002) A gross and histopathological study of an ectopic white line development in equine laminitis. *J. Vet. Med. Sci.* **64**, 893–900

Murray, R., Dyson, S., Schramme, M., Branch, M. (2003) Magnetic resonance imaging of the equine digit with chronic laminitis. *Vet. Radiol. Ultrasound* **44**, 609–617

Parks, A.H., O'Grady, S.E. (2003) Chronic laminitis: current treatment strategies. *Vet. Clin. N. Am.: Equine Pract*. **19**, 393–416

Peloso, J.G., Cohen, N.D., Walker, M.A., Watkins, J.P., Gayle, J.M., Moyer, W. (1996) Case control study of risk factors for the development of laminits in the contralateral limb in Equidae with unilateral lameness. *J. Am. Vet. Med. Ass.* **209**, 1746–1749

Pollit, C. (2010) The anatomy and physiology of the suspensory apparatus of the distal phalanx. *Vet. Clin. N. Am.: Equine Pract* **26**, 29–49

Redden, R. (2001) A technique for performing digital venography in the standing horse. *Equine Vet. Educ.* **5**, 172–178

Rucker, A., Redden, R., Arthur, E. et al. (2006) How to perform the digital venogram. *Proc. Am. Ass. Equine Pract.* **52**, 526–530

Rucker, A. (2010) Clinical applications of digital venography. *J. Equine Vet. Sci.* **30**, 491–503

Rucker, A. (2010) Equine venography and its clinical application in North America. *Vet. Clin. N. Am.: Equine Pract*. **26**, 167–177

Sherlock, C., Parks, A. (2013) Radiographic and radiological assessment of laminitis. *Equine Vet. Educ.* **25**, 524–535

Stick, J.A., Jann, H.W., Scott, E.A., Robinson, N.E. (1982) Pedal bone rotation as an indicator of laminitis in horses. *J. Am. Vet. Med. Ass.* **180**, 251–253

Wagner, I., Hood, D. (1997) Cause of air lines associated with acute and chronic laminitis. *Proc. Am. Ass. Equine Pract.* **43**, 363–366

NAVICULAR BONE

Bathe, A., Joyner, S. (2003) Limitations and improvements in the quality of navicular flexor view radiographs. *Proc. Am. Ass. Equine Pract.* **49**, 317–319

Downloaded From Vet-eBooks.com

Benninger, M., Deiss, E., and Ueltschi, G. (2005) Bipartite distal phalanx and navicular bone in an Andalusian stallion. *Vet. Radiol. Ultrasound* **46**, 69–71

Berry, C., Pool, R., Stover, S. *et al*. (1992) Radiographic/morphologic investigation of a radiolucent crescent within the flexor central eminence of the navicular bone in Thoroughbreds. *Am. J. Vet. Res.* **53**, 1604–1611

Biggi, M., Dyson, S. (2010) Comparison between radiological and magnetic resonance imaging lesions in the distal border of the navicular bone with particular reference to distal border fragments and osseous cyst-like lesions. *Equine Vet. J.* **42**, 707–712

Biggi, M., Dyson, S. (2011) High-field magnetic resonance imaging investigation of distal border fragments of the navicular bone in horses with foot pain. *Equine Vet. J.* **43**, 302–308

Biggi, M., Blunden, T., Dyson, S. (2012) Can distal border fragments of the navicular bone be a primary cause of lameness? *Equine Vet. Educ*. **25**, 347–351

Biggi, M., Dyson, S. (2013) Unusual navicular bone fractures in hindlimbs: clinical and imaging findings. *J. Equine Vet. Sci.* **33**, 1082–1087

Blunden, T., Dyson, S., Murray, R., Schramme, M. (2006) Histopathological findings in horses with chronic palmar foot pain and age-matched control horses Part 1: the navicular bone & related structures. *Equine Vet. J.* **38**, 15–22

Brounts, S., Adams, S., Vemireddi, V., Holland, C. (2008) A malignant glomus tumour in the foot of a horse. *Equine Vet. Educ.* **20**, 24–27

Busoni, V., Denoix, J.-M. (2001) Ultrasonography of the podotrochlear apparatus in the horse using a transcuneal approach: technique and reference images. *Vet. Radiol. Ultrasound* **42**, 534–540

Claerhoudt, S., Pille, F., Vanderperren, K. et al. (2011) Association between navicular bone fragmentation and shape in Belgian Warmblood horses. *Vet. Comp. Orthop. Traumatol.* **24**, 132–136

Claerhoudt, S., Bergman, H., van der Veen, V. et al. (2012) Differences in the morphology of distal border synovial invaginations of the distal sesamoid bone in the horse as evaluated by computed tomography compared with radiography. *Equine Vet. J.* **44**, 679–683

Colles C.M., Garner H.E., & Coffman J.R. (1979) The blood supply of the horse's foot. Proc 25th Am. Assoc. Eq. Pract, 385–398

Colles C.M. (1982) The pathogenesis and treatment of navicular disease in the horse. *PhD Thesis*, University of London

Colles C.M. (1982) Navicular disease and its treatment. *In Practice* **4**(2), 29–36

Colles C.M. (2001) How to repair navicular bone fractures in the horse *Proc. Am. Assoc. Equine Pract.* **47**, 270–277

Colles C.M., Hickman, J. (1977) The arterial supply of the navicular bone and its variations in navicular disease. *Equine Vet. J.* **9**, 150–154

Colles C.M. (2011) Navicular bone fractures in the horse. *Equine Vet. Educ.* **23**, 255–261

De Clerq, T., Verschooten, F., Ysebaert, M. (2000) A comparison of the palmaroproximal-palmarodistal oblique view of the isolated navicular bone to other views. *Vet. Radiol. Ultrasound* **41**, 525–533

Dik, K., Broeck, J. van den (1995) Role of navicular bone shape in the pathogenesis of navicular disease: a radiological study. *Equine Vet. J.* **27**, 390–393

Dik. K., van den Belt, A., Enzerink, E., van Weeren, R. (2001a) The radiographic development of the distal and proximal double contours of the equine navicular bone on dorsoproximal-palmarodistal oblique (upright pedal) radiographs, from age 1 to 11 months. *Equine Vet. J.* **33**, 70–74

Dik. K., van den Belt, A., van den Broek, J. (2001b) Relationships of age and shape of the navicular bone to the development of navicular disease: a radiological study. *Equine Vet. J.* **33**, 172–175

Dyson, S. (2011) Radiological interpretation of the navicular bone. *Equine Vet. Educ.* **23**, 73–87

Dyson, S., Murray, R., Schramme, M., Branch, M. (2003) Lameness in 46 horses associated with deep digital flexor tendonitis in the horse: diagnosis confirmed with magnetic resonance imaging. *Equine Vet. J.* **35**, 681–690

Dyson, S., Murray, R., Blunden, T., Schramme, M. (2011) Current concepts of navicular disease. *Equine Vet. Educ.* **23**, 27–39

Frecklington, P., Rose, R. (1981) An unusual case of fracture of the navicular bone in the hindlimb of a horse. *Austr. Vet. Pract.* **11**, 57–59

Heitzmann, A., Denoix, J.-M. (2007) Rupture of the distal sesamoidean impar ligament with proximal displacement of the distal sesamoid bone in a steeplechaser. *Equine Vet. Educ.* **19**, 117–120

Hoegaerts, M., Pille, F., De Clerq, T., Fulton, I., Saunders, J. (2005) Comminuted fracture of the distal sesamoid bone and distal rupture of the deep digital flexor tendon. *Vet. Radiol. Ultrasound* **46**, 234–237

Lillich, J., Ruggles, A., Gabel, A., Bramlage, L., Schneider, R. (1995) Fracture of the distal sesamoid bone in horses: 17 cases (1982–1992). *J. Am. Vet. Med. Ass.* **207**, 924–927

MacGregor, C.M. (1986) Radiographic assessment of navicular bones based on change in the distal nutrient foramina. *Equine Vet. J.* **18**, 203–206

Murray, R., Schramme, M., Dyson, S., Blunden, A. (2006) MRI characteristics of the foot in horses with palmar foot pain and control horses. *Vet. Radiol. Ultrasound*, **47**, 1–16

Murray, R., Blunden, A., Schramme, M., Dyson, S. (2006) How does magnetic resonance imaging represent histological findings in the equine digit? *Vet. Radiol. Ultrasound* **47**, 17–31

O'Brien, T.R., Millman, T.M., Pool, R.R., Suter, P.F. (1975) Navicular disease in the Thoroughbred horse: a morphologic investigation relative to a new radiographic projection. *J. Am. Vet. Rad. Soc.* **16**, 39–50

Downloaded From Vet-eBooks.com

Oxspring, G.E. (1935) The radiology of navicular disease, with observations on its pathology. *Vet. Rec.* **48**, 1445–1454

Poulos, P. (1983) Correlation of radiographic signs and histological changes in the navicular bone. *Proc. Am. Ass. Equine Pract.* **29**, 241–255

Poulos, P. (1988) The nature of enlarged 'vascular channels' in the navicular bone of the horse. *Vet. Radiol.* **29**, 60–64

Puchalski, S., Galuppo, L. Hornof, W., and Wisner, E. (2007) Intra-arterial contrast-enhanced computed tomography of the equine distal extremity. *Vet. Radiol. Ultrasound* **48**, 21–29

Richardson, G., O'Brien, T. (1985) Puncture wounds into the navicular bursa of the horse: their radiological evaluation. *Vet. Radiol.* **26**, 203–207

Stock, K., Distl, O. (2006) Genetic analysis of the radiographic appearance of the distal sesamoid bone in Hanoverian Warmblood horses. *Am. J. Vet. Res.* **67**, 1013–1019

Vaughan, L.C. (1961) Fracture of the navicular bone in the horse. *Vet. Rec.* **73**, 895–897

Verschooten, F., Roels, J., Lampo, P., DeMoor, A., Picavet, T. (1989) Radiographic measurements from the lateromedial projection of the equine foot with navicular disease. *Res. Vet. Sci.* **46**, 15–21

Watering, C.C. van de and Morgan, J.P. (1975) Chip fractures as a radiological finding in navicular disease of the horse. *J. Am. Vet. Rad. Soc.* **16**, 206–210

Widmer, W., Buckwalter, K., Fessler, J., Hill, M., Van Sickle, D., Ivancevich, S. (2000) Use of radiography, computed tomography and magnetic resonance imaging for evaluation of navicular syndrome in the horse. *Vet. Radiol. Ultrasound* **41**, 108–117

Wong, D., Scaratt, W., Maxwell, V., Moon, M. (2003) Incomplete ossification of the carpal, tarsal and navicular bones in a dysmature foal. *Equine Vet. Educ.* **15**, 72–81

Wright, I. (1993) A study of 118 cases of navicular disease: radiological features. *Equine Vet. J.* **25**, 493–500

Wurfel, C., Hertsch, B. (2005) Study on the diagnostic values of contrast radiography of the navicular bone. *Pferheilkunde*, **21**, 4–12

Yorke, E., Judy, C., Saveraid, T. et al. (2013) Distal border fragments of the equine navicular bone: association between magnetic resonance imaging characteritics and clinical lameness. *Vet. Radiol. Ultrasound* **53**, 35–40

SPACE-OCCUPYING LESIONS: KERATOMATA AND TUMOURS

Attenburrow, D., Heyse-Moore, G. (1982) Non-ossifying fibroma in a phalanx of a Thoroughbred yearling. *Equine Vet. J.* **14**, 59–61

Berry, C., O'Brien, T., Pool, R. (1991) Squamous cell carcinoma of the hoof wall in a stallion. *J. Am. Vet. Med. Ass.* **199**, 90–92

Brounts, S., Adams, S., Vemireddi, V., Holland, C. (2008) A malignant glomus tumour in the foot of a horse. *Equine Vet. Educ.* **20**, 24–27

Gasiorowski, J., Getman, L., Richardson, D. (2011) Supracoronary approach for keratoma removal in horses: two cases. *Equine Vet. Educ.* **23**, 489–493

Gelatt, K.L., Neuwirth, L., Hawkins, D.L., Woodard, J.C. (1996) Hemangioma of the distal phalanx in a colt. *Vet. Radiol. Ultrasound* **37**, 275–280

Getman, L., Davidson, E., Ross, M. et al. (2011) Computed tomography or magnetic resonance imaging-assisted partial hoof wall resection for keratoma removal. *Vet. Surg.* **40**, 708–714

Honnas, C., Liskey, C., Meagher, D., Brown, D., Luck, E. (1990) Malignant melanoma in the foot of a horse. *J. Am. Vet. Med. Ass.* **197**, 756–758

Mair, T., Linnenkohl, W. (2012) Low-field magnetic resonance imaging of keratomas of the hoof wall. *Equine Vet. Educ.* **24**, 459–468

Oosterlinck, M., Raes, E., Verbraecken, S. et al. (2011) Severe lameness caused by metastatic renal adenocarcinoma of the third phalanx in a Warmblood mare. *Equine Vet. Educ.* **23**, 512–516

Pickersgill, C. (2000) Recurrent white line abscessation associated with a keratoma in a pony. *Equine Vet. Educ.* **12**, 286–291

Downloaded From Vet-eBooks.com

Downloaded From Vet-eBooks.com

Chapter 4
The proximal and middle phalanges and the proximal interphalangeal joint

The proximal aspect of the proximal phalanx is also discussed in Chapter 5.

RADIOGRAPHIC TECHNIQUE

Equipment

Radiographs of the proximal and middle phalanges (pastern region) can easily be obtained using portable machines. Using digital radiography or conventional film–screen combinations, high-definition screen and appropriate film combinations can be used even with portable equipment, since movement blur is seldom a problem. It is unnecessary to use a grid even in large horses.

Positioning

Survey radiographs of the proximal and middle phalanges are often obtained as part of the examination of the foot or fetlock. Specific views of this area are best obtained with the horse bearing weight on the limb, and should include lateromedial, dorsopalmar and two oblique views (to show medial and lateral aspects). When evaluating the dorsal joint margins, lateromedial (flexed) and oblique (flexed) views may be more useful (see Chapter 3, 'Distal phalanx – Other oblique views' and Figure 3.6).

For all views, a horizontal x-ray beam is centered midway between the fetlock and coronary band. The x-ray beam should normally be aligned with reference to the bulbs of the heel in order to obtain correct lateromedial or dorsopalmar images. Dorsal 5–10° proximal-palmarodistal oblique views may be obtained with the x-ray beam aligned at right angles to the dorsal surface of the pastern, and angling the cassette accordingly. This view results in less distortion, and is particularly useful for assessment of the middle phalanx and the proximal interphalangeal joint.

Chip fractures of the phalanges are best visualised on oblique images. Fractures of the body of the phalanges are frequently spiral, and a series of oblique radiographs may be required to determine their course. Fractures, separate centres of ossification or osteochondrosis or developmental orthopaedic lesions of the proximal palmar aspect of the proximal phalanx may best be evaluated (and/or detected) using dorsal 30° proximal 70° lateral-palmarodistomedial oblique or dorsal 30° proximal 70° medial-palmarodistolateral oblique views (see Chapter 5 and Figure 5.2b).

Clinical Radiology of the Horse, Fourth Edition. Janet A. Butler, Christopher M. Colles, Sue J. Dyson, Svend E. Kold and Paul W. Poulos.
© 2017 John Wiley & Sons, Ltd. Published 2017 by John Wiley & Sons, Ltd.
Companion website: www.clinical-radiology-horse.com

Downloaded From Vet-eBooks.com

Subtle osteophyte formation is sometimes best evaluated on flexed oblique (dorsolateral-palmaromedial and dorsomedial-palmarolateral oblique [flexed]) views. These are obtained with the toe of the foot placed in a navicular block or on a flat block (Figure 3.6), with the sole of the foot approximately vertical (see Chapter 3, 'Distal phalanx – Other oblique views').

NORMAL ANATOMY

Immature horse

The proximal and middle phalanges both ossify from three centres. In both bones the distal epiphysis unites with the shaft before birth. In foals that are skeletally immature at birth, a lucent crescent is occasionally noted in the distal metaphysis of the bone, which represents a non-mineralised cartilage remnant of the distal physis. The proximal physis closes at about 1 year of age in the proximal phalanx, and at 8–12 months in the middle phalanx.

Skeletally mature horse

There is an area relatively devoid of trabeculae in the central part of the proximal and middle phalanges. This is a marrow or fat cavity, and is of variable size. It appears as a lucent zone, best seen on dorsopalmar images, although the clarity with which it is seen will depend upon a number of radiographic factors. It may not be visible in the middle phalanx.

On dorsopalmar views of the proximal phalanx there are relatively opaque lines on the medial and lateral aspects of this lucent area, which extend proximally and distally. These are the areas of insertion of the oblique sesamoidean ligaments (Figures 4.1 and 4.2).

On dorsopalmar radiographs, the ergot may be recognised as a circumscribed opacity superimposed on the proximal aspect of the proximal phalanx. This opacity may have radiolucent lines across it.

Both the proximal and middle phalanges have a horizontal row of nutrient foramina at their proximal and distal ends. These may be seen to varying degrees on dorsopalmar images depending on the angle of projection, and are a normal finding. Care should be exercised, when interpreting radiographs of the navicular bone, that the foramina of the middle phalanx are not superimposed over the navicular bone, giving the appearance of abnormal proximal nutrient foramina.

On lateromedial images of the proximal phalanx, a small irregularity may be evident on the palmar aspect of the bone at approximately one-third of the length of the bone from the distal end. This is the apex of the area of insertion of the oblique sesamoidean ligaments. The irregular bone may extend proximally in an oblique lateral and/or medial direction following the line of insertion of the ligaments, and is seen more readily on oblique radiographic images. This finding tends to be more prominent in older and/or large horses.

There may be a small circular radiolucent area or a slightly oblique radiolucent line in the centre of the middle or proximal phalanx on dorsopalmar and oblique images. This represents the normal nutrient foramen of the bone.

Downloaded From Vet-eBooks.com



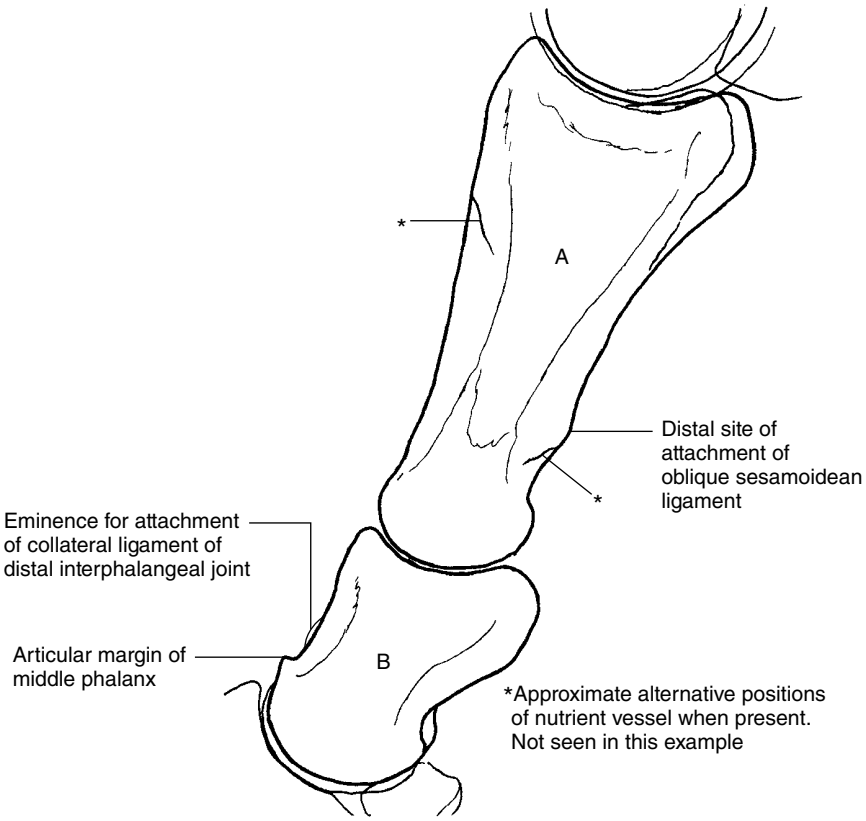


Figure 4.1 Lateromedial radiograph and diagram of the proximal and middle phalanges of a normal adult horse. A = proximal phalanx, B = middle phalanx.

Downloaded From Vet-eBooks.com



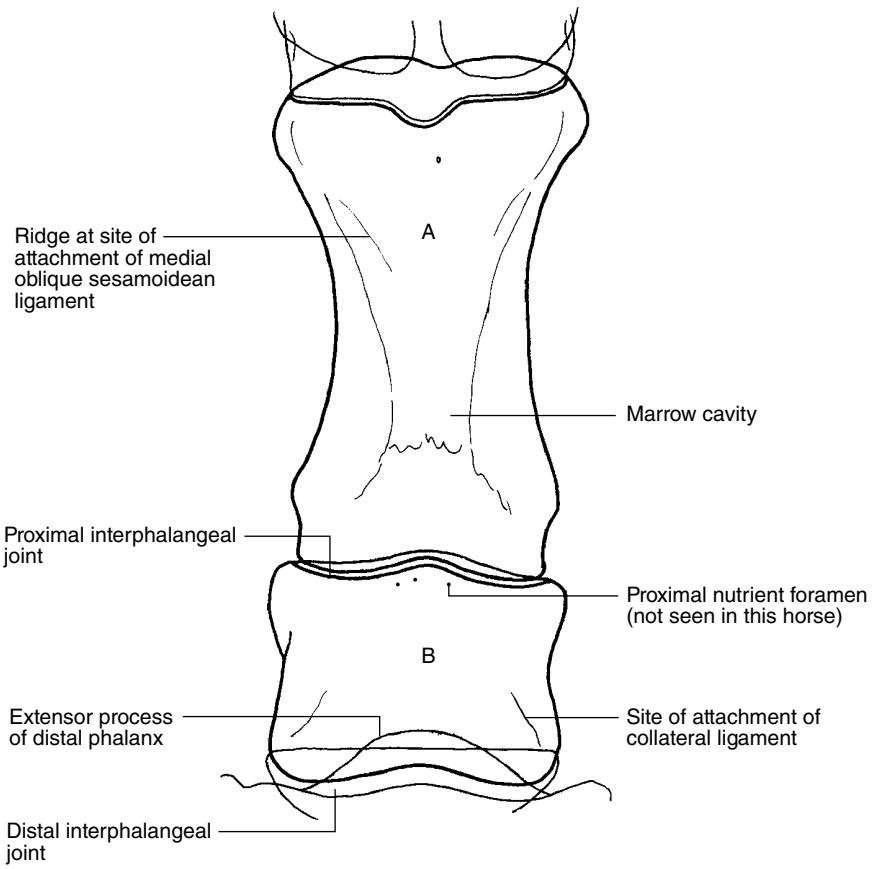


Figure 4.2 Dorsopalmar radiograph and diagram of the proximal and middle phalanges of a normal adult horse. A = proximal phalanx, B = middle phalanx.

Downloaded From Vet-eBooks.com

The middle phalanx is approximately half the length of the proximal phalanx. There are two prominent bony ridges, either side of the distal dorsal aspect of the bone, where the collateral ligaments of the distal interphalangeal joint originate. These are particularly obvious on slightly oblique views. The bony eminences at ligament insertions tend to be more prominent in large horses.

The articular surface of the distal end of the middle phalanx normally has a smooth curved outline, which extends dorsally into a point (Figure 4.1). The central third of the articular surface may be relatively flatter than the more dorsal and palmar aspects. The articular surfaces of the proximal and middle phalanges in the proximal interphalangeal joint are reasonably congruous (Figure 4.1).

NORMAL VARIATIONS AND INCIDENTAL FINDINGS

There is often new bone formation (entheseophyte formation) at the origins or insertions of a number of ligaments, on the palmar, palmaromedial and palmarolateral aspects of the proximal phalanx and on the dorsomedial and dorsolateral aspects of the middle phalanx. This is usually of no long-term significance, but indicates that the ligaments have undergone acute or chronic trauma at some time prior to radiography. Entheseophyte formation is seen most commonly at the attachments of the proximal and distal digital annular ligaments, the oblique sesamoidean ligaments, the collateral ligaments of the proximal and distal interphalangeal joints, the ligaments between the proximal phalanx and the ungular cartilages and the palmar ligaments of the proximal interphalangeal joint. It is important to be aware of the sites of attachment of tendons, ligaments and joint capsules (Figures 4.3a–c and 4.4a–c; Table 4.1) in order to be able to interpret the significance of new bone formation at particular sites. Entheseophytes should alert the clinician to a potential soft-tissue problem although this may be historic. Entheseophyte formation at the attachment of the ligament between the ungular cartilage and the palmaromedial or palmarolateral aspect of the proximal phalanx is most commonly seen in association with extensive ossification of the ungular cartilage.

A small mineralised opacity may occasionally be present at the dorsal aspect of the proximal articular surface of the middle phalanx. Local analgesia may be required to assess its clinical significance.

Occasionally there are one or two small, smoothly outlined, discrete opacities on the palmar proximal aspect of the proximal phalanx. These are present within the oblique sesamoidean ligaments, and their origin is uncertain. They may represent fabellae, small chip fractures sustained early in life, or mineralisation within the ligaments. Provided that they are smooth and opaque and do not involve the joint surface, they may be regarded as an incidental finding. They should not be confused with so-called Birkeland fractures (see below).

A small rounded osseous opacity is sometimes seen at the dorsoproximal aspect of the proximal phalanx. This may be unilateral or bilateral. If small (less than approximately 2 mm in diameter) and uniformly opaque, it may be an incidental finding (see Figure 5.31). Intra-articular analgesia may be required to establish its significance.

Downloaded From Vet-eBooks.com

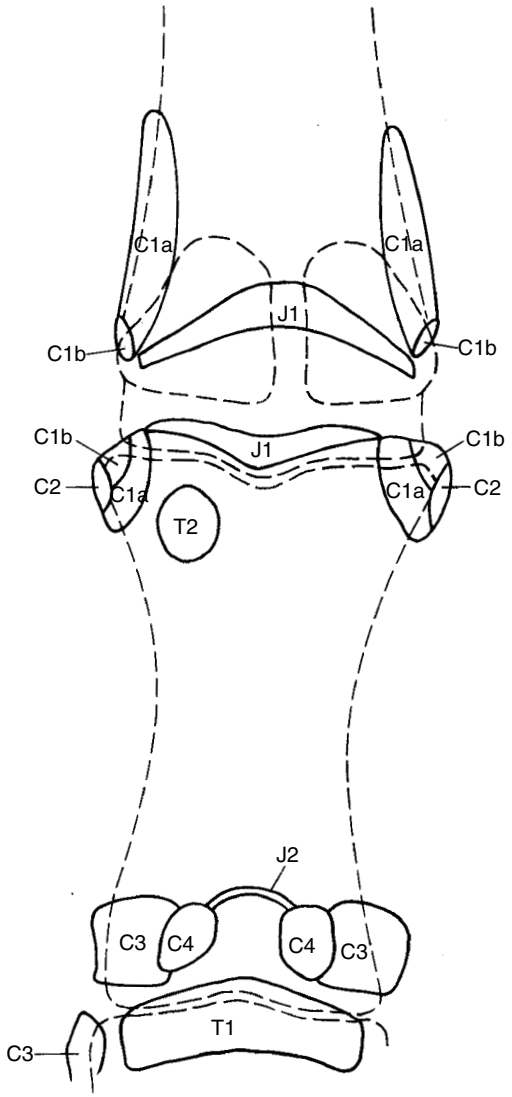


Figure 4.3(a) Diagram of a dorsal 15° proximal-palmarodistal oblique image of the fetlock and pastern regions, to illustrate the sites of attachment for those soft-tissue structures attaching to surfaces seen from the dorsal aspect. Refer to Table 4.1. Source: Adapted from Weaver, Stover and O'Brien, 1992, *Equine Veterinary Journal*.

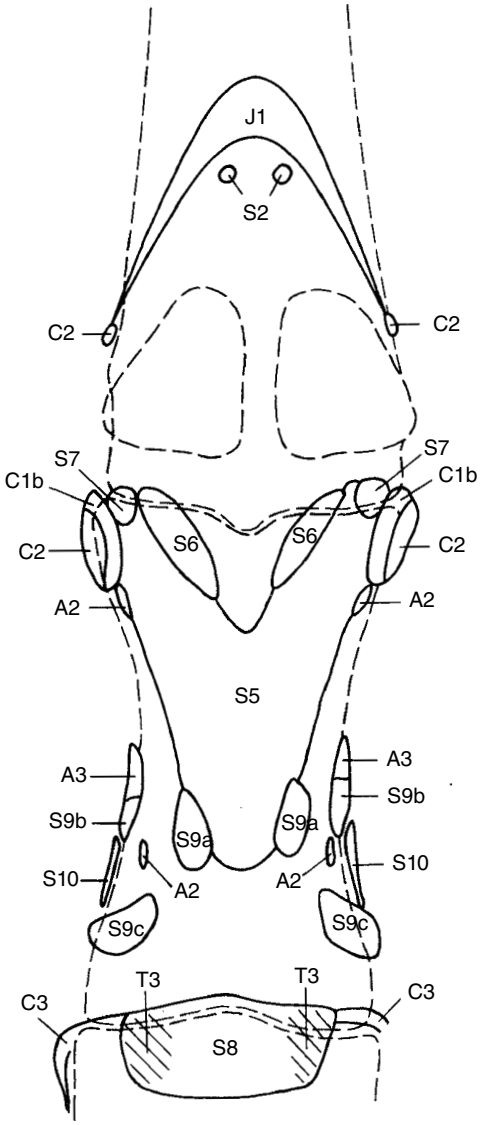


Figure 4.3(b) Diagram of a dorsal 15° proximal-palmarodistal oblique image of the fetlock and pastern regions, illustrating the site of soft-tissue attachments seen from the palmar aspect. See Table 4.1. Source: Adapted from Weaver, Stover and O'Brien, 1992, *Equine Veterinary Journal*.

On lateromedial radiographs, the distal end of the proximal phalanx may appear to be displaced dorsally relative to the proximal aspect of the middle phalanx. Although this can give the impression of subluxation, it has not been associated with any clinical abnormalities, and is most commonly seen in horses with upright conformation. The impression of subluxation of this joint may also be seen in radiographs obtained with the limb non-weight-bearing (see also 'Subluxation of the proximal interphalangeal joint').

Small periarticular osteophytes are frequently seen on the dorsoproximal aspect of the middle phalanx. Because this joint is relatively immobile, small changes may not have any clinical significance, but they cannot be differentiated from the early signs of degenerative joint disease and so should be viewed with suspicion (Figure 4.5).

Downloaded From Vet-eBooks.com

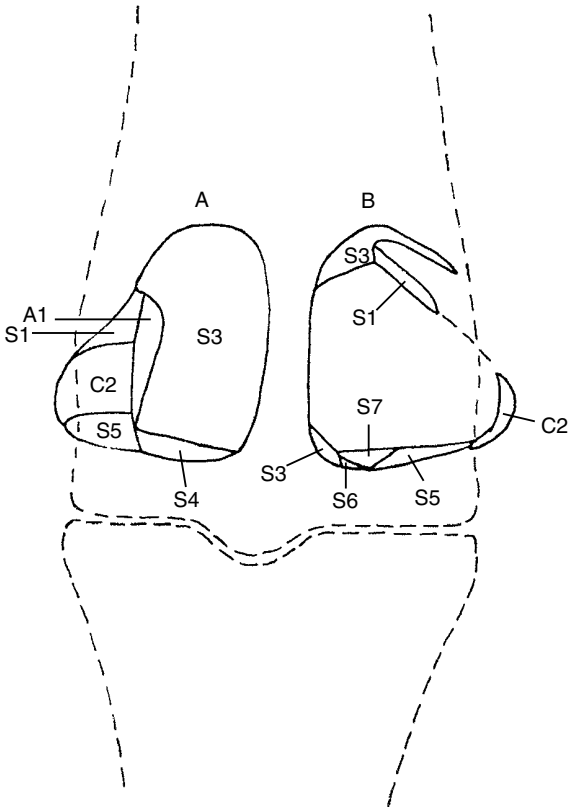


Figure 4.3(c) Diagram of a dorsal 15° proximal-palmarodistal oblique image of a fetlock joint illustrating the sites of attachment of soft-tissue structures to the palmar (A) or dorsal (B) aspects of the proximal sesamoid bones. See Table 4.1. Source: Adapted from Weaver, Stover and O'Brien, 1992, *Equine Veterinary Journal*.

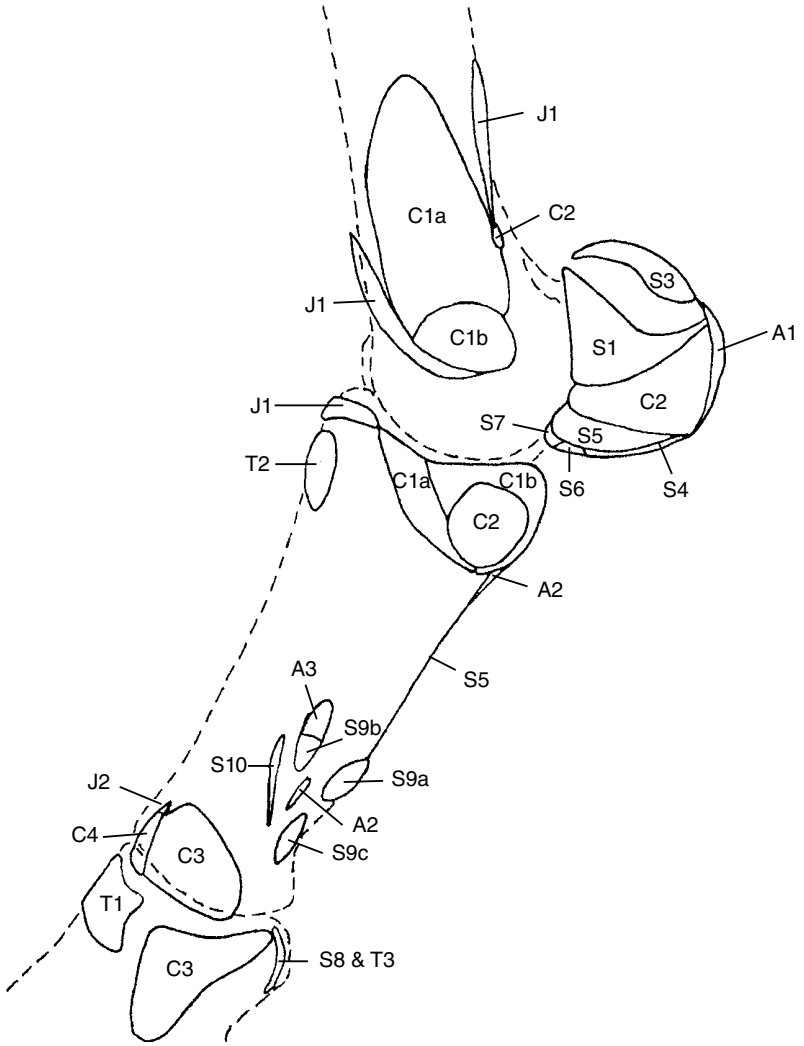


Figure 4.4(a) Diagram of a lateromedial image of the fetlock and pastern regions showing the sites of attachment of soft-tissue structures. See Table 4.1. Source: Adapted from Weaver, Stover and O'Brien, 1992, *Equine Veterinary Journal*.

Downloaded From Vet-eBooks.com

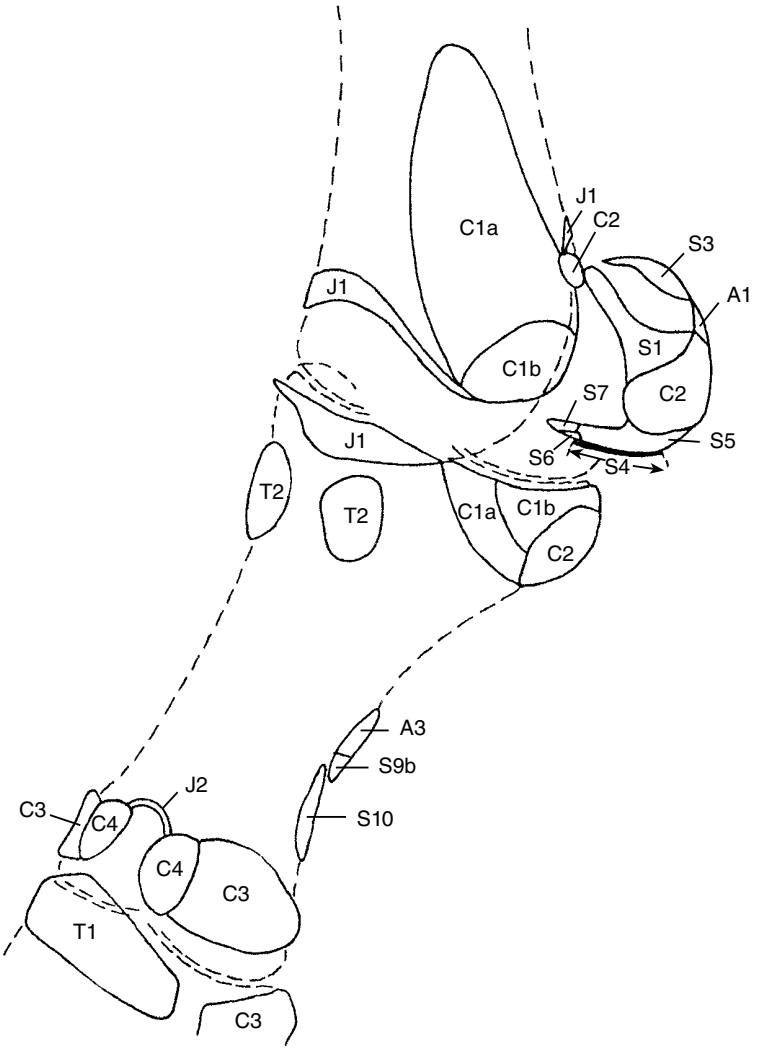


Figure 4.4(b) Diagram of an oblique image of the fetlock and pastern regions to illustrate soft-tissue attachments seen from the dorsomedial or dorsolateral aspects. See Table 4.1. Source: Adapted from Weaver, Stover and O'Brien, 1992, *Equine Veterinary Journal*.

A smoothly outlined spur may be present on the palmar aspect of the proximal epiphysis of the middle phalanx, pointing distally. The significance of this is uncertain, and it has been seen in lame and sound horses (Figure 4.6).

The position of the nutrient foramen is variable: it is seen on lateromedial views to enter dorsoproximally or palmarodistally in different horses.

There is a depression between the condyles on the palmar distal aspect of the proximal phalanx that can appear as a radiolucent zone on dorsopalmar images and should not be confused with a lesion. Osseous cyst-like lesions in the distal aspect of the proximal phalanx or the proximal or distal aspects of the middle phalanx are occasionally seen as incidental findings, but should be evaluated carefully because they may be the cause of lameness (see 'Osseous cyst-like lesions', below).

In heavy cob-type and draught horses there are often thick folds of skin on the palmar aspect of the pastern. These can create potentially confusing opacities when superimposed over the phalanges in dorsal and oblique projections.

Downloaded From Vet-eBooks.com

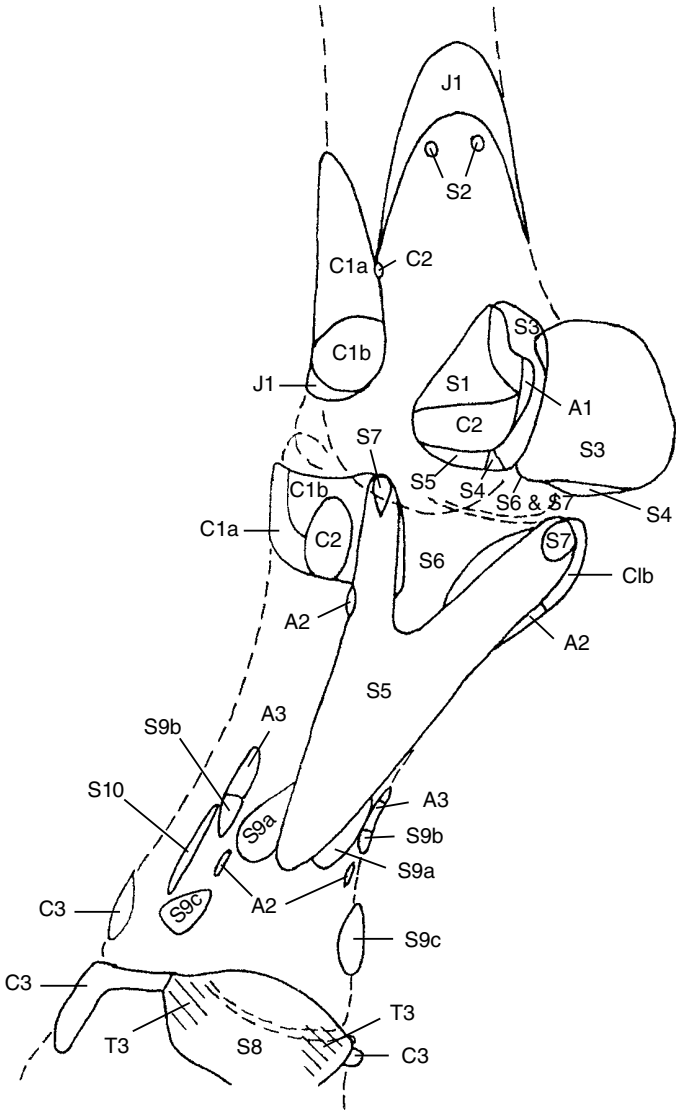


Figure 4.4(c) Diagram of an oblique image of the fetlock and pastern regions illustrating the site of soft-tissue attachments seen from the palmarolateral or palmaromedial aspects. See Table 4.1. Source: Adapted from Weaver, Stover and O'Brien, 1992, *Equine Veterinary Journal*.

SIGNIFICANT FINDINGS

A number of the findings mentioned above as incidental may at some time have been significant. These include small discrete opacities close to the joint margins, small osteophytes (lipping) at the dorsal aspect of the proximal interphalangeal joint, and new bone formation (entheseophytes) at the attachments of ligaments (Figures 4.7a and 4.7b). All of these findings probably result from trauma which occurred at least 3–6 weeks prior to radiography. An active osteophyte or entheseophyte may be less opaque than the parent bone and have an irregular or 'fuzzy' outline (Figure 4.14). It is not possible to age smoothly outlined and uniformly opaque osteophytes or entheseophytes. These lesions may be regarded as an indicator of potential problems, but in chronic lameness should only be incriminated if they can be shown by other techniques to be causing pain and lameness.

Downloaded From Vet-eBooks.com

Table 4.1 Legends for the soft tissue structures indicated in Figures 4.3 and 4.4

J1	Metacarpophalangeal (fetlock) joint capsule
J2	Proximal interphalangeal (pastern) joint capsule
C1a	Superficial part of the collateral ligaments of the metacarpophalangeal joint
C1b	Deep part of the collateral ligaments of the metacarpophalangeal joint
C2	Collateral sesamoidean ligaments of the proximal sesamoid bones
C3	Collateral ligaments of the proximal interphalangeal joint
C4	Collateral sesamoidean ligaments of the distal sesamoidean (navicular) bone
S1	Suspensory ligament
S2	Metacarpointersesamoidean ligament
S3	Intersesamoidean ligament; proximal scutum; palmar ligament of the metacarpophalangeal joint
S4	Straight sesamoidean ligament
S5	Oblique sesamoidean ligaments
S6	Cruciate sesamoidean ligaments
S7	Short sesamoidean ligaments
S8	Middle scutum
S9a	Axial palmar ligaments of the proximal interphalangeal joint
S9b	Superficial abaxial palmar ligaments of the proximal interphalangeal joint
S9c	Deep abaxial palmar ligaments of the proximal interphalangeal joint
S10	Ligaments to the ungular cartilage of the distal phalanx
A1	Palmar annular ligament
A2	Proximal digital annular ligament
A3	Distal digital annular ligament
T1	Common digital extensor tendon
T2	Lateral digital extensor tendon
T3	Superficial digital flexor tendon



Figure 4.5 Lateromedial image of a proximal interphalangeal joint, showing a small periarticular osteophyte on the dorsoproximal aspect of the middle phalanx (arrow). These are often asymptomatic.

Dysplasia of the proximal interphalangeal joint

Dysplasia of the proximal interphalangeal joint (Figure 4w.8a) is a rare condition which may result in an abnormal shape of the pastern in a young horse. Although an unbroken horse may be sound, lameness usually ensues once work starts because of joint instability, injuries of the supporting soft tissue structures on the palmar aspect of the joint and secondary osseous abnormalities (Figure 4w.8b).

Downloaded From Vet-eBooks.com



Figure 4.6 Lateromedial image of a pastern showing a 'spur' on the palmaroproximal aspect of the middle phalanx. Note the pronounced bony ridge at the region of origin of the collateral ligaments of the distal interphalangeal joint on the dorsal aspect of the middle phalanx (arrow).



Figure 4.7(a) Dorsolateral-palmaromedial oblique image of a metacarpophalangeal joint and proximal phalanx of a 9-year-old crossbred. There is smoothly marginated new bone on the palmarolateral aspect of the proximal phalanx at the region of insertion of the oblique sesamoidean ligament, representing entheseophyte formation (white arrow). There is also periarticular osteophyte formation on the dorsoproximal medial aspect of the proximal phalanx consistent with degenerative joint disease of the metacarpophalangeal joint (black arrow).



Figure 4.7(b) Dorsomedial-palmarolateral oblique image of a metacarpophalangeal joint and proximal phalanx of a 9-year-old crossbred, the same limb as in Figure 4.7(a). There is extensive smoothly marginated new bone on the palmaromedial aspect of the proximal phalanx at the region of insertion of the oblique sesamoidean ligament, the distal digital annular ligament, the axial palmar ligament of the proximal interphalangeal joint and the superficial abaxial ligament of the proximal interphalangeal joint, representing entheseophyte formation (white arrow). There is also periarticular osteophyte formation on the dorsoproximal lateral aspect of the proximal phalanx consistent with degenerative joint disease of the metacarpophalangeal joint (black arrow).

Downloaded From Vet-eBooks.com



Figure 4.9 Lateromedial image of a pastern and foot of a hindlimb of a 5-year-old Arab, with a history of an audible click associated with the pastern of approximately 8 months' duration. The horse occasionally stumbled, but no lameness was detectable. The distal aspect of the proximal phalanx is positioned slightly dorsal relative to the middle phalanx, i.e. there is subluxation of the proximal interphalangeal joint.

Subluxation of the proximal interphalangeal joint

Subluxation of the proximal interphalangeal joint occurs most commonly in hindlimbs and may be unilateral or bilateral. It is generally seen in young horses (up to 5 years of age), but is occasionally seen in older horses. The horse may superficially appear normal at rest, although in some horses the dorsal contour of the proximal interphalangeal joint appears abnormal when viewed from the side. At the walk, abnormal dorsal displacement of the distal end of the proximal phalanx may be apparent. At faster gaits no abnormality can usually be seen. Lateromedial radiographic views confirm slight dorsal displacement of the distal aspect of the proximal phalanx (Figure 4.9). Other radiographic abnormalities are occasionally seen in older horses in which subluxation may develop secondary to injury of the straight sesamoidean ligament or palmar ligaments of the proximal interphalangeal joint. In these cases entheseous new bone may be seen at their attachments on the proximal and middle phalanges, and ultrasonographic examination of the palmar soft tissues of the pastern is indicated. In some horses the condition resolves spontaneously, but assessment of foot balance and tone in the flexor muscle groups may aid in treatment. Desmotomy of the accessory ligament of the deep digital flexor tendon has been successful in both young and mature horses with subluxation of the proximal interphalangeal joint in hindlimbs that did not respond to conservative management.

Osseous cyst-like lesions

Osseous cyst-like lesions in the distal aspect of the proximal phalanx or the proximal aspect of the middle phalanx can be seen as incidental radiological abnormalities, but may be associated with lameness. In a study of 321 foals examined at 6 and 18 months of age, an osseous cyst-like lesion was seen in

Downloaded From Vet-eBooks.com

6.2% of horses, with a similar frequency in Warmbloods, Thoroughbreds and French Trotters. The majority were in the distal condyles of the proximal phalanx in hindlimbs. Six of 15 lesions identified at 6 months of age disappeared by 10 months; none progressed. Forty percent of lesions identified at 18 months were not detectable at 6 months of age. Incidental osseous cyst-like lesions are detected more commonly using magnetic resonance imaging than radiography.

Single osseous cyst-like lesions associated with lameness occur in both middle and proximal phalanges, usually in the subchondral bone close to the proximal interphalangeal joint and frequently eccentrically in the joint. They may originate as shallow depressions in the subchondral bone which progressively enlarge into an osseous cyst-like lesion, which may or may not be surrounded by a rim of increased opacity. In some horses a radiolucent 'neck' can be seen between the osseous cyst-like lesion and the chondral margin. Less commonly a large osseous cyst-like lesion may occur in the trabecular bone distal to the proximal subchondral bone plate of the middle phalanx. Osseous cyst-like lesions causing lameness may respond to conservative or surgical treatment.

Multiple small osseous cyst-like lesions may be associated with degenerative joint disease in the proximal interphalangeal joint and warrant a poor prognosis. This has been described as juvenile degenerative joint disease following osteochondrosis in young horses but is not a common observation. Despite the relative immobility of this joint, the prognosis is poor without surgical intervention and guarded with surgical arthrodesis. The prognosis is better in a hindlimb than in a forelimb.

An osseous cyst-like lesion is occasionally seen adjacent to the origin of a collateral ligament of the distal interphalangeal joint in association with ipsilateral collateral desmitis.

Degenerative joint disease of the proximal interphalangeal joint

In early cases of degenerative joint disease of the proximal interphalangeal joint, there may be small osteophytes on the dorsoproximal aspect of the middle phalanx. These are evident on lateromedial and dorsolateral-palmaromedial and dorsomedial-palmarolateral oblique radiographs, and careful examination of the dorsopalmar view often reveals other subtle changes at the joint margins. In some cases, osteophyte formation may be best evaluated in flexed oblique (dorsolateral-palmaromedial and dorsomedial-palmarolateral oblique [flexed]) images (see Chapter 3, 'Distal phalanx – Other oblique views'). With more advanced disease there may be narrowing of the joint space, radiolucent areas in the subchondral bone, endosteal irregularity, increased opacity of the adjacent trabecular bone and more extensive marginal osteophyte formation. If there is extensive periarticular new bone formation superimposed over the proximal interphalangeal joint assessment of the subchondral bone can be challenging. Joint space width is best assessed on dorsopalmar radiographs (Figure 4.10). In advanced cases, there may be extensive new bone forming from the proximal aspect of the middle phalanx and the distal aspect of the proximal phalanx, preceding ankylosis of the proximal interphalangeal joint.

Downloaded From Vet-eBooks.com

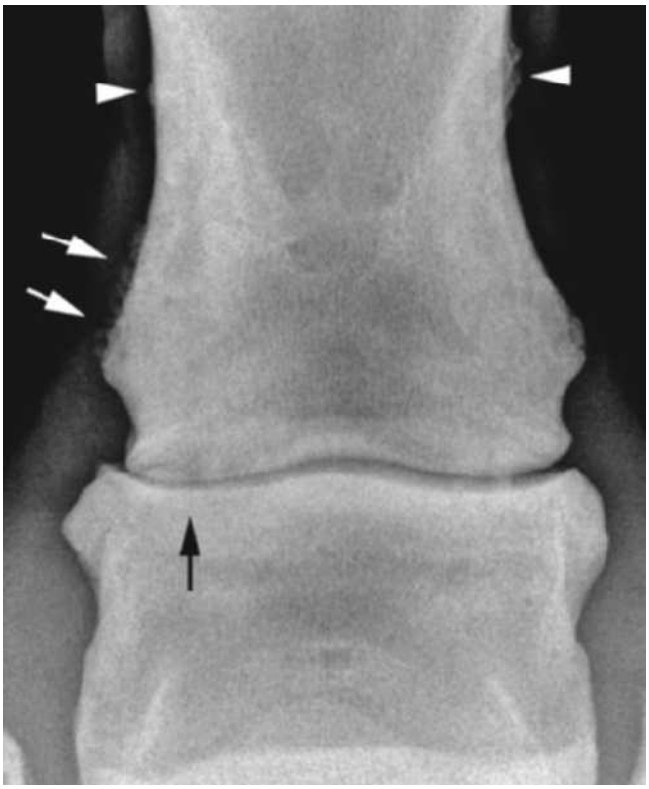


Figure 4.10 Dorsoplantar image of a proximal interphalangeal joint of a 14-year-old Irish Sports horse, with lameness of 3 months' duration. Medial is to the left. There is narrowing of the medial aspect of the proximal interphalangeal joint (black arrow), consistent with degenerative joint disease. There is irregular new bone on the distal medial metaphyseal region of the proximal phalanx (white arrows) representing enthesopathy at the origin of the ligament to the medial ungular cartilage. There is also smoothly outlined new bone on the medial and lateral aspects of the proximal phalanx at the proximal attachment of the distal digital annular ligament (arrowheads).

Once radiographic changes are established the prognosis for spontaneous resolution of lameness and the response to intra-articular medication are poor. Surgical arthrodesis is an option, but the prognosis for competition horses is guarded.

New bone formation

The term ringbone is widely used to describe any new bone formed distal to the fetlock. It is an imprecise term, and should be avoided.

There are many causes of new bone formation in the pastern region. These include entheseophytes at tendon and ligament insertions, localised trauma, localised infection, degenerative joint disease (see above), sagittal fracture of the proximal or middle phalanx (see 'Fractures', below), and hypertrophic osteopathy (see Chapter 1, 'Hypertrophic osteopathy').

Extensive modelling of the dorsal articular margins of the proximal interphalangeal joint can be seen alone, or in association with chronic oblique or straight sesamoidean desmitis (Figure 4.11). It may not be synonymous with degenerative joint disease and, although dramatic in radiographic appearance, may be asymptomatic. Diagnostic analgesia is necessary to determine its

Downloaded From Vet-eBooks.com



Figure 4.11 Dorsolateral-palmaromedial oblique (flexed) radiographic image of the proximal interphalangeal joint of the right forelimb of a 12-year-old show jumper. There is extensive periarticular new bone on the dorsomedial aspect of the proximal interphalangeal joint, although no intra-articular abnormalities were seen. Lameness was not alleviated by intra-articular analgesia. There was evidence of chronic desmitis of the oblique sesamoidean ligaments. The current lameness was associated with a complex of soft-tissue injuries within the hoof capsule.

clinical significance. Ultrasonographic examination of the palmar soft tissues of the pastern is indicated.

There is often entheseous new bone at the attachments of several structures which may reflect multifocal injury, e.g. a collateral ligament of the proximal interphalangeal joint, the distal digital annular ligament (Figure 4.10), the palmar abaxial ligament of the proximal interphalangeal joint and the ligaments between the proximal phalanx and ungular cartilage (Figures 3w.37c–e). Secondary degenerative joint disease may ensue. Entheseophyte formation may be seen at the dorsomedial or dorsolateral aspect of the middle phalanx at the origin of the collateral ligaments of the distal interphalangeal joint in association with ipsilateral collateral desmitis.

Focal, usually unilateral, new bone seen in localised areas on the diaphysis of the proximal or middle phalanges at sites unrelated to ligament or joint capsule attachments is probably due to periostitis as a result of trauma. This may be associated with lameness. The bone normally remodels and the lameness resolves, unless the bone is forming in a position prone to repeated trauma, e.g. on the medial aspect of the limb where it is constantly struck by the contralateral limb (Figure 4.12).

Irregularly outlined palisading new bone is sometimes seen on the dorsal diaphysis of the middle phalanx in a lateromedial image (Figure 4.13, see also Figure 3.41). This is generally associated with lameness relieved by intra-articular analgesia of the distal interphalangeal joint. The aetiology is

Downloaded From Vet-eBooks.com

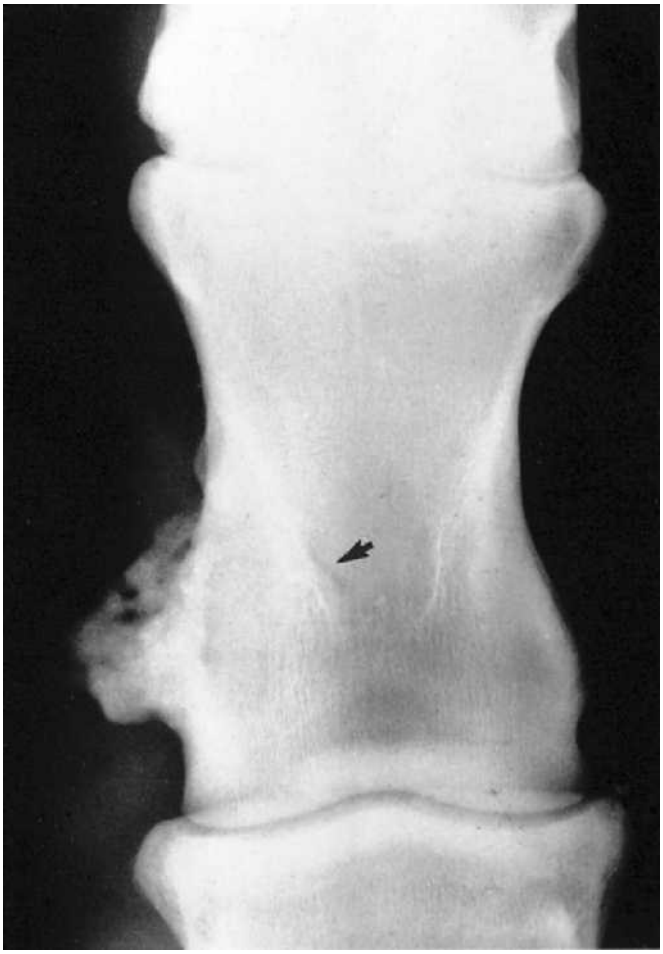


Figure 4.12 Dorsopalmar image of a pastern (medial is to the left), showing new bone on the distal medial aspect of the proximal phalanx caused by repeated trauma (the oblique radiolucent line, arrowed, represents a nutrient vessel).

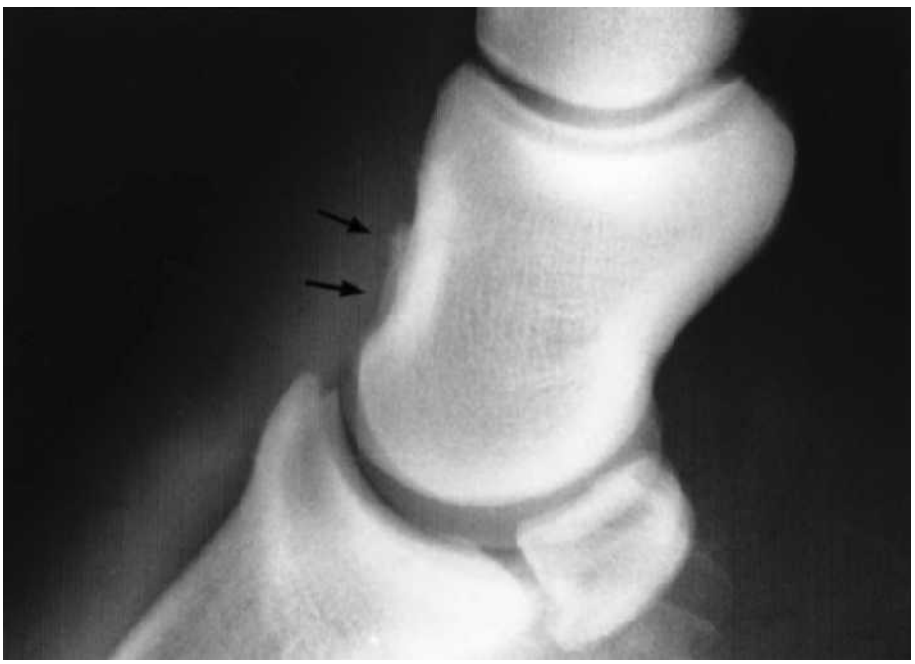


Figure 4.13 Lateromedial image of the proximal and distal interphalangeal joints of an 8-year-old horse, with lameness alleviated by intra-articular analgesia of the distal interphalangeal joint. There is palisading new bone (arrows) on the dorsal cortex of the diaphyseal region of the middle phalanx, within the distal interphalangeal joint capsule.

Downloaded From Vet-eBooks.com



Figure 4.14 Dorsolateral-palmaromedial oblique radiographic image of the proximal aspect of a pastern of a 6-year-old dressage horse. There is irregular new bone on the proximopalmar lateral aspect of the proximal phalanx (arrows), at the site of insertion of the proximal digital annular ligament. The horse resented digital pressure applied to this area. The soft tissue opacity distal to the lateral proximal sesamoid bone is the ergot. Note the concave depression in the skin contour palmar to the ergot.

uncertain, although such new bone is often seen in association with degenerative joint disease. The bone lies within the dorsoproximal outpouching of the distal interphalangeal joint capsule and surgical debridement of this new bone may result in resolution of lameness. Occasionally smoothly outlined new bone is seen at the same site unassociated with clinical signs.

New bone unassociated with the interphalangeal joints may develop, encircling the phalanges. The aetiology is unknown. It is usually associated with chronic lameness.

New bone on the dorsoproximal aspect of the proximal or middle phalanges must be differentiated from that associated with a partial or complete sagittal fracture of the proximal or middle phalanges (see 'Fractures', below and Figure 4.18).

New bone (entheseophytes) is often seen at the region of insertion of the oblique sesamoidean ligaments on the palmar aspect of the proximal phalanx. This is probably due to chronic or acute stress on the ligaments (see Figure 4.7). It may cause lameness initially while actively forming, but is not of long-term clinical significance, unless there is ongoing desmitis. It should alert the clinician to the possibility of soft-tissue injury. Ultrasonography may be used to assess the ligaments. New bone may be seen at the attachments of the proximal or distal digital annular ligaments to the medial and lateral aspects of the proximal and middle phalanges respectively, reflecting enthesopathy (see Figure 4.3b and Figure 4.14).

Downloaded From Vet-eBooks.com

'Scalping' injury of the proximal or middle phalanx

A 'scalping' injury of the proximal or middle phalanx is usually the result of another horse galloping alongside and striking into the horse, resulting in a 'scooped out' concave defect in the dorsal cortex of the bone. Although initially causing severe lameness, such lesions usually resolve spontaneously.

Collateral ligament injury of the proximal interphalangeal joint

Modelling of the distal eminence of the proximal phalanx medially and/or laterally or focal bone resorption usually reflects collateral ligament injury. With a severe injury there may be detectable soft-tissue swelling on the ipsilateral side of the proximal interphalangeal joint. Ultrasonographic examination of the collateral ligaments may be indicated. With severe injuries there may be associated subchondral bone trauma detectable using magnetic resonance imaging, which may result in secondary degenerative joint disease.

Rupture of the straight sesamoidean ligament

Rupture of the straight sesamoidean ligament is an unusual injury which results in sudden over extension of the proximal interphalangeal joint, but has no other radiological signs. The joint should be inspected carefully for other concurrent injuries.

Subchondral bone trauma of the proximal axial aspect of the proximal phalanx

Lesions of the condyles of the proximal aspect of the proximal phalanx are discussed in Chapter 5. Trauma of the subchondral bone of the sagittal groove of the proximal phalanx may result in either a small incomplete fissure fracture (see 'Fractures', below, and Figure 5w.9c) or the development of an ill-defined radiolucent area in the subchondral bone (Figure 4w.15). The subchondral bone plate at the sagittal groove may be thickened and have an irregular endosteal margin. The extent of such lesions may be better defined using magnetic resonance imaging. These lesions, which may occur unilaterally or bilaterally, are usually associated with increased radiopharmaceutical uptake. They may be the result of repetitive loading rather than a single traumatic event. Lameness may resolve with rest, but radiological abnormalities may persist. Occasionally small incomplete fissures are seen as an incidental finding with normal radiopharmaceutical uptake.

Subchondral bone trauma of the proximal interphalangeal joint

Sudden-onset, severe lameness may be followed by the development of an ill-defined radiolucent area in the subchondral bone of the distal aspect of the proximal phalanx or more commonly the proximal aspect of the middle phalanx (Figure 4w.16). Such lesions may be an ill-defined horizontal lesion parallel to the articular surface or a more focal circular region of reduced opacity. These lesions may extend over time into the adjacent trabecular bone. Periosteal new bone may develop on the ipsilateral cortex of the

Downloaded From Vet-eBooks.com

affected bone. Periarticular new bone may develop, reflecting secondary degenerative joint disease. These lesions are thought to arise as a result of focal cartilage and subchondral bone trauma. In the acute phase magnetic resonance imaging may give more information than radiography. Such lesions are associated with intense focal increased radiopharmaceutical uptake. The prognosis is guarded.

Subchondral bone trauma of the distal dorsal aspect of the middle phalanx

There is a syndrome characterised by lameness associated with a diffuse area of increased signal intensity in fat-suppressed magnetic resonance images in the distal dorsal aspect of the middle phalanx, either medially or laterally. This is thought to reflect bone trauma. There are usually no associated detectable radiological abnormalities at any stage of this condition.

Fractures

Fractures of the proximal and middle phalanges are relatively common (see Figure 5.30). Small chip fractures of the proximal aspect of the proximal phalanx are described elsewhere (see Chapter 5, 'Osteochondrosis, developmental orthopaedic disease and osteochondral fragments') and are of variable significance.

Osteochondral fragments on the dorsal or palmar aspect of the proximal interphalangeal joint are not common, but can be seen as incidental radiological findings or can be associated with lameness. In a study of pre-sales radiographs of 3,749 German Warmbloods an osteochondral fragment was identified in the proximal interphalangeal joint in 0.9% of horses. The significance of a fragment therefore needs to be verified by intra-articular analgesia. Midline palmar fragments may represent an avulsion of the insertion of either the straight sesamoidean ligament or the axial palmar ligaments of the proximal interphalangeal joint. Fragments adjacent to the lateral or medial palmar eminence may represent an avulsion of the insertion of the abaxial palmar ligament of the proximal interphalangeal joint or the proximal attachment of the distal digital annular ligament. Fragments believed to be a cause of lameness can be removed arthroscopically with a reasonable prognosis, assuming that there is not severe concurrent ligamentous injury.

Midline sagittal fractures occur in both bones, but are more common in the proximal phalanx. Although such fractures occur most commonly in racehorses, they also occur in sports horses. They frequently follow a spiral course and are generally seen as a double radiolucent line extending through the diaphysis of the bone. Each line represents cortical discontinuity (Figure 4.17). There are three principal types of midline sagittal fracture:

1 A fracture extending from the proximal to the distal joint, and entering both joints.

2 A fracture extending from either joint and exiting through the cortex.

3 An incomplete sagittal fracture extending from one of the two joints into the diaphysis of the bone (Figures 4.18a and 4.18b). These may only involve the dorsal cortex and most commonly affect the proximal phalanx. Fractures may be associated with either articular comminution or mid-diaphyseal comminution.

Downloaded From Vet-eBooks.com



Figure 4.17 Dorsopalmar image of a pastern, showing a complete sagittal fracture of the proximal phalanx (note the double lucent line which represents the fracture through the dorsal and palmar cortices).

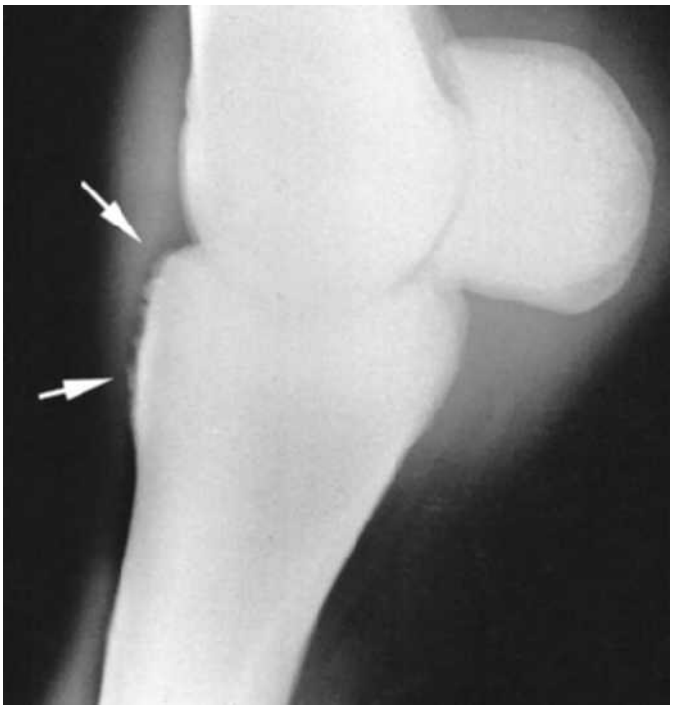


Figure 4.18(a) Lateromedial image of the pastern, showing new bone on the dorsoproximal aspect of the proximal phalanx (arrows) secondary to an incomplete sagittal fracture of approximately 6 weeks' duration.

Initially there may be little or no displacement and surprisingly limited clinical signs. The fracture may also be difficult to detect, and therefore a series of oblique views should be obtained if there is any suspicion that such a fracture may be present. A series of oblique views may also be needed to determine the exact configuration of a fracture. In the acute stage radiography frequently underestimates the complexity of fracture configuration. Radiographs acquired more than 10–14 days after injury may reveal additional fracture lines and/or elongation of previously detected fracture lines, presumably because of either osteoclastic resorption making fracture lines more obvious or fracture propagation. Non-displaced sagittal fractures may be accompanied by remarkably little lameness, and this has led to such cases being returned to work undiagnosed, sometimes with catastrophic results.

Incomplete fractures of the proximal aspect of the proximal phalanx can be very difficult to detect in the acute stage. If the horse is exercised however, such fractures can propagate into catastrophic comminuted fractures.

Downloaded From Vet-eBooks.com



Figure 4.18(b) Dorsopalmar image of a pastern, showing an incomplete sagittal fracture of the proximal phalanx (arrow) of approximately 6 weeks' duration. Note that much of the fracture line is superimposed over the distal end of the third metacarpal bone. Arrowheads highlight the dorsoproximal aspect of the proximal phalanx. There is some increased opacity around the fracture in the proximal phalanx.



Figure 4.18(c) Dorsoproximal-plantarodistal oblique image of the left metatarsophalangeal joint of an 8-year-old sports horse. There is an incomplete articular fracture of the proximal aspect of the proximal phalanx in the sagittal groove. No abnormality was detected in a lateromedial image.

If a fracture is suspected on clinical grounds the horse should be rested and re-radiographed after 10 days, when rarefaction along the fracture line may be more obvious. Nuclear scintigraphy may be useful. Some horses never develop any associated radiographic abnormality. In others, an incomplete fracture may not be detected radiographically until callus forms as part of the normal healing process. This is seen as new bone on the dorsoproximal aspect of the proximal phalanx (Figures 4.18a and 4.18b) and may be best detected on lateromedial radiographs. Reduced exposures are needed to demonstrate this poorly mineralised new bone. In some cases there is only increased opacity in the midline of the proximal aspect of the proximal phalanx seen in a dorsoproximal-palmarodistal oblique view. Incomplete fractures have a good prognosis with conservative treatment, but repeat radiographs should be obtained to ensure healing does take place. Although most incomplete fractures of the proximal aspect of the proximal phalanx involve the dorsal cortex, less commonly they occur as sagittal fissures midway between the dorsal and palmar cortices (Figure 4.18c), and may sometimes

Downloaded From Vet-eBooks.com



Figure 4.19 Dorsomedial-palmarolateral oblique image of a metacarpophalangeal joint, showing a slightly displaced articular fracture of the medial palmar process of the proximal phalanx. There are some ill-defined opacities in the dorsal aspect of the joint.

be seen as an ill-defined lucent area in the most proximal aspect of the proximal phalanx in a dorsoproximal-palmarodistal oblique view (see 'Subchondral bone trauma of the proximal aspect of the proximal phalanx', above).

There is growing evidence that in Thoroughbred racehorses some parasagittal fractures of the proximal aspect of the proximal phalanx may be the result of stress-related bone injury and there are prodromal radiological abnormalities including increased thickness of the subchondral bone plate at the sagittal groove. Nuclear scintigraphy or magnetic resonance imaging may be more sensitive than radiography for detection of prodromal abnormalities in some horses.

Simple fractures of the proximal or middle phalanx respond well to internal fixation, but comminuted fractures are common and may be so extensive that any treatment is hopeless. Use of an external fixator for severely comminuted fractures or internal fixation and arthrodesis can occasionally save an animal for breeding purposes.

Fractures of the dorsal and palmar/plantar aspects of the proximal epiphysis of the proximal phalanx occasionally occur. Dorsal 30° proximal 70° lateral-palmarodistomedial oblique and dorsal 30° proximal 70°medial-palmarodistolateral oblique images are helpful for identification of such fractures (see Chapter 5, 'Radiographic technique – Special oblique views'). These may occur as simple fractures or in combination with sagittal fractures.

Palmar or, more commonly, plantar fractures frequently involve either the medial or lateral tuberosity of the proximal phalanx (Figure 4.19). It is possible for both tuberosities to fracture separately or for a complete fracture of the palmar/plantar aspect of the bone to occur. Fractures of the tuberosity usually involve only a proximal fragment, but occasionally extend down the diaphysis. They may be articular or non-articular, and may require surgical fixation.

Small fragments on the palmar or plantar articular margin of the proximal phalanx (Figure 4.20) occur on the axial aspect of the medial or lateral

Downloaded From Vet-eBooks.com



Figure 4.20 Oblique lateromedial radiographic image of the left metatarsophalangeal joint of an 8-year-old Thoroughbred purchased 1 week previously. There was soft-tissue swelling on the dorsal aspect of the fetlock and mild lameness, which was not altered by distal limb flexion. There is a small articular fragment displaced from the medial plantar tuberosity of the proximal phalanx (black arrows). There is a large smoothly outlined osseous opacity (white arrow) plantar to the lateral plantar tuberosity of the proximal phalanx. There is a small mineralised opacity on the dorsal aspect of the metatarsophalangeal joint.

tuberosity, near the insertion of the cruciate sesamoidean ligaments. These are more common in hindlimbs and have been referred to as Birkeland fractures. However, some workers suggest that these fragments are associated with osteochondrosis. Surgical removal of these fragments may be indicated.

Dorsal frontal fractures also occur predominantly in hindlimbs. They are often incomplete. Incomplete fractures have a good prognosis with conservative treatment, but complete fractures usually require surgical treatment. Articular fractures of the distal medial or distal lateral aspect of the middle phalanx, close to the site of insertion of the collateral ligament of the distal interphalangeal joint, sometimes occur. Multiple flexed oblique views may be required to identify the fracture (Figure 4.21). Surgical removal usually results in a satisfactory outcome.

Dystrophic mineralisation

Dystrophic mineralisation occasionally occurs in the sesamoidean ligaments. Its significance is equivocal. Ultrasonography may be useful.

Tumours

Neoplastic lesions in the pastern are rare, but osteosarcoma has been recorded.

Downloaded From Vet-eBooks.com



Figure 4.21 Dorsal 45° medial-plantarolateral (flexed) oblique image of the foot and pastern of a horse with acute-onset, severe lameness. There is an articular fracture (arrow) of the distal aspect of the lateral condyle of the middle phalanx. The shoe had not been removed for clinical reasons.

Additional figures

The book companion website at www.clinical-radiology-horse.com includes additional figures that are not included in the printed book or e-book formats. Please see '**About the Companion Website**' at the start of the book for details on how to access the website. These figures are prefixed with the letter 'w' in the printed book, e.g. Figures 1w.4c–f.

FURTHER READING

Brasche, S., Rick, M., Herthel, D. (2004) Treatment of a horse with osteomyelitis following repair of a middle phalangeal fracture via pastern arthrodesis. *Equine Vet. Educ.* **16**, 262–266

Caston, S., McClure, S., Beug, J. et al. (2013) Retrospective evaluation of facilitated pastern ankylosis using intra-articular ethanol injections: 34 cases (2006–2012). *Equine Vet. J.* **45**, 442–447

Cillan-Garcia, E., Kearns, L., Hetze, U. et al. (2010) Osteosarcoma of the middle phalanx in a horse. *Equine Vet. Educ.* **22**, 535–539

Contino, E., Park, R., McIlwraith, C. W. (2011) Prevalence of radiographic changes in yearling and 2-year-old Quarter Horses intended for cutting. *Equine Vet. J.* **44**, 185–195

Doran, R., White, N., Allen, D. (1987) Use of a bone plate for treatment of middle phalangeal fractures in horses: 7 cases (1979–1984). *J. Am. Vet. Med. Ass.* **191**, 575–578

Dowling, B., Dart, A., Hodgson, D. (1998) Subchondral cystic lesion involving the second phalanx in two horses. *Aust. Vet. J.* **76**, 328–331

Downloaded From Vet-eBooks.com

Dyson, S., Nagy, A., Murray, R. (2011) Clinical and diagnostic imaging findings in horses with subchondral bone trauma of the sagittal groove of the proximal phalanx. *Vet. Radiol. Ultrasound* **52**, 596–604

Ellis, D., Simpson, D., Greenwood, R., Crowhurst, J. (1987) Observations and management of fractures of the proximal phalanx in young Thoroughbreds. *Equine Vet. J.* **19**, 43–49

Ellis, D., Greenwood, R. (1985) Six cases of degenerative joint disease of the proximal interphalangeal joint of young thoroughbreds. *Equine Vet. J.* **17**, 66–68

Fjordbakk, C., Strand, E., Milde, A. et al. (2007) Osteochondral fragments involving the dorsomedial aspect of the proximal interphalangeal joint in young horses: 6 cases (1997–2006). *J. Am. Vet. Med. Ass.* **230**, 1498–1501

Holcombe, S.J., Schneider, R.K., Bramlage, L.R., Gabel, A.A., Bertone A.L., Beard, W.L. (1995) Lag screw fixation of non-comminuted sagittal fractures of the proximal phalanx in racehorses: 59 cases (1973–1991). *J. Am. Vet. Med. Ass.* **206**, 1195–1199

Jacquet, S., Robert, C., Valette, J.-P., et al. (2013) Evolution of radiological findings detected in the limbs of 321 young horses between the ages of 6 and 18 months. *Vet. J.* **197**, 58–64

Jones, P., Delco, M., Beard, W., et al. (2009) A limited surgical approach for pastern arthrodesis in horses with severe osteoarthritis: 11 horses, 2000–2007. *Vet. Comp. Orthop. Traumatol.* **22**, 303–308

Kamm, J., Goodrich, L., Werpy, N. et al. (2012) A descriptive study of the equine proximal interphalangeal joint using magnetic resonance imaging, contrast arthrography, and arthroscopy. *Vet. Surg.* **41**, 677–684

Kraus, B., Richardson, D., Nunamaker, D., Ross, M. (2004) Management of comminuted fractures of the proximal phalanx in horses: 64 cases (1983–2001). *J. Am. Vet. Med. Ass.* **224**, 254–263

Knox, P., Watkins, J. (2006) Proximal interphalangeal joint arthrodesis using a combination plate–screw technique in 53 horses (1994–2003). *Equine Vet. J.* **38**, 538–542

Kold, S., Killingbeck, J. (1998) The use of autogenous cancellous bone graft for the treatment of subchondral bone cysts in the distal phalanges; three cases. *Equine Vet. Educ.* **10**, 307–312

Markel, M., Richardson, D. (1985) Non comminuted fractures of the proximal phalanx in 69 horses. *J. Am. Vet. Med. Ass.* **186**, 573–579

Markel, M., Martin, B., Richardson, D. (1985) Dorsal frontal fractures of the first phalanx in the horse. *Vet. Surg.* **14**, 36–40

Markel, M., Richardson, D., Nunamaker, D. (1985) Comminuted first phalanx fractures in 30 horses. *Surgical versus non-surgical treatments. Vet. Surg.* **14**, 135–140

Olive, J., Mair, T., Charles, B. (2009) Use of standing low-field magnetic resonance imaging to diagnose middle phalanx lesions in horses. *Equine Vet. Educ.* **21**, 116–123

Pizzigatti, D., Hussni, C., Rodrigues, C. et al. (2013) Bilateral dorsal subluxation of the proximal interphalangeal joint in a mare: case report. *J. Equine Vet. Sci.* **33**, 746–750

Pudadera, J., Dart, A. (2010) Using magnetic resonance imaging to diagnose non-displaced fractures of the second phalanx in horses. *Aust. Vet. J.* **88**, 439–442

Radcliff, R., Cheetham, J., Bezuidenhout, A. et al. (2008) Arthroscopic removal of palmar/plantar osteochondral fragments from the proximal interphalangeal joint in four horses. *Vet. Surg.* **37**, 733–740

Ramzan, P., Powell, S. (2010) Clinical and imaging features of suspected prodromal fracture of the proximal phalanx in three Thoroughbred racehorses. *Equine Vet. J.* **42**, 164–169

Schaer, T., Bramlage, L., Embertson, R., Hance, S. (2001) Proximal interphalangeal arthrodesis in 22 horses. *Equine Vet. J.* **33**, 360–365

Sherlock, C., Mair, T. (2011) Osseous cyst-like lesions/subchondral bone cysts of the phalanges. *Equine Vet. Educ.* **23**, 191–204

Shiroma, J., Engel, H., Watrous, B. (1989) Dorsal subluxation of the proximal interphalangeal joint in the pelvic limb of three horses. *J. Am. Vet. Med. Ass.* **195**, 777–780

Smith, M., Wright, I. (2014) Radiographic configuration and healing of 121 fractures of the proximal phalanx in 120 Thoroughbred racehorses (2007–2011). *Equine Vet. J.* **46**, 81–87

Smith, M., Wright, I. (2014) Are there radiologically identifiable prodromal changes in Thoroughbred racehorses with parasagittal fractures of the proximal phalanx? *Equine Vet. J.* **46**, 88–91

Stock, K., Hamann, H., Distl, O. (2005) Prevalence of osseous fragments in distal and proximal interphalangeal, metacarpo- and metatarsophalangeal and tarsocrural joints of Hanoverian Warmblood horses. *J. Vet. Med. A* **52**, 388–394

Trotter, G., McIlwraith, C., Nordin, R., Turner, A. (1982) Degenerative joint disease with osteochondrosis of the proximal interphalangeal joint in young horses. *J. Am. Vet. Med. Ass.* **180**, 1312–1318

Weaver, J., Stover, S., O'Brien, T. (1992) Radiographic anatomy of soft tissue attachments in the equine metacarpophalangeal and proximal phalangeal region. *Equine Vet. J.* **24**, 310–315

Downloaded From Vet-eBooks.com

Downloaded From Vet-eBooks.com

Chapter 5
Metacarpophalangeal and metatarsophalangeal (fetlock) joints

RADIOGRAPHIC TECHNIQUE

Although this chapter refers to the metacarpophalangeal joint, it applies equally well to the metatarsophalangeal joint. A standard examination includes lateromedial, dorsolateral-palmaromedial oblique (D45°L-PaMO), dorsomedial-palmarolateral oblique (D45°M-PaLO) and dorsoproximal-palmarodistal oblique images. Lateromedial (flexed) images potentially give more information than weight-bearing lateromedial images. Additional views may be required to identify specific lesions, especially in racehorses.

Equipment

Radiographs of the metacarpophalangeal joint are readily obtained with portable equipment and do not require the use of a grid. Digital systems, or high-definition screens and compatible film are recommended when available.

Positioning

Lateromedial, dorsal 45° lateral-palmaromedial oblique, dorsal 45° medial-palmarolateral oblique and dorsoproximal-palmarodistal oblique views

Standard views of the metacarpophalangeal joint are obtained with the horse weight bearing, using a horizontal x-ray beam for the lateromedial and oblique images. Initial exposures should give good visualisation of the trabecular pattern of the distal aspect of the third metacarpal bone, but may be reduced for evaluation of soft tissues, chip fractures or new bone. Although only four standard views need to be obtained during a routine examination, dorsal 60° lateral-palmaromedial oblique and dorsal 60° medial-palmarolateral oblique views may be necessary for better assessment of lesions on the dorsal joint margins. Superimposition of the proximal sesamoid bones over the metacarpophalangeal joint space is avoided by angling the x-ray beam proximodistally at least 10° for a dorsopalmar view (dorsal 10° proximal-palmarodistal oblique) and at least 15° for a dorsoplantar view (dorsal 15° proximal-plantarodistal oblique). The precise angle depends on both the foot pastern axis and the position of the limb. The position of the limb (forelimb or hindlimb) markedly influences the position of the proximal

Clinical Radiology of the Horse, Fourth Edition. Janet A. Butler, Christopher M. Colles, Sue J. Dyson, Svend E. Kold and Paul W. Poulos.
© 2017 John Wiley & Sons, Ltd. Published 2017 by John Wiley & Sons, Ltd.
Companion website: www.clinical-radiology-horse.com

Downloaded From Vet-eBooks.com

sesamoid bones relative to the third metacarpal or metatarsal bone and the proximal phalanx for all views. Whilst ideally the fetlock should be extended, with the limb as far back as possible while weight bearing (in order to 'lift' the proximal sesamoid bones), the horse may stand more comfortably and be less likely to move if the metacarpal/metatarsal regions are vertical.

If there is some rotation of the distal aspect of the limb, it can be difficult to achieve a true lateromedial image. The position of the metacarpophalangeal joint relative to the foot should be assessed. Usually aligning the x-ray beam from the lateral aspect 5° palmar to a line tangential to the bulbs of the heel (i.e. lateral 5° palmar-medial dorsal oblique) will result in a true lateromedial view, but this may need to be adjusted in the light of results. It may help to palpate the relative positions of the medial and lateral epicondyles of the third metacarpal bone. This is particularly important in hindlimbs, since many horses stand with the limb rotated outwards. A true lateromedial projection is required for proper assessment of the sagittal ridge of the third metacarpal bone, but slightly oblique views may sometimes be helpful for assessment of suspect lesions elsewhere in the joint.

Examination of the proximal sesamoid bones is only partially achieved on the standard views described above. A dorsopalmar view acquired at higher kilovoltage is required to assess the axial surface of the bones. Further oblique views may also be required (see below).

Lateromedial (flexed) view

A lateromedial (flexed) view of the metacarpophalangeal joint gives better visualisation of the articular surfaces of the proximal sesamoid bones and of the sagittal ridge of the third metacarpal bone than a weight-bearing image. Lesions of the dorsodistal aspect of the sagittal ridge of the third metacarpal bone may be missed in a weight-bearing lateromedial image. If slightly oblique, the flexed view may aid in determining the extent of chip fractures of the base of the proximal sesamoid bones. These radiographs may be enhanced by reducing the mAs slightly from that normally required for the third metacarpal bone. The lateromedial (flexed) view is obtained by resting the horse's toe on a block, preferably 20–25 cm high, with the metacarpophalangeal joint flexed (or positioning the joint similarly, holding the limb at the toe). The x-ray beam is centred on the centre of the radius of curvature of the distal articular surface of the third metacarpal bone. The alignment of the beam may be difficult, as slight abnormalities in conformation result in oblique images. It is most practical to acquire one image and realign the beam if necessary.

Special oblique views

Standard D45°L-PaMO and D45°M-PaLO views highlight the lateral and medial proximal sesamoid bones respectively, allowing assessment of their shape, internal architecture and the apex, dorsal, palmar and distal borders. Additional information can also be obtained from a lateral 45° proximal-medial distal oblique view (L45°Pr-MDiO) (Figure 5.1a), to highlight the abaxial surface of the medial proximal sesamoid bone (Figure 5.1b) and a medial 45° proximal-lateral distal oblique view (M45°Pr-LDiO) to highlight the abaxial surface of the lateral proximal sesamoid bone.

Downloaded From Vet-eBooks.com

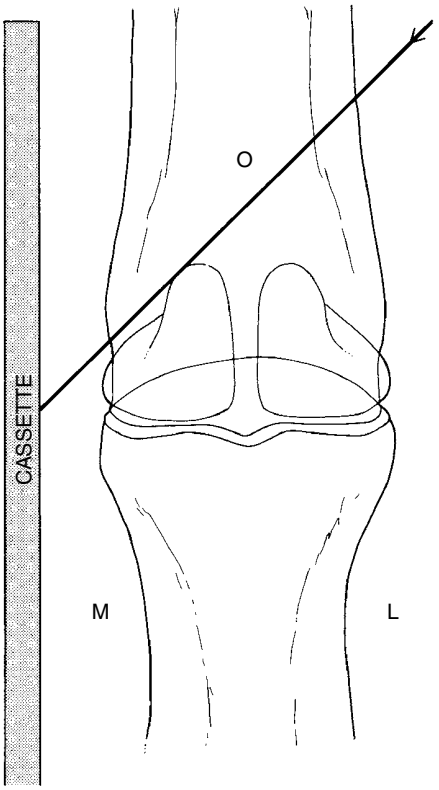


Figure 5.1(a) Technique to obtain lateral 45° proximal-medial distal oblique view to skyline the abaxial surface of the medial proximal sesamoid bone.

Evaluation of the proximal palmar (plantar) articular margins of the palmar (plantar) process of the proximal phalanx is sometimes best achieved using a dorsal 30° proximal 70° lateral-palmar distal medial oblique view (D30°Pr70°L-PaDiMO) (Figure 5.2a) or a dorsal 30° proximal 70° medial-palmar distal lateral oblique view (D30°Pr70°M-PaDiLO). This view is particularly useful for identification of palmar (plantar) fragments, and determining their source (see 'Osteochondrosis, developmental orthopaedic disease and osteochondral fragments', below). The D30°Pr70°L-PaDiMO view projects the lateral proximal sesamoid bone distal to the medial proximal sesamoid bone, and highlights the lateral palmar (plantar) process of the proximal phalanx (Figure 5.2b).

Assessment of the palmar (plantar) aspect of the lateral and medial condyles of the third metacarpal (metatarsal) bone may be facilitated by using a dorsal 45° proximal 45° lateral-palmar distal medial oblique view (D45°Pr45°L-PaDiMO), to project the lateral condyle distal to the medial condyle (Figure 5.3). This view is particularly useful for identification of stress reactions (radiolucency or increased radiopacity) in the lateral (or medial) condyle of the third metacarpal or metatarsal bone (see 'Stress-related bone injury', below).

Tangential dorsopalmar views

The articular surface of the distal aspect of the third metacarpal bone curves through 180°. On dorsopalmar views, only a limited part of the bone and joint tangential to the beam is clearly visualised. This means that when third metacarpal condylar fractures or osteochondral lesions are suspected, several dorsoproximal-palmarodistal or dorsodistal-palmaroproximal tangential views can be useful for determining the extent of such fractures

Downloaded From Vet-eBooks.com

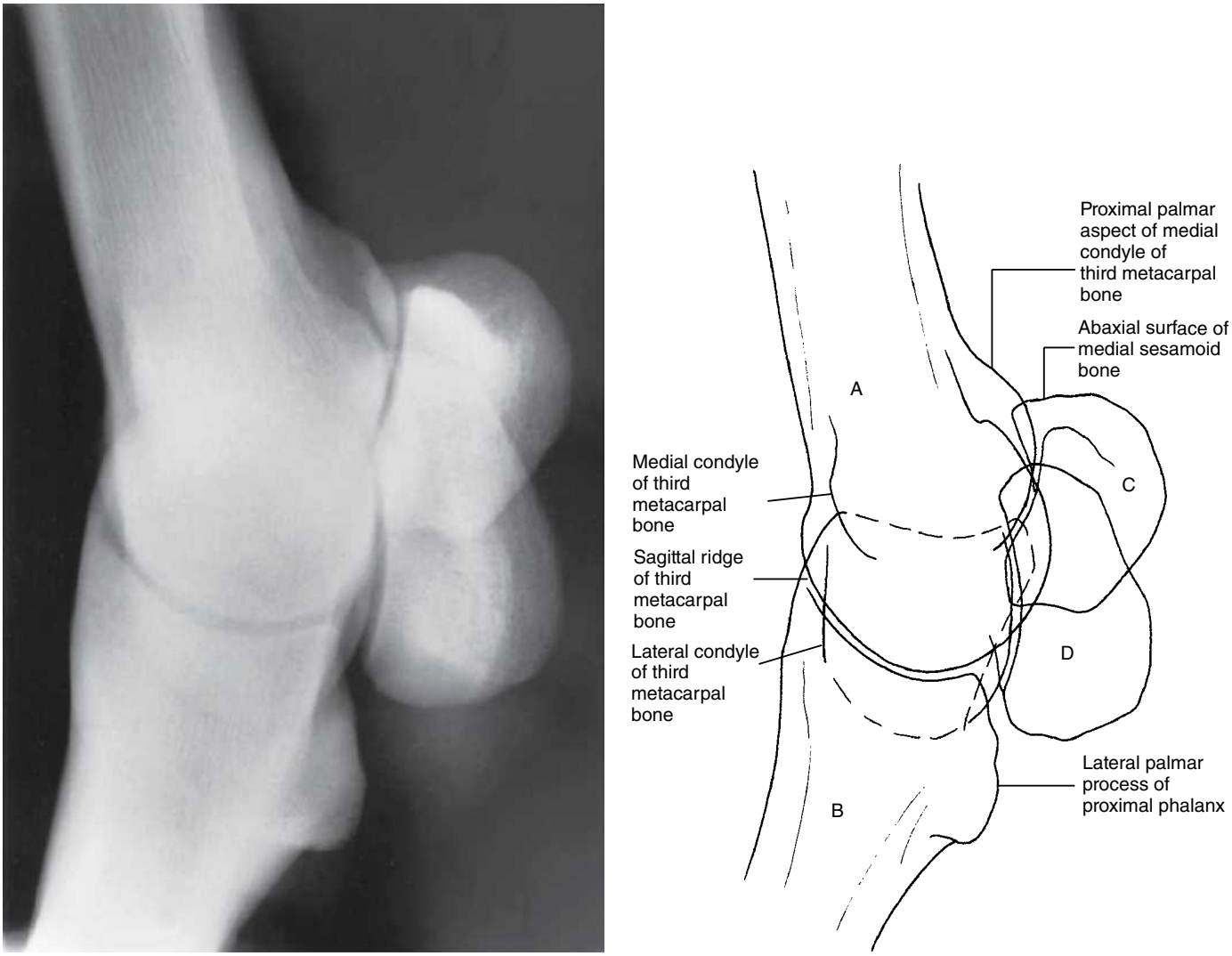


Figure 5.1(b) Lateral 45° proximal-medial distal oblique radiographic image and diagram of the metacarpophalangeal joint of a normal adult horse. A = third metacarpal bone, B = proximal phalanx, C = medial proximal sesamoid bone, D = lateral proximal sesamoid bone.

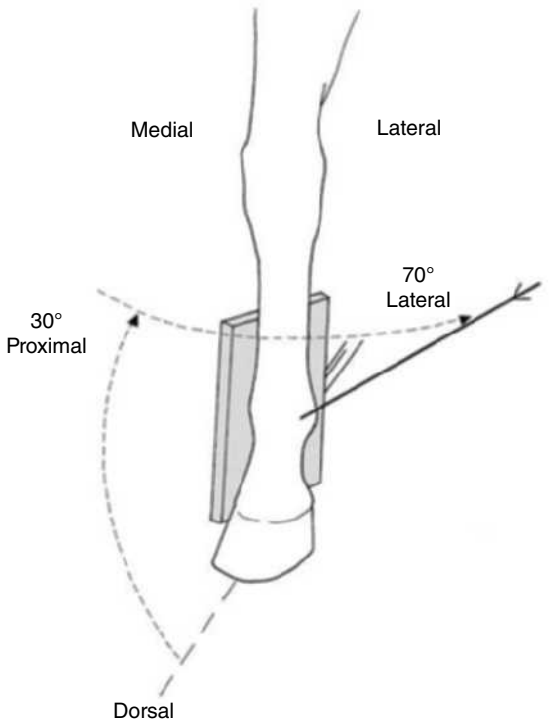


Figure 5.2(a) Positioning to obtain a dorsal 30° proximal 70° lateral-palmarodistal medial oblique view of the metacarpophalangeal joint, to highlight the lateral palmar process of the proximal phalanx.

Downloaded From Vet-eBooks.com

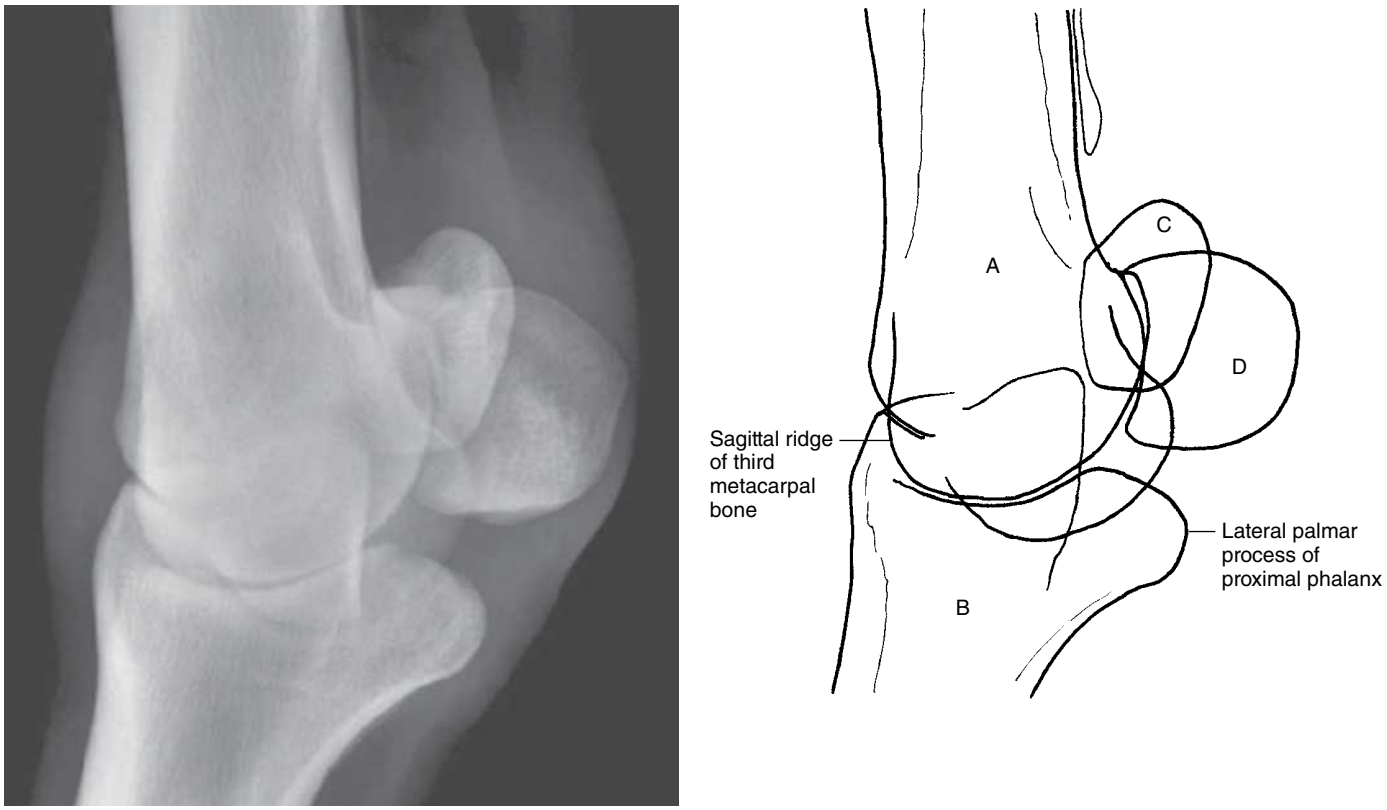


Figure 5.2(b) Dorsal 30° proximal 70° lateral-palmarodistal medial oblique radiographic image and diagram of the metacarpophalangeal joint of a normal adult horse. A = third metacarpal bone, B = proximal phalanx, C = medial proximal sesamoid bone, D = lateral proximal sesamoid bone.

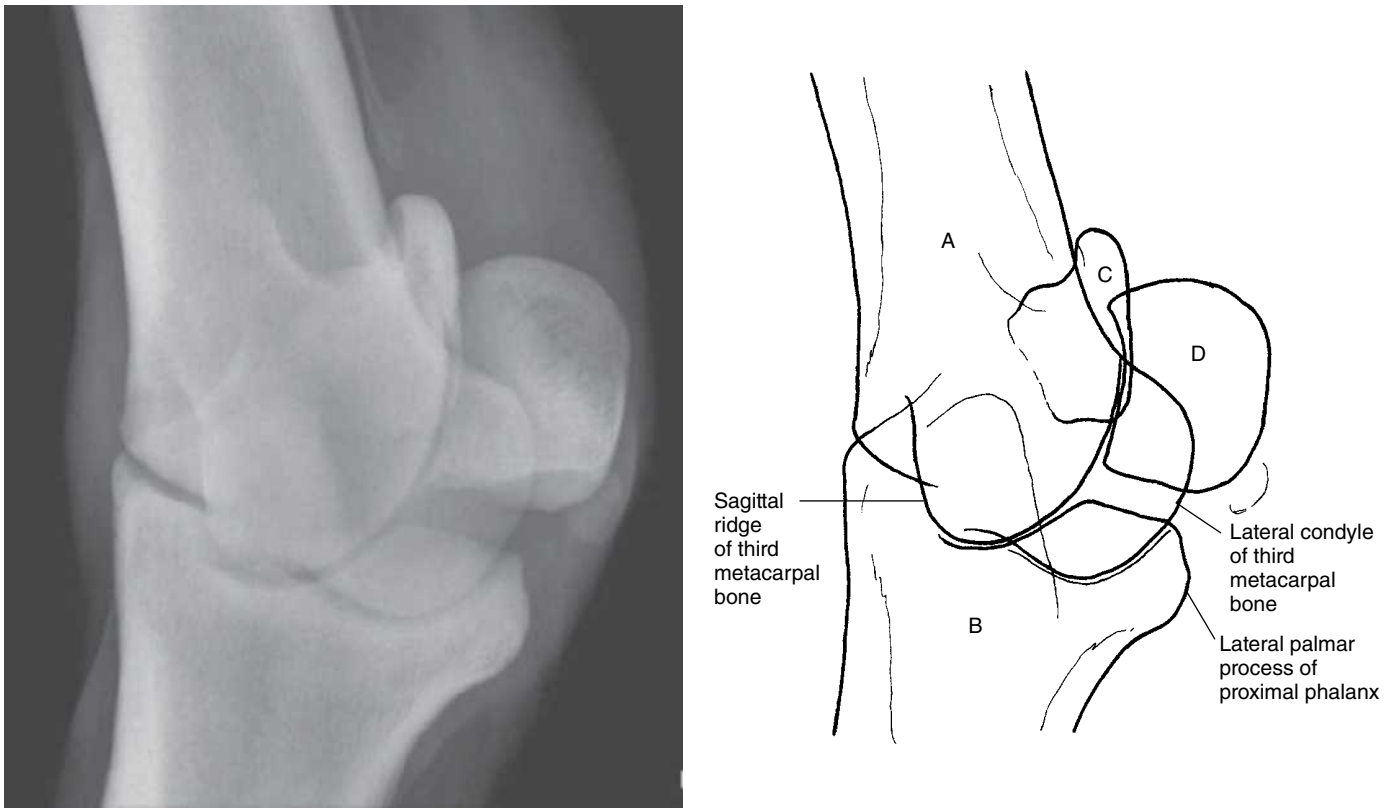


Figure 5.3 Dorsal 45° proximal 45° lateral-palmarodistal medial oblique radiographic image and diagram of the metacarpophalangeal joint of a normal adult horse. A = third metacarpal bone, B = proximal phalanx, C = medial proximal sesamoid bone, D = lateral proximal sesamoid bone.

Downloaded From Vet-eBooks.com

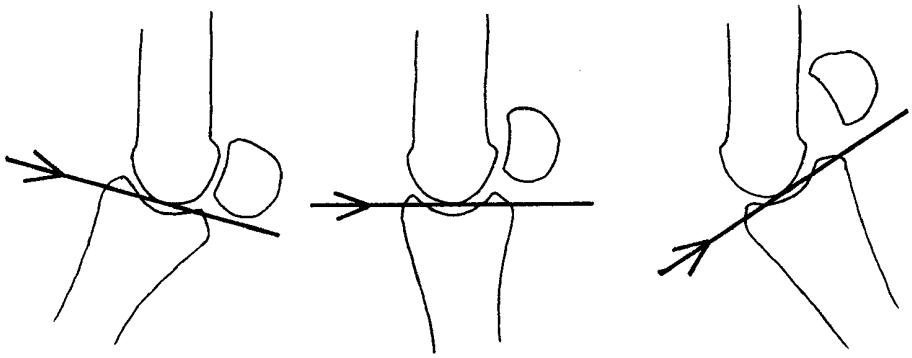


Figure 5.4 Technique to obtain dorsoproximal-palmarodistal oblique, dorsopalmar (flexed) and dorsodistal-palmaroproximal (flexed) oblique views of the metacarpophalangeal joint. Note the different angles made by the x-ray beam to the long axis of the third metacarpal bone, in order to skyline different areas of the third metacarpal bone.

and confirming possible comminution (Figure 5.4). Improved assessment may be achieved by flexing the metacarpophalangeal joint. The toe of the foot is placed in the standard navicular block (see Figures 3.63c and 5.5a), with the metacarpal region vertical. With the metacarpal region vertical it makes the technique easy to repeat for follow-up examinations, keeping the same angle of the x-ray beam relative to the third metacarpal bone. A horizontal x-ray beam is centred on the joint. The cassette is positioned perpendicular to the x-ray beam. This view moves the proximal sesamoid bones further proximally (see Figure 6.2c), and is particularly useful when evaluating their axial margins. With the limb in the same position the x-ray beam can also be directed distoproximally to assess a more palmar aspect of the articular surface of the metacarpal condyles.

The palmar articular surface may be assessed better with the limb partially extended, with the foot on a flat block (see Figure 6.3). This technique has the disadvantage of resulting in magnification and geometric distortion. The cassette is positioned approximately vertically. The x-ray beam is directed distoproximally, in the plane of rotation of the metacarpophalangeal joint, at approximately 125° to the metacarpal region. If the limb and x-ray beam are correctly aligned, between one-quarter and one-third of the proximal sesamoid bones is projected below the joint space (see Figure 6.2d). This view is particularly important when evaluating a vertical condylar fracture. Comminution of the palmar articular surface of the third metacarpal bone is usually only identifiable in this projection. It is also useful for detecting lucent lesions in the palmar aspect of the condyles of the third metacarpal bone (see 'Stress-related bone injury', below).

Dorsoproximal-dorsodistal (flexed) view

A dorsoproximal-dorsodistal (flexed) view of the metacarpophalangeal joint may be a useful view to detect subtle lesions of the dorsal half of the distal articular surface of the third metacarpal bone. The horse is positioned with the metacarpophalangeal joint flexed and the metacarpal region vertical. The cassette is placed distal to the joint and parallel to the floor. The x-ray tube is positioned dorsal to the limb, with the x-ray beam centred on the metacarpophalangeal joint, angled dorsal 45–70° proximal-dorsodistal. A series of radiographs may be obtained at slightly different angles to assess different areas of the joint (Figure 5.5).

Downloaded From Vet-eBooks.com

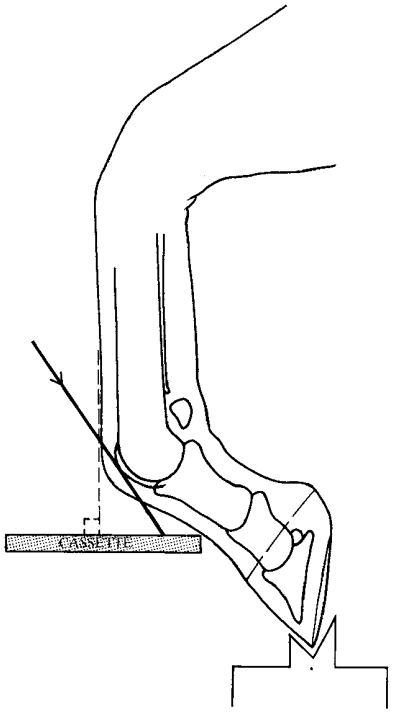


Figure 5.5(a) Positioning to obtain a dorsoproximal-dorsodistal (flexed) oblique view of the metacarpophalangeal joint, to highlight the dorsal aspect of the sagittal ridge of the third metacarpal bone.

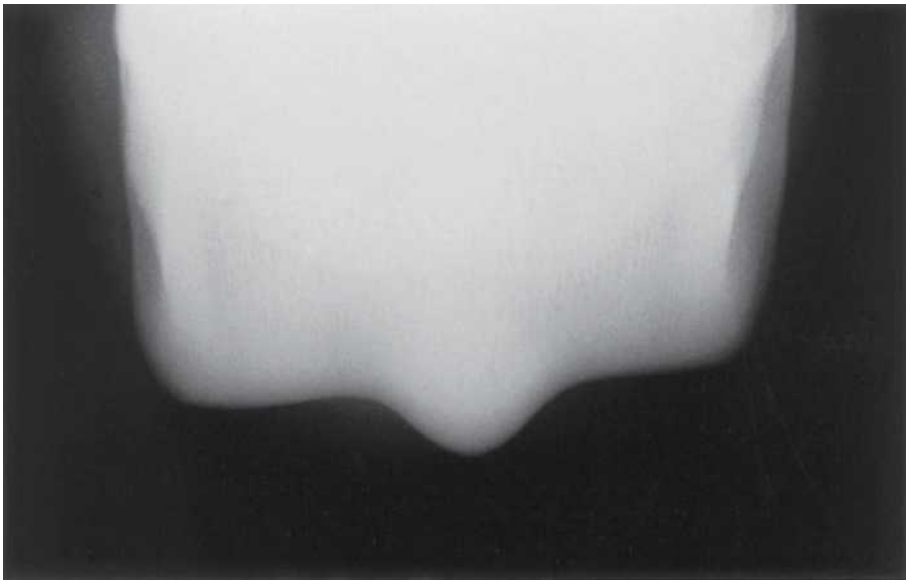


Figure 5.5(b) Dorsoproximal-dorsodistal (flexed) oblique image of a metacarpophalangeal joint, to highlight the sagittal ridge and condyles of the third metacarpal bone.

Palmaroproximal-palmarodistal oblique view of the proximal sesamoid bones

A palmaroproximal-palmarodistal oblique view of the proximal sesamoid bones is most useful for evaluation of their axial and abaxial margins and for defining the presence of an abaxial fragment and whether or not it is articular. The horse is positioned with the fetlock extended with the limb to be examined palmar to the contralateral limb. The horse stands on a cassette tunnel. The x-ray machine is placed almost vertically above the proximal sesamoid bones. Palmar 85° proximal 15° lateral-palmarodistal medial oblique and palmar 85° proximal 15° medial-palmarodistal lateral oblique views highlight the abaxial aspects of the medial and lateral proximal sesamoid bones respectively (Figure 5.6).

NORMAL ANATOMY

Immature horse

Prior to fusion of the distal physis of the third metacarpal/metatarsal bone at about 6–8 months of age, the distal metaphysis usually appears irregular (Figures 5.7a and 5.7b). The proximal physis of the proximal phalanx fuses at about 12 months of age.

Each proximal sesamoid bone usually ossifies from a single centre, which in the very young animal may have a slightly irregular margin. In a small

Downloaded From Vet-eBooks.com

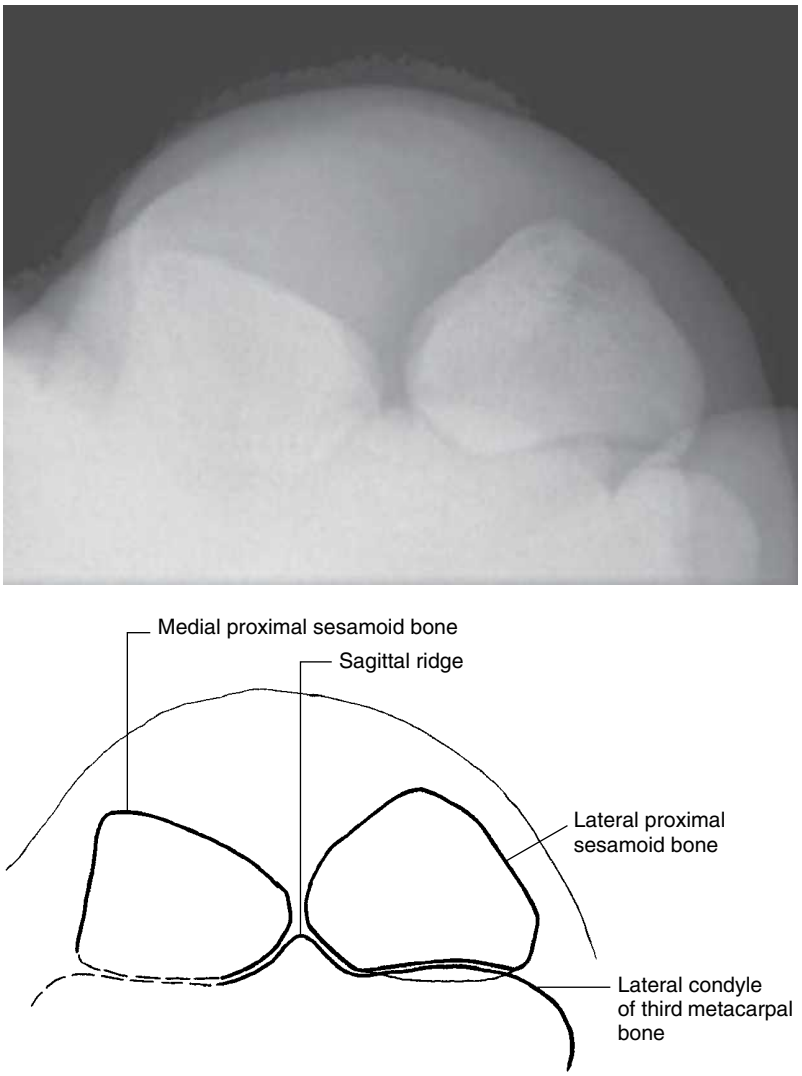


Figure 5.6 Palmar 85° proximal lateral-palmarodistal medial oblique image of a normal metacarpophalangeal joint. Lateral is to the right. The palmar, axial and abaxial aspects of the proximal sesamoid bones and the palmar aspect of the sagittal ridge of the third metacarpal bone are highlighted.

percentage of foals there are two ossification centres, one for the proximal one-third and one for the distal two-thirds of the bone. This may occur in one or several proximal sesamoid bones of the same foal. Fusion usually occurs by approximately 60 days of age. This should not be confused with a fracture of the proximal sesamoid bone (see 'Fractures of the proximal sesamoid bones', below). The cartilage precursor is fully ossified by about 3–4 months, although the bones may continue to enlarge until 18 months of age.

Skeletally mature horse

On a lateromedial view, the joint surface of the distal epiphysis of the third metacarpal bone describes a smooth curve, which flattens slightly on the palmarodistal aspect (Figure 5.8a). The third metacarpal bone articulates with the proximal phalanx and the proximal sesamoid bones. The distal metaphysis of the third metacarpal bone may have some irregularity at the level of the fused physis (physeal scar). The appearance of the dorsoproximal

Downloaded From Vet-eBooks.com



Figure 5.7(a) Dorsopalmar image of a metacarpophalangeal joint of a normal foal 6 weeks of age.



Figure 5.7(b) Lateromedial image of a metacarpophalangeal joint of a normal foal 8 weeks of age. Note also the separate centre of ossification of the distal aspect of the fourth metacarpal bone.

aspect of the sagittal ridge of the third metacarpal bone is rather variable. It may be smooth, smoothly irregular, have a small notch or a small radiolucent area (Figure 5w.8b). Immediately distal to this the sagittal ridge may be smoothly convex or flattened (Figure 5w.8c). Smoothly outlined new bone on the distal dorsal aspect of the third metacarpal bone may reflect previous tearing of the joint capsule attachment.

On dorsopalmar radiographs, the metacarpophalangeal joint is approximately symmetrical about the prominent sagittal ridge of the distal aspect of the third metacarpal bone, although the medial condyle is slightly wider than the lateral (Figure 5.9a). The sagittal ridge articulates with a groove in the proximal phalanx; the fit between the sagittal ridge and the groove should be congruous. The distal axial aspect of the third metacarpal bone between the proximal sesamoid bones may be more opaque than elsewhere (Figure 5w.9b). The joint space is approximately at right angles to the long axis of the third metacarpal bone and should have uniform thickness. Immediately proximal to the joint, the medial and lateral aspects of the third metacarpal bone have a smooth depression, above which the cortex has slightly greater opacity. Slight obliquity of a dorsopalmar view may result in

Downloaded From Vet-eBooks.com

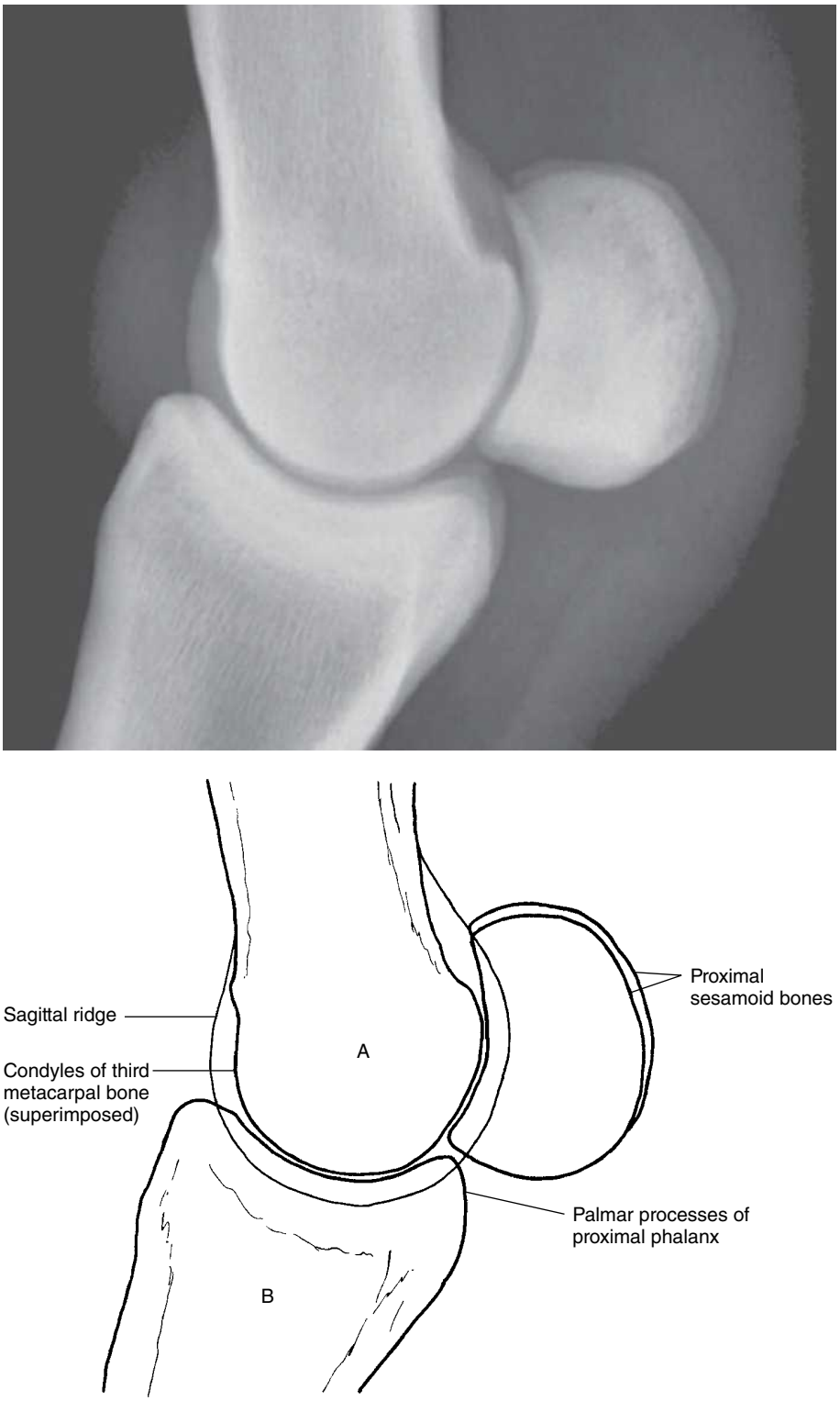


Figure 5.8(a) Radiograph and diagram of a lateromedial image of a normal adult metacarpophalangeal joint. A = third metacarpal bone, B = proximal phalanx.

a proximal sesamoid bone being superimposed over the epicondyle of the third metacarpal bone, which may result in a well-defined radiolucent area mimicking an osseous cyst-like lesion.

The proximal subchondral bone plate of the proximal phalanx is best evaluated in a dorsopalmar projection. There is usually a clear demarcation between

Downloaded From Vet-eBooks.com

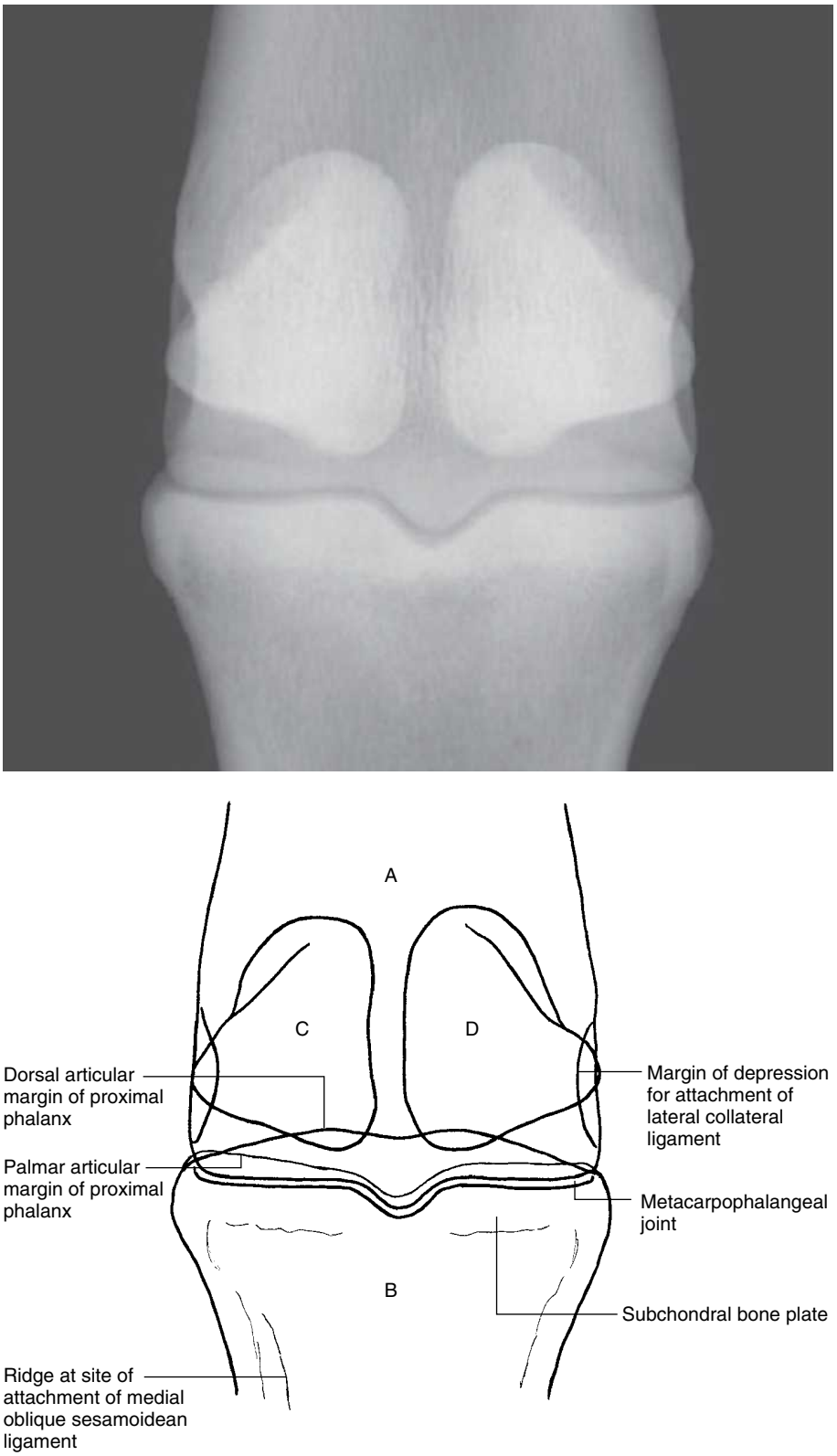


Figure 5.9(a) Dorsal 10° proximal-palmarodistal oblique radiographic image and diagram of a normal adult fetlock. Medial is to the left. A = third metacarpal bone, B = proximal phalanx, C = medial proximal sesamoid bone, D = lateral proximal sesamoid bone.

the subchondral bone plate and the underlying cancellous bone. The subchondral bone plate is of fairly uniform thickness, sometimes slightly thicker laterally than medially. The ergot is superimposed over the proximal phalanx, which may result in an approximately circular region of increased opacity, or occasionally

Downloaded From Vet-eBooks.com

an area of increased opacity and a short radiolucent line that may mimic a fracture (see Figures 1w.7b and 1w.7c). A short radiolucent line in the subchondral bone of the sagittal groove of the proximal phalanx can be an incidental finding (Figure 5w.9c), but may represent a fracture (see Chapter 4). A radiolucent area within the subchondral bone of the proximal phalanx in the sagittal groove may be seen as an incidental finding, but has also been seen as a progressive lesion causing lameness (see Figure 4w.15). There may be a relatively radiolucent area distal to the subchondral bone of the sagittal groove of the proximal phalanx (Figure 5w.9b).

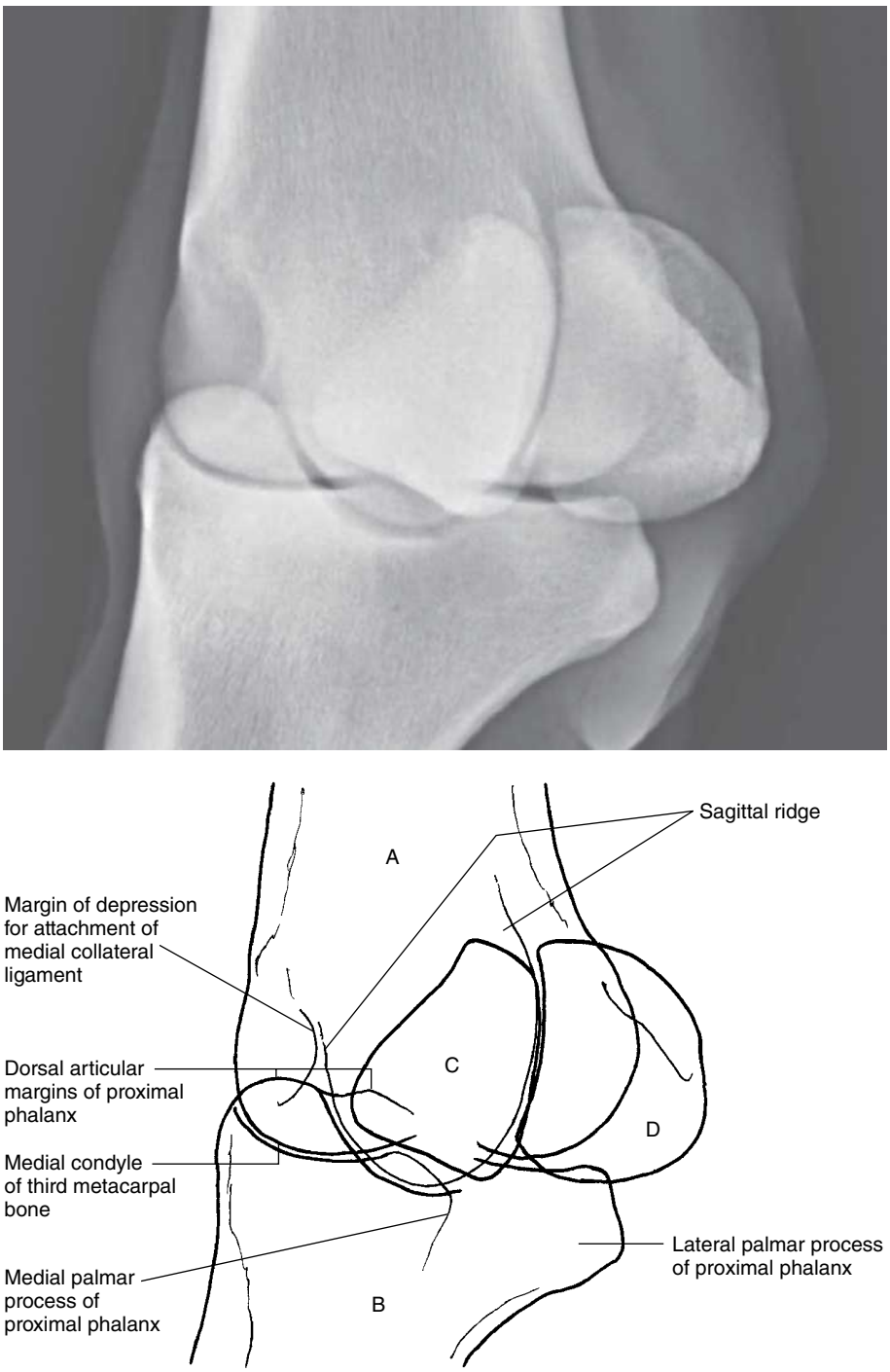


Figure 5.10 Radiograph and diagram of a dorsolateral-palmaromedial oblique image of a normal adult metacarpophalangeal joint. A = third metacarpal bone, B = proximal phalanx, C = medial proximal sesamoid, D = lateral proximal sesamoid.

Downloaded From Vet-eBooks.com



Figure 5.11 Lateromedial (flexed) image of a normal adult metacarpophalangeal joint. Note how the proximal sesamoid bones lift away from the palmar aspect of the third metacarpal bone.

The proximal sesamoid bones are difficult to see clearly, because on most views they are superimposed over other bones. They are most clearly seen on the dorsolateral-palmaromedial and dorsomedial-palmarolateral oblique views (Figure 5.10). They normally have a smooth outline, rounded over their palmar aspects. The axial and abaxial surfaces may have some unevenness, being areas of ligament insertion, but should not have marked roughening. There are faint radiating lucent lines within the bones. On lateromedial (flexed) views, the proximal sesamoid bones are lifted away from the palmar distal aspect of the third metacarpal bone (Figure 5.11).

NORMAL VARIATIONS AND INCIDENTAL FINDINGS

Slight modelling of the dorsoproximal articular margins of the proximal phalanx is a common incidental finding in older horses and is often unassociated with detectable clinical signs, although it may reflect degenerative joint disease (see 'Degenerative joint disease', below). Entheseous new bone on the proximal metaphyseal region of the proximal phalanx may occur at the insertion of the lateral digital extensor tendon and can be seen in a lateromedial image (Figure 5.12). A small, smoothly rounded osseous opacity at the dorsoproximal aspect of the proximal phalanx sometimes occurs in one or more fetlocks (see 'Osteochondrosis, developmental orthopaedic disease and osteochondral fragments', below). Small palmar or plantar osteochondral fragments and an ununited palmar or plantar process (see 'Osteochondrosis, developmental orthopaedic disease and osteochondral fragments', below) are frequently not associated with clinical signs, but they may affect performance or longevity of career in competition horses and racehorses. There are breed differences in the frequency of occurrence of fragments. Fragments were identified in

Downloaded From Vet-eBooks.com



Figure 5.12 Lateromedial (flexed) image of an adult metacarpophalangeal joint. There is entheseous new bone at the insertion of the lateral digital extensor tendon (arrow) and dystrophic mineralisation in the tendon proximal to it.



Figure 5.13 Lateromedial image of a metacarpophalangeal joint of an adult horse. There are several small, smoothly rounded mineralised opacities distal to the proximal sesamoid bones, which are unlikely to be of clinical significance. Note that this is not a true lateromedial projection. The condyles of the third metacarpal bone are not superimposed, because the horse was not standing squarely on the limb.

20.7% of mature German Warmbloods undergoing pre-sales radiographic examination. In a survey of 321 foals (French trotters, Thoroughbreds and French Warmbloods) examined at 6 and 18 months of age, dorsal fragments were seen in 10% (most commonly in Warmbloods) and plantar fragments in 9% (most commonly in trotters). Some fragments were present at 6 months but had disappeared by 18 months of age, whereas some new fragments were identified at 18 months of age. These were not long-term longitudinal studies so the potential clinical significance of the fragments is not known. Smoothly rounded osseous opacities are sometimes seen distal to one or both proximal sesamoid bones (Figure 5.13), presumably within the sesamoidean ligaments. They are usually asymptomatic and may reflect avulsion fractures sustained as a foal, or dystrophic mineralisation.

Downloaded From Vet-eBooks.com

The number of radiolucent vascular channels and their width in the proximal sesamoid bones varies among horses. Normal vascular channels are considered to have parallel sides. An unusually long proximal sesamoid bone usually indicates previous fracture of the bone in the neonatal period (see 'Fractures of the proximal sesamoid bones', below). The presence of entheseous new bone on a margin of a proximal sesamoid bone may reflect abnormal stress at the insertion of a variety of soft tissue structures including the suspensory ligament, the palmar annular ligament, the straight, oblique, cruciate or short sesamoidean ligaments and the collateral ligaments of the proximal sesamoid bones (Figure 5w.14). The apices of the proximal sesamoid bones in hindlimbs are usually more pointed than in forelimbs.

A number of grading systems have been developed to score radiological variants of the proximal sesamoid bones in yearling Thoroughbreds in order to try to determine if radiological appearance can be used to predict future racing performance or the development of suspensory branch injury. These are based on the presence or absence of vascular channels, the width of the vascular channels (<2 mm or ≥ 2 mm), and whether the vascular channels have parallel or divergent sides. The presence of entheseous new bone, elongation of the bone or abaxial radiolucent areas were considered separately. Depending on the grading scale used there is some evidence to suggest that the greater the number of abnormalities the less likely a horse is to race as many times as their peers, and that the risk of suspensory ligament branch injury is greater.

In maximally flexed lateromedial views, especially of hind fetlocks, a focal radiolucent area may be seen superimposed over the distal aspect of the sagittal ridge of the third metacarpal/metatarsal bone. This is a 'gas artefact' caused by maximal flexion of the joint, and disappears with reduced flexion.

In some horses prominent radiolucent lines representing vascular channels are seen at the level of the distal physis of the third metacarpal (metatarsal) bone. These may be seen alone or in association with stress-related bone injury.

Intra-articular analgesia of the fetlock joint is often associated with air being introduced into the joint. If radiography is performed within a few hours, radiolucent areas may be seen in the proximal recesses of the joint capsule, and in some views these are superimposed over the third metacarpal bone and mimic lesions (see Figure 1.13). Such artefacts disappear within 24–48 hours.

SIGNIFICANT FINDINGS

Soft-tissue swelling

Soft-tissue swelling in the fetlock region has many causes and may be detected radiographically, either alone or with other radiographic abnormalities. The cause of swelling often cannot be determined radiographically and ultrasonographic evaluation may therefore be indicated. The metacarpophalangeal joint is prone to soft-tissue injury, and although initial radiographs may show only soft-tissue swelling, radiographs obtained 3–6 weeks later may demonstrate new bone at the articular margins, at the points of attachment of the joint capsule and/or collateral ligaments. Entheseophytes and periarticular osteophytes may also develop on the proximal sesamoid bones. Accurate knowledge of the anatomy of soft-tissue attachments is essential for determination of the likely cause of

Downloaded From Vet-eBooks.com

entheseophyte formation. It is important to recognise how far proximal the origin of the proximal portions of the collateral ligaments of the metacarpophalangeal joint are located (Figures 4.3 and 4.4).

Synovitis is a common problem, visualised radiographically as distension of the metacarpophalangeal joint capsule. This is most easily seen on the dorsal aspect of the joint on a lateromedial image. Abnormal stress at the joint capsule attachments may result in entheseous new bone, particularly on the distal dorsal aspect of the third metacarpal bone and the proximodorsal aspect of the proximal phalanx. Thickening of the joint capsule may be detected ultrasonographically. Chronic proliferative synovitis (so-called 'villonodular' hypertrophic synovitis) may result in modelling of the proximodorsal aspect of the sagittal ridge of the third metacarpal bone and the area just proximal to this. This is associated with soft-tissue swelling seen on a lateromedial image. In the early stages a depression may be noted just proximal to the sagittal ridge. There may be new bone just proximal to the depression, representing entheseous new bone at the capsular attachment (Figure 5.15a). In advanced cases, an increased opacity may be evident dorsal to the depression, due to dystrophic mineralisation or osseous metaplasia. These changes are most easily identified on a lateromedial (flexed) view. The soft tissues can be assessed ultrasonographically, but differentiation between a thickened joint capsule and an intra-articular soft tissue mass can be challenging. The use of intra-articular

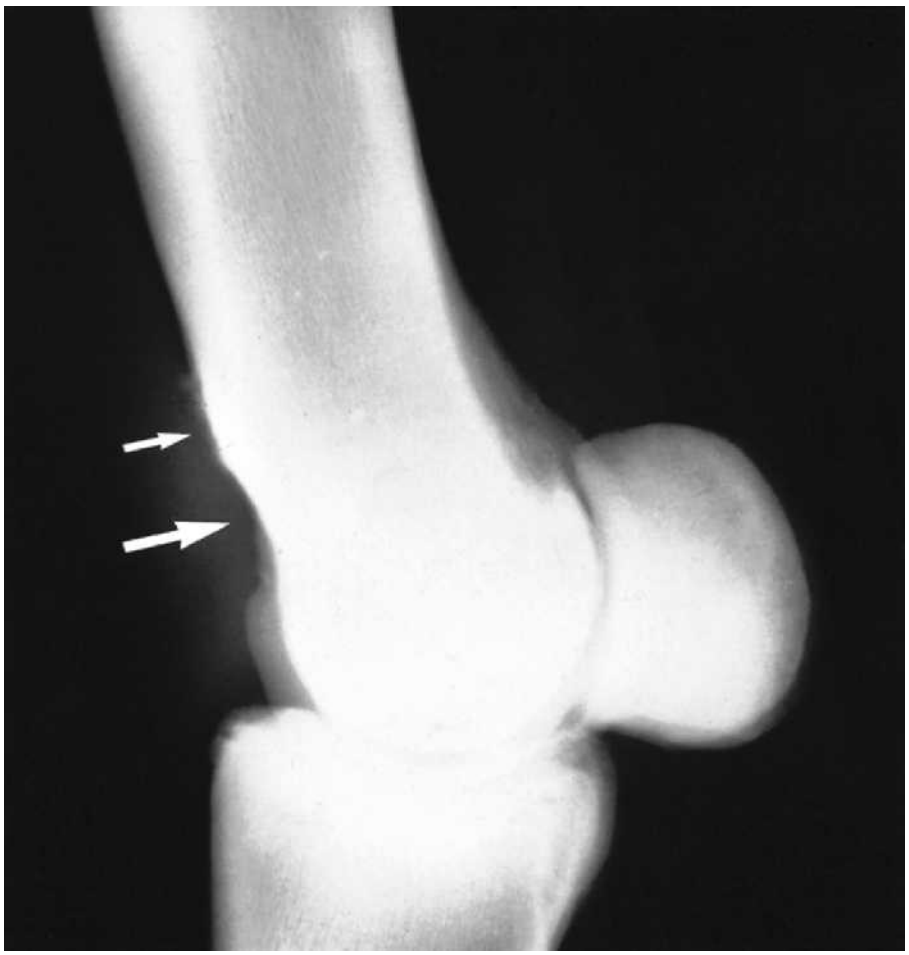


Figure 5.15(a) Chronic proliferative synovitis. Lateromedial image of a metacarpophalangeal joint, showing radiographic changes associated with chronic proliferative synovitis. There is a depression proximal to the sagittal ridge of the third metacarpal bone (large arrow). Proximal to this is periosteal new bone at the site of the capsular attachment (small arrow). This modelling of the dorsal distal aspect of the third metacarpal bone usually relates to chronic proliferative synovitis. The radiograph is deliberately underexposed to demonstrate these abnormalities.

Downloaded From Vet-eBooks.com



Figure 5.15(b) Chronic proliferative synovitis. Lateromedial image of a metacarpophalangeal joint, with contrast medium in the joint (slightly oblique view). Note the filling defect (arrows) in the dorsal pouch of the joint.

radiodense (positive) contrast medium may outline the soft-tissue mass more accurately (Figure 5.15b). Clinically there is enlargement of the dorsal pouch of the metacarpophalangeal joint. Treatment is by surgical removal of the mass and adequate rest to allow the joint inflammation to resolve.

A soft-tissue mass in the plantar recess of the metatarsophalangeal joint has been recorded secondary to haemarthrosis. The mass had similarities to human villonodular pigmented synovitis and resulted in severe supracondylar lysis with no other osseous pathology. Surgical removal resulted in a successful outcome.

Supracondylar lysis has also been seen in association with chronic suspensory branch injuries and synovial proliferation and adhesion formation in the plantar recess of the metatarsophalangeal joint (Figure 5.16).

Soft-tissue swelling medially or laterally may reflect injury of a collateral ligament. With severe lameness and marked swelling, stressed dorsopalmar radiographs should be obtained to determine the stability of the joint (see 'Luxation', below). Occasionally there may be an avulsion fracture from the origin of the collateral ligament, which may be substantially displaced distally. Collateral desmitis can occur without obvious swelling and should be considered if pain causing lameness is localised to the fetlock region, but there is no response to intra-articular analgesia. In the acute stage radiographs may appear normal, although entheseophyte formation may develop subsequently. Ultrasonography helps diagnosis.

Downloaded From Vet-eBooks.com



Figure 5.16 Lateromedial image of the left metatarsophalangeal joint of a 6-year-old Appaloosa with degenerative suspensory desmopathy, resulting in an abnormally low position of the proximal sesamoid bones. There is supracondylar lysis of the plantar distal aspect of the third metatarsal bone (arrows). This was associated with proliferative synovitis in the plantar recess of the metatarsophalangeal joint. There was no evidence of degenerative joint disease at post mortem examination. Note the ill-defined osseous cyst-like lesion distal to the subchondral bone of the proximal phalanx, surrounded by a thin rim of more opaque bone, an incidental finding.

Soft-tissue swelling on the palmar proximal aspect of the metacarpophalangeal joint may be due to distension of the digital flexor tendon sheath. Swelling may arise after trauma to the region and results in lameness, which may resolve with rest or may require surgical treatment, depending on the underlying pathology. On lateromedial views a depression in the palmar contour of this swelling may indicate functional constriction by the palmar annular ligament. Occasionally mineralisation in the sheath or the digital flexor tendon, or abnormalities of the proximal sesamoid bones, are seen. Ultrasonographic examination may give additional information about the associated soft-tissue structures.

Intrathecal radiodense contrast medium can be used to demonstrate tears of the manica flexoria, which are particularly prevalent in hindlimbs, or marginal tears of the deep digital flexor tendon. In a normal horse the manica flexoria is outlined in a lateromedial image by two parallel lines of radiodense contrast medium which taper distally (Figure 5w.17a). An isolated area of radiodense contrast medium overlying the dorsal border of the deep digital flexor tendon, or the absence of the parallel lines outlining the manica flexoria, are indicative of a manica flexoria tear (Figure 5w.17b). A line of radiodense contrast medium coursing within the outline of the deep digital flexor tendon obliquely proximodistally is indicative of a marginal tear of the tendon (Figure 5w.17c). The prognosis depends on the underlying pathology; manica flexoria tears have a good prognosis whereas tears of the deep digital flexor tendon have a guarded prognosis.

Distension of the digital flexor tendon sheath and the metacarpophalangeal joint capsule may also be seen in association with infectious or traumatic osteitis of one or both proximal sesamoid bones (see 'Infectious and

Downloaded From Vet-eBooks.com

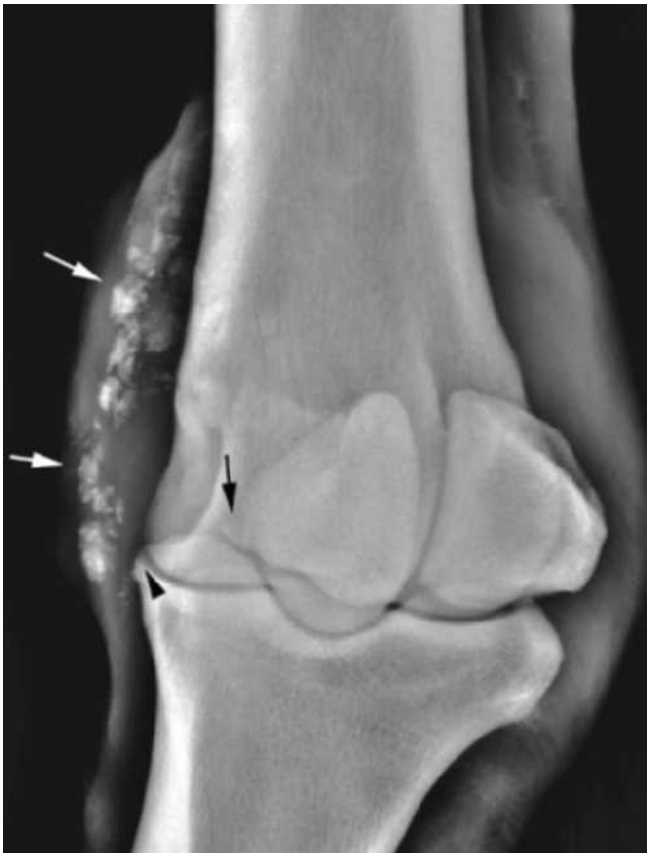


Figure 5.18 Dorsolateral-plantaromedial oblique image of a metatarsophalangeal joint of a 10-year-old Thoroughbred general-purpose riding horse. There is periarticular dystrophic mineralisation around the joint (white arrows), the result of a chronic subcutaneous periarticular abscess. There is modelling of the dorsoproximal medial aspect of the proximal phalanx (arrowhead) reflecting degenerative joint disease and an osseous fragment proximal to the dorsoproximal aspect of the proximal phalanx (black arrow).

traumatic osteitis of the axial aspect of the proximal sesamoid bones', below). Swelling may arise after trauma to the region and results in lameness, which may resolve with prolonged rest or may require surgical treatment. The prognosis depends on the underlying pathology. Ultrasonographic examination may give additional information about the associated soft-tissue structures.

Dystrophic mineralisation is occasionally seen within one or both suspensory ligament branches, usually reflecting chronic injury. The distal aspect of the second and fourth metacarpal bones should be evaluated carefully, because modelling and or fracture frequently occurs in association with chronic suspensory branch injuries (Figures 6w.21a and 6w.21b).

Periarticular dystrophic mineralisation is occasionally seen on the dorsal aspect of the joint as the result of chronic infection (Figure 5.18).

Degenerative joint disease

On lateromedial and/or oblique views, modelling of the proximodorsal aspects of the proximal phalanx may involve the articular margins, and indicate degenerative joint disease (Figure 5.19a). The proximomedial aspect of the proximal phalanx is usually affected first reflecting the way in which the joint is loaded. Periarticular osteophytes are best seen in oblique projections and vary from thin, sharply angled periarticular margins ('spurs') to large, more rounded protuberances of bone. As disease progresses, there may be increased opacity and thickness of the subchondral bone, an irregular endosteal margin and loss of normal trabecular architecture. The distal

Downloaded From Vet-eBooks.com



Figure 5.19(a) Degenerative joint disease. Dorsolateral-palmaromedial oblique image of a metacarpophalangeal joint, showing early changes associated with degenerative joint disease. There is modelling of the dorsomedial aspect of the proximal phalanx (arrow).



Figure 5.19(b) Advanced degenerative joint disease. Lateromedial (flexed) image of a metatarsophalangeal joint of a 4-year-old riding horse, with effusion in the joint, resentment of passive flexion and moderate lameness. There is modelling of the apices of the proximal sesamoid bones (white arrow), the dorsoproximal aspect of the proximal phalanx (black arrowhead) and the dorsal and palmar distal aspects of the third metatarsal bone proximal to the sagittal ridge (black arrows). The loss of bone proximal to the condyles on the plantar aspect of the third metatarsal bone is consistent with supracondylar lysis. The dorsoproximal aspect of the sagittal ridge of the third metatarsal bone is irregular.

dorsal aspect of the third metacarpal bone may also change in shape (Figures 5.19b and 5w.19c and d). The proximal dorsal attachments of the joint capsule are close to the proximal end of the sagittal ridge of the third metacarpal bone, and entheseophyte formation at this point may result from joint trauma or chronic joint capsule distension. This is not synonymous with degenerative joint disease but may be seen in association with it.

On dorsopalmar images, osteophytes may be seen at the articular margins on the medial or lateral aspects of the proximal phalanx and indicate degenerative joint disease. Entheseophytes at the insertion of the joint capsule develop slightly distal to a periarticular osteophyte, and indicate strain or tension of the capsular attachment. It is often difficult to differentiate between these two types of new bone formation at this location, and careful clinical assessment of their significance is required. There may be lack of congruity between the distal aspect of the sagittal ridge of the third metacarpal (metatarsal) bone and the sagittal groove of the proximal phalanx (Figure 5.20).

Downloaded From Vet-eBooks.com

In advanced degenerative joint disease, periarticular osteophytes on the proximal and distal margins of the proximal sesamoid bones may be seen. Associated with this there may be a depression in the distal palmar aspect of the third metacarpal bone, proximal to the condyles. This so-called 'supracondylar lysis' is associated with fibrous proliferation of the synovial membrane in this region (Figures 5.19b and 5w.19d). Positive contrast studies may demonstrate a filling defect in this area.

The joint space is best assessed on a dorsopalmar view. Narrowing of the joint space, particularly unilateral narrowing (usually of the medial side), is significant and reflects advanced articular cartilage pathology. It is important, however, that this is assessed on weight-bearing views, with the horse standing evenly on all four feet, since the joint can open on either side if unevenly loaded. Narrowing of one side of the joint space may be the only radiographic abnormality detectable in any view in some horses with advanced degenerative joint disease (Figure 5.20). The relatively opaque subchondral bone should be of even thickness. Change in thickness or opacity of the subchondral bone of the third metacarpal bone or the proximal phalanx has been associated with degenerative joint disease. There may also be decreased demarcation between the subchondral bone and the



Figure 5.20 Dorsal 15° proximal-palmarodistal oblique radiographic image of a metacarpophalangeal joint of a 12-year-old showjumper. There is marked narrowing of the medial aspect of the metacarpophalangeal joint, reflecting substantial loss of the articular cartilage. Note also the lack of congruity between the sagittal ridge of the third metacarpal bone and the sagittal groove of the proximal phalanx. There was no periarticular modelling, but such joint space narrowing reflects advanced degenerative joint disease.

Downloaded From Vet-eBooks.com

underlying cancellous bone and occasionally a single small osseous cyst-like lesion underlying abnormal subchondral bone.

Subchondral bone trauma

Subchondral and trabecular bone trauma of the distal dorsal aspect of the third metacarpal bone and/or the proximal aspect of the proximal phalanx may result in abnormal mineralisation of the subchondral and trabecular bone, evident on magnetic resonance images as areas of reduced signal intensity in T1 and T2 weighted images. Such areas, if extensive, can be seen as areas of increased radiopacity on radiographs (Figures 5w.21a and 5w.21b).

Acute injuries of the proximal aspect of the proximal phalanx causing severe lameness may result in a focal ill-defined radiolucent line or an osseous cyst-like lesion in the subchondral bone, and subsequent development of a diffuse area of increased opacity distally (Figure 5w.22a). They are often associated with the development of periosteal new bone formation on the proximal epiphyseal and metaphyseal regions of the ipsilateral aspect of the proximal phalanx (Figure 5w.22b). These lesions have been called 'focal impact fractures' resulting in focal collapse of the articular cartilage and necrosis of the underlying subchondral and trabecular bone. Such lesions have a poor prognosis.

Osteochondrosis, developmental orthopaedic disease and osteochondral fragments

The aetiology of some changes in the metacarpophalangeal and metatarsophalangeal joints still remains open to debate, although recent publications are helping to clarify the findings. Some abnormalities formerly thought to be due to osteochondrosis or developmental orthopaedic disease may be traumatic in origin. There appear to be breed differences in the incidence of these abnormalities and their clinical significance is not always easy to determine. Included in this group are fragments arising from the dorsal aspect of the sagittal ridge of the third metacarpal (metatarsal) bone, fragments on the dorsoproximal aspect of the proximal phalanx, palmar or plantar osteochondral fragments, an ununited palmar or plantar eminence of the proximal phalanx and flattening of the palmar or plantar condyle of the third metacarpal or metatarsal bone.

Osteochondrosis of the sagittal ridge may be seen anywhere on the ridge, but is most often seen dorsally on the proximal or middle third (Figure 5.23a and b) in both forelimbs and hindlimbs. A mild lesion is seen as flattening or concavity of the ridge. Such lesions may resolve spontaneously. More severe lesions may result in marked irregularity of the dorsal contour of the sagittal ridge and the presence of osteochondral fragments. These lesions are best seen on a lateromedial (flexed) image (Figure 5.23b) and may involve all four fetlocks. The prognosis is favourable with surgical management. Lesions restricted to the distal aspect of the sagittal ridge are more common in forelimbs and are usually characterised by radiolucent areas in the subchondral bone (Figure 5w.24a and b). Such lesions are only detectable in lateromedial

Downloaded From Vet-eBooks.com



Figure 5.23(a) Lateromedial radiographic image of a metacarpophalangeal joint of a yearling Thoroughbred, obtained as part of a routine screening. There is slightly heterogeneous opacity where the sagittal ridge of the third metacarpal bone is superimposed over the proximal aspect of the proximal phalanx dorsally. Compare with Figure 5.23(b).



Figure 5.23(b) Lateromedial (flexed) image of the same fetlock as Figure 5.23(a). There is a large defect in the dorsal aspect of the sagittal ridge of the third metacarpal bone (arrows). This is osteochondrosis.

(flexed) and dorsoproximal-palmarodistal oblique images. They are usually associated with lameness in young horses and respond well to surgical debridement. Occasionally traumatic injury to a fetlock can result in a fracture of the dorsal aspect of the sagittal ridge of the third metacarpal bone of similar appearance to osteochondrosis fragments.

Small, well-rounded fragments on the dorsoproximal aspect of the proximal phalanx (Figure 5.31), readily identifiable on a lateromedial projection, are a common radiographic finding, frequently not associated with clinical signs. They may be present in one or several fetlocks and are usually seen dorsomedially. Their aetiology is unknown but they may result from separate centres of ossification or possibly be a manifestation of developmental orthopaedic disease. Although often asymptomatic, in 50% of 117 Warmbloods the majority of which were sound, there was arthroscopic evidence of synovitis ± cartilage fibrillation. The presence of more than one fragment or a fragment in a horse greater than 7 years of age were risk factors for related lameness. In a study involving several breeds, some fragments disappeared between 6 and 18 months of age, some appeared between 6 and 18 months of age, and some were present at 6 months of age and persisted unchanged. Occasionally fragments are associated with synovial effusion and lameness, in which case surgical removal is indicated. A good prognosis is usually warranted. In Thoroughbred racehorses some fragments are thought to represent chip fractures.

So-called osteochondrosis involving the palmar (plantar) aspect of the condyles of the third metacarpal (metatarsal) bones usually occurs slightly palmar (plantar) to the transverse ridge. Initially the radiographic changes are flattening and increased opacity of the subchondral bone in the affected

Downloaded From Vet-eBooks.com

area. This may be followed by resorptive changes, resulting in focal radiolucent areas of variable shape. Although this lesion was formerly classified as osteochondrosis, it now seems probable that it is a traumatic lesion and only seen in athletic horses (see 'Stress-related bone injury', below).

Palmar or plantar osteochondral fragments (Figure 5.25a) are usually seen medially or laterally (or both together) at the site of attachment of the short sesamoidean ligaments, and occur most commonly in hindlimbs. They have also been referred to as Birkeland fractures. They are best identified in D30°Pr70°L-PaDiMO or D30°Pr70°M-PaDiLO views. Medial fragments are most common. These are believed to represent avulsion fractures, sustained as a foal, and are frequently asymptomatic, although they may compromise performance at high speed. Such fragments have also been a cause of lameness in sports horses, especially when seen in conjunction with periarticular modelling and surgical removal may be warranted. An ununited palmar or plantar process of the proximal phalanx (Figure 5.25b) usually occurs laterally, either alone or in association with a palmar or plantar osteochondral fragment. It occurs most commonly in hindlimbs and may be articular or non-articular. In some horses it may represent an avulsion fracture of the collateral ligament. Collateral



Figure 5.25(a) Dorsal 30° proximal 70° medial-plantarodistal lateral oblique image of a metatarsophalangeal joint of an 8-year-old Danish Warmblood. There is a non-articular osteochondral fragment from the proximoplantar aspect of the medial plantar process of the proximal phalanx.



Figure 5.25(b) Dorsolateral-plantaromedial oblique image of a metatarsophalangeal joint of a 7-year-old Thoroughbred. There are two smoothly rounded osseous opacities in close apposition to the plantar aspect of the lateral plantar process of the proximal phalanx. Each has a trabecular pattern. This is an ununited lateral plantar process of the proximal phalanx.

Downloaded From Vet-eBooks.com

ligament avulsions are usually associated with lameness, but other fragments are frequently asymptomatic. Asymptomatic fragments may become significant with increasing levels of work.

Physitis

Physitis (epiphysitis) of the distal physis of the third metacarpal bone occurs predominantly in rapidly growing foals. Radiographically the physis is widened and irregular in thickness, frequently with new bone (lipping) at its margins. On dorsopalmar views an angular limb deviation may be evident. The usual clinical history is of a limb deviation developing distal to the metacarpophalangeal joint. Treatment of this condition must be radical and rapid, because of the early closure of the distal physis. Usually restriction of diet and exercise, coupled with corrective trimming of the foot, will be sufficient. In some cases, periosteal elevation, physeal stimulation or transphyseal bridging may be needed.

Osseous cyst-like lesions

Osseous cyst-like lesions occur near the metacarpophalangeal joint, most commonly in the third metacarpal bone, but also in the proximal phalanx. Accurate identification of these may require a dorsoproximal-palmarodistal angulation of the x-ray beam. Lesions often start as focal flattening of the subchondral bone and develop through an elliptical lucent area to an oval-shaped lucency, with progressive development of surrounding increased radiopacity. Conservative treatments warrant a guarded prognosis, but surgical treatment may show more favourable results in the third metacarpal bone.

Ill-defined radiolucent areas in the medial or lateral condyles of the third metacarpal bone (Figure 5.26a) or in the medial or lateral condyles of the proximal aspect of the proximal phalanx (Figure 5.26b) may also develop as a sequel to trauma (e.g. falling). Lameness is usually persistent with conservative management. The success of surgical debridement of lesions in the distal aspect of the third metacarpal bone depends on accessibility based on the location of the lesion relative to the major weight-bearing surface of the bone.

Sesamoiditis

Sesamoiditis is a widely used term that encompasses lucent areas within the proximal sesamoid bones and new bone production. Radiographic abnormalities are best assessed in D45°M-PaLO and D45°L-PaMO views. The radiographic appearance is variable, ranging from a number of radiolucent areas along the palmar aspect of the bones, with minimal new bone formation, to extensive new bone on the axial and abaxial surfaces, with an apparently normal internal structure of the bone. There is often poor correlation between radiological abnormalities and clinical signs.

The lucent areas are sometimes referred to as vascular channels. The number of sharply demarcated vascular channels in a normal horse may vary according to breed and work history. Wide or abnormally shaped lucent areas are likely to be associated with lameness (Figure 5.27a). In racing Thoroughbreds the presence of two or more vascular channels of

Downloaded From Vet-eBooks.com



Figure 5.26(a) Dorsal 15° proximal-palmarodistal oblique radiographic image of the right metacarpophalangeal joint of a 7-year-old event horse. Medial is to the left. There is an ill-defined radiolucent area in the distal medial aspect of the third metacarpal bone (arrows). There was moderate lameness associated with distension of the joint capsule and exacerbation of lameness by flexion. Arthroscopic examination revealed a large full-thickness cartilage defect extending into a crater in the subchondral bone on the weight-bearing surface of the third metacarpal bone and extensive cartilage fibrillation of the medial condyle of both the third metacarpal bone and the proximal phalanx.



Figure 5.26(b) Dorsal 10° proximal-palmarodistal oblique image of a metacarpophalangeal joint of a 13-year-old pony with lameness localised to the joint. Lateral is to the right. There is an ill-defined radiolucent area in the proximal subchondral bone plate of the proximal phalanx lateral to the sagittal groove (arrow). The well-circumscribed circular radiolucent area distal to the subchondral bone of the sagittal groove of the proximal phalanx is a normal finding.

irregular width as yearlings has been associated with decreased performance when compared with horses with normal vascular channels (Figure 5.27b). The greater the number of vascular channels, the more likely there is to be associated lameness. New bone on the abaxial and distal surfaces of the bone is often associated with strain of the suspensory ligament and sesamoidean ligaments (Figure 5.27c). The lucent zones adjacent to the vascular channels, but outside the normal bone, are areas of fibrous

Downloaded From Vet-eBooks.com



Figure 5.27(a) Dorsolateral-palmaromedial oblique radiographic image of the left metacarpophalangeal joint of a 12-year-old hunter with severe desmitis of the lateral branch of the suspensory ligament. The lateral proximal sesamoid bone has multiple broad radiating lucent lines representing enlarged vascular channels in the proximal one half of the bone. There is mild modelling of the palmar aspect of the bone.

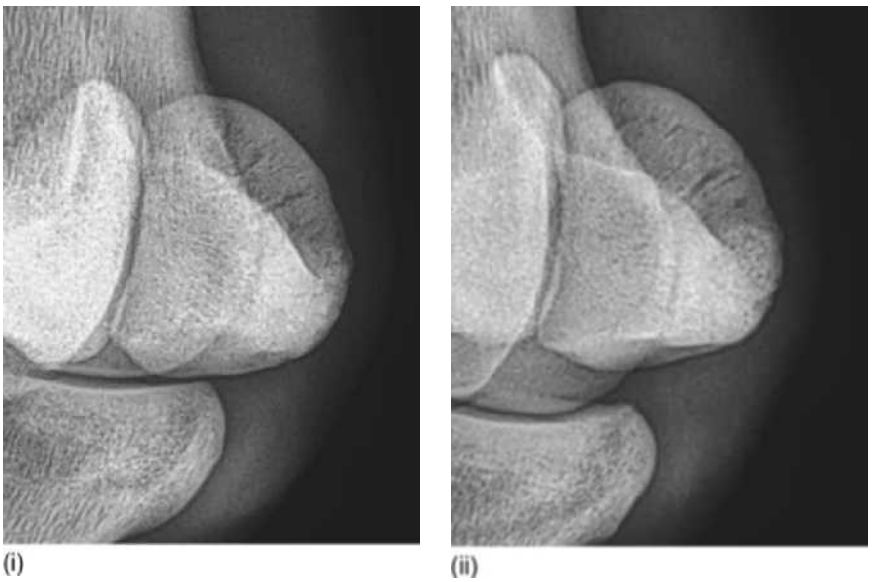


Figure 5.27(b) (i) Dorsomedial-palmarolateral oblique image of the left metacarpophalangeal joint of a 2-year-old Thoroughbred highlighting the medial proximal sesamoid bone. There are several radiating lucent lines of consistent width in the bone. (ii) Dorsomedial-palmarolateral oblique image of the right metacarpophalangeal joint of a 2-year-old Thoroughbred highlighting the medial proximal sesamoid bone. There are several radiating lucent lines, one of which is much wider than the others.



Figure 5.27(c) Dorsomedial-palmarolateral oblique radiographic image of the right metacarpophalangeal joint of an 8-year-old Thoroughbred steeplechaser. There is extensive soft-tissue swelling of the dorsal aspect of the joint. There is irregular new bone on the abaxial (black arrow) and palmarodistal (white arrows) aspects of the medial proximal sesamoid bone. There are ill-defined lucent areas in the proximal half of the medial proximal sesamoid bone. There was a large core lesion in the medial branch of the suspensory ligament.

Downloaded From Vet-eBooks.com

tissue around nutrient vessels. The fibrous tissue resists encroachment of entheseophytes and gives a radiographic appearance of enlarged vascular channels.

In a young horse (less than 3 years of age) where lucent lesions are the predominant radiographic abnormality, a fair prognosis can be given if the horse receives adequate rest (although the radiographic lesions will persist). The prognosis may be more guarded when these lesions develop in older horses. Radiating lucent zones may also be seen in association with desmitis of a suspensory ligament branch ± entheseous new bone.

In horses where new bone formation is the predominant radiological finding, there has probably been an associated soft-tissue injury. Ultrasonographic examination of the suspensory apparatus and palmar (plantar) annular ligament in these cases may be useful. The prognosis depends on the amount of new bone formed and the extent of the accompanying soft-tissue injuries. Periarticular osteophytes seen on the articular margins of the proximal sesamoid bones are an indication of degenerative joint disease. This may be best identified on a lateromedial (flexed) view (Figure 5.19b) (see 'Degenerative joint disease', above). A discrete lucent zone in the palmar aspect of a proximal sesamoid bone may reflect enthesopathy of the palmar annular ligament. The ligament should also be evaluated ultrasonographically.

Lucent zones restricted to the axial aspect of the proximal sesamoid bones are easily overlooked, unless a dorsopalmar radiographic view is overexposed. For accurate evaluation of the axial margins of the proximal sesamoid bones a dorsopalmar (flexed) view is extremely useful.



Figure 5.27(d) Dorsolateral-palmaromedial oblique radiographic image of the left metacarpophalangeal joint of a 7-year-old Thoroughbred steeplechaser. There is a large ill-defined radiolucent area in the proximal palmar aspect of the lateral proximal sesamoid bone (arrows), with irregular new bone on the palmar aspect of the proximal sesamoid bone distal to it (arrowhead). There are also several narrow radiating radiolucent lines in the bone, normal vascular channels. The horse had sustained an apparently innocuous puncture wound on the palmar aspect of the fetlock 8 weeks previously, but had recently developed a deteriorating lameness. There was marked pain on focal pressure applied to the palmar aspect of the lateral proximal sesamoid bone. Surgical exploration revealed necrotic bone, which was debrided. Note also mild modelling of the dorsoproximal-medial aspect of the proximal phalanx.

Downloaded From Vet-eBooks.com

Infectious osteitis of the palmar or abaxial aspect of a proximal sesamoid bone

A discrete, progressively enlarging radiolucent area on the palmar or abaxial aspect of a proximal sesamoid bone may be the result of a penetrating injury and infectious osteitis (Figure 5.27d). This is associated with severe lameness and focal pain on pressure over the lesion. Prognosis is favourable with surgical debridement.

Infectious and traumatic osteitis of the axial aspect of the proximal sesamoid bones

Lucent zones restricted to the axial aspect of the proximal sesamoid bones are easily overlooked, unless a dorsopalmar radiographic view is overexposed. For accurate evaluation of the axial margins of the proximal sesamoid bones a dorsopalmar (flexed) view is extremely useful.

Lucent lesions on the axial aspect of the proximal sesamoid bones (Figure 5.28) have been associated with infectious osteitis in horses that have presented with severe lameness, often with distension of the digital flexor tendon sheath. The prognosis is guarded.

An irregular axial margin of one or both of the proximal sesamoid bones with lucent areas extending into the bone has also been seen with or without desmitis of the intersesamoidean ligament and is assumed to be of traumatic origin. Hindlimbs are more commonly affected than forelimbs. Although lesions have been seen in many breeds, the Friesian breed appears to be particularly susceptible. Ultrasonographic examination is



Figure 5.28 Dorsoplantar (flexed) image of a metatarsophalangeal joint of a 3-year-old Thoroughbred with sudden onset of severe lameness 6 weeks previously, associated with diffuse swelling on the plantar aspects of the fetlock and pastern. There is an indistinct axial margin with underlying ill-defined lucent zones, involving the proximal half of the medial and lateral proximal sesamoid bones (arrows). This is the result of infection.

Downloaded From Vet-eBooks.com

indicated. The prognosis is guarded with conservative management, but surgical debridement may be indicated in selected cases.

Osseous cyst-like lesion in the proximal aspect of a proximal sesamoid bone

A well-circumscribed osseous cyst-like lesion in the apex of a proximal sesamoid bone has been described as a cause of acute-onset severe lameness. There was enlargement of the ipsilateral branch of the suspensory ligament but no disruption of its internal architecture. Surgical debridement resulted in a successful outcome.

Abnormal position of the proximal sesamoid bones

The position of the proximal sesamoid bones relative to the metacarpophalangeal (metatarsophalangeal) joint should be carefully assessed. Failure of the suspensory apparatus in the metacarpal or, more commonly, metatarsal regions results in an abnormally low position of the proximal sesamoid bones on all weight-bearing radiographs (see Figure 5.16) and is a poor prognostic indicator. Severe injury of the superficial digital flexor tendon results in hyperextension of the entire fetlock joint, thus the proximal sesamoid bones will be lower. Complete disruption of the sesamoidean ligaments results in proximal displacement of the proximal sesamoid bones. Ultrasonographic evaluation is indicated.

Luxation

Luxation of the metacarpophalangeal joint can occur in lateromedial or dorsopalmar directions. The injury may be obvious radiographically, but it may be necessary to obtain radiographs with the distal aspect of the limb under stress (see Figures 1.25a and 1.25b). The radiographs must be carefully examined for concurrent fractures. The prognosis for return to athletic function is poor. Degenerative joint disease is an inevitable sequel, with associated lameness. Development of degenerative joint disease of the proximal interphalangeal joint has also been observed, presumably secondary to trauma which induced luxation of the fetlock. Some horses have subsequently been used for pleasure riding or breeding. Conservative management and surgical treatment have been described.

Stress-related bone injury

Stress-related bone injury occurs commonly in the condyles of the third metacarpal and third metatarsal bones in Thoroughbred and Standardbred racehorses and occasionally in sports horses. Hindlimbs are more commonly affected than forelimbs. Although the palmar (plantar) aspect of the lateral condyle is most frequently affected, experience with magnetic resonance imaging reveals that evidence of bone trauma may be more widespread throughout the condyles. Care must be taken with interpretation, as the subchondral bone on the palmar (plantar) aspect of the condyle is normally

Downloaded From Vet-eBooks.com



Figure 5.29 Lateromedial radiographic image of the left metatarsophalangeal joint of a 4-year-old Thoroughbred flat racehorse with bilateral hindlimb lameness. There is increased opacity of the plantar aspect of the condyles of the third metatarsal bone, consistent with abnormal mineralisation. There were no localising clinical signs. Lameness was abolished by a 'low four-point block' at the plantar and plantar metatarsal nerves, but only slightly improved by intra-articular analgesia, a response typical of subchondral bone pain.

slightly flatter than the remainder of the condyle. Flattening of the condyle, or a triangular-shaped area of increased opacity in the subchondral bone (Figure 5.29), are best assessed on a lateromedial or lateromedial (flexed) view, or the dorsal 45° proximal 45° lateral-palmar distal medial oblique view. Dorsopalmar (flexed) images should be assessed carefully for alteration in trabecular architecture and opacity. In more advanced disease there may also be focal radiolucent areas reflecting bone necrosis. Nuclear scintigraphy is more sensitive for detection of early and less severe reactions. These lesions may occur bilaterally, especially in the hindlimbs, causing a variable degree of lameness or loss of performance. It is usually difficult to keep horses that have radiographic abnormalities sound enough to withstand training. However paddock turnout for 3 months may allow time for osseous modelling with some horses returning to training.

Fractures

The common fracture sites of the phalanges and metacarpophalangeal joint are shown in Figure 5.30.

Downloaded From Vet-eBooks.com

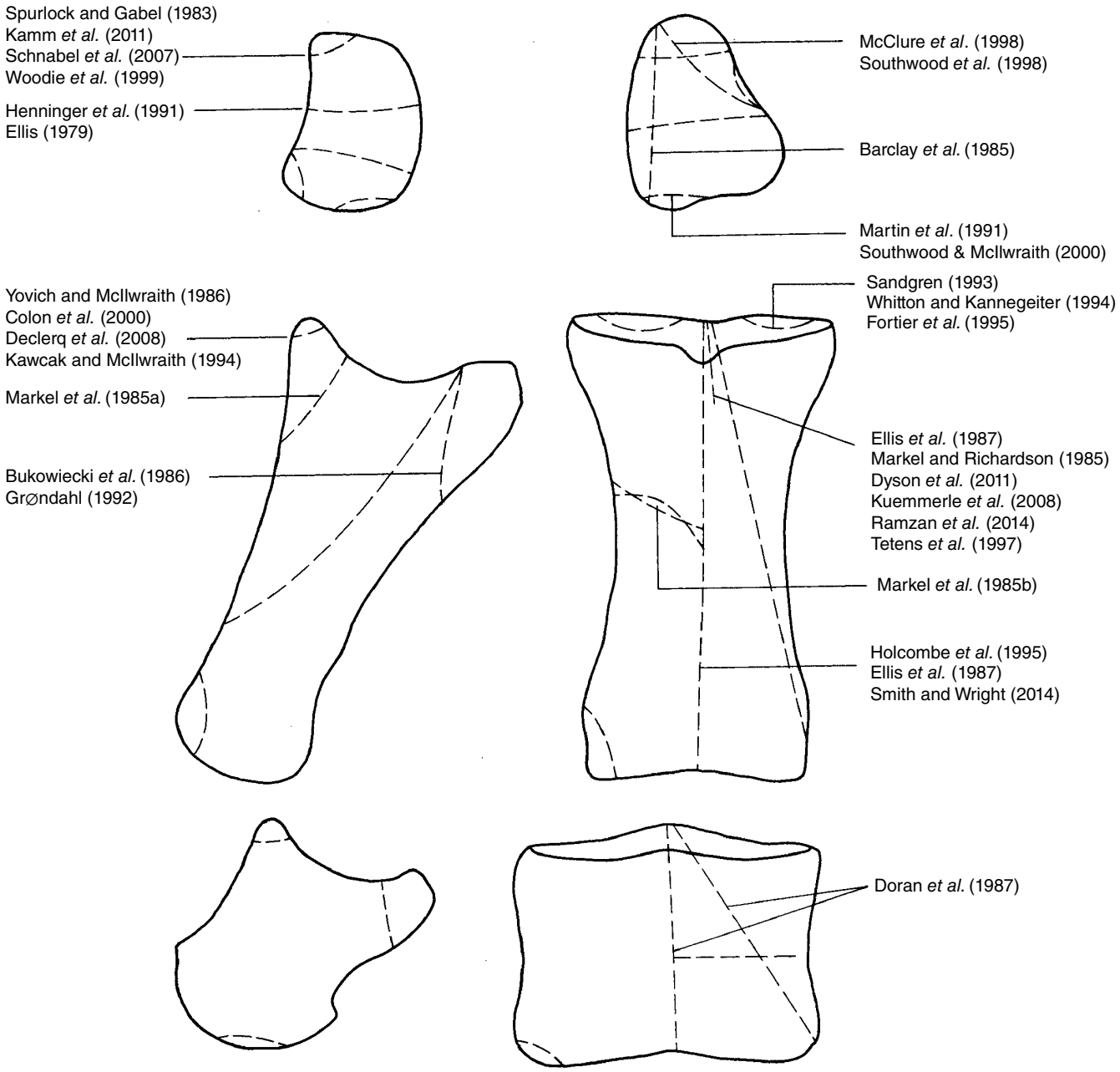


Figure 5.30 The common fracture sites for the phalanges and metacarpophalangeal joint.

Fractures of the proximal aspect of the proximal phalanx

Small radiopaque bodies at the joint margins may be an incidental finding (Figure 5.31 and 'Osteochondrosis, developmental orthopaedic disease and osteochondral fragments, above).

Chip fractures of the proximodorsal and proximopalmar aspects of the proximal phalanx, involving the joint surface, are relatively common and, if only 2–3 mm in diameter, lameness frequently resolves with rest, although it may be recurrent. Larger fragments, fragments associated with recurrent lameness, or fragments of bone with a roughened appearance or

Downloaded From Vet-eBooks.com



Figure 5.31 Lateromedial radiographic image of a metacarpophalangeal joint. There is a small, well-rounded mineralised opacity on the dorsoproximal aspect of the proximal phalanx. This was an incidental finding at a pre-purchase examination of this 7-year-old intermediate event horse.

irregular and lucent base usually need surgical removal. Other fractures of the proximal phalanx are referred to under 'Fractures' in Chapter 4. See also 'Osteochondral fragments', above.

Fractures of the proximal sesamoid bones

Fractures of the proximal sesamoid bones occur frequently, and their significance depends on their position and the degree of associated soft-tissue injury. They may occur in association with fractures of the third metacarpal bone and phalanges, and should not be overlooked.

Fractures of the abaxial surface of the bone are best seen on oblique tangential views (see Figures 5.1a and 5.1b). Prognosis depends on the degree of suspensory ligament pathology, but is often guarded; surgical removal of large fragments may be required.

Fractures of the apical region involving less than one-third of the bone generally respond well to surgical removal of the fragment (Figure 5w.32a). These fractures occur in all types of horses, particularly in racing Thoroughbreds. Fracture size and configuration does not alter the outcome.

Larger fragments should normally be treated by internal fixation or bone grafting, preferably within 10 days of fracture. Even with prompt treatment, the prognosis for these fractures is guarded. Basilar fragments of bone (Figure 5w.32b) may be removed surgically, but even with improved arthroscopic techniques, some disruption of the sesamoidean ligaments is inevitable, resulting in a guarded prognosis. Not all fragments are surgically accessible. Sometimes the entire distal

Downloaded From Vet-eBooks.com

border of the bone appears to have 'crumbled' with the presence of multiple small osseous opacities.

A triangular-shaped radiopacity distal to the proximal sesamoid bone usually reflects an avulsion fracture of the oblique sesamoidean ligament (Figure 5w.33). Such fractures may occur in Thoroughbreds as foals, reducing their earning potential as 2- and 3-year-olds compared with maternal siblings. Radiopacities of other shapes may represent dystrophic mineralisation (Figure 5.13).

Parasagittal fractures of the proximal sesamoid bones also occur, usually concurrent with other fractures. They warrant a guarded prognosis.

Occasionally an avulsion fracture at the attachment of the palmar annular ligament occurs (Figure 5.34). These have a favourable outcome with either conservative management or surgical removal.

Care should be taken when interpreting radiographs of foals. The proximal sesamoid bones are not fully mineralised until 3 months of age and the cartilage precursors may tear. This may not be seen radiographically until the sesamoid bones are more completely ossified, when the bones may appear elongated or be seen as two separated fragments (Figures 5.35a and 5w.35b). This is a common injury in foals under 1 month of age and may involve all four limbs. It is often seen in slightly premature foals that have exercised excessively and is associated with mild, transient lameness. With confinement and stall rest, bony union usually develops. The resulting proximal sesamoid bone is usually larger than normal but the prognosis is good if treated promptly. The altered length of the bone may however predispose to sesamoiditis.

Fractures of the third metacarpal (metatarsal) bone

Fractures of the distal aspect of the third metacarpal bone are described in Chapter 6.



Figure 5.34 Dorsolateral-palmaromedial oblique image of a metacarpophalangeal joint of a mature riding horse with lameness of 4 weeks' duration and pain on palpation of the lateral proximal sesamoid bone. There is an osseous opacity palmar to the lateral proximal sesamoid bone, consistent with an avulsion of the insertion of the palmar annular ligament. This was verified ultrasonographically. The horse was managed conservatively and made a complete functional recovery.

Downloaded From Vet-eBooks.com



Figure 5.35(a) Lateromedial image of a metacarpophalangeal joint of a foal 8 weeks of age, one day after the onset of mild lameness associated with pain on palpation over the medial proximal sesamoid bone and mild localised soft tissue swelling. There is a non-displaced apical fracture of the medial proximal sesamoid bone (arrow). Compare with Figure 5w.35b.

Additional figures

The book companion website at www.clinical-radiology-horse.com includes additional figures that are not included in the printed book or e-book formats. Please see '**About the Companion Website**' at the start of the book for details on how to access the website. These figures are prefixed with the letter 'w' in the printed book, e.g. Figures 1w.4c–f.

FURTHER READING

Anthenill, L., Stover, S., Gardner, I., et al. (2006) Association between findings on palmarodorsal radiographic images and detection of a fracture in the proximal sesamoid bones of forelimbs obtained from cadavers of racing Thoroughbreds *Am. J. Vet. Res*. **67**, 858–868

Barbee, D., Allen, J., Grant, B., Crawley, G., Sande. R. (1987) Detection by computerized tomography of occult osteochondral defects in the fetlock of a horse. *Equine Vet. J.* **19**, 556–558

Barclay, W., Foerner, J., Phillips, T. (1985) Axial sesamoid fractures associated with lateral condylar fractures. *J. Am. Vet. Med. Ass.* **186**, 278–279

Barclay, W., Foerner, J., Phillips, T. (1987) Lameness attributable to osteochondral fragmentation of the plantar aspect of the proximal phalanx: 19 cases. *J. Am. Vet. Med. Ass.* **191**, 855–857

Barr, E., Clegg, P., Senior, M., Singer, E. (2005) Destructive lesions of the proximal sesamoid bones as a complication of dorsal metatarsal artery catheterisation in three horses. *Vet. Surg.* **34**, 159–166

Barrett, E., Rodgerson, D. (2014) Ultrasound assisted arthroscopic approach for removal of basilar sesamoid fragments of the proximal sesamoid bones. *Vet. Surg.* **43**, 712–714

Beccati, F., Pepe, M., Di Meo, A., et al. (2011) Radiographic evaluation of changes in the proximal phalanx of Thoroughbreds in race training. *Am. J. Vet. Res.* **72**, 1482–1488

Birkeland, R. (1972) Chip fractures of the first phalanx in the metacarpophalangeal joint. *Acta Radiol. Suppl.* **39**, 73–77

Bukowiecki, C., Bramlage, L., Gabel, A. (1986) Palmar/plantar process fractures of the proximal phalanx in 15 horses. *Vet. Surg.* **15**, 383–388

Downloaded From Vet-eBooks.com

Carlsten, J., Sandgren, B., Dalin, J. (1993) Development of osteochondrosis in the tarsocrural joints and osteochondral fragments in the fetlock joint in Standardbred trotters. 1. A radiological survey. *Equine Vet. J.* **25** (Suppl. 16), 42–47

Cohen, N., Carter, G., Watkins, J., O'Conor, M. (2006) Association of racing performance with specific abnormal radiographic findings in Thoroughbred yearlings sold in Texas. *J. Equine Vet. Sci.* **26**, 462–474

Colon, J., Bramlage, L., Hance, S., Embertson, R. (2000) Qualitative and quantitative documentation of the racing performance of 461 Thoroughbred racehorses after arthroscopic removal of dorsoproximal first phalanx osteochondral fractures (1986–1995). *Equine Vet. J.* **32**, 475–481

Courouce-Malblanc, A., Leleu, C., Bouchilloux, M., Geffroy, O. (2006) Abnormal radiographic findings in 865 French Standardbred trotters and their relationship to racing performance. *Equine Vet. J. Suppl.* **36**, 417–422

Cullimore, A., Finnie, J., Marmion, W., et al. (2009) Severe lameness associated with an impact fracture of the proximal phalanx in a filly. *Equine Vet. Educ.* **21**, 247–251

Dabareiner, R., Watkins, J., Carter, G., Honnas, C., Eastman, T. (2001) Osteitis of the axial border of the proximal sesamoid bones in horses: 8 cases (1993–1999). *J. Am. Vet. Med. Ass.* **219**, 82–86

Dabareiner, R., White, N., Sullins, K. (1996) Metacarpopha langeal joint synovial pad fibrotic proliferation in 63 horses. *Vet. Surg.* **25**, 199–206

Dalin, G., Sandgren, B., Carlsten, J. (1993) Plantar osteochondral fragments in the metatarsophalangeal joints in Standardbred trotters: result of osteochondrosis or trauma? *Equine Vet. J. Suppl*. **25** (Suppl. 16), 62–65

Declerq, J., Martens, A., Maes, D.,al. (2008) Dorsoproximal proximal phalanx osteochondral fragmentation in 117 Warmblood horses. *Vet. Comp. Orthop. Traumatol.* **22**, 1–6

Dik, K.J. (1985) Special radiographic projections for the equine proximal sesamoid bones and the caudoproximal extremity of the first phalanx. *Equine Vet. J.* **17**, 244–247

Dyson, S., Murray, R. (2006) Osseous trauma in the fetlock region of mature sports horses. *Proc. Am. Ass. Equine Pract.* **52**, 443–456

Dyson, S., Murray, R. (2007) Magnetic resonance imaging of the equine fetlock. *Clin. Techniques in Equine Pract.* **6**, 62–77

Dyson, S., Nagy, A., Murray, R. (2011) Clinical and diagnostic imaging findings in horses with subchondral bone trauma of the sagittal groove of the proximal phalanx. *Vet. Radiol. Ultrasound* **52**, 596–604

Ellis, D. (1979) Fractures of the proximal sesamoid bones in Thoroughbred foals. *Equine Vet. J.* **11**, 48–52

Enzerink, E., Dik, K. (2001) Palmar/plantar ligament insertion injury: a report of 4 cases. *Equine Vet. Educ.* **13**, 75–80

Fiske-Jackson, A., Barker, W., Eliahsar, E., et al. (2013) The use of intrathecal analgesia and contrast radiography as preoperative diagnostic methods for digital flexor tendon sheath pathology. *Equine Vet. J.* **45**, 36–40

Fortier, L., Foerner, J., Nixon, A. (1995) Arthroscopic removal of axial osteochondral fragments of the plantar/palmar proximal aspect of the proximal phalanx in horses: 119 cases (1988–1992). *J. Am. Vet. Med. Ass.* **206**, 71–74

Gonzalez, L., Schramme, M., Robertson, I., et al. (2010) MRI features of meacarpo(tarso)phalangeal region lameness in 40 horses. *Vet. Radiol. Ultrasound* **51**, 404–414

Grøndahl, A. (1992) Incidence and development of ununited proximoplantar tuberosity of the proximal phalanx in Standardbred trotters. *Vet. Radiol. Ultrasound* **33**, 18–21

Grøndahl, A., Gaustad, G., Engeland, A. (1994) Progression and association with lameness and racing performance of radiographic changes in the proximal sesamoid bones of young Standardbred trotters. *Equine Vet. J.* **26**, 152–155

Hardy, J., Marcoux, M., Breton, L. (1991) Clinical relevance of radiographic findings in proximal sesamoid bones of two-year-old Standardbreds in their first year of race training. *J. Am. Vet. Med. Ass.* **198**, 2089–2094

Hauspie, S., Martens, A., Declerq, J., et al. (2010) Radiographic features of the dorsal condylar sagittal ridge of the third metacarpal and metatarsal bones in young Warmblood stallions. *Vet. Comp. Orthop. Traumatol.* **23**, 411–416

Hauspie, S., Forsyth, R., Vanderperren, K., et al. (2012) The histological appearance of the proximal aspect of the dorsal condylar sagittal ridge of the third metacarpal and metatarsal bone in young Warmblood horses: normal appearance and correlation with detected radiographic findings. *Anat. Histol. Embryol.* **42**, 232–238

Haynes, P., Root, C., Clabough, Q., Roberts, E. (1981) Palmar supracondylar lysis of the third metacarpal bone. *Proc. Am. Ass. Equine Pract.*, **27**, 185–193

Henninger, R., Bramlage, L., Schneider, R., Gabel, A. (1991) Lag screw and cancellous bone graft fixation of transverse proximal sesamoid fractures in horses: 25 cases (1983–1989). *J. Am. Vet. Med. Ass.* **199**, 606–612

Hinnigan, G., Papoula-Pereira, R., Hetzel, U., et al. (2014) Severe supracondylar lysis of the third metatarsal bone due to intra-articular haemorrhage with similarities to human pigmented villonodular synovitis: A differential diagnosis to intra-articular neoplasia. *Equine Vet. Educ*. doi: 10.1111/eve.12071

Hogan, P., McIlwraith, C., Honnas, C., et al. (1997) Surgical treatment of subchondral cystic lesions of the third metacarpal bone: results in 15 horses (1986–1994). *Equine Vet. J*, **29**, 477–482

Hornhof, W.J., O'Brien, T.R. (1980) Radiographic evaluation of the palmar aspect of the equine metacarpal condyles: a new projection. *Vet. Radiol.* **21**, 161–167

Jacklin, B., Wright, I. (2012) Frequency distribution of 174 fractures of the distal condyles of the third metacarpal and metatarsal bones in 167 Thoroughbred racehorses (1999–2009). *Equine Vet. J.* **44**, 707–713

Jacquet, S., Robert, C., Valette, J.-P., et al. (2013) Evolution of radiological findings detected in the limbs of 321 young horses between the ages of 6 and 18 months. *Vet. J.* **197**, 58–64

Downloaded From Vet-eBooks.com

Kamm, J., Bramlage, L., Schnabel, L., et al. (2011) Size and geometry of apical sesamoid fracture fragments as a determinant of prognosis in Thoroughbred racehorses. *Equine Vet. J.* **43**, 412–417

Kane, A., Park, R., McIlwraith, C., Rantanen, N., Morehead, J., Bramlage, L. (2003a) Radiographic changes in Thoroughbred yearlings. Part 1: Prevalence at the time of sales. *Equine Vet. J.* **35**, 354–365

Kane, A., McIlwraith, C., Park, R., Rantanen, N., Morehead, J., Bramlage, L. (2003b) Radiographic changes in Thoroughbred yearlings. Part 2: Association with racing performance. *Equine Vet. J.* **35**, 366–374

Kawcak, C., McIlwraith, C.W. (1994) Proximodorsal first phalanx osteochondral chip fragmentation in 336 horses. *Equine Vet. J.* **26**, 392–396

Kawcak, C., Bramlage, L., Embertson, D. (1995) Diagnosis and management of incomplete fracture of the distal palmar aspect of the third metacarpal bone in five horses. *J. Am. Vet. Med. Ass.* **206**, 335–338

King, J., Zubrod, C., Schneider, R., et al. (2012) MRI findings in 232 horses with lameness localised to the metacarpo(tarso) phalangeal region and without a radiographic diagnosis. *Vet. Radiol. Ultrasound* **54**, 36–47

Kuemmerle,.J, Auer, J., Racdemacher, N., et al. (2008) Short incomplete sagittal fractures of the proximal phalanx in 10 horses not used for racing. *Vet. Surg.* **37**, 193–200

Lykkjen, S., Olsen, H., Dolvik, N., et al. (2014) Heritability estimates of tarsocrural osteochondrosis and palmar/plantar first phalanx osteochondral fragments in Standardbred trotters. *Equine Vet. J.* **46**, 32–37

McCall, D.J.M., Kneller, S.K. (1989) Proximodorsal-distodorsal view of the equine metacarpophalangeal joint. *Vet. Technician* **10**, 617–621

McClure, S., Watkins, J., Glickman, N., et al. (1998) Complete fracture of the third metacarpal or metatarsal bone in horses: 25 cases (1980–1986). *J. Am. Vet. Med. Ass.* **213**, 847–850

McLellan, J., Plevin, S. (2013) Do radiographic signs of sesamoiditis in yearling Thoroughbreds predispose the development of suspensory ligament branch injury? *Equine Vet. J.* doi: 10.1111/evj.12154

Mair, T., Tucker, R. (2004) Hypertrophic osteopathy (Marie's disease) in horses. *Equine Vet. Educ.* **16**, 308–311

Marneris, D., Dyson, S. (2014) Clinical features, diagnostic imaging findings and concurrent injuries in 71 sports horses with suspensory branch injuries. *Equine Vet. Educ.* **26**, 312–321

Martin, B., Nunamaker, D., Evans, L., Orsini, J., Palmer, S. (1991) Circumferential wiring of mid-body and large basilar fractures of the proximal sesamoid bones in 15 horses. *Vet. Surg.* **20**, 9–14

Medina, L., Wheat, J., Morgan, J., Pool, R. (1950) Treatment of basal fractures of the sesamoid bones using autogenous bone grafts. *Proc. Am. Ass. Equine Pract.* **26**, 345–380

Menarim, B., Vasconcelos, V., Alvarez, L., et al. (2012) Radiographic abnormalities in barrel racing horses with lameness referable to the metacarpophalangeal joint. *J. Equine Vet. Sci.* **32**, 216–221.

Morgan, J., Santschi, E., Zekas, L., et al. (2006) Comparison of radiography and computer tomography to evaluate metacarpo/metatarsophalangeal joint pathology of paired limbs of Thoroughbred racehorses with severe condylar fractures. *Vet. Surg.* **35**, 611–617

Nickels, J.F., Grant, B.D., Lincoln, S.C. (1975) Villonodular synovitis of the equine metacarpophalangeal joint. *J. Am. Vet. Med. Ass.* **168**, 1043–1046

Nixon, A., Pool, R. (1995) Histologic appearance of axial osteochondral fragments from the proximoplantar/proximopalmar aspect of the proximal phalanx. *J. Am. Vet. Med. Ass.* **207**, 1076–1080

O'Brien, T.R., Morgan, J.P., Wheat, J.D., Suter, P.F. (1971) Sesamoiditis in the thoroughbred: a radiographic study. *J. Am. Vet. Res.* **12**, 75–87

O'Brien, T.R., Hornhof, W., Meagher, D. (1981) Radiographic detection and characterisation of palmar lesions in the fetlock joint. *J. Am. Vet. Med. Ass.* **178**, 231–237

Palmar, S.E. (1982) Radiography of the abaxial surface of the proximal sesamoid bones of the horse. *J. Am. Vet. Ass.* **181**, 264–265

Poulos, P. (1988) Radiographic and histologic assessment of proximal sesamoid bone changes in young and working horses. *Prox. Am. Ass. Equine Pract.* **34**, 347–358

Powell, S. (2012) Low-field standing magnetic resonance imaging findings of the metacarpo/metatarsophalangeal joint of racing Thoroughbreds with lameness localised to the region: A retrospective study of 131 horses. *Equine Vet. J.* **44**, 169–177

Preston, S., Brown, M., Trumble, T., et al. (2012) Effects of various presale radiographic findings for yearling Thoroughbreds on 2-year-old racing performance. *J. Am. Vet. Med. Ass.* **241**, 1505–1513

Ramzan, P., Powell, S. (2010) Clinical and imaging features of suspected prodromal fracture of the proximal phalanx in three Thoroughbred racehorses. *Equine Vet. J.* **42**, 164–169

Ramzan, P., Palmer, L., Powell, S. (2014) Unicortical condylar fracture of the Thoroughbred fetlock: 45 cases (2006–2013). *Equine Vet. J.* doi: 10:1111/evj.12349

Rebsamen, E., Furst, A., Hagen, R., et al. (2011) Outcome and radiographic assessment of the development of osteoarthritis in 15 horses with rupture of collateral ligaments and joint instability in metacarpophalangeal or metatarsophalangeal joints. *Pferdheilkunde* **27**, 141–146

Rick, M., O'Brien, T., Pool, R., Meagher, D. (1983) Condylar fractures of the third metacarpal bone and third metatarsal bone in 75 horses: radiographic features, treatment and outcome. *J. Am. Vet. Med. Ass.* **183**, 287–296

Riggs, C. (1999) Aetiopathogenesis of parasagittal fractures of the distal condyles of the third metacarpal and third metatarsal bones: review of the literature. *Equine Vet. J.* **31**, 116–121

Downloaded From Vet-eBooks.com

Riggs, C., Whitehouse, G., Boyde, A. (1999a) Structural variation of the distal condyles of the third metacarpal bone and third metatarsal bone in the horse. *Equine Vet. J.* **31**, 130–139

Riggs, C., Whitehouse, G., Boyde, A. (1999b) Pathology of the distal condyles of the third metacarpal bone and third metatarsal bone in the horse. *Equine Vet. J.* **31**, 140–149

Ross, M., Nolan, P., Palmer, J., et al. (1991) The importance of the metatarsophalangeal joint in Standardbred lameness. *Proc. Am. Ass. Equine Pract.* **37**, 741–756

Ross, M. (1998) Scintigraphic and clinical findings in the Standardbred metatarsophalangeal joint: 114 cases (1993–1995). *Equine Vet. J.* **30**, 131–138

Sandgren, B. (1993) Osteochondrosis in the tarsocrural joint and osteochondral fragments in the metacarpo/metatarsophalangeal joints in young Standardbreds. PhD Thesis, University of Uppsala, Sweden

Schnabel, L., Bramlage, L., Mohammed, H., Embertson, R., Ruggles, A., Hopper, S. (2006) Racing performance after arthroscopic removal of apical sesamoid fractures in Thoroughbred horses age ≥2 years: 84 cases (1998–2002). *Equine Vet. J.* **38**, 446–453

Schnabel, L., Bramlage, L., Mohammed, H., Embertson, R., Ruggles, A., Hopper, S. (2007) Racing performance after arthroscopic removal of apical sesamoid fractures in Thoroughbred horses age <2 years: 151 cases (1998–2002). *Equine Vet. J.* **39**, 64–68

Schleining, J., Voss, E. (2004) Hypertrophic osteopathy secondary to gastric squamous cell carcinoma in a horse. *Equine Vet. Educ.* **16**, 304–307

Shepherd, M., Pilsworth, R. (1997) Stress reactions in the plantarolateral condyles of MT III in UK Thoroughbreds: 26 cases. *Proc. Am. Ass. Equine Pract.* **43**, 128–131

Smith, M., Wright, I. (2014) Radiographic configuration and healing of 121 fractures of the proximal phalanx in 120 Thoroughbred racehorses (2007–2011). *Equine Vet. J.* **46**, 81–87

Smith, M., Wright, I. (2014) Are there radiologically identifiable prodromal changes in Thoroughbred racehorses with parasagittal fractures of the proximal phalanx? *Equine Vet. J.* **46**, 88–91

Smith, R.K., Coumbe, A., Schramme, M.C. (1995) Bilateral synovial chondromatosis of the metatarsophalangeal joints in a pony. *Equine Vet. J.* **27**, 234–238

Southwood, L., Trotter, G., McIlwraith, C. (1998) Arthroscopic removal of abaxial fracture fragments of the proximal sesamoid bone in horses: 47 cases (1989–1997). *J. Am. Vet. Med. Ass.* **213**, 1016–1021

Southwood, L., McIlwraith, C. (2000) Arthroscopic removal of fracture fragments involving a portion of the base of the proximal sesamoid bone in horses: 26 cases (1984–1997). *J. Am. Vet. Med. Ass.* **217**, 236–240

Spike, D., Bramlage, L., Howard, B., et al. (1997) Radiographic proximal sesamoiditis in Thoroughbred sales yearlings. *Proc. Am. Ass. Equine Pract.* **43**, 132–137

Spike-Pierce, D., Bramlage, L. (2003) Correlation of racing performance with radiographic changes in the proximal sesamoid bones of 487 Thoroughbred yearlings. *Equine Vet. J.* **35**, 350–353

Spurlock, G., Gabel, A. (1983) Apical sesamoid fractures in the proximal sesamoid bones in 109 Standardbred horses. *J. Am. Vet. Med. Ass.* **183**, 76–79

Stock, K., Hamann, H., Distl, O. (2005) Prevalence of osseous fragments in distal and proximal interphalangeal, metacarpo- and metatarsophalangeal and tarsocrural joints of Hanoverian Warmblood horses. *J. Vet. Med. A* **52**, 388–394

Storgaard, J., Jorgensen, H., Proschowsky, H., Falke-Ronne, J., Willeberg, P., Hesselholt, M. (1997) The significance of routine radiographic findings with respect to racing performance and longevity in Standardbred trotters. *Equine Vet. J.* **29**, 55–59

Tetens, J., Ross, M., Lloyd, J. (1997) Comparison of racing performance before and after treatment of incomplete midsagittal fractures of the proximal phalanx in Standardbreds. *J. Am. Vet. Med. Ass.* **210**, 82–86

Thompson, K., Rooney, J. (1994) Bipartite proximal sesamoid bones in young Thoroughbred horses. *Vet. Radiol. Ultrasound* **35**, 368–370

Tull, T., Bramlage, L. (2011) Racing prognosis after cumulative stress-induced injury of the distal portion of the third metacarpal and third metatarsal bones in Thoroughbred racehorses: 55 cases (2000–2009). *J. Am. Vet. Med. Ass.* **238**, 1316–1322

Vanderperren, K., Bergman, H., Spoormakers, T., et al. (2014) Clinical, radiographic, ultrasonographic and computed tomographic fractures of nonseptic osteitis of the axial border of the proximal sesamoid bones. *Equine Vet. J.* doi: 10.1111/evj.12141

Varela, A., Patipa, L., Eggleston, R. (2014) Subchondral bone cyst of the apical portion of the proximal sesamoid bone as a cause of severe lameness in a Warmblood filly. *Equine Vet. Educ.* **26**, 126–131

Verwilghen, D., Janssens, S., Busoni, V., et al. (2013) Do developmental orthopaedic disorders influence future jumping performance in Warmblood stallions? *Equine Vet. J.* doi:10.1111/evj.12027

Whitton, C., Kannegeiter, N. (1994) Osteochondral fragmentation of the plantar/palmar proximal aspect of the proximal phalanx in racing horses. *Austr. Vet. J.* **71**, 318–321

Winberg, F., Petterson, H. (1994) Diagnosis and treatment of lesions of the intersesamoidean ligament and its adjoining structures. *Vet. Surg.* **23**, 215

Woodie, J., Ruggles, A., Bertone, A., Hardy, J., Schneider, R. (1999) Apical fractures of the proximal sesamoid bone in Standardbred horses: 43 cases (1990–1996). *J. Am. Vet. Med. Ass.* **214**, 1653–1656

Wright, I., Minshall G. (2014) Identification and treatment of osteochondritis dissecans of the distal sagittal ridge of the third metacarpal bone. *Equine Vet. J.* 10.1111/evj.12187

Yovich, J., McIlwraith, C., Stashak, T. (1985) Osteochondrosis dissecans of the sagittal ridge of the third metacarpal and metatarsal bones in horses. *J. Am. Vet. Med. Ass.* **186**, 1186–1191

Downloaded From Vet-eBooks.com

Yovich, J., McIlwraith, C. (1986) Arthroscopic surgery for osteochondral fractures of the proximal phalanx of the metacarpophalangeal and metatarsophalangeal (fetlock) joints in horses. *J. Am. Vet. Med. Ass.* **188**, 273–279

Zekas, L., Bramlage, L., Embertson, R., Hance, S. (1999a) Characterisation of the type and location of fractures of the third metacarpal/metatarsal condyles in 135 horses in central Kentucky (1986–1994). *Equine Vet. J.* **31**, 304–308

Zekas, L., Bramlage, L., Embertson, R., Hance, S. (1999b) Results of treatment of 145 fractures of the third metacarpal/metatarsal condyles in 135 horses in central Kentucky (1986–1994). *Equine Vet. J.* **31**, 309–313

Zubrod, C., Schneider, R., Tucker, R., et al. (2004) Use of magnetic resonance imaging for identifying subchondral bone damage in horses: 11 cases (1999–2003). *J. Am. Vet. Med. Ass.* **224**, 411–418

Downloaded From Vet-eBooks.com

Downloaded From Vet-eBooks.com

Chapter 6
The metacarpal and metatarsal regions

Throughout this chapter, although reference is made to the metacarpal region it also applies to the metatarsal region. Significant differences of the metatarsal region are highlighted.

A standard radiographic examination of the metacarpal region comprises lateromedial, dorsopalmar, dorsolateral-palmaromedial oblique and dorsomedial-palmarolateral oblique views. In selected cases dorsoproximal-palmarodistal oblique views may yield valuable additional information about the distal aspect of the third metacarpal bone (see Chapter 5, 'Tangential dorsopalmar views'). Occasionally a lateromedial (flexed) view of the proximal metacarpal region is helpful for identifying avulsion fractures at the origin of the suspensory ligament. Special projections for evaluating the proximal sesamoid bones are discussed in Chapter 5 ('Special oblique views').

In many instances the clinical examination will suggest which views are necessary and at which level the x-ray beam should be centred. In some cases a complete examination is not required, although many views with only slight differences in angle of projection may be needed (e.g. for evaluation of a dorsal cortical fatigue fracture of the third metacarpal bone). It is difficult to evaluate the entire length of the metacarpal region properly using small (30 cm) cassettes.

RADIOGRAPHIC TECHNIQUE

Lateromedial, dorsopalmar and oblique views

The metacarpal region may be radiographed using a portable x-ray machine and either digital imaging plates or high-definition or rare earth screens and compatible film. A grid is unnecessary. All the standard projections are ideally obtained with the horse bearing full weight on the limb, with the metacarpal region vertical. To assess the proximal half of the palmar (plantar) cortex of the third metacarpal (metatarsal) bones a lateral 15° palmar (plantar)–medial dorsal oblique image is preferred to a lateromedial image (compare Figures 6.1a and 6.1b). The second and fourth metacarpal bones are best evaluated using dorsomedial-palmarolateral oblique and dorsolateral-palmaromedial oblique views, respectively. The x-ray beam is centred on the area of principal interest. In some cases it may be helpful to use a long (43 cm) cassette so that the entire length of the metacarpal region can be seen on a single radiograph, but in an adult horse some obliquity of

Clinical Radiology of the Horse, Fourth Edition. Janet A. Butler, Christopher M. Colles, Sue J. Dyson, Svend E. Kold and Paul W. Poulos.
© 2017 John Wiley & Sons, Ltd. Published 2017 by John Wiley & Sons, Ltd.
Companion website: www.clinical-radiology-horse.com

Downloaded From Vet-eBooks.com



Figure 6.1(a) Lateromedial image of the proximal half of the metatarsal region of a normal adult horse. The second metatarsal bone is partially superimposed over the third metatarsal bone and the dorsal surface of the plantar cortex of the third metatarsal bone is not well-defined. Compare with Figure 6.1(b).



Figure 6.1(b) Lateral 15° plantar- dorsomedial oblique image of the same limb as in Figure 6.1(a). The plantar cortex of the third metatarsal bone is clearly demarcated. The second and fourth metatarsal bones are superimposed and the interosseous space between them and the third metatarsal bone is seen distinctly.

projection at the extremities of the bones is inevitable (see Figure 6.4). Therefore it is usually preferable to use more than one projection and create a 'jigsaw' of the length of the bone.

Many of the radiographic abnormalities in this region are subtle and are only visible with correct angulation of the x-ray beam and appropriate exposure factors. Fatigue (stress) fractures of the dorsal cortex of the third metacarpal bone are easily missed unless multiple oblique views are obtained. Early periosteal proliferative reactions, less opaque than the parent bone (e.g. a 'splint') are easily overexposed. Thus reduced exposure factors should be used. The timing of the radiographic examination is also critical, because many radiographic abnormalities will not be present until at least 7–21 days after the onset of clinical signs. Sequential radiographic examinations may therefore be helpful.

Downloaded From Vet-eBooks.com

Dorsoproximal-palmarodistal oblique views

In a dorsopalmar image of the distal aspect of the metacarpal region, the proximal sesamoid bones are projected over the distal aspect of the third metacarpal bone (Figure 6.2a) and lesions involving the condyles may easily be missed (e.g. an incomplete vertical condylar fracture). The proximal sesamoid bones are projected further proximally if the x-ray beam is angled proximodistally at least 10°, i.e. a dorsal 10° proximal-palmarodistal oblique (D10°Pr-PaDiO) view (Figure 6.2b). This view is particularly important for the identification of incomplete, vertical articular condylar fractures, although these lesions may still be difficult to detect. Improved visualisation may be achieved by flexing the metacarpophalangeal joint. The toe of the foot is placed in the standard navicular block (see Figure 3.63c), with the metacarpal region vertical. A horizontal x-ray beam is centred on the joint. The cassette is positioned as near perpendicular to the x-ray beam as possible. This positions the proximal sesamoid bones further proximally (Figure 6.2c). If the x-ray beam is directed dorsodistal-palmaroproximal a more palmar region of the articular surface can be examined.

The palmar articular surface may be assessed better with the limb partially extended with the foot on a flat block (Figure 6.3). The cassette or imaging plate is held approximately parallel to the metacarpal region.



Figure 6.2(a) Horizontal dorsopalmar image of the distal metacarpal region of a normal adult horse. The proximal sesamoid bones are superimposed over the condyles of the third metacarpal bone. Note the curved outline of the medial and lateral aspects of the distal end of the third metacarpal bone (arrows) and the variable opacity in these areas. This may be exaggerated in a slightly oblique projection.



Figure 6.2(b) Dorsal 10° proximal-palmarodistal oblique image of the distal metacarpal region of a normal adult horse. The proximal sesamoid bones are projected proximally giving excellent visualisation of the metacarpal condyles.

Downloaded From Vet-eBooks.com



Figure 6.2(c) Dorsopalmar (flexed) image of the distal metacarpal region of a normal adult horse. The proximal sesamoid bones are projected more proximally than in Figure 6.2(b). This view highlights a more distal articular margin of the condyles of the third metacarpal bone.



Figure 6.2(d) Dorsodistal-palmaroproximal oblique image of the distal metacarpal region of a normal adult horse. The proximal sesamoid bones are superimposed over the metacarpophalangeal joint, but this view gives visualisation of the palmar aspect of the metacarpal condyles.

The x-ray beam is directed dorsodistal-palmaroproximally in the plane of rotation of the metacarpophalangeal joint, at approximately 125° to the third metacarpal bone. If the limb and the x-ray beam are correctly aligned, between one-quarter and one-third of the proximal sesamoid bones are projected below the joint space (Figure 6.2d). This view is especially important when evaluating a vertical condylar fracture; comminution of the palmar articular surface of the third metacarpal bone is usually only identifiable in this projection. It is also useful for detecting lucent lesions in the palmar aspect of the third metacarpal bone condyles (see Chapter 5, 'Stress-related bone injury'). Other oblique views of the condyles of the third metacarpal bone and the proximal sesamoid bones are described in detail in Chapter 5. (See 'Special oblique views', 'Tangential dorsopalmar views', 'Dorsoproximal-dorsodistal (flexed) view' and 'Palmaroproximal-palmarodistal oblique view of the proximal sesamoid bones'.)

Other imaging techniques

Nuclear scintigraphy offers a more sensitive method than radiography for detection of acute stress (fatigue) fractures. Ultrasonography provides a means of evaluating the metacarpal soft-tissue structures. It must be remembered that bony and soft-tissue lesions may occur concurrently and this may have an important bearing on the prognosis (e.g. fractures of the

Downloaded From Vet-eBooks.com

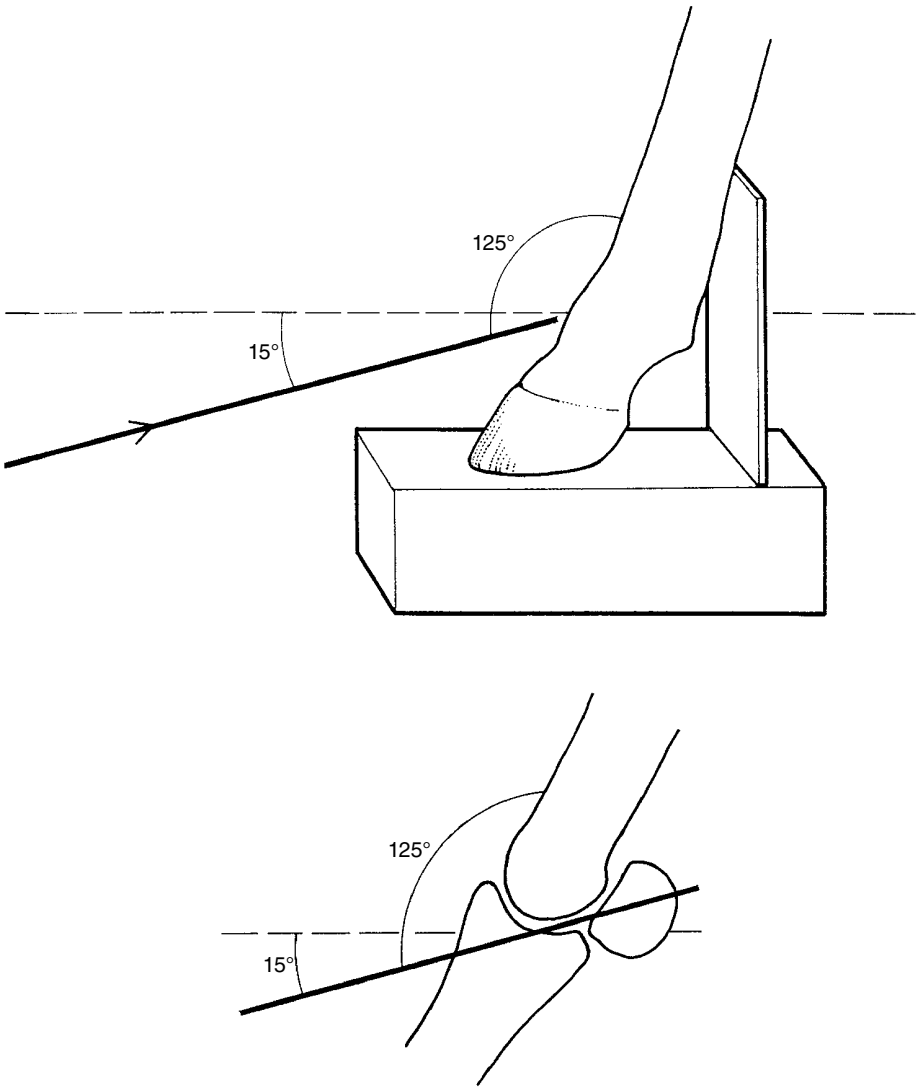


Figure 6.3 Position of the limb, x-ray machine and cassette to obtain a dorsodistal-palmaroproximal oblique view of the distal metacarpal region (see Figure 6.2d).

distal one-third of the second or fourth metacarpal bones often occur together with suspensory desmitis). Magnetic resonance imaging has the potential to identify both soft-tissue and osseous lesions that are not detectable using other imaging techniques. Computed tomography may help to demonstrate the configuration of complex fractures and to detect entheseous new bone at the origin of the suspensory ligament.

NORMAL RADIOGRAPHIC ANATOMY: ITS VARIATIONS AND INCIDENTAL FINDINGS

Lateromedial view

The dorsal cortical contour of the third metacarpal bone is usually straight, but that of the third metatarsal bone is relatively convex particularly in its distal third (Figures 6.4a and 6.4b). The dorsal cortex is thicker than the palmar (plantar) cortex, especially on the dorsomedial aspect of the forelimb. The smoothness of the dorsal cortex should always be evaluated carefully under high-intensity illumination or by using the windowing of a digital

Downloaded From Vet-eBooks.com



Figure 6.4(a) Lateromedial image of a normal adult metacarpal region. Note the obliquity of projection at the distal end of the bone. To evaluate this area better, an image centred on this region is required.



Figure 6.4(b) Lateromedial image of a normal adult metatarsal region. Due to the increased length of the bone relative to the metacarpal region there is greater obliquity at the proximal and distal extremities of the bone. Note the slightly convex contour of the dorsal cortex of the third metatarsal bone.

Downloaded From Vet-eBooks.com

system. The dorsal cortices of the third metacarpal or metatarsal bones may be unusually convex and thicker than normal as a result of previous trauma, or adaptation to previous work. Small, uniformly opaque, clinically silent osteophytes or entheseophytes are sometimes seen on the dorsoproximal aspect of the third metatarsal bone (see Chapter 9, 'Radiographic anatomy: normal variations and incidental findings – Lateromedial view' and Figures 9.7a and 9.7b). The principal nutrient canal is frequently seen in the palmar cortex, at approximately the distal margin of the proximal third of the bone. It may course horizontally, or curve proximally.

Dorsopalmar view

The proximal articular surface of the third metacarpal bone is concave, therefore part of the carpometacarpal joint is superimposed over the third carpal bone (Figure 6.5b). The subchondral bone plate is a relatively opaque band of uniform thickness. A series of small, circular lucent zones, nutrient foramina, may be seen in the subchondral bone of the proximal aspect of the third metacarpal bone depending on the angle of projection (Figure 6.5b). The proximal and distal quarters of the third metacarpal bone have a relatively coarse, but uniformly opaque trabecular pattern (see Figures 6.2a–c, 6.5b and 6.19c). The trabeculae are orientated approximately parallel to the long axis of the bone. In some horses there is a narrow, vertical, more opaque line in the middle of the proximal quarter of the third metacarpal bone, representing a ridge between the heads of the suspensory ligament. This is seen more commonly in hindlimbs (Figure 6.5c). Increased opacity of the proximolateral aspect of the third metatarsal bone may be a response to normal biomechanical loading (Figure 6.5d). The principal nutrient foramen is usually seen as an oval-shaped lucent area superimposed on the medullary cavity, at the junction between the proximal and middle thirds of the bone (Figure 6.5a). Occasionally it may be linear in appearance, or there may be more than one nutrient foramen.

In this view and some oblique projections the second and fourth metacarpal bones are partially superimposed over the third metacarpal bone, and this may result in some confusing lucent lines. These lucent lines (Mach lines or bands) are due to edge enhancement, the effect of one bone edge crossing another (Figure 6.6), and should not be confused with fractures. This appearance may be more marked with digital images, where computerised edge enhancement of images may take place. The second and fourth metacarpal bones are most readily evaluated in the oblique views.

The proximal metacarpal physis is closed at birth. The distal metacarpal physis closes radiographically at approximately 3–6 months of age, but 'functionally' at a much earlier stage (Figure 6.7).

The proximal sesamoid bones are superimposed over the distal end of the third metacarpal bone. Their position depends on the angle of projection (see Figures 6.2a–d). Radiographic features of these bones are discussed in Chapter 5.

Dorsolateral-palmaromedial oblique and dorsomedial-palmarolateral oblique views

The dorsolateral-palmaromedial oblique view (Figure 6.8) highlights the dorsomedial cortex of the third metacarpal bone and the fourth metacarpal bone. The fourth metacarpal bone may have a proximal extension

Downloaded From Vet-eBooks.com



Figure 6.5(a) Dorsopalmar image of the metacarpal region of a normal adult horse. Medial is to the left. Note the vertical lucent line on the axial aspect of the fourth metacarpal bone (arrowheads) created by an edge effect. The lucent zone in the middle of the third metacarpal bone (arrow) represents the principal nutrient foramen.



Figure 6.5(b) Dorsopalmar image of the proximal third of the metacarpal region of a normal adult horse. Medial is to the left.



Figure 6.5(c) Dorsoplantar image of the proximal metatarsal region of a 7-year-old Warmblood. Medial is to the left. There is a linear region of increased radiopacity in the proximal axial aspect of the third metatarsal bone, a normal variant.

Downloaded From Vet-eBooks.com



Figure 6.5(d) Dorsoplantar image of the proximal metatarsal region of a 9-year-old Warmblood. Medial is to the left. There is mild diffuse increased radiopacity of the proximolateral aspect of the third metatarsal bone. This may be of no clinical significance.

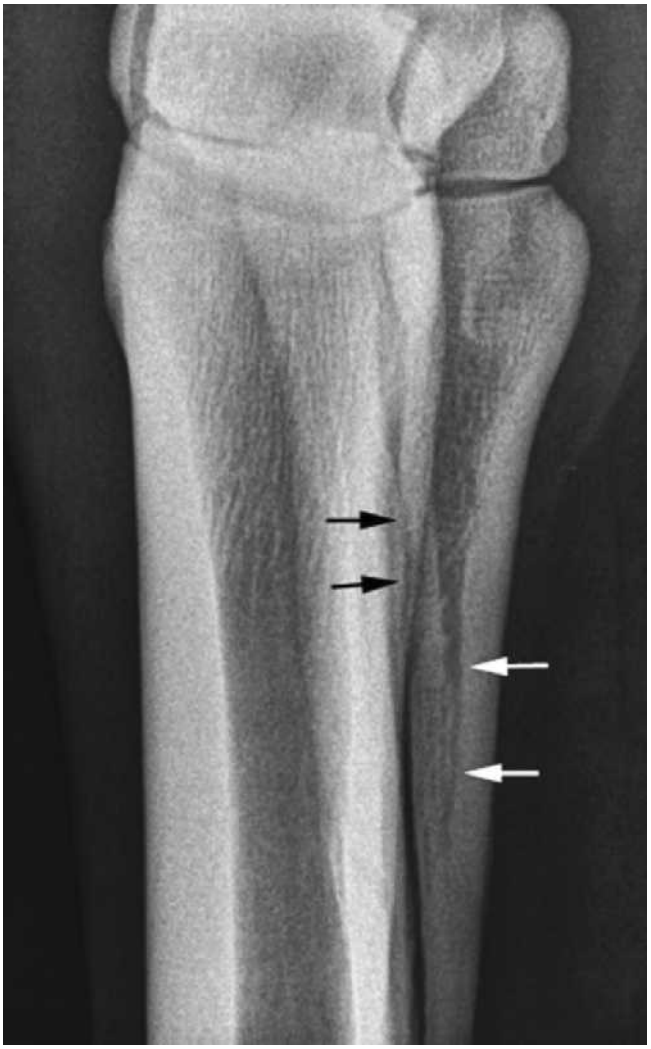


Figure 6.6 Palmarolateral-dorsomedial oblique image of a normal adult metacarpal region. Note the approximately vertical lucent line in the third metacarpal bone on the dorsal aspect of the second metacarpal bone which is the result of edge enhancement (a Mach line) (black arrows). There is a lucent line (white arrows) in the proximal one-third of the second metacarpal bone which represents a nutrient foramen.

(Figure 6w.9a) which occasionally has several radiolucent areas in the most proximal aspect. The second metacarpal bone is superimposed over the third. The proximal end or base of the fourth metacarpal bone articulates with the fourth carpal bone. The base of the fourth metatarsal bone articulates with the fourth tarsal bone (see Figures 6w.9b and 9.10a). It may have a prominent plantar protuberance. Occasionally this protuberance has a small bony spur on its plantar aspect (Figure 6w.9b) which in the authors' experience is usually of no significance, although it may reflect previous injury. The fourth metacarpal and metatarsal bones occasionally have a separate centre of ossification distally.

Downloaded From Vet-eBooks.com

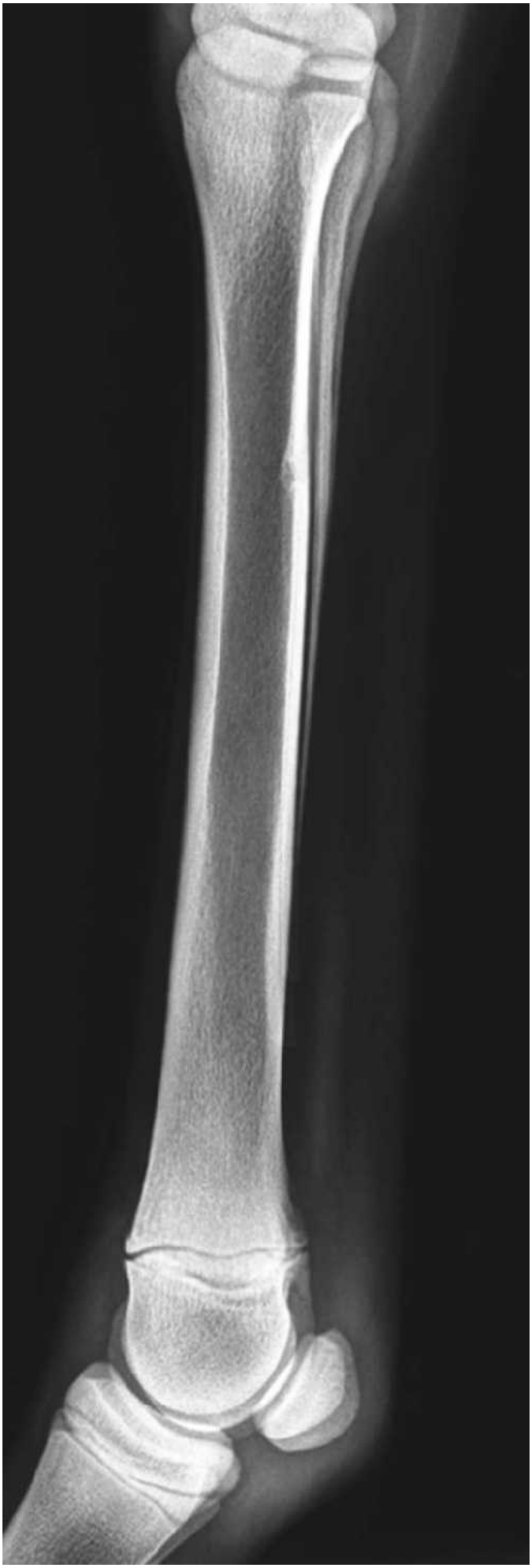


Figure 6.7 Lateromedial image of the metacarpal region of a normal foal of 1 day of age.

Downloaded From Vet-eBooks.com



Figure 6.8 Dorsolateral-palmaromedial oblique image of a normal adult metacarpal region. The fourth metacarpal bone is highlighted. A first carpal bone is present.



Figure 6.10 Dorsomedial-palmarolateral oblique image of a normal adult metacarpal region. The second metacarpal bone, which articulates with both the second and third carpal bones, is highlighted.

Downloaded From Vet-eBooks.com

The dorsomedial-palmarolateral oblique view (Figure 6.10) highlights the dorsolateral cortex of the third metacarpal bone and the second metacarpal bone. The second metacarpal bone articulates with the second and third carpal bones. The second metatarsal bone articulates with the first and second tarsal bones (these are usually fused). Occasionally there is a separate centre of ossification at the distal aspect of the second metacarpal and metatarsal bones.

The principal nutrient foramen of the third metacarpal bone may be projected as a lucent line across the second or fourth metacarpal bones and should not be confused with a fracture (Figure 6.11). The second and fourth metacarpal bones are relatively straight, but may curve away from the third metacarpal bone distally. There is considerable variation in their length and shape. In Finnhorses there may be thickening of the entire length of the bones, of no clinical significance. There is a variably sized and shaped enlargement on the distal ends of the second and fourth metacarpal bones (this is particularly marked, but clinically insignificant, in certain breed lines of the Irish Draught horse); the distal epiphyses are cartilaginous at birth and gradually ossify (Figure 6.7), but are separate from the rest of the bone until approximately 1–9 months of age.

The contour of the second and fourth metacarpal bones is clearly defined, but many horses have smoothly outlined exostoses reflecting previous trauma to the bone (Figure 6.12a). Sometimes there is irregular periosteal new bone with distinct margins; this must not be misinterpreted as an active periosteal reaction (compare Figure 6.12b with Figure 6.15).

In some horses there is a large exostosis on the proximolateral aspect of the third and fourth metatarsal bones (Figure 6.13). This is usually smoothly demarcated and of no clinical significance, despite usually being associated with intense focal increased radiopharmaceutical uptake. There may be associated mineralisation of the interosseous ligament between the third and fourth metatarsal bones.

With the correct obliquity of the x-ray beam, and provided that there is no mineralisation or ossification of the interosseous ligaments, a lucent space may be seen between the second and third, and fourth and third metacarpal bones. In some horses it may be necessary to obtain several views at slightly different angles in order to evaluate the entire interosseous space. Most adult horses have some mineralisation or ossification of the interosseous ligaments (Figure 6.14). Occasionally ossification is complete. There may be one or more ill-defined lucent zones in the base (head) of the second metacarpal bone. This is usually seen in association with the presence of a first carpal bone (see Figure 7.13b).

In some horses there is a lucent line in the proximal one-third of either or both of the second and fourth metacarpal bones. This extends distally from the medullary cavity and ends on the dorsal aspect of the bone (Figure 6.6); it represents a nutrient foramen and should not be misinterpreted as a fracture.

An old fracture of the 'button' of the distal end of the second or fourth metacarpal (metatarsal) bones may persist as a slightly displaced fragment with no surrounding osseous reaction. These are usually clinically insignificant.

Downloaded From Vet-eBooks.com



Figure 6.11 Dorsolateral-plantaromedial oblique image of a normal adult metatarsal region. Note the radiolucent line crossing the second metatarsal bone, a nutrient foramen. The interosseous space between the third and fourth metatarsal bones is uniformly radiolucent.

Downloaded From Vet-eBooks.com



Figure 6.12(a) Dorsomedial-palmarolateral oblique image of an adult metacarpal region. There is a smoothly outlined exostosis on the second metacarpal bone and some mineralisation in the interosseous space, of no clinical significance.



Figure 6.12(b) Dorsomedial-palmarolateral oblique image of an adult metacarpal region. The mid diaphysis of the second metacarpal bone is enlarged. There is irregular periosteal new bone with distinct margins in this region (compare with Figures 6.15a and 6.15b). Despite the irregularity the margin is distinct, which makes it likely that this change is inactive. There is also mineralisation in the interosseous space. These osseous abnormalities were not of current clinical significance.

Downloaded From Vet-eBooks.com



Figure 6.13 Dorsoplantar image of the proximal metatarsal region of a 9-year-old event horse. There is a smoothly marginated exostosis on the proximolateral aspect of the third metatarsal bone. The interior of the exostosis has a heterogeneous opacity. There is an ill-defined oblique radiolucent line in the cortex of the third metatarsal bone. This exostosis was cool and non-painful and not associated with lameness.

SIGNIFICANT RADIOLOGICAL ABNORMALITIES

Periostitis

Periostitis resulting from direct trauma to bone

Direct trauma to any of the metacarpal bones may result in inflammation of the periosteum and/or a subperiosteal haematoma and subsequent periosteal new bone. The smoothness of the margin and the opacity of the new bone help to determine the activity and age of the lesion. New bone is usually not detectable for at least 14 days and appears first as a slightly opaque area in the soft tissues adjacent to the metacarpal bone, with an irregular margin (Figures 6.15a and 6.15b). The new bone becomes progressively more opaque and smoother in outline as it is modelled (see Figures 6.12a and 6.12b). Trauma to the bone may alternatively be detected ultrasonographically as early as 5 days after the injury.

The second and fourth metacarpal bones seem particularly susceptible to production of very irregular new bone. Pillars of relatively opaque bone may be separated by more lucent bone. This palisade-like appearance, which may be due to invasion of the proliferative new bone by fibrous tissue, may persist when the lesion has become inactive (Figure 6.12b). The pattern of mineralisation can result in a lucent line, or lines, which traverse the periosteal reaction and may mimic a fracture (Figure 6.15b), although a primary fracture line may sometimes be present.

Downloaded From Vet-eBooks.com



Figure 6.14 Dorsomedial-palmarolateral oblique image of an adult metacarpal region. There is mineralisation between the third and second metacarpal bones of no clinical significance.

Provided that there is no further trauma to the bone, an active periosteal reaction usually becomes quiescent within 6–12 weeks. A horse with an active periosteal reaction usually resents pressure applied to the lesion but may not be lame. It is likely that the reaction will heal most quickly if the horse is confined to box rest.

Periostitis produced in response to micro-fractures

Sore shins or 'bucked shins' is a relatively common syndrome in racing Thoroughbreds and Quarter Horses, resulting in localised heat, pain and swelling and a variable degree of lameness.

Cortical modelling is an adaptive response to increased loading during normal exercise. During training of 2- and 3-year-old horses, cortical modelling is particularly intense and often creates focal areas of porosity in the cortex. Cyclic loading of the immature third metacarpal bone may ultimately result in

Downloaded From Vet-eBooks.com



Figure 6.15(a) Dorsolateral-palmaromedial oblique image of the mid metacarpal region of a 6-year-old event horse. There is soft tissue swelling overlying an ill-defined exostosis (arrows) on the abaxial aspect of the fourth metacarpal bone. There was focal pain on pressure over this area and mild lameness.



Figure 6.15(b) Dorsomedial-palmarolateral oblique image of the metacarpal region of an 8-year-old Warmblood with mild lameness evident only on a circle. There is soft-tissue swelling overlying a large generally well-defined old exostosis involving the diaphysis of the second metacarpal bone. Within the exostosis are relatively lucent lines. These are the result of new bone formation and should not be confused with fractures. On the distal palmar aspect of the exostosis there is less well defined active periosteal new bone (arrow).

Downloaded From Vet-eBooks.com

fatigue micro-fractures in the middle or distal thirds of the dorsal cortex, which are not detectable radiographically. They may also be seen occasionally in older horses that have not previously undergone training. Micro-fractures may result in only periosteal and endosteal reactions, and if the training programme is moderated a fracture may never be detected radiographically. If early clinical signs are overlooked and the horse is kept in training, an overt, radiographically detectable fracture may result. Alternatively acute fractures do occur without any preceding periosteal reaction.

When clinical signs are first recognised, high-quality radiographs are essential to identify radiographic abnormalities. Nuclear scintigraphy usually demonstrates focal increased radiopharmaceutical uptake. Intracortical fissures or indistinct lucent areas in the dorsal cortex are sometimes demonstrable, with or without localised periostitis and an endosteal reaction. Periostitis is not detectable using plain radiography until at least 2 weeks after the onset of the clinical signs.

Using high-quality radiographic technique and multiple oblique views it may be possible to detect small fractures in the dorsal cortex of the bone. Most fractures traverse distoproximally at an angle of approximately 30° to the long axis of the bone and end at the junction of the middle and inner one-thirds of the cortex (Figures 6.16a and 6.16b). Some fractures extend to form a complete semi-circle or 'saucer'; occasionally only the proximal half of the saucer can be seen. Multiple fractures sometimes occur. These may occur after new bone has been laid down on the dorsal cortex of the third metacarpal bone as a response to training; this immature bone may be susceptible to multifocal fractures if overloaded prematurely.

Vertical radiolucent lines may develop within the cortical bone of the diaphysis of the third metacarpal bone (Figure 6.17). It is postulated that these form as the result of fractures along the cement line between bone which had developed as a yearling and that which developed subsequently, because the bone is of different density and stiffness.

Rest results in resolution of clinical signs, but follow-up radiography or nuclear scintigraphy is important to monitor bone healing. Some fractures heal satisfactorily within 8–12 weeks and training can be resumed, but in some horses there appears to be minimal change in the radiographic appearance of the fracture and, in selected cases, surgical intervention may be necessary. In order to monitor healing it is very important to obtain identical radiographic views to those that initially demonstrated the lesion best.

Syndesmopathy between the second and third or fourth and third metacarpal bones (splints)

A syndesmosis is a slightly movable articulation where the contiguous bony surfaces are united by an interosseous ligament, e.g. the articulations between the second and third and fourth and third metacarpal bones. Synostosis means fusion of two bones. Focal or diffuse ossification of the interosseous ligament results in synostosis. Syndesmopathy refers to injury of the syndesmosis between the second and third and third and fourth metacarpal (metatarsal) bones and alteration in adjacent cortical or trabecular architecture (Figure 6w.18), with or without osseous spurs developing on the dorsal or palmar articular margins. If seen in association with focal increased radiopharmaceutical uptake there is reasonable evidence that the

Downloaded From Vet-eBooks.com



Figure 6.16(a) Lateromedial image of the metacarpal region of a 3-year-old Thoroughbred flat racehorse. There is an oblique radiolucent line in the dorsal cortex of the third metacarpal bone (arrows), a dorsal cortical stress fracture. There is subtle periosteal and endosteal new bone at the same level and overlying soft tissue swelling. Note also the smoothly marginated exostosis involving the diaphyseal region of the fourth metacarpal bone. See also Figure 6.16(b).



Figure 6.16(b) Dorsolateral-palmaromedial oblique image of the metacarpal region of the same limb as in Figure 6.16(a). In this view much more extensive periosteal new bone can be seen in the region of the incomplete dorsal cortical fracture of the third metacarpal bone.

Downloaded From Vet-eBooks.com

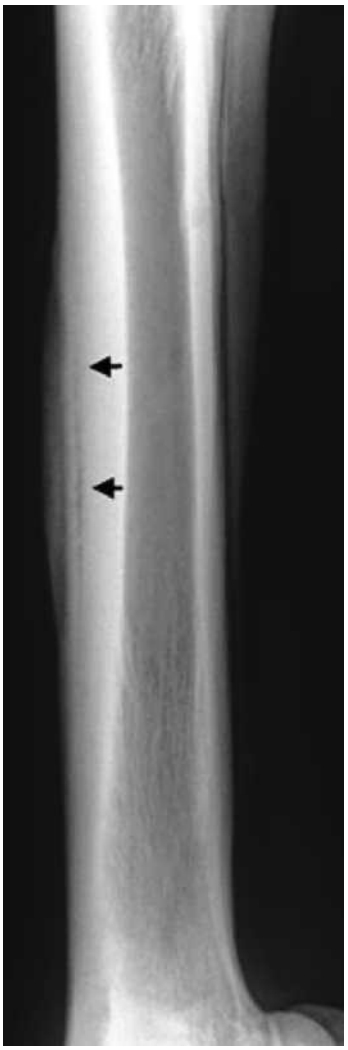


Figure 6.17 Lateral 15° dorsal-medial palmar oblique image of the mid metacarpal region of a 2-year-old Thoroughbred. There is smoothly outlined new bone on the dorsomedial aspect of the diaphysis of the third metacarpal bone. There is a vertical radiolucent line within the dorsal cortex of the third metacarpal bone (arrows). It is postulated that this is the result of fracture along the cement line between bone which had developed as a yearling and that which developed subsequently, because the bone is of different density and stiffness. Source: Reproduced with permission of Dr L. Bramlage.

lesion is active and associated with lameness. Ultrasonography may be more sensitive than radiography for identification of osseous modelling on the palmar aspect, but magnetic resonance imaging is probably superior for definitive diagnosis of proximal lesions present without palpable abnormalities. Injuries are seen most commonly involving the second and third metacarpal bones in the proximal one-third of the metacarpus. Syndesmopathy is often seen in association with ossification between the bones (synostosis) further distally.

When palpable new bone develops between the second and third or fourth and third metacarpal bones secondary to damage to the interosseous ligament, it is known colloquially as a 'splint'. Splints develop most frequently between the second and third metacarpal bones in the forelimb and the fourth and third metatarsal bones in the hindlimb. Several oblique views may be necessary in order to evaluate the interosseous space properly. This condition occurs most commonly in young horses when regular work commences, but is also seen in older horses. There may be associated lameness, deteriorating with work. Careful palpation reveals a localised area

Downloaded From Vet-eBooks.com

of pain. If the metacarpal region is offset laterally relative to the central axis of the antebrachium and carpus, or there is an angular limb deformity, the horse is particularly prone to the development of both ossification between the second and third metacarpal bones, and new bone on the medial aspect of the second metacarpal bone, as the bones model according to Wolff's law. This often develops without associated lameness. New bone formation may also occur suddenly in older horses without lameness.

In an early lesion there is some slightly opaque bone between the two metacarpal bones and cortical bone modelling may be detectable. With time the periosteal new bone becomes more opaque and will eventually look uniform in opacity. The amount of periosteal new bone produced is extremely variable and sometimes an active bony reaction may mimic a fracture with associated callus. It is not possible to differentiate radiographically between this condition and periostitis developing secondary to direct trauma. With rest the active bone reaction usually settles within 6 weeks, but can take several months. The new bone may model once it is no longer active. Lameness will recur if work is resumed while the periosteal reaction is still active.

Occasionally, if extensive new bone develops on the axial surface of the second or fourth metacarpal bones, this may result in associated suspensory ligament desmitis and adhesion formation. The significance of the new bone must be assessed in the light of clinical signs and ultrasonographic examination. Surgical treatment is usually necessary. Occasionally magnetic resonance imaging may also be helpful if the results of ultrasonography are equivocal.

An exostoses or 'splint' may also develop secondary to trauma to the second or fourth metacarpal bones, with or without the presence of a fracture and unassociated with the interosseous ligament. Axial progression may interfere with the suspensory ligament. Modelling often occurs with time and rest, but is sometimes incomplete and leaves a smoothly outlined osseous mass.

Exostoses on the proximolateral aspect of the third and fourth metatarsal bones are usually incidental findings (see 'Normal radiographic anatomy: its variations and incidental findings', above and Figure 6.13).

Endosteal reaction and entheseophyte formation in the area of attachment of the suspensory ligament

The suspensory ligament originates from the proximal palmar aspect of the third metacarpal bone. Tearing of the attachment may result in entheseophyte formation (periostitis), due to subperiosteal haematoma formation, or endosteal new bone formation (Figure 6w.19f). Radiographic examination may reveal a localised area of increased opacity in the proximal aspect of the bone with or without small patchy lucent zones. In the early stages this is seen only in high-quality dorsopalmar/dorsoplantar images (compare Figures 6.19c and d), and comparison with the contralateral limb is often helpful. Endosteal new bone is seen as a region of increased opacity of the palmar subcortical bone in a true lateromedial view (see below). Compare Figures 6.19a and b. The presence of radiological abnormalities associated with proximal suspensory desmopathy is seen more commonly in hindlimbs (Figures 6.19b and 6.19d and Figures 6w.19e and 6w.19f) than forelimbs and is usually a sign of chronicity. However, increased opacity of the proximal

Downloaded From Vet-eBooks.com



Figure 6.19(a) Lateromedial image of the proximal metatarsal region of a normal adult horse. Note the regular, linear orientation of the trabeculae and the definition between the cortical and medullary bone.



Figure 6.19(b) Lateromedial image of the proximal metatarsal region of a 6-year-old Thoroughbred event horse with chronic proximal suspensory desmopathy. There is endosteal new bone on the proximoplantar aspect of the third metatarsal bone (arrows). Note also the small osteophyte on the dorsoproximal aspect of the third metatarsal bone.

aspect of the third metatarsal bone may be seen as an incidental finding in dorsoplantar projections and is not necessarily synonymous with active desmopathy. In the forelimb the lesions predominantly involve the medial half of the third metacarpal bone, whereas in the hindlimb the lateral half of the third metatarsal bone is more frequently involved. In dorsopalmar views it is difficult to differentiate between endosteal and periosteal new bone; ultrasonography can be a more sensitive way of detecting entheseous new bone. If entheseophyte formation is extensive it may also be seen in a lateromedial image as an area of increased opacity superimposed over the second or fourth metacarpal bones. Computed tomography gives most accurate information about entheseous new bone.

Increased opacity seen in a dorsopalmar image may also be due to increased opacity of the trabeculae, which may be seen in the subcortical bone in a lateromedial view, i.e. endosteal new bone (Figure 6.19b). The trabeculae may be orientated more obliquely than usual. The suspensory ligament *per se* should be evaluated ultrasonographically. Nuclear scintigraphy may also be helpful to determine the degree of bony activity. In some horses injury appears to be principally entheseous, with little or no detectable abnormality of the suspensory ligament itself. There may be focal increased radiopharmaceutical uptake, or signal alterations in the third metacarpal bone at the ligament's origin seen on magnetic resonance images, but

Downloaded From Vet-eBooks.com



Figure 6.19(c) Dorsoplantar image of the proximal metatarsal region of a normal adult horse. Note the regular linear orientation of the trabeculae and the clear definition between the proximal subchondral bone plate and the medulla.



Figure 6.19(d) Dorsoplantar image of the proximal metatarsal region of a 6-year-old Thoroughbred event horse with chronic proximal suspensory desmopathy. There are generalised patchy areas of increased opacity in the proximal aspect of the third metatarsal bone which may reflect entheseous new bone. The apparent narrowing of the lateral aspect of the centrodistal joint space is an artefact.

no detectable radiographic abnormality. Severe trauma may result in an avulsion fracture of the origin of the suspensory ligament from the third metacarpal bone (see 'Metaphyseal and diaphyseal fractures' and Figure 6.31).

Longitudinal, incomplete fatigue (stress) fractures of the palmar cortex of the third metacarpal bone can result in increased opacity of the proximomedial aspect of the third metacarpal bone and a lucent vertical or oblique line or lines may be detectable (Figure 6.32). The opaque region may extend further distally compared with that associated with proximal suspensory desmitis and abnormalities are usually not detectable on a lateromedial projection. However, occasionally with an extensive fracture, periosteal callus will develop on the palmar aspect of the third metacarpal bone. These fractures are not related to suspensory ligament injury.

Focal increased opacity in the proximomedial aspect of the third metacarpal bone could represent an osseous spur. Such spurs have been verified using magnetic resonance imaging or computed tomography and are medial to and unrelated to the suspensory ligament. Their aetiology is unknown. Surgical removal has resulted in resolution of lameness.

Downloaded From Vet-eBooks.com

Periosteal new bone on the proximal third of the second or fourth metacarpal bones

Extensive palisading periosteal new bone involving the base (head) and proximal metaphyseal region of the second or fourth metacarpal bones can be seen in association with localised narrowing of the carpometacarpal joint (Figure 6.20). It is usually associated with chronic lameness (see Chapter 7, 'Degenerative joint disease').

Modelling of the second and fourth metacarpal bones in association with suspensory body or branch injury

The distal third of the second and fourth metacarpal bones have a close anatomical relationship with the suspensory body and branches. Changes may occur in the distal third of the second and fourth metacarpal bones in association with injury of the suspensory body or branches. These include change in shape with deviation away from the cortex of the third metacarpal bone (Figure 6w.21a), thickening of the bone, development of irregular margins, and a fracture at the junction of the middle and distal thirds of the bone or occasionally further distally (Figure 6w.21b).

The suspensory branches have a close anatomical relationship with the palmar recess of the metacarpophalangeal joint and with chronic injury there may be extensive synovial proliferation resulting in secondary supracondylar lysis of the third metacarpal bone.



Figure 6.20 Dorsolateral-palmaromedial oblique image of the proximal metacarpal region of an aged pleasure horse, with lameness associated with pain in this area. There is narrowing of the carpometacarpal joint medially (black arrow) and an ill-defined radiolucent area in the distal aspect of the second carpal bone. There is generalised increased opacity of the trabecular bone of the second carpal bone and the proximomedial aspect of the third metacarpal bone. There is irregular periosteal new bone on the proximomedial aspect of the third metacarpal bone (white arrow), with mild overlying soft tissue swelling. These abnormalities are typical of degenerative joint disease of the carpometacarpal joint.

Downloaded From Vet-eBooks.com

Exostoses on the palmar aspect of the distal half of the third metacarpal bone

Exostoses on the palmar (plantar) aspect of the third metacarpal (metatarsal) bone at the junction of the middle and distal one-thirds appear as linear radiopacities in the middle of the bone in a dorsopalmar (plantar) image (Figure 6w.22). If extensive the new bone extends beyond the palmar cortex of the third metacarpal bone and can also be seen in a lateromedial image. Exostoses may occur unilaterally or bilaterally and have been seen as incidental findings in some horses, but also associated with lameness. When lameness occurred it was thought to be associated with the result of impingement of the exostosis on the dorsal aspect of the suspensory ligament, verified by ultrasonography. It has been speculated that such exostoses develop because hyperextension of the metacarpophalangeal or metatarsophalangeal joint creates tension at the metacarpal or metatarsal attachment of the intersesamoidean ligament, which may result in partial tearing and the formation of an exostosis at the ligament's attachment on the third metacarpal or metatarsal bone. Hyperextension of the fetlock joint also causes distal and dorsal displacement of the proximal sesamoid bones, which induces tension and dorsal movement of the suspensory ligament with the potential for impingement of the exostosis on the suspensory ligament. Lameness has been described as resolving with either surgical or conservative management.

Infectious osteitis and osteomyelitis

The third metacarpal bone is only protected by a thin layer of soft tissues and is therefore susceptible to infection following severe skin wounds and trauma to the bone. An open fracture of any of the metacarpal bones may also result in infection. The thick dorsal cortex of the diaphysis of the third metacarpal bone may predispose it to sequestrum formation in its outer one-third, since trauma to the bone may deprive it of its periosteal blood supply and leave it dependent on medullary vessels traversing the cortex.

Radiographic signs of osteitis are not detectable until at least 7–14 days after the injury when subtle lucent areas may be seen in the cortex. These may be restricted to lucent lines parallel to the margin of the bone, in the outer one-third of the cortex, followed by the development of periosteal reaction and more diffuse areas of reduced opacity in the cortex (Figure 6.23a). Earlier diagnosis of infectious osteitis may be possible using ultrasonography. In some cases this initial appearance progresses to sequestrum formation; a central opaque piece of bone (the sequestrum) is surrounded by a lucent zone (purulent material or granulation tissue) which in turn is bordered by more radiopaque bone (the involucrum) (Figures 6.23b and 6.23c). Periostitis may develop proximal and distal to the sequestrum, but does not involve the sequestrum itself. Although antimicrobial therapy may control clinical signs, removal of the sequestrum is usually required for complete recovery.

Angular limb deformities originating from the diaphysis of the third metacarpal or metatarsal bone

An angular limb deformity originating from the diaphysis of the third metacarpal or metatarsal bone is a rare condition, which may be congenital. The abnormal limb angulation is noted clinically, but the site of deformity

Downloaded From Vet-eBooks.com



Figure 6.23(a) Dorsopalmar image of a metacarpal region of an 11-year-old Draught cross which had been kicked 1 month previously. There was a discharging wound on the medial aspect of the mid metacarpal region. Medial is to the left. There is soft tissue swelling overlying ill-defined periosteal new bone on the medial aspect of the diaphysis of the third metacarpal bone (arrows); a lucent line can be seen between this new bone and the third metacarpal bone and there are ill defined lucent areas in the cortex of the third metacarpal bones. This is early infectious osteitis.



Figure 6.23(b) Dorsolateral-palmaromedial oblique image of a metacarpal region of a 5-year-old crossbred horse which had been kicked 2 months previously. There is soft-tissue swelling overlying ill-defined periosteal new bone. In the cortex of the third metacarpal bone there is an oval-shaped radiolucent area with a central area of further reduced opacity, reflecting infection.

is confirmed radiologically. The limb deviation usually originates in the proximal one-third of the third metacarpal or metatarsal bone. There may be cortical thickening on the concave side of the bone. To correct the condition wedge osteotomy may be considered. A deformity of the distal aspect of the third metatarsal bone occurs occasionally, in which the bone describes a smooth 'bend', either laterally or medially. Treatment must be instituted as early as possible, using corrective trimming and shoe extensions. The limb may remodel adequately as it grows if sufficiently aggressive treatment is started early enough in life.

Downloaded From Vet-eBooks.com

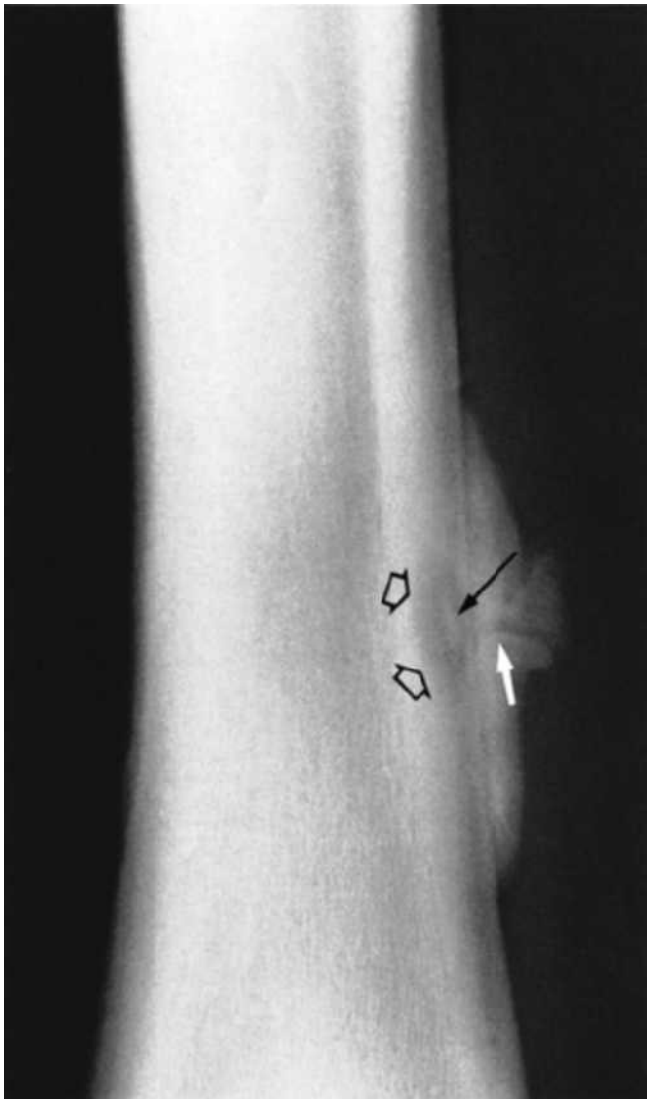


Figure 6.23(c) Dorsopalmar image of a metacarpal region. There is a sequestrum (filled black arrow) and involucrum (open arrows), and extensive periosteal new bone formation with a lucent cloaca (white arrow) and overlying soft-tissue swelling.

Physitis of the third metacarpal bone

Physitis (physeal dysplasia) of the distal physis of the third metacarpal bone may result in enlargement of the bone and an angular limb deformity of the metacarpophalangeal joint. Radiographically the metaphysis of the bone is broadened and asymmetrical. There is increased opacity of the metaphysis adjacent to the physis, which may be more irregular in appearance than normal, with narrow vertical radiolucent lines or conical areas representing retained cartilage cones. The cortices of the bone may be abnormally thick. The epiphysis may appear wedge shaped. Correction of the deviation using radical trimming and or shoeing of the foot may be successful, but it should be stressed that should surgical correction of the deviation may be needed, it should be performed before 8 weeks of age, despite the 'open' radiographic appearance of the physis.

Downloaded From Vet-eBooks.com

Mineralisation in the soft tissues

Dystrophic mineralisation may occur in the soft tissues, particularly in the suspensory ligament or the digital flexor tendons, as the result of trauma or injection of a medicament. This may or may not be of clinical significance. A thorough clinical appraisal of the structure involved and ultrasonographic examination are indicated. Dystrophic mineralisation seen in association with a solid soft-tissue mass unrelated to a specific anatomical structure is suggestive of a mast cell tumour (mastocytosis).

Hypertrophic osteopathy

Shifting limb lameness associated with variable oedematous swelling of a limb or limbs is the most common clinical feature of hypertrophic osteopathy (Marie's disease) (see 'Hypertrophic osteopathy' in Chapter 1). Careful palpation of the metaphyses and diaphyses of the bones may reveal unusual heat and tenderness. Radiologically the disease is typified by periosteal new bone, which often appears active and extends along the metaphyses and diaphyses (see Figure 1.19a). The third metacarpal and metatarsal bones are frequently involved. The periosteal reaction must be differentiated from other causes of periostitis and osteitis. Thoracic or abdominal opacities may or may not be detectable.

Enostosis-like lesions and panosteitis

Enostosis-like lesions have a characteristic radiological appearance: a focal area of increased opacity close to the nutrient foramen and contiguous with the endosteum, but with no cortical or periosteal reaction (Figure 6w.24a). This coincides with focal increased radiopharmaceutical uptake of variable intensity. In many horses these lesions appear to be incidental abnormalities, although they may be associated with lameness. Lesions may be restricted to a single bone or be present in several bones in lame and non-lame limbs. Acute, severe lameness has been seen in horses with lesions in the third metacarpal bone (Figure 6w.24b). Lameness usually resolves with rest and time, but may subsequently recur due to other lesions in either the same or another limb.

Panosteitis is a poorly understood condition, which may or may not be related to enostosis-like lesions. It is characterised by new bone on the endosteal surface of the metaphyseal and diaphyseal regions of the third metacarpal (metatarsal) bone (Figure 6w.25).

Fractures

Third metacarpal bone

FRACTURES OF THE DISTAL PHYSIS

Fractures of the distal physes of the third metacarpal and metatarsal bones in foals are quite common and usually have a Salter-Harris type II configuration (see 'Fractures' in Chapter 1). Internal fixation is probably the treatment of choice and, provided that the foal is not less than 8 weeks of age, the

Downloaded From Vet-eBooks.com

longitudinal growth of the bone should not be compromised. Immobilisation of the limb in a full-limb cast has been successful in some cases.

FATIGUE FRACTURES OF THE DORSAL CORTEX ('SAUCER' FRACTURES)

Fatigue fractures of the dorsal cortex have been discussed previously (see 'Periostitis in response to microfractures', above).

CONDYLAR FRACTURES

Fracture of either the medial or, more commonly, the lateral condyle is a common injury in racehorses (Thoroughbreds, Standardbreds and Quarter Horses) and elite endurance horses. If the fracture is complete there is usually distension of the metacarpophalangeal joint capsule, pain on flexion of the joint, and moderate to severe lameness. If the fracture is incomplete there may be no localising clinical signs and lameness may resolve temporarily following rest. The fractures either occur in the condylar groove (Figure 6.27), in the condyle adjacent to the sagittal ridge (Figure 6.26), or mid condyle (see Figure 6.28), and may be incomplete with minimal displacement or complete. Incomplete fractures may only involve the palmar cortex of the bone (unicortical fracture) and will be missed unless a dorsodistal-palmaroproximal (plantarodorsal) oblique (dorsopalmar/plantarodorsal [flexed]) image is acquired (Figure 6.28). Some bicortical fractures extend longitudinally through the diaphysis, in the same parasagittal plane or spiralling proximally (Figure 6.27). Many fractures are complete and 'break out' through the cortex approximately 5–8 cm proximal to the articular surface. Any fracture extending longer than 7.5 cm is likely to be complete. In both the forelimbs and the hindlimbs the lateral condyle is most commonly involved (Figure 6.26). Medial condylar fractures are more often incomplete and extend into the diaphysis, especially in hindlimbs.

If the fracture extends proximally and is incomplete it is very important to examine the entire metacarpal region. Fractures involving both the medial and lateral condyles occasionally occur. A concurrent parasagittal fracture of a proximal sesamoid bone may also be seen, usually in the lateral proximal sesamoid bone associated with a lateral condylar fracture. This is a very poor prognostic indicator. All the standard views should be used, and extra oblique views at 5° increments may be necessary to establish whether the metacarpal fracture extends into the diaphysis. Even with radiographs of excellent quality it may not be possible to identify all the components of the fracture. A dorsodistal-palmaroproximal oblique view to examine the palmar articular surface is important to identify comminution, which cannot be detected in standard views. The proximal sesamoid bones should also be inspected carefully. Computed tomography or magnetic resonance imaging may give more information than radiography. Some incomplete, non-displaced fractures are extremely difficult to detect radiologically in the acute stage, and nuclear scintigraphy may be useful to confirm the results of trauma to bone. Follow-up radiographs obtained after 7–10 days may demonstrate the fracture. Simple, non-displaced fractures may be successfully treated by lag screw fixation or, in selected cases, immobilisation in a cast and box rest. Displaced fractures require reduction and internal fixation. The presence of Y-shaped fragments at the articular surface (Figure 6.28) is

Downloaded From Vet-eBooks.com



Figure 6.26 Flexed dorsopalmar image of the metacarpophalangeal joint of a 3-year-old Thoroughbred flat racehorse. Medial is to the left. There is an incomplete lateral condylar fracture of the third metacarpal bone (arrows). The fracture could not be seen in other views. Ideally a dorsodistal-palmaroproximal oblique view is also required to evaluate better the articular surface to establish whether or not there is comminution.



Figure 6.27 Dorsopalmar image of a metacarpal region of a 10-year-old Thoroughbred, acquired after a fall. Lateral is to the right. There is an incomplete lateral condylar fracture of the third metacarpal bone which spirals proximally in the diaphysis. The two radiolucent lines represent the fracture passing through the dorsal and palmar cortices of the bone. There is mild soft tissue swelling on the distal lateral aspect of the metacarpal region.

Downloaded From Vet-eBooks.com



Figure 6.28 Dorsodistal-palmaroproximal (extended) oblique image of the metacarpophalangeal joint of a 5-year-old Thoroughbred racehorse with acute onset forelimb lameness of 2 weeks' duration. Lateral is to the right. There is a fracture of the lateral condyle of the third metacarpal bone. Note the Y-shaped comminution (arrows) at the articular surface. This is not visible in standard projections.

associated with a poorer prognosis. Long-term persistence of a radiologically detectable lucent fracture line is associated with reduced performance compared with horses in which the fracture line disappears.

METAPHYSEAL AND DIAPHYSEAL FRACTURES

Incomplete transverse fractures through the palmar or dorsal aspect of the distal diaphysis or metaphysis occur occasionally and may be bilateral (Figures 1.23 and 6.29a–d). They are associated with moderate to severe lameness and pain can be induced by applying pressure on the palmar or dorsal cortex. These fractures, which are usually incomplete, are best seen in lateromedial and oblique projections. Usually a lucent line traverses the bone horizontally from either the palmar or the dorsal cortex. Within 7–10 days some callus may be identified at the site where the fracture passes through the cortex. In some horses, periosteal callus develops before a radiolucent fracture line is detectable, and paradoxically a line of increased opacity may be seen traversing the third metacarpal bone before a radiolucent line is seen. With extensive periosteal callus the distal aspect of the second or fourth metacarpal bones may become distorted in shape. These fractures heal satisfactorily with rest. Extensive periosteal callus will model with time and reduce remarkably in size.

Downloaded From Vet-eBooks.com



Figure 6.29(a) Dorsolateral-palmaromedial oblique image of the distal metacarpal region of a 4-year-old polo pony with acute onset of moderate lameness of 2 weeks' duration and considerable swelling in the distal metacarpal and fetlock regions, but no joint effusion. There is extensive periosteal new bone on the palmarolateral-distal diaphyseal and proximal metaphyseal regions of the third metacarpal bone (white arrows). Note also the horizontal line of increased opacity traversing the third metacarpal bone (black arrows). This was an incomplete horizontal fracture of the palmar aspect of the third metacarpal bone. The distal aspect of the fourth metacarpal bone is distorted because of the soft-tissue swelling. Compare with Figures 6.29(b–d).



Figure 6.29(b) Dorsolateral-palmaromedial oblique image of the same limb as in Figure 6.29(a), obtained 5 weeks later. There is very well consolidated callus and a more obvious radiolucent line traversing the metaphyseal region of the third metacarpal bone. There is slight modelling of the distorted distal aspect of the fourth metacarpal bone.

Fractures of the diaphysis of the third metacarpal bone usually occur in transverse, spiral or comminuted configurations and are often compound. Clinical signs include severe lameness, readily detectable crepitus and possibly swelling of the fetlock joint, but in some cases non-displaced fractures may be very difficult to detect clinically. Radiography is used to confirm the orientation of the fractures. Many oblique views may be needed to follow the complete course of the fracture(s). The radiographs should be inspected carefully to establish whether involvement of the nutrient foramen has occurred, because this will adversely influence the prognosis. Internal fixation using dynamic compression plates and lag screws may result in complete recovery.

Downloaded From Vet-eBooks.com



Figure 6.29(c) Dorsolateral-palmaromedial oblique image of the same limb as Figures 6.29(a and b), obtained 4½ months after the onset of lameness. There has been further modelling of the callus. An ill-defined horizontal radiopaque line is seen in the metaphyseal region of the third metacarpal bone.



Figure 6.29(d) Dorsolateral-palmaromedial oblique image of the same limb as Figures 6.29(a–c), 13 months after initial injury. There has been remarkable modelling of the callus and the distal aspect of the fourth metacarpal bone. A faint linear horizontal radiopaque line persists in the third metacarpal bone at the fracture site.

Mid diaphyseal incomplete longitudinal fractures of the palmar cortex of the third metacarpal bone sometimes occur in sports horses. They can be difficult to identify radiologically in the acute stage. However, periosteal callus results in a linear area of increased opacity during healing (Figure 6w.30). Periosteal callus may also be detected ultrasonographically. Nuclear scintigraphy may be helpful for fracture identification in the acute stage. These injuries have a good prognosis.

Incomplete oblique sagittal dorsal cortical fractures occur occasionally in young Thoroughbred racehorses. These fractures are orientated in a proximolateral-distomedial direction, within the dorsal cortex, at an angle of 20–30° to the long axis of the bone. They are best identified in palmarodorsal views.

Avulsion fractures of the origin of the suspensory ligament from the palmar cortex of the third metacarpal bone cause a variable degree of lameness that may be relieved by subcarpal local analgesia. Radiographically, in a dorsopalmar image, these fractures are identified as lucent crescent-shaped lesions in the metaphysis, or as a 'punched-out' radiopacity (Figure 6.31). In a lateromedial or a flexed lateromedial projection they are sometimes seen as separate bone

Downloaded From Vet-eBooks.com



Figure 6.31 Dorsopalmar image of a metacarpal region of a 6-year-old steeplechaser with sudden onset of lameness 12 days previously. Lameness was alleviated by subcarpal analgesia. There is a curved lucent line in the third metacarpal bone (arrow) which represents an incomplete avulsion fracture of the origin of the suspensory ligament. The horse was treated conservatively and made a complete recovery.

fragments on the palmar aspect. They occur in both the forelimb and the hindlimb. Ultrasonography may be more sensitive in identifying some small avulsed fragments and is helpful to determine the presence of concurrent suspensory desmitis. Lameness usually resolves satisfactorily with rest, although in racing trotters the prognosis with rest alone is less favourable and surgery may be required.

Incomplete longitudinal stress fractures of the palmar cortex of the third metacarpal bone occur in racehorses and sports horses. They may occur unilaterally or bilaterally. Lameness is usually sudden in onset, and often there are no localising clinical signs (Figure 1W.11a). These fractures occur medially in the proximal one-third of the bone. They are evident radiographically in a dorsopalmar image as vertical or slightly obliquely orientated lucent lines (the fracture seen 'end-on') in the metaphyseal region, sometimes extending distally into the diaphysis, usually with surrounding increased opacity of the trabecular bone (Figure 6.32). Sometimes no fracture line is detectable, only diffuse increased opacity. This is particularly so in the less lame limb of a bilaterally lame horse. Development of increased opacity, the result of micro-fractures, may precede the onset of lameness.

Downloaded From Vet-eBooks.com



Figure 6.32 Dorsopalmar image of a metacarpal region of a 5-year-old hurdler with recurrent lameness of several weeks' duration. Lameness was alleviated by subcarpal analgesia. There is an ill-defined approximately vertical lucent line (arrows) in the medial half of the third metacarpal bone with surrounding increased opacity of the trabecular bone. This is an incomplete palmar cortical fatigue or stress fracture of the third metacarpal bone. The horse was treated conservatively and made a complete recovery.

Less commonly the fracture is seen only in an oblique view, although increased opacity is seen on a dorsopalmar projection. Increased opacity should be differentiated from that associated with chronic proximal suspensory desmitis (see 'Endosteal reaction and entheseophyte formation in the area of attachment of the suspensory ligament', above). Nuclear scintigraphy enables earlier detection of these fractures and may also aid interpretation of subtle alterations in the trabecular pattern of the bone. It also permits detection of some fractures that never become radiologically apparent. Lameness usually resolves satisfactorily with rest (3 months).

Articular fractures of the dorsoproximal medial aspect of the third metacarpal bone have been identified in Standardbred racehorses (pacers). These fractures are best identified in a dorsolateral-palmaromedial projection. Satisfactory healing usually occurs with conservative management.

COMPRESSION FRACTURE OF THE DISTAL THIRD METACARPAL BONE PHYSIS

A compression fracture of the distal third metacarpal bone physis has to date only been documented in elite endurance horses and may occur unilaterally or bilaterally. It is characterised radiologically by increased opacity of the physis, and a slight step at the lateral margin with or without periosteal callus (Figure 6.33). Dorsopalmar radiographic images are most useful for its identification.

Downloaded From Vet-eBooks.com



Figure 6.33 Dorsopalmar image of the distal aspect of the metacarpal region of an 8-year-old Arab endurance horse. There is an irregular radiopaque line in the distal aspect of the third metacarpal bone, which crossed from the medial to lateral cortices. This represents a transverse compression fracture of the distal aspect of the third metacarpal bone. Source: Reproduced with permission of Dr M. Misheff.



Figure 6.34 Lateral 10° plantar-dorsomedial oblique image of the hock and proximal metatarsal region of a 2-year-old Thoroughbred flat racehorse. There is an incomplete articular stress fracture of the dorsoproximal aspect of the third metatarsal bone (black arrows). There is extensive active-appearing periosteal new bone on the dorsoproximal aspect of the third metatarsal bone (white arrows) and a large periarticular osteophyte.

Third metatarsal bone

Incomplete articular fractures of the dorsoproximal aspect of the third metatarsal bone have been seen in association with osteophyte formation on the dorsal aspect of the tarsometatarsal joint in young Thoroughbred racehorses and occasionally in older performance horses. These fractures are difficult to identify radiologically unless the x-ray beam passes through the fracture plane. They are usually best seen in a projection that superimposes the lateral and medial trochlea tali. Similar complete fractures have been identified in Standardbred racehorses. Lameness is moderate but acute in onset, and is alleviated either by intra-articular analgesia of the tarsometatarsal joint or by perineural analgesia of the fibular and tibial nerves. Nuclear scintigraphy may be useful to focus attention on the proximal metatarsal region. In both Thoroughbreds and Standardbreds there is frequently pre-existing periarticular new bone formation on the dorsoproximal aspect of the third metatarsal bone (Figure 6.34). Abnormal bone may predispose to fracture. The prognosis for return to full athletic function without recurrent lameness is guarded. Although the fracture may heal, there is often further development of periarticular new bone or degenerative changes within the tarsometatarsal joint.

Downloaded From Vet-eBooks.com

Second and fourth metacarpal/metatarsal bones

Fractures involving the proximal half of the second and fourth metacarpal bones are usually the result of external trauma and may be comminuted. There is a risk of secondary infection, especially if the fracture is open. Ultrasonography may be useful for assessment. Surgical stabilisation may be required, since weight is transmitted through the second and fourth metacarpal bones. Surgical stabilisation may also be needed if there is tearing of the collateral ligaments of the carpometacarpal joint. The carpal bones should be inspected for evidence of a concurrent fracture, which will adversely influence the prognosis (see also Chapter 7, 'Carpal fractures'). However, fractures



Figure 6.35(a) Dorsolateral-plantaromedial oblique image of the proximal metatarsal region of a 7-year-old showjumper that had been kicked 8 hours previously. There is a comminuted non-displaced fracture of the fourth metatarsal bone. There is overlying soft-tissue swelling and a radiolucent line extends from the skin surface to the bone representing gas in an open wound. The horse was treated conservatively and made an excellent recovery.



Figure 6.35(b) Dorsomedial-plantarolateral oblique image of the proximal metatarsal region of a Thoroughbred gelding, kicked 5 weeks previously. There was mild lameness and localised soft-tissue swelling over the second metatarsal bone. There is a healing fracture of the proximal aspect of the second metatarsal bone.

Downloaded From Vet-eBooks.com

of the proximal third of the second or fourth metatarsal bones can usually be treated conservatively, with complete success (Figure 6.35a and 6.35b).

A fracture at the junction between the middle and distal thirds of the second or fourth metacarpal bones is often seen in association with suspensory desmitis, but may be the result of external trauma. The fracture may not be detectable clinically without radiographic examination, especially if there is widespread swelling. The suspensory ligament should be carefully assessed ultrasonographically and the proximal sesamoid bones radiographed if indicated. If the fracture is displaced (Figure 6.36a), a non-union may result. The distal fracture fragment often does not cause a problem if left *in situ*, but may be removed surgically. The majority of fractures that are treated conservatively do heal within 2 months (Figure 6.36b), although there may be considerable callus formation (Figure 6.36c) and small lucent defects may persist. The callus models and often reduces in size, but some enlargement of the bone persists. Simple fractures of the second and fourth metacarpal (metatarsal) bones have a good prognosis, but associated suspensory ligament desmitis warrants a more guarded prognosis. Surgical removal of the distal aspect of the affected bone from a site proximal to the fracture may be indicated if there is a malunion or adhesion to the suspensory ligament.

Figure 6.37 summarises common fracture sites in the metacarpal and the metatarsal regions.

Tumours

Neoplastic lesions in the metacarpal or metatarsal regions are rare. A benign fibro-osseous tumour developing from the second or fourth metacarpal bones has been described, characterised by an expansile osseous mass of heterogeneous opacity. Dystrophic mineralisation seen in association with a solid soft tissue mass unrelated to a specific anatomical structure is suggestive of a mast cell tumour (mastocytosis).

Additional figures

The book companion website at www.clinical-radiology-horse.com includes additional figures that are not included in the printed book or e-book formats. Please see '**About the Companion Website**' at the start of the book for details on how to access the website. These figures are prefixed with the letter 'w' in the printed book, e.g. Figures 1w.4c–f.

Downloaded From Vet-eBooks.com



Figure 6.36(a) Dorsolateral-plantaromedial oblique image of a metatarsal region. The horse had sustained a wound on the plantarolateral aspect of the metatarsal region 4 months previously. Radiographs acquired 6 days later revealed a displaced fracture of the distal aspect of the fourth metatarsal bone. There is mild soft-tissue swelling overlying an old displaced non-union fracture of the fourth metatarsal bone.



Figure 6.36(b) Dorsomedial-palmarolateral oblique image of a metacarpal region. There is a healed fracture of the distal aspect of the second metacarpal bone. Note also the rather curved configuration of the bone, suggestive of possible adhesions with adjacent soft tissues.

Downloaded From Vet-eBooks.com



Figure 6.36(c) Dorsomedial-palmarolateral oblique image of a metacarpal region. There is considerable modelling of the distal end of the second metacarpal bone, the result of a previous fracture and excessive callus formation. Note also the mineralisation proximal to the proximal sesamoid bones reflecting associated suspensory desmitis.

Downloaded From Vet-eBooks.com

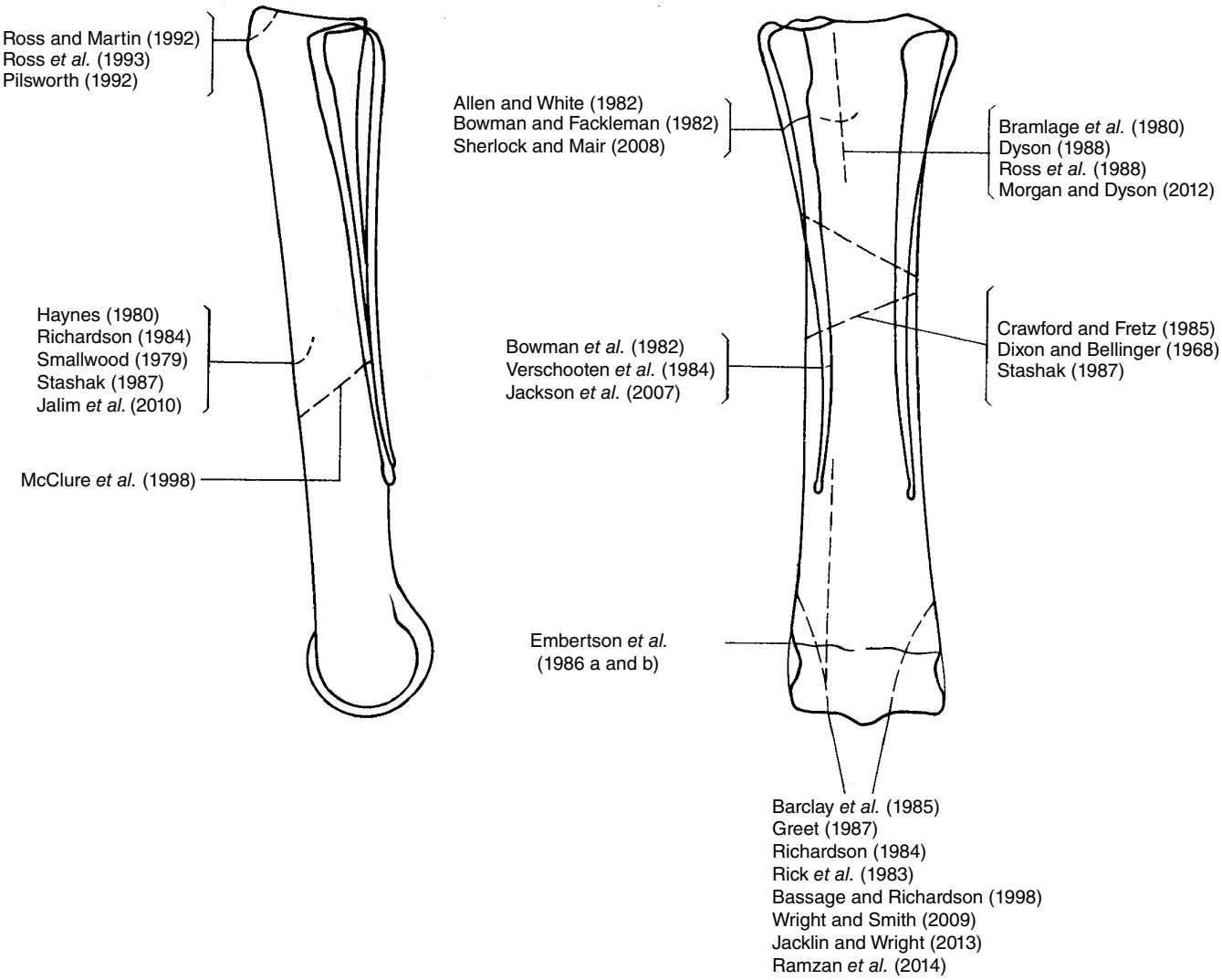


Figure 6.37 Common fracture sites in the metacarpal and metatarsal regions, and recommended references (see 'Further reading').

FURTHER READING

Allen, D., White, N. (1982) Management of proximal splint fractures and exostoses in the horse. *Proc. Am. Ass. Equine Pract.* **28**, 89–95

Ahern, B., Boston, R., Ross, M. (2010) Enostosis-like lesions in 79 horses. *Proc. Am. Ass. Equine Pract.* **56**, 392

Barclay, W., Foerner, J., Phillips, T. (1985) Axial sesamoid injuries associated with lateral condylar fractures in horses. *J. Am. Vet. Med. Ass.* **186**, 278–279

Bassage, L., Richardson, D. (1998) Longitudinal fractures of the condyles of the third metacarpal and metatarsal bones in racehorses: 224 cases (1986–1995). *J. Am. Vet. Med. Ass.* **212**, 1757–1764

Bassage, L., Ross, M. (1998) Enostosis-like lesions in the long bones of 10 horses: scintigraphic and radiographic features. *Equine Vet. J.* **30**, 35–42

Baxter, G., Doron, R., Allen, D. (1992) Complete excision of a fractured fourth metacarpal bone in eight horses. *Vet. Surg.* **21**, 273–278

Bertoni, l., Forresu, D., Coudry, V., et al. (2012) Exostoses on the palmar or plantar aspect of the diaphysis of the third metacarpal or metatarsal bone in horses: 16 cases (2001–2010). *J. Am. Vet. Med. Ass.* **240**, 740–747

Bischofberger, A., Furst, A., Auer, J., et al. (2009) Surgical management of complete diaphyseal third metacarpal and metatarsal bone fractures: clinical outcome in 10 mature horses and 11 foals. *Equine Vet. J.* **41**, 465–473

Booth, L. (1998) Superficial septic osteitis and sequestrum formation in the horse. *Equine Vet. Educ.* **10**, 233–237

Bowman, K., Fackleman, G. (1982) Surgical treatment of complicated fractures of the splint bones in horses. *Vet. Surg.* **11**, 121–124

Downloaded From Vet-eBooks.com

Bowman, K., Evans, L., Herring, M. (1982) Evaluation of surgical removal of fractured distal splint bones in the horse. *Vet. Surg.* **11**, 116–120

Bowman, K., Sweeney, C., Tate, L. (1987) Compression plating of a medial condylar fracture of the third metatarsal bone in a Thoroughbred filly. *J. Am. Vet. Med. Ass.* **190**, 305–307

Bramlage, L., Gabel, A., Hackett, R. (1980) Avulsion fractures of the origin of the suspensory ligament in the horse. *J. Am. Vet. Med. Ass.* **176**, 1004–1010

Bramlage, L. (2013) Response of bone necessitated by high-speed exercise. *Proc. Amer. Assoc. Equine Pract.*, **59**, 412–422.

Caron, J., Barber, S., Doige, C., Pharr, J. (1987) The radiographic and histologic appearance of controlled surgical manipulation of the equine periosteum. *Vet. Surg.* **16**, 13–20

Cole, R., Chesen, B., Pool, R., Watkins, J. (2007) Imaging diagnosis – mast cell tumour. *Vet. Radiol. Ultrasound* **48**, 32–34

Coudry, V., Denoix, J.-M., Didierlaurent, D. et al. (2008) Use of magnetic resonance imaging to diagnose the cause of proximal metacarpal pain in a standardbred trotter. *Vet. Rec.* **162**, 790–791

Dixon, R., Bellinger, C. (1968) Fissure fractures of the equine metacarpus and metatarsus. *J. Am. Vet. Med. Ass.* **153**, 1289–1291

Dyson, S. (1988) Some observations on lameness associated with the proximal metacarpal region in the horse. *Equine Vet. J. Suppl.* **6**, 43–52

Dyson, S. (1991) Proximal suspensory desmitis: clinical, radiographic and ultrasonographic features. *Equine Vet. J.* **23**, 25–31

Dyson, S. (1994) Proximal desmitis in the hindlimb: 42 cases. *Br. Vet. J.* **150**, 279–291

Dyson, S. (2003) Proximal metacarpal and metatarsal pain: a diagnostic challenge. *Equine Vet. Educ.* **15**, 134–138

Dyson, S. (2011) The enigma of enostosis-like lesions in the horse. *Vet. Rec.* **168**, 324–325

Embertson, R., Bramlage, L., Gabel, A. (1986a) Physeal fractures in the horse: Management and outcome. *Vet. Surg.* **15**, 230–236

Embertson, R., Bramlage, L., Herring, D., Gabel, A. (1986b) Physeal fractures in the horse: classification and incidence. *Vet. Surg.* **15**, 223–229

Enright, K., Tobin, E., Katz, L. (2011) A review of 14 cases of hypertrophic osteopathy (Marie's disease) in horses in the Republic of Ireland. *Equine Vet. Educ.* **23**, 224–230

Fairburn, A., Dyson, S., Murray, R. (2010) Clinical significance of osseous spurs on the dorsoproximal aspect of the third metatarsal bone. *Equine Vet. J.* **47**, 591–599

Greet, T. (1987) Condylar fractures of the cannon bone with axial sesamoid fracture in 3 horses. *Vet. Rec.* **120**, 223–225

Hornhof, W., O'Brien, T. (1980) Radiographic evaluation of the palmar aspect of the equine metacarpal condyles: a new projection. *Vet. Radiol.* **21**, 161–167

Jacklin, B, Wright, I. (2013) Frequency distribution of 174 fractures of the distal condyles of the third metacarpal and metatarsal bones in 167 Thoroughbred racehorses (1999–2009). *Equine Vet. J.* **44**, 707–713

Jackson, N., Furst, A., Hassig, M., Auer, J. (2007) Splint bone fractures in the horse: a retrospective study 1992–2001. *Equine Vet. Educ.* **19**, 324–335

Jalim, S., McIlwraith, C., W., Goodman, N., et al. (2010) Lag screw fixation of dorsal cortical stress fractures of the third metacarpal bone in 116 racehorses. *Equine Vet. J.* **42**, 586–590

Jensen, P., Gaughan, E., Lillich, J., Bryant, J. (2004) Segmental ostectomy of the second and fourth metacarpal and metatarsal bones in horses: 17 cases (1993–2002). *J. Am. Vet. Med. Ass.* **224**, 271–274

Kawcak, C., Bramlage, L., Embertson, D. (1995) Diagnosis and management of incomplete fracture of the distal palmar aspect of the third metacarpal bone in five horses. *J. Am. Vet. Med. Ass.* **206**, 335–337

Launois, M., Vandeweerd, J., Perrin, R., et al. (2009) Use of computed tomography to diagnose new bone formation associated with desmitis of the proximal aspect of the suspensory ligament in third metacarpal or third metatarsal bones of three horses. *J. Am. Vet. Med. Ass.* **234**, 514–518

Launois, T., Desbrosse, F., Perrin, R. (2003) Percutaneous osteostixis as treatment of the palmar/plantar third metacarpal/metatarsal cortex at the origin of the suspensory ligament in 29 horses. *Equine Vet. Educ.* **15**, 126–138

Lloyd, K., Koblik, P., Ragle, C., Wheat, J., Lakritz, J. (1988) Incomplete palmar fractures of the proximal extremity of the third metacarpal bone in the horse: ten cases (1981–1986). *J. Am. Vet. Med. Ass.* **192**(6), 798–803

Madron, M., McClure, S., Yaeger, M. (2013) Fibro-osseous tumour of the second metacarpal bone in a Thoroughbred filly. *Equine Vet. Educ.* **25**, 231–234

Mair, T., Tucker, R. (2004) Hypertrophic osteopathy (Marie's disease) in horses. *Equine Vet. Educ.* **16**, 308–311

Mair, T., Krudewig, C. (2008) Mast cell tumours (mastocytosis) in the horse: a review of the literature and report of 11 cases. *Equine Vet. Educ.* **20**, 177–182

McClure, S., Watkins, J., Glickman, N., et al. (1998) Complete fracture of the third metacarpal or metatarsal bone in horses: 25 cases (1980–1986). *J. Am. Vet. Med. Ass.* **213**, 847–850

Moens, Y., Verschooten, F., De Moor, A., Wouters, L. (1980) Bone sequestration as a consequence of limb wounds in the horse. *Vet. Radiol.* **21**, 40–44

Momiya, N., Tagami, M., Tsunoda, N., Taniyama, H. (1999) Aneurysmal bone cyst in a colt. *Equine Vet. Educ.* **11**, 243–246

Morgan, R., Dyson, S. (2012) Incomplete longitudinal fractures and fatigue injury of the proximopalmar medial aspect of the third metacarpal bone in 55 horses. *Equine Vet. J.* **44**, 64–70

Nagy, A., Dyson, S. (2012) Magnetic resonance imaging findings in the carpus and proximal metacarpal region of 50 lame horses. *Equine Vet. J.* **44**, 163–168

Downloaded From Vet-eBooks.com

O'Neill, H., Bladon, B. (2011) Retrospective study of scintigraphic and radiological findings in 21 cases of enostosis-like lesions in horses. *Vet. Rec.* **168**, 326

O'Sullivan, C., Lumsden, J. (2002) Distal third metacarpal bone palmar cortical stress fractures in four Thoroughbred racehorses. *Equine Vet. Educ.* **14**, 70–73

Pieber, K., Kuebber-Heiss, A., Kuebber, P., et al. (2010) Fibro-osseous tumour of the fourth metacarpal bone in a horse: clinical, radiographic and long-term post operative findings. *Equine Vet. Educ.* **22**, 62–65

Pilsworth, R. (1992) Incomplete fracture of the dorsal aspect of the proximal cortex of the third metatarsal bone as a cause of hindlimb lameness in the racing Thoroughbred: a review of 3 cases. *Equine Vet. J.* **24**, 147–150

Pilsworth, R., Hopes, R., Greet, T. (1988) Use of a flexed dorsopalmar (plantar) projection of the fetlock joint to demonstrate lesions of the distal third metacarpal (tarsal) bone in the horse. *Vet. Rec.* **122**, 332–333

Pinchbeck, G., Kriz, N. (2001) Two cases of incomplete longitudinal fracture of the proximopalmar aspect of the third metacarpal bone. *Equine Vet. Educ.* **13**, 187–194

Ramzan, P. (2002) Enostosis-like lesions: 12 cases. *Equine Vet. Educ.* **14**, 143–148

Ramzan, P. (2009) Transverse stress fractures of the distal diaphysis of the third metacarpus in six Thoroughbred racehorses. *Equine Vet. J.* **41**, 602–605

Ramzan, P., Palmer, L., Powell, S. (2014) Unicortical condylar fracture of the Thoroughbred fetlock: 45 cases (2006–2013). Equine Vet. J. doi: 10:1111/evj.12349

Richardson, D. (1984) Dorsal cortical fractures of the equine metacarpus. *Comp. Cont. Educ.* **6**, S248–254

Richardson, D. (1984) Medial condylar fractures of the third metatarsal bone in horses. *J. Am. Vet. Med. Ass.* **185**, 761–765

Rick, M., O'Brien, T., Pool, R., Meagher, D. (1983) Condylar fractures of the third metacarpal bone and third metatarsal bone in 75 horses: radiographic features, treatments and outcome. *J. Am. Vet. Med. Ass.* **183**, 287–296

Rose, R. (1978) Surgical treatment of osteomyelitis in the metacarpal and metatarsal bones of the horse. *Vet. Rec.* **102**, 498–500

Ross, M., Martin, B. (1992) Dorsomedial articular fracture of the proximal aspect of the third metacarpal bone in Standardbred racehorses: seven cases (1978–1990). *J. Am. Vet. Med. Ass.* **201**, 332–335

Ross, M., Ford, T., Orsini, P. (1988) Incomplete longitudinal fracture of the proximal palmar cortex of the third metacarpal bone in horses. *Vet. Surg.* **17**, 82–86

Ross, M., Sponseller, M., Gill, H., Moyer, W. (1993) Articular fracture of the dorsoproximolateral aspect of the third metatarsal bone in five Standardbred racehorses. *J. Am. Vet. Med. Ass.* **203**, 698–700

Russell, T., Maclean, A. (2006) Standing surgical repair of propagating metacarpal and metatarsal condylar fractures in racehorses. *Equine Vet. J.* **38**, 423–427

Sammi, V., O'Brien, T., Stannard, A. (1997) Radiographic features of mastocytosis in the equine limb. *Equine Vet. J.* **29**, 63–66

Sampson, S., Tucker, R. (2007) Magnetic resonance imaging of the proximal metacarpal and metatarsal regions. *Clin. Techniq. Equine Pract.*, **6**, 78–85

Sherlock, C., Mair, T. (2008) A retrospective study comparing conservative and surgical treatments of open comminuted fractures of the fourth metatarsal bone in horses. *Equine Vet. Educ.* **20**, 373–379

Verschooten, F., Gasthuys, F., De Moor, A. (1984) Distal splint bone fractures in the horse: an experimental and clinical study. *Equine Vet. J.* **16**, 532–536

Watt, B., Foerner, J., Haines, G. (1998) incomplete oblique sagittal fracture of the dorsal cortex of the third metacarpal bone in six horses. *Vet. Surg.* **27**, 337–341

White, K. (1983) Diaphyseal angular limb deformities in 3 foals. *J. Am. Vet. Med. Ass.* **182**, 272–279

Wright, I., Smith, M. (2009) A lateral approach to the repair of propagating fractures of the medial condyle of the third metacarpal bone and metatarsal bones in 18 racehorses. *Vet. Surg.* **38**, 689–695

Zubrod, C., Schneider, R., Tucker, R. (2004) Use of magnetic resonance imaging to identify suspensory desmitis and adhesions between exostoses of the second metacarpal bone and the suspensory ligament in four horses. *J. Am. Vet. Med. Ass.* **224**, 1815–1819

Downloaded From Vet-eBooks.com

Downloaded From Vet-eBooks.com

Chapter 7
The carpus and antebrachium

RADIOGRAPHIC TECHNIQUE

The carpus consists of three principal joints: antebrachiocarpal (radiocarpal), middle carpal (intercarpal) and carpometacarpal. Articulations also exist between adjacent bones in each row of carpal bones. This causes overlying images that may confuse interpretation. Therefore it is necessary to obtain at least five standard views.

The distal aspect of the radius is included in standard views of the carpus, but to evaluate the majority of the radius four standard views centred on the area of interest are required.

Equipment

Portable x-ray machines are adequate for radiography of the carpus and antebrachial regions and a grid is not required. Using conventional radiography, high-definition screens and films are preferable, although rare earth screens and compatible films can be used. The faster screen and film combinations tend to lack contrast and definition. A grid may be useful if the carpal region is very swollen.

Positioning for the carpus

Examinations are best carried out with the horse standing. Sedation may be required in fractious animals.

All examinations should include lateromedial, dorsopalmar, dorsal 45° lateral-palmaromedial oblique and dorsal 45° medial-palmarolateral oblique views. Lateromedial (flexed) views are very helpful in many cases, to separate the dorsodistal margin of the radial and intermediate carpal bones, where bone fragmentation and alteration in subchondral bone opacity frequently occur in racehorses. If degenerative joint disease is suspected it may also be helpful to obtain dorsal 75° lateral-palmaromedial oblique and dorsal 75° medial-palmarolateral oblique views to evaluate the entire joint margins better. These views are required for Thoroughbred pre-sales radiographs and may highlight early periarticular modelling. For suspected fractures, it is often necessary to acquire further oblique views at different angles, as well as dorsoproximal-dorsodistal oblique (flexed) ('skyline') views. Consistency of the angle of the views will greatly aid film reading.

Clinical Radiology of the Horse, Fourth Edition. Janet A. Butler, Christopher M. Colles, Sue J. Dyson, Svend E. Kold and Paul W. Poulos.
© 2017 John Wiley & Sons, Ltd. Published 2017 by John Wiley & Sons, Ltd.
Companion website: www.clinical-radiology-horse.com

Downloaded From Vet-eBooks.com

Lateromedial, dorsopalmar and oblique views

Lateromedial, dorsopalmar and oblique views are all obtained with the horse standing bearing weight evenly on all four limbs, with the limb to be radiographed vertical. Dorsopalmar and most oblique views are obtained with the x-ray beam aligned horizontally and the cassette held vertically, at right angles to the beam. The joints slope distally to a varying degree towards their lateral or medial aspects. For this reason the x-ray beam may need to be angled slightly up or down in order to give good visualisation of the joints on lateromedial images. The x-ray beam should be centred on the middle carpal joint or on a site of particular interest. In order to obtain true lateromedial and dorsopalmar views of the joints the x-ray beam should be orientated relative to the limb, rather than the trunk of the horse.

Lateromedial (flexed) views

The lateromedial (flexed) view is of great assistance to separate some of the overlying bone images. Chip fractures and alterations in subchondral bone opacity are often most easily seen on this view.

The horse should stand squarely on all four limbs. The limb to be radiographed is then lifted by an assistant who stands against, or just behind, the shoulder of the horse, facing in the same direction as the horse. The toe of the foot is rested on the assistant's leg to help keep the limb steady and also to enable the limb to be repositioned accurately if subsequent films are needed. It is important not to rotate the limb and the foot should be supported vertically below the elbow (Figure 7.1). The x-ray beam is initially maintained horizontal, at right angles to the long axis of the limb. Slight changes in alignment of the x-ray beam may need to be made subsequently to allow better visualisation of specific lesions.

Dorsoproximal-dorsodistal oblique (flexed) 'skyline' views

Dorsoproximal-dorsodistal oblique (flexed) views of the carpus are essential to identify some slab fractures, to establish their extent and to detect pathology not apparent in the standard views (see also below, 'Degenerative

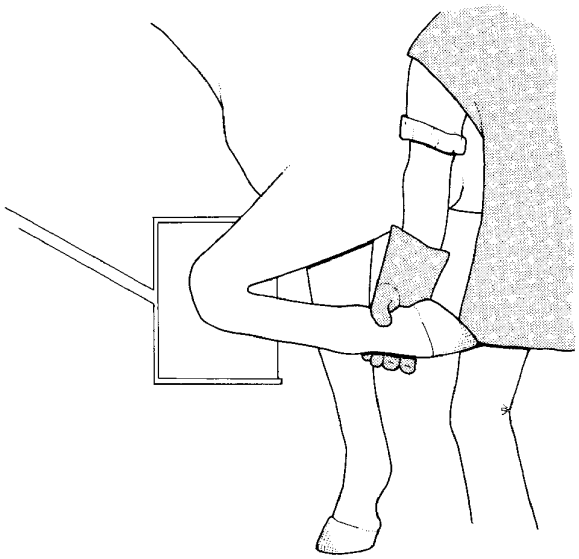


Figure 7.1 Positioning to obtain a lateromedial (flexed) view of the carpus.

Downloaded From Vet-eBooks.com

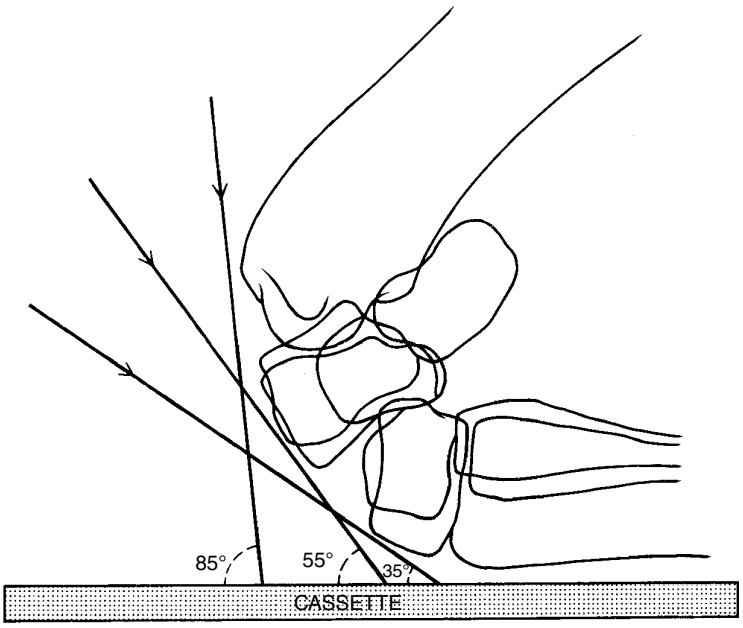


Figure 7.2 Positioning to obtain dorsoproximal-dorsodistal oblique (flexed) views of the carpus. The three different angles of the x-ray beam allow assessment of the distal aspect of the radius, the proximal row of carpal bones, or the distal row of carpal bones.

joint disease', 'Sclerosis of the third carpal bone' and 'Sagittal fracture of the third carpal bone').

An assistant holds the limb to be examined with the carpus flexed and slightly in front of the carpus of the contralateral limb, trying to keep the metacarpal region horizontal (Figure 7.2). The imaging plate/cassette is placed against the dorsal aspect of the third metacarpal bone, with its centre level with the carpus. Alternatively the flexed limb and cassette may be placed on a block of sufficient height, with restraint of the limb at the toe. This can help to reduce movement and standardise the degree of flexion. The degree of flexion of the carpus that can be achieved depends on the amount of pain induced by flexion. The angle of the x-ray beam required to examine the distal aspect of the radius and the proximal and distal rows of carpal bones is therefore variable. The radiographer must try to visualise the positions of the radius and the carpal bones in relation to the degree of flexion. In a fully flexed carpus the following guide can be given (Figure 7.2):

- To project an image of the distal aspect of the radius, the x-ray beam is aligned at approximately 85° to the cassette, pointing obliquely downward through the flexed carpus. This is often most easily achieved if the carpus is allowed to drop towards the ground
- To project an image of the proximal row of carpal bones, the beam is aligned at approximately 55° to the cassette
- To project an image of the distal row of bones, the beam is aligned at approximately 35° to the cassette.

Positioning for the antebrachium (radius)

The horse should stand bearing full weight with the antebrachium positioned vertically. The most common reason to be examining this region is to determine the presence of an incomplete fracture of the radius following

Downloaded From Vet-eBooks.com

a kick injury. The x-ray beam should initially be centred at the site of suspected trauma, but if a fracture line is identified, additional more proximal views may be required to determine the full extent of the fracture. Craniocaudal, lateromedial and several oblique views are normally required.

NORMAL ANATOMY

Immature horse

The distal aspect of the radius has two ossification centres. The lateral styloid process (morphologically the distal end of the ulna) is separate at birth and fuses with the epiphysis in the first year of life. Oblique views of the carpus in a skeletally mature horse may demonstrate a radiolucent line between the styloid process and the distal aspect of the radius. This line is more pronounced in young horses, but may persist to varying degrees throughout life. The distal radial physis closes at about 20 months of age.

At birth the joint spaces appear wider than in a mature horse, because endochondral ossification is incomplete and therefore the cartilage is thicker (Figures 7.3a and 7.3b). The carpal bones should be approximately cuboidal. Rounded margins to the bones indicate that they are incompletely ossified (see below, 'Incomplete carpal ossification').

Each of the carpal bones ossifies from a single centre and is fully developed by 18 months of age.

The third metacarpal bone has a proximal epiphysis, which is fused with the metaphysis at birth.

Skeletally mature horse

The carpus is complex and it may be necessary to compare images from several different views to ensure that suspected lesions are not due to overlying images of bones.

Lateromedial image

The distal aspect of the radius has a prominent transverse ridge caudally, to which, medially and laterally, the medial and lateral collateral ligaments of the carpus attach. Immediately distal to the ridge are depressions for attachment of carpal ligaments. This transverse ridge is not the origin of the accessory ligament of the superficial digital flexor tendon, which arises from a longitudinal ridge approximately 10–15 cm proximal to the antebrachiocarpal joint.

In a lateromedial image (Figure 7.4) the two rows of carpal bones are clearly delineated by the antebrachiocarpal, middle carpal and carpometacarpal joints. These joints are represented by double lucent lines, as they undulate, rather than forming flat parallel planes. It is possible to eliminate the double line in local areas by altering the angle of the beam and/or the point at which it is centred.

Downloaded From Vet-eBooks.com



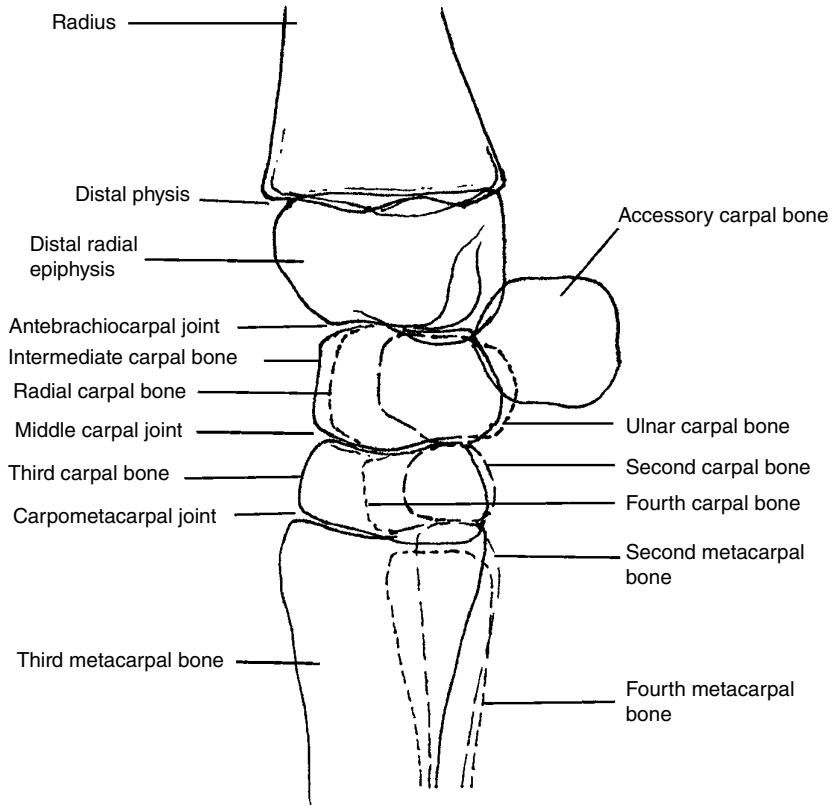


Figure 7.3(a) Lateromedial image and diagram of a carpus of a normal 5-day-old foal.

Downloaded From Vet-eBooks.com



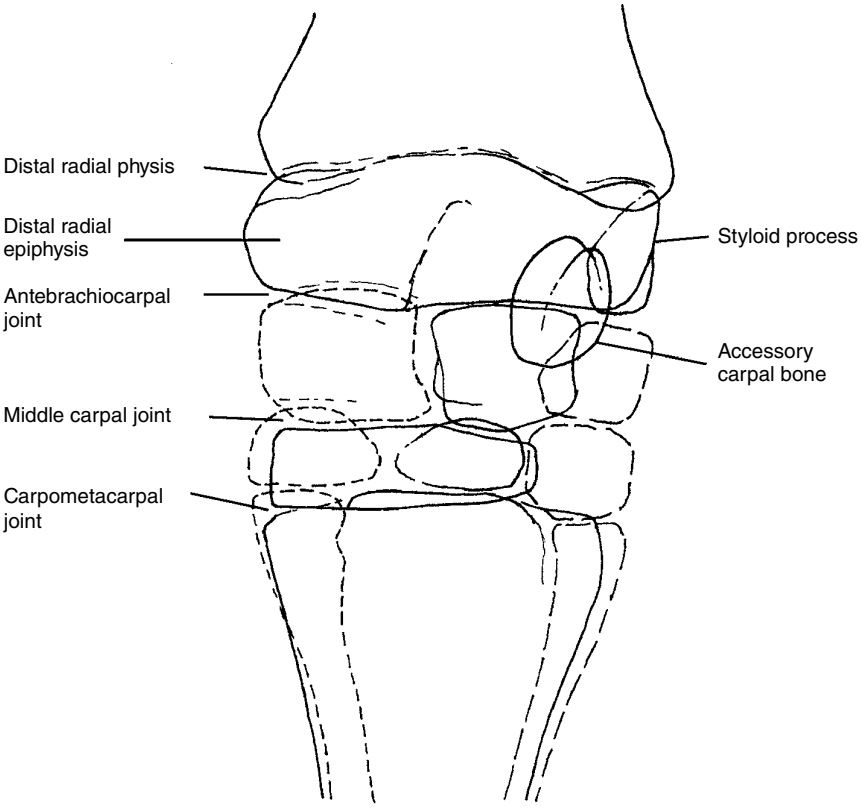


Figure 7.3(b) Dorsopalmar image and diagram of a carpus of a normal 5-day-old foal. Lateral is to the right.

Downloaded From Vet-eBooks.com



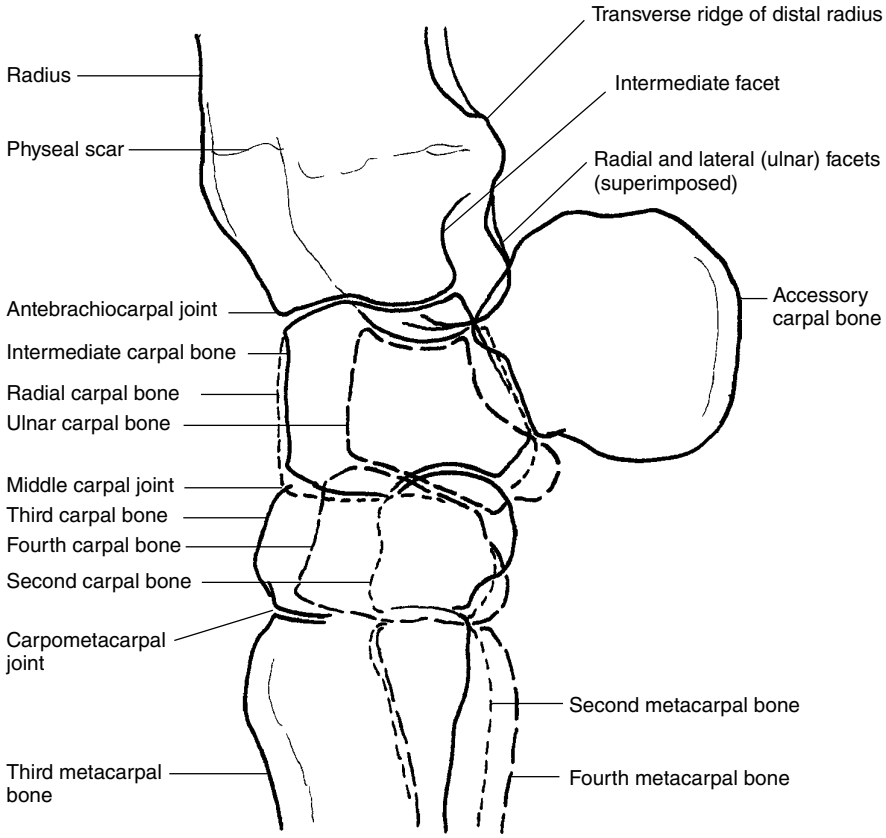


Figure 7.4 Lateromedial image and diagram of a normal adult carpus. Note the focal radiolucencies on the dorsal aspect of the antebrachiocarpal joint, representing fat pads.

Downloaded From Vet-eBooks.com

On a true lateromedial image, the bone projected most dorsally in the proximal row of carpal bones is the intermediate carpal. This bone has a relatively straight dorsal border, well defined proximally and distally where it meets the articular surfaces at approximately a right angle. Very slight dorsolateral-palmaromedial obliquity will make the radial carpal bone most prominent.

The most dorsal of the distal row of carpal bones is the third carpal bone. The middle third of this bone often protrudes dorsally. The dorsal surface meets the articular surfaces at approximately a right angle.

The accessory carpal bone is relatively thin, but thickens at its palmar aspect where there are tendon and ligament insertions. There is a vertical radiolucent line close to the palmar surface caused by edge enhancement.

One or two focal radiolucencies may be seen in the soft tissues on the dorsal aspect of the antebrachiocarpal joint. These represent fat in the joint capsule and lie palmar to the synovial sheath of the extensor carpi radialis tendon. Distension of the joint capsule may obscure these lucent areas.

Dorsopalmar image

There is a large approximately circular lucent zone in the centre of the distal end of the radius, which is caused by a depression (between the medial and lateral styloid processes) in the caudal surface of the bone.

Figure 7.5 shows the individual carpal bones seen on the dorsopalmar radiograph and the reader is referred to this figure for their identification. A radiolucent canal is normally seen between the radial and intermediate carpal bones on this projection.

Oblique images

Standard oblique views are shown in Figures 7.6 and 7.7, but their appearance is greatly affected by the degree of obliquity. Interpretation of oblique radiographs is therefore facilitated by comparison with an anatomical specimen.

Superimposition of the chestnut over the radius should not be confused with a pathological opacity.

Lateromedial (flexed) image

In a lateromedial (flexed) image (Figure 7.8) the distal end of the radius is normally projected as three distinct articular surfaces, that with the largest radius of curvature being the radial facet, the smallest the intermediate facet, and the lateral or ulnar facet having an intermediate radius of curvature.

As the carpus is flexed, the accessory carpal bone gradually rotates around a horizontal axis, and so appears slightly shorter in a proximal to distal direction than on a standing lateromedial image.

The majority of carpal flexion occurs at the antebrachiocarpal joint, with some flexion at the middle carpal joint. As the carpus flexes, the intermediate carpal bone moves proximally relative to the radial carpal bone. The proximal

Downloaded From Vet-eBooks.com



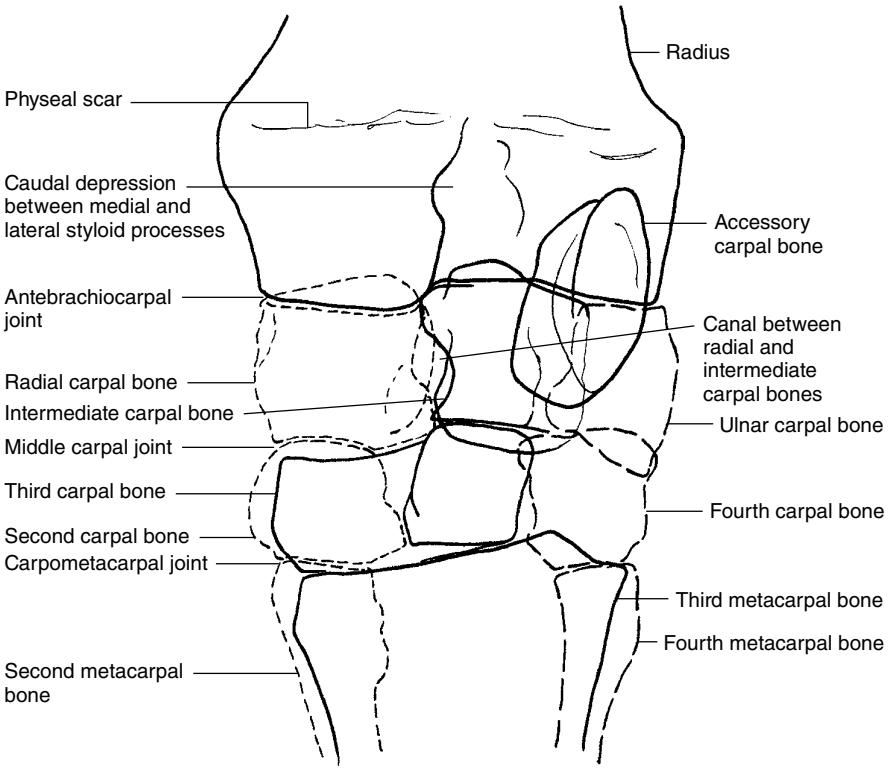


Figure 7.5 Dorsopalmar image and diagram of a normal adult carpus. Lateral is to the right.

Downloaded From Vet-eBooks.com



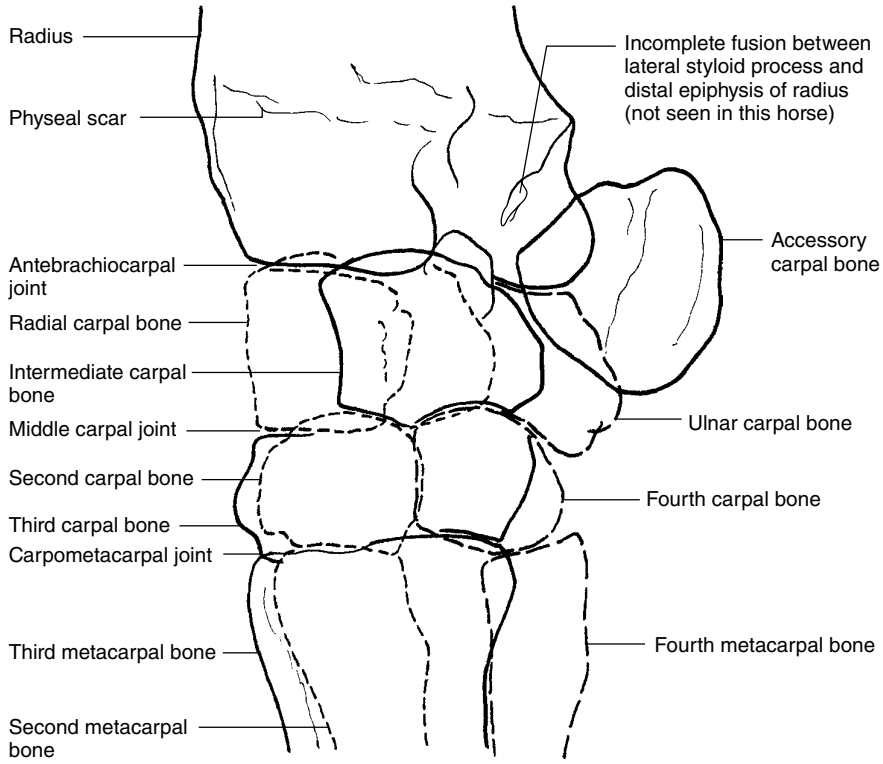


Figure 7.6 Dorsal 45° lateral-palmaromedial oblique image and diagram of a normal adult carpus.

Downloaded From Vet-eBooks.com



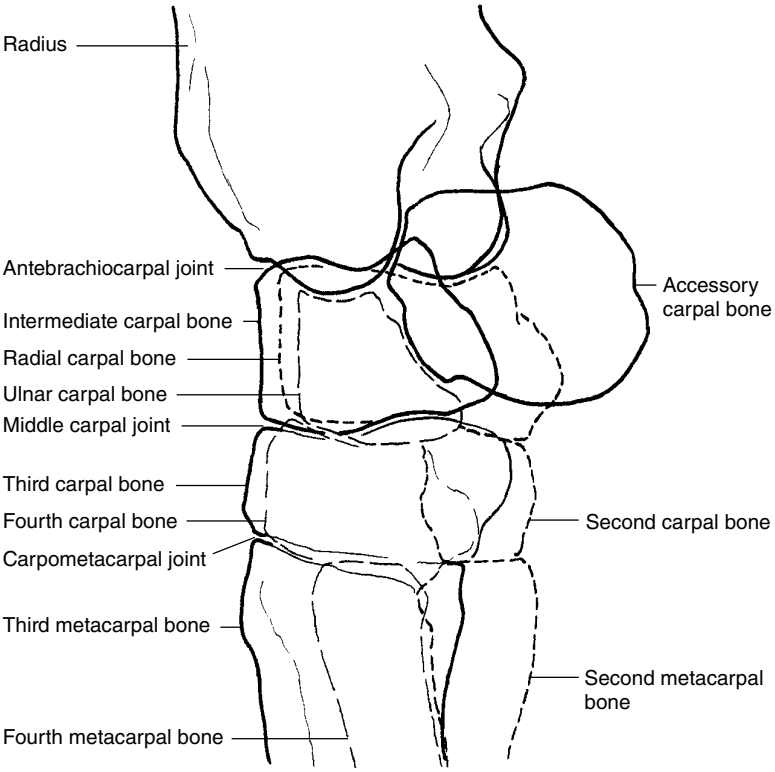


Figure 7.7 Dorsal 45° medial-palmarolateral oblique image and diagram of a normal adult carpus.

Downloaded From Vet-eBooks.com



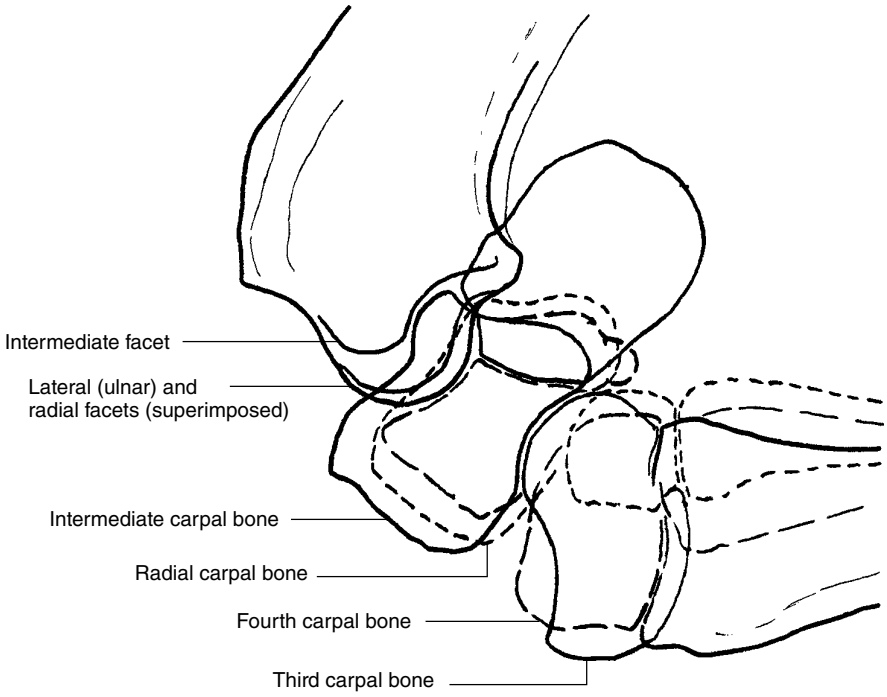


Figure 7.8 Lateromedial (flexed) image and diagram of a normal adult carpus.

Downloaded From Vet-eBooks.com

border of the fourth carpal bone is seen proximal to the third, and the dorsal surface of the third is dorsal to the fourth. The carpometacarpal joint does not open appreciably during flexion. The first and/or the fifth carpal bones, if present, are easily seen.

Dorsoproximal-dorsodistal oblique (flexed) views

It is necessary to obtain separate views to evaluate the distal aspect of the radius and the proximal and distal rows of carpal bones.

The distal aspect of the radius has a continuous outline, with two distinct grooves on the dorsal aspect (Figure 7.9a). The outline of the proximal row of carpal bones may be seen superimposed on the image of the radius on overexposed radiographs.

In the proximal row of carpal bones (Figure 7.9b) the dorsal borders of the radial and intermediate carpal bones are clearly outlined, with their articulation near the midline. The ulnar carpal bone can be seen laterally.

In the distal row of carpal bones (Figure 7.9c) the third carpal bone is central, with the second and fourth carpal bones at the medial and lateral aspects respectively.

Each carpal bone should have a smooth outline, with an even trabecular pattern and a sharply defined border between compact and trabecular bone.

NORMAL VARIATIONS AND INCIDENTAL FINDINGS

In a lateromedial or slightly oblique lateromedial image there is a smoothly outlined prominence on the caudolateral and caudomedial aspects of the radius at the level of the fused physis. The distal caudal aspect of the radius proximal to the physis may have a rather irregular outline (Figure 7.10). The transverse ridge on the distal caudal aspect of the radius often appears slightly roughened and does not reflect previous tearing of the accessory ligament of the superficial digital flexor tendon (superior check ligament), which arises further proximally from a longitudinal ridge approximately 10–15 cm proximal to the antebrachiocarpal joint. Oblique images may demonstrate an incomplete lucent line in the distal lateral aspect of the radius, representing incomplete fusion between the lateral styloid process and the distal epiphysis of the radius (Figure 7.11a).

Although the distal end of the ulna is vestigial in the horse, it may continue to the distal tuberosity of the radius as a fibrous cord. In approximately 35% of horses it is partially ossified, and is clearly seen radiologically. It is variable in size and appearance (Figures 7.11a and 7.11b). In some small pony breeds, e.g. the Shetland, a complete ulna may be present.

The palmar aspect of the ulnar carpal bone is variable in shape, but is usually bilaterally symmetrical (Figure 7w.12). Occasionally there is a separate centre of ossification on its distal palmar aspect. A lucent zone is sometimes seen in the ulnar carpal bone, with or without an adjacent osseous opacity (Figure 7w.12e). Such lucent zones may possibly be associated with previous intercarpal ligament avulsion. They are not generally associated with lameness in sports horses, but have been associated with lameness in racehorses (see 'Osseous cyst-like lesions', below) and arthroscopic assessment may be indicated. Osseous cyst-like lesions are also occasionally seen in conjunction with an extra small bone on the palmarolateral aspect of the proximal row of carpal bones.

Downloaded From Vet-eBooks.com



(a)



(b)



(c)

Figure 7.9 Dorsoproximal-dorsodistal oblique (flexed) images and diagrams of a carpus of a normal adult horse, showing: (a) the distal aspect of the radius; (b) the proximal row of carpal bones; (c) the distal row of carpal bones. Lateral is to the right.

Downloaded From Vet-eBooks.com

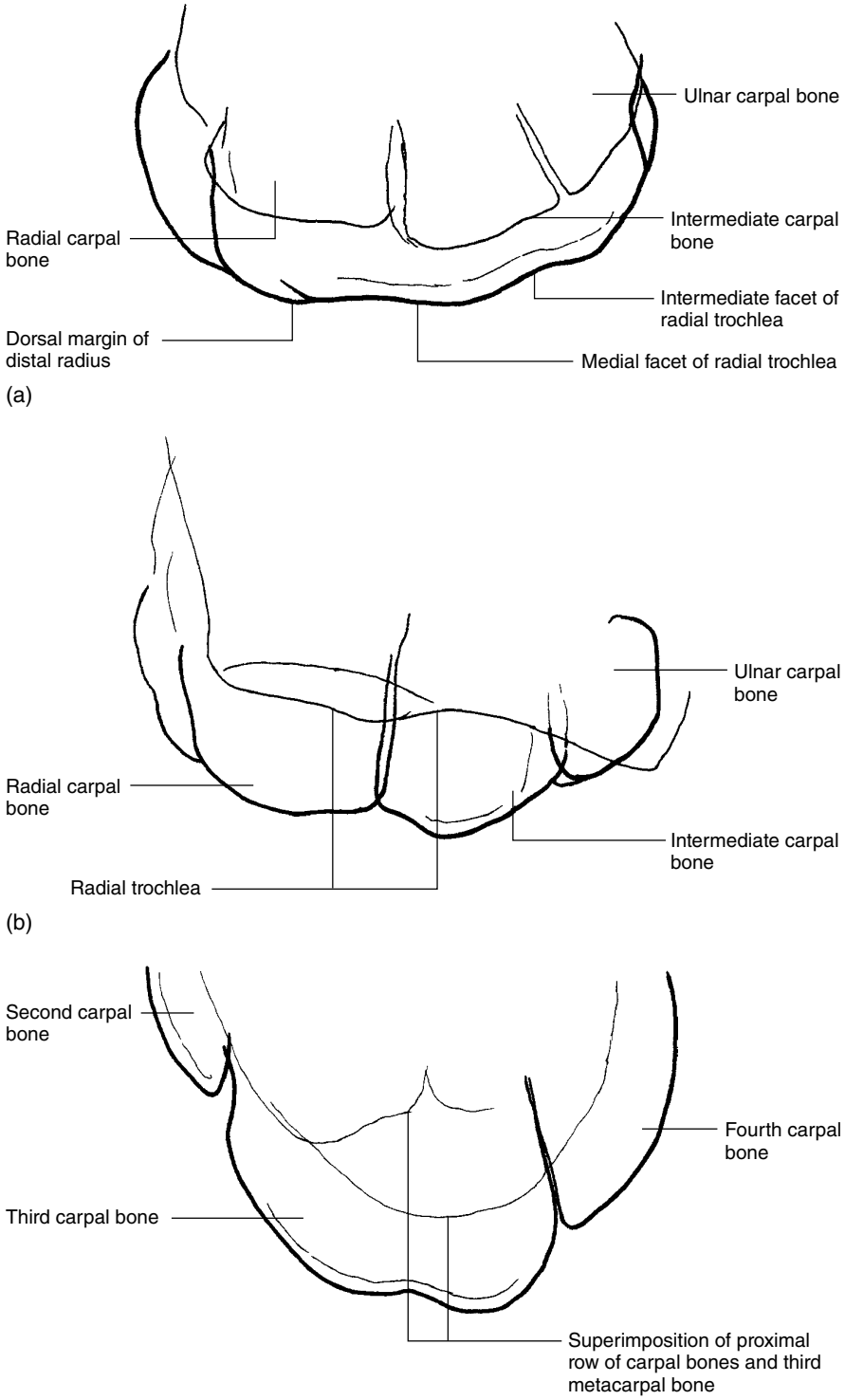


Figure 7.9 *Cont'd*

Downloaded From Vet-eBooks.com



Figure 7.10 Lateromedial image of a carpus from a normal adult horse, showing the contour of the distal caudal aspect of the radius. At the level of the fused distal radial physis there are several bony protuberances.

The first carpal bone is seen in approximately one-third of horses in one, or more commonly, both limbs. It is variable in size, ranging from pinpoint to 12–15 mm in diameter. It may, but need not, articulate with the second carpal bone (Figure 7.13a–c), and also with the second metacarpal bone. If it is separated from the second carpal bone, it usually has a uniformly opaque appearance. If the first carpal bone is in close proximity to the second carpal or second metacarpal bones, these bones may have focal lucent areas within them.

Occasionally, in less than 2% of horses, a fifth carpal bone is present on the palmarolateral aspect of the distal row of carpal bones.

Very occasionally there is a separate ossification centre in the proximal row of carpal bones. The size, shape and articulations of these bones are variable, but they are usually uniformly opaque. These separate ossification centres should not be confused with fractures.

In some horses in a dorsomedial-palmarolateral oblique image there is mineralisation between the second and third carpal bones (Figure 7.14a), which may be present in association with ossification of the interosseous ligament between the second and third metacarpal bones. The clinical significance of this is uncertain. Irregularity of the adjacent margins of the second and third carpal bones can be seen in a dorsopalmar image (Figure 7.14b). Although these radiological changes have been associated with interosseous ligament injury, they can also be seen as incidental findings.

Mild increased opacity of the radial facet of the third carpal bone may be seen in dorsoproximal-dorsodistal oblique (flexed) images of horses in full

Downloaded From Vet-eBooks.com



Figure 7.11 Dorsolateral-palmaromedial oblique images of the distal aspect of a radius and proximal aspect of a carpus of normal adult horses showing: (a) a curvilinear opacity (white arrow) adjacent to the distal lateral aspect of the radius, a vestigial distal ulna. There is also a radiolucent zone (black arrow) in the distal lateral aspect of the radius which represents incomplete fusion of the lateral styloid process, which is an incidental finding; (b) a linear osseous opacity parallel to the radius, a vestigial distal ulna (arrows). There is also a clearly demarcated opacity (arrowhead) in the soft tissues caudal to the radius, representing the torus carpeus (chestnut).

work; this is generally bilaterally symmetrical and is considered a normal adaptation to training. Marginal osteophyte formation may be seen, particularly on the medial aspect of the antebrachiocarpal and middle carpal joints in older horses with conformational abnormalities of the distal aspect of the limb. This is most common if the metacarpal region is set on lateral to the central axis of the antebrachium. It is not necessarily associated with lameness, but this may depend on the athletic demands placed on the horse. Proximal extension of the proximal aspect of the fourth metacarpal bone is occasionally seen (Figure 6w.9a).

SIGNIFICANT FINDINGS

Soft-tissue swelling

Soft-tissue injury and swelling of the carpus is common. It can generally be appreciated radiographically but it is frequently not possible to determine its cause. The site of maximum swelling may be located near the site of the injury, but frequently the swelling is too extensive for this to be of diagnostic

Downloaded From Vet-eBooks.com



(a)



(b)



(c)

Figure 7.13 Dorsomedial-palmarolateral oblique images of a carpus of normal horses, showing variations of the first carpal bone. (a) The first carpal bone (arrow) is a rounded uniformly opaque osseous body well separated from the second carpal bone. (b) The first carpal bone (arrow) appears to articulate with both the second carpal bone and the second metacarpal bone. The distal palmar aspect of the second carpal bone and the proximal palmar aspect of the second metacarpal bone are relatively lucent. Note also the narrowing of the interosseous space between the second and third carpal bones and ossification of the interosseous space between the proximal aspects of the third and second metacarpal bones. (c) The first carpal bone appears to articulate with the second carpal bone. The distal palmar aspect of the second carpal bone is relatively lucent. There are ill-defined lucent areas within the first carpal bone. Note also narrowing of the interosseous space between the proximal aspects of the third and second metacarpal bones.

Downloaded From Vet-eBooks.com



Figure 7.14(a) Dorsomedial-palmarolateral oblique image of a carpus. The dorsal aspect of the second carpal bone is irregular (arrow) in the region of insertion of the interosseous ligament between the second and third carpal bones.



Figure 7.14(b) Dorsopalmar image of the carpus in Figure 7.14(a). There is irregularity of the contour of the lateral aspect of the second carpal bone (arrow) in the region of insertion of the interosseous ligament between the second and third carpal bones. Compare with Figure 7.5.

assistance. Gravity will also change the appearance of the swelling. Swelling may be restricted to, or by, periarticular structures or involve the carpal joint capsules. It may indicate the presence of synovitis and/or infection, or result from contusion or ligament strains.

The antebrachiocarpal (radiocarpal) joint usually does not communicate with the middle carpal joint. Synovitis of these joints may therefore occur separately. Distension of the antebrachiocarpal joint capsule may obscure the focal radiolucencies, which represent fat, on the dorsal aspect of the joint. If there is swelling of the middle carpal joint capsule, a dorsoproximal-dorsodistal oblique view of the distal row of carpal bones should be obtained (see below, 'Sclerosis of the third carpal bone').

Diffuse soft-tissue swelling on the dorsal aspect of the carpus may be due to a hygroma, an acquired bursa. Usually there are no associated radiographic abnormalities other than the soft-tissue swelling. Occasionally herniation of a joint capsule may occur, to cause a synoviocoele, usually on either the dorsolateral or dorsomedial aspect of the carpus.

Distension of the tendon sheath of the extensor carpi radialis, common digital extensor or lateral digital extensor may result in a chronic longitudinal swelling over the dorsal aspect of the carpus. Occasionally communication

Downloaded From Vet-eBooks.com

develops between two of the above structures. Positive and double contrast radiographic techniques (see Chapter 16) are useful to aid differentiation of these swellings, and to identify filling defects due to synovial proliferation or adhesion formation. Ultrasonography may yield additional information. Chronic distension of the tendon sheath of the extensor carpi radialis is often seen in association with irregular periosteal new bone formation on the distal cranial aspect of the radius. This new bone is not necessarily of clinical significance.

Kick injuries of the distal aspect of the antebrachium may result in sharp spikes of bone on the distal cranial aspect of the radius and severe trauma to the extensor carpi radialis tendon. Occasionally resection of the tendon is required, but the bone spike can often be managed conservatively.

Distension of the carpal sheath may be associated with a primary soft-tissue injury best assessed ultrasonographically, but radiographic assessment of the caudodistal aspect of the radius is important to rule out an osteochondroma or distal radial exostoses. The accessory carpal bone forms part of the carpal canal and is integrally related to the carpal sheath and should also be evaluated carefully.

Intercarpal ligament desmitis

Each of the carpal bones is connected to the adjacent bone by horizontally orientated intercarpal ligaments, within the joint. In addition there are medial and lateral palmar intercarpal ligaments connecting the proximal and distal rows of carpal bones, closely related to the palmar carpal ligament. There are also dorsal intercarpal ligaments connecting the dorsal aspect of adjacent carpal bones.

Palmar intercarpal ligament desmitis has been recognised both ultrasonographically and arthroscopically unassociated with detectable radiographic abnormality. Partial tearing of the palmar carpal ligament may result in overextension of the carpus and widening of the palmar aspect of the middle carpal joint in a weight-bearing true lateromedial image. Rupture of the palmar carpal ligament is a rare injury resulting in severe overextension of the carpus.

Dorsal intercarpal ligament injury is associated with the development of entheseous new bone on the dorsal aspect of affected bones (Figures 7.15a and 7.15b), often the radial and intermediate carpal bones in racehorses. It may reflect a degree of carpal instability.

Desmitis of the horizontal intra-articular intercarpal ligaments may be associated with entheseous new bone on the axial aspects of the affected carpal bones, especially the second and third carpal bones (Figures 7.14 and 7w.16). It is occasionally associated with the development of an osseous cyst-like lesion in one of the bones. There may be no detectable radiological abnormality and diagnosis may be dependent on magnetic resonance imaging.

Degenerative joint disease

The radiological changes associated with degenerative joint disease are described elsewhere (see 'Degenerative joint disease' in Chapter 1). The most frequent abnormalities identified in the carpus are periarticular

Downloaded From Vet-eBooks.com



Figure 7.15(a) Dorsolateral-palmaromedial oblique image of a carpus. There is irregularly outlined entheseous new bone on the dorsal aspect of the radial carpal bone (arrow) at the site of the dorsal intercarpal ligament attachment. This is often not of long-term clinical significance, but reflects previous carpal instability. Note the rounded contour of the distal dorsal aspect of the radial carpal bone.



Figure 7.15(b) Dorsolateral-palmaromedial oblique image of a carpus of a 3-year-old Thoroughbred flat racehorse, with lameness which was improved by intra-articular analgesia of the middle carpal joint. There is extensive irregular entheseophyte formation on the dorsal aspect of the radial carpal bone (white arrow), at the attachment of the dorsal intercarpal ligament. There is reduced opacity of the distal dorsal aspect of the radial carpal bone (arrowhead) and mild modelling of the proximodorsal aspect of the third carpal bone (grey arrow). Diagnostic arthroscopy of the middle carpal joint revealed extensive cartilage degeneration on the radial facet of the third carpal bone.

osteophytes, rounding of the normally right-angled shape of the articular margins of the carpal bones and increased opacity of or lucent zones within the subchondral or trabecular bone (Figure 7.17a–e). The antebrachiocarpal and middle carpal joints are most commonly affected, especially the antebrachiocarpal joint in sports horses and the middle carpal joint in racehorses, while the carpometacarpal joint is occasionally affected especially in old horses.

Periarticular osteophytes are most commonly seen at the proximal and distal dorsal aspects of the radial carpal bone, the proximodorsal aspect of the third carpal bone and, less commonly, the proximodorsal aspect of the intermediate carpal bone. Because of this positioning, examinations for degenerative joint disease of the carpus should always include dorsal 45° lateral-palmaromedial and dorsal 75° lateral-palmaromedial oblique views as well as lateromedial views (flexed). Care should also be taken to evaluate the palmar margins of the joints, since periarticular osteophyte formation may also develop here, especially in more advanced cases of degenerative joint disease. Small bone spurs or modelling of the joint margins may be found in apparently sound horses in work, and their significance must be assessed in relation to the age of the horse, conformation, the work previously carried out, current lameness and future work required. Thus these would be of more

Downloaded From Vet-eBooks.com



(a)



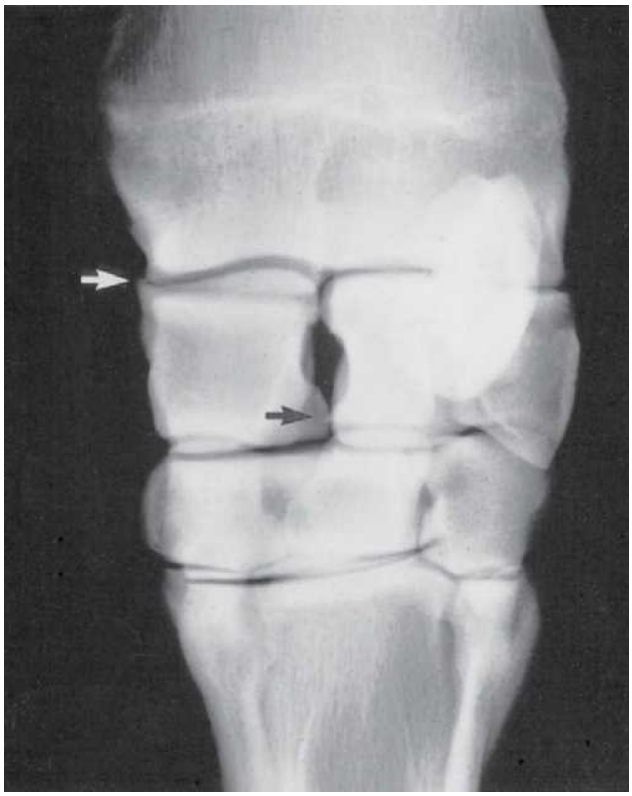
(b)



(c)

Figure 7.17 Radiographs of the carpus of adult horses, showing changes associated with early degenerative joint disease (the significance of these radiographic abnormalities must be determined in the light of the clinical examination).
(a) Dorsolateral-palmaromedial oblique image of a carpus of a 2-year-old Thoroughbred flat racehorse. There is mild periarticular osteophyte formation on the dorsoproximal aspect of the radial carpal bone. Lameness was improved by intra-articular analgesia of the antebrachiocarpal joint. Arthroscopy revealed fibrillated cartilage overlying soft subchondral bone on the medial aspect of the radial carpal bone. (b) Dorsolateral-palmaromedial oblique image of a carpus of a 2-year-old Thoroughbred flat racehorse. There is mild periarticular osteophyte formation on the dorsodistal aspect of the radial carpal bone. There is entheseophyte formation on the dorsal aspect of the radial carpal bone. The dorsoproximal aspect of the third carpal bone is rounded. Lameness was improved by intra-articular analgesia of the middle carpal joint. Image courtesy of Bruce Bladon.
(c) Dorsolateral-palmaromedial oblique image of a carpus of a 5-year-old Thoroughbred ex-flat racehorse, now a hurdler. There is soft tissue swelling on the dorsomedial aspect of the carpus overlying irregular entheseous new bone on the dorsomedial aspect of the radial carpal bone. There is mild modelling of the distal dorsal aspect of the radial carpal bone with loss of trabecular architecture and subtle modelling of the dorsoproximal aspect of the third carpal bone. Lameness was improved by intra-articular analgesia of the middle carpal joint. Note also the mild modelling of the dorsoproximal medial aspect of the third metacarpal bone.

Downloaded From Vet-eBooks.com



(d)

Figure 7.17(d) Dorsopalmar image of a carpus of a 14-year-old Thoroughbred. Lateral is to the right. There is osteophyte formation on the distal medial aspect of the radius and the proximal aspect of the radial carpal bone (white arrow). There is a small clearly outlined spur on the distal medial aspect of the intermediate carpal bone (black arrow), the clinical significance of which is unknown.



(e)

Figure 7.17(e) Dorsolateral-palmaromedial oblique image of a carpus of a 5-year-old Thoroughbred. There is osteophyte formation on the proximal dorsomedial aspect of the radial carpal bone (arrow), reflecting degenerative joint disease of the antebrachiocarpal joint. The dorsal aspect of the radial carpal bone has smoothly marginated entheseous new bone at the site of the intercarpal ligament attachments (arrowhead).

significance if found at a pre-purchase examination of a young top-grade performance horse, than if seen as an incidental finding in an old pleasure horse. Quite extensive abnormalities of the antebrachiocarpal joint in sports and pleasure horses can be present without lameness, although there is often restricted flexion of the joint and pain induced by flexion. Radiographic abnormalities of either the antebrachiocarpal or middle carpal joint are more likely to be associated with lameness in racehorses.

In the young Thoroughbred in training, subtle modelling changes of the radial and third carpal bones may have important consequences. Initially there may be slight loss of opacity on the dorsal distal aspect of the radial carpal bone (Figure 7.15b). The distal articular margin becomes more rounded and 'cut back' ('ski-slope') (Figure 7.15a). This effectively moves the articulation with the third carpal bone in a slightly palmar direction. Subsequently the dorsoproximal aspect of the third carpal bone becomes

Downloaded From Vet-eBooks.com

more opaque. This modelling may predispose to fracture of the third carpal bone. Subtle lucent areas on the distal dorsal aspect of the radial carpal bone (Figure 7.18a and b) are usually associated with significant cartilage and subchondral pathology and may lead to fragmentation or the development of a large area of subchondral bone injury extending into the spongiosa (Figure 7.18c). Intra-articular medication has variable efficacy for lameness management, depending on the extent of cartilage pathology and possible instability of the joint.

Narrowing of a joint space or ankylosis are rarely seen except in the carpometacarpal joint (Figure 6.20).

Degenerative changes are sometimes seen involving only part of the carpometacarpal joint, either the articulation between the second carpal and second metacarpal bone, or the fourth carpal and fourth metacarpal bone. There is narrowing of the joint space and subchondral lucent zones or increased radiopacity, often in association with irregular periosteal new bone on the metaphysis and proximal diaphysis of the second or fourth metacarpal bone (Figure 6.20). This is most commonly seen in old horses and ponies and is associated with a variable degree of chronic lameness. Conservative management is usually unsuccessful, although analgesic management may alleviate symptoms. Surgical arthrodesis has been described.

New bone formation

New bone formation is seen in several locations:

- New bone formed at the margins of the joints (periarticular osteophytes) is associated with degenerative joint disease (see above)
- New bone formed on the dorsal aspect of one or more carpal bones, not involving the joint margins, may be associated with tearing or strain of the intercarpal ligaments (entheseophyte formation, Figures 7.15a and 7.15b), or direct trauma to the periosteum (periosteal osteophytes). Its significance will depend to some extent on its activity at the time of examination, as well as on the amount of bone formed. The new bone will gradually remodel, but may remain irregular. If it has well-defined, smooth, opaque margins it is unlikely to be of long-term significance. Entheseophyte formation on the dorsal aspects of the carpal bones is sometimes seen in association with degenerative joint disease, but may also be seen as an incidental observation in young Thoroughbreds in training. Entheseophyte formation reflects ligamentous damage, resulting in slight instability of the joints. This may cause secondary degenerative joint disease, but need not do so
- New bone formation is quite often seen on the transverse ridge of the distal caudal aspect of the radius, unassociated with clinical signs
- Mineralisation or new bone beginning to bridge the antebrachiocarpal, middle carpal and/or carpometacarpal joints, as well as new bone between the carpal bones in either row, is rare but usually the result of infection or repeated intra-articular administration of corticosteroids (so-called steroid arthropathy). Both steroid arthropathy and infection result in destruction of bone and thus irregular lucent areas in the bones. Infection is usually associated with increased radiopacity, and either condition may result in spontaneous

Downloaded From Vet-eBooks.com



Figure 7.18(a) Lateromedial (flexed) image of a carpus of a 4-year-old Thoroughbred flat racing horse. Dorsal is to the left. The horse had shown intermittent lameness for many months but had been kept in training and had raced successfully. There is an ill-defined small radiolucent area in the distal dorsal aspect of the radial carpal bone (arrow), which has a smoothly irregular contour.



Figure 7.18(b) Lateromedial (flexed) image of a carpus of a 2-year-old Thoroughbred flat racing horse, with bilateral forelimb lameness. Dorsal is to the left. There is an ill-defined small radiolucent area in the distal dorsal aspect of the radial carpal bone (arrow). See also Figure 7.20(b).

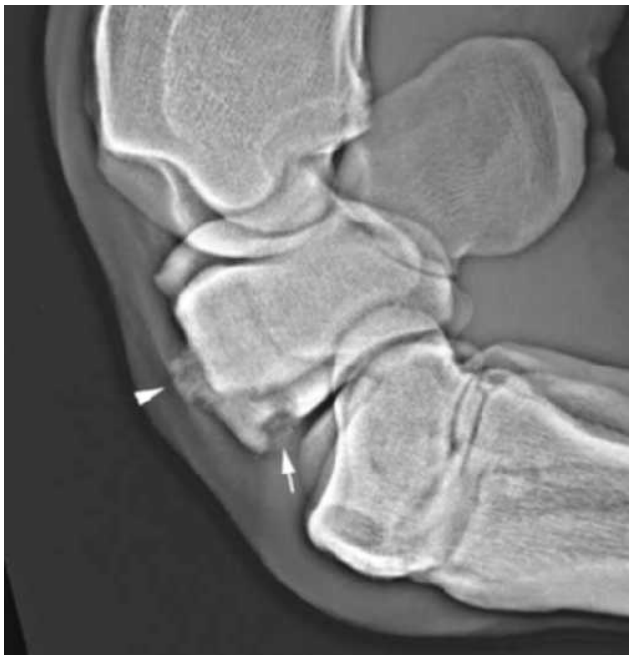


Figure 7.18(c) Lateromedial (flexed) image of a carpus of a 6-year-old former Thoroughbred racehorse, now used as a general-purpose riding horse, with recent acute onset lameness. There is a large lucent defect in the distal aspect of the radial carpal bone extending deeply into the subchondral bone (arrow). There is heterogeneous opacity of the surrounding trabecular bone. The distal subchondral bone of the radial carpal bone has increased opacity palmar to the defect. There is irregular, poorly marginated entheseous new bone on the dorsal aspect of the radial carpal bone (arrow head) with overlying soft tissue swelling.

Downloaded From Vet-eBooks.com

attempts of natural ankylosis of joints and extensive new bone formation. In either case, a hopeless prognosis must be given

- New bone formation occasionally occurs at the origin of the accessory ligament of the superficial flexor tendon (superior check ligament) on the caudodistal aspect of the radius. Its significance should be assessed in the light of clinical signs. Lameness, if present, will usually resolve with rest. Ultrasonographic evaluation is important to assess the integrity of the ligament
- A small exostosis on the caudal aspect of the radius at the level of the distal physis may be subtle and difficult to detect radiologically but can cause an impingement lesion on the deep digital flexor tendon and cause severe episodic lameness, with or without distension of the carpal sheath (Figure 7.19). Ultrasonography may be necessary to confirm the diagnosis. Surgical removal usually has a successful outcome
- Distension of the carpal sheath, lameness and resentment of pressure applied to the distal caudal aspect of the radius may be associated with an osteochondroma on the distal diaphysis or metaphysis of the radius. Radiographically this appears as a variably shaped bony protuberance on the distocaudal aspect of the radius (see Figure 7.26). This mass has a thin cortex that appears to be continuous with the cortex of the radius. Sequential radiographs may demonstrate progressive enlargement of the mass. Ultrasonography usually reveals disruption of the dorsal aspect of the deep digital flexor tendon. Treatment by surgical removal of the osteochondroma is usually successful in resolving both the lameness and carpal sheath swelling



Figure 7.19 Lateromedial image of the distal aspect of a radius and proximal aspect of a carpus of an 8-year-old Warmblood dressage horse with sporadic lameness. When present the lameness was accentuated by carpal flexion, in association with mild distension of the carpal sheath. Cranial is to the left. There is an exostosis on the caudal aspect of the radius at the level of the distal radial physis (arrow). Ultrasonographic examination confirmed that this spike was impinging on the deep digital flexor tendon. Note also the slightly irregular periosteal new bone on the caudal aspect of the radius proximal to the physis (arrow heads).

Downloaded From Vet-eBooks.com

- New bone formation may occur on the distal cranial aspect of the radius, often in conjunction with distension of the tendon sheath of the extensor carpi radialis. This is usually the result of repeated trauma, but is rarely of long-term significance. Occasionally surgical debridement is indicated
- Calcinosis circumscripta has occasionally been recognised in the carpus
- Synovial osteochondromatosis (development of multiple abnormal cartilage growths that undergo endochondral ossification within a synovial lined cavity) has been seen in the middle carpal joint associated with palpable nodular swelling and lameness and is characterised radiologically as multiple mineralised opacities within the joint.

Sclerosis of the third carpal bone

A mild degree of increased opacity of the third carpal bone is believed to be a normal modelling feature in young Thoroughbred and Standardbred racehorses in training, as well as in endurance horses. It usually involves the radial facet. These changes can only be appreciated radiologically in dorsoproximal-dorsodistal oblique (flexed) images, which highlight the third carpal bone. Small round radiolucent areas in the spongiosa reflect blood vessels (Figure 7.20a). Enlargement of these vascular canals can occur in association with increased radiopacity. Marginal radiolucent areas involving the dorsal compact bone are more likely to be of clinical significance. Marked increased opacity (which has been shown histologically to be consistent with sclerosis) of either the radial (Figure 7.20b) and/or intermediate facet is abnormal. This change is appreciated radiologically as a loss of both the trabecular structure and the definition between the dorsal compact bone and the spongiosa. There may be associated distension of the middle carpal joint capsule, a finding that should lead to further evaluation of the third carpal bone. Small poorly



Figure 7.20(a) Dorsoproximal-dorsodistal oblique (flexed) image of the distal row of carpal bones of a 5-year-old Thoroughbred cross event horse. Medial is to the left. There is mild increased opacity of the radial facet of the third carpal bone and two small discrete radiolucencies (arrows) in the spongiosa. Lameness was abolished by median and ulnar nerve blocks; magnetic resonance imaging demonstrated abnormal mineralisation in both the radial and third carpal bones.

Downloaded From Vet-eBooks.com



Figure 7.20(b) Dorsoproximal-dorsodistal oblique (flexed) image of the distal row of carpal bones of a 2-year-old Thoroughbred flat racing horse. Medial is to the left. There is extensive increased opacity (sclerosis) of the radial facet of the third carpal bone. There are several ill-defined lucent lines within the sclerotic bone. The dorsal margin of the bone is slightly irregular medially. Lameness was improved by intra-articular analgesia of the middle carpal joint. Compare with the trabecular structure of the fourth carpal bone. See also Figure 7.18(b).



Figure 7.20(c) Dorsoproximal-dorsodistal oblique (flexed) image of the distal row of carpal bones of a 3-year-old Thoroughbred racehorse. Medial is to the left. There is extensive increased opacity (sclerosis) of the radial facet of the third carpal bone and multiple lucent zones on the dorsal aspect of the bone. Lameness was partially improved by intra-articular analgesia of the middle carpal joint and abolished by perineural analgesia of the median and ulnar nerves.

circumscribed lucent zones are abnormal (Figure 7.20c) and may be a precursor to either a dorsal slab fracture (Figure 7.29) or a parasagittal fracture (Figure 7.30). The third carpal bone should be compared carefully with the fourth carpal bone since the trabecular pattern of the latter is generally normal. If the fourth carpal bone appears to have increased opacity the radiograph is probably underexposed and should be repeated. The radial facet can also be

Downloaded From Vet-eBooks.com

compared with the remainder of the third carpal bone. Sclerosis of the third carpal bone can be seen in conjunction with lameness improved or alleviated by intra-articular analgesia of the middle carpal joint, with no other identifiable abnormality. In many horses with clinically significant sclerosis of the spongiosa of the third carpal bone there is associated increased radiopharmaceutical uptake. Increased radiopharmaceutical uptake however can be seen in the absence of a detectable radiological abnormality, highlighting the presence of third carpal bone disease. With end-stage sclerosis, radiopharmaceutical uptake may be within the normal range.

Lameness usually resolves with rest (paddock turnout is recommended) and the sclerotic bone may slowly remodel over approximately 6 months, although lameness may recur when full work is resumed. Magnetic resonance imaging and computed tomography have demonstrated that lesions may be more extensive than appreciated radiologically, involving bones more proximal and distal in the same sagittal plane, e.g. the distal aspect of the radius, the radial carpal bone and the third metacarpal bone. Excessive sclerosis in the radial facet of the third carpal bone has been shown to predispose to subsequent fracture. Sometimes intra-articular analgesia does not alleviate the lameness associated with third carpal bone sclerosis, but nuclear scintigraphic examination reveals increased modelling activity in the third carpal bone.

Sclerosis of the radial facet of the third carpal bone has occasionally been identified as the cause of lameness in sports horses.

Osseous cyst-like lesions

Osseous cyst-like lesions have been described in all the carpal bones, as well as at the proximal end of all three metacarpal bones and the distal aspect of the radius. Osseous cyst-like lesions in the carpal bones are frequently, but not always, incidental findings unassociated with lameness. However, in young foals osseous cyst-like lesions may represent C-type osteomyelitis (see 'Infectious arthritis' in Chapter 1) and should lead to further diagnostic tests for infectious arthritis (Figures 7.21a and 7.21b). Aggressive broad-spectrum antimicrobial therapy may be required. Very large osseous cyst-like lesions close to a joint margin are probably more likely to be associated with lameness (see 'Subchondral bone cysts and osseous cyst-like lesions' in Chapter 1). Significant lesions may become clinically silent with conservative treatment or may require surgery.

Osseous cyst-like lesions in the axial aspect of the ulnar carpal bone, with avulsion fragments at the insertion of the interosseous ligament, have been seen as a cause of lameness in racehorses. However, similar lesions have been seen in sports horses as incidental abnormalities unassociated with lameness. Occasionally osseous cyst-like lesions are seen in any of the carpal bones associated with interosseous desmitis, a diagnosis that can be confirmed using magnetic resonance imaging.

Osseous cyst-like lesions in the distal aspect of the radius, close to the subchondral bone, have been associated with lameness (Figure 7w.22). In immature horses with conservative management, such lesions may spontaneously 'fill-in' radiographically. This is usually accompanied by resolution of lameness. In mature horses osseous cyst-like lesions tend to persist, and

Downloaded From Vet-eBooks.com



Figure 7.21(a) Lateromedial image of a carpus of a 2.5-month-old crossbred foal. Dorsal is to the left. There is massive soft-tissue swelling on the dorsal and palmar aspects of the carpus centred around the middle carpal joint. There is a large radiolucent area in the third carpal bone (arrows), consistent with type C osteomyelitis. Synovial fluid from the middle carpal joint contained 97% neutrophils.



Figure 7.21(b) Dorsopalmar image of a carpus of the same foal as Figure 7.21(a). Medial is to the left. There is an ill-defined radiolucent lesion in the third carpal bone (arrows).

surgical treatment may be necessary. The antebrachiocarpal joint should be examined carefully for evidence of pre-existing degenerative joint disease.

Polydactyly

Polydactyly has been recorded in the horse, arising from the carpus or distally, and often represents a non-rudimentary second or fourth metacarpal bone. The extra appendage tends to cause limb deviation and therefore requires surgical removal at an early age, with good results.

Physitis

The radiological appearance of physitis is described fully under 'Physitis (epiphysitis)' in Chapter 1. Physitis is relatively common in the distal radial physis of rapidly growing yearlings or occasionally in young racehorses as they commence work.

Downloaded From Vet-eBooks.com



Figure 7.23 Craniocaudal image of the distal aspect of the radius and the carpus of a 14-month-old potential event horse. Medial is to the left. The medial aspect of the distal radial physis is broader than laterally. The distal metaphyseal region is flared medially. The central axes of the radius and the metacarpal regions are not in alignment.

Physitis is characterised radiographically by an irregular widening of the physis (Figure 7.23). There may be new bone bridging the physis medially and/or laterally. Frequently limb deviation will also result. Clinically the limb may be swollen immediately proximal to the carpus, and may be hot and painful to palpation. Treatment is by restricting feed and exercise and appropriate foot trimming until an adequate clinical response is seen.

Carpal angular limb deformities

Many limb deviations arise from the distal aspect of the radius or the carpus and may be congenital or acquired. If a deviation is severe, or a moderate deviation fails to respond to conservative treatment, radiographic examination is indicated. For valgus and varus deviations, dorsopalmar views on long (43 cm) cassettes are most useful. The extent of the deviation can be measured

Downloaded From Vet-eBooks.com



Figure 7.24 Dorsopalmar image of a carpus of a 2-month-old foal with a mild carpal valgus deformity. Medial is to the left. Lines bisecting the radius and third metacarpal bone intersect at the distal radial physis. The angle between them is 5°. This mild deformity will self correct.

Downloaded From Vet-eBooks.com

and monitored by drawing the lines that bisect the radius and third metacarpal bones. These will intersect at or near the point at which the deviation arises, and the angle at the point of intersection indicates the degree of deviation (Figure 7.24). Subsequent films to evaluate change in angle must be identical in position to the first set.

Radiological abnormalities may include one or more of the following:

- Irregularity in width of the distal radial physis
- A wedge-shaped distal radial epiphysis
- Incomplete ossification of one or more carpal bones (see below)
- Malformation of one or more carpal bones. This probably results from weight bearing on incompletely ossified bones
- Delayed development of the lateral styloid process.

The radiographs should also be inspected carefully to assess the presence of other pathological abnormalities of the physis which may influence management (Figure 1w.11 g–i). If the limb deformity is related to changes in the distal physis or epiphysis, treatment carries a reasonable prognosis if carried out well before closure of the physis. Malformation of the carpal bones warrants a poor prognosis. Incomplete ossification requires early identification and treatment for a successful outcome (see below). An angular limb deformity may be coexistent with rotation (usually outwards) of the limb, which should be assessed clinically. Radiographs can give limited information about rotation and the direction of the x-ray beam must be governed by this clinical assessment. In general terms, if a limb is outwardly rotated and a radiograph is obtained in line with the antebrachium, the carpal bones will appear slightly superimposed upon one another. If the x-ray beam is in line with the carpus however, the bones will be separated normally.

Incomplete carpal ossification

Incomplete ossification of the carpal bones is seen in very young foals (often dysmature or twins) and often with a carpal angular limb deformity. On radiographs the distal radial physis usually appears normal, but one or more of the carpal bones will be small and rounded, lacking the normal cuboidal shape (Figure 7.25).

Successful treatment requires prompt action in the first days of life to support (and if necessary straighten) the limb in a cast, until ossification of the affected bones is normal.

Osteochondroma

Osteochondromata are most frequently identified radiographically, on the caudodistal aspect of the radius in the metaphyseal region in the middle one-third of the bone. They are variable in size and shape, and may have an irregular outline (Figure 7.26). It may be possible to identify a communication with the marrow cavity of the radius. Although they may be benign and not associated with clinical signs, they may result in lameness, often with distension of the carpal sheath and lacerations of the deep digital flexor tendon. The latter can be identified ultrasonographically. These lesions are usually solitary, but may be associated with lesions elsewhere. They can be removed surgically, with a good prognosis for return to work.

Downloaded From Vet-eBooks.com



Figure 7.25 Dorsopalmar image of a carpus of a Quarterhorse foal, born at 323 days of gestation, obtained 6 days after birth. Lateral is to the right. The carpal bones are incompletely ossified; note their rounded contour. Note also the incompletely ossified separate centre of ossification of the lateral styloid process of the ulna.

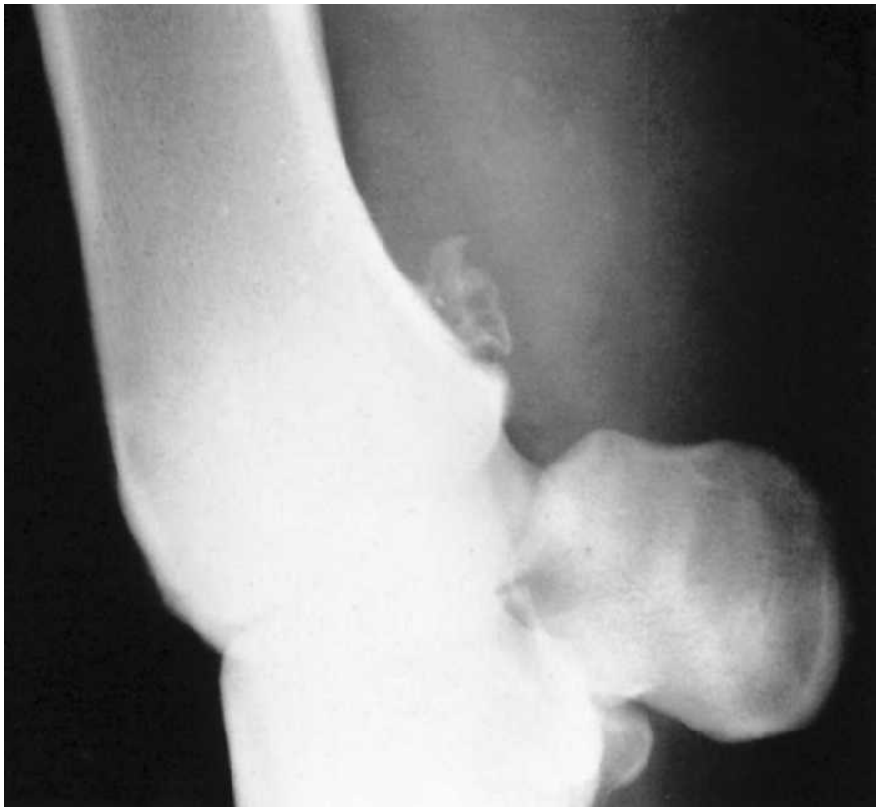


Figure 7.26 Lateromedial image of the distal aspect of a radius of a mature horse. There is a solitary osteochondroma on the caudal distal aspect of the radius, which was associated with distension of the carpal sheath and severe lameness. After surgical removal of the osteochondroma the clinical signs resolved.

Downloaded From Vet-eBooks.com

Carpal subluxation

Carpal subluxation is rare and may occur at the antebrachiocarpal, middle carpal or carpometacarpal joints. The latter site is most common. There may be concurrent fractures of several bones resulting in carpal instability. Occasionally stressed radiographic views are required to confirm the diagnosis. The prognosis for athletic function is poor.

Carpal fractures

Chip fractures of the carpal bones

Chip fractures occur frequently, most commonly in racehorses (Figure 7.27), but they also occur in sports horses, especially event horses and endurance horses. They may be defined as fractures that involve only one joint surface of the bone. Identification may require several oblique views, although they may be most readily observed on a lateromedial (flexed) image.

The most common sites for chip fractures are:

- The distal border of the dorsal aspect of the radius
- The distal dorsal aspect of the radial carpal bone (slightly to the medial side of the midline) and the opposing radial facet of the third carpal bone
- The distal dorsal aspect of the intermediate carpal bone.

Less commonly fractures occur in the proximal aspect of the radial and intermediate carpal bones.



Figure 7.27 Lateromedial (flexed) image of a carpus, showing a non-displaced chip fracture of the distal dorsal aspect of the radial carpal bone (arrows). The fracture was poorly demonstrated on other views. Note the entheseous new bone on the dorsal aspect of the intermediate carpal bone (arrow head).

Downloaded From Vet-eBooks.com

Lameness due to small fracture fragments may resolve with rest. Surgical removal should always be considered in cases in which horses are required to return to athletic performance, and in cases with larger fragments. A good prognosis can generally be given, provided that no other lesions are present. A degree of cartilage damage will have occurred and degenerative joint disease may subsequently develop. The integrity of the palmar intercarpal ligaments is important. The response of the parent bone is also important. The development of a radiopaque line for example, on the distal dorsal aspect of the radial carpal bone, represents secondary bone healing and is a poor prognostic sign. Chip fractures can also involve the lateral, medial and palmar aspects of the carpal bones. These are less common and carry a more guarded prognosis.

Large carpal chip fractures with good osseous infrastructure may be best treated using internal fixation, to minimise disruption of the articular surface of the bone. Osteochondral fragments on the palmar aspect of the joint may be seen in conjunction with dorsal fragments in racehorses. They may also arise dorsally and migrate palmad. Multiple small fragments warrant a more guarded prognosis for return to racing.

Degenerative joint disease (see above, 'Degenerative joint disease') may be pre-existing and may have predisposed to a fracture. The radiographs should be carefully scrutinised to evaluate the entire carpus, both for evidence of degenerative joint disease and for the presence of more than one fracture. Since fractures frequently occur bilaterally, both carpi should be examined radiographically.

Fractures on the palmar aspect of the carpal joints alone are usually the result of trauma, for example a fall or poor recovery from general anaesthesia (Figure 7.28a). However, they have also occurred during recovery from general anaesthesia when no untoward event has been seen, despite careful observation. Fractures usually involve the palmar aspect of the radial and/or intermediate carpal bones, and may be chip fractures or frontal plane fractures. They may initially be minimally distracted and are easily missed. Clinical signs may be overlooked unless the reaction to flexion of the carpus is assessed. Acquisition of both weight-bearing and lateromedial (flexed) and oblique images is recommended. More than one bone may be fractured. During flexion, minimally displaced fragments may be pulled in a palmar direction, facilitating their identification (Figure 7.28b). There may also be 'crush' injuries of the palmar aspect of the radial or intermediate carpal bones, resulting in ill-defined radiolucent areas in the palmar aspect of the bone. Although such fragments can be removed surgically, rapid onset of degenerative joint disease often occurs.

Slab fractures

Slab fractures (involving both proximal and distal articular surfaces) occur most commonly at the dorsal aspect of the third, fourth or radial carpal bones (Figure 7.29). These fractures can usually be detected on lateromedial radiographs, but dorsoproximal-dorsodistal oblique (flexed) views should always be obtained to ascertain the extent and degree of comminution of the fracture. This view will also show fractures that are not easily recognised on lateromedial views, and may show increased opacity of the third carpal bone (see 'Sclerosis of the third carpal bone', above). Slab fractures have also been recorded at the palmar aspect of the third carpal bone.

Downloaded From Vet-eBooks.com

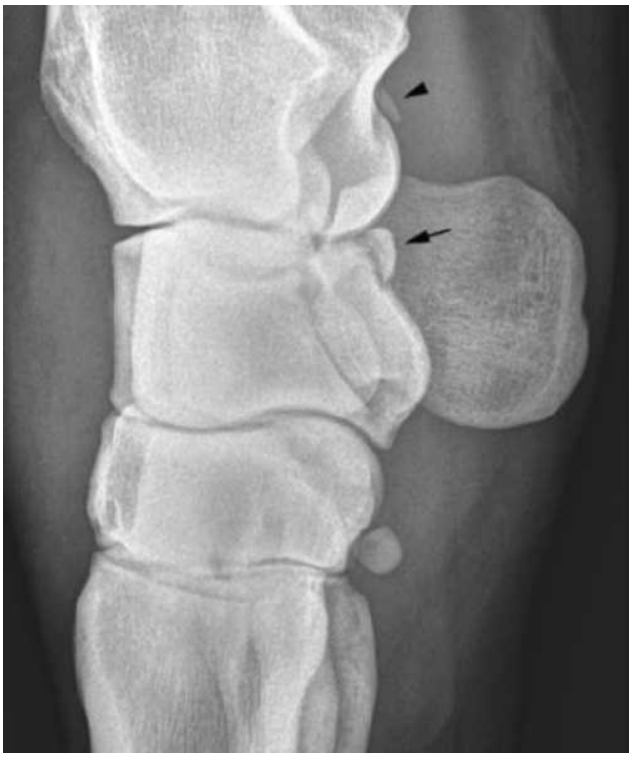


Figure 7.28(a) Dorsal 75° medial-palmarolateral oblique image of a carpus of an 8-year-old Warmblood dressage horse. The horse had undergone general anaesthesia for unrelated surgery 5 weeks previously and showed forelimb lameness accentuated by carpal flexion when undergoing routine reexamination. There is a discrete osseous opacity on the distal caudal aspect of the radius (arrow head) and a slightly displaced fragment on the proximopalmar aspect of the radial carpal bone (arrow). Note also the presence of a first carpal bone.



Figure 7.28(b) Lateromedial (flexed) image of the same carpus as in Figure 7.28(a). There are osseous fragments on the proximopalmar aspects of both the radial and intermediate carpal bones (arrows). Note also the small opacity proximal to the accessory carpal bone.

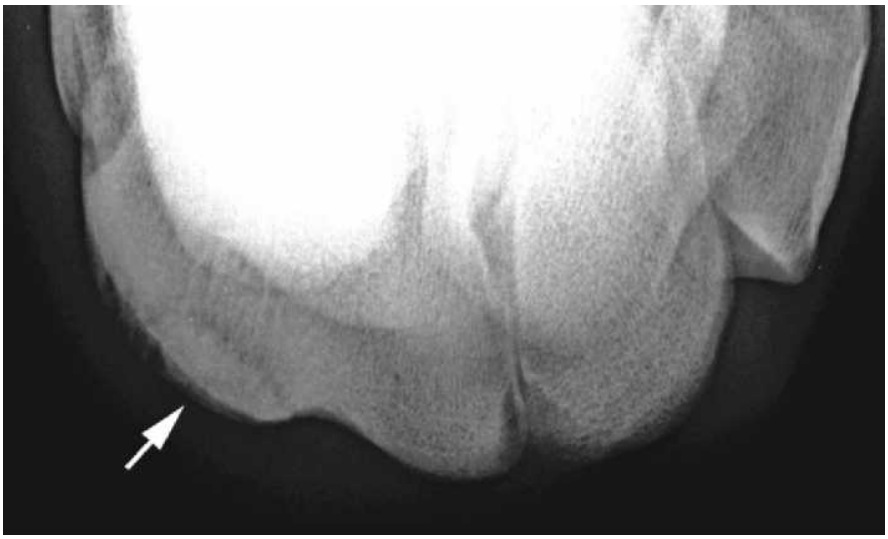


Figure 7.29 Dorsoproximal-dorsodistal oblique (flexed) image of the distal row of carpal bones of a 5-year-old Thoroughbred hurdler. Lateral is to the right. There is a diffuse increased opacity and loss of trabecular architecture of the radial facet of the third carpal bone and a non-displaced dorsal (slab) fracture of the third carpal bone (arrow). Compare the trabecular pattern of the medial aspect of the third carpal bone with that of the fourth (see also Figure 7.20).

Downloaded From Vet-eBooks.com



Figure 7.30 Dorsoproximal-dorsodistal oblique (flexed) image of the distal row of carpal bones of a 6-year-old Thoroughbred hurdler. Lateral is to the right. There is intense diffuse increased opacity of the radial facet of the third carpal bone. There is an incomplete parasagittal fracture on the medial aspect of the radial facet of the third carpal bone (arrow). The radiolucent line is not sharp indicating some chronicity of the fracture.

Dorsal or oblique slab fractures of the radial and third carpal bones are usually repaired by lag screw fixation, but if the fracture fragment is very thin it may be removed.

Parasagittal fractures of the third carpal bone are generally only detectable on dorsoproximal-dorsodistal oblique (flexed) images (Figure 7.30). Internal fixation is possible, but a fair prognosis can be given for conservative treatment provided that there is minimal displacement and no degenerative joint disease.

Fractures of the accessory carpal bone

The most common fractures of the accessory carpal bone occur in a vertical or slightly oblique plane just palmar to the groove for the tendon of ulnaris lateralis, and may be the result of a fall or occur during exercise. There is often distension of the carpal sheath. The fractures may be simple or comminuted. Comminution may occur proximally and distally, often resulting in triangular-shaped fragments that may become displaced, especially during carpal flexion (Figure 7w.31a). Displacement between the main pieces of bone is more obvious during flexion. The flexor tendons that insert on the palmar aspect of the bone may result in the palmar fragment being pulled proximally and medially. Although the main fracture may be readily detected in a weight-bearing lateromedial image, comprehensive examination of the carpus is advised so that displaced fragments are not overlooked. Fragments may become displaced distally to the distal aspect of the carpal sheath, therefore radiographic examination of the metacarpus may also be indicated. Bone fragments may impinge on the deep digital flexor tendon, therefore ultrasonographic examination of the carpal sheath is also recommended. Tenoscopic removal of fragments may be indicated.

With prolonged rest (6–8 months), initially in a sleeve cast to limit carpal flexion, and restricted exercise, approximately 80% of horses with uncomplicated fractures return to work. Healing is usually by fibrous union and a lucent line persists. Some horses develop chronic lameness, and tenoscopic

Downloaded From Vet-eBooks.com

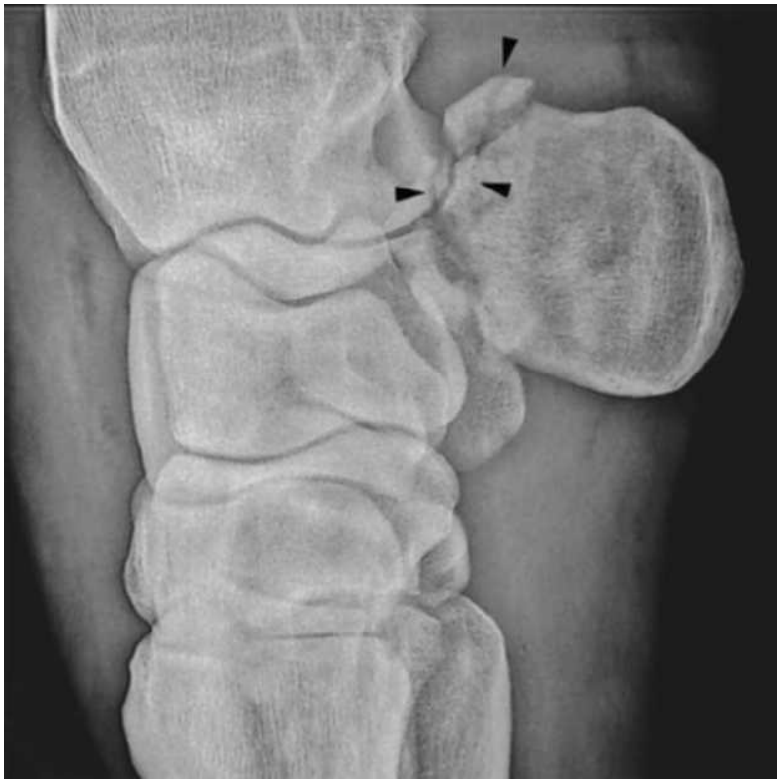


Figure 7.31(b) Dorsal 80° lateral-palmaromedial oblique image of a carpus of an 8-year-old Thoroughbred steeplechaser with acute onset of lameness after a fall, of 3 weeks' duration. There is a comminuted articular fracture (arrow heads) of the accessory carpal bone. The dorsal aspect of the accessory carpal bone has a rather heterogeneous opacity.

assessment of the carpal sheath and transection of the palmar retinaculum may be indicated. Internal fixation has been performed with variable results.

Articular chip fractures of the accessory carpal bone may occur involving either the articulation with the radius or the ulnar carpal bone. Fractures may be simple or comminuted. In some horses there may be a suspicion of a fracture in a lateromedial image, however the fracture may be partially superimposed over other carpal bones, and a dorsal 80° lateral-palmaromedial oblique view may give better visualisation (Figure 7.31b). The distal caudal aspect of the radius should be inspected carefully; focal radiolucent areas in the bone may reflect secondary degeneration or be the result of bone trauma at the time of initial injury (Figure 7w.31c). Surgical removal of articular chip fractures is usually required to prevent the rapid development of degenerative joint disease. If lameness persists, transection of the carpal retinaculum may be indicated.

Fractures of the second or fourth carpal bones

Fractures of the second or fourth carpal bones are often comminuted. These fractures are often accompanied by fractures of the proximal aspect of the second or fourth metacarpal bones. This will result in marked lateromedial instability of the carpometacarpal joint. Non-comminuted fractures require internal fixation but carry a guarded prognosis (see also 'Metacarpal fractures' in Chapter 6).

Downloaded From Vet-eBooks.com

Complex fractures of the carpus

Occasionally a horse sustains complex injuries of the carpus, with fractures of several bones. Accurate identification of all the fractures can be challenging because of the normal overlap between bones resulting in confusing radiolucent lines. One or more bones may be displaced, with resultant marked instability of the carpus. More accurate information can be obtained from computed tomography; however, the prognosis is extremely poor.

Fractures of the radius

Fractures of the radius are discussed in Chapter 8.

Additional figures

The book companion website at www.clinical-radiology-horse.com includes additional figures that are not included in the printed book or e-book formats. Please see '**About the Companion Website**' at the start of the book for details on how to access the website. These figures are prefixed with the letter 'w' in the printed book, e.g. Figures 1w.4c–f.

FURTHER READING

Auer, J., Smallwood, J., Morris, E., et al. (1982) The developing equine carpus from birth to 6 months. *A radiographic study. Equine Pract.* **4**, 35–55

Auer, J., Watkins, J., White, N., et al. (1986) Slab fractures of the fourth and intermediate carpal bones in 5 horses. *J. Am. Vet. Med. Assoc.* **188**, 595–601

Bailey, J., Barber, S., Fretz, P., Jacobs, K. (1984) Subluxation of the carpus in thirteen horses. *Can. Vet. J.* **25**, 311–314

Barba, M., McMaster, M., Valeria, A., et al. (2014) Carpal hyperextension in a percheron caused by palmar carpal ligament tear. *Equine Vet. Educ.* doi: 10:1111/eve.12073

Barr, A., Sinnott, M., Denny, H. (1990) Fractures of the accessory carpal bone in the horse. *Vet. Rec.* **127**, 432–434

Beinlich, C., Nixon, A. (2004) Radiographic and pathologic characterization of lateral palmar intercarpal ligament avulsion fracture in the horse. *Vet. Radiol. Ultrasound* **45**, 532–537

Bramlage, L., Schneider, R., Gabel, A. (1988) A clinical perspective on lameness originating in the carpus. *Equine Vet. J. Suppl.* **6**, 12–18

Dabareiner, R., White, N., Sullins, K. (1996) Radiographic and arthroscopic findings associated with subchondral lucency of the distal radial carpal bone in 71 horses. *Equine Vet. J.* **28**, 93–97

De Haan, C., O'Brien, T., Koblick, P. (1987) A radiographic investigation of third carpal bone injury in 42 racing thoroughbreds. *Vet. Radiol.* **28**, 88–92

Derungs, S., Fuerst, A., Haas, C., et al. (2001) Fissure fractures of the radius and tibia in 23 horses: a retrospective study. *Equine Vet. Educ.* **13**, 313–318

Dietze, A., Rendano, V. (1984) Fat opacities dorsal to the equine antebrachiocarpal joint. *Vet. Radiol.* **25**, 205–209

Dyson, S. (1988) Some observations on lameness associated with pain in the proximal metacarpal region. *Equine Vet. J. Suppl.* **6**, 43–52

Dyson, S. (1990) Fractures of the accessory carpal bone. *Equine Vet. Educ.* **2**(4), 188–190

Ellis, D. (1985) Some observations on bone cysts in the carpal bones of young thoroughbreds. *Equine Vet. J.* **17**, 63–65

Fischer, A., Stover, S. (1987) Sagittal fractures of the third carpal bone in horses: 12 cases (1977–1985). *J. Am. Vet. Med. Ass.* **191**, 106–108

Gertson, K.E., Dawson, H.A. (1976) Sagittal fracture of the third carpal bone in a horse. *J. Am. Vet. Med. Ass.* **169**, 633–634

Getman, L., Southwood, L., Richardson, D. (2006) Palmar carpal osteochondral fragments in racehorses: 31 cases (1994–2004). *J. Am. Vet. Med. Ass.* **228**, 1551–1558

Hopper, B., Steel, C., Richardson, L., Alexander, G., Robertson, I. (2004) Radiographic evaluation of sclerosis of the third carpal bone associated with exercise and the development of lameness in Standardbred horses. *Equine Vet. J.* **36**, 441–446

Kraus, B., Ross, M., Boston, R. (2005) Surgical and nonsurgical management of sagittal slab fractures of the third carpal bone in racehorses: 32 cases. *J. Am. Vet. Med. Ass.* **226**, 945–950

Lacourt, M., MacDonald, M., Rossier, Y., et al. (2013) Equine articular synovial cysts: 16 cases. *Vet. Surg.* **42**, 99–106

Lang, H., Nixon, A. (2015) Arthroscopic removal of discrete palmar carpal osteochondral fragments in horses: 25 cases (1999–2013). *J. Am. Vet. Med. Assoc.* **246**, 998–1004

Downloaded From Vet-eBooks.com

Lucas, J., Ross, M., Richardson, D. (1999) Postoperative performance of racing Standardbreds treated arthroscopically for carpal chip fractures: 176 cases (1986–1993). *Equine Vet. J.* **31**, 48–52

Magnusson, L., Ekman, S. (2001) Osteoarthritis of the antebrachiocarpal joint of 7 riding horses. *Acta. Vet. Scand.* **42**, 429–434

Malone, E., Les, C., Turner, T. (2003) Severe carpometacarpal osteoarthritis in older Arabian horses. *Vet. Surg.* **32**, 191–195

Martens, P. (1999) Identification of an ossicle associated with the palmar aspect of the carpus in a horse. *Vet. Radiol. Ultrasound* **40**, 342–345

Mason, T.A., Bourke, J.M. (1973) Closure of the distal radial epiphysis and its relationship to unsoundness in two year old thoroughbreds. *Aust. Vet. J.* **49**, 221–228

May, K., Holmes, L., Moll, H., Jones, J. (2001) Computed tomographic imaging of comminuted carpal fractures in a gelding. *Equine Vet. Educ.* **13**, 303–308

Mayrhofer, W., Stanek, C., Lutz, H., Hiedbrink, U. (2006) Wertigkeit klinischer, radiologischer und computertomographischer Befunde bei der Diagnostik von Karpalgelenkserkrankungen beim Pferd. *Pferdeheilkunde* **22**, 773–784

Minshall, G., Wright, I. (2014) Frontal plane fractures of the accessory carpal bone and implications for the carpal sheath of the digital flexor tendons. *Equine Vet. J.* doi:10:1111/evj.122003

Murray, R. (2007) Magnetic resonance imaging of the equine carpus. *Clin. Techniques Equine Pract.* **6**, 86–95

Myers, V.S. (1965) Confusing radiological variation at the distal end of the radius of the horse. *J. Am. Vet. Med. Ass.* **147**, 1310–1312

Nagy, A., Dyson, S. (2012) Magnetic resonance imaging findings in the carpus and proximal metacarpal region of 50 lame horses. *Equine Vet. J.* **44**, 163–168

Newman, J.C., Lustgarten, M., Berman, K.G., Vivrette, S., Redding, W.R. (2013) Surgical treatment of synovial osteochondromatosis in the middle carpal joint of a pony. *Equine Vet. Educ*. **26**, doi:10.1111/eve.12093

Nixon, A., Schachter, B., Pool, R. (2004) Exostoses of the caudal perimeter of the radial physis as a cause of carpal synovial sheath tenosynovitis and lameness in horses: 10 cases (1999–2003). *J. Am. Vet. Med. Ass.* **224**, 264–270

Oosterlinck, M., Pille, F., Gasthuys, F., et al. (2009) Spontaneous ankylosis of the carpometacarpal joint in a Paint Horse. *Equine Vet. Educ.* **21**, 452–454

Park, R.D., Morgan, J.P., O'Brien, T. (1970) Chip fractures in the carpus of the horse; a radiographic study of their incidence and location. *J. Am. Vet. Med. Ass.* **157**, 1305–1312

Pepe, M., Becatti, F., Giallet, R., et al. (2013) Bilateral rupture of the palmar carpal ligament in a horse suffering from acute diaphragmatic hernia. *J. Equine Vet. Sci.* **33**, 57–61

Platt, D., Wright, I. (1997) Chronic tenosynovitis of the carpal extensor tendon sheaths in 15 horses. *Equine Vet. J.* **29**, 11–17

Schneider, R., Bramlage, A., Barone, L., Kantrowitz, B. (1988) Incidence, location and classification of 371 third carpal bone fractures in 313 horses. *Equine Vet. J.* **20** (Suppl. 6), 33–42

Schroeder, O., Aceto, H., Boyle, A. (2013) A field study of kick injuries to the radius and tibia in 51 horses (2000–2010). *Can. Vet. J.* **54**, 271–275

Simon, V., Dyson, S. (2010) Radiologic anatomic variation of the carpus in horses with carpal lameness and control horses. *Vet. Radiol. Ultrasound* **51**, 601–606

Simon, V., Dyson, S. (2012) Radiological and scintigraphic evaluation of the third carpal bone of control and horses with carpal lameness. *Vet. Radiol. Ultrasound* **53**, 465–473

Specht, T., Nixon, A., Colahan, P. (1988) Subchondral cyst-like lesions in the distal portion of the radius in 4 horses. *J. Am. Vet. Med. Assoc.* **193**, 949–952

Stephens, P., Richardson, D., Spencer, F. (1988) Slab fractures of the third carpal bone in Standardbreds and Thoroughbreds: 155 cases (1977–1984). *J. Am. Vet. Med. Assoc.* **193**, 353–358

Ter Braake, F., Rijkenhuizen, A. (2001) Endoscopic removal of osteochondroma at the caudodistal aspect of the radius: and evaluation in 4 cases. *Equine Vet. Educ.* **13**, 90–93

Toth, F., Schumacher, J., Newman, S. (2009) Calcinosis circumscripta in the antebrachiocarpal joint of a horse. *Equine Vet. Educ.* **21**, 584–588

Thrall, D.E., Lebel, J.L., O'Brien, T.R. (1971) A five-year survey of the incidence and location of equine carpal chip fractures. *J. Am. Vet. Med. Ass.* **158**, 1366–1368

Uhlorn, H., Ekman, S., Haglund, A., Carlsten, A. (1998) The accuracy of the dorsoproximal-dorsodistal projection in assessing third carpal bone sclerosis in Standardbred trotters. *Vet. Radiol. Ultrasound* **39**, 412–417

Uhlorn, H., Carlsten, J. (1999) Retrospective study of subchondral sclerosis and lucency in the third carpal bone of Standardbred trotters. *Equine Vet. J.* **31**, 500–505

Waselau, M., Bertone, A., Green, W. (2006) Computed tomographic documentation of a comminuted fourth carpal bone fracture associated with carpal instability treated by partial carpal arthrodesis in an Arabian filly. *Vet. Surg.* **35**, 618–625

Whitton, C., Kannegeiter, N., Rose, R. (1997) The intercarpal ligaments of the equine mid carpal joint. Part 3. Clinical observations in 32 racing horses with midcarpal joint disease. *Vet. Surg.* **26**, 374–381

Wilke, M., Nixon, A., Malark, J., et al. (2001) Fractures of the palmar aspect of the carpal bones in horses: 10 cases (1984–2000). *J. Am. Vet. Med. Ass.* **219**, 801–804

Wong, D., Scaratt, W., Maxwell, V., Moon, M. (2003) Incomplete ossification of the carpal, tarsal and navicular bones in a dysmature foal. *Equine Vet. Educ.* **15**, 72–81

Wright, I., Minshall, G. (2012) Clinical, radiological and ultrasonographic features in 22 horses with caudal distal radial osteochondromata. *Equine Vet. J.* **44**, 319–324

Wright, I., Smith, M. (2011) The use of small (2.7 mm) screws for arthroscopically guided repair of carpal chip fractures. *Equine Vet. J.* **43**, 270–279

Young, A., O'Brien, T., Pool, R. (1988) Exercise related sclerosis in the third carpal bone of the racing thoroughbred. *Proc. Am. Ass. Equine Pract.* **34**, 339–346

Downloaded From Vet-eBooks.com

Downloaded From Vet-eBooks.com

Chapter 8
The shoulder, humerus, elbow and radius

Scapulohumeral (shoulder) joint and humerus

RADIOGRAPHIC TECHNIQUE

Equipment

The scapulohumeral joint may be radiographed with the horse standing if a high-output x-ray machine is available. Better-quality radiographs are generally obtained with the horse under general anaesthesia in lateral recumbency. With the horse anaesthetised, positioning is easier and longer exposure times can be used without risk of movement, so a lower output x-ray machine may be used. The radiation hazard to personnel is also reduced. Digital systems, or rare earth screens and appropriate film, are essential due to the high exposures required to penetrate the large muscle mass in this area. Whether using conventional film–screen combinations or digital imaging, a grid is recommended to reduce the effects of scattered radiation, and lead should be placed behind the cassette to limit backscatter. There is less soft tissue to penetrate cranially, and therefore it may be necessary to repeat a view with different exposure factors in order to assess both the cranioproximal aspect of the humerus and the more caudally situated scapulohumeral joint. For mediolateral (extended) radiographs obtained with the horse standing, the cassette should be mounted in a holder and not be hand-held. Both mediolateral (extended) and oblique (extended) views are required for a complete assessment of the scapulohumeral joint, and in selected cases arthrography may yield valuable additional information.

Positioning

Mediolateral (extended) view

STANDING

The forelimb to be examined is positioned next to the cassette/imaging plate and the limb is protracted as much as the horse will comfortably allow, to avoid superimposition of the left and right scapulohumeral (shoulder) joints (Figure 8.1). The toe of the foot should be rested on the handler's knee, or a stand, to minimise movement and allow repeat radiographs to be obtained

Clinical Radiology of the Horse, Fourth Edition. Janet A. Butler, Christopher M. Colles, Sue J. Dyson, Svend E. Kold and Paul W. Poulos.
© 2017 John Wiley & Sons, Ltd. Published 2017 by John Wiley & Sons, Ltd.
Companion website: www.clinical-radiology-horse.com

Downloaded From Vet-eBooks.com

CHAPTER 8
The shoulder, humerus, elbow and radius

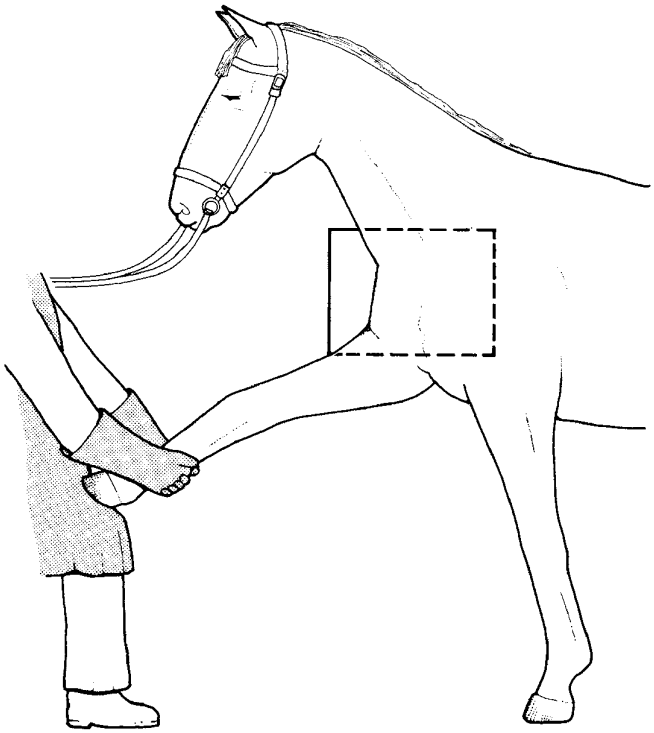


Figure 8.1 Positioning of the horse and cassette/imaging plate to obtain a mediolateral (extended) image of the scapulohumeral joint. The forelimb to be examined should be extended, but without lifting it too high to avoid superimposition of the cervical vertebrae.

with a minimum of change in positioning. If possible the shoulder joint should be superimposed over the trachea, to provide the best image. Some horses resist protraction of the limb and this may result in movement blur and partial superimposition of the left and right shoulder joints. Light sedation or analgesia may be helpful, but the horse may relax and lower its neck so that a larger proportion of the distal aspect of the scapula is superimposed over the cervical and thoracic vertebrae. Raising the head and neck and supporting the head can help to minimise this. If the limb is raised excessively the caudal neck vertebrae may be partially superimposed over the shoulder. The use of an analgesic such as butorphanol facilitates the examination of horses suffering severe pain when protracting the limb.

The x-ray beam is centered on the trachea, 5-8 cm in front of the cranial border of the scapula, on the weight-bearing limb. The beam will be centered approximately on the greater tubercle of the humerus of the raised limb. It is recommended that a small marker is placed on the skin where the beam is centered, so that it can be accurately repositioned if repeat radiographs are required.

The distal two-thirds of the humerus is examined using a similar technique, but centering further distally. This examination is usually only indicated when a fracture is suspected and associated pain often makes protraction of the limb very difficult. High exposure factors may therefore be required in order to obtain adequate penetration of the large muscle mass.

LATERAL RECUMBENCY

The anaesthetised horse is placed in lateral recumbency, lying on the limb to be radiographed. This limb is protracted, the contralateral forelimb is retracted and the neck is extended. It may be helpful to restrain the forelimbs using ropes. The position of the endotracheal tube is adjusted so

Downloaded From Vet-eBooks.com

that its distal end is not superimposed over the scapulohumeral joint. The examination is performed most easily if the horse is lying on a cassette tunnel, to avoid having to lift the horse in order to place the cassette beneath it. With appropriate sedation a foal may be restrained in lateral recumbency without the need for general anaesthesia.

The x-ray beam is centered approximately 10cm cranial to the distal aspect of the scapular spine of the limb contralateral to that being radiographed. This is approximately equivalent to centering at the level of the greater tubercle of the humerus of the protracted limb. It is helpful to mark the point on the skin where the beam is centered (e.g. with sticky tape) so that appropriate corrections can be made for subsequent exposures.

If the scapulohumeral joint is positioned distal to the trachea, up to one-third of the distal aspect of the scapula can be seen without superimposition of the cervical and thoracic vertebrae and the ribs. Evaluation of the proximal two-thirds of the scapula is difficult because of the superimposed bones and the thinness of the scapula. If either the medial or lateral aspects of the margins of the glenoid cavity of the scapula or the proximal articular surface of the humerus are superimposed over the proximal or distal borders of the trachea, the summation of opacities makes interpretation difficult and additional radiographs may be required. It is always helpful to position the scapulohumeral joint over the trachea. This can be achieved in the standing horse, although it may be easier if the horse is anaesthetised.

The distal two-thirds of the humerus is examined using a similar technique, but centering further distally. This examination is usually only indicated when a fracture is suspected, which may mean that anaesthesia is contra-indicated.

Cranial 45° medial-caudolateral oblique (extended) view

The cranial 45° medial-craniolateral oblique (extended) view is most easily obtained with the horse standing. The forelimb to be examined is protracted and the cassette is held caudal to the shoulder muscle mass in order to position it sufficiently far medially (Figure 8.2). This inevitably results in some magnification. A grid is unnecessary, which allows lower exposure factors. The x-ray beam is centered at the level of the greater tubercle of the humerus.

Alternatively a caudolateral-craniomedial oblique (extended) view may be obtained, depending largely on the radiographer's preference.

Caudolateral-craniomedial oblique view

The caudolateral-craniomedial oblique view is obtained with the horse weight bearing on the affected limb. The x-ray machine is positioned close to the thorax, behind the shoulder to be examined. A horizontal x-ray beam is used, angled at approximately 40° lateral to the sagittal midline (i.e. caudal 40° lateral-craniomedial oblique view). The x-ray cassette is positioned cranial to the shoulder, against the horse's neck, perpendicular to the x-ray beam.

Cranial 45° medial-caudolateral oblique and caudal 40°lateral-craniomedial oblique views help to clarify some intra-articular lesions, especially those in the sagittal plane. They also permit identification of some fractures not visible in a mediolateral (extended) projection and help to determine the direction of a luxation of the humerus.

Downloaded From Vet-eBooks.com



Figure 8.2 Positioning of the horse and imaging plate to acquire a cranial 45° medial-caudolateral oblique (extended) image of the scapulohumeral joint. The forelimb to be examined is protracted, but less extension is needed compared to the position required for a mediolateral image.

Cranioproximal-craniodistal oblique (flexed) 'skyline' view of the proximal aspect of the humerus

The cranioproximal-craniodistal oblique (flexed) view can be obtained either in the standing horse (as described) or with the horse under general anaesthesia (when equivalent positioning needs to be achieved). The limb is held with the carpus and elbow flexed (Figure 8.3), with the x-ray cassette positioned horizontally distal to the humeral tubercles. The horse's head and neck are turned away from the limb to be examined. The x-ray machine is positioned proximal to the shoulder and the x-ray beam is directed ventrally, centered on the humeral tubercles. This view helps to identify a variety of lesions, including fractures of the greater and lesser tubercles of the humerus, which may be difficult to identify in other projections.

Downloaded From Vet-eBooks.com

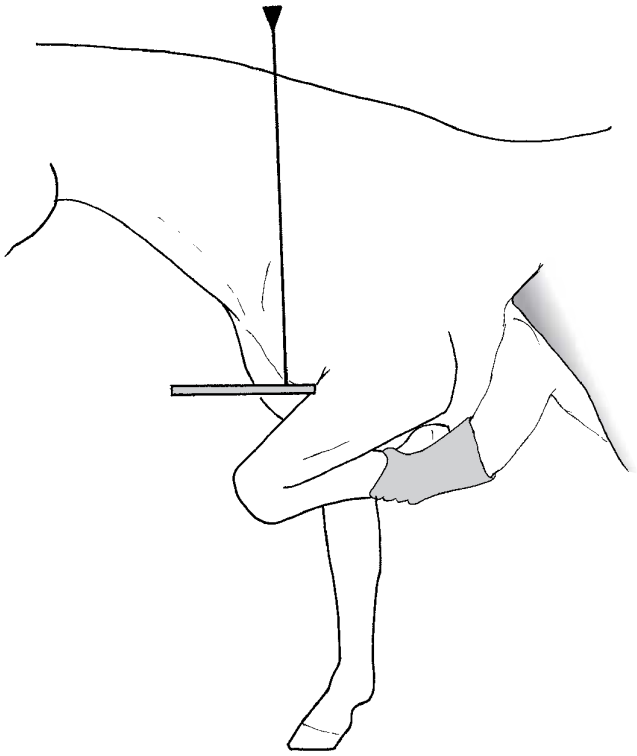


Figure 8.3 Positioning to obtain a cranioproximal-craniodistal oblique (flexed) view of the proximal aspect of the humerus. The limb is held with the carpus flexed maximally. The imaging plate is held horizontally distal to the shoulder. The horse's head and neck are turned away from the limb to be examined. The x-ray beam is directed ventrally.

Arthrography

Arthrography can be performed with the horse standing or in lateral recumbency under general anaesthesia. In the latter position the technique is more complicated because, after injecting the contrast medium with the limb to be examined uppermost, the horse must then be turned over for radiography. A small volume (7–10ml) of a 60% mixture of sodium and meglumine amidotrizoate (Urografin 60%, Schering AG) is recommended. Dilution of the contrast agent with a balanced polyionic electrolyte solution may help definition of the articular cartilage. The technique can be used to highlight articular cartilage defects and subtle bone lesions and to identify dissecting cartilage flaps in cases of osteochondrosis.

RADIOGRAPHIC ANATOMY, NORMAL VARIATIONS AND INCIDENTAL FINDINGS

Birth to 3 years old

Scapula

The scapula has four centres of ossification: the scapular cartilage, the body of the scapula, the cranial part of the glenoid cavity of the scapula and the supraglenoid tubercle (Figure 8.4). The latter two may be incompletely ossified at birth and have a fuzzy, irregular outline. The cranial part of the glenoid cavity of the scapula fuses with the body by 5 months after birth. The physis of the supraglenoid tubercle closes by 12–24 months after birth.

Downloaded From Vet-eBooks.com

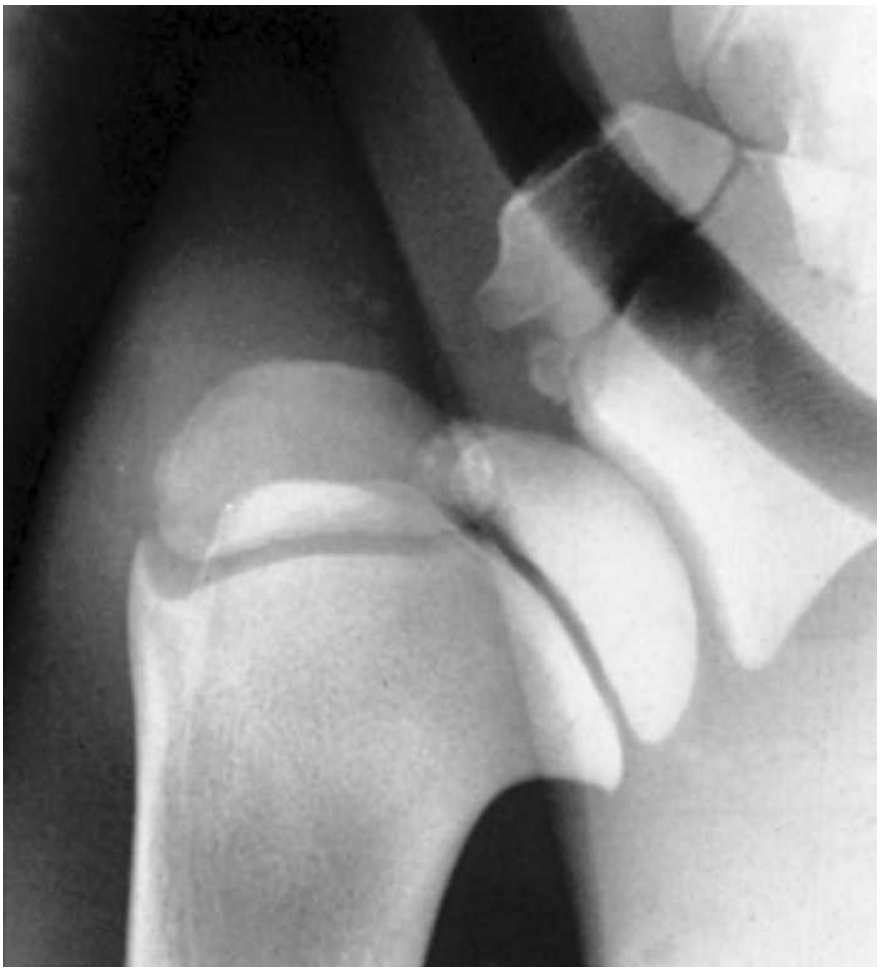


Figure 8.4 Mediolateral (extended) image and diagram of a shoulder of a 12-day-old foal. The cranial centre of ossification of the glenoid cavity of the scapula and the lesser tubercle of the humerus are incompletely ossified. The curvature of the glenoid cavity of the scapula is more shallow and the ventral angle is more rounded compared with an adult shoulder.

Humerus

The proximal aspect of the humerus ossifies from three centres: the diaphysis, the humeral head and the greater tubercle. The lesser tubercle develops from the same ossification centre as the humeral head. It is usually incompletely ossified at birth and has a fuzzy outline and a granular opacity. The centres of ossification of the proximal humeral epiphysis merge by 3–4 months of age and gradually assume a more adult shape; the proximal humeral physis closes by 24–36 months.

Skeletally mature horse

Mediolateral (extended) image

There is little variation in the normal radiographic anatomy of the scapulo-humeral joint except as a result of positioning. The medial aspect of the periphery of the glenoid cavity of the scapula is projected proximal to the lateral aspect and is smoothly curved (Figure 8.5a). Its caudal edge, the ventral angle of the scapula, is sharply pointed. The lateral aspect of the glenoid cavity of the scapula is seen as a relatively less opaque area immediately distal to the medial aspect and may make the latter appear poorly defined. It may be superimposed over the humeral head, resulting in a relatively lucent, roughly

Downloaded From Vet-eBooks.com

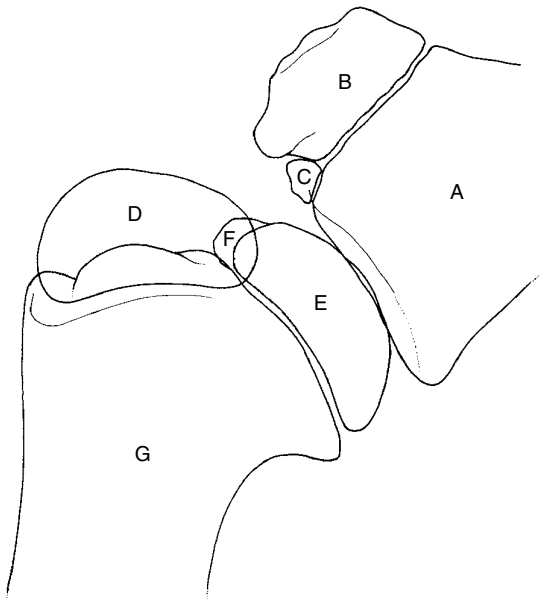


Figure 8.4 *Cont'd* A = body of scapula, B = ossification centre for the supraglenoid tubercle and coracoid process, C = ossification centre for the cranial part of the glenoid of the scapula, D = ossification centre for the greater tubercle of the humerus, E = ossification centre for the humeral head and lesser tubercle, F = incompletely ossified lesser tubercle, G = diaphysis of humerus.

triangular area in the cranial part of the humeral head which should not be mistaken for a lucent lesion in the subchondral bone of the humeral head (Figure 8.5b). The lateral aspect of the glenoid cavity forms the proximal border of this lucency.

There is a clearly demarcated band of radiopaque bone, of uniform width, around the caudal two-thirds of the glenoid cavity of the scapula. In approximately 5% of horses there is a small lucent zone (up to 0.5 cm diameter) in the middle of the glenoid cavity of the scapula within the opaque band (Figure 8.6). A faint vertical lucent line is sometimes seen at the junction of the cranial and middle thirds of the glenoid cavity. This represents the glenoid notch. Cranial to the glenoid notch the opaque band is usually narrower.

The outline of the humeral head is smoothly curved. The greater, lesser and intermediate tubercles may be slightly separated or superimposed upon each other depending on the positioning of the humerus (Figures 8.5a and 8.7).

There is reasonable congruity between the outlines of the glenoid cavity of the scapula and the humeral head, although in some horses the glenoid cavity of the scapula is more curved, resulting in apparent widening of the joint space in the middle of the joint.

Cranial 45° medial-caudolateral oblique (extended) image

In a cranial 45° medial-caudolateral oblique (extended) image the width of the scapulohumeral joint space is more variable than in a mediolateral image. The cranial eminence of the lesser tubercle, the intermediate tubercle and the intertubercular groove are highlighted and the deltoid tuberosity is outlined (Figure 8.8). The 'lip' of the deltoid tuberosity, which curves caudolaterally, may be projected in this view and should not be confused with a chip fracture (Figure 8.9). Occasionally there is a smoothly outlined concave depression in the centre of the humeral head, with no alteration in the underlying bone architecture, and should be considered an incidental abnormality (Figure 8.10).

Downloaded From Vet-eBooks.com

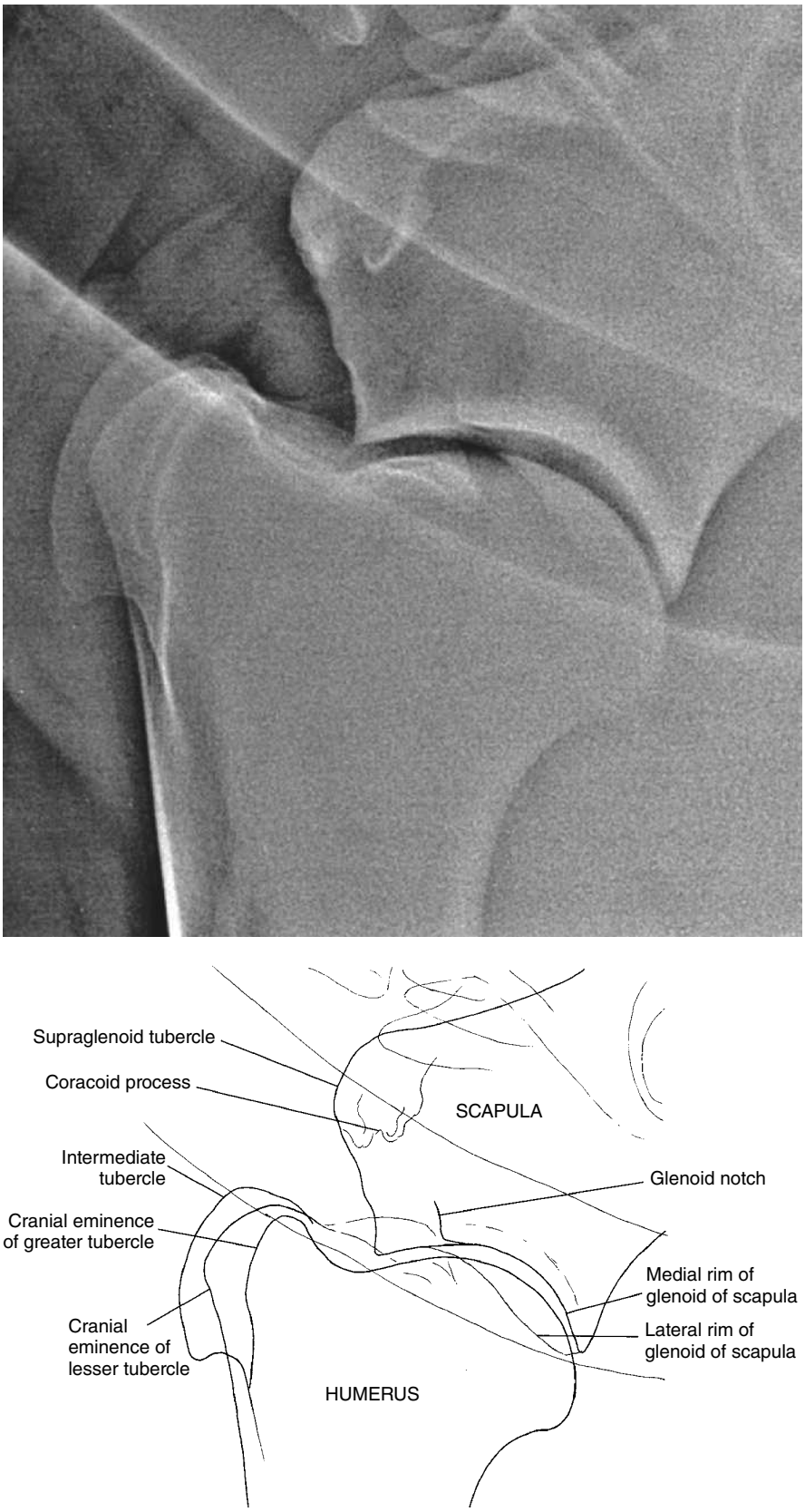


Figure 8.5(a) Mediolateral (extended) image and diagram of a normal adult scapulohumeral joint (compare with Figure 8.7). See text regarding normal anatomy, above.

Downloaded From Vet-eBooks.com



Figure 8.5(b) Coned down mediolateral (extended) image of a normal scapulohumeral joint, superimposed over the trachea. Note the congruity of the articulation between the scapula and the humerus and the sharply pointed ventral angle of the scapula (white arrow). The lucent line (black arrows) traversing the humeral head is normal, an edge effect created by the overlying lateral rim of the glenoid cavity of the scapula.

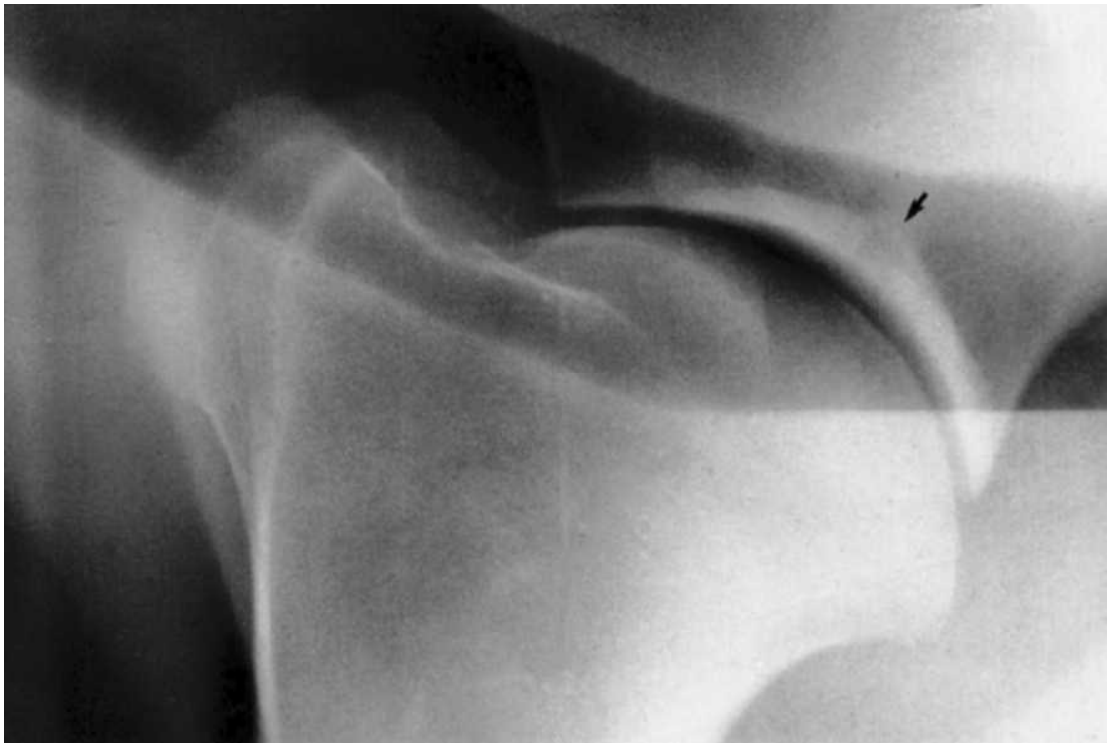


Figure 8.6 Mediolateral (extended) image of a normal adult scapulohumeral joint. There is an irregularly shaped radiolucent area (arrow) in the subchondral bone of the middle of the glenoid cavity of the scapula. This can be an incidental abnormality.

Downloaded From Vet-eBooks.com

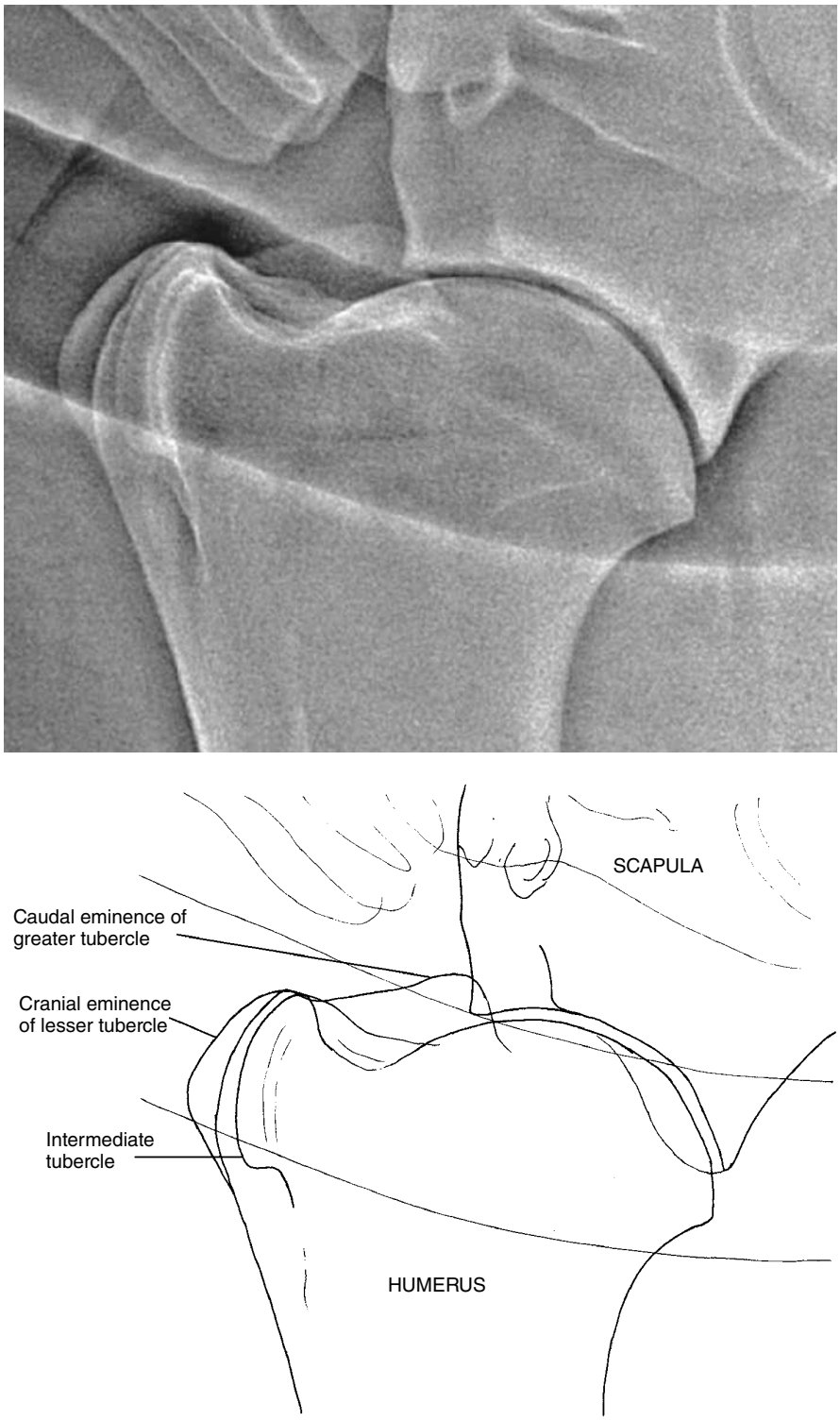


Figure 8.7 Mediolateral (extended) image and diagram of a normal adult scapulohumeral joint (compare with Figure 8.5a). Due to slight differences in position of the proximal aspect of the humerus, the greater tubercle appears more prominent.

Downloaded From Vet-eBooks.com



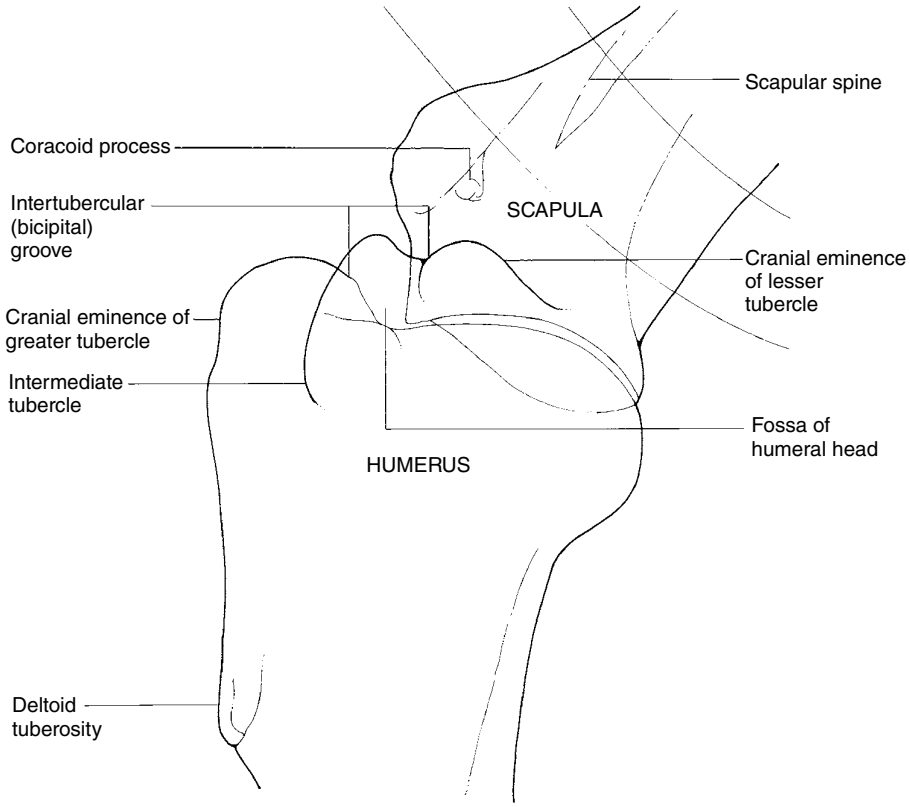


Figure 8.8 Cranial 45° medial-caudolateral oblique image and diagram of a normal adult scapulohumeral joint.

Downloaded From Vet-eBooks.com



Figure 8.9 Craniomedial-caudolateral oblique (extended) image of a normal adult humerus. The 'lip' of the deltoid tuberosity is projected (arrow) and should not be confused with a chip fracture.

Cranioproximal-craniodistal oblique (flexed) image of the proximal aspect of the humerus

The cranioproximal-craniodistal oblique (flexed) view skylines the humeral tubercles, the medial (lesser), intermediate and lateral (greater), which should have a smooth contour (Figure 8.11).

Arthrography

A narrow band of contrast medium outlines the articular surfaces of the scapula and humerus (Figure 8.12). Some contrast medium may also be superimposed over the distal aspect of the scapula and the humeral

Downloaded From Vet-eBooks.com



Figure 8.10 Craniomedial-caudolateral oblique (extended) image of an adult scapulohumeral joint of a 10-year-old Warmblood showjumper. There is a smoothly marginated depression in the proximal aspect of the humerus (arrow) which was an incidental finding.

head. This outlines the proximal cul-de-sac of the scapulohumeral joint capsule and distal aspect of the joint capsule, respectively. In a small proportion of normal horses, arthrography will demonstrate communication between the scapulohumeral joint capsule and the intertubercular (bicipital) bursa.

SIGNIFICANT RADIOLOGICAL ABNORMALITIES

Osteochondrosis

Radiographic abnormalities associated with osteochondrosis are identified in the scapula, the humerus or both. The changes predominantly involve the caudal half of the joint and result in loss of congruity between the subchondral

Downloaded From Vet-eBooks.com

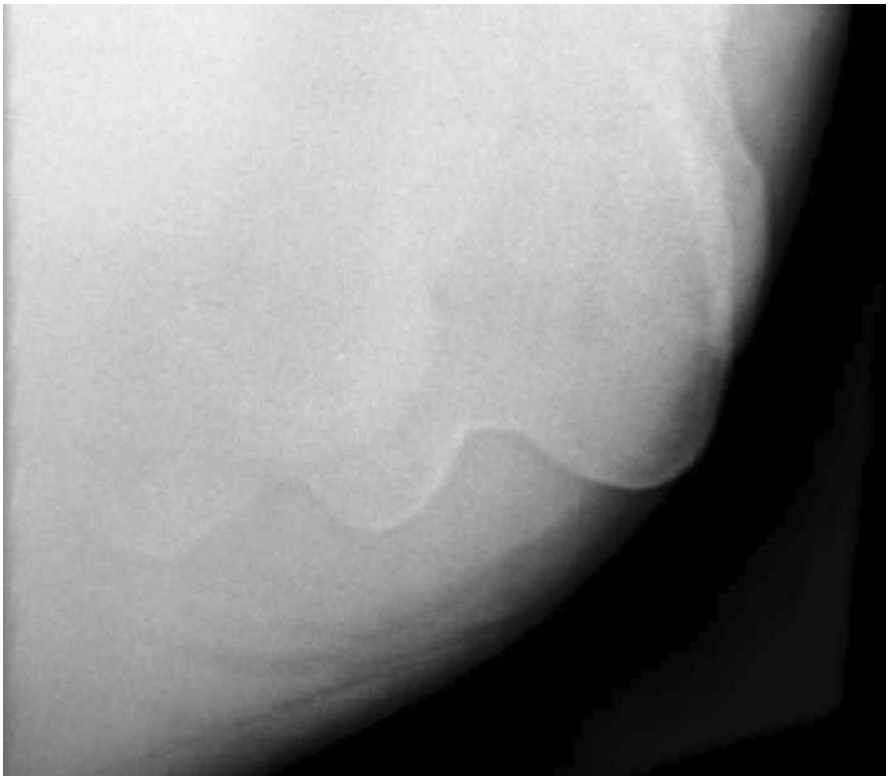


Figure 8.11 Cranioproximal-craniodistal oblique (flexed) image of the humeral tubercles of a normal adult horse (medial is to the left).

bone adjacent to the articular surfaces of the scapula and humerus. In some cases there is only subtle variation in contour of the articular surfaces (Figure 8.13a). In other cases there are extensive, irregularly outlined lucent zones in the subchondral bone, which may be surrounded by areas of increased opacity (Figure 8.13b). There is often flattening of the subchondral bone of the humeral head and/or the glenoid cavity of the scapula (Figure 8.13c). The caudoventral angle of the scapula, which is usually sharply pointed, may be modelled so that it is more bulbous, a sign of degenerative joint disease. The rim of the glenoid cavity of the scapula may have a blurred outline. Some of the modelling of the scapula and the humerus is due to secondary degenerative joint disease. Osteochondrosis may occur unilaterally or bilaterally, usually in horses less than 3 years of age. It causes a variable degree of lameness. Lameness may or may not be improved by intra-articular anaesthesia.

The majority of horses treated conservatively remain lame. Surgical treatment has given encouraging results in immature horses.

In older horses focal osteochondral lesions in the distal aspect of the scapula and the proximal aspect of the humeral head have been associated with lameness. Lesions include focal increased opacity proximal to the subchondral bone of the distal aspect of the scapula, small focal radiolucent zones at the distal aspect of the scapula and focal flattening of the humeral head. Arthroscopy invariably reveals associated cartilage defects. The aetiology of these lesions is uncertain; they may be the result of osteochondrosis or trauma. Surgical treatment is recommended.

Downloaded From Vet-eBooks.com



Figure 8.12 Mediolateral arthrogram of a normal adult scapulohumeral joint. This image was acquired with screen-film technology and a grid; the grid lines are prominent.

Osseous cyst-like lesions

Poorly defined lucent zones of irregular shape in the subchondral bone of either the scapula or the humerus are a manifestation of osteochondrosis (Figure 8.13b), but distinct, large, circular lucent areas (osseous cyst-like lesions) may be a different clinical condition (or conditions) and are considered separately here.

A small lucent area within the radiopaque rim of subchondral bone of the glenoid cavity of the scapula, mid-way between its cranial and caudal margins, has been identified in normal horses (Figure 8.6) and is of questionable clinical significance. However, horses have been reported which were rendered sound by intra-articular anaesthesia and had this as the only detectable radiographic 'abnormality'. Subsequent arthroscopic evaluation revealed focal lesions.

Downloaded From Vet-eBooks.com



Figure 8.13(a) Mediolateral (extended) image of the scapulohumeral joint of a 3-year-old Thoroughbred with osteochondrosis. There is a slight depression in the humeral head (arrow). Lameness was improved by both intra-articular anaesthesia and medication.

Osseous cyst-like lesions are not common. They may occur singly or there may be more than one (Figures 8.14a and 8.14b). They occur most frequently either in the middle of the distal aspect of the scapula or the middle of the humeral epiphysis, and are usually surrounded by a rim of radiopaque bone. Associated lameness is usually improved by intra-articular anaesthesia, although it may not be abolished. Lesions in the distal aspect of the scapula are usually close to the articular surface when first recognised, but appear to move further away with time and become surrounded by a broader rim of opaque bone, associated with which there may be improvement in lameness. Osseous cyst-like lesions in the distal aspect of the scapula occur most commonly in young horses, but are occasionally seen in association with sudden-onset lameness in mature horses. In older horses the cyst-like lesions are often more difficult to detect radiographically and may be easily missed if the radiograph is underexposed (Figure 8.14c). Secondary modelling of the ventral angle of the scapula is a variable feature. Not all osseous cyst-like lesions behave similarly and some in the proximal aspect of the humerus 'fill in' radiographically with resolution of lameness. Some young

Downloaded From Vet-eBooks.com



Figure 8.13(b) Mediolateral (extended) image of the scapulohumeral joint of a yearling Thoroughbred with osteochondrosis. There are extensive lucent areas in the subchondral bone of the distal aspect of the scapula with surrounding increased radiopacity. There is considerable modelling of the caudal one-third of the glenoid cavity of the scapula and its ventral angle, resulting in loss of congruity between the scapula and humerus. There is an ill-defined lucent area in the subchondral bone of the middle of the humeral head, but at post-mortem examination the overlying cartilage was intact and firmly adherent to the subchondral bone.



Figure 8.13(c) Mediolateral (extended) image of the scapulohumeral joint of a yearling Thoroughbred with osteochondrosis. There is extensive modelling of the distal aspect of the scapula and the proximal aspect of the humerus. The outline of the caudal aspect of the glenoid cavity and of the ventral angle of the scapula is rather blurred due to new bone formation. There are ill-defined lucent zones in the caudal distal aspect of the scapula.

Downloaded From Vet-eBooks.com



Figure 8.14(a) Mediolateral (extended) image of a scapulohumeral joint of a 2-year-old Thoroughbred. There is a well-defined single osseous cyst-like lesion in the distal aspect of the scapula, surrounded by a rim of increased radiopacity. When first identified several months previously, the lesion was smaller, closer to the articular surface and less well demarcated without a rim of increased opacity. There is no detectable modelling of the scapula (compare with Figure 8.14b)). Post-mortem examination revealed a true subchondral bone cyst.



Figure 8.14(b) Mediolateral (extended) image of a scapulohumeral joint of a 2-year-old Thoroughbred with two large osseous cyst-like lesions in the distal aspect of the scapula. Note the modelling of the ventral angle of the scapula. The horse ultimately raced successfully despite radiographic persistence of the lesions.

Downloaded From Vet-eBooks.com

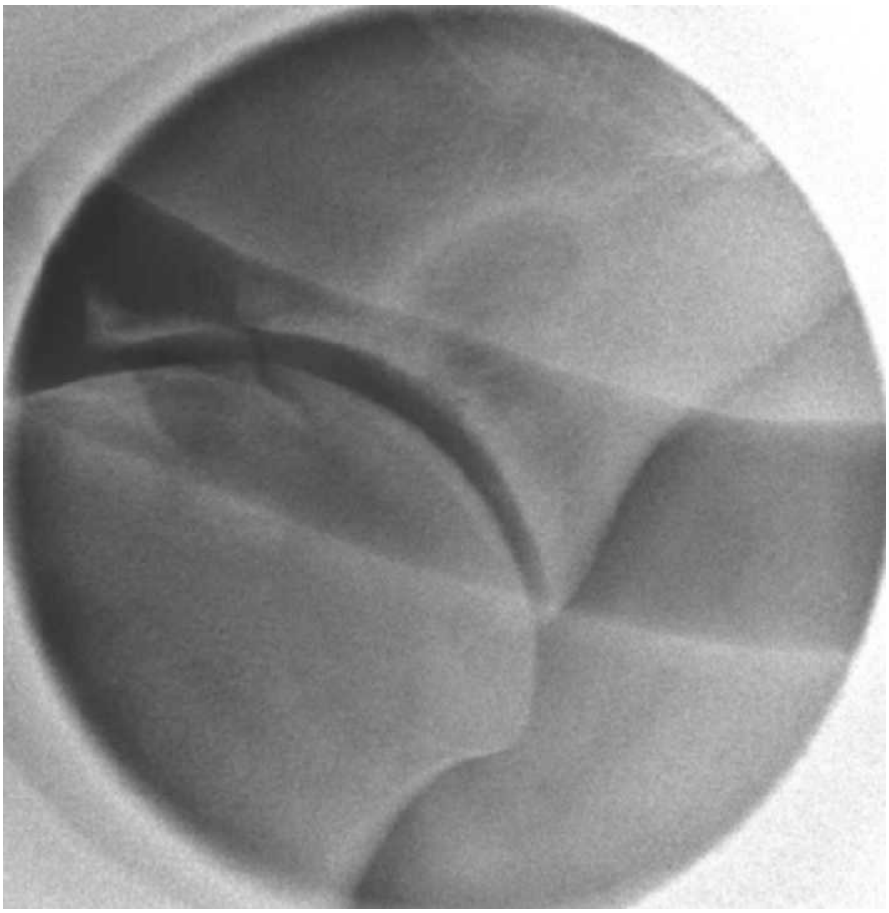


Figure 8.14(c) Coned mediolateral image of the left scapulohumeral joint of a 9-year-old Warmblood showjumper with sporadic lameness, which was also variable in severity. There is a large, well defined osseous cyst-like lesion in the centre of the distal aspect of the scapula, caudal to which are two less well defined areas of reduced radiopacity. Lameness was improved by intra-articular analgesia of the scapulohumeral joint.

horses with osseous cyst-like lesions in the middle of the distal aspect of the scapula have shown resolution of lameness following intra-articular medication with corticosteroids, but the response in adult horses has been poor. Occasionally modelling of the distal aspect of the scapula is seen in association with an osseous cyst-like lesion in the proximal aspect of the humerus.

Poorly defined osseous cyst-like lesions have also been seen to develop in the cranioproximal aspect of the humerus, caudal to the humeral tubercles, following known trauma to the shoulder region (Figure 8.15). Associated lameness has generally resolved with conservative management. Some lesions have not been detectable in a mediolateral projection, but have been seen in a craniomedial-caudolateral oblique image. Such lesions are usually not improved by intra-articular analgesia or intrathecal analgesia of the intertubercular bursa, but are associated with focal increased radiopharmaceutical uptake.

Degenerative joint disease

Degenerative joint disease of the scapulohumeral joint occurs rarely compared with the incidence in other joints, except as a sequel to osteochondrosis, trauma, infection or an intra-articular fracture in which cases it inevitably follows rapidly. Some of the modelling of the scapula and humerus described

Downloaded From Vet-eBooks.com



Figure 8.15 Cranial 45° medial-caudolateral oblique (extended) image of a scapulohumeral joint and proximal aspect of the humerus of an 8-year-old Thoroughbred gelding with moderate lameness, unaltered by any local analgesic technique. There was focal intense increased radiopharmaceutical uptake in the cranioproximal aspect of the humerus. There is an ill-defined radiolucent area, an osseous cyst-like lesion, in the cranioproximal aspect of the humerus (arrows), which coincided with the region of increased radiopharmaceutical uptake. No radiographic abnormality was detectable in a mediolateral projection.

in conjunction with osteochondrosis is due to secondary degenerative joint disease. Radiographic features of degenerative joint disease include loss of congruity between the outlines of the distal aspect of the scapula and the proximal aspect of the humerus due to flattening of the humeral head and/or modelling of the ventral angle of the scapula (Figure 8.16). Subtle abnormalities of the cranial aspects of the joint may also be seen, including small periarticular osteophytes, especially on the craniodistal aspect of the scapula. In addition there may be variations in opacity of the subchondral bone. Narrowing of the joint space may be seen in advanced cases. The prognosis for return to athletic function is extremely poor.

Mineralisation in the tendon of biceps brachii

Mineralisation in the tendon of biceps brachii can occur as a sequel to a fracture of the supraglenoid tubercle (Figure 8.17), but has also been described as a bilateral condition in association with degenerative joint disease of the scapulohumeral joints. It can also occur as a sequel to chronic tendonitis of biceps brachii. Extensive unilateral mineralisation of uncertain aetiology has also been seen in association with lameness in young horses with no history of trauma or previously recognised lameness (Figure 8w.18). Mineralisation is most easily identified radiographically in a mediolateral view and is seen as a variably sized opacity in the soft tissues cranioproximal to the tubercles of the humerus. If chronic there may be secondary modelling changes of the humeral tubercles. Ultrasonography may give additional information. The prognosis for future soundness is guarded.

Downloaded From Vet-eBooks.com



Figure 8.16 Mediolateral (extended) image of the left scapulohumeral joint of a 5-year-old Warmblood dressage horse which had become lame within 3 weeks of purchase from a dealer. The lameness was not altered by any local analgesic technique. There was mild increased radiopharmaceutical uptake in the distal caudal aspect of the scapula. There is extensive modelling of the ventral angle of the scapula and the proximal caudal aspect of the humerus. There is loss of joint surface congruity caudally in the scapulohumeral joint, due to flattening of the caudal aspect of the humerus. This is degenerative joint disease, probably secondary to osteochondrosis.

Lesions of the humeral tubercles

Trauma to the cranial aspect of the shoulder may result in radiolucent lesions of the humeral tubercles that may be difficult to identify in standard radiographic projections of the shoulder (Figure 8w.19). Similar lesions can also occur with no known history of trauma. Nuclear scintigraphy may be necessary to suggest the presence of a lesion and indicate the need for radiographic assessment. A defect in the cortical bone may be detected in some horses using a cranioproximal-craniodistal oblique (flexed) 'skyline' view. The intermediate tubercle is most commonly affected. In other horses ultrasonography has been required to identify the lesion. Lameness is usually acute in onset and not responsive to any local analgesic technique. Conservative management usually results in resolution of the lameness.

Congenital abnormalities of the bicipital apparatus

Congenital abnormalities of the tubercles of the humerus have been identified rarely in mature horses with chronic forelimb lameness. These include an abnormal shape (usually narrowed) of the intertubercular sulcus seen in a mediolateral view. Absence of the lesser tubercle or hypoplasia is best seen in a cranioproximal-craniodistal oblique (flexed) 'skyline' view of the tubercles. Radiographic evidence of secondary osteoarthritis of the scapulohumeral

Downloaded From Vet-eBooks.com

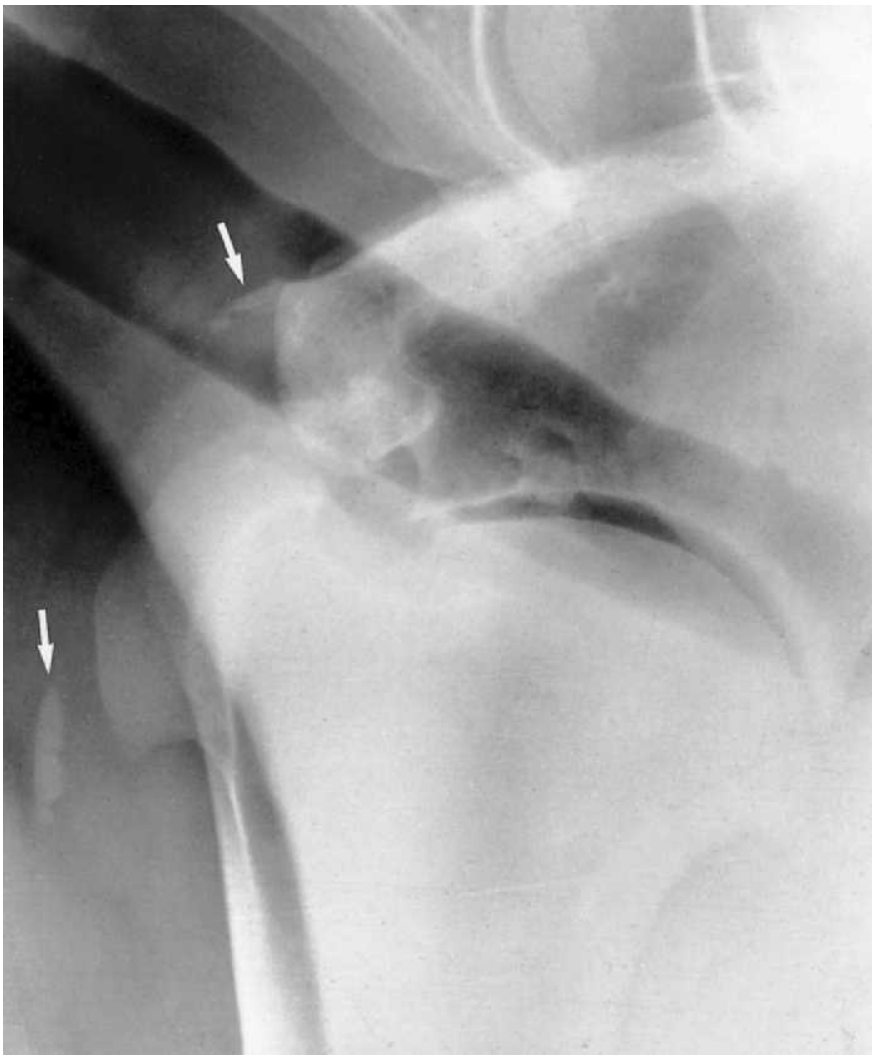


Figure 8.17 Mediolateral (extended) image of a scapulohumeral joint of an aged horse. There are discrete mineralised areas (arrows) in the tendon of biceps brachii. Note the modelled supraglenoid tubercle, subsequent to previous fracture, the articular fracture fragment and the abnormally pointed distal cranial aspect of the scapula.

joint may also be seen. Ultrasonography is useful to assess the intertubercular bursa and tendon of biceps brachii, which is usually luxated medially.

Heterotopic ossification

Heterotopic ossification (myositis ossificans) is the presence of bone in locations where it is not usually seen, and in humans there is an association between repetitive local trauma, surgery, burns and brain or spinal cord injuries. It has been described in the horse and was characterised by a thin, broad, curvilinear mineralised radiopacity, convex cranially, cranial to biceps brachii, which represented a thin plate of bone with spiked edges (Figures 8w.20a and 8w.20b).

Abnormalities of the scapulohumeral joint in Shetland Ponies and Miniature Horses

Dysplasia of the scapulohumeral joint, with or without subluxation of the scapulohumeral joint or secondary degenerative joint disease, has been seen in both Shetland Ponies and Miniature Horses (Figure 8.21). Unilateral or

Downloaded From Vet-eBooks.com



Figure 8.21(b) Mediolateral (extended) image of a scapulohumeral joint of a 5-year-old Shetland Pony. The joint surfaces of the scapula and humerus are abnormally flat and there is subluxation of the joint. There is extensive new bone on the caudoventral aspect of the scapula, and a separate mineralised opacity caudally.

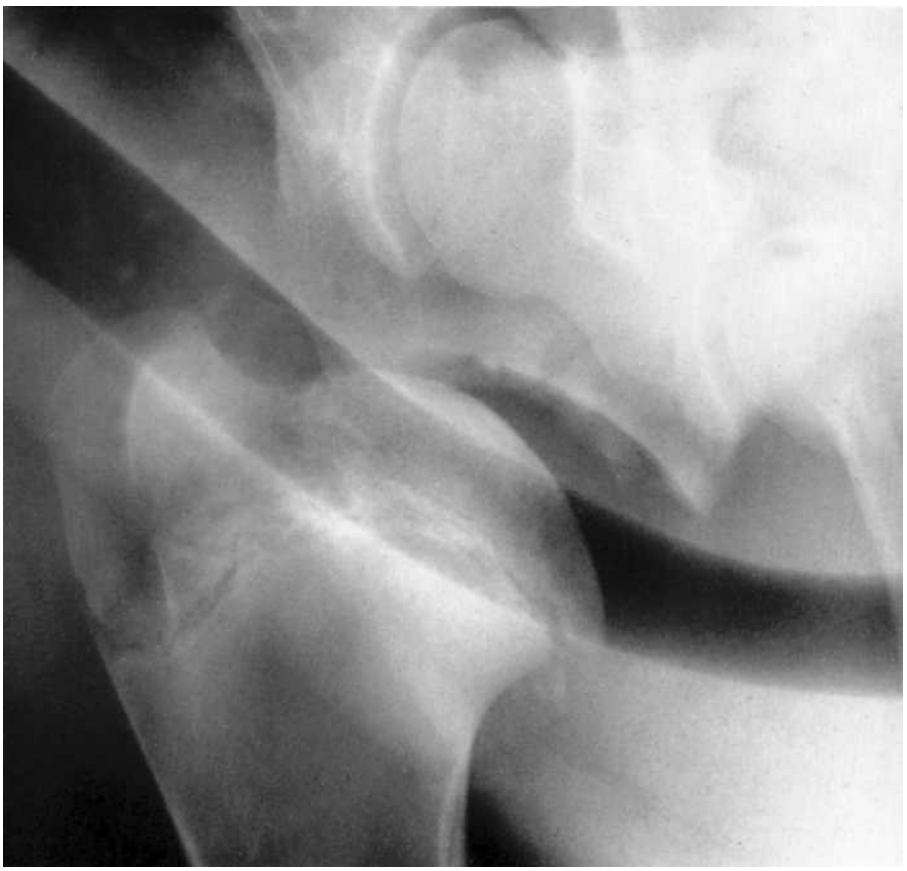


Figure 8.22 Mediolateral (extended) image of a scapulohumeral joint of a 7-month-old Thoroughbred with osteomyelitis of the distal aspect of the scapula and the proximal aspect of the humerus and infectious arthritis. Note the ill-defined lucent zones in the distal aspect of the scapula, the flattened shape of the humeral head due to its partial collapse and the widened joint space. There is periosteal new bone around the ventral angle of the scapula.

Downloaded From Vet-eBooks.com

focal or extend along the entire width of the physis, with or without new bone at the cortices. These changes must be differentiated from those due to osteochondrosis. Septic arthritis may result in apparent widening of the joint space due to excess synovial fluid. The granular opacity and irregular outline of incompletely ossified bones (see Figure 8.4) should not be confused with the results of infection.

Septic physitis in the proximal humeral physis has also been recognised in 2-year-old Thoroughbreds in race training with sudden onset of forelimb lameness. Radiographs are characterised by a large radiolucent zone in the caudal aspect of the physis, with surrounding increased opacity and periosteal new bone on the caudal physeal and metaphyseal regions of the proximal aspect of the humerus. Long-term antimicrobial therapy may be successful in the treatment of this condition.

Luxation of the scapulohumeral joint

Luxation of the scapulohumeral joint causes firm swelling in the shoulder region and severe lameness. The humerus may be displaced proximally and cranially (Figure 8.23) or proximally and caudally and is readily seen



Figure 8.23 Mediolateral (extended) image of a scapulohumeral joint of a mature pony with cranioproximal luxation of the humerus. Craniomedial-caudolateral oblique (extended) views should also be obtained to ensure that there is no concurrent fracture. This luxation was successfully reduced and the pony ultimately resumed full athletic function.

Downloaded From Vet-eBooks.com

radiographically in a mediolateral (extended) projection. The proximal aspect of the humerus is superimposed over the distal aspect of the scapula. An oblique view is invaluable for determining whether the luxation is medial or lateral and for identification of any concurrent fracture. A simple luxation must be reduced rapidly, with the horse anaesthetised. Full return to athletic function has been recorded, but generally the prognosis is poor. The presence of a concurrent fracture also warrants a guarded prognosis.

Enostosis-like lesions

The humerus is a relatively common site for enostosis-like lesions, characterised radiologically by areas of increased opacity, which are usually well-demarcated, adjacent to a nutrient vessel and close to the endosteum.

Fractures

Fractures of the shoulder region are usually the result of a fall, a kick or a collision with a solid object. They cause moderate to severe lameness with a variable amount of soft-tissue swelling, with or without audible or palpable crepitus.

Fracture of the supraglenoid tubercle

A fracture of the supraglenoid tubercle is the most common fracture in the shoulder region (Figures 8.24a, 8w.24b and 8w.24c). The fracture may be simple or comminuted and there is often an articular component. There may be a separate fracture through the glenoid notch (this represents the separate centre of ossification of the cranial part of the glenoid cavity of the scapula). The supraglenoid tubercle is usually displaced cranially and distally resulting in a non-union fracture. Lameness may initially improve, but usually persists unless the fracture is treated surgically. Mineralisation in the tendon of biceps brachii may be a sequel in addition to secondary degenerative joint disease.

Other fractures

Other common sites of fractures are illustrated in Figure 8.25. Fractures restricted to the glenoid cavity of the scapula may be difficult to identify in a mediolateral (extended) view, but may be seen in an oblique (extended) projection.

Fractures of the body or neck of the scapula are not uncommon and may be articular. Short fractures of the neck and body are easily overlooked due to superimposition of the cervical and thoracic vertebrae and the ribs.

Stress fractures of the distal aspect of the scapula usually occur distal to or adjacent to the scapular spine in Thoroughbred and Quarterhorse racehorses. These are usually best identified scintigraphically, and may not be

Downloaded From Vet-eBooks.com



Figure 8.24(a) Mediolateral (extended) image of a scapulohumeral joint of a 2-month-old pony foal with acute onset lameness. Cranial is to the left. There is a displaced, comminuted articular fracture of the supraglenoid tubercle of the scapula. The physis between the ossification centre for the cranial part of the glenoid of the scapula and the body of the scapula (arrow) is still open, as are the physes between the humeral tubercles, the humeral head and the metaphysis of the humerus.

detectable radiologically. In some horses a cortical defect and periosteal callus can be identified using ultrasonography.

A traumatically induced fracture of the scapular spine may be very difficult to identify radiographically except in tangential views. Ultrasonography may be more sensitive for identification of these fractures. Such fractures are sometimes associated with a chronic draining sinus due to sequestrum formation.

Fractures of the cranioproximal aspect of the humerus, the deltoid tuberosity and the greater, lesser and intermediate tubercles of the humerus may only be identifiable in a craniomedial-caudolateral oblique (extended) projection (Figure 8.26), cranioproximal-craniodistal oblique (flexed) view or, for the greater tubercle, a caudolateral-craniomedial oblique view.

Downloaded From Vet-eBooks.com

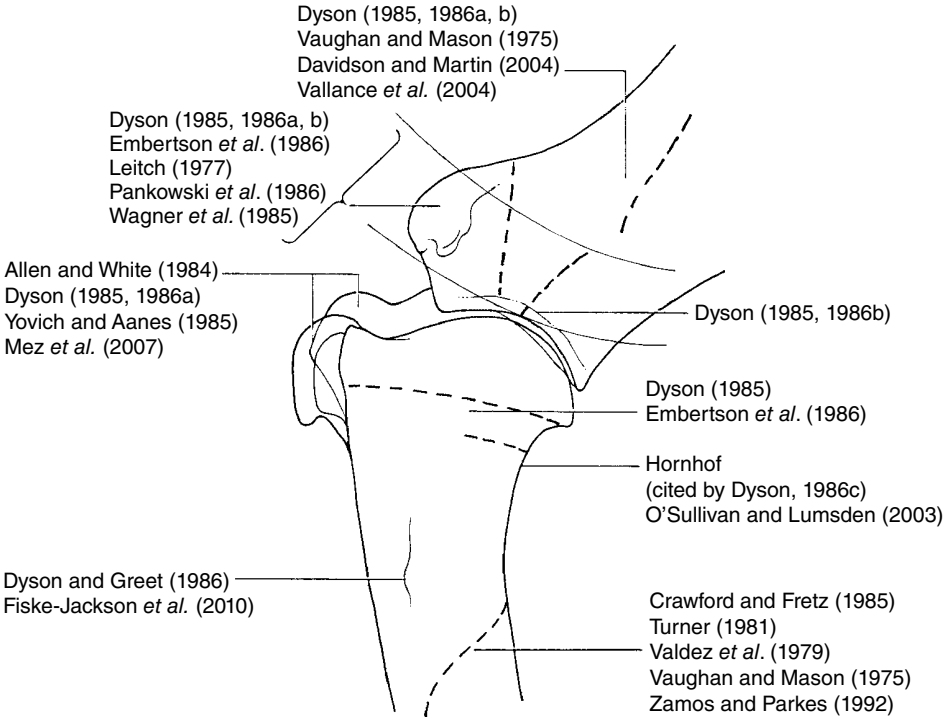


Figure 8.25 Location of common fractures of the scapula and humerus, and recommended references (see 'Further reading').

Chip fractures of the deltoid tuberosity are usually the result of kick injuries and result in acute-onset severe lameness. In acute injuries there is focal pain and swelling. Fractures may be missed on mediolateral images, but are consistently seen in a craniomedial-caudolateral oblique (extended) image or using ultrasonography. These fractures have an excellent prognosis with conservative management.

Stress fractures of the caudal aspect of the proximal humeral metaphysis or cranial aspect of the distal humeral metaphysis (Figure 8.27) occur occasionally. They can be difficult to identify radiographically in the acute phase, although they may be demonstrable using nuclear scintigraphy. If chronic there may be periosteal callus ± endosteal callus on the caudal aspect of the proximal humeral metaphysis or the cranial aspect of the distal humeral metaphysis.

Crush fractures of the humeral head can be extraordinarily difficult to detect radiologically in either the acute phase or in follow-up radiographs, but are associated with acute-onset severe lameness. There is intense increased radiopharmaceutical uptake in the humeral head. Evidence of secondary degenerative joint disease develops with time, usually characterised by modelling of the ventral angle of the scapula (Figure 8w.28a). Ultrasonography can be used to demonstrate marked irregularity in contour of the humeral head (Figure 8w.28b).

Fractures of the humeral diaphysis are usually oblique or spiral with considerable overriding, with or without comminution. The prognosis for a fracture in the shoulder region depends on its location and configuration, and readers are advised to consult the references listed under 'Further reading'.

Downloaded From Vet-eBooks.com



Figure 8.26 Craniomedial-caudolateral oblique (extended) image of the proximal aspect of a humerus of a 3-year-old Thoroughbred. There is a non-displaced fracture of the cranioproximal aspect of the humerus. No abnormality was detectable in a mediolateral view. The filly was treated conservatively and made a complete recovery, but did develop an asymptomatic osseous cyst-like lesion in the cranioproximal aspect of the humerus.

Bone fragility syndrome

Bone fragility syndrome is a condition characterised by acute onset of unilateral or multilimb lameness or chronic intermittent lameness in one or more limbs. There is often shoulder muscle atrophy and there may be lateral bowing of the scapulae. There is multifocal increased radiopharmaceutical uptake in the scapulae and other bones, especially the ribs and pelvis. Radiographic features include fractures of the scapulae, osteolytic areas and periosteal new bone. The prognosis is hopeless.

Downloaded From Vet-eBooks.com



Figure 8.27 Mediolateral (flexed) image of the elbow of a 3-year-old Thoroughbred flat racehorse with left forelimb lameness of 2 weeks' duration. Cranial is to the top. There is periosteal callus on the distal cranial aspect of the humerus (arrows), reflecting a humeral stress fracture. This was associated with intense increased radiopharmaceutical uptake.

Humeroradial, humeroulnar and radioulnar (elbow or cubital) joints and radius

RADIOGRAPHIC TECHNIQUE

Equipment

The elbow joint and the radius are readily examined radiographically using a portable machine, with the horse standing. Sedation and administration of analgesics may facilitate positioning of the limb. Digital systems or fast screens are recommended, but a grid is not essential. It may be necessary to acquire two mediolateral (flexed) views to ensure correct exposures of both the olecranon of the ulna and the humeroradial joint.

Positioning

Mediolateral (flexed) view

For radiography of the elbow the horse is positioned with the limb to be radiographed next to the cassette. The x-ray machine is placed on the opposite side of the horse. The forelimb to be examined is protracted so that the olecranon of the ulna is cranial to the muscles of the contralateral limb. The x-ray beam is centred approximately at the junction between the cranial two-thirds and caudal one-third of the forearm, at the level of the proximal articular surface of the radius.

The majority of the radius can be examined radiographically with the horse bearing weight on the limb. The x-ray beam is centred at the point of interest and is aligned at right angles to the limb.

Downloaded From Vet-eBooks.com

Craniocaudal views

Craniocaudal radiographic views of the elbow joint are usually obtained with the horse bearing weight on the limb, and the cassette held caudal to the forearm, with the edge of the cassette against the thorax. It is helpful to rotate the cassette so that it can be held as high under the thorax as possible. It may be necessary to direct the x-ray beam approximately 10–15° from cranioproximally to caudodistally, depending on the shape of the rib cage, in order to examine the distal aspect of the humerus and the humeroradial joint properly. Unfortunately this technique will cause some distortion of the radiographic image.

Alternatively the limb may be protracted, the cassette held parallel with the ulna and the x-ray beam directed perpendicular to it. There is more likely to be movement blur using this technique, and if there is a fracture of the ulna it may be difficult to straighten the limb adequately. Good-quality craniocaudal views, with minimal distortion, are obtained more readily with the horse anaesthetised.

The radius is radiographed with the horse bearing weight on the limb. The beam is centred at the area of interest.

Oblique views

A craniomedial-caudolateral oblique view is the easiest oblique view to obtain with the horse bearing weight on the limb (see Figure 8.33). A craniolateral-caudomedial oblique view of the proximal aspect of the radius is feasible, but due to the relative positions of the sternum and distal aspect of the humerus, it is impractical to obtain a similar view of the humerus. In some horses it may be easier to obtain images with the limb semi-flexed.

RADIOGRAPHIC ANATOMY, NORMAL VARIATIONS AND INCIDENTAL FINDINGS

Birth to 3 years old

The distal aspect of the humerus develops from three ossification centres: the diaphysis, the distal epiphysis and the epiphysis of the medial epicondyle. The radius has a single proximal epiphysis and the ulna has a single proximal apophysis (Figure 8.29); the ulna may also have a separate centre of ossification for the anconeal process (Figure 8.30). At birth the ossification centres are rounded and may be irregular in outline because they are incompletely ossified. The apophysis of the ulna is small and widely separated from the metaphysis. It gradually enlarges to cover the proximal ulnar metaphysis by 10–12 months. The physis appears very irregular (Figure 8.30) and remains open until 24–36 months after birth. The distal humeral physes and the proximal radial physis close between 11 and 24 months. The distal radial physis closes between 22 and 42 months of age; there is a separate centre of ossification of the lateral styloid process which fuses with the rest of the distal epiphysis within the first year of life.

Skeletally mature horse

Mediolateral (flexed) view

There is little variation in the normal radiographic appearance of the adult elbow except as a result of positioning (Figure 8.31). The anconeal process of the ulna may be sharply pointed or rounded. The trochlear notch of the ulna

Downloaded From Vet-eBooks.com



Figure 8.29 Mediolateral (flexed) image and diagram of a normal elbow of a 12-day-old foal. Note the position of the incompletely ossified proximal apophysis of the ulna.

Downloaded From Vet-eBooks.com

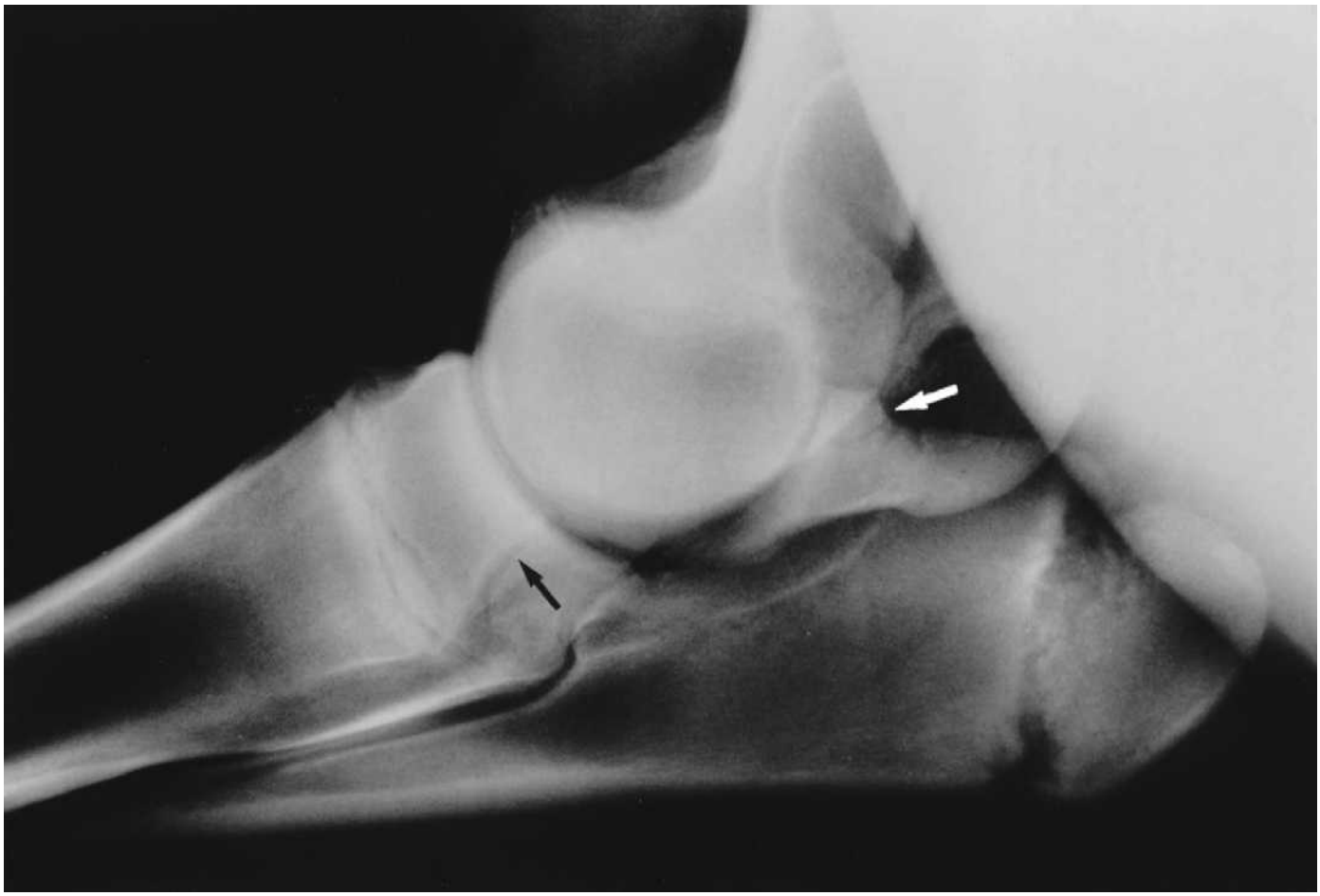


Figure 8.30 Mediolateral (flexed) image of a normal elbow of an 11-month-old filly. The proximal ulnar apophysis has enlarged compared with Figure 8.29 and is fusing with the metaphysis, but the physis is extremely irregular. There is a radiolucent line (black arrow) in the caudal aspect of the proximal radial physis which represents part of the radioulnar articulation. Positioning is not ideal, since the opacity of the pectoral muscles is superimposed over the proximal aspect of the ulna. The anconeal process (white arrow) is a separate centre of ossification.

is divided into an articular zone proximally and a synovial fossa distally, separated by a distinct ridge. It is important to differentiate between these two areas when assessing a fracture involving the trochlear notch. The interosseous space between the ulna and radius may be clearly or poorly defined, depending upon the angle of projection. The ulna is incomplete in the majority of horses and fuses distally with the radius. Some horses have a vestigial distal ulna (see Figures 7.11a and 7.11b) and occasionally the ulna is complete. The cranial margin of the proximal articular surface of the radius has several 'lips' or overlapping edges which must not be confused with osteophyte formation. The radial tuberosity is smoothly outlined, but may appear irregular in a slightly oblique mediolateral projection. The medial aspect of the head of the radius is wider craniocaudally than the lateral aspect. Therefore the radioulnar articulation is not in a single plane, and in a mediolateral view the articulation of the lateral aspect of the ulna with the proximal aspect of the radius is seen as a lucent line through the caudal aspect of the radius (Figures 8.30 and 8.31).

Downloaded From Vet-eBooks.com

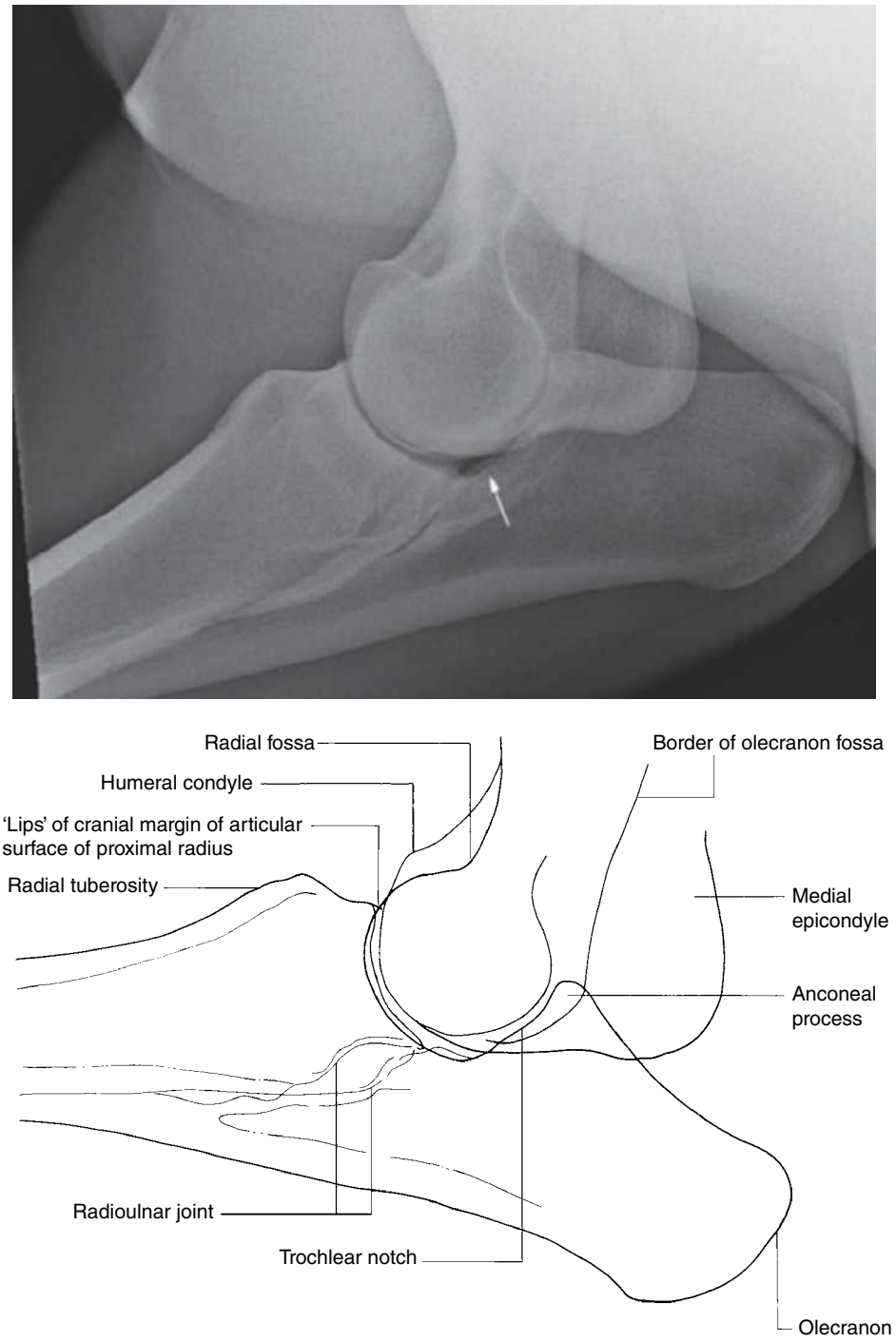


Figure 8.31 Mediolateral (flexed) image and diagram of a normal adult elbow. The non-articular portion of the trochlear notch of the ulna is arrowed.

There is an irregularly outlined bony prominence, the transverse crest, on the distocaudal aspect of the radius. Its size depends on the angle of projection, since slight obliquity will enhance it. The mottled opacity of the torus carpeus (chestnut) on the caudal aspect of the radius must not be confused with dystrophic mineralisation of soft tissues. Other radiographic characteristics of the distal aspect of the radius are discussed in Chapter 7.

Downloaded From Vet-eBooks.com

Craniocaudal views

The humeroradial joint space often appears wider medially than laterally. There are smoothly outlined eminences on the distal medial and lateral aspects of the humerus and proximal medial and lateral aspects of the radius for attachment of the collateral ligaments (Figures 8.32 and 8.33).

SIGNIFICANT RADIOLOGICAL ABNORMALITIES

Osteochondrosis

Osteochondrosis of the elbow in the horse is rare. It has been documented at post-mortem examination to involve the medial condyle of the humerus and the medial proximal aspect of the radius. Lameness associated with a separate bone fragment detached from the anconeal process of the ulna has been described in a 2-year-old Standardbred. The lameness was relieved by intra-articular anaesthesia of the elbow. The anconeal process is best assessed in a mediolateral (flexed) view, and detachment of its apex may be an osteochondritic lesion. Care must be taken in the assessment of young foals in which the anconeal process may be a separate centre of ossification.

Osseous cyst-like lesions

Osseous cyst-like lesions occasionally occur close to the elbow joint and are usually seen in young horses. They occur most commonly in the medial aspect of the proximal radial epiphysis, often in association with periosteal reactions at the site of insertion of the medial collateral ligament of the humeroradial joint (Figures 8w.34a and 8w.34b). These cyst-like lesions may ultimately 'fill-in' radiographically, but degenerative joint disease may be a sequel. The response to conservative treatment has been variable; some horses respond well to intra-articular medication. Surgical treatment might yield better results. The joint should be inspected carefully for evidence of secondary degenerative joint disease before contemplating surgery.

Osseous cyst-like lesions occur less commonly in the distal aspect of the radius. Surgical treatment may be successful.

Degenerative joint disease

Degenerative joint disease of the humeroradial, humeroulnar and radioulnar joints usually occurs as a sequel to an osseous cyst-like lesion, collateral ligament damage or an articular fracture, but may develop as a primary condition. In a mediolateral view the 'lips' of the proximal articular surface of the radius (see above, 'Skeletally mature horse/Mediolateral view') should not be confused with osteophytes. Craniocaudal views are more helpful for the diagnosis of degenerative joint disease. Typically, osteophyte formation is seen on the distal medial and lateral aspects of the humerus and/or the proximal aspect of the radius (Figures 8.35a and 8.35b). In advanced cases there may be narrowing of the humeroradial joint space with increased opacity of the subchondral bone. The long-term prognosis for return to athletic function is poor; transient improvement may be achieved with intra-articular medication.

Downloaded From Vet-eBooks.com



Figure 8.32 Craniocaudal image and diagram of a normal adult elbow. Lateral is to the right.

Downloaded From Vet-eBooks.com

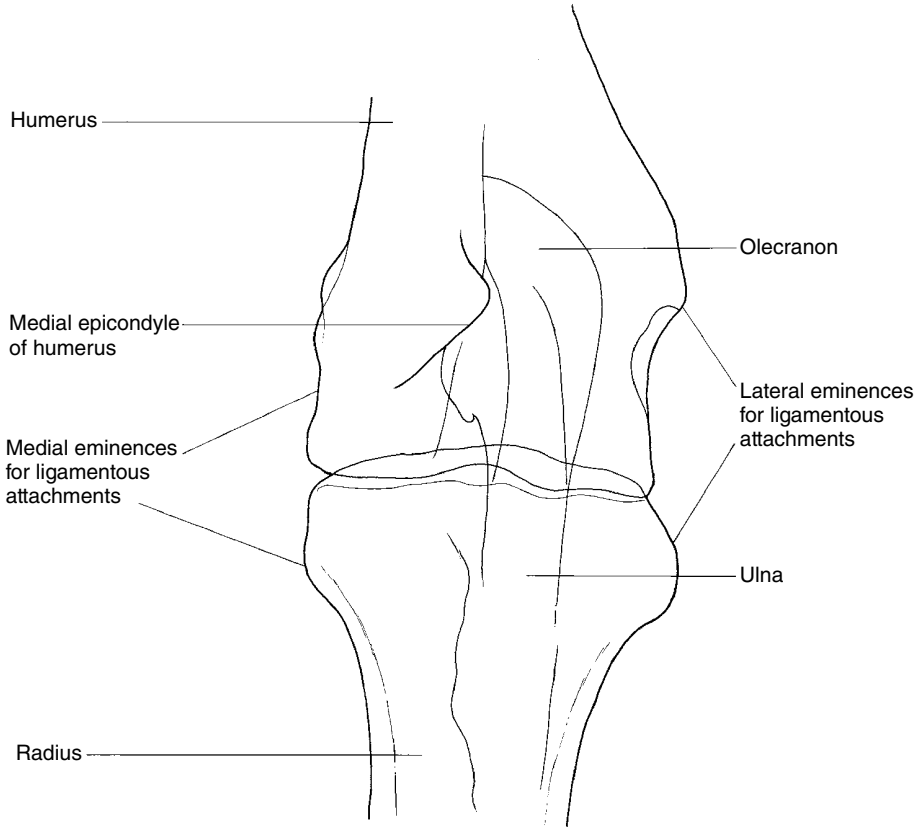


Figure 8.32 *Cont'd*



Figure 8.33 Craniomedial-caudolateral oblique image of a normal adult elbow.

Downloaded From Vet-eBooks.com

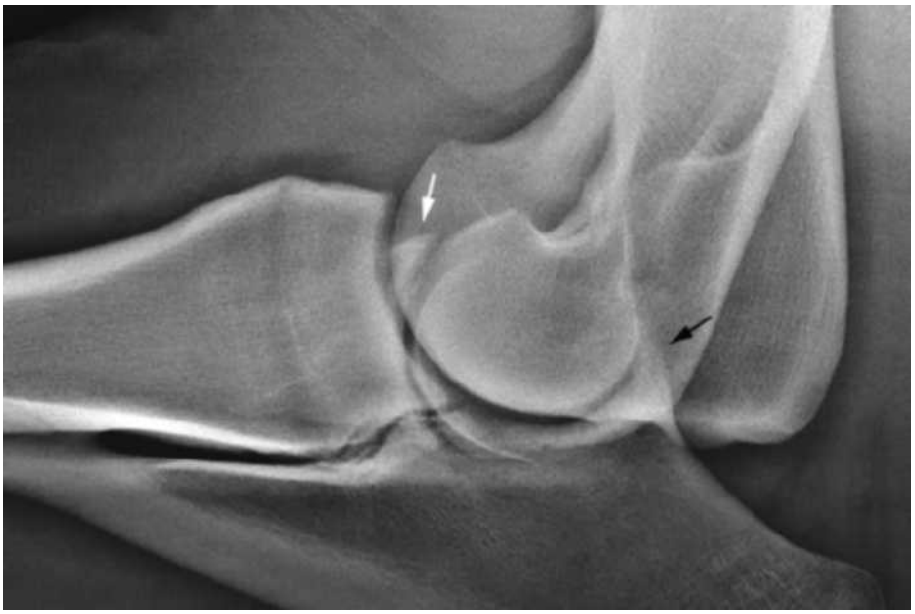


Figure 8.35(a) Oblique mediolateral (flexed) image of an elbow joint of 17-year-old pleasure riding horse with radiographic evidence of degenerative joint disease. Cranial is to the top. There is osteophyte formation on the cranioproximal aspect of the radius (white arrow) (compare with Figure 8.31) and modelling of the anconeal process of the ulna (black arrow). Lameness was substantially improved by intra-articular analgesia.



Figure 8.35(b) Craniocaudal image of an elbow (same horse as Figure 8.35a). Lateral is to the right. There is periarticular osteophyte formation on the medial aspect of the humeroradial joint (arrows). There is ill-defined new bone on the proximomedial aspect of the radius at the level of the physis (arrow head), at the region of insertion of the medial collateral ligament of the humeroradial joint. Ultrasonographic examination confirmed injuries of both the medial and lateral collateral ligaments of the humeroradial joint.

Downloaded From Vet-eBooks.com

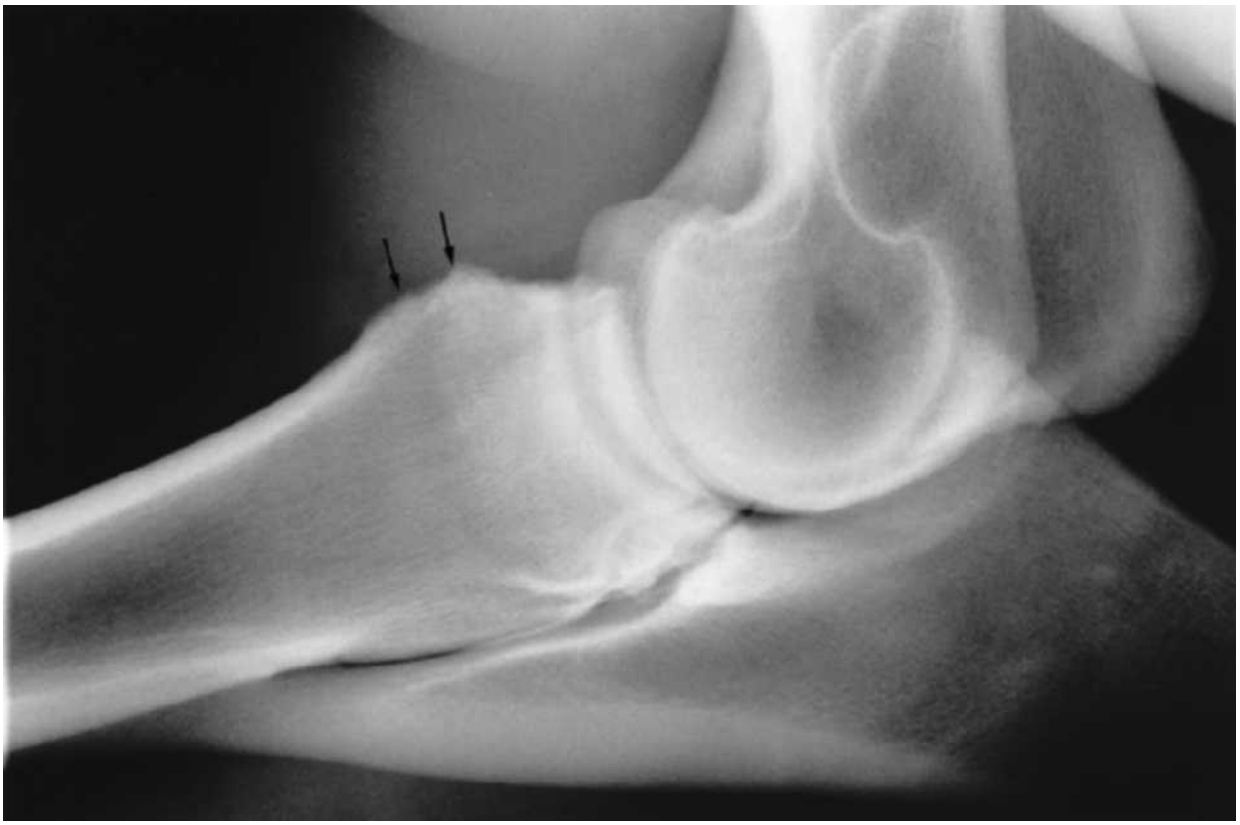


Figure 8.36 Mediolateral (flexed) image of an elbow of a 7-year-old advanced event horse, with lameness of several months' duration. Cranial is to the top. There is periosteal new bone formation on the cranioproximal aspect of the radius (arrows), which represents entheseophyte formation at the insertion of biceps brachii.

Periosteal proliferative reactions (enthesopathy) at the site of insertion of biceps brachii on the radial tuberosity

Entheseous new bone, with or without discrete bony fragments, may develop at the insertion of biceps brachii on the radial tuberosity, and is best seen on a mediolateral (flexed) view (Figure 8.36). New bone may not be identifiable until 3–6 weeks after the onset of lameness, so nuclear scintigraphy is more sensitive in the acute phase and may help to interpret the significance of entheseous new bone in a horse with more chronic lameness. In the acute phase there may be some pain on manipulation of the joint, but in more chronic cases there may be no localising signs. Lameness may resolve with rest, but often persists; the biceps brachii should be assessed ultrasonographically in its entirety.

Entheseous new bone at the sites of attachment of the collateral ligaments of the humeroradial joint

Sprain of the lateral collateral (or, less commonly, the medial collateral) ligament of the humeroradial joint may be followed by the development of entheseous new bone on the humeral epicondyles and proximal aspect of the radius, best seen in a craniocaudal projection (Figure 8.37). Occasionally a fragment may be avulsed, especially from the proximal attachment. With chronic injury there is frequently dystrophic mineralisation within the injured ligament. Diagnostic ultrasonography is useful to determine the

Downloaded From Vet-eBooks.com



Figure 8.37 Craniocaudal image of an elbow of a 10-year-old riding school pony with chronic lameness. Lateral is to the right. There is extensive new bone on the lateral aspect of the epicondyle of the humerus (arrow heads). There is periosteal roughening and new bone on the proximal lateral and medial aspects of the radius (small white arrows). This is entheseophyte formation at the sites of attachment of the collateral ligaments of the humeroradial joint. There is also mineralisation in the soft tissues laterally (large white arrow). There was also slight osteophyte formation on the articular margins of the joint, seen only in a mediolateral view.

degree of ligamentous damage. Chronic instability of the joint makes degenerative joint disease a likely sequel.

Avulsion of the deep digital flexor muscle from the medial epicondyle of the humerus

Avulsion of the deep digital flexor muscle from the medial epicondyle of the humerus is an unusual injury which may result in mild displacement of a fragment of bone (Figure 8.38), with or without subsequent development of dystrophic mineralisation within the muscle.

Avulsion of the origin of ulnaris lateralis

Avulsion of the origin of ulnaris lateralis results in displacement of a fragment of bone from the distal lateral aspect of the humerus from a site caudal and distal to the origin of the lateral collateral ligament of the humeroradial joint. Ultrasonography reveals enlargement of the tendon of origin of ulnaris lateralis.

Downloaded From Vet-eBooks.com



Figure 8.38 Craniomedial-caudolateral oblique (flexed) image of an elbow of a 7-year-old polo pony. Cranial is to the left. There is a poorly marginated osseous mass of heterogeneous opacity distal (arrow) to the medial epicondyle of the humerus and a second smaller opacity proximocaudal to the larger mass. There is a defect in the distal aspect of the medial epicondyle of the humerus. This represents a chronic avulsion of the origin of the humeral head of the deep digital flexor tendon. Source: Reproduced with permission of Stefano Tassan.

Periosteal reaction at the site of origin of the accessory ligament of the superficial digital flexor tendon

Periostitis may develop proximal to the transverse ridge, on the distal caudomedial aspect of the radius, secondary to tearing of the attachment of the accessory ligament of the superficial digital flexor tendon (the superior or radial check ligament). Clinical signs include lameness, sometimes associated with distension of the carpal sheath in acute cases. This injury may occur concurrently with injury of the accessory ligament of the superficial digital flexor tendon and/or superficial digital flexor tendonitis and therefore these structures should be examined ultrasonographically. Radiographic changes are usually only detectable in chronic cases, and rest generally results in resolution of clinical signs.

Luxation of the elbow joint

Luxation of the elbow joint is not common and has only been reported concurrent with a fracture of the radius or ulna.

Downloaded From Vet-eBooks.com

Infection

Infection occurs most commonly in young foals but, because the lateral aspect of the radius is poorly protected by soft tissues, a deep wound in this area may penetrate the elbow joint capsule or cause localised infection. This may spread to the joint or result in osteomyelitis of the radius or ulna in an adult horse. If the degree of lameness associated with a wound in the elbow region is unexpectedly severe, or if there is a discharging sinus, radiographic examination is indicated. Injection of as much radiodense contrast medium as possible, via a Foley catheter, should establish whether a sinus communicates with the joint capsule or with sequestrated bone (Figure 16.10b). It may also demonstrate a filling defect representing a foreign body. Ultrasonographic evaluation may also be helpful.

Osteochondroma of the distal aspect of the radius

Distension of the carpal sheath, lameness and resentment of pressure applied to the distal caudal aspect of the radius may be associated with an osteochondroma on the distal diaphysis or the metaphysis of the radius. Radiographically this appears as a variably shaped bony protuberance on the distocaudal aspect of the radius, usually proximal to the physeal scar midway from medial to lateral (see Figure 7.26). This mass has a thin cortex which appears to be continuous with the cortex of the radius. Sequential radiographs may demonstrate progressive enlargement of the mass. Ultrasonography will usually reveal a tear in the cranial or dorsal aspect of the deep digital flexor tendon. Treatment by surgical removal of the abnormal bone is usually successful in resolving both the lameness and carpal sheath swelling.

Hereditary multiple exostosis

Hereditary multiple exostosis is a rare condition characterised by multiple bony projections on growing long bones, the ribs, the pelvic bones and the spinous processes of the thoracic and lumbar vertebrae. These swellings are present at birth and may enlarge progressively until skeletal maturity. They may be asymptomatic unless impinging upon adjacent soft tissues, but may cause distension of synovial structures. The radiographic appearance is similar to that of solitary osteochondroma. There is no known treatment. This hereditary condition is transmitted by an autosomal dominant gene.

Hypertrophic osteopathy

This condition is discussed in detail under 'Hypertrophic osteopathy' in Chapter 1. Periosteal new bone along the diaphysis and the metaphyses of the radius may be due to hypertrophic osteopathy. The multifocal nature of the disease should help to differentiate it from other causes of periostitis.

Downloaded From Vet-eBooks.com

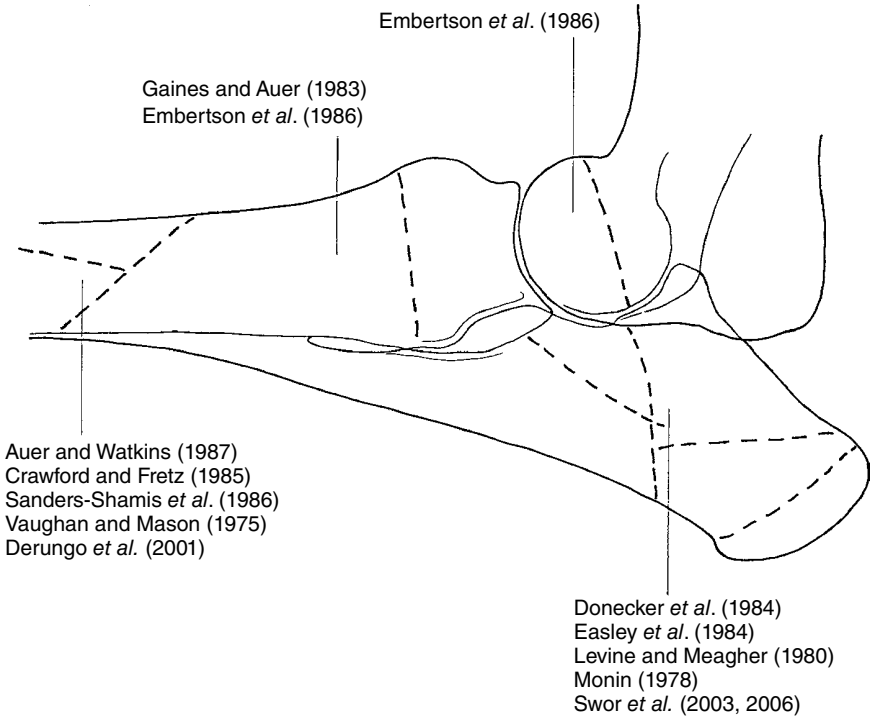


Figure 8.39 Location of common fractures in the elbow region, and recommended references (see 'Further reading').

Fractures (Figure 8.39; see also Figure 8.27)

Physeal fractures

Fractures of the distal physis of the humerus occur occasionally and warrant a poor prognosis. In an immature horse, the open proximal physis of the ulna should not be confused with a fracture. The apophysis may be displaced proximally (Salter-Harris type I fracture) (see 'Fractures' in Chapter 1) and it is important to compare its position with a horse of similar age. Radiographic examination of the contralateral limb provides an ideal comparison, provided the horse will bear weight sufficiently on the limb in question. These fractures and both proximal and physeal fractures of the radius have a fair prognosis.

Ulnar fractures

Fracture of the olecranon of the ulna is a common sequel to trauma in the elbow region. Lameness is usually severe and the horse may stand with the elbow 'dropped'. There may or may not be associated soft-tissue swelling. Radiographic examination of a suspected fracture should include both mediolateral (flexed) and craniocaudal views in order to assess its configuration accurately. A fracture which enters the trochlear notch must be assessed carefully to determine whether or not it involves the articular or non-articular region (Figure 8.40). Provided that ulnar fractures are recognised and treated early, the prognosis depends on whether the fracture is simple or compound, the extent of comminution and the degree of displacement of the fracture fragments. Internal fixation offers the best chance for full return to athletic function.

Radial fractures

Radial fractures are a common result of trauma and occur in many configurations, incomplete parasagittal, comminuted, transverse and physeal being

Downloaded From Vet-eBooks.com



Figure 8.40 Mediolateral (flexed) image of an adult elbow of a pony with a comminuted non-displaced fracture of the olecranon, following a kick. Cranial is to the top. Although one of the fracture lines enters the trochlear notch of the ulna, it involves a non-weight bearing area. For financial reasons the fracture was managed conservatively, but subsequently the fracture became displaced and developed into a non-union.

the most frequent. Multiple radiographic views may be necessary to assess the full extent of a fracture. Seemingly innocuous kick injuries on the medial aspect of the antebrachium have the potential to result in incomplete vertical and/or oblique fractures of the radius (Figures 1.22, 8.41a and 8.41b) because of the lack of soft tissues covering the bone. At the time of the initial injury the horse may not be very lame, but radiographic examination is warranted. Fractures may not be detectable radiographically initially, but such fractures have the propensity to propagate, and if the horse is allowed free exercise this can be potentially catastrophic. Horses should be confined to box rest and follow-up x-rays obtained after approximately 10 days. False negative results have been recorded up to 16 days after injury. Endosteal or periosteal reaction can be seen in some horses from approximately 8 days after injury. Alternatively nuclear scintigraphic examination should be considered. Repair of a complete fracture may be successful in immature horses, but the prognosis in adult horses for complete fractures is extremely guarded. Incomplete fissure (stress) fractures or incomplete fractures resulting from kick injuries often heal with conservative treatment (3–6 months' box rest ± splinting and/or cross tying).

Fatigue or stress fractures of the radial diaphysis occur in young (2- and 3-year-old) Thoroughbreds in training. Although they may not be detectable radiographically in the acute phase, there may be localised increased opacity of the medulla. Nuclear scintigraphy is a more sensitive diagnostic technique. Increased opacity in the medulla in the mid-diaphyseal region reflects endosteal callus and should be differentiated from an enostosis-like lesion.

Downloaded From Vet-eBooks.com



Figure 8.41(a) Craniomedial-caudolateral oblique radiographic image of the radius of a 16-year-old hunter, which had been kicked on the antebrachium 2 weeks previously. There was a discharging wound and the horse was non-weight-bearing on the limb. There is an oblique radiolucent line (arrows), representing an incomplete fissure fracture.



Figure 8.41(b) Craniomedial-caudolateral oblique image of the same horse as in Figure 8.41(a), obtained 10 days later. The fracture line is now much more obvious (arrows), extends much further proximally than was previously apparent and is surrounded by some more opaque bone, representing callus.

Downloaded From Vet-eBooks.com

Enostosis-like lesions

The radius is one of the more common sites for enostosis-like lesions, which are seen most commonly in young Thoroughbred racehorses, but also occasionally occur in mature sports horses. These lesions are often associated with acute severe lameness. There are usually no localising clinical signs and diagnosis is usually dependent on the identification of focal increased radiopharmaceutical uptake in the radial diaphysis, often close to the nutrient foramen. Radiographic examination reveals focal increased opacity often close to the nutrient foramen. Lameness usually resolves with time, although in some horses it shifts between limbs.

Tumours

Osteosarcoma and an aneurysmal bone cyst have been reported in the humerus and radius respectively.

Additional figures

The book companion website at www.clinical-radiology-horse.com includes additional figures that are not included in the printed book or e-book formats. Please see '**About the Companion Website**' at the start of the book for details on how to access the website. These figures are prefixed with the letter 'w' in the printed book, e.g. Figures 1w.4c–f.

FURTHER READING

ELBOW AND RADIUS

Anderson, J., Galuppo, L., Barr, B., et al. (2008) Clinical and scintigraphic findings in horses with a bone fragility disorder: 16 cases (1980–2006). *J. Am. Vet. Med. Ass.* **232**, 1694–1699

Auer, J., Watkins, J. (1987) Treatment of radial fractures in adult horses: an analysis of 15 clinical cases. *Equine Vet. J.* **19**, 103–110

Bassage, L., Ross, M. (1998) Enostosis-like lesions in the long bones of 10 horses: scintigraphic and radiographic features. *Equine Vet. J.* **30**, 35–42

Bertone, A., McIlwraith, C., Powers, P., Stashak, T., Aanes, W., Turner, A. (1986) Subchondral osseous cystic lesions of the elbow of horses: conservative versus surgical treatment. *J. Am. Vet. Med. Ass.* **189**, 540–546

Brown, M., MacCallum, F. (1974) Anconeal process of ulna: separate centre of ossification in the horse. *Br. Vet. J.* **130**, 434–438

Chopin, J., Wright, J., Melville, L., Robinson, W. (1997) Lateral collateral ligament avulsion of the humeroradial joint in a horse. *Vet Radiol. Ultrasound* **38**, 50–54

Crawley, G., Grant, B. (1986) Repair of elbow joint luxation without concomitant fracture in a horse. *Equine Pract.* **8**(5), 19–26

Dabareiner, R., Chaffin, M.K., Quirham, H., et al. (2013) Enthesopathy and desmitis of the medial collateral ligament of the cubital joint in 4 horses. *J. Am. Vet. Med. Ass.* **242**, 1152–1158

Derungs, S., Fuerst, A., Haas, C., Geissbuhler, U., Auer, J. (2001) Fissure fractures of the radius and tibia in 23 horses: a retrospective study. *Equine Vet. Educ.* **13**, 313–318

Donecker, J., Bramlage, L., Gabel, A. (1984) Retrospective analysis of 29 fractures of the olecranon process of the equine ulna. *J. Am. Vet. Med. Ass.* **185**, 183–189

Easley, K., Schneider, J., Guffy, M., Boero, M. (1984) Equine ulnar fractures: a review of 25 clinical cases. *Equine Vet. Sci.* **3**(1), 5–12

Edwards, G., Vaughan, L. (1978) Infective arthritis of the elbow joint in the horse. *Vet. Rec.* **103**, 227–229

Fitch, G., Martinelli, M. (1998) Conservative management of a sequestrum involving the radial cortex in 2 horses. *Equine Vet. Educ.* **10**, 228–232

Hardy, J., Marcoux, M., Eisenberg, H. (1986) Osteochondrosis-like lesion of the anconeal process in 2 horses. *J. Am. Vet. Med. Ass.* **189**, 802–803

Levine, S., Meagher, D. (1980) Repair of an ulnar fracture with radial luxation in a horse. *Vet. Surg.* **9**, 58–60

Downloaded From Vet-eBooks.com

Mackey, V., Trout, D., Meagher, D., Hornhof, W. (1987) Stress fractures of the humerus, radius and tibia in horses. *Vet. Radiol.* **28**, 26–31

Oikawa, M., Narama, I. (1998) Enthesopathy of the radial tuberosity in two Thoroughbred racehorses. *J. Comp. Path.* **118**, 135–143

O'Neill, H., Bladon, B. (2011) Retrospective study of scintigraphic and radiological findings in 21 cases of enostosis-like lesions in horses. *Vet Rec.* **168**, 326

Ordidge, R. (2001) Pathological fracture of the radius secondary to an aneurysmal bone cyst. *Equine Vet. Educ.* **13**, 239–242

Ramzan, P. (2002) Enostosis-like lesions: 12 cases. *Equine Vet. Educ.* **14**, 143–148

Sanders-Shamis, M., Bramlage, L., Gabel, A. (1986) Radius fractures in the horse: a retrospective study of 47 cases. *Equine Vet. J.* **18**, 432–437

Schroeder, O., Aceto, H., Boyle, A. (2013) A field study of kick injuries to the radius and tibia in 51 horses (2000–2010). *Can. Vet. J.* **54**, 271–275

Swineboard, E., Dabareiner, R., Swor, T., et al. (2003) Osteomyelitis secondary to trauma involving the proximal end of the radius in horses: five cases (1987–2001). *J. Am. Vet. Med. Ass.* **223**, 486–491

Swor, T., Watkins, J., Bahr, A., Honnas, C. (2003) Results of plate fixation of type 1b olecranon fractures in 24 horses. *Equine Vet. J.* **35**, 670–675

Swor, T., Watkins, J., Bahr, A., Epstein, K., Honnas, C. (2006) Results of plate fixation of type 5 olecranon fractures in 20 horses. *Equine Vet. J.* **37**, 30–34

SHOULDER AND HUMERUS

Ahern B., Boston, R., Ross, M. (2014) Enostosis-like lesions in equids: 79 cases (1997–2009). *J. Am. Vet. Med. Assoc.* **245**, 1042–1047

Allen, D., White, N. (1984) Chip fracture of the greater tubercle of a horse. *Comp. Cont. Educ.* **6**, S39–41

Anderson, J., Galuppo, L., Barr, B., et al. (2008) Clinical and scintigraphic findings in horses with a bone fragility disorder: 16 cases (1980–2006). *J. Am. Vet. Med. Ass.* **232**, 1694–1699

Arnold, C., Chaffin, M., Honnas, C. et al. (2008) Diagnosis and surgical management of a subchondral bone cyst within the intermediate tubercle of the humerus in a horse. *Equine Vet. Educ.* **20**, 310–315

Bassage, L., Ross, M. (1998) Enostosis-like lesions in the long bones of 10 horses: scintigraphic and radiographic features. *Equine Vet. J.* **30**, 35–42

Bohn, A., Papageorges, M., Grant, B. (1992) Ultrasonographic evaluation and surgical treatment of humeral osteitis and bicipital tenosynovitis in a horse. *J. Am. Vet. Med. Ass.* **201**, 305–306

Booth, T. (1999) Lameness associated with the bicipital bursa in an Arab stallion. *Vet. Rec.* **145**, 194–198

Boswell, J., Schramme, M., Wilson, A., May, S. (2000) Radiological study to evaluate suspected scapulohumeral joint dysplasia in Shetland ponies. *Equine Vet. J.* **32**, 510–514

Boys Smith, S., Singer, E. (2007) Mineralisation of the biceps brachii tendon in a 6-year-old Cob mare. *Equine Vet. Educ.* **19**, 74–79

Coudry, V., Allen, K., Denoix, J.-M. (2005) Congenital abnormalities of the bicipital apparatus in four mature horses. *Equine Vet. J.* **37**, 272–275

Davidson, E., Martin, B. (2004) Stress fracture of the scapula in 2 horses. *Vet. Radiol. Ultrasound* **45**, 407–410

Denoix, J.-M. (2014) Dysplasia of the sulcus intertubercularis with medial luxation of the proximal tendon of biceps brachii. *Equine Vet. Educ*. doi: 10.1111/eve/12203

Doyle, P., White, N. (2000) Diagnostic findings and prognosis following arthroscopic treatment of subtle osteochondral lesions in the shoulder joint of horses. *J. Am. Vet. Med. Ass.* **217**, 1878–1882

Dyson, S. (1985) Sixteen fractures of the shoulder region in the horse. *Equine Vet. J.* **17**, 104–110

Dyson, S. (1986a) Shoulder lameness in the horse: an analysis of 58 suspected cases. *Equine Vet. J.* **18**, 29–36

Dyson, S. (1986b) The differential diagnosis of shoulder lameness in the horse. Thesis, Fellowship of the Royal College of Veterinary Surgeons.

Dyson, S. (2009) Lesions of the proximal aspect of the humerus and the tendon of biceps brachii. *Equine Vet. Educ.* **21**, 67–70.

Dyson, S. (2011) The enigma of enostosis-like lesions in the horse. *Vet. Rec.* **168**, 324–325

Dyson, S. (2014) Intermuscular heterotopic ossification in the shoulder region associated with a hopping-type forelimb lameness. *J. Equine Vet. Sci.* **34**, 532–537

Dyson, S., Greet, T. (1986) Repair of a fracture of the deltoid tuberosity of the humerus in a pony. *Equine Vet. J.* **18**, 230–232

Embertson, R., Bramlage, L., Gabel, A. (1986) Physeal fractures in the horse II: management and outcome. *Vet. Surg.* **14**, 295–302

Firth, E., Dik, K., Goedegebuure, S., et al. (1980) Polyarthritis and bone infection in foals. *Zbl. Vet. Med.* **B27**, 102–124

Fiske-Jackson, A., Crawford, A., Archer, R.M., et al. (2010) Diagnosis, management and outcome in 19 horses with deltoid tuberosity fractures. *Vet. Surg.* **39**, 1005–1010

Forresu, D., Lepage, O., Cauvin, D. (2006) Septic bicipital bursitis, tendonitis and arthritis of the scapulohumeral joint in a mare. *Vet. Rec.* **159**, 352–354

Fugaro, M., Adams, S. (2002) Biceps brachii tenotomy or tenectomy for the treatment of bicipital bursitis, tendonitis and humeral osteitis in 3 horses. *J. Am. Vet. Med. Ass.* **220**, 1508–1511

Gaines, J., Auer, J. (1983) Treatment of a Salter Harris Type III epiphyseal fracture in a young horse. *Comp. Cont. Educ.* **5**, S102–106

Hahn, J., Geburek, F., Stadler, P., et al. (2011) Closed reduction of scapulohumeral joint luxation in an Icelandic horse after general anaesthesia. *Equine Vet. Educ.* **23**, 163–168

Downloaded From Vet-eBooks.com

Kay, A. (2006) An acute subchondral cystic lesion of the equine shoulder causing lameness. *Equine Vet. Educ.* **18**, 316–319

Koch, E., Pack, L., Zwicker, A. et al. (2014) Osteosarcoma in the proximal humerus of a mare. *Equine Vet. Educ.* doi:10.1111/eve/12148

Leitch, M. (1977) A review of treatment of tuber scapulae fractures in the horse. *J. Equine Med. Surg.* **1**, 234–240

Little, D., Redding, R., Gerard, M. (2009) Osseous cyst-like lesions of the lateral intertubercular groove of the proximal humerus: a report of 5 cases. *Equine Vet. Educ.* **21**, 60–66

Lund, C.M., Ragle, H.C., Rice, H.C., Wilkinson, T.E. (2014) Bilateral hypoplasia of the minor tubercle of the humerus with medial luxation of the biceps tendon in two quarter horses. *Equine Vet. Educ.* **26**, 467–477.

Mackey, V., Trout, D., Meagher, D., Hornhof, W. (1987) Stress fractures of the humerus, radius and tibia in horses. *Vet. Radiol.* **28**, 26–31

Meagher, D., Pool, R., Brown, M. (1979) Bilateral ossification of the tendon of biceps brachii muscle in the horse. *J. Am. Vet. Med. Ass.* **174**, 282–285

Mez, J., Dabareiner, R., Cole, R., Watkins, J. (2007) Fracture of the greater tubercle of the humerus in horses: 15 cases (1986–2004). *J. Am. Vet. Med. Assoc.* **230**, 1350–1355

Nixon, A., Stashak, T., McIlwraith, W., Aanes, W., Martin, G. (1985) A muscle separating approach to the equine shoulder joint for the treatment of osteochondritis dissecans. *Vet. Surg.* **5**, 247–256

Nyack, B., Morgan, J., Pool, R., Meagher, D. (1981) Osteochondrosis of the shoulder joint of the horse. *Cornell Vet.* **71**, 149–163

O'Neill, H., Bladon, B. (2011) Retrospective study of scintigraphic and radiological findings in 21 cases of enostosis-like lesions in horses. *Vet Rec.* **168**, 326

O'Sullivan, C., Lumsden, J. (2003) Stress fractures of the tibia and humerus in Thoroughbred racehorses: 99 cases (1992–2000). *J. Am. Vet. Med. Ass.* **222**, 491–498

Pankowski, R., Grant, B., Sande, R., Nickels, F. (1986) Fracture of the supraglenoid tubercle: treatment and results in 5 horses. *Vet. Surg.* **15**, 33–39

Parks, A., Nickels, F. (1986) Scapular sequestrum in a horse: a case report. *Vet. Surg.* **15**, 389–391

Ramzan, P., Pilsworth, R. (2001) Suspected septic physitis of the proximal humerus in two cases of Thoroughbred horses age two years. *Equine Vet. J.* **33**, 514–518

Ramzan, P. (2002) Enostosis-like lesions: 12 cases. *Equine Vet. Educ.* **14**, 143–148

Ramzan, P. (2004) Osseous cyst-like lesion of the intermediate tubercle of a horse. *Vet. Rec.* **154**, 534–536

Semevolos, S., Watkins, J., Auer, J. (2003) Scapulohumeral arthrodesis in Miniature horses. *Vet. Surg.* **32**, 416–420

Tudor, R., Crosier, M., Love, N., Bowman, K. (2001) Radiographic diagnosis: fracture of the caudal aspect of the greater tubercle of the humerus in a horse. *Vet. Radiol. Ultrasound* **42**, 244–245

Vaughan, L., Mason, B. (1975) A Clinicopathological Study of Racing Accidents in Horses, Adlard & Son, Bartholomew Press, Dorking, Surrey

Vallance, S., Lumsden, J., O'Sullivan, C. (2009) Scapula stress fractures in Thoroughbred racehorses: eight cases (1997–2006). *Equine Vet. Educ.* **21**, 554–559

Wagner, P., Watrous, B., Shires, G., Riebold, T. (1985) Resection of the supraglenoid tubercle of the scapula in a colt. *Comp. Cont. Educ.* **7**, S36–40

Wilson, R., Reynolds, W. (1984) Scapulohumeral joint luxation with treatment by closed reduction in a horse. *Aust. Vet. J.* **61**, 300–301

Yovich, J., Aanes, W. (1985) Fracture of the greater tubercle of the humerus in a filly. *J. Am. Vet. Med. Ass.* **187**, 74–75

Zamos, D., Parks, A. (1992) Comparison of surgical and non-surgical treatment of humeral fractures in horses: 22 cases (1980–1989). *J. Am. Vet. Med. Ass.* **201**, 114–116

Downloaded From Vet-eBooks.com

Chapter 9
The tarsus

RADIOGRAPHIC TECHNIQUE

Equipment

Radiographic examination of the tarsus (hock) is easily performed using a portable x-ray machine and high-definition screens or digital systems. A grid is unnecessary unless there is considerable periarticular soft-tissue swelling. A minimum of four views, lateromedial, dorsoplantar, dorsolateral-plantaromedial oblique and dorsomedial-plantarolateral oblique (or plantarolateral-dorsomedial oblique), is required. In selected cases, lateromedial (flexed) and dorsoplantar (flexed) views yield valuable additional information. The first four views are best obtained with the horse bearing full weight on the limb, with the metatarsal region positioned vertically (compare Figures 1.3a and 1.3b). It is preferable for the horse to bear weight evenly on both hindlimbs. If the horse is reluctant to bear full weight on the limb due to excessive pain, administration of an analgesic such as butorphanol may be helpful. Sedation with detomidine or other alpha-2 agonist ± butorphanol may facilitate examination of a difficult horse, which may otherwise refuse to stand still, or may kick repeatedly.

The hindlimbs should be spread apart sufficiently to allow positioning of the cassette without it touching either limb. The person holding the cassette can position it more accurately if the horse's tail is tied in a knot and the hock is not obscured. A long-handled cassette/imaging plate holder should be used. Care should be taken to ensure that both the proximal border of the tuber calcis and the tarsometatarsal joints are included on the images.

Positioning

Lateromedial view

The talocalcaneal-centroquartal (proximal intertarsal), the centrodistal (distal intertarsal) and the tarsometatarsal joints are not horizontal, but slope proximodistally, from laterally to medially. In order to avoid confusing overlap of the joint spaces it is helpful to angle the x-ray beam approximately 5-10° proximodistally (i.e. L5-10°Pr-MDiO view), centring at the approximate level of the centrodistal joint. Alternatively a horizontal x-ray beam is centred at the level of the talus (tibiotarsal bone), thus making use of a divergent x-ray beam through the lower joints of the hock. For a true lateromedial

Clinical Radiology of the Horse, Fourth Edition. Janet A. Butler, Christopher M. Colles, Sue J. Dyson, Svend E. Kold and Paul W. Poulos.
© 2017 John Wiley & Sons, Ltd. Published 2017 by John Wiley & Sons, Ltd.
Companion website: www.clinical-radiology-horse.com

Downloaded From Vet-eBooks.com

view the x-ray beam is directed parallel to a line joining the medial and lateral malleoli of the tibia, or to a line tangential to the heel of the foot.

LATEROMEDIAL (FLEXED) VIEW

A lateromedial (flexed) view can be useful to evaluate the proximal aspects of the trochlear ridges of the talus, the coracoid process of the calcaneus and the plantar distal aspect of the tibia (see Figure 9.4b). An assistant stands beside the horse's abdomen facing the tail and holds the distal aspect of the metatarsus so that the angle between the tibia and the third metatarsal bone is approximately 50°. Care should be taken to hold the limb close to the horse's body, to avoid rotation of the tarsus. If the tip of the toe is rested on the assistant's knee or thigh, this helps holding the limb steady, and also helps reposition the limb if necessary for further images. The x-ray beam is centred on the talus.

Dorsoplantar view

Many horses stand slightly 'toe-out', which is helpful because it obviates the need to position the x-ray machine beneath the horse's abdomen in order to obtain a dorsoplantar view. A horizontal x-ray beam is used, centred at the centrodistal joint. However, if one side of the centrodistal joint appears narrow this may be an artefact, especially if the talocalcaneal-centroquartal and/or tarsometatarsal joints also appear narrower on one side (Figures 9.1a and 9.1b). In some horses it is impossible for all of the centrodistal joint to be assessed simultaneously, due to the slope of the distal joints of the hock: two views may be required. If the x-ray beam is horizontal and centred at the centrodistal joint, the lateral side of the joint may appear normal but the medial side may appear abnormally narrow. If the x-ray beam is angled 5–10° proximodistally (i.e. dorsal 5° proximal-plantarodistal oblique), the medial side of the centrodistal joint may then look normal. Abnormalities of the medial and lateral malleoli may be missed in a dorsoplantar projection. A dorsal 15° medial-plantarolateral oblique view is useful to assess the lateral malleolus, and a dorsal 15° lateral-plantaromedial oblique projection is helpful to evaluate the medial malleolus (see Figure 9.8c).

Oblique views

Due to the complex structure of the equine tarsus, changes in the degree of obliquity of the x-ray beam can result in considerable alteration in the radiographs obtained. It is therefore essential to establish a consistent technique (e.g. dorsal 35° lateral-plantaromedial oblique). The x-ray beam is centred at the site of principal interest (often the centrodistal joint). A horizontal beam is employed. It may be safer to obtain a plantarolateral-dorsomedial oblique, rather than a dorsomedial-plantarolateral oblique view, although either technique can be used.

Dorsoplantar (flexed) view

The hindlimb is held flexed with the hock as far behind the horse as possible (Figure 9.2). Many horses in which this view is required resent flexion of the limb and administration of an analgesic such as butorphanol will

Downloaded From Vet-eBooks.com



Figure 9.1(a) Dorsoplantar image of a normal adult hock. Lateral is to the right. The lateral half of the talocalcaneal-centroquartal, centrodistal and tarsometatarsal joints appear narrow compared with medially. It would be very unusual for this to reflect pathological change. It may reflect the way in which the horse is standing (the metatarsal region should be vertical) or the orientation of the x-ray beam.



Figure 9.1(b) Dorsoplantar image of the same hock as Figure 9.1(a). The joint spaces of the talocalcaneal-centroquartal, centrodistal and tarsometatarsal joints are more uniform in width. The horse was load bearing more equally between the hindlimbs with the metatarsal regions vertical. It is sometimes necessary to angle the x-ray beam 5-10° proximodistally to determine that the joint spaces are normal.

facilitate this examination. The cassette is held parallel to the plantar aspect of the tuber calcanei and the x-ray beam is directed as nearly perpendicular to it as possible. It may be easier to obtain a plantarodorsal (flexed) view in some cases if only limited flexion of the hock can be achieved. These projections are particularly useful for evaluation of the tuber calcanei, the sustentaculum tali of the calcaneus and part of the talocalcaneal joint.

Downloaded From Vet-eBooks.com

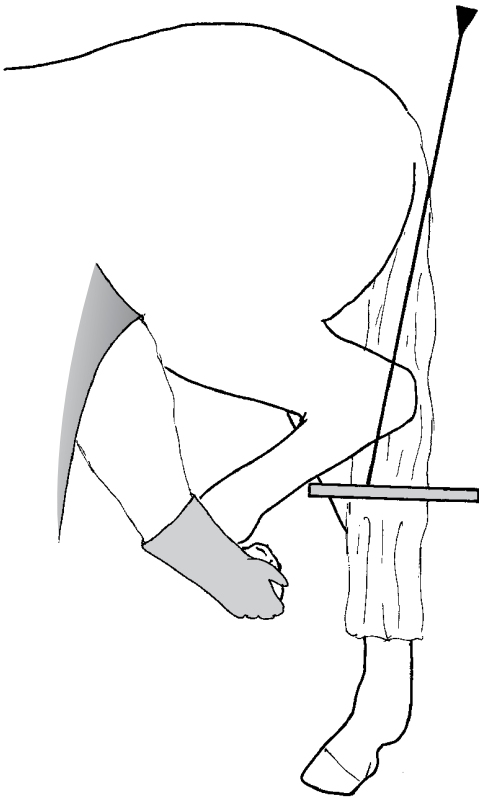


Figure 9.2 Positioning of the limb, cassette and x-ray machine to obtain a dorsoplantar (flexed) view of the calcaneus and sustentaculum tali of the fibular tarsal bone.

RADIOGRAPHIC ANATOMY: NORMAL VARIATIONS AND INCIDENTAL FINDINGS

It is important to recognise that some of the variations in radiographic appearance discussed below are the result of a previous problem that is now clinically silent. They cannot be regarded as normal, but are unlikely to be of clinical significance.

Immature horse

At birth the malleoli of the tibia and the trochlear ridges may be incompletely ossified and have an irregular, rough contour and a granular opacity (Figures 9.3a and 9.3b). There is a separate ossification centre for the lateral malleolus of the tibia, which represents the distal epiphysis of the fibula. This well-circumscribed, oval opacity fuses to the tibia by 3 months of age and should not be misinterpreted as a fracture. Adult features such as the medial proximal and distal tubercles of the talus are undeveloped. There is a separate ossification centre for the tuber calcanei, which may be absent at birth but gradually ossifies and fuses to the calcaneus by 16–24 months of age. The centres of ossification have rounded margins, especially those of the central and third tarsal bones. The joint spaces appear wider than in an adult, because there is proportionally more cartilage present. The first and second tarsal bones may be unfused. The proximal physis of the third metatarsal bone is closed at birth.

Downloaded From Vet-eBooks.com

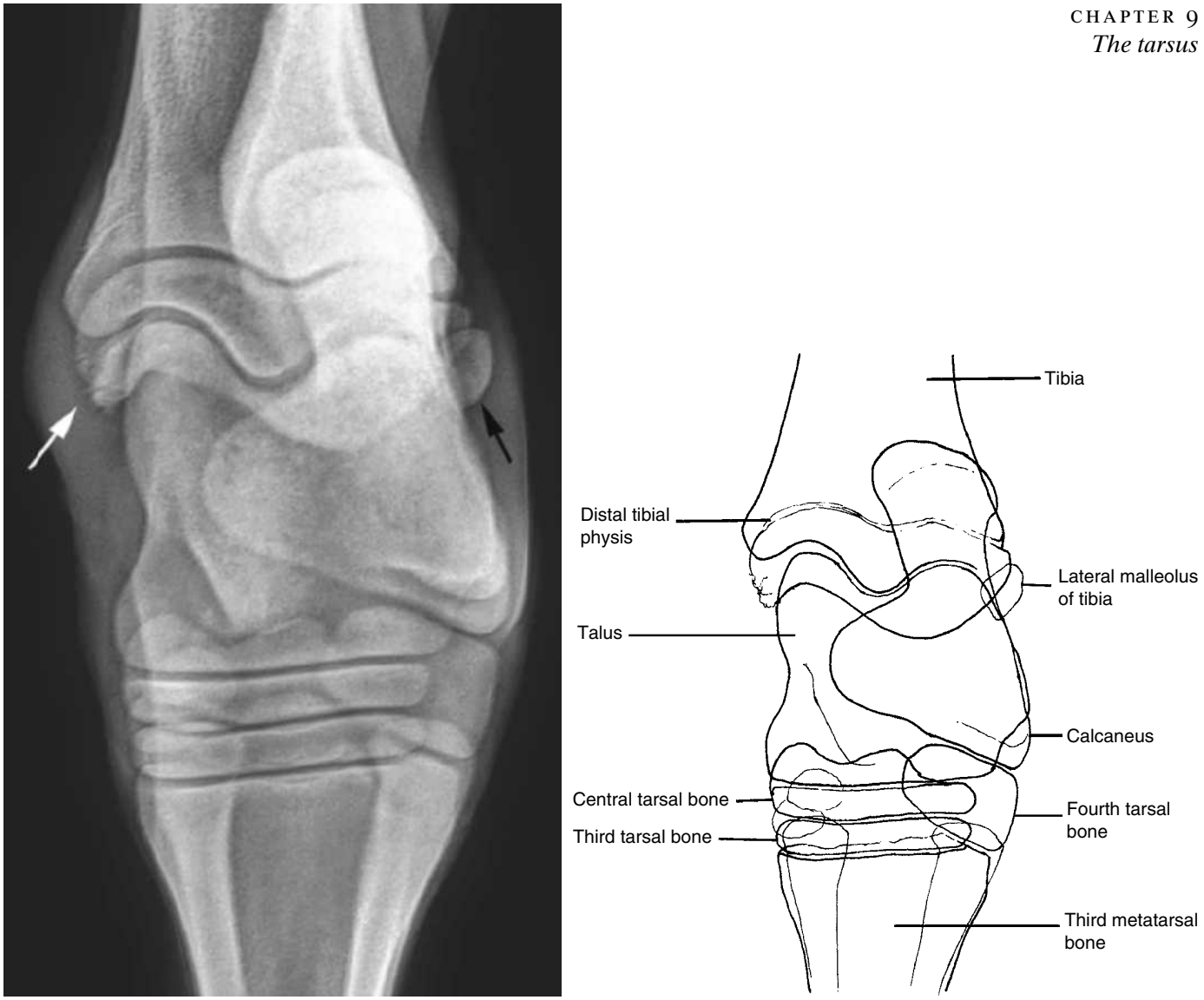


Figure 9.3(a) Dorsoplantar image and diagram of a hock of a 5-day-old foal. Lateral is to the right. The small tarsal bones are rounded and the joint spaces wide compared with those of an adult. The medial malleolus of the tibia (white arrow) is incompletely ossified. There is a separate ossification centre of the lateral malleolus of the tibia (black arrow).

Skeletally mature horse

In order to understand the complicated radiographic anatomy of the tarsus it is useful to compare the radiographs with a bone specimen and to examine the shapes of the individual, disarticulated bones (see Figures 9.4a, 9.8a, 9.10a and 9.11).

Lateromedial view

A normal lateromedial image and a lateromedial (flexed) image are illustrated in Figures 9.4a and 9.4b. Poorly-marginated areas of increased opacity are occasionally seen in the distal metaphysis of the tibia as an incidental finding. The distal cranial aspect of the tibia may be smoothly irregular. In some horses there is a separate bony fragment at the craniodistal aspect of the tibia: its exact

Downloaded From Vet-eBooks.com



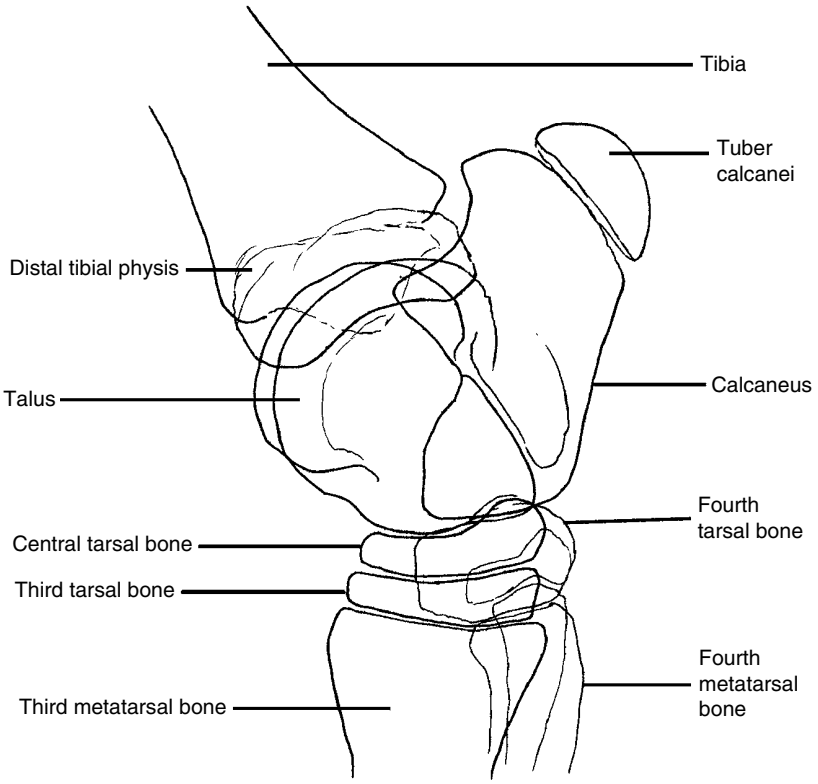


Figure 9.3(b) Lateromedial image and diagram of a hock of a 5-day-old foal. Note the relatively flat contour of the trochlear ridges of the talus compared with those of an adult, the widened joint spaces and the incompletely ossified tuber calcanei.

Downloaded From Vet-eBooks.com

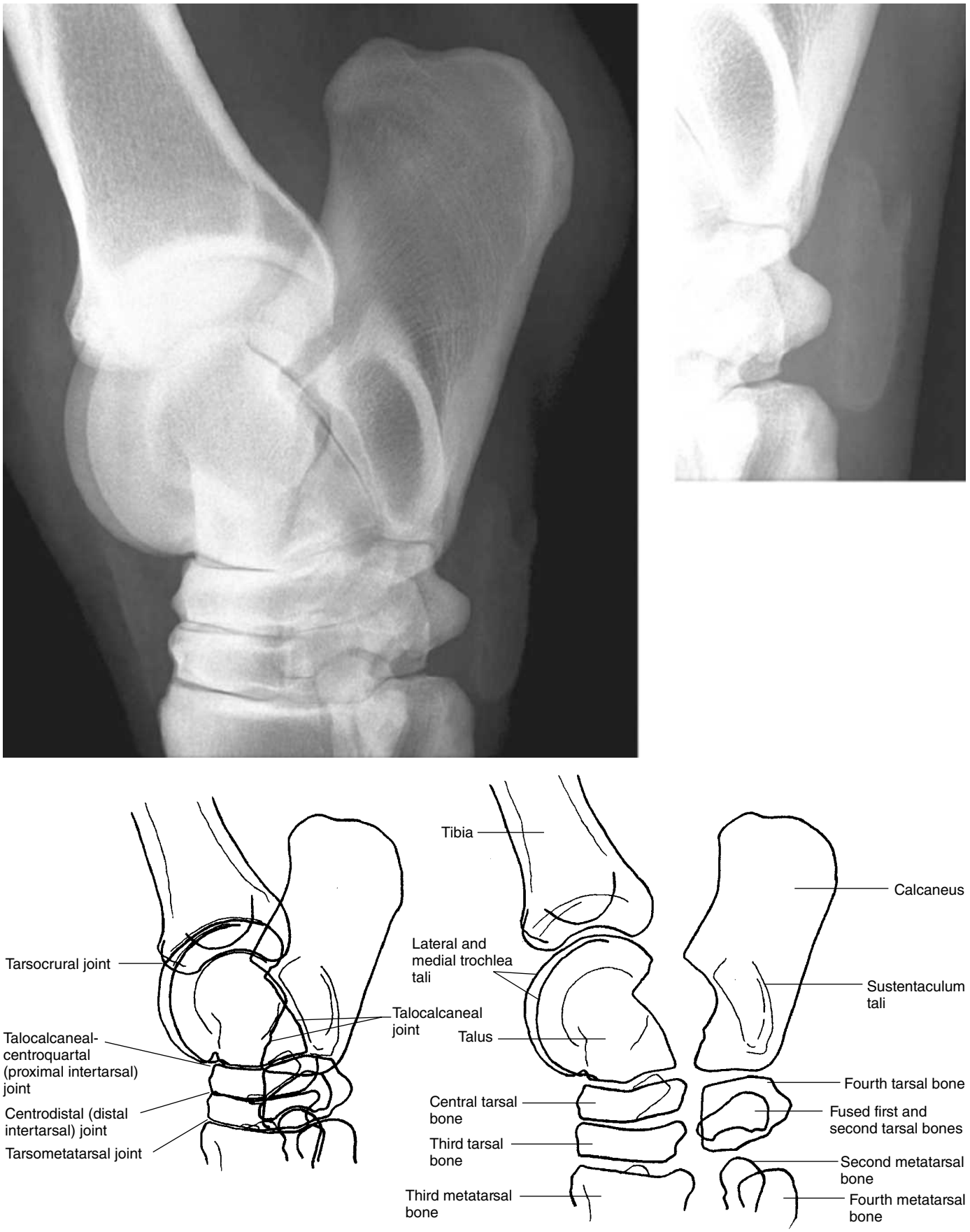


Figure 9.4(a) Lateromedial image and diagram of a normal adult hock. On a soft exposure (inset) the torus tarseus (chestnut) is readily seen.

Downloaded From Vet-eBooks.com

location is established from the oblique views, the most common site being the craniodistal aspect of the intermediate ridge of the tibia (see Figure 9.18). This is likely to be a manifestation of osteochondrosis. It is often clinically silent, particularly if small, although its presence may be associated with distension of the tarsocrural joint capsule (bog spavin), with or without lameness. The medial and lateral trochlear ridges of the talus are smoothly curved, but may be slightly flattened in the mid-region (Figure 9w.4c), especially in Warmblood and heavy horse breeds. There is sometimes a smoothly outlined depression in the middle one-third of the lateral trochlear ridge of the talus, with normal subchondral bone opacity or slight increased opacity seen in either a lateromedial or dorsomedial-plantarolateral oblique view (Figure 9w.4d). There is some controversy as to whether these represent a manifestation of osteochondrosis; however, they are invariably asymptomatic. There may be an ill-defined narrow lucent area in the subchondral bone of the medial trochlea representing the presence of a synovial fossa. The lateral trochlear ridge has a distinct large notch at its distal end, whereas the medial ridge has a variably sized protuberance distally. This protuberance may be small, with or without a lucent line (a nutrient vessel) extending through it, or may be large and rounded or pointed. Sometimes there are one or two discrete bony opacities distal to it (Figure 9.5), which should not be confused with fractures. The two trochlear ridges are more widely separated in the oblique views.

Depending on the exposure factors used, a variable number of lucent lines can be identified in the region where the calcaneus and talus are superimposed. These represent the talocalcaneal and tarsocrural articulations and should not be confused with fractures.



Figure 9.4(b) Lateromedial (flexed) image of a hock of an adult horse. There is slight modelling of the dorsoproximal aspect of the third metatarsal bone, of no clinical significance in this horse.

Downloaded From Vet-eBooks.com

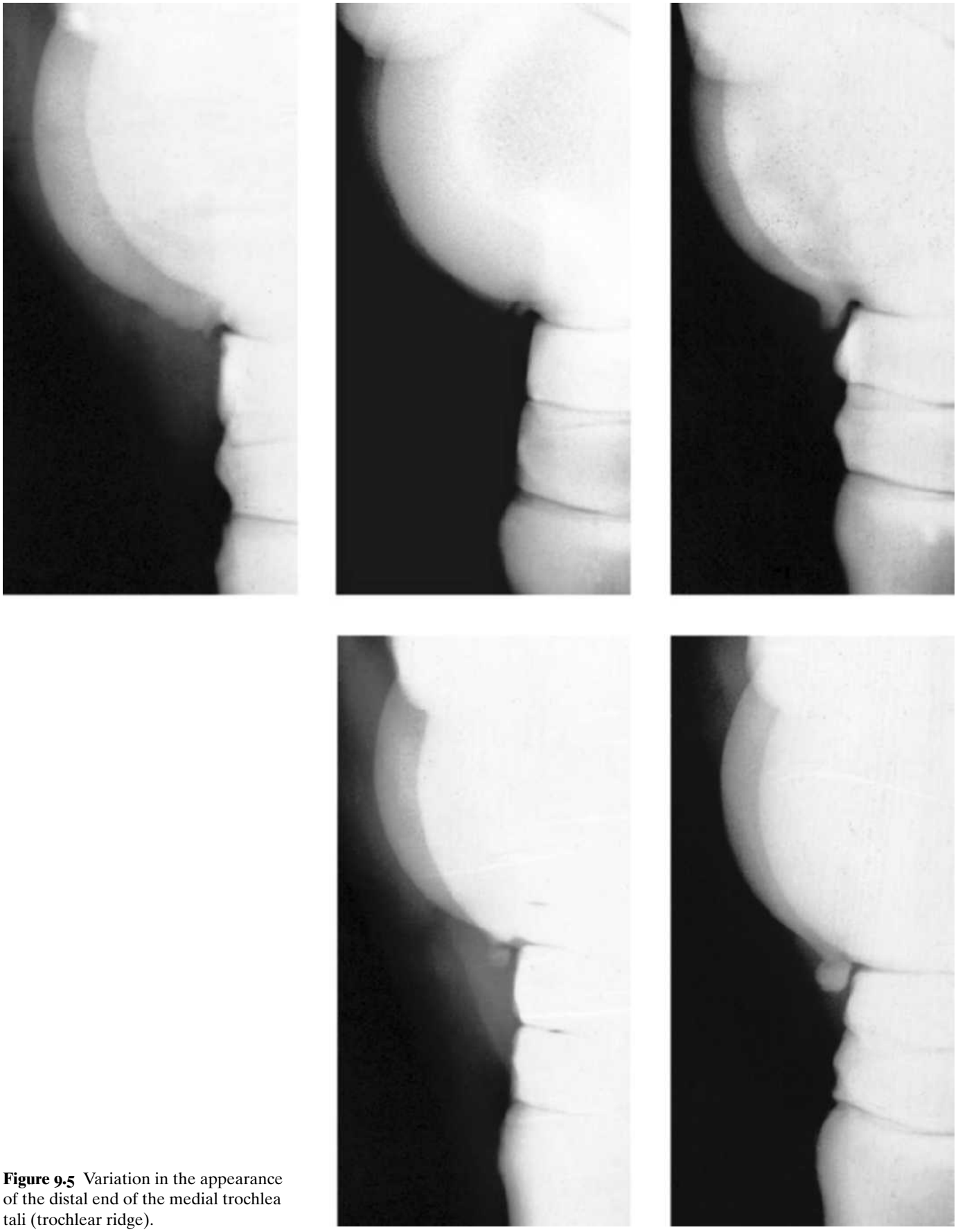


Figure 9.5 Variation in the appearance of the distal end of the medial trochlea tali (trochlear ridge).

Downloaded From Vet-eBooks.com



Figure 9.6 Lateromedial image of a hock of a 10-year-old showjumper. There is a well-defined entheseophyte (arrow) on the plantar aspect of the calcaneus at the origin of the long plantar ligament. This was of no clinical significance.

Entheseophyte formation on the proximoplantar aspect of the calcaneus is sometimes seen as an incidental finding (Figure 9.6).

The central and third tarsal bones are fairly regular in height (proximodistally) from their dorsal to plantar aspects. The first, second and fourth tarsal bones are projected superimposed upon each other; the smoothly irregular plantar contour of the fourth tarsal bone is highlighted in this view. The plantar surfaces of the calcaneus and fourth tarsal and metatarsal bones are sometimes smoothly modelled, reflecting previous tearing of the attachment of the plantar ligament ('curb').

There is sometimes a small osseous 'spur' on the dorsoproximal aspect of the third metatarsal bone (Figures 9.7a–f). This may be an osteophyte or an entheseophyte at the site of attachment of the dorsal tarsometatarsal ligament, fibularis (peroneus) tertius, or the cranial tibial tendon, reflecting a previous injury. In the absence of other radiological abnormalities, an osteophyte or an entheseophyte does not necessarily signify degenerative joint disease, although they may have an association. An osteophyte of no significance should have a smooth margin and be of uniform opacity (Figures 9.7a and 9.7b). An irregular margin or variable opacity (both of which may only be discernible when the radiograph is viewed over high-intensity illumination or windowed appropriately) suggests bony activity (Figures 9.7c and 9.7d). Dystrophic mineralisation in the tendon of fibularis tertius or tibialis cranialis is usually an incidental finding (Figure 9.7g).

Downloaded From Vet-eBooks.com



Figure 9.7(a) Lateromedial image of the left hock of an 11-year-old Warmblood showjumper with a good competition record. There is a uniformly opaque spur on the dorsoproximal aspect of the third metatarsal bone. This radiograph was obtained at a pre-purchase examination. There was no detectable lameness, although mild lameness was induced by flexion. The horse was purchased and has remained sound and in full work.



Figure 9.7(b) Slightly oblique lateromedial image of the right hock of a 7-year-old Thoroughbred cross gelding used for unaffiliated competition. There is a well-consolidated periarticular osteophyte on the dorsoproximal aspect of the third metatarsal bone. Lameness was associated with proximal suspensory desmopathy. Intra-articular analgesia of the tarsometatarsal joint did not alter the lameness.



Figure 9.7(c) Lateromedial image of the left hock of a 13-year-old Thoroughbred used for general purposes. There is a large osteophyte on the dorsoproximal aspect of the third metatarsal bone which is less opaque than the parent bone. This is an active lesion. There is also subtle modelling of the distal dorsal aspect of the third tarsal bone. Lameness was improved by intra-articular analgesia of the tarsometatarsal joint.

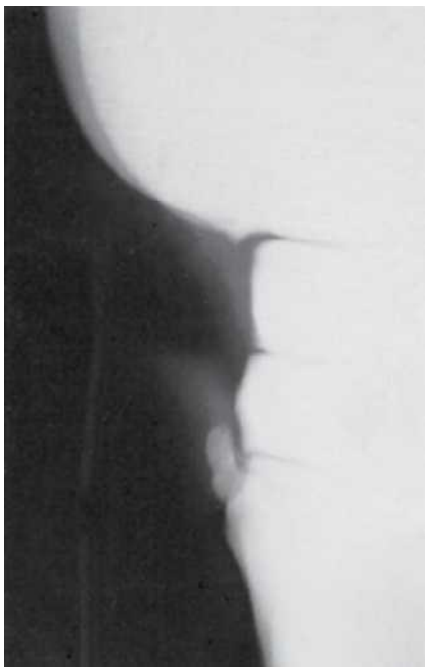


Figure 9.7(d) Lateromedial image of an adult hock. There is an active entheseophyte on the dorsoproximal aspect of the third metatarsal bone.

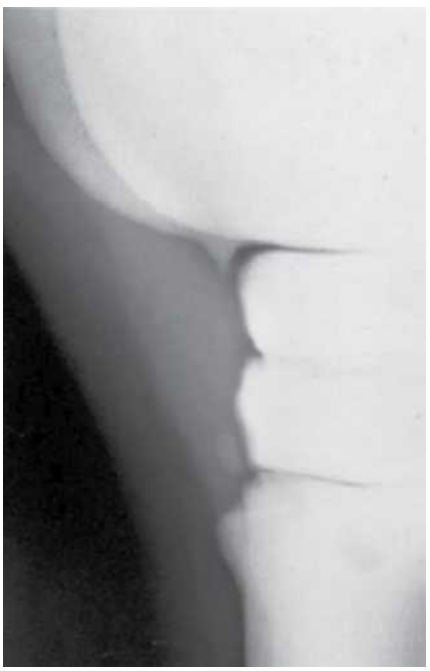


Figure 9.7(e) Lateromedial image of an adult hock. There is dystrophic mineralisation in the cranial tibial tendon.

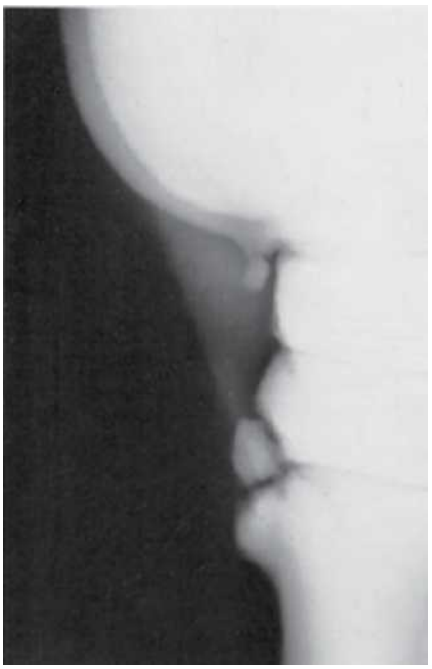


Figure 9.7(f) Fracture of a large entheseophyte on the dorsoproximal aspect of the third metatarsal bone. Note also the osseous opacity distal to the medial trochlea tali.

Downloaded From Vet-eBooks.com



Figure 9.7(g) Dorsomedial-plantarolateral oblique image of a hock. There is dystrophic mineralisation in the tendon of fibularis tertius (arrow).



Figure 9.8(a) Dorsoplantar image and diagrams of a normal adult hock. Lateral is to the right. Note the relatively lucent areas in the central and third tarsal bones in the middle of the centrodistal joint (arrows), the centrodistal interosseous space, a normal finding. There is a similar interosseous space between the third tarsal bone and third metatarsal bone.

Downloaded From Vet-eBooks.com

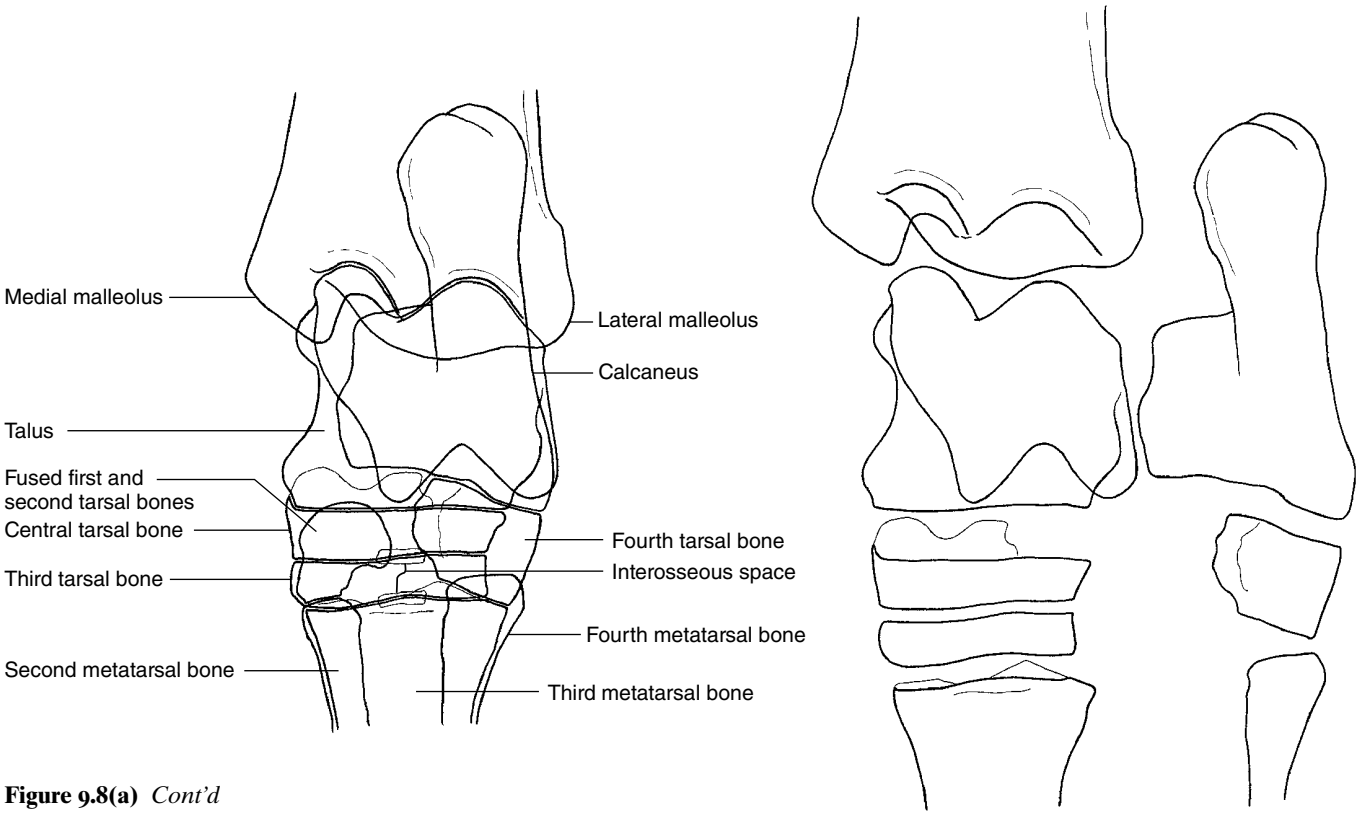


Figure 9.8(a) *Cont'd*

The mottled opacity of the torus tarseus (chestnut) may be seen overlying the plantar aspect of the fourth tarsal bone (Figure 9.4a) and must not be confused with pathological mineralisation of the soft tissues.

Dorsoplantar view

The medial and lateral malleoli are seen as smoothly rounded protuberances of the distal aspect of the tibia (Figure 9.8a). Smooth irregularity of outline may reflect previous damage to the attachment of the collateral ligaments of the tarsocrural joint. A well-defined oval-shaped radiolucent area adjacent to the distal lateral aspect of the talus is a normal finding, the presence of which depends on the angle of projection (Figures 9.8b and 9.20d). This is created by slight overlap of the talus and the calcaneus and an oval-shaped space between them, the sinus tarsi. It should not be misinterpreted as an osseous cyst-like lesion.

The concave proximal articular surface of the central tarsal bone results in its plantar aspect being superimposed over the talus. There are many confusing opacities and lucent lines in the region of the central and third tarsal bones because of superimposition of the first, second and fourth tarsal bones and the bases (proximal ends) of the second and fourth metatarsal bones. The bases of the latter two bones are sloping and their articulations with the fused first and second tarsal bone and the fourth tarsal bone, respectively, are superimposed over the proximal one-third of the third tarsal bone. The resultant lucent lines should not be confused with pathological lesions. There are sometimes well-defined oval lucent areas bordered by a thin rim of radiopaque bone, between the talocalcaneal-centroquartal, centrodistal and

Downloaded From Vet-eBooks.com



Figure 9.8(b) Slightly oblique dorsoplantar image of the right hock of a 12-year-old Thoroughbred cross Warmblood advanced event horse. Lateral is to the right. There is a well-circumscribed radiolucent area lateral to the distal lateral aspect of the talus (arrow). This radiolucent area represents the sinus tarsi between the talus and fibular tarsal bone, a normal finding which should not be confused as an osseous cyst-like lesion.



Figure 9.8(c) Dorsal 15° lateral-plantaromedial oblique image of a normal adult tarsus. This degree of obliquity allows assessment of the distal and axial aspects of the medial malleolus. Compare with Figures 9.8(a) and 9.17(b).

tarsometatarsal joints. These represent non-articular depressions, the interosseous spaces, and should not be confused with osseous cyst-like lesions. Small, well-defined osseous cyst-like lesions are sometimes seen in isolation in the spongiosa of either the central or third tarsal bones and are usually of no clinical significance (Figure 9.9a).

The dorsoplantar view is the best for evaluating the width of the intertarsal articulations, provided that these joints are in the centre of the radiograph and bearing in mind the limitations imposed by the slope of the articular surfaces mentioned above. Sometimes one side of the joint space appears narrowed, but this may be an artefact. The view should be repeated, angling the x-ray beam 5–10° proximodistally (i.e. dorsal 5° proximal-plantarodistal oblique). Usually this 'opens up' the apparently narrowed side of the joint. Poor technique can also mimic a narrow joint space (Figure 9.1). Complete or, more often, incomplete ankylosis of the centrodistal and/or tarsometatarsal joints, in the absence of subchondral bone lysis, is sometimes seen without associated lameness.

Entheseous new bone on the proximal medial tubercle of talus may be seen as an incidental finding. A radiolucent line may traverse obliquely the central and third tarsal bones. This is a Mach line created by the

Downloaded From Vet-eBooks.com



Figure 9.9(a) Dorsomedial-plantarolateral oblique image of the left hock of a 6-year-old Warmblood. There is a well-circumscribed radiolucent osseous cyst-like lesion in the plantar aspect of the third tarsal bone (arrows) of questionable clinical significance. There is also a very small spur on the dorsoproximal aspect of the third metatarsal bone.



Figure 9.9(b) Dorsoplantar image of the hock of a 12-year-old Connemara gelding. Lateral is to the right. The centrodistal joint is markedly narrowed and effectively fused. There is an oblique radiolucent line traversing the central and third tarsal bones from proximomedially to distolaterally (arrows), mimicking a fracture of the fused bones. This is an artefact and is a Mach line on the lateral aspect of the fused first and second tarsal bones superimposed on the central and third tarsal bones. The line persisted in dorsoproximal-plantarodistal oblique images and in dorsal 5°lateral–plantaromedial oblique images. None of these observations were of clinical significance.

superimposition of the lateral border of the fused first and second tarsal bones (Figure 9.9b). This should not be confused with a fracture.

An exostosis on the proximolateral aspect of the third metatarsal bone is seen in some horses. This may have a heterogeneous opacity (see Figure 6.13), but is usually smoothly outlined. Such exostoses, despite invariably being associated with focal, intense increased radiopharmaceutical uptake, are generally of no clinical significance.

Dorsolateral-plantaromedial oblique view

The dorsolateral-plantaromedial oblique view (Figure 9.10a) highlights the medial malleolus of the tibia, the medial trochlear tali and the dorsomedial aspects of the intertarsal joints. There is a variably sized and shaped lucent area in the proximal part of the tarsal groove which represents a synovial fossa. Similar areas in the corresponding articular surface of the tibia are not seen radiographically. The distally located medial tuberosity of the talus is usually smoothly rounded; it may be smoothly irregular, reflecting previous

Downloaded From Vet-eBooks.com



Figure 9.10(a) Dorsolateral-plantaromedial oblique image and diagrams of a normal adult hock. There is a radiolucent area (black arrow), a synovial fossa, in the intertrochlear groove of the talus. The third tarsal bone has a medial prominence. The dorsal opening of the tarsal canal is clearly outlined (white arrow). Note the oval lucent area between the talus and calcaneus, the sinus tarsi.

tearing of the attachment of the medial short collateral ligament. The sinus tarsi, a non-articular area between the talus and calcaneus, is seen as a relatively lucent line or oval-shaped area between the two bones, and varies with the angle of projection. There may be a smoothly demarcated, shallow, concave depression in the outline of the medial trochlea of the talus with normal architecture of the underlying trabecular bone.

There is a bony prominence on the dorsomedial aspect of the third tarsal bone at the site of attachment of one of the dorsal tarsal ligaments. The subchondral bone of the distal aspect of the talus, the central and third tarsal bones and the proximal aspect of the third metatarsal bone is relatively opaque. There are non-articular depressions on the opposing surfaces of the talus, central and third tarsal bones and third metatarsal bones that result in relatively lucent areas in the centre of the centrodistal and tarsometatarsal

Downloaded From Vet-eBooks.com

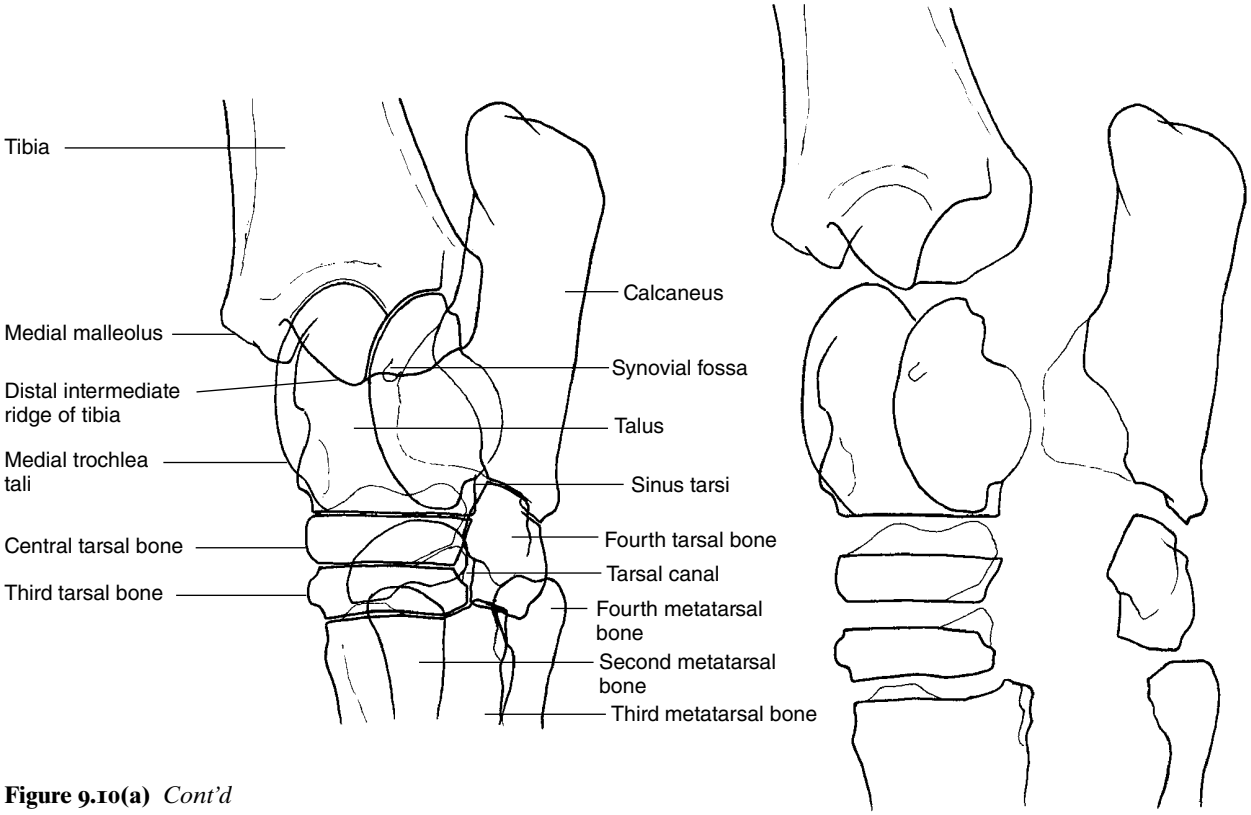


Figure 9.10(a) *Cont'd*



Figure 9.10(b) Lateromedial image of a mature horse. There is a smoothly outlined concave depression in the lateral trochlea of the talus (arrow), of no clinical significance. Note the bifid protuberance on the distal aspect of the medial trochlea, another normal variant. There is also subtle modelling of the dorsoproximal aspect of the third tarsal bone.

joints. These are sites of intertarsal interosseous ligaments. Each radiolucent area is surrounded by a rim of more opaque bone of uniform thickness, which is well-demarcated from the adjacent trabecular bone of the spongiosa. Occasionally there is mineralisation within the centre of the radiolucent space.

Downloaded From Vet-eBooks.com

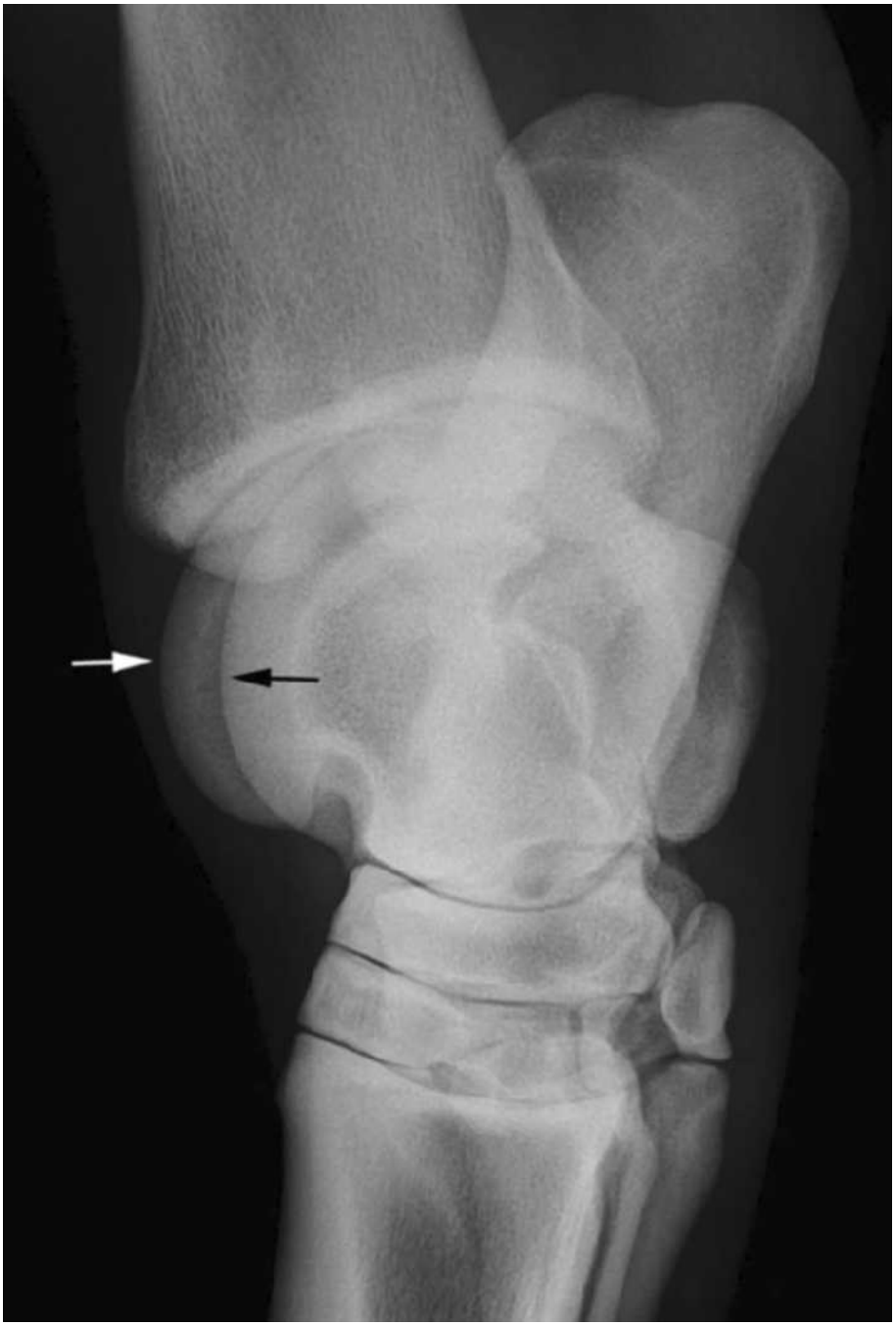


Figure 9.11 Plantarolateral-dorsomedial oblique image and diagrams of a normal adult hock. The medial trochlea tali (black arrow) and the lateral trochlea tali (white arrow) are clearly separated. The sustentaculum tali is highlighted on the plantar aspect of the talus. Note the inverted flask-shaped joint space between the third and fused first and second tarsal bones.

In a well-positioned dorsolateral-plantaromedial oblique view, the dorsal opening of the tarsal canal, through which passes the perforating tarsal artery and a branch of the deep fibular (peroneal) nerve, is seen as a well-defined lucent area. The canal is not in the sagittal plane but courses slightly obliquely; therefore, unless the x-ray beam is parallel with the long axis of the canal, its walls will be seen as bone encroaching into the canal. This must

Downloaded From Vet-eBooks.com

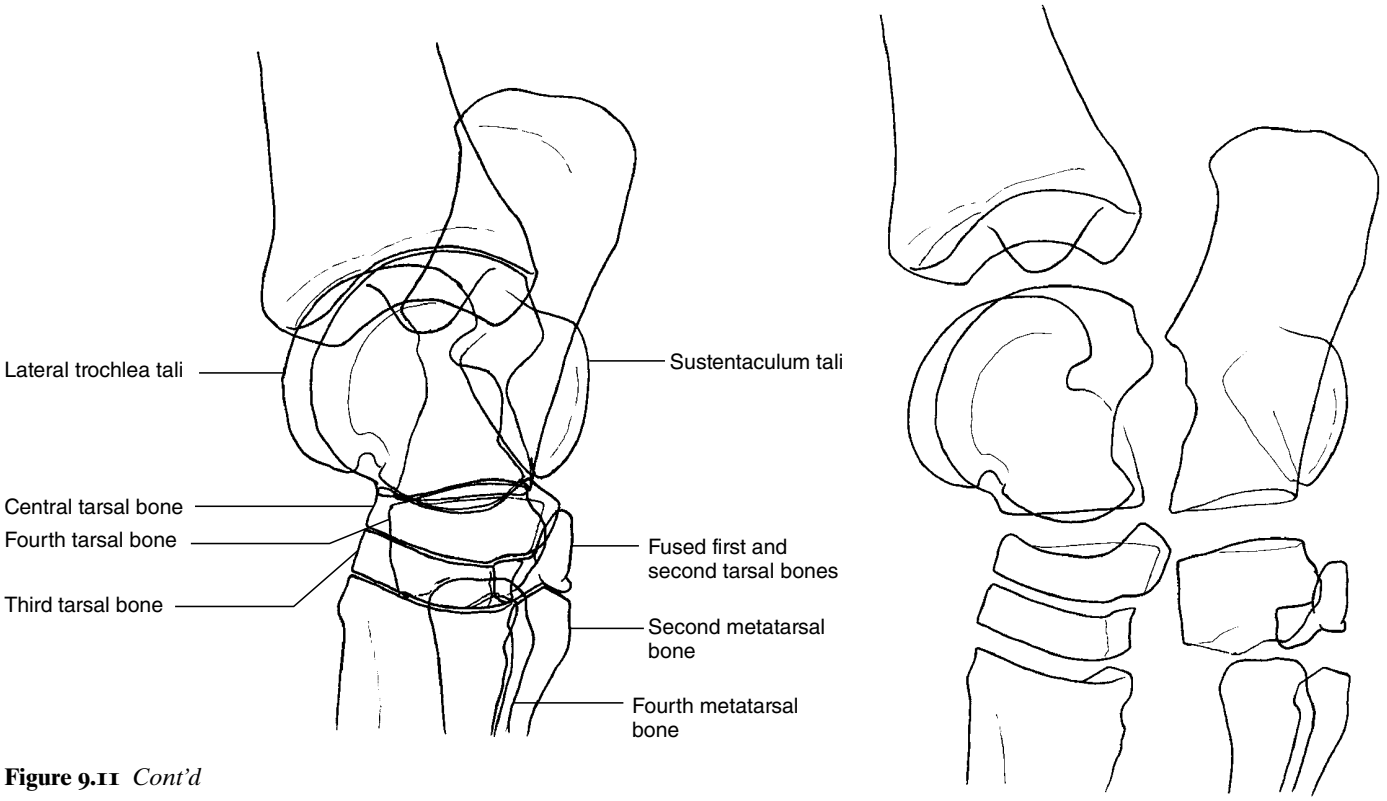


Figure 9.11 *Cont'd*

be differentiated from new bone on the lateral aspect of the centrodistal joint (see Figure 9.23a). This new bone can usually also be seen in a dorsoplantar view. The plantar opening of the tarsal canal appears as a relatively lucent area superimposed over the fourth tarsal bone.

Occasionally there is a separate centre of ossification on the proximal aspect of the fourth metatarsal bone or an osseous spur on the proximoplantar aspect of the fourth metatarsal bone.

Dorsomedial-plantarolateral oblique view

The dorsomedial-plantarolateral oblique view (Figure 9.11) highlights the sustentaculum tali, the lateral trochlea tali, the dorsolateral aspects of the intertarsal joints, and the plantar aspect of the sustentaculum tali and the central, first and second tarsal bones. Occasionally the distal end of an incompletely ossified fibula is seen. A separate bony fragment from the craniodistal aspect of the intermediate ridge of the tibia is often best seen in this view which may or may not be clinically significant (see 'Osteochondrosis', below). Such lesions were seen in 9.6% of 3794 mature German Warmblood horses undergoing presales radiographic examination. There is also a high frequency of occurrence in trotters, ranging from 7.2% to 15% in a variety of studies. The normal contour of the distal aspect of the intermediate ridge of the tibia is flat or smoothly convex. A flattened or concave contour is suggestive of osteochondrosis or possibly previous fragment removal (Figure 9.19b). Sometimes ill-defined radiopacities persist distal to the intermediate ridge of the tibia (Figure 9w.12). Occasionally a well-defined osseous cyst-like lesion is seen in the distal subchondral bone plate of the tibia, either unilaterally or bilaterally (Figure 9w.13a). Rarely there is a well-defined entheseophyte on the distal

Downloaded From Vet-eBooks.com

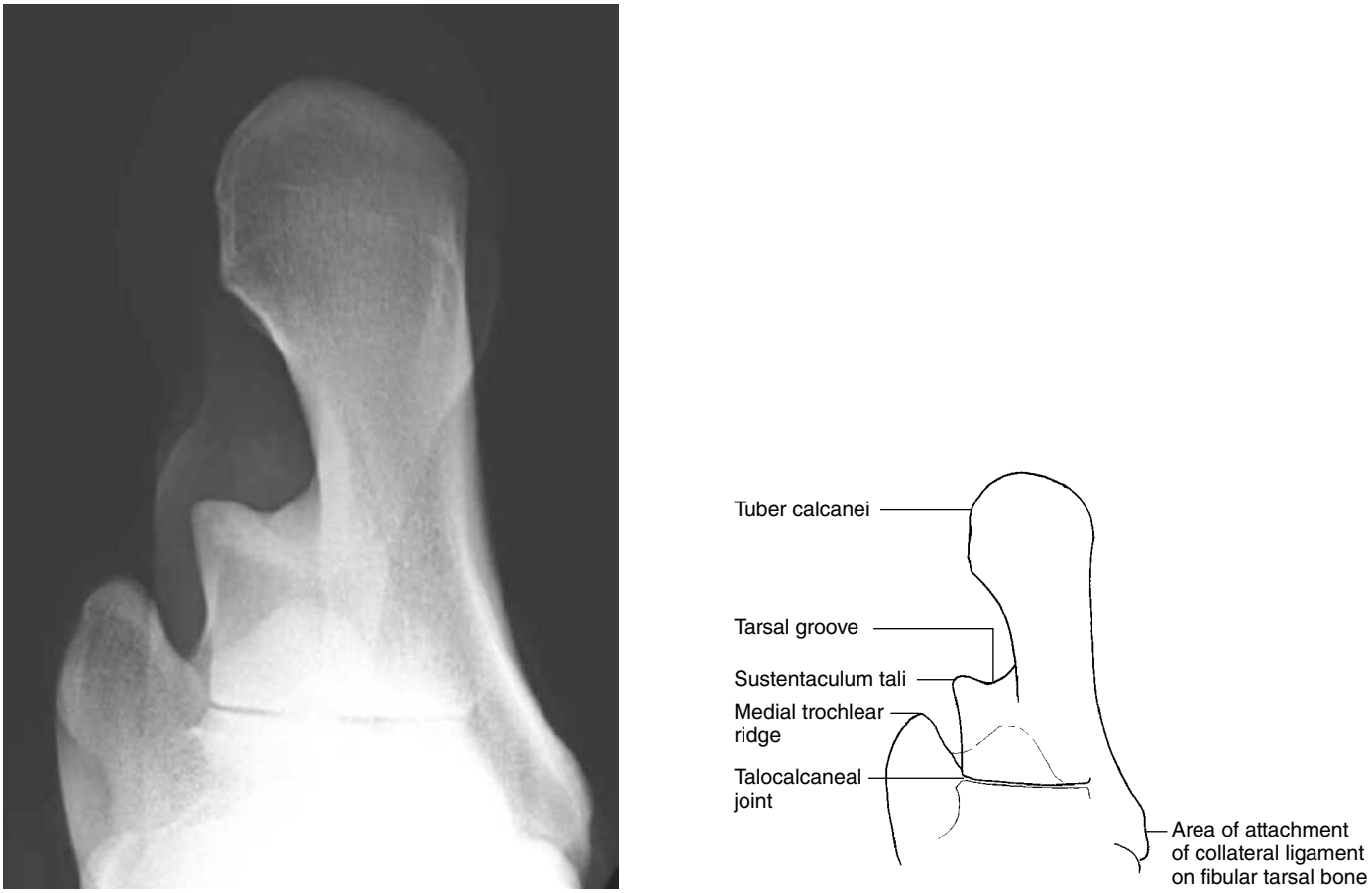


Figure 9.14 Dorsoplantar (flexed) image and diagram of a normal hock. Lateral is to the right.

aspect of the sustentaculum tali (Figure 9w.13b). There may be a smoothly-demarcated, shallow, concave depression in the outline of the lateral trochlea of the talus with normal architecture of the underlying trabecular bone (Figures 9.10b and 9w.4d).

Dorsoplantar (flexed) view

The proximal parts of the medial trochlear ridge, the sustentaculum tali, the tarsal groove, the tuber calcanei and the talocalcaneal joint are highlighted in the dorsoplantar (flexed) view (Figure 9.14). Other structures are underexposed and cannot be assessed properly.

SIGNIFICANT RADIOLOGICAL ABNORMALITIES

Congenital abnormalities

Congenital malformation of the sustentaculum tali of the calcaneus (fibular tarsal bone) occurs in Saddlebreds and occasionally in Thoroughbreds (Figure 9.15). Flattening of the proximal aspect of the sustentaculum tali results in the deep digital flexor tendon slipping dorsally and medially. Clinically the plantar aspect of the tarsal region appears broader than usual and there is tarsal valgus. Radiographic abnormalities are detectable only in a dorsoplantar (flexed) image, in which the contour of the sustentaculum tali appears flattened.

Downloaded From Vet-eBooks.com



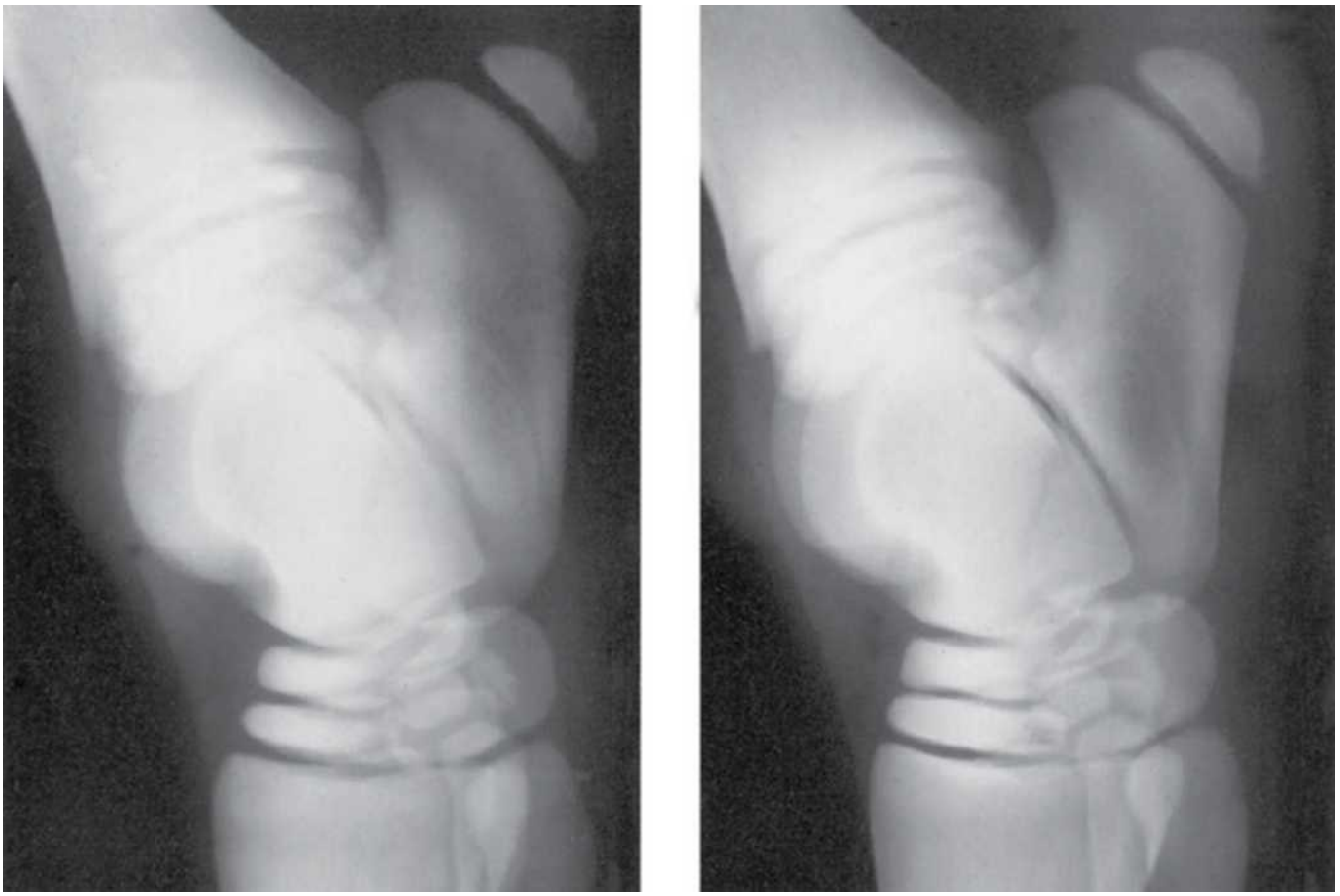
Figure 9.15 Dorsoplantar (flexed) oblique image of the hock of a 3-week-old Thoroughbred foal with a malformed hock. Lateral is to the right. There is flattening of the sustentaculum tali (arrow).

Tarsal bone collapse

Tarsal bone collapse may be recognised radiographically in neonatal foals, in older foals or young adults. In a neonate the tarsal bones appear relatively immature; they are smaller and more rounded than usual due to incomplete ossification (Figure 9.16a). They may have a granular opacity (the bone is comprised of opaque granules). Clinically the neonatal foal shows excessive flexion of the hocks (sickled and 'curby' hock conformation) and/or tarsal valgus deformities. The condition is most common in premature foals or those born one of a twin. Unless the limbs are supported from the first days of life (e.g.in cylinder tube casts) until ossification has progressed further, normal weight bearing will result in compression of either or both the central and third tarsal bones. The compressed bones appear wedge-shaped in both lateromedial and dorsoplantar images, and may have fragmentation and narrowing of the joint spaces. This condition has also been seen in neonatal foals in association with osteomyelitis of the third and central tarsal bones, in which case the bone may have a mottled opacity due to lucent areas within the bone. Since tarsal collapse is often bilateral, both hocks should be examined radiographically.

Tarsal collapse may pass unrecognised until the horse starts work, when there may be an acute onset of unilateral or bilateral hindlimb lameness or stiffness (Figure 1w.9). Radiographic examination reveals wedge-shaped central and/or third tarsal bones (Figures 9.16b and 9.16c) and there may be

Downloaded From Vet-eBooks.com



(i) (ii)

Figure 9.16(a) Lateromedial images of a premature Thoroughbred foal born at a gestational age of 318 days. The radiographs were obtained (i) 6 days and (ii) 12 days post partum, i.e. at 324 and 330 days' gestation. Note the rounded edges of the incompletely ossified tarsal bones and the wide joint spaces and the progressive enlargement of the bones and decrease in width of the joint spaces.

evidence of secondary degenerative joint disease (e.g. collapse of the joint spaces and periarticular new bone). In less severe cases there may only be a slight wedge-shaped appearance of the third tarsal bone. Compare the height of the bone dorsally with the plantar aspect.

In the neonate, provision of external support to the limb permits endochondral ossification to proceed without deformation of the bones and, provided treatment is started early, the prognosis is fair to good. In the adult, the prognosis is usually poor for performance animals; ankylosis of the bones may ultimately occur, although not necessarily so.

Osteochondrosis

Radiographic abnormalities which are thought to be a manifestation of osteochondrosis include:

1 A lucent area on the axial aspect of the medial malleolus (Figure 9.17a) or separation of a bony fragment at either the medial (Figure 9.17b) or (less commonly) the lateral malleolus of the tibia, or the craniodistal aspect of the intermediate ridge of the tibia (Figure 9.18).

Downloaded From Vet-eBooks.com



Figure 9.16(b) Lateromedial image of a hock of a 5-month-old Thoroughbred foal. The foal presented with lameness and swelling on the distal dorsal aspect of the hock. There is deformation of the third tarsal bone with narrowing of the height of the bone plantar to the dorsal articular margin. There is diffuse increase in opacity of the spongiosa. However despite mild joint space narrowing of the centrodistal and tarsometatarsal joints dorsally, there remains congruity between the articular margins of the central and third tarsal bones and the third metatarsal bone.



Figure 9.16(c) Lateromedial image of the left hock of a 9-year-old Thoroughbred cross with mild left hindlimb lameness, improved by intra-articular analgesia of the tarsometatarsal joint. The dorsal aspect of the central tarsal bone is narrow from proximally to distally and has increased opacity. There is mild modelling of the dorsal aspect of the central tarsal bone and a small osteophyte on the dorsoproximal aspect of the third tarsal bone. The dorsal aspect of the third tarsal bone also has increased opacity.

2 Bony fragments at the distal end of the medial trochlear ridge of the talus (see Figure 9.5) or the lateral trochlear ridge of the talus (Figures 9.19a and b).
3 Separation of a bony fragment from the medial proximal tubercle of the talus.
4 An irregular, flattened contour of the medial and/or lateral trochlear ridges of the talus with or without radiolucent zones in the underlying subchondral bone (Figure 9.10b).

Bony fragments of the medial and lateral malleoli of the tibia must be differentiated from avulsion fractures. Some medial malleolar articular fragments are not detectable in a dorsoplantar projection; a dorsal 15° lateral-plantaromedial oblique view may be required (Figure 9.17b; compare with Figure 9.17a). Fragments distal to the distal end of the trochlear ridges may have originated from the distal aspect of the tibia and have fallen distally. Lesions frequently occur bilaterally. Fragments at the craniodistal aspect of the intermediate ridge of the tibia are most common and can be detected at less than 3 months of age.

Downloaded From Vet-eBooks.com



Figure 9.17(a) Dorsolateral-plantaromedial oblique image of a yearling Thoroughbred with sudden onset of tarsocrural joint effusion. There is a radiolucent area in the subchondral bone of the medial malleolus of the tibia (arrows), a manifestation of osteochondrosis.



Figure 9.17(b) Dorsal 15° lateral-plantaromedial oblique image of the right hock of a yearling Warmblood with marked distension of the tarsocrural joint, but no detectable lameness. There is an osteochondral fragment on the axial aspect of the medial malleolus (arrows), a manifestation of osteochondrosis.

They vary considerably in size and shape, but are often bilaterally symmetrical. More than one fragment may be present; a large fragment may also become fractured. There may be an obvious lucent defect in the adjacent subchondral bone. The majority occur on the craniodistal lateral aspect of the intermediate ridge of the tibia and are readily seen in plantarolateral-dorsomedial oblique views. Medial lesions occasionally occur however, and are seen in a slightly more plantar position in this oblique view and are easily missed. Lesions of the trochleas of the talus are usually in the distal one-half and may be restricted to the most distal aspect (Figure 9.19b). Osteochondrosis lesions may cause release of inflammatory debris into the joint and resultant synovitis and distension of the tarsocrural joint, which can be seen on radiographs.

Downloaded From Vet-eBooks.com



Figure 9.18 Dorsomedial-plantarolateral oblique image of the right hock of a 7-year-old Warmblood showjumper with distension of the tarsocrural joint, but no lameness. There appears to be a single large osteochondral fragment on the craniodistal aspect of the intermediate ridge of the tibia and a smaller fragment immediately cranial to it. These osteochondrosis fragments were removed surgically and three pieces were found.



Figure 9.19(a) Dorsomedial-plantarolateral oblique image of the right hock of a weanling Thoroughbred with distension of the tarsocrural joint. There is an irregular outline of the lateral trochlea of the talus and multiple mineralised fragments, a manifestation of osteochondrosis.



Figure 9.19(b) Dorsomedial-plantarolateral oblique image of a hock. There is fragmentation of the distal aspect of the lateral trochlea of the talus, reflecting osteochondrosis. There is a concave contour of the distocranial aspect of the intermediate ridge of the tibia, suggestive of previous removal of an osteochondral fragment.

Downloaded From Vet-eBooks.com

The incidence of osteochondrosis in the tarsus is particularly high in certain breeds (e.g. Standardbreds, Warmbloods and some heavy horse breeds) and there may be a hereditary predisposition to the condition. A number of surveys in different breeds have been carried out. In a survey of 392 foals, fragments on the craniodistal aspect of the intermediate ridge of the tibia were identified in 9.9% of French trotters, 8.2% of Selle Francais and 1.5% of Thoroughbreds. Fragmentation of the lateral trochlea of the talus was seen in 5% of French trotters. In a survey of 3749 young Warmbloods undergoing pre-sales radiography, fragments in the tarsocrural joint were identified in 9.6%. Surveys have shown that lesions seen in young foals may disappear by maturity, and in others lesions appear later in life, usually before 18 months of age. In a French study 58.6% of lesions of the craniodistal aspect of the intermediate ridge of the tibia were stable between 6 and 18 months of age, whereas only 13.7% disappeared and a small number of new lesions were seen at 18 months of age that had not been detected at 6 months.

In Dutch Warmbloods it has been shown that fragments at the craniodistal aspect of the intermediate ridge of the tibia are frequent (>65%) at 1 month of age, but in the majority (80%) the radiographic appearance is normal at 1 year of age. Lesions of the lateral trochlear ridge of the talus are less frequent (30%) at 1 month of age, but the majority (97%) are normal at 1 year of age. A lesion present at 5 months of age in either location is likely to persist.

The clinical significance of fragments must be based on clinical assessment of each case. Lameness may or may not be present, or may develop at a later stage.

Lameness is more likely in association with large or mobile fragments. Chronic distension of the tarsocrural joint capsule may lead to degenerative joint disease and ultimately lameness. In Standardbreds, these lesions have been associated with subtle hindlimb gait abnormalities at high speeds. In Warmbloods, performance at high levels may be compromised. Lesions of the trochlear ridges of the talus are more often associated with mild to moderate lameness, but not invariably so. The potential significance of osteochondrosis lesions as a cause of lameness must be assessed carefully. Surgical treatment may be indicated, with variable outcome. Although distension of the tarsocrural joint may resolve, a good cosmetic result cannot be guaranteed, despite good functional results.

Physitis or physeal dysplasia

Physitis or physeal dysplasia, which is possibly related to osteochondrosis, can cause enlargement of the distal end of the tibia, stiffness and sometimes an angular limb deformity in young foals. Radiographically the metaphysis of the bone is broadened and asymmetrical. There is increased opacity of the metaphysis adjacent to the physis, which may be more irregular in appearance than normal. The cortices of the metaphysis may be abnormally thick. Most cases resolve spontaneously with appropriate management of diet and exercise, although an angular limb deformity may persist in severe cases.

Downloaded From Vet-eBooks.com

Degenerative joint disease

In many horses there is a poor correlation between pain associated with the distal joints of the hock and the radiographic abnormalities. There may be lameness and no detectable radiographic changes. Alternatively there may be extensive radiographic changes and no apparent associated lameness. In some horses the radiographic changes are quite advanced when clinical signs are first recognised. Radiographic examination of horses with obvious enlargements on the medial aspects of the distal joints of the hocks often reveals that this is caused primarily by soft-tissue swelling. Perineural and intra-articular anaesthesia are helpful to establish the significance of radiographic abnormalities and to define the source of pain if no lesions are detectable. This may be combined with anaesthesia of the cunean bursa in selected cases.

The centrodistal (distal intertarsal) and tarsometatarsal joints are affected most frequently, either alone or in combination. The condition often occurs bilaterally. The talocalcaneal–centroquartal (proximal intertarsal) joint is less commonly involved, but is often associated with distension of the tarsocrural joint capsule because of the communication between these two joints. Degenerative joint disease of the talocalcaneal joint or tarsocrural joint occurs rarely.

There is considerable variation among horses in the type, extent and progression of radiographic abnormalities that develop. These changes include periarticular osteophytes (Figures 9.20a-d), periosteal new bone (Figure 9.21), subchondral bone lysis (Figures 9.22a-c) and/or increased opacity of the spongiosa, decreased compactospongious demarcation and narrowing or loss of the joint space (spaces) (Figures 9.23a and 9.23b). There may be alteration of the interosseous space between the central and third



Figure 9.20(a) Lateromedial image of a hock of a 6-year-old Warmblood dressage horse. There is a large curved osteophyte on the dorsoproximal aspect of the third metatarsal bone; the proximal aspect of the spur of bone is less opaque than further distally, which suggests that this spur may be active. Lameness was alleviated by intra-articular analgesia of the tarsometatarsal joint. Note that the dorsal aspect of the third tarsal bone is slightly less thick from proximal to distal dorsally compared with the plantar aspect.

Downloaded From Vet-eBooks.com

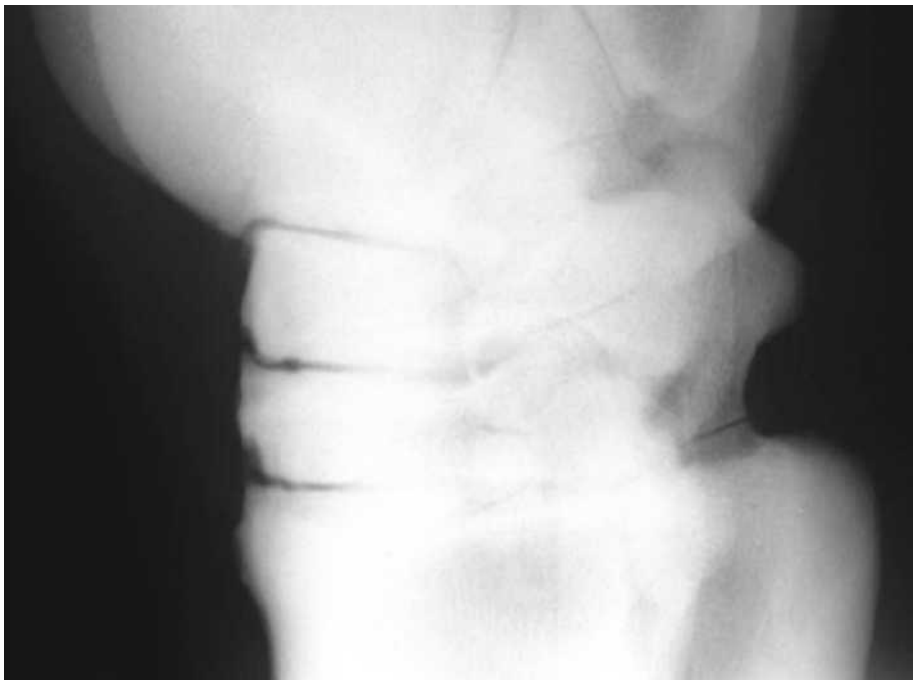


Figure 9.20(b) Lateromedial image of a hock of a mature horse with osteophyte formation involving the centrodistal and tarsometatarsal joints. The radiograph is underexposed to highlight the periarticular new bone.



Figure 9.20(c) Plantarolateral-dorsomedial oblique image of a hock of a mature horse with periarticular osteophyte formation involving the centrodistal and tarsometatarsal joints. Note also the modelling of the dorsal aspect of the third tarsal bone and the irregular opacity of the proximodorsal aspect of the third metatarsal bone. The radiograph is underexposed to highlight the periarticular new bone.

Downloaded From Vet-eBooks.com



Figure 9.20(d) Dorsoplantar image of the left hock of a 7-year-old Arab cross Thoroughbred show horse. Lameness was improved by tibial and fibular nerve blocks or intra-articular analgesia of the tarsometatarsal joint. There is a periarticular osteophyte on the distal lateral aspect of the central tarsal bone (white arrow). Note also the radiolucent area adjacent to the distal lateral aspect of the talus (black arrow). This is created by slight overlap of the talus and the calcaneus and the oval-shaped space between them, the sinus tarsi, which should not be confused as an osseous cyst-like lesion.



Figure 9.21 Dorsoplantar image of a hock of an 11-year-old pleasure riding horse with degenerative joint disease of the tarsometatarsal joint. Lateral is to the right. The tarsometatarsal joint is narrowed and there is extensive periosteal new bone on the medial aspect of the joint. The horse had been lame approximately 1 year and joint space narrowing had progressed during this period.

Downloaded From Vet-eBooks.com



Figure 9.22(a) Lateromedial image of the left hock of a 7-year-old riding horse. There is narrowing of the centrodistal joint space. There are ill-defined lucent zones on the distal dorsal aspect of the central tarsal bone and the proximodorsal aspect of the third tarsal bone (arrows). The region of the interosseous space and intertarsal ligament between the central and third tarsal bones is poorly defined (arrowheads).

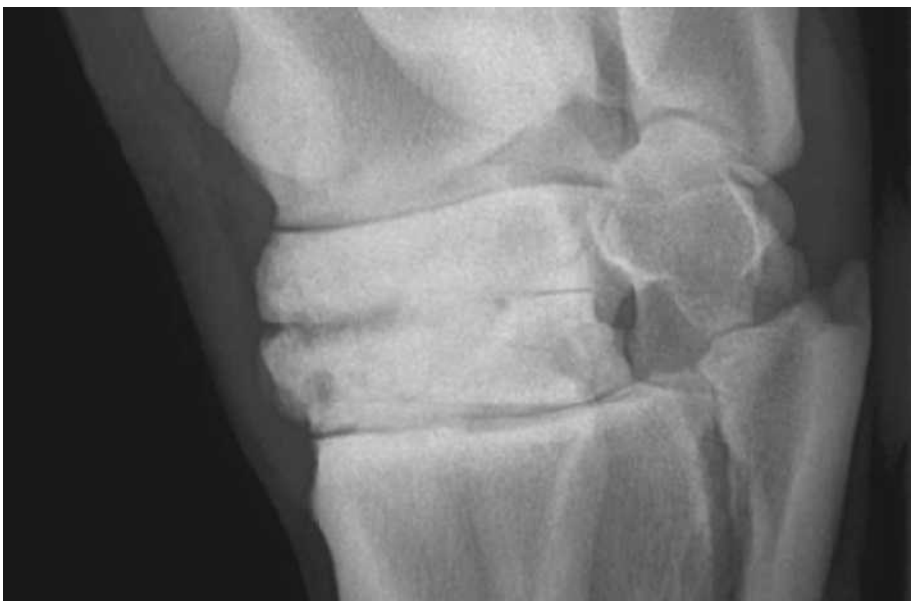


Figure 9.22(b) Dorsolateral-plantaromedial oblique image of the left hock of a 7-year-old Warmblood cross purchased 3 weeks previously. The horse showed mild lameness, markedly exacerbated by proximal limb flexion. There is partial obliteration of the centrodistal joint space, especially in the region of the interosseous space and intertarsal ligament, and extensive subchondral bone lysis adjacent to the joint dorsomedially. There is generalised increased opacity of the central and third tarsal bones and an ill-defined lucent zone in the distal dorsal aspect of the third tarsal bone.

Downloaded From Vet-eBooks.com



Figure 9.22(c) Lateromedial image of the same hock as in Figure 9.22(b). There is narrowing of the centrodistal joint space, subchondral bone lysis dorsally, extensive increased opacity of the central and third tarsal bones and modelling on the dorsal aspect of each bone.



Figure 9.23(a) Dorsolateral-plantaromedial oblique image of a hock of a 9-year-old Warmblood. There is narrowing of the centrodistal joint space, almost complete obliteration of the interosseous space and osteophyte formation on the distal lateral aspect of the central tarsal bone (arrow), bridging the centrodistal joint and encroaching upon the tarsal canal.

Downloaded From Vet-eBooks.com



Figure 9.23(b) Lateromedial image of the right hock of a 9-year-old Warmblood dressage horse with lameness improved by intra-articular analgesia of the tarsometatarsal joint, and abolished by perineural analgesia of the fibular and tibial nerves. There is marked narrowing of the centrodistal joint space and some increased opacity of the dorsal aspect of the central and third tarsal bones.



Figure 9.24(a) Dorsolateral-plantaromedial oblique image of a hock of a 12-year-old Warmblood dressage horse. There is complete obliteration of the interosseous space between the central and third tarsal bones, with increased opacity in the surrounding trabecular bone (black arrows). The centrodistal joint space is narrowed dorsal and plantar to the obliterated interosseous space. There is bone bridging the dorsomedial aspect of the centrodistal joint (white arrow). There is ill-defined new bone on the proximodorsal aspect of the central tarsal bone.

Downloaded From Vet-eBooks.com



Figure 9.24(b) Dorsolateral-plantaromedial oblique image of a hock of an 11-year-old Warmblood dressage horse. There is increased opacity within the centrodistal interosseous space, reflecting mineralisation. There are no other detectable radiological abnormalities. This was an incidental radiological finding.

tarsal bones and/or the third tarsal and third metatarsal bones. The space can be completely ossified, surrounded by ill-defined bone of increased opacity (Figure 9.24a), or in less-advanced cases there is patchy opacity within the normal lucent space (Figure 9.24b), with irregular margins of the surrounding band of radiopaque bone.

In the early stages of the disease the lesions may be subtle and only detectable in a single radiographic view. For this reason, it is important that a complete radiographic examination is carried out. Even in more advanced cases the radiographic abnormalities are occasionally visible on only one of the four standard projections. Since small osteophytes and periosteal new bone are less opaque than the parent bone, they are easily overlooked. The radiographs should always be viewed over high-intensity illumination to study the bone margins, or if obtained digitally the images should be manipulated to permit evaluation of the bone margins. Both hocks should be examined radiographically if changes are found in one limb. It may be necessary to repeat a view at different exposures in order to evaluate both the compactospongious demarcation and the trabecular pattern properly, and to identify marginal osteophytes.

Spur formation on the dorsoproximal aspect of the third metatarsal bone (see Figures 9.7a and 9.7b) may not reflect significant intra-articular disease and its significance must be interpreted with care. This may be an entheseophyte associated with the insertion of the cranial tibial tendon, fibularis (peroneus) tertius, or the dorsal tarsometatarsal ligament; however, an osteophyte may reflect degenerative joint disease. Osteophyte formation may also be associated with an incomplete or complete articular fracture of the dorsoproximal aspect of the third metatarsal bone (see 'Fractures – Third metatarsal bone' in Chapter 6 and Figure 6.34). Osteophyte formation

Downloaded From Vet-eBooks.com

involving the dorsal aspects of the centrodistal joint (Figures 9.20b and 9.20c) or the lateral aspect of this joint (Figure 9.23a) is often associated with lameness. Osteophytes on the lateral aspect of the centrodistal joint are best seen in dorsoplantar and dorsolateral–plantaromedial oblique views, encroaching upon the tarsal canal (Figures 9.20d and 9.23a). Large osteophytes on the proximal aspect of the third metatarsal bone do occasionally fracture; a fracture fragment (see Figure 9.7f) should not be confused with dystrophic mineralisation in the cranial tibial tendon (see Figure 9.7e).

Irregular periosteal new bone occurs most commonly on the dorsomedial aspects of the joints, and usually signifies degenerative joint disease. It may be seen alone or in combination with destructive lesions of bone. Destructive lesions may result in irregular margins of the central and third tarsal bones and the third metatarsal bone and/or lucent zones in the subchondral bone. If there are extensive lucent areas in the subchondral bone, lameness is usually persistent. There are sometimes discrete osseous cyst-like lesions in the subchondral bone.

Narrowing of the joint spaces (Figures 9.23a and 9.23b) can occur with any of these changes and is most accurately assessed on appropriately positioned dorsoplantar views, but should be verified on other views. Care should be taken not to diagnose joint narrowing from poorly positioned radiographs. An additional view at a slightly different angle (e.g. dorsal 5° proximal-plantarodistal oblique) may show no evidence of narrowing. Occasionally, narrowing of the joint space is the only radiographic abnormality detectable. Conventional radiographs will underestimate the degree of functional ankylosis. The joint spaces may become obliterated completely, resulting in ankylosis of the bones and resolution of lameness. Persistence of lameness may be due to continued subchondral bone pain, or to early changes in more proximal or distal joints. Nuclear scintigraphy is useful in determining active bone modelling. In other cases there is extensive extra-articular inactive bone bridging the joints with some loss of joint space.

Occasionally a horse will have acute onset of very severe unilateral hindlimb lameness with pain localised to the hock region. There may be no detectable radiological abnormalities at this stage; however, there is intense increased radiopharmaceutical uptake in the central and third tarsal bones. Follow-up radiographs obtained after 8 weeks may show evidence of rapidly progressive degenerative joint disease.

The shape of the central and third tarsal bones should be assessed carefully, in order to detect cases in which degenerative joint disease has developed secondarily to tarsal bone collapse (see 'Tarsal bone collapse', above, and Figures 1w.9 and 9.16c).

Degenerative joint disease of the talocalcaneal joint is usually seen in isolation, unassociated with lesions of the centrodistal or tarsometatarsal joints (Figure 9.26c). There are usually no localising clinical signs and the response to intra-articular analgesia is poor. Lesions may be missed unless tibial and fibular nerve blocks are performed. Although radiological abnormalities can usually be detected, characterised by joint space narrowing and subchondral bone lysis with or without increased opacity of the adjacent trabecular bone, in a small proportion of affected horses lesions can only be detected by magnetic resonance imaging or computed tomography. These lesions are usually associated with a typical linear pattern of increased radiopharmaceutical uptake in the subchondral bone.

Downloaded From Vet-eBooks.com

Occasionally degenerative joint disease of the tarsocrural joint is detectable radiologically; however, extensive articular cartilage pathology can be present in the absence of detectable osseous changes. Degenerative joint disease is characterised by periarticular osteophyte formation on the distal aspects of the tibia and talus (Figure 9w.25).

The speed of progression of changes in the centrodistal and tarsometatarsal joints is both variable and unpredictable, and it is unusual to be able to monitor progressive fusion of the joints radiographically. Some horses may be treated conservatively either by intra-articular medication or by administration of anti-inflammatory analgesics and corrective shoeing. Surgical or chemical arthrodesis of the affected joints can be an effective treatment, particularly for those with extensive lytic lesions. Surgical or chemical fusion of the centrodistal and tarsometatarsal joints can be followed by fracture of the fused bones or subsequent development of degenerative joint disease of the talocalcaneal-centroquartal joint. Involvement of the talocalcaneal–centroquartal (proximal intertarsal) joint (Figures 9.26a and 9w.26b) or the talocalcaneal joint (Figure 9.26c) warrants a guarded prognosis.

Mineralisation of the central or third tarsal bone

In a small number of sports horses lameness has been associated with diffuse increased opacity of the central and/or third tarsal bone (Figure 9w.27). This has been associated with diffuse intense increased radiopharmaceutical uptake in the affected bone(s). Magnetic resonance imaging has confirmed diffuse areas of low signal intensity in T1 and T2 weighted images, consistent with mineralisation of the spongiosa.

Occasionally such lesions have also been seen together with a small osseous cyst–like lesion in the proximal subchondral bone plate.

Bone trauma

Acute-onset lameness associated with the tarsus may be present in the absence of detectable radiological abnormality. This may be associated with bone trauma, which may be identified using magnetic resonance imaging, and is characterised by areas of increased signal intensity in the trabecular bone in fat-suppressed images.

Periosteal proliferative reactions at the sites of attachment of ligaments and joint capsules

Twisting or wrenching the hock during exercise, or as the result of a fall, may result in a sprain of one or more of the soft-tissue structures of the hock and cause severe lameness. There is usually localised periarticular soft tissue swelling and distension of the tarsocrural joint capsule. Radiographic examination may only show soft-tissue swelling initially, with no osseous abnormality, but is important to rule out a fracture. Diagnostic ultrasonography may be useful to evaluate the joint capsule and collateral ligaments of the tarsocrural joint. Nuclear scintigraphy may identify areas of increased

Downloaded From Vet-eBooks.com



Figure 9.26(a) Dorsolateral-plantaromedial oblique image of the right hock of an 8-year-old Connemara cross with lameness of 4 months' duration and distension of the tarsocrural joint. Lameness was accentuated by proximal limb flexion. There is narrowing of the talocalcaneal-centroquartal joint, new bone on the distal medial tuberosity of the talus, modelling of the dorsomedial articular margins of the talocalcaneal-centroquartal joint and periarticular osteophyte formation on the distal dorsomedial aspect of the central tarsal bone.



Figure 9.26(c) Lateromedial image of the right hock of a 15-year-old dressage horse with moderate lameness abolished by fibular and tibial nerve blocks and improved by intra-articular analgesia of the tarsocrural joint. There is narrowing of the talocalcaneal joint space and subchondral lysis (arrows) consistent with degenerative joint disease.

radiopharmaceutical uptake indicating site(s) of injury. After approximately 3–6 weeks, extensive periosteal reactions may develop at the sites of attachment of the joint capsules, collateral ligaments and/or intertarsal ligaments (Figure 9.28). The sites of periosteal reactions should be correlated carefully with the sites of soft-tissue attachments to confirm which structures may have been damaged. These changes may be progressive and follow-up examination after a further 6–8 weeks may give a better indication of the extent of the damage. Lameness may take a considerable time to resolve, and if new bone involves the articulations of the hock, or if there is extensive joint

Downloaded From Vet-eBooks.com



Figure 9.28 Dorsal 10° lateral-plantaromedial oblique image of a hock of a 4-year-old Thoroughbred flat racehorse. Lateral is to the right. There is irregular entheseous new bone formation on the lateral aspect of the calcaneus (arrows) at the sites of insertion of components of the deep (short) and superficial (long) lateral collateral ligaments of the tarsocrural joint. This was associated with focal linear intense increased radiopharmaceutical uptake and some disruption of ligament architecture seen ultrasonographically.

capsule fibrosis and pericapsular reaction, lameness may be persistent. Acute injuries of the collateral ligaments of the tarsocrural joint may heal without complications, with a favourable prognosis for athletic function.

An avulsion fracture of either the medial or, more commonly, the lateral malleolus of the tibia (Figure 9.29a) may occur in association with sprain of the collateral ligaments of the tarsocrural joint. The fracture may be simple or comminuted. Fracture fragments may be displaced and rotated. It may be helpful to obtain a dorsal 15° medial-plantarolateral oblique view to highlight the fragment(s) (Figure 9.29b). In contrast to the osteochondral fragments of osteochondrosis, a recent fracture is more irregular in shape. Ultrasonography can be useful to identify the precise location of a fracture in the frontal plane and to assess the collateral ligaments. Periosteal new bone may develop on the distal cranial aspect of the tibia, and entheseous new bone at the insertion of the collateral ligaments on the talus. Conservative treatment offers a moderate prognosis while surgical removal offers the best prognosis.

A fracture of the lateral malleolus of the tibia can also occur as a result of direct blunt trauma, for example a kick. The force of the injury may be translated across the distal tibia, resulting in the development of periosteal new bone medially.

Downloaded From Vet-eBooks.com



Figure 9.29(a) Dorsoplantar image of the left hock of a 6-year-old steeplechase horse. There are at least two osseous fragments of the lateral malleolus of the tibia. Compare with Figure 9.29(b).



Figure 9.29(b) Dorsal 15° medial-plantarolateral oblique image of the same hock as in Figure 9.29(a). Comminution of the fracture of the lateral malleolus is more easily seen.

Fragmentation of the proximal tubercle of the talus

Fragmentation of the proximal tubercle of the talus may be seen as an incidental radiological abnormality, often in association with a pre-purchase examination, but has occasionally been seen in association with acute onset of lameness. The fragments are best seen in a dorsomedial-plantarolateral oblique image (Figure 9.30a) and a dorsoplantar (flexed) image (Figure 9.30b). They usually occur unilaterally, but have been seen bilaterally. The fragments are variable in shape and may be of heterogeneous opacity. It is speculated that these fragments are the result of avulsion of the attachment of the short medial collateral ligament of the tarsocrural joint, the medial talocalcaneal ligament or the tarsal plantar ligament. They might possibly represent a rare manifestation of osteochondrosis. A fragment located medial to the proximal tubercle of the talus could also be the result of direct trauma.

Downloaded From Vet-eBooks.com



Figure 9.30(a) Dorsomedial-plantarolateral oblique image of a hock of a mature riding horse. There is an irregular outline of the plantar aspect of the proximal tubercle of the talus, which is of heterogeneous opacity (arrows). Compare with Figure 9.30(b). It is speculated that these fragments are the result of avulsion of the attachment of the short medial collateral ligament of the tarsocrural joint, the medial talocalcaneal ligament or the tarsal plantar ligament. This was an incidental finding.



Figure 9.30(b) Dorsoplantar (flexed) image of the calcaneus, sustentaculum tali and the plantar aspect of the talus of the same hock as in Figure 9.30(a). Lateral is to the right. There is a well-rounded fragment of heterogeneous opacity (arrow) on the plantarolateral aspect of the proximal tubercle of the talus.

Luxation

Luxation of the tarsus is not common but may occur at any of the joints. The horse shows a severe, non-weight-bearing lameness, a variable degree of soft-tissue swelling and obvious instability of the tarsus. Radiographic examination is performed to establish which joint is involved and the extent of concurrent damage (Figure 9.31). 'Stressed' views may be helpful. The majority of, but not all, luxations are associated with fractures of one or more tarsal bones. The prognosis for luxation of the tarsocrural joint is poor, but closed reduction and external immobilisation has been successful in treating luxations of the talocalcaneal–centroquartal (proximal intertarsal) or tarsometatarsal joints in horses which resumed light work, or were used for breeding.

Distension of the tarsal sheath and synoviocoeles (Thoroughpin)

Persistent lameness and swelling of the tarsal sheath proximal to the hock (so-called 'true thoroughpin') may be associated with lesions of the sustentaculum tali of the calcaneus and/or mineralisation in the soft tissues (Figure 9.32a). Although the latter may be identified in the standard radiographic

Downloaded From Vet-eBooks.com



Figure 9.31 Flexed and stressed lateromedial radiograph of a right hock of a 7-year-old Cob with severe lameness. There is abnormal opening of the dorsal aspect of the tarsometatarsal joint reflecting subluxation.

views (particularly the plantarolateral-dorsomedial oblique view), lesions of the sustentaculum tali are often only visible in the dorsoplantar (flexed) view (Figure 9.32b). Ultrasonography is useful for assessing the tarsal sheath and its contents and osseous contours. The presence of radiographic changes (e.g. lesions of the sustentaculum tali, mineralisation within the sheath or filling defects in the sheath) associated with distension of the tarsal sheath warrants a guarded prognosis.

Herniation of the tarsal sheath may result in a synoviocoele, (so-called 'false thoroughpin'), a fluid-filled swelling just proximal to the hock. This may or may not be associated with lameness. Some of these swellings resolve spontaneously, but others persist and may be associated with chronic lameness. Contrast radiography may be useful to determine whether or not there is communication between the synoviocoele and the tarsal sheath (Figure 9.32c); a communication can sometimes be detected

Downloaded From Vet-eBooks.com



Figure 9.32(a) Plantarolateral-dorsomedial oblique image of a hock. There is considerable modelling of the sustentaculum tali (black arrows) which was associated with distension of the tarsal sheath and severe lameness. Note also the heterogeneous opacity of the chestnut (white arrow) which is partially superimposed.

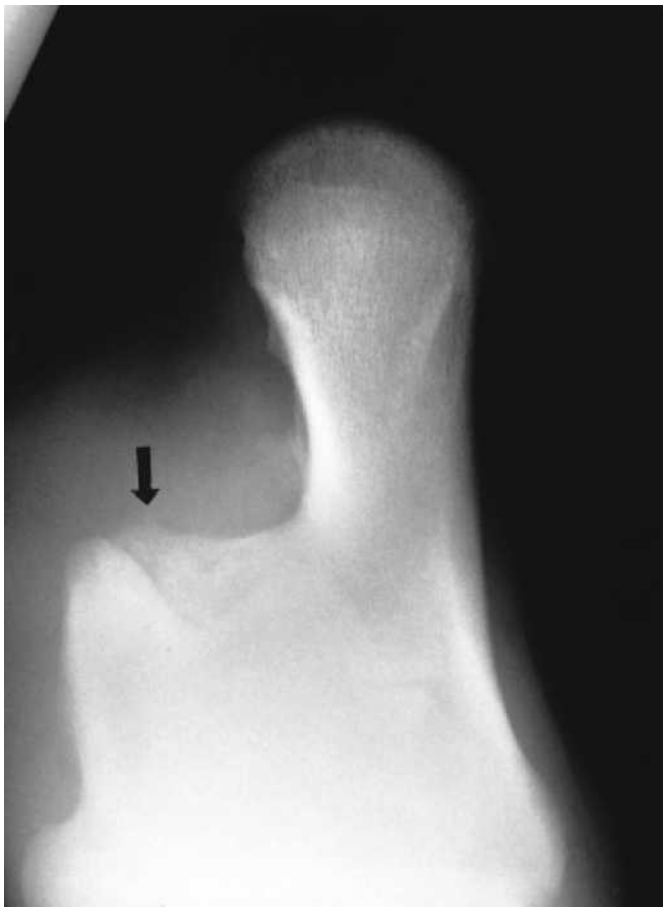


Figure 9.32(b) Dorsoplantar (flexed) image of the same hock as Figure 9.32(a). Lateral is to the right. Note the irregular contour of the surface of the sustentaculum tali (arrow) over which the lateral digital flexor tendon passes, and the poorly defined opacities in the soft tissues medial to the calcaneus.

ultrasonographically and confirmed endoscopically. Endoscopic enlargement of the defect in the tarsal sheath wall may improve lameness.

Infectious arthritis and osteomyelitis

Infectious arthritis occurs most commonly in young foals, but may be a sequel to trauma in an adult, and occasionally develops without an apparent cause. The tarsocrural joint is most commonly affected, resulting in distension of the joint capsule and lameness. The lower joints may be involved alone or in combination and, especially in young foals, the central and third tarsal bones must be inspected carefully for evidence of lucent zones indicative of concurrent osteomyelitis (type T osteomyelitis, see 'Infectious arthritis' in Chapter 1). In foals the distal tibial physis and epiphysis should also be evaluated with care, since in the majority of cases type P osteomyelitis is present.

Trauma in the region of the calcaneus may result in a chronically draining wound and severe lameness. Osteomyelitis of the tuber calcanei may be a sequel, but radiographic abnormalities may only be detectable in a dorsoplantar (flexed) view. Sinography may be helpful to establish if a draining sinus communicates with the bone. Ultrasonography may permit

Downloaded From Vet-eBooks.com



Figure 9.32(c) Lateromedial image of the right tarsal region of a 6-year-old Connemara riding horse centred at the level of the distal aspect of the tibia. The horse had developed a thoroughpin on the lateral aspect of the limb 8 weeks previously, subsequent to which the horse had become mildly lame. Radiodense contrast medium was injected into the thoroughpin, together with local anaesthetic solution. There is a clearly demarcated contrast-medium-filled mass with radiolucent filling defects, which were occupied by echogenic material when examined ultrasonographically. There is also contrast medium in the tarsal sheath outlining the lateral digital flexor tendon. The thoroughpin is a synoviocoele caused by a defect in the wall of the tarsal sheath; in some horses there is a one-way valve so that, unlike in this horse, communication between the tarsal sheath and the synoviocoele cannot be demonstrated. Lameness was not changed by intrasynovial analgesia. The thoroughpin was an incidental finding. Lameness was caused by proximal suspensory desmopathy.

identification of osseous lesions much earlier than radiography. A guarded prognosis is warranted even with surgical treatment.

In the acute stage, lesions of the tuber calcanei can cause lameness that cannot readily be localised to the hock. There may however be a radiolucent defect visible (Figures 9.33a and 9.33b).

Osseous cyst-like lesions

Single (Figure 9.34a) or multiloculated (Figure 9.34b) osseous cyst-like lesions occur occasionally, most commonly in the distal aspect of the tibia and the talus, occasionally in the calcaneus (Figures 9w.34c and 9w.34d) and rarely in the third metatarsal bone. They are generally, but not always, associated with lameness. They usually occur unilaterally. Their aetiology is uncertain.

Downloaded From Vet-eBooks.com



Figure 9.33(a) Dorsomedial-plantarolateral oblique image of the right hock of a pony foal 6 months of age, with acute-onset severe lameness and subtle soft-tissue swelling on the plantar aspect of the hock. There is an ill-defined radiolucent area in the proximoplantar aspect of the apophysis of the calcaneus (arrows). Compare with Figure 9.33(b) acquired 5 days later. The overlying soft tissue structures appeared normal ultrasonographically and no bone defect could be detected.

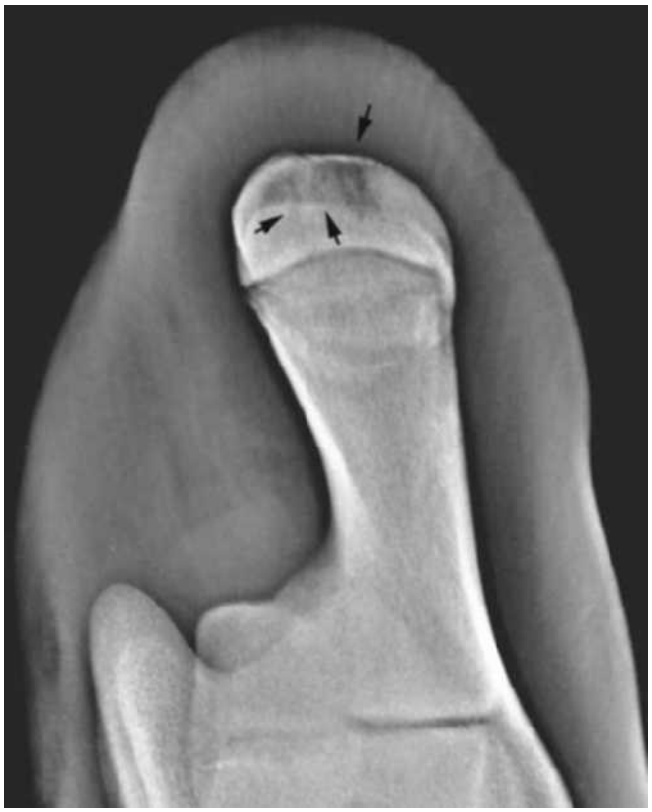


Figure 9.33(b) Dorsoplantar (flexed) image of the same hock as in Figure 9.33(a) acquired 5 days later. There are more extensive lucent areas in the tuber calcanei (arrows) associated with infectious osteitis. The overlying soft tissue structures appeared normal ultrasonographically and no bone defect could be detected.

Although some are identifiable radiographically, some osseous cyst-like lesions in the distal aspect of the tibia or proximal aspect of the talus (close to the intertrochlear groove of the talus) have only been seen using computed tomography and/or during arthroscopic surgery. They are invariably associated with focal increased radiopharmaceutical uptake. Horses with clinically significant osseous cyst-like lesions in the distal aspect of the tibia, the talus, or in the proximoplantar aspect of the calcaneus generally have a guarded prognosis for return to full athletic function.

Small and moderately-sized osseous cyst-like lesions in the subchondral bone of the proximal aspect of the lateral trochlea of the talus have been seen in association with osteochondrosis of the distal aspect of the intermediate ridge of the tibia or the medial malleolus of the tibia (Figures 9w.35a and 9w.35b). These may be the result of defective endochondral ossification. Occasionally small subchondral osseous cysts-like lesions have been seen as an incidental finding in the medial trochlea of the talus (Figure 9w.36).

Osseous cyst-like lesions may occur in the central and third tarsal bones in association with degenerative joint disease (see 'Degenerative joint disease', above). They may also occur in isolation, when they may be of no clinical significance, particularly if contained within the spongiosa (Figure 9.9a).

Downloaded From Vet-eBooks.com



Figure 9.34(a) Dorsolateral-plantaromedial oblique image of a hock of an 8-year-old Warmblood showjumper with severe lameness improved by fibular and tibial nerve blocks. There is a well-circumscribed osseous cyst-like lesion (arrow) in the distal subchondral bone plate of the tibia, communicating with the tarsocrural joint.



Figure 9.34(b) Dorsolateral-plantaromedial oblique image of a hock of a 9-year-old Warmblood showjumper with severe lameness improved by fibular and tibial nerve blocks. There is a well-circumscribed osseous cyst-like lesion (arrow) in the distal subchondral bone plate of the tibia, communicating with the tarsocrural joint. This is surrounded proximally by a rim of increased opacity. Proximal to this is a much larger cyst-like lesion (arrowheads). There was intense increased radiopharmaceutical uptake in the distal aspect of the tibia.

Hypertrophic osteopathy

See 'Hypertrophic osteopathy' in Chapter 1 and Figure 1w.19b.

Fractures

Because of the complex radiographic anatomy of the tarsus, detection of fractures is sometimes difficult. The support afforded by the intertarsal ligaments and collateral ligaments often results in minimal distraction of the fracture fragments. A slab fracture of the central or the third tarsal bone may be completely overlooked unless follow-up radiographs are obtained 7–10 days after the onset of lameness, when rarefaction along the fracture line will

Downloaded From Vet-eBooks.com



Figure 9.37(a) Dorsomedial-plantarolateral oblique image of the left hock of a 3-year-old Thoroughbred flat racehorse. There is a frontal plane slab fracture of the third tarsal bone. The fracture traverses the narrowest part of the bone. Note the increased opacity of the dorsal aspect of the central and third tarsal bones.



Figure 9.37(b) Dorsomedial-plantarolateral oblique image of a hock of a 10-year-old elite Arab endurance horse with recent-onset lameness which was markedly improved by intra-articular analgesia of the tarsometatarsal joint. There is a curved radiolucent line in the plantar aspect of the third tarsal bone consistent with a recent fracture (arrows). This was associated with intense increased radiopharmaceutical uptake in the third tarsal bone.

make it more obvious (Figure 9.37a). Many oblique views may be required in order to identify the fracture. In young Thoroughbred racehorses a wedge-shaped conformation of the dorsolateral aspect of the third tarsal bone may be a risk factor for fracture. Other fractures of the central and third tarsal bones also occur (Figure 9.37b). Nuclear scintigraphy may be useful in acute cases in which a fracture is suspected. Increased radiopharmaceutical uptake may demonstrate results of trauma to the central and third tarsal bones, but in some cases a fracture is not subsequently identifiable. Computed tomography may demonstrate fractures that cannot be identified radiologically.

Downloaded From Vet-eBooks.com

Magnetic resonance imaging may demonstrate both fractures and other evidence of bone trauma. Treatment of slab fractures by internal fixation offers the best prognosis for future soundness, although secondary degenerative joint disease may be a sequel. Non-displaced incomplete fractures can be managed conservatively.

Sagittal fractures of the talus cause acute-onset severe lameness. They may be very difficult to detect in the acute stage. They are associated with focal intense increased radiopharmaceutical uptake in the talus. Sequential radiographic examinations may reveal the radiolucent fracture line in dorsoplantar or slightly oblique dorsoplantar radiographic views. The prognosis with conservative management is usually favourable.

There are many types of fractures within the tarsus (Figure 9.38). The prognosis depends on the site of the fracture and its configuration, but is generally guarded. Large fractures involving the distal third of the lateral trochlea of the talus respond well to surgical removal of the fracture fragment because this part of the bone is not a major weight-bearing component of the joint. The dorsoplantar (flexed) view may be necessary to identify fractures of the sustentaculum tali. Readers are advised to consult the references given under 'Further reading' for additional information about specific fracture types (Figure 9.38).

Fractures of the distal tibial physis are quite common in foals and yearlings, Salter-Harris type II (see 'Fractures' in Chapter 10) occurring most frequently. Treatment either by immobilisation in a cast or by internal fixation has been successful in some cases. Malleolar fractures of the distal

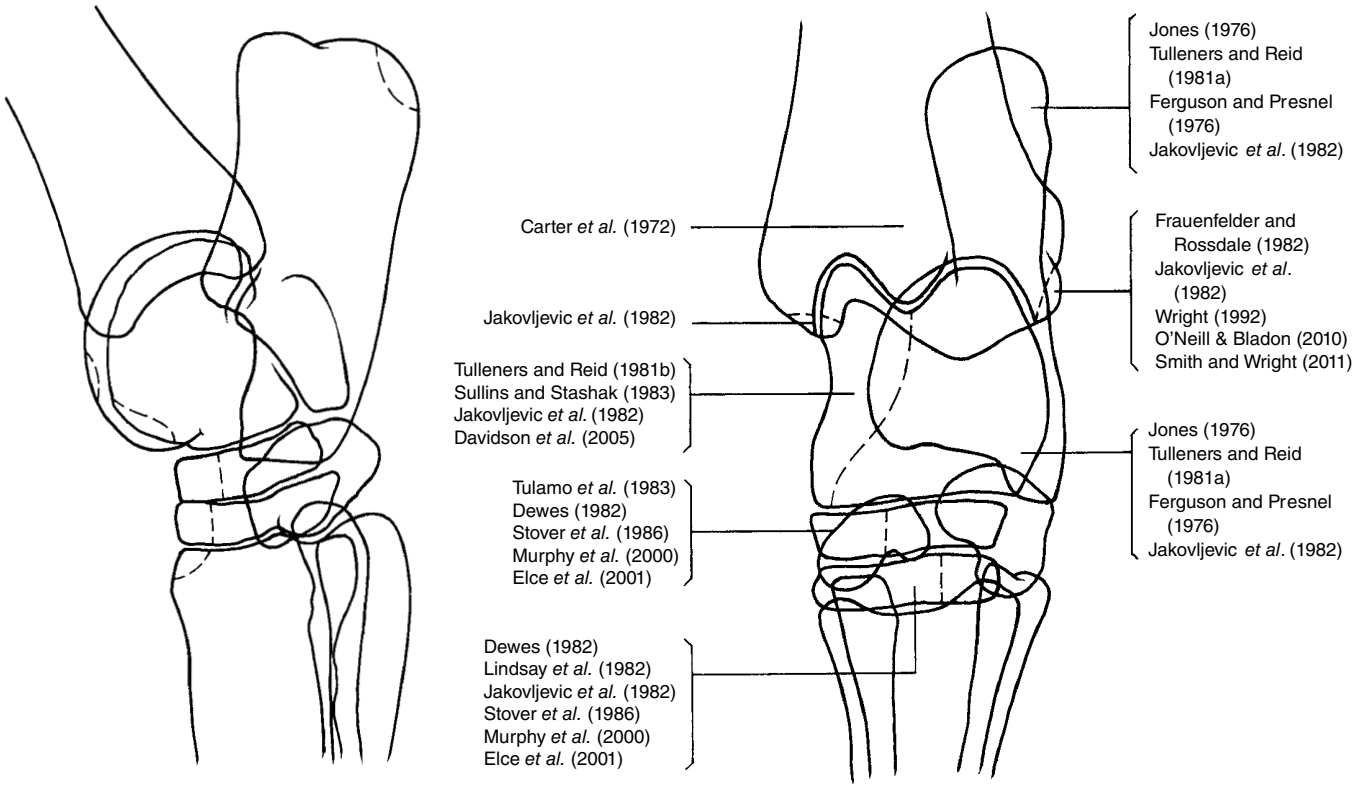


Figure 9.38 Location of common fracture sites in the hock and suggested references (see 'Further reading').

Downloaded From Vet-eBooks.com

aspect of the tibia are discussed under 'Periosteal proliferative reactions at the sites of attachment of ligaments and joint capsules', above.

Tumours

Neoplastic lesions in the hock region are rare. Osteosarcoma and mastocytosis have been reported.

Additional figures

The book companion website at www.clinical-radiology-horse.com includes additional figures that are not included in the printed book or e-book formats. Please see '**About the Companion Website**' at the start of the book for details on how to access the website. These figures are prefixed with the letter 'w' in the printed book, e.g. Figures 1w.4c–f.

FURTHER READING

Abuja, G., Bubecj, K., Quinteros, D., et al. (2013) Surgical treatment of distal tarsal joint luxations in three horses. *Vet. Comp. Orthop. Traumatol.* **26**, 304–310

Amitrano, F., Austin, S., Kay, A. (2014) Osteomyelitis of the medial trochlear ridge of the talus in a horse. *Equine Vet. Educ*. Doi: 10.1111/eve.12152

Axelsson, M., Bjornsdottir, S., Eksell, P., Haggstrom, J., Sigurdsson, H., Carlsten, J. (2001) Risk factors associated with hindlimb lameness and degenerative joint disease in the distal tarsus of Icelandic horses. *Equine Vet. J.* **33**, 84–90

Baird, D., Pilsworth, R. (2001) Wedge-shaped conformation of the dorsolateral aspect of the third tarsal bone in the Thoroughbred racehorse is associated with development of slab fractures in this site. *Equine Vet. J.* **33**, 617–620

Ball, M., Allen, D., Parks, A. (1996) Surgical treatment of subchondral cyst-like lesions in the tibia of an adult pony. *J. Am. Vet. Med. Ass.* **208**, 704–706

Barker, W., Smith, M., Minshall, G., et al. (2013) Soft tissue injuries of the tarsocrural joint: a retrospective analysis of 30 cases evaluated arthroscopically. *Equine Vet. J.* **45**, 435–441

Barneveld, A. (1983) Equine bone spavin. PhD Thesis, University of Utrecht

Bassage, L., Garcia-Lopez, J., Currid, E. (2000) Osteolytic lesions of the tuber calcanei in 2 horses. *J. Am. Vet. Med. Ass.* **217**, 710–716

Beard, W., Bramlage, L., Schneider, R., Embertson, R. (1994) Postoperative racing performance in Standardbreds and Thoroughbreds with osteochondrosis of the tarsocrural joint: 109 cases (1984–1990). *J. Am. Vet. Med. Ass.* **204**, 1655–1659

Biggi., M., Zani, D., De Zani, D., et al. (2012) Magnetic resonance imaging findings of bone marrow lesions in the equine distal tarsus. *Equine Vet. Educ.* **24**, 236–241

Bjonsdottir, S., Axelsson, M., Eksell, P., Sigurdsson, H., Carlsten, J. (2000) Radiographic and clinical survey of degenerative joint disease in the distal tarsal joints in Icelandic horses. *Equine Vet. J.* **32**, 263–267

Blaik, M., Hansen, R., Kincaid, S., Hathcock, J., et al. (2000) Low-field magnetic resonance imaging of the equine tarsus: normal anatomy *Vet. Radiol. Ultrasound* **41**, 131–141

Boero, M., Kneller, S., Baker, G., Metcalf, M., Twardock, A. (1988) Clinical, radiographic and scintigraphic findings associated with enthesitis of the lateral collateral ligaments of the tarsocrural joint in Standardbred racehorses. *Equine Vet. J.* **20** (Suppl. 6), 53–59

Carlsten, J., Sandgren, B., Dalin, J. (1993) Development of osteochondrosis in the tarsocrural joints and osteochondral fragments in the fetlock joint in Standardbred trotters. I. A radiological survey. *Equine Vet. J.* **25** (Suppl. 16), 42–47

Cohen, N., Carter, G., Watkins, J., O'Conor, M. (2006) Association of racing performance with specific abnormal radiographic findings in Thoroughbred yearlings sold in Texas. *J. Equine Vet. Sci.* **26**, 462–474

Courouce-Malblanc, A., Leleu, C., Bouchilloux, M., Geffroy, O. (2006) Abnormal radiographic findings in 865 French Standardbred trotters and their relationship to racing performance. *Equine Vet. J. Suppl.* **36**, 417–422

Daniel, A., Judy, C., Rick, M., et al. (2012) Comparison of radiography, nuclear scintigraphy, and magnetic resonance imaging for detection of specific conditions of the distal tarsal bones of horses: 20 cases (2006–2010). *J. Am. Vet. Med. Ass.* **240**, 1109–1114

Davidson, E., Ross, M., Parente, E. (2005) Incomplete sagittal fracture of the talus in 11 racehorses: outcome. *Equine Vet. J.* **37**, 457–461

De Moor, A., Verschooten, F., Desmet, P., Steenhaut, M., Hooreens, J., Wolf, G. (1972) Osteochondritis dissecans of the tibiotarsal joint in the horse. *Equine Vet. J.* **4**, 139–143

Denoix, J.-M., Jacquet, S., Lepeule, J., et al. (2013) Radiographic findings of juvenile osteochondral conditions detected in 392 foals using a field radiographic protocol. *Vet. J.* **197**, 44–51

Dewes, H. (1982) The onset and consequence of tarsal bone fractures in foals. *N.Z. Vet. J.* **30**, 129–135

Dik, K., Merkens, H. (1987) Unilateral distension of the tarsal sheath in the horse: a report of 11 cases. *Equine Vet. J.* **19**, 307–313

Dik. K. Keg, P. (1990) The efficacy of contrast radiography to demonstrate 'false thoroughpins' in five horses. *Equine Vet. J.* **22**, 223–225.

Dik, K., Enzerink, E. (1999) The radiographic development of osteochondral abnormalities in the hock and stifle of Dutch Warmblood foals from 1 to 11 months of age. *Equine Vet. J.* **31** (Suppl. 31), 9–15

Dusterdieck, K., May, K., Pleasant, S., Howard, R. (2002) Distal intertarsal joint subluxation in a pony. *Equine Vet. Educ.* **14**, 12–15

Dyson, S. (2013) Lameness associated with mineralisation of the central tarsal bone and a small osseous cyst-like lesion in two sport horses. *J. Equine Vet. Sci.* **33**, 51–56

Edwards, G. (1978) Changes in the sustentaculum tali associated with distension of the tarsal sheath (thoroughpin). *Equine Vet. J.* **10**, 97–100

Eksell, P., Uhlhorn, H., Carlsten, J. (1999) Evaluation of different projections for radiographic detection of tarsal degenerative joint disease in Icelandic horses. *Vet. Radiol. Ultrasound* **40**, 228–232

Elce, Y., Ross, M., Woodford, A., Arensberg, C. (2001) A review of central and third tarsal bone slab fractures in 57 horses. *Proc. Am. Assoc. Equine Pract.* **47**, 488–490

Espinosa, P., Lacourt, M., Alexander, K., et al. (2013) Fragmentation of the proximal tubercle of the talus in horses: 9 cases (2004–2010). *J. Am. Vet. Med. Ass.* **242**, 984–991

Fairburn, A., Dyson, S., Murray, R. (2010) Clinical significance of osseous spurs on the dorsoproximal aspect of the third metatarsal bone. *Equine Vet. J.* **47**, 591–599

Farrow, C., McNeel, S., Morgan, J., Resch, R. (1976) Visualisation of the tuber calcis and sustentaculum in the horse. *Calif. Vet.* **30**, 14–15

Ferguson, J., Presnel, K. (1976) Tension band plating of a fractured equine fibular tarsal bone. *Can. Vet. J.* **17**, 314–317

Firth, E., Dik, K., Goedegebuure, S., et al. (1980) Polyarthritis and bone infection in foals. *Vet. Med.* **B27**, 102–124

Firth, E., Goedegebuure, S., Dik, K., Poulos, P. (1985) Tarsal osteomyelitis in foals. *Vet. Rec.* **116**, 261–266

Fleck, S., Dyson, S. (2012) Lameness associated with tarsocrural joint pathology in 17 mature horses (1997–2010). *Equine Vet. Educ.* **24**, 628–638

Garcia-Lopez, J., Kirker-Head, C. (2004) Occult osseous cyst-like lesions of the equine tarsocrural joint. *Vet. Surg.* **564**, 557–564

Grondahl, A., Jansen, J., Terge, J. (1996) Accessory ossification centres associated with osteochondral fragments in the extremities of horses. *J. Comp. Path.* **114**, 385–398

Grondahl, A., Engeland, A. (1995) Progression and association with lameness and racing performance in Standardbred trotters. *Equine Vet. J.* **26**, 152–155

Gross, D. (1984) Tarsal luxation and fracture in a pony. *Mod. Vet. Pract.* **45**, 68–69

Gutierrez-Nibeyro, S., Sullins, K., Powers, B. (2010) Treatment of appendicular osteosarcoma in a horse. *Equine Vet. Educ.* **22**, 540–544

Hand, D., Watkins, J., Honnas, C. (2001) Osteomyelitis of the sustentaculum tali in horses: 10 cases (1992–1998). *J. Am. Vet. Med. Ass.* **219**, 341–345

Hartung, K., Munzer, B., Keller, H. (1983) Radiologic evaluation of spavin in young trotters. *Vet. Radiol.*, **24**, 153–155

Hoppe, F. (1984) Osteochondrosis in Swedish horses. Thesis, Sveriges Lantbruksuniversitet, Uppsala

Jakovljevic, S., Gibbs, C., Yeats, J. (1982) Traumatic fractures of the equine hock: a report of 13 cases. *Equine Vet. J.* **14**, 62–68)

Jacquet, S., Robert, C., Valette, J.-P., Denoix, J.-M. (2013) Evolution of radiological findings detected in the limbs of 321 young horses between the ages of 6 and 18 months. *Vet. J.* **197**, 58–64

Janicek, J., Cook, J., Wilson, D., et al. (2010) Multiple osteochondral autografts for treatment of a medial trochlear ridge subchondral cystic lesion in the equine tarsus. *Vet. Surg.* **39**, 95–101

Jenner, F., Solano, M., Gliatto, J., Lavallee, S., Kirker-Head, C. (2003) Osteosarcoma of the tarsus in a horse. *Equine Vet. J.* **35**, 214–216

Jones, R. (1976) The diagnosis and treatment of avulsion fractures of the sustentaculum tali in a horse. *Can. Vet. J.* **17**, 287–290

Kane, A., Park, D., McIlwraith, C., Rantanen, N., Morehead, J., Bramlage, L. (2003) Radiographic changes in Thoroughbred yearlings. Part 1: Prevalence at the time of sales. *Equine Vet. J.* **35**, 354–365

Kane, A., McIlwraith, C., Park, R., Rantanen, N., Morehead, J., Bramlage, L. (2003) Radiographic changes in Thoroughbred yearlings. Part 2: Association with racing performance. *Equine Vet. J.* **35**, 366–374

Kearney, C., McAllister, H., Jenner, F. (2010) Conservative management of a comminuted central tarsal bone fracture and joint instability in a horse. *Equine Vet. Educ.* **22**, 107–111

Labens, R., Innocent, G., Voute, L. (2007) Repeatability of a quantitative rating scale for assessment of horses with distal tarsal osteoarthritis. *Vet. Radiol. Ultrasound* **48**, 204–211

Lamas, L., Edmonds, J., Hodge, W., et al. (2012) Use of ethanol in the treatment of distal tarsal joint osteoarthritis: 24 cases. *Equine Vet. J.* **44**, 339–403

Lamb, L., Zubrod, C, Hague, B., et al. (2012) Clinical outcome of collateral ligament injuries of the tarsus. *Can. Vet. J.* **53**, 518–524

Laws, E., Richardson, D., Ross, M., Moyer, W. (1993) Racing performance of Standardbreds after conservative and surgical treatment for tarsocrural osteochondrosis. *Equine Vet. J.* **25**, 199–202

Lindsay, W., McMartin, R., McClure, J. (1982) Management of slab fractures of the third tarsal bone in 5 horses. *Equine Vet. J.* **14**, 55–58

MacDonald, M., Honnas, C., Meagher, D. (1989) Osteomyelitis of the calcaneus in horses: 28 cases (1972–1987). *J. Am. Vet. Med. Ass.* **194**, 1317–1320

McCoy, A., Ralston, S., McCue, N. (2014) Short- and long-term racing performance of Standardbred pacers and trotters after early surgical intervention for tarsal osteochondrosis. *Equine Vet. J.* doi: 10.1111/evj/12297

Minshall, G., Wright, I. (2012) Synoviocoeles associated with the tarsal sheath: description of the lesion and treatment in 15 horses. *Equine Vet. J.* **44**, 71–75

Moll, H., Slane, D., Humburg, J., Jagar, J. (1987) Traumatic tarsal luxation repaired without internal fixation in three horses and three ponies. *J. Am. Vet. Med. Ass.* **190**, 297–300

Montgomery, L., Juzwiak, J. (2009) Subchondral cyst-like lesions in the talus of four horses. *Equine Vet. Educ.* **21**, 629–637

Moreau, H., Denoix, J.-M. (1994) Calcification of the medial collateral ligament of the hock in a jumping horse. *Pract. Vet. Equine* **26**, 219–220

Murphy, E., Schneider, R., Adams, S., et al. (2000) Long-term outcome on conservative management of tarsal slab fractures in 25 horses (1976–1999). *J. Am. Vet. Med. Ass.* **216**, 1949–1954

O'Neill, H., Bladon, B. (2010) Arthroscopic removal of fractures of the lateral malleolus of the tibia in the tarsocrural joint: a retrospective study of 13 cases. *Equine Vet. J.* **42**, 558 – 562

Poulin Braim, A., Bell, R., Textor, J., et al. (2010) Computed tomography of proximal metatarsal and concurrent third tarsal bone fractures in a Thoroughbred racehorse. *Equine Vet. Educ.* **22**, 290–295

Pilsworth, R. (1992) Incomplete fracture of the dorsal aspect of the third metatarsal bone as a cause of hindlimb lameness in racing Thoroughbreds: a review of three cases. *Equine Vet. J.* **24**, 147–150

Post, E., Singer, E., Clegg, P., et al. (2003) Retrospective study of 24 cases of septic calcaneal bursitis in the horse. *Equine Vet. J.* **35**, 662–668

Raes, E., Bergman, H., Van Ryssen, B., et al. (2014) Computed tomographic features of lesions detected in horses with tarsal lameness. *Equine Vet. J.* **46**,189–193

Rose, P., Moore, I. (2003) Imaging diagnosis – avulsion of the medial collateral ligament of the tarsus in a horse. *Vet. Radiol. Ultrasound* **44**, 657–659

Ross, M., Sponseller, M., Gill, H., Moyer, W. (1993) Articular fracture of the dorsoproximal aspect of the third metatarsal bone in five Standardbred racehorses. *J. Am. Vet. Med. Ass.* **203**, 698–700

Sandgren, B. (1993) Osteochondrosis in the tarsocrural joint and osteochondral fragments in the metacarpo/metatarsophalangeal joints in young Standardbreds. PhD Thesis, University of Uppsala

Santschi, E., Adams, S., Fessler, J., et al. (1997) Treatment of bacterial tarsal tenosynovitis and osteitis of the sustentaculum tali of the calcaneus in 5 horses. *Equine Vet. J.* **29**, 244–247

Schougaard, H., Falk Ronne, J., Philipson, J. (1990) A radiographic survey of tibiotarsal osteochondrosis in a selected population of trotting horses in Denmark and its possible genetic significance. *Equine Vet. J.* **22**, 288–289

Sherlock. C., Eggleston, R., Peroni, J., et al. (2012) Desmitis of the medial tarsal collateral ligament in 7 horses. *Equine Vet. Educ.* **24**, 72–80

Shively, M. (1982) Correct anatomic nomenclature for the joints of the equine tarsus. *Equine Pract.* **4**(4), 9–13

Shively, M., Smallwood, J. (1980) Radiographic and xeroradiographic anatomy of the equine tarsus. *Equine Pract.* **2**(4), 19–34

Skelly-Smith, E., Ireland, J., Dyson, S. (2015) The centrodistal joint interosseous ligament region in the tarsus of the horse: normal appearance, abnormalities and possible association with other tarsal lesions, including osteoarthritis. *Equine Vet. J.* doi 10.1111/evj.12457

Smith, M., Wright, I. (2011) Arthroscopic treatment of fractures of the lateral malleolus of the tibia: 26 cases. *Equine Vet. J.* **43**, 28–287

Smith, R., Dyson, S., Schramme, M., et al. (2005) Osteoarthritis of the talocalcaneal joint in 18 horses. *Equine Vet. J.* **37**, 166–171

Sprackman, L., Dakin, S., May, S., Weller, R. (2015) Relationship between the shape of the central and third tarsal bones and the presence of tarsal osteoarthritis. *Vet. J.* **204**, 94–98

Stock, K., Hamann, H., Distl, O. (2005) Prevalence of osseous fragments in distal and proximal interphalangeal, metacarpo- and metatarsophalangeal and tarsocrural joints of Hanoverian Warmblood horses. *J. Vet. Med. A* **52**, 388–394

Storgaard, J., Jorgensen, H., Proschowsky, H., Falke-Ronne, J., Willeberg, P., Hesselholt, M. (1997) The significance of routine radiographic findings with respect to racing performance and longevity in Standardbred trotters. *Equine Vet. J.* **29**, 55–59

Stover, S., Hornhof, W., Richardson, G., Meagher, D. (1986) Bone scintigraphy as an aid to diagnosis of occult distal tarsal bone trauma in 3 horses. *J. Am. Vet. Med. Ass.* **182**, 624–627

Stromberg, B., Rejno, S. (1978) Osteochondritis in the horse: a clinical and radiological investigation of the knee and hock joints. *Acta Vet. Scand. Suppl.* **358**, 139–152

Sullins, K., Stashak, T. (1983) An unusual fracture of the tibiotarsal bone in a mare. *J. Am. Vet. Med. Ass.* **182**, 1395–1396

Taylor, S., Martinelli, M.J., Trostle, S.S., Kemper, T. (2005) Articular mastocytosis in the tarsocrural joint of a horse. *Equine Vet. Educ.***17**, 207–211.

Tomlinson, J., Redding, W., Berry, C., Smallwood, J. (2003) Computed tomographic anatomy of the equine tarsus. *Vet. Radiol. Ultrasound* **44**, 174–178

Tulamo, R., Bramlage, L., Gabel, A. (1983) Fractures of the central and third tarsal bones in horses. *J. Am. Vet. Med. Ass.* **182**, 1234–1238

Tulleners, E., Reid, C. (1981a) Osteomyelitis of the sustentaculum talus in a pony. *J. Am. Vet. Med. Ass.* **178**, 290–291

Tulleners, E., Reid, C. (1981b) An unusual fracture of the tarsus in two horses. *J. Am. Vet. Med. Ass.* **178**, 291–294

Verwilghen, D., Janssens, S., Busoni, V., et al. (2013) Do developmental orthopaedic disorders influence future jumping performance in Warmblood stallions? *Equine Vet. J.* doi:10.1111/evj.12027

Whitcomb, M. (2006) Ultrasonography of the equine tarsus. *Proc. Am. Assoc. Equine Pract.* **52**, 13–17

Wong, D., Scaratt, W., Maxwell, V., Moon, M. (2003) Incomplete ossification of the carpal, tarsal and navicular bones in a dysmature foal. *Equine Vet. Educ.* **15**, 72–81

Wright, I. (1992) Fractures of the lateral malleolus of the tibia in 16 horses. *Equine Vet. J.* **24**, 424–429

Chapter 10
The stifle and tibia

Stifle

RADIOGRAPHIC TECHNIQUE

Five radiographic views are necessary for complete evaluation of the stifle joint:

1. Lateromedial and/or flexed lateromedial.
2. Caudocranial.
3. Caudal 60° lateral-craniomedial oblique.
4. Craniolateral-caudomedial oblique/caudomedial-craniolateral oblique.
5. Cranioproximal-craniodistal (flexed) oblique.

In many horses sufficient information can be obtained using views 1,2 and 3.

Equipment

For caudocranial views of the stifle in mature horses, an x-ray machine with a minimum output of 90 kV and 20 mAs is required. Radiography should only be attempted with the horse standing if it is co-operative. A fractious horse may inflict serious damage to personnel and equipment, and will result in unacceptably high radiation hazards. If the horse cannot be calmed using sedation and/or a twitch, general anaesthesia should be used, although with modern sedatives this is rarely necessary.

Digital systems or fast rare earth screens and films are recommended. Large imaging plates or cassettes (35 cm × 43 cm) are advisable in order to examine an adequate length of the femur and tibia. A cassette holder should ideally be used; however, holders of this size are cumbersome and difficult to hold still. For this reason the cassette is often hand-held. Using these large cassettes, and with adequate collimation of the x-ray beam, the holder's gloved hands should be well away from the primary x-ray beam. The difficulty in aligning the cassette and x-ray beam in the standing horse makes it advisable to dispense with the use of a grid. Under general anaesthesia, the quality of the radiographs can be enhanced by using a grid.

Clinical Radiology of the Horse, Fourth Edition. Janet A. Butler, Christopher M. Colles, Sue J. Dyson, Svend E. Kold and Paul W. Poulos.
© 2017 John Wiley & Sons, Ltd. Published 2017 by John Wiley & Sons, Ltd.
Companion website: www.clinical-radiology-horse.com

Positioning

Lateromedial view

A true lateromedial view may be required if osseous irregularities near the distal insertion of the cranial cruciate ligament are suspected. The limb to be examined should be positioned caudal to the contralateral limb, fully weight bearing. This facilitates positioning of the cassette on the medial aspect of the stifle. The cassette usually has to be hand-held, as high in the groin region as possible. The x-ray beam should be centred on the femorotibial joint. Palpate the tibial crest and centre immediately proximal to it, approximately 10 cm caudal to the cranial aspect of the limb. To obtain lateromedial alignment, the beam should initially be aligned parallel to a tangent to the bulbs of the heel, but this may require alteration on subsequent films.

Flexion of the stifle, either with the limb lifted and retracted or with the horse resting the toe on the ground, 'drops' the stifle and facilitates obtaining a true lateromedial radiograph. Some horses will not tolerate a cassette on the medial aspect of the hindlimb with the limb weight bearing, but will accept it if the limb is flexed. This view requires an extra person to flex the limb.

A lateromedial (flexed) view (see Figure 10.7c) also potentially gives extra room in which to position the cassette. Other advantages of the flexed lateromedial view include better visualisation of the proximal aspect of the tibia in the region of the intercondylar eminences, assessment of the proximal aspect of the trochlear ridges of the femur, without superimposition of the patella, and a clearer view of the apex of the patella.

Caudolateral-craniomedial oblique view

A caudal 60° lateral-craniomedial oblique (Cd 60°L-CrMO) view may give more information than a lateromedial view and be easier to acquire. In an oblique view the trochlear ridges and the condyles of the femur are not superimposed. The large adductor muscle mass on the medial aspect of the horse's thigh, together with the testicles in entire males, make accurate positioning of the cassette for a true lateromedial view difficult. With a caudal 60° lateral-craniomedial oblique view, the cassette can be positioned slightly more cranial to the joint (Figure 10.1).

Angling the x-ray beam 10–15° proximodistally (downwards) further facilitates alignment of the beam and the cassette and enables better assessment of the trochlear ridges. The x-ray beam should be centred approximately 10 cm caudal to the cranial aspect of the limb, at the level of the femorotibial joint, which is readily palpable immediately proximal to the tibial crest.

An alternative technique is to position the cassette lateral to the stifle, with the x-ray machine medial. The x-ray beam passes under the ventral aspect of the abdomen to obtain a cranial 60° medial 15° distal-caudolateral proximal oblique view of the stifle. This technique allows easier positioning of the cassette and is accepted more readily by a fractious horse. It is impractical in a stallion or a horse with a low abdominal wall.

Further obliquity (Cd45°L-CrMO) gives better separation of the femoral condyles (see Figure 10.9).

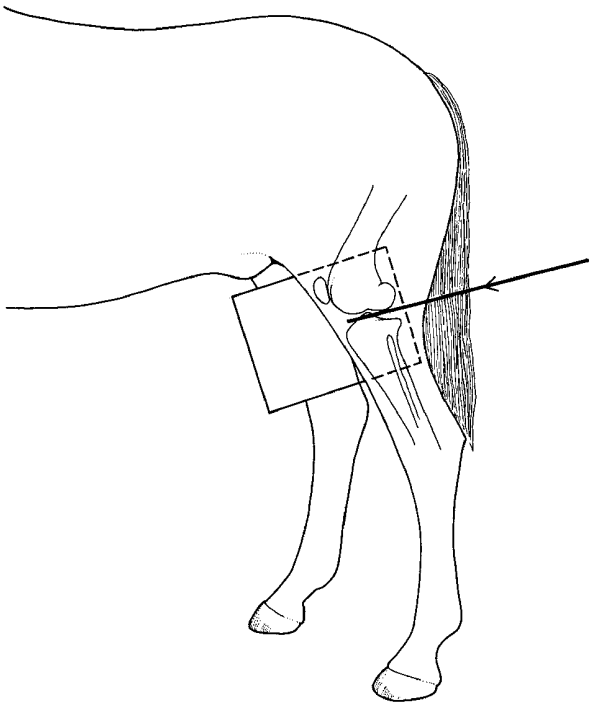


Figure 10.1 Positioning of the limb, cassette and x-ray beam to obtain a caudal 60° lateral-craniomedial oblique view of the stifle.

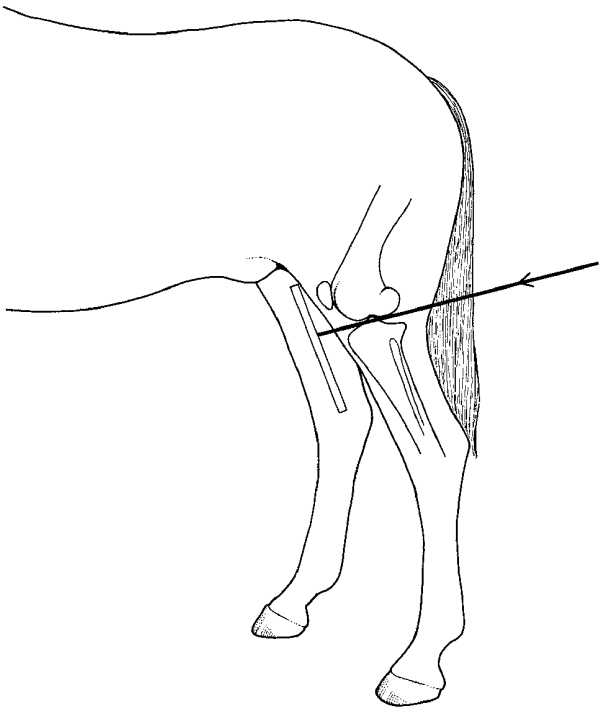


Figure 10.2 Positioning of the limb, cassette and x-ray beam to obtain a caudoproximal-craniodistal oblique view of the stifle.

Caudocranial or caudal 10° proximal-craniodistal oblique views

The caudocranial view is preferred to a craniocaudal view, because positioning is easier, and the imaging plate is closer to the joint. It does put the equipment and the radiographer at risk, but with experienced handlers, correct imaging plate positioning and sedation, these problems can be minimised. Positioning the horse with the limb positioned caudally and angling the x-ray beam 10–20° proximodistally, may facilitate placement of the cassette perpendicular to the x-ray beam and in close apposition to the limb (technically this is a caudal 10° proximal-craniodistal oblique image). Make sure that the heel of the foot is on the ground, because slight elevation of the heel may result in artefactual narrowing of the femorotibial joint space. The cassette can be positioned without touching the flank, and this aids correct alignment of cassette and x-ray beam (Figure 10.2). The cassette should be slowly advanced medially until the radiographer can see the edge of the cassette between the hindlimbs. Care should be taken not to touch the sheath in male horses. The x-ray beam should be centred on a line bisecting the limb, i.e. approximately between the semimembranosus and semitendinosus muscles, at the level of the distal third of these muscles. Alternatively the exit point of the beam from the cranial aspect of the joint should be at the level of the tibial crest.

Overexposure of the fibula may occur using conventional film–screen combinations, particularly in younger animals in which the fibula is predominantly cartilaginous.

Craniolateral-caudomedial oblique/caudomedial-craniolateral oblique view

A craniolateral-caudomedial oblique view or caudomedial-craniolateral oblique view may be required. With a craniolateral-caudomedial oblique image there is potentially more magnification because the imaging plate is further away from the bones because of the overlying musculature compared with a caudomedial-craniolateral oblique image.

Cranioproximal-craniodistal (flexed) oblique view

The cranioproximal-craniodistal (flexed) oblique view is primarily employed to assess the patella, the trochlear ridges, and the intertrochlear groove of the femur. It is essential for diagnosis of some patellar fractures.

With a standing horse, the limb should be held semi-flexed behind the horse (as if for shoeing), with the femorotibial joint at right angles and the tibia horizontal. The cassette is held approximately horizontal, with its caudal edge against the cranial aspect of the tibia, centred just proximal to the tibial crest (Figure 10.3a). It is not possible to align the x-ray beam perpendicular to the cassette, but satisfactory images are obtained by angling the x-ray beam in a cranial 45° proximal 10° lateral-distal medial oblique direction to avoid the abdominal wall. Adducting the flexed lame limb may facilitate positioning by rotating the stifle outwards.

This view is sometimes more easily obtained with the horse under general anaesthesia. The horse is placed in dorsal recumbency with the limb fully flexed. The x-ray beam is directed in a craniodistal-cranioproximal direction and is centred on the femoropatellar articulation, i.e. approximately 8 cm distal to the profile of the flexed joint. The cassette is positioned along the cranial aspect of the femur (Figure 10.3b).

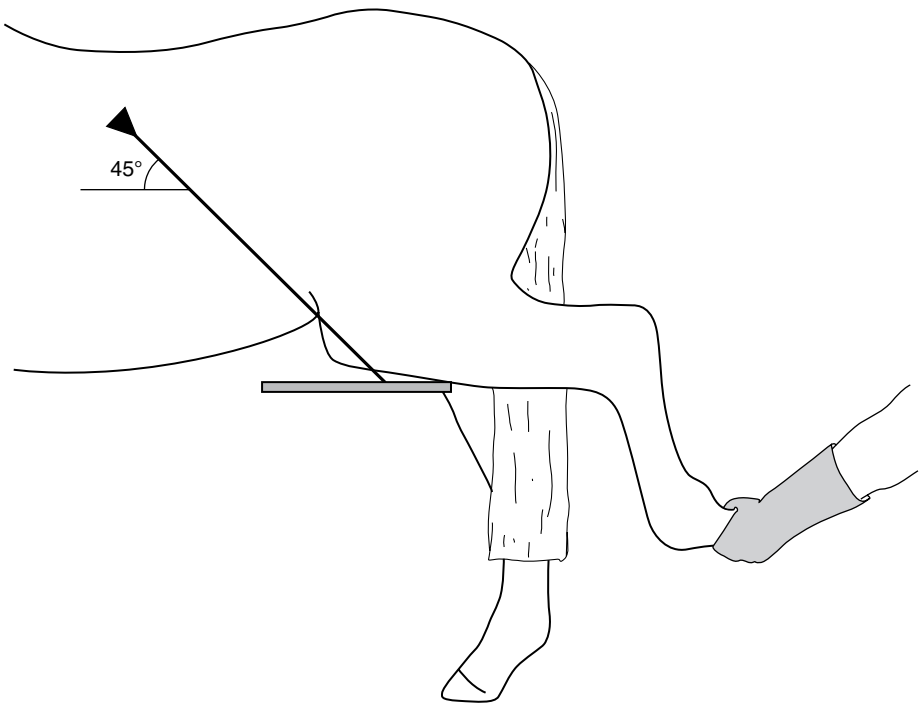


Figure 10.3(a) Positioning of the limb, cassette and x-ray beam to obtain a cranioproximal-craniodistal (flexed) oblique view of the patella with the horse standing. It may be necessary to angle the x-ray beam slightly from lateral to medial.

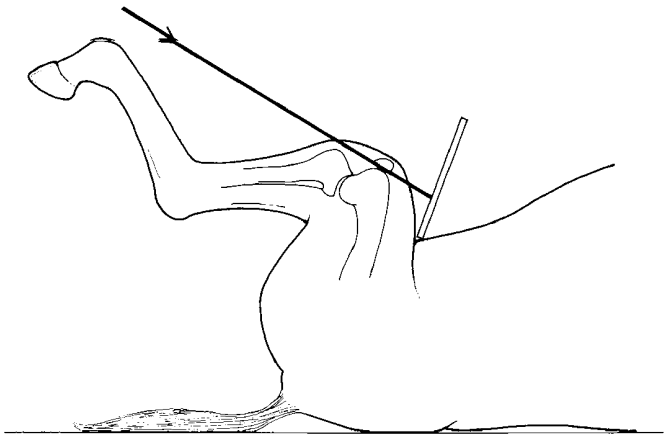


Figure 10.3(b) Positioning of the limb, cassette and x-ray beam to obtain a craniodistal-cranioproximal (flexed) oblique view of the patella with the horse in dorsal recumbency.

NORMAL ANATOMY, VARIATIONS AND INCIDENTAL FINDINGS

Immature horse

Important radiographic changes occur in the stifle during growth. Six centres of ossification are present at birth (Figures 10.4a and 10.4b): the metaphysis and distal epiphysis of the femur, the proximal epiphysis and metaphysis of the tibia, the tibial tuberosity (apophysis) and the patella.

At birth, the patella is a triangular shape, which becomes more complex with age. Initially it has an irregular contour and granular compact bone opacity due to incomplete ossification. The articular surface is concave. The patella is usually fully ossified by 4 months of age.

At birth, the lateral and the medial trochlear ridges of the femur are similar in size. The proximal parts of these ridges have an irregular contour and granular subchondral bone opacity. This appearance is normally present until 3 months of age but may persist until 5 months. It is caused by irregular subchondral ossification and should be differentiated from infectious arthritis (joint-ill), which can have a similar radiographic appearance (see Figure 10.27b). At approximately 2 months of age, the medial trochlear ridge becomes more prominent than the lateral ridge at its proximal part, becoming wider and rounder with a smoothly contoured shoulder (Figure 10.5).

The distal femoral physis is wavy and irregular in outline. It closes at 24–30 months of age. The femoral condyles are smoothly outlined. Irregularity of the condyles should be interpreted as pathological at any age. The femorotibial joint space appears wide at birth due to incomplete ossification of the epiphyses. This incomplete ossification results in apparent sloping of the tibial condyles (Figure 10.4b), which later become more horizontal. The intercondylar eminences (lateral and medial) of the tibia are also incompletely developed, appearing small and blunted. The corresponding intercondylar fossa is shallow.

At birth, the apophysis (centre of ossification of the tibial tuberosity) is separated from the proximal tibial epiphysis as well as from the proximal tibial metaphysis. The apophyseal–metaphyseal physis is seen on lateromedial images as an oblique lucent line of irregular width, and on craniocaudal images as a V-shaped lucent line overlying the proximal tibial metaphysis. The apophyseal–epiphyseal physis closes between 9 and 12 months of age, and the apophyseal–metaphyseal physis closes at



Figure 10.4(a) Lateromedial image of a stifle of a normal 5-day-old foal. Cranial is to the left. Note the irregular contour and granular opacity of the proximal part of the femoral trochlea and of the patella. The physes are relatively wide. The lateral and medial trochlear ridges of the femur are of similar size. There is an approximately triangular lucent area cranial to the femoropatellar joint representing fat. Note also the separate centre of ossification of the tibial crest (the tibial apophysis).



Figure 10.4(b) Caudocranial image of the stifle of a normal 5-day-old foal. Lateral is to the right. Incomplete ossification of the proximal tibial epiphysis gives the impression of slanting of the tibial condyles. The femorotibial joint space is wide compared with that of the adult. The tibial apophysis and its physis can be identified superimposed on the tibial metaphysis (arrow).

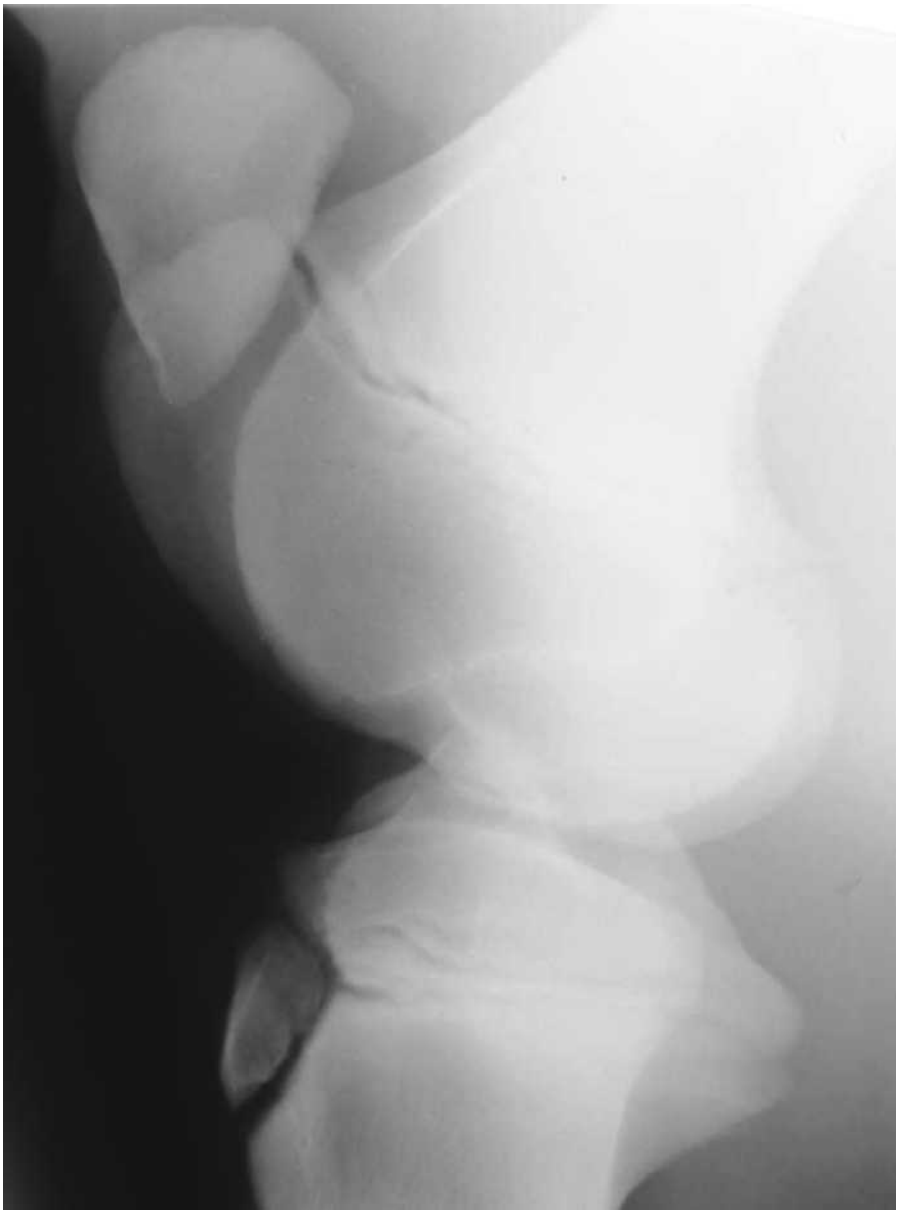


Figure 10.5 Lateromedial image of the stifle of a normal 2-month-old foal. Cranial is to the left. The proximal part of the medial trochlear ridge of the femur and the patella are still incompletely ossified and therefore have an irregular outline. The shape of the trochlea of the femur and the patella, however, is more similar to an adult than to a neonatal foal (compare with Figure 10.4a).

30–36 months. The proximal tibial physis (epiphyseal–metaphyseal physis) closes at 24–30 months of age.

The fibula has little ossification until 1–2 months of age, at which time ossification occurs from one or more centres (Figures 10.6a-d). This ossification may remain incomplete, resulting in horizontal or oblique radiolucent lines in the fibula (Figure 10.6f and Figures 10w.11a-c). These should not be confused with fractures.

Skeletally mature horse

Lateromedial view

With the exception of a slight degree of obliquity, the principal radiographic features of the lateromedial view (Figure 10.7a) are the same as those described in detail below for the caudal 60° lateral-craniomedial oblique view.



Figure 10.6 Caudomedial-craniolateral oblique images of the fibulas of seven horses of variable age; lateral is to the right: (a)–(d) are skeletally immature horses and show progressive ossification occurring with increasing age; (e)–(g) are skeletally mature horses. Ossification often occurs from more than one centre of ossification which may never fuse, resulting in persistent lucent lines traversing the fibula (f and g).

Caudal 60° lateral-craniomedial oblique view

The large medial trochlear ridge of the femur is positioned proximal and cranial to the smaller lateral trochlear ridge (Figure 10.7b). The trochlear ridges are smoothly curved in outline. Proximally the medial trochlear ridge has a small flattened area at its junction with the metaphysis of the femur. The distal two-thirds of the medial ridge are flatter than the lateral trochlea. There is a small notch where the medial trochlear ridge merges with the medial femoral condyle. From this notch an irregular radiopaque line traverses the condyles in a caudal and slightly proximal direction. This is the intercondylar fossa. Immediately above the notch, the convergence of two radiopaque lines indicates the extensor fossa. There is a radiopaque line parallel to the trochlear ridges, which represents the base of the intertrochlear groove. On the lateral trochlear ridge there is a flattened area at its transition into the lateral condyle. Neither this, nor the poorly developed area of decreased opacity immediately proximal to this area should be interpreted as an osteochondral defect. If the x-ray beam is angled from too far cranially, the lateral trochlear ridge may appear flattened. The most proximal part of the ridge may have an indistinct margin (Figure 10.8) which should not be



(e) (f) (g)

Figure 10.6 *Cont'd*

confused with a manifestation of osteochondrosis. The femoral condyles have a smooth convex outline. On the Cd 60°L-CrM oblique view the condyles are partly superimposed, the medial condyle being projected slightly caudal to the lateral condyle. Fabellae occasionally occur proximal to the caudal aspect of the femoral condyles.

The position of the patella in relation to the distal femur changes with the degree of flexion/extension of the femorotibial joint. When the horse is bearing weight, the patella is positioned over the proximal aspect of the medial trochlear ridge. With flexion of the femorotibial joint, the patella moves distally which aids assessment of the proximal aspect of the trochlea. Softly exposed radiographs may demonstrate the patellar ligaments.

The femoral condyles and the intercondylar eminences of the tibia are superimposed on this view. The tibial tuberosity and tibial crest are recognised cranially.

A soft-tissue opacity is often seen at the cranial aspect of the femorotibial joint, cranial to the site of insertion of the cranial cruciate ligament.

Caudal 45° lateral-craniomedial oblique view

The femoral condyles are further separated in the caudal 45° lateral-craniomedial oblique view (Figure 10.9), compared with a Cd 60°L-CrMO view.



Figure 10.7(a) True lateromedial image of the stifle of a normal adult horse. Cranial is to the left. The larger medial trochlea of the femur is projected cranial to the lateral trochlea.

Caudocranial or caudal 10°proximal-craniodistal oblique views

The patella is seen partly superimposed upon the lateral cortex of the diaphysis of the femur (Figure 10.10a). The medial ridge of the supracondylar fossa and the border of the extensor fossa on the lateral surface of the lateral femoral condyle can also be evaluated.

Deviations from a true caudocranial image may outline slight osseous irregularities along either the medial or the lateral femoral epicondyles. An oval area of decreased opacity is frequently seen at the proximolateral aspect of the intercondylar fossa of the femur, as is a flask-shaped lucent area distal and slightly lateral to the intercondylar eminences of the tibia. They occur as the result of superimposition, and should not be interpreted as cystic lesions in the bone. The border of the intercondylar fossa is relatively opaque.

The medial femoral condyle is rounder than the lateral, but slight flattening of the medial femoral condyle or slight concavity of bone outline (a 'dimple') (Figure 10w.10b) may be within the normal range provided the trabecular pattern of the subchondral bone is normal. The shape of the femoral condyles and the width of the femorotibial joint change with the angle of projection of the radiograph.



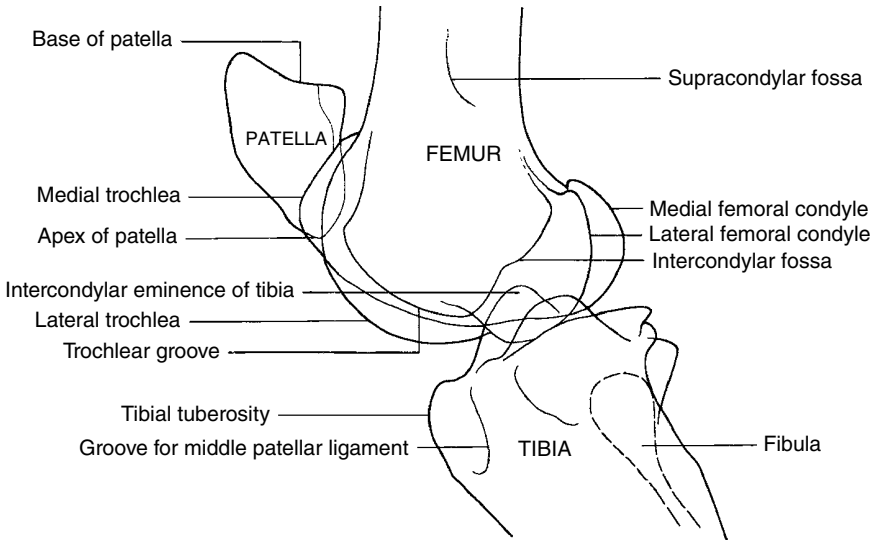


Figure 10.7(b) Caudal 60° lateral-craniomedial oblique image and diagram of a normal adult stifle. Cranial is to the left. Note the smooth curved contour of the lateral and medial trochlear ridges of the femur. The medial trochlea is larger than the lateral. Compare with Figure 10.9.



Figure 10.7(c) Lateromedial (flexed) image of the stifle of a normal adult horse. Cranial is to the left. Compared with a weight-bearing view the patella has moved distally and the cranial aspect of the femorotibial joint is opened.



Figure 10.8 Lateromedial image of the stifle of a normal yearling Thoroughbred. Cranial is to the left. The contour of the proximal aspect of the lateral trochlea of the femur is slightly flattened and ill-defined (arrow). This is the result of angulation of the x-ray beam from too far cranially and does not represent a pathological abnormality. Compare with Figures 10.7(a) (normal) and 10.16 (osteochondrosis).



Figure 10.9 Caudal 45° lateral-craniomedial oblique image of the stifle of a normal mature horse. Cranial is to the left. Compare with Figures 10.7(a) and 10.7(b).

The lateral condyle of the femur has a proximomedial-distolateral inclination. The lateral joint space of the femorotibial joint is narrower than the medial space; this does not indicate collapse of the lateral meniscus. The femorotibial joint space width medially and laterally appears to vary depending on the way in which the horse is standing, and narrowing should be interpreted with extreme caution unless it can be reproduced in several views. There is a variable shape of the proximomedial aspect of the tibia, which is usually bilaterally symmetrical (Figure 10w.10c).

The medial intercondylar eminence of the tibia is larger and more pointed than the lateral eminence (Figures 10.10a and 10.10d). The lateral condyle of the tibia has a proximomedial-distolateral inclination to mirror the outline of the lateral femoral condyle. Superimposed on the lateral condyle and metaphysis are the tibial tuberosity and tibial crest. There are focal areas of reduced opacity distal to the intercondylar eminences and proximal to the tuberosity of the tibia. The fibula articulates with the lateral aspect of the tibia.

Craniolateral-caudomedial oblique/caudomedial-craniolateral oblique view

The medial trochlea of the femur and the fibula and its articulation with the tibia are highlighted in this image (Figure 10w.11a). Occasionally there is fusion between the proximal aspects of the tibia and fibula (Figure 10w.11b)



Figure 10.10(a) Caudoproximal-craniodistal oblique image and diagram of a normal adult stifle. Lateral is to the right. Note the different shapes of lateral and medial femoral condyles. The intercondylar fossa has a well-defined margin. The medial intercondylar eminence is larger than the lateral and more sharply pointed. Note the poorly defined lucent area distal to it.

or osseous irregularity of the tibia adjacent to the articulation between the tibia and fibula (Figure 10w.11c).

Cranioproximal-craniodistal (flexed) oblique view

The medial trochlear ridge is larger and rounder than the lateral and is separated from it by the trochlear groove (Figure 10.12). The patella is approximately triangular and its medial angle is more pointed than the lateral. The patella has a uniform opacity with a distinct subchondral bone plate and a smooth articular outline.

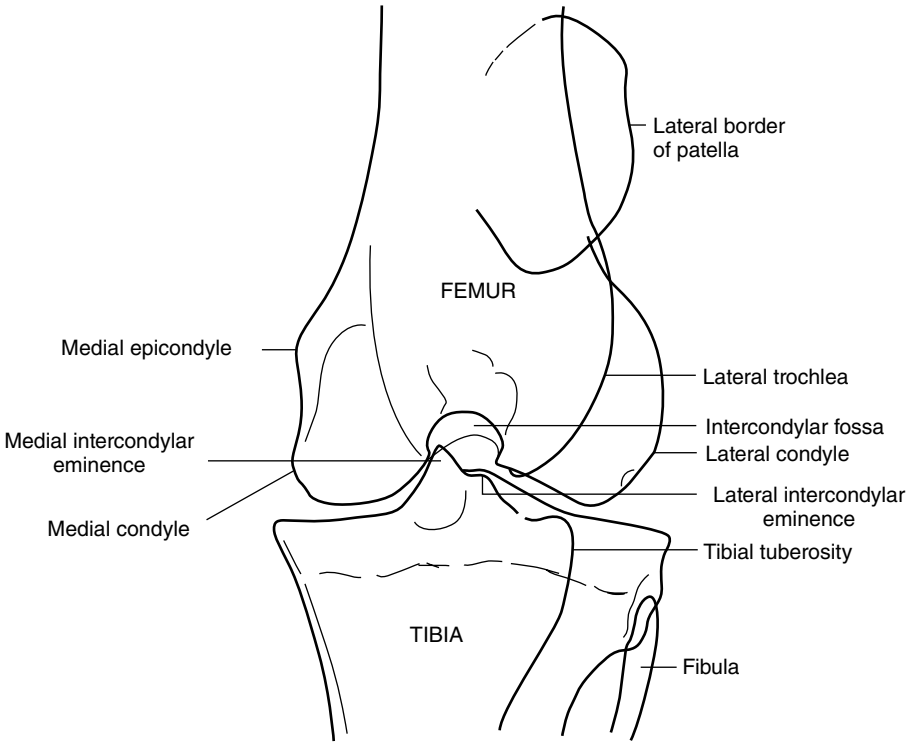


Figure 10.10(a) *Cont'd*



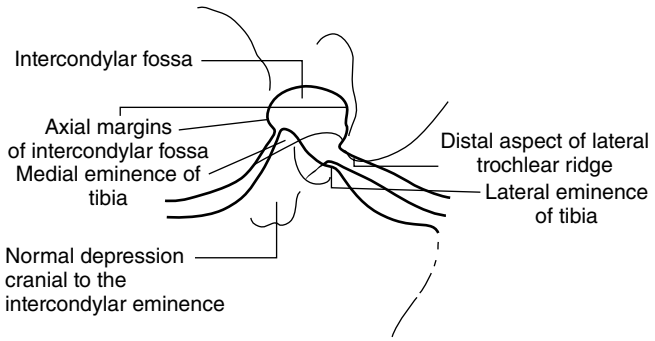


Figure 10.10(d) Caudocranial image of the axial aspect of the femorotibial joint of a normal mature horse. Lateral is to the right.



Figure 10.12 Cranioproximal-craniodistal oblique (flexed) image of the patella and femoral trochleas of a normal adult horse. Lateral is to the right. The medial aspect of the patella is more pointed than laterally. The medial trochlea of the femur is larger and more convex than the lateral trochlea. Note the congruity of the articular surfaces.

Other structures are poorly defined on this view.

Knowledge of the sites of soft-tissue attachments in the stifle region is an important prerequisite for accurate radiographic interpretation (Figures 10.13, 10.14 and 10.15, Table 10.1).

SIGNIFICANT FINDINGS

Osteochondrosis

In this text, subchondral bone cysts (osseous cyst-like lesions) are regarded as a separate entity from osteochondrosis, although they are considered by some workers to be part of the same syndrome (see 'Osseous cyst-like lesions', below).

In the stifle, osteochondrosis is most commonly recognised radiographically involving the lateral trochlear ridge of the femur. Lesions are also seen restricted to the articular surface of the patella. Less commonly, lesions may also involve the medial trochlear ridge and the trochlear groove. Osteochondrosis frequently occurs bilaterally and both stifles should be radiographed.

Radiographic indications of osteochondrosis of the lateral trochlear ridge are most easily detected on a caudal 60° lateral-craniomedial oblique image, and may include:

1 Flattening, especially of the middle third of the ridge (Figure 10.16).

2 An irregular contour of the ridge, usually limited to the middle third, but occasionally involving as much as two-thirds of the ridge. There may be one or more subchondral lucent defects extending for up to 2 cm into the ridge (Figures 10.17a and 10.17b). These may have a margin with increased opacity and are easily demonstrated on slightly more oblique views.

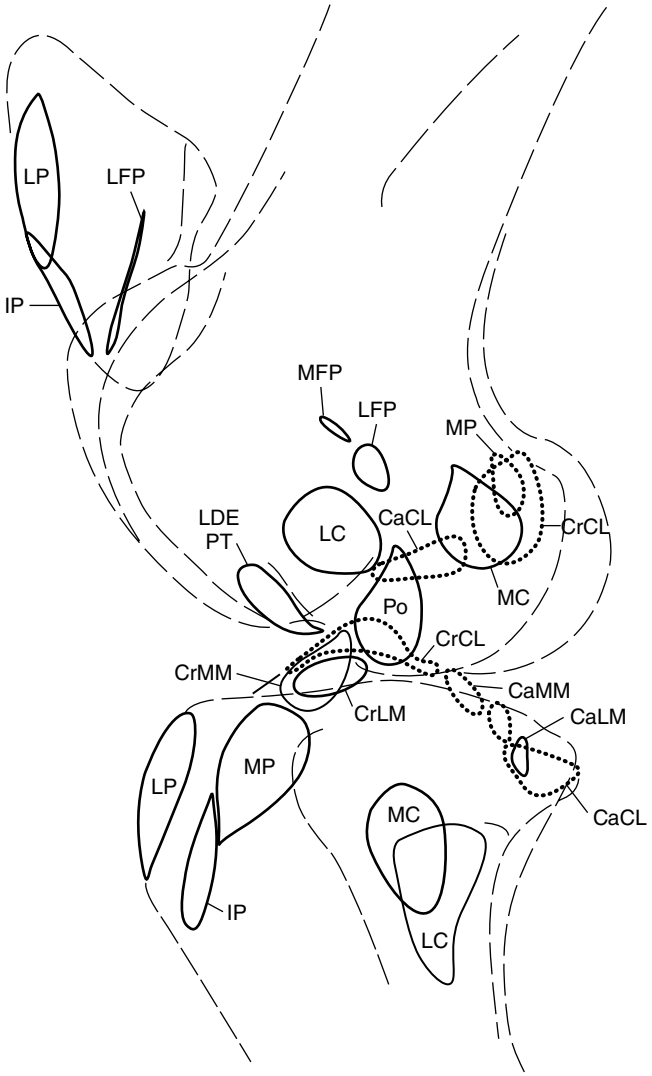


Figure 10.13(a) Diagram of a caudal 60° lateral-craniomedial oblique view of the stifle illustrating the sites of ligament and tendon attachments. The areas of attachment situated within the intercondylar area are marked with dotted lines. See Table 10.1. Source: Reproduced from Maulet et al., 2005, *Equine Vetinary Education*.

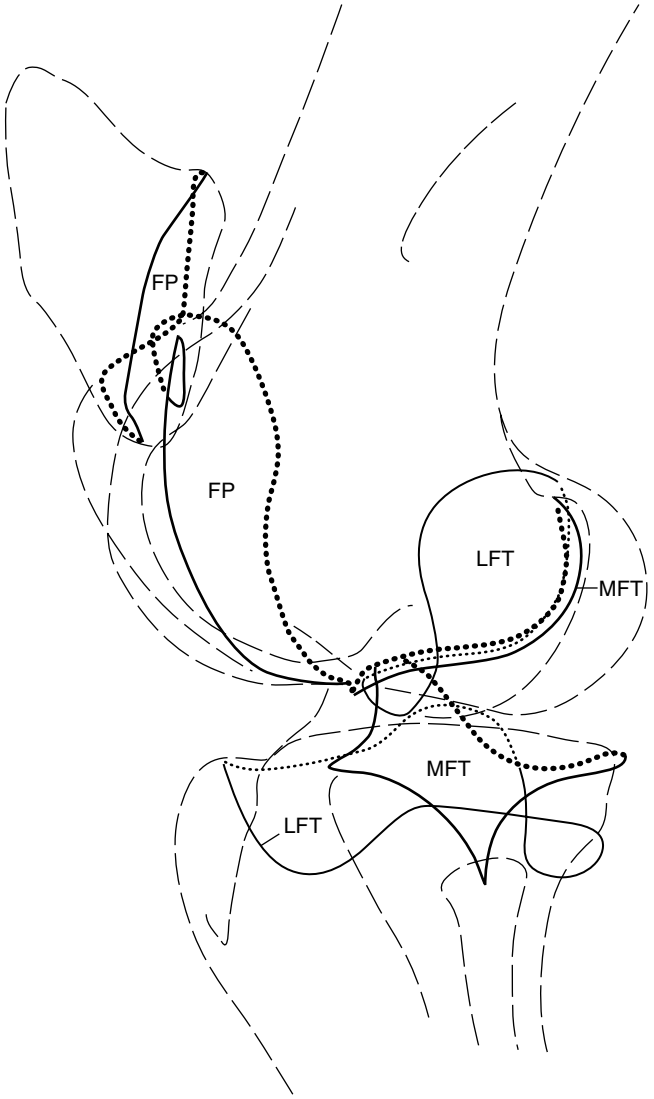


Figure 10.13(b) Diagram of a caudal 60° lateral-craniomedial oblique view of the stifle illustrating the sites of joint capsule attachments. The attachments situated on the medial aspect of the patella and femur are marked with dotted lines. See Table 10.1. Source: Reproduced from Maulet et al., 2005, *Equine Vetinary Education*.

3 Radiopaque fragments may be present within a defect in the ridge (Figure 10.18).

4 In long-standing cases, the lateral trochlear ridge may be grossly undersized but have a regular outline (Figure 10w.19b). This is normally due to fragmentation and remodelling. There may be one or more rounded, radiopaque fragments within the femoropatellar joint or attached to the joint capsule. Occasionally similar changes are identified in the medial trochlea of the femur. Very severe under sizing of the lateral trochlea may predispose to secondary luxation of the patella and osteoarthritis.

5 The articular surface of the patella may be irregular (Figure 10.19a), most commonly near the apex. Other patellar changes include subchondral lucent zones, with or without surrounding increased opacity, dystrophic new bone

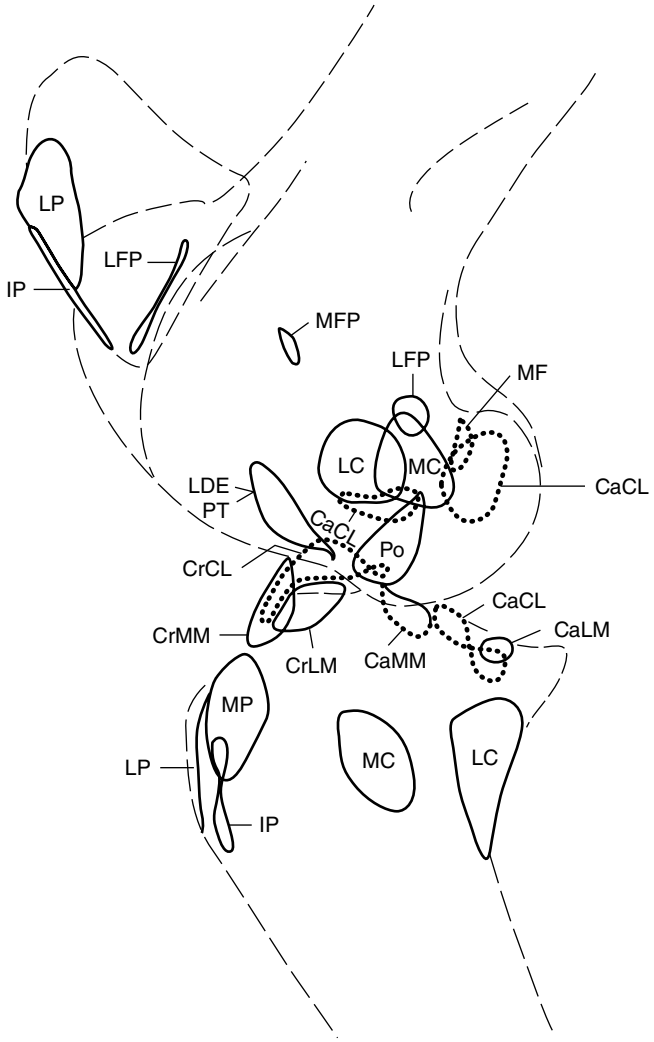


Figure 10.14(a) Diagram of a lateromedial view of the stifle illustrating the sites of ligament and tendon attachments. The areas of attachment situated within the intercondylar area are marked with dotted lines. See Table 10.1. Source: Reproduced from Maulet et al., 2005, *Equine Vetinary Education*.

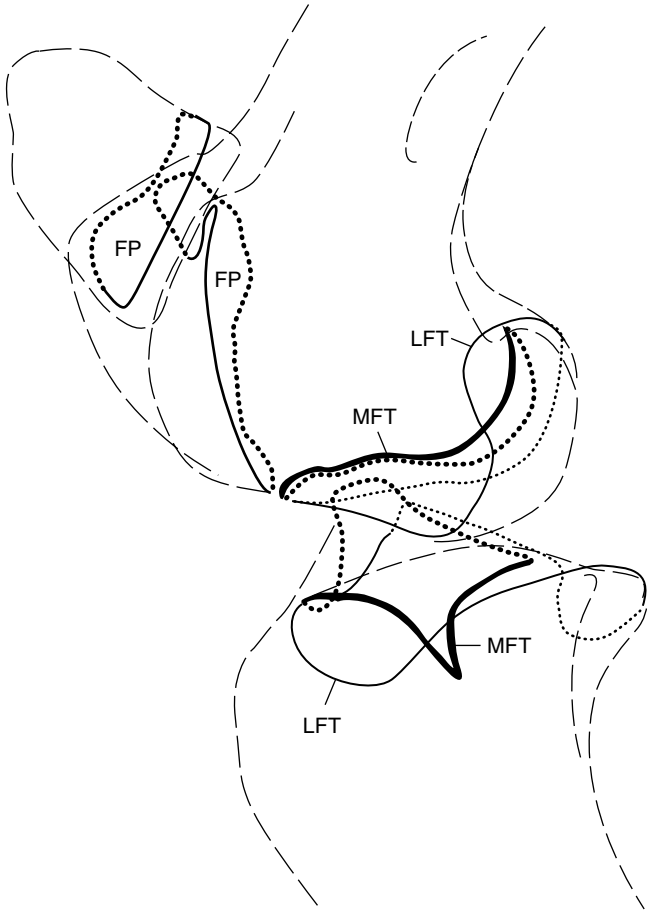


Figure 10.14(b) Diagram of a lateromedial view of the stifle illustrating the sites of joint capsule attachments. The attachments of the femoropatellar joint on the medial aspect and of the femorotibial joint within the intercondylar area are marked with dotted lines. See Table 10.1. Source: Reproduced from Maulet et al., 2005, *Equine Vetinary Education*.

distal to the patella (Figure 10w.19b), possibly secondary to mal-tracking of the patella, and proliferative new bone on the distal aspect of the patella (Figure 10w.19c). These changes are rare, and may occur alone or in association with lesions of the lateral trochlear ridge. A fragment occasionally occurs in isolation at the base of the patella at its articular margin. It is important to ensure that the whole of the patella is seen on radiographs and the proximal part is not missed. The aetiology of these fragments has not been confirmed. Lesions of the patella may warrant a more guarded prognosis.

Simultaneous involvement of more than one structure in the joint has been suggested as indicative of a poor prognosis. Radiography tends to underestimate the degree of pathological abnormality which may be detected arthroscopically.

Osteochondrosis cannot be detected radiographically until a moderate degree of subchondral bone change is present, normally by 3 to 4 months

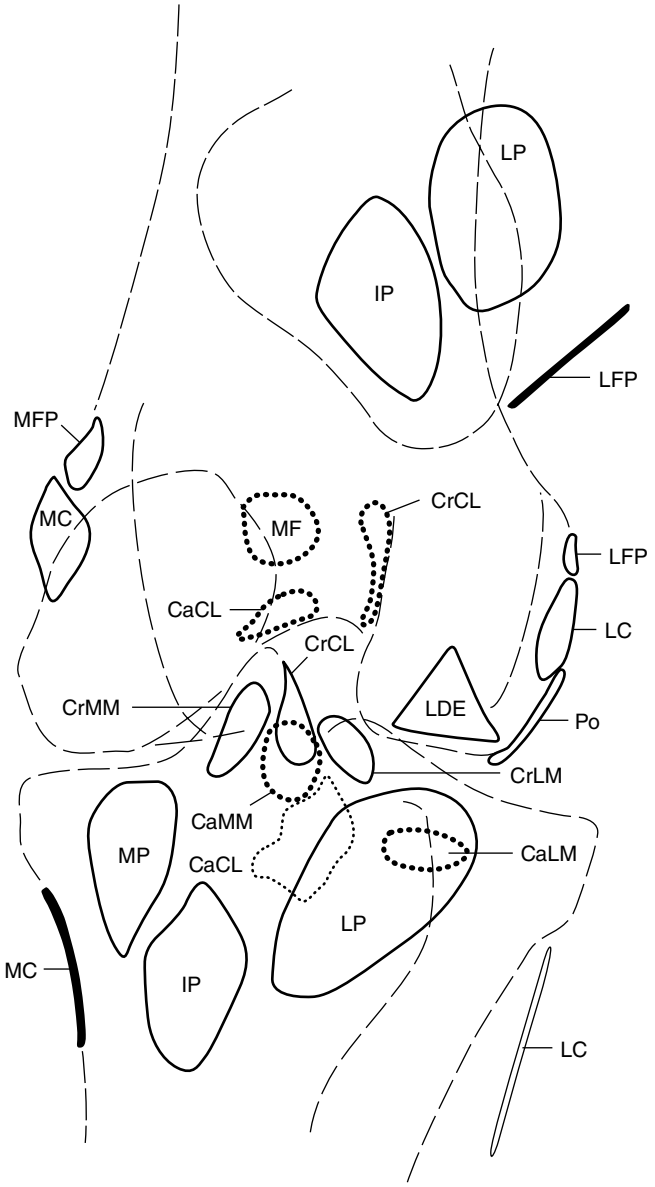


Figure 10.15(a) Diagram of a caudocranial view of the stifle illustrating the sites of ligament and tendon attachments. The areas of attachment situated on the caudal aspect of the femur and tibia are marked with dotted lines. See Table 10.1. Source: Reproduced from Maulet et al., 2005, *Equine Veterinary Education*.

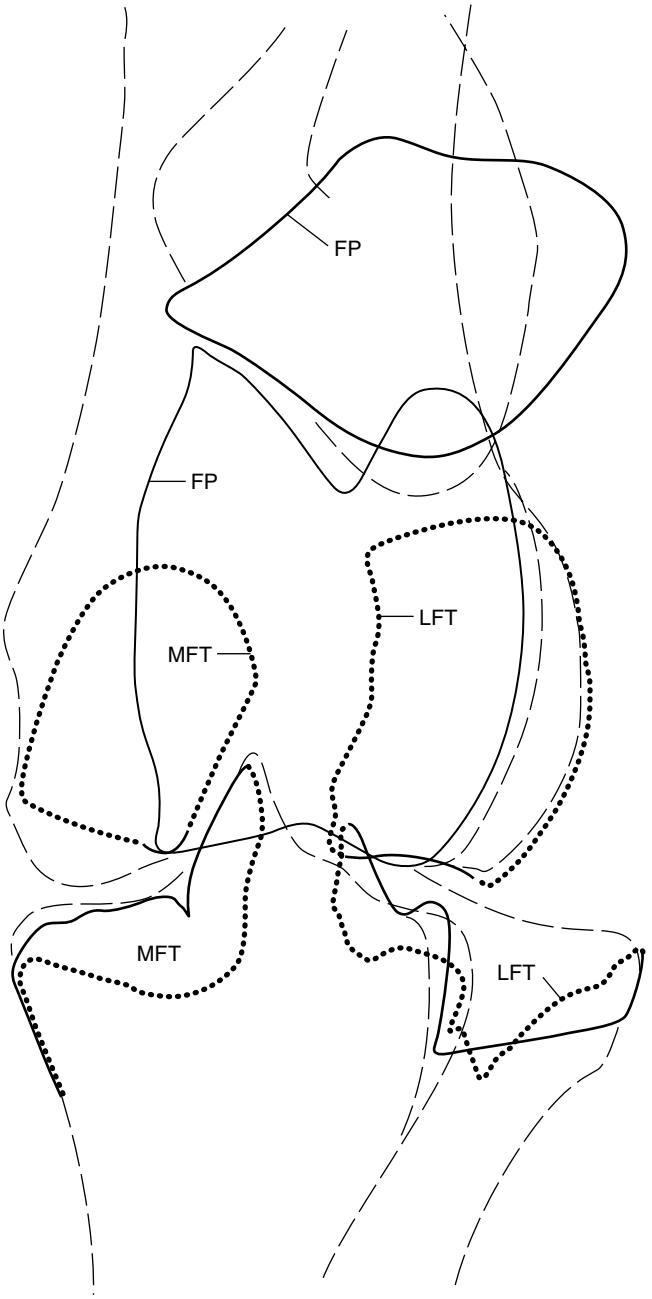


Figure 10.15(b) Diagram of a caudocranial view of the stifle illustrating the sites of joint capsule attachments. The areas of attachment situated on the caudal aspect of the femur and tibia are marked with dotted lines. See Table 10.1. Source: Reproduced from Maulet et al., 2005, *Equine Veterinary Education*.

of age. It is important that oblique views are included and care should be taken not to overlook subchondral lucencies on overexposed films. Slight flattening of the lateral trochlear ridge need not be accompanied by clinical symptoms, and is occasionally seen with increased opacity of the subchondral bone as an incidental finding in older horses. A small proportion of lesions may be missed by radiographic assessment, but may be detected using ultrasonography.

Table 10.1 Legends for the soft-tissue structures indicated in Figures 10.13, 10.14 and 10.15.

LP	Lateral patellar ligament
IP	Intermediate patellar ligament
MP	Medial patellar ligament
LFP	Lateral femoropatellar ligament
MFP	Medial femoropatellar ligament
LC	Lateral collateral ligament of the femorotibial joint
MC	Medial collateral ligament of the femorotibial joint
CrLM	Cranial tibial ligament of the lateral meniscus
CrMM	Cranial tibial ligament of the medial meniscus
CaLM	Caudal tibial ligament of the lateral meniscus
CaMM	Caudal tibial ligament of the medial meniscus
MF	Meniscofemoral ligament of the lateral meniscus
CrCL	Cranial cruciate ligament
CaCL	Caudal cruciate ligament
Po	Tendon of the popliteus muscle
PT	Tendon of origin of fibularis (peroneus) tertius
LDE	Tendon of origin of the long digital extensor muscle
FP	Femoropatellar joint capsule
LFT	Lateral sac of the femorotibial joint capsule
MFT	Medial sac of the femorotibial joint capsule

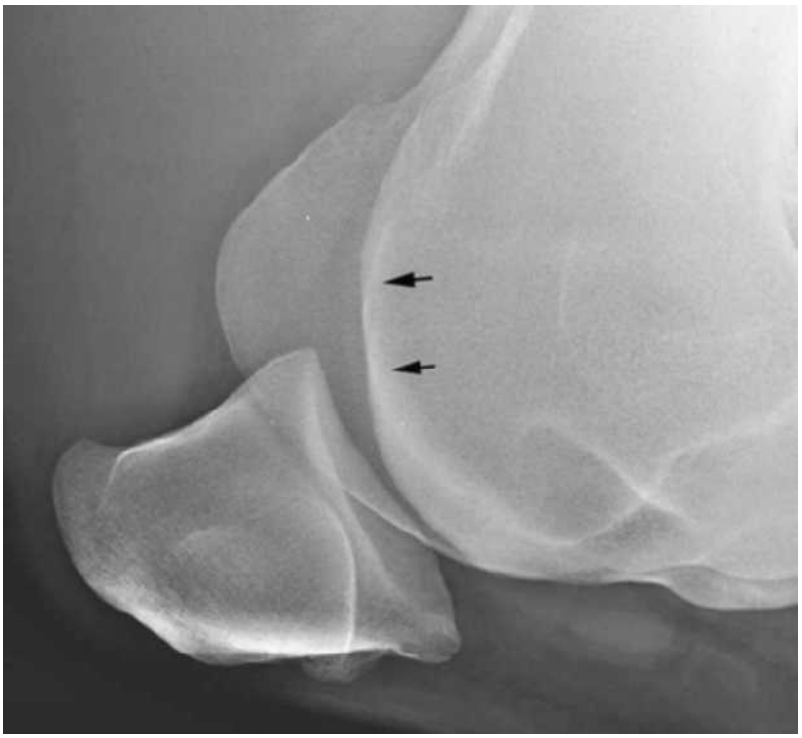


Figure 10.16 Lateromedial (flexed) image of a stifle of an adult horse. Cranial is to the left. There is flattening of the middle one-third of the lateral trochlear ridge of the femur (arrows) (compare with Figure 10.7a), consistent with chronic osteochondrosis. This advanced event horse had a component of femoropatellar joint pain contributing to lameness.

In early mild cases, conservative management may be adequate, and spontaneous resolution of such lesions often occurs, usually by 8 months of age. Radiological changes seen at 18 months of age are usually permanent. In a study of 321 foals examined at 6 and 18 months of age (Warmbloods, French trotters and Thoroughbreds) lesions of the lateral trochlea of the femur were present in 13.7% of horses (Thoroughbreds and Warmbloods more than trotters); by 18 months approximately 61% of lesions had



Figure 10.17(a) Lateromedial image of a stifle of a 10-month-old Thoroughbred foal. Cranial is to the left. The middle one-third of the lateral trochlear ridge of the femur is smoothly irregular and flattened. In the underlying subchondral bone there are ill-defined areas of decreased opacity and generalised increased opacity (black arrows). In addition, there is a subtle depression in the outline of the middle of the medial trochlear ridge (arrow head). Similar changes were present in the contralateral limb. The foal showed only slight hindlimb stiffness, but experienced great difficulty in getting up. Fragments were identified in the defect during exploratory arthroscopy. Ultrasonography may be more accurate for fragment detection than radiography. These abnormalities are typical of osteochondrosis. Note also the separate ossification centre of the apophysis of the tibia.



Figure 10.17(b) Caudal 60°lateral-craniomedial oblique image of the left stifle of a yearling Warmblood, with an upright hindlimb posture and effusion in the femoropatellar joints (the same horse as Figure 10.18). Cranial is to the left. The middle third of the lateral trochlea of the femur has a slightly concave contour and the underlying subchondral bone has heterogeneous opacity, with ill-defined areas of reduced opacity surrounded by areas of increased opacity. There are 5 discrete mineralised opacities aligned linearly cranial to the lateral trochlea. These abnormalities are typical of osteochondrosis. There is also modelling of the apex of the patella.

resolved. In Dutch Warmbloods approximately 86% of lesions of the lateral trochlear ridge present at 6 months of age resolved spontaneously by 18 months. Once distension of the joint capsule and lameness are present, surgical intervention may be recommended, depending on the age of the horse. Post-operatively, there will be some modelling of the defect, but even in clinically successful cases the radiographic appearance will remain abnormal. Approximately 66% of horses treated by arthroscopic surgery have returned to full function as either racehorses or sports horses. The presence of lesions at several sites had a negative effect on outcome.



Figure 10.18 Caudal 60° lateral-craniomedial oblique image of the right stifle of a yearling Warmblood, with an upright hindlimb posture and effusion in the femoropatellar joints (the same horse as Figure 10.17b). Cranial is to the left. There is a focal concave defect in the lateral trochlea of the femur, with mineralised opacities within the defect. These abnormalities are typical of osteochondrosis.

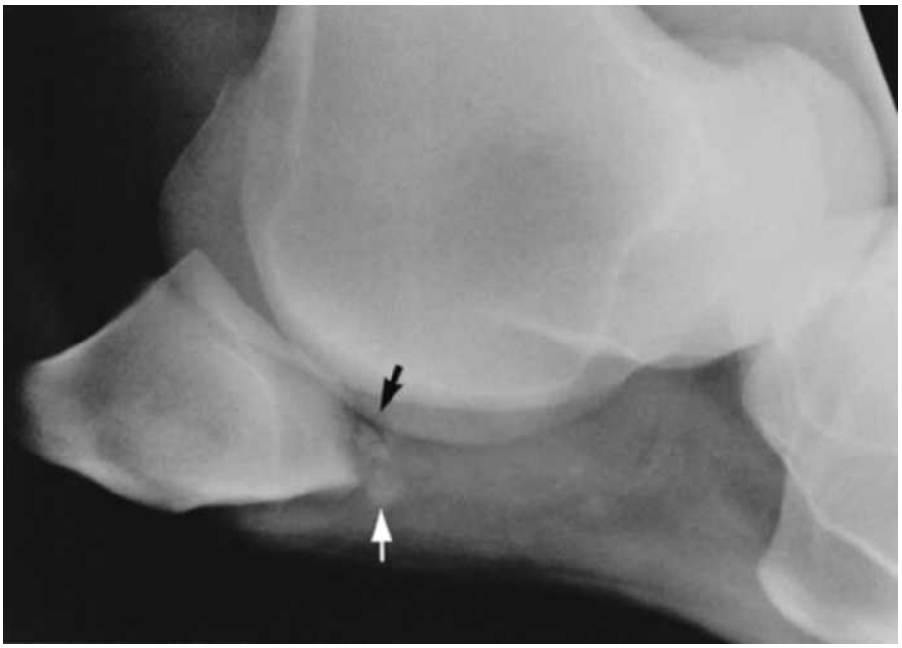


Figure 10.19(a) Lateromedial (flexed) image of a stifle of a 2-year-old Thoroughbred. Cranial is to the left. The distal quarter of the articular surface of the patella is markedly irregular with extensive subchondral fragmentation towards the apex (arrows). These changes may be part of the osteochondrosis syndrome. Similar, usually less severe, changes may develop secondary to medial patellar desmotomy.

Osteochondrosis may remain asymptomatic throughout the horse's life, or may become symptomatic late in life. In older horses there are usually discrete bony opacities in association with a shallow defect and increased opacity of the subchondral bone. In these cases the bony fragments must be removed in order to provide a congruent articulation and prevent the development of secondary degenerative joint disease. However, if secondary degenerative joint disease is already present the prognosis is more guarded, but this may not be radiographically apparent. Detection of severe cartilage pathology may be detected by ultrasonography in some horses, but exploratory arthroscopy is most reliable. In association with chronic osteochondrosis there may be modelling of the patella, especially the distal aspect (Figure 10w.19c), which probably reflects chronic instability of the femoropatellar articulation. Such lesions warrant a guarded prognosis.

Osseous cyst-like lesions

Subchondral bone cysts

Although subchondral bone cysts are considered by some authors to be part of the osteochondrosis syndrome, they are referred to in this text as a separate lesion. An experimentally-induced elliptical full-thickness cartilage plus subchondral bone defect, at the region of maximum weight bearing in the medial femoral condyle, will result in the development of an osseous cyst-like lesion within 3 weeks, which may progressively enlarge over the following 9 weeks. This supports clinical evidence of subchondral bone cysts developing in the medial femoral condyle of mature horses following known trauma. Concurrent osteochondrosis lesions of the lateral trochlear ridge, and medial or lateral femoral condyle subchondral bone cysts, have been seen in a small number of horses (Figures 10w.20a and 10w.20b).

Subchondral bone cysts in the stifle occur almost exclusively in the medial femoral condyle. They frequently develop bilaterally, although the horse may present with a unilateral lameness, therefore both hindlimbs should be examined radiographically. A fully developed subchondral bone cyst is seen as an almost circular or oval lucent area within the subchondral bone, usually surrounded by a narrow rim of more opaque bone. It is best seen on a caudocranial image and may be difficult to see on weight-bearing lateral or oblique images due to superimposition of the condyles. A subchondral bone cyst may be seen more readily in a flexed oblique image or a caudolateral-craniomedial oblique image.

The cyst initially develops from a saucer-shaped radiolucent area proximal to the articular cartilage (Figure 10.21a). This lucent zone gradually enlarges to become dome-shaped, with a flat base in close apposition to the articular surface (Figures 10.21b and 10.21c). If a cyst develops prior to skeletal maturity, continued growth and endochondral ossification of the epiphysis gives the impression that the cyst moves proximally into the condyle. The cyst becomes more rounded (Figure 10.22a) and a communicating lucent channel develops



(a)



(b)



(c)

Figure 10.21 Caudocranial images (lateral is to the right) of one stifle of an Arab horse, showing the development of a dome-shaped subchondral bone cyst in the medial femoral condyle from a crescent-shaped subchondral defect: (a) 12 months of age; (b) 18 months of age; (c) 21 months of age. Note the rim of increased radiopacity surrounding the defect.



Figure 10.22(a) Caudocranial image of a stifle of a 2-year-old horse. Lateral is to the right. There is a large oval subchondral bone cyst in the medial femoral condyle. There is a thin rim of increased radiopacity surrounding the cyst and apparent reformation of a subchondral bone plate between the cyst and the medial femorotibial joint.



Figure 10.22(b) Caudocranial image of the left stifle of a 9-year-old Thoroughbred cross intermediate event horse, with intermittent lameness of variable severity. Medial is to the left. There is a subchondral bone cyst in the medial femoral condyle, with a clearly defined 'neck' through the subchondral bone. The subchondral bone cyst has a rim of mildly increased radiopacity.

or remains between the cyst and the medial femorotibial joint (Figure 10.22b). This channel is formed by infolding of the articular cartilage and subchondral bone plate. An almost complete subchondral bone plate may become re-established at the medial femorotibial articulation.

Shallow saucer-shaped radiolucent lesions proximal to the articular cartilage do not necessarily develop into subchondral bone cysts. They need

not cause pain, although many are believed to cause lameness at some time. A number of caudocranial views with varying proximodistal inclination of the x-ray beam are necessary to evaluate the subchondral trabecular pattern and the depth of the lesion. When a subchondral bone cyst is present in one limb, a shallow saucer-shaped lesion is occasionally present in the contralateral limb. This may remain quiescent or develop as discussed above.

Shallow saucer-shaped lesions when associated with lameness may respond to conservative treatment. Surgical treatment has yielded inconsistent results. When well-developed subchondral bone cysts are present, the radiographs should be carefully assessed for evidence of degenerative joint disease (see below), which may warrant a more guarded prognosis. An association between subchondral bone cysts in the medial femoral condyle and medial meniscal injuries has been noted, with injuries being recognised in both structures at the initial examination, or meniscal injuries developing subsequent to arthroscopic debridement of a cyst. Therefore ultrasonographic assessment of the joint is recommended before deciding on a treatment plan. Conservative treatment may restore clinical soundness in approximately 20–50% of horses, despite little radiographic change except for the formation of a rim of radiopaque bone around the periphery of the cyst. Long-standing cysts may be seen radiographically as incidental findings in mature horses, but their future clinical significance is uncertain.

Surgical treatment of subchondral bone cysts by debridement with or without the use of a cancellous bone graft, or a chondrocyte graft or hydroxyapatite, results in up to 60% of cases returning to normal work. The prognosis is more favourable in horses up to 3 years of age compared with older horses. Injection of the cyst lining with corticosteroids has produced favourable results in horses of all ages, with approximately 67% returning to full athletic function.

There is little correlation between clinical progress and the post-operative radiographic appearance of a cyst, although in some cases progressive enlargement of the cyst has been noted, associated with persistent lameness. Radiographic resolution of the lesion is not necessary for a satisfactory clinical outcome.

Focal flattening of the subchondral bone of the medial femoral condyle is a frequent finding in yearling Thoroughbreds, but is not believed to influence performance. Focal flattening or mild concavity of the subchondral bone of the medial femoral condyle, with or without altered trabecular architecture or an underlying semicircular zone of increased radiopacity, has been seen in some older horses with pain associated with the medial femorotibial joint (Figure 10w.23). Arthroscopic evaluation usually reveals abnormalities of the overlying articular cartilage.

Other osseous cyst-like lesions

Osseous cyst-like lesions may occur in the lateral femoral condyle and the proximal epiphysis of the tibia (Figure 10.24a). Osseous cyst-like lesions in the proximal aspect of the tibia may be surrounded by a rim of radiopaque bone. These have been identified in both the medial and lateral condyles of the tibia either alone (in immature horses) or in conjunction with other signs of degenerative joint disease (in mature horses) (Figure 10.24b). Medical or surgical treatment has been successful in some young horses, but the

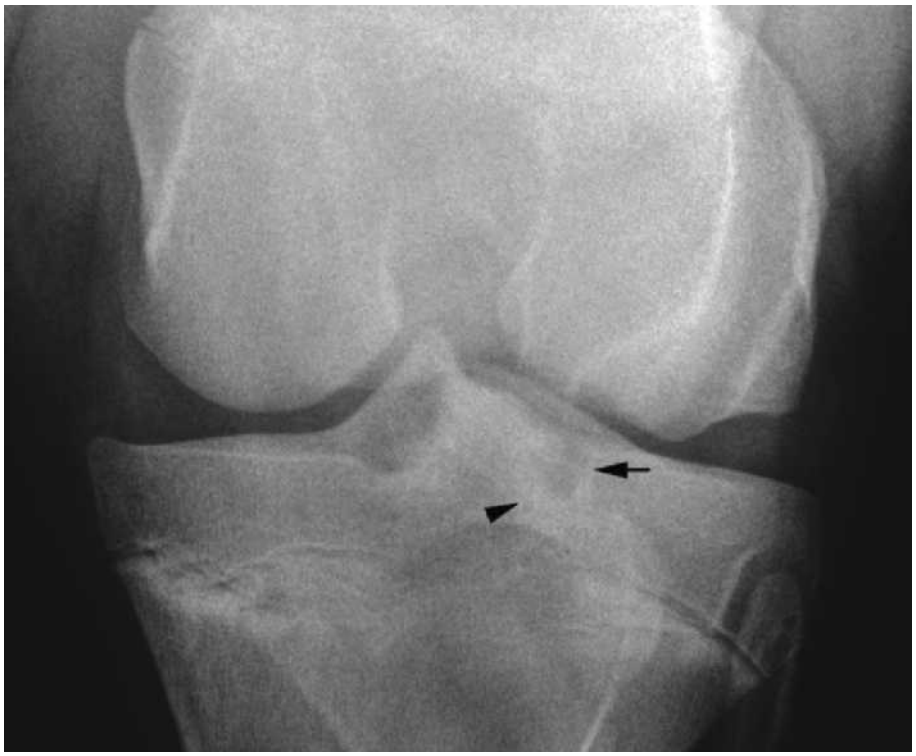


Figure 10.24(a) Caudocranial image of a stifle of a 1-year-old Arab. Lateral is to the right. There is a well-circumscribed osseous cyst-like lesion (arrow) in the subchondral bone of the proximolateral aspect of the tibia, surrounded by a broad rim of increased radiopacity (arrow head).



Figure 10.24(b) Caudocranial image of the left stifle of a 12-year-old Grand Prix showjumper. Lameness was partially improved by intra-articular analgesia of the medial femorotibial joint. Medial is to the left. There is a large osseous cyst-like lesion in the proximomedial aspect of the tibia, surrounded by a broad rim of increased radiopacity (arrows). There is modelling of the distal medial aspect of the femur and the proximomedial aspect of the tibia consistent with degenerative joint disease.

prognosis in adult horses is guarded. Osseous cyst-like lesions distal to the intercondylar eminences may be associated with cruciate ligament injuries (see Figure 10.30a) or tearing of cranial meniscal ligaments (Figure 10.30b).

Isolated osseous cyst-like lesions are occasionally seen in the patella as the result of trauma. Foals appear particularly susceptible (Figure 10.25). Such lesions should be differentiated from radiolucent areas which are the result of infection.

Necrosis of the femoral condyles

Necrosis of the femoral condyles is an unusual injury of unknown aetiology and has been reported in a young foal and also seen in a small number of adult horses, either alone or in association with meniscal injury. It has been characterised by heterogeneous opacity of the trabecular bone, with the medial femoral condyle being most commonly affected.

Bone trauma

There is a slowly growing body of information based on scintigraphy and magnetic resonance imaging that bone trauma of the femur and tibia can occur without detectable radiological abnormalities.



Figure 10.25 Lateromedial (flexed) image of a stifle of a 4-week-old Thoroughbred foal 2 weeks after a fall, since which the foal had been lame. Cranial is to the left. There is a well-demarcated osseous cyst-like lesion in the patella. The principle differential diagnosis would be infection. The proximal half of the medial trochlea of the femur is irregular in outline because of incomplete ossification.

Physitis

Physitis is associated with irregular widening of the physis, usually involving the distal femoral physis. The incidence in the stifle is very low. Bilateral physitis may result in an upright hindlimb stance and a stiff and stilted gait. The differential diagnosis should include osteochondrosis.

Degenerative joint disease

Degenerative joint disease of the femorotibial joint is best recognised radiographically on a caudocranial image (Figures 10.26a–c). A lateromedial image is more useful for the femoropatellar joint. Changes include:

- Periarticular osteophyte formation
- Flattening of the articular surface
- Irregularity of the subchondral bone plate and increased opacity of the adjacent trabecular bone
- Lucent zones in the subchondral bone
- Narrowing of the femorotibial joint space
- Modelling of the medial intercondylar eminence of the tibia
- Modelling of the supracondylar fossa of the femur.

Osteophytes on the tibial condyles, best seen on caudocranial images, are not necessarily associated with lameness, although they may reflect the presence of joint disease. They occur most often on the medial tibial condyle. It is helpful to compare the radiographs of suspected lesions with radiographs of the contralateral joint. Degenerative joint disease may develop secondarily to trauma to other structures of the stifle, and the radiographs should be inspected carefully for evidence of meniscal damage, cruciate ligament injury or collateral ligament injury (see below). Diagnostic ultrasonography is essential for evaluating soft-tissue pathology, including damage of the meniscal cartilages, the patellar ligaments and the collateral



Figure 10.26(a) Caudocranial image of the right stifle of a 14-year-old Welsh Cob cross Thoroughbred with lameness of 9 months' duration. Medial is to the left. There is marked modelling of the proximomedial aspect of the tibia and a large periarticular osteophyte, consistent with degenerative joint disease. Surgical exploration revealed a tear of the cranial aspect of the medial meniscus and extensive fibrillation of the cranial meniscal ligament of the medial meniscus.



Figure 10.26(b) Caudocranial image of the left stifle of a 12-year-old Welsh Cob mare with sudden onset, severe lameness, markedly improved by intra-articular analgesia of the medial femorotibial joint. Medial is to the left. There is modelling of the distal medial aspect of the femur and the proximomedial aspect of the tibia consistent with degenerative joint disease. There was intense increased radiopharmaceutical uptake in the medial femoral condyle. Surgical exploration revealed profound widespread degeneration of the articular cartilage. There was only temporary response to intra-articular medication. Follow-up radiography 3 months later revealed no change. However post-mortem examination revealed extensive subchondral bone necrosis in the medial femoral condyle.



Figure 10.26(c) Caudocranial image of a stifle of an 8-year-old horse. Lateral is to the right. There is irregularity in the contour of the lateral aspect of the intercondylar fossa (black arrow) and new bone formation on the most axial aspect of the lateral femoral condyle (open arrow). There is a suggestion of a discrete mineralised opacity proximal to the medial intercondylar eminence of the tibia. The circular lucent zone with a more opaque centre, distal to the medial intercondylar eminence, is abnormal (compare with Figure 10.10a). These changes are indicative of degenerative joint disease and probably result from trauma to either the cranial cruciate ligament and/or a cranial meniscal ligament (see Figure 10.29).

ligaments of the joint, and is also more sensitive for detection of periarticular osteophytes than radiography. If the degree of lameness and the extent of radiographic and ultrasonographic abnormalities are not well correlated, either contrast-enhanced computed tomography or exploratory arthroscopy is indicated. There may be widespread articular cartilage and associated intra-articular soft-tissue pathology in association with relatively minor radiographic abnormalities.

A poor prognosis is warranted for advanced degenerative joint disease of the stifle, although in early disease intra-articular medication with corticosteroids, polysulphated glycosaminoglycans, interleukin-1 receptor antagonist protein (IRAP) or mesenchymal stem cells may resolve the lameness, although this may not be permanent.

Infection

Septic arthritis (type S) and osteomyelitis in foals (types E and P) frequently affect the femorotibial joint and the femoral condyles (the medial condyle being most commonly affected Figure 10.27a). Lateromedial radiographs may reveal patchy lucencies in the subchondral bone of the trochlear ridges of the femur and the patella due to destruction and collapse of the cartilage and the subchondral bone. An irregular joint surface is therefore seen (Figure 10.27b). This should not be confused with the radiographic appearance of incomplete ossification normally seen in young foals (see Figure 10.4a). The femoral condyles in foals are normally smoothly outlined with no patchy lucencies. Radiographic changes within the femoral condyles are therefore



Figure 10.27(a) Caudoproximal-craniodistal oblique image of a stifle of a 3-month-old foal. Lateral is to the right. There are poorly defined lucent zones in the medial femoral condyle, surrounded by more radiopaque bone. There is a suggestion of a discrete fragment (arrow) extending from the medial aspect of the intercondylar fossa medially, which may represent a sequestrum or a pathological fracture. These radiographic abnormalities are consistent with severe type E osteomyelitis.

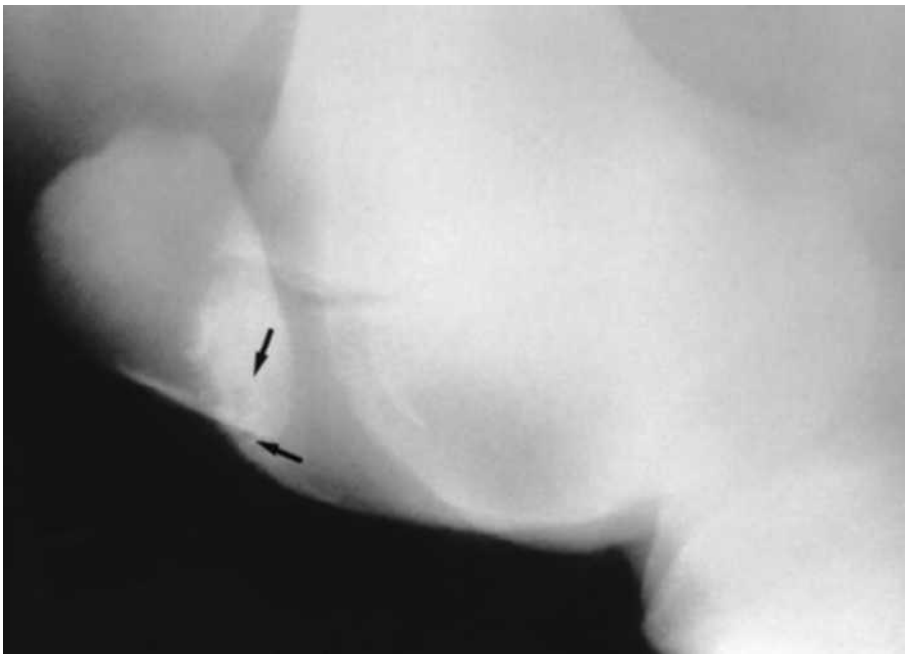


Figure 10.27(b) Slightly oblique lateromedial image of a stifle of an approximately 4-week-old Thoroughbred foal. Cranial is to the left. The foal had distension of the femoropatellar joint capsule and synovial fluid analysis confirmed a diagnosis of septic arthritis. The apex of the patella and the trochlear ridges of the femur are incompletely ossified, as is normal for a foal of this age. There are also poorly defined lucent zones (arrows) in the subchondral bone of the medial trochlear ridge indicative of osteomyelitis.

significant in all ages of foals and are best detected in caudocranial images. Changes may also be recognised within the tibial epiphysis and are usually best demonstrated on caudocranial views.

Infectious osteitis of the patella may occur in horses of any age. It is usually the result of direct trauma to the region and is often associated with a draining sinus. Although radiographic changes may be seen in a lateromedial image, a cranioproximal-craniodistal oblique image may be required. Contrast radiography and/or ultrasonographic examination of cases with a discharging sinus may be useful.

Miscellaneous soft-tissue injuries

In addition to the collateral ligaments common to most joints, the femorotibial joint includes lateral and medial menisci and associated ligaments, as well as cranial and caudal cruciate ligaments.

Collateral ligaments

The collateral ligaments of the femorotibial joint originate from the femoral epicondyles. In most normal horses, the outline of the epicondyles may be smoothly irregular on caudocranial radiographs. Sprain of these ligaments may result in increased irregularity due to new bone production. There may also be entheseophyte formation at their insertions on the proximal aspect of the tibia. Occasionally avulsion fractures occur. Further information may be obtained from ultrasonographic examination. If rupture of a collateral ligament is suspected, radiographs should be obtained with the joint under lateromedial stress, in order to confirm unilateral widening of the femorotibial joint space. Avulsion fracture at the origin of the lateral collateral ligament has been described in association with medial patellar fractures, highlighting the importance of a comprehensive radiographic assessment of the stifle even if one injury has already been identified.

Meniscal damage

The true incidence of damage to the medial or lateral meniscus, or the supporting cranial and caudal ligaments, is unknown, but with the development of ultrasonography, contrast-enhanced computed tomography, magnetic resonance imaging and exploratory arthroscopy an increasing number of injuries are being identified, frequently not associated with any detectable radiological abnormality. Some cases of degenerative joint disease (see above, 'Degenerative joint disease') develop secondarily to meniscal instability or meniscal tears. An association between meniscal injuries and subchondral bone cysts in the medial femoral condyle has also been documented. Traumatic injuries severe enough to damage the menisci may also result in damage to other structures, such as the collateral and meniscal ligaments. Plain and contrast radiographs are of limited value in outlining a meniscal tear, but meniscal damage may result in narrowing of the joint space. This is best assessed on caudocranial weight-bearing radiographs which may be difficult to obtain, as resting pain is often present. It is helpful to compare the width of the joint space with that of the contralateral stifle, but exact replication of the images is essential. Mineralisation, with or without slight displacement, of a damaged meniscus has been recognised (Figure 10.28). Lucent zones distal to the intercondylar eminences of the proximal tibia may be seen in association with tears of the cranial meniscal ligaments (Figure 10.30a).

Surgical debridement of tears of the axial aspect of a meniscus may have favourable results, but prognosis for other meniscal injuries is poor.

Cruciate ligaments

Rupture of the cranial and caudal cruciate ligaments has been described and has a poor prognosis.



Figure 10.28 Caudocranial image of a stifle of a 13-year-old hunter with moderate lameness and some effusion in the femoropatellar and medial femorotibial joints. Lateral is to the right. There is a large mineralised opacity on the medial aspect of the femorotibial joint (white arrow), associated with a chronic tear of the medial meniscus. There is a large periarticular osteophyte on the proximomedial aspect of the tibia (black arrow head) and entheseous new bone on the medial epicondyle of the femur and the proximomedial aspect of the tibia at the attachments of the medial collateral ligament of the femorotibial joint (black arrows). The distal subchondral bone of the medial femoral condyle is irregular in outline and the trabecular bone proximal to this has reduced opacity.

Sprain of the cruciate ligaments with or without partial detachment of the distal insertion of the cranial cruciate ligament occurs more frequently. This ligament inserts with the cranial ligaments of the menisci immediately cranial to the intercondylar eminences. A discrete soft-tissue radiopacity immediately cranial and proximal to the site of insertion may indicate damage to the cruciate ligament. If seen on a lateromedial view, it should not be confused with the area of increased opacity seen on the cranial aspect of the normal femorotibial joint. In chronic cases there may be proliferative bony changes (Figure 10.29), often best seen on a lateromedial (flexed) image. Osseous cyst-like lesions may occur at the sites of origin and insertion of the cruciate ligaments. They are seen proximal to the intercondylar fossa, superimposed on the femoral condyles and/or distal to the intercondylar eminences of the tibia (Figure 10.30a). Apparently detached osseous fragments may be evident in the intercondylar fossa, often in association with irregularities in the contour of the intercondylar eminences (Figure 10.30b). These do not necessarily reflect cruciate ligament injury. Lesions of the cruciate ligaments have a guarded prognosis. A fracture of the medial intercondylar eminence may be seen in association with cruciate ligament injury, but is not synonymous with it. A fracture may be seen in isolation, with surgical removal resulting in a satisfactory outcome (Figure 10w.31).

Other soft-tissue injuries

Caudal 60° lateral-craniomedial oblique radiographs, obtained with low kilovoltage, may reveal increased opacity of the patellar ligaments, especially on digital images. New bone formation near the proximal ligament

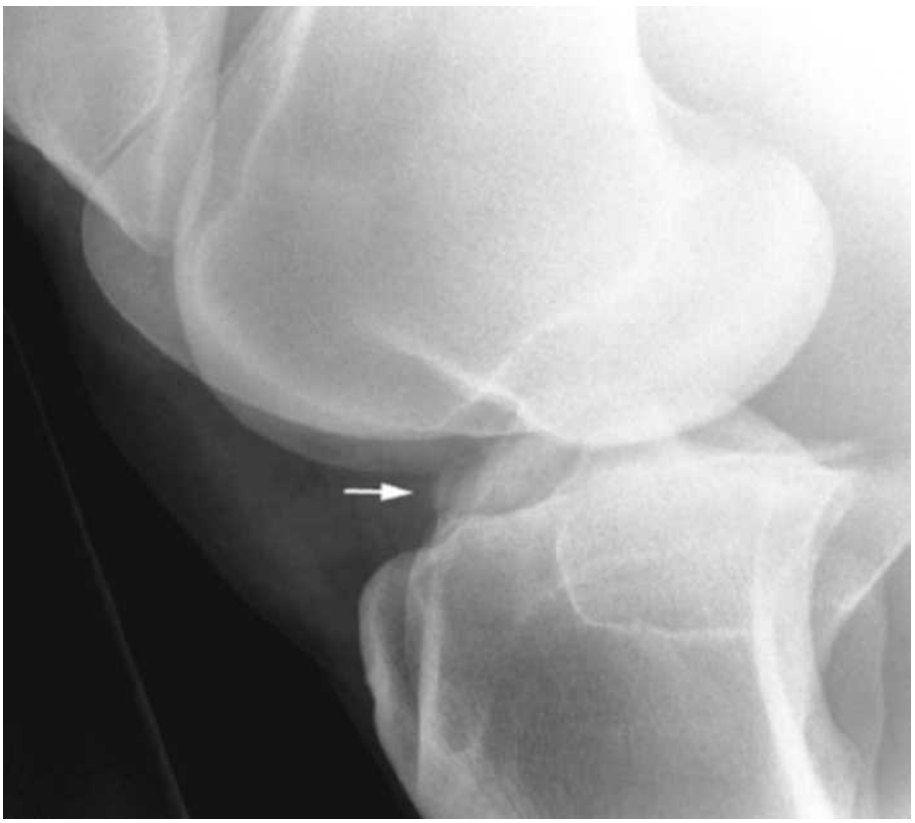


Figure 10.29 Lateromedial image of the right stifle of a 7-year-old polo pony with distension of the femoropatellar joint and moderate lameness. Cranial is to the left. There is entheseous new bone on the cranioproximal aspect of the tibia at the insertion of either the cranial cruciate ligament or the cranial ligament of the medial meniscus (arrow).



Figure 10.30(a) Caudocranial image of the proximal aspect of the tibia of an 11-year-old Thoroughbred cross horse. Lateral is to the right. There is a poorly defined area of reduced radiopacity immediately distal to the intercondylar eminences. The area is circumscribed by a thick rim of increased opacity. Osseous cyst-like lesions occurring at this site have been associated with damage to the insertion of the cranial cruciate ligament or a cranial meniscal ligament. There is slight modelling of the medial aspect of the medial tibial condyle. The circular opacity on the lateral aspect of the femorotibial joint is a screen artefact.



Figure 10.30(b) Caudocranial image of a stifle of a 10-year-old Thoroughbred cross Welsh dressage horse. Medial is to the left. There is a mineralised opacity slightly superimposed over the proximal aspect of the medial intercondylar eminence (black arrow). There is a periarticular osteophyte on the proximomedial aspect of the tibia (white arrow). There is a large ill-defined radiolucent area distal to the intercondylar eminences of the tibia (black arrow heads) in the region of insertion of the cranial meniscal ligaments.

insertions on the patella may also occur. These changes normally follow injury to the patella. The prognosis for this type of injury is good following rest. However, primary patellar ligament injuries can occur without any associated radiological abnormality. Ultrasonography is indicated to assess the integrity of the patellar ligaments. Injuries of the middle patellar

ligament occur more frequently than medial or lateral ligament injuries but injuries can occur in combination. Desmitis of the middle patellar ligament may be associated with increased radiopharmaceutical uptake at the insertion on the tibial crest.

Periosteal proliferation may be seen on the cranial aspect of the tibia, close to the distal aspect of the tibial crest, with or without cortical lucency. Sometimes a lucent line parallel to the cortical surface is seen, with or without a radiopaque fragment (Figure 10.32a). These changes have been seen in young Thoroughbreds, with focal pain on pressure to the area, and probably reflect an insertional enthesopathy of semitendinosus. However, such changes are occasionally seen as incidental abnormalities in older horses.

Injury of the origin of the gastrocnemius muscle on the caudal distal diaphyseal region of the femur occasionally results in focal periosteal new bone formation. Ultrasonography is more useful for assessing the integrity of the gastrocnemius tendon and muscle and for identification of early new bone formation. In foals, avulsion fractures may occur at the origin of the lateral head of gastrocnemius.

Occasionally an avulsion fracture occurs at the origin of fibularis tertius resulting in a displaced fragment from the craniolateral aspect of the femur (Figure 10.32b).



Figure 10.32(a) Lateromedial image of the proximal aspect of a tibia of 3-year-old Thoroughbred racehorse. Cranial is to the left. There is an osseous fragment (white arrow) at the tibial site of insertion of semitendinosus. The cranial cortex has a slightly irregular outline and there is a parallel lucent line in the cortical bone (black arrow).



Figure 10.32(b) Lateromedial (flexed) image of a stifle of a 6-month-old foal which developed lameness after rearing up and falling over backwards while being restrained for a farrier. The foal was immediately lame. This radiograph was acquired 3 days later. Cranial is to the left. There is an avulsion fracture of fibularis tertius (arrow) from the distal craniolateral aspect of the femur.

Modelling of the apex of the patella

Modelling of the apex of the patella may develop within weeks of performing a medial patellar desmotomy to treat intermittent upward fixation of the patella. Radiographic changes include spur formation at the apex of the patella, an irregular outline or fragmentation. Lameness may resolve with surgical debridement.

Modelling of the patella may also reflect chronic instability of the femoropatellar joint associated with chronic osteochondrosis and secondary degenerative joint disease, or hypoplasia of the femoral trochleas (Figure 10.19a and Figures 10w.19b and c). Hypoplasia of the femoral trochleas may be congenital or a sequel to severe osteochondrosis. The apex of the patella is best assessed in a flexed lateromedial image.

Calcinosis circumscripta

Calcinosis circumscripta (tumoral calcinosis) is a condition characterised by the formation of one or more hard, circumscribed subcutaneous swellings, typically formed at the lateral aspect of the femorotibial joint. Lameness is not usually present with smaller lesions. Caudocranial radiographs demonstrate the lesion as a distinctly outlined mass of soft-tissue opacity irregularly infiltrated with small, highly opaque, amorphous granules (Figure 10.33). If lameness is present, surgery may be necessary.

Patellar luxation

Lateral luxation of the patella occurs occasionally in foals, but rarely in adults other than miniature breeds (including Shetlands), except secondary to severe osteochondrosis with reduced size of the lateral trochlear ridge, or hypoplasia of the femoral trochleas. Radiography may help to diagnose this



Figure 10.33 Caudocranial image of the proximal aspect of the tibia of a 9-year-old Thoroughbred cross intermediate event horse (the same horse as in Figure 10.22b). Medial is to the left. There is an approximately rectangular area of heterogeneous opacity laterally, partially overlying the fibula. This is the typical appearance and location of calcinosis circumscripta.

condition. The radiographs should be inspected carefully to determine if there is primary hypoplasia of the trochlear ridges of the femur. The position and orientation of the patella are assessed most accurately on caudocranial images. Surgical treatment may be successful.

Upward fixation of the patella is a relatively common condition, in which radiography is of little value. Lameness sometimes develops after treatment by medial patellar desmotomy. This is usually associated with modelling of the apex and cranial distal surface of the patella, best seen in caudal 60° lateral-craniomedial oblique or lateromedial (flexed) images.

Distal luxation of the patella is a rare injury resulting in the limb being locked in flexion. Radiography is useful to verify the position of the patella and to exclude concurrent injuries.

Infectious osteitis of the patella

Infectious osteitis of the patella usually follows known trauma and a penetrating wound. There may be a detectable radiolucent tract running from the skin surface to the cranial aspect of the patella, which develops both lytic lesions and some new bone formation. A sequestrum and involucrum may develop. Diagnostic ultrasonography may be a more sensitive diagnostic technique early in the disease process.

Chondromalacia of the patella

Chondromalacia of the patella has been described, characterised by softening and fibrillation of the articular cartilage. Its aetiology is unknown. There are usually no detectable radiological abnormalities and diagnosis is reliant on arthroscopy.

Fractures

The presence of bone fragments in the femorotibial or femoropatellar joints may indicate the presence of a fracture or fractures, but it is not always possible to identify where the fragments have originated from. They should not be confused with fragments associated with osteochondrosis.

Patella

Patellar fractures may be recognised or suspected on lateromedial images (Figure 10.34a), but a cranioproximal-craniodistal (flexed) oblique view is essential to ascertain the location and extent of a fracture, to determine if there is more than one fracture, and to determine if comminution is present (Figure 10.34b).

Small fragments separated from the base of the patella are often slightly displaced proximally and are best seen on lateromedial images (Figure 10w.35a). They are usually avulsion fractures at the insertion of the quadriceps muscle and seldom cause persistent lameness. Some persist radiographically, but others disappear.



Figure 10.34(a) Caudal 60°lateral-craniomedial oblique image of a stifle of a 7-year-old horse which hit a fixed cross-country fence. Cranial is to the left. There is a fracture of the base of the patella. A cranioproximal-craniodistal oblique view should be obtained to evaluate the patella more fully (see Figure 10.34b).



Figure 10.34(b) Cranioproximal-craniodistal (flexed) oblique image of a patella of a 7-year-old eventer. Lateral is to the right. There is a displaced articular fracture of the medial aspect of the patella (arrow). The horse was treated by surgical removal of this fragment and made a complete recovery. The fragment detached from the base of the patella (See Figure 10.34a) was not removed.



Figure 10.36 Lateromedial (flexed) image of a stifle of an adult horse. Cranial is to the left. There is a fracture of the distal aspect of the lateral trochlear ridge (arrow). Note the more distal location of this fracture compared with the typical site of osteochondrosis. Cranioproximal-craniodistal oblique views also demonstrated a slightly displaced avulsion fracture of the medial aspect of the patella.

Avulsion fractures of the medial angle of the patella (Figure 10.34b and Figure 10w.35) are sometimes displaced proximally or medially. Lateromedial and cranioproximal-craniodistal (flexed) oblique views are required to determine the location and extent of these fractures. Occasionally an articular chip fracture occurs, which may only be detectable in cranioproximal-craniodistal (flexed) oblique images (Figures 10w.35a and 10w.35b). Surgical removal of the avulsed fragment, sometimes together with the attached fibrocartilage, normally ensures a satisfactory clinical outcome, provided that there is no evidence of degenerative joint disease and no other soft-tissue injury. Ultrasonographic assessment of the stifle is recommended to determine if there are concurrent injuries.

Sagittal patellar fractures involving the medial pole are sometimes seen in association with fractures of the lateral trochlear ridge of the femur (Figure 10.36) and this may affect the prognosis, unless recognised and treated accordingly.

Sagittal fractures of the patella involving more than the medial one-third of the bone carry a much poorer prognosis. Transverse fractures of the patella occur less commonly and are readily identifiable in lateromedial images. Treatment by internal fixation offers the best prognosis.

Femur

Fractures of the trochlear ridges and the caudal aspect of the femoral condyles can be demonstrated on caudal 60° lateral-craniomedial and craniolateral-caudomedial oblique images (Figure 10.36). They may be accompanied by fractures of the patella.

Fractures of the caudal aspect of the femoral condyles can be identified on lateromedial and oblique images, and usually occur with other injuries to the joint, which may seriously affect the prognosis. Care must be taken not to mistake fabellae (which are occasionally present at this location) for fractures.

Salter-Harris fractures of the distal femoral physis occur occasionally. Lateromedial and caudocranial views should be obtained. These fractures have a guarded prognosis, although internal fixation may be possible in younger animals.

Avulsion of the origin of fibularis (peroneus) tertius from the lateral extensor fossa of the femur occurs occasionally, usually in foals (see Figure 10.32b) and rarely in adult horses, resulting in loss of function of the reciprocal apparatus of the hindlimb and lameness. One or more fragments may be avulsed and are usually displaced cranially and distally. The prognosis is poor in adults and guarded in foals, although removal of the fragments and prolonged rest have been successful in some horses.

Avulsion of the origin of the gastrocnemius tendon on the distal caudal aspect of the femur occasionally occurs in foals; in adult horses muscle failure is more common. It results in inability to bear weight on the limb and dropping of the hock with partial weight bearing.

Tibia

Fractures of the tibial tuberosity or fractures of the tibial crest are best seen on a caudolateral-craniomedial oblique image (Figures 10.37a, 10w.37b and 10w.37c). They are frequently the result of direct trauma, e.g. hitting a fixed fence. Care must be taken in horses less than 3 years of age to differentiate fractures from the normal apophyseal–metaphyseal physis (see 'Normal anatomy, variations and incidental findings – Immature horse', above). The radiographs should be inspected carefully to determine the presence of comminution and to relate the precise fracture location to the insertion of the patellar ligaments. Ultrasonography can be helpful in deciding this. Conservative treatment of non-displaced fractures may be adequate, although healing may be prolonged. If there is significant separation of the fracture, surgical repair or fragment removal may be required; care should be taken to exclude distal spiralling of the fracture before general anaesthesia is contemplated.

Fractures of the medial intercondylar eminence may be associated with damage to the cranial cruciate ligament (see above, 'Cruciate ligaments'),



Figure 10.37(a) Caudolateral-craniomedial oblique image of the proximal aspect of the tibia of a 6-year-old Thoroughbred event horse, 2 days after the onset of lameness, after hitting a fixed fence. Cranial is to the left. There is a slightly displaced fracture of the tibial crest (white arrows). The horse was treated conservatively and made a complete recovery. There is also a multiloculated radiolucent area in the proximal metaphyseal region of the tibia (black arrows), an incidental finding.

but not necessarily so. In the absence of cruciate ligament injury, surgical removal of the fragment warrants a fair prognosis.

Fractures of the proximal physis of the tibia are rare.

Fibula

Fractures of the fibula may give rise to lameness (Figure 10.38). Care should be taken not to interpret normal lucent lines across the shaft of the fibula as fractures (see 'Normal anatomy, variations and incidental findings – Immature horse' and Figure 10.6). Fracture lines tend to run obliquely across the fibula and are normally subsequently associated with both resorption and callus. Lucent lines through the head of the fibula, especially if entering the tibiofibular articulation, are more likely to be a fracture than a lucent line between separate centres of ossification.

Tibia

RADIOGRAPHIC TECHNIQUE

Good-quality radiographs of the tibia may be obtained using a portable x-ray machine and digital systems, or rare earth or high-definition screens with appropriate film. Large cassettes are useful but it may be necessary to obtain radiographs of the proximal and distal halves of the tibia separately.

There is less muscle surrounding the distal half of the tibia, so exposure factors should be reduced accordingly. A complete assessment requires four views: lateromedial, caudocranial (or craniocaudal), craniolateral-caudomedial



Figure 10.38 Craniolateral-caudomedial oblique image of a stifle of a mature Arab horse with lameness of 2 months' duration. There is a chronic slightly displaced simple complete fracture of the proximal aspect of the fibula (arrow). There is loss of opacity adjacent to the fracture line in the proximal aspect of the bone; the fracture gap is slightly irregular in width; distal to the fracture gap there is increased opacity in the bone. There is also a transverse radiolucent line distally at the junction between separate centres of ossification.

oblique and caudolateral-craniomedial oblique. The caudocranial view is best obtained by holding the cassette parallel to the cranial aspect of the bone and directing the x-ray beam perpendicularly to the cassette, i.e. obliquely downward. This is therefore more correctly termed a caudoproximal-craniodistal oblique view.

NORMAL ANATOMY, VARIATIONS AND INCIDENTAL FINDINGS

The proximal and distal aspects of the tibia are described above, 'Normal anatomy, variations and incidental findings' and in Chapter 9 ('Radiographic anatomy: normal variations and incidental findings'). In the caudocranial view the tibial crest is superimposed over the lateral proximal aspect of the tibia, and in an immature horse the lucent line of the open physis should not be confused with a fracture. Lateral to the tibial crest is an obliquely orientated narrow or broad lucent line, the nutrient canal, which extends through the metaphysis and proximal diaphysis (Figure 10.39). There is a prominent ridge on the medial aspect of the proximal tibial metaphysis and this may be outlined in a caudocranial projection as a smooth irregularity of the medial cortex. Its outline will depend upon the angle of projection.



Figure 10.39 Caudocranial image of the proximal two-thirds of a normal adult tibia and fibula. Lateral is to the right. Note the oblique broad lucent line surrounded by mild increased opacity in the diaphysis of the tibia which represents the principal nutrient foramen.

SIGNIFICANT RADIOLOGICAL ABNORMALITIES

Enostosis-like lesions and other focal opacities

Enostosis is defined as a mass of proliferating bone within a bone and is a general term sometimes used synonymously with bone islands in man and panosteitis in the dog. Equine enostosis-like lesions have been characterised radiographically as focal or multifocal intramedullary increased opacity in the diaphyseal region of long bones, near the nutrient foramen, often along the endosteal surface of the bone. In the horse they have been recognised

most commonly in the tibia (Figure 10w.40), humerus, radius and the third metacarpal and metatarsal bones. Their clinical significance is unclear, although in some horses they are associated with lameness that generally resolves with time. They should not be confused with endosteal callus secondary to a fatigue or stress fracture.

Small focal rounded radiopacities (Figure 10w.41) have been seen in the proximal aspect of the tibia. Their aetiology and clinical significance are unknown.

Fractures

Proximal and distal physeal fractures are considered in Chapter 9.

Complete diaphyseal fractures of the tibia are usually either mid-shaft oblique fractures or spiral fractures, and result in severe, non-weight-bearing lameness, soft-tissue swelling and crepitus. A complete radiographic examination should be performed if surgical repair is contemplated, in order to determine whether the fracture is single or comminuted and to determine its precise orientation. Surgical repair may be successful in foals, but in older horses the prognosis is very poor.

Kick injuries to the medial aspect of the crus have a high risk of causing an incomplete oblique or vertical fracture of the tibia because of the paucity of overlying soft tissues. At the time of the initial injury the horse will not necessarily be very lame, but radiographic examination may be warranted. Initially fractures may not be detectable radiographically, but they do have the propensity to propagate, and if the horse is allowed free exercise this can be potentially catastrophic. Horses should be confined to box rest and follow-up x-rays obtained after approximately 10 days. False negative results have been recorded up to 16 days after injury. Endosteal or periosteal reaction can be seen in some horses from approximately 8 days after injury. Alternatively nuclear scintigraphic examination should be considered.

Incomplete metaphyseal and diaphyseal stress fractures occur most commonly in young Thoroughbred horses and Standardbreds, and are associated with an acute onset of lameness, which may resolve rapidly. Careful palpation of the medial aspect of the tibia, where there is a minimum of overlying soft tissues, may identify a focus of pain. Swelling is often minimal and clinical diagnosis may be extremely difficult in the acute stage, without the use of nuclear scintigraphy. Radiographic examination in the acute stage may be similarly unrewarding. Repeat radiographic examination after 7–10 days may reveal a fracture line and slight callus formation may be evident where the fracture passes through the cortex (Figure 10.42). Alternatively, increased opacity of endosteal bone may be the only radiographic abnormality. However, in some horses radiographic abnormalities are never detectable. In the Thoroughbred the proximolateral or proximocaudal aspects of the tibia are the most common sites for these fractures, which may spiral distally. Fractures also occur on the mid-caudal diaphysis and the distal metaphyseal region of the tibia in Thoroughbreds. In Standardbreds oblique mid-diaphyseal fractures are most common, with no tendency to spiral. Nuclear scintigraphy is generally a more sensitive indicator of trauma to the bone than radiography and increased radiopharmaceutical uptake may be detected bilaterally, reflecting bilateral injury despite unilateral lameness. Most incomplete



Figure 10.42(a) Caudocranial image of the proximal aspect of the right tibia of a 3-year-old Thoroughbred flat racehorse with sudden onset bilateral hindlimb lameness, which improved rapidly with rest. Medial is to the left. The radiograph was obtained 14 days after the recognition of lameness. There was focal intense increased radiopharmaceutical uptake in the proximocaudal aspect of the tibia. There is extensive periosteal callus associated with an incomplete proximocaudal stress fracture. Compare with Figure 10.42(b).



Figure 10.42(b) Slightly oblique lateromedial image of the proximal aspect of the tibia of the same horse as Figure 10.42(a). There is an ill-defined approximately horizontal fracture (arrows) of the proximocaudal aspect of the tibia, with extensive periosteal callus. Note also that the cranial aspect of the physis of the apophysis of the tibia is not fully closed.

fractures heal satisfactorily if treated conservatively, although internal fixation has been used in selected cases to minimise the risk of the fracture becoming complete and possibly compound.

Additional figures

The book companion website at www.clinical-radiology-horse.com includes additional figures that are not included in the printed book or e-book formats. Please see '**About the Companion Website**' at the start of the book for details on how to access the website. These figures are prefixed with the letter 'w' in the printed book, e.g. Figures 1w.4c–f.

FURTHER READING

Arnold, C., Schaer, T., Baird, D., Martin, B. (2003) Conservative management of 17 horses with nonarticular fractures of the tibial tuberosity. *Equine Vet. J.* **35**, 202–208

Baker, G., Moustafa, M., Boero, M., Foreman, J. Wilson, O. (1987) Caudal cruciate ligament function and injury in the horse. *Vet. Rec.* **121**, 131–321

Barr, E., Pinchbeck, G., Clegg, P., Singer, E. (2006) Accuracy of diagnostic techniques used in the investigation of stifle lameness in horses – 40 cases. *Equine Vet. Educ.* **18**, 326–332

Bassage, L. and Ross, M. (1998) Enostosis-like lesions in the long bones of 10 horses: scintigraphic and radiographic findings. *Equine Vet. J.* **30**, 35–42

Beccati, F., Chalmers, H., Dante, S., et al. (2013) Diagnostic sensitivity and interobserver agreement of radiography and ultrasonography for detecting trochlear ridge osteochondrosis lesions in the equine stifle. *Vet. Radiol. Ultrasound* **54**, 176–184

Bergman, E. (2007) Computed tomography and computed tomography arthrography of the equine stifle: technique and preliminary results in 16 clinical cases. *Proc. Am. Assoc. Equine Pract.* **53**, 46–55

Bourzac, C., Alexander, K., Rossier, Y., et al. (2009) Comparison of radiography and ultrasonography for the diagnosis of osteochondritis dissecans in the equine femoropatellar joint. *Equine Vet. J.* **41**, 686–692

Clarke, K., Reardon, R., Russell, T. (2015) Treatment of osteochondritis dissecans in the stifle and tarsus of juvenile Thoroughbred horses. *Vet. Surg.* **44**, 297–303.

Cohen, J., Richardson, D., McKnight, A., et al. (2009) Long-term outcome in 44 horses with stifle lameness after arthroscopic exploration and debridement. *Vet. Surg.* **38**, 543–551

Colbern, G., Moore, J. (1984) Surgical management of proximal articular fracture of the patella in a horse. *J. Am. Vet. Med. Ass.* **185**(5), 543–546

Crijns, C., Gielen, I., van Bree, H., et al. (2010) The use of CT and CT arthrography in diagnosing equine stifle injury in a Rheinlander gelding. *Equine Vet. J.* **42**, 367–371

De Busscher, V., Verwilghen, D., Bolen, G., et al. (2006) Meniscal damage diagnosed by ultrasonography in horses: a retrospective study of 74 femorotibial ultrasonographic examinations (2000–2005) *J. Equine Vet. Sci*. **26**, 453–461

De Moor, A., Verschooten, F. (1983) Subchondrale Knochenzysten und verwandte Läsionen beim Pferd. In Orthopädie bei Huf- und Klauentieren (edited by P.F. Knezevic), Schlutersche, Hannover, West Germany, pp. 244–250

Derungs, S., Fuerst, A., Haas, C., et al. (2001) Fissure fractures of the radius and tibia in 23 horses: a retrospective study. *Equine Vet. Educ.* **13**, 313–318

Dik, K.J. and Nemeth, F. (1983) Traumatic patellar fractures in the horse. *Equine Vet. J.* **15**, 244–247

Dik, K., Enzerink, E., van Weeren, P. (1999) Radiographic development of osteochondral abnormalities in the hock and stifle of Dutch Warmblood foals from age 1 to 11 months. *Equine Vet. J.* **31** (Suppl. 31), 9–15

Dyson, S., Wright, I., Kold, S., Vatistas, N. (1992) Clinical and radiographic features, treatment and outcome in 15 horses with fracture of the medial aspect of the patella. *Equine Vet. J.* **24**, 264–268

Embertson, R., Bramlage, L., Gabel, A. (1986) Physeal fractures in the horse 2. Management and outcome. *Vet. Surg.* **15**(3), 230–236

Embertson, R., Bramlage, L., Herring, W., Gabel, A. (1986) Physeal fractures in the horse 1. Classification and incidence. *Vet. Surg.* **15**(3), 223–229

Ferris, D., Frisbie, D., Kisiday, J., et al. (2013) Clinical outcome after intra-articular administration of bone marrow derived mesenchymal stem cells in 33 horses with stifle injury. *Vet. Surg.* **43**, 9–11

Firth, E.C. (1983) Studies of the morphology of the immature equine radius and metacarpus, and its relationship to chondro-osseous disease. PhD Thesis, University of Utrecht

Foerner, J., Juzwiak, J., Watt, B., et al. (2006) Injection of equine subchondral bone cysts with triamcinolone: 73 horses (1999–2005). *Proc. Am. Assoc. Equine Pract.* **52**, 412–413

Foland, J., McIlwraith, C.W., Trotter, G. (1992) Arthroscopic surgery for osteochondritis dissecans of the femoropatellar joint of the horse. *Equine Vet. J.* **24**, 419–423

Goulden, B.E., O'Callaghan, M.K. (1980) Tumoral calcinosis in the horse. *N.Z. Vet. J.* **27**, 217–219

Haggett, E., Foote, A., Head, M., et al. (2012) Necrosis of the femoral condyles in a four-week-old foal: clinical, imaging and histopathological features. *Equine Vet. J.* **44** (Suppl. 41), 91–95

Hall, M., Jalim, S., Russell, T. (2010) Distal luxation of the patella in a horse. *Austr. Vet. J.* **88**, 396–398

Haynes, P., Watters, J., McClure, R., French, W. (1980) Incomplete tibial fractures in three horses. *J. Am. Vet. Med. Ass.* **177**, 1143–1145

Hendrix, S., Baxter, G., McIlwraith, C.W., et al. (2010) Concurrent or sequential development of medial meniscal and subchondral cystic lesions within the medial femorotibial joint in horses (1996–2006). *Equine Vet. J*. **42**, 5–9.

Hermans, P., Kersjes, A., Van der Mey, G., Dik, K. (1987) Investigation into the heredity of congenital lateral patellar subluxation in the Shetland pony. *Vet. Qtly.* **9**(1), 1–8

Hertsch, B. (1980) Die Ossifikationsvorgänge am Kniegelenk beim jungen Pferde. *Zbl. Vet. Med. A*, **27**, 279–289

Hoegarts, M., Nicaise, M., van Bree, H., Saunders, J. (2005) Cross-sectional related anatomy and comparative ultrasonography of the equine medial femorotibial joint and its related structures. *Equine Vet. J.* **37**, 520–529

Howard, R., McIlwraith, C.W., Trotter, G. (1995) Arthroscopic surgery for subchondral cystic lesions of the medial femoral condyle in horses: 41 cases (1988–1991). *J. Am. Vet. Med. Ass.*, **206**, 842–850

Jacquet, S., Robert, C., Valette, J.-P., et al. (2013) Evolution of radiological findings detected in the limbs of 321 young horses between the ages of 6 and 18 months. *Vet. J.* **197**, 58–64

Jeffcott, L.B., Kold, S.E. (1982) Stifle lameness in the horse; a survey of 86 referred cases. *Equine Vet. J.* **14**, 31–39

Jeffcott, L.B., Kold, S.E. (1982) Clinical and radiological aspects of stifle bone cysts in the horse. *Equine Vet. J.* **14**, 40–46

Kee, S., Kim, B-H., Seo, E., et al. (2014) Lameness caused by osteoma cutis in a Thoroughbred colt. *Equine Vet. Educ*. doi: 10.1111.eve.12225

Kidd, J., Bradshaw, J. (2002) Bilateral non-ossifying fibromas in the proximal tibiae of a yearling Thoroughbred filly. *Equine Vet. J.* **34**, 317–320

La Faunae, N., Lerner, D. and O'Brien T. (1971) Bilateral congenital lateral patellar luxation in a foal. *Can. Vet. J.* **12**, 119–120

McIlwraith, C. (1990) Osteochondral fragmentation of the distal aspect of the patella in horses. *Equine Vet. J.* **22**, 157–163

McLellan, J., Plevin, S., Hammock, P., et al. (2009) Comparison of radiography, scintigraphy and ultrasonography in the diagnosis of patellar chondromalacia in a horse, confirmed by arthroscopy. *Equine Vet. Educ.* **21**, 642–647

McLellan, J., Plevin, S., Taylor, E. (2012) Concurrent patellar fracture and lateral collateral ligament avulsion as a result of trauma in three horses. *J. Am.Vet. Med. Ass*. **240,** 1218–1222

Mackay, V., Trout, W., Meagher, W., Hornhof, W. (1987) Stress fractures of the humerus, radius and tibia in horses. *Vet. Radiol.* **28**, 26–31

Marble, G., Sullins, K. (2000) Arthroscopic removal of patellar fracture fragments in horses: five cases (1989–1998). *J. Am. Vet. Med. Ass.*, **216**, 1799–1801

Maulet, B., Mayhew, I., Jones, E., Booth, T. (2005) Radiographic anatomy of the soft tissue attachments of the stifle. *Equine Vet. J.* **37**, 530–535

Nickels, F.A., Sande, R. (1982) Radiographic and arthroscopic findings in the equine stifle. *J. Am. Vet. Med. Ass.* **181**, 918–924

Ortved, K., Nixon, A., Mohammed, H., et al. (2012) Treatment of subchondral cystic lesions of the medial femoral condyle of mature horses with growth factor enhanced chondrocyte grafts: a retrospective study of 49 cases. *Equine Vet. J.* **44**, 606–613

O'Sullivan, C., Lumsden, J. (2003) Stress fractures of the tibia and humerus in Thoroughbred racehorses: 99 cases (1992–2000). *J. Am. Vet. Med. Ass.*, **222**,491–498

Pascoe, J.R., Pool, R.R., Wheat, J.D., O'Brien, T.R. (1984) Osteochondral defects of the lateral trochlear ridge of the distal femur of the horse. Clinical, radiographic and pathological examination, and results of surgical treatment. *Vet. Surg.* **13**, 99–110

Prades, M., Grant, B., Turner, T., Nixon, A., Brown, M. (1989) Injuries to the caudal cruciate ligament and associated structures: summary of clinical, radiographic, arthroscopic and pathological findings. *Equine Vet. J.* **21**, 354–357

Ramzan, P. (2002) Enostosis-like lesions: 12 cases. *Equine Vet. Educ.* **14**, 143–148

Rejno, S., Stromberg, B. (1978) Osteochondrosis in the horse II. Pathology. In *Osteochondrosis in Domestic Animals, 1* (edited by S.E. Olsson). *Acta Radiol*. Suppl. **358**, pp. 153–178

Ruggles, A., Moore, R., Bertone, A., et al. (1996) Tibial stress fractures in racing Standardbreds: 13 cases (1989–1993). *J. Am. Vet. Med. Ass.* **209**, 634–637

Sanders-Shamis, M., Bukowiecki, C., Biller, D. (1988) Cruciate and collateral ligament failure in the equine stifle: seven cases. *J. Am. Vet. Med. Ass.* **193**, 573–576

Sandler, E., Bramlage, L., Embertson, R., et al. (2002) Correlation of lesion size with racing performance in Thoroughbreds after arthroscopic treatment of subchondral cystic lesions of the medial femoral condyle: 150 cases (1989–2000). *Proc. Am. Ass. Equine Pract.* **48**, 255–256

Santschi, E., Williams, J., Morgan, J., Johnson, C., et al. (2015) Preliminary investigation of the treatment of equine medial femoral condylar subchondral cystic lesions with a transcondylar screw. *Vet. Surg.* **44**, 281–188.

Schneider, R., Jenson, P., Moore, R. (1997) Evaluation of cartilage lesions on the medial femoral condyle as a cause of lameness: 11 cases (1988–1994*). J. Am. Vet. Med. Ass.* **210**, 1649–1652

Schroeder, O., Aceto, H., Boyle, A. (2013) A field study of kick injuries to the radius and tibia in 51 horses (2000–2010). *Can. Vet. J.* **54**, 271–275

Scott, G., Crawford, W., Colahan, P. (2004) Arthroscopic findings in horses with subtle radiographic evidence of osteochondral lesions of the medial femoral condyle: 15 cases (1995–2002). *J. Am. Vet. Med. Ass.* **224**, 1821–1826

Shanis, L., Auer. J. (1985) Complete ulnas and fibulas in a pony. *J. Am. Vet. Med. Ass.* **186**, 802–804

Smith, B., Auer, J., Watkins, J. (1990) Surgical repair of tibial tuberosity avulsion fractures in 4 horses. *Vet. Surg.* **19**, 117–121

Smith, M., Walmsley, J., Phillips, T., et al. (2005) Effect of age at presentation on outcome following arthroscopic debridement of subchondral cystic lesions of the medial femoral condyle. *Equine Vet. J.* **37**, 175–180

Squire, K., Blevins, W., Frederick, M., Fessler, J. (1990) Radiographic changes in an equine patella following medial patellar desmotomy. *Vet. Radiol. Ultrasound* **31**, 208–209

Stromberg, B. (1976) Osteochondrosis dissecans of the stifle joint in the horse. A clinical, radiographic and pathological study. *J. Am. Vet. Radiol. Soc.* **17**, 117–124

Swor, T., Schneider, R., Ross, M., Hammer, E., Tucker, R. (2001) Injury to the origin of the gastrocnemius muscle as a possible cause of lameness in four horses. *J. Am. Vet. Med. Ass.* **219**, 215–219

Textor, J., Nixon, A., Lumsden, J., Ducharme, N. (2001) Subchondral cystic lesions of the proximal extremity of the tibia in horses: 12 cases (1983–2000). *J. Am. Vet. Med. Ass.* **218**, 408–413

UpRichard, K., Elce,Y., Piat, P., et al. (2013) Outcome after arthroscopic treatment of lateral femoral trochlear ridge osteochondrosis in sport horses: A retrospective study of 37 horses. *Vet. Comp. Orthop. Traumatol.* **26**, 105–109

Verschooten, F., De Moor, A. (1982) Subchondral cystic and related lesions affecting the equine pedal bone and stifle. *Equine Vet. J.* **14**, 47–54

Wallis, T., Goodrich, L., McIlwraith, C., et al. (2008) Arthroscopic injection of corticosteroids into the fibrous lining of subchondral cystic lesions of the medial femoral condyle in horses: a retrospective study of 52 cases (2001–2006). *Equine Vet. J.* **40**,461–467

Walmsley, J., Phillips, T., Townsend, H. (2003) Meniscal tears in horses: an evaluation of clinical signs and arthroscopic treatment of 80 cases. *Equine Vet. J.* **35**, 402–406

Wright, I., Montesso, F., Kidd, L. (1995) Surgical treatment of fractures of the tibial tuberosity in 6 adult horses. *Equine Vet. J.* **27**, 96–102

Chapter 11
The head

RADIOGRAPHIC TECHNIQUE

The head is a difficult area to radiograph, because it is mobile and high off the ground. A technique is described for obtaining radiographs of all parts of the head, but details on positioning, anatomy and significant findings are given under headings for individual areas. The use of tranquillisers (e.g. xylazine, romifidine or detomidine) may be beneficial, both for their sedative action and also because the head will be lowered, making the examination physically easier. The use of a headstand can steady the head and reduce motion.

The head has a complex three-dimensional anatomy which frequently results in superimposition that can obscure certain lesions on radiographs and nuclear scintigraphy. The anatomy lends itself to cross-sectional imaging techniques such as computed tomography (CT) or magnetic resonance imaging (MRI). CT is most useful for the identification of pathology involving dental and/or osseous structures. MRI is more valuable for evaluation of the central nervous system and other soft tissues of the head.

Equipment

It is quite possible to obtain satisfactory radiographs with portable equipment. Because the head is anatomically complex, large imaging plates or cassettes (35 cm × 43 cm) should be used when possible in order to maintain spatial relationships when evaluating the radiograph. If only a small cassette or imaging plate is available, depending on the region of interest, two adjacent radiographs of each projection can be acquired to ensure all of the relevant anatomy is included in the examination. It is often helpful to use both right (left to right) and left (right to left) lateral-lateral projections in order to take advantage of both image sharpness and magnification for localisation of the side of a lesion.

When obtaining radiographs of the head of a standing horse it is important to recognise that the holder of the horse is close to the primary x-ray beam. It is therefore essential to collimate the x-ray beam as much as possible. The horse holder should wear lead gloves and a thyroid protector in addition to a lead gown. A leather head collar and its buckles may be superimposed over an area of interest, so the use of a rope halter may be preferable. With digital systems, even a rope halter may result in confusing artefacts. The imaging plate must be held by some mechanical device to reduce the

Clinical Radiology of the Horse, Fourth Edition. Janet A. Butler, Christopher M. Colles, Sue J. Dyson, Svend E. Kold and Paul W. Poulos.
© 2017 John Wiley & Sons, Ltd. Published 2017 by John Wiley & Sons, Ltd.
Companion website: www.clinical-radiology-horse.com

radiation hazard to personnel and to minimise movement. A plate holder can easily be fixed to a wall, using vertical runners to allow adjustment for height, or it can be hung from a drip stand.

All views can generally be obtained in the standing horse, but the dorsoventral (DV) view can prove challenging. Adequate penetration of the DV view may not be possible using portable equipment, but can generally be obtained with stationary equipment. A dorsoventral view of the caudal portion of the head or occipito-atlantal joint may require general anaesthesia. In the standing horse, occlusal views are generally possible, although some patients can be difficult.

A grid may be beneficial in all views of the head, except occlusal views. With portable x-ray machines, it is best to use either digital systems or standard rate rare earth screens and compatible film.

GENERAL POSITIONING OF THE PATIENT

Lateral-lateral view

A lateral-lateral view is normally obtained with the horse standing. The position for centering and the exposure factors depend on the area to be examined, e.g. the paranasal sinuses or the mandibular cheek teeth. If the horse is in lateral recumbency it is necessary to support the rostral end of the head to keep the midline of the head parallel with the cassette. Care must be taken that the head does not rotate along a rostral–caudal axis (i.e. turn sideways), and some support under the angle of the jaw may be required. Radiolucent padding (foam) can be used to achieve this whilst the horse is under general anaesthesia.

Dorsoventral or ventrodorsal views

The dorsoventral view can be obtained in many standing horses if appropriate positioning can be achieved. In general this requires heavy sedation so that the horse drops its head toward the ground and the nose is extended. The imaging plate is placed along the ventral aspect of the mandibles or further caudally depending on the area of interest. In the standing position, the caudal portion of the skull can be imaged to the level of the first cervical vertebra in many horses, but some patients will not tolerate this technique, and general anaesthesia may be required. The x-ray generator is positioned dorsal and slightly caudal to a line perpendicular to the frontal bone.

For examination under general anaesthesia, the horse is placed in dorsal recumbency and the head extended. Generally it is not possible to bring the dorsal surface of the head to a horizontal position. For this reason, if the cassette or imaging plate is to be placed against the dorsal surface of the head (the preferred position), and not oblique to the head, a pad may be necessary under the cassette at the rostral end of the head to hold the cassette in position. If the cassette is to be placed far enough caudally to assess the occipital bone, it may be necessary to raise the poll on a small radiolucent pad. Alternatively, the head is positioned obliquely relative to the cassette for the most caudal images of the skull and upper neck. The x-ray beam is aligned from the ventral aspect, in the midline, and perpendicular to the cassette. It is centered over the point of interest (Figure 11.1). The dorsoventral plane

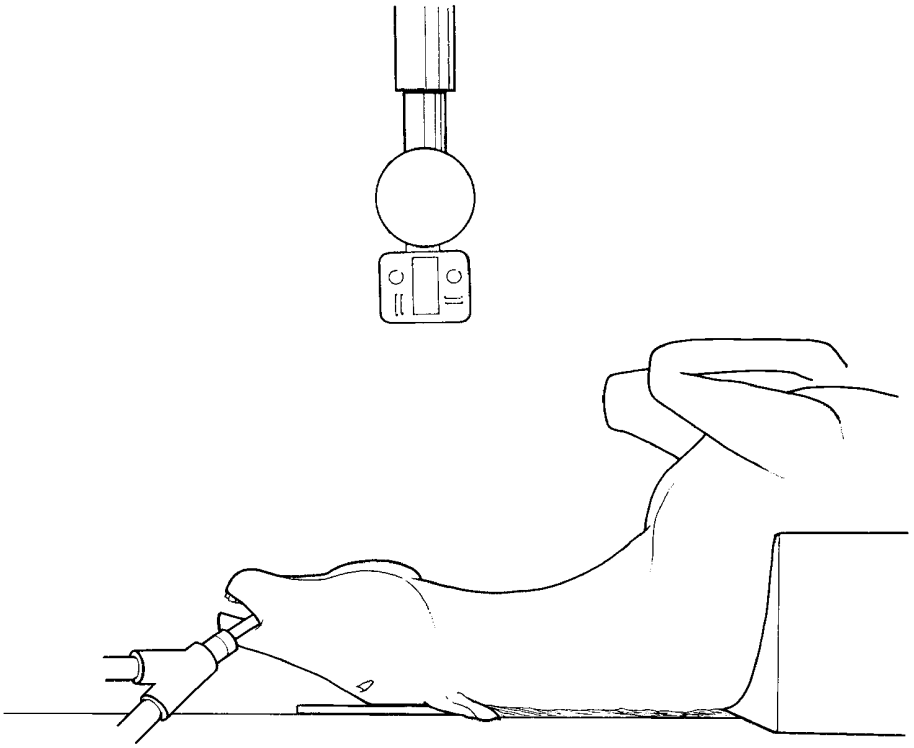


Figure 11.1 Positioning of the horse and cassette to obtain a ventrodorsal view of the head.

of the skull must be maintained vertical, because any degree of obliquity results in loss of information on the radiograph. It may be helpful to withdraw the endotracheal tube, if one is used, as this can mask abnormalities.

Oblique views

Oblique views are essential for evaluation of tooth roots, some fractures, and for separation of the temporomandibular joints. In a standing patient, the horse should be sedated and the head allowed to rest on a stand to minimise movement. Oblique views may be obtained by angling the x-ray beam and the cassette while keeping the head and neck of the horse straight. For some anatomical regions (temporomandibular joints, temporohyoid joints) a combination of angling the x-ray beam and rotating the head results in good separation and imaging of the particular anatomy. Rotation of the horse's head towards or away from a cassette or imaging plate can make it simpler to obtain the correct positioning, but will make it more difficult to reproduce positioning accurately.

If the horse is anaesthetised, risk to personnel is minimised, the angle of obliquity can be more carefully controlled and repeat views can be accurately reproduced. The horse is positioned in lateral recumbency and the x-ray beam is angled relative to the head.

Cranium

This section covers the bony structures at the base of the skull, which can all be seen on one radiograph. It includes the cranial vault and the bony skull caudal to it. Also included are the ethmoid bones, part of the frontal bones,

part of the vertical rami of the mandibles, and the atlas. The general positioning of the horse and equipment are discussed above.

RADIOGRAPHIC TECHNIQUE

Lateral-lateral view

The x-ray beam is centered approximately 5 cm caudal to the orbit, and aligned at right angles to the midline of the head (and the cassette). When obtaining radiographs of the occiput it may be useful to pull the ears forwards to avoid their superimposition over the region of insertion of the nuchal ligament (see Figure 11.8b). This can be done in a sedated horse by attaching sticky tape to the ears in order to pull them forwards.

Ventrodorsal view

The x-ray beam is centered on the larynx and aligned at right angles to the cassette.

Oblique views

Oblique views are recommended to examine the temporomandibular joints (see 'General positioning of the patient', above for information regarding positioning) and the temporohyoid joints, as well as parts of the skull which are superimposed over the vertical ramus of the mandible, or that are masked by the dense petrous temporal bone. They can also be used to determine on which side of the skull a lesion is present.

NORMAL ANATOMY, VARIATIONS AND INCIDENTAL FINDINGS

Immature horse

The skull is a complex structure; at birth a number of bones are not fully ossified and many sutures are not fused. The ages at which these bones fuse and sutures are obliterated are given in Table 11.1.

At birth, the cranium is rather more domed than in the adult and on a lateral-lateral radiograph a 'fontanelle' is evident as a radiolucency between the frontal bones at the rostral third of the cranial vault (Figure 11.2). This closes at 3–4 months. Also evident at birth is the nasofrontal suture, which becomes less evident over the first 6 months of life.

The spheno-occipital suture at the base of the cranium is seen on radiographs until about 5 years of age (Figure 11.2). It becomes a progressively less prominent feature as the foal ages. The position of the teeth in the maxillary sinus changes with age and varies from that in an adult (see Figures 11.25a and 11.25b).

Skeletally mature horse

Figures 11.3a, 11.3b and 11.4 show normal lateral-lateral and dorsoventral images of the cranium of an adult horse.

Table 11.1 Fusion times for bones of skull.

Bone	Ossification centres at birth	Fusion of suture	Obliteration of suture
Occipital			
Parieto-occipital	1. Squamous	2 and 3 by 4 months	5 years
Spheno-occipital	2. Lateral		5 years
Occipitomastoid	3. Basilar	2/3 with 1, 12–24 months	Aged
Sphenoid			
Spheno-occipital	1. Presphenoid 2. Postsphenoid	Uncertain, but as foal	5 years
Ethmoid	1. Perpendicular 2. Cribriform	Uncertain, soon after birth	
Parietal			
Parietal suture	One centre		4 years
Parieto-occipital			5 years
Premaxilla			
Left and right	One centre		4th year
Nasal			
Left and right	One centre		Do not fuse
Nasofrontal			1 year
Mandible			
Left and right	Two halves		3 months



Figure 11.2 Slightly oblique lateral-lateral image of the cranium of a 1-month-old Thoroughbred. Rostral is to the left. Note the radiolucency in the cortex of the frontal bones, an open fontanelle (black arrow). This normal feature closes by 3–4 months of age. Note also the clearly demarcated spheno-occipital suture line between the basioccipital and basisphenoid bones (white arrow). This is usually closed by approximately 5 years of age. There are unerupted caudal molar teeth.



Figure 11.3(a) Lateral-lateral image and diagram of the cranium of a normal mature horse. Dorsal is to the left. There is slight rotation of the mandible resulting in separation of the right and left condylar and coronoid processes.

On lateral-lateral radiographs the cranial cavity is evident as a large oval structure. The dorsal aspect has a rather irregular appearance due to the internal contour of the cranium. Ventrally the base of the cranial cavity is superimposed on the radiopaque articulations of the mandibles, the coronoid processes and the zygomatic arch, and is difficult to identify. At the caudal aspect of the cranial cavity, the two petrous temporal bones are evident as opaque, irregular, roughly circular bony masses.

The nuchal crest is a well-defined structure on the caudal aspect of the squamous part of the occipital bone, the latter having a well-defined medulla

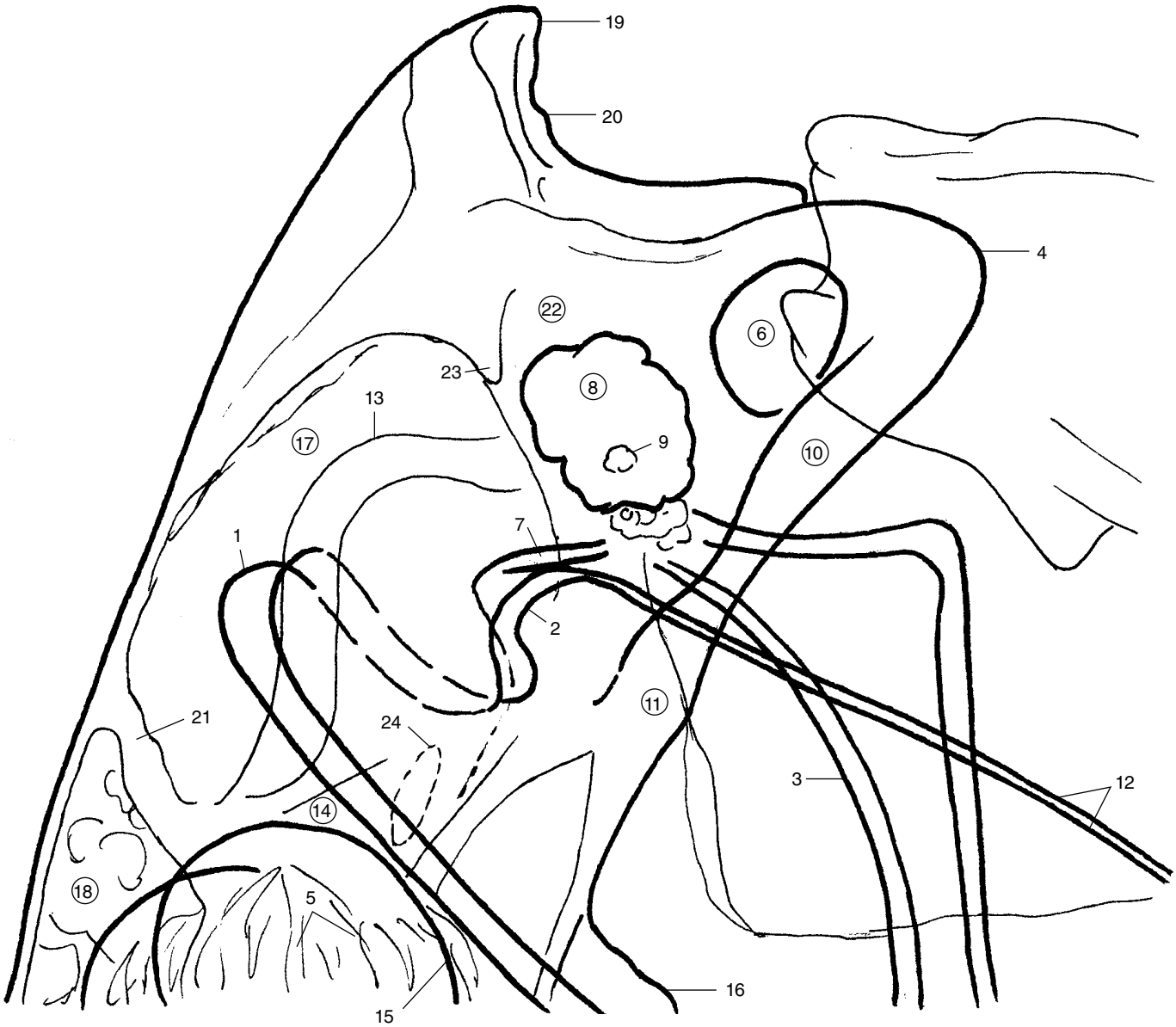


Figure 11.3(a) *Cont'd* 1 = coronoid process, 2 = condyloid process, 3 = stylohyoid, 4 = occipital condyle, 5 = ethmoid turbinates, 6 = hypoglossal foramen, 7 = temporomandibular articulation, 8 = petrous temporal bone, 9 = external acoustic meatus, 10 = basioccipital bone, 11 = body of basisphenoid, 12 = rami of mandibles, 13 = zygomatic process of temporal bone, 14 = zygomatic process of frontal bone, 15 = orbit, 16 = pterygoid process, 17 = cranium, 18 = frontal sinus, 19 = external occipital protuberance, 20 = external occipital crest, 21 = internal plate of frontal bone, 22 = caudal fossa of cranium, 23 = osseous temporal process, 24 = site of sphenopalatine sinus.

and smooth opaque cortices. New bone formation at the site of attachment of the nuchal ligament may be seen as an incidental abnormality, but less commonly may be associated with clinical signs (see 'Entheseophyte formation on the occiput associated with the nuchal ligament', below). Ventral to the temporal bones, the basilar part of the occipital bone also has a well-defined medulla, extending caudally to form the occipital condyles. The condyles have a smooth oval outline. Slightly oblique radiographs may reveal a small smooth depression in the caudal aspect of the condyles. This is a normal finding.

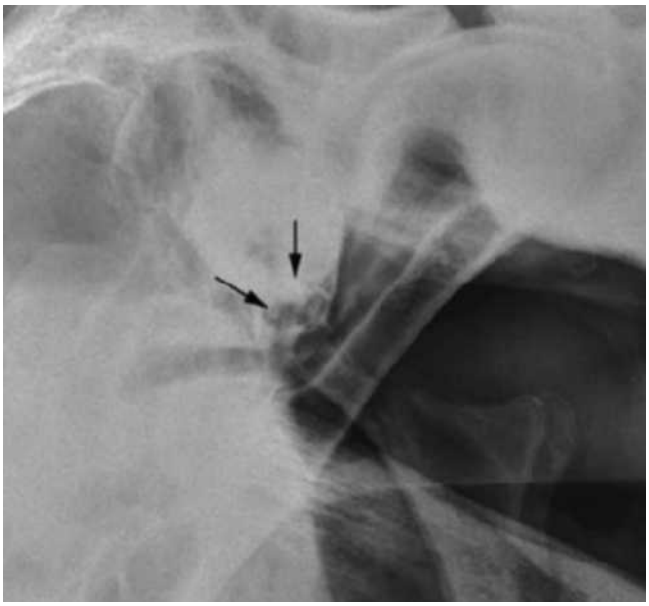


Figure 11.3(b) Close-up slightly oblique lateral-lateral radiographic image of the caudal aspect of the cranium centred on the temporohyoid articulation (arrows). Rostral is to the left.

Rostral to the cranial cavity are the ethmoid turbinate bones which have a brush-like appearance. Their caudal aspect is more opaque, roughly circular and surrounded by even more opaque bone, the ethmoid plate. The rostral aspect of the ethmoid bones is superimposed over the maxillary sinus and additional radiographs may be required for satisfactory assessment.

Dorsal to the ethmoid turbinate bones are the frontal sinus and the overlying frontal bones.

Ventral to the occipital and sphenoid bones are the lucent Eustachian tube diverticula (guttural pouches; see 'Pharynx, larynx and Eustachian tube diverticulum', below), partly superimposed on the vertical rami of the mandibles. The outline of the trachea, pharynx, larynx and hyoid apparatus may also be seen.

SIGNIFICANT FINDINGS

Dentigerous cysts

Dentigerous cysts (or temporal teratomata) are of highly variable shape and size and may be found in many positions (Figure 11.5). They frequently have an opaque core, composed of dental tissue, but may have less radiopaque tissue surrounding it. They are frequently found around the base of the ear and in close apposition to the petrous temporal bones.

Dentigerous cysts are usually identified clinically as a mass or a discharging sinus close to an ear. The introduction of a probe or contrast medium into the sinus is helpful in locating the site of the cyst. Dentigerous cysts can normally be removed surgically, the difficulty of the operation depending upon their position.

Choanal restriction or atresia

The choanae form the junction between the nasal and nasopharyngeal airways. Choanal restriction is uncommon. Congenital total obstruction of the choanae may occur unilaterally or bilaterally, due to a bony or

membranous septum, resulting in an abnormal respiratory noise, severe dyspnoea or death in a neonatal foal. A bony septum may be visible in a ventrodorsal radiographic image. If an obstructive membranous septum is suspected from endoscopic examination, it can be confirmed radiographically by observing blockage of radiodense contrast medium placed in the nasal cavities.

Narrowing of the caudal aspect of one or both nasal airways can occur, with or without deviation of the nasal septum, resulting in respiratory noise. Carefully positioned ventrodorsal radiographic images are required to document narrowing, with comparisons made between the two sides of the head, and with horses of similar breed, age and size.

Abnormalities of the nasal septum

The normal nasal septum can have a mildly undulating appearance. Deviation of the nasal septum may be congenital, but is more commonly acquired and may result in respiratory compromise. Acquired deformity is usually the result of an adjacent space-occupying mass and is usually readily identifiable in a well-positioned dorsoventral or ventrodorsal radiograph. In a young horse with septal malformation, much of the distortion may be due to abnormalities of the soft tissues overlying the bone which may not be detectable radiographically, but may be identified using magnetic resonance imaging. Abnormalities of the bones of the skull are most accurately assessed with CT or MRI, and abnormalities of the septum identified radiographically, either congenital or acquired, may require final evaluation using one of these techniques.

Ethmoid haematoma and diseases of the Eustachian tube diverticulum (guttural pouch)

See 'Pharynx, larynx and Eustachian tube diverticulum', below.

Temporohyoid osteoarthropathy

The cause of temporohyoid osteoarthropathy is not known but otitis media/interna, age-related degeneration and biomechanical strain on the temporohyoid joint have been proposed. Clinical signs typical of peripheral vestibular disease and facial nerve paralysis are sometimes associated with specific radiographic changes, including an irregular increased opacity in the region of the acoustic meatus and articulation of the hyoid and petrous temporal bones, with or without fracture of the stylohyoid bone. Bony proliferation in the region of the temporohyoid joint may be seen in an oblique projection (Figures 11.6a and 11.6b). Once osseous proliferative changes have developed at the temporohyoid joint, normal movement of the stylohyoid bone (hyoid apparatus) is restricted and physiologic movements may result in traumatic injury, including haemorrhage into the middle and inner ear. This may cause recurrence or exacerbation of clinical signs. Surgical resection of part of the stylohyoid bone may give improvement of the clinical signs.



Figure 11.4 Ventrodorsal image and diagram of the cranium of a normal mature horse.

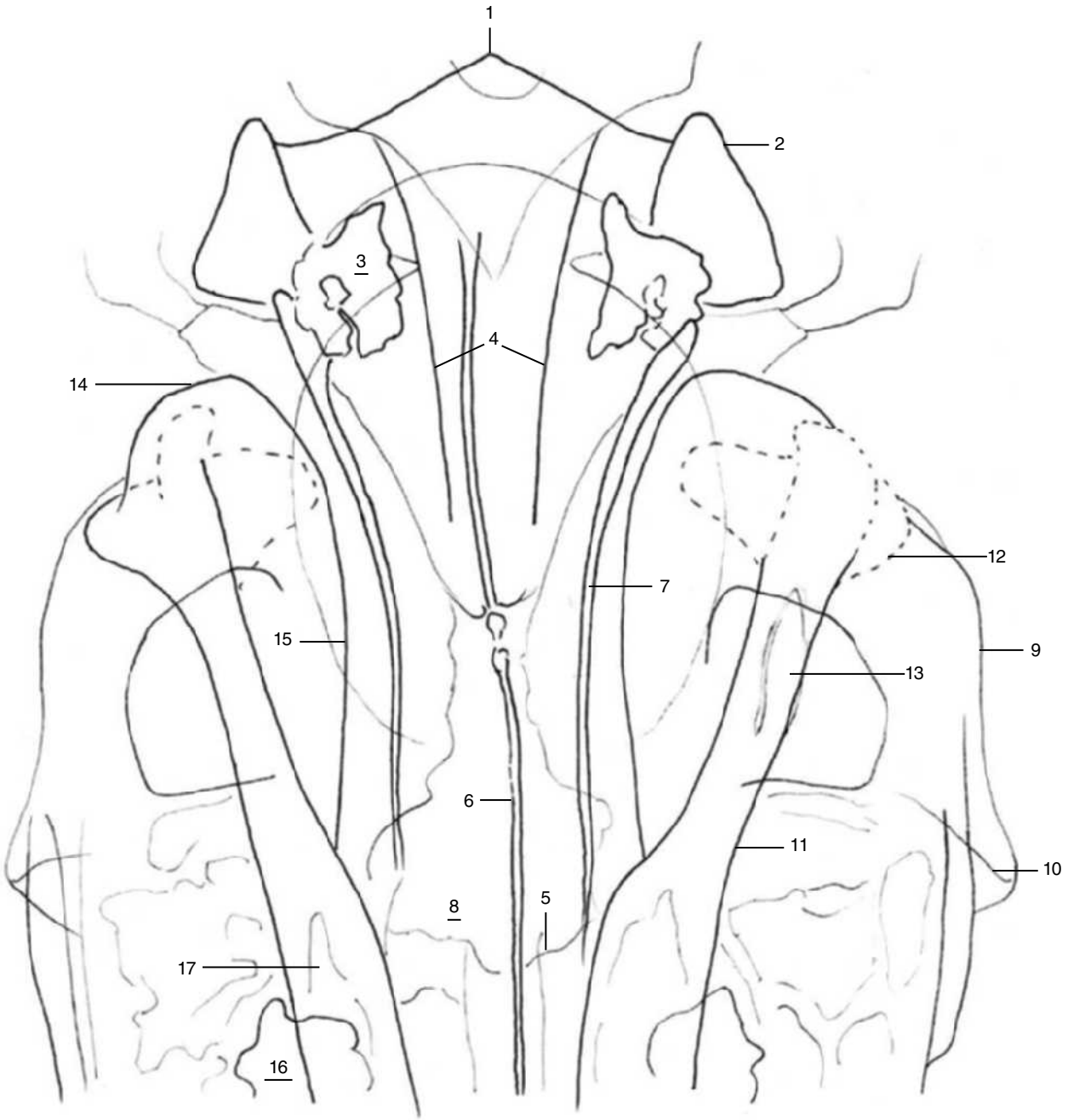


Figure 11.4 *Cont'd* 1 = nuchal crest, 2 = jugular process, 3 = tympanic bulla, 4 = basilar part of occipital bone, 5 = rostral border of choanae, 6 = vomer, 7 = stylohoid, 8 = ethmoid turbinate region, 9 = zygomatic arch, 10 = caudal margin of orbit, 11 = mandible, 12 = condylar process of mandible, 13 = coronoid process of mandible, 14 = caudal border of ramus of mandible, 15 = axial margin of angle of mandible, 16 = third upper molar tooth, 17 = third lower molar tooth.



Figure 11.5 Lateral-lateral image of the occipital region of a young Thoroughbred foal with a firm swelling ventral to the ear. Rostral is to the left. Within the mass a tooth-like structure can be seen (black arrow). This mass is a dentigerous cyst. Note also the clearly demarcated spheno-occipital suture line between the basioccipital and basisphenoid bones (white arrow). This is usually closed by approximately 5 years of age.



Figure 11.6(a) Lateral-lateral image of the caudal aspect of the head of an 8-year-old Warmblood with sudden onset of left-sided facial nerve paralysis, peripheral vestibular signs and kerato-conjunctivitis sicca. Rostral is to the left. There is a poorly defined area of increased opacity in the region of the temporohyoid joint. The stylohyoid bone is thickened and has increased opacity (arrows). See also Figure 11.6(b).

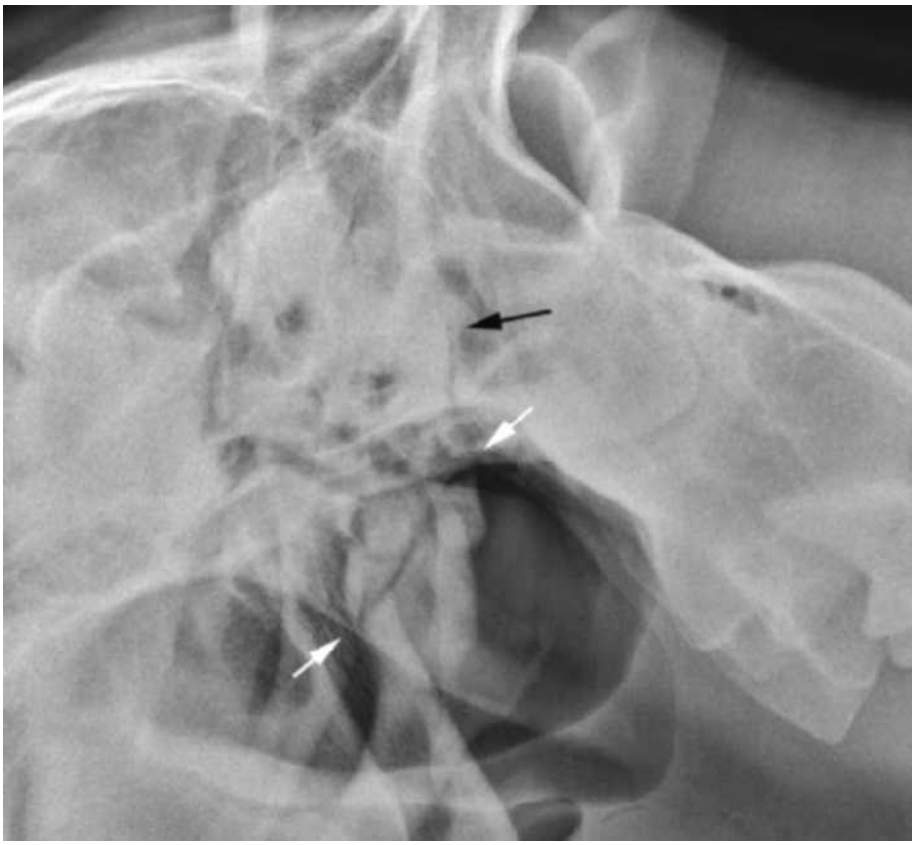


Figure 11.6(b) Oblique image of the caudal aspect of the head, separating the two hyoid bones, the rami of the mandibles and the guttural pouches. Rostral is to the left. There is a fracture of the thickened stylohyoid bone (white arrows), which is more easily seen than in the lateral-lateral image (compare with Figure 11.6a). The acoustic meatus (black arrow) is more dorsal. A piece of the stylohyoid bone was removed surgically. The bony mass regressed considerably and the horse made a complete functional recovery.

Nasal polyps

Nasal polyps are soft-tissue masses that may partially occlude the airway and result in abnormal respiratory noise and/or nasal discharge. They appear radiographically as smoothly marginated soft-tissue opacities (Figure 11.7). They should be distinguished from soft-tissue opacities within a sinus, or an ethmoid haematoma, which may extend into the nasal cavities.

Hydrocephalus

Hydrocephalus in the horse is usually a clinical diagnosis, but may be confirmed by radiography. The cranial vault has a domed appearance, the overlying bones being thin with loss of the normal, irregular, internal surface of the cranium. The cranial cavity has a homogeneous appearance. This condition is most common in miniature breeds.

Entheseophyte formation on the occiput associated with the nuchal ligament

New bone formation may occur in the region of insertion of the nuchal ligament on the occiput (Figures 11.8a and 11.8b), also extending slightly dorsal and ventral to the site of insertion. This may be seen as an incidental finding, most commonly in Warmbloods. Clinically affected horses tend to resist the reins, find difficulty in flexion at the poll and may rear or head shake.



Figure 11.7 Lateral-lateral radiograph of the head of a 4-year-old horse with a 10-week history of a bilateral nasal discharge. Dorsal is to the left. Within the nasal cavity are several (at least three) well-circumscribed soft-tissue opacities (arrows). These are nasal polyps. The paranasal sinuses are normal.

However, these are non-specific clinical signs and the significance of any bony abnormality should be determined by local infiltration of local anaesthetic solution. Treatment by local infiltration of corticosteroids and local anaesthetic solution, combined with modification of the training programme, has variable results. Treatment using osteopathic techniques may also be beneficial.



Figure 11.8(a) Lateral-lateral radiographic image of the caudal aspect of the head of a 7-year-old dressage horse. Rostral is to the left. When ridden the horse would episodically throw its head in the air almost vertically. There is entheseous new bone on the caudal aspect of the occiput (arrows) at the insertion of the nuchal ligament. The horse's behaviour when ridden was markedly improved by infiltration of local anaesthetic solution around this entheseous new bone. Note that the opacity of the ears is superimposed over this entheseous new bone. Compare with Figure 11.8(b). Entheseous new bone at this site can also be seen as an incidental abnormality.

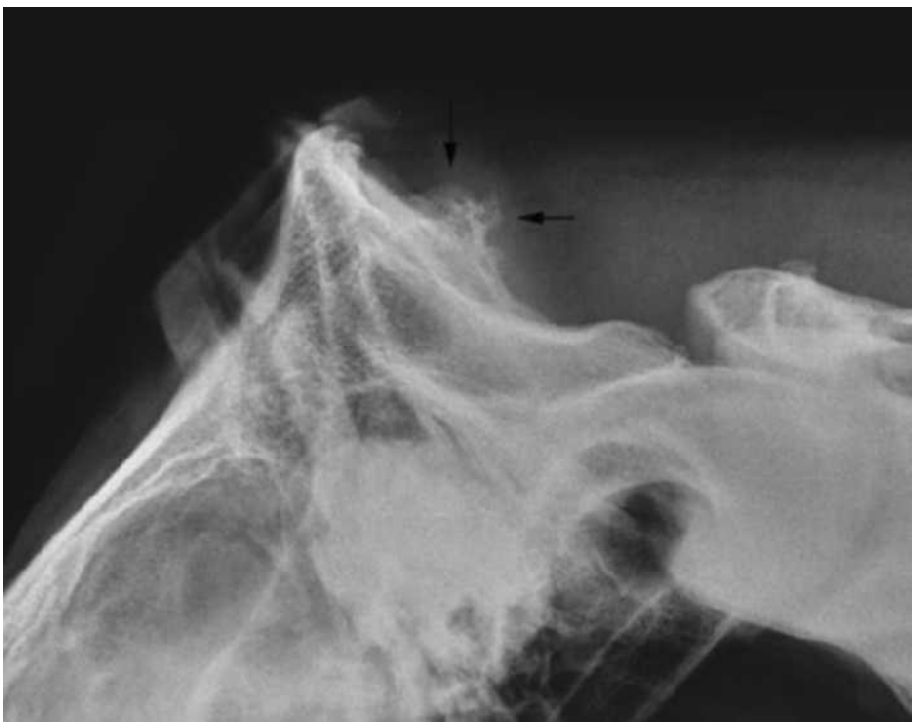


Figure 11.8(b) Lateral-lateral radiographic image of the caudal aspect of the head of a 7-year-old Irish Sports event horse. Rostral is to the left. The ears have been pulled forwards and taped. There is irregularly outlined entheseous new bone on the caudal aspect of the occiput (arrows). Compare with Figure 11.8(a). The horse had a recent onset of head-shaking behaviour coinciding with the onset of sunny weather. The entheseous new bone is probably an incidental abnormality.

Fractures

Frontal bone

Depression fractures of the frontal bone are relatively common after trauma to the head. They can be seen on lateral-lateral or slightly oblique lateral images, and are best seen when the exposure is set for the sinuses

(see 'Paranasal sinuses [frontal, maxillary, conchal] and maxilla', below). With an acute fracture an area of bone is pushed ventrally relative to the remainder of the dorsal surface of the face. It is important to check for possible sequestra in more chronic cases, which should also be assessed for concurrent fluid accumulation within the sinuses (haemorrhage or sinusitis) and possible involvement of the bony orbit and lacrimal duct.

If treated conservatively, there is generally good functional healing, provided that sequestra do not form. It is possible to raise these fractures surgically to give more aesthetically pleasing healing.

Nasofrontal suture separation/exostosis

Nasofrontal suture separation/exostosis is relatively common in young horses but can also be seen in adults (Figure 11.9). There is frequently no history of trauma, but a hard swelling forms across the dorsal aspect of the head, level with or just rostral to the rostral aspect of the orbits. On radiographs this is apparent on lateral-lateral images as a radiopaque protuberance of callus forming in the region of the nasofrontal suture. The callus can protrude both externally and internally, into the associated sinuses or nasal passage. Typically the bone has greater opacity on either side of the suture, and initially a radiolucent suture line may be evident traversing the new bone. There may be concurrent involvement of the nasolacrimal suture. Occasionally haemorrhage occurs, leaving a fluid line within the maxillary sinus. A degree of



Figure 11.9 Slightly oblique lateral-lateral image of the nasofrontal region of a 6-year-old event horse which had recently developed a firm swelling on the dorsal midline of the head, distal to the eyes. Dorsal is to the left. There is separation at the nasofrontal suture, slight displacement and associated incomplete periosteal and endosteal bridging callus, with overlying soft tissue swelling. There are fluid lines within the maxillary sinus.

epiphora may be present temporarily, or permanently, if the area of suture affected involves the nasolacrimal duct. This lesion is of little clinical significance, but usually results in permanent disfigurement of the head.

Basioccipito–basisphenoid suture separation

Basioccipito-basisphenoid suture separation or fracture usually occurs after direct trauma, typically a horse falling over backwards and hitting its head on the ground. It is most commonly seen in young horses, when the suture is not closed, and radiological confirmation of separation may therefore be very difficult. It is generally best identified on good lateral-lateral and oblique images. Signs of separation include widening of the suture or the formation of a step deformity; however, fractures with minimal displacement may not be detectable. In chronic injuries callus can occasionally be detected. Computed tomography may be a more sensitive means of detection.

Clinical signs reflect cranial nerve involvement and may include blindness, incoordination and slight nasal haemorrhage. The condition carries a very guarded prognosis, depending on the degree of clinical signs seen.

Avulsion fracture of the rectus capitis ventralis major and minor muscles from the basioccipital and basisphenoid bones

Avulsion fracture of the rectus capitis ventralis major and minor muscles from the basioccipital and basisphenoid bones is an unusual fracture that may occur if a horse falls over backwards and hits the poll, with the ventral neck muscles in tension. This results in traction forces being applied to the base of the skull by the paired rectus capitis ventralis major muscles that insert on tubercles at the junction between the basioccipital and basisphenoid bones. There is usually associated haemorrhage, which may result in haematoma formation in the retropharyngeal space. Bone fragments may be seen ventral to the basisphenoid bone, sometimes close to the stylohyoid bone. There may be a step deformity at the sphenoccipital suture. Bone fragments may puncture the guttural pouch and haemorrhage may pool in the pouch. Increased soft-tissue opacity in the retropharyngeal region and guttural pouch area may obliterate the normal air-filled guttural pouches seen radiographically. Gas can accumulate in the subarachnoid and epidural spaces. In some horses fracture fragments cannot be identified, but a presumptive diagnosis can be made based upon the other radiological abnormalities.

Avulsion fracture of the nuchal crest

Avulsion fracture of the nuchal crest is an unusual finding. It is associated with trauma and results in stiffness of the neck. A small radiopaque fragment may be seen caudal to the nuchal crest on lateral-lateral radiographs. An optimistic prognosis can be given with conservative treatment.

Fractures involving the orbit

Fractures involving the zygomatic arch occur as the result of trauma to the region of the eye. They are generally difficult to detect on radiographs, but are most easily seen on lateral-lateral images of the cranial

region. It is often helpful to separate the two arches by directing the beam obliquely, and tangential to the orbital rim. Fractures may be simple or comminuted, with varying degrees of displacement. Although the prognosis for simple non-displaced fractures is quite good, displacement and comminution, causing modelling of the orbit, often causes chronic ophthalmitis. Surgery to reduce displacement and remove sequestra may be required.

Fracture of the mandible

Fractures of the vertical ramus of the mandible are usually seen on lateral-lateral or slightly oblique lateral images (see Figure 11.39b). The ramus of the mandible is relatively thin, therefore fractures may be difficult to delineate and several different exposures may be required for complete assessment. The prognosis varies depending on the configuration of the fracture and the age of the horse. Fractures of the horizontal ramus are discussed elsewhere (see 'Teeth and mandible', below) (Figure 11.39a).

Paranasal sinuses (frontal, maxillary, conchal) and maxilla

RADIOGRAPHIC TECHNIQUE

Lateral-lateral view

The x-ray beam is centered midway between the orbit and the lateral opening of the infraorbital canal, about 2.5 cm dorsal to the facial crest. It is aligned at right angles to the midline of the head and the cassette.

Ventrodorsal view

The x-ray beam is centered in the midline between the horizontal rami of the mandible, approximately one-third of the distance from the caudal aspect of the rami towards the rostral aspect of the mandible. It is aligned at right angles to the cassette.

Dorsoventral views can be obtained in a well-sedated horse, but careful collimation of the x-ray beam is essential to ensure safety of personnel. The x-ray tube is positioned in front of the head, with the beam angled obliquely downwards, perpendicular to the cassette. The cassette is held ventral to the mandible and parallel to it.

It is difficult to evaluate the more caudal structures of the head (caudal to the maxillary sinuses) using this technique, even with deep sedation, and general anaesthesia may be required. Great care is needed to obtain true dorsoventral views and to avoid a degree of obliquity.

Oblique views

Oblique views, in addition to lateral-lateral views, are recommended for examining the sinuses, in order to separate the left and right sides. Carefully positioned oblique views from the left and right sides provide a control

image when pathology is localised to one side. Oblique images are frequently required to determine the primary cause of sinusitis, especially to evaluate the teeth roots.

NORMAL ANATOMY, VARIATIONS AND INCIDENTAL FINDINGS

A lateral-lateral image allows identification of lesions involving the frontal sinus, maxillary sinus, conchal sinus and nasal cavity (Figure 11.10).

The frontal sinus appears triangular on lateral-lateral radiographs and is seen dorsal to the turbinate bones and rostral to the cranial vault. There are normally two distinct septa positioned in a dorsoventral direction across the sinus.

The maxillary sinus is immediately dorsal to the cheek teeth, which form the ventral border of the sinus. The appearance of this varies with the stage of development of the teeth. The sinus extends from the orbit caudally to include the last three or four cheek teeth rostrally (depending partly on the age of the animal). The dorsal border of the sinus is difficult to see on radiographs, but runs parallel to the facial crest, along a line roughly level with the infraorbital foramen. The sinus is divided into rostral and caudal parts by a septum lying obliquely across the centre of the sinus.

The nasal cavities are medial and dorsal to the maxillary sinus.

The ventral and dorsal conchal sinuses or conchae are medial to the maxillary sinus and can be seen on a lateral-lateral image. The ease of assessment depends on the age of the horse and the position of the maxillary cheek teeth. The dorsal conchal sinus communicates with the frontal sinus and is often termed the conchofrontal sinus. The dorsal concha is dorsal to the middle meatus and maxillary cheek teeth. The rostral margin of the dorsal concha is rounded and identified at the level of the second or third maxillary cheek teeth in an adult horse. The ventral conchal sinus communicates with the rostral maxillary sinus, and is medial to the maxillary sinus and teeth, and ventral to the middle meatus. The rostral margin of the ventral conchal sinus is rounded and identified at the level of the second maxillary cheek teeth. The ventral conchal bulla is the caudal extension of the ventral conchal sinus. It is identified by the thin, osseous septa with a round, caudodorsal margin that is dorsal and caudal to the rostral maxillary sinus.

On ventrodorsal or dorsoventral (Figure 11.11) images, the two horizontal rami of the mandible and the cheek teeth are the dominant features. The narrow nasal septum runs a straight course in the midline, between the two rami. The nasal cavity, conchal sinuses and turbinates are located on either side of the septum. A small portion of the maxillary sinus can be seen lateral to the mandible and maxillary cheek teeth.

SIGNIFICANT FINDINGS

Sinusitis

Sinusitis in the maxillary (Figure 11.12) or frontal sinuses usually results in increased opacity of the sinus on lateral-lateral radiographs. The radiograph must be correctly exposed, otherwise an increase in opacity may be missed.



Figure 11.10 Lateral-lateral image and diagram of the nasofrontal region of a normal adult horse, exposed to evaluate the paranasal sinuses rather than the tooth roots. Dorsal is to the left.



Figure 11.10 *Cont'd* 1 = nasomaxillary notch, 2 = nasal bone, 3 = frontal bone, 4 = orbit, 5 = facial crest, 6 = internal plate of frontal bone, 7 = dorsal nasal meatus, 8 = middle nasal meatus, 9 = ventral nasal meatus, 10 = infraorbital canal, 11 = conchal sinus septum, 12 = conchofrontal sinus, 13 = recess of dorsal nasal concha, 14 = sinus of ventral nasal concha, 15 = recess of ventral nasal concha, 16 = frontal sinus, 17 = margin of maxillary sinus, 18 = ethmoid turbinates, 19 = third upper molar tooth, 20 = cranial aspect of ramus of mandible.



Figure 11.11 Dorsoventral radiographic image and diagram of the head to show the paranasal sinuses to the left and to the right, the rami of the mandibles and the nasal septum of a clinically normal adult horse. The well-circumscribed radiolucent area represents air in the pharynx, rostral to the ethmoid turbinates, demarcated rostrally by the caudal aspect of the hard palate. Rostral to this radiolucent area the nasal septum is deviated slightly to the left of the image.

On standing radiographs, one or more horizontal fluid lines are generally visible in the sinuses (Figure 11.12). When viewing the radiographs, they should be positioned at the same angle as when exposed, if the fluid lines are to be horizontal. The radiograph should be carefully evaluated to determine if there is more than one fluid line, reflecting involvement of more than one sinus cavity. The fluid is generally of uniform opacity, unless there is inspissated

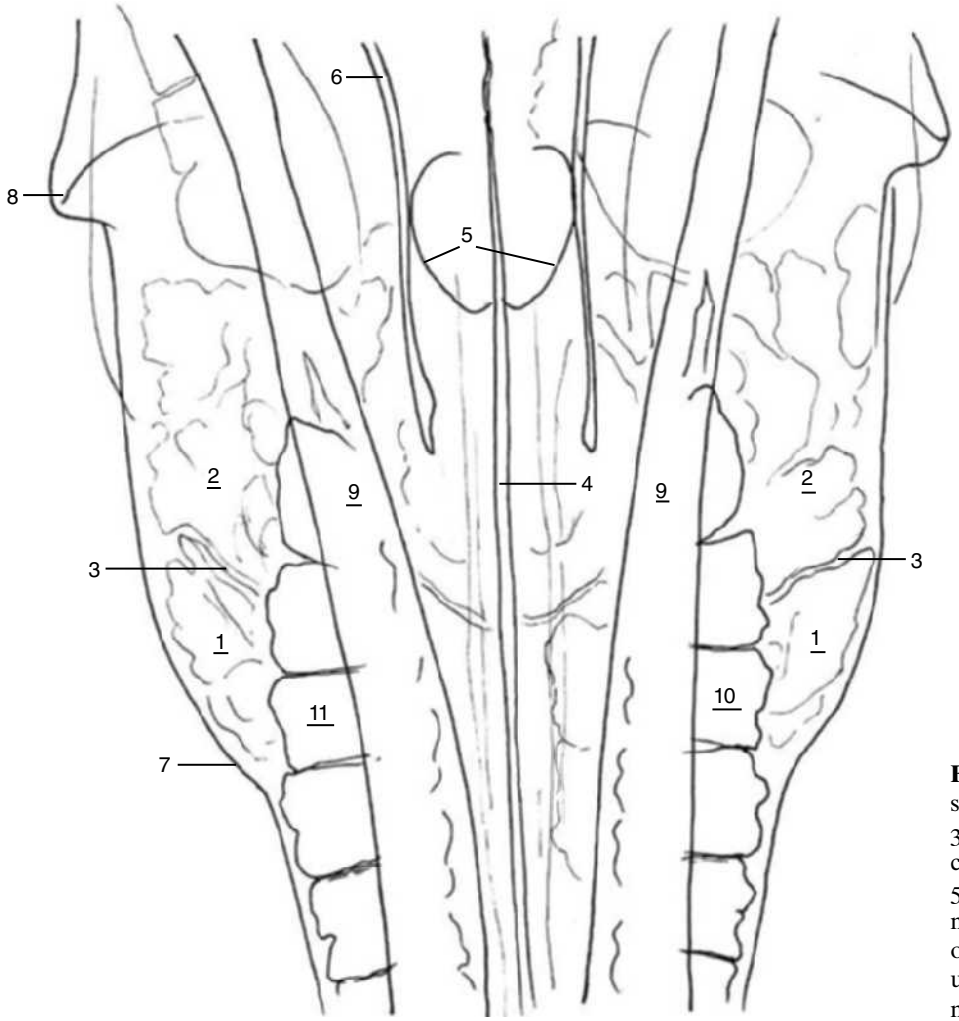


Figure 11.11 *Cont'd* 1 = rostral maxillary sinus, 2 = caudal maxillary sinus, 3 = bony septum between rostral and caudal maxillary sinus, 4 = nasal septum, 5 = choanae, 6 = stylohyoid, 7 = rostral margin of facial crest, 8 = caudal margin of orbit, 9 = mandible, 10 = first left upper molar (109), 11 = first right upper molar (209).

pus, when it may be heterogeneous. Inspissated pus often has a mixed pattern of fragmented gas contained within a soft tissue mass. When associated with dental disease and within the conchal bulla, inspissated pus can have a confusing radiographic appearance, the inflammatory debris taking on a 'soft tissue mass'-like appearance. This should be distinguished from other masses such as a maxillary cyst or a dental tumour (see 'Maxillary sinus cyst' and 'Other causes of opacity of the maxillary sinus', below). Inspissated pus within the ventral conchal bulla occurs secondary to chronic dental disease and is important to recognise radiographically. Ventral conchal bulla sinusitis has been implicated as a nidus for persistent infection and clinical signs including nasal discharge. Pus within the ventral conchal bulla often requires a specific surgical approach as well as medical management for resolution.

It should be remembered that sinusitis in the horse is generally secondary to other conditions, e.g. tooth root abscess, ethmoid haematoma, maxillary sinus cysts, or a fracture. The radiographs should be carefully examined for possible causative conditions. It may be necessary to drain the sinus and obtain further radiographs before the primary cause can be identified.

Clinically, sinusitis is usually associated with a unilateral nasal discharge, frequently of a purulent and malodorous nature. Although some cases of

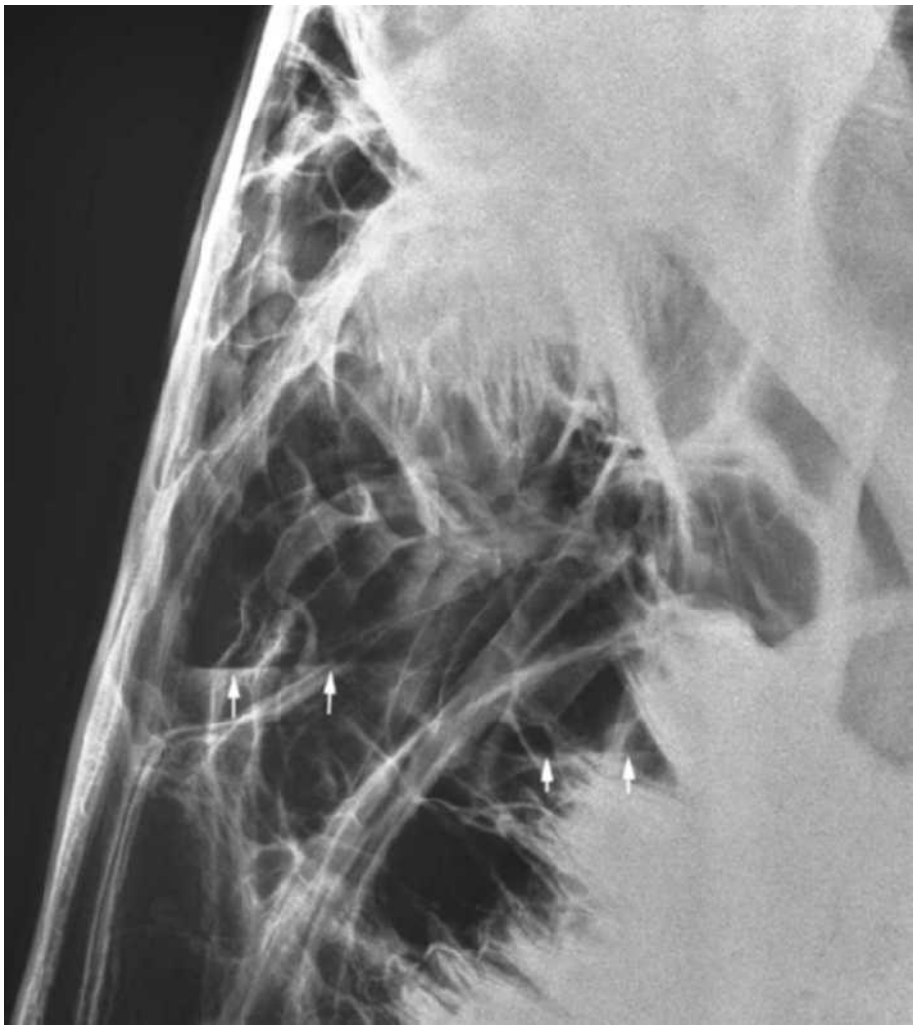


Figure 11.12 Right lateral-lateral image of the head of an 8-year-old Irish Sports Horse with a unilateral nasal discharge of 3 weeks' duration that had not responded to antimicrobial therapy. Dorsal is to the left. There are fluid lines (arrows) in the conchofrontal and maxillary sinuses, typical of sinusitis.

sinusitis will respond to treatment with antibiotics, surgical drainage and correction of the underlying cause are often required.

Submucosal cyst

A submucosal cyst may result in deformity of the facial bones and new bone production. A soft-tissue mass is identifiable radiographically (Figure 11.13). Clinically the facial deformity should be differentiated from that due to a previous fracture, a sinus cyst or a tumour. The soft-tissue opacity should also be differentiated from an ethmoid haematoma, sinusitis, or other causes of sinus opacity. In contrast to sinusitis, a horizontal fluid line usually cannot be identified.

Maxillary sinus cyst

A maxillary sinus cyst is not uncommon, but can be difficult to diagnose with certainty, especially in the early stages. It usually occurs in young horses (up to 5 years old), but is occasionally seen in older animals. The presenting signs are usually facial swelling, respiratory noise or unilateral nasal discharge.

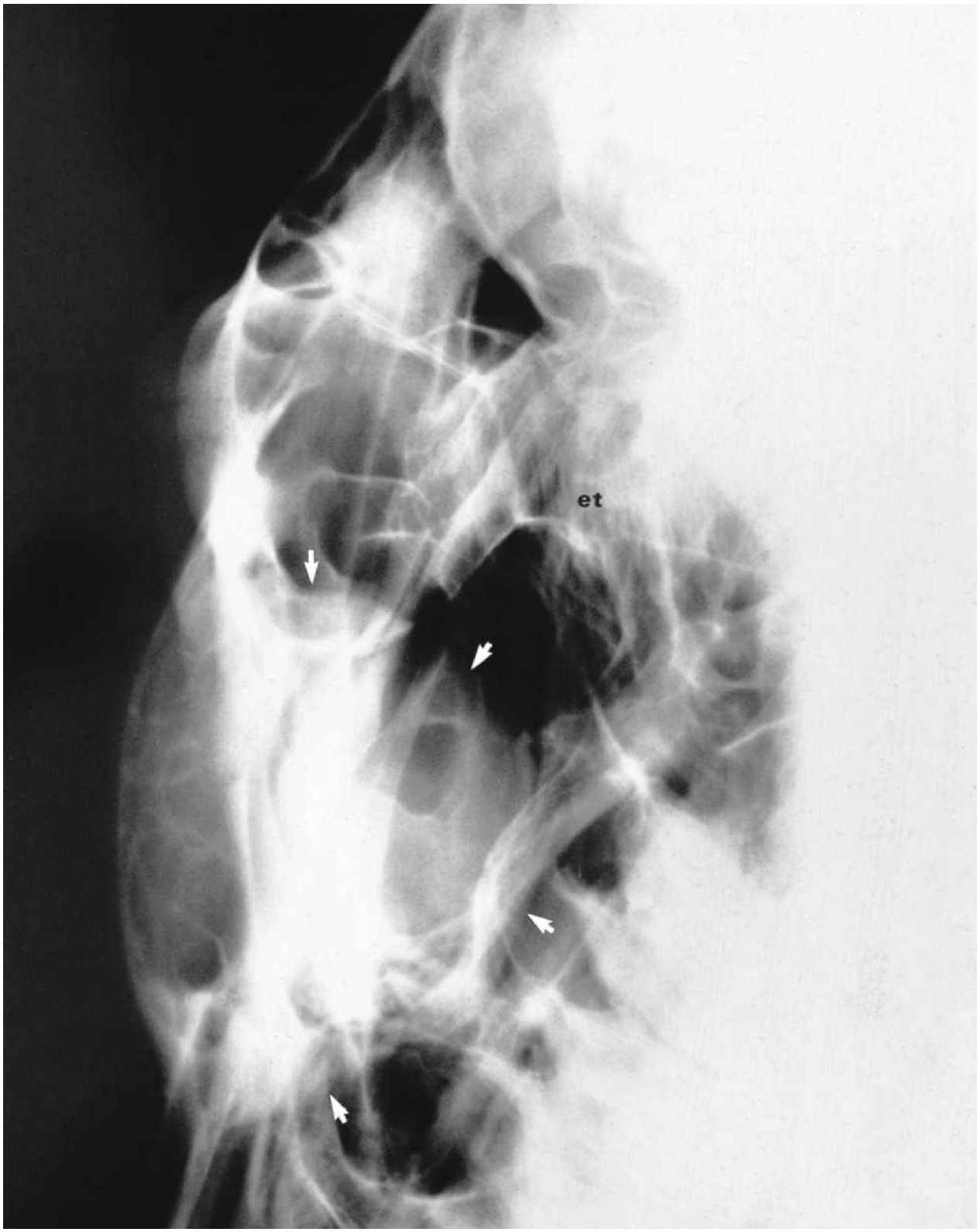


Figure 11.13 Right oblique view of the frontal area of a 10-year-old Quarterhorse with a history of a slowly progressive deformity of the facial bones on the right side. Dorsal is to the left. There is a well-circumscribed soft-tissue mass (arrows) rostral to the ethmoid turbinates (et), extending dorsally and deforming the nasal and maxillary bones. This soft-tissue mass is a submucosal cyst. The sinuses appear otherwise normal.

A secretory lining is present in the sinus and this is fluid filled. In the early stages this may pass undetected on lateral-lateral radiographs, causing only a slight increase in the opacity of the sinus. The cyst may be loculated, facilitating differentiation from sinusitis, and may completely fill the sinus. The cyst may gradually enlarge and can cause distortion of the surrounding bone. Usually the medial wall of the sinus is gradually pushed towards the midline (mesially), and this may cause gradual progressive obstruction of the nasal passages and obstruction of the airway – this can be seen on ventrodorsal images (Figure 11.14). On a ventrodorsal image the opacity of the parts of the sinus seen lateral to the mandibular rami can be compared. In more advanced cases, there may also be dorsolateral displacement of the maxilla, causing a gradual 'swelling' of the face of the horse. Treatment is by surgical resection of the cyst, including its lining.

Maxillary cysts

Multiple cystic lesions of the maxilla, usually involving the tooth roots, sometimes occur in young foals. Their origin is uncertain. Maxillary cysts may be seen on lateral-lateral images, but ventrodorsal images are also useful to assess the extent of involvement of the maxilla hidden radiographically by the superimposition of the very opaque outline of the teeth. Multiple radiolucent, sometimes multiloculated cystic lesions are present, often with enlargement in size of the maxilla. In extensive cases there may be little bone surrounding the cysts. Treatment is by surgical drainage, but the prognosis is guarded, depending on the extent of the lesion.

Ethmoid haematoma

An ethmoid haematoma is usually characterised clinically by intermittent nasal haemorrhage, usually unilateral. Strictly speaking it is a condition of the nasal chamber and only affects the sinuses in advanced cases. It is most easily diagnosed endoscopically, but it may be detected on radiographs, and these may help ascertain the size of the lesion and effects on adjacent bones (Figures 11.15a and 11.15b). The lesion is of soft tissues and is therefore seen only as a slight increase in radiopacity. In early cases the lesion is seen on lateral-lateral images overlying the maxillary sinus immediately rostral to the ethmoid bone. It may be more easily seen on ventrodorsal images, where the opacity of the two sides of the head can be compared. In advanced cases there may be modelling of the turbinate bones and nasal septum. The lesion may also invade the sinuses, including the sphenopalatine sinus in some cases. CT (or MRI) scanning is useful for more complete delineation of the lesion's extent, particularly when there is invasion of the mass into the sinuses or the presence of bilateral disease.

The condition can be treated by surgical resection or intra-lesional injection of formaldehyde, and has a fair to guarded prognosis.

Other causes of opacity of the maxillary sinus

The most common cause of opacity of the maxillary sinus is undoubtedly sinusitis. Frequently this is associated with tooth disease. In some cases, however, the tooth root may become surrounded by fibrous tissue, and this has



Figure 11.14 Ventrodorsal image of the head of a yearling Thoroughbred with stertorous breathing and an intermittent right-sided nasal discharge. Right is to the left. There is a large, well-circumscribed radiopacity in the right maxillary sinus (solid arrows), axial to the molar teeth. Note the deviation of the nasal septum to the left. There is also an ill-defined opacity (open arrows) abaxial to the molar teeth (compare with the left side). Diagnosis: maxillary sinus cyst.



Figure 11.15(a) A left to right lateral-lateral image of the nasofrontal region of a yearling. Dorsal is to the left. There is a soft-tissue opacity (arrows) dorsal to the most caudal upper cheek tooth, adjacent to, and summating with, the ethmoid turbinates. The mass is an ethmoid haematoma. Note that this projection is slightly oblique: the cheek teeth are at different levels.

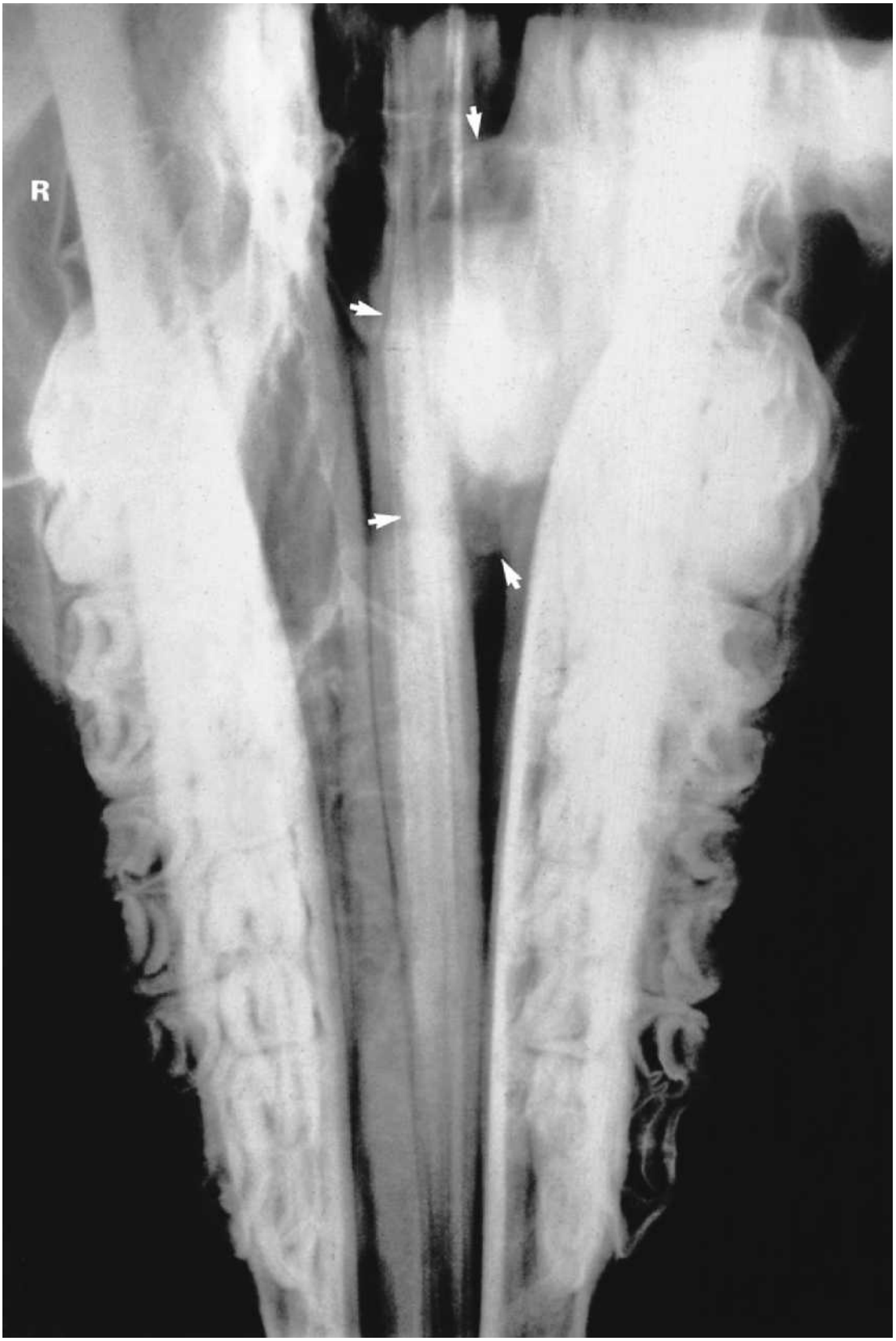


Figure 11.15(b) Ventrodorsal image of the same horse as in Figure 11.15(a) demonstrating much more clearly the soft-tissue opacity (arrows) axial to the most caudal left cheek tooth. Left is to the right. There is slight deviation of the nasal septum towards the right (R). The mass is an ethmoid haematoma.

been seen to extend into the maxillary sinus and may completely fill the sinus on one side. In rare cases this fibrous reaction may become mineralised, resulting in discrete areas of more radiopaque material within the sinus (Figure 11.16). These abnormalities can be seen on lateral-lateral radiographs, but ventrodorsal views are needed to determine the extent of the lesion. Surgical treatment is required.

Although neoplasia is generally rare in the horse, tumours are more common in the head than elsewhere. Carcinomas (adeno- and squamous cell), sarcomas (osteo-, myxo-, haemangio- and anaplastic sarcoma) (Figure 11w.17), neuroendocrine, odontoma and melanoma may occur in this region. The imaging characteristics are variable depending on tumour type and location, but usually show some of the characteristics of neoplasia, as described in Chapter 1.

An ameloblastoma (formerly called an adamantinoma) and an ameloblastic odontoma are tumours derived from the enamel organ (the embryological precursor of a tooth), and are seen in young horses. Radiographically they appear as lesions of the maxilla or mandible and have a variable

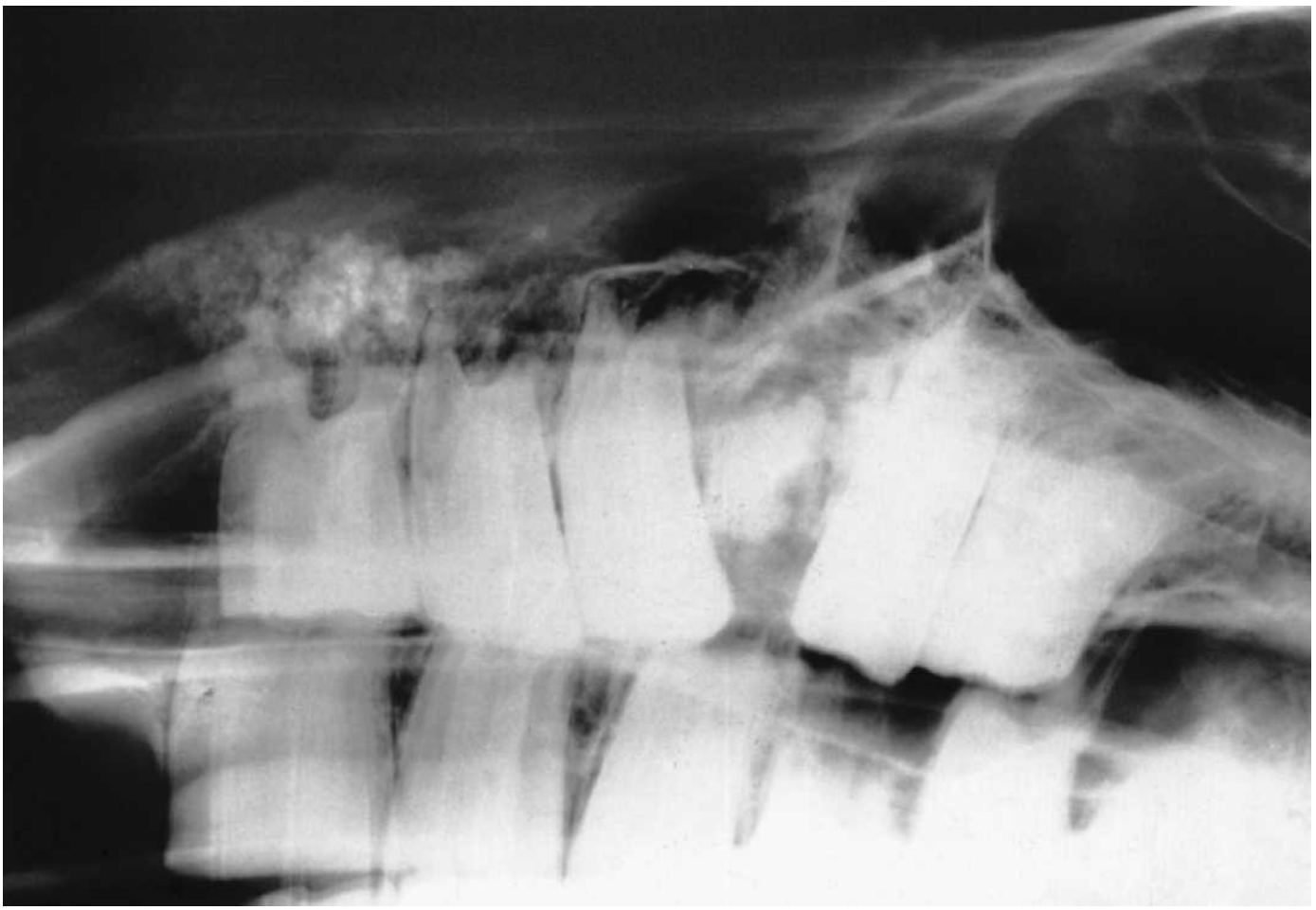


Figure 11.16 Right lateral oblique image of the maxillary region of a 10-year-old Standardbred. Rostral is to the left. The horse had previously had the bulk of the fourth upper right cheek tooth removed, but a piece remains. There is periapical lysis (rarefaction) around the caudal root of the third upper cheek tooth. Dorsal to the first upper right cheek tooth is an area of dystrophic mineralisation within the conchal sinus. The rostral maxillary sinus and the ventral conchal sinus communicate via the conchomaxillary opening. Such dystrophic mineralisation ('coral') is invariably the result of chronic infection (usually dental in origin).

appearance. An ameloblastoma remains as primarily a well-demarcated soft-tissue mass and has a septate configuration, resulting in a 'foamy' 'soap bubble' appearance (Figures 11.18a and 11.18b). An odontoma is derived from dental residues and tends to have a more opaque, tooth-like structure (Figure 11.18c).

Osteomas are benign, smoothly outlined, opaque tumours. They may become very large before being detected, as they grow slowly and cause few clinical signs. They have been associated with head shaking.

Adenocarcinomas occur in the frontal sinus and the nasal cavity. They occur in older animals and are very destructive. They grow rapidly and tend to be ill-defined. There is usually an associated unilateral nasal discharge.

Increased lucency of the maxillary sinus

Increased lucency of the bone surrounding the maxillary sinus has been seen associated with neoplasia (see above, 'Other causes of opacity of the maxillary sinus') and maxillary cysts (see above, 'Maxillary cysts').



Figure 11.18(a) Slightly oblique left lateral image of the head of a 4-year-old Thoroughbred. Dorsal is to the left. There is a well-demarcated partially mineralised soft tissue mass in the maxilla partially superimposed over the upper first two cheek teeth. The mass is of heterogeneous opacity, often described as a 'foamy' appearance. Biopsy revealed this to be an odontogenic tumour.



Figure 11.18(b) Ventrodorsal image of the same horse as Figure 11.18a. Right is to the left. There is a well-demarcated partially mineralised soft-tissue mass in the maxilla partially superimposed over the upper first two cheek teeth and extending mesially towards the nasal septum. The mass is of heterogeneous opacity, often described as a 'foamy' appearance. Biopsy revealed this to be an odontogenic tumour.

Cyst-like lesions of the incisive bone (premaxilla)

Cyst-like lesions occasionally develop in the incisive bone (premaxilla). These are expansile lesions that usually result in distortion of the facial contour and thinning of the overlying cortex (Figures 11.19a and 11.19b).

Teeth and mandible

Indications for evaluation of the teeth include quidding, weight loss, facial swelling, unilateral or bilateral nasal discharge, oral malodour, difficulties in eating, oral discomfort, reluctance to accept the bit and head shaking.

The Triadan system of tooth numbering has been adopted by veterinarians dealing with dentistry, thus replacing the terms incisor, canine, premolar and molar (cheek) teeth. This can be confusing to the uninformed. The teeth are numbered sequentially 1–11 from the central incisor caudally; the right maxillary teeth are prefixed 1, the left maxillary cheek teeth are prefixed 2, the left mandibular teeth are prefixed 3 and the right mandibular teeth are prefixed 4

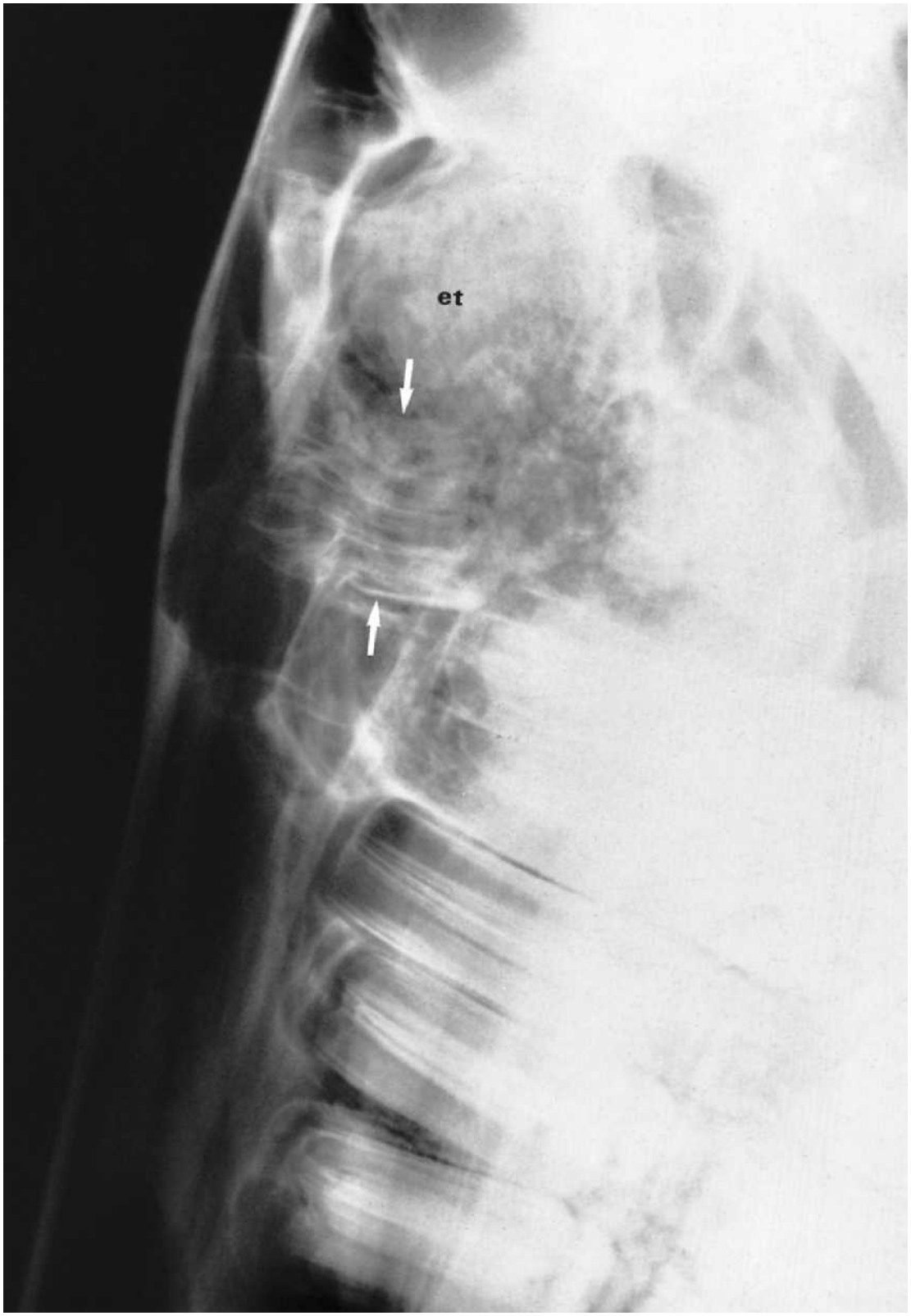


Figure 11.18(c) Slightly oblique left lateral image of the nasofrontal region of a 3-year-old Thoroughbred with a recent history of swelling below the left eye, left-sided mucoid nasal discharge and dyspnoea. Dorsal is to the left. There is a large mass of irregular opacity in the region of the most caudal upper cheek tooth. Within the mass are several opacities resembling teeth (arrows); et = ethmoid turbinates. Post-mortem examination confirmed that the mass was an ameloblastic odontoma.



Figure 11.19(a) Right oblique image of the rostral aspect of the head region of an aged pony with a slowly enlarging facial swelling. Rostral is to the left. There is a cyst-like lesion in the incisive bone (premaxilla), distorting its dorsal contour. The overlying cortex is thinned and has a slightly scalloped appearance caudally.

(Table 11.2). We have maintained traditional terminology in this text, but provide this table as a reference source.

RADIOGRAPHIC TECHNIQUE

Mandible

The views described below for the teeth, and above (see 'Cranium') for the cranium, are also used to assess the mandible. The exposure factors required for teeth and bone, however, are very different, and several radiographs may be needed of each area to acquire all the available information.

Temporomandibular joint

The temporomandibular joint can be examined using lateral-lateral views obtained with the head in the sagittal plane or rotated to facilitate separation of the left and right sides. However, to avoid superimposition, a skyline view can be used to assess the left and right joints independently. The horse's head is supported on a stand with adjustable height so that the poll is extended and the

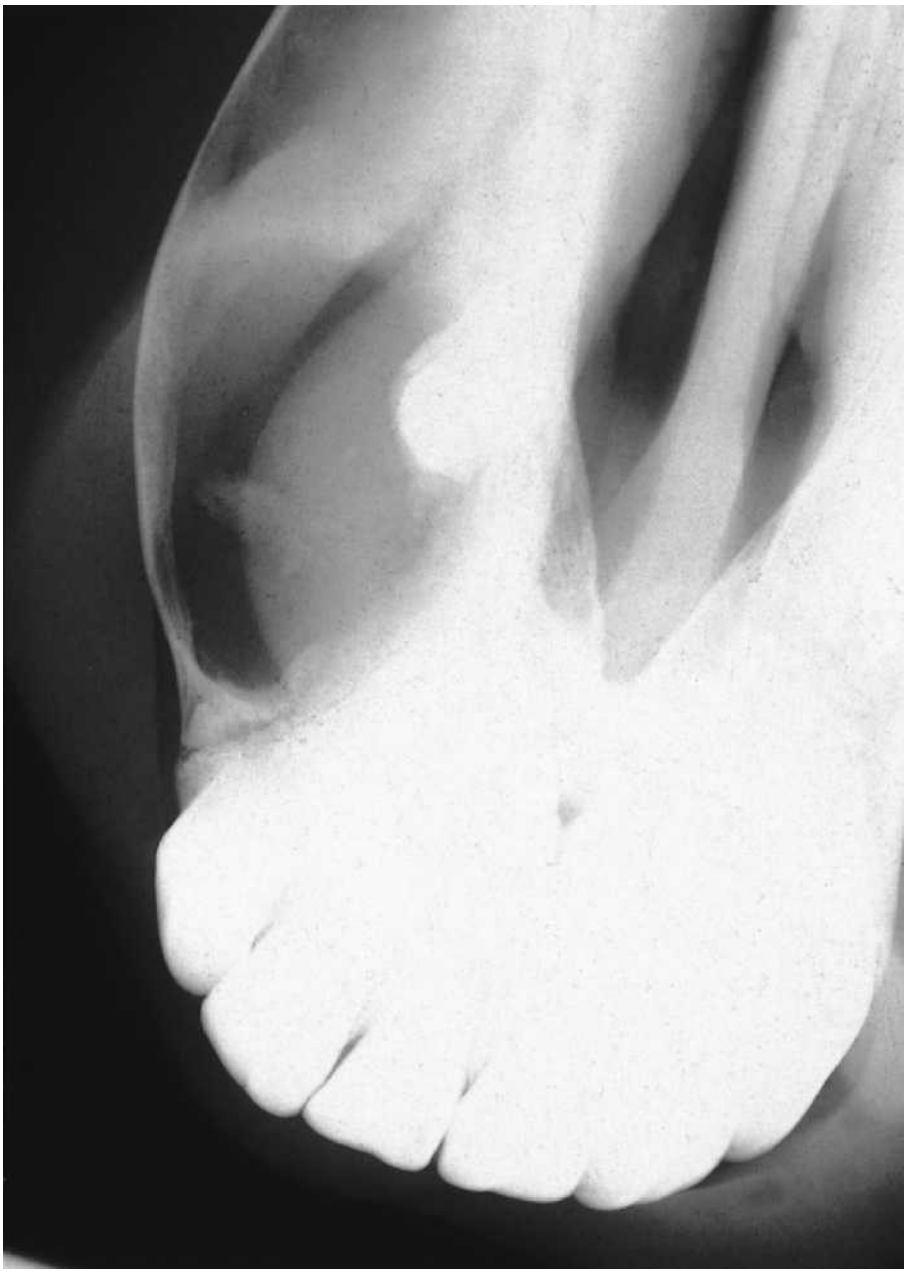


Figure 11.19(b) Slightly oblique dorsoventral, occlusal image of the incisive region (the same horse as in Figure 11.19a). Right is to the left. The cyst-like lesion is well defined. There are ill-defined opacities within it. The right canine tooth is partially superimposed over the axial aspect of the cyst-like lesion.

Table 11.2 The Triadan method of tooth numbering.

	Maxillary teeth		Mandibular teeth	
Tooth	Right	Left	Right	Left
Central incisor	101	201	401	301
Middle incisor	102	202	402	302
Corner incisor	103	203	403	303
Canine (tush)	104	204	404	304
Vestigial 1st premolar/wolf tooth	105	205	(405)	(305)
2nd premolar/1st cheek tooth	106	206	406	306
3rd premolar/2nd cheek tooth	107	207	407	307
4th premolar/3rd cheek tooth	108	208	408	308
1st molar/4th cheek tooth	109	209	409	309
2nd molar/5th cheek tooth	110	210	410	310
3rd molar/6th cheek tooth	111	211	411	311

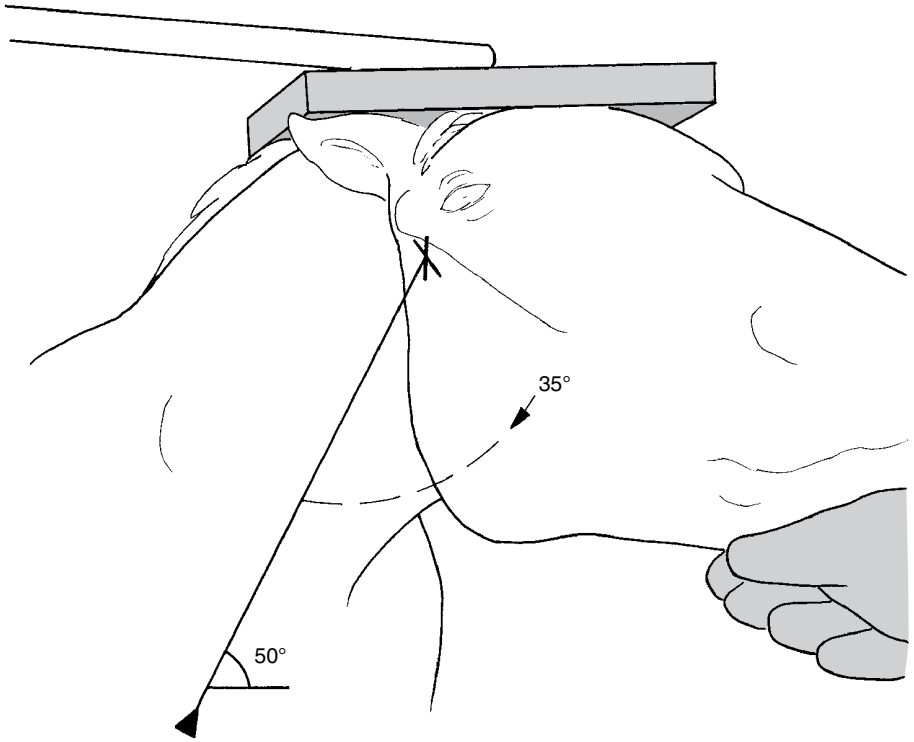


Figure 11.20 Positioning of the horse, x-ray beam and imaging plate to obtain a rostral 35° lateral 50° ventral-caudodorsal oblique view of the temporomandibular joint.

muzzle is almost horizontal (Figure 11.20). The x-ray tube is positioned below and to the side of the head to be examined, directed caudally. The x-ray beam is directed at an angle of 35° to the long axis of the head and 50° ventrally. A cassette is positioned horizontally above the poll, held in a cassette holder. The x-ray beam should be well-collimated and personnel should wear lead gloves. This rostral 35° lateral 50° ventral-caudodorsal oblique view allows good assessment of the lateral aspect of the temporomandibular joint (Figure 11.27).

Cheek teeth

Lateral-lateral view

Satisfactory lateral-lateral views can usually be obtained with the horse standing. The x-ray beam is centered at the point where the first molars (fourth cheek teeth) of the upper and lower jaws meet. The x-ray beam is aligned at right angles to the midline of the head and the cassette.

Ventrodorsal view

A ventrodorsal view may be obtained under sedation, but may be best and most safely obtained with the horse in dorsal recumbency under general anaesthesia if this is an option. It is important to ensure that the midline of the head is positioned vertically, to avoid oblique views. The x-ray beam is centered in the midline between the horizontal rami of the two mandibles, at the level of the first molars.

In a standing horse, dorsoventral radiographic views of adequate quality can be obtained in a co-operative patient, using the technique described above (see 'Frontal and maxillary sinuses and maxilla'). It is more difficult to evaluate the most caudal cheek teeth using this method. In order to evaluate

the caudal cheek teeth, the beam should be directed in a dorsocaudal to ventrorostral direction. The beam should be oriented so that the x-ray generator is caudal and pointing down, behind a line perpendicular to the dorsal surface of the frontal bone, centered immediately rostral to the naso-frontal suture.

Oblique views

Oblique views are essential to view the roots of the teeth satisfactorily, since their density precludes examination of one tooth superimposed over another. The best views are obtained with the horse under general anaesthesia, but the current trend towards dental procedures being carried out under sedation rather than anaesthesia may mean that general anaesthesia cannot be justified for the acquisition of radiographic images. The best radiographs are obtained with the teeth of interest against the cassette. To view the teeth against the cassette, the x-ray beam is angled dorsally 30° (lateral 30°dorsal-lateral ventral oblique) to assess the maxillary roots or ventrally 30° (lateral 30°ventral-lateral dorsal oblique) to assess the mandibular roots (Figure 11.21). In order to image the interdental spaces, the x-ray beam should be moved caudally 10–15° for the caudal maxillary cheek teeth; this angle should be reduced for the more rostral teeth within the arcade. The x-ray beam should be centered on the root to be examined. If the tooth of interest is on the side away from the imaging plate, then the angulation of the x-ray beam is reversed.

In a standing horse, radiography is facilitated by use of a head stand. To separate the left and right tooth arcades with the horse standing, for maximum safety the x-ray beam should be collimated as tightly as possible. It is usually easiest to use a horizontal x-ray beam, and rotate the horse's head towards or away from the cassette, which is positioned vertically. If the head is turned towards the cassette, the maxillary cheek teeth nearest the x-ray tube and the mandibular cheek teeth roots nearest the cassette can be assessed.

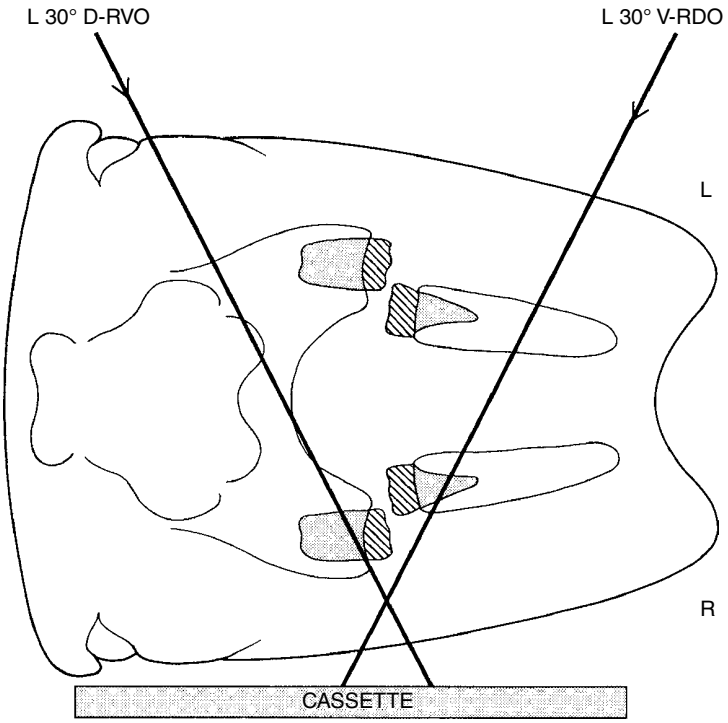


Figure 11.21 Diagrammatic transverse section of head to show angulation of the x-ray beam to obtain views of the right maxillary (L30°D-RVO) and mandibular (L30°V-RDO) cheek teeth roots with the horse in right lateral recumbency under general anaesthesia.

Alternatively, the head can be maintained in a neutral position. The tooth roots to be examined are positioned closest to the cassette, which is positioned perpendicular to the angle of the x-ray beam. To examine the roots of the maxillary cheek teeth, the x-ray beam is angled obliquely from midline in front of the head, 60° to the side away from the cassette, 30° proximal towards the cassette (Figure 11.22). For the roots of the mandibular cheek teeth, the obliquity of the x-ray beam is reversed. When using this second technique it is easier to reproduce the angle of projection accurately. The precise angle of the x-ray beam needed to evaluate the mandibular cheek teeth varies depending on the intermandibular width; a more horizontal x-ray beam is required for a broad head and a more vertical x-ray beam for a narrow head.

Open-mouth oblique views

Open-mouth oblique views are necessary to view the occlusal surfaces of the erupted crowns of the maxillary and mandibular cheek teeth. The horse is sedated and the mouth is held open using a Butler's gag, or preferably a non-radiopaque object such as a PVC cylinder or a piece of wood placed between the incisors. The degree to which the mouth is opened will depend on the size of the pony or horse. The head is held straight and the cassette, supported in a cassette holder, is positioned parallel to the long axis of the horse's head. The x-ray beam is carefully collimated and is

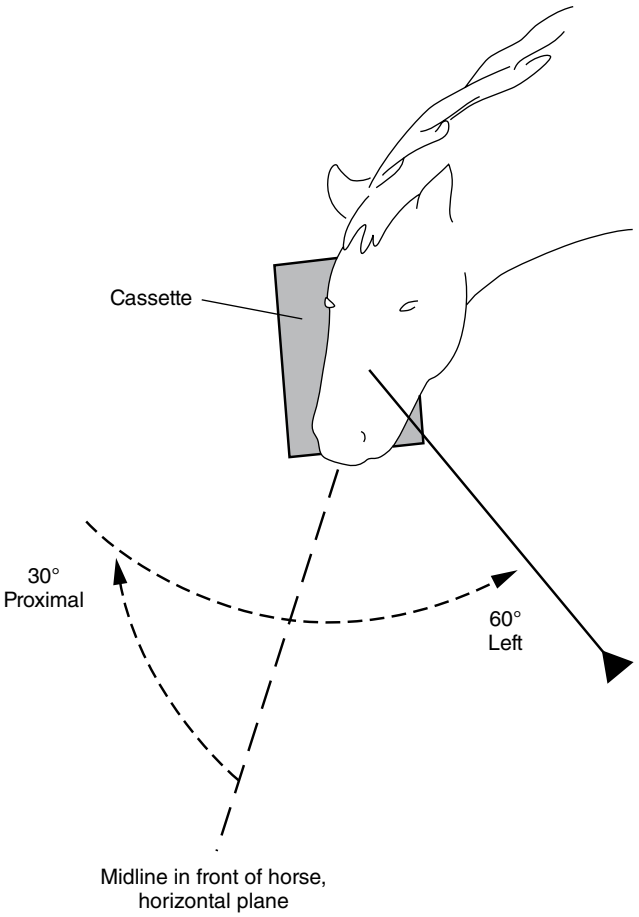


Figure 11.22 Positioning to obtain oblique views of the upper cheek teeth in a standing horse, with the head in a neutral position. The teeth to be examined are closest to the cassette. The x-ray beam must be tightly collimated to ensure safety of personnel.

directed perpendicular to the long axis of the horse's head, centered at the rostral extremity of the facial crest, at the level of the occlusal surfaces of the cheek teeth (Figure 11.23). Angling the beam 10–15° dorsal or ventral projects the occlusal surfaces clear of the bulk of the teeth (Figure 11.26). A lateral 15° ventral view is used to evaluate the contralateral maxillary cheek teeth and a lateral 10° dorsal view is used to image the contralateral mandibular cheek teeth. The precise angles for optimal evaluation of the cheek teeth crowns are variable depending on a number of factors such as mandibular width and tooth wear. It is frequently not possible to view all the tooth surfaces on one image, and a number of views of slightly differing obliquity may be needed. Angulation depends upon the absolute size of the skull, the length of the erupted crown, the presence of abnormalities of wear and the degree of angulation of the curve of Spee (the dorsal curvature of the occlusal surface of the caudal three cheek teeth). If the x-ray beam is not perpendicular to the long axis of the horse's head this may result in distortion and overlapping of the cheek teeth crowns.

Incisors

Lateral-lateral view

The x-ray beam is centered at the rostral aspect of the head, on the occlusal surfaces of the incisor teeth. It is aligned at right angles to the midline of the head and the cassette.

Ventrodorsal view

In an anaesthetised horse a ventrodorsal view is obtained with the x-ray beam centered on the ventral aspect of the muzzle of the horse, and the x-ray cassette against the dorsal aspect of the head. It is also possible to obtain occlusal images of the incisor teeth, placing the cassette in the oral cavity, so that only the upper or lower teeth are seen on the film. In a standing patient a dorsoventral view is easier to acquire. Occlusal images can be acquired in a conscious sedated patient, but do require patience to obtain, and great care must be taken to maintain adequate radiation safety.

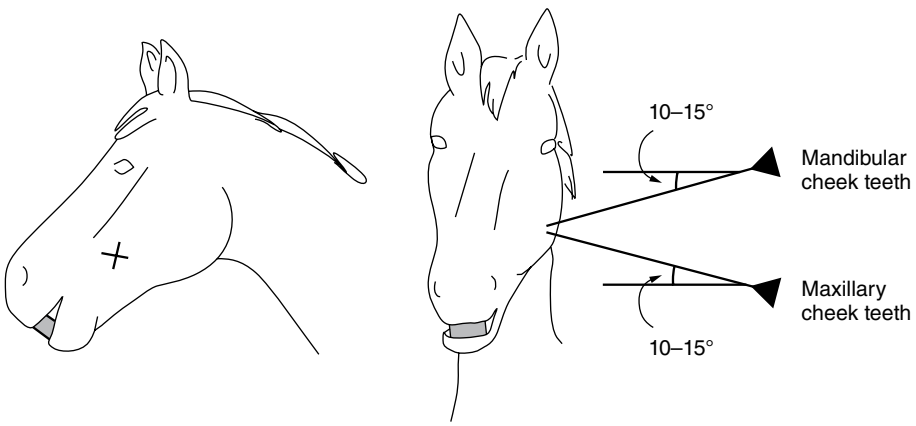


Figure 11.23 Technique for obtaining open-mouth oblique views of the occlusal surface of the teeth. The mouth is held open as far as possible. The imaging plate is positioned parallel to the long axis of the horse's head. The x-ray beam is directed 10–15° to evaluate the contralateral mandibular or maxillary cheek teeth.

Oblique views

Oblique views are not essential for routine examination of the incisor teeth, because the occlusal images give excellent visualisation. They are, however sometimes needed to separate the incisor roots, particularly in younger patients. Oblique projections are acquired being mindful of the curved nature of the incisor orientation. Oblique views may also be beneficial for examination of specific lesions, especially in conscious patients.

NORMAL ANATOMY AND VARIATIONS

In lateral-lateral images of the rostral part of the mandible there is an oval-shaped relatively lucent area, at the caudal aspect of which is an irregular opacity (Figure 11.24a). This region of the mandibular symphysis is variable in appearance and should not be confused with a lesion. The horse has four premolars and three molars (Figures 11.25a–c). The first premolar (the wolf tooth) is frequently absent or is vestigial. Enamel is the most radiodense material in the body, making examination of the structure within the teeth difficult; however, the internal structure of teeth can be evaluated with digital radiographs. The increasing use of open mouth oblique views, reducing superimposition of the contralateral arcades allows for much greater definition of the roots, pulp chambers and variable dental densities of the crown. The teeth develop and erupt from the gums as shown in Table 11.3. The developing tooth is first seen as a lucent area within the mandible or maxilla. As the enamel is laid down, the tooth itself becomes evident, the enamel gradually becoming folded, so that the tooth has its typical structure by the time it erupts from the gum. As the tooth erupts, the lamina dura develops a cystic and distended appearance. This should not be confused with a tooth root abscess, which has a similar appearance (see 'Tooth root infection', below). The lamina dura of an erupting tooth is more regular in outline and is surrounded by smoothly marginated bone of normal opacity. Anatomically the roots do not form until the tooth has erupted, when the base of the tooth becomes narrowed and more distinctly outlined. The roots of the premolars are aligned roughly at right angles to the long axis of the horizontal ramus of the mandible. The molars have progressive angulation, with the roots being more caudal than the crowns towards the caudal aspect of the jaw.

As the teeth develop, the appearance of the mandible changes considerably. In the young horse the teeth are deeply embedded in the bone, which accordingly is rather thick. At about 2 years of age the ventral aspect of the mandible is often somewhat irregular, because the roots of the cheek teeth cause 'swellings' along the horizontal ramus. In an adult horse the ventral surface of the mandible is smooth and the bone is somewhat thinner, as the teeth are extruded from the bone.

In a normal horse, the erupted crowns of the maxillary and mandibular cheek teeth are closely apposed (Figure 11.25). The length of the reserve crown decreases with age. Compare Figures 11.25 a and b with Figure 11.31b.

The incisor teeth gradually change their angle throughout life, the occlusal surfaces becoming more rostral with age (Figures 11.24a and 11.24b).

The canine teeth (tushes or false wolf teeth) may be vestigial or absent, but are more common in geldings and stallions than in mares. They generally erupt at about 4–5 years of age, approximately in the middle of the interdental space (the gap between the incisors and premolars).

'Wolf teeth' are vestigial remnants of the first premolars. They are frequently absent or there may be up to four present. They tend to be placed close to the rostral aspect of the second premolar and generally have a roughly conical crown. There may be little or no apparent root to these teeth, or they may have a root penetrating variable depths into the bone. The teeth frequently do not penetrate the gum and can only be detected on x-ray or by palpation.

The rostral 35° lateral 50° ventral-caudodorsal oblique view of the temporomandibular joint permits assessment of the lateral aspect of the joint (Figure 11.27). Structures axial to the plane of the coronoid process are superimposed with the calvarium. The temporal condyle of the squamous temporal bone has a flat or slightly concave ventral border and is confluent dorsally with the superimposed opacity of the zygomatic arch. The mandibular condyle is a shelf of bone slightly convex dorsally, especially axially. The joint space is clearly seen between these structures.

SIGNIFICANT FINDINGS

Brachygnathia and prognathia

Brachygnathia and prognathia are generally congenital and can be seen on lateral-lateral radiographs. While it is not necessary to radiograph patients to make these diagnoses, radiographs of the cheek teeth may be valuable to check for sharp points where there is irregular wear, e.g. in brachygnathia the lower jaw is shorter than the upper, and there tend to be sharp points on the rostral aspect of the upper second premolar and caudal aspect of the lower third molar teeth.

Polydontia

Polydontia is the presence of teeth in excess of the normal dental formula. It most commonly results from persistence of the temporary dentition, particularly the incisors. Incisors are usually displaced labially or lingually and cause little trouble, although they may result in ulceration of the gum or lip. With the cheek teeth, the demand made for additional space by supernumerary teeth tends to result in teeth being rotated or adjacent teeth being displaced. This results in disturbance of the wear patterns, resulting in sharp spikes on the teeth and resultant damage to soft tissues. Frequently, supernumerary teeth are associated with tooth root infection (apical abscessation) and associated secondary disease including sinusitis. Radiography is not really necessary to diagnose this condition, but it may be helpful in differentiating between deciduous and permanent teeth. Radiographs should also be used to assess the surrounding teeth, tooth roots and maxilla or mandible to check for secondary disease. If secondary disease is associated with the additional teeth, extraction may be necessary. Radiographs are useful to define the structure of the surrounding bone and to ascertain if the supernumerary tooth shares a socket with the adjacent tooth or has a separate socket.

Oligodontia

Oligodontia, the congenital absence of a tooth, is of little clinical significance, although it may lead to sharp points on teeth, caused by uneven wear.



Figure 11.24(a) Lateral-lateral image and diagram of the rostral aspect of the head of a normal mature horse. Dorsal is to the left.

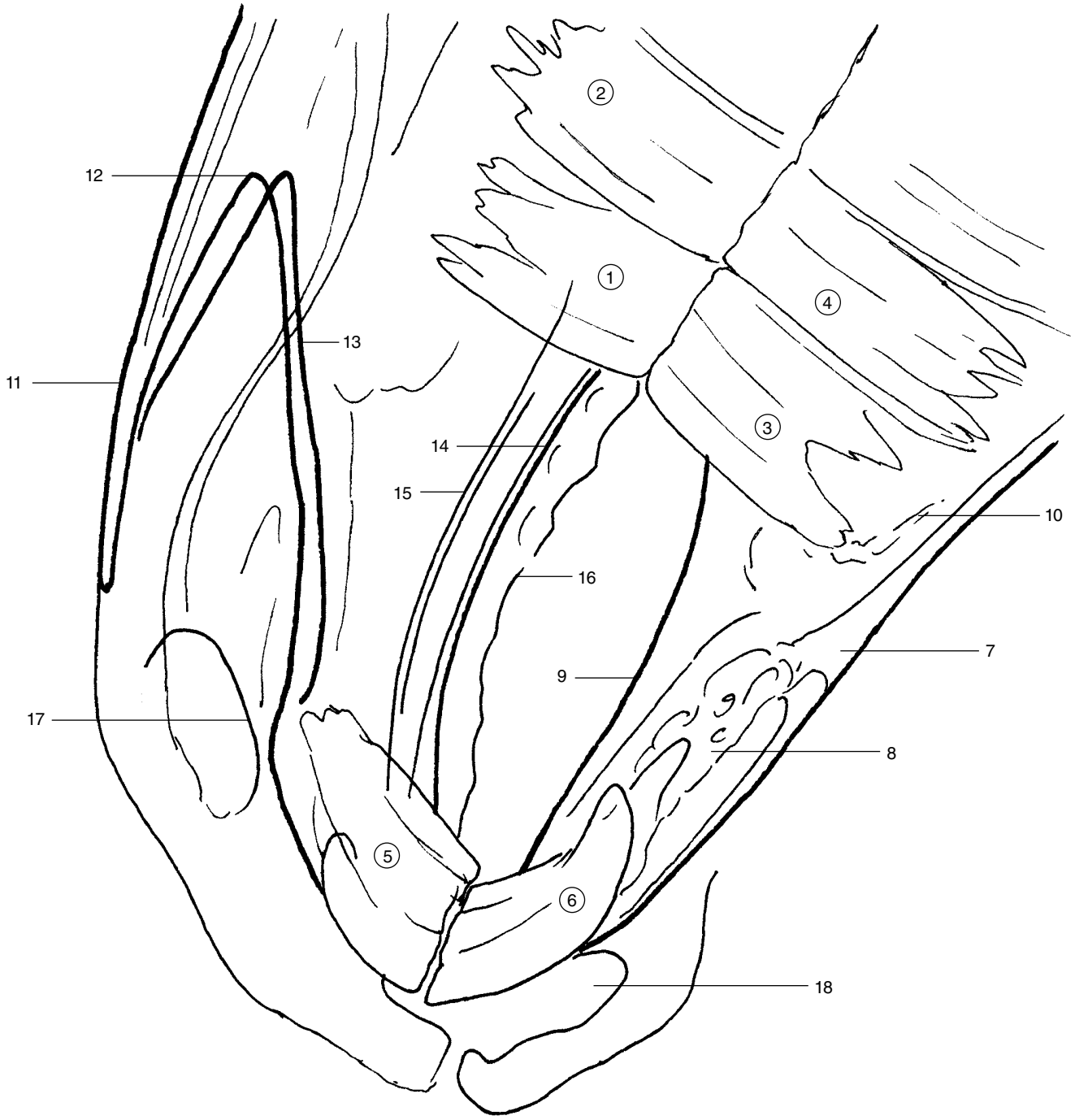


Figure 11.24(a) *Cont'd* 1 = second upper premolars, 2 = third upper premolars, 3 = second lower premolars, 4 = third lower premolars, 5 = upper incisor teeth, 6 = lower incisor teeth, 7 = body of mandible, 8 = area of mandibular symphysis, 9 = interalveolar margin of mandible, 10 = mandibular canal, 11 = nasal process, 12 = nasomaxillary notch, 13 = dorsal border of nasal process of incisive bone, 14 = interalveolar border of incisive bone, 15 = palatine process of incisive bone, 16 = ridge of hard palate, 17 = nostril, 18 = vestibulum oris.

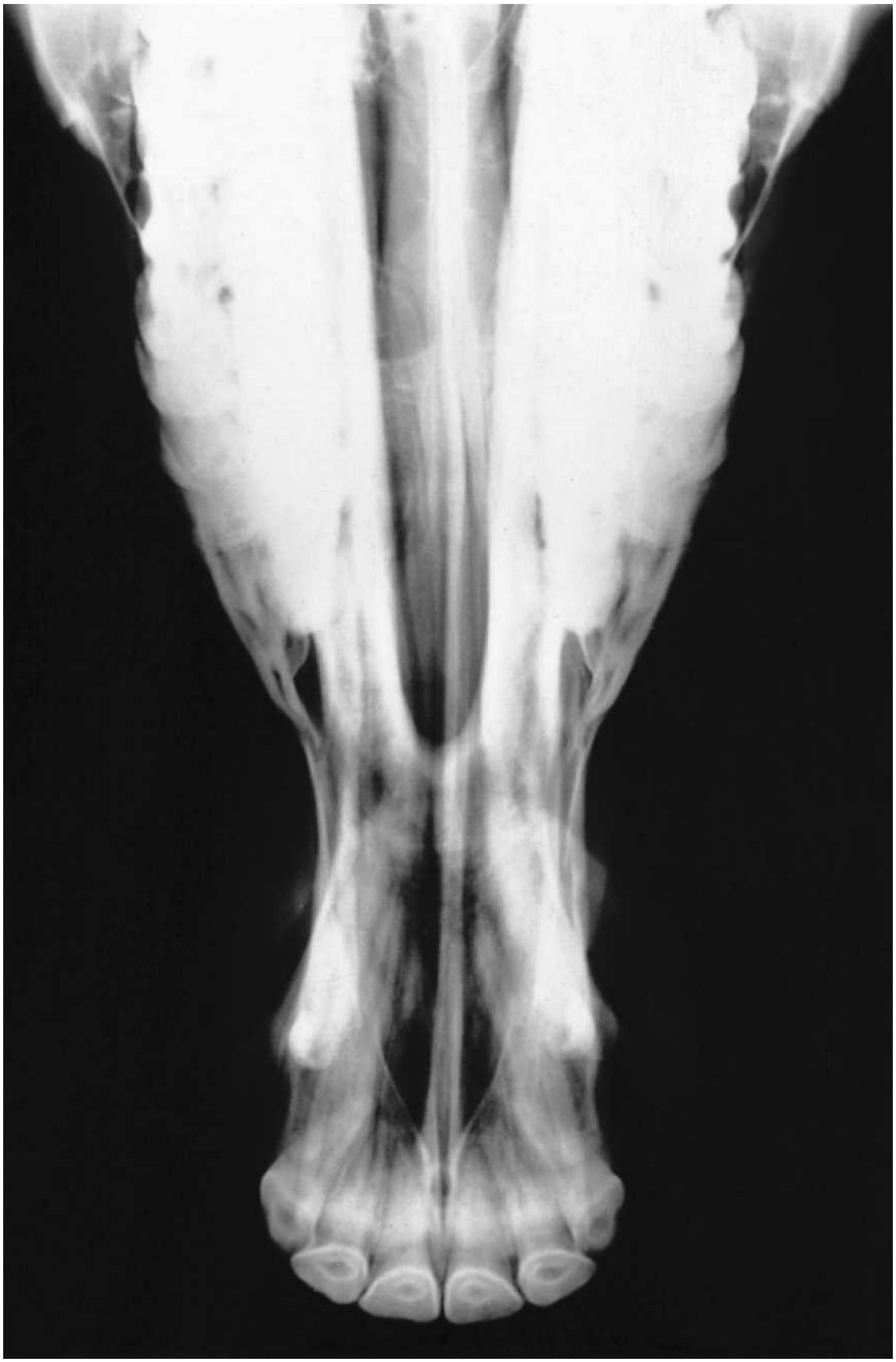


Figure 11.24(b) Ventrodorsal image and diagram of the rostral aspect of the head of a normal mature horse.

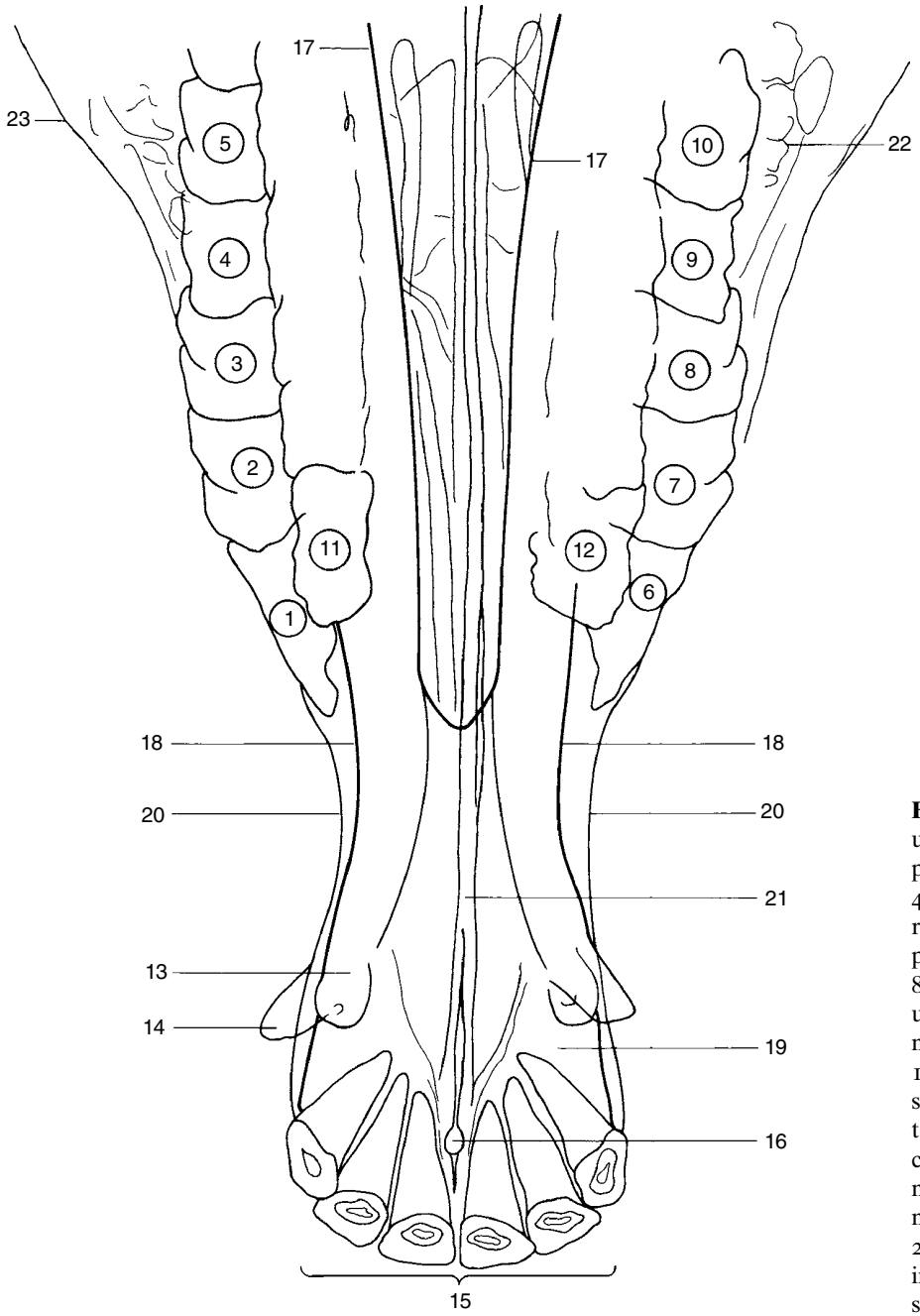


Figure 11.24(b) *Cont'd* 1 = second right upper premolar, 2 = third right upper premolar, 3 = fourth right upper premolar, 4 = first right upper molar, 5 = second right upper molar, 6 = second left upper premolar, 7 = third left upper premolar, 8 = fourth left upper premolar, 9 = first left upper molar, 10 = second left upper molar, 11 = second right lower premolar, 12 = second left lower premolar, 13 = incisive canine tooth, 14 = mandibular canine tooth, 15 = incisor teeth, 16 = interincisive canal, 17 = medial border of molar part of mandible, 18 = lateral border of body of mandible, 19 = body of incisive bone, 20 = lateral border of nasal process of incisive bone, 21 = vomer, 22 = maxillary sinus, 23 = facial crest.

Tumours of dental origin

An ameloblastoma (formerly known as an adamantinoma) and an ameloblastic odontoma are tumours derived from the enamel organ (the embryological precursor of a tooth). They are generally recognised in young horses and are discussed above ('Other causes of opacity of the maxillary sinus') (Figures 11.18 a–c).

Equine odontoclastic tooth resorption and hypercementosis (EOTRH)

Incisor radiographs are critical in the diagnosis of equine odontoclastic tooth resorption and hypercementosis (EOTRH). This condition, seen in



Figure 11.25(a) Right lateral-lateral image of the maxillary region of a normal 2-year-old Thoroughbred. Rostral is to the left. Note the well-defined periapical lucent zones which represent the normal dental sacs and the deciduous teeth (caps) on the occlusal surfaces of the premolar teeth. The lamina dura are well delineated (compare with Figure 11.30).

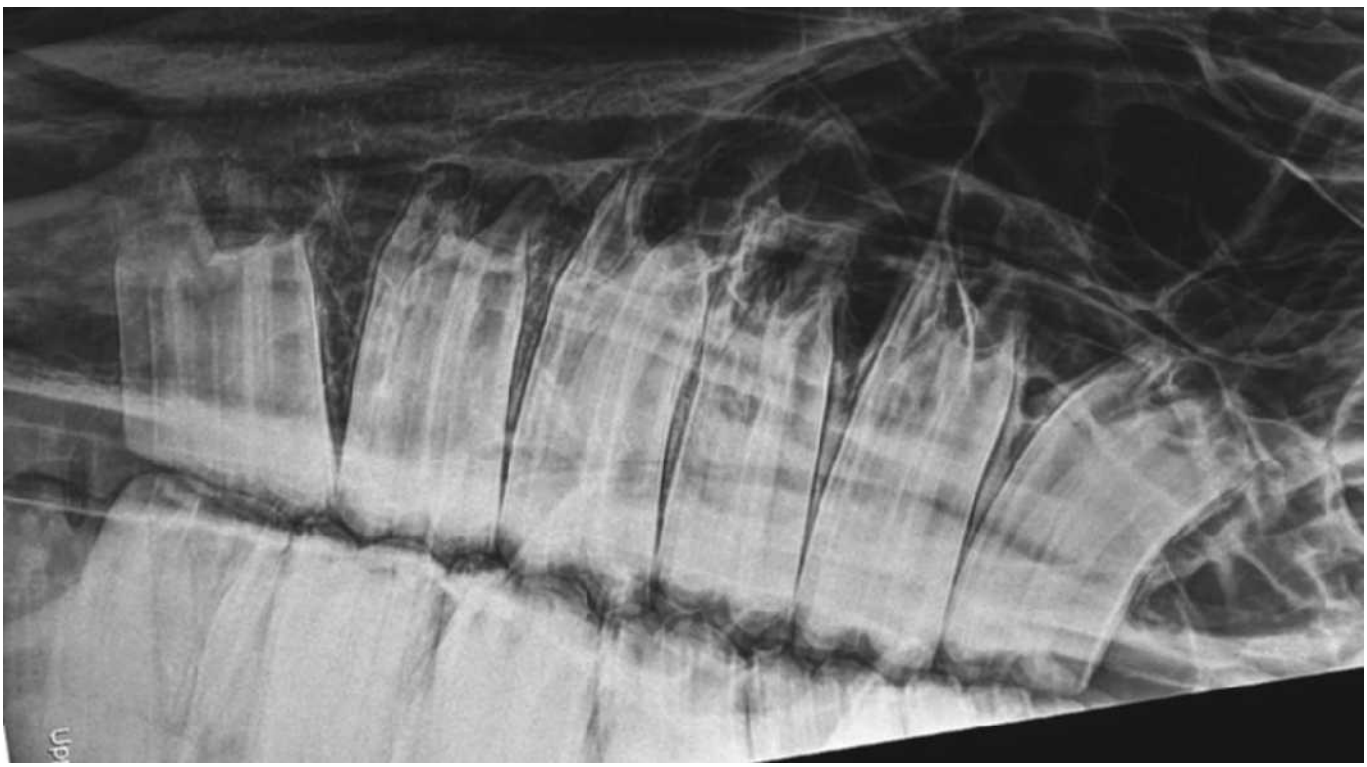


Figure 11.25(b) Right oblique image and diagram of the maxillary region of a normal 9-year-old Warmblood. Rostral is to the left. The exposure was selected to highlight the detail of the tooth roots.

old horses, usually results in dysphagia. Intra-oral radiographs demonstrate tooth resorption or proliferation of cementum or a combination of both. This predominantly involves the incisors, but may also involve the canine teeth. EOTRH can be associated with widening of the periodontal and periapical spaces, surrounding osteolysis and increased opacity, and dental displacement and occasionally fracture. Any number of incisor teeth can be affected in the same horse. Tooth resorption is highly variable in appearance, with irregularly margined zones of dental tissue lysis (Figure 11.28a). Similarly, hypercementosis can have a variable appearance, from regions of irregularly margined increase of cementum, to large bulbous mass-like lesions of cementum surrounding the incisor roots (Figure 11.28b). Treatment depends on the severity and clinical presentation but the prognosis is guarded and many horses require incisor extraction to alleviate the clinical signs of dysphagia and oral pain.

Dental fractures

Radiographs play an important role in the characterisation of dental fractures, particularly when they occur in the incisor teeth. Uncomplicated crown fractures of the incisor teeth can be identified on intra-oral

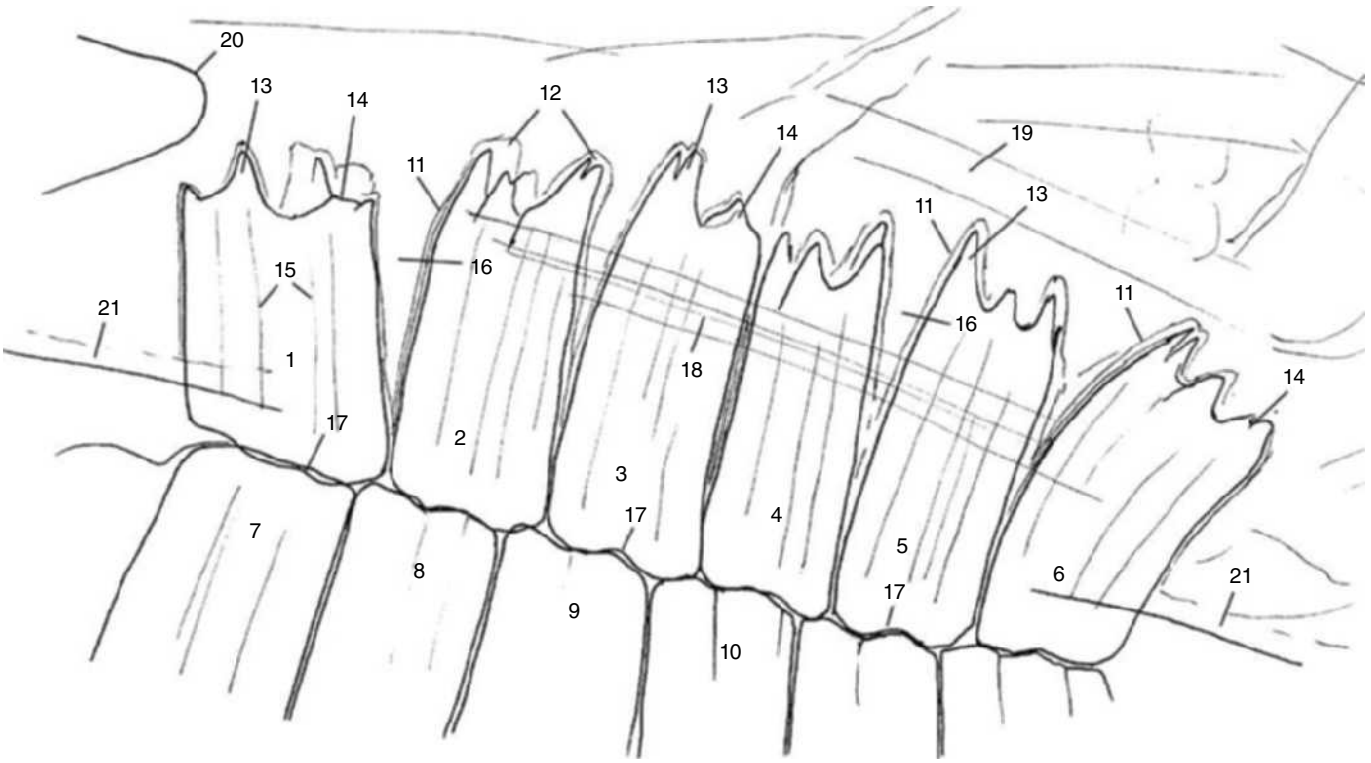


Figure 11.25(b) *Cont'd* 1 = second right upper premolar, 2 = third right upper premolar, 3 = fourth right upper premolar, 4 = first right upper molar, 5 = second right upper molar, 6 = third right upper molar, 7 = second right lower premolar, 8 = third right lower premolar, 9 = fourth right lower premolar, 10 = first right lower molar, 11 = lamina dura, 12 = socket, 13 = rostral root, 14 = caudal root, 15 = buccal longitudinal crest and folds of peripheral enamel, 16 = interalveolar septum, 17 = occlusal surface, 18 = middle nasal meatus, 19 = infraorbital canal, 20 = nasomaxillary notch, 21 = hard palate.

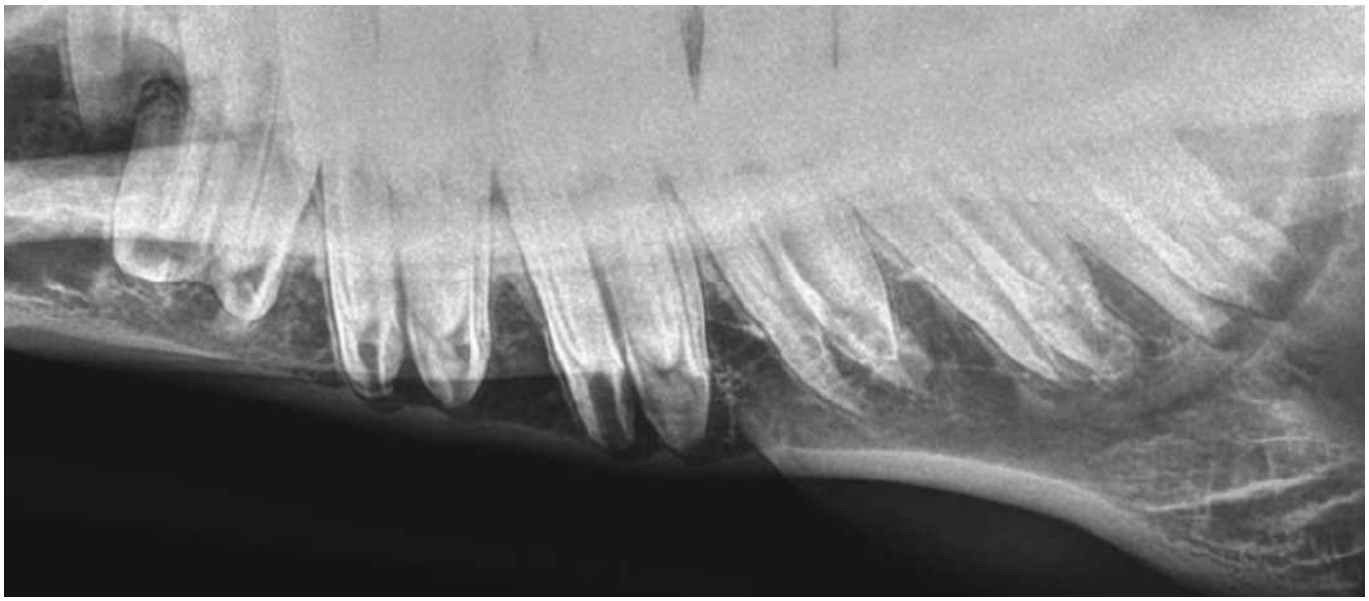


Figure 11.25(c) Right oblique image of the mandible of a normal adult Lusitano, to show the tooth roots. Rostral is to the left.

Table 11.3 Tooth development.

Tooth	Precursor present	Erupt from gum	Come into wear	Tooth lost
Deciduous				
1st incisor	N/A	1st week	1 month	2½ years
2nd incisor	At birth	4–6 weeks	By 3 months	3½ years
3rd incisor	?	6–9 months	By 1 year	4½ years
Canine: inconsistent and do not erupt				
1st cheek tooth	N/A	0–2 weeks	By 1 year	2½ years
2nd cheek tooth	N/A	0–2 weeks	By 1 year	3 years
3rd cheek tooth	N/A	0–2 weeks	By 1 year	4 years
Permanent				
1st incisor	Approx. 20 months	2½ years	3 years	
2nd incisor	Approx. 30 months	3½ years	4 years	
3rd incisor	Approx. 42 months	4½ years	5 years	
Canine?	4–5 yr – inconsistent			
1st premolar (wolf tooth)	Inconsistent			
2nd premolar	Approx. 15 months	2½ years		
3rd premolar				
Upper	Approx. 17 months	3 years		
Lower	Approx. 15 months	2½ years		
4th premolar				
Upper	Approx. 25 months	4 years		
Lower	Approx. 25 months	3½ years		
1st molar	Approx. 3 months	9–12 months		
2nd molar	Approx. 10 months	2 years		
3rd molar	Approx. 30 months	4 years		

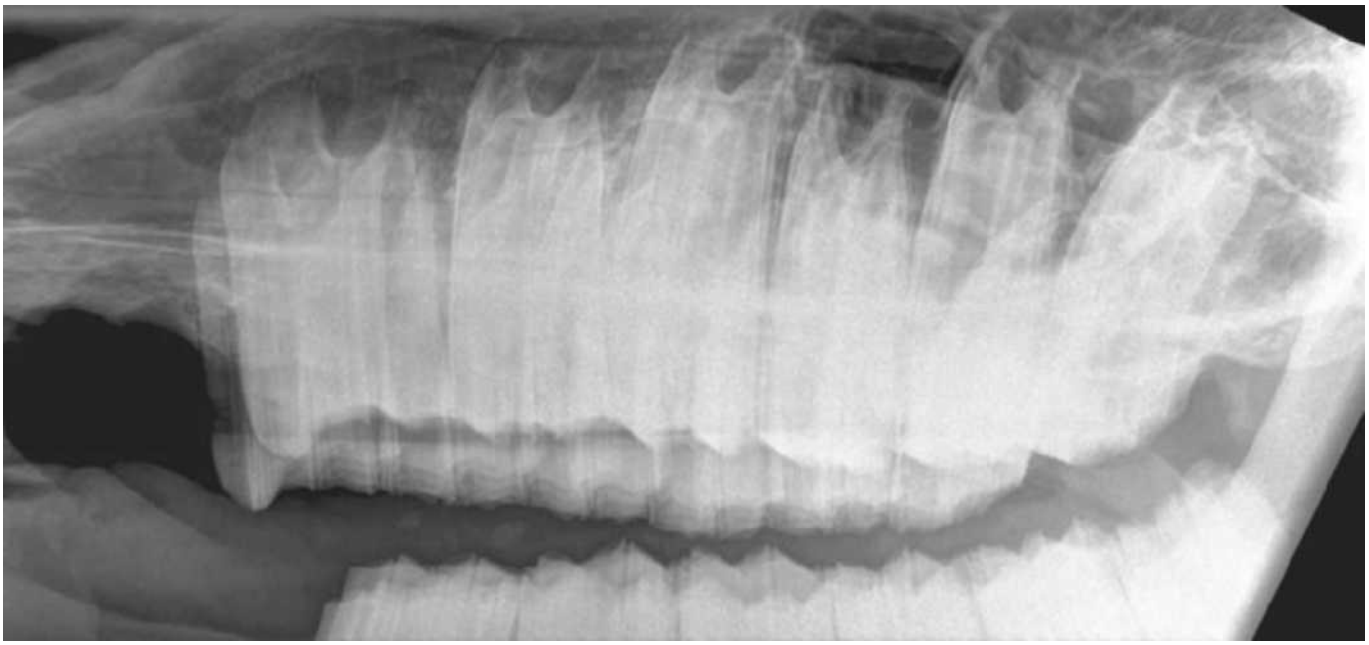


Figure 11.26 Open-mouth oblique image of the maxillary cheek teeth of an adult horse with no history of medical problems. Rostral is to the left. There are hooks on the rostral aspect of the first upper cheek teeth.



Figure 11.27 Rostral 35° lateral 50° ventral-caudodorsal oblique image of the lateral aspect of the right temporomandibular joint (arrows) of a normal adult horse.

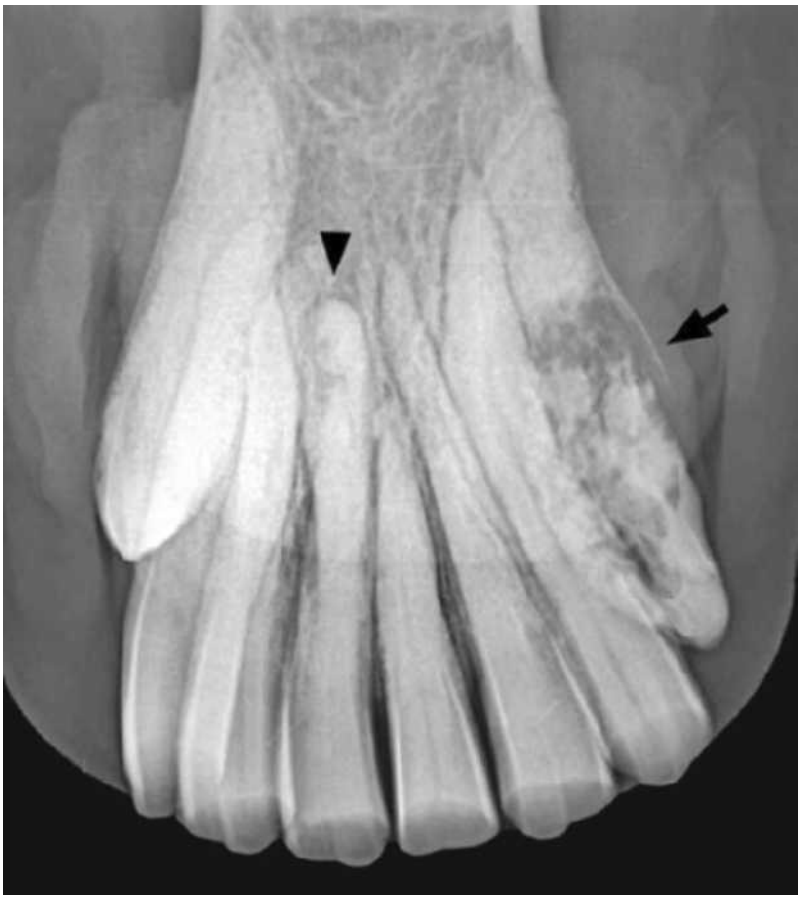


Figure 11.28(a) Intraoral image of the mandibular incisors; left is to the right. There is marked irregular loss of opacity (dental substance) of the left canine tooth (204, arrow), typical of equine odontoclastic tooth resorption and hypercementosis (EOTRH). A combination of hypercementosis, demonstrated as a bulbous shape of the right first (central, 101) incisor root (arrowhead), and irregular resorption is also present. The right canine tooth has smoothly margined cementum proliferation.



Figure 11.28(b) Intraoral radiograph of the maxillary incisors and canines. Right is to the right. Note the large bulbous mass-like lesions of cementum surrounding the incisor and canine roots characteristic of hypercementosis, part of the equine odontoclastic tooth resorption and hypercementosis complex.

radiographs as fracture lines that do not penetrate the pulp. Complicated crown fractures often extend into the vital tissue (pulp) and result in apical widening and periapical infection. Similarly, crown fractures of the cheek teeth can be identified on open-mouth oblique images as defects on the occlusal surfaces. It is more difficult to determine pulp involvement in the cheek teeth except by the identification of secondary signs related to endodontal disease, i.e. periapical abscessation and/or sinusitis. Sagittal or parasagittal fractures of the cheek teeth may be identified on dorsoventral images by the presence of a lucent line and displacement of the fracture fragment. Complicated dental fractures result in pulp exposure and pulpitis. If the pulpitis is irreversible, root abscessation ensues and the tooth must be removed.

Tooth root infection

Infections of the tooth roots vary in their appearance and can be difficult to distinguish on radiographs. There are a number of changes progressing through: widening of the periodontal space; loss of detail of the lamina dura; lysis of the periapical bone, possibly with increased opacity of the surrounding bone; destruction of the apex of the tooth root, giving it an irregular margin or marked change (often blunted) in shape. Tooth root infections are typically secondary to endodontal or periodontal disease. Endodontal disease occurs when a breech in enamel allows for exposure of the pulp to the environment, for example with an incomplete dental fracture or a defect in the secondary dentin. Computed tomography (CT) is a very accurate means of identifying infected teeth and the underlying cause. The cross-sectional nature of CT allows for the differentiation of the internal architecture of the teeth, thereby allowing for the identification of pulp abnormalities including gas accumulation within the pulp horns, roots or in the periapical space. CT also identifies all of the aforementioned signs of tooth root infection with greater sensitivity and overall accuracy than routine radiographs. Nuclear scintigraphy is sometimes helpful for identification of the affected tooth (teeth) through the indirect identification of associated osseous abnormalities. Ultrasonography is useful in the evaluation of soft-tissue swellings associated with mandibular teeth infections but ultrasound does not penetrate bone or dental surfaces.

Infections of the teeth in the mandible tend to present clinically as swellings on the lower jaw (Figure 11.29). These may be very slow to develop and eventually a discharging sinus may occur at the ventral aspect of the swelling.

Infections of the upper teeth may develop similarly (Figures 11.30a–d), with swelling and discharge from the maxilla or periorbital area. More usually, if the upper molars (and occasionally fourth premolar) are involved, there will be either a nasal discharge or a purulent sinusitis (see above, 'Sinusitis'). Infection of the maxillary teeth is sometimes accompanied by quite extensive fibrous reactions in the maxillary sinus, possibly including areas of local mineralisation. If such changes are found in the maxillary sinus, tooth root infection or periodontal disease should always be considered a likely cause (see Figure 11.16).

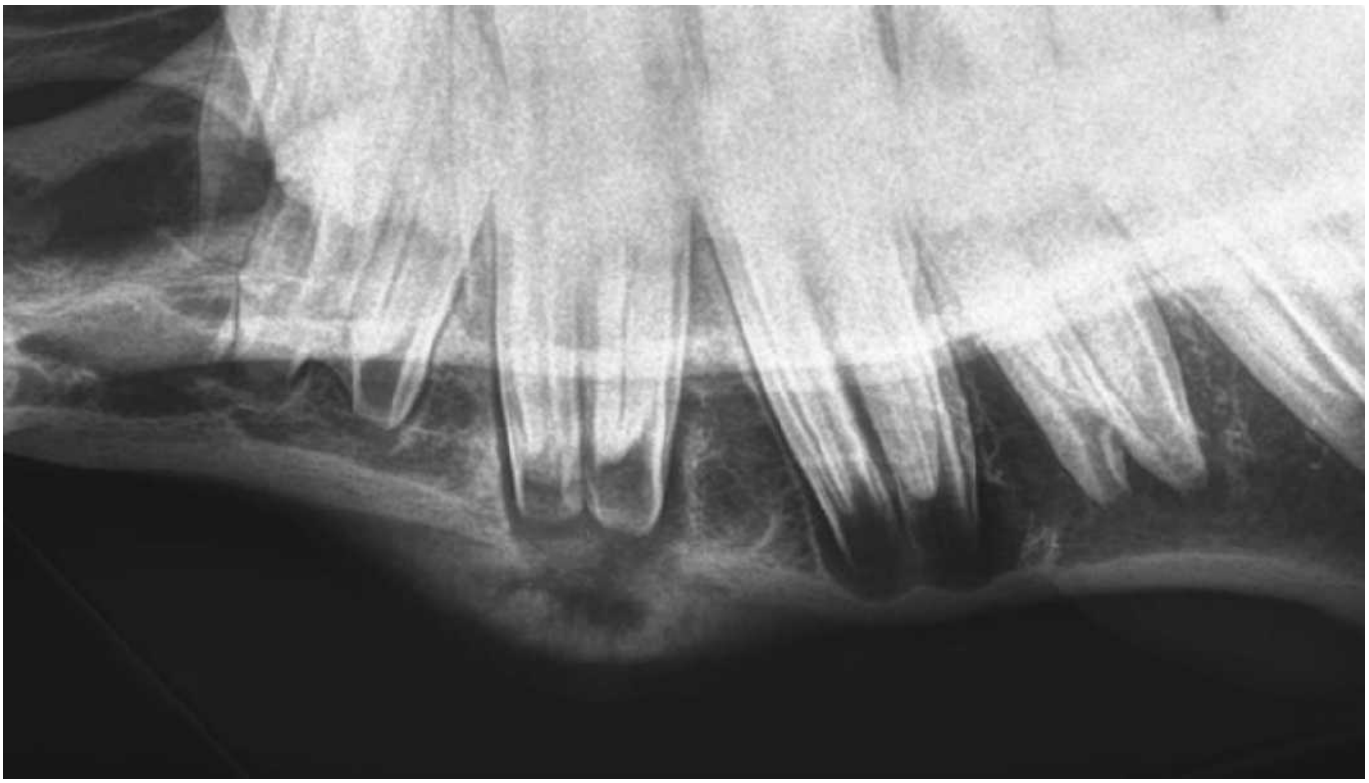


Figure 11.29 Right-left oblique image of the mandible of an 8-year-old Thoroughbred with a history of a painful swelling developing in the left mandibular region over the previous 6 weeks. Rostral is to the left. There is soft-tissue swelling overlying radiating poorly marginated, active periosteal new bone formation, bridging an area where there is complete disruption of the ventral cortex of the mandible. There is loss of detail of the lamina dura and a suggestion of blunting of the tooth roots of the second lower cheek tooth (307) with considerable lysis of the periapical bone. There is a suggestion of slight increased opacity of the surrounding bone rostrally. These abnormalities are typical of tooth root infection.

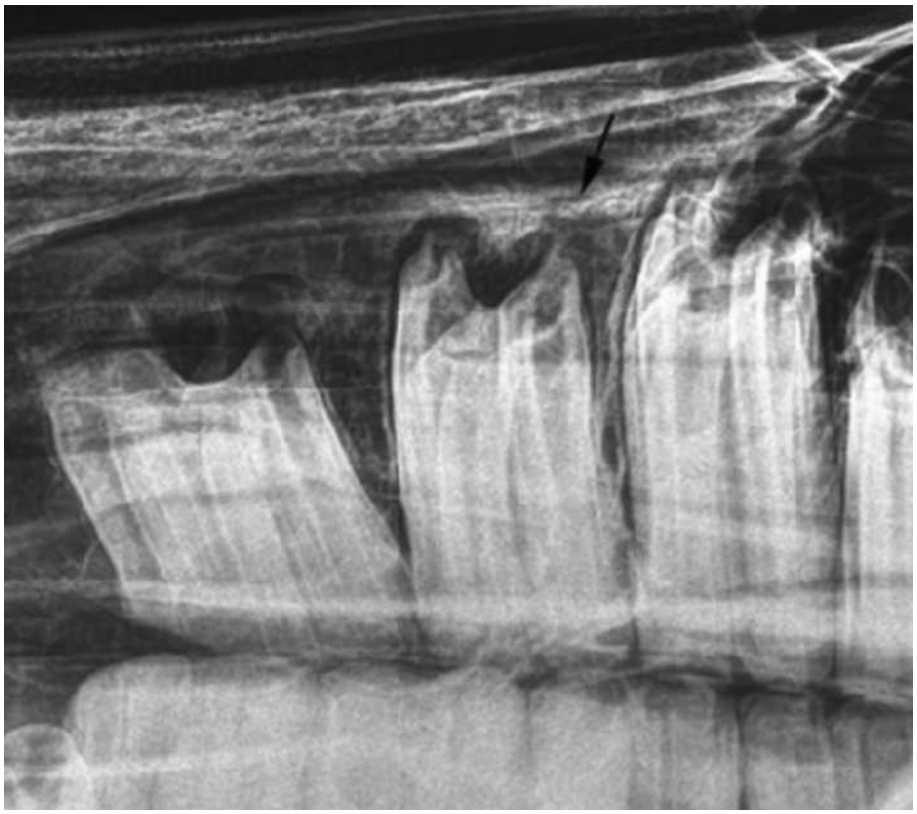


Figure 11.30(a) Left-right oblique image of the upper cheek teeth of a 7-year-old Thoroughbred with a firm swelling of approximately 3 months' duration. Rostral is to the left. The caudal tooth roots of the second upper cheek tooth (107) (arrow) are poorly defined and the lamina dura is less well-defined caudally. The tooth was extracted and the caudal tooth root was filled with purulent material.

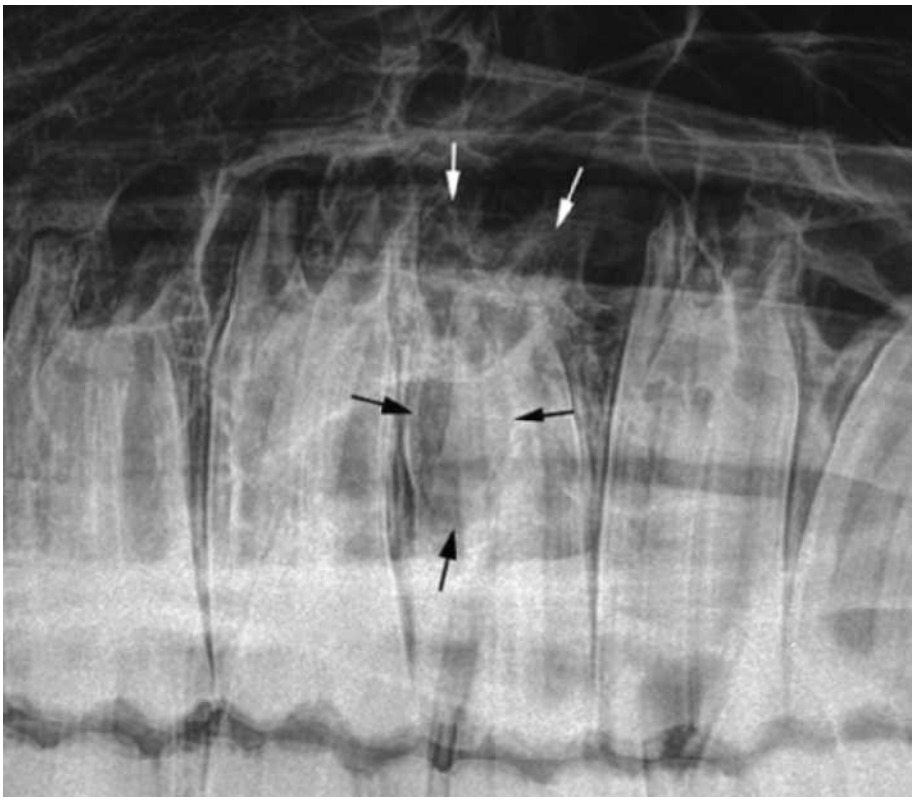


Figure 11.30(b) Right-left oblique image of the upper tooth arcade of a 9-year-old Warmblood. Rostral is to the left. There is modelling of the apices of the tooth roots of the first upper molar (209) (white arrows). There is also a radiolucent area (black arrows) within the tooth. Oral examination revealed large rostral infundibular caries with adjacent pulp exposure.

By the time these infections have been diagnosed it is usually necessary to extract the affected teeth. Although attempts have been made to drain these infections and operate on or fill the tooth roots, this is generally unsuccessful, uneconomic and, in view of the reasonable prognosis for conventional treatment, unnecessary.

Periodontal disease

Periodontal disease is more common in the maxillary teeth than in the mandibular teeth. The radiographic signs are similar to those for root infections, but there tends to be more reaction in the alveolar bone. Although periodontal disease is frequently accompanied by, or the result of, food material packing around the teeth, and even passing up into the maxillary sinus, it may be accompanied by little detectable oral discomfort.

Disorders of the erupted crowns

A diastema is a space between two adjacent teeth which may be congenital or acquired. An acquired diastema occurs due to tooth loss, fracture or through uneven overgrowth of the opposing dental arcade. Diastemata can result in impeded mastication of food, which becomes trapped, putrefies and leads to gingivitis, gingival recession and ultimately to periodontal disease and pain.

Diastemata can occur in young horses due to insufficient angulation of the rostral and caudal cheek teeth, or when the tooth buds develop too far apart. In older horses multiple diastemata may develop because the cheek

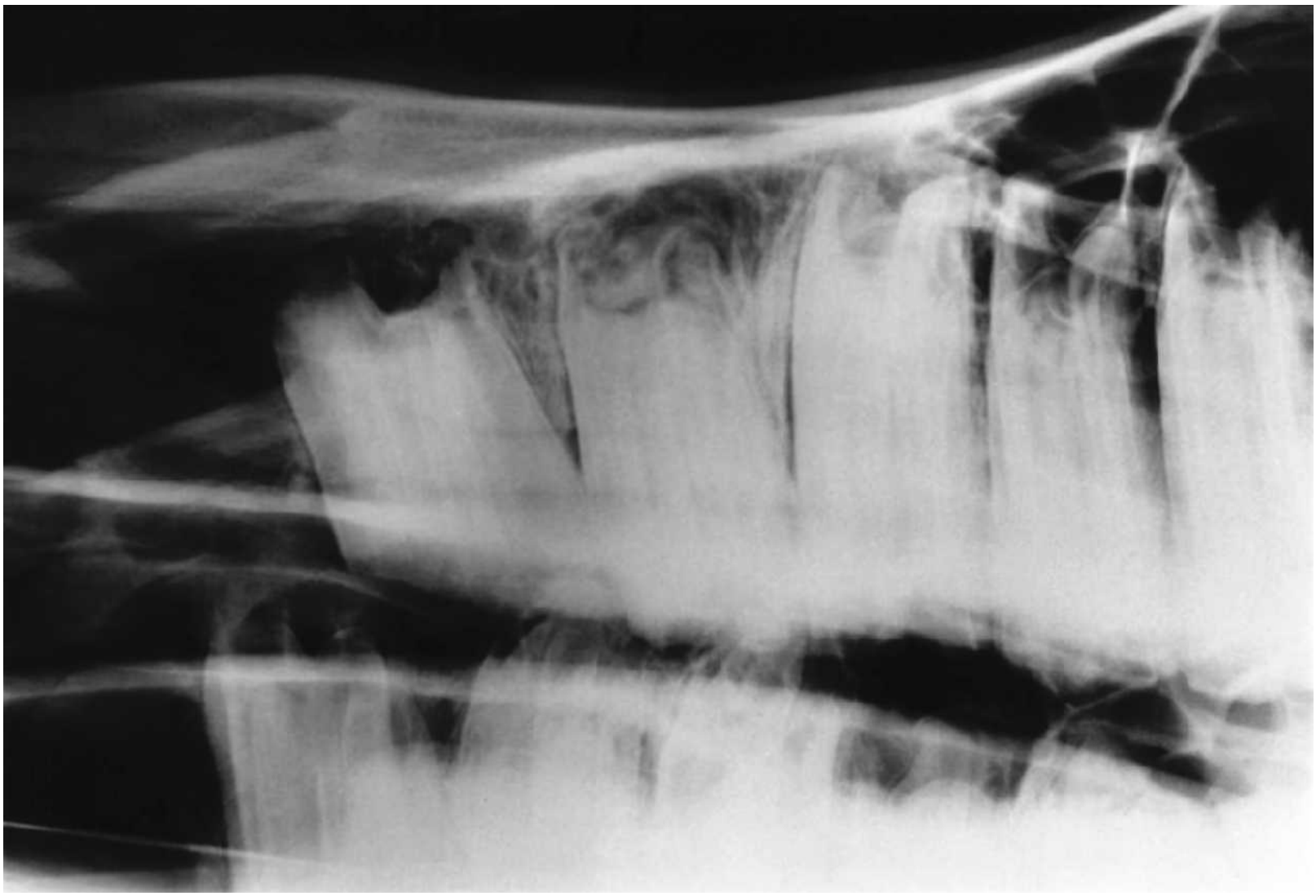


Figure 11.30(c) Left-right oblique image of the right upper cheek tooth arcade. Rostral is to the left. There is loss of definition of the lamina dura of the second upper cheek tooth (107), with a nodular opacity dorsal to it within an area of increased opacity. This is a finding associated with chronic tooth root infection. Compare with Figures 11.30(a) and 11.30(b).

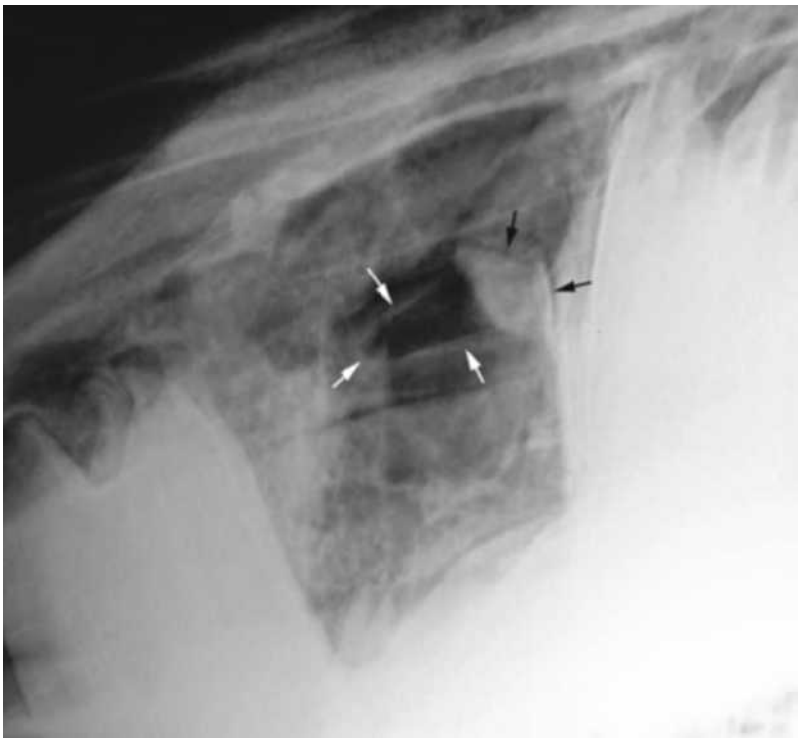


Figure 11.30(d) Right-left oblique image of the rostral upper cheek teeth 2 months after removal of the left third upper premolar. A chronic nasal discharge has persisted. There is a fragment of tooth (black arrows) rostral to which is a radiolucent area, surrounded by a more radiopaque rim (white arrows). Note also the diffuse, somewhat reticular opacity in the remainder of the space formerly occupied by the tooth.

teeth narrow towards their apices and therefore the rostrocaudal width of the exposed crown decreases with age and wear. Diastemata are difficult to detect clinically and cannot be seen in standard oblique views. Open-mouth oblique views are essential for diagnosis (Figure 11.31a). Treatment of a single diastema causing severe periodontal pain may require removal of a single tooth on one side of the diastema. Conservative treatment should be attempted initially, particularly if multiple diastemata are present.

Other abnormalities of the erupted crowns include traumatic or idiopathic fractures, abnormalities of wear such as exaggerated transverse ridges, wavemouth (Figure 11.31b) or stepmouth, supernumerary or reduced number of cheek teeth and the presence of retained and impacted deciduous cheek tooth remnants which may be confirmed on oblique open-mouth views. They may however be better detected by clinical examination.

Mandibular periostitis

Periostitis of the mandible is characterised radiologically as periosteal new bone formation, usually on the ventral surface of the mandible. It can be the result of trauma, with an incomplete fracture of the cortex of the mandible, or develop subsequent to chronic bruising, e.g. as a result of tight-fitting tack or repeated contusion from looking over a high door. The soreness will resolve once the inciting factor is removed, although some change in contour of the mandible is likely to remain. This condition should be differentiated from a tooth root abscess and a tumour of the mandible.

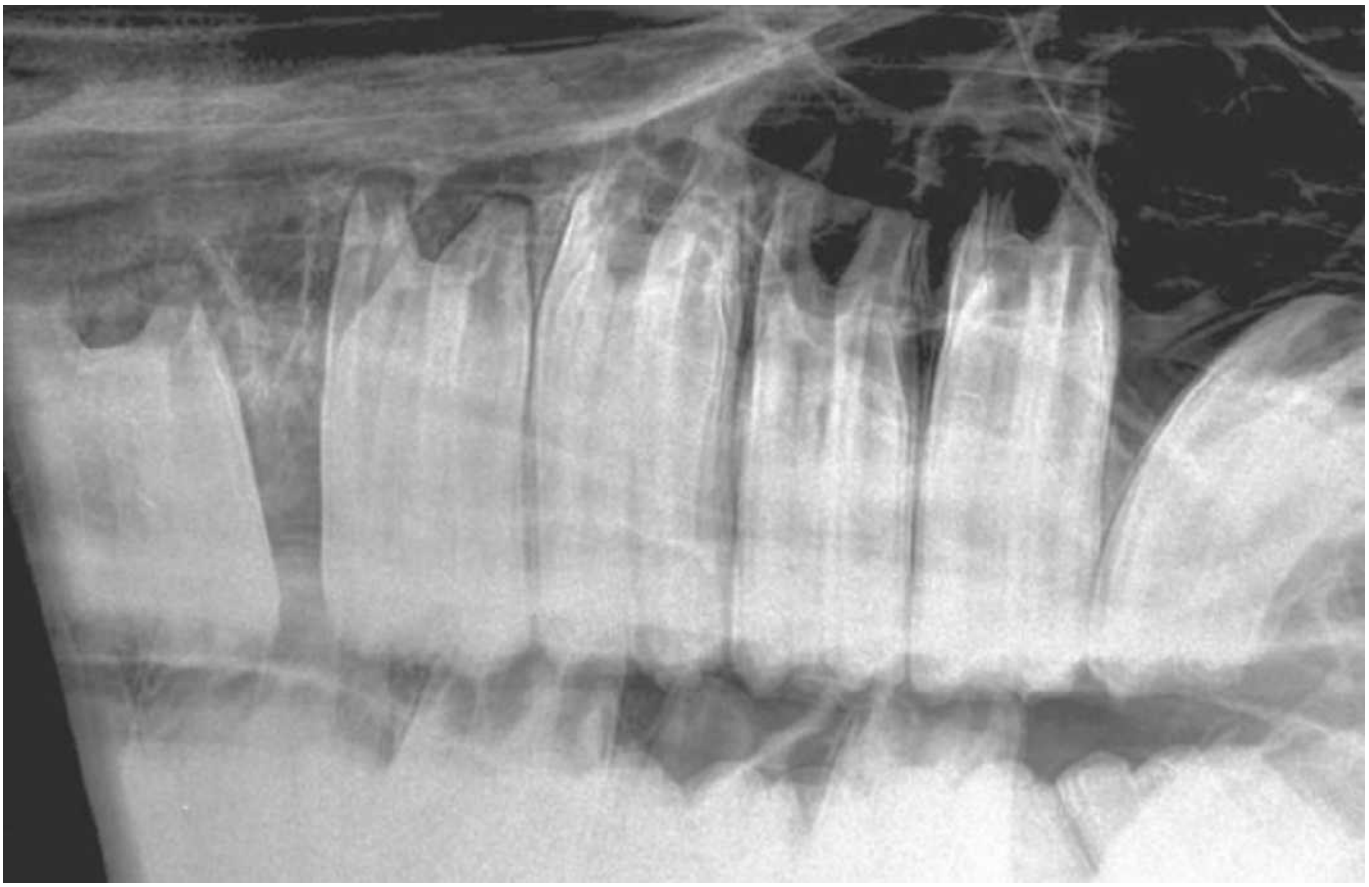


Figure 11.31(a) Open-mouth oblique image of the right upper cheek teeth of a 6-year-old Appaloosa which presented with facial swelling and marked gingivitis. Rostral is to the left. There is a space, a diastema, between the rostral two cheek teeth, 106 and 107.

Osteomyelitis

Osteomyelitis of the mandible is not uncommon and is characterised radiographically by destruction of bone with or without new bone formation (Figure 11.32). It is sometimes difficult to distinguish radiographically extensive infection from a tumour. Small lesions may be treated surgically, but extensive lesions carry a guarded prognosis.

Mandibular cysts

Multiple cystic lesions of the mandible, usually involving the tooth roots, are not uncommon in young foals (Figure 11w.33). They generally involve the rostral half or two-thirds of the horizontal ramus. Their origin is uncertain. This lesion is easily recognised on lateral-lateral radiographs as multiple radiolucent cystic lesions in the mandible, often with enlargement in size of the mandible. In extensive cases there may be minimal remaining bone surrounding the cysts.

Clinically there is swelling of the mandible, often with a rather bulbous or even lobulate appearance. In extensive cases, the teeth may be loose within the jaw and the horse may have difficulty eating. Differential diagnoses include ameloblastoma, cystic fibrosis and infection. Treatment is by surgical drainage, but the prognosis is guarded, depending on the extent of the lesion.



Figure 11.31(b) Open-mouth oblique image of the right cheek teeth of an aged Welsh pony. Two maxillary cheek teeth had previously been removed from the left side, but nasal discharge persisted. There is a very irregular alignment of the occlusal surface of the maxillary cheek teeth. This is wavemouth. Note the relatively short lengths of the reserve crowns typical of ageing horses.

Craniomandibular osteopathy

A condition resembling craniomandibular osteopathy in the dog has been recognised in the horse, resulting in large, firm, non-painful swellings on the ventral aspect of the rami of the mandibles of a young horse. Radiographically this is due to extensive periosteal new bone formation extending from the ventral cortices of the bones (Figure 11w.34). Bone biopsies show similar histological changes to craniomandibular osteopathy in the dog. There is some degree of spontaneous regression of the lesions over 1 year. The lesions do not interfere with mastication.

Tumours

The mandible is one of the more common sites for a tumour in bone in the horse, including osteosarcomas, ameloblastomas and ossifying fibromas. Most tumours result in widespread destruction of bone (Figures 11.35 and 11.36) and carry a poor prognosis. It is usually not possible to identify a specific tumour type by its radiographic appearance. Tumours must be differentiated from osteomyelitis (see Figure 11.32).

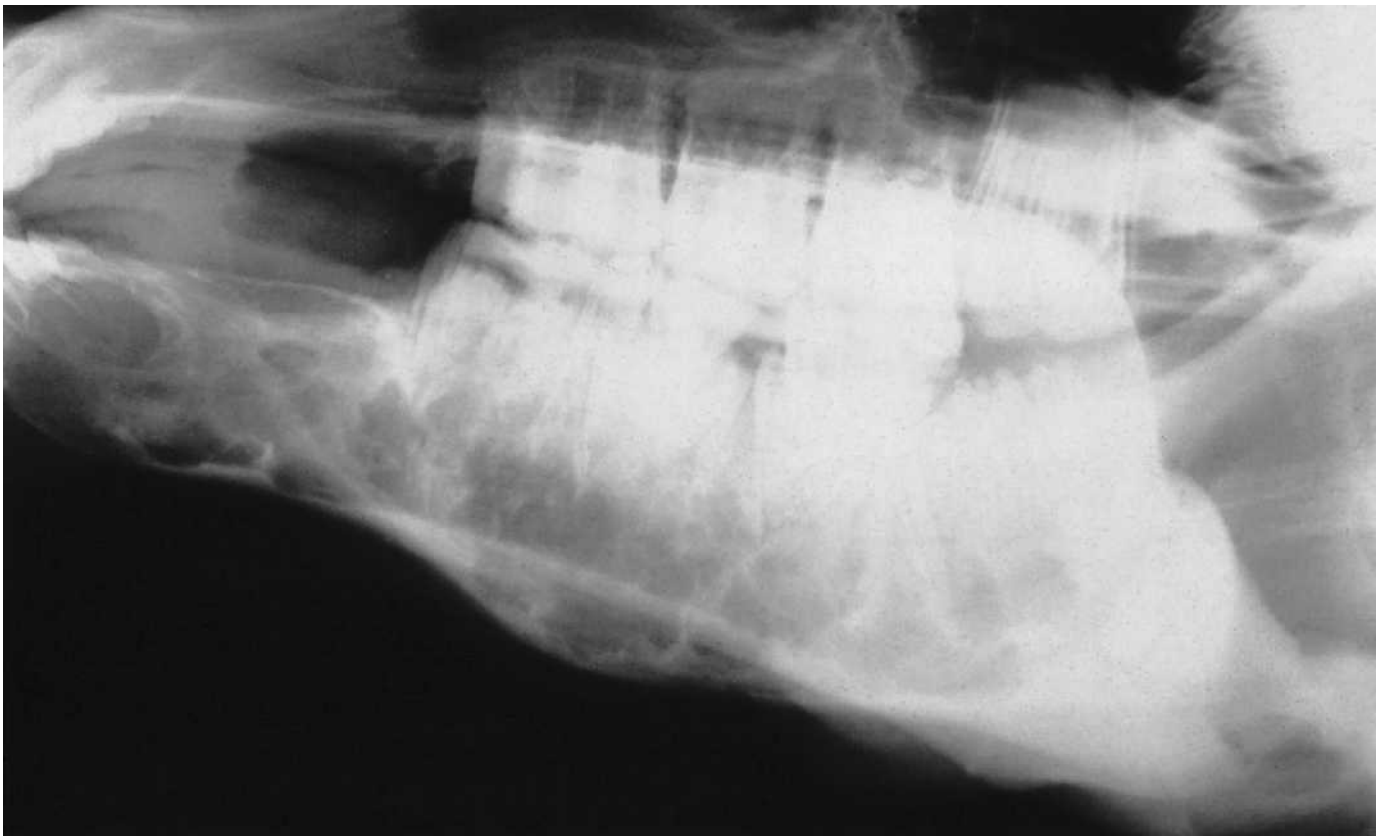


Figure 11.32 Slightly oblique right-left lateral image of the mandible of a weanling Morgan with a history of a small mass developing on the mandible 6 weeks previously and enlarging progressively despite antimicrobial therapy. Rostral is to the left. There is a large expansile lesion of the mandible that has a reticulate or 'foamy' appearance. Post-mortem examination confirmed that this was the result of osteomyelitis, although its radiographic appearance was similar to that of an odontoma, a reparative granuloma or an aneurysmal bone cyst.

Tumour-like lesions are also seen, including osseous cyst-like lesions, mycetoma and an intraosseous epidermoid cyst.

Temporomandibular joint degenerative joint disease

Degenerative joint disease of the temporomandibular joint is a poorly understood condition that can vary considerably in severity. Clinical signs can vary from bitting or performance problems to severe pain and swelling. The radiographic changes seen are similar to those seen in any other joint disease (see end of Chapter 1, 'Degenerative joint disease') and vary with aetiology. Infectious or traumatic arthritis may have proliferative new bone around the joint accompanied by bone lysis. The oblique anatomy of the joint may conceal mild or early lesions in horses with mild clinical symptoms. Ultrasonography may be more sensitive for detection of early periarticular osteophyte formation and for assessment of the meniscal cartilage. CT and MRI are useful for the complete assessment of these joints. In horses with osteoarthritis, these techniques may identify periarticular osteophyte formation, increased opacity of the subchondral bone, subchondral osseous cyst like lesions and misshapen mandibular condyles. The condition is very painful when advanced, resulting in dysphagia and weight loss. Arthroscopic

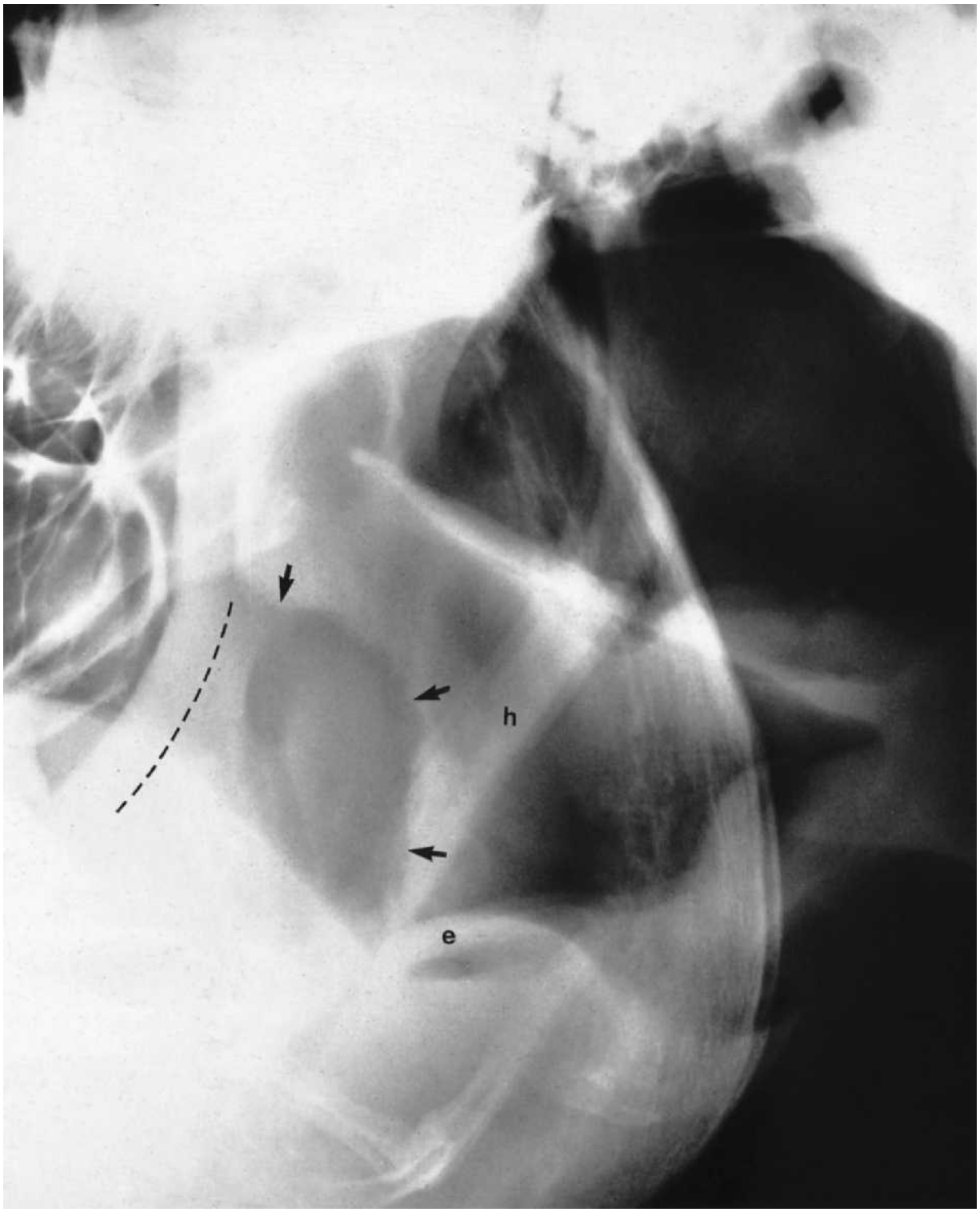


Figure 11.35 Slightly oblique right-left lateral radiograph of the skull of a 7-year-old Quarterhorse with a 3-month history of swelling in the region of the left mandible and difficulty in chewing. Rostral is to the left. There is a large lucent area (arrows) in the cranial angle of the left mandible. The bone adjacent to the margins of the defect appears lytic and irregular. The left stylohyoid bone (h) cannot be evaluated totally, but appears to be involved in the process. The approximate location of the normal cranial angle of the mandible is marked with a dotted line. The epiglottis (e) is normal. Post-mortem examination confirmed the presence of a squamous cell carcinoma.



Figure 11.36 Right-left lateral-lateral image of the rostral maxilla and mandible of a yearling Thoroughbred. Dorsal is to the left. A firm lump was noted on the rostral aspect of the left mandible 2 months previously. There is a large multiloculated expansile mass in the left mandible which is displacing the incisor teeth. The mass was excised surgically and histological examination revealed that this was fibrous dysplasia with reactive new bone, but no evidence of malignancy.

surgery may be useful in early cases. The prognosis for advanced cases of infectious arthritis is poor, although condylectomy has been described and may be beneficial.

Luxation of the temporomandibular joint

Temporomandibular joint luxation (Figure 11w.37) is usually the result of trauma and may occur unilaterally or bilaterally. There may be associated fractures. Oblique radiographic views may be required to separate the two joints. There is usually associated malocclusion of the molars. The radiographs should be inspected carefully for the presence of concurrent fractures.

Fractures

Fractures of the rostral aspect of the mandible are common, especially in foals and young horses (Figure 11.38). They frequently involve a fracture at, or immediately caudal to, the third incisor. They may result in one or more teeth being broken or torn from the body of the mandible, usually with some associated bone. Injuries may involve only one side, or both mandibles may be fractured. These fractures generally require surgical intervention, either



Figure 11.38 Intra-oral ventrodorsal image of the rostral mandible of a show pony. Right is to the left. There is a displaced fracture of the mandible involving the tooth roots of the right corner (103) and intermediate (middle, 102) incisors. Note that the root of the corner incisor is fractured.

to remove loose fragments or to stabilise the fracture by internal fixation or, more commonly, by intra-oral fixation using cerclage wire. They carry a good prognosis with surgical treatment, although some brachygnathia may result or develop with growth.

Fractures of the horizontal ramus of the mandible (Figure 11.39a) may occur at any point, although they frequently involve the interdental space. They generally respond to conservative treatment if unilateral, but some may benefit from internal fixation. Internal fixation may not be practical if the tooth roots are too closely involved with the fracture line, and in some cases in young horses the tooth roots may involve too much of the bone for fixation to be possible, although wiring adjacent teeth together may help give some increased stability to the jaw. Fractures of the horizontal ramus of the mandible often open into the oral cavity, with some risk of developing osteomyelitis.

Fractures of the vertical ramus of the mandible (Figure11.39b) are often best identified on the view previously described for examination of the cranium (see 'Cranium – Radiographic technique', above). They are usually unilateral and may be difficult to delineate. They may require several different exposures for complete evaluation. Internal fixation is not generally practical

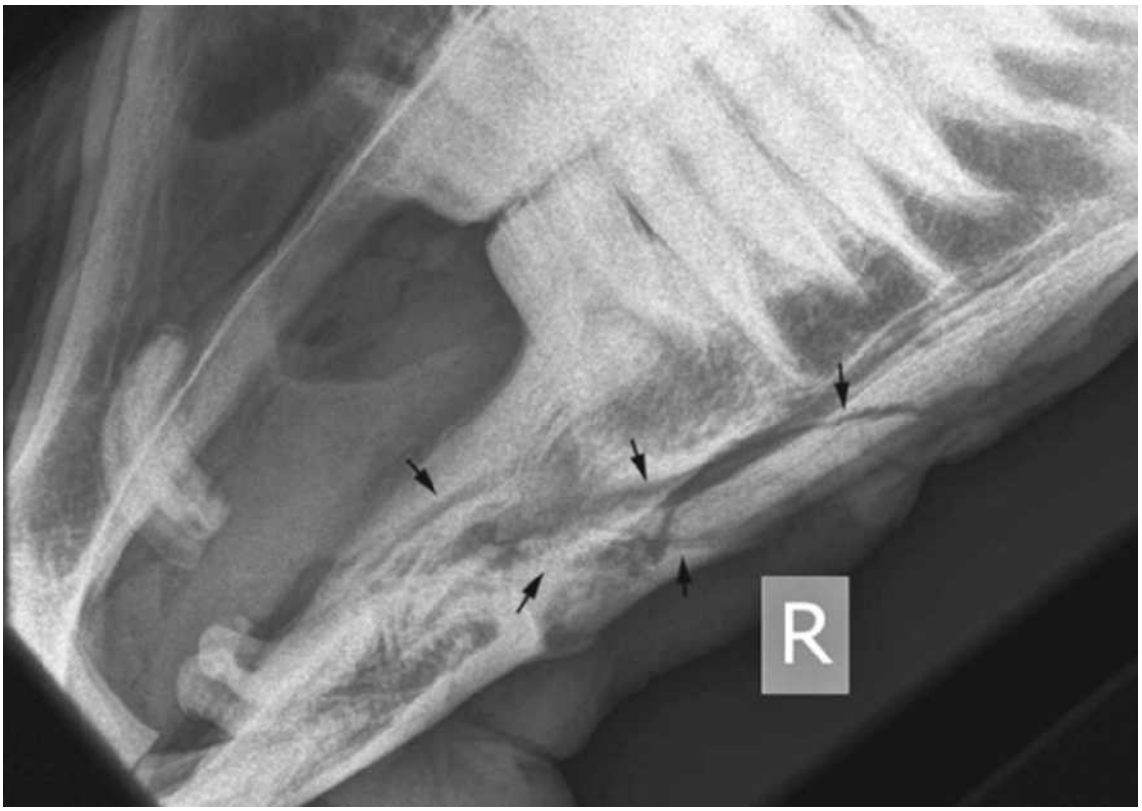


Figure 11.39(a) Lateral-lateral image of the rostral aspect of the head of a 16-year-old riding horse which had been kicked the previous day. Dorsal is to the left. The horse was dysphagic and there was a discharging wound. There is a comminuted fracture of the horizontal ramus of the mandible (arrows), with overlying soft tissue swelling. An intra-oral radiograph more accurately defined the degree of comminution of the fracture.

or necessary, because if the horse can feed adequately the fractures usually heal with conservative treatment. The prognosis is good, provided that the fracture does not enter the temporomandibular joint.

The radiographs should be carefully examined to exclude concurrent dislocation of the temporomandibular joint.

Sequestrum of the interdental space

The mandibular interdental space is relatively poorly covered by soft tissues and is potentially at risk to trauma from the bit. This may predispose it to sequestrum formation. Radiographically there are typical signs of sequestrum formation (see Chapter 1, 'Infectious osteitis and infectious osteomyelitis'), usually immediately rostral to the first premolar (Figure 11.40). Oblique views are necessary to separate the two horizontal rami of the mandible. This can be achieved by turning the horse's head slightly towards or away from the x-ray machine.

Clinical signs include depressed appetite, oral discomfort, slight swelling on the ventral and lateral aspects of the mandible, and sometimes a draining sinus. Surgical treatment carries a good prognosis.

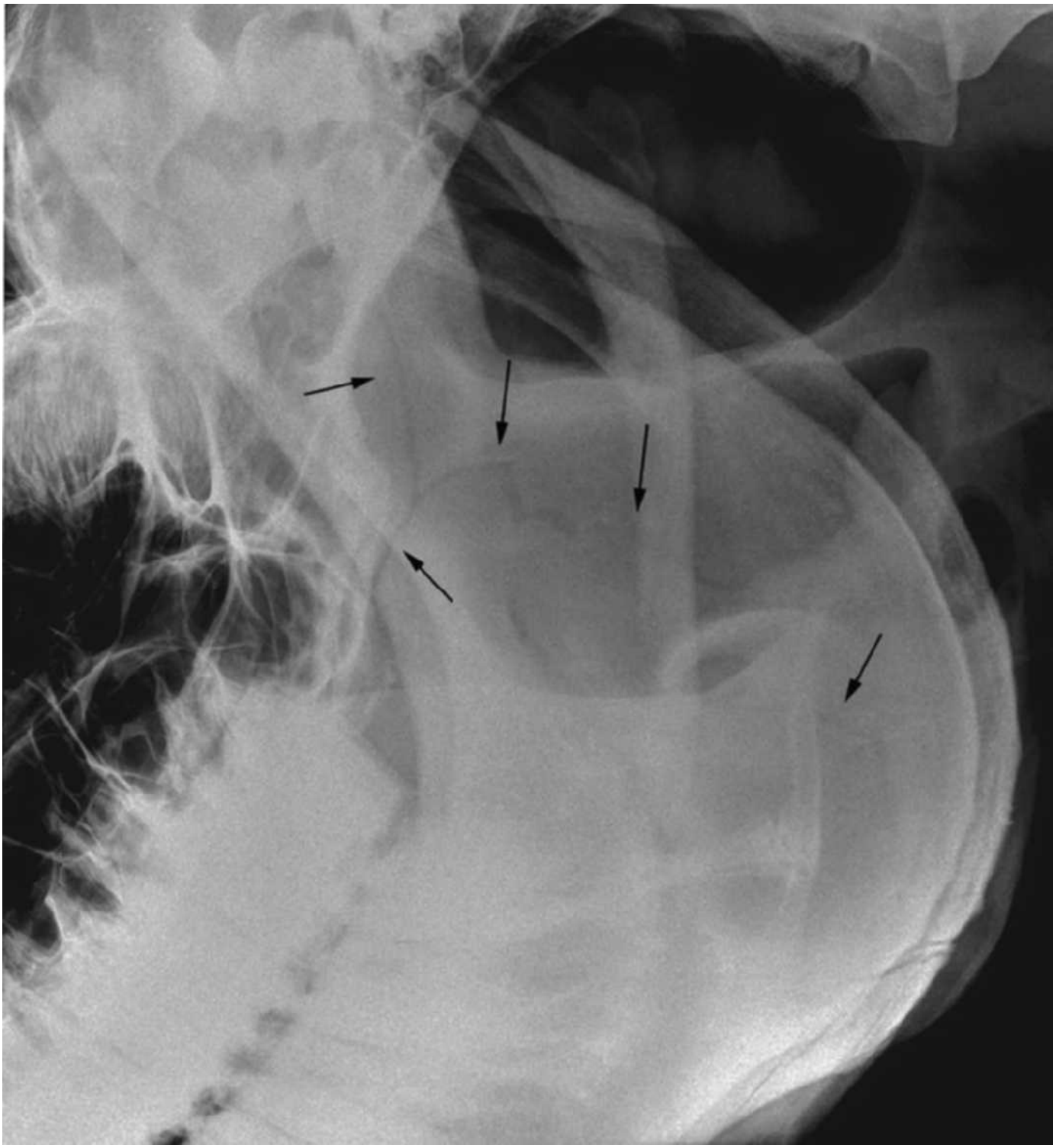


Figure 11.39(b) Slightly oblique lateral-lateral image of the mandibular region of a 14-year-old Arab which had fallen in the stable and showed bleeding from the mouth and nose. Rostral is to the left. There is a comminuted fracture of the vertical ramus of the mandible (arrows).

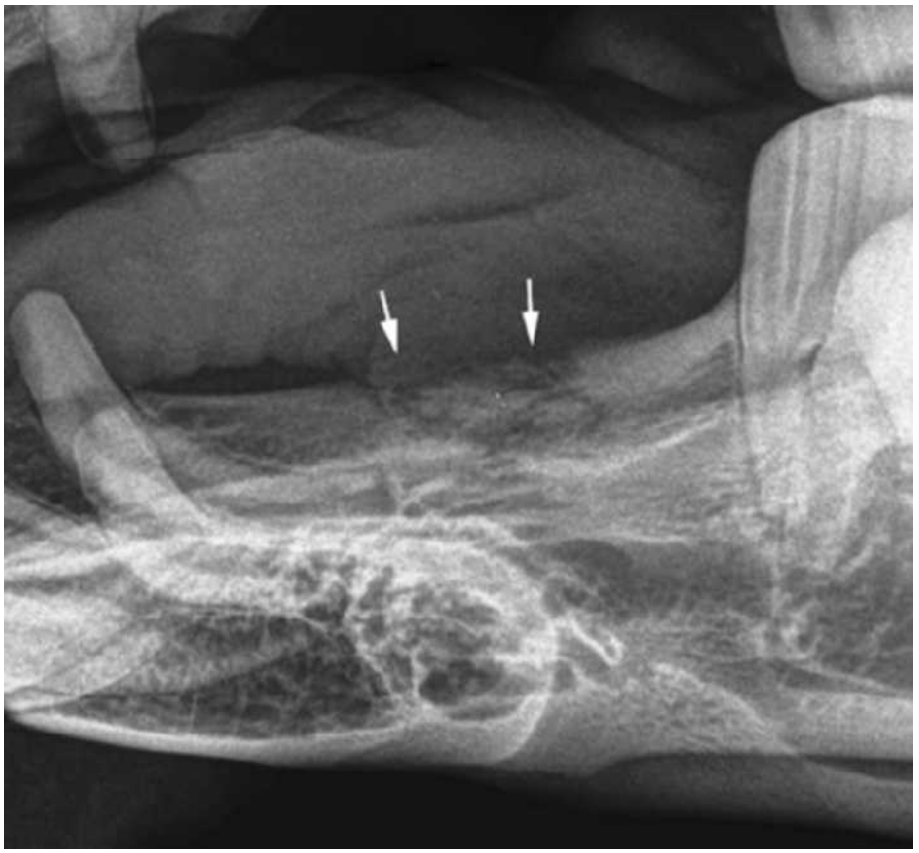


Figure 11.40 Slightly oblique lateral-lateral image of the horizontal ramus of the mandible of a 9-year-old Oldenburg who would not 'take the bit' on the right rein. Rostral is to the left. The dorsal cortex in the interdental space is poorly defined with loss of opacity (arrows), typical of a sequestrum.

Pharynx, larynx and Eustachian tube diverticulum

The pharyngeal area includes structures that are an integral part of the respiratory system and the reader may also want to refer to Chapter 14. Radiographs of this area permit assessment of the soft palate, epiglottis, hyoid apparatus, nasopharynx and Eustachian tube diverticulum (guttural pouch).

RADIOGRAPHIC TECHNIQUE

Lateral-lateral view

Evaluation of this area is almost always limited to lateral-lateral views, normally obtained with the horse standing. The x-ray beam is centered between the base of the ear and the angle of the mandible, and aligned at right angles to the midline of the head and the cassette. When the Eustachian tube diverticulum (guttural pouch) is being evaluated, it is often advantageous to obtain both right (left to right) and left (right to left) lateral-lateral radiographs in order to determine the side of involvement. Exposures appropriate for soft tissues should be used.

Ventrodorsal view

Although ventrodorsal images of this area can be acquired under sedation, this area is perhaps best and most safely examined under general anaesthesia. It is difficult to obtain ventrodorsal images without some degree of rotation. The horse is placed in dorsal recumbency and the head extended. The poll is placed on a small pad, so that the x-ray cassette can be placed in contact with the dorsal aspect of the skull, and be placed far enough caudally to visualise the Eustachian tube diverticulum and pharynx. The dorsoventral plane of the skull must be maintained vertical, in order that diagnostic radiographs are obtained. It may be necessary to reposition the head to obtain straight ventrodorsal views, as any obliquity results in loss of information on the radiograph. It may also be helpful in some cases to withdraw the endotracheal tube, if one is used, because this can mask abnormalities.

NORMAL ANATOMY, VARIATIONS AND INCIDENTAL FINDINGS

When examining radiographs of this area it is important to remember that the soft-tissue structures are constantly moving. Radiographs only indicate the position of the structure for a fraction of a second in the life of the patient, and must be interpreted on this basis. For this reason, assessment of the relationship of structures such as the soft palate or epiglottis to other structures must be interpreted with care (Figures 11.41a and 11.41b). Repeat radiographs of the same region can help provide confirmation of abnormal radiographic findings. Sedation can result in altered pharyngeal function; for

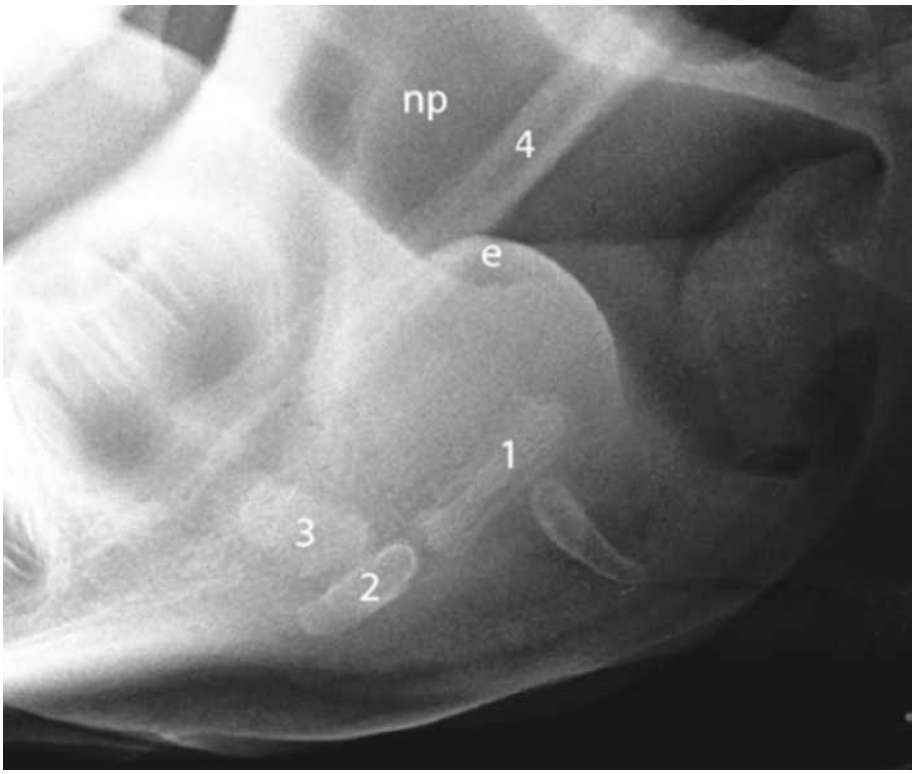


Figure 11.41(a) Well-collimated lateral-lateral image of a normal pharynx of an immature horse. Rostral is to the left. The nasopharynx (np) contains air. Note the epiglottis (e), thyrohyoid (1), basihyoid (2), ceratohyoid (3) and stylohyoid (4).

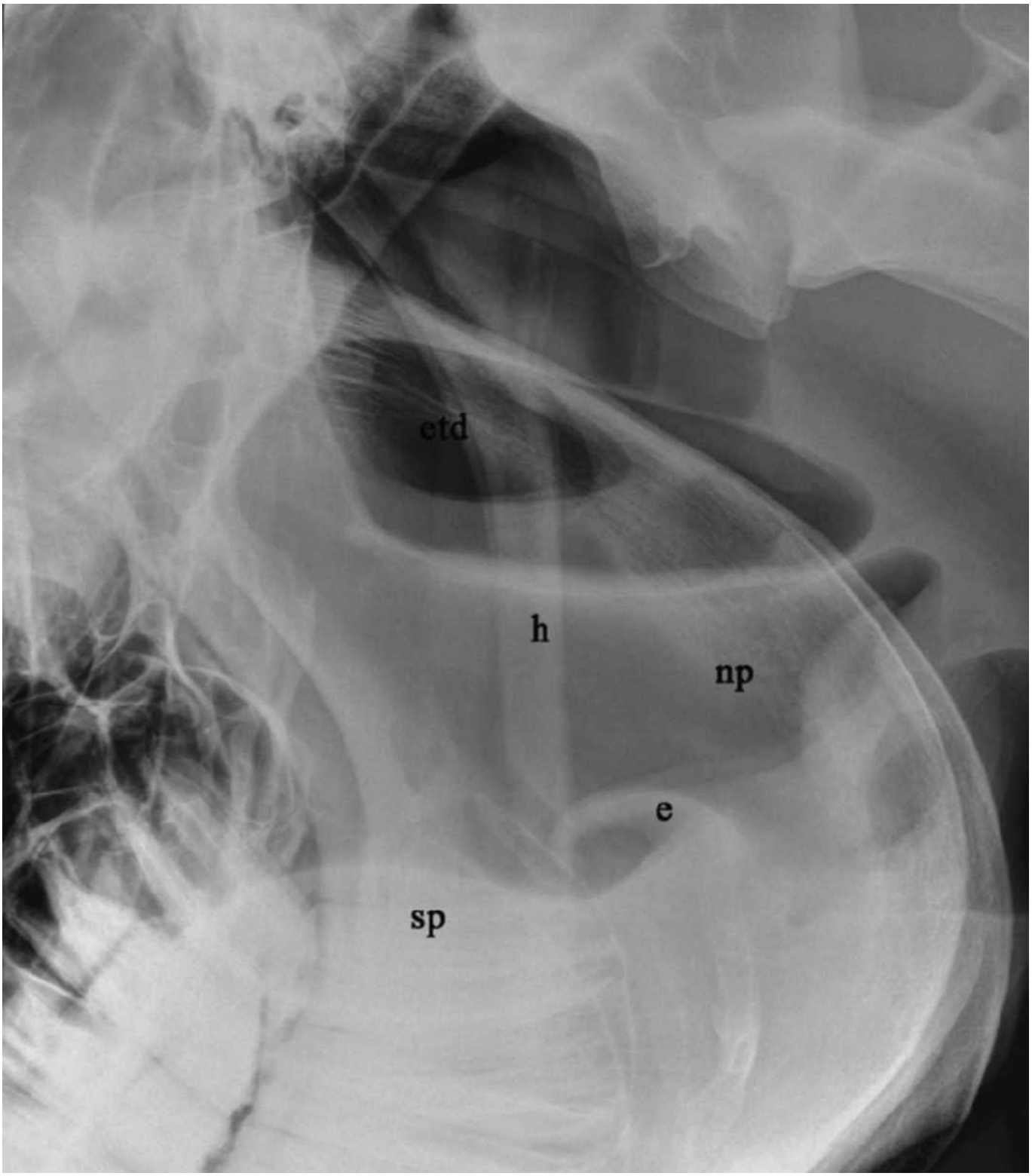


Figure 11.41(b) Slightly oblique lateral-lateral image and diagram of the pharyngeal region of a normal adult horse. Rostral is to the left. Note that the caudal angles of the left and right mandibles are slightly separated, indicating slight obliquity. There is gas in the Eustachian tube diverticulum (etd) and the nasopharynx (np). The epiglottis (e), soft palate (sp) and stylohyoid bones (h) are clearly demarcated.



Figure 11.41(b) *Cont'd* 1 = petrous temporal bone, 2 = external acoustic meatus, 3 = basioccipital bone, 4 = body of basisphenoid bone, 5 = pterygoid process, 6 = maxillary tuberosity, 7 = third upper molar tooth, 8 = third lower molar tooth, 9 = stylohyoid angle, 10 = stylohyoid, 11 = ceratohyoid, 12 = basihyoid, 13 = thyrohyoid, 14 = condyloid process of mandible, 15 = ramus of mandible, cranial edge, 16 = ramus of mandible, caudal edge, 17 = angle of mandible, 18 = mandibular foramen, 19 = mandibular canal, 20 = dorsal wall of pharynx, 21 = aryepiglottic fold, 22 = arytenoid cartilage, 23 = epiglottis, 24 = cranial wall of Eustachian tube diverticulum (guttural pouch), 25 = caudal wall of Eustachian tube diverticulum (guttural pouch), 26 = plica salpingopharyngea, 27 = laryngeal ventricles, 28 = soft palate, 29 = atlas (first cervical vertebra), 30 = dens, 31 = axis (second cervical vertebra).

example, dorsal displacement of the soft palate is common in horses receiving alpha-2 agonists as a sedative.

The most obvious structures on this view are the radiolucent Eustachian tube diverticula (guttural pouches) (Figure 11.41b). The dorsal aspect of the pouches is in contact with the base of the skull and the atlas. The caudal border lies approximately below the articulation of the atlas and axis. The ventral border forms the roof of the pharynx, and lies approximately level with the dorsal aspect of the arytenoid cartilages and the rostral aspect of the ethmoid bone. The ventral cranial third of the Eustachian tube diverticulum lies between the vertical rami of the mandible. The caudal and ventral borders of each Eustachian tube diverticulum are apparent as double lines, because the two pouches are seldom positioned exactly over one another on the radiograph. The greater cornua of the stylohyoid bones cross the diverticulum between the medial and lateral compartments.

The soft palate is at the rostral aspect of the pharynx. Rostrally it is seen caudal to the last upper molars, generally positioned about midway between the crown and root of the teeth. It follows a smooth S-shaped course over the back of the tongue, to lie under the epiglottis caudally. There is sometimes a small triangular area of air between the soft palate and the base of the tongue.

The epiglottis is clearly seen caudal to the last lower molar, the opening formed by the epiglottis and arytenoid cartilages forming a smooth continuation of the tracheal lumen into the nasopharynx. The epiglottis is markedly curved (dorsally convex), nearly forming a complete semicircle. Its base is approximately vertical, while the tip lies nearly at a right angle to the dorsal surface of the soft palate.

A small lucent gas shadow may be seen at the base of the epiglottis, in the trachea (the middle ventricle of the larynx), and two further lucent crescents are seen below the base of the arytenoid cartilages (the lateral ventricles).

The tracheal rings are clearly delineated. Dorsal to the trachea, immediately caudal to the tip of the arytenoid cartilage, a small lucent linear air shadow may occasionally be seen in the cranial part of the oesophagus. This should not extend more than 2–5 cm in length in a normal horse.

Mineralisation of the laryngeal cartilages, hyoid apparatus and tracheal rings may occur as a normal variation in some older horses.

SIGNIFICANT FINDINGS

Eustachian tube diverticulum empyema

Although probably becoming a less common condition, Eustachian tube diverticulum empyema may be seen in areas with a large population of horses. It usually follows a streptococcal infection, particularly *Streptococcus equi*. Clinically there is usually a unilateral purulent nasal discharge. Empyema may fill one or both pouches (Figure 11.42), giving an increase in radiopacity of the diverticulum. There is normally a fluid line in the diverticulum, which aids differentiation from a soft-tissue mass. It is possible to determine if the condition involves one or both pouches by obtaining ventrodorsal views. It may be easier, however, to obtain lateral-lateral radiographs from the left and right sides. The radiographs are compared for magnification and sharpness of

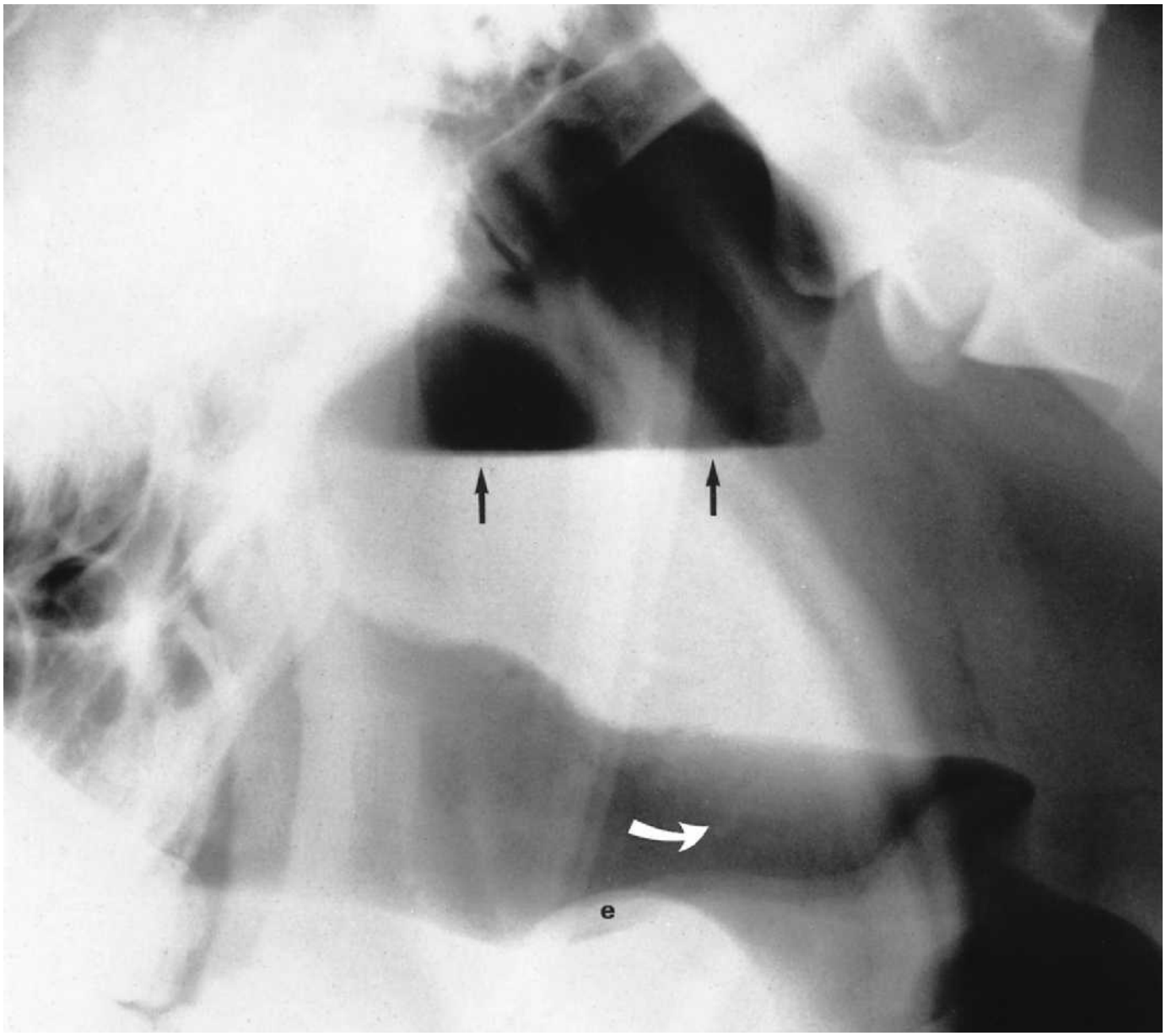


Figure 11.42 Lateral-lateral image of the pharyngeal region of a 2-year-old Thoroughbred with a history of nasal discharge and an occasional cough. Rostral is to the left. There is a fluid line (straight arrows) in one or both Eustachian tube diverticula. The ventral half of the diverticulum is uniformly opaque due to the accumulation of pus, i.e. empyema. In the original radiograph there was a clearly irregular outline of the dorsal pharyngeal wall and the fine mottled opacities (curved arrow) in the dorsal nasal pharynx which represented pharyngeal lymphoid hyperplasia, but this cannot be seen in this reproduction. The epiglottis (e) is normal.

the fluid line. The air cap appears larger and less sharp when away from the cassette. It is often possible to obtain a further radiograph with the nose of the horse elevated. This moves the fluid within the diverticulum and allows assessment of the thickness of the cranial ventral margins. The thickness of the diverticular walls at this point gives some indication of the nature of the fluid and the chronicity of the condition.

The condition should initially be treated conservatively, but surgical drainage may be needed. A reasonable prognosis can be given for early cases, but if surgery is required the prognosis is guarded.

Eustachian tube diverticulum chondrosis

Eustachian tube diverticulum chondrosis normally results from chronic empyema that has been inadequately treated. Clinical signs of nasal discharge may or may not persist after resolution of other signs of upper respiratory infection. If it occurs as a sequel to strangles, the horse may be a permanent carrier and potential shedder of *Streptococcus equi*. The chondroids seen on radiographs are smooth, irregularly shaped radiopaque masses within the diverticula (Figure 11.43). Although some cases are asymptomatic, removal of the chondroids may be indicated, especially if *Streptococcus equi* is cultured.

Eustachian tube diverticulum tympany

Tympany of the Eustachian tube diverticulum is most commonly seen in young animals. It generally presents clinically as a soft fluctuant swelling in the parotid area. In severe cases it may cause respiratory distress.



Figure 11.43 Lateral-lateral image of the pharyngeal region of an 8-year-old pony. Rostral is to the left. There are many well circumscribed opaque masses within the Eustachian tube diverticulum. These are chondroids, a sequel to *Streptococcus equi* infection.

Radiographically it presents as a grossly enlarged Eustachian tube diverticulum, extending caudal to the atlas (Figure 11.44). There is some rounding of the outline of the diverticulum and often narrowing of the nasopharynx. Generally the condition is unilateral so that two distinct diverticular outlines can be seen. Occasionally bilateral cases occur.

The condition may arise from the presence of excessive soft tissue at the pharyngeal orifice, which acts as a valve and allows air into the pouch during deglutition but does not allow for the exit of air. As a sequel to the condition, there may be respiratory distress due to narrowing of the pharynx, and in some cases aspiration pneumonia. For this reason, radiographs of the thorax should also be obtained. Cases may resolve spontaneously as the horse ages,

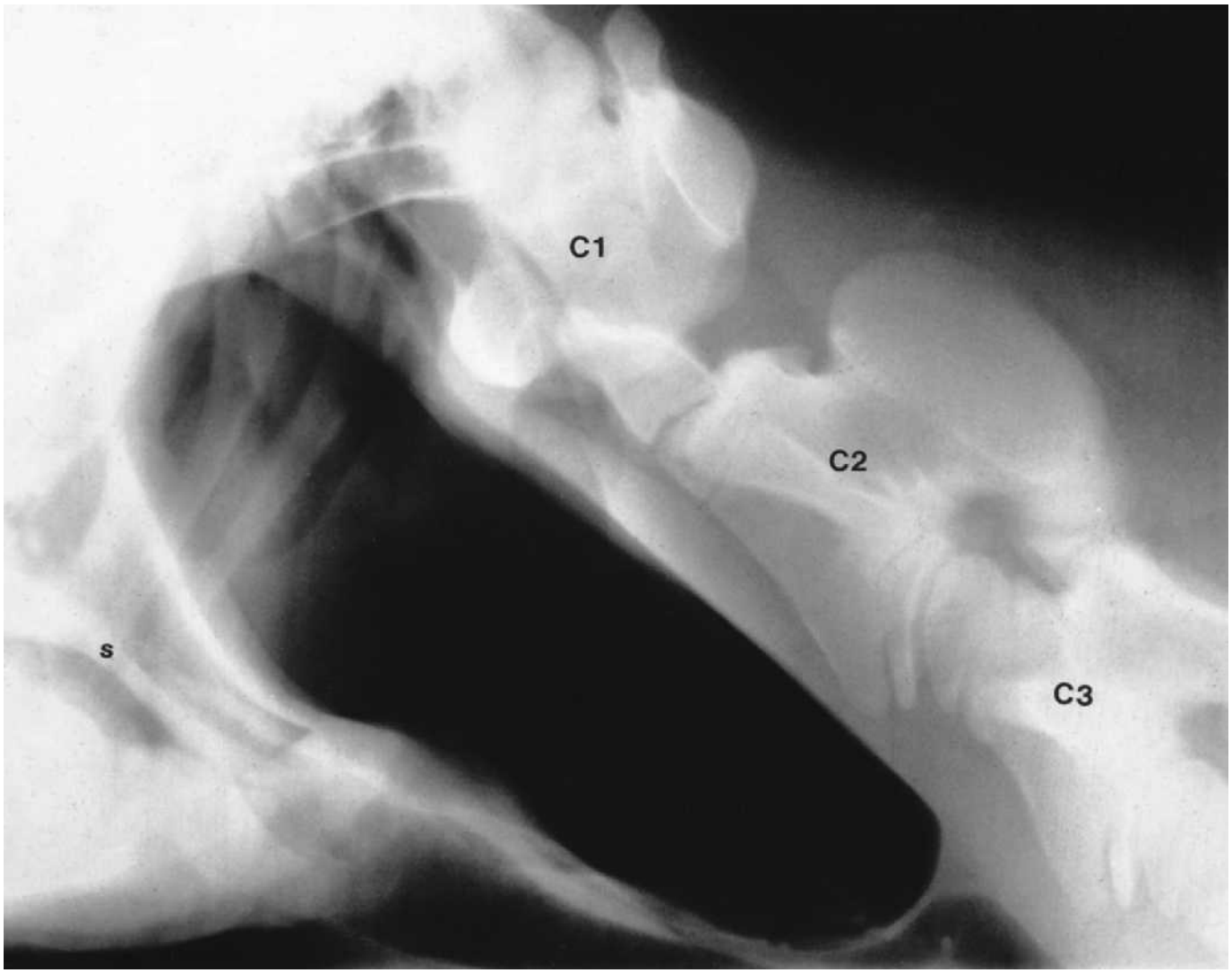


Figure 11.44 Right lateral-lateral image of the pharyngeal region of a 1-month-old Arab. Cranial is to the left. The soft tissues in the parotid region were noted to be enlarged soon after birth and progressively enlarged and became more fluctuant. Both Eustachian tube diverticula are markedly distended with gas (air) and extend caudally to the level of the middle of the third cervical vertebra (C_3). This is consistent with bilateral Eustachian tube diverticula tympany. Note also gas in the oesophagus just caudal to the distended diverticula. The soft palate (s) is delineated by air in the oropharynx. The epiglottis is flat against the soft palate.

but usually require treatment. This may simply mean placement of an indwelling catheter for several weeks, but some cases require surgery.

Eustachian tube diverticulum mycosis

Plain radiographs of the guttural pouch are generally unrewarding for the diagnosis of Eustachian tube diverticulum mycosis, which potentially causes haemorrhage. Fluid lines may be seen in the Eustachian tube diverticulum, or there may be no radiological abnormality on plain radiographs. This is a life-threatening condition, and angiography of the carotid tree may be useful in diagnosis and treatment (see Chapter 16, 'Angiography').

The condition can present as slight or massive spontaneous epistaxis, usually when at rest. In a minority of cases it may present as difficulty in deglutition, Horner's syndrome, or as other signs of damage to the cranial nerves. The condition is thought to result from mycotic infection of an aneurysm, which generally but not always involves the internal carotid artery.

Eustachian tube diverticulum masses

A number of masses are seen in association with the Eustachian tube diverticulum. The most common is enlargement of the parotid or retropharyngeal lymph nodes (Figure 11.45), which may impinge on the wall of the diverticulum and give the appearance of a mass involving the Eustachian tube diverticulum. Similarly, cysts and abscesses may result in this appearance.

Tumours of the pouch have been recorded, the most common being a squamous cell carcinoma and melanoma.

Pharyngeal lymphoid hyperplasia

Pharyngeal lymphoid hyperplasia is seen radiographically as a diffuse mottled increase in soft-tissue opacity of the pharyngeal wall. This is frequently recognised in racing Thoroughbreds, but may be a normal phenomenon in the development of all young horses. It may cause some respiratory noise and respiratory obstruction, but its effect on performance is uncertain. Treatment is by conservative management and the long-term prognosis is good.

Fracture of the hyoid apparatus

Fractures of the hyoid apparatus can occur as a result of external trauma, trauma applied via tongue traction, or secondary to osteomyelitis of the stylohyoid bone, followed by pathological fracture. Stylohyoid fracture can be identified on lateral-lateral radiographs, although slightly oblique views may be necessary to determine whether the left or right bone is involved. Fracture of the stylohyoid bone can also be seen in isolation (Figure 11.46). Computed tomography or MRI is generally necessary to identify fractures of other portions of the hyoid apparatus.

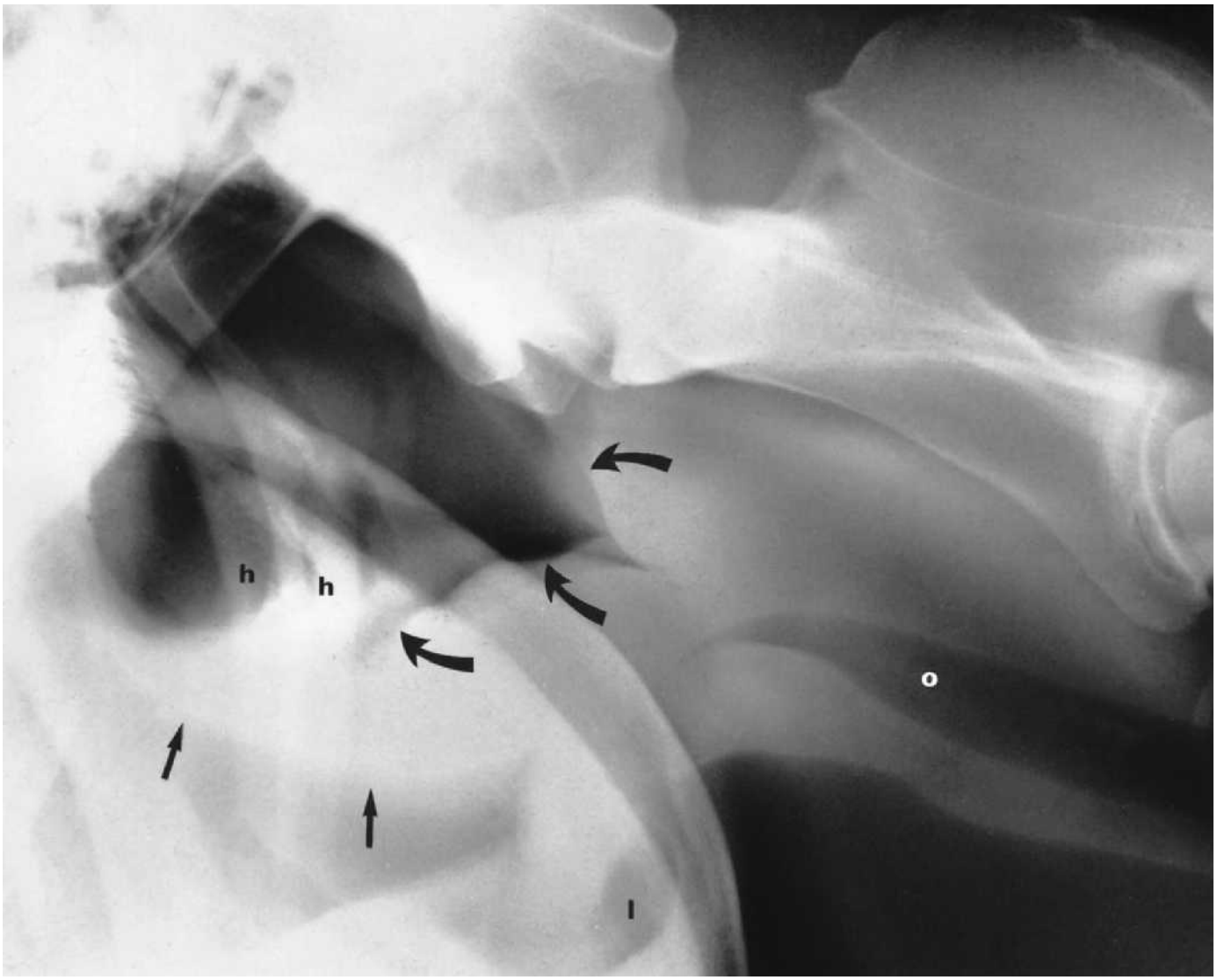


Figure 11.45 Lateral-lateral image of the pharyngeal region of a 4-year-old Quarterhorse with a 3-day history of dysphagia. Rostral is to the left. Clinical examination revealed eighth and ninth cranial nerve deficits and bilateral nasal discharge containing food. The ventral margins of the Eustachian tube diverticula (ETD) are irregular (straight arrows) and there is soft-tissue swelling in the retropharyngeal area impinging on the ventral caudal aspect of the ETD (curved arrows). There is air in the oesophagus (o) and the lateral saccules (l). The stylohyoid bones (h) are normal. The caudal ventral soft-tissue mass is due to retropharyngeal lymphadenopathy and local inflammation, caused by infection with *Streptococcus equi*. Compare with Figure 11.43.

Epiglottic entrapment

With epiglottic entrapment the apex and lateral margins of the epiglottis become enveloped by the ventral mucosa and aryepiglottic folds (Figure 11.47). The radiographic appearance is varied, but the epiglottis always appears blunted and shortened. It should be confirmed by endoscopy and must be differentiated from epiglottic shortening (see below). There may be concurrent dorsal displacement of the soft palate, but this is inconsistent.

Clinically the horse shows exercise intolerance and abnormal respiratory sounds at high speeds, but is asymptomatic at rest. Treatment is surgical and there is a reasonable prognosis.

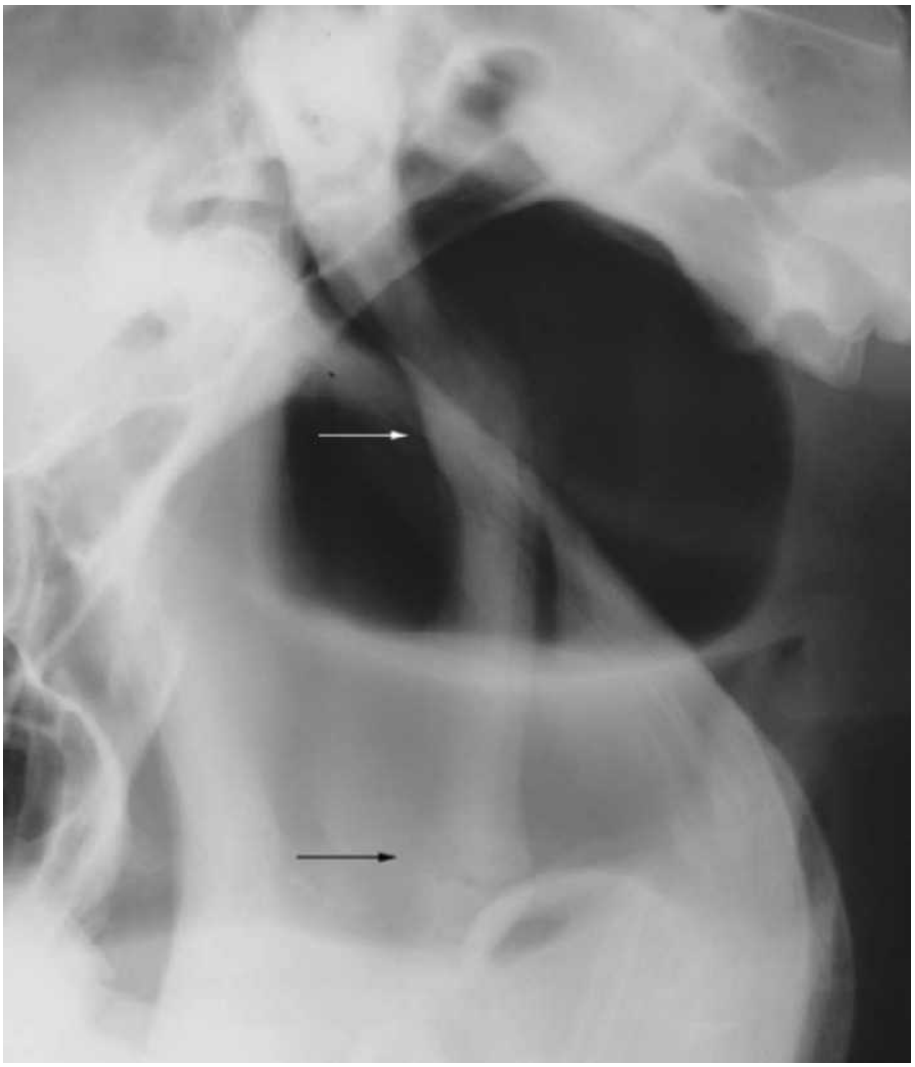


Figure 11.46 Lateral-lateral radiograph of the pharyngeal region of a 15-year-old Quarterhorse. Rostral is to the left. The mare had exhibited transient facial nerve paralysis 12 months previously, which had recently recurred. There is bony proliferation on the stylohyoid (white arrow). Such bony proliferation may be visible endoscopically via the guttural pouch. There is also a pathological, delayed union fracture with callus further distally (black arrow), which is unable to heal due to constant movement of the stylohyoid bone. Note the flaring of the ends of the bone at the fracture site (black arrow) and slight increased opacity along the fracture margins, typical of a delayed union. A normal epiglottis is partially superimposed over the distal fracture piece.

Epiglottic shortening

Abnormal shortness of the epiglottis may predispose to dorsal displacement of the soft palate or entrapment of the epiglottis by the aryepiglottic folds. The length of the epiglottis can only be assessed objectively on radiographs by taking magnification into account. Radiodense markers of known length (A*l* and A*r)* must be taped to the right and left sides of the horse's neck. The length of these markers on a lateral-lateral radiograph should be measured (R*l* and R*r*), together with the distance between the tip of the epiglottis and the thyroid cartilage (R*e*). The formula for correction for magnification to determine the actual epiglottic length (A*e*) is as follows:

$$Ae / Re = \left(Al / Rl + Ar / Rr\right) / 2$$

Normal values have been recorded for the Thoroughbred (8.76 ± 0.44 cm) and Standardbred (8.74 ± 0.38 cm).

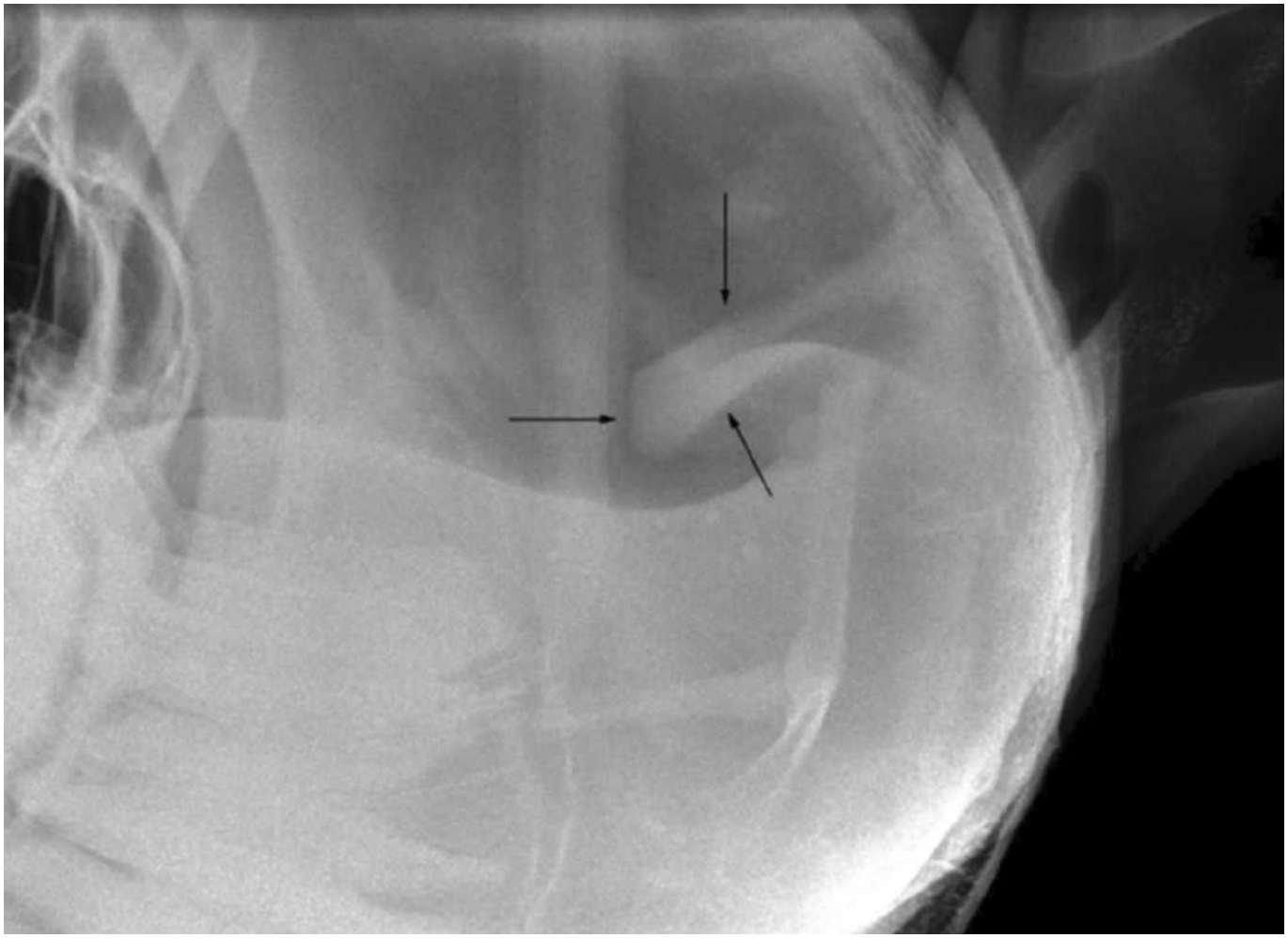


Figure 11.47 Lateral-lateral image of the pharynx of an 11-year-old Thoroughbred with a history of persistent salivation and food reflux. Rostral is to the left. There is entrapment of the epiglottis by the aryepiglottic folds (arrows). Endoscopic examination revealed marked thickening and ulceration of the aryepiglottic folds, and confirmed entrapment of the epiglottis. There was also moderate, diffuse pharyngitis. There is some ill-defined mineralisation within the arytenoid cartilages.

A horse with an abnormally short epiglottis is usually asymptomatic at rest, but may show exercise intolerance and make an abnormal respiratory noise at high-speed exercise.

Sub-epiglottic cysts

Sub-epiglottic cysts are believed to arise from remnants of the thyroglossal duct (Figures 11.48a and 11.48b). They are well-circumscribed radiopaque (soft-tissue) masses under the ventral aspect of the base of the epiglottis which displace the epiglottis in a caudodorsal direction. Treatment is surgical and the prognosis is reasonable.

Arytenoid chondritis

Arytenoid chondritis causes exercise intolerance and abnormal respiratory noise. The arytenoid cartilages may have a mottled increase in opacity or an irregular outline, particularly of the cranial margin of the cartilage

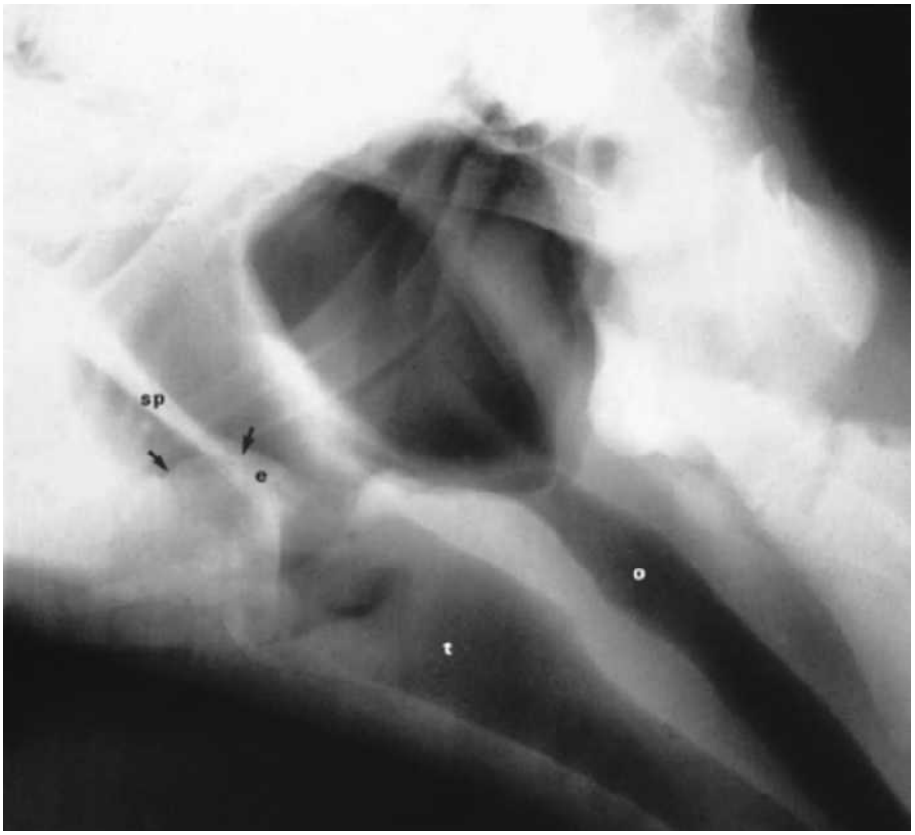


Figure 11.48(a) Lateral-lateral image of the pharyngeal region of a 1-month-old Standardbred colt, with a history of dyspnoea following suckling or strenuous exercise. Rostral is to the left. There is a smoothly outlined soft-tissue opacity (arrows), ventral to the epiglottis (e), in the oropharynx. The mass, a subepiglottic cyst, appears to displace the soft palate (sp) dorsally above the epiglottis, but the area between the soft palate, epiglottis and subepiglottic cyst cannot be defined. Note air in the oesophagus (o) and the trachea (t).

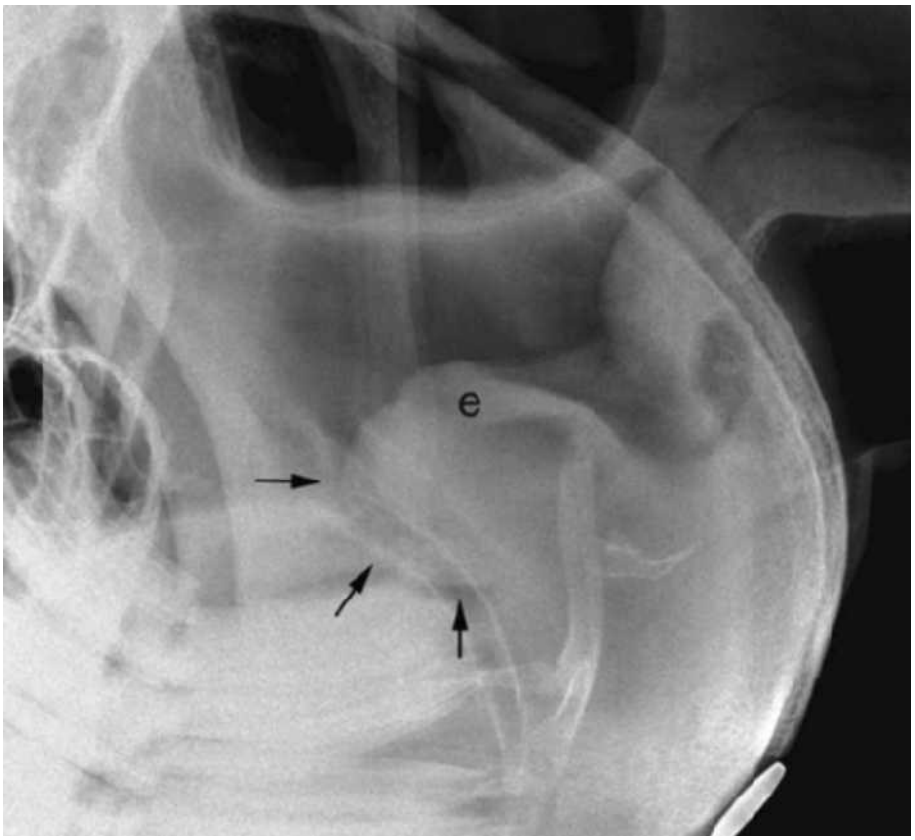


Figure 11.48(b) Lateral-lateral radiographic view of the pharynx of a 6-year-old Thoroughbred cross Cob with a 4-month history of coughing and reflux of food. Rostral is to the left. There is a large radiopaque mass (arrows) ventral to the epiglottis (e), a subepiglottic cyst.



Figure 11.49 Lateral-lateral image of the pharyngeal region of an 11-year-old hunter with a history of exercise intolerance and an abnormal respiratory noise. Rostral is to the left. Endoscopic examination of the larynx revealed distortion in shape of the arytenoid cartilages, i.e. arytenoid chondropathy (chondritis). Radiographically there is extensive well-defined soft-tissue swelling (arrows) on the craniodorsal aspect of the larynx. There is some ill-defined mineralisation within the arytenoid cartilages (arrowheads).

(Figure 11.49). They may also have some mineralisation, which may occasionally be seen incidentally in old animals, where there is more generalised involvement throughout the laryngeal cartilages (Figure 11w.50). Ultrasonography of the larynx reveals enlargement and changes in echogenicity (hyperechogenicity) of the arytenoid cartilage. If the condition is unilateral in a breeding horse it may be treated conservatively, but surgery is usually required to return a horse to athletic function or if the condition is bilateral.

Other laryngeal disorders

Radiography is not generally useful for the diagnosis of recurrent laryngeal hemiplegia or laryngeal dysplasia. Ultrasonography, MRI and CT can identify abnormalities (atrophy) of the cricoarytenoideus lateralis (ultrasonography) and cricoarytenoideus dorsalis (MRI and CT) muscles, abnormalities associated with recurrent laryngeal neuropathy. Ultrasonography and MRI demonstrate laryngeal dysplasia through the characterisation of abnormal laryngeal anatomy.

Dorsal displacement of the soft palate

Dorsal displacement of the soft palate may be intermittent or persistent, with the soft palate located dorsal to the epiglottis (Figure 11.51). The presence of air between the tongue and soft palate is usually the first radiographic

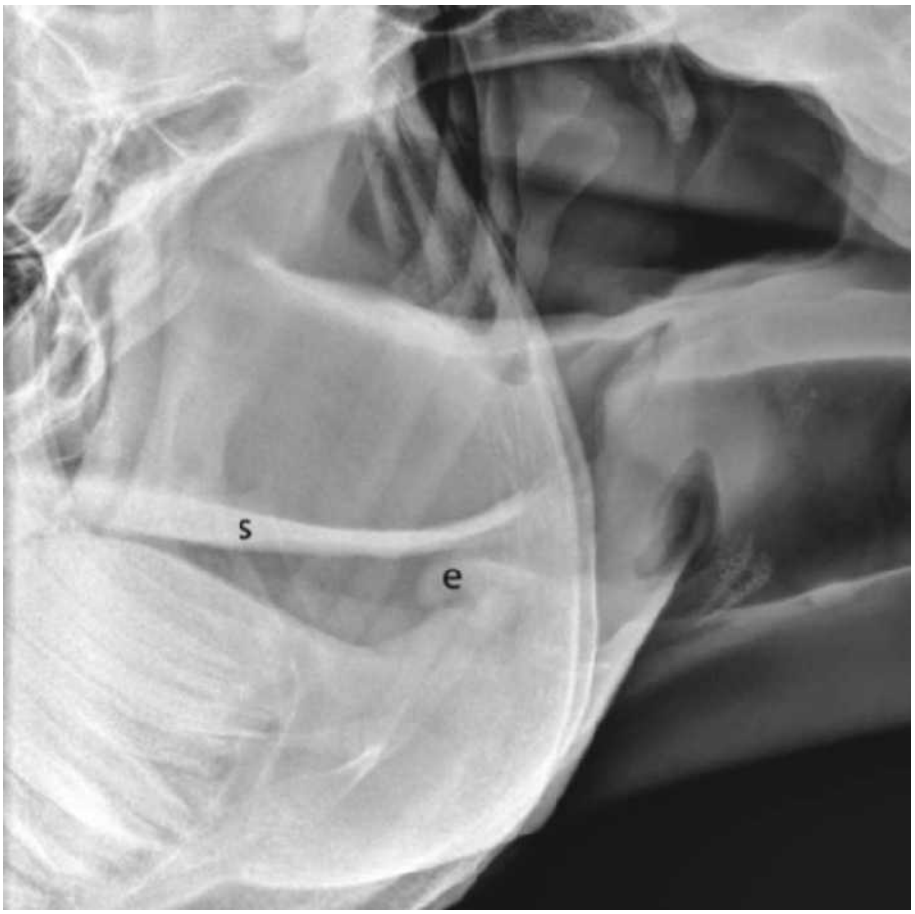


Figure 11.51 Lateral-lateral image of the pharyngeal region of an aged Thoroughbred. Rostral is to the left. The soft palate (s) is displaced dorsal to the epiglottis (e).

abnormality noticed. Careful examination of the radiograph may show the caudal part of the soft palate lying over the epiglottis. This is a dynamic condition and so may not be seen on plain radiographs. It is most likely to be demonstrated immediately after the horse swallows and may be more easily confirmed by endoscopy. This condition has been reported in horses that have shown no clinical signs of exercise intolerance.

Cleft palate

Cleft palate is most commonly seen in foals, but may not be diagnosed in some animals until quite late in life. Careful evaluation of lateral-lateral radiographs may reveal the presence of a double soft palate image. Positive contrast studies (barium swallows; see Chapter 15, 'Oesophagus – Contrast examination of the oesophagus') may reveal the presence of contrast medium dorsal to the soft palate (Figure 11w.52). If clinically significant, horses with a cleft palate frequently develop aspiration pneumonia, so radiographic assessment of the thorax should also be carried out.

Confirmation of the diagnosis by endoscopy is necessary to determine the extent of the cleft. In mild cases, conservative treatment is often sufficient. In more extensive cases, surgery may be necessary but does carry a very guarded prognosis.

Multilobular osteoma (chondroma rodens)

Multilobular osteoma is not common, but has a characteristic radiographic appearance. It is a well-defined mass with clearly demarcated undulating borders and a homogeneous stippled internal radiopacity. Clinical signs depend on the location of the mass in the skull. The mass usually enlarges slowly. Surgical removal is indicated.

Aneurysmal bone cyst

Aneurysmal bone cysts are rare in the horse, but have been reported in the mandible and the long bones. The lesion is characterised radiographically by an expansile relatively lucent lesion, traversed by opaque incomplete septa. The overlying cortex is thinned and there is usually extensive periosteal new bone formation. Surgical debridement and bone grafting can be attempted.

Additional figures

The book companion website at www.clinical-radiology-horse.com includes additional figures that are not included in the printed book or e-book formats. Please see '**About the Companion Website**' at the start of the book for details on how to access the website. These figures are prefixed with the letter 'w' in the printed book, e.g. Figures 1w.4c–f.

FURTHER READING

NORMAL ANATOMY

Ackerman, N., Coffman, J. Corley, E.A. (1974) The sphenooccipital suture of the horse: its normal radiographic appearance. *J. Am. Vet. Rad. Soc.* **15**, 79–81

Arenchibia, A., Vazquez, J., Jaber, R., et al. (2000) Magnetic resonance imaging and cross-sectional anatomy of the normal equine sinuses and nasal passages. *Vet. Radiol. Ultrasound* **41**, 313–319

Bahar, S., Bolat, D., Dayan, M.O., Paksoy, Y. (2014). Two and three-dimensional anatomy of paranasal sinuses in Arabian foals. *J. Vet. Med. Sci.* **76**, 37–44

Brinkschulte, M., Bienert-Zeit, A., Lupke, M., et al. (2014). The sinonasal communication in the horse: examinations using computerized three-dimensional reformatted renderings of computed-tomography datasets. *BMC Vet. Res.* **10**, 72

Brinkschulte, M., Bienert-Zeit, A., Lupke, M., Hellige, M., Staszyk, C., Ohnesorge, B. (2013) Using semi-automated segmentation of computed tomography datasets for three-dimensional visualization and volume measurements of equine paranasal sinuses. *Vet. Radiol. Ultrasound* **54**, 582–590

Carmalt, J., Kneissi, S., Rawlinson, J., et al. (2016) Computed tomographic appearance of the temporomandibular joint in 1018 asymptomatic horses: a multi-institution study. *Vet. Radiol. Ultrasound* **57**, 237–245

Cook, W. (1973) The auditory tube diverticulum (guttural pouch) in the horse. Its radiographic examination. *J. Am. Vet. Rad. Ass.* **14**, 51–71

D'Aout, C., Nisolle, J., Navez, M., et al. (2014) Computed tomography and magnetic resonance anatomy of the normal orbit and eye of the horse. *Anat Histol. Embryol.* doi: 10.1111/ahe. 12149

De Zani, D., Borgonovo, S., Biggi, M., et al. (2010) Topographic comparative study of paranasal sinuses in adult horses by computed technology, sinuscopy, and sectional anatomy. *Vet. Res. Commun.* **34**, S13–16

Finnegan, C., Townsend, N., Barnett, T., Barakzi, S. (2011) Radiographic identification of the equine ventral conchal bulla. *Vet. Rec.* **169**, 683

Ebling, A., McKnight, A.L., Seiler, G., Kircher, P. (2009) A complementary radiographic projection of the equine temporomandibular joint. *Vet. Radiol. Ultrasound* **50**, 385–91

Gibbs, C., Lane, J.G. (1987) Radiographic examinations of the facial, nasal and paranasal sinus regions of the horse. (ii) Radiological findings. *Equine Vet. J.* **19**, 474–482

Lacombe, V., Sogaro-Robinson, C., Reed, S. (2010) Diagnostic utility of computed tomography imaging in equine intracranial conditions. *Equine Vet. J.* **42**, 393–399

Latimer, C., Wyman, C., Dresem, C., Burt, J. (1984) Radiographic and gross anatomy of the nasolacrimal duct of the horse. *Am. J. Vet. Res.* **46**, 451–458

Morrow, K., Park, R., Spurgeon, T., Stashak, T., Arceneaux, B. (2000) Computed tomographic imaging of the equine head. *Vet. Radiol. Ultrasound* **41**, 491–498

Nykamp, S., Scrivani, P., Pease, A. (2004) Computed tomography dacrocystography evaluation of the nasolacrimal apparatus. *Vet. Radiol. Ultrasound* **45**, 23–28

Ramzan, P., Marr, C., Meehan J., Thompson, A. (2008) Novel oblique radiographic projection of the temporomandibular articulation of horses. *Vet. Rec.* **162**, 714–716

Smallwood, J., Wood, B., Taylor, W., Tate, L. (2002) Anatomic reference for computed tomography of the head of a foal. *Vet. Radiol. Ultrasound* **43**, 99–117

Stilson, A.E., Hening, D.S., Robertson, J.T. (1985) Contribution of the nasal septum to the radiographic anatomy of the equine nasal cavity. *J. Am. Vet. Med. Ass.* **186**, 590–592

Townsend, N., Cotton, J.C., Barakzai, S. (2009) A tangential radiographic projection for investigation of the equine temporomandibular joint. *Vet. Surg.* **38**, 601–606

TUMOURS AND CYSTS

Acland, H.M., Orsini, J.A., Elkins, S., Lee, J.W., Lein, D.H., Morris, D.D. (1984) Congenital ethmoid carcinoma in a foal. *J. Am. Vet. Med. Ass.* **184**, 979–981

Camus, A., Burba, D., Valdes, M., Taylor, H. (1996) Intraosseous epidermoid cyst in a horse. *J. Am. Vet. Med. Ass.* **209**, 632–633

Cissel, D., Wisner, E., Textor, J., Mohr, F., Scrivani, P., Theon, A. (2012) Computed tomographic appearance of equine sinonasal neoplasia. *Vet Radiol. Ultrasound* **53**, 245–251

Dixon, J., Smith, K., Sherlock, C., et al. (2016) Computed tomographic appearance of melanomas in the equine head. *Vet. Radiol. Ultrasound* **57**, 246–252

Naylor, R., Dunkel, B., Dyson, S., Paz-Penuelas, M., Dobson, J. (2010) A retrobulbar meningioma as a cause of unilateral exophthalmus and blindness in a horse. *Equine Vet. Educ.* **22**, 503–510

Robert, M.C., Groenendyk, S.L., Kelly, W.R. (1978) Ameloblastic odontoma in a foal. *Equine Vet. J.* **10**, 91–93

Stephenson, R. (2005) An unusual case of headshaking caused by a premaxillary bone cyst. *Equine Vet. Educ.* **17**, 79–82

Walker, M., Schumacher, J., Schmitz, D., et al. (1998) Cobalt 60 radiotherapy for treatment of squamous cell carcinoma of the nasal cavity and paranasal sinuses in three horses. *J. Am. Vet. Med. Ass.* **212**, 848–851

Woodford, N., Lane, J. (2006) Long-term retrospective study of 52 horses with sinonasal cysts. *Equine Vet. J.* **38**, 198–202

FRACTURES

Anderson, J., Hecht, S., Kalck, K.A. (2012) What is your diagnosis? Skull fracture in a foal. *J. Am. Vet. Med. Assoc.* **241**, 181–183

Gerding, J., Clode, A., Gilger, B.C., Montgomery, K. (2014) Equine orbital fractures: a review of 10 cases (2006–2013). *Vet. Ophthalmol.* **17**, 97–106

Henninger, R., Beard, W., Schneider, R., Bramlage, L., Burkhardt, H. (1999) Fractures of the rostral portion of the mandible in horses: 89 cases (1979–1997). *J. Am. Vet. Med. Ass.* **214**, 1648–1652

Lim, C., Saulez, M.N., Viljoen, A., Carstens, A. (2013) Basilar skull fracture in a Thoroughbred colt: radiography or computed tomography? *J. S. Afr. Vet. Assoc.* **84**, E1–5

Lischer, C., Walliser, U., Witzmann, P., Wehrlieser, M., Ohlerth, S. (2005) Fracture of the paracondylar process in four horses: advantages of CT imaging. *Equine Vet. J.* **37**, 483–487

Pownder, S., Scrivani, P.V., Bezuidenhout, A., Divers, T.J., Ducharme, N. (2010) Computed tomography of temporal bone fractures and temporal region anatomy in horses. *J Vet. Intern. Med.* **24**, 398–406

Ramirez, O., Jorgensen, J., Thrall, D. (1998) Imaging basilar skull fractures in the horse: a review. *Vet. Radiol. Ultrasound* **39**, 391–395

TEETH

Barakzai, S., Dixon, P. (2003) A study of open-mouthed oblique radiographic projections for evaluating lesions of the erupted (clinical) crown. *Equine Vet. Educ.* **15**, 143–148

Caldwell, L. (2006) A review of diagnosis, treatment and sequelae of incisor-luxation fractures in horses (from a dentist's point of view). *Proc. Am. Ass. Equine Pract.* **52**, 559–564

Carmult, J. (2003) Understanding the equine diastema. *Equine Vet. Educ.* **15**, 34–37

Dacre, I., Kempson, S., Dixon, P. (2007) Equine idiopathic cheek tooth fractures. Part 1: Pathological studies on 35 fractured cheek teeth. *Equine Vet. J.* **39**, 310–321

Dixon, P., Tremaine, H., Pickles, K., et al. (1999) Equine dental disease Part 1: a long-term study of 400 cases: disorders of incisor, canine and first premolar teeth. *Equine Vet. J.* **31**, 369–377

Dixon, P., Tremaine, H., Pickles, K., et al. (1999) Equine dental disease Part 2: a long-term study of 400 cases: disorders of development and eruption and variations in position of the cheek teeth. *Equine Vet. J.* **31**, 519–528

Dixon, P., Tremaine, H., Pickles, K., et al. (2000) Equine dental disease Part 3: a long-term study of 400 cases: disorders of wear, traumatic damage and idiopathic fractures, tumours and miscellaneous disorders of the cheek teeth. *Equine Vet. J.* **32**, 9–18

Dixon, P., Tremaine, H., Pickles, K., et al. (2000) Equine dental disease Part 4: a long-term study of 400 cases: apical infections of cheek teeth. *Equine Vet. J.* **32**, 182–194

Dixon, P., Dacre, I., Tremaine, H., McCann, J., Barakzai, S. (2005) Standing oral extraction of cheek teeth in 100 horses (1998–2003). *Equine Vet. J.* **37**, 105–112

Dixon, P., Barakzai, S., Collins, N., Yates, J. (2007) Equine idiopathic cheek tooth fractures: Part 3. *Equine Vet. J.* **39**, 327–333

Earley, E., Rawlinson, J. (2013) A new understanding of oral and dental disorders of the equine incisor and canine teeth. *Vet. Clin. North Am.: Equine Pract*. **29**, 273–300

Easley, J., Freeman, D. (2013) New ways to diagnose and treat equine dental-related sinus disease. *Vet. Clin. North Am.: Equine Pract*. **29**, 467–485

Gayle, J., Redding, W., Vacek, J., Bowman, K. (1999) Diagnosis and surgical treatment of periapical infection of the third mandibular molar in five horses. *J. Am. Vet. Med. Ass.* **215**, 829–832

Gibb, S. (2000) Dental imaging. In: *Equine dentistry*. Eds. Baker, G., Easley, J., pp. 220–249 W.B. Saunders, Philadelphia

Gift L., DeBowes, R., Clem, M., Rasmir-Raven, A., Nyrop, K. (1992) Brachygnathia in horses: 20 cases (1979–1989). *J. Am. Vet. Med. Ass.* **200**, 715–719

Quinn, G., Tremaine, H., Lane, J. (2005) Supernumerary cheek teeth (n = 24): clinical features, diagnosis, treatment and outcome in 15 horses. *Equine Vet. J.* **37**, 505–509

Prichard, M., Hackett, R., Erb, H. (1992) Long-term outcome of tooth repulsion in horses – a retrospective study of 61 cases. *Vet. Surg.* **21**, 145–149

Robert, M.C., Groenendyk, S.L., Kelly, W.R. (1978) Ameloblastic odontoma in a foal. *Equine Vet. J.* **10**, 91–93

Robert, M., Gangl, M.C., Lepage, O. (2010) A case of facial deformity due to bilateral developmental maxillary cheek teeth displacement in an adult horse. *Can. Vet. J.* **51**, 1152–1156

Selberg, K., Easley, J. (2013) Advanced imaging in equine dental disease. *Vet. Clin. North Am.: Equine Pract*. **29,** 397–409

Taylor, L., Dixon, P. (2007) Equine idiopathic cheek teeth fractures: Part 2: A practice based survey of 147 affected horses in Britain and Ireland. *Equine Vet. J.* **39**, 322–326

Weller, R., Livesey, L., Maierl, J., et al. (2001) Comparison of radiography and scintigraphy in the diagnosis of dental disorders in the horse. *Equine Vet. J.* **33**, 49–58

PARANASAL SINUSES

Beard, W., Hardy, J. (2001) Diagnosis of conditions of the paranasal sinuses in the horse. *Equine Vet. J.* **13**, 265

Beard, W., Robertson, J., Leeth, B. (1990) Bilateral congenital cysts in the frontal sinuses of a horse. *J. Am. Vet. Med. Ass.* **196**, 453–454

Behrens, E., Schumacher, J., Morris, E. (1991) Contrast paranasal sinusography for evaluation of disease of the paranasal sinuses of five horses. *Vet. Radiol.* **32**, 105–109

Dixon, P., Froydenlund, T., Luiti, T., Kane-Smyth, J., Horbal, A., Reardon, R. (2014) Empyema of the nasal conchal bulla as a cause of chronic unilateral nasal discharge in the horse: 10 cases (2013–2014). *Equine Vet J.* doi: 10.1111/evj.12322

Dixon, P., Parkin, T., Collins, N., et al. (2012) Equine paranasal sinus disease: a long-term study of 200 cases (1997–2009): ancillary diagnostic findings and involvement of the various sinus compartments. *Equine Vet. J.* **44**, 267–271

Easley, J., Freeman, D. (2013) New ways to diagnose and treat equine dental-related sinus disease. *Vet. Clin. North Am.: Equine Pract*. **29**, 467–485

Gibbs, C., Lane, J.G. (1987) Radiographic examinations of the facial, nasal and paranasal sinus regions of the horse. (ii) Radiological findings. *Equine Vet. J.* **19**, 474–482

Gibbs, C., Lane, J.G., Meynink, S.E., Steele, F.C. (1987) Radiographic examinations of the facial, nasal and paranasal sinus regions of the horse. (i) Indications and procedures in 235 cases. *Equine Vet. J.* **19**, 466–473

Henninger, W., Frame, E., Willman, M., et al. (2003) CT features of alveolitis and sinusitis in horses. *Vet. Radiol. Ultrasound* **44**, 269–276

Lane, J., Gibbs, C., Meynink, S., Steele, F. (1987) Radiographic examination of the facial, nasal and paranasal regions of the horse: I. Indications and procedures in 235 cases. *Equine Vet. J.* **19**, 466–473

Lane, J., Longstaff, J., Gibbs, C. (1987) Equine paranasal sinus cysts: a report of 15 cases. *Equine Vet. J.* **19**, 537–544

Montgomery, J., Carmalt, J. (2013) Radiographic appearances of maxillary sinus feed impaction in a horse. *J. Vet. Dent.* **30,** 158–160

Schmotzer, W.B., Haltgren, B.D., Watrous, B.J., Wagner, P.C., Kaneps, A.J. (1987) Nasomaxillary fibrosarcomas in three young horses. *J. Am. Vet. Med. Ass.* **191**, 437–439

Schumacher, J., Smith, B., Morgan, S. (1988) Osteoma of paranasal sinuses of a horse. *J. Am. Vet. Med. Ass.* **192**, 1449–1450

Tessier, C., Bruhschwein, A., Lang, J., et al. (2013) Magnetic resonance imaging features of sinonasal disorders in horses. *Vet Radiol. Utrasound* **54**, 54–60

Tremaine, H., Dixon, P. (2001) A long-term study of 277 cases of equine sinonasal disease. Part 1: Details of horses, historical, clinical and ancillary diagnostic findings. *Equine Vet. J.* **33**, 274–282

Tremaine, H., Dixon, P. (2001) A long-term study of 277 cases of equine sinonasal disease. Part 2: Treatment and results of treatment. *Equine Vet. J.* **33**, 283–289

Woodford, N., Lane, J. (2006) Long-term retrospective study of 52 horses with sinonasal cysts. *Equine Vet. J.* **38**, 198–202

LARYNX AND PHARYNX

Blythe, L., Watrous, B., Schmitz, J., Kaneps, A. (1984) Vestibular syndrome associated with temporohyoid joint fusion and temporal bone fracture in three horses. *J. Am. Vet. Med. Ass.* **185**, 775–781

Boles, C.L. (1975) Epiglottic entrapment and follicular pharyngitis: diagnosis and treatment. *Proc. Am. Ass. Equine Pract.* **21**, 29–34

Boles, C.L., Raker, C.W., Wheat, J.D. (1978) Epiglottic entrapment by aryteno-epiglottic folds in the horse. *J. Am. Vet. Med. Ass.* **172**, 338–342

Dixon, P., McGorum, B., Railton, D., et al. (2001) Laryngeal paralysis: a study of 375 cases in a mixed-breed population of horses. *Equine Vet. J.* **33**, 452–458

Evans, L.H. (1981) Entrapment of the epiglottis. *Proc. Am. Ass. Equine Pract.* **27**, 61–62

Ferraro, G.L. (1981) Equine follicular pharyngitis. *Proc. Am. Ass. Equine Pract.* **27**, 55–56

Haynes, P.F. (1981) Persistent dorsal displacement of the soft palate associated with epiglottic shortening in two horses. *J. Am. Vet. Med. Ass.* **197**, 677–681

Haynes, P.F., Snider, T.G., McClure, J.R., McClure, J.J. (1980) Chronic chondritis of the equine arytenoid cartilage. *J. Am. Vet. Med. Ass.* **177**, 1135–1142

Linford, R., O'Brien, T., Wheat, J., et al. (1983) Radiographic assessment of epiglottic length and pharyngeal and laryngeal diameters in the Thoroughbred. *Am. J. Vet. Res.* **44**, 1660–1666

Naylor, R., Perkins, J., Allen, S. et al. (2010) Histopathology and computed tomography of age-associated degeneration of the equine temporohyoid joint. *Equine Vet. J.* **42**, 425–430

Tulleners, E. (1991) Correlation of performance with endoscopic and radiographic assessment of epiglottic hypoplasia in racehorses with epiglottic entrapment corrected by use of contact neodymium: ytrium aluminum laser. *J. Am. Vet. Med. Ass.* **198**, 621–626

MISCELLANEOUS CONDITIONS

Dixon, P., Loh, N., Barakzai, S. (2014). Swellings of the angle of the mandible in 32 horses (1997–2011). *Vet. J.* **199**, 97–102

Dunkel, B., Corley, K., Johnson, A.L., et al. (2013) Pneumocephalus in five horses. *Equine Vet. J.* **45**, 367–371

Ferrell, E., Gavin, P., Tucker, R., Sellon, D., Hines, M. (2002) Magnetic resonance for evaluation of neurologic disease in 12 horses. *Vet. Radiol. Ultrasound* **43**, 510–517

Frame, E., Riihimaki, M., Berger, M., Vatne, M., McEvoy, F. (2005) Scintigraphic findings in a case of temporohyoid osteoarthropathy in a horse. *Equine Vet. Educ.* **17**, 11–13

Freeman, D. (2006) Guttural pouch tympany – a rare and difficult disease. *Equine Vet. Educ.* **18**, 234–238

Gasser, A., Love, N., Tate, L. (2000) Ethmoid haematoma. *Vet. Radiol. Ultrasound* **41**, 247–249

Jackman, B., Baxter, G. (1992) Treatment of a mandibular bone cyst by use of a corticancellous bone graft in a horse. *J. Am. Vet. Med. Ass.* **201**, 892–894

Jubb, K.V.F., Kennedy, P.C., Palmer, N. (1985) *Pathology of Domestic Animals*, 3rd edn, Academic Press, Orlando

Kiper, M., Wrigley, R., Traub-Dragatz, J., Bennett, D. (1992) Metallic foreign bodies in the mouth or pharynx of horses: seven cases (1983–1989). *J. Am. Vet. Med. Ass.* **200**, 91–93

Lamb, C., Schelling, S. (1989) Congenital aneurysmal bone cyst in the mandible of a foal. *Equine Vet. J.* **21**, 130–132

Lane, J.G. (1989) The management of guttural pouch mycosis. *Equine Vet. J.* **21**, 321–324

Latimer, C., Wyman, C. (1984) Atresia of the nasolacrimal duct in three horses. *J. Am. Vet. Med. Ass.* **184**, 989–992

Lavach, J.D., Severin, G.A. (1977) Neoplasia of the equine eye, adnexa and orbit: a review of 68 cases. *J. Am. Vet. Med. Ass.* **170**, 202–203

Manso-Diaz, G., Dyson, S., Dennis, R., et al. (2014) Magnetic resonance imaging characteristics of equine head disorders: a review of 84 cases (2000–2013). *Vet Radiol. Ultrasound* doi: 10.1111/vru.12210

Manso-Diaz, G., Taeymans, O. (2012) Imaging diagnosis – nasofrontal suture exostosis in a horse. *Vet. Radiol. Ultrasound* **53**, 573–575

Oey, L., Muller, J.-M.V., Klopmann, T., Jacobsen, B., Beineke, A., Feige, K. (2011) Diagnosis of internal and external hydrocephalus in a Warmblood foal using magnetic resonance imaging. *Tierarztl Prax Ausg G Grosstiere Nutziere* **39**, 41–45

Orsini, J., Baird, D., Ruggles, A. (2004) Radiotherapy of a recurrent ossifying fibroma in the paranasal sinuses of a horse. *J. Am. Vet. Med. Ass.* **224**, 1483–1486

Readford, P., Lester, G.D., Secombe, C.J. (2013) Temporohyoid osteoarthropathy in two young horses. *Aust. Vet J.* **91**, 209–121

Richardson, J., Lane, J.G., Day, M. (1994) Congenital choanal restriction in 3 horses. *Equine Vet. J.* **26**, 162–165

Santos, M., Gutierrez-Nibeyro, S., Stewart, A., Hyde, R., Rodgerson, D. (2012) Identification of a periorbital wooden foreign body as the cause of chronic ocular discharge in a horse. *Aust. Vet. J.* **90**, 84–87

Schambourg, M., Marcoux, M., Celeste, C. (2006) Salingoscopy for the treatment of recurrent guttural pouch tympany in a filly. *Equine Vet. Educ.* **18**, 231–233

Taylor, D., Wisner, E., Kuesis, B., Smith, S., O'Brien, T. (1993) Gas accumulation in the subarachnoid space resulting from blunt trauma to the occipital region of a horse. *Vet. Radiol. Ultrasound* **34**, 191–193

Trostle, S., Rantanen, N., Andersen, M., Taylor, S., Vrono, D. (2005) Juvenile ossifying fibroma in a 12 week old foal. *Equine Vet. Educ.* **17**, 284–286

Tudor, R., Ramiriz, O., Tate, L., Gerard, M. (1999) A congenital malformation of the maxilla of a horse. *Vet. Radiol. Ultrasound* **40**, 353–356

Viu, J., Armengou, L., Jose-Cunilleras, E., Cesarini, C., Pumarola, C., Monreal, L. (2010) Cranioencephalic malformation with atlanto-occipital luxation in an Andalusian neonate foal. *J. Vet. Intern. Med.* **24**, 398–406

Walker, M., Sellon, D., Cornelisse, C., Hines, M., Ragle, C., Schott, H. (2002) Temporohyoid osteoarthropathy in 33 horses (1993–2000). *J. Vet. Intern. Med.* **16**, 697–703

Weller, R., Taylor, S., Maierl, J., Cauvin, E., May, S. (1999) Ultrasonographic anatomy of the equine temporomandibular joint. *Equine Vet. J.* **31**, 529–535

Chapter 12
The vertebral column

Cervical vertebrae

The usual indications for radiographic examination of the cervical vertebrae include abnormal head and/or neck posture, swelling, stiffness or pain of the neck or back, trauma to the neck, ataxia, inability to stand and horses sub-performing. Other less common indications include forelimb lameness which is not altered by diagnostic analgesia, abnormal forelimb posture, clinical signs suggestive of nerve root compression such as dermatomal sweating, forelimb weakness, shortened cranial phase of the step, and toe drag or instability of the carpus. Radiographic assessment of such cases requires at least lateral-lateral radiographs of the occipital bone, all cervical vertebrae and the first thoracic vertebra. Lateral-lateral radiographs are best acquired with the horse standing, but can be acquired with the horse in lateral recumbency, under general anaesthesia. Lateroventral-laterodorsal oblique images may be needed to provide additional information in selected horses, and are also readily acquired in a standing patient. Ventrodorsal (dorsoventral) views of the cranial aspect of the neck can sometimes be acquired in a standing horse; however, there are potential radiation safety risks. Caudal ventrodorsal images can only be obtained in a recumbent horse. As in humans, relating radiographic findings in the vertebral column to clinical symptoms may be extremely difficult.

RADIOGRAPHIC TECHNIQUE

Equipment

Good-quality images of the cranial and mid-neck regions are within the capability of portable x-ray machines, but images of the seventh cervical (C7) and first thoracic (T1) vertebrae require more powerful equipment in all but the smallest horses. Digital systems or fast rare earth screens and appropriate film are recommended. A grid, although beneficial, is not essential for the cranial part of the neck, but is necessary for the caudal one-third if using conventional film–screen techniques.

In order to assess the relative alignment of the cervical vertebrae it is helpful to use large imaging plates or cassettes (35 cm × 43 cm) so that parts of at least three vertebrae are projected on each film. The cassette should be

Clinical Radiology of the Horse, Fourth Edition. Janet A. Butler, Christopher M. Colles, Sue J. Dyson, Svend E. Kold and Paul W. Poulos.
© 2017 John Wiley & Sons, Ltd. Published 2017 by John Wiley & Sons, Ltd.
Companion website: www.clinical-radiology-horse.com

supported in a cassette holder, which is mounted on a wall or on a set of stocks or a mobile stand. If the cassette holder is not linked to the x-ray machine, alignment can be difficult, and it is helpful to mark the neck on both sides at the sites where the x-ray beam is being centered. This is easily done using sticky tape. If using smaller imaging plates, placing metallic markers on the neck can help in accurate identification of the third, fourth and fifth cervical vertebrae.

Positioning

Radiography of the head and neck in the standing horse renders the handler particularly at risk of exposure to radiation, and appropriate precautions, including wearing lead gloves, are important. If the area to be radiographed involves the occipito-atlantal articulation, a rope halter should be used rather than a head collar, in order to avoid artefacts from metal buckles.

The standing horse

Slightly oblique radiographic images are difficult to interpret, and in most circumstances true lateral-lateral images are essential, especially if measurements of vertebral dimensions are to be obtained. The handler should try to ensure the neck is positioned naturally (neutral position), and in line with the thoracolumbar vertebrae of the horse. It may be helpful if the horse handler pulls gently forwards on the halter, but this may result in changes in the alignment of the cervical vertebrae. Many horses are apprehensive of the x-ray machine and the cassette, especially when these are close to the head. The use of blinkers and ear plugs may be helpful. To minimise movement of the horse it may be helpful to restrain it in stocks; sedation may be helpful, not only to reduce movement, but also because it causes the horse to lower its head and neck. However, sedation may alter the alignment of the vertebrae relative to an unsedated horse and when examining the caudal cervical vertebrae it may be necessary to raise the head and neck to avoid superimposition of the seventh cervical and first thoracic vertebrae over the scapula or shoulder joint. Supporting the head on a stand may help to stabilise the position of the neck and reduce the risk of movement during image acquisition. Support of the head is particularly useful for the acquisition of lateroventral-laterodorsal images, when it is beneficial to have the head resting on the stand at approximately the horse's shoulder level.

Sedation of an ataxic horse should be carried out with care because it is likely that the ataxia will be exacerbated. A sedated horse usually moves less and is more likely to hold the head and neck in the sagittal plane. It has the disadvantage that the neck may be flexed relative to the normal standing position; thus the alignment of the vertebrae is altered. In some horses it is not possible to obtain true lateral-lateral projections of all the cervical vertebrae, despite appropriate positioning. This usually either reflects abnormal muscle tone in the neck associated with pain, or is the result of abnormal asymmetrical modelling of the caudal articular process joints, which results in a permanent slight rotation of the more cranial vertebrae. Using an oblique x-ray beam angled from dorsally or ventrally may help to acquire a true lateral-lateral image (Figures 12w.29b and c).

LATERAL-LATERAL IMAGES

Complete radiographic assessment of the cervical vertebrae (C1–C7) of an adult horse usually requires at least four views: the occiput and C1 (atlas); C1–C3; C3–C5; and C5–T1. In most cases a fifth view is required to evaluate the seventh cervical vertebra and its articulation with the first thoracic vertebra. In some horses valuable information can be gained by assessment of the first two thoracic vertebrae and the cranial ribs.

Radiographs are obtained with the horse standing square with its head and neck in the sagittal plane. The x-ray beam is aligned horizontally, and perpendicular to the neck. In the caudal half of the neck the cervical vertebrae are situated ventrally and the x-ray beam should be centered accordingly. It is usually easiest to radiograph the mid-neck region first and then the more caudal area, before examining the cranial part. This allows the horse to become familiar with the equipment before it is placed close to the head. Ideally the imaging plate should be as close to the neck as possible to minimise magnification, but in the caudal aspect of the neck the shoulder gets in the way. Divergence of the x-ray beam means that the margins of structures on the periphery of the image may distorted, and if any potential abnormality is detected the image should be repeated with the area of interest in the centre of the image. Lead markers placed on the skin of the neck above the level of the vertebrae can be helpful for orientation when acquiring and interpreting radiographs.

It is sometimes helpful to obtain both left to right and right to left projections in order to establish on which side of the neck a lesion is situated. The lesion is smaller and more clearly defined when closer to the cassette. It may also allow identification of a lesion that might otherwise be missed (Figures 12w.23a and 12w.23b).

When obtaining radiographs of the occiput it may be useful to pull the ears forwards to avoid superimposition of the cartilages of the ears over the region of insertion of the nuchal ligament (see Figure 11.8b). This is easily achieved in a sedated horse by attaching sticky tape to the ears in order to pull them cranially.

LATEROVENTRAL-LATERODORSAL IMAGES

Lateroventral-laterodorsal images should be acquired from left to right and from right to left to separate the joints of the left and right articular processes. The precise angle of projection depends on the level at which the images are being acquired. Usually it is the caudal neck vertebrae that are examined and the angles are approximately: for C4–C5, lateral 50–55° ventral-laterodorsal oblique; for C5–C6 and C6–C7 lateral 45–55° ventral-laterodorsal oblique (Figure 12.1). The articular process joints closest to the x-ray machine are projected dorsally (Figure 12.15a). It is equally possible to acquire images with the x-ray beam orientated from dorsal to ventral, in which case the articular process joints closest to the imaging plate are projected dorsally (Figure 12.15b).

The anaesthetised horse

In order to obtain true lateral-lateral projections when the horse is in lateral recumbency, it is necessary to support the head and neck, using radiolucent cushions, so that the vertebral column is horizontal from the shoulder

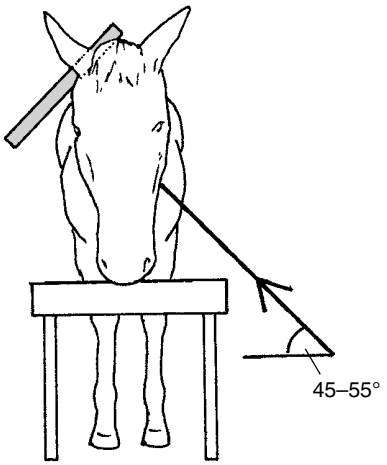


Figure 12.1 Positioning to acquire lateroventral-laterodorsal images. Images should be acquired from left to right and from right to left to separate the joints of the left and right articular processes. The precise angle of projection depends on the level at which the images are being acquired: for C4–5, lateral 50–55° ventral-laterodorsal oblique; for C5–6 and C6–7, lateral 45–55° ventral-laterodorsal oblique. The articular process joints closest to the x-ray machine are projected dorsally.

to the head. Aligning the x-ray machine and the cassette with the horse in this position may be difficult, but longer exposure times can be used. The neck may be flexed passively in order to accentuate a subluxation seen in a lateral-lateral view, but care must be taken not to kink the endotracheal tube, to displace a fracture, or to exacerbate a potential spinal cord compression.

Ventrodorsal views can usually only be obtained safely in a recumbent horse. Even with high-output x-ray machines it is difficult to get good-quality radiographs caudal to the fifth cervical vertebra because of the surrounding muscle mass. Myelography is discussed in the section 'Myelography' in Chapter 16.

NORMAL ANATOMY, VARIATIONS AND INCIDENTAL FINDINGS

There are seven cervical vertebrae (C1–C7). In the resting position the neck is S-shaped with a smooth transition of angulation between the vertebrae, from slight flexion (dorsal convexity) cranially, to slight extension (dorsal concavity) caudally. This is more marked in foals and small ponies. Apparent hyperflexion/subluxation at the articulation between the second and third or third and fourth vertebrae (see Figure 12w.2d) may occur without clinical signs, in horses with a wide dorsoventral diameter of the vertebral foramen (minimum sagittal diameter).

Lateral-lateral images

It is important to be able to differentiate between obliquity of a lateral-lateral image and lack of superimposition of the articular process joints because of asymmetrical enlargement (Figures 12.2a–c). In a true lateral-lateral image

of C3–C6 the transverse processes of the left and right sides are superimposed. If the neck was not entirely straight during image acquisition, the transverse processes are seen separately, and the articular process joints, the left and right sides of the vertebral arch and the lamina are not superimposed. With asymmetrical enlargement of articular process joints it is possible to acquire a true lateral-lateral image of the vertebral body, with the



Figure 12.2(a) A poor-quality lateral-lateral image of the third to fifth cervical vertebrae of a mature horse. Cranial is to the left. There is some obliquity of the image because the horse's neck was not completely straight during image acquisition. The left and right articular process joints and transverse processes are not superimposed. Obliquity makes it impossible to accurately assess the articular process joints and the intervertebral foramina. Compare with Figure 12.2(b). A similar image may be acquired in a horse with natural rotation of the cervical vertebrae due to asymmetric enlargement and/or orientation of the articular processes.



Figure 12.2(b) A lateral-lateral image of the third to fifth cervical vertebrae of a mature horse, the same as in Figure 12.2(a). Cranial is to the left. This is a superior quality image. There is better superimposition of the left and right articular process joints and transverse processes. Note that the pedicles of the vertebrae are relatively short so that the articular process joints are low slung and the intervertebral foramina are small. The vertebral foramen of the fourth cervical vertebra is wedge shaped, having a narrower dorsoventral diameter cranially compared with caudally. The caudodorsal aspect of each vertebral body has a 'ski jump' appearance.



Figure 12.2(c) Lateral-lateral image of the sixth and seventh cervical vertebrae of a 7-year-old Warmblood. Cranial is to the left. There is slight asymmetry in size of the articular process joints. There is a radiolucent band (arrows) which represents a non-articular groove on the axial aspect of the caudal articular process of the sixth cervical vertebra, a normal finding.

transverse processes superimposed, but the articular process joints are seen only partially superimposed. It may be necessary to acquire both left to right and right to left views or oblique images to confirm this enlargement.

The cervical vertebrae, other than the atlas, have a similar basic shape. The two sides of the vertebral arch (pedicles), its roof (lamina) and the body of each vertebra form the vertebral foramen in which lies the spinal cord (Figure 12.3). The series of vertebral foramina together constitute the vertebral canal. Within each vertebra the vertebral foramen appears approximately rectangular in shape (Figure 12.4).

Narrowing (stenosis) of the vertebral foramen may be significant (see below, 'Vertebral stenosis'), and objective measurement of the dorsoventral diameter may be required. Normal values for various measurement techniques are found in Tables 12.1 to 12.4.

Minimum sagittal diameter

Measurement of the height of the foramen can be made directly from a lateral-lateral image. Measurement should be made across the narrowest part of the foramen in a dorsoventral direction. The absolute minimum sagittal diameter (MSD) (or minimum median diameter) (Figure 12.4b) may be useful for comparison among vertebrae in one horse, but its use for comparison among horses is potentially unreliable due to variations in magnification

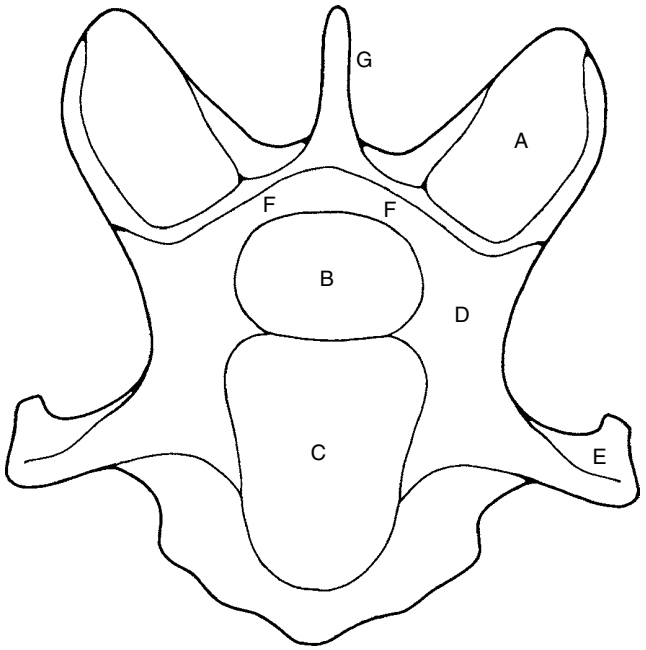


Figure 12.3 Craniocaudal diagram of the seventh cervical vertebra of an adult horse. A = facet of cranial articular process, B = vertebral foramen, C = head of vertebral body, D = lateral vertebral arch or pedicle, E = transverse process, F = dorsal lamina, forming dorsal arch, G = spinous process.

Table 12.1 Minimum sagittal diameter (mm) of the vertebral foramen, measured from radiographs of clinically normal horses. Source: Adapted from Mayhew, Whitlock and de Lahunta 1978, Table IV.1. Reproduced with permission of *The Cornell Veterinarian*.

	Less than 320 kg body weight					
	C2	C3	C4	C5	C6	C7
Mean	23.8	19.8	18.7	19.7	21.1	22.9
Standard deviation	1.5	0.9	1.0	1.2	1.5	1.6
Reference	20.8	18.1	16.7	17.3	18.3	19.8
limits*	26.8	21.5	20.7	22.1	23.9	26.1
	More than 320 kg body weight					
	C2	C3	C4	C5	C6	C7
Mean	26.7	22.2	21.3	22.4	24.1	27.4
Standard deviation	2.3	1.8	1.8	1.8	2.5	2.6
Reference	22.1	18.5	17.7	18.7	19.0	22.6
limits*	31.3	25.9	24.9	26.1	29.1	32.6

* Minimum and maximum sagittal diameter which can be considered normal.

and patient size. Comparison should only be made between horses of a similar size (Table 12.1). In horses with severe stenosis of the vertebral canal, MSD measurements may be sufficiently accurate to differentiate between normal and affected horses, but diagnosis can be difficult and unreliable, unless combined with other subjective criteria.

Intravertebral sagittal ratio

The problem of variable magnification among horses, can be largely eliminated by calculation of a ratio of measurements, rather than absolute measurements. This helps to standardise the assessment of MSD among horses. Dividing the MSD by the dorsoventral height of the body of the same vertebra



Figure 12.4(a) Lateral-lateral radiographic image of the mid-neck region (cervical vertebrae C4–C6) of a normal mature horse. Cranial is to the left. The vertebral foramen is approximately rectangular in shape. The small bony protuberance on the craniodorsal aspect of the vertebral bodies is a normal variant.

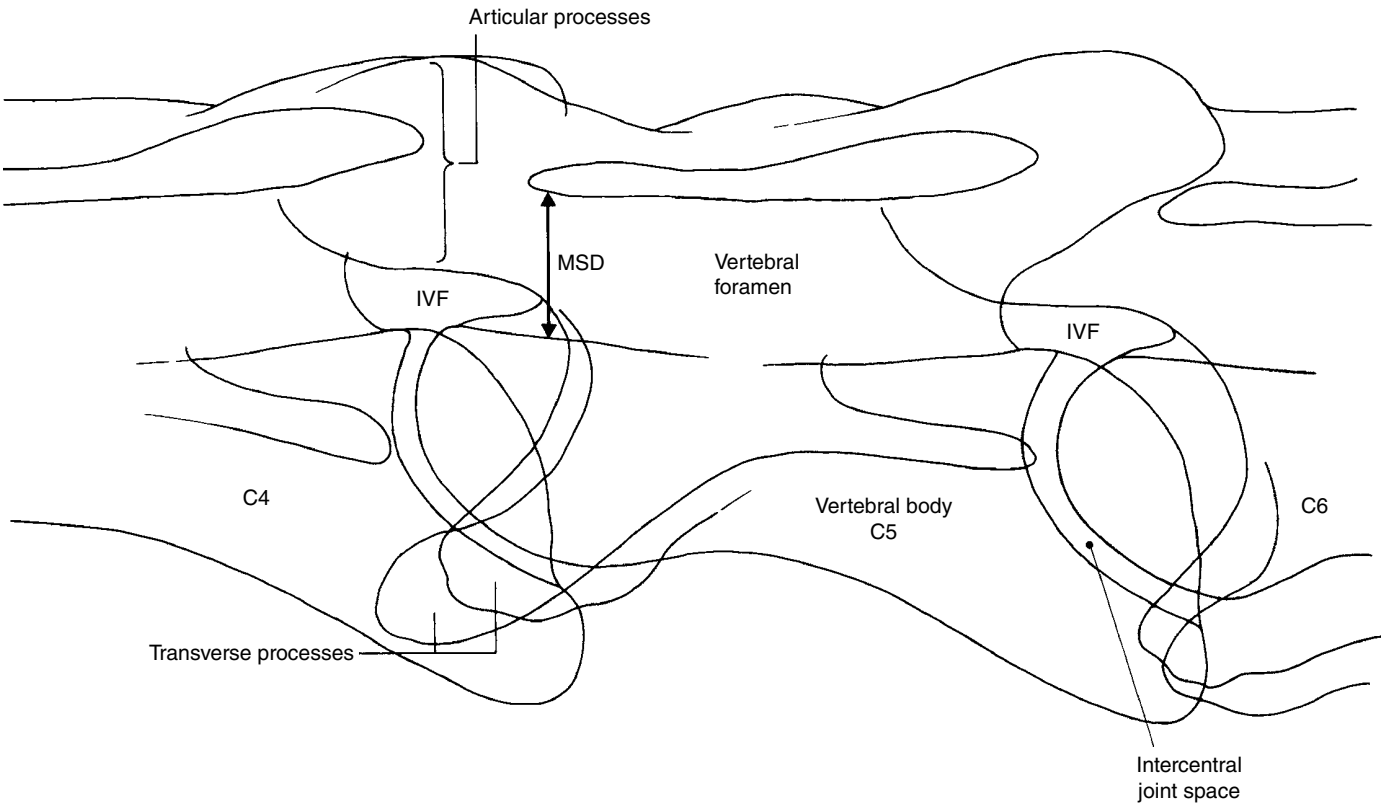


Figure 12.4(b) Diagram of Figure 12.4(a). IVF = intervertebral foramen, MSD = minimum sagittal diameter, C_4 = fourth cervical vertebra, C_5 = fifth cervical vertebra, C6 = sixth cervical vertebra.

(at the same level) gives the intravertebral sagittal ratio. The height of the vertebral body is measured at the maximum height of the cranial physis of the vertebral body (Figure 12.5a). Normal figures are given in Table 12.4.

Intervertebral sagittal diameter ratio

Intervertebral sagittal diameter ratio is the ratio of the MSD between adjacent vertebrae to the height of the vertebral body (Figure 12.5b). The height of the foramen between adjacent vertebrae is measured between the most dorsal aspect of the cranial physis of the vertebral body, and the ventrocaudal aspect of the lamina of the vertebral body immediately cranial.

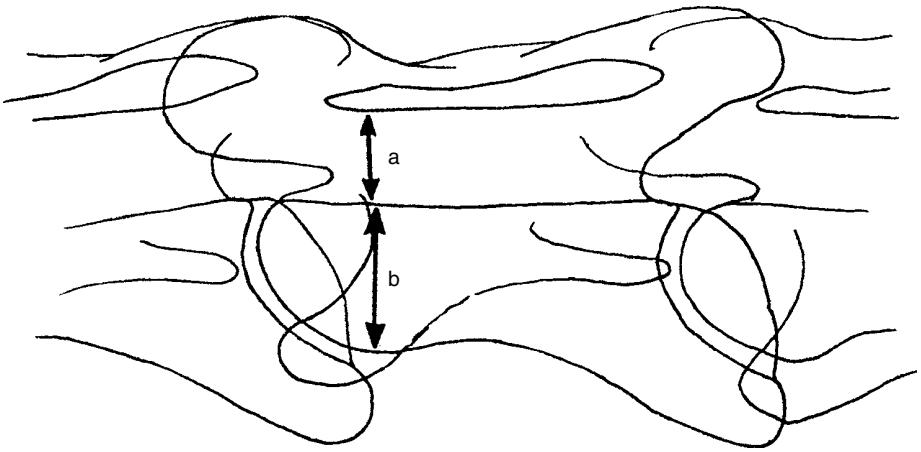


Figure 12.5(a) Method to obtain the sagittal ratio of the vertebral foramen. Divide the minimum sagittal diameter (MSD) (a) by the dorsoventral height (b) of the corresponding vertebral body at biggest point of its cranial aspect.

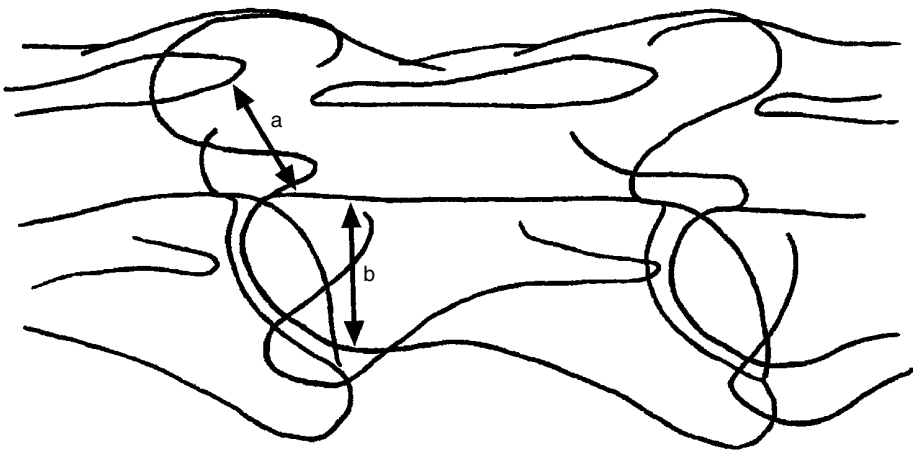


Figure 12.5(b) Measurement of the intervertebral diameter, the distance between the cranioproximal aspect of the physis of the cranial aspect of the vertebral body and the ventrocaudal aspect of the lamina of the immediately cranial vertebra (a). The height of the widest part of the cranial aspect of the vertebral head (b) is also measured. The intervertebral sagittal ratio is calculated by dividing the minimum intervertebral distance by the maximum height.

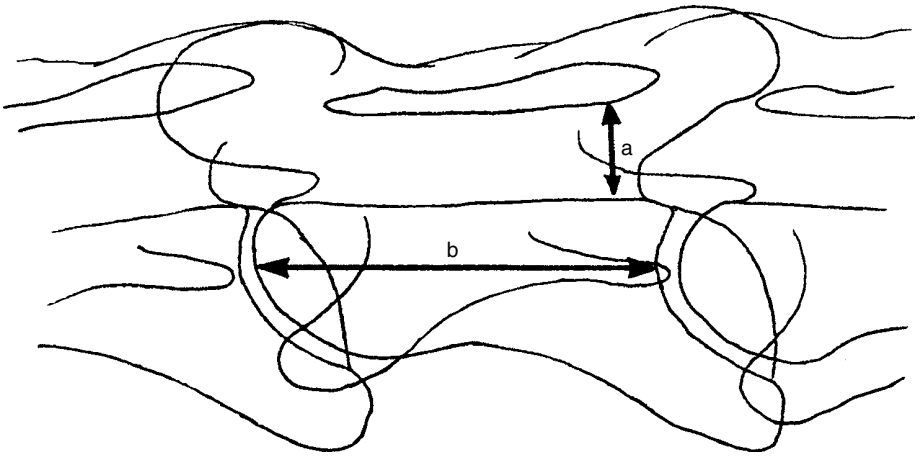


Figure 12.5(c) Method to obtain a corrected minimum sagittal diameter (cMSD). The absolute (measured) MSD (a) is divided by the length (b) of the corresponding vertebral body.

Table 12.2 Normal values for radiographic minimum sagittal diameter (MSD) (mm) and corrected MSD (cMSD) (%) for Thoroughbred foals, 3–7 months of age. Source: Mayhew et al. 1993, Table 2. *Equine Veterinary Journal*.

	Cervical vertebral site										
	C2	C2–C3	C3	C3–C4	C4	C4–C5	C5	C5–C6	C6	C6–C7	C7
MSD	23	28	20	25	20	25	21	26	21	31	23
Standard deviation	1	4	1	2	1	2	1	3	1	5	1
cMSD	18	33	24	30	24	31	25	34	27	46	35
Standard deviation	1	2	2	2	2	2	2	3	2	5	2

Corrected mean sagittal diameter

The corrected MSD has primarily been used to assess vertebrae in Thoroughbred foals 3–7 months old. It is the ratio of absolute MSD divided by the length of the vertebral body (Figure 12.5c; Table 12.2).

The sagittal diameter of the vertebral canal tends to be slightly smaller in the mid-cervical region compared with more cranial and caudal levels. If both the intervertebral and intravertebral minimum sagittal ratios are calculated the results are more likely to differentiate between horses with ataxia associated with cervical vertebral malformation than those with ataxia due to other causes and to predict accurately a site of spinal cord compression due to cervical vertebral malformation. Intervertebral sagittal ratios are more likely to predict at least one site of spinal cord compression than intravertebral minimum sagittal diameter ratios. However, it must also be borne in mind that it has been demonstrated that there are differences among observers for estimation of both intervertebral and intravertebral ratios, which can vary between 5 and 10%, which may lead to misdiagnosis.

Characteristics of the cervical vertebrae

C1: The atlas has no body or articular processes. It develops in two lateral halves which gradually ossify. In a ventrodorsal view of a neonate there is a longitudinal lucent line between the two halves.

C2: The axis has separate centres of ossification for the dens (odontoid peg), head, body and caudal epiphysis (Figure 12.6). The dens fuses with the head at approximately 7 months of age (Figure 12.7). The cranial arch of C2 bears lateral vertebral foramina, the cranial borders of which are incomplete in young horses (Figure 12.9), and may become complete, or remain as a notch in the adult. The dorsal spine usually has a smooth contour, but its cranial and caudal edges are often slightly irregular. Occasionally a small bony spur is seen apparently on the dorsal aspect of the caudal epiphysis (Figure 12.8 and Figure 12w.10ii) projecting into the vertebral canal; this is actually superimposition of the caudal extension of a transverse process and is an incidental finding.

C3 to C7: The third, fourth and fifth cervical vertebrae are approximately similar in shape (Figure 12.4), although there are variations specific to certain vertebrae (see below). The sixth and seventh cervical vertebrae have distinctive characteristics. The bodies of the vertebrae have cranial and caudal epiphyses. Closure of the physes occurs gradually, the time varying among individuals. Closure of the cranial physes starts ventrally (Figure 12.9) and is



Figure 12.6 Lateral-lateral image of the cranial cervical vertebrae (C1–C3) of a 5-day-old foal. Cranial is to the left. Note the separate centre of ossification (arrow) of the dens of the axis (C2). The cranial and caudal physes of C2 and C3 are open.



Figure 12.7 Lateral-lateral image of the occiput and cranial cervical vertebrae (C1 and C2) of a normal adult horse. Cranial is to the left. Note the complete foramina in the cranial aspect of the axis (compare with Figure 12.9). There is slight rotation of the atlas.



Figure 12.8 Lateral-lateral image of the cranial cervical vertebrae of a normal adult horse. Cranial is to the left. There is a large spur (arrow) which appears to be on the dorsocaudal aspect of the vertebral body of the axis (C2), protruding into the vertebral canal. It is actually part of the transverse process and is an incidental radiological finding.

complete by approximately 2 years after birth. The caudal physes remain open until 4–5 years of age, closure starting dorsally (Figure 12.9).

The convex cranial articular surface of each vertebral body is usually smoothly curved or slightly flattened, and reasonably congruous with the concave caudal articular surface (caudal fossa) of the adjacent vertebra. The latter has a relatively opaque subchondral bone plate. Flattening of the joint surfaces or irregularity in width of an intercentral articulation should be



Figure 12.9 Lateral-lateral image of the cranial cervical vertebrae (C1–C3) of a normal Warmblood yearling. Cranial is to the left. The cranial borders of the vertebral foramina of the axis (C2) are incomplete. The physes of C2 and C3 are not fully closed.

regarded as abnormal (see 'Degenerative changes of the intercentral articulations' and 'Discospondylitis'). It may be helpful to compare the shape of adjacent vertebrae.

The third to seventh cervical vertebrae each have pairs of cranial and caudal articular processes projecting from the borders of the vertebral arch; the second cervical vertebra has a caudal articular process only. The extremities of these processes carry articular surfaces, which articulate with those of adjacent vertebrae, forming the articular process joints. The shape of the articular process joints between the second and third cervical vertebrae is variable (Figure 12w.10). There is a non-articular groove on the axial surface of the caudal articular process of each vertebra which results in a crescent-shaped relatively radiolucent area in the articular processes seen in a lateral-lateral radiographic image (Figure 12.11). This is not the joint space.

The dorsal aspect of C3 may be variable in its convexity.

The sixth cervical vertebra (**C6**) is slightly shorter than C5. It has a trifid transverse process, which has an extra ventral lamina or process projecting ventrally (and caudally). The two ventral parts of the processes give the ventral surface of the vertebra a relatively concave shape (Figure 12.12). Sometimes one or both of these ventral processes may be transposed on to the ventral surface of the seventh cervical vertebra (**C7**) (see Figures 12.22a, 12w.22b and 12.24) or very rarely onto C5. When this transposition on to C7 occurs bilaterally, the ventral aspect of C6 has the same profile as C5.



Figure 12.11 Lateral-lateral image of the sixth and seventh cervical vertebrae of an adult horse. Cranial is to the left. There is a radiolucent band (arrows) which represents a non-articular groove on the axial aspect of the caudal articular process of the sixth cervical vertebra, a normal finding. The articular process joints are enlarged with ventral buttressing onto the caudodorsal aspect of the vertebral body of the sixth cervical vertebra. The intervertebral foramen is small. Note also a small spur on the ventral aspect of the articular processes. The seventh cervical vertebra has a small spinous process.



Figure 12.12 Lateral-lateral image of the caudal cervical vertebrae (C5–C7) of a normal adult horse. Cranial is to the left. The articular process joints between the sixth and seventh cervical vertebrae are larger than those of the fifth and sixth cervical vertebrae, but are within the normal range. There is a small spinous process on the dorsal aspect of the seventh cervical vertebra. Note also the small spur on the dorsal aspect of the head of the vertebral body of the sixth cervical vertebra.



Figure 12.13 Lateral-lateral radiographic image of the cervicothoracic junction (C6–T1) of a normal adult horse. Cranial is to the left. Note the smooth ventral aspect of the vertebral body of the seventh cervical vertebra and the large spinous process of the first thoracic vertebra. Note also the large circular intervertebral foramina between the first and second thoracic vertebrae.

(Figure 12w.22b). There may be associated asymmetry of the articular process joints. The ventral processes of C6, and occasionally of other vertebrae, have small centres of ossification at their caudal limits that should not be confused with fractures (see Figure 12.15b and Figure 12.20).

The seventh cervical vertebra is shorter than C6 and may have a small spinous process dorsally; this varies in size, shape and position among horses (Figure 12.12). On lateral-lateral radiographs this may be superimposed over the articular process joints between C6 and C7, and should not be confused with new bone associated with degenerative joint disease.

The first thoracic vertebra has a larger spinous process (Figure 12.13). The orientation of the articular process joints in the cranial thoracic region differs from the caudal cervical vertebrae, with larger intervertebral foramina especially between the first and second thoracic vertebrae (Figure 12.14).

In older horses, small spondylitic spurs are sometimes seen as incidental findings on the ventral surface of the vertebral bodies adjacent to one or more intercentral articulations.

Modelling of the articular process joints of the fifth and sixth and the sixth and seventh cervical vertebrae occurs commonly (see Figure 12.22) and is considered in more detail below ('Modelling of the articular process joints').

Lateroventral-laterodorsal images

For a lateroventral-laterodorsal image the articular process joint closest to the x-ray machine is projected dorsally and the contralateral side is projected ventrally (Figure 12.15a). With a laterodorsal-lateroventral image the articular process joint closest to the imaging plate is projected dorsally (Figure 12.15b). Assessment of the relative size and shape of the left and



Figure 12.14 Lateral-lateral radiographic image of the cervicothoracic junction (C7–T2) of a normal adult horse. Cranial is to the left. Note the large oval-shaped intervertebral foramina between the first and second thoracic vertebrae.



Figure 12.15(a) Lateral 50° ventral-laterodorsal oblique image and diagram of the fourth to sixth cervical vertebrae acquired from left to right of a normal adult horse. Cranial is to the left. The left articular process joints are projected at the top of the image and are smoothly marginated. The intervertebral foramina are large and well-demarcated. Note that the right articular process joints are not of uniform width, tending to be wider cranially. However, each articular process is of similar craniocaudal length and the subchondral bone plates are of uniform opacity.

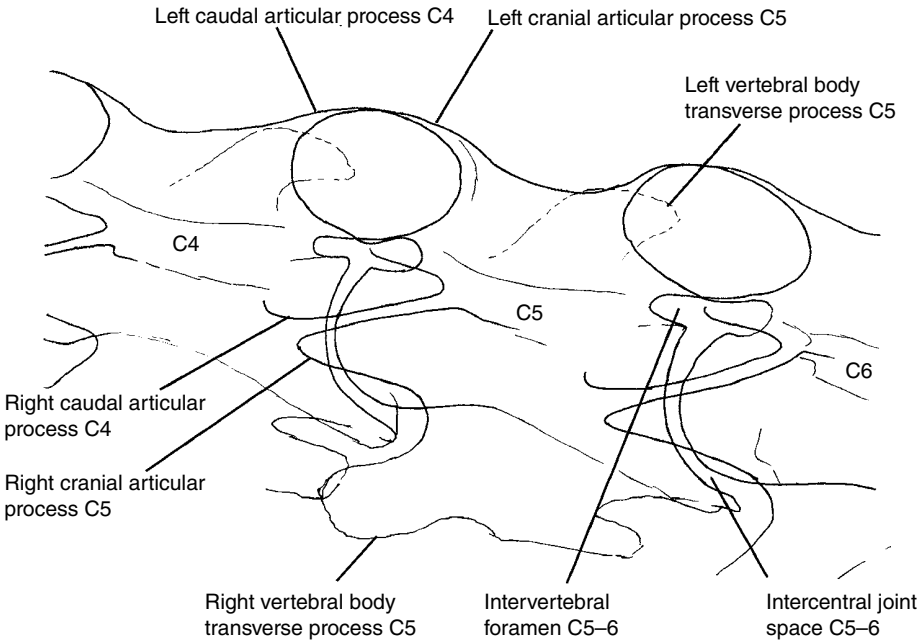


Figure 12.15(a) *Cont'd*

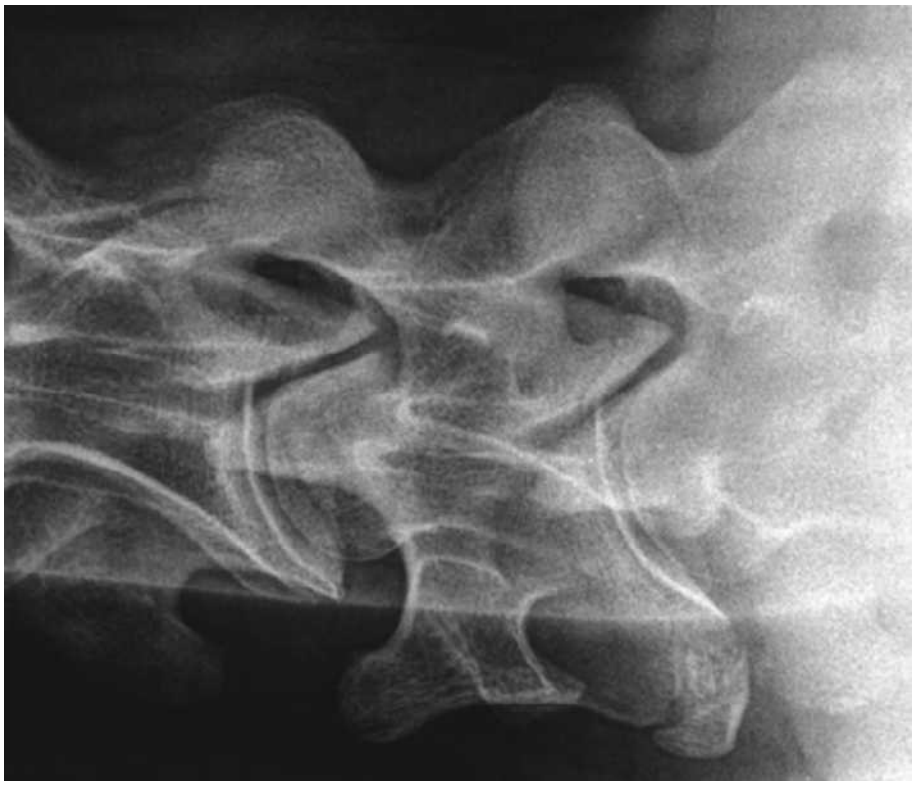


Figure 12.15(b) Lateral 50° dorsal-lateroventral oblique image of the fifth to seventh cervical vertebrae acquired from left to right of a normal adult horse. Cranial is to the left. The right articular process joints are projected at the top of the image. Note that there is a separate centre of ossification on the ventrocaudal aspect of the vertebral body of the sixth cervical vertebra, a normal variant.

right articular process joints can be made by comparing images acquired from left to right and from right to left. The dorsally projected articular process joints appear approximately round to oval in shape (Figures 12.15a and 12.15b). The presence of periarticular modelling can be assessed (Figure 12.16a). The ventrally projected articular process joints can be assessed for symmetry and congruity of each articular process (Figures 12.15a and 12.15b). The joint margins and regularity of the subchondral bone plate can also be evaluated (Figure 12.16b).



Figure 12.16(a) Lateral 50° dorsal-lateroventral oblique image of the fifth to seventh cervical vertebrae acquired from right to left of a 13-year-old Thoroughbred with mild hindlimb ataxia, left-sided weakness and mild forelimb lameness. Cranial is to the left. The left articular process joints are projected at the top of the image. The left articular process joint between the sixth and seventh cervical vertebrae is enlarged with irregular periarticular new bone formation (arrows); the intervertebral foramen is narrowed.

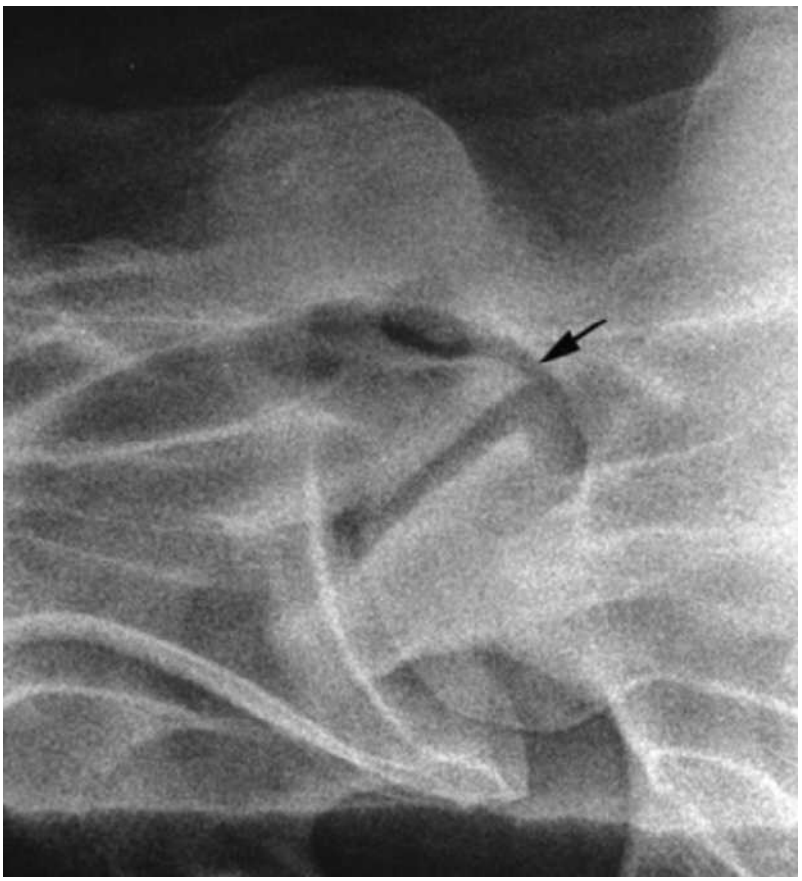


Figure 12.16(b) Lateral 50° dorsal-lateroventral oblique image of the sixth to seventh cervical vertebrae acquired from right to left of a 7-year-old Thoroughbred. The right articular process joint is abnormal with an irregular joint surface of the caudal articular process of the sixth cervical vertebra, and modelling of its caudal margin (arrow).

When assessing radiographs of the neck it is important not only to examine each vertebra, but also to consider the neck as a whole and to evaluate the shape of the vertebral canal, the alignment of the vertebral bodies, the shape and size of the epiphyses, the regularity of both the intercentral articulations and the articular process joints, and the size of the intervertebral foramina. Comparison with radiographs of a normal horse of similar age, and with bone specimens, is often helpful. When the results of lateral-lateral survey radiographs are negative or equivocal it may be necessary to obtain latero-ventral–laterodorsal oblique images, ventrodorsal (or, less commonly, dorsoventral) views and/or to perform myelography (see 'Myelography' in Chapter 16). As in humans, there is often a poor correlation between radiographic findings in the vertebral column and clinical symptoms.

Congenital abnormalities

Vertebral malformations are rare and, although neck stiffness, distortion of the neck and/or ataxia may be seen soon after birth, some lesions are not clinically apparent unless the spinal cord becomes compromised.

Occipito-atlanto-axial malformation (OAAM)

Occipito-atlanto-axial malformation is the most common congenital abnormality, and is most often seen in Arab horses (in which it is thought to be familial) although it does occur in other breeds. The vertebral defects may be symmetrical or asymmetrical and include fusion and a variety of distorted shapes (Figure 12.17). Lateral and ventrodorsal radiographic views are needed for proper assessment of this abnormality.

Vertebral fusion

Vertebral fusion may involve two or more vertebrae (Figure 12w.18). Absence of irregular bony callus helps to distinguish congenital fusion from fusion following a fracture in a foal, but in an older horse the two may be indistinguishable once the callus has modelled.

Developmental abnormalities

The cervical vertebrae undergo modelling during growth, influenced by the biomechanical stresses placed upon them and the rate of bone turnover. Abnormalities may occur; the cause and time of onset of such changes are uncertain, but they result in one or more of a variety of cervical abnormalities, considered together as developmental abnormalities. These may predispose to, or cause, compression of the spinal cord and thus ataxia. Some of the changes described may be related to osteochondrosis. These changes may in part be reversed in foals by restriction of feed intake and exercise. It should be noted that any of these variants, alone or in combination, can be seen in clinically normal horses. The greater both the number of abnormal variants and their severity, the more likely there are to be associated clinical signs. Vertebral stenosis and vertebral angulation are most likely to be associated

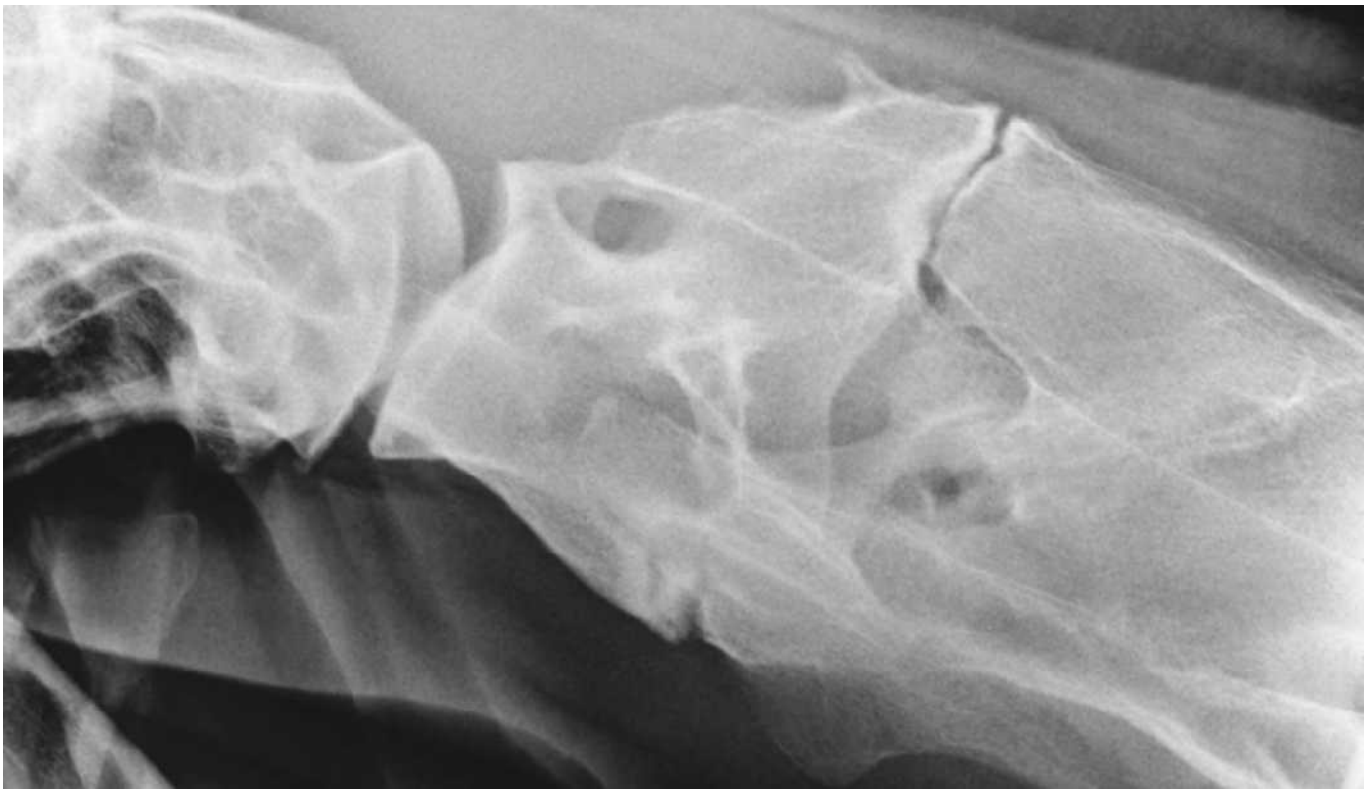


Figure 12.17 Lateral-lateral image of the occiput and the cranial cervical vertebrae (C1–C2) of a 6-year-old Warmblood gelding showjumper with neck stiffness. The horse had to straddle its forelimbs in order to graze. The atlas (C1) is fused to the occiput and the axis (C2) is partially duplicated and misshapen – an occipito-atlanto-axial malformation. Compare with Figure 12.7. Source: Reproduced with permission of Ana Stela Fonseca.

with spinal cord compression, followed by enlargement of a caudal epiphysis and caudal extension of the arch of the vertebral canal over the cranial aspect of the next vertebra.

A semi-quantitative method of assessing cervical radiographs includes documentation of encroachment of the caudal epiphyses dorsally into the vertebral canal ('ski jumps') (Figure 12.19), caudal extension of the dorsal aspect of the arch of the vertebral canal, intervertebral malalignment, abnormal ossification of the articular processes, and degenerative joint disease of the articular process joints (see below).

A study compared subjective assessment of plain radiographs, semi-quantitative scoring of plain radiographs and myelography (positive results defined as ≥50% reduction in dorsal contrast medium column) in two groups of horses. In one group, the horses had histologically confirmed spinal cord disease due to cervical vertebral malformation. The second group had other causes of spinal cord disease. The semi-quantitative method was most accurate for identification of horses with spinal cord compression due to cervical vertebral malformation (Tables 12.3 and 12.4). Semi-quantitative measurements resulted in a higher sensitivity (87%) and specificity (94%) as well as more powerful positive predictive value (95%) and negative predictive value (84%) than either of the other techniques.



Figure 12.19 Lateral-lateral image of the third to fifth cervical vertebrae of a 2-year-old Warmblood which underwent radiography as part of a pre-purchase examination. There is enlargement of the dorsocaudal aspects of the epiphyses of the third and fourth cervical vertebrae (arrows), 'ski jumps'. Note also that the ventral aspect of the caudal physes are still open.

Table 12.3 Accuracy parameters for diagnosing cervical vertebral malformation from radiographs. Source: Mayhew and Green 2000, Table 1. *Equine Veterinary Journal*.

Parameter	Plain films ($n=77$)	Scored films ($n=77$)	Myelograms ($n=50$)
Sensitivity	0.59	0.87	0.56
Positive predictive value	0.79	0.95	0.86
Negative predictive value	0.56	0.84	0.52

77 cases of histologically confirmed CVM and 31 cases of pathologically confirmed 'other than CVM' were analysed. Techniques used were subjective analysis (plain films), semiquantitative scoring including minimum sagittal diameter measurements (scored films) and ≥50% reduction of the dorsal contrast medium column (myelograms).

Table 12.4 Cervical intervertebral and intravertebral sagittal ratio measurements for 18 horses with spinal cord disease determined histologically not to be due to cervical vertebral malformation. Source: Mayhew and Green 2000, Table 2. *Equine Veterinary Journal*.

	C2	C2–3	C3	C3–4	C4	C4–5	C5	C5–6	C6	C6–7*	C7
Median	73	93	60	71	58	73	60	81	58	71	62
Mean	72	90	61	71	59	73	61	80	60	70	63
Standard deviation (SD	8	12	5	9	6	11	6	10	6	9	5
Mean –2 SD	56	66	51	53	47	51	49	60	48	52	53
Maximum	83	108	70	92	83	90	75	100	75	86	72
Minimum	55	63	52	60	49	56	52	63	54	58	55

* Measured in reverse from dorsocaudal aspect of the body of C6 to the cranial aspect of the dorsal lamina of the vertebral arch of C7.
Note that in some horses the intravertebral minimal sagittal ratio was <50%, but the intervertebral sagittal ratio was within the normal range.

Enlargement of the caudal epiphyses

The caudal epiphyses of C2–C7 form the most caudal part of the floor of each vertebral foramen. Dorsal enlargement of one or more of the caudal epiphyses (a 'ski jump') can reduce the sagittal diameter of the vertebral foramen (see Figure 12.19), resulting in compression of the spinal cord and ataxia. This usually develops within the first year of life.

Vertebral stenosis

Short vertebral pedicles (the lateral walls of the vertebral foramen) result in reduction of the minimum sagittal diameter (MSD) (median diameter) of the vertebral foramen. The articular processes have only marginal clearance of the intervertebral foramina (Figure 12.20), which therefore appear reduced in size. The stenosis is usually more pronounced towards the cranial aspect of the vertebra, resulting in a wedge-shaped vertebral foramen. The condition is the basis for many cases of spinal cord compression and occurs most commonly in young male Thoroughbreds. Intravertebral and intervertebral sagittal ratio measurements or corrected MSD values are thought to be more accurate than absolute MSD values for detection of generalised vertebral stenosis (see 'Normal anatomy, variations and incidental findings', above). An intravertebral sagittal ratio at any vertebra from C4 to C6 of ≤50% (≤52% at C7) is a good predictor (26.1–41.5 times the odds more likely) of the horse having cervical vertebral malformation. However, a small number of clinically normal horses and those with ataxia unrelated to cervical vertebral malformation have intravertebral sagittal ratios of <50% (Table 12.4). If both the intervertebral and intravertebral minimum sagittal ratios are calculated, the results are more likely to differentiate between horses with ataxia associated with cervical vertebral malformation and those with ataxia due to other causes. Using both measurements also helps to increase the accuracy of predicting a site of spinal cord compression due to cervical vertebral malformation. Intervertebral sagittal ratios are more likely to predict at least one site of spinal cord compression than intravertebral minimum sagittal diameter ratios.

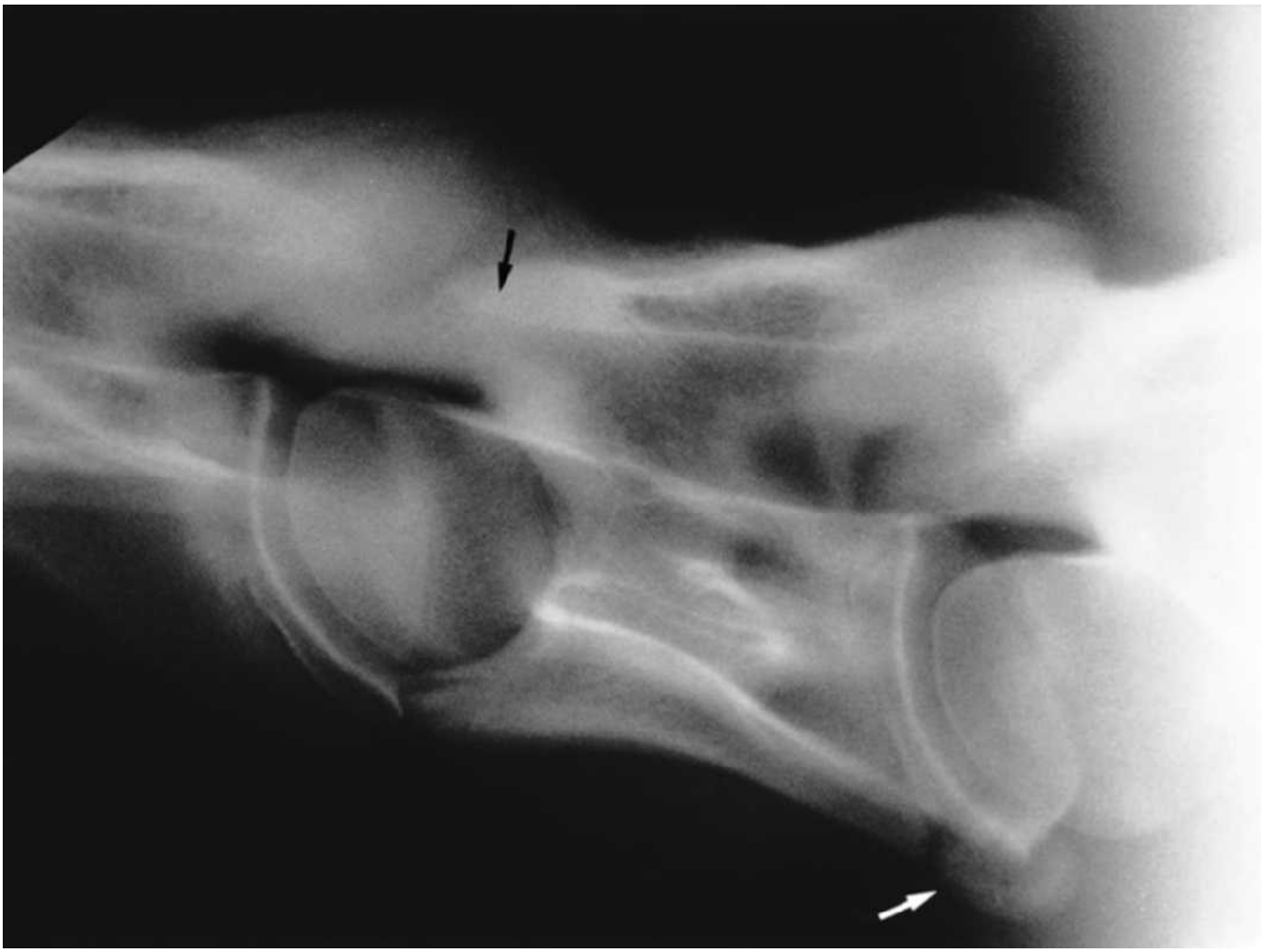


Figure 12.20 Lateral-lateral image of the caudal cervical vertebrae (C_5–C_7) of an ataxic yearling Thoroughbred colt. Cranial is to the left. There is stenosis of the cranial orifice of C6 (black arrow) due to short vertebral pedicles. This causes the vertebral foramen to assume a wedge shape (compare with Figure 12.12) and causes a reduction in size of the intervertebral foramina. Note the separate centre of ossification (white arrow) on the caudal aspect of the ventral processes of C6. This is normal and should not be confused with a fracture.

Vertebral instability, subluxation or angulation

Vertebral instability, subluxation or angulation occurs most commonly at the C_3–C_4 articulation (Figure 12.21a). The apparent subluxation is often present in the resting position and is exaggerated by flexion. Other developmental abnormalities (see 'OAAM', above, 'Vertebral stenosis', above, and 'Modelling of the cervical articular process joints', below) are often present concurrently, resulting in narrowing of the sagittal diameter of the vertebral foramen and spinal cord compression, possibly at more than one site. Occasionally there is reciprocal hyperextension at a more caudal articulation, resulting in a 'zig-zag' orientation of the cervical vertebrae (Figure 12.21b). Slight malalignment of two adjacent vertebrae occurs commonly and may have no clinical significance, especially if the minimum sagittal diameter of the vertebral canal is relatively wide (Figure 12w.2d). Dynamic malalignment may be associated with hypoplasia of the vertebral body and caudal fossa, so

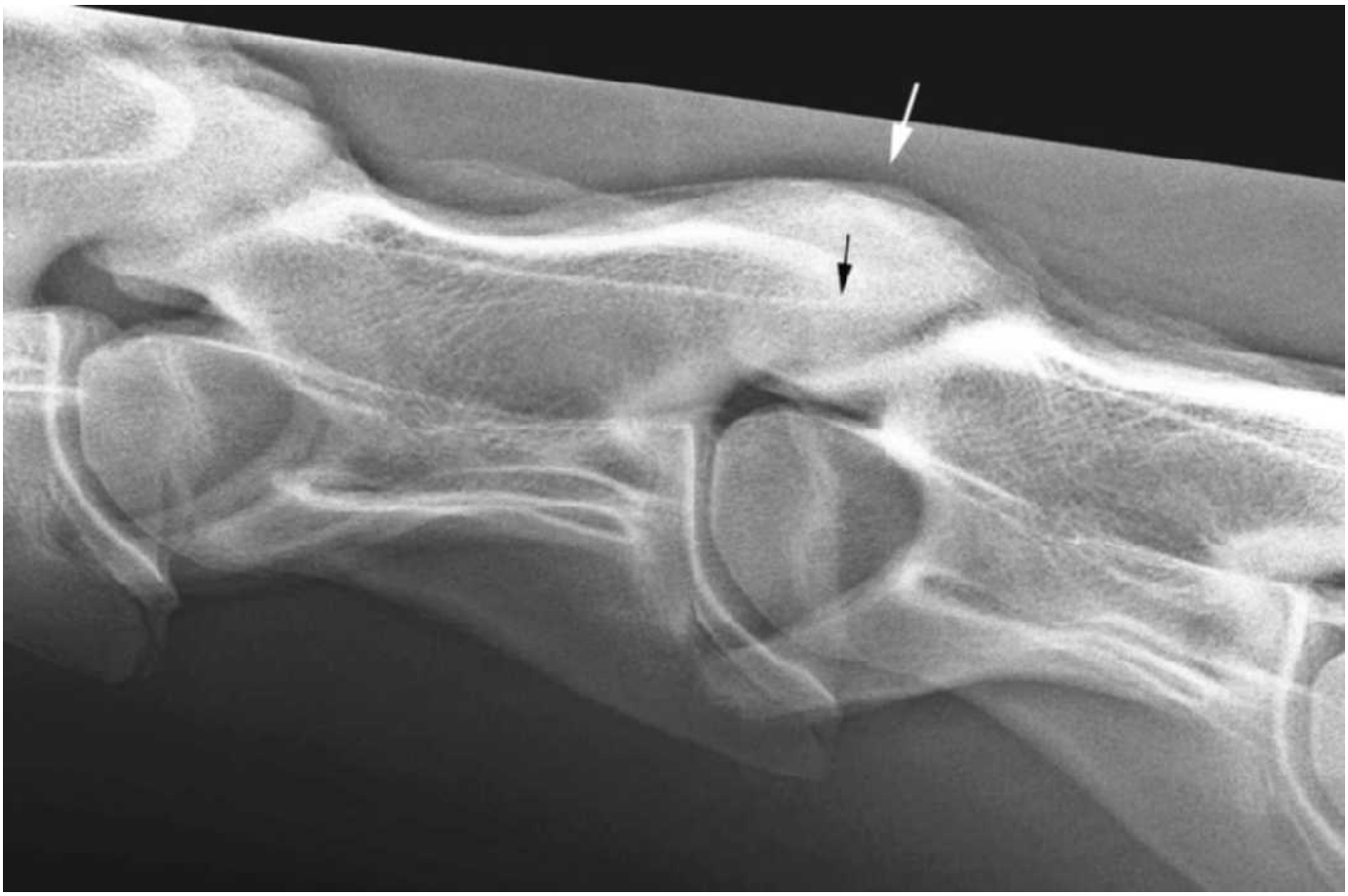


Figure 12.21(a) Lateral-lateral image of the second to fifth cervical vertebrae of a 6-year-old Warmblood stallion with mild hindlimb ataxia, obtained with the horse standing normally. Cranial is to the left. There is subluxation of the third and fourth cervical vertebrae (white arrow) with narrowing of the minimal sagittal diameter of the vertebral canal. Note also the severe caudal extension of the vertebral arch of the third cervical vertebra (black arrow), which extends beyond the cranial physis of the vertebral body of the fourth cervical vertebra, and the 'ski jump' appearance of the dorsocaudal aspect of the vertebral body of the third cervical vertebra.

their shapes should be evaluated carefully. The radiographs must be examined and interpreted in the light of the clinical signs, and if there is any doubt about the potential significance of a lesion it is helpful to obtain flexed lateral-lateral views, to measure intravertebral and intervertebral sagittal ratios (see above) and possibly to perform myelography. Also refer to Rooney type I lesions ('Modelling of the cervical articular process joints', below).

Caudal extension of the arch of the vertebral canal

In a normal vertebra the dorsal aspect of the arch of the vertebral canal (the dorsal lamina) reaches, but does not extend over, the cranial epiphysis of the next caudal vertebra. Caudal extension of the arch of the vertebral canal is identified by drawing a line perpendicular to the longitudinal aspect of the vertebral canal from the caudal tip of the vertebral arch (dorsal lamina) (Figure 12.21a). If this line extends on to the dorsal aspect of the cranial epiphysis of the next caudal vertebra, this is defined as mild caudal extension. Severe caudal extension is present if the line reaches the cranial physis of the vertebra. Such caudal extension may predispose the horse to compression of the spinal cord.



Figure 12.21(b) Lateral-lateral image of the caudal cervical vertebrae (C5–C7) and first thoracic vertebra of a 6-year-old Thoroughbred novice event horse presented because of difficult behaviour and poor performance. Clinical examination revealed mild hindlimb ataxia and weakness. Cranial is to the left. There is dorsal subluxation of the seventh cervical vertebra and reciprocal extension between the seventh cervical and first thoracic vertebrae. The articular process joints between the sixth and seventh cervical vertebrae are enlarged and have focal radiolucent areas. The intervertebral foramina are narrowed caudally. The vertebral foramen of the seventh cervical vertebra is wedge-shaped, narrower cranially.

Modelling of the cervical articular process joints

Rooney (1963) described two distinct lesions of the articular process joints (see 'Further reading'). Type 1 occurs at the C2–C3 articulation, associated with malalignment of the articular processes. It results in hyperflexion and stenosis of the vertebral foramen and usually causes ataxia. If the vertebrae are fused, however, it is possible for quite a marked stenosis to be present without signs of ataxia. In a Rooney type 2 lesion there is medial (axial) enlargement of the articular processes of C4, or occasionally C5, and this may cause spinal compression, especially in foals. This lesion cannot be detected radiographically on a plain lateral-lateral view and is difficult to identify on a ventrodorsal view.

The articular processes of C5–C6 and C6–C7 are frequently enlarged and modelled in mature horses, resulting in alteration of the normally smooth contours of their articulations (Figure 12.22a and 12w.22b). This probably reflects the stresses placed on these highly mobile joints, but the comparatively wide vertebral canal at this point means that stenosis of the

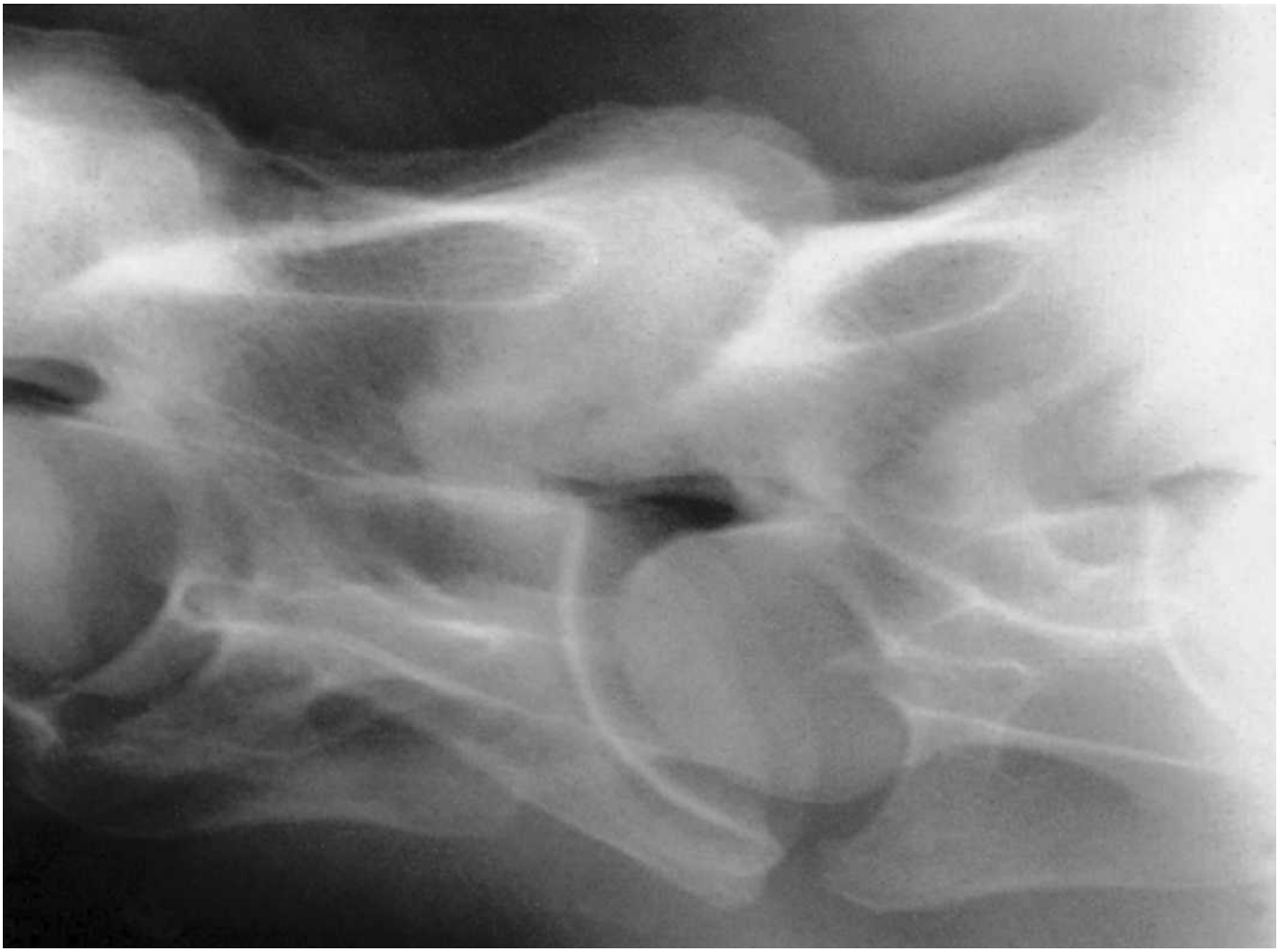


Figure 12.22(a) Lateral-lateral image of the sixth and seventh cervical vertebrae of a clinically normal adult horse. Cranial is to the left. There is modelling and enlargement of the articular process joints, a common incidental finding. Note the absence of buttresses (compare with Figure 12.25). C6 appears slightly rotated. There is transposition of one ventral process from C6 to C7.

vertebral canal usually does not occur, and so it is often of no clinical significance. These modelling changes, however, are the prerequisite for development of an epidural synovial bursa or 'cyst', which can intermittently or permanently compress the spinal cord and cause ataxia. Such modelling changes may also result in low-grade neck pain or stiffness.

The articular processes may be dysplastic with asymmetry between the left and right sides; such dysplasia may make the joint spaces more evident and cause abnormal alignment (Figure 12w.23). This has biomechanical implications and may predispose to progressive degenerative joint disease.

Periarticular new bone can be produced in association with articular cartilage lesions and this may be of clinical significance in a horse with neck stiffness or ataxia. Small lucent zones in the region of the articular processes represent deep pits in the vertebral pedicles (Figure 12.24). These are usually indicative of a clinically significant lesion. Associated chronic synovitis may result in the development of radiolucent areas in the pedicle cranial to the articular process joint(s) (Figure 12.27).

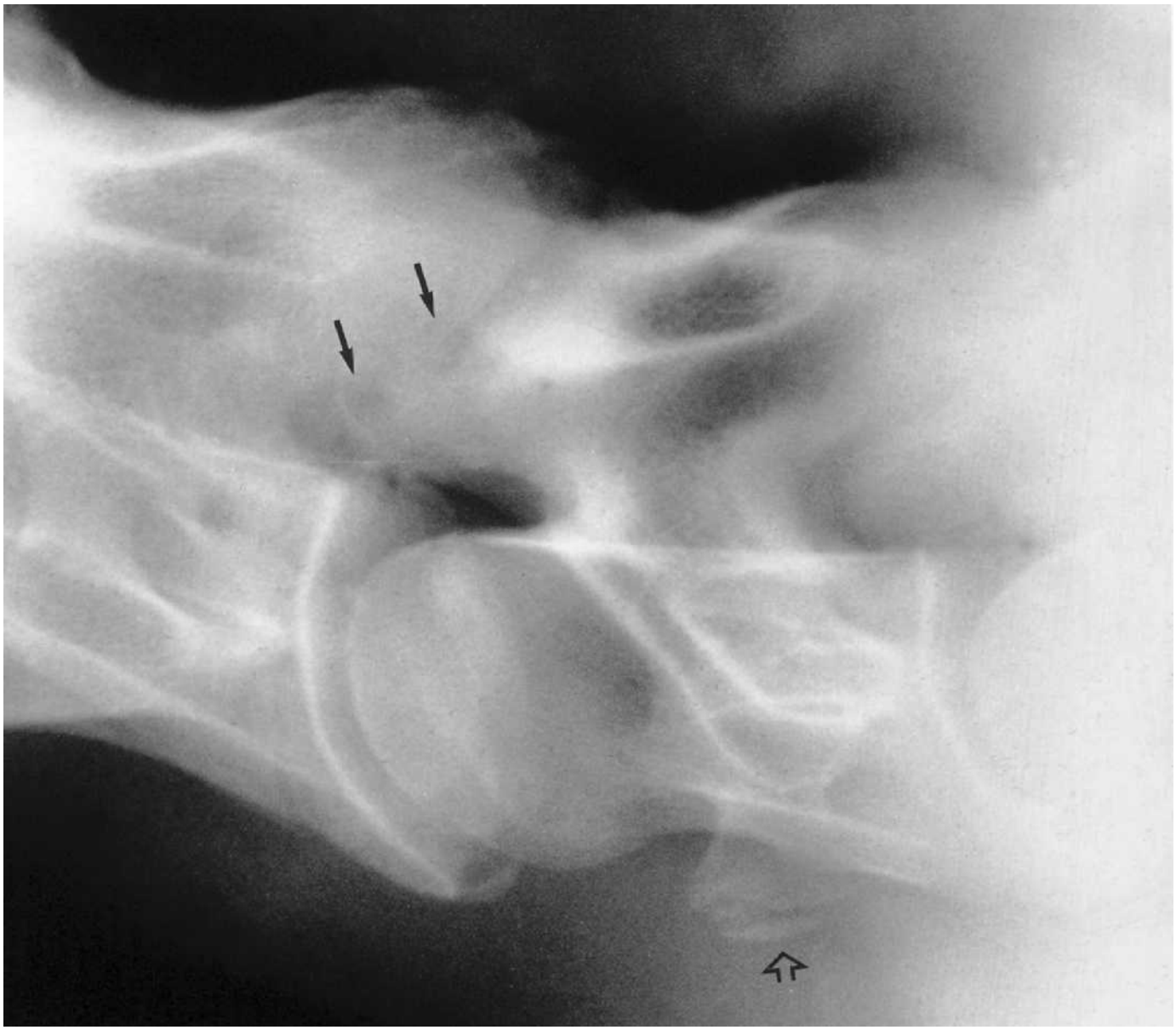


Figure 12.24 Lateral-lateral image of the caudal cervical vertebrae (C6 and C7) of an ataxic yearling Thoroughbred filly. Cranial is to the left. There is extensive modelling of the articular process joints of C6–C7 and an irregular joint contour. Radiolucent areas (solid arrows) represent pits in the vertebral pedicles. Spinal cord compression was confirmed at C6–C7, associated with a synovial cyst. One ventral process, with a separate centre of ossification, was transposed from C6 to C7 (open arrow).

A bony 'buttress' may be seen on the ventral aspect of one or both cranial articular processes, in normal and ataxic horses. If well-developed this buttress impinges on the body or arch of the more cranial vertebra and forms a false joint. (Figures 12.25a and 12.25b). Radiographically the buttress partially or completely obliterates the intervertebral foramen (Figures 12.25a and 12.25b). This may be of no clinical significance unless the joint capsule bulges axially and compresses the spinal cord, or new bone results in nerve root impingement.

Massive enlargement of the articular process joints of C4–C5, C5–C6, and C6–C7 has been seen in association with unilateral forelimb lameness (Figures 12.26a and 12w.26b–d). Nerve root impingement associated with atrophy of the caudal cervical musculature has been documented by



Figure 12.25(a) Lateral-lateral image of the caudal cervical vertebrae (C5–C7) of a 7-year-old Warmblood with generalised stiffness. Cranial is to the left. There is considerable enlargement of the articular process joints between the fifth and sixth and sixth and seventh cervical vertebrae, with almost complete obliteration of the intervertebral foramina.

contrast-enhanced computed tomography at C4–C5 and C5–C6, associated with severe degenerative joint disease of the articular process joints. In a horse with unilateral forelimb lameness of unknown cause, comparison of left to right and right to left lateral-lateral radiographs and acquisition of lateroventral-laterodorsal images from left to right and from right to left may be helpful (Figures 12w.26c and 12w.26d).

A pathological fracture may develop secondarily to modelling of a cervical articular process joint. There is usually minimal displacement of the fracture fragments, but a lucent line is detectable radiographically (Figure 12.27). Fractures may occur unilaterally or bilaterally. This is difficult to assess on lateral-lateral radiographs, but can be determined from lateroventral-laterodorsal images. An associated ataxia warrants a poor prognosis, but healed fractures have been found at post mortem in apparently clinically normal animals or in horses with articular process arthropathy.

There is a growing body of evidence that radiography underestimates the degree of osseous change present in articular process joints. However, there is also clear evidence that many radiological abnormalities are asymptomatic.



Figure 12.25(b) Lateral-lateral image of the caudal cervical vertebrae (C6–T1) of an 8-year-old Selle Français gelding. Cranial is to the left. The horse had a history of neck stiffness and poor performance and intermittently the neck locked in a low position with the horse unable to move. This usually resolved spontaneously. There is massive enlargement of the articular process joints between the sixth and seventh cervical vertebrae; the ventral aspect of the articulation extends to the vertebral bodies. This is ventral buttressing. There is also buttressing at the articulation between the seventh cervical and first thoracic vertebrae. The intervertebral foramina are very small. The horse also had clinical evidence of back pain and sacroiliac joint region pain and had radiographic evidence of impinging spinous processes of the seventeenth and eighteenth thoracic vertebrae and osteoarthritis of the articular process joints at the same level. Performance was markedly improved by analgesia of the impinging spinous processes and caudal thoracic articular process joints together with the sacroiliac joint region. The radiographic abnormalities of the neck may result in episodic nerve root impingement and severe pain, causing the locking of the neck.

Modelling of the caudal cervical articular process joints is common in mature horses and, unless radiographic abnormalities are dramatic, ascribing clinical significance to them can be difficult. Nuclear scintigraphy is often not helpful because there is frequently little change in the normal pattern of radiopharmaceutical uptake (which is always greater in the caudal neck region compared with the mid neck). Ultrasonography can be useful to identify joint capsule thickening and increased amounts of synovial fluid, but such abnormalities are not necessarily associated with pain. Ultrasound-guided local analgesia of the articular process joint is the most reliable method of confirming the presence of pain and the clinical significance of any radiological abnormality. Contrast-enhanced computed tomography



Figure 12.26(a) Lateral-lateral image of the caudal cervical vertebrae (C5–C7) of a 4-year-old Warmblood dressage horse, which was stiffer to the right and exhibited right forelimb lameness. Cranial is to the left. The sixth cervical vertebra appears slightly rotated because of asymmetrical enlargement of the articular process joints between the sixth and seventh cervical vertebrae. Note also the large spurs (arrows) projecting from the ventral aspect of the articulations of both C5 and C6 and C6 and C7. Right forelimb lameness was abolished by intra-articular analgesia of the right C6–C7 articular process joint.

provides the opportunity for three-dimensional images of the vertebrae, to demonstrate axial enlargement of the articular process joints ± impingement on the spinal cord, encroachment of bone on the intervertebral foramina and nerve root impingement.

Subluxation of the atlantoaxial joint

Subluxation of the atlantoaxial joint may occur in foals or less commonly in an adult horse, associated with damage to the ventral ligaments of the dens. It results in an abnormal extended neck posture, with or without ataxia. The abnormal position of the vertebra is easily seen on a lateral-lateral radiographic view (Figure 12.28), which should be scrutinised carefully for a concurrent fracture. The distance between the dorsal lamina of the first



Figure 12.27 Lateral-lateral image of the fifth and sixth cervical vertebrae of an ataxic 9-year-old Thoroughbred cross riding horse. Cranial is to the left. There is a chronic fracture involving the articular process of C5–C6 (arrows). The articular process joints are enlarged with ventral buttressing and obliteration of the intervertebral foramen. Note the well-defined radiolucent area in the pedicle of the fifth cervical vertebra.

cervical vertebra and the dorsal aspect of the dens should be measured and compared with normal values. In most horses the dens is displaced proximally and the prognosis is poor. Successful reduction of a ventral luxation in an adult horse has been recorded.

Subluxation of the caudal cervical and first thoracic vertebrae

Subluxation of the fifth and sixth, sixth and seventh cervical or seventh cervical and first thoracic vertebrae is sometimes seen in mature horses with poor performance and low-grade ataxia. Dorsal subluxation is most common (Figure 12.21b), but ventral subluxation does occur (Figure 12.29a). There may be associated modelling of the articular process joints (Figures 12w.29b and c). Vertebral stabilisation could be considered.

Entheseophyte formation on the occiput associated with the nuchal ligament

New bone formation may occur in the region of insertion of the nuchal ligament on the occiput, also extending slightly dorsal and ventral to the site of insertion (Figure 11.8). It can be seen as an incidental finding, especially in Warmbloods. Clinically affected horses tend to resist the reins, find difficulty in flexion at the poll and may rear or head-shake. The significance of the bony abnormality may be determined by local infiltration of local



Figure 12.28 Lateral-lateral image of the cranial cervical vertebrae (C1–C2) of a 9-year-old advanced event horse with severe neck stiffness and an audible click associated with these vertebrae. Cranial is to the left. There is subluxation of the atlantoaxial joint. Note the narrowed space between the dorsal aspect of the odontoid peg of the axis and the ventral aspect of the dorsal lamina of the atlas (arrowed). There is slight irregularity of the dorsal contour of the odontoid peg. Post mortem examination confirmed complete rupture of the ligament of the dens. Compare with Figure 12.7.

anaesthetic solution although only a positive block will be of assistance. Treatment by osteopathic manipulation or local infiltration of corticosteroids and local anaesthetic solution, combined with modification of the training programme, has shown variable results.

Degenerative changes of the intercentral articulations

A survey of the cervical intervertebral discs of 103 horses from birth to 23 years of age confirmed that they consisted solely of fibrocartilage, with no nucleus pulposus. Age-related degenerative changes were common, but not associated with clinical signs. The strong longitudinal ligament dorsal to the intervertebral discs prevents herniation into the vertebral canal. Narrowing of an intercentral articulation due to primary degeneration of an intervertebral fibrocartilage (disc) is rarely seen (see 'Discospondylitis', below), but degenerative changes of the joint may occur secondary to trauma. Radiographic abnormalities include narrowing of the intercentral joint space, change in shape of the joint surfaces and change in the subchondral bone opacity (Figure 12.31).



Figure 12.29(a) Lateral-lateral image of the caudal cervical vertebrae (C6–C7) of a 15-year-old Thoroughbred stallion with a history of difficulty in mounting mares and a non-specific hindlimb gait abnormality. Cranial is to the left. Clinical examination revealed mild hindlimb ataxia and weakness. There is ventral subluxation of the head of the seventh cervical vertebra. The intercentral joint space is narrowed ventrally. There is periarticular new bone on the caudoventral aspect of the body of the sixth cervical vertebra and modelling of the dorsal articular margin consistent with degenerative joint disease. There is enlargement of the articular process joints between the sixth and seventh cervical vertebrae with ventral buttressing.

Osteomyelitis

In foals, systemic infections may localise in cancellous bone, often in the vertebral bodies. This usually results in neck stiffness and recurrent pyrexia. Focal lucent areas are the first identifiable radiographic change, but if the foal survives, areas of increased opacity may develop. In older horses local extension of a chronic soft-tissue infection (e.g. avian tuberculosis) can result in osteomyelitis and neck stiffness. Radiolucent areas, usually surrounded by more opaque margins, are seen within the vertebral bodies (Figure 12.30).

Discospondylitis

Discospondylitis (inflammation of the vertebral body and the associated intervertebral disc) is rare and is usually associated with infection, although it may be of unknown or traumatic aetiology (see above, 'Degenerative changes of the intercentral articulations'). Clinical signs may include neck pain and stiffness, with or without ataxia or forelimb lameness, cervical hyperaesthesia or muscle twitching. Radiological recognition of discospondylitis at the cervico-thoracic junction however has been seen unassociated with clinical signs of either lameness or abnormal neck posture. Non-infected cases are characterised by narrowing of the intercentral joint space with modelling of the ends of the adjacent vertebral bodies (Figure 12.31). At the

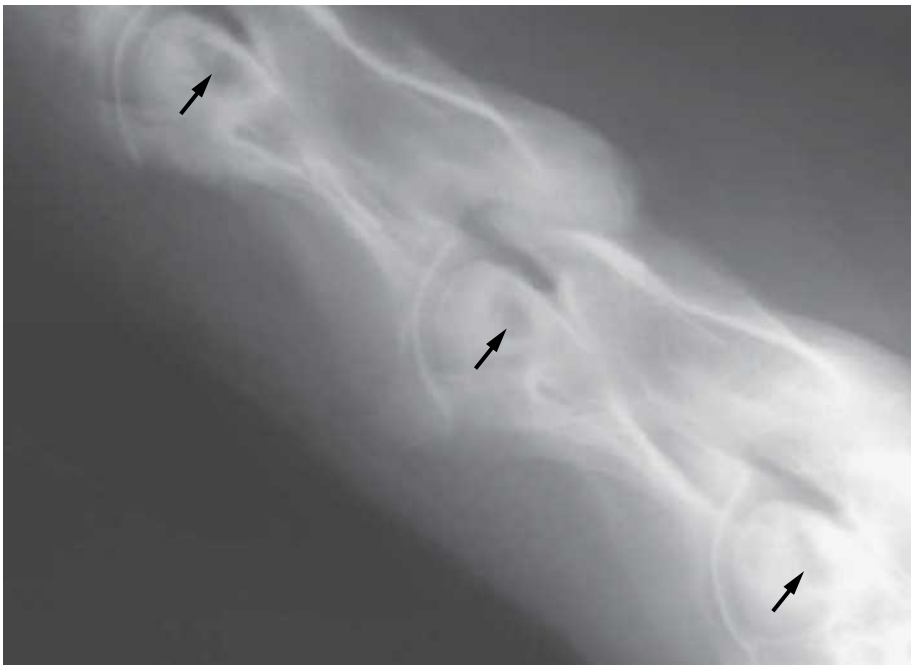


Figure 12.30 Lateral-lateral image of the third to sixth cervical vertebrae of a 5-year-old Thoroughbred mare with severe neck stiffness, persistent leucocytosis and neutrophilia, and an increase in β_2 globulins. Cranial is to the left. There are irregular radiolucent areas in the vertebral bodies (arrows) surrounded by bone of increased opacity. Tuberculous osteomyelitis was confirmed post-mortem.

time of onset of clinical signs radiography may be unrewarding for lesions associated with infection, but follow-up radiographs usually reveal abnormalities. Focal or more diffuse radiolucent zones and some increased opacity are seen in the caudal end plate of one cervical vertebra and/or the cranial aspect of the adjacent vertebra, with or without alteration of the width of the disc space. Ultrasonographic examination may be useful to identify fluid accumulation typical of abscess formation. The prognosis with conservative management is poor, but successful surgical management has been recorded.

Osseous cyst-like lesions

Occasionally, single or several well-demarcated radiolucent zones are identified in one or more adjacent vertebrae, associated with profound neck pain, with or without forelimb lameness. These lesions have not been proved to be caused by osteomyelitis or myeloma, although a definitive diagnosis has not always been possible by bone biopsy or post-mortem examination. One horse with extremely severe neck pain and forelimb lameness had radiolucent zones in the fifth and sixth cervical vertebrae, and bone biopsy revealed accumulation of abnormal plasma cells, but the horse made a most spectacular and complete recovery after exploratory surgery and returned to international showjumping. A show pony had a large cyst-like lesion in the fourth cervical vertebra with profound neck pain and left forelimb lameness. Post-mortem examination revealed a cavity filled with granulation tissue, surrounded by a large area of bone necrosis, but no suggestion of the underlying cause.



Figure 12.31 Lateral-lateral image of the sixth cervical to second thoracic vertebrae of a 4-year-old pony with severe neck stiffness and great difficulty in lowering its head to graze. Cranial is to the left. There is complete loss of the intercentral joint space between the seventh cervical (C7) and first thoracic (T1) vertebrae. The caudal end plate of C7 and the head of the vertebral body of T1 are misshapen. There is a lucent area in the head of T1 with generalised surrounding increased opacity. The dorsal profile of the vertebral body of C7 is of abnormal shape. There is transposition of a ventral process onto the vertebral body of C7. There is also considerable enlargement of the articular process joints between the seventh cervical and first thoracic vertebrae. The pony's ability to lower the neck was improved after intra-articular analgesia of the articular process joints between C7 and T1. Source: Reproduced with permission of Annamaria Nagy.

Neoplasia

Neoplastic invasion of cervical vertebrae is rare, but may present clinically as neck stiffness, neck pain or ataxia (Figure 12.32a). Pressure caused by an expanding soft-tissue mass may cause smooth modelling of the bone. Neurofibromatosis can cause enlargement of the transverse and intervertebral foramina and cavitation of the vertebral arch, resulting in a large well defined radiolucent zone (Figure 12w.32b). A mottled opacity of the vertebral bodies may be suggestive of neoplastic invasion of the bone marrow (e.g. lymphosarcoma, plasma cell myeloma), which may result in osteomalacia and pathological fractures. It may be difficult to differentiate radiographically between the effects of neoplasia, infection and trauma.



Figure 12.32(a) Lateral-lateral image of the first to third cervical vertebrae of a 24-year-old pony with sudden-onset ataxia and neck stiffness. Cranial is to the left. There is multifocal osteolysis in the vertebral body of the second cervical vertebra, suggestive of neoplasia. Post-mortem examination confirmed the presence of a large extradural soft tissue mass at the level of C2 within the right side of the vertebral canal, displacing and compressing the spinal cord towards the left and slightly dorsally. The mass was confirmed as lymphosarcoma. Source: Reproduced with permission of Lucy Meehan.

Soft-tissue lesions

Mineralisation in the soft tissues should not be confused with lesions involving the vertebrae. This may occur secondary to an intramuscular injection (Figure 12w.33a) or as the result of previous trauma. A common site is in the ligamentum nuchae, caudal to the occiput. This dystrophic mineralisation is readily identifiable radiographically (Figure 12w.33b), but may not be of long-term clinical significance.

Tearing of muscle and ligamentous insertions on the ventral aspect of the vertebral bodies may result in entheseophyte formation, readily identifiable radiographically on a lateral-lateral projection. This may be of no long-term clinical significance.

Spondylosis

Spondylosis of the cervical vertebrae is rare. Two cases have been described, both in mature Quarterhorses. Spondylosis was extensive, involving the second cervical to first thoracic vertebrae and the third to seventh cervical vertebrae, respectively. Both horses had severe neck stiffness.

Scoliosis

Scoliosis may be congenital associated with vertebral malformation. Acquired scoliosis is an unusual condition in adult horses but has been described. There may be no detectable radiological abnormality of the cervical vertebrae. Although traumatic subluxation has been assumed to be a cause, a neurological basis has been the best documented, associated with *Parelaphostrongylus tenuis* migration.

Fractures

Fractures are usually the result of trauma (e.g. a fall or a collision) but may occur secondary to a pre-existing lesion (e.g. modelling of a cervical articular process joint; Figure 12.27). They result in neck pain and stiffness, and may cause ataxia. In young horses separation occasionally occurs along unfused physes and this occurs most often in the axis. The prognosis depends on the site of the fracture, particularly with reference to the vertebral foramen, the degree of fracture displacement and the amount of callus that develops subsequently. Fractures may involve the articular process joints, the pedicle or the vertebral body or a combination (Figures 12w.34a, 12w.34b, 12.35 and 12.36).

In the acute stage it is often difficult to make an accurate prognosis based on the clinical signs or the radiographic appearance of the fracture (Figures 12.35a, 12.35b and 12.36). Initial ataxia may resolve, only to recur if callus impinges on the spinal cord. Fusion of adjacent vertebrae may develop and cause neck stiffness. Generally, fractures involving the bone surrounding the vertebral foramen or the articular process warrant a guarded prognosis.

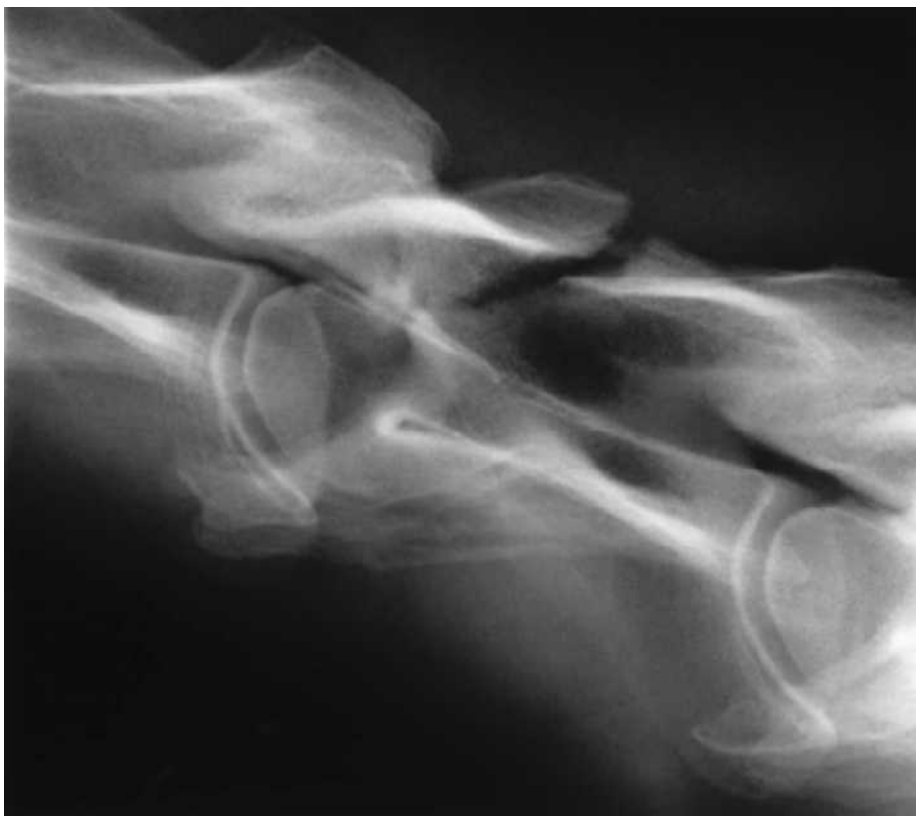


Figure 12.35(a) Lateral-lateral image of the third to fifth cervical vertebrae of a 9-year-old Dutch Warmblood dressage horse with severe neck pain and stiffness, and incoordination following a fall in a field 12 days previously. Cranial is to the left. There is a comminuted, slightly displaced fracture of the dorsal arch of the fourth cervical vertebra.

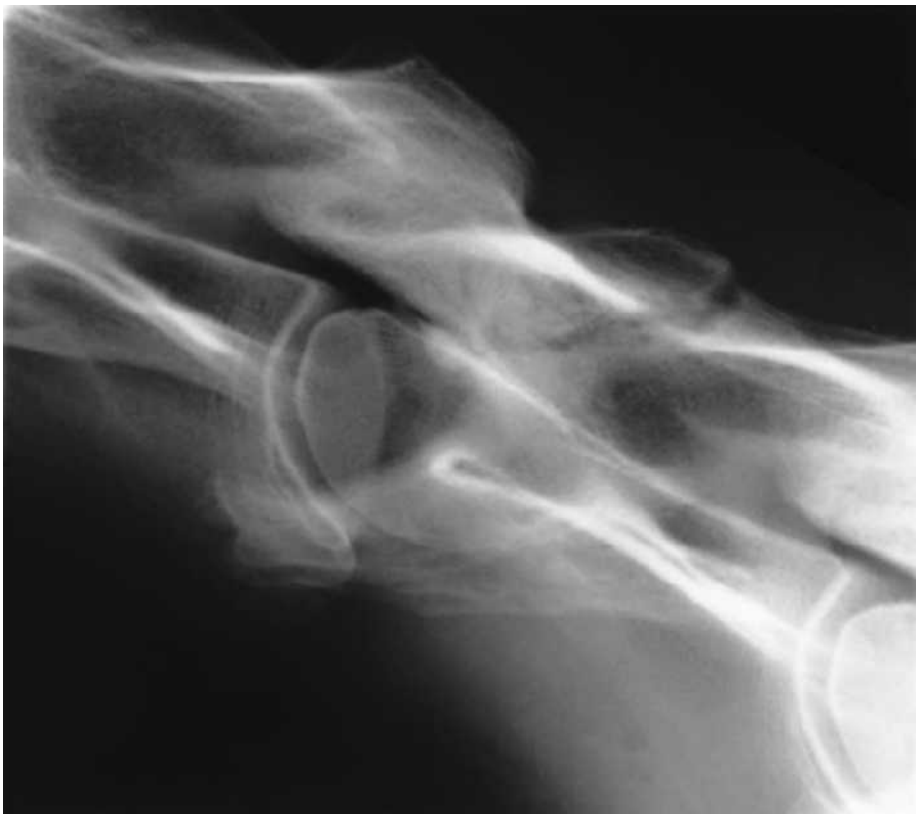


Figure 12.35(b) Lateral-lateral image of the third to fifth cervical vertebrae of the same horse as in Figure 12.35(a), obtained 6 weeks later. Cranial is to the left. There is evidence of some bony union. The horse made a complete functional recovery.



Figure 12.36 Lateral-lateral image of the sixth cervical to first thoracic vertebrae of a 10-year-old event horse with sudden-onset severe hindlimb ataxia and caudal neck pain. Cranial is to the left. There is considerable asymmetric enlargement of the articular process joints of the sixth and seventh cervical and seventh cervical and first thoracic vertebrae. There is a recent fracture extending from one of the articular processes through one of the pedicles of the seventh cervical vertebra (arrows). The head of the first thoracic vertebra is aligned slightly dorsal relative to the vertebral body of the seventh cervical vertebra.

Occasionally a fracture of a caudal cervical vertebra may be associated with unilateral forelimb lameness.

Thoracolumbar vertebrae

RADIOGRAPHIC TECHNIQUE

Equipment

Radiography of the thoracolumbar vertebrae in adult horses poses a number of technical problems. The thickness of the back requires radiographic equipment with an output of 75–120 kV and 100–250 mAs, and the large mass of soft tissues causes considerable scattered radiation that must be controlled to obtain diagnostic radiographs.

Ideally the x-ray tube is mounted on an overhead gantry with a linked cassette holder to ensure alignment of the x-ray beam and the imaging plate. If a cassette holder is not linked to an overhead gantry, it is best mounted on the horizontal beam of a set of stocks, or directly on a wall. This improves safety and helps to reduce movement. Stocks are recommended not only to restrain the horse but also to ensure that it is standing straight, so that true lateral-lateral images are obtained.

Digital systems or rare earth screens and appropriate film are necessary. The effect of scattered radiation must be controlled and the use of an appropriate grid is recommended. In addition, a lead sheet (at least 0.01 mm lead equivalent) should be placed behind the cassette to prevent backscatter. These measures are particularly important for radiographs of the lumbar spine. A sheet of lead can be placed dorsally on the horse's back to reduce scattered radiation. This can be particularly useful in the lumbar region and is well tolerated by all but the most sensitive horses. With the above equipment, it is technically possible to obtain radiographs of the thoracolumbar vertebral column from the first thoracic (T1) to approximately the third or fourth lumbar vertebrae (L3/L4), depending on the size and thickness of the horse. Further caudally, the lumbosacral vertebrae and ilial wings are superimposed, making interpretation impossible (except in foals and small, thin ponies). In the lumbar region, the mass of soft tissues results in considerable scattered radiation, so that without the use of an appropriate grid, detail and contrast are lost.

To minimise movement of the patient, tranquillisation is usually necessary. Radiographs are best obtained at the end of expiration. Only lateral-lateral and lateral oblique radiographs of the thoracolumbar vertebrae can be obtained with the horse standing. Ventrodorsal radiographs of the caudal thoracic vertebrae may be obtained under general anaesthesia. Ventrodorsal views of the lumbar region are discussed elsewhere (see Chapter 13, 'Radiographic technique').

To evaluate the thoracolumbar vertebrae (T2–L3) adequately, it is necessary to use large cassettes (35 cm × 43 cm), and to obtain at least four to six radiographs. To help identify individual vertebrae on successive radiographs, it is helpful to tape small radiodense markers (e.g. lead arrows) to the skin on the midline of the back. Four or five (more if using smaller imaging plates) of these should be evenly spaced between the withers and the croup.

Positioning

The horse should stand squarely, taking weight evenly on all four limbs, with the head and neck straight. Resting a limb causes rotation of the vertebrae, resulting in radiographic images that are difficult to interpret. The first radiograph is normally obtained in the mid-thoracic region (approximately T9–T15). For routine lateral-lateral radiographs, the x-ray beam is centered at the level of the vertebral canal (approximately 15–20 cm below the dorsal midline of the back in an adult Thoroughbred horse), and aligned at right angles to the long axis of the trunk. Successive radiographs are similarly aligned, centering cranial or caudal to the previous view. Adjacent radiographic images should overlap, as this greatly aids identification of vertebrae. At the withers, the x-ray beam needs to be centered in a way that the top of the cassette is just above the highest point of the withers. The imaging plate should be orientated vertically as close as possible to the horse; anything else will result in distortion (most often elongation) of the spinous processes in particular and should be avoided.

For all areas of the thoracolumbar vertebrae, at least two differently exposed films are needed, even when using digital systems: one to examine the spinous processes and a second to examine the vertebral bodies and their articulations. Assessment of the articular processes and their articulations (articular process or facet joints) requires high-quality, well-collimated radiographs. Additional information about the left and right articular process joints and the vertebral bodies can be obtained using oblique radiographic views. It is important to be able to assess the entire length of the spinous processes, the articular process joints and the vertebral bodies for complete evaluation. Assessment of the summits of the spinous processes may be enhanced by the use of exposures at reduced kilovoltage, without a grid.

If linked equipment is not available, it is often helpful to mark the horse on each side with an adhesive label where each radiograph is centered, to aid alignment of the cassette.

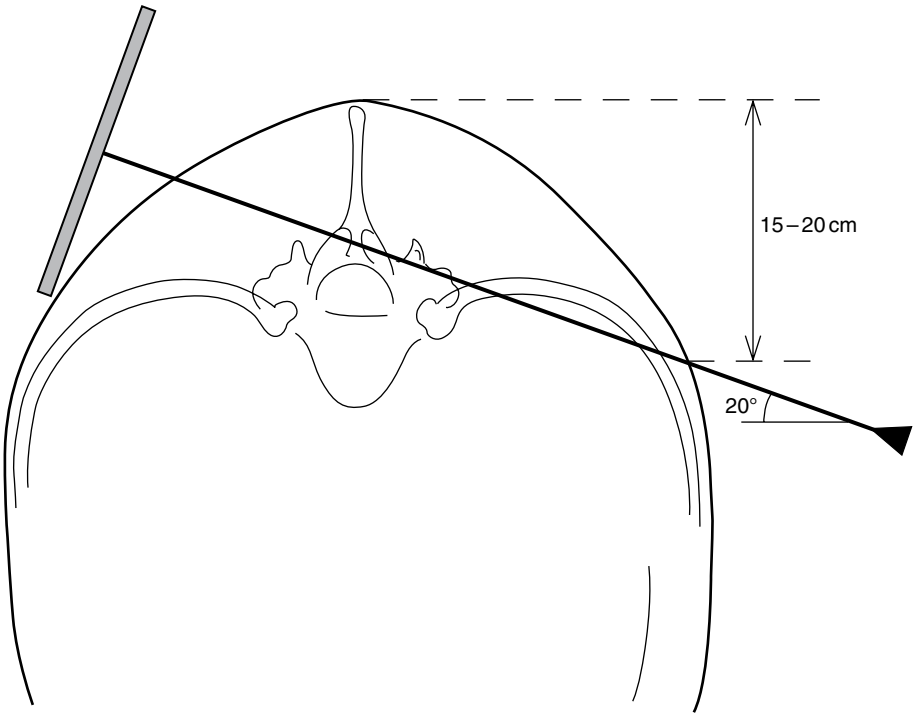


Figure 12.37 Positioning of the horse, imaging plate and x-ray beam to obtain a lateral 20° ventral-laterodorsal oblique view of the thoracic articular process joints. The x-ray beam, angled 20° ventral from horizontal, is centered at the level of the articular process joints, 15–20 cm distal to the dorsal midline depending on the size of the horse. The imaging plate is aligned perpendicular to the x-ray beam and positioned as close to the horse as possible.

To obtain oblique radiographic images of the articular process joints and vertebral bodies, the x-ray tube is aligned 20° ventral to the horizontal (Figure 12.37). The imaging plate is aligned perpendicular to the x-ray beam. The x-ray beam is centered at the approximate level of the articular process joints. Radiographs are best obtained at the end of expiration to avoid the diaphragm being superimposed over the caudal thoracic articular process joints. Radiographs should be obtained from left to right and right to left. However, such views are only useful in the thoracic region because caudal to the diaphragm abdominal structures are superimposed over the articular process joints. Particular care with radiation safety should be taken whenever the x-ray beam is angled upwards, as most x-ray facilities are designed for vertical (down) or horizontal x-ray beams.

NORMAL ANATOMY, VARIATIONS AND INCIDENTAL FINDINGS

Immature horse

At birth the thoracolumbar vertebral column is dorsally convex and remains so until it becomes straight at about 6 months of age. All the vertebral bodies have cranial and caudal physes, the cranial physes closing at about 6–12 months of age and the caudal physes between 2 and 4 years of age (Figures 12.38a and 12.38b).

At approximately 12 months of age the cranial thoracic spinous processes (T2–T8) develop separate centres of ossification within their cartilaginous summits. This ossification is gradual. These centres of ossification have an irregular outline and mottled opacity, and usually remain separate from the parent bone and incompletely ossified throughout life (Figure 12.39).

Skeletally mature horse

The horse normally has 18 thoracic vertebrae. The number of lumbar and sacral vertebrae varies among horses. Most horses have six lumbar vertebrae and five sacral vertebrae, but a significant number of horses have only five lumbar vertebrae, or may have six sacral vertebrae. There may be congenital fusion of the lumbosacral joint. The donkey has only five lumbar vertebrae and four to six sacral vertebrae. The vertebral bodies are approximately rectangular in shape, cranially convex and caudally concave. They articulate at the intercentral joints, which are uniform in width. Care should be taken not to interpret overlying lung opacities as modelling of the vertebral bodies. The vertebral canal is of similar height throughout the thoracolumbar vertebral column. The articular process joints are difficult to evaluate and higher exposures may be required (Figure 12.40). Large, well-muscled horses are easier to examine than smaller, fatter horses. These articulations are identified as oblique radiolucent lines dorsal to the vertebral canal (Figure 12.41a). The articular process joints in the lumbar region are larger than in the thoracic region; they appear more radiopaque and have a more irregular outline (see Figure 12.45). There are marked variations in shape of the articular process joints from the cranial thoracic region to the caudal lumbar region (Figures 12w.41b, 12.41c and 12.45), and comparison with articulated bone specimens is invaluable. In the thoracic region the mammillary processes are

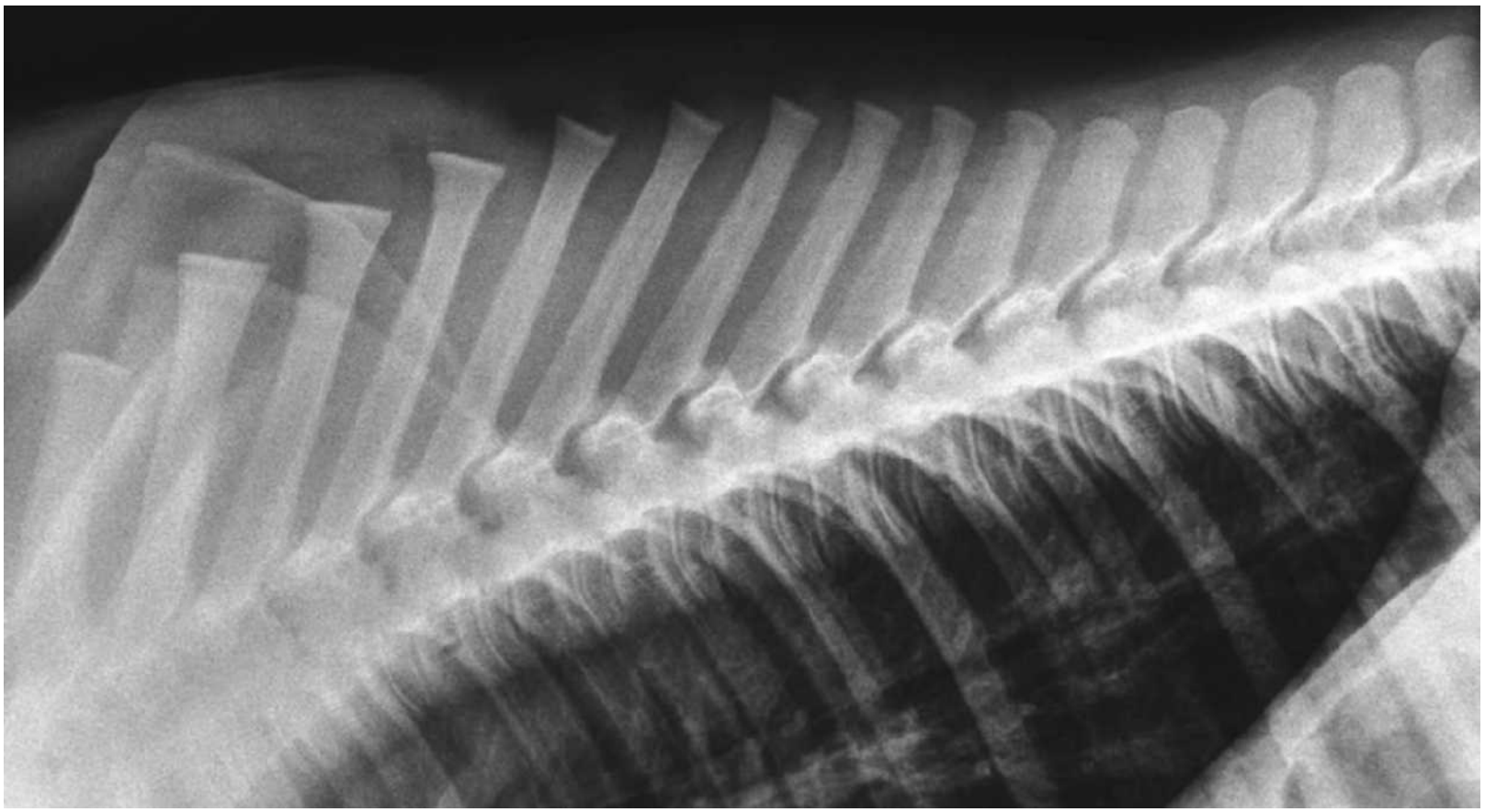


Figure 12.38(a) Lateral-lateral image of the thoracic vertebrae of a normal 1-day-old Thoroughbred foal. Note the absence of mineralisation of the separate centres of ossification of the spinous processes of the more cranial vertebrae compared with an adult horse (Figure 12.39). Cranial is to the left. The cranial and caudal physes of the vertebral bodies are clearly seen.

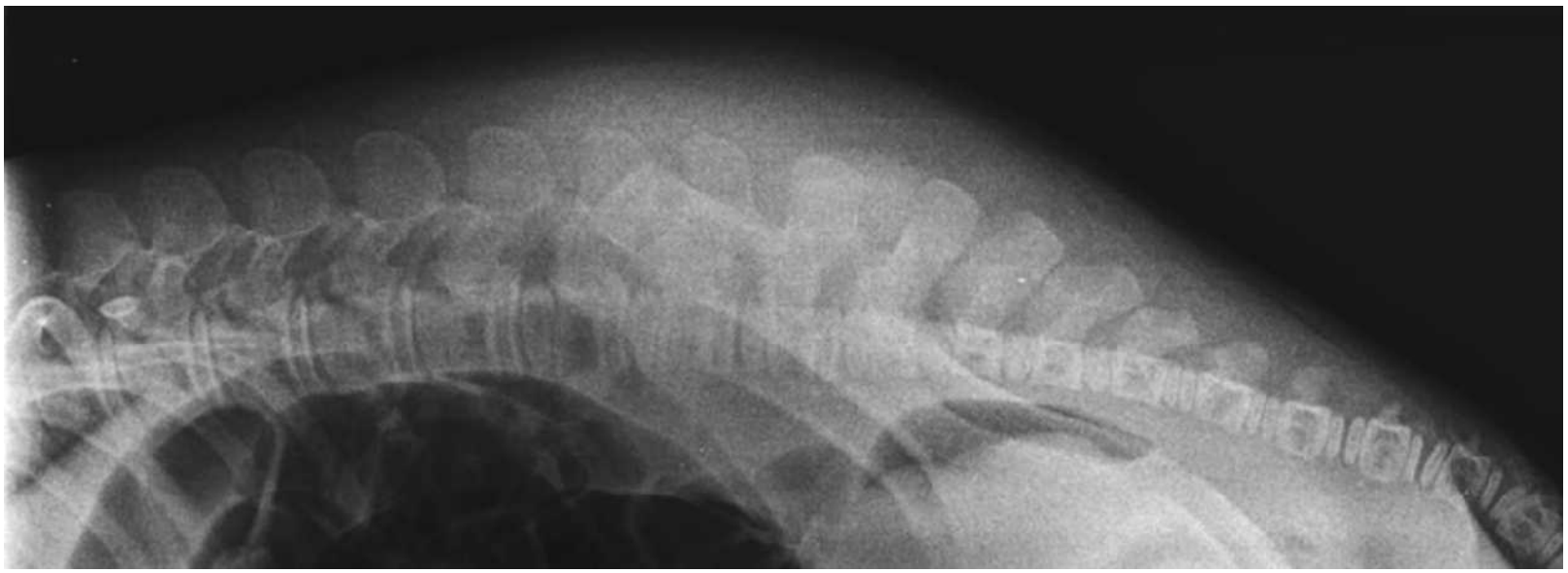


Figure 12.38(b) Lateral-lateral image of the caudal thoracic, lumbar, sacral and coccygeal vertebrae of a 2-day-old Thoroughbred foal. Cranial is to the left. The cranial and caudal physes of the vertebral bodies are clearly seen.



Figure 12.39 Lateral-lateral image of the cranial thoracic spinous processes of the withers region (T2–T8) of a normal adult horse. Cranial is to the left. Note the uneven opacity of the separate centres of ossification of the summits of the spinous processes. This appearance persists throughout life. Note also the smooth contour of the cranial and caudal margins of each spinous process.



Figure 12.40 Lateral-lateral image of the articular process joints in the mid to caudal thoracic region of a normal adult horse. Cranial is to the left. Note the relatively opaque articular processes (arrows) crossed by a lucent line (the joints) coursing from caudodorsally to cranioventrally. The vertebral canal is obscured by superimposition of the ribs. In some horses with very highly curved ribs, the articular process joints may also be obscured.

partially superimposed, which can potentially confound assessment of the articular process joints (Figure 12.41a). The ribs articulate dorsal to the intercentral articulations and initially course dorsally and caudally, but then turn ventrally (Figure 12.40). If the ribs are 'highly sprung' they will be superimposed over the articular process joints, prohibiting evaluation of the joints on lateral-lateral images.

The spinous process of T1 has a triangular shape and is considerably shorter than that of T2. The spinous process of T2 is noticeably shorter than T3 and more rectangular than T1. There is marked variation in width among individuals. T1 has no separate dorsal ossification centre, but there are separate ossification centres from T2 to T7 or T8. These are usually single centres, but occasionally two are present. Further caudally the summit of each spinous process is smoothly rounded. Smoothly outlined, irregular new bone formation on the summit of a spinous process may reflect previous supraspinous enthesopathy. There is frequently rather irregular new bone on the cranial and caudal aspect of the body of one or more spinous processes in the cranial thoracic region (T2–10), possibly reflecting entheseous reaction at the attachment of the interspinous ligament (Figures 12.42 and 12w.50a). However, when affecting more caudal thoracic vertebrae it is more likely to be of clinical significance and may be associated with increased radiopharmaceutical uptake (see Figures 12.50b and 12.50c).

The spinous processes at the withers (approximately T2–T10) are long and slender and slope caudally (Figure 12.39). Their cranial aspects frequently have a smoothly outlined irregular border. Caudal to the seventh thoracic vertebra, the processes become shorter, more upright and broader (Figure 12.42). The spinous processes are approximately parallel and any

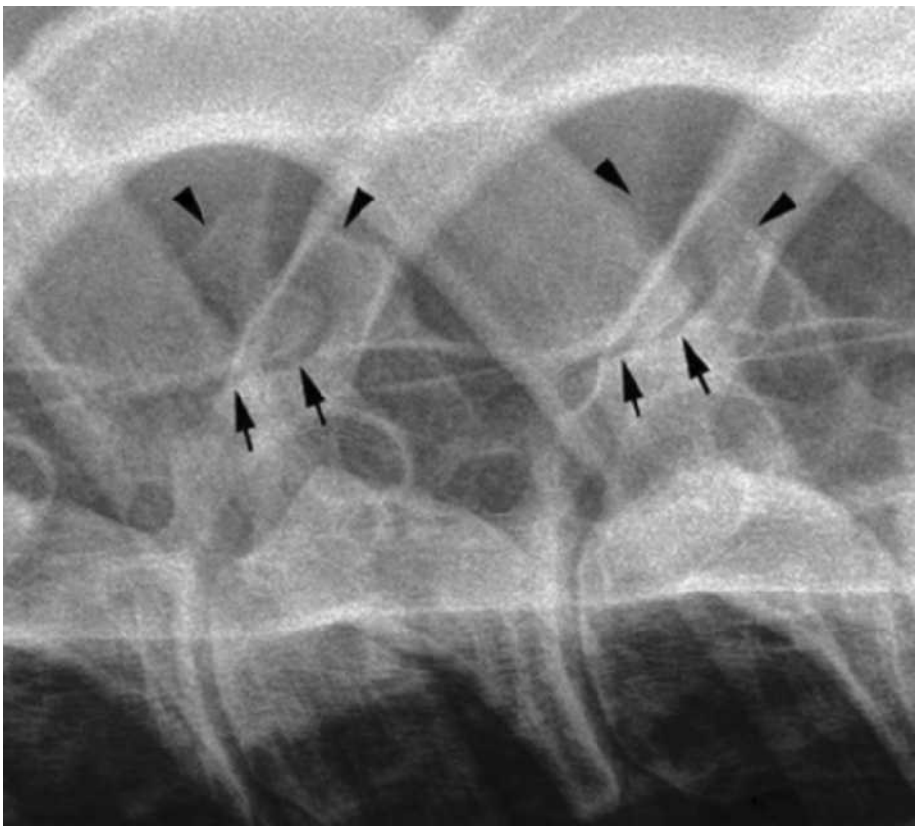


Figure 12.41(a) Close-up lateral 20° ventral-laterodorsal image of the articular process joints (facet joints) between the thirteenth and fourteenth and fourteenth and fifteenth thoracic vertebrae (arrows) of a normal adult horse. Cranial is to the left. Note the oblique orientation of the joint spaces and the regularity of joint space width. The mammillary processes (arrowheads) and ribs are partially superimposed.

marked deviation from this indicates that the vertebral bodies and intervertebral articular process joints should be examined carefully. The anticlinal vertebra (which has a vertical spinous process) is usually T15 or T16. Caudal to this the spinous processes slope cranially. There is considerable variation among horses in the shape of the thoracic spinous processes and therefore in their spacing in the mid to caudal thoracic region (Figures 12.43a and 12.43b). On either side of the anticlinal vertebra the spinous processes tend to be closer together (see Figure 12w.48 and Figures 12w.52a–d). The spinous processes may be in apposition, especially in short-coupled horses. The space between adjacent spinous processes may in part be breed dependent, with Thoroughbreds having closer spinous processes than Warmbloods. Based on a study of Swedish Warmbloods it was suggested that a space of <4 mm could be considered abnormal; however, in our experience many clinically normal horses have spinous processes which are closer. Normally the spinous processes have smooth margins of the compact bone throughout their length. The width of each spinous process is similar, despite variations in shape and overall contour. Smoothly irregular new bone or less-smooth bone is frequently seen on the cranial and caudal aspects of the spinous processes of the second to tenth thoracic vertebrae, despite a wide interspinous gap and unassociated with obvious clinical signs. It is less common to see new bone formation on more caudal thoracic dorsal spinous processes in clinically normal horses. There is sometimes a cranially directed 'beak' on the summits of the spinous processes in the caudal thoracic region.

The spinous processes of the lumbar vertebrae resemble those of the caudal thoracic region (Figure 12.44); however, their orientation varies. In horses with five lumbar vertebrae, the spinous processes tend to be parallel, whereas in horses with six lumbar vertebrae there may be divergence of the two most caudal spinous processes.

The thoracic vertebrae have relatively small transverse processes compared with the lumbar vertebrae where the transverse processes are large and flattened, and can be identified on lateral-lateral radiographs (Figure 12.45).

Identification of individual vertebrae is most easily made by identifying the spinous processes of T1, and numbering caudally. As a rough guide, the following structures can be used:

1 The separate centre of ossification on the spinous process of T3 is broad and triangular shaped.

2 Separate centres of ossification are present on the spinous processes of T2–T7/T8.

3 The spinous process of T6 (or T7) normally forms the highest point of the withers.

4 T15 is normally the anticlinal vertebra.

5 Except in full inspiration, the image of the diaphragm usually lies over the vertebral body of T16 or T17, although in fat horses the diaphragm may overlie T15.

Osseous opacities may be seen overlying spinous processes caused by eosinophilic nodular dermatitis (Figure 12.46).

It is important to recognise that radiography of the thoracolumbar region has limitations. Many osseous abnormalities may be present that cannot be detected, for example asymmetry of the articular process joints (Figure 12.47a), new bone encroaching on intervertebral foramina, and modelling of the intercentral articulations (Figure 12.47b). In a standing horse the orientation and articulations of the lumbar transverse processes cannot be assessed.

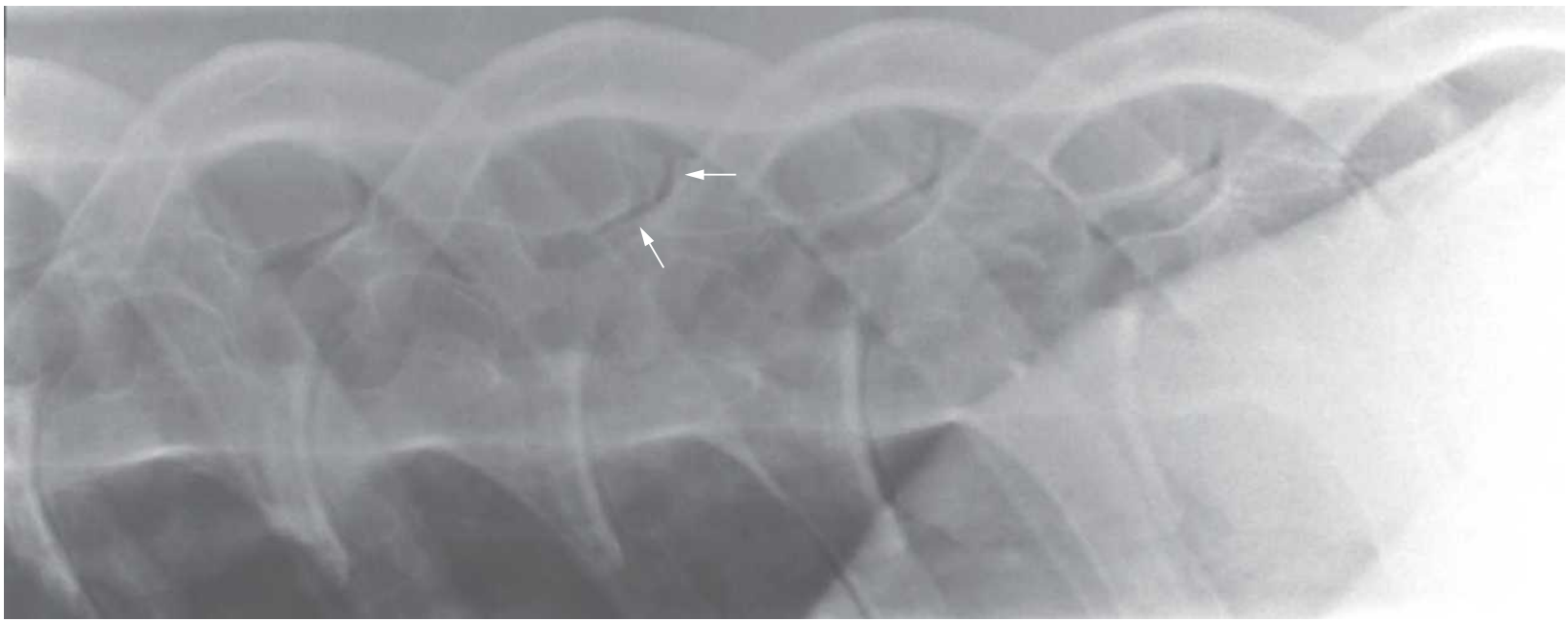


Figure 12.41(c) Lateral 20° ventral-laterodorsal oblique image and diagram of the caudal thoracic region (T13–T18) of a normal adult horse. Cranial is to the left. The articular process joints between T15–T16, T16–T17 and T17–T18 are approximately a rotated L-shape, with both oblique and vertical components (arrows).

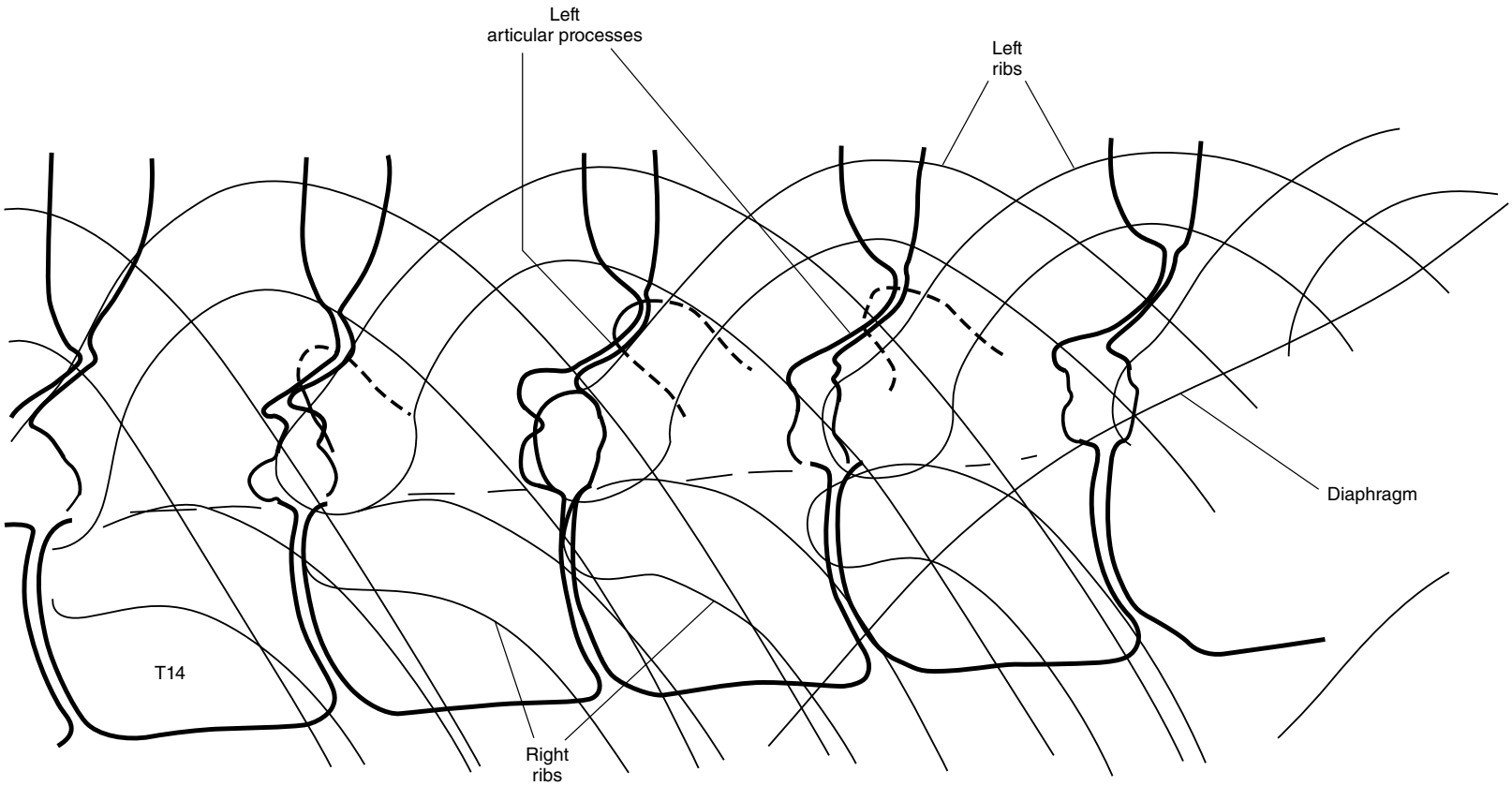


Figure 12.41(c) *Cont'd*

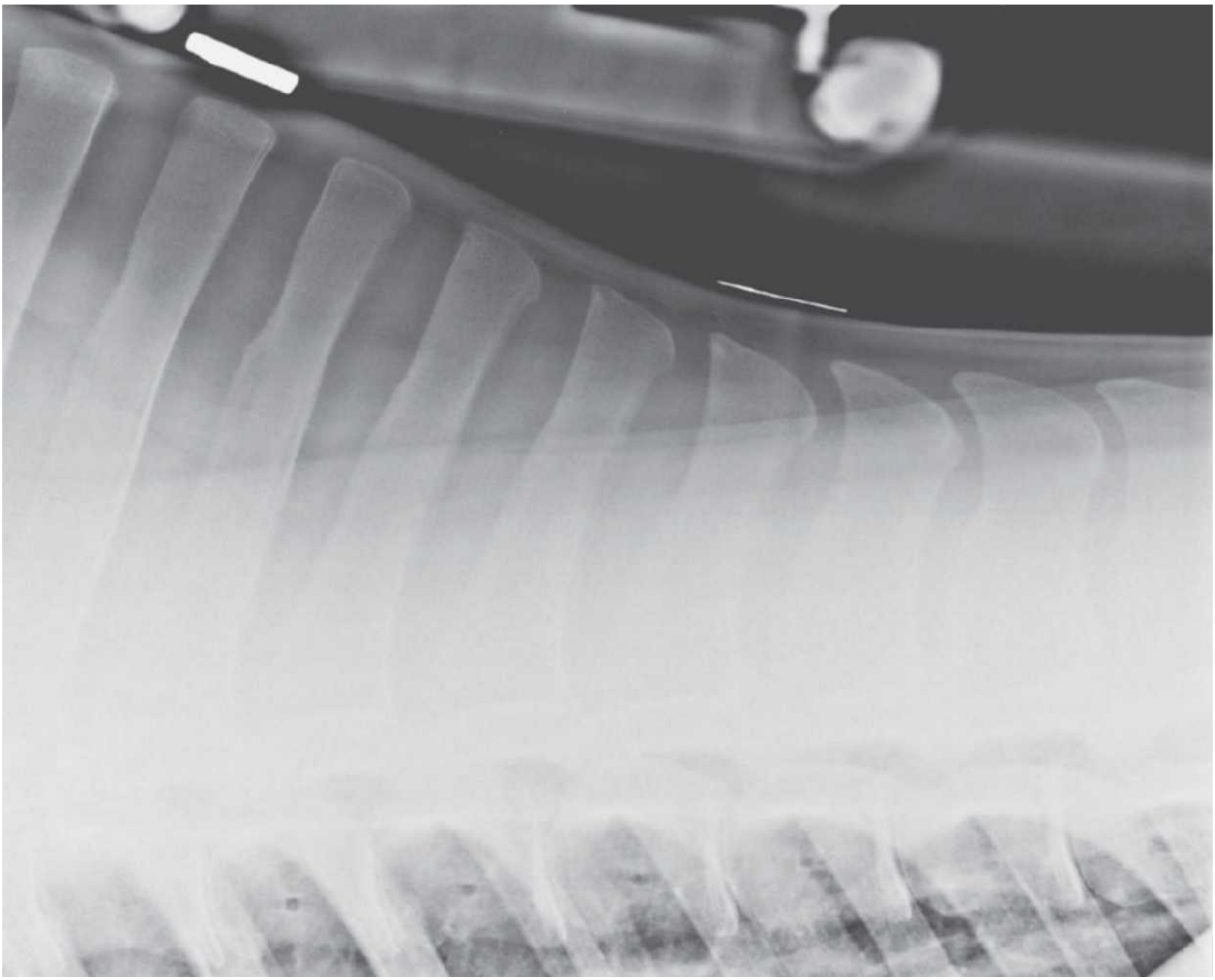


Figure 12.42 Lateral-lateral image of the mid-thoracic spinous processes (T7–T15) of a normal adult horse. Cranial is to the left. The radiograph was obtained using an aluminium wedge filter and there are lead markers on the skin. The spinous processes in this region are completely ossified (compare with Figure 12.39). Note the rather irregular margin of the cranial and caudal aspects of the more cranial spinous processes. The articular process joints are underexposed and cannot be evaluated.

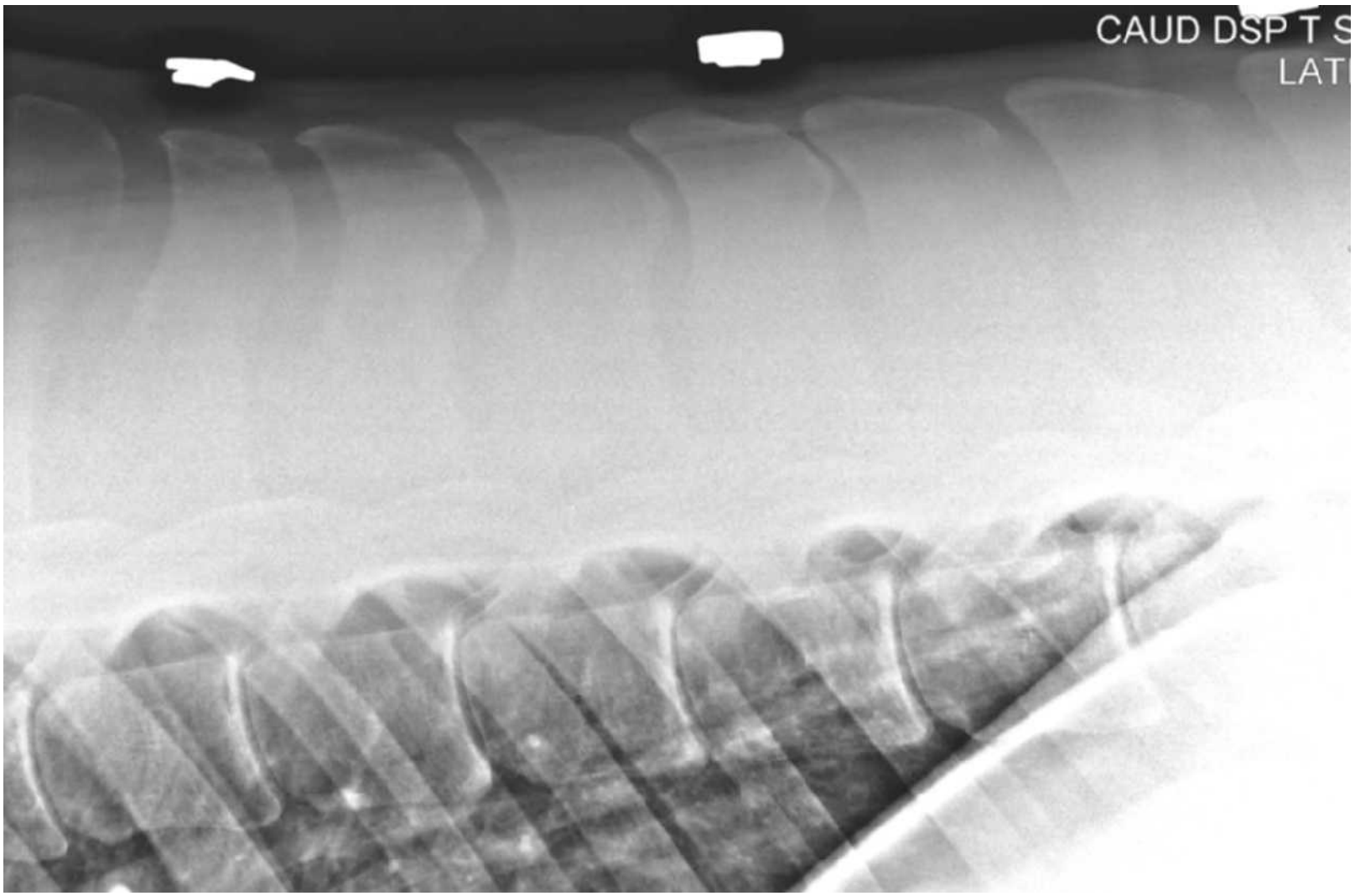


Figure 12.43(a) Lateral-lateral image of the caudal thoracic spinous processes (T12–T18) of a normal adult horse. Cranial is to the left. The spinous processes are well spaced; they are closer in some normal horses. Note that the dorsal cranial aspect of each spinous process is somewhat beak-shaped, contoured over the summit of the more cranial spinous process, a normal variant. The articular process joints are obscured by the highly sprung ribs. The diaphragm crosses the vertebral bodies of T17 and T18.

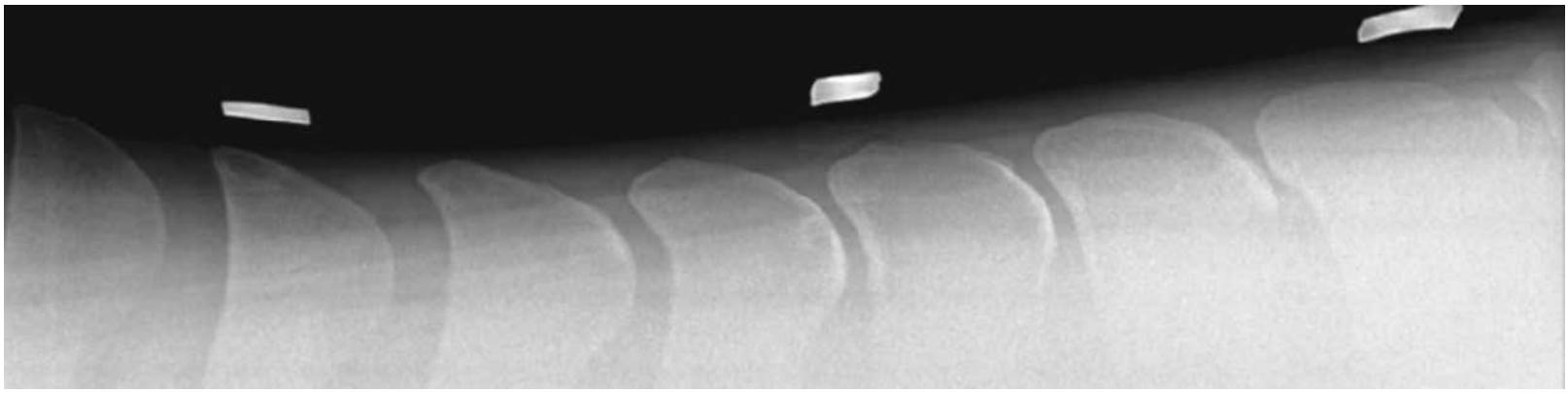


Figure 12.43(b) Lateral-lateral image of the proximal half of the spinous processes of the 11th to 17th thoracic vertebrae of a clinically normal horse. Cranial is to the left. The spinous processes are well spaced, but there is a radiolucent zone in the subcortical bone on the caudal aspect of T14. There is mild increased opacity of the compact bone of the caudal aspect of T14, T15 and T16. The cranial aspect of the spinous process of T13 and 14 is slightly beak-shaped.

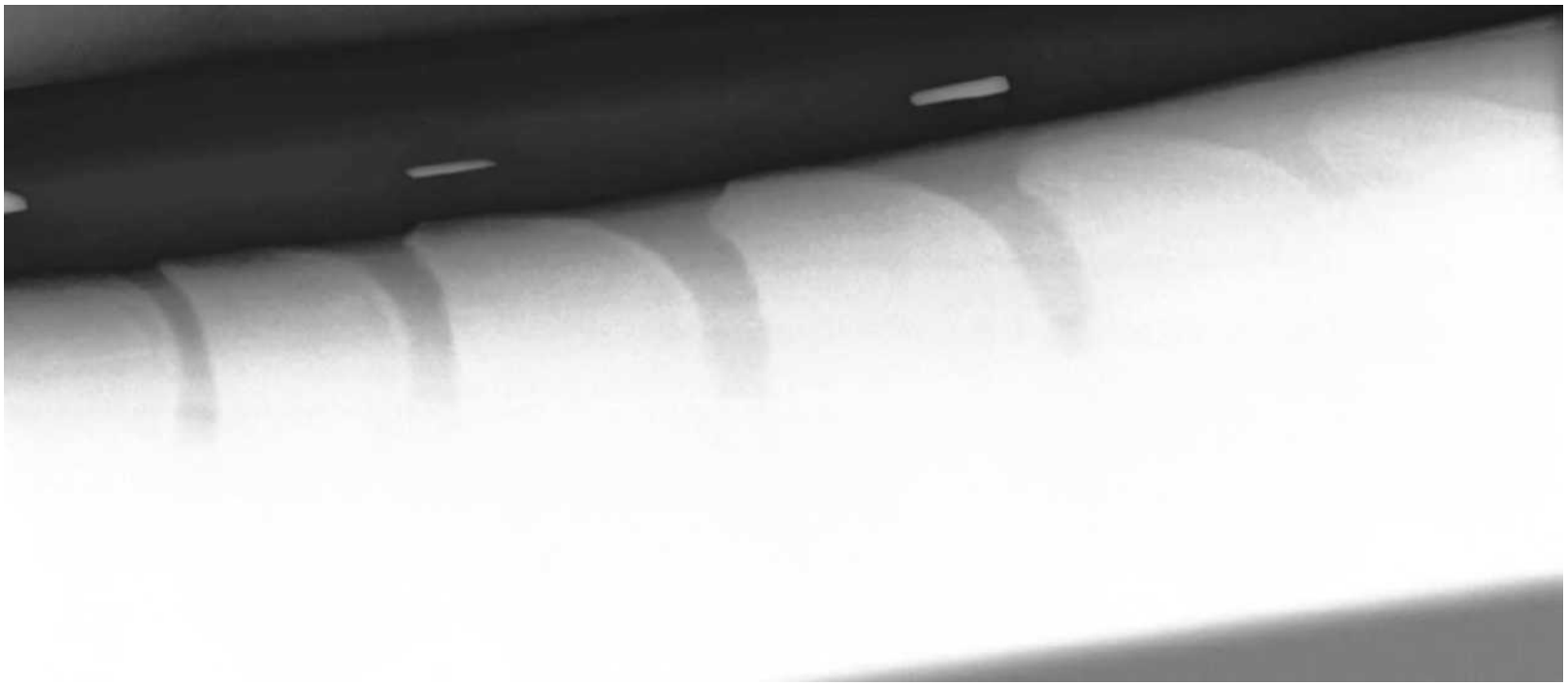


Figure 12.44 Lateral-lateral image of the spinous processes of the lumbar vertebrae of a normal adult horse. Cranial is to the left. The spinous processes are well spaced. Different exposures are required for assessment of the articular process joints and vertebral bodies.

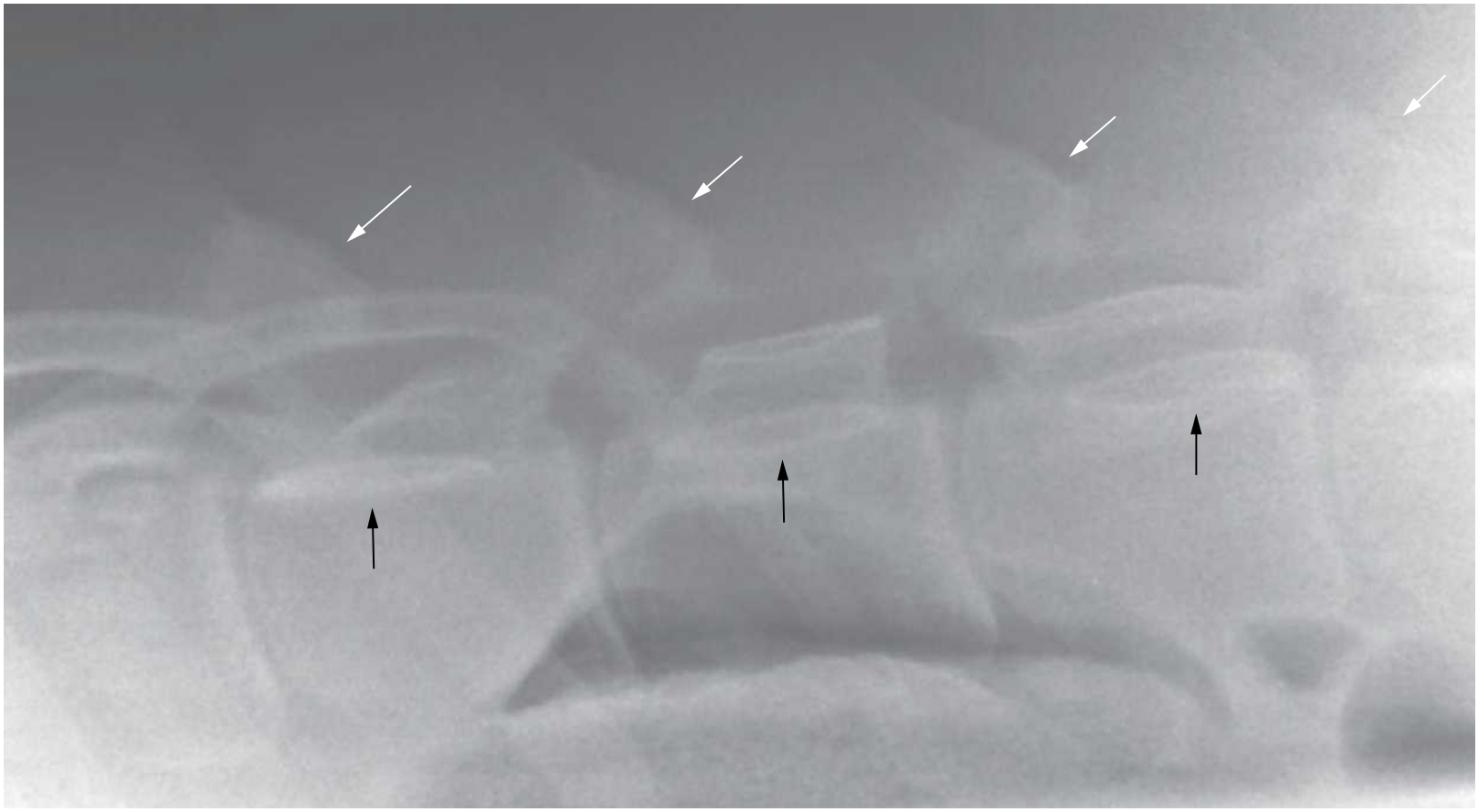


Figure 12.45 Lateral-lateral image of the articular process joints and vertebral bodies of the cranial lumbar vertebrae. Cranial is to the left. Superimposed over the more cranial vertebrae are the caudal ribs and abdominal viscera. Note the relatively opaque appearance of the articular process joints (white arrows) through which a faint lucent line courses from caudodorsal to cranioventral. The oval-shaped opaque area (black arrows) on the dorsal aspect of each vertebral body represents a transverse process. Note the opaque caudal subchondral bone plate of each vertebral body.

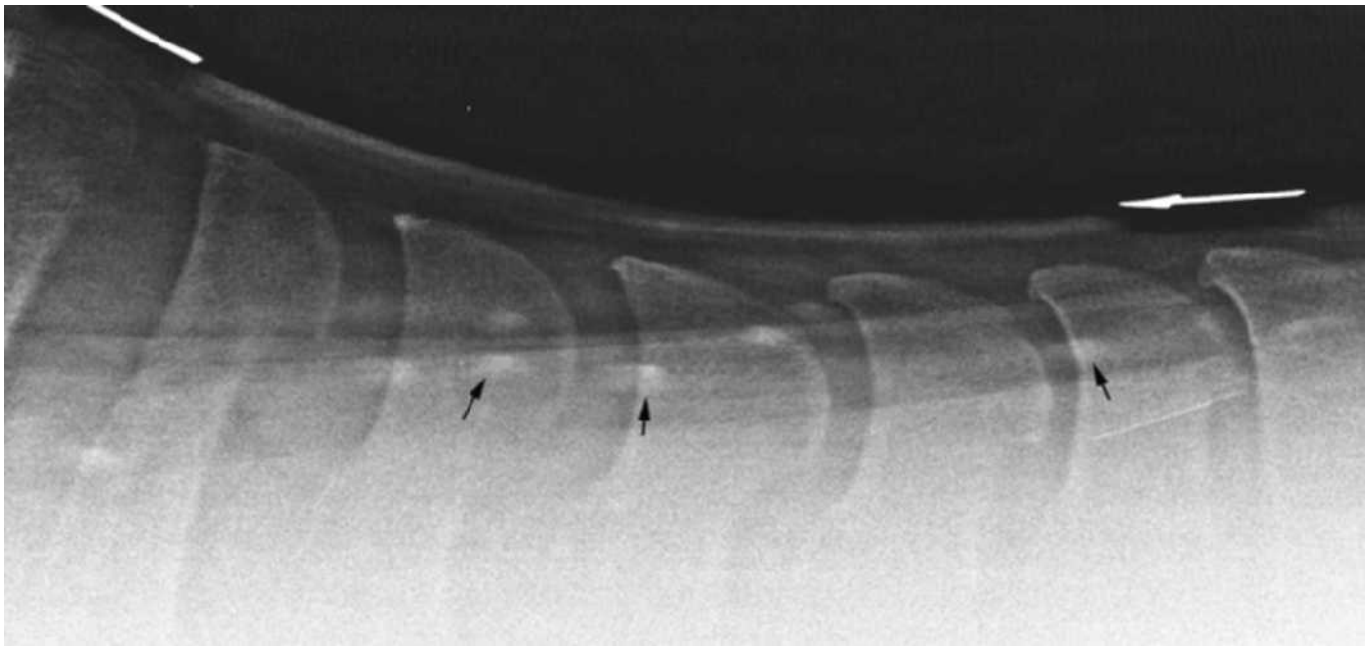


Figure 12.46 Lateral-lateral image of the spinous processes of the tenth to sixteenth thoracic vertebrae. Cranial is to the left. There are numerous opacities superimposed over the spinous processes (arrows). These represent dermal swellings, the result of chronic eosinophilic nodular dermatitis.



Figure 12.47(a) The caudal aspect of the eighteenth thoracic vertebra of a 10-year-old event horse with thoracolumbar pain, sacroiliac joint region pain and bilateral hindlimb proximal suspensory desmopathy. There was radiographic evidence of osteoarthritis of the articular process joints between the sixteenth and seventeenth and seventeenth and eighteenth thoracic vertebrae, but the articulations between the eighteenth thoracic and first lumbar vertebrae were obscured by the diaphragm. Right is to the right. Note the huge asymmetry in size of the articular processes (right > left) and the periarticular new bone around the ventral parts of the intercentral joint surface, features that were missed by radiographic assessment. Compare with Figure 12.47(b).



Figure 12.47(b) Lateral image of the eighteenth thoracic and first lumbar vertebrae of the same horse as in Figure 12.47(a). Cranial is to the left. There is extensive new bone bridging the left side of the intercentral joint, a feature that was missed by radiographic assessment. This was not detected radiographically because of superimposition of the diaphragm.

SIGNIFICANT FINDINGS

It is important to recognise that several radiographic abnormalities of the thoracolumbar vertebrae may occur concurrently, which may influence treatment and prognosis. It is therefore important to evaluate the vertebrae in their entirety, not just for example the spinous processes. Radiographic abnormalities are not always of clinical significance (Figure 12w.48) and must be interpreted in the light of clinical findings and, where appropriate, the response to local analgesia. Nuclear scintigraphic evaluation can be helpful in identifying which radiographic abnormalities are likely to be of clinical significance, although a negative result does not preclude the existence of back pain, nor does a positive result imply that the area is a source of pain. Ultrasonography may also be useful.

Sprain of the supraspinous ligament

The supraspinous ligament is a functional continuation of the nuchal ligament of the neck. It attaches to the periosteum of the summits of the spinous processes from T10/T11, caudally to the last lumbar vertebra. If these attachments are sprained following severe trauma such as a fall, there may be 'lifting' of the periosteum at the dorsal aspect of successive processes. This may be seen on softly exposed radiographs as a small radiopaque 'flake' dorsal to, parallel with and in close proximity to the summit of the spinous process (Figure 12.49). Alternatively, entheseous new bone may develop on the summit of the spinous process. The condition is most frequently seen in the T10–T13 or L1–L3 regions. Ultrasonographic evaluation of the supraspinous ligament may be helpful and should be performed, but architectural variations and abnormalities, for example from previous injuries, can be seen in some asymptomatic horses. The condition can cause symptoms of back pain for several months; it often has an acute onset. Satisfactory improvement normally occurs with rest, but the radiographic appearance does not necessarily alter, and these changes may therefore be an incidental radiographic finding. Nuclear scintigraphic evaluation may help to determine the presence of active bone modelling and thus the likely clinical significance; primary soft-tissue pain may also be present in some horses.

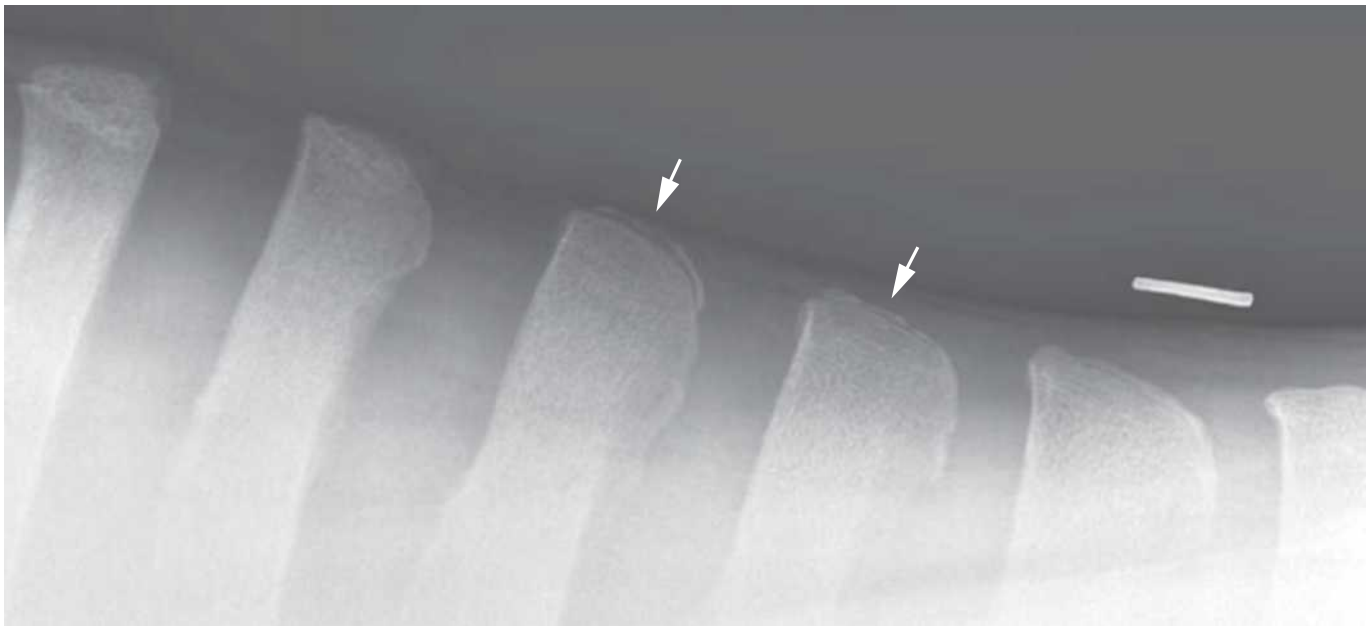


Figure 12.49 Lateral-lateral image of the summits of the spinous processes of the mid-thoracic region (T8–T13). Cranial is to the left. This 7-year-old Warmblood had chronic back pain. There is separation of a thin radiopaque flake on the dorsal aspect of two spinous processes (T10 and T11, arrows), which is believed to reflect elevation of the periosteum following damage to the supraspinous ligament. Note also the mild irregular entheseous new bone on the bodies of the spinous processes of T9 and T10, normal variants.

Interspinous ligament enthesopathy

Smoothly irregular new bone formation on the cranial and caudal aspects of the spinous processes of the first 8–10 thoracic vertebrae is a common incidental finding (see Figures 12.42, 12.49, 12w.50a), but new bone formation on the spinous processes of more caudal vertebrae is more likely to be of clinical significance (Figures 12.50b, 12.50c, 12.51a and 12.51b), reflecting interspinous ligament enthesopathy. It may be seen alone or together with either impinging spinous processes or degenerative joint disease of the articular process joints.

Impingement and overriding of the spinous processes

There is inconsistency in the terminology used to describe the various manifestations of closely positioned spinous processes. In this text we have chosen to use the term impinging (so-called 'kissing spines') to mean that two adjacent spinous processes are touching (Figures 12w.52a and 12w.52b). This does not however imply that this is of clinical significance. Overriding (overlapping) describes the presence of bone formation from one spinous process extending on the right and/or left sides of the adjacent spinous process (Figure 12w.52c). This may reflect superimposition of modelled spinous processes, with pseudo-joint formation or occasionally fusion. In some horses the proximal aspect of each spinous process has a cranially pointing 'beak-shaped' projection which extends over the dorsal aspect of the adjacent spinous process (Figures 12.42, 12.43a and b, 12w.52d).

There has been some debate about whether impinging spinous processes is a congenital or acquired condition. In a small study of 25 Warmblood foals no interspinous space was <4 mm in width, suggesting that if impingement



Figure 12.50(b) Lateral-lateral image of the spinous processes of the twelfth to fifteenth thoracic vertebrae of a 9-year-old Warmblood dressage horse with back stiffness. Cranial is the left. There is extensive entheseous new bone at the attachment of the interspinous ligament on the caudal aspect of the spinous process of the thirteenth thoracic vertebra (arrows).

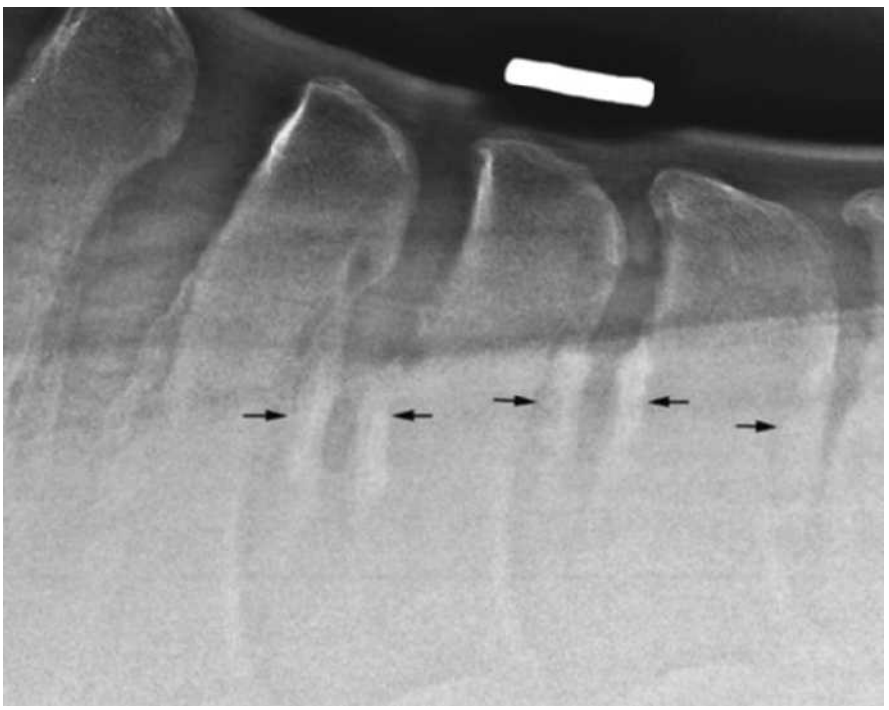


Figure 12.50(c) Lateral-lateral image of the spinous processes of the tenth to fourteenth thoracic vertebrae of a 10-year-old Warmblood dressage horse with back stiffness. Cranial is the left. There is extensive entheseous new bone at the attachment of the interspinous ligament on the cranial and caudal aspects of the spinous processes (arrows).

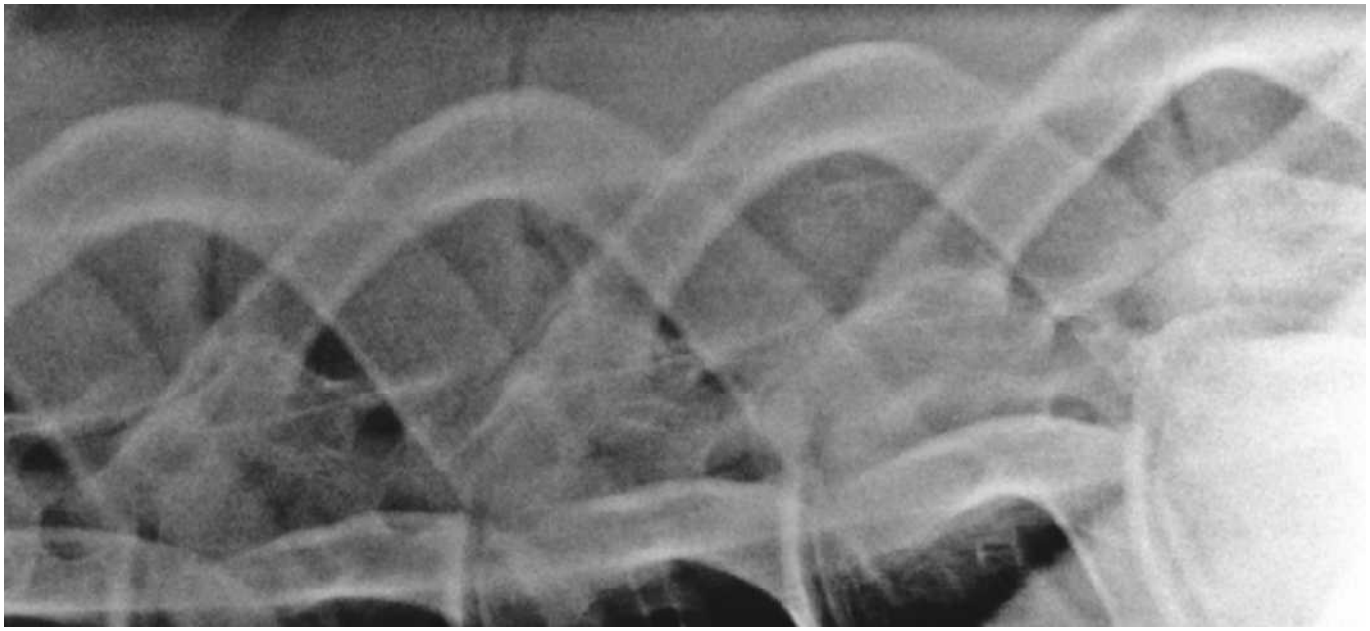


Figure 12.51(a) Lateral 20° ventral-laterodorsal oblique image of the caudal thoracic articular process joints (T13–T17) of a 9-year-old Warmblood with back stiffness and reluctance to work. Cranial is to the left. The bases of the spinous processes are all close. There is substantial periarticular new bone involving the articular process joints between the 15th and 16th and 16th and 17th thoracic vertebrae.

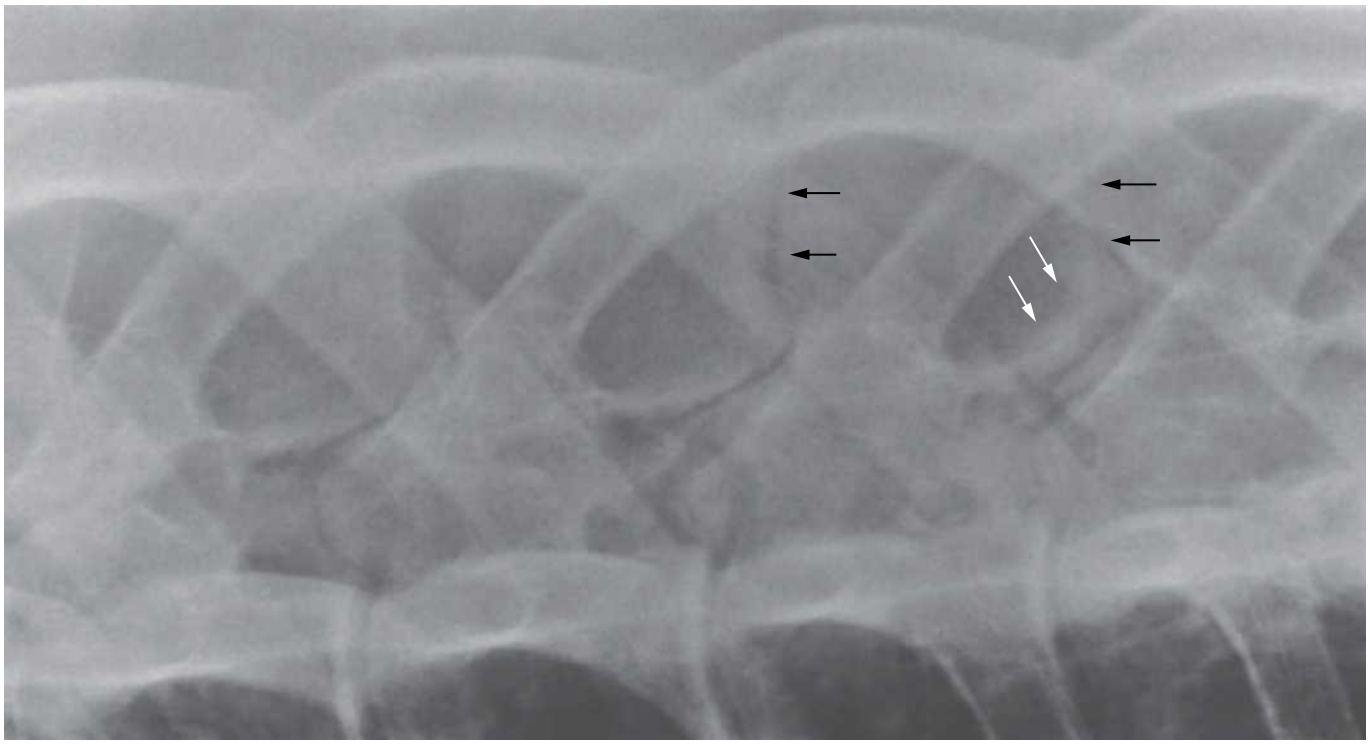


Figure 12.51(b) Lateral 20° ventral-laterodorsal oblique image of the caudal thoracic articular process joints (T13–T16) and spinous processes of a 16-year-old general-purpose Cob with marked back stiffness. Cranial is to the left. The bases of the spinous processes of T14, T15 and T16 are very close, with increased opacity (black arrows). There is also thickening of the subchondral bone plate of the articular process joint between T15 and T16 (white arrows). There was also bony bridging further proximally between the spinous processes of T13 and T14.

developed later in life it would be an acquired condition. However, the propensity to develop impingement will obviously, to a degree, depend on the baseline proximity of spinous processes. There is evidence that there is an association between age and the severity of radiological abnormalities; older horses have more extensive lesions than young horses. There is also an association between osteoarthritis of the articular process joints and impinging spinous processes. In a radiographic study of 604 horses, the severity of lesions of the spinous processes was significantly positively associated with the presence of osteoarthritis of the articular process joints. When assessing the interspinous spaces, care should be taken in interpretation of space width at the margins of the image (see Figure 1.5). Reliable measurements can only be acquired from the central portion of an image.

It is important to be aware that impingement and overriding of the summits of the thoracic spinous processes is a fairly common radiological observation, even in clinically normal horses or at least in horses with no known or proven pain or clinical problem (Figures 12w.48 and 12w.52). Radiographic changes should be looked upon with some caution and must be interpreted in the light of a comprehensive clinical examination of the horse at rest and at work. It is not possible to relate the radiographic changes to the degree of clinical signs exhibited. In a study of 582 horses, only 46% with radiological abnormalities of the spinous processes had clinical evidence of primary thoracolumbar pain. However, crowding of the spinous processes may reduce the patient's athletic potential and can alter the biomechanics of the thoracolumbar region and predispose to the development of other pathological lesions that may cause pain. A change in stance, with slight hollowing (extension) of the back, may also result in crowding of the spinous processes, which may therefore be secondary to some other cause of back pain. Atrophy of the epaxial muscles and poor core muscle strength can result in the development of clinical signs in a previously asymptomatic horse. Clinical significance is also influenced by the athletic demands placed on the horse (Figures 12.53a and b).

Radiographic examination can be misleading if only a limited part of the thoracolumbar region is evaluated and the radiographic quality is not

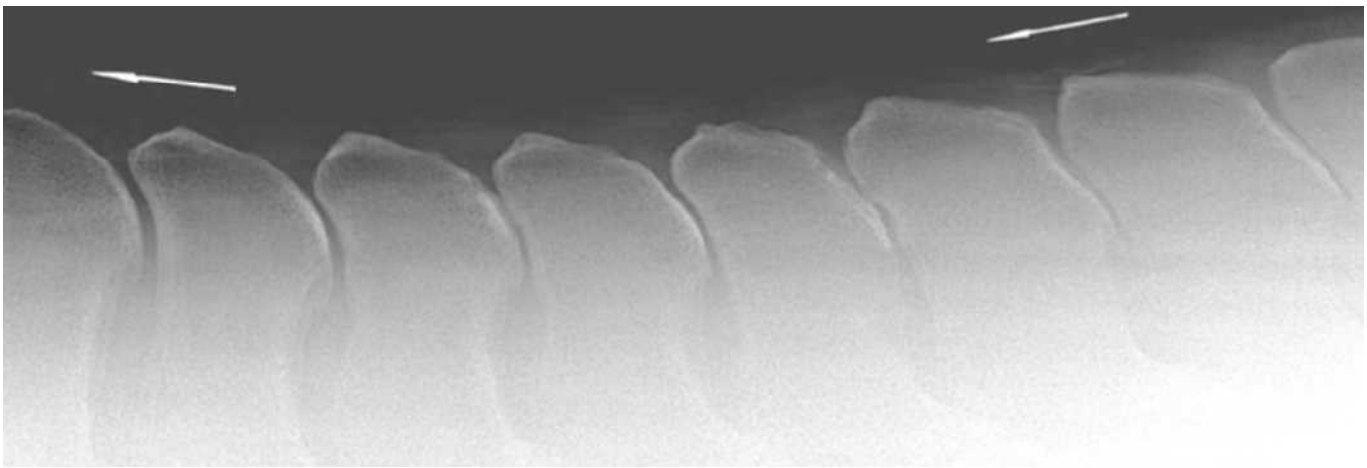


Figure 12.53(a) Lateral-lateral image of the spinous processes of the caudal thoracic and cranial lumbar region (T13–L2) of a 6-year-old Andalusian cross gelding with a stiff back, poor hindlimb impulsion and engagement and reluctance to canter. Cranial is to the left. The summits of the spinous processes are very close or impinging, with mild increased opacity of the compact bone. There was intense increased radiopharmaceutical uptake associated with these spinous processes.

adequate. Clinically significant impingement or overriding spinous processes often occurs in the mid and caudal thoracic regions. Abnormalities can extend throughout the lumbar region, or even occur exclusively in the lumbar region. The dorsoventral extent of radiological abnormalities varies considerably and it is important that the entire length of each spinous process is assessed. Radiographs are generally acquired with horses sedated, resulting in lowering of the head and neck and slight flexion of the thoracolumbar vertebral column, which causes slight separation of the spinous processes. In contrast, when a horse is ridden, the back is relatively extended, the amount in part depending on the development and strength of the epaxial and abdominal muscles and the weight and skill of the rider. This mild extension results in the spinous processes potentially being slightly closer together. These factors must be considered when interpreting radiographs.

Impingement may result in secondary osseous changes, including discrete lucent zones in the compact and trabecular bone and periosteal reaction with new bone formation (Figure 12.53b). There may also be increased opacity and modelling of the opposing surfaces of the spinous processes (Figure 12.53b). The cranial aspect of the summit of one spinous process may model to envelop the caudal aspect of the adjacent cranial spinous process (overriding). Rarely, two adjacent spinous processes may become fused (Figure 12w.54). Closeness or impingement of the summits of adjacent spinous processes is frequently seen, but need not be of clinical significance. The entire length of each spinous process should be evaluated; although in many horses radiological abnormalities are restricted to the dorsal quarter, in others the entire length of the spinous process is involved (Figure 12.55). It is probably true to say that the larger the number of impinging spinous processes, especially with secondary osseous reaction, the more likely they are to be of clinical significance. In a study of 582 horses, there was an association between both the number of spinous processes involved and the severity of radiological abnormalities and the presence of thoracolumbar

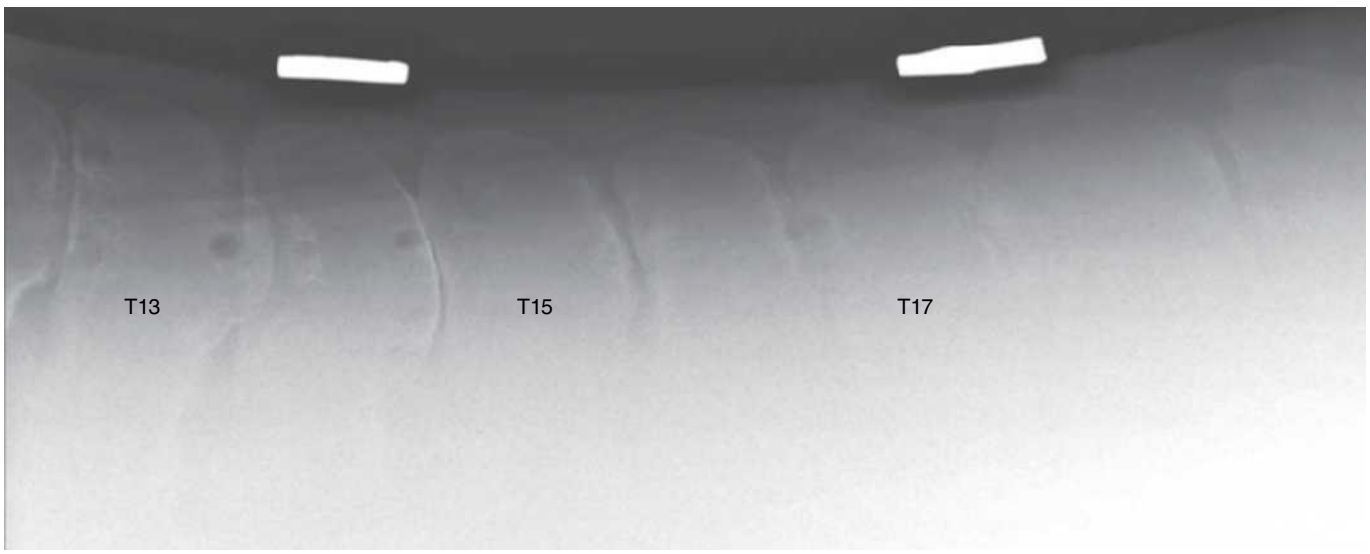


Figure 12.53(b) Lateral-lateral image of the caudal thoracic and cranial lumbar region (T12–L1) of a 9-year-old Irish Thoroughbred with stiffness, poor hindlimb impulsion, reluctance to go forwards and episodic explosions. Cranial is to the left. The summits of the spinous processes are very variable in craniocaudal width. The spinous processes are impinging or overlapping. There is mild increased opacity of the compact bone and adjacent extensive radiolucent areas.



Figure 12.55 Lateral-lateral image of the spinous processes of the fourteenth to seventeenth thoracic vertebrae of a mature horse with back pain and stiffness, which was substantially improved by infiltration of local anaesthetic solution around the impinging spinous processes. Cranial is to the left. The spinous processes are very close throughout their dorsoventral length.

pain. However, the frequency of occurrence of the most severe radiological abnormalities and total radiological grade was higher in horses with sacroiliac joint region pain ± lameness, than in horses with primary thoracolumbar pain. It is possible that in these horses the impinging spinous processes predisposed to the development of sacroiliac joint region pain, which then became the predominant clinical problem.

Nuclear scintigraphic evaluation is helpful in some horses, but false-negative results occur and increased radiopharmaceutical uptake can be seen in the summits of one or more spinous processes in some horses without evidence of pain and no apparent impingement. Increased radiopharmaceutical uptake may reflect injury of the supraspinous ligament and secondary osseous reaction. In some cases where overt back pain is absent, 'overcrowding' of the processes (reduced interspinous spaces without marked reaction of the opposing bone surfaces) may reduce the flexibility of the back, and hence reduce performance at the highest levels of competition. The greater the number of spinous processes involved, the higher the likelihood of associated clinical signs. The clinical significance of radiological evidence of impinging spinous processes may be determined by infiltration of local anaesthetic solution around the spinous processes and reassessing the horse's performance, preferably ridden. It is important to remember however that such infiltration may desensitise structures other than the spinous processes.

Infiltration of corticosteroids may give the rider a longer period to assess any effect on the horse's performance, but the response is also non-specific.

Conservative management (rest, ground work and physiotherapy to improve core muscle strength) frequently results in clinical improvement, although there is generally little or no change in the radiographic appearance. Local infiltration with corticosteroids and/or pain-modifying drugs, shock wave treatment, acupuncture or osteopathic manipulation may help to control pain, but effects may be temporary in some horses. Surgical treatment by complete or partial resection of the summits of one or more spinous processes, or possibly transection of the interspinous ligament, should be contemplated in severe or intractable cases, but again results may only be temporary. Case selection is key to success; verification of the clinical significance of impinging spinous processes by local analgesia is recommended. It is important to evaluate the vertebrae in their entirety, to preclude other co-existing pathological changes of likely significance, which will adversely influence the prognosis. In a study of 582 horses, those with radiological abnormalities of the spinous processes and concurrent osseous pathology were more likely to have clinical signs of thoracolumbar pain than horses with lesions of the spinous processes or osteoarthritis of the articular process joints alone. However, horses with osteoarthritis of the articular process joints alone were more likely to have thoracolumbar region pain than horses with lesions of the spinous processes alone.

Other abnormalities of the spinous processes

The alignment of the spinous process in the sagittal plane is best appreciated clinically and abnormalities can be verified using dorsal scintigraphic images. Deviation of a spinous process to the left or the right may be associated with uneven muscle tone between the two sides of the back, and or asymmetry of the articular process joints between left and right sides, but may be associated with other pathological abnormalities of the adjacent vertebrae (see also 'Lordosis, kyphosis and scoliosis', below). Radiographs of the entire group of vertebrae should be carefully inspected. The summits of the spinous processes generally follow a smooth curve; an abrupt change in height between two adjacent spinous processes is not normal and may be congenital or acquired. It is likely to be associated with other pathological abnormalities which compromise performance.

Bridges of bone between adjacent spinous processes are occasionally seen and are probably congenital in origin; if widespread they are likely to compromise movement of the thoracolumbar region and predispose to the development of other pathological changes. Huge variation in width of adjacent spinous processes (Figures 12.53b and 12w.56) is also a congenital abnormality which is usually associated with abnormalities of the vertebral bodies and the articular process joints.

Vertebral fusion

Vertebral fusion may involve two or more vertebrae, but is rare in the thoracolumbar vertebral column. The absence of irregular bony callus helps to distinguish a congenital abnormality from fusion following a recent fracture. A fracture that occurred a year or more previously may be indistinguishable from congenital fusion, due to modelling of the callus.

Lordosis, kyphosis and scoliosis

Varying degrees of lordosis, kyphosis and, occasionally, scoliosis occur. Although minor deviations may result from uneven muscle tone in the epaxial muscles possibly resulting from trauma (and may be treated), severe deviations resulting from congenital malformations have a poor prognosis, although some horses perform well despite the problem. Wedge-shaped vertebral bodies may be seen on lateral-lateral or dorsoventral radiographs.

Lordosis may be the result of congenital hypoplastic articular processes, but may also be an acquired defect. Marked lordosis of the thoracolumbar spine is recognised radiographically as a ventral convexity (dipping) of the thoracolumbar vertebral column, and may adversely affect performance, although it does not necessarily do so.

Kyphosis may also be congenital or acquired. It is recognised radiographically as a dorsal convexity (arching) of the thoracolumbar vertebral column. A similar posture may be adopted by young horses with bilateral osteochondrosis of the femoropatellar articulations, and this must be considered as a differential diagnosis.

Congenital scoliosis may occur. On lateral-lateral radiographs, twisting of the vertebral column results in asymmetry of the positioning of the ribs and an apparent variation in the length of the vertebral bodies (Figure 12w.57).

Mild degrees of lordosis and kyphosis are frequently seen and are not necessarily associated with poor performance, although they may be of significance in horses undertaking particular athletic activities. Scoliosis may be of sufficient severity to interfere with any type of performance.

Degenerative joint disease

The articular processes (facets) in the thoracic region form simple arthrodial joints with small and flat articular surfaces which become angulated caudally (see Figures 12.40 and 12.41). In the lumbar region, the articular processes are hinge-like and have a slightly different radiographic appearance (see Figure 12.45). True lateral-lateral projections and oblique views that 'cut through' the joints (Figure 12.41a) are essential for assessment of any abnormality involving these structures. Lesions may be missed on lateral-lateral images. Evaluation of the joints on lateral-lateral images can be extremely difficult if the ribs are 'highly sprung'. The articulations between the eighteenth thoracic and first lumbar vertebrae may be obscured by the diaphragm. The joints under suspicion must be in the middle of the radiograph, and it may be helpful to compare the size and shape of the adjacent articular process joints. Adequate visualisation of these joints in the lumbar region of large horses may not be possible.

Degenerative joint disease of the articulations of the articular processes (articular process [facet] joints) (Figure 12.58a) is difficult to diagnose and requires high-quality radiographs, with good definition. Good collimation will markedly enhance radiographic quality (see Figure 2w.3). The condition was formerly thought to be a rare cause of back pain, but with improved radiographic technique, and also the use of nuclear scintigraphy, is now being recognised more frequently. There is some evidence that it may be a more important cause of pain than impinging spinous processes. Radiographic evidence of degenerative joint disease is not common in horses with no

clinical signs of thoracolumbar region pain. Degenerative joint disease of the articular process joints most often affects the caudal thoracic and cranial lumbar vertebrae. Radiographic abnormalities include (Figure 12.58b):

- Alteration in joint space width, usually narrowing
- Osteolysis in the articular processes or dorsal to the articular process joint
- Thickened subchondral bone plate
- Increased opacity of the articular processes
- Dorsal periarticular proliferation, resulting in increased size of the joint. This is most easily recognised in the caudal thoracic and lumbar regions. Care must be taken to differentiate overlying mammillary processes. There may be reduced space between the spinous processes ventrally, especially in the caudal thoracic region
- Ventral periarticular proliferation. This can only be recognised in the lumbar region, due to the superimposition of the ribs in the thoracic region
- Ankylosis.

Comparison of left and right oblique images helps to determine if the radiographic abnormalities are unilateral or bilateral. Bilateral lesions are common. Lesions occur most commonly between the fifteenth thoracic and first lumbar vertebrae (Figure 12.58a and 12.58b); however, more cranial (Figure 12w.58c) and more caudal (Figure 12w.58d) lesions do occur. In a study of 77 horses with back pain and degenerative joint disease of the articular process joints, there was a median of three levels of lesion per horse. Degenerative joint disease can be a primary condition

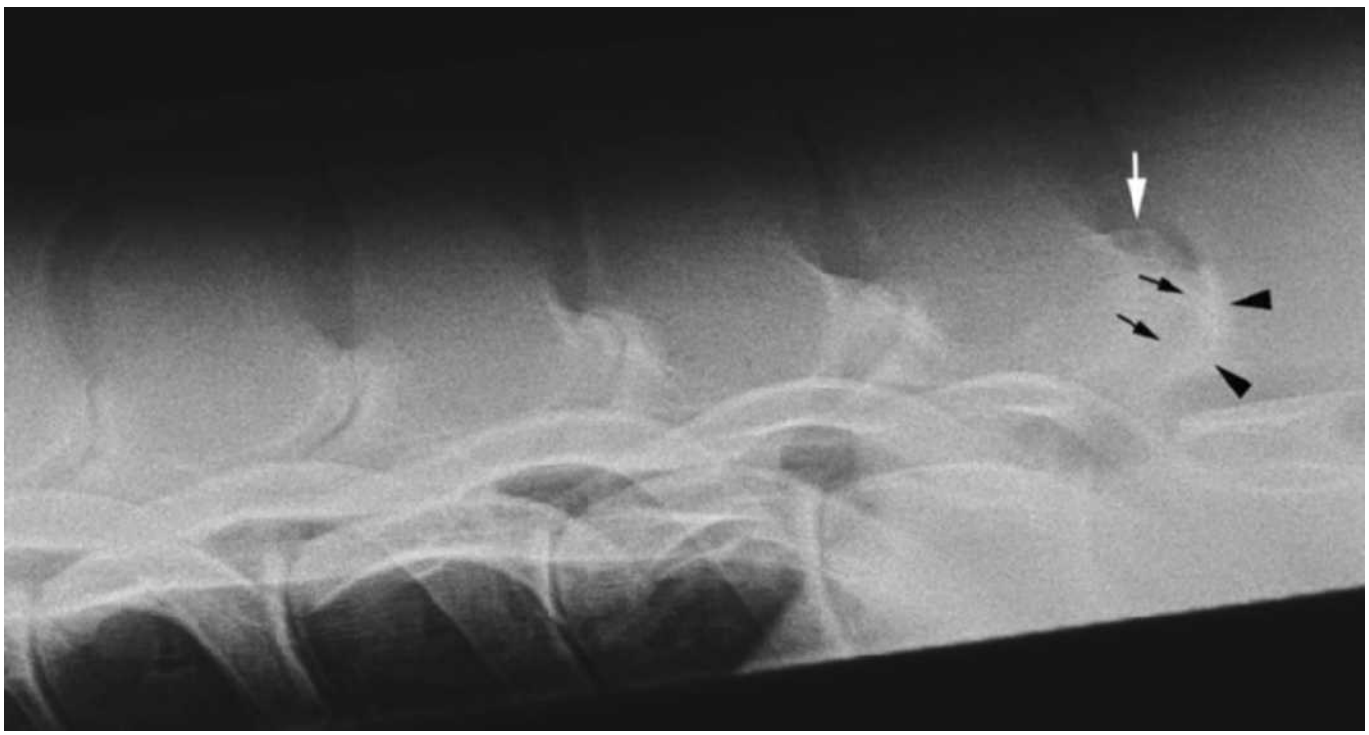


Figure 12.58(a) Lateral-lateral image of the caudal thoracic and cranial lumbar vertebrae of an 8-year-old horse with chronic back pain. Cranial is to the left. There is degenerative joint disease of the articular process joints characterised by periarticular new bone formation at T18–L1 (white arrow), thickening of the subchondral bone plate (arrowheads) and loss of joint space (black arrows). The changes are most advanced caudally.

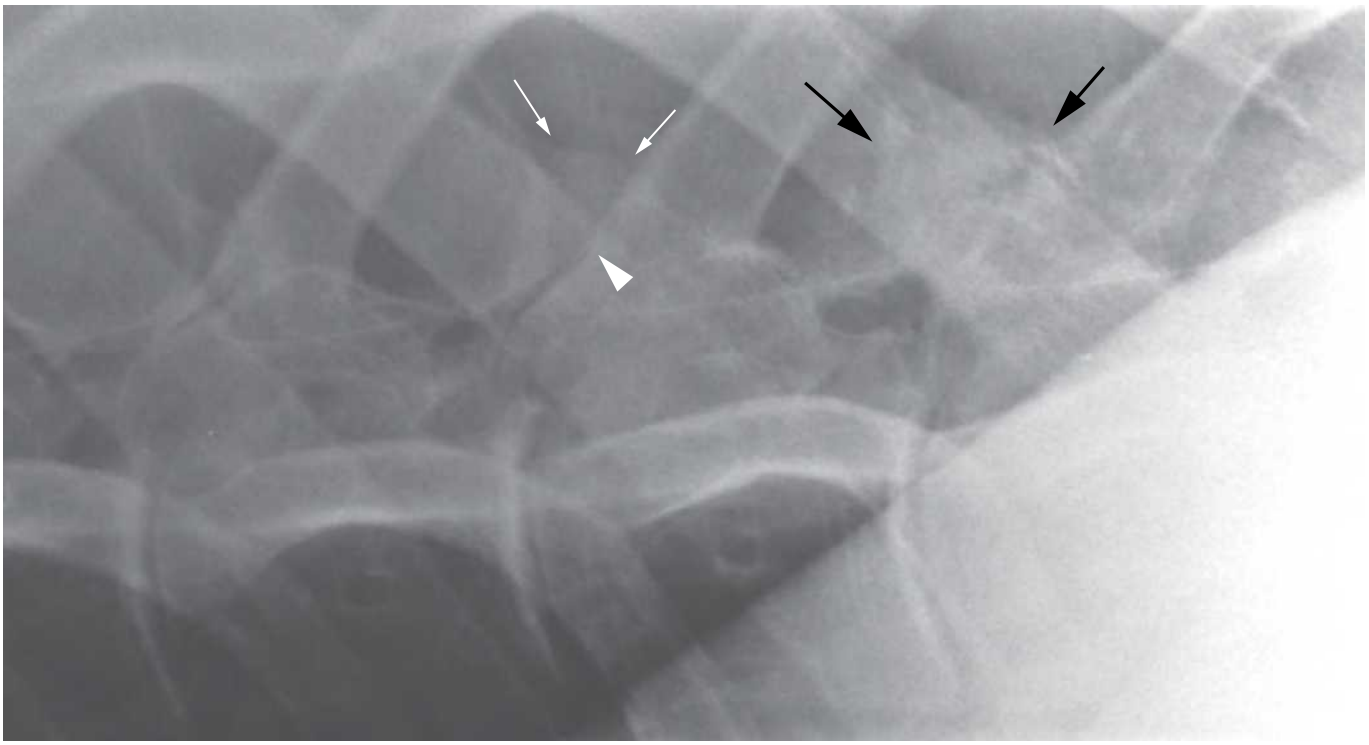


Figure 12.58(b) Lateral 20° ventral-laterodorsal oblique image of the caudal thoracic vertebrae (T15–T18). Cranial is to the left. There is degenerative joint disease characterised by narrowing of the articular process joint between T16 and T17 proximally (white arrowhead) and periarticular new bone dorsally (white arrows). There is extensive increased opacity of the subchondral bone and periarticular new bone around the articular process joints between the seventeenth and eighteenth thoracic vertebrae (black arrows) and complete loss of joint space.

or may occur secondary to a stress fracture of an articular process, seen most commonly in the lumbar region in young Thoroughbred racehorses. Ultrasonography may also be helpful in some horses, especially in the lumbar region, for identification of the laterality of lesions. Although periarticular new bone can be detected ultrasonographically, there is the potential for false-negative results because accurate assessment of joint space width, subchondral bone pathology and dorsal extension of the joint cannot be performed. Ultrasonography is not a substitute for radiography. With low-grade radiographic abnormalities the results of nuclear scintigraphic examination may be normal in mature horses. Severe degenerative changes are often associated with moderately or intensely increased radiopharmaceutical uptake. In young Thoroughbreds there may be focal intensely increased radiopharmaceutical uptake associated with a stress fracture of the dorsal lamina in the cranial lumbar region. Ultrasound-guided paravertebral local analgesia can be helpful to verify the significance of equivocal radiological abnormalities.

Occasionally concurrent abnormalities of the intercentral articulations are identified, which probably reflect previous trauma, or new bone may extend proximally between the spinous processes, reflecting interspinous enthesopathy (Figures 12.51a and 12.51b). This is most commonly seen in association with impinging spinous processes.

Ossifying spondylosis (spondylosis deformans)

Spondylosis is a relatively uncommon condition in the horse, the aetiology of which is not known. In a review of 670 horses with thoracolumbar region pain which underwent comprehensive radiographic assessment, spondylosis was identified in 3.4% (23). Of these horses 61% had more than one intercentral articulation affected. Spondylosis was identified as the only osseous pathology in only 9 of 23 horses. A higher prevalence of spondylosis has been described in a post-mortem study, which may suggest limitations of radiography for detection of small spondyles. Spondylosis is consistently found in the caudal half of the thoracic region (T10–T16). It may be multifocal, usually at adjacent articulations, and in some horses reflects ventral ligament enthesopathy.

Osteophytes (spondyles) arise from the ventral aspects of the vertebral bodies near the intercentral articulations. The osteophytes usually extend across the intercentral joint towards similar osteophytes on adjacent vertebrae (Figure 12.59a). Frequently a slightly irregular radiolucent line of varying width remains between the opposing spondyles as an apparent continuation of the intercentral joint (Figures 12.59b and 12.59c), but complete bridging between adjacent vertebrae often occurs with time (Figure 12.59d). There is considerable variation in the degree of spondylosis which develops, and the clinical significance of the changes has not yet been well established. Although spondylosis is usually seen in lateral-lateral radiographs, occasionally it can only be demonstrated on oblique radiographs and it is therefore helpful to include the ventral margin of the vertebral bodies on oblique radiographs. Nuclear scintigraphy has low sensitivity but high specificity for prediction of radiological evidence of spondylosis.

Once spondylosis has started to form, it frequently, but not always, progresses in caudal and cranial directions. Spondylosis may occur without obvious clinical signs. This may depend on the athletic demands placed on the horse. Some horses with associated back pain have been able to perform acceptably with controlled medication, although only limited athletic pursuits are possible.

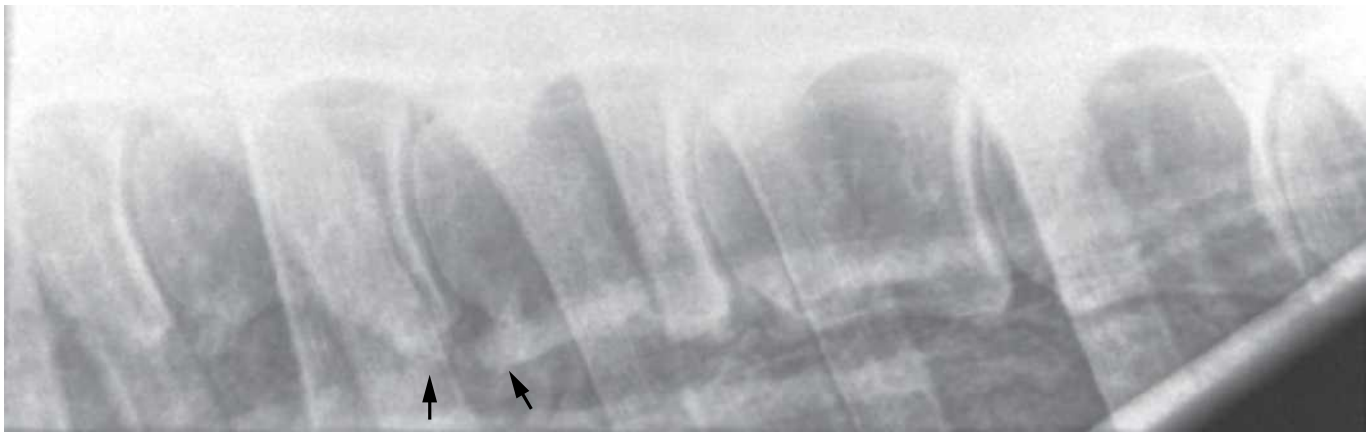


Figure 12.59(a) Lateral-lateral image of the vertebral bodies of the caudal thoracic region (T13–T18). Cranial is to the left. There is new bone reflecting early spondylosis involving the ventral aspect of the vertebral bodies of T14 and T15 (arrows). This 8-year-old Thoroughbred event horse had recently begun stopping and also had moderate impinging spinous processes in the same region. Care must always be taken to differentiate genuine new bone formation from superimposed lung opacities.

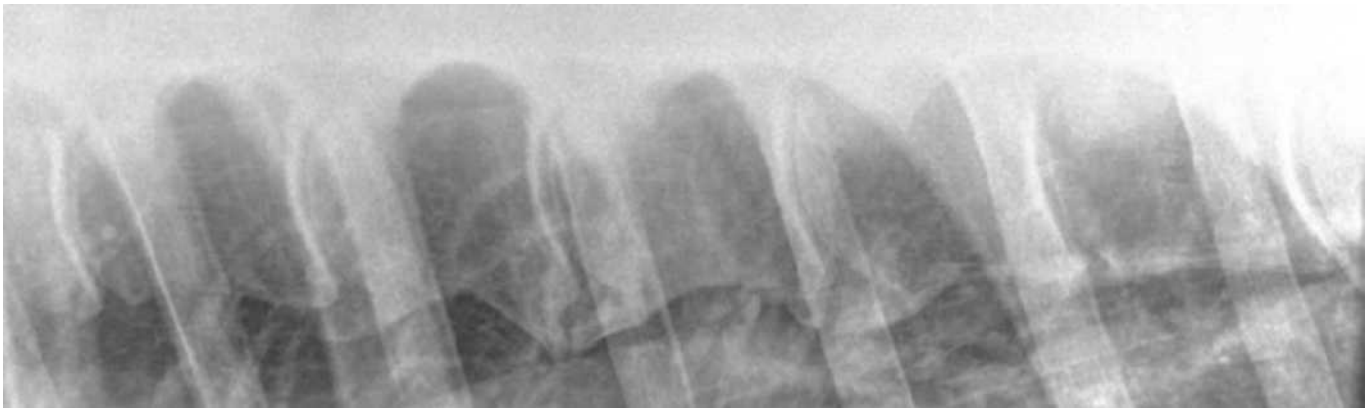


Figure 12.59(b) Lateral-lateral image of the vertebral bodies of the tenth to sixteenth thoracic vertebrae of an 8-year-old Irish Draught cross gelding with a history of an unspecified back injury 6 months previously, after which the horse had been reluctant to walk for several weeks. Currently the horse was stiff, short-striding and reluctant to canter. Cranial is to the left. There is new bone on the cranial and caudal ventral aspects of the vertebral body of T12 and the cranial ventral aspect of T13. There is a large bridge of bone extending between the fourteenth and thirteenth thoracic vertebrae. There is slight modelling of the caudal ventral aspect of the vertebral body of T14 and the cranial ventral aspect of T15. This represents extensive spondylosis. The intercentral joints appear normal. Compare with Figure 12.59(c).



Figure 12.59(c) Oblique image of the vertebral bodies of the twelfth to fifteenth thoracic vertebrae of the same horse as in Figure 12.59(b). Cranial is to the left. Note the large spondyles which effectively extend the intercentral articulations.



Figure 12.59(d) Lateral-lateral image of the vertebral bodies of the mid-thoracic vertebrae (T11–T16) of a 12-year-old Thoroughbred advanced event horse. Cranial is to the left. The horse was stiff and evasive and short stepping. There is advanced spondylosis with bone bridging between the twelfth to fourteenth thoracic vertebrae. The horse also had bilateral forelimb and hindlimb proximal suspensory desmitis and osteoarthritis of the centrodistal joint of the left hindlimb.

Spondylosis has also been seen concurrent with other abnormalities, such as impinging spinous processes and degenerative joint disease of the caudal thoracic articular process joints.

A grading system has been proposed:

0 No osteophytes present.

1 Osteophyte from one vertebral body, not bridging the intervertebral space.

2 Osteophyte from 2 adjacent vertebral bodies, not meeting.

3 Osteophyte from 2 adjacent vertebral bodies, meeting but no evidence of increased opacity at opposing borders.

4 Osteophyte from 2 adjacent vertebral bodies, meeting and evidence of increased opacity at opposing borders.

5 Complete bridging of intervertebral space.

Infectious osteitis

Systemic infections may localise in the vertebral bodies, although this is a rare finding. This may result in some stiffness of the back and intermittent pyrexia. Radiographically, focal lucent areas, sometimes surrounded by a rim of increased opacity, are seen. While a number of systemic infections may cause this condition in foals, including *Rhodococcus equi*, the most common cause in an adult horse is tuberculosis. Neoplastic metastases may give a similar radiographic appearance. Negative radiographic findings do not preclude the possibility of vertebral infection. Nuclear scintigraphy may be more sensitive.

Infection in the withers region (fistulous withers) may involve the spinous processes. This may appear as lucency in the compact bone and periosteal new bone formation. It should not be confused with the normal radiographic appearance of the spinous processes in this region (see Figure 12.39). Positive contrast fistulograms and/or diagnostic ultrasonography may be helpful to determine whether a draining tract is associated with infectious osteitis. This condition has become less common in the United Kingdom in recent years, probably due to the reduced incidence of brucellosis, with which it was commonly associated. Topical treatment with metronidazole has been found helpful in some cases. Surgery may be required, but some cases remain refractory to treatment.

Discospondylitis

Discospondylitis (inflammation of the vertebral body and associated intervertebral disc) has been seen either as a primary condition or in association with infection, but is rare. It may be characterised by back stiffness and an abnormal stance and gait, with or without ataxia. Serum fibrinogen may be elevated if the underlying cause is infection. Radiographically there is alteration in the intercentral joint space: either narrowing or obliteration of the intervertebral joint space, ± new bone on the ventral and/or dorsal aspect of the vertebral bodies. In association with infection there may be increased opacity and lysis of the vertebral endplates. There may be some malalignment of the vertebrae. Successful treatment with antimicrobial drugs has been reported.

Luxation

Subluxation or luxation of a vertebra in the thoracolumbar region is rare and is associated with severe pain, with or without ataxia. Luxation occurs most commonly in the lumbar region, where radiographic evaluation of the vertebral bodies is most difficult. The alignment of the vertebrae and the width of the intercentral articulations must be assessed carefully (Figure 12w.60). The prognosis for athletic function is extremely poor.

Fractures

Fractures involving the bodies of the thoracolumbar vertebrae are relatively uncommon. They normally cause or are accompanied by damage to the spinal cord, which often results in immediate paraplegia. They are often compression-type fractures (Figure 12w.61). Significant radiological signs of a vertebral fracture include: (a) apparent shortening of the length of the vertebral body; (b) a change in shape of the intercentral articulations, possibly with dorsal (upward) displacement of the vertebra; (c) callus formation.

Hairline fractures with minimal displacement may prove impossible to detect radiographically, but may be detected using nuclear scintigraphy.

Stress fractures occur in young Thoroughbred racehorses in training, usually involving an articular process joint in the lumbar region. These are characterised scintigraphically by focal intense increased radiopharmaceutical uptake, which is usually unilateral. Radiographically the affected facet joint is usually enlarged, but identification of a fracture may be challenging.

In young animals, pathological fractures of vertebrae may occur secondarily to osteomyelitis following destructive and resorptive changes in the vertebral body.

Fracture of a vertebral body generally has a grave prognosis.

Fractures of the spinous processes usually occur at the withers as the result of a fall. Displacement of the fragments is often present (Figure 12.62a). Complete osseous healing rarely occurs and there is often deformation of the spinous processes. A good prognosis for future performance can be given, although a special saddle may be required due to the flattened and broader outline of the withers. Fractures involving more caudal thoracic spinous processes occasionally occur as the result of trying to escape through a narrow space e.g., jumping over a stable door or getting stuck in a trailer side door (Figure 12w.62b). An isolated fracture of a lumbar spinous process has occasionally been seen (Figure 12w.62c).

Other fractures occur, but may be difficult to identify on radiographs.

Fracture of the ribs may present clinically as back pain. Fracture of the first rib may result in forelimb lameness or a neurological gait deficit (see Chapter 14, Trauma or rib fractures).

Neoplasia

Neoplastic lesions of the thoracolumbar vertebrae are rare and include melanomata and squamous cell carcinoma. Lesions in the lumbosacral region may be associated with unusual hindlimb gait abnormalities. Ultrasonography may be useful for identification of soft tissue masses.

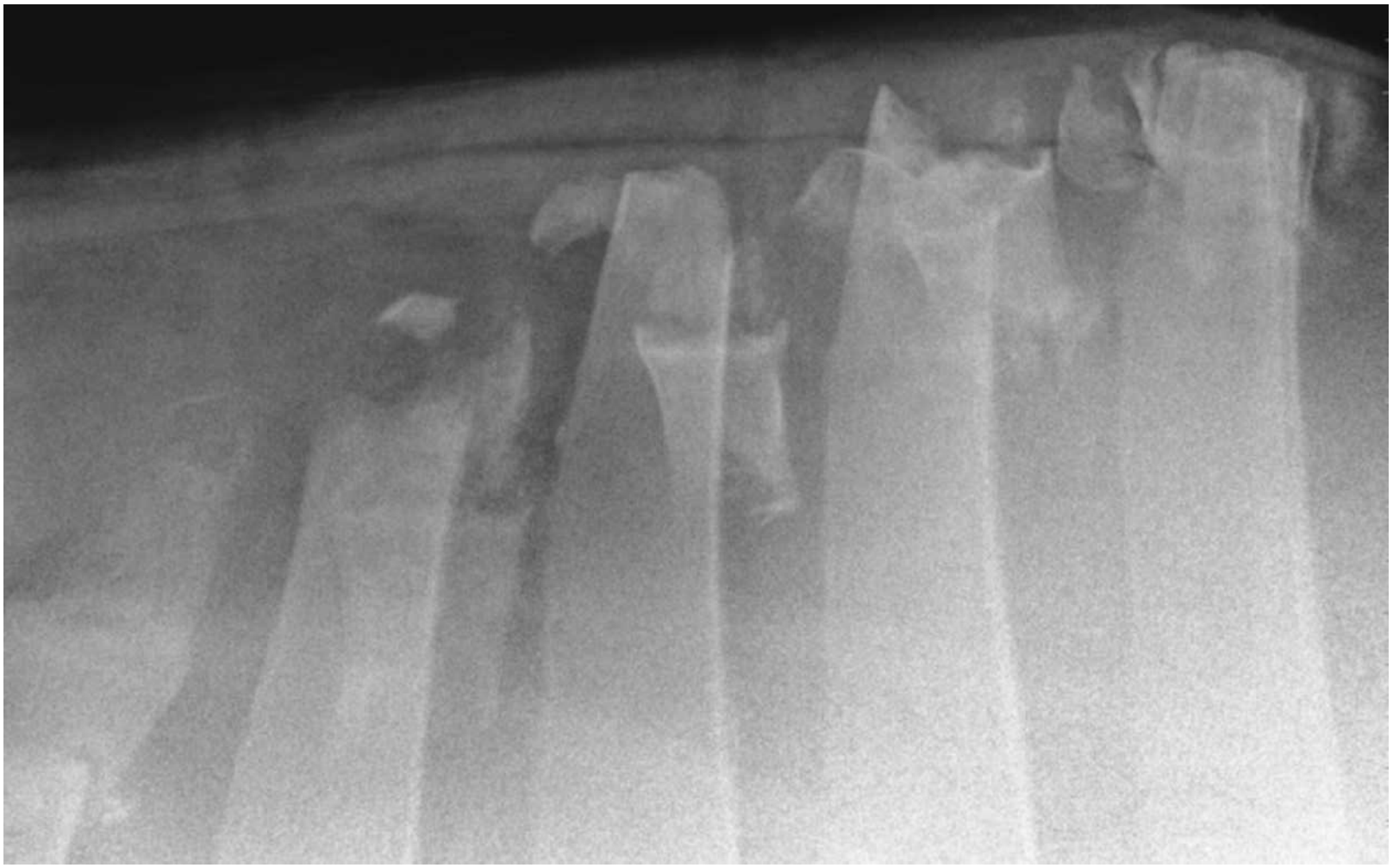


Figure 12.62(a) Lateral-lateral image of the spinous processes of the second to sixth thoracic vertebrae of an advanced event horse with acute onset of pain in the withers region following a fall in water, and subsequently becoming cast in a stable within 24 hours. Cranial is to to the left. There are displaced comminuted fractures of the spinous processes of T2–T6 (also 7–9, not shown). The horse was treated conservatively and made a complete functional recovery, although slight malformation of the withers region persisted.

SACRUM AND COCCYGEAL VERTEBRAE

Lateral-lateral radiographs of the sacrum and coccygeal vertebrae are obtained similarly to those of the thoracolumbar vertebrae. Definition of the body of the sacrum is often poor due to the overlying soft tissues and the resulting scattered radiation. Ventrodorsal views can be obtained with the horse in dorsal recumbency under general anaesthesia (see 'Pelvis' in Chapter 13).

On a lateral-lateral view of a normal horse, the sacrum is poorly defined, but its ventral border is seen as a linear opacity (Figure 12.63). The coccygeal vertebrae are aligned in a curvilinear manner (Figure 12.64).

Occasionally pain is associated with impinging spinous processes of the sacrum (Figure 12.65).

Sacral fractures are often displaced in a dorsoventral direction, and thus are best identified in a lateral-lateral projection. Clinically these fractures may result in a change in conformation of the hindquarters and neurological abnormalities. Ultrasonographic examination both externally and per rectum may be useful for verifying the diagnosis.

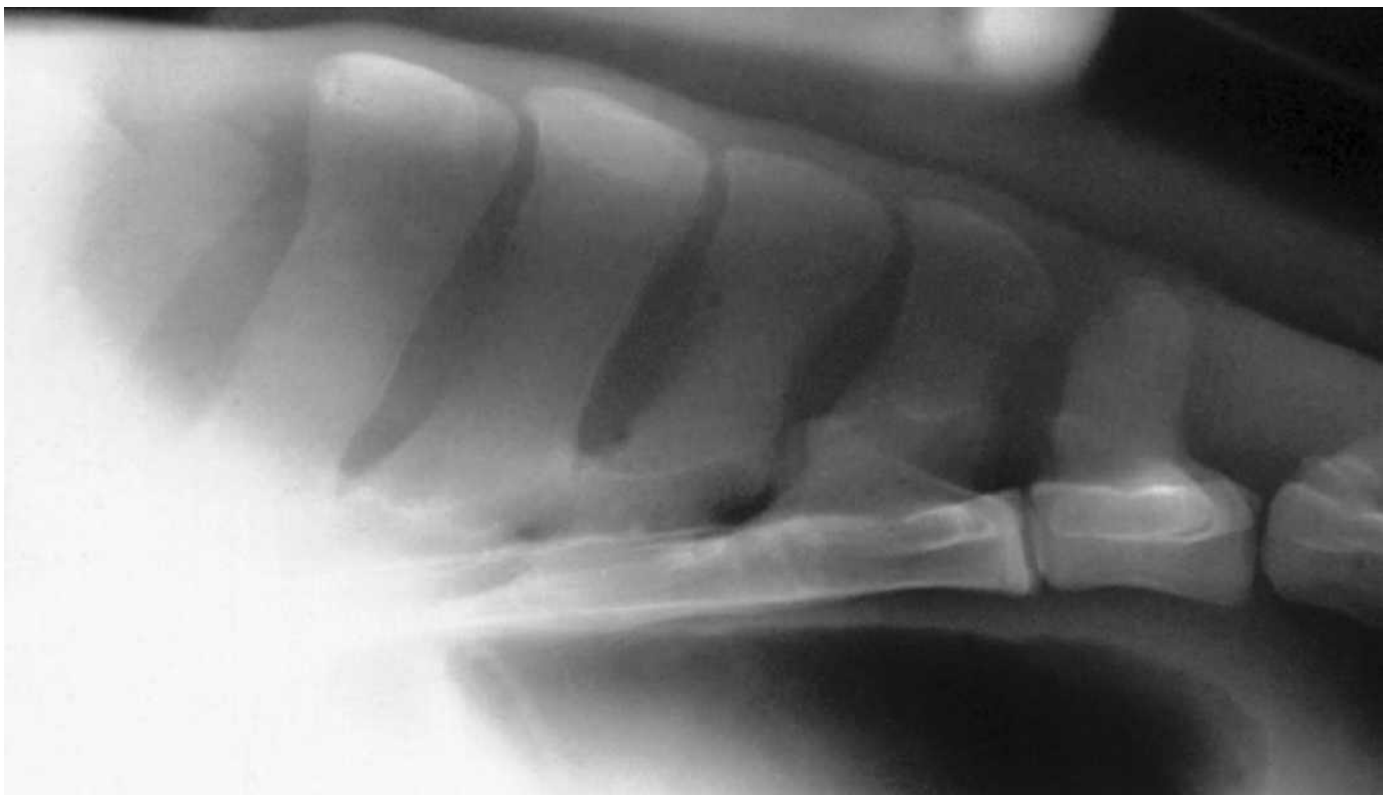


Figure 12.63 Lateral-lateral image of the sacrum and cranial coccygeal vertebrae of a normal adult horse. Cranial is to the left. The horse was poorly muscled over its dorsal midline and the sacrum is defined better than in the majority of horses. The radiograph was obtained using an aluminium wedge filter.

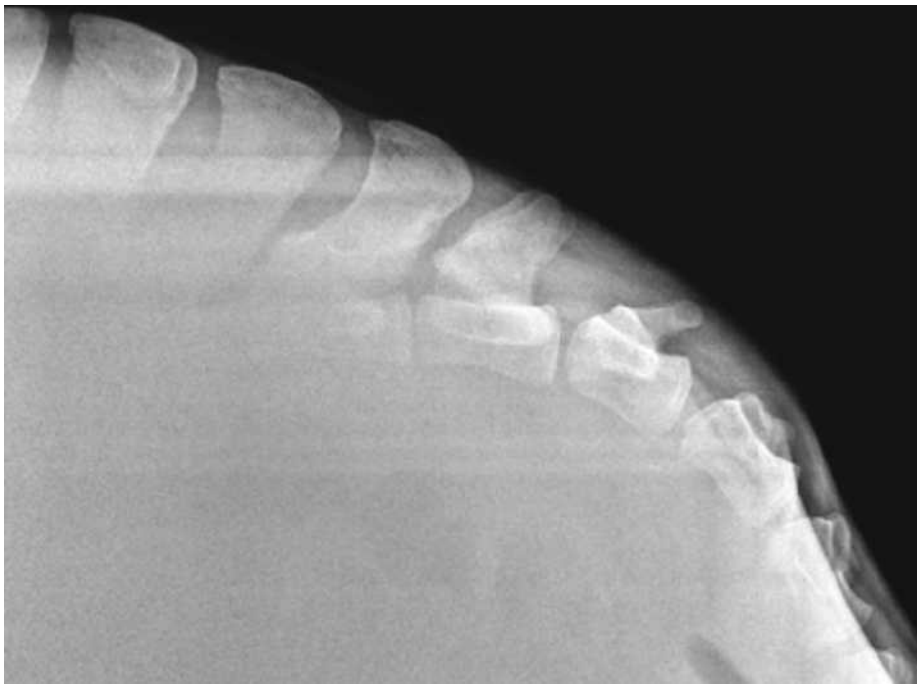


Figure 12.64 Lateral-lateral image of the caudal aspect of the sacrum and the cranial coccygeal vertebrae (CO1–CO5) of a normal adult horse. Cranial is to the left. Note the different shape of each coccygeal vertebra.

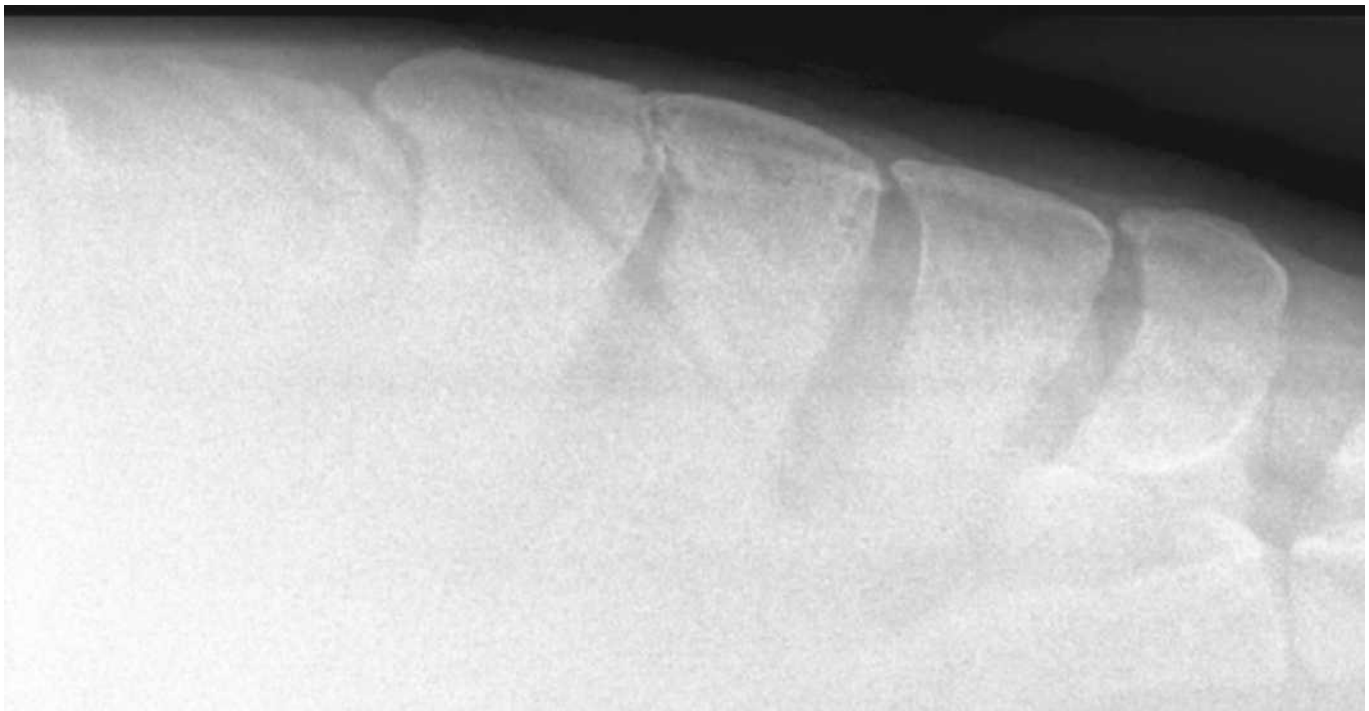


Figure 12.65 Lateral-lateral image of the spinous processes of the sacrum of a 14-year-old Arab endurance horse with poor performance and a reluctance to canter. The horse was painful to palpation throughout the thoracolumbar and sacral regions. There is overriding of three sacral spinous processes. There were also some architectural changes of the supraspinous ligament seen ultrasonographically.

Additional figures

The book companion website at www.clinical-radiology-horse.com includes additional figures that are not included in the printed book or e-book formats. Please see '**About the Companion Website**' at the start of the book for details on how to access the website. These figures are prefixed with the letter 'w' in the printed book, e.g. Figures 1w.4c–f.

FURTHER READING

CERVICAL VERTEBRAE

Adams, A., Steckel, R., Blevins, W. (1985) Diskospondylitis in five horses. *J. Am. Vet. Med. Ass.* **186**, 270–272

Alitalio, I., Karkkainen, M. (1983) Osteochondrotic changes in the vertebrae of four ataxic horses suffering from cervical vertebral malformation. *Nord. Vet. Med.* **35**, 468–474

Berg, L., Nielsen, J., Thoefner, M., et al. (2003) Ultrasonography of the equine cervical region: a descriptive study in eight horses. *Equine Vet. J.* **35**, 647–655

Birmingham, S., Reed, S., Mattoon, J., et al. (2010) Qualitative assessment of corticosteroid cervical articular facet injection in symptomatic horses. *Equine Vet. Educ.* **22**, 77–82

Bollwein, A., Hanichen, T. (1989) Age related changes in the intervertebral disks of the cervical vertebral column in the horse. *Tierarztl. Prax;.* **17**, 73–76

Claridge, H., Piercy, R., Parry, A., et al. (2010) The 3D anatomy of the cervical articular process joints in the horse and their topographical relationship to the spinal cord. *Equine Vet. J.* **42**, 726–731

Colles, C., Nevin, A., Brooks, J. (2014) The osteopathic treatment of somatic dysfunction causing gait abnormality in 51 horses. *Equine Vet. Educ.* **24**, 148–155

Cunha dos Santos, F., de Lourdes, M., Fernandes, C., et al. (2014) Cervical extradural haematoma in an ataxic horse. *Equine Vet. Educ.* **26**, 306–309

DeRouen, A., Spriet, M., Aleman, M. (2016) Prevalance of anatomical variation of the sixth cervical vertebra and association with vertebral canal stenosis and articular process osteoarthritis in the horse. *Vet. Radiol. Ultrasound* **57**, 253–258

Didierlaurent, V., Contremoulins, V., Denoix, H-M., Audigié, F. (2009) Scintigraphic pattern of uptake of 99mtechnetium by the cervical vertebrae of sound horses. *Vet. Rec.* **164**, 809–813

Dimock, A., Puchalski, S. (2010) Cervical radiology. *Equine Vet. Educ.* **22**, 83–87

Down, S., Henson, F. (2009) Radiographic retrospective study of the caudal cervical articular process joints in the horse. *Equine Vet. J.* **41**, 518–524

Draper, A., Finno, C. (2014) Cervical spondylosis deformans in two horses. *Equine Vet. Educ*. doi: 10.1111/eve.12167

Dyson, S. (2011) Lesions of the equine neck resulting in lameness or poor performance. *Vet. Clin. N. Am.: Equine Pract.* **27**, 417–437

Funk, K., Erickson, E. (1968) A case of atlanto-axial subluxation in a horse. *Can. Vet. J.* **9**, 120–123

Garcia-Lopez, J., Jenei, T., Chope, K., Bubeck, K. (2010) Diagnosis and management of cranial and caudal nuchal bursitis in four horses. *J. Am. Vet. Med. Ass.* **237**, 823–829

Gerlach, K., Muggli, L., Lempe, A., et al. (2012) Successful closed reduction of an atlantoaxial subluxation in a mature Warmblood horse. *Equine Vet. Educ.* **24**, 294–296

Greet, T.R.C., Jeffcott, L.B., Whitwell, K.E., Cook, W.R. (1980) The slap test for laryngeal adduction function in horses with suspected cervical spinal cord damage. *Equine Vet. J.* **12**, 127–131

Guffy, M., Coffman, J., Strafuss, A. (1969) Atlantoaxial luxation in a foal. *J. Am. Vet. Med. Ass.* **155**, 754–757

Hahn, C., Handel, I., Green, S., et al. (2008) Assessment of the utility of using intra- and intervertebral minimum sagittal diameter ratios in the diagnosis of cervical vertebral malformation in horses. *Vet. Radiol. Ultrasound* **49**, 1–6

Hirsch, J., Grant, B., Linovitz, R., et al. (2009) Diagnosis and surgical treatment of epidural neoplasms in two ataxic horses. *Equine Vet. Educ.* **21**, 564–568

Hoffman, C., Clark, C. (2013) Prognosis for racing with conservative management of cervical vertebral malformation in Thoroughbreds: 103 cases (2002–2010) *J. Vet. Intern. Med.* **27**, 317–323

Hudson, N., Mayhew, I. (2005) Radiographic and myelographic assessment of the equine cervical vertebral column and spinal cord. *Equine Vet. Educ.* **17**, 34–38

Janes, J., Garrett, K., McQuerry, K., et al. (2014) Comparison of magnetic resonance imaging with standing cervical radiographs for evaluation of vertebral canal stenosis in equine cervical stenotic myelopathy. *Equine Vet. J.* doi: 10:1111/evj.12221

Leipold, H., Brandt, G., Guffy, M., Blauch, B. (1974) Congenital atlanto-occipital fusion in a foal. *Vet. Med./Small Anim. Clin.* **69**, 1312–1316

Levine, J., Scrivani, P., Divers, T., et al. (2010) Multicenter case-control study of signalment, diagnostic features and outcome associated with cervical vertebral malformation-malarticulation in horses. *J. Am. Vet. Med. Assoc.* **237**, 812–822

Levine, J., Adam, E., MacKay, R., et al. (2007) Confirmed and presumptive cervical vertebral compressive myelopathy in

older horses: a retrospective study (1992–2004). *J. Vet. Intern. Med.* **21**, 812–819

Lischer, C., Withers, J., Parkin, T. (2010) Accuracy of radiographic measurements of the cervical articular process joints of the horse. *Pferdheilkunde* **26**, 553–558

Matoon, J., Drost, W., Weisbrode, S. (2004) Technique for equine cervical articular process joint injection. *Vet. Radiol. Ultrasound* **45**, 238–240

Mayhew, I. (1978) Congenital occipitoatlantoaxial malformations in the horse. *Equine Vet. J.* **10**, 103–113

Mayhew, I. (2009) Cervical vertebral fractures. *Equine Vet. Educ.* **21**, 536–539

Mayhew, I., DeLahunta, A., Georgi, J., Aspros, A. (1976) Naturally occurring cerebrospinal parelaphostrongylosis. *Cornell Vet.* **66**, 56–72

Mayhew, I., Whitlock, R., de Lahunta, A. (1978) Spinal cord disease in the horse. *Cornell Vet.* **68**, Suppl. 6, 44–68

Mayhew, I., Donawick, W., Green, S., et al. (1993) Diagnosis and prediction of cervical vertebral malformation in Thoroughbred foals based on semi-quantitative radiographic indicators. *Equine Vet. J.* **25**, 435–440

Mayhew, I., Green, S. (2000) Accuracy of diagnosing CVM from radiographs. *Proc.* 39th Annual Congress of the British Equine Vet. Assoc. 74–75

McKelvey, W., Owen, R. (1979) Acquired torticollis in 11 horses. *J. Am. Vet. Med. Ass.* **175**, 295–297

McCoy, D., Shires, P., Beadle, R. (1974) Ventral approach for stabilisation of atlantoaxial subluxation secondary to odontoid fracture in a foal. *J. Am. Vet. Med. Ass.* **185**, 545–549

Mitchell, C., Nykamp, S., Foster, R., et al. (2012) The use of magnetic resonance imaging in evaluating horses with spinal ataxia. *Vet. Radiol. Ultrasound* **53**, 613–620

Moore, B., Holbrook, T., Stefanacci, J., et al. (1992) Contrast-enhanced computed tomography in six horses with cervical stenotic myelopathy. *Equine Vet. J.* **24**, 197–202

Moore, B., Reed, S., Biller, D., et al. (1994) Assessment of vertebral canal diameter and bony malformations of the spine in horses with cervical sclerotic myelopathy. *Am. J. Vet. Res.* **55**, 5–13

Muno, J., Samii, V., Robertson, J., et al. (2009) Cervical vertebral fracture in a Thoroughbred filly with minimal neurological dysfunction. *Equine Vet. Educ.* **21**, 527–531

Nielsen, J., Berg, L., Thoefner, M., Thomsen, P. (2003) Accuracy of ultrasound-guided intra-articular injection of cervical facet joints in horses: a cadaveric study. *Equine Vet. J.* **35**, 657–661

Nout, Y., Reed, S. (2003) Cervical vertebral stenotic myelopathy. *Equine Vet. Educ.* **15**, 212–223

Olchowy, T. (1994) Vertebral body osteomyelitis due to *Rhodococcus equi* in 2 Arabian foals. *Equine Vet. J.* **26**, 79–80

Owen, R., Smith-Maxie, L. (1978) Repair of fractured dens of the axis in a foal. *J. Am. Vet. Med. Ass.* **173**, 854–856

Oswald, J., Love, S., Parkin, T., et al. (2010) Prevalence of cervical stenotic myelopathy in a population of thoroughbred horses. *Vet. Rec.* **166**, 82–83

Pinchbeck, G., Murphy, D. (2001) Cervical vertebral fracture in three foals. *Equine Vet. Educ.* **13**, 8–12

Prange, T., Carr, E., Stick, J., et al. (2012) Cervical vertebral canal endoscopy in a horse with cervical vertebral stenotic myelopathy. *Equine Vet. J.* **44**, 116–119

Randelhoff, A. (1997) Pathologische anatomische und histologische Untersuchungen zur Pathogenese von Wirbelsáulenveránderungen bei Pferden. Doctorate Thesis, Berlin

Rantanen, N., Gavin, P., Barbee, S., Sande, R. (1981) Ataxia and paresis in horses, Part 2: Radiographic and myelographic examination of the cervical vertebral column. *Comp. Cont. Educ.* **3**, 161–171

Ricardi, G., Dyson, S. (1993) Forelimb lameness associated with radiographic abnormalities of the cervical vertebrae. *Equine Vet. J.* **25**, 422–426

Richardson, D. (1986) *Eikenella corrodens* osteomyelitis of the axis in a foal. *J. Am. Vet. Med. Ass.* **188**, 298–299

Rooney, J.R. (1963) Equine incoordination 1. Gross morphology. *Cornell Vet.* **53**, 411–422

Scrivani, P., Levine, J., Holmes, N., et al. (2011) Observer agreement study of cervical-vertebral ratios in horses. *Equine Vet. J* **43**, 399–403

Sweers, L., Carsten, A. (2006) Imaging features of discospondylitis in two horses. *Vet. Radiol. Ultrasound* **47**, 159–164

Speltz, M., Olson, E., Hunt, L., Pool, R., Wilson, J., Carlson, M. (2006) Equine intervertebral disk disease: a case report. *J. Equine Vet. Sci.* **26**, 413–419

Thomsen, L., Berg, L., Markussen, B., et al. (2013) Synovial folds in equine articular process joints. *Equine Vet. J.* **45**, 448–453

Van Biervliet, J., de Lahunta, A., Ennulat, D., Oglesbee, M., Summers, B. (2003) Acquired cervical scoliosis in six horses associated with dorsal grey column chronic myelitis. *Equine Vet. J.* **35**, 86–92

Van Biervliet, J., Scrivani, P., Divers, T., et al. (2004) Evaluation of decision of spinal cord compression based on cervical myelography in horses: 38 cases (1981–2001). *Equine Vet. J.* **36**, 14–20

Vaughan, L., Mason, B. (1975) A Clinicopathological Study of Racing Accidents in Horses, Adlard & Son, Bartholomew Press, Dorking, Surrey

Voigt, A., Saulez, M., Donnellan, C. (2009) Nuchal crest avulsion fracture in 2 horses: a cause of headshaking. *J. S. Afr. Vet. Ass.* **80**, 111–113

Whitwell, K. (1980) Causes of ataxia in horses. *In Practice* **2**, 17–24

Whitwell, K., Dyson, S. (1987) Interpreting radiographs 8: Equine cervical vertebrae. *Equine Vet. J.* **19**, 8–14

Wilson, W., Hughes, S., Ghoshal, N., McNeel, S. (1985) Occipitoatlantoaxial malformation in two non Arabian horses. *J. Am. Vet. Med. Ass.* **187**, 36–40

Withers, J., Voute, L., Hammond, G., et al. (2009) Radiographic anatomy of the articular process joints of the caudal cervical vertebrae in the horse on lateral and oblique projections. *Equine Vet. J.* **41**, 895–902

Witte, S., Alexander, K., Bucellato, M., Sofaly, C., Fife, W., Hinchclife, K. (2005) Congenital atlantoaxial luxation associated with malformation of the dens in a Quarter horse foal. *Equine Vet. Educ.* **17**, 175–178

Alward, A., Pease, A., Jones, S. (2007) Thoracic discospondylitis with associated epaxial muscle atrophy in a Quarter Horse gelding. *Equine Vet. Educ.* **19**, 67–71

Berner, D., Winter, K., Brehm, W., et al. (2012) Influence of head and neck position on radiographic measurement of intervertebral distances between thoracic dorsal spinous processes in clinically sound horses. *Equine Vet. J.* **44** (Suppl. 43), 21–26

Colles, C., Nevin, A., Brooks, J. (2014) The osteopathic treatment of somatic dysfunction causing gait abnormality in 51 horses. *Equine Vet. Educ.* **24**, 148–155

Coomer, R., McKane, S., Smith, N., et al. (2012) A controlled study evaluating a novel surgical treatment for kissing spines in standing sedated horses. *Vet. Surg.* **41**, 890–897

Cousty, M., Retureau, C., Tricaud, C., et al. (2010) Location of radiological lesions of the thoracolumbar column in French trotters with and without signs of back pain. *Vet. Rec.* **166**, 41–45

De Heer, N., Nout, Y. (2011) Congenital kyphosis secondary to lumbar vertebral hypoplasia causing paraparesis in a Friesian foal. *Equine Vet. Educ.* **23**, 231–234

Denoix, J.-M. (2005) Thoracolumbar malformations or injuries and neurological manifestations. *Equine Vet. Educ.* **17**, 191–194

Denoix, J.-M. (2007) Discovertebral pathology in horses. *Equine Vet. Educ.* **19**, 72–73

Finding, E., Ciasca, T., Pinilla, M., et al. (2014) Diagnosis, treatment and outcome of spinal lymphoma in a pony. *Equine Vet. Educ.* **26**, 303–305

Erichsen, C., Eksell, P., Roethlisberger Hol, K., Johnston, C. (2004) Relationship between scintigraphic and radiographic evaluation of spinous processes in the thoracolumbar spine in riding horses without clinical signs of back problems. *Equine Vet. J.* **36**, 458–465

Giguere, S., Lavoie, J. (1994) *Rhodococcus equi* vertebral osteomyelitis in 3 Quarter Horses. *Equine Vet. J.* **26**, 74–78

Gillen, A., Dyson, S., Murray, R. (2009) Nuclear scintigraphic assessment of thoracolumbar synovial intervertebral articulations. *Equine Vet. J.* **41**, 534–540

Giroudroux, M., Dyson, S., Murray, R. (2009) Osteoarthritis of the thoracolumbar synovial intervertebral articulations: clinical and radiographic features in 77 horses with poor performance and back pain. *Equine Vet. J.* **41**, 130–138

Haussler, K., Stover, S. (1998) Stress fractures of the vertebral lamina and pelvis in Thoroughbred racehorses. *Equine Vet. J.* **30**, 374–383

Haussler, K., Stover, S., Willits, N. (1997) Developmental variation in lumbosacropelvic anatomy of Thoroughbred horses. *Am. J. Vet. Res.* **58**, 1083–1091

Hawkins, J., Fessler, J. (2000) Treatment of supraspinous bursitis by use of debridement in standing horses: 10 cases (1968–1999). *J. Am. Vet. Med. Ass.* **217**, 74–78

Henson, F., Lamas, L., Knezevic, S., et al. (2007) Ultrasonographic evaluation of the supraspinous ligament in a series of ridden and unridden horses and horses with unrelated back pathology. *BMC Vet. Res.* **3**, 3

Jacklin, B., Minshall, G., Wright, I. (2014) A new technique for subtotal (cranial wedge) ostectomy in the treatment of impinging/overriding spinous processes: Description of technique and outcome in 25 cases. *Equine Vet J.* **46**, 339–344

Jeffcott, L.B. (1975) The diagnosis of diseases of the horse's back. *Equine Vet. J.* **7**, 67–78

Jeffcott, L.B. (1979) Radiographic examination of the equine vertebral column. *Vet. Radiol.* **20**, 135–139

Jeffcott, L.B. (1979) Radiographic features of the normal equine thoracolumbar spine. *Vet. Radiol.* **20**, 140–147

Jeffcott, L.B. (1979) Back problems in the horse – a look at past, present and future progress. *Equine Vet. J.* **11**, 129–136

Jeffcott, L.B. (1980) Disorders of the thoracolumbar spine of the horse – a survey of 443 cases. *Equine Vet. J.* **12**, 197–210

Jeffcott, L.B., Dalin, G. (1980) Natural rigidity of the horse's backbone. *Equine Vet. J.* **12**, 101–108

Jeffcott, L.B., Hickman, J. (1975) The treatment of horses with chronic back pain by resecting the summits of the impinging dorsal spinous processes. *Equine Vet. J.* **7**, 115–119

Kothstein, T., Eashmir-Raven, A., Thomas, M., Brashier, M. (2000) Radiographic diagnosis: thoracic spinal fracture resulting in kyphosis in a horse. *Vet. Radiol. Ultrasound* **41**, 44–45

Meehan, L., Dyson, S., Murray, R. (2009) Radiographic and scintigraphic evaluation of spondylosis in the equine thoracolumbar spine: a retrospective study. *Equine Vet J.* **41**, 800–807

Perkins, J., Schumacher, J., Kelly, G., Pollock, P., Harty, M. (2005) Subtotal ostectomy of dorsal spinous processes performed in nine standing horses. *Vet. Surg.* **34**, 625–629

Piat, P., Blond, L., Spriet, M., et al. (2012) Fractures of the withers in horses. *Equine Vet. Educ.* **24**, 582–588

Rashmir-Raven, A., Thomas, M., Brashier, M. (2000) Radiographic diagnosis: Thoracic spinal fracture resulting in kyphosis in a horse. *Vet. Radiol. Ultrasound* **41**, 44–45

Rooney, J.R., Prickett, M.E. (1966) Congenital lordosis of the horse. *Cornell Vet.* **57**, 417–428

Sinding, M., Berg, L. (2010) Distances between thoracic spinous processes in Warmblood foals: a radiographic study. *Equine Vet J.* **42**, 500–503

Smythe, R.H. (1962) Ankylosis of the equine spine; pathologic or biologic? *Mod. Vet. Pract.* **43**, 50–51

Sweers, L., Carstens, A. (2006) Imaging features of discospondylitis in two horses. *Vet. Radiol. Ultrasound* **47**, 159–164

Unt, V., Piercy, R. (2009) Vertebral embryology and equine congenital vertebral anomalies. *Equine Vet. Educ.* **21**, 212–214

Walmsley, J., Pettersson, H., Winberg, F., McEvoy, F. (2002) Impingement of the dorsal spinous processes in two

hundred and fifteen horses: case selection, surgical technique and results. *Equine Vet. J.* **34**, 23–28

Wong, D., Scarratt, W., Rohleder, J. (2005) Hindlimb paresis associated with kyphosis, hemivertebrae and multiple thoracic vertebral malformations in a Quarterhorse gelding. *Equine Vet. Educ.* **17**, 187–191

Zimmerman, M., Dyson, S., Murray, R. (2012) Close, impinging and overriding spinous processes in the thoracolumbar spine: The relationship between radiological and scintigraphic findings and clinical signs. *Equine Vet. J.* **44**, 178–184

Zimmerman, M., Dyson, S., Murray, R. (2011) Comparison of radiographic and scintigraphic findings of the spinous processes in the equine thoracolumbar region. *Vet. Radiol. Ultrasound* **52**, 661–671

SACRUM AND COCCYGEAL VERTEBRAE

Taylor, S., Murray, R., Donovan, T., Scott, C. (2002) Conservative management of a sacrococcygeal fracture/luxation in a horse. *Equine Vet. Educ.*, **14**, 63–70

Chapter 13
The pelvis and femur

Pelvis

The primary indications for radiography of the pelvis are:
1 Asymmetry of the pelvis, assessed by comparison of the tubera coxae and tubera sacrale.
2 Hindlimb lameness in the absence of clinical and radiographic abnormalities of the more distal aspects of the limb and exclusion of the more distal aspects of the limb as a source of pain by diagnostic analgesia.
3 Audible or palpable crepitus in the pelvic region associated with hindlimb lameness (radiography performed with the horse under general anaesthesia should be postponed in these circumstances for at least 6 weeks – see 'Fractures', below). It should be noted that diagnostic ultrasonography, performed transcutaneously or per rectum, can be useful to identify some but not all fractures, especially those of the ilial wing.
4 Positive nuclear scintigraphic findings.

RADIOGRAPHIC TECHNIQUE

Equipment

Radiographs of the pelvis require radiographic equipment with an output in excess of 100 kV and 200 mAs. Digital systems or rare earth screens and films are required. Large (35 cm × 43 cm) cassettes are recommended.

Oblique lateral radiographic views of the pelvis in a standing horse can be obtained and yield adequate diagnostic information in foals, ponies and Thoroughbred-type horses, but their diagnostic value in large horses is more limited.

Standing ventrodorsal oblique radiographs can be obtained and may be useful to diagnose obvious lesions of the coxofemoral joint and the ischium, particularly when general anaesthesia is clinically undesirable. Strict control of personnel is essential to minimise the radiation hazard. Standing radiographs may underestimate the degree of pathological abnormality. It is not possible to assess the ilial wings and sacroiliac joints using this technique.

Lateral 30° dorsal-lateroventral oblique images of the pubis, coxofemoral joint and ischium can be obtained in some ponies and small horses.

Customised oblique images of the tubera coxae and tubera ischii can also be acquired.

Clinical Radiology of the Horse, Fourth Edition. Janet A. Butler, Christopher M. Colles, Sue J. Dyson, Svend E. Kold and Paul W. Poulos.
© 2017 John Wiley & Sons, Ltd. Published 2017 by John Wiley & Sons, Ltd.
Companion website: www.clinical-radiology-horse.com

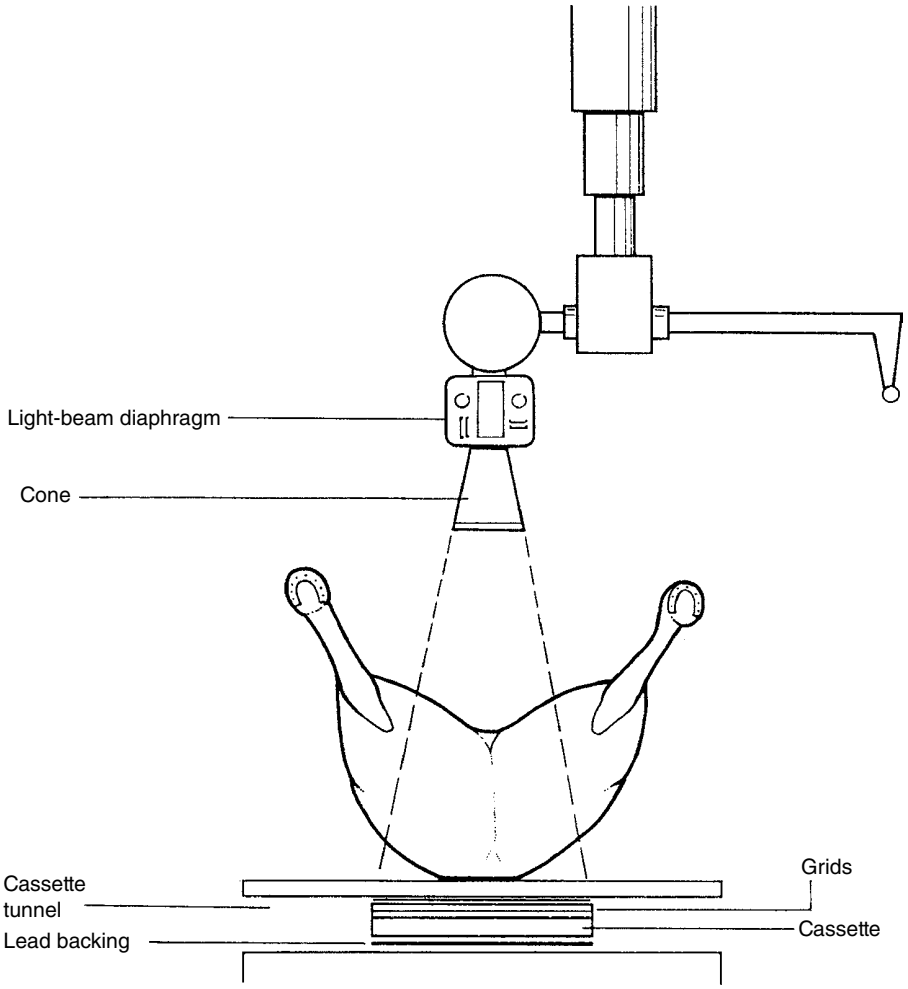


Figure 13.1 Positioning of the x-ray machine, horse and cassette to obtain ventrodorsal radiographic views of the pelvis and lumbar vertebrae (not to scale).

Much more detailed, high-quality radiographs of the entire pelvic region are obtained with the horse in dorsal recumbency under general anaesthesia. Because of the large exposures required, no personnel should be in the x-ray room during radiography. It is preferable to have an x-ray table that incorporates a cassette tunnel, because accurate positioning of the cassettes directly under a recumbent horse is difficult (Figure 13.1).

Because of the large amount of soft tissue present, scattered radiation is a serious problem. It must be carefully controlled using one or more of the following:

- Precise collimation of the primary x-ray beam, using a light-beam diaphragm
- A focused grid (12:1 ratio), or ideally two focused grids with grid lines at right angles to each other (this will markedly increase the exposure required)
- A lead-intensifying screen (lead equivalent 0.002 cm) placed in front of the grid(s) to absorb low-energy radiation
- A sheet of lead (0.01 mm lead equivalent) placed behind the cassette in order to reduce backscatter
- A lead cone in addition to a light-beam diaphragm is helpful to collimate the primary beam fully
- When acquiring standing oblique images of the pelvis, the use of an air gap can be helpful, but does cause magnification problems.

Positioning

Ventrodorsal views of the pelvis with the horse in dorsal recumbency

For accurate assessment of pelvic radiographs it is important that the horse is positioned symmetrically in dorsal recumbency in the so-called 'frog-leg' position, i.e. with the caudal aspect of the lumbar vertebral column and the sacrum in a straight line, and the hindlimbs flexed and abducted. In horses with unilateral atrophy of the muscles of the hindquarters and/or severe asymmetry of the pelvis, positioning can be difficult. The best guide to ensure that positioning is correct is to assess the linea alba, which should be straight and lie vertically above the spine. Extra padding (non radiodense) may need to be placed under the horse if there is pronounced unilateral muscle atrophy of the hindquarters, to aid correct positioning. The position of the flexed hindlimbs, and in particular the points of the hocks, can be deceptive. All the radiographs are obtained with the x-ray beam aligned perpendicular to the table on which the horse is supported.

For complete assessment of the pelvis of an adult horse, at least seven standard overlapping radiographic views are recommended (using 35 cm × 43 cm cassettes) (Figure 13.2).

Three views are obtained along the midline of the pelvis. The x-ray beam in each case is centered on the linea alba.

1 To examine the tubera ischii, the caudal edge of the cassette is positioned immediately caudal to the tubera ischii.

2 To examine the region of the coxofemoral joints and obturator foramina, the cassette is moved cranially so that the two radiographic images overlap by about 5 cm. This also gives visualisation of the caudal part of the sacrum.

3 To examine the sacroiliac and lumbosacral joints and the cranial part of the sacrum, the cassette is moved cranially, to overlap the previous position by about 5 cm.

Separate views are obtained of each tuber coxae. The cassette is positioned 5–10 cm cranial to the most cranial view of the pelvic canal, but is centered approximately 20 cm to the right or left of the midline. This view may aid definition of the individual sacroiliac joints.

For examination of the left and right coxofemoral joints, the horse should be rolled slightly so that the limb on the side to be radiographed is tilted nearer to the table, forming an angle of 10–15° with the horizontal. The cassette is positioned about 10 cm cranial to the position for the caudal pelvic view, and the x-ray beam is centered 5–10 cm lateral to the linea alba. This view also gives good visualisation of the proximal aspect of the femur.

Demonstration of specific lesions may require non-standard views. Subluxation of the coxofemoral joint may not be apparent in the frog-leg position and it may be necessary to extend the limb to demonstrate this abnormality. Oblique views are best obtained by rolling the horse, rather than angling the x-ray beam, in order to avoid grid cut-off.

Superimposition of gas- and ingesta-filled viscera over the pelvis is a problem. Routine starvation prior to general anaesthesia and radiography unfortunately has little effect upon this. During radiography rectal manipulation of the viscera and manual emptying of the rectum can be tried, but tend to be ineffective in moving the intestinal contents significantly.

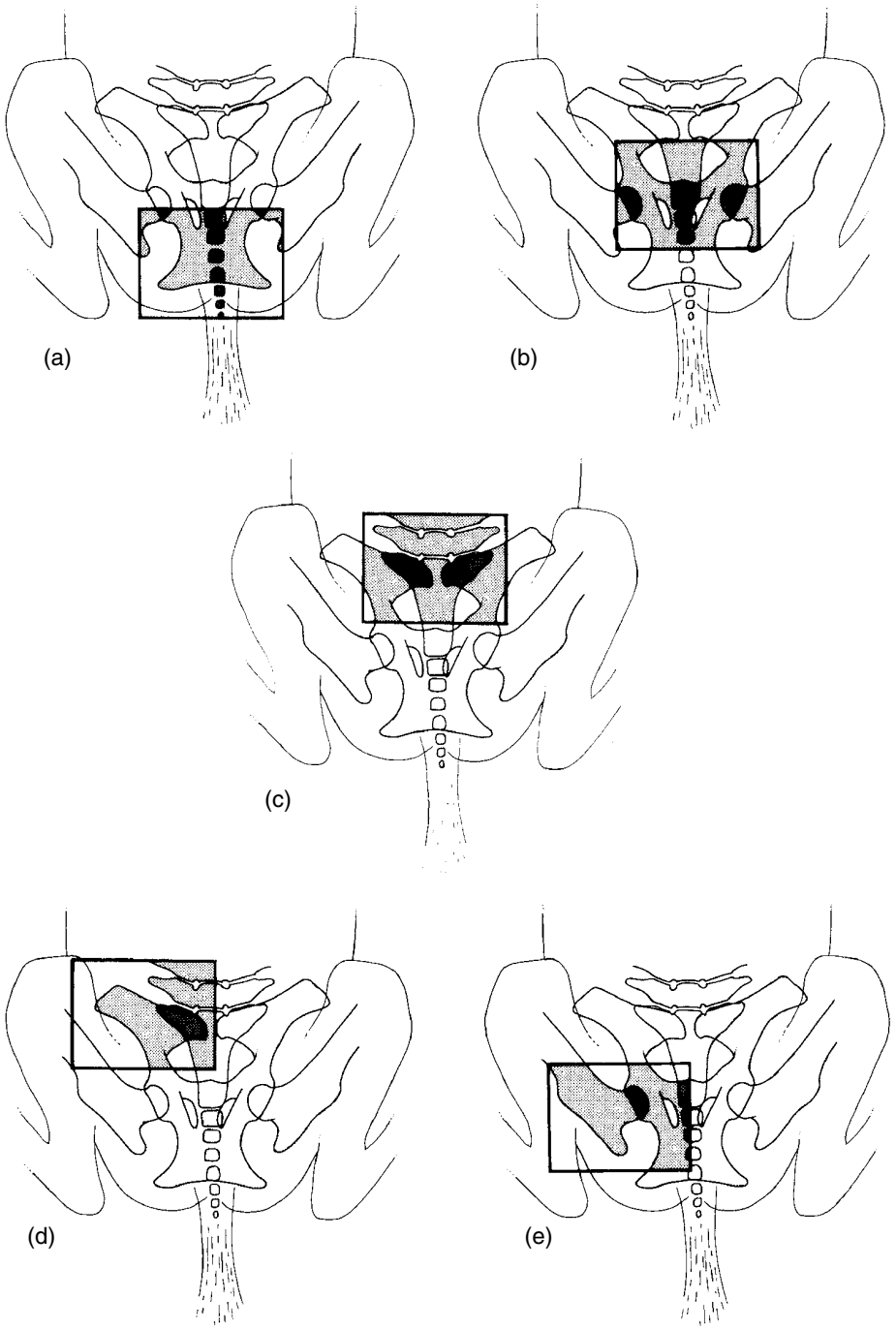


Figure 13.2 Positioning the cassette relative to the horse to obtain ventrodorsal views of (a) the tubera ischii, (b) the pelvic canal, (c) the sacroiliac joints, (d) an iliac wing and (e) a coxofemoral joint. The latter is obtained with the horse rocked towards the side to be examined.

Lateral 30° dorsal–lateroventral oblique views of the pelvis in the standing horse

Lateral 30° dorsal-lateroventral oblique views of the pelvis can provide adequate diagnostic information in foals, ponies and some Thoroughbred-type horses. Their diagnostic value in larger horses is limited. The horse should stand squarely on all four limbs; however, many horses with fractures of the pelvic region are not able to bear full weight on the lame limb. Rectal examination, including ultrasonographic examination, of the osseous structures of the pelvis is recommended to obtain further information about the possible site of

fracture. Evacuation of faeces from the rectum helps avoid artefacts created by overlying faecal material. It is also beneficial to inject air into the rectum to provide better contrast for the assessment of overlying osseous structures.

A vertically positioned cassette supported by a cassette holder is positioned against the side of the pelvis to be examined (Figure 13.3). The x-ray machine is angled 30° ventrally from the horizontal (i.e. angled from dorsal to ventral), centering the x-ray beam between the level of the greater trochanter of the femur and the base of the tail, approximately two-thirds of the distance between the ipsilateral tuber sacrale and tuber ischii. If the horse is unable to bear weight on the limb to be examined the pelvis is tipped ventrally on that side, so the x-ray beam must be angled a further 5–10° ventrally and centered several centimetres further ventrally. The height of the cassette is adjusted accordingly. The precise craniocaudal position of the cassette and x-ray machine depends on the area of clinical interest.

Rare earth screens, or a digital system, and a stationary parallel grid aligned perpendicular to the x-ray beam give best results. This view permits evaluation of the caudal half of the ilial shaft, the ischium, the greater trochanter of the femur, the femoral head, the acetabulum and the coxofemoral joint. It permits the identification of displaced fractures, extensive periarticular new bone and lack of congruence of the coxofemoral joint. However, it is not possible to detect more subtle radiographic abnormalities, such as periarticular osteophyte formation. Little information can be gained about the ilial wings and the tubera coxae.

This technique involves high exposure factors and the minimum number of personnel should be present.

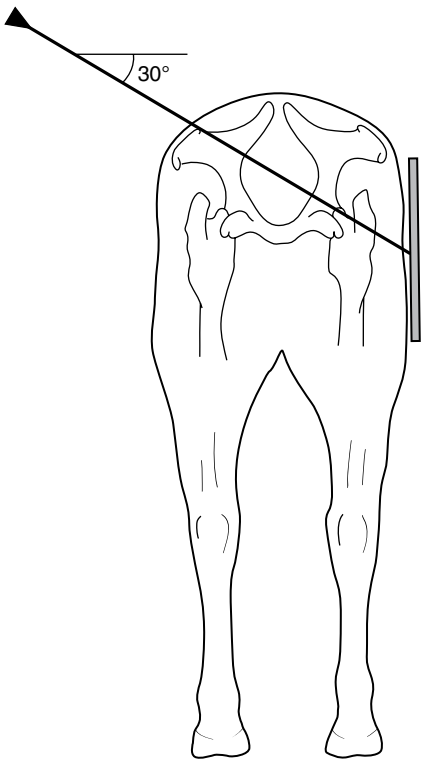


Figure 13.3 Positioning the x-ray beam and cassette to obtain a lateral oblique view of the coxofemoral joint in a standing horse. The cassette is positioned as close as possible to the horse, centered at the level of the coxofemoral joint. The x-ray beam is angled 30° ventrally and centered between the greater trochanter of the femur and the tail head, approximately two-thirds of the distance between the tuber sacrale and tuber ischii.

Cranioventral-caudodorsal views of the pelvis in the standing horse

It is essential that the horse is adequately sedated. It should stand with the hindlimbs abducted as far as is compatible with standing both comfortably and still. A cassette and cross-hatch grid are placed dorsal to the pelvic region, angled so that they will be perpendicular to the x-ray beam. The x-ray tube is then positioned ventral to the horse's abdomen, cranial to the hindlimbs, and the beam is angled dorsally 10–25° caudad. The cassette and cross-hatch grid are positioned over the hindquarter to be examined, or over the dorsal midline to examine both sides simultaneously (Figure 13.4). The cassette and the x-ray tube can be moved caudally, cranially or laterally to assess the coxofemoral joints, the caudal aspect of the pelvic canal and the tubera ischii. It is important to recognise the potential risk to personnel in the room, with the large exposure factors required (up to 150 kV, 400 mAs for a 500 kg horse). The use of a vertically mounted Bucky and cassette holder is highly recommended. The cassette should never be hand-held.

NORMAL ANATOMY, VARIATIONS AND INCIDENTAL FINDINGS

Immature horse

The pelvis consists of three paired bones (left and right): the ilium, pubis and ischium (Figure 13.5). At birth the symphyseal branches of the pubis and ischium are fused to each other, but ossification of their shafts, and fusion

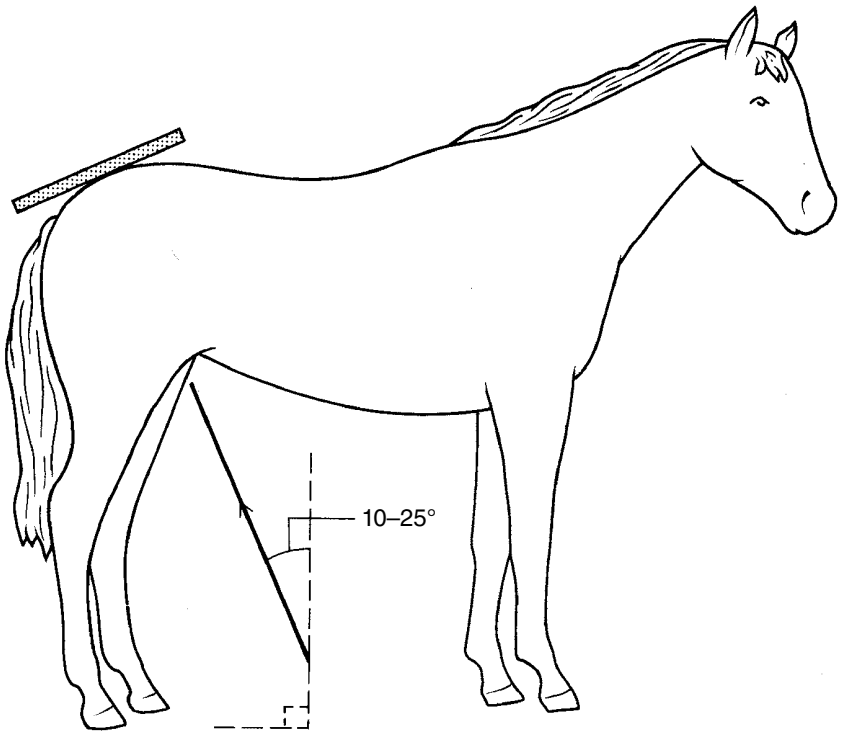


Figure 13.4 Positioning to obtain ventrodorsal views of the pelvis in the standing horse.

with the ilium to complete the acetabulum, does not occur until about 1 year of age (Appendix A, 'Fusion times of physes and suture lines'). In foals and yearlings the points of the tubera ischii are irregular and bluntly outlined due to incomplete ossification.

Separate ossification centres occur in each of the bones:

- ilium – iliac crest and tuber coxae
- pubis – acetabular portion of the shaft
- ischium – caudal portion of the bone and tubera ischii.

The separate centres of ossification of the pelvis fuse by about 10–12 months, but the symphysis pubis remains unfused throughout life.

The proximal aspect of the femur has separate centres of ossification for the femoral head, the trochanter major and the trochanter minor. The physis of the femoral head closes between 24 and 36 months, and the trochanter major fuses with the femoral shaft between 18 and 30 months. Fusion of the trochanter minor is less consistent, usually occurring at about 2 years.

Skeletally mature horse: ventrodorsal views

When examining radiographs of the pelvis it is useful to start by assessing the obturator foramina (Figures 13.5, 13.6a and 13.6b). If the horse is correctly positioned, these should appear symmetrical. If the foramina appear asymmetrical, this may be due to poor positioning or to traumatic damage to the pelvis. Asymmetry of the foramina is frequently seen in combination with pubic, ischial or acetabular fractures.

The symphysis pubis remains evident throughout life (Figures 13.5, 13.6a and 13.6b). It is relatively straight. Occasionally a bony protuberance is evident at the cranial aspect of the pubic symphysis. The pubic bones should be aligned, with no step at the pelvic brim. Roughening on

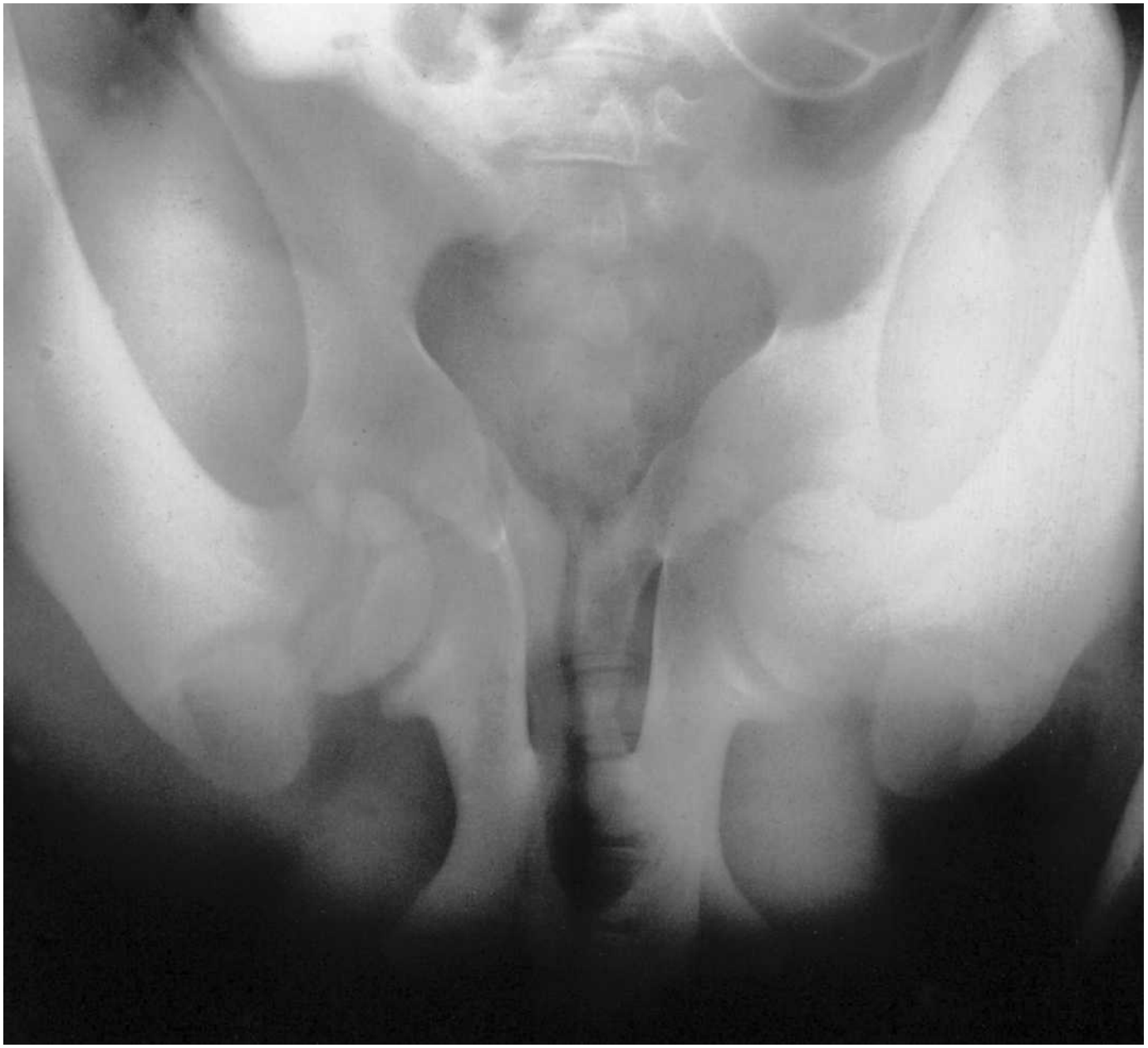


Figure 13.5 Ventrodorsal view of the pelvis, caudal lumbar vertebrae and sacrum of a normal foal of 11 days of age (compare with Figures 13.6(a–c). Cranial is to the top. Note the position of the symphyses between the ilium and pubis, and the ischium and the ilium, the wide pubic symphysis and the physis of the femoral head.

the cranial aspect of the pubis in the region of the pubic tubercle and iliopubic eminence may be seen.

The outline of the tubera ischii varies slightly among individuals, but should always be regular (Figure 13.6a).

The shaft of the ilium is smooth, with some roughening of the psoas tubercle. The ilium broadens cranially to form the body of the ilium and tuber coxae laterally, and the tuber sacrale medially (Figure 13.6d).

To compare the left and right coxofemoral joints, it is important that the pelvis is symmetrically positioned with similar rotation and abduction of the

femurs. This can be evaluated on radiographs by comparing the angle formed between the trochanter major and the acetabular branch of the ischium.

The acetabulum is formed by fusion of the ilium, ischium and pubis. The dorsal rim has a smooth outline (Figures 13.5 and 13.6e). The ventral rim has, at its deepest point, a depression – the acetabular fossa – for attachment of the ligament of the femoral head (teres ligament). At the site of attachment of this ligament on the femoral head, a small focal lucent area – the fovea capitis – can sometimes be seen, opposite the acetabular fossa.

The sacroiliac joints (left and right) provide the only articulation between the pelvis and the spine, and have little movement (Figure 13.6c). They are atypical diarthrodial joints with flattened joint surfaces which are angled at approximately 30° to the horizontal plane. The size and contour of the joints vary among individual animals. The joints are difficult to identify on a ventrodorsal projection, due to their angle and superimposition of abdominal viscera. It may be helpful to locate the narrowest (caudal) part of the sacrum between the shafts of the ilia and follow the diverging outlines of the sacrum cranially towards the external angle of the lumbosacral joint (Figure 13.6c). The sacroiliac joints are located where these lines are superimposed upon the wings of the ilia.

The five sacral vertebrae are fused, but have separate spinous processes which are seen as oval-shaped opacities in the midline, superimposed on the body of the sacrum (Figure 13.6c). The body of the sacrum broadens cranially. The first sacral vertebra has transverse processes which articulate with the transverse processes of the most caudal (usually the sixth) lumbar vertebra. The lumbosacral joints are easily seen on dorsoventral radiographs (Figure 13.6c). The sacral body has intervertebral foramina between the adjacent vertebrae, but these can be difficult to identify radiographically. The intervertebral foramina between the sacrum and the most caudal lumbar vertebra and adjacent lumbar vertebrae are clearly seen as approximately circular lucent zones on the left and right sides of the intercentral articulations. The intercentral articulations are slightly variable in width and often appear wider in the sagittal midline than at the periphery of the joints, because the caudal articular surfaces are more curved than the cranial articular surface of the adjacent vertebra. The caudal subchondral bone plate of each lumbar vertebra is relatively more opaque.

Articulations between the transverse processes of the lumbar vertebrae are variable and may be asymmetrical. There is no relationship between age and the number of articulations, or the presence of ankylosis. The size and width of intertransverse articulations tends to be greatest at the lumbosacral joint and decreases craniad. The articulations between the transverse processes of adjacent lumbar vertebrae are often slightly irregular in outline. Occasionally irregular lucent zones and areas of increased radiopacity are seen in the cortical bone opposing the joints. The lumbosacral joint, and in some horses the intercentral joints between the fifth and sixth and fourth and fifth lumbar vertebrae and the intertransverse articulations, can also be assessed by ultrasonography per rectum.

Less commonly there may be fusion of the intercentral joints between either the most caudal lumbar vertebrae or, more commonly, between the sixth lumbar vertebra and the sacrum. The clinical significance of these changes is uncertain. Fusion may alter the biomechanical function of the thoracolumbosacral spine and predispose to other lesions of the thoracolumbar and sacroiliac regions.

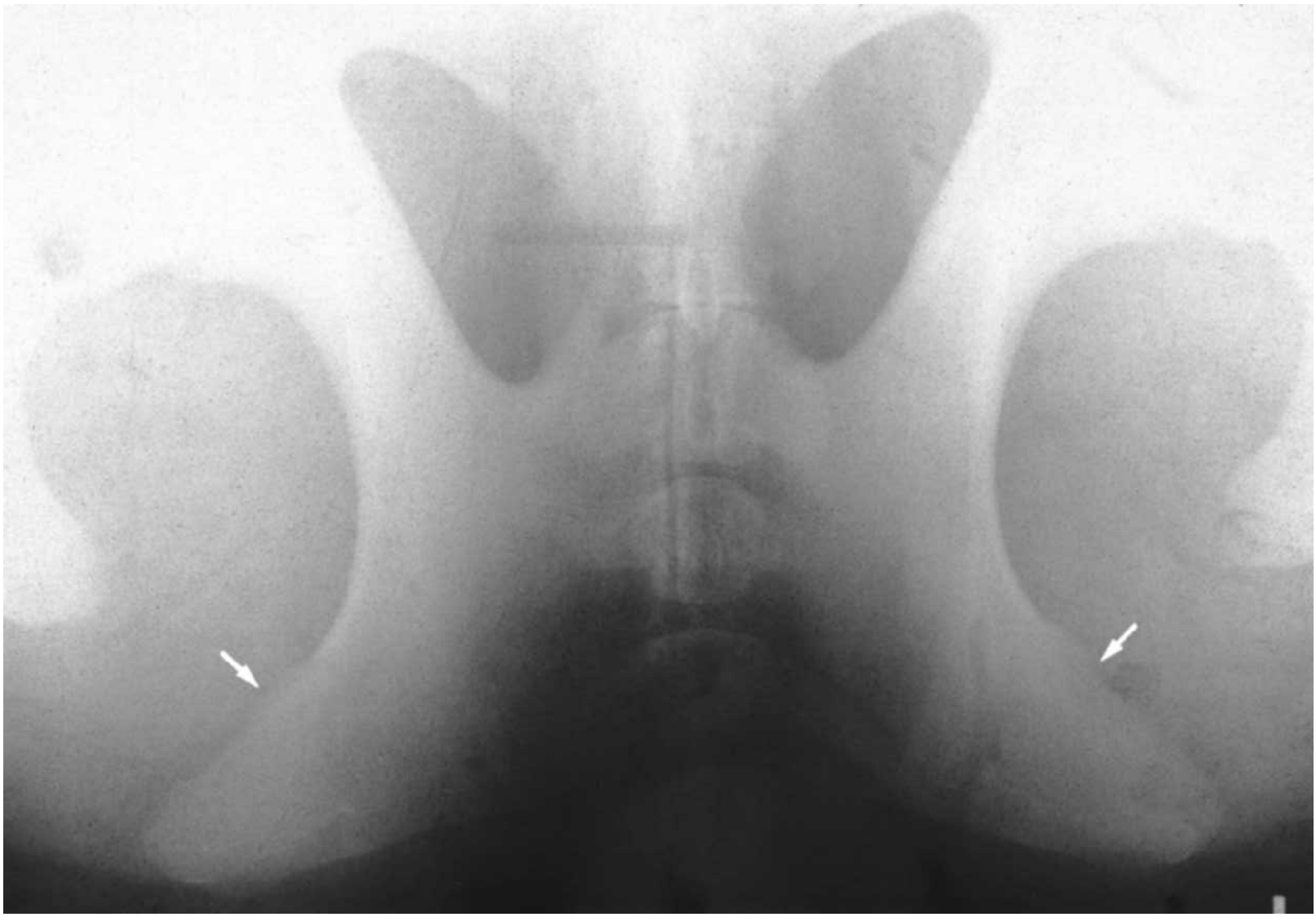
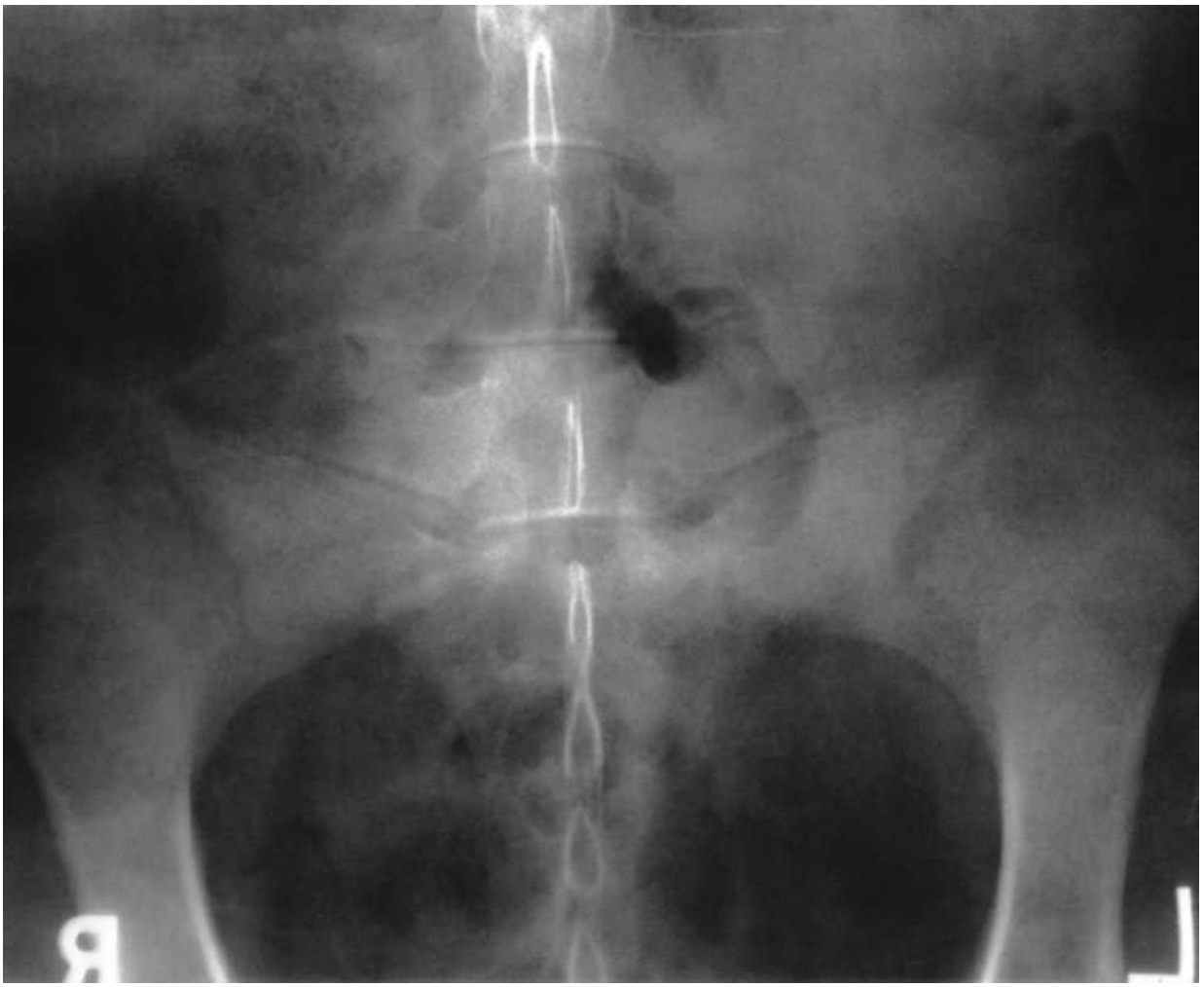


Figure 13.6(a) Ventrodorsal image of the caudal aspect of the pelvis of a normal adult horse. Cranial is to the top. The cranial coccygeal vertebrae are superimposed over the pubic symphysis. Note the slight irregularity in outline of the cranial edge of each tuber ischium (arrows), a normal variant.



Figure 13.6(b) Ventrodorsal image of the pelvic canal of a normal adult horse. Cranial is to the top. The oval-shaped opacities in the midline (open arrows) represent the spinous processes of the sacrum. Superimposed abdominal viscera cause the gas shadows. Note the symmetry of the obturator foramina, apparent widening of each coxofemoral joint in the region of the insertion of the ligament of the femoral head (teres ligament) (closed arrows) and the flat appearance of the outline of the opposing femoral heads.



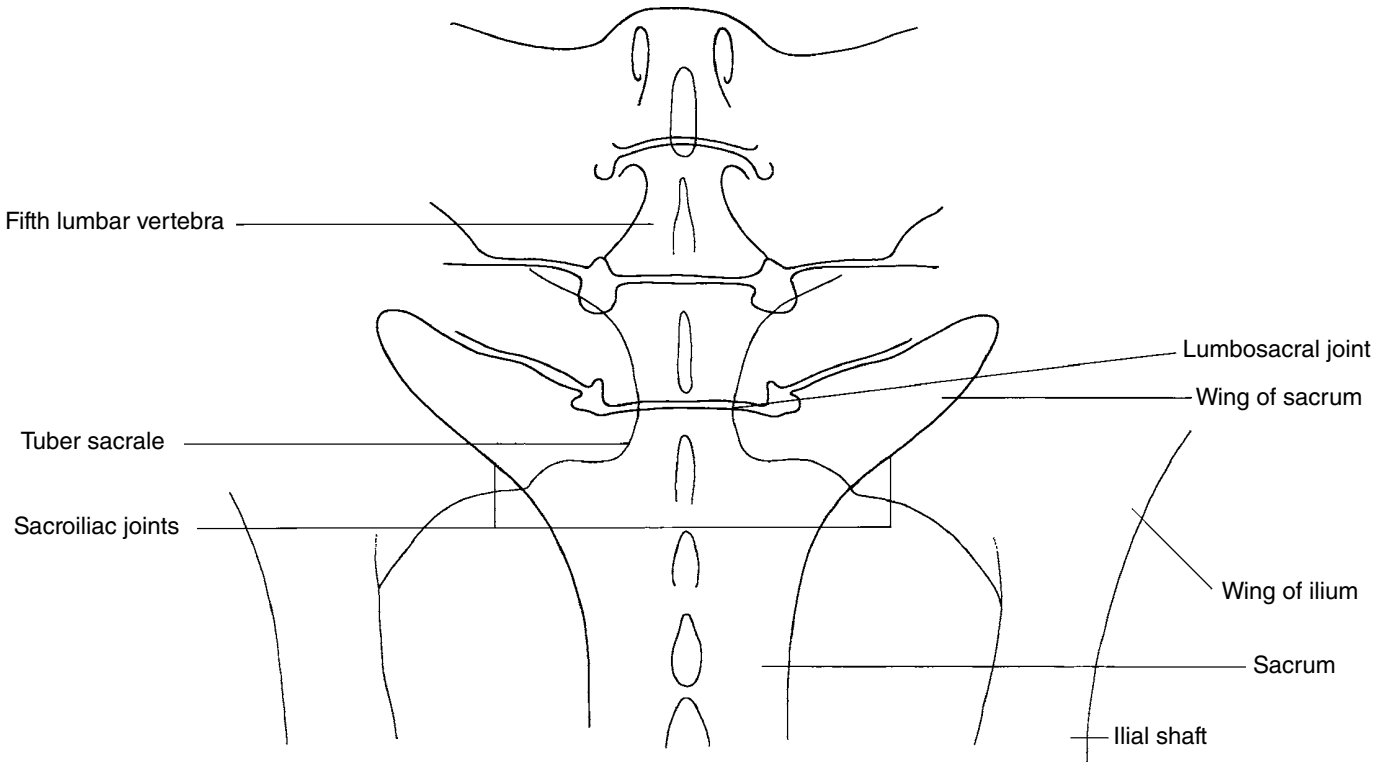


Figure 13.6(c) Radiograph (above) and diagram of a ventrodorsal image of the lumbosacral region of a normal adult horse. Cranial is to the top and left is to the right. Note the changing shape of the intercentral articulations of the lumbar vertebrae from cranially to caudally and the wider lumbosacral joint. The articulations between the transverse processes of the caudal lumbar vertebrae and the sacrum are well defined. The sacroiliac joint is less well defined on the left side due to superimposition of abdominal viscera.



Figure 13.6(d) Ventrodorsal image of the right iliac wing and shaft of a normal 4-year-old horse. Cranial is to the top. Note the incomplete fusion of the separate centre of ossification of the tuber coxae (arrow). The right sacroiliac joint is underexposed and therefore poorly defined.



Figure 13.6(e) Ventrodorsal image of a coxofemoral joint of a normal adult horse. Cranial is to the top. Note the slightly irregular margin of the cranial proximal aspect of the femur (arrow), which should not be confused with new bone formation.

In a standing horse acceptable images of the caudal aspect of the ilium and the ischium, the acetabulum and femoral head and neck can be obtained. Views of the obturator foramen are oblique compared with images obtained with the horse under general anaesthesia, resulting in foreshortening. Caudal abdominal contents are superimposed over the pubis, making evaluation difficult. Evaluation of the ilia and sacroiliac joints is impossible.

Skeletally mature horse: lateral 30° dorsal-lateroventral oblique views

In small standing horses, acceptable images of the ilial shaft, the coxofemoral joint, the greater trochanter of the femur, the femoral neck and the ischium can be obtained. Because of the obliquity of the x-ray beam they appear somewhat distorted (Figure 13.7). Knowledge of normal anatomy is essential, because in a horse that is unwilling to bear full weight on the lame limb, the radiographic images of the left and right sides will not be symmetrical. They are therefore not suitable for comparison to determine normality or abnormality.

SIGNIFICANT FINDINGS

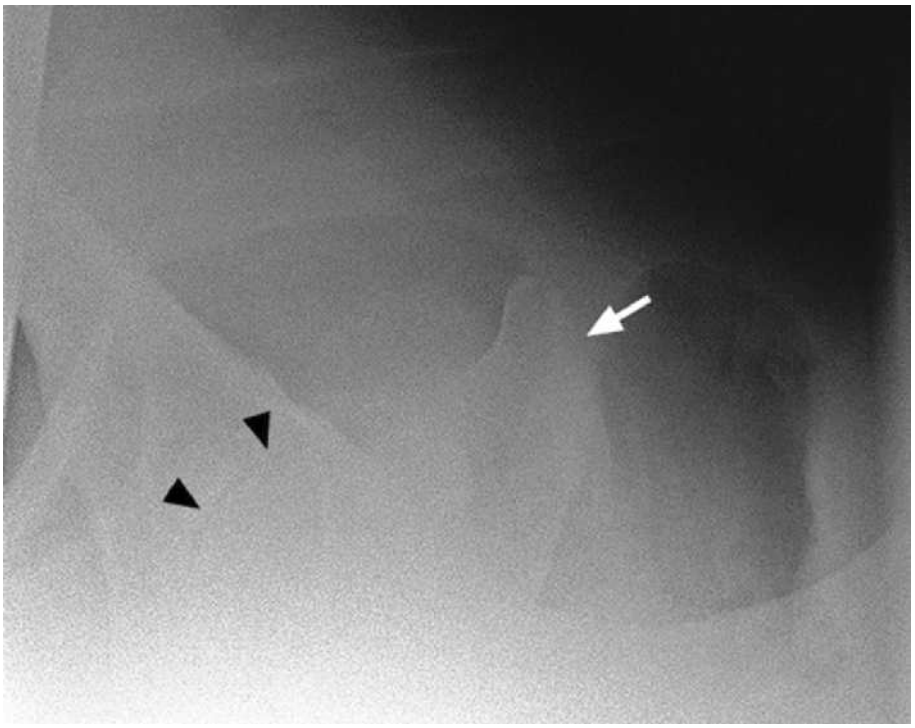
Hip dysplasia

Hip dysplasia occurs very infrequently. Radiographic evidence includes flattening of the acetabulum, deformation of the femoral head and neck, subluxation and secondary degenerative changes in the joint. Such changes can only be appreciated on radiographs obtained with the horse under general anaesthesia. Even then care must be taken when evaluating radiographs, since relatively small changes in the position of the horse, or angle of the x-ray beam, can cause artefacts, especially in the region of attachment of the ligament of the femoral head (teres ligament).

Subluxation of the coxofemoral joint

Subluxation of the coxofemoral joint has been described in association with malformation of the acetabulum and femoral head. Although the latter may be developmental in origin, it is also thought to occur secondarily to trauma and hip dysplasia (see above). The condition is characterised radiographically by flattening of the contour of the acetabulum and the femoral head, and an increase in the width of the joint space. These features can generally only be appreciated in radiographs obtained with the horse in dorsal recumbency under general anaesthesia.

Traumatically induced subluxation associated with partial tearing of the ligament of the femoral head (teres ligament) can be a challenge to identify because, in the frog-leg position in dorsal recumbency, or in lateral oblique views obtained in a standing horse loading the limb, the joint may appear to be in normal alignment. Subluxation can be demonstrated in dorsal recumbency by extending the limb. If chronic there is usually also evidence of



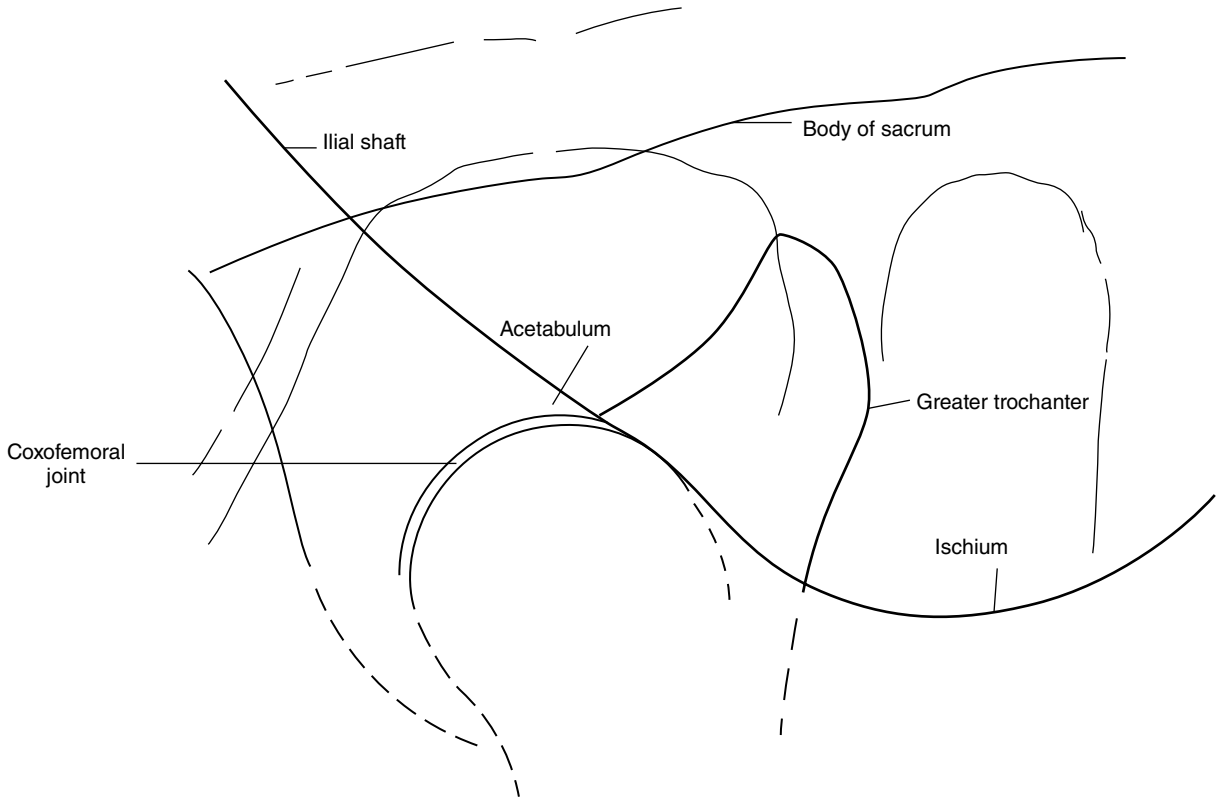


Figure 13.7 Lateral 30°dorsal-lateroventral oblique radiographic image and diagram of the pelvic region of a 3-year-old normal Thoroughbred. Cranial is to the left. The coxofemoral joint (arrowheads) and greater trochanter of the femur (arrow) can be identified. The ilial shaft extends to the left and the ischium to the right.

degenerative joint disease. There may be associated fracture(s). In a standing horse if the horse rests the limb then subluxation may be demonstrated. Transcutaneous ultrasonography is also useful for diagnosis.

Luxation of the coxofemoral joint

Luxation of the coxofemoral joint is rare and is usually the result of trauma with craniodorsal displacement of the femoral head. It can also be seen in association with multifocal stress fractures of the ilial shaft, pubis and ischium in young Thoroughbreds. It has been recognised in association with permanent upward fixation of the patella. Radiographically there is superimposition of the acetabulum and the femoral head. The radiographs should be inspected carefully for evidence of concurrent fractures of the femoral head and acetabulum. Luxation of the coxofemoral joint should be detectable on standing oblique views of the coxofemoral joint. The condition is characterised clinically by moderately severe to non-weight-bearing lameness, a tendency to abduct the stifle and foot, disparity in height of the hocks and dorsal displacement of the trochanter major of the femur. There is often audible and palpable crepitus. Ultrasonography may also be useful for diagnosis. Surgical treatment has been successful in some cases, but the prognosis is generally poor.

Infectious arthritis/osteomyelitis

Infectious arthritis and osteomyelitis complex occurs occasionally in the coxofemoral joint of young horses. It is characterised radiographically by widening of the joint space, and productive and destructive bone changes involving both the acetabulum and the femoral head. The proximal femoral physis may also be involved in type P osteomyelitis (see 'Infectious arthritis' in Chapter 1).

Degenerative joint disease

Degenerative joint disease of the coxofemoral joint is an unusual cause of lameness in the horse. In some cases it is secondary to hip dysplasia, an acetabular fracture or damage to the ligament of the head of the femur (teres ligament). Radiographic changes include: (a) modelling of the acetabulum, with osteophyte formation on the cranial and caudal margins (Figure 13.8); (b) flattening of the femoral head; (c) irregular width of joint space; (d) changes in subchondral bone opacity; (e) new bone formation on the neck of the femur.

Low-grade radiographic abnormalities are only detectable in radiographs obtained with the horse under general anaesthesia. More advanced radiographic abnormalities may be detectable in lateral 30° dorsal-lateroventral oblique radiographs obtained in a standing horse. Ultrasonography may permit the identification of thickening of the joint capsule, presence of an abnormal amount of fluid especially in the cranioventral recess of the joint capsule, and dorsal periarticular osteophytes. Nuclear scintigraphy may reveal increased radiopharmaceutical uptake, which may prompt more detailed radiographic examination.



Figure 13.8 Ventrodorsal image of the right coxofemoral joint of a 14-year-old part Thoroughbred with evidence of degenerative joint disease. Cranial is to the top. The cranial half of the acetabulum is poorly defined due to osteophyte formation (arrow) (compare with Figure 13.6e); there is also slight loss of definition of the caudal half of the acetabulum.

The prognosis for future athletic function is hopeless in mature animals, but some horses may be sound enough to be retired for breeding purposes.

Sacroiliac joint disease

The radiographic features associated with a chronic sacroiliac lesion are usually minimal or absent. Occasionally there may be increase of the width of the joint space (Figure 13.9), or asymmetry of the two joints. The relative positions of the tubera sacrale and the summits of the sacral spinous processes may be altered. In advanced cases, periarticular osteophytes near the most caudal margin of the joint can be seen, disrupting the relatively smooth caudal outline of the medial aspect of the wing of the ilium. It is not possible to demonstrate radiographic abnormalities in the majority of cases where clinical signs are suggestive of lameness or poor performance associated with the sacroiliac joints.

Linear tomography has shown potential for examining the lumbosacral region, including abnormalities of the sacroiliac joint. This equipment is only available at a very small number of clinics and therefore is not discussed further.

Nuclear scintigraphic examination may also be valuable; asymmetry of radiopharmaceutical uptake in the sacroiliac joint regions is not normal. However, sacroiliac joint region pain can occur without increased radiopharmaceutical uptake and asymmetry of the pelvic muscles may confound interpretation. Transrectal ultrasonography can give limited information about the caudal aspect of the joint space and reveal alteration in joint space width and bone contour.

The tubera sacrale are not easily examined radiographically, but ultrasonography may reveal altered bone contour reflecting enthesopathy and structural abnormalities of the dorsal sacroiliac ligament. These changes may or may not be associated with lameness.

Osseous cyst-like lesions

Osseous cyst-like lesions have been recorded in the femoral head and the acetabulum. There is insufficient information for any prognosis or treatment to be recommended.

Osteochondrosis

The coxofemoral joint is an unusual site for osteochondrosis. Radiographic abnormalities have been described in both the acetabulum and the femoral head, and include poorly defined lucent zones in the subchondral bone, with or without a surrounding rim of increased radiopacity. Circular lucent zones in the subchondral bone have been referred to as subchondral bone cysts, but there is little evidence to show whether these are true subchondral bone cysts. Modelling of the caudal aspect of the acetabulum without associated lucent zones in the subchondral bone has also been described. The prognosis for further athletic soundness is generally considered to be poor.



Figure 13.9 Ventrodorsal image of the sacrum and right ilial wing of a 5-year-old Arab with asymmetry of the tubera sacrale and right hindlimb lameness. Cranial is to the top. The right sacroiliac joint is abnormal in shape and widened irregularly (arrows). There is no evidence of new bone formation on the caudal aspect of the joint.

Osteochondroma of the pubis

There is considerable variation among horses in the osseous contours of the pubis. Osteochondroma of the pubis has been described as a cause of exercise-induced haematuria. Diagnosis of an osteochondroma of the pubis can be achieved by ultrasonographic examination performed per rectum.

Fractures

If a fracture of the pelvis is suspected, standing radiography may be useful in some cases. Percutaneous and transrectal ultrasonography may yield diagnostic information. If radiographs are to be obtained with the horse in dorsal recumbency, it is recommended that anaesthesia should be delayed for at least 6 weeks in order to avoid further displacement of the fracture during induction and recovery.

Although severe direct trauma is normally required to fracture the pelvis, 'spontaneous' fracture (often of the wing or shaft of the ilium) is a common stress-related bone injury in young Thoroughbred racehorses in training, and occasionally can result in complete fracture during exercise. Spontaneous fractures are more common in females. With the more routine use of nuclear scintigraphic evaluation combined with diagnostic ultrasonography, stress fractures have been detected earlier and the incidence of complete fractures has decreased. Stress fractures occur less commonly in the pubis.

The most common sites of fractures are the ilium (including the tuber coxae), acetabulum and ischium (Figure 13.10). As a general rule the prognosis is considerably worse if there is an articular component to the fracture (coxofemoral or sacroiliac), due to subsequent secondary degenerative joint disease.

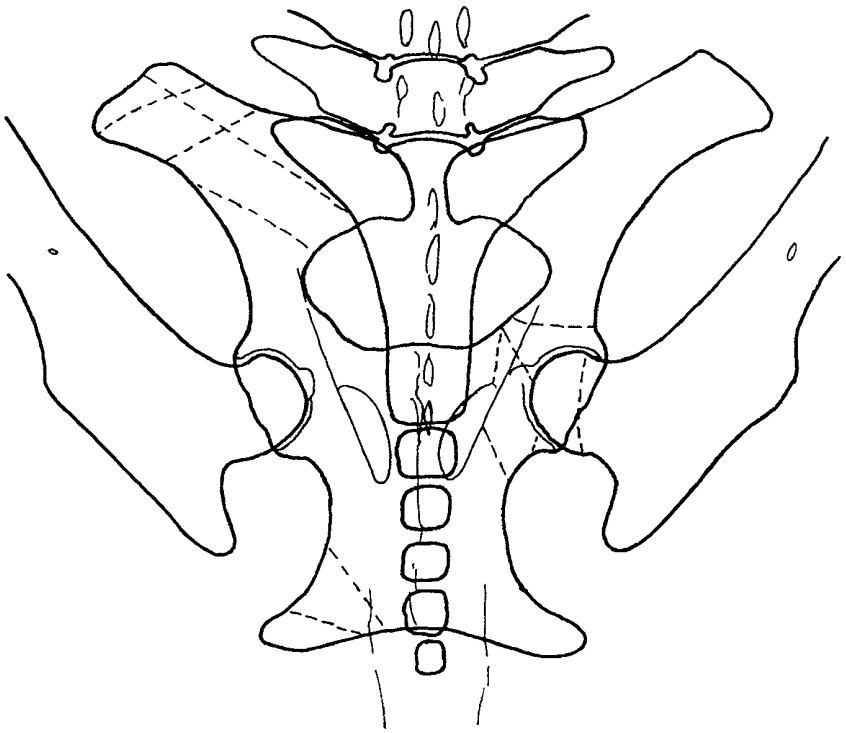


Figure 13.10 Common fracture sites of the pelvis. Compare with the position of the symphyses of the immature horse in Figure 13.5. See also Little and Hilbert (1987), Rutowski and Richardson (1989), Pilsworth et al. (1994), Anderson et al. (2008), Dabareiner and Cole (2009) and Hennessy et al. (2013).

Fractures of the ilium

Fractures of the tuber coxae alone are recognised by a slight palpable irregularity of the external angle of the ilium, and seldom require radiography for diagnosis. On radiographs the tuber coxae appears blunted but the displaced fragment may not be visible. These fractures have a good prognosis. Oblique radiographic views of the affected tuber coxae can be obtained in a standing horse, but ultrasonography is generally easier and equally informative. A lateral 50° dorsal-lateroventral oblique view can be obtained, with the x-ray machine positioned on the opposite side to the injured limb, and the x-ray beam centered several centimetres from the dorsal midline towards the side of the injury. Ideally the horse should bear weight on the injured limb and rest the contralateral limb, thereby tilting the pelvis. The imaging plate is positioned as near to right angles to the x-ray beam as possible, ventral to the tuber coxae under examination.

Complete fractures of the ilial wing frequently extend obliquely in a craniocaudal direction. There is often displacement due to the action of the muscle masses that attach to the tuber coxae. Large fissures which frequently ramify towards the centre of the wing (Figure 13.11) can occur with minimal

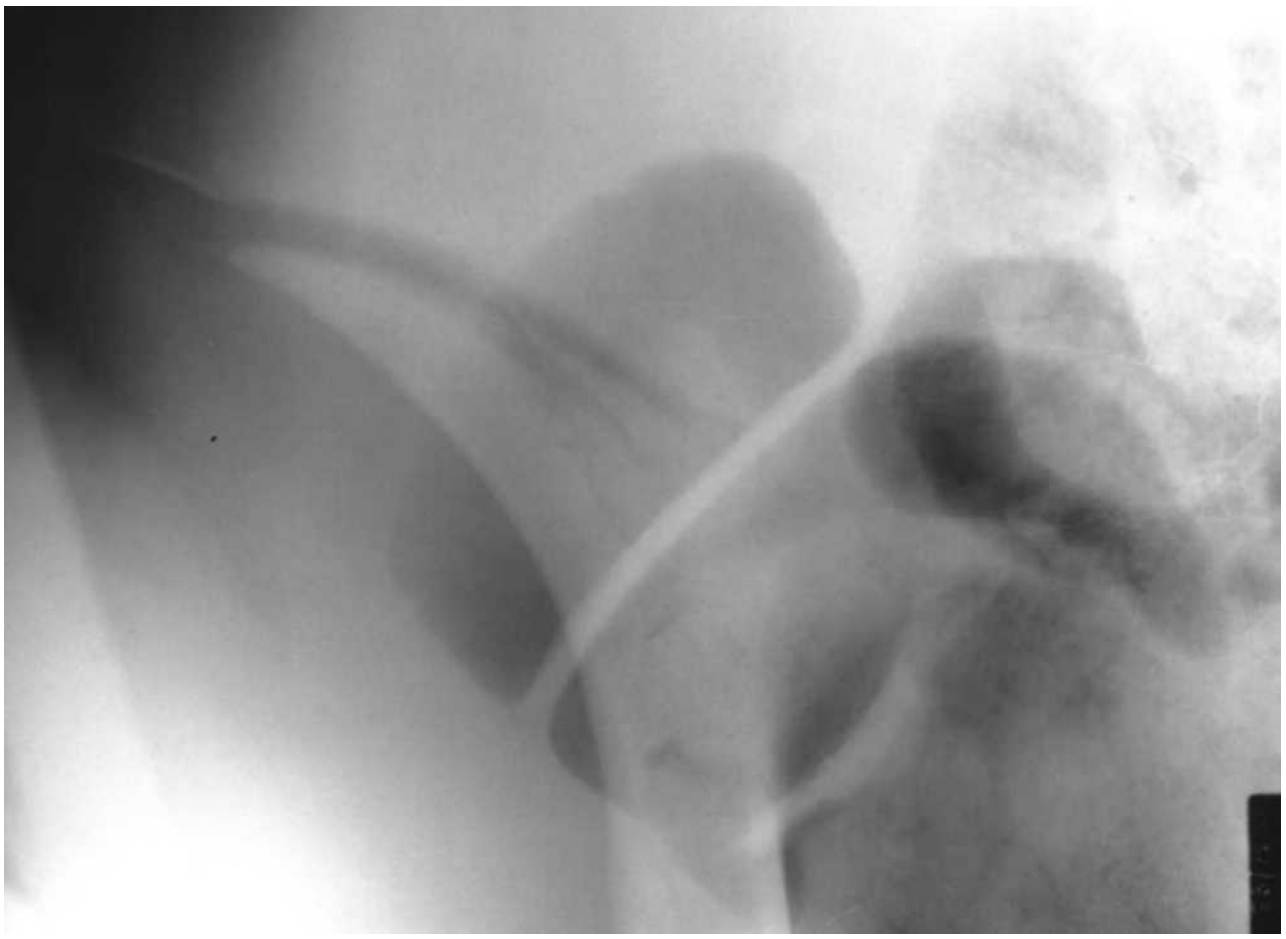


Figure 13.11 Ventrodorsal image of the right ilium of a 2-year-old Thoroughbred mare with a history of acute onset severe right hindlimb lameness after work 6 weeks previously. Cranial is to the top. There is a displaced fracture of the right ilial wing, ramifying towards the ilial shaft. There is no bony union. The right sacroiliac joint is obscured by superimposed abdominal viscera. The radiograph was obtained using an aluminium wedge filter.

displacement of the ilium. These may extend towards and sometimes involve the sacroiliac joint. Such fractures can usually be demonstrated using transcutaneous diagnostic ultrasonography.

Incomplete fractures have a good prognosis. Complete fractures of the ilial wing alone carry a fair prognosis if there is osseous union, but fibrous union accompanied by continual lameness may occur. If the fractures involve the sacroiliac joint, the prognosis is guarded to poor.

Stress fractures of the ilial shaft in young Thoroughbreds are less common than ilial wing stress fractures and are sometimes scintigraphically silent or associated with only mildly increased radiopharmaceutical uptake. If a fracture becomes complete then diagnosis may be possible using lateral 30° dorsal-lateroventral oblique radiographic views obtained in a standing horse. Such fractures may also occur as a result of a fall. Fractures of the shaft of the ilium may be articular (see below). The prognosis is poor.

Fractures involving the coxofemoral joint

Fractures of the bones comprising the acetabulum are frequently accompanied by deformation of the ipsilateral side of the pelvis due to the severity of the initiating trauma. It must be borne in mind that the large forces required to create a fracture may result in multifocal fractures and identification of all the fractures may be important for prognosis. The most common site is at or close to the symphysis between the ilium and pubis. Some fractures are difficult to detect in lateral oblique radiographs in a standing horse, but may be detectable by transrectal ultrasonography, or in ventrodorsal radiographs obtained under general anaesthesia. In a study comparing standing radiography and ultrasonography in Warmblood horses, radiography was superior to ultrasonography for the detection of acetabular fractures. If the fracture involves only a small part of the acetabulum in a skeletally immature horse, satisfactory modelling of the joint may occur without radiographic evidence of degenerative joint disease. Such an animal may be capable of an athletic career. If large parts of the acetabular surface are involved, particularly in a skeletally mature animal, and/or articular incongruity exists, secondary degenerative joint disease is inevitable. This may be recognised radiographically within 4–5 weeks.

Fractures of the proximal femoral physis occasionally occur in foals. If a complete Salter-Harris type 1 fracture occurs, this may result in displacement of the femoral head (Figure 13.12). Internal fixation may be attempted, but with a very guarded prognosis. Secondary degenerative changes may ensue. Fracture of the femoral head may follow severe trauma in an adult. The prognosis is hopeless. Fracture of the greater trochanter of the femur is a rare injury and diagnosis is usually made using nuclear scintigraphy and ultrasonography.

If there is marked deformation of the pelvis, even without articular involvement, changes in apposition of the joint surfaces of the coxofemoral or sacroiliac joints may result in a change in gait or lameness.

Fracture of the ischium

The acetabular branch of the ischium is frequently involved in fractures of the acetabulum (see above). Fractures of the tuber ischii occur separately and are often related either to direct trauma or to the distracting



Figure 13.12 Ventrodorsal image of a coxofemoral joint of a yearling Thoroughbred with lameness of approximately 2½ months' duration. Cranial is to the top. There is a displaced fracture of the femoral head through the physis (Salter-Harris type 1) with secondary changes in the femoral head and degenerative joint disease. Note the increased opacity of the femoral head adjacent to the physis.

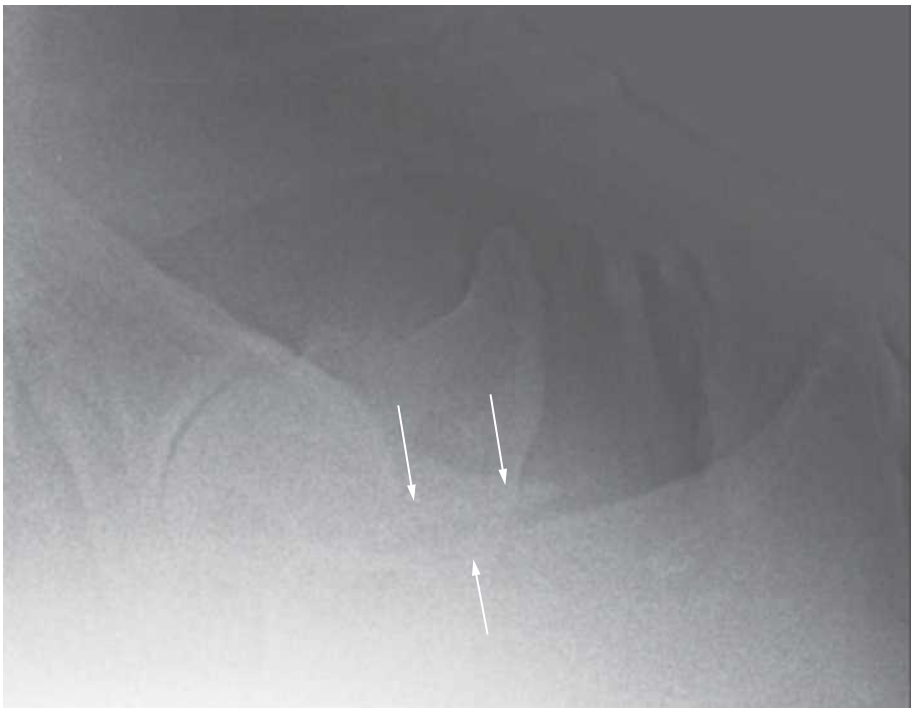


Figure 13.13(a) Lateral 30°dorsal-lateroventral oblique radiographic image of a 2-year-old Thoroughbred flat racehorse with acute onset of right hindlimb lameness. Cranial is to the left. There is a displaced fracture of the cranial aspect of the ischium (arrows).

effect of the semitendinosus and semimembranosus muscles, which originate on the ventral surface of this bone. There is often slight displacement of the most peripheral 5–7 cm of the tuber ischii. The prognosis for this fracture is usually good, the majority responding satisfactorily to 3–6 months of rest. Osseous healing with slight deformation of the tuber usually occurs, although occasionally lameness resolves despite lack of bony union. Non-union fractures with continual lameness rarely occur. Sequestration with sinus discharge occasionally occurs. A fracture of the tuber ischii is usually detectable using nuclear scintigraphy and ultrasonography, but can be confirmed radiographically. Increased radiopharmaceutical uptake is not synonymous with a recent injury, because after a previous fracture increased radiopharmaceutical uptake may persist long term.

Less commonly, a fracture of the body of the ischium occurs, usually the result of a fall when jumping at speed. Such fractures are usually complete and displaced and can be detected in lateral oblique radiographs of the ischium obtained in a standing horse (Figures 13.13a and 13.13b).

Femur

RADIOGRAPHIC TECHNIQUE

Equipment

The proximal two-thirds of the femur are best radiographed with the horse under general anaesthesia. It is not easy to obtain more than one view with the horse in a single position. High-output x-ray equipment and digital systems or fast rare earth screens are essential, and a grid is beneficial, because

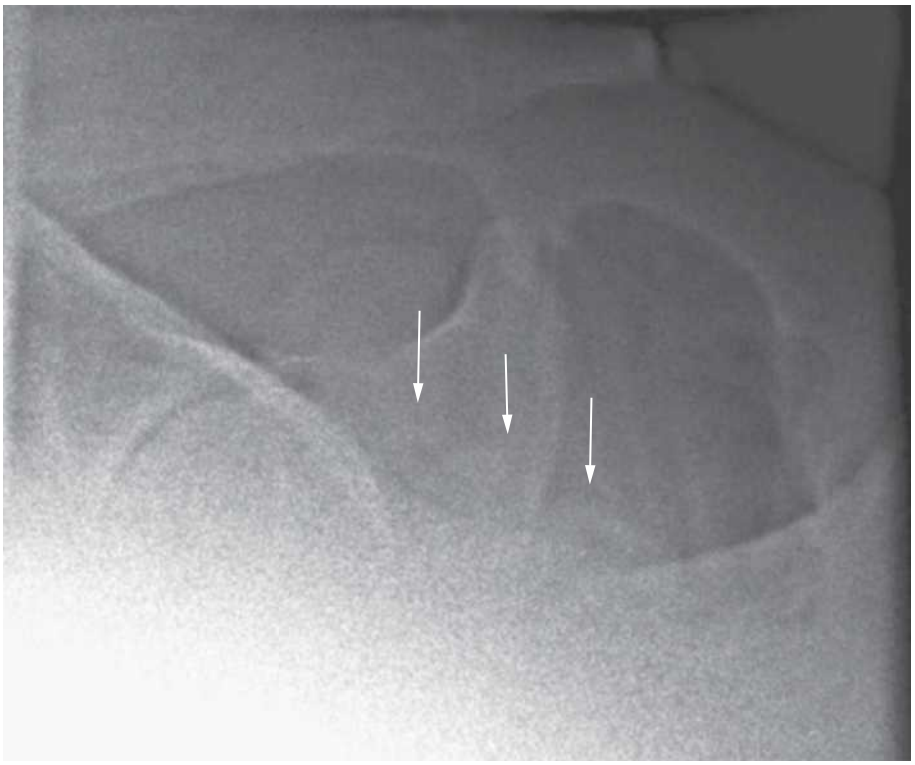


Figure 13.13(b) Lateral 30°dorsal-lateroventral oblique radiographic image of the same horse as in Figure 13.13(a), obtained 6 weeks later. Cranial is to the left. There is extensive callus bridging the fracture site (arrows).

of the large muscle mass which must be penetrated. The third trochanter of the femur can be examined in a standing horse.

Positioning

A craniolateral-caudomedial oblique view is the easiest to obtain. The horse is positioned in dorsal recumbency, tipped towards the limb to be examined, as described for radiography of the coxofemoral joint (see 'Pelvis – Radiographic technique – Positioning'). It is usually necessary in an adult horse to obtain more than one radiograph in order to assess the entire length of the femur. It is difficult to obtain other projections, but this can be done by adjusting the position of the horse and limb.

An alternative technique is to place the horse in lateral recumbency, lying on the limb to be examined. This limb is then extended caudally and the contralateral limb extended cranially. This technique does not give such good results for the most proximal aspect of the femur.

The distal one-third of the femur may be radiographed using the same techniques as for the stifle joint (see 'Stifle – Radiographic technique' in Chapter 10) and caudocranial, lateromedial and oblique views are readily obtained either with the horse standing or under general anaesthesia.

RADIOGRAPHIC ANATOMY

For details of the anatomy of the proximal and distal aspects of the femur, the reader is referred to the coxofemoral joint (see above) and the stifle joint (see Chapter 10).

The proximal aspect of the femur has separate centres of ossification for the femoral head, the trochanter major and the trochanter minor. The physis of the femoral head closes between 24 and 36 months, and the trochanter major fuses with the femoral shaft between 18 and 30 months. Fusion of the trochanter minor is less consistent, usually occurring at about 2 years of age.

The distal femoral physis is wavy and irregular in outline, closing at 24–30 months of age. The greater and lesser trochanters and the third trochanter of the femur are readily seen in a craniolateral-caudomedial oblique view.

RADIOGRAPHIC ABNORMALITIES

Enostosis-like lesions

The femur is a rare site for enostosis-like lesions, but associated lameness has been described and the lesion verified post mortem. Radiographically the lesion was a well-circumscribed opacity in the medulla of the femoral diaphysis.

Fractures of the femur

Fractures involving the proximal and distal epiphyses are discussed in conjunction with the coxofemoral joint (see 'Pelvis – Significant findings – Fractures', above) and the stifle joint (see Chapter 10, 'Stifle – Significant findings – Fractures').

Diaphyseal fractures of the femur

Diaphyseal fractures are relatively uncommon and result in a non-weight-bearing lameness. In immature or small horses it may be possible to detect crepitus, but in adult horses this may be concealed by the large muscle mass and soft-tissue swelling. In young horses the fractures are usually simple and oblique, but in adults the fractures are generally comminuted. There is often considerable overriding of the fracture fragments. Surgical repair of simple diaphyseal fractures may be attempted in foals, provided that the nutrient foramen is not involved. In older horses the prognosis is extremely poor.

Fracture of the greater trochanter of the femur

Fracture of the greater trochanter of the femur is an unusual cause of lameness. There may be localised soft-tissue swelling, but in well-muscled horses it may not be possible to localise clinical signs. Nuclear scintigraphy is helpful for diagnosis and may indicate that there is cranial displacement of the proximal fragment. The fracture can be confirmed using both ultrasonography and radiography in a standing horse. Fracture occurs through the physis of the greater trochanter in young horses. The prognosis with conservative management is guarded.

Fracture of the third trochanter

Fracture of the third trochanter of the femur occasionally occurs (Figure 13.14). There may be acute onset of severe lameness, which rapidly



Figure 13.14 Caudocranial image of a femur of an 8-year-old advanced event horse, with acute-onset hindlimb lameness of 2 weeks' duration, after being cast. There is a fracture of the third trochanter of the femur (arrows). The horse made a complete recovery.

improves to a moderate to mild lameness. There may be palpable crepitus, although this may be difficult to detect in a well-muscled horse. Nuclear scintigraphic examination may help to identify such fractures. Increased radiopharmaceutical uptake in the third trochanter of the femur could also be the result of entheseous trauma. Differentiation is usually possible using ultrasonography. Fractures may be demonstrated radiographically in a standing horse using a cranial 25° lateral-caudomedial oblique view. Although some fractures heal only by fibrous union, most horses are able to return to full athletic function.

FURTHER READING

Amitrano, F., Gutierrez-Nibeyro, S., Joslyn, S. (2014) Radiographic diagnosis of craniodorsal coxofemoral luxation in standing equids. *Equine Vet. Educ*. doi:10.1111/eve 12156

Anderson, J., Galuppo. L., Barr, B., et al. (2008) Clinical and scintigraphic findings in horses with a bone fragility disorder: 16 cases (1980–2006). *J. Am. Vet. Med. Ass.* **232**, 1694–1699

Barr, A. (2013) Diaphyseal femoral fractures in young horses. *Equine Vet. Educ.* **26**, 32–33

Barrett, E., Talbot, A., Driver, A., et al. (2006) A technique for pelvic radiography in the standing horse. *Equine Vet. J.*, **38**, 266–270

Barstow, A., Dyson, S. (2015) Clinical features and diagnosis of sacroiliac joint region pain in 296 horses: 2004–2014. *Equine Vet. Educ*. **27**, 637–647

Beccati, F., Pepe, M., Nannarone, S., et al. (2012) Apophyseal avulsion fracture of the greater trochanter of the femur in a Thoroughbred filly. *Vet. Comp. Orthop. Traumatol.* **25**, 342–347

Bennet, D., Campbell, J., Rawlinson, J. (1977) Coxofemoral luxation complicated by upward fixation of the patella in the pony. *Equine Vet. J.* **9**, 192–194

Bertoni, L., Seignour, M., de Mira, M., et al. (2013) Fractures of the third trochanter in horses: 8 cases. *J. Am. Vet. Med. Ass.* **243**, 261–266

Brenner, S., Whitcomb, M. (2009) Ultrasonographic diagnosis of coxofemoral subluxation in horses. *Vet. Radiol. Ultrasound* **50**, 423–428

Dabareiner, R., Cole, R. (2009) Fractures of the tuber coxae of the ilium in horses: 29 cases (1996–2007). *J. Am. Vet. Med. Ass*. **234**, 1303–1307

Dalin, G., Jeffcott, J. (1986) Sacroiliac joint of the horse: 1. Gross morphology. *Anat. Histol. Embryol.* **15**, 80–94

Dalin, G., Jeffcott, J. (1986) Sacroiliac joint of the horse: 2. Morphometric features. *Anat. Histol. Embryol.* **15**, 97–107

Davenport-Goodall, C., Ross, M. (2004) Scintigraphic abnormalities of the pelvic region in horses examined because of lameness or poor performance: 128 cases (1993–2000). *J. Am. Vet. Med. Ass.* **224**, 88–95

Davison, P. (1967) A case of coxofemoral subluxation in a Welsh pony. *Vet. Rec.* **80**, 441–443

Driver, A., Nagy, A. (2008) Fracture of the ischium in an eight-year-old Arabian gelding: a diagnostic challenge. *Equine Vet. Educ.* **20**, 127–130

Dyson, S., Murray, R., Branch, M., et al. (2003) The sacroiliac joints: evaluation using nuclear scintigraphy. Part 1: The normal horse. *Equine Vet. J.* **35**, 226–232

Dyson, S., Murray, R., Branch, M., Harding, E. (2003) The sacroiliac joints: evaluation using nuclear scintigraphy. Part 2: lame horses. *Equine Vet. J.* **35**, 233–239

Garcia-Lopez, J., Boudrieau, R., Provost, P. (2001) Surgical repair of coxofemoral joint luxation in a horse. *J. Am. Vet. Med. Ass.* **219**, 1254–1258

Garcia-Lopez, J. (2010) Coxofemoral luxations in the horse: surgical options and challenges. *Equine Vet. Educ.* **22**, 554–556

Geburek, F., Rotting, A., Stadler, P. (2009) Comparison of the diagnostic value of ultrasonography and standing radiography for pelvic-femoral disorders in horses. *Vet. Surg.* **38**, 310–317

Gorgas, D., Kircher, P., Doherr, M., et al. (2007) Radiographic technique and anatomy of the equine sacroiliac region. *Vet. Radiol. Ultrasound* **48**, 501–506

Hance, S.R., Bramlage, L.R., Schneider, R.K., Embertson, R.M. (1992) Retrospective study of 38 cases of femur fractures in horses less than one year of age. *Equine Vet. J.* **24**, 357–363

Haussler, K., Stover, S., Willits, N. (1997) Developmental variation in lumbosacropelvic anatomy of Thoroughbred horses. *Am. J. Vet. Res.* **58**, 1083–1091

Haussler, K., Stover, S. (1998) Stress fractures of the vertebral lamina and pelvis in Thoroughbred racehorses. *Equine Vet. J.* **30**, 374–383

Hennessy, S., Muurlink, M., Anderson, G., et al. (2013) Effect of displaced versus non-displaced pelvic fractures on long-term racing performance in 31 Thoroughbred racehorses. *Austr. Vet. J.* **91**, 246–250

Hesse, K., Verheyen, K. (2010) Associations between physiotherapy findings and subsequent diagnosis of pelvic or hindlimb fracture in racing Thoroughbreds. *Equine Vet. J.* **43**, 234–239

Huggons, N., Andrea, R., Grant, B., Duncan, C. (2010) Total hip arthroplasty in the horse: overview, technical considerations and case report. *Equine Vet. Educ.* **22**, 547–553

Hunt, D.A., Snyder, J.R., Morgan, J.P., et al. (1990) Femoral capital physeal fractures in 25 foals. *Vet. Surg.* **19**, 41–49

Jeffcott, L.B. (1982) Pelvic lameness in the horse. *Equine Pract.* **4**, 21–47

Jeffcott, L.B. (1983) Technique of linear tomography for the pelvic region of the horse. *Vet. Radiol.* **24**, 194–200

Jeffcott, L.B. (1983) Radiographic appearance of equine lumbosacral and pelvic abnormalities by linear tomography. *Vet. Radiol.* **24**, 201–213

Kuemmerle, J., Furst, A. (2011) Treatment of a coxofemoral luxation in a pony using a prosthetic capsule technique. *Vet. Surg.* **40**, 631–635

Little, C., Hilbert, B. (1987) Pelvic fractures in horses: 19 cases. *J. Am. Vet. Med. Ass.* **190**, 1203–1205

Mahne, A., Marais, H., Rubio-Martinez, L., Williams, J. (2012) Severe hindlimb lameness and pathological femur fracture in a horse secondary to haemangiosarcoma. *Equine Vet. Educ*. doi:10.1111/j.2042-3292.2012.00442.x

May, S., Patterson, J., Peacock, J., Edwards, G. (1991) Radiographic technique for the pelvis in the standing horse. *Equine Vet. J.* **23**, 312–314

Miller, C., Todhunter, R. (1987) Acetabular osteochondrosis dissecans in a foal. *Cornell Vet.* **77**, 75–83

Nagy, A., Dyson, S., Barr, A. (2010) Ultrasonographic findings in the lumbosacral joint of 43 horses with no clinical signs indicative of back pain or hindlimb lameness. *Vet. Radiol. Ultrasound* **51**, 533–539

Nixon, A., Adams, R., Teigland, M. (1988) Subchondral cystic lesions (osteochondrosis) of the femoral heads in a horse. *J. Am. Vet. Med. Ass.* **192**, 360–362

Pilsworth, R.C., Shepherd, M.C., Herinckx, B.M.B., Holmes, M.A. (1994) Fracture of the wing of the ilium, adjacent to the sacroiliac joint in Thoroughbred racehorses. *Equine Vet. J.* **26**, 94–99

Roneus, B., Svanholm, R., Carlson, J. (1987) Diagnostik, etiologi och prognos vid skadar i backenregionen hos häster. *Svensk Veterinärtidning* **39**, 315–323

Rebsamen, E., Geyer, H., Furst, A., et al. (2012) Haematuria in two geldings caused by osteochondroma of the os pubis: case reports and anatomic study of the os pubis. *Equine Vet. Educ.* **24**, 30–37

Rose, J., Rose, E., Smylie, D. (1981) Case history: acetabular osteochondrosis in a yearling thoroughbred. *Equine Vet. Surg.* **1**, 173–174

Rottensteiner, U., Palm, F., Kofler, J. (2012) Ultrasonographic evaluation of the coxofemoral joint region in young foals. *Vet. J.* **191**, 193–198

Rutowski, J., Richardson, D. (1989) A retrospective study of 100 pelvic fractures in horses. *Equine Vet. J.* **21**, 256–259

Skidell, J. (1987) Backenfractur hos häst – en litteratursammanstallning och beskrivning av 33 fall. *Svensk Veterinärtidning* **39**, 326–333

Smyth, G., Taylor, G. (1992) Stabilization of a proximal femoral physeal fracture in a filly by use of cancellous bone screws. *J. Am. Vet. Med. Ass.* **210**, 895–898

Speitz, V.C., Wrigley, R. (1979) A case of bilateral hip dysplasia in a foal. *Equine Vet. J*, **11**, 202–204

Stecher, R., Goss, L. (1961) Ankylosing lesions of the spine of the horse. *J. Am. Vet. Med. Ass.* **138**, 248–255

Stubbs, N., Riggs, C., Hodges, P., et al. (2010) Osseous spinal pathology and epaxial muscle ultrasonography in Thoroughbred racehorses. *Equine Vet. J.* **42** (Suppl 38), 654–661

Stieger-Vanegas, S., Kippenes-Skogmo, H., Nilsson, E. (2009) Imaging diagnosis – Enostosis-like lesion in the femur of a horse. *Vet, Radiol. Ultrasound* **50**, 509–512

Swor, T., Schneider, R., Ross, M., Hammer, E., Tucker, R. (2001) Injury to the origin of the gastrocnemius muscle as a possible cause of lameness in four horses. *J. Am. Vet. Med. Ass.* **219**, 215–219

Trump, M., Kircher, P., Furst, A. (2011) The use of computed tomography in the diagnosis of pelvic fractures involving the acetabulum in two fillies. *Vet. Comp. Orthop. Traumatol.* **24**, 68–71

Turner, A., Milne, D., Hohn, R., Rouse, G. (1979) Surgical repair of fractured capital epiphysis in three foals. *J. Am. Vet. Med. Ass.*, **175**, 1198–1202

Walker, W., Werpy, N., Goodrich, L. (2012) Procedure for the transrectal and transcutaneous ultrasonographic diagnosis of pelvic fractures in the horse. *J. Equine Vet. Sci.* **32**, 222–230

Whitcomb, M., Vaughan, B., Katzman, S., Hersman, J. (2016) Ultrasound-guided injections in horses with cranioventral distension of the coxofemoral joint capsule: feasibility for a cranioventral approach. *Vet. Radiol. Ultrasound* doi:10.1111/vru.12323

Chapter 14
The thorax

RADIOGRAPHIC TECHNIQUE

Equipment

Complete radiographic examination of the thorax of adult horses is only possible with high output x-ray units. Although advances in digital image processing have reduced the dependency on grids or Bucky systems, highest image quality is achieved with a grid and digital image processing. If conventional film–screen combinations are being used, then fast film–screen combinations are essential. A 10: 1 ratio grid (or suitable equivalent for digital systems) is recommended. If a grid is not available the effects of scattered radiation can be reduced by leaving an air gap between the patient and the cassette. This technique should be avoided whenever possible because of the increased parallax and magnification that occurs. A short exposure time is required, usually timed to coincide with full inspiration, to minimise movement blur.

Large cassettes/digital imaging plates (35 cm × 43 cm) are required to achieve complete imaging of the entire adult equine thorax. Usually four images are required, to provide complete coverage of the thorax, and to include recognisable anatomical reference points in all images. The use of digital radiography can make assessment of lung opacity more difficult than when using conventional film, because digital image processing systems vary among manufacturers and result in a variable appearance of pulmonary parenchyma. The ability to alter brightness and contrast when viewing acquired images can also inadvertently override the correct image appearance. Care should be taken by the viewer to adjust to each system's appearance prior to the interpretation of thoracic radiographs, particularly when assessing pulmonary opacities.

Positioning

Depending on their size, young foals can occasionally be radiographed in lateral and dorsal recumbency by placing them on a cassette and grid on the floor, or by using a machine with an x-ray table incorporating a Bucky grid.

An adult horse should be radiographed standing, positioned with the forelimbs slightly forward in order to decrease the amount of muscle mass over the cranial aspect of the thorax. The radiographs should be obtained at full inspiration (see 'Normal anatomy – Mature horse', below). Expiratory radiographs are of value for comparison with inspiratory radiographs to

Clinical Radiology of the Horse, Fourth Edition. Janet A. Butler, Christopher M. Colles, Sue J. Dyson, Svend E. Kold and Paul W. Poulos.
© 2017 John Wiley & Sons, Ltd. Published 2017 by John Wiley & Sons, Ltd.
Companion website: www.clinical-radiology-horse.com

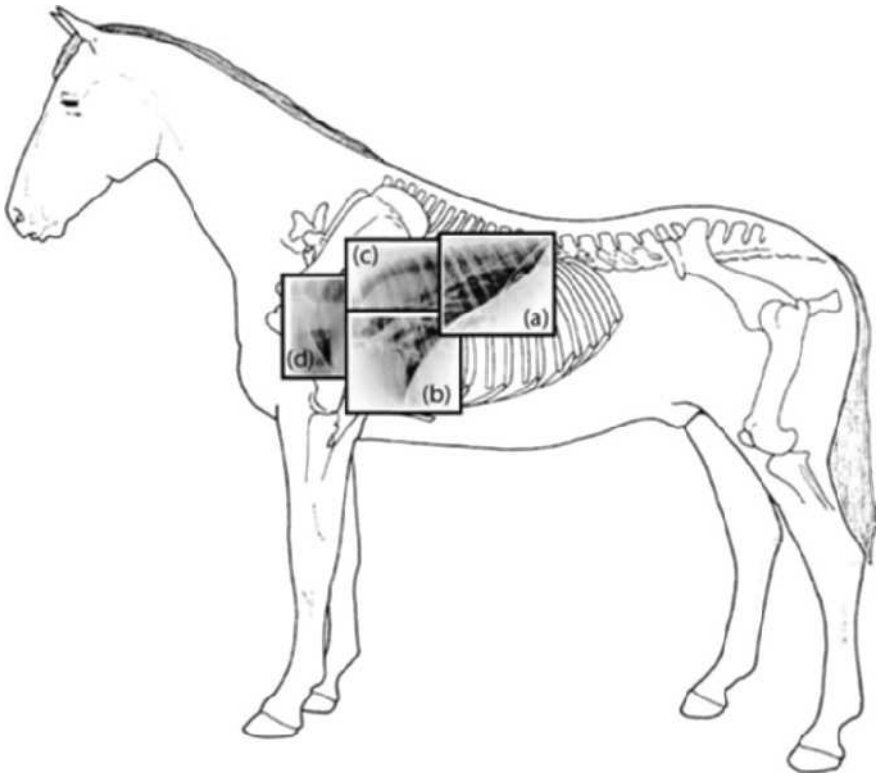


Figure 14.1 Placement of cassettes for the four overlapping views of the thorax.

assess the effect of respiration on tracheal diameter, or for evaluation of obstructive lung disease. It is recommended that four large (35 cm × 43 cm) lateral-lateral radiographs of the thorax be obtained with overlap of the fields (Figure 14.1): (a) dorsocaudal, (b) ventrocaudal, (c) dorsocranial and (d) ventrocranial (Figures 14.1a–d). Fields (a) and (b) can be acquired with large mobile units, but fields (c) and (d) usually require larger equipment in order to penetrate the greater muscle mass in this area. The entire thorax may sometimes be evaluated on one or two radiographs in foals (Figure 14.2), ponies and small horses (Figures 14.3a and 14.3b).

In order to compensate for parallax and magnification, views (a) and (b) should be obtained with the right side (right lateral projection) and then the left side (left lateral projection) of the thorax next to the cassette. Parallax and magnification are major problems in evaluation of the equine thorax, but they can be used to advantage by utilising the changes in position, size and image sharpness to determine the location of the lesion (left side versus right side). Structures close to the cassette will be well-demarcated and have sharp margins, whereas those away from the cassette will be magnified and less distinct due to the larger object–film distance (Figures 14.4a and 14.4b). It is recommended that if possible thoracic radiographs be obtained using a focal-film distance of at least 100–120 cm.

Examination of neonates or miniature horses in lateral recumbency should include both right and left lateral-lateral recumbent views. Ventrodorsal views should be obtained when possible. When obtaining recumbent lateral-lateral radiographs, care must be exercised not to extend the forelimbs excessively as this will cause the chest to rotate and a true lateral-lateral radiograph will not be acquired.

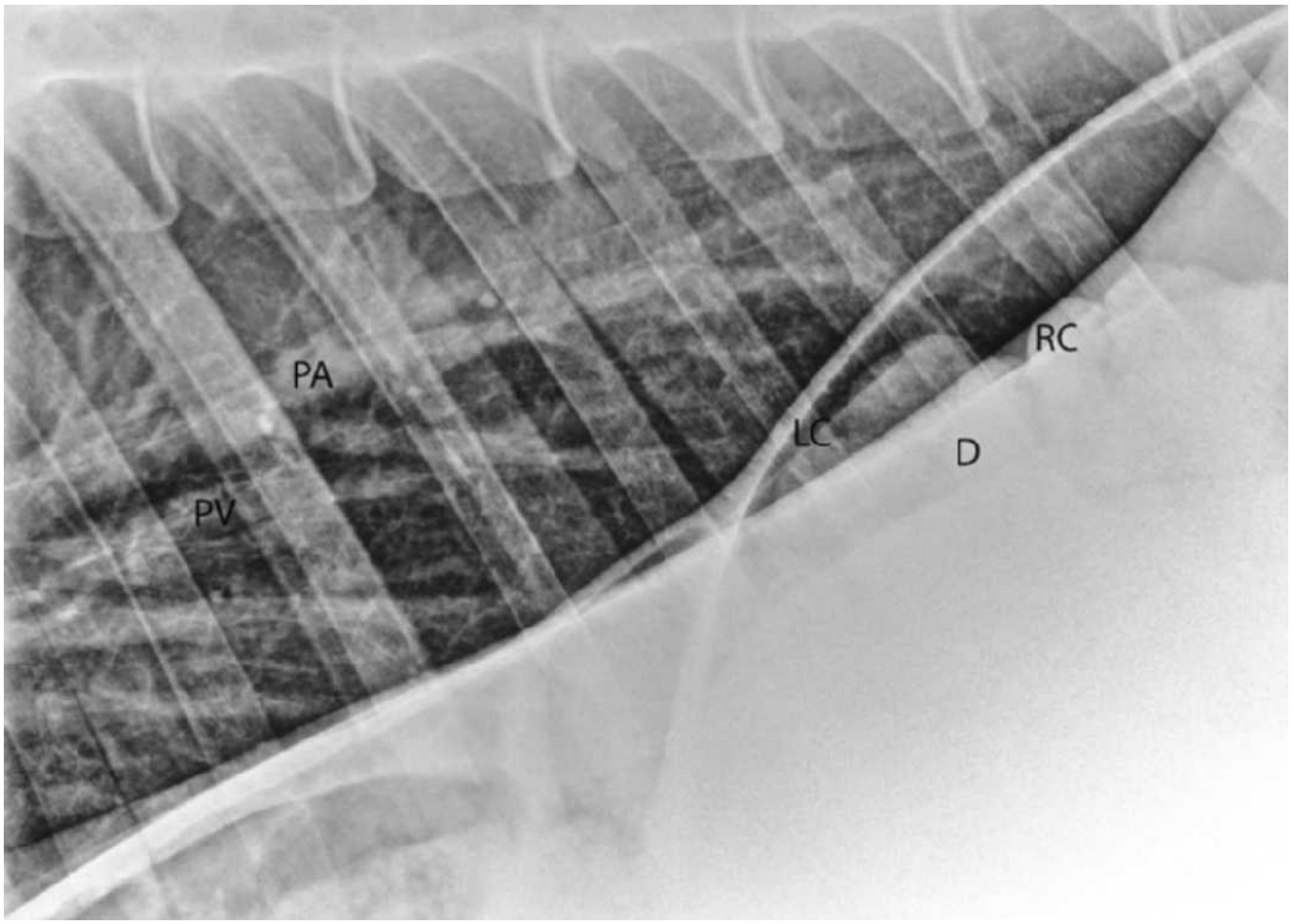


Figure 14.1(a) Dorsocaudal portion of the thorax of a normal adult horse. Cranial is to the left. The branching pulmonary arteries (PA) and pulmonary veins (PV) pass dorsocaudad. The diaphragm (D) is separated into the left crus (LC) which overlies the major portion of the gastric gas cap which is also partially seen below the right crus (RC).

Other imaging techniques

Nuclear scintigraphy

Nuclear scintigraphy of the thorax is a useful adjunctive technique to provide a functional assessment of the thoracic anatomy and pulmonary parenchyma when coupled with radiography. This technique has been utilised for the evaluation of diseases such as recurrent airway obstruction (RAO) and exercise-induced pulmonary haemorrhage (EIPH) or diseases with ventilation perfusion (V/Q) mismatch (see below). Nuclear scintigraphy requires special equipment, radiopharmaceuticals, and licensing, in addition to trained personnel, to be of maximum value.

Ultrasonography

Ultrasonography is complementary to radiography for the complete assessment of intra-thoracic disease. The method of image generation along with the greater availability, economy and safety of ultrasonography make it more

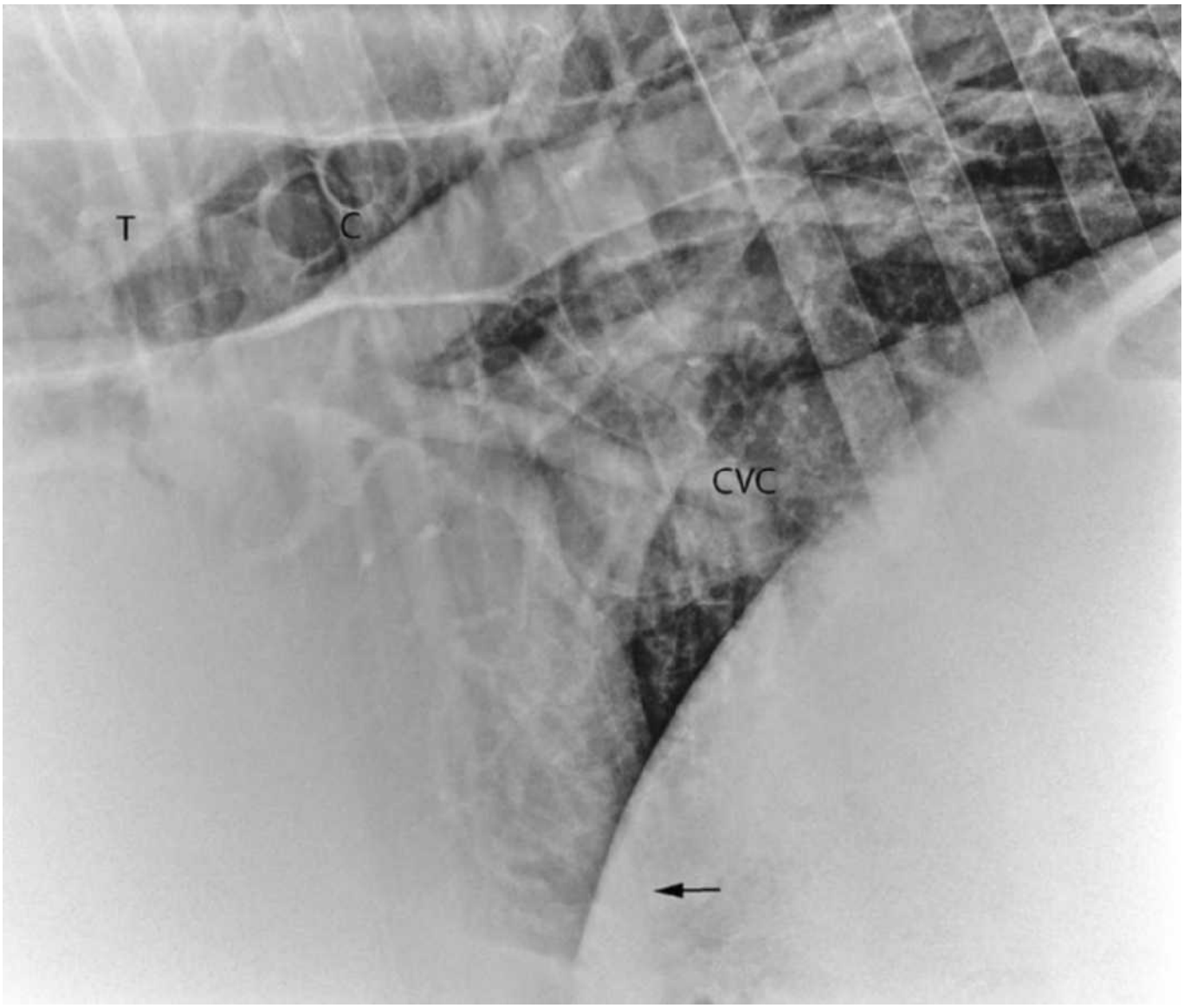


Figure 14.1(b) Ventrocaudal portion of the thorax of a normal adult horse. Cranial is to the left. The caudal border of the heart overlaps the right diaphragmatic crus and is marked by the black arrow. The pulmonary vessels overlie the caudal margin of the cardiac silhouette. The cranial portion of the cardiac silhouette is obscured by muscle mass which is not penetrated on this film. The caudal vena cava (CVC) is clearly delineated below the pulmonary arteries and veins as they exit and enter the heart, respectively. The trachea (T) passes caudally over the base of the heart and bifurcates at the carina (C).

useful than radiography for the evaluation of some conditions, particularly cardiac and pleural disease.

Diagnostic ultrasonography, in contrast to radiography, is capable of differentiating and characterising fluid and soft-tissue structures more fully. It is therefore indicated for the evaluation of pleural, pericardial and cardiac disease, including chamber size, myocardial contractility, and valvular disease.

The acoustic properties of bone (ribs) and air (normal lung) prevent the use of ultrasonography for many pulmonary diseases; however, peripheral pulmonary lesions (e.g. nodules and consolidation) may be more fully assessed and differentiated using this technique compared with radiography

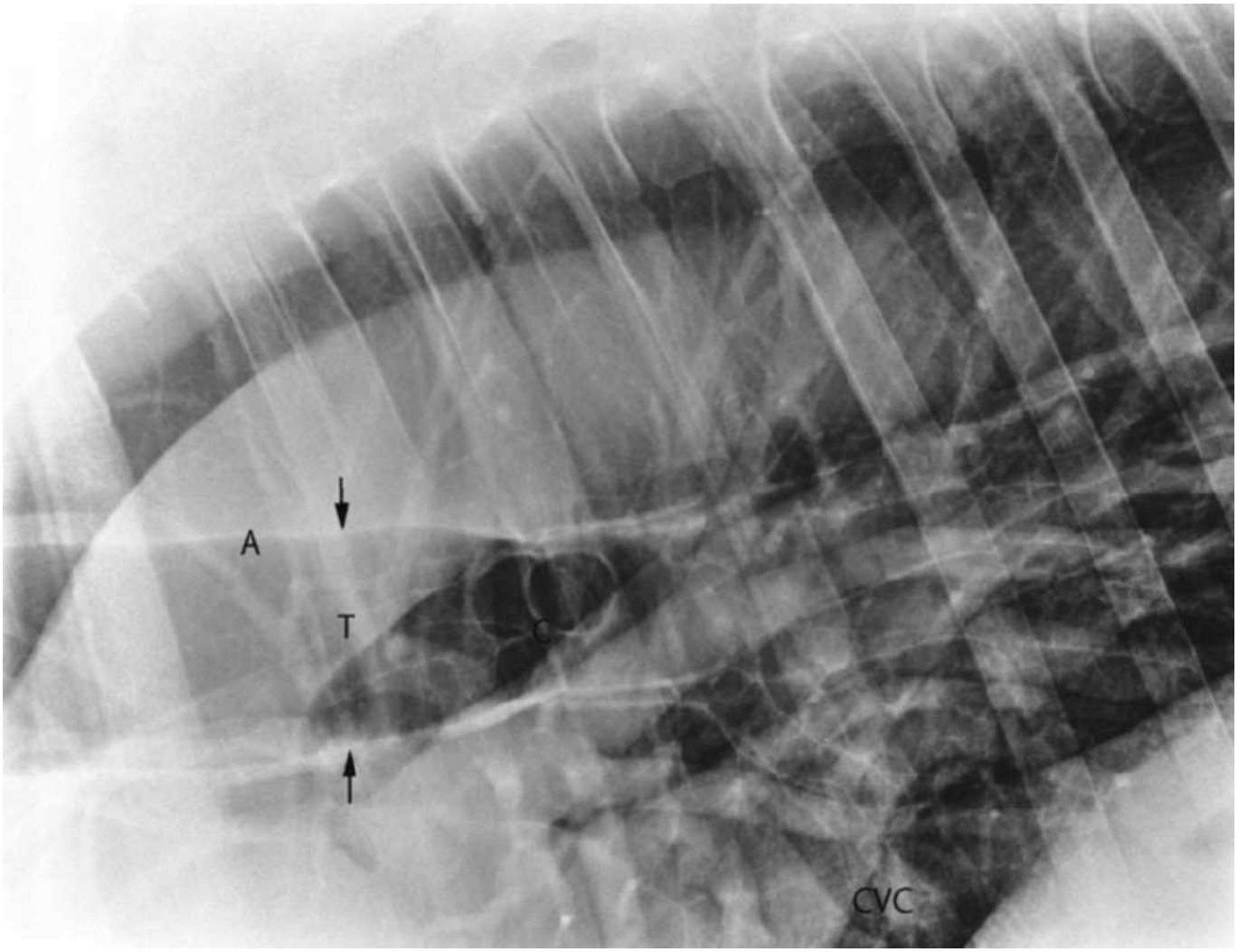


Figure 14.1(c) Dorsocranial portion of the thorax of a normal adult horse. Cranial is to the left. The aorta (A) arises from the base of the heart and passes dorsocaudad. The great pulmonary vessels arise from and enter the heart between the aorta and the caudal vena cava (CVC). The trachea (T) lies between the black arrows as it passes caudad and ends at the carina (C), where the mainstem bronchi branch.

or auscultation. Diagnostic ultrasonography is an invaluable addition for evaluation of intra-thoracic disease in the presence of pleural fluid, allowing for the differentiation of pulmonary abscesses, granulomata and tumours or masses, provided that these masses are in contact with the pleural surface. Through the characterisation of the pleura at the visceral interface, ultrasonography can also be used to identify pneumonic changes in the underlying lung. 'Comet tail' artefact is a useful phenomenon that occurs when the underlying lung has focal consolidation or a lack of aeration. Masses that are within the lung and surrounded by air cannot be adequately assessed because of attenuation of the ultrasound beam by air.

Computed tomography

Computed tomography (CT) has great potential in the few equids small enough to fit through the circular CT gantry. Typically, this is limited to foals and miniature horses or donkeys. Computed tomography images

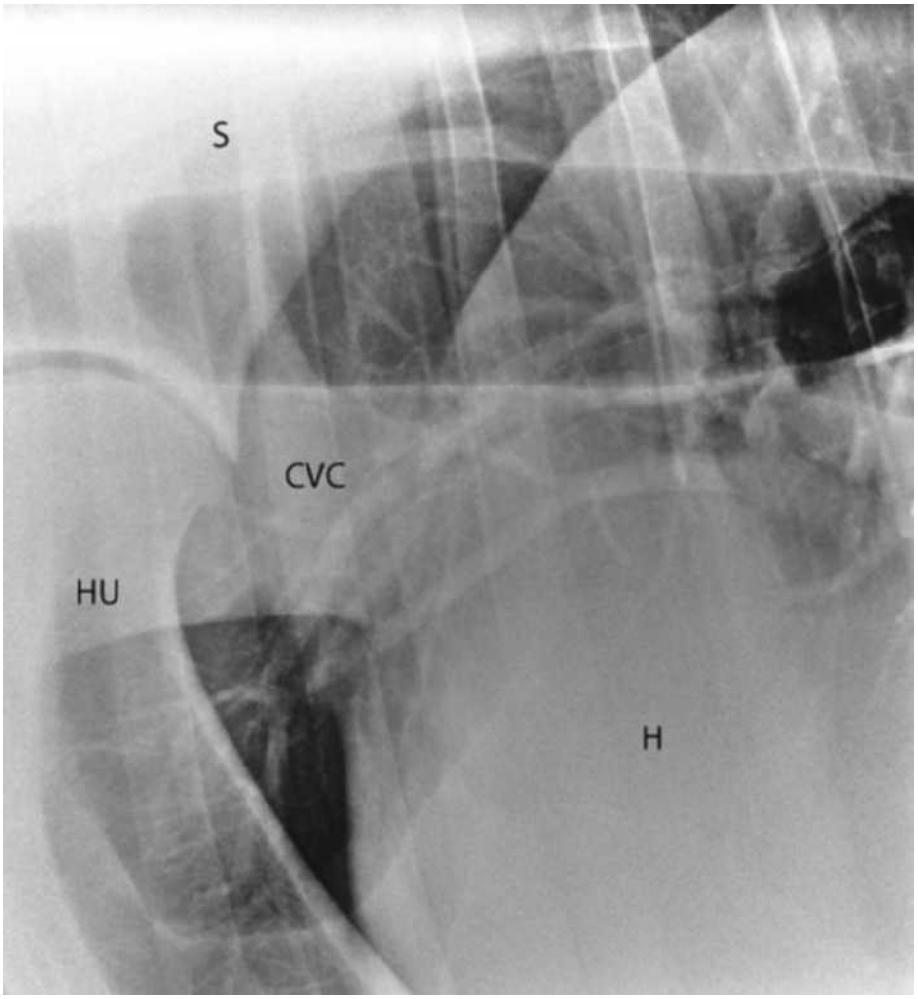


Figure 14.1(d) Ventrocranial portion of the thorax of a normal adult horse. Cranial is to the left. High exposure factors are required to penetrate the muscle mass, humerus (HU) and scapula (S). The trachea is dorsal to the cranial vena cava (CVC). The cranial margin of the heart (H) is clearly visible and vessels arch over the top of the cardiac silhouette.

have high spatial resolution and perform well in regions with high inherent contrast resolution such as the thorax, where there is variation in tissue density from gas (lung) to mineral (ribs). Thoracic wall, pleural, pulmonary, mediastinal and cardiac diseases can all be more fully characterised than with radiographs (due to the absence of superimposition) or ultrasound (due to the ability to image gas and mineral). Computed tomography can be particularly useful in the evaluation of bacterial (*Rhodococcus* sp.) pneumonia in foals and its sequelae, including pulmonary and lymph node abscessation.

Monitoring pulmonary and pleural disease

Radiography and ultrasonography can provide important information regarding disease progression and resolution that affects treatment decisions and prognosis. Imaging is an adjunct to auscultation and clinicopathological testing that can provide additional, important information. For example, radiographic signs of pneumonia in a foal may be present earlier and persist longer than auscultation or haematological abnormalities indicate. The onset of radiographic signs of pulmonary disease often lags behind the clinical

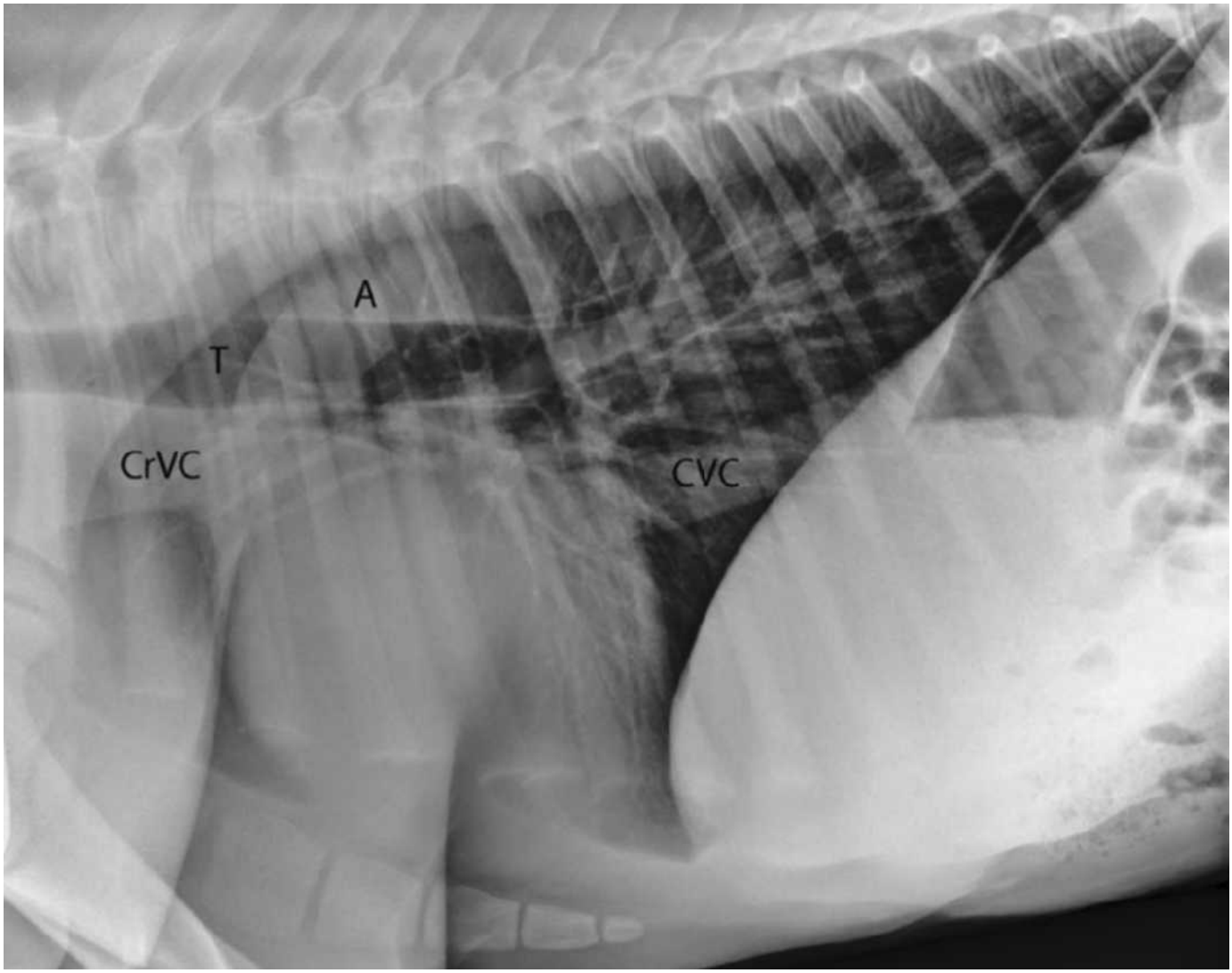
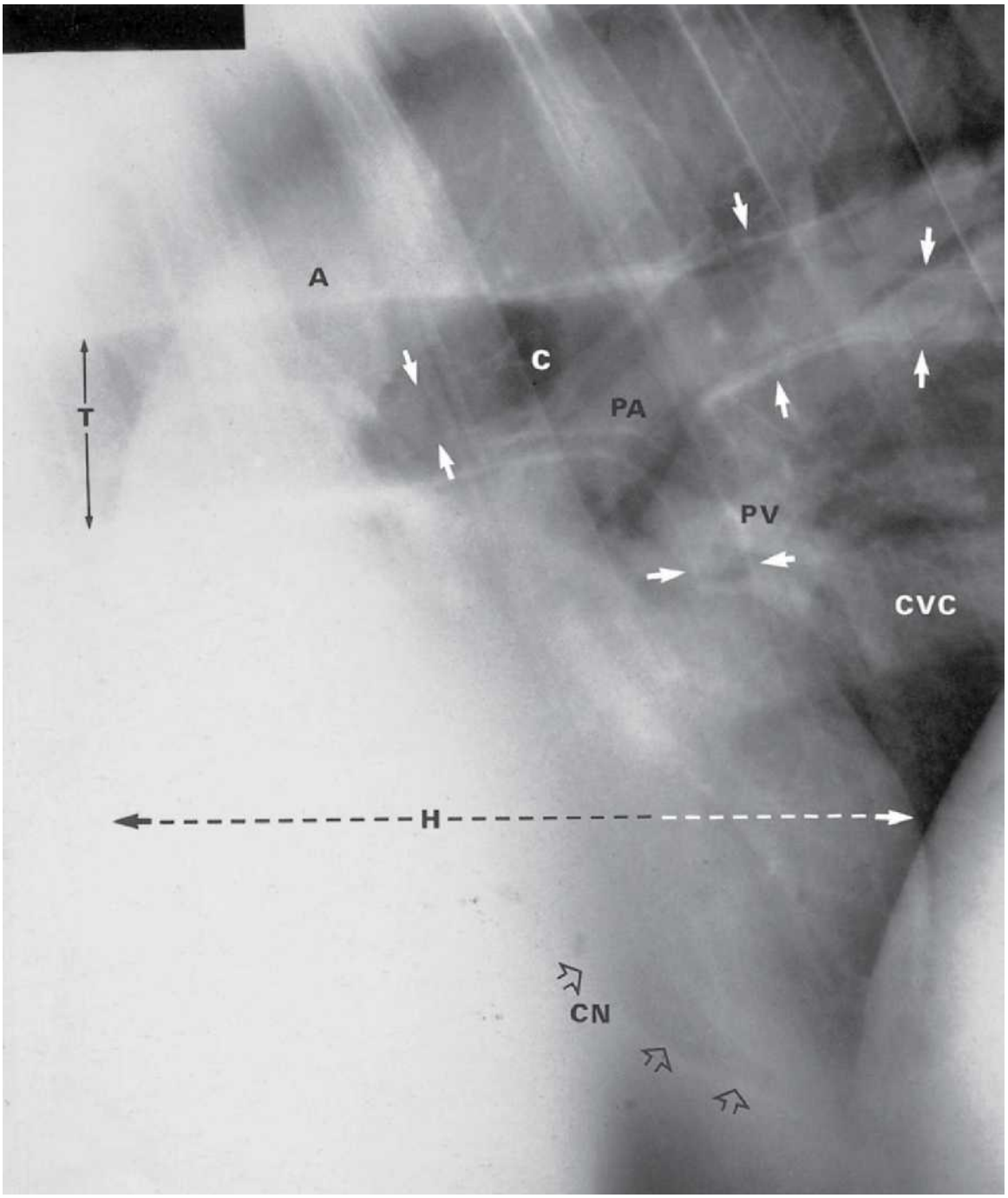


Figure 14.2 A normal 1-day-old Arabian colt. Lateral-lateral image of the thorax and cranial aspect of the abdomen; cranial is to the left. The portions of the abdomen which are seen on this film are also normal. Note the position of the trachea (T), and the inability to see the margins of the aorta (A) beyond the caudal cardiac margin. The cranial vena cava (CrVC) and caudal vena cava (CVC) are clearly seen.

signs, particularly in adult horses with inflammatory disease. Similarly, radiographic signs of improvement may lag behind clinical improvement in both immature and mature horses.

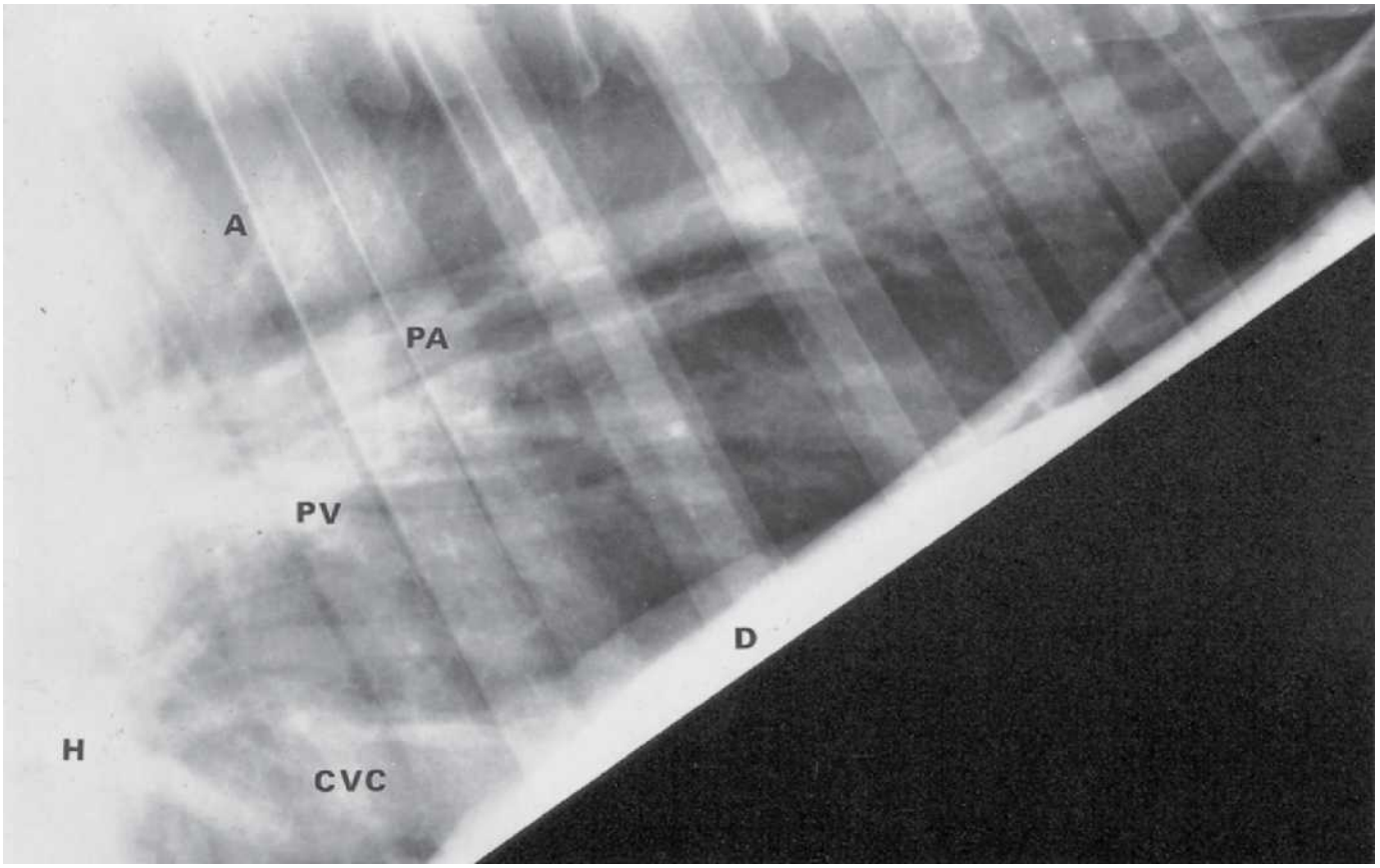
NORMAL ANATOMY

The age of the horse, its size, body condition, the width of the thorax, the phase of respiration at which images are acquired, the exposure factors, and the digital imaging system and processing will all influence the radiographic appearance of the lungs. Scattered radiation reduces contrast and resolution, especially in the ventral lung fields. Thoracic wall, visceral and parietal pleura and mediastinal structures all contribute to the overall tissue density. Digital imaging provides a more uniform image opacity of thoracic radiographs, compensating in part for errors of under- and overexposure. Errors of exposure however do still occur with digital images. Overexposure can lead



(a)

Figure 14.3 Normal adult thorax. Cranial is to the left. Due to the small size of the patient, the entire thorax was obtained on two radiographs, both right lateral-lateral projections. Portions of the dorsocranial and ventrocranial thorax as well as a portion of the ventrocaudal thorax are demonstrated in (a), whereas (b) demonstrates the normal dorsocaudal thorax and a portion of the ventrocaudal thorax. (a) The tracheal diameter (T) is marked by solid arrows. The trachea bifurcates at the carina (C). Some of the major bronchi are marked between short white arrows. The cranial to caudal dimension of the cardiac silhouette is defined by (H) and arrows. Major pulmonary vessels can be seen and include the aorta (A), pulmonary arteries (PA), pulmonary veins (PV) and the caudal vena cava (CVC). The caudal ventral lung margin can be seen over the cardiac notch (CN) and is marked by open arrows. Fine vascular structures are readily identified over the caudal margin of the heart, aorta and vertebral bodies.



(b)

Figure 14.3 *Cont'd* (b) Normal adult thorax. Cranial is to the left. The caudodorsal lung fields are clear, and close inspection allows detection of fine bronchial structures with parallel walls. Fine vascular structures can be seen over the vertebral bodies and ribs where the x-ray beam is attenuated. The margins of the aorta (A) are no longer seen caudally. The pulmonary arteries (PA) and pulmonary veins (PV) can be seen exiting and entering the heart (H) above the caudal vena cava (CVC), which can be seen passing from the heart to the diaphragm (D). Dorsocaudally the gas in the stomach can be seen against the left diaphragmatic crus, while the right crus is flatter and lies over the hepatic shadow. Many pulmonary vascular structures can be seen centrally, but are lost caudodorsally due to beam penetration.

to 'clipping' artefact, where the normal fine structural detail of aerated lung is lost. Underexposure leads to a degradation of image quality, and loss of image resolution through the introduction and amplification of image noise. Interpretation of pulmonary patterns is not easy and even experienced radiologists may interpret radiographs of the thorax differently.

If digital imaging is not available, high-speed film–screen combinations are required, but this does result in some loss of resolution. Underexposure may create artefactual lung opacities, whereas overexposure may mask lesions. Using a high kV, low mA technique helps to reduce artefacts created by exposure factors.

For comparison of radiographs among horses, and for serial examinations of the same horse, it is critically important to utilise the same exposure techniques, positioning and radiographic views in addition to using the same exposure indices on digital systems.

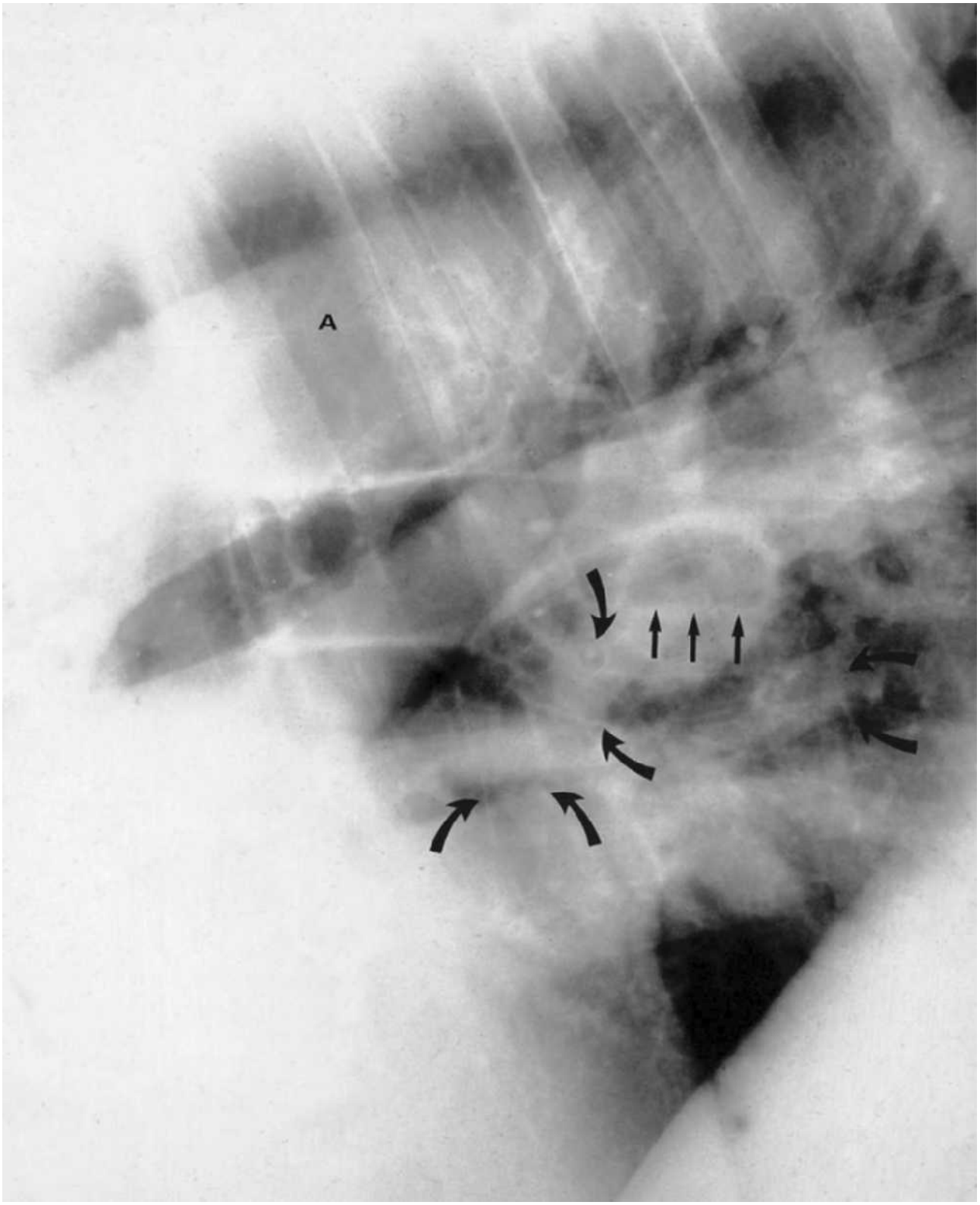


Figure 14.4(a) Right lateral-lateral radiograph of a 10-year-old Standardbred stallion with a history of pulmonary disease. Cranial is to the left. There was mucus and pus in the trachea. There is a solitary cavitary pulmonary lesion, seen as a well-circumscribed mass containing both air and fluid. The air–fluid interface (straight arrows) is demonstrated in both (a) and (b - left lateral-lateral image). The lungs are normal and fine vascular structures can be seen in the dorsal lung fields and over the aorta (A). Bronchial walls and end-on bronchi (curved arrows) are also seen.

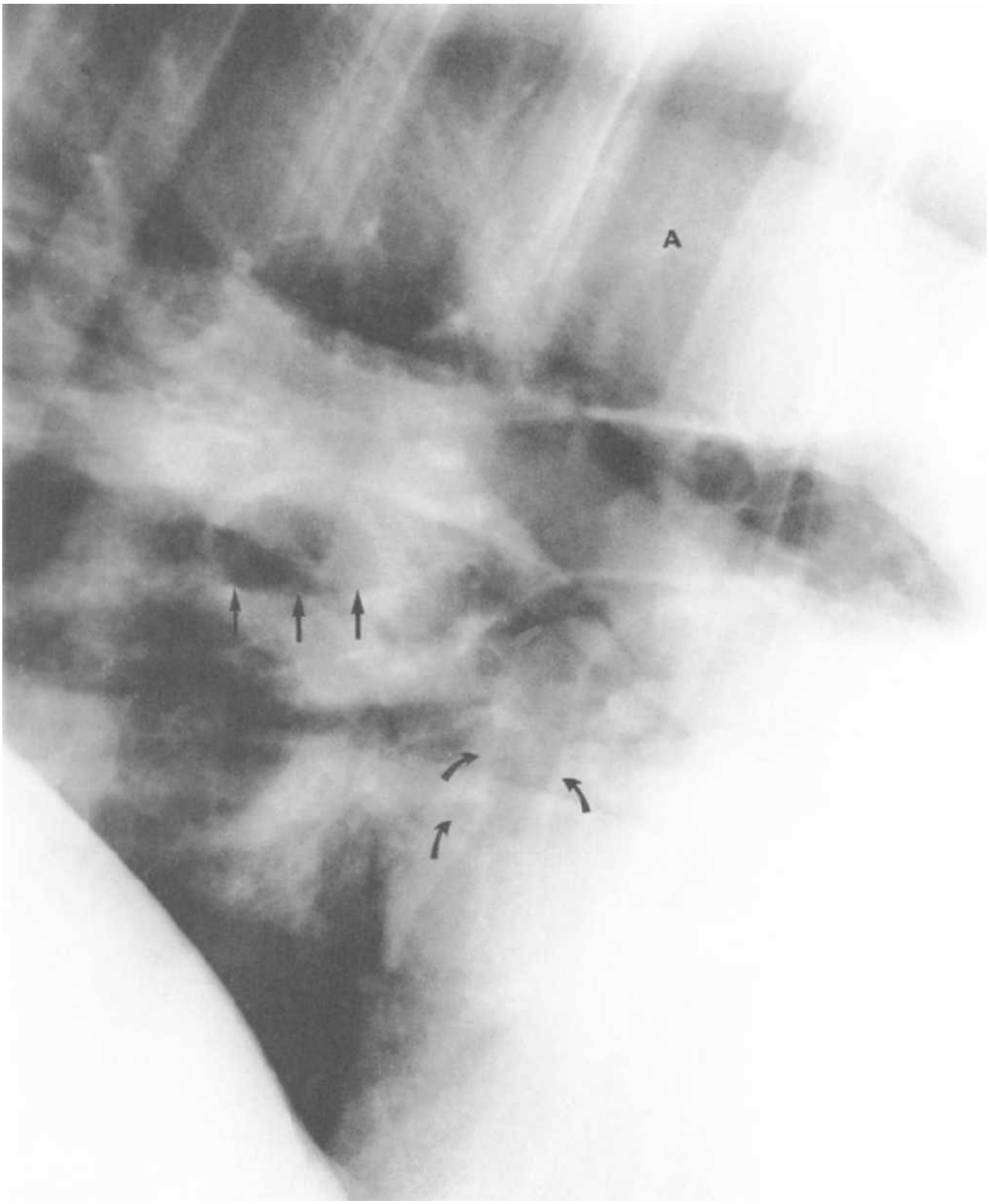


Figure 14.4(b) Left lateral-lateral projection of the same area as Figure 14.4(a) (cranial is to the right) also demonstrates the cavitary pulmonary lesion; however, the margins of the fluid line and mass are less well-defined and slightly magnified, indicating that the lesion is in the right hemithorax. On both images, bronchial walls and end-on bronchi are also identifiable (curved arrows).

Immature horse

The cardiac silhouette occupies a greater proportion of the thoracic cavity in the neonate than in the adult (compare Figures 14.1b and d 14.2 and 14.3a). In a normal foal the craniocaudal dimension should be between 5.6 and 6.3 times the length of a mid-thoracic vertebra, and the apicobasilar dimension should be 6.7–7.8 times the length of a mid-thoracic vertebra. Radiographs of the thorax of foals obtained within the first few hours of birth usually have a generalised interstitial opacity due to incomplete inflation. Within 12 hours the lungs become more lucent as the foal becomes active and the lungs are more completely inflated. The initial increased opacity leads to some diagnostic challenges during the first few days of life, because premature (see Figure 14.22) and septicaemic foals also have increased interstitial opacity. Foals with questionable abnormalities should therefore be re-evaluated in 24 and 48 hours.

Mature horse

Normal lung should appear lucent with well-defined vascular structures that are largest at the heart base and taper gradually to the periphery of the lungs. These vessels should be most opaque over their greatest dimension and gradually decrease in opacity as they progress peripherally. The trachea enters the thoracic inlet as a lucent tubular structure that has well-defined tracheal cartilages within the wall. The outer wall cannot be differentiated from other mediastinal soft tissues. The tracheal cartilages are not usually seen in young animals because they lack mineral content, which develops with age. The trachea terminates at the carina (point of bifurcation) at the base of the heart (Figure 14.1b), where it becomes the right and left mainstem bronchi. The mainstem bronchi if seen end-on are round, well-demarcated structures at the base of the heart; in longitudinal plane their linear, opaque, well-defined walls are seen. Bronchi are not normally seen much beyond the bifurcation (carina) (Figures 14.1c and 14.3a). The left mainstem bronchus is more dorsal than the right because of its close association with the left atrium.

A lucent triangle of normal lung tissue is usually identifiable caudoventrally in radiographs obtained at full inspiration. The sides of the triangle are made up of the caudal vena cava dorsally, the cardiac silhouette cranially and the diaphragm caudally. This triangle should be evaluated to determine the degree of inspiration. At peak inspiration, the apex of the triangle may be slightly blunted because the diaphragm and the cardiac silhouette separate, and the apex is then formed by the sternum.

The cardiac notch in both the right and left lungs leaves an area overlying the mid-ventral heart that is not covered by lung tissue; thus this area over the cardiac silhouette is devoid of pulmonary vessels. Care must be taken not to confuse the lack of vessels in this area with consolidated lung which might, in another location, have a similar appearance.

Dorsocaudal lung field (field A)

A portion of the aorta is usually observed just below or slightly overlapping the bodies of the thoracic vertebrae. The caudal portion of the aortic silhouette is only seen when the radiograph is obtained at peak inspiration. This is because the aortic silhouette becomes incorporated in the increasing lung

opacity in the dorsocaudal aspect of the lung, when the lungs contain less air (expiration). The pulmonary artery and vein extend from the base of the heart towards the vertebral bodies. Small pulmonary vessels are seen at the periphery of the lungs and can best be evaluated over the vertebral bodies, the cardiac silhouette and the diaphragm (see Figure 14.1a).

Ventrocaudal lung field (field B)

The dorsal portion of this radiographic image should overlap field (a). The caudal edge is defined by the silhouette of the diaphragm while the ventral side is defined by the diaphragm, sternum and the caudal aspect of the heart. The caudal vena cava is best evaluated in the right lateral projection because it lies on the right side of the thorax (see Figure 14.1b).

Dorsocranial lung field (field C)

The dorsocranial region overlaps portions of fields (a) and (b) but extends craniad. The aortic arch is the most prominent structure in this view and only a small amount of lung tissue, which is not obscured by the base of the heart and the muscle mass over the shoulders, is seen. A part of the trachea and the carina can be seen just above the cardiac silhouette. The great vessels can be evaluated as they leave the base of the heart (see Figure 14.1c).

Ventrocranial lung field (field D)

In this view the ventrocranial aspect of the thorax can be evaluated, but the lungs are often obscured by the forelimbs cranially and by the cardiac silhouette caudally. This can be improved by extending and pulling forward the limb that is closest to the x-ray tube. There is some overlap with the other three fields at the dorsocaudal portion of this view. This is usually the least useful of the four views (see Figure 14.1d).

NORMAL VARIATIONS AND INCIDENTAL FINDINGS

An increase in lung opacity (interstitial opacity) may be noted as horses age, resulting in an inability to see the fine vascular structures and in loss of structural detail. This change in appearance is due to chronic pulmonary fibrosis, an age-related change. Excessive body condition (extra-thoracic fat) also causes the appearance of increased pulmonary interstitial opacity through increased scattered radiation. With increasing age, the mainstem bronchi and tracheal rings may be more visible due to cartilage mineralisation.

Factors influencing interpretation

A single set of radiographs of the equine thorax represents the status at the time the radiographs are obtained. Many diseases will pass through similar stages during progression or regression, and radiographic findings will often, but not always, lag behind the clinical signs. Underexposed thoracic radiographs give the appearance of increased lung opacity, while overexposure results in apparent decreased opacity and digital clipping artefact.

Digital radiographs are less susceptible to errors of under- and overexposure compared with conventionally acquired images, and mild variations from optimal exposure are less critical to the evaluation of thoracic radiographs. The digital age has however introduced new problems with interpretation of radiographs. Different systems use different degrees and types of processing, making comparison between radiographs acquired on different systems very difficult. Excessive post-processing, particularly edge enhancement, can create false radiographic findings. Most systems compensate for a small degree of over- or underexposure; however, underexposure can result in a lower quality of radiograph, with marginal blurring, and a false impression of increased interstitial opacity. Gross overexposure can render the radiolucent portions of the lung (particularly the dorsocaudal region) non-diagnostic. When acquiring digital thoracic radiographs, the exposure indices offered by the various manufacturers should be used.

Expiratory radiographs (radiographs obtained at end expiration) give the appearance of increased lung opacity because the air to tissue ratio is decreased; thus the soft tissues summate, and result in a false interstitial pattern. The same phenomenon occurs when there is a large amount of intra-abdominal fluid or an abdominal mass, both of which interfere with normal diaphragmatic excursion and thus prevent peak inspiration.

Interpretation of thoracic radiographs is based on a thorough understanding of the patterns that make up the various thoracic diseases, as well as their pathophysiology and the effect of positioning.

When evaluating lateral-lateral recumbent thoracic radiographs of young or small horses, it is important to understand that the image and its interpretation are slightly altered by position compared with images acquired standing. The sharpest image will be in the upper lung because the dependent lung will partially collapse. This partial collapse obscures opacities within the lung because of the lack of adjacent air to contrast with them. Concurrently the well-aerated upper lung allows for better definition of structures despite parallax and magnification artefacts. Both left-right and right-left lateral-lateral projections should therefore be obtained in recumbent as well as standing patients.

SIGNIFICANT FINDINGS

Patterns of lung disease

Interstitial

Within the connective tissue framework of the lungs are the arteries, veins, lymphatics, nerves and the bronchi. The walls of the bronchi and the alveoli separate the interstitium from the air space. Thus, any inflammatory or infiltrative disease that affects any of these structures will result in what is referred to as an interstitial pattern (Figures 14.5 and 14.6). Although the pattern may vary to some degree depending upon the pathogenesis of the disease process, the typical appearance of an unstructured interstitial pattern is an increase in background opacity that results in the loss of the fine vascular structure that typifies a normal, well-inflated (aerated) lung. Structured interstitial patterns, including miliary or nodular patterns, occur

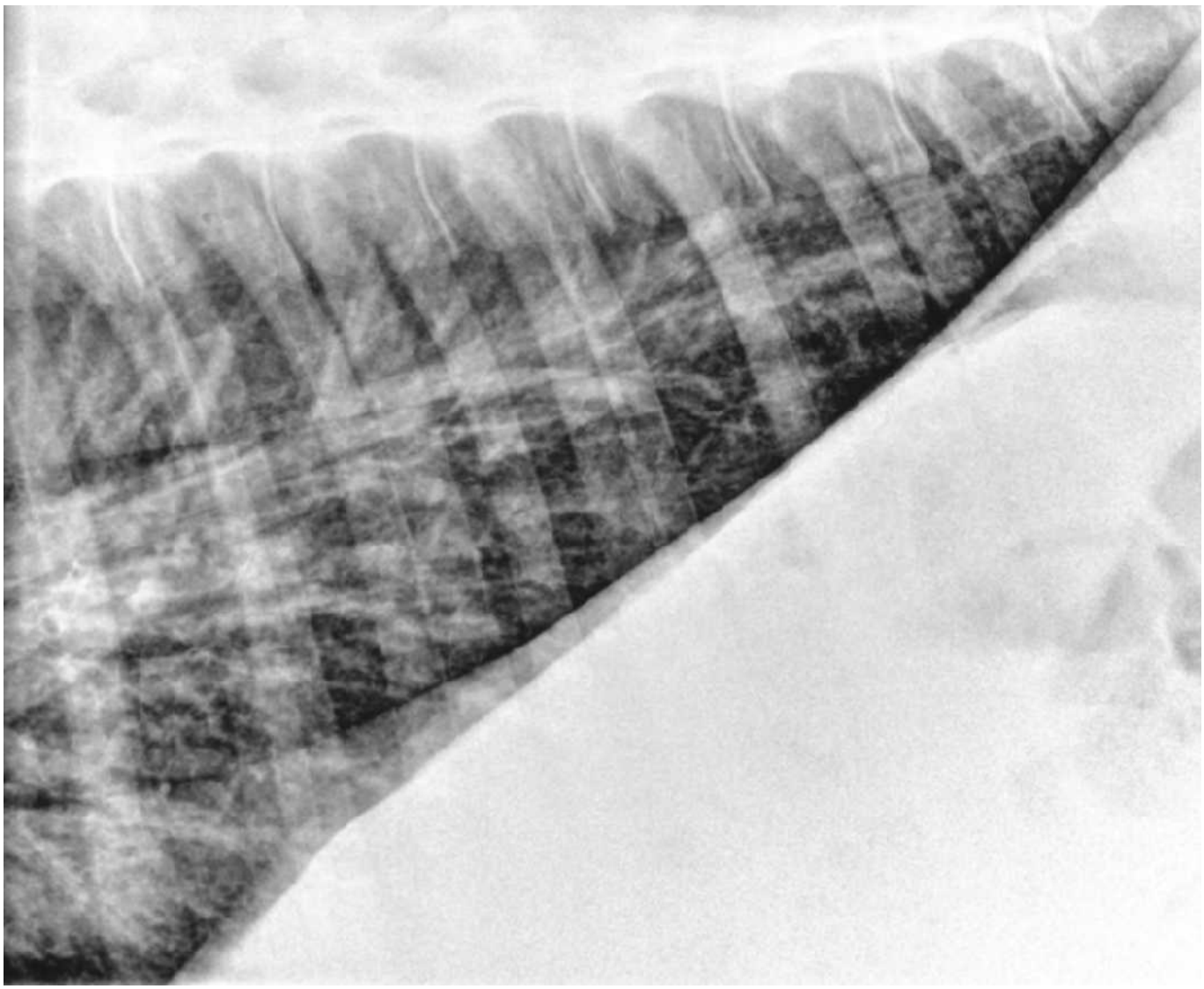


Figure 14.5 Lateral-lateral image of the dorsocaudal aspect of the thorax; cranial is to the left. Five-month-old Thoroughbred colt admitted with severe acute dyspnoea. There are pulmonary interstitial infiltrates, characterised by a generalised increased lung opacity and the inability to see the fine vascular markings. The major vessels are less clearly demarcated compared with normal. These findings are consistent with bronchointerstitial pneumonia.

when the interstitial infiltrates coalesce and form structured tissues. Because of the variety of tissues involved, a changed interstitial pattern is the predominant pattern noted in the early stages of most pulmonary disease, including: infectious inflammatory disease (viral, bacterial, mycotic and parasitic), inflammatory disease (hypersensitive and eosinophilic), haemorrhagic, neoplastic and pulmonary oedema (cardiogenic and non-cardiogenic). In a foal an interstitial pattern is seen in both septicaemic and immature patients. (See 'Bronchointerstitial pneumonia of foals/acute respiratory distress syndrome/acute lung injury', below.)

A generalised interstitial pattern is non-specific and can be associated with a broad range of differential diagnoses ranging from cardiogenic pulmonary oedema, to early infectious pneumonia or pneumonitis, to chronic pulmonary fibrosis. A true interstitial pattern must be differentiated from artefactual increases in pulmonary opacity seen with radiographs acquired

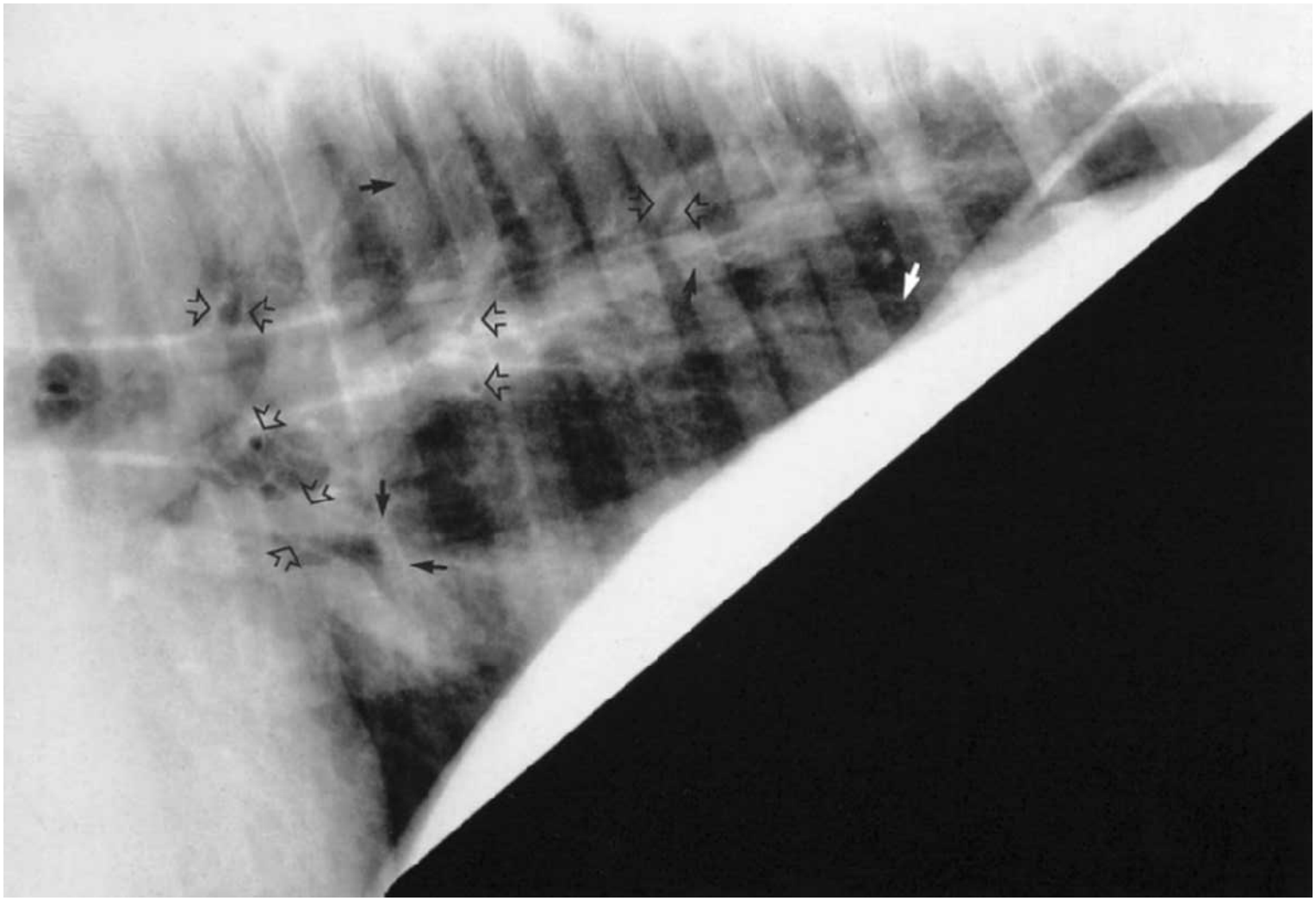


Figure 14.6 Lateral-lateral image of the dorsocaudal aspect of the thorax; cranial is to the left. Three-month-old Thoroughbred colt which had previously had guttural pouch empyema with a recent 2-week history of pneumonia and nasal discharge. The nasal discharge had improved within the previous 3–4 days. The radiograph demonstrates interstitial and bronchial pattern due to bacterial pneumonia. There is a generalised increase in interstitial opacity, of which a major component is a bronchial pattern. The bronchial markings are prominent and well-circumscribed end-on bronchi are seen. Some of the larger bronchi are marked with open arrows. Note the width of the bronchus and prominent bronchial walls. Solid arrows mark small bronchi in the periphery.

during expiration, high body condition score, underexposure or inappropriate digital processing. A granular or nodular interstitial pattern when present should promote differential diagnoses such as granulomatous inflammatory disease, mycotic disease or metastatic neoplasia. Many pulmonary diseases start within the interstitium, before involving the air spaces, so the presence of this pattern alone is not pathognomonic for any disease. Follow-up radiographs are always advisable.

Vascular

There are vessels within the interstitium which can only be differentiated prior to the accumulation of interstitial fluid (oedema) or infiltrate. Interstitial infiltrates mask the underlying fine vascular structures or give them an indistinct outline. A vascular pattern is primarily characterised by changes in size or shape of the pulmonary veins or arteries. Because of the close relationship of the vasculature to the interstitium, it can be difficult to identify these changes clearly. Increased size of the pulmonary vasculature may be associated with congenital or acquired cardiac disease or inflammatory lung disease. This is particularly evident late in the disease process if there is increased pulmonary vascular resistance. Pulmonary vessels are most easily recognised as round to ovoid fluid opacities of varying size, that lie over the other vessels as they are seen end-on in the peripheral lung tissue.

Bronchial

The bronchi are housed within the interstitium but are part of the air conducting system and are therefore generally considered separately from interstitial diseases. A bronchial pattern on radiographs is characterised primarily by the appearance of bronchial wall thickening (bronchial pattern, Figure 14.6). The apparent thickening can be the result of true wall thickening, the accumulation of mucus and mucosal thickening, or more often, peribronchial infiltrates. Airway wall thickening occurs with recurrent airway obstruction due to smooth muscle and mucous-cell hyperplasia. Peribronchial infiltrates are more consistent with acute or chronic inflammatory conditions, including inflammatory airway disease (IAD). Chronic airway disease can also include increases in size or shape of the bronchi, with bronchiectasis (i.e. dilation and thickening) as the bronchial walls become progressively more abnormal (see Figure 14.14).

Airway thickening or peribronchial infiltrates can be recognised as linear thickening when observing airways along their length or a peribronchial cuffing or increased opacity surrounding end on airways. Many digital systems enhance the appearance of normal, thin bronchial walls. This can result in false-positive interpretation of a bronchial pattern that is primarily due to increased visibility of the bronchi and not pathology.

Alveolar

When the terminal air spaces fill with fluid (transudate, exudate or blood) or tissue, the alveoli assume a soft-tissue opacity rather than normal lucency of air. In the early stages when few alveoli are involved, the structures that are normally seen will be obscured by fluffy or cloudy fluid (soft tissue) opacities.

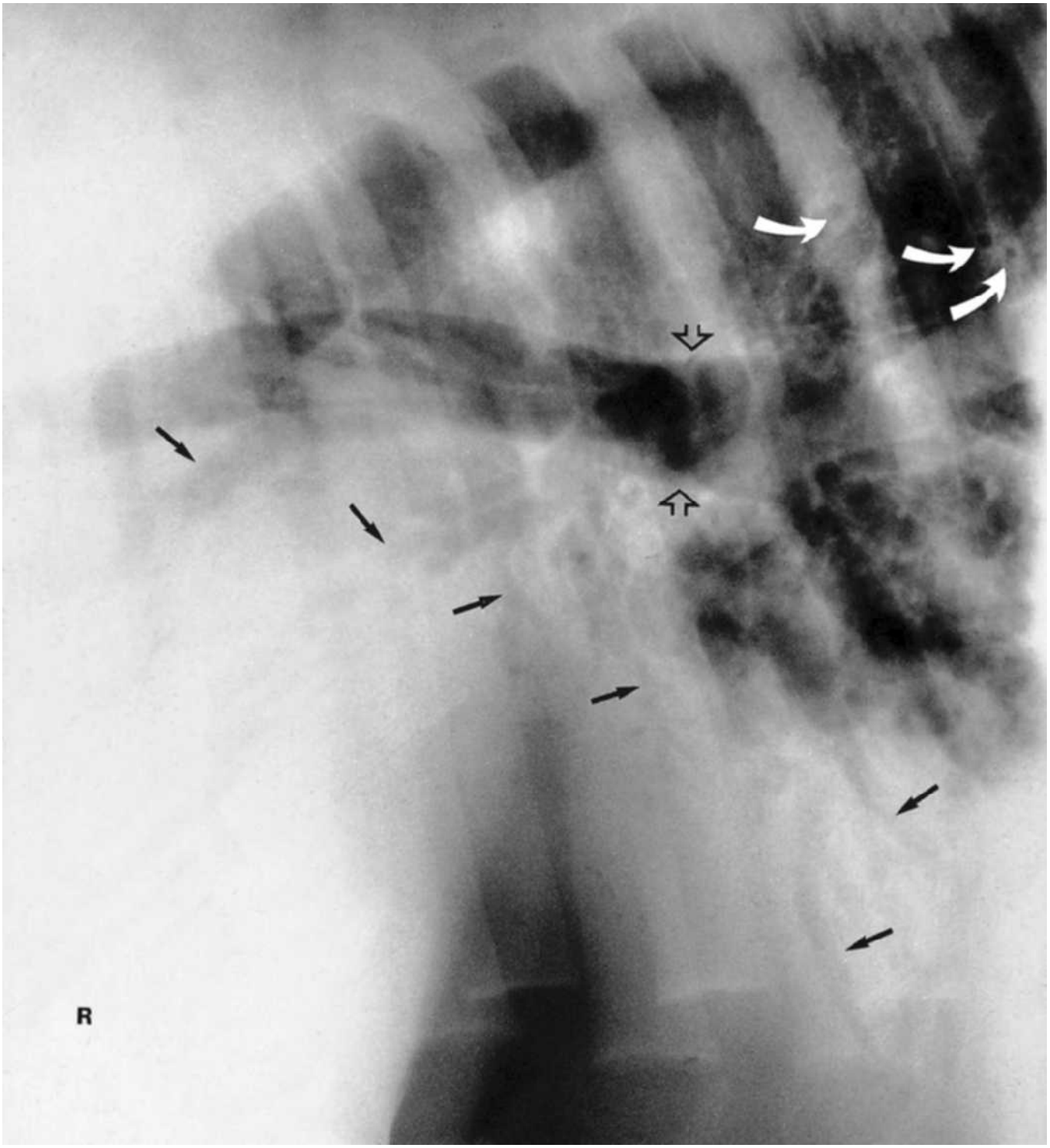


Figure 14.7 Three-month-old Thoroughbred filly with a history of acute onset of respiratory distress. Lateral-lateral image of the thorax; cranial is to the left. There is an irregular fluid opacity which involves the entire ventrocaudal aspect of the thorax and obscures the cardiac silhouette. Air bronchograms (black solid arrows) are readily seen. Dilatation of the caudal aspect of the trachea at the carina (open arrows) is indicative of maximal inspiratory effort and dyspnoea. Peribronchial changes are noted dorsal to the carina (white curved arrows). These changes are typical of either severe aspiration or bacterial pneumonia. The air bronchograms branch as they extend towards the periphery and are indicative of alveolar infiltrate and consolidation. Diagnosis: bacterial and aspiration pneumonia.

Disease progression results in increasing numbers of opaque alveoli, coalescence and summation of the opacities and pathological consolidation. When the normally lucent aerated alveoli are filled with soft tissue or fluid and the bronchi are air-filled, the radiographs show air bronchograms. An air bronchogram is a lucent branching structure within an opaque (consolidated) lung field (Figure 14.7; see also Figure 14.20). Air bronchograms are indicative of almost complete alveolar filling; the only remaining air space is the bronchi, which are visible as dark branching structures in a background of grey. At this stage the distribution of the air bronchograms within the lung field can aid in the differentiation among various causes of pulmonary consolidation. The differential diagnosis includes: bacterial, mycotic and aspiration pneumonia, and pulmonary oedema of both cardiogenic and non-cardiogenic origin (see 'Diseases of the lung', below).

Cavitary pulmonary lesions

A cavitary pulmonary lesion is a term used to describe a cavity that occurs in the lung (see also 'Cavitary pulmonary lesions', below) (Figures 14.4a and b, 14w.10b, 14w.21 and 14.23). In the horse the most common form is the result of abscess formation, liquefaction and loss of the fluid centre through a communicating bronchus. These are usually seen in young horses and have a thick opaque wall. Other abscesses or granulomata may also be seen. An air–fluid interface is often present. Other causes include neoplasia, traumatic and congenital cavitary lesions or bullae.

Pulmonary masses

Pulmonary masses are described in more detail in 'Diseases of the lung', below. Masses may be single (nodular) or multiple (miliary). (See 'Patterns of lung disease – Interstitial', above.)

Diseases of the pleural space and mediastinum

Pleural effusion

Radiography and ultrasonography should be used as complementary tools for the evaluation of pleural fluid and concurrent lung disease. Ultrasonography is much more sensitive than radiography for the detection of small amounts of fluid within the pleural space. Ultrasonography is also more useful than radiography for the characterisation of pleural fluid and the identification of associated underlying pulmonary disease, particularly when pleural effusion obscures the ventral aspect of the thorax on radiographs. On radiographs, small amounts of fluid in the pleural space may be seen as fluid opacities, which occupy the pleural fissures (Figure 14.8). With increased amounts of fluid there is a diffuse fluid opacity in the ventrocaudal aspect of the thorax of a standing patient. The presence of large amounts of fluid results in a loss of definition between the heart and the diaphragm (Figure 14.9). This fluid line is poorly demarcated because of the capillary action of the pleural space and is only sharply delineated when there is concurrent pneumothorax. The loss of definition progresses dorsally with increasing amounts of fluid, which may at times be defined by the lung



Figure 14.8 Yearling Thoroughbred colt with a history of thoracic disease. Lateral-lateral image of the thorax. Cranial is to the left. There is a small irregular fluid opacity in the ventrocaudal aspect of the thorax over the cardiac silhouette (arrows). The remainder of the thorax is normal. This opacity represents a small amount of free pleural fluid at the base of the ventrocaudal lung adjacent to the cardiac notch.

margins as they begin to retract dorsally. Abnormal (pneumonic) tissue tends to remain more ventral and summate with the fluid. Abnormal lung can be identified and characterised through the pleural effusion, using ultrasonography. Pleural effusion often causes ventral pulmonary atelectasis that can be differentiated from consolidation using ultrasonography.

All types of pleural effusion appear similar on radiographs and although pleuropneumonia is the most common cause of pleural effusion in horses, other types of effusion including transudate, modified transudate, exudate, haemorrhage and lymph (chyle) should be considered. They have a uniform

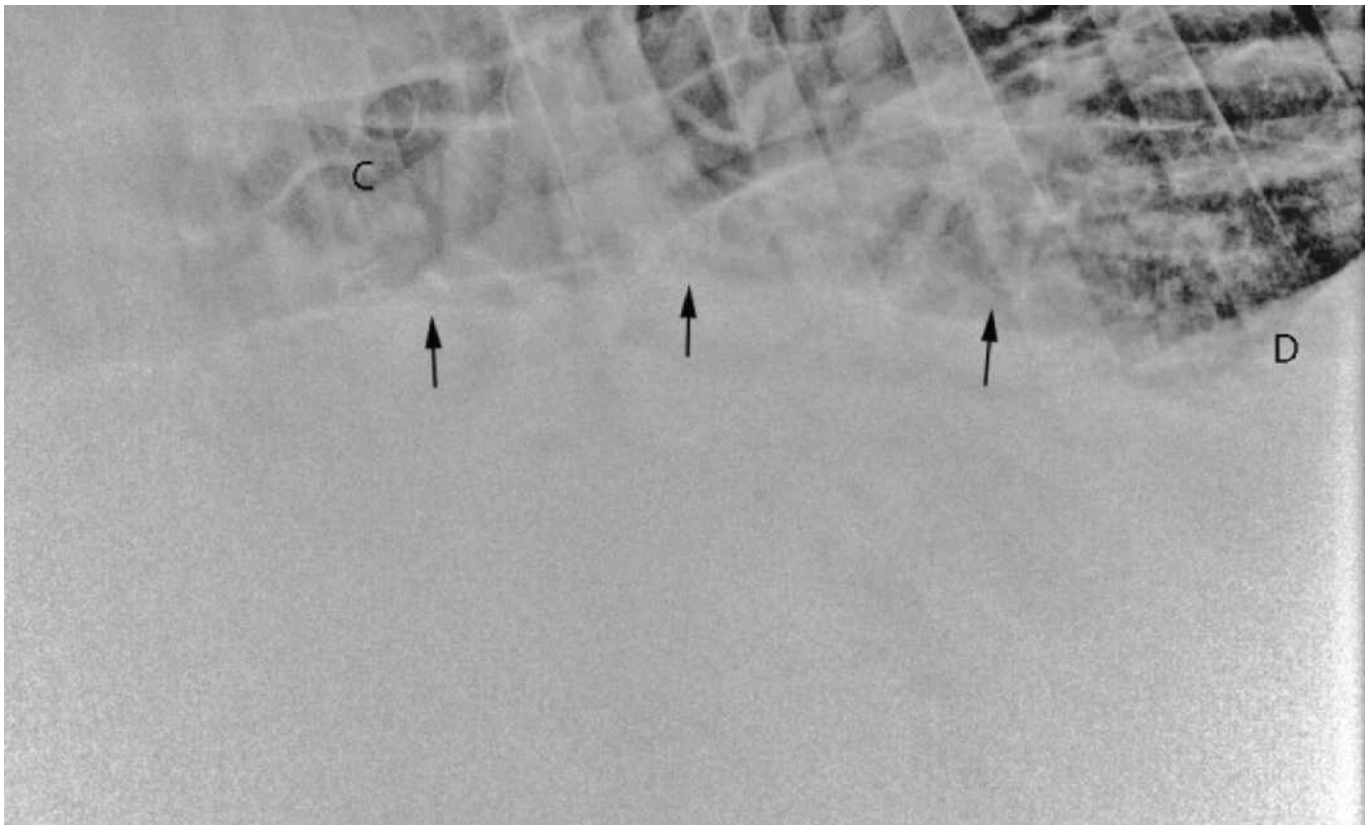


Figure 14.9 Six-year-old Thoroughbred stallion with respiratory distress. Lateral-lateral image of the thorax. Cranial is to the left. There is an irregular fluid level (black solid arrows) ventral to the carina (C) and extending to the diaphragm (D). The cardiac silhouette and ventral aspect of the thorax are completely obscured by the fluid opacity. The lung cannot expand normally, which has resulted in increased interstitial pattern in all lung lobes. These findings are consistent with pleuropneumonia.

ground-glass appearance similar to the cardiac silhouette or the diaphragm and underlying liver. Malignant mesothelioma must be considered in the differential diagnosis when pleural fluid is present. In these cases the pericardial sac may also be involved and result in pericardial effusion. A final diagnosis must rely on additional techniques such as ultrasonography and pleurocentesis. Diagnostic ultrasonography adds to the study of pleural disease by occasionally defining the character of the fluid; it also allows identification of fibrin, adhesions or concurrent cardiac disease, pericardial disease, pericardial effusion, lung consolidation and occasionally masses or abscesses within the consolidated lung.

It is advisable to re-radiograph the thorax after the removal of pleural fluid in order to evaluate the lungs both for possible causes and for involvement of areas that could not be evaluated in the presence of the fluid.

Pneumothorax

Free air in the pleural space rapidly collects dorsally, in the paraspinal recess and the dorsal caudal reflection of the pleura adjacent to the diaphragm at the highest portion of the paraspinal recess. The dorsocaudal area of the thorax is, therefore, the most important area to evaluate when small amounts of gas are expected. Radiographically the lung margins are retracted both from the diaphragm caudally and the vertebral bodies dorsally, thus allowing

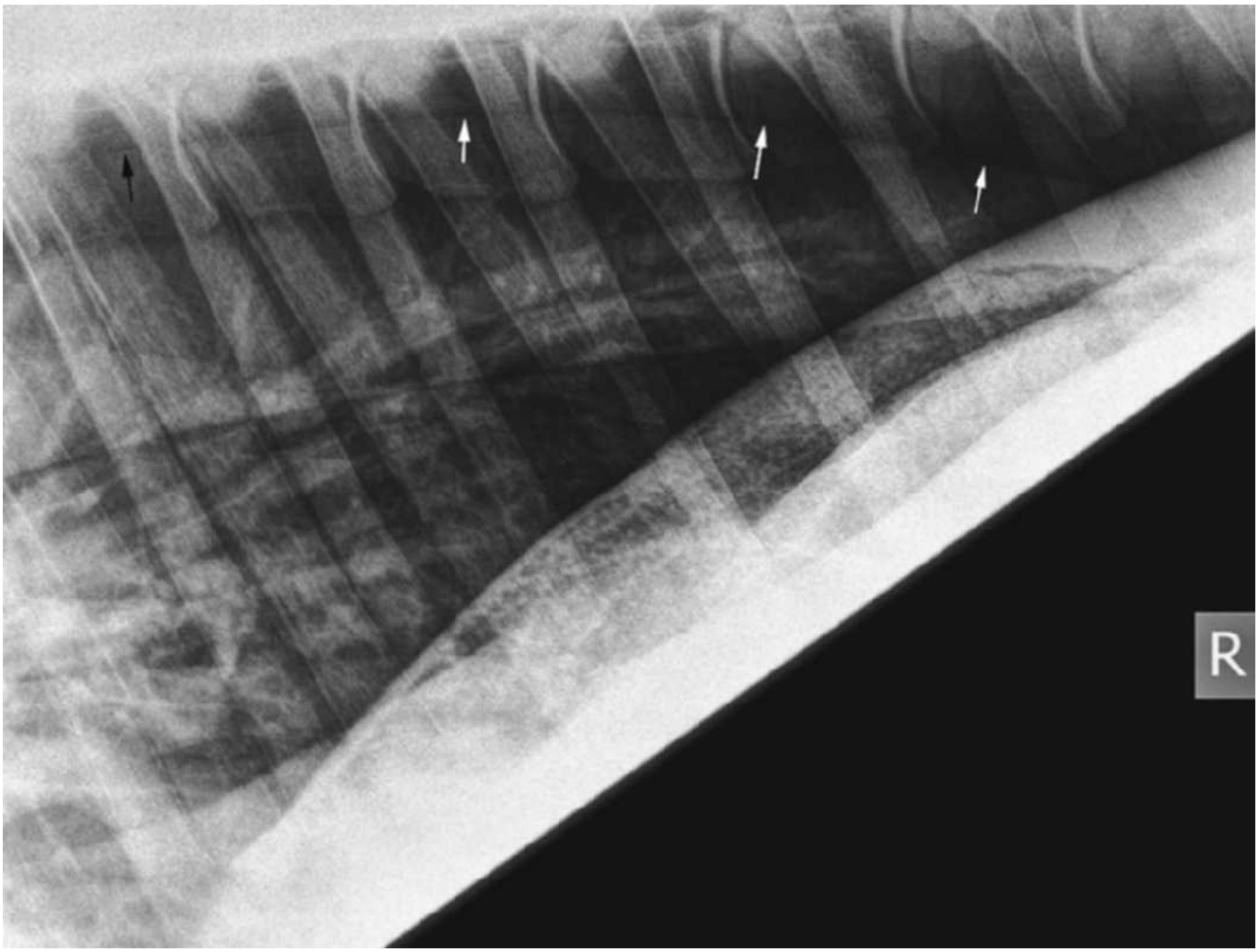


Figure 14.10(a) Right lateral-lateral image of a thorax with evidence of pneumothorax. Cranial is to the left. The radiograph was acquired three days after a traumatic wound to the thorax of this 8-year-old Thoroughbred. Ultrasonographic examination revealed rib fractures. The right lung is retracted ventrally and cranially from the thoracic margins and the diaphragm, respectively. The dorsum of the right lung is identified by arrows. Note that vessels are not seen over the majority of the vertebral bodies (compare with Figure 14.1a).

the pleural surface of the lung to be seen (Figure 14.10a and 14w.10b). Unilateral pneumothorax may occur, and in these cases it is possible to see one lung margin retracted and to see the vessels in the contralateral lung. In cases of bilateral pneumothorax, both lung lobes are retracted. In cases of pleural effusion and iatrogenic pneumothorax, the pleura can be assessed for qualitative changes such as thickening, or a lobular margination that can occur with chronic inflammatory conditions. The line caused by the gas–fluid interface created by the pneumothorax may give some information regarding the nature of the fluid.

Pneumothorax can arise from disruption of the thoracic wall, lung or, mediastinum. Thoracic wall lesions including penetrating trauma or rib fractures, can introduce air to the pleural space via communication with the external environment or through subsequent pulmonary trauma. Lung disruption can occur through rupture of lung lesions such as bullae, blebs or abscesses, or through inhaled foreign bodies. Pneumomediastinum can occur iatrogenically or via trauma such as axillary skin wounds. Whenever

spontaneous pneumothorax is present, the entire thorax should be scrutinised for signs of concurrent pathology such as rib fractures, foreign bodies and pulmonary disease.

Pneumomediastinum

Radiographically, pneumomediastinum is seen as tracks of air outlining mediastinal structures. Both sides of the trachea are clearly defined together with other structures that cannot normally be seen within the mediastinum, such as the oesophagus and the great vessels at the base of the heart (Figure 14.11).

Pneumomediastinum may be progressive, extending into the pleural space and resulting in a pneumothorax. The converse is never true; an increase in intrathoracic pressure compresses the mediastinum, thus preventing the entrance of air into the potential mediastinal space. Pneumothorax and pneumomediastinum can exist concurrently, usually as the result of trauma.

Free air in the mediastinum may result from rupture of a tracheal ring, a penetrating wound or an abscess, or may be iatrogenic following techniques such as a transtracheal wash or intravenous fluid administration.

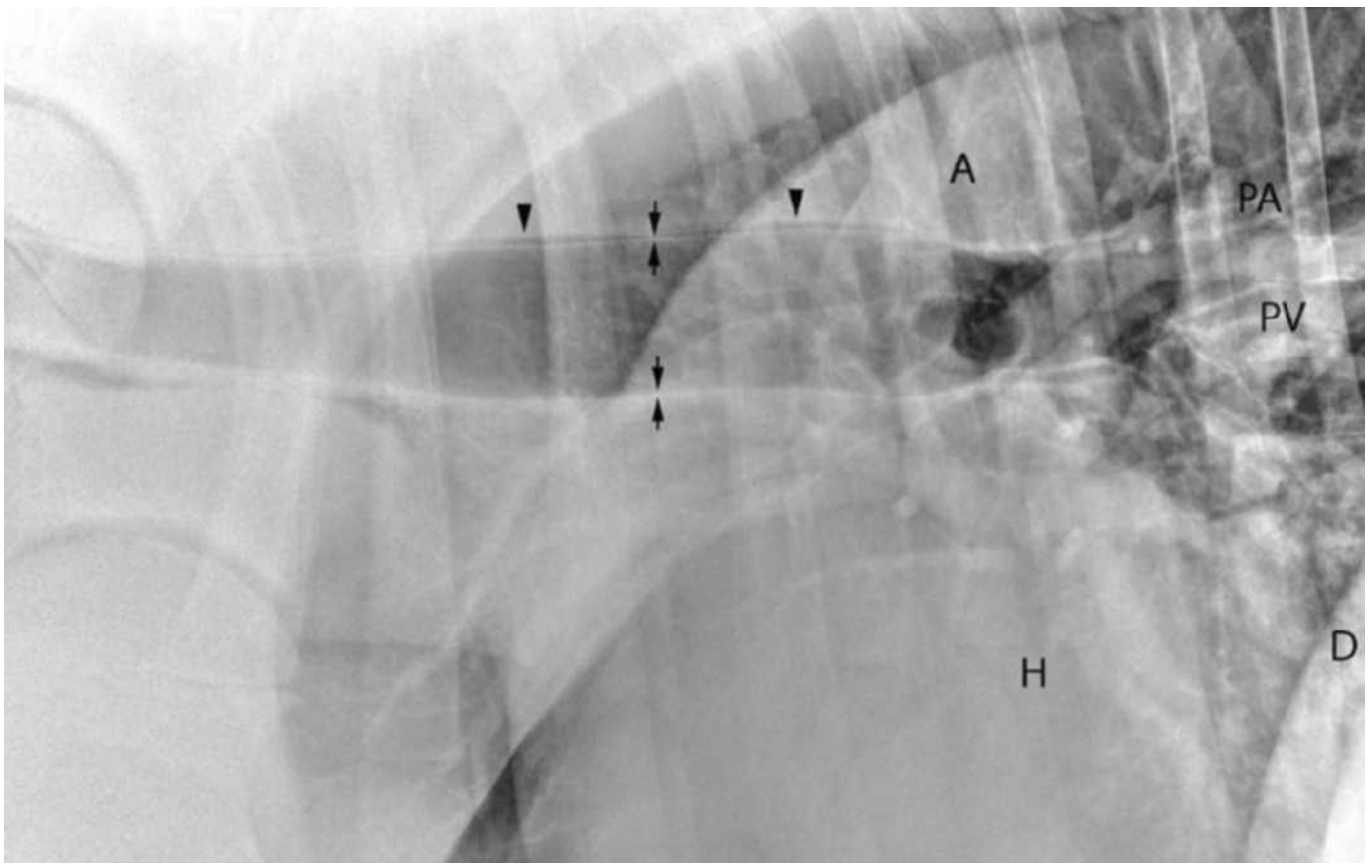


Figure 14.11 Yearling female Quarterhorse which was in a trailer accident and had multiple head and neck lacerations, resulting in pneumomediastinum. Lateral-lateral image of the thorax; cranial is to the left. There is free air in the mediastinum which outlines both sides of the tracheal wall (between black arrows). Air in the mediastinum is seen between the dorsal tracheal wall and the black arrowheads. Air in the mediastinum highlights the major pulmonary vascular structures. The aorta (A), pulmonary arteries (PA) and the pulmonary veins (PV) are easily seen. The pulmonary arteries and veins to the caudal ventral lung lobes are seen over the heart (H). The diaphragm is identified (D).

Mediastinal masses

Mediastinal masses are difficult to detect and are often identified because of mass effect, i.e. displacement of other, adjacent mediastinal structures such as the trachea, great vessels or heart. Masses in the mediastinum are rare, but when present are most often caused by lymphadenopathy. Diseases affecting the lymphatic system should therefore be considered first, followed by infectious inflammatory lesions including bacterial and fungal aetiologies, neoplasia including lymphoma or other disseminated diseases, and some non-infectious inflammatory diseases. Mediastinal masses are often associated with pleural effusion, making identification more difficult. In these cases, ultrasound-guided pleurocentesis, drainage of the pleural effusion and occasionally tissue sampling through biopsy are helpful.

The oesophagus is a mediastinal structure that can cause mass effect on the surrounding structures, but is discussed in Chapter 15.

Tracheal collapse and stenosis

The radiographic diagnosis of tracheal collapse is aided by the acquisition of inspiratory and expiratory thoracic radiographs for comparison of tracheal dimensions. Tracheal collapse, along with tracheal hypoplasia (Figure 14.12), are conditions recognised in miniature horses and donkeys, causing airway-related signs, such as coughing, 'honking' and increased expiratory effort. Tracheal collapse is a rare cause of exercise intolerance in an exercising Thoroughbred horse and radiographs in conjunction with endoscopy are needed for diagnosis.

Tracheal (or airway) stenosis should be subdivided into luminal, mural and extraluminal causes. The air column within the tracheal lumen aids in the identification of luminal and mural causes of stenosis (Figure 14.13). Extraluminal causes may include any mass lesions (mass effect) from other mediastinal structures such as the oesophagus or mediastinal lymph nodes.

Diseases of the lung

Inflammatory airway disease (IAD) (bronchitis and bronchiolitis)

Inflammatory airway disease is characterised by poor performance, exercise intolerance (or coughing with non-septic inflammation in bronchoalveolar lavage fluid), pulmonary dysfunction without evidence of systemic disease, or increased respiratory effort. It is considered separately from recurrent airway obstruction or heaves, and radiographs are considered supportive of the diagnosis. A diffuse or regional bronchial pattern with or without mild interstitial infiltrates can be seen on radiographs in horses with IAD.

Recurrent airway obstruction (RAO) or heaves (previously termed chronic obstructive pulmonary disease)

Recurrent airway obstruction (RAO) (heaves), or summer pasture-associated RAO, are associated with a cough, laboured breathing, exercise intolerance, nasal discharge and abnormal lung sounds. The clinical signs wax and wane and can be associated with environmental triggers. This condition is



Figure 14.12 Lateral-lateral image of the caudal cervical and cranial thoracic regions; cranial is to the left. Fourteen-year-old miniature horse with a history of chronic inspiratory stridor and, when exercised, a 'honking' sound on expiration. There is severe collapse of the cervical and thoracic trachea. The cardiac silhouette appears to be slightly enlarged. Diagnosis: hypoplastic trachea.

characterised by airway hyper-reactivity and pulmonary function tests consistent with increased airway resistance. A generalised bronchial pattern may be seen, resulting from smooth muscle hyperplasia with excess mucus production (mucous-cell hyperplasia and metaplasia), and mucus accumulation, in addition to inflammatory infiltrates and fibroplasia surrounding the airways. A patchy bronchial pattern can also be seen, with regions of airway involved showing oriented, but unstructured, interstitial opacity. As with IAD, radiographic findings are considered supportive of the diagnosis. Late in the course of the disease, airway wall changes can progress to bronchiectasis (Figure 14.14) and occasionally emphysema, or air being trapped in parts of the lung, showing as increased pulmonary lucency.

Equine multinodular pulmonary fibrosis

Equine multinodular pulmonary fibrosis is associated with two radiographic patterns reflecting the underlying pathology. The more common form has multifocal, coalescing 1–5 cm opaque (fibrotic) nodules throughout the interstitium, accompanied by a diffuse, interstitial pattern. When present at

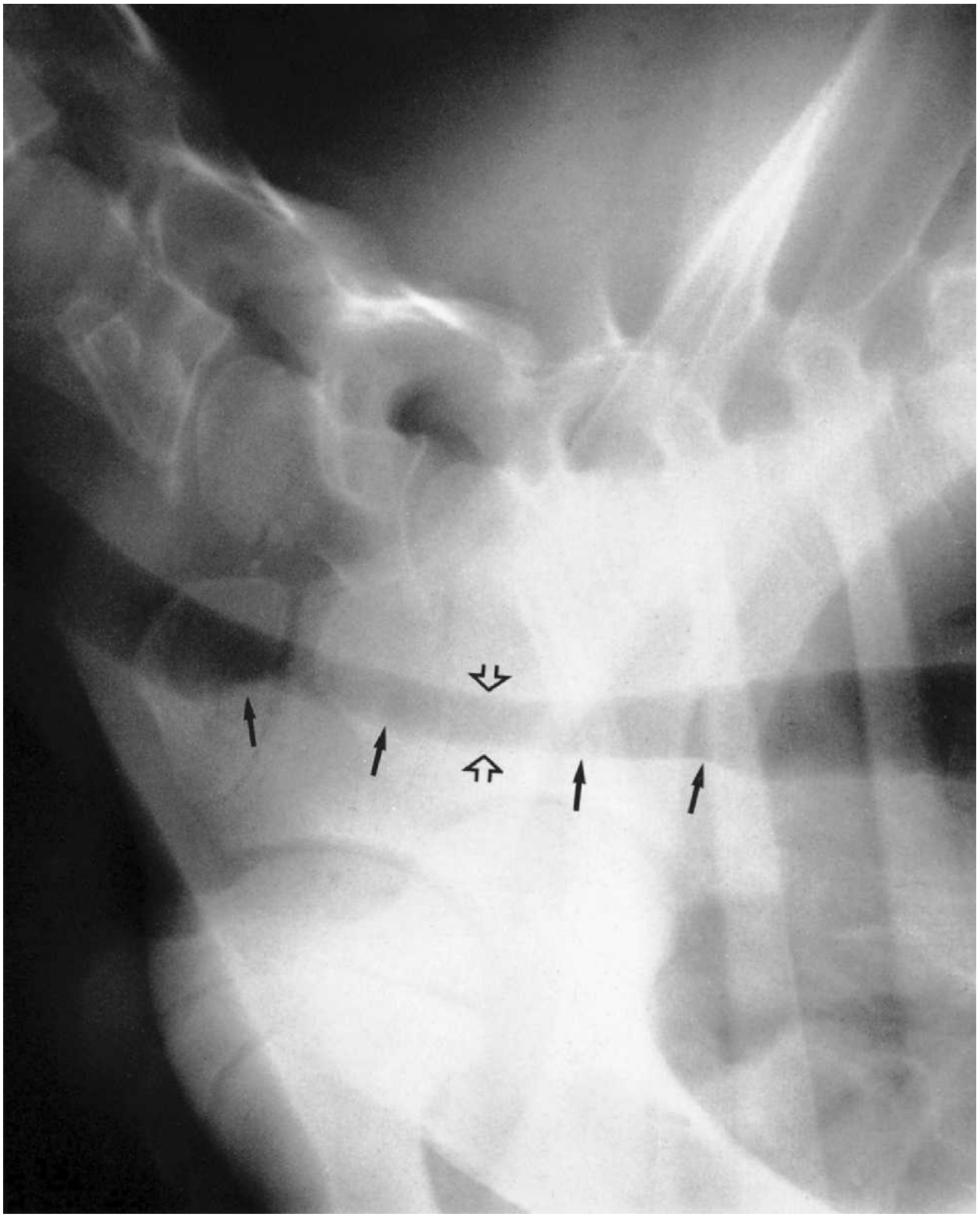


Figure 14.13 Lateral-lateral image of the thoracic inlet and cranial aspect of the thorax; cranial is to the left. Three-month-old Arab colt with chronic pneumonia. There is narrowing of the trachea to approximately 50% of its diameter (open arrows). A tracheal mass is demonstrated on the ventral tracheal wall (solid arrows). This mass may represent either a true intraluminal mass or material that is being expectorated. Note the open physes of the scapulae and humeri. Diagnosis: material in the trachea that is being expectorated from the lungs.

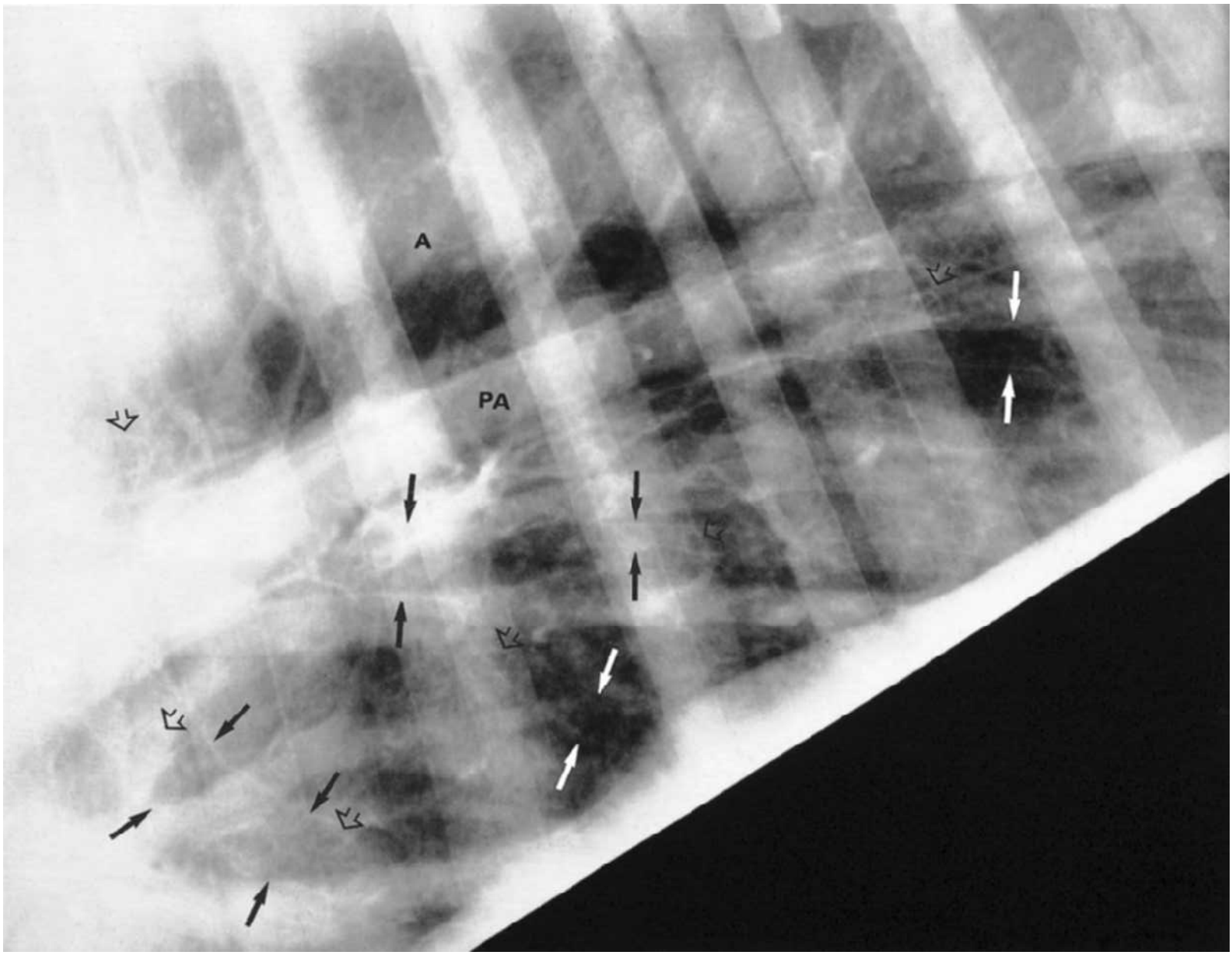


Figure 14.14 Lateral-lateral image of the caudal thoracic region; cranial is to the left. A 23-year-old Friesian mare with bronchiectasis and emphysema. The lungs are markedly overinflated and have large tortuous bronchi, between solid arrows (black and white). Thin-walled end-on bronchial structures are marked with open arrows. Only a few of the bronchi are marked. The aorta (A) and the pulmonary arteries (PA) are readily seen extending caudal to the periphery.

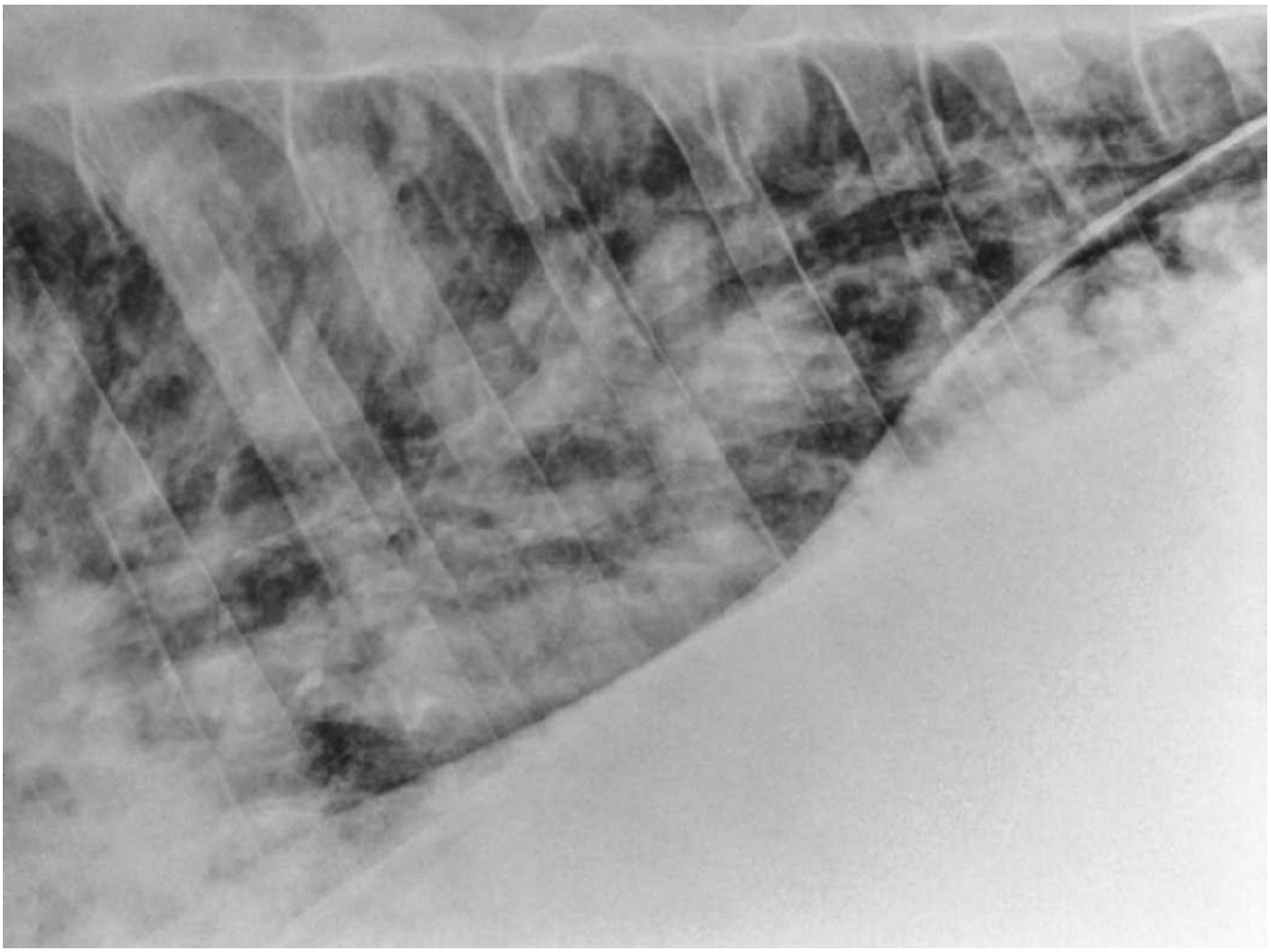


Figure 14.15 Lateral-lateral image of the dorsocaudal aspect of the thorax of a mature horse with dyspnoea. Cranial is to the left. There are multi-focal, opaque (fibrotic) nodules throughout the interstitium, and a diffuse interstitial pattern. The aorta is obscured. These abnormalities are consistent with multinodular pulmonary fibrosis.

the periphery of the lung, the nodules can be identified and characterised using ultrasonography. The less common form has larger, less numerous nodules to masses up to 8–10cm in diameter surrounded by more normal lung (Figure 14.15). This disease is associated with equine herpes virus-5.

Eosinophilic pneumonia

Idiopathic equine eosinophilic pneumonia can be difficult to differentiate from RAO clinically. Radiographs reveal a diffuse granular or miliary interstitial pattern (Figure 14.16). The identification of this pattern should prompt a diagnostic work-up to differentiate this from fungal pneumonia, neoplasia or silicosis (depending on geographic location).

Bacterial pneumonia

The radiographic appearance of bacterial pneumonia varies with the patient age, aetiological agent and route of transmission. In foals with pneumonia, including those associated with failure of passive antibody transfer or

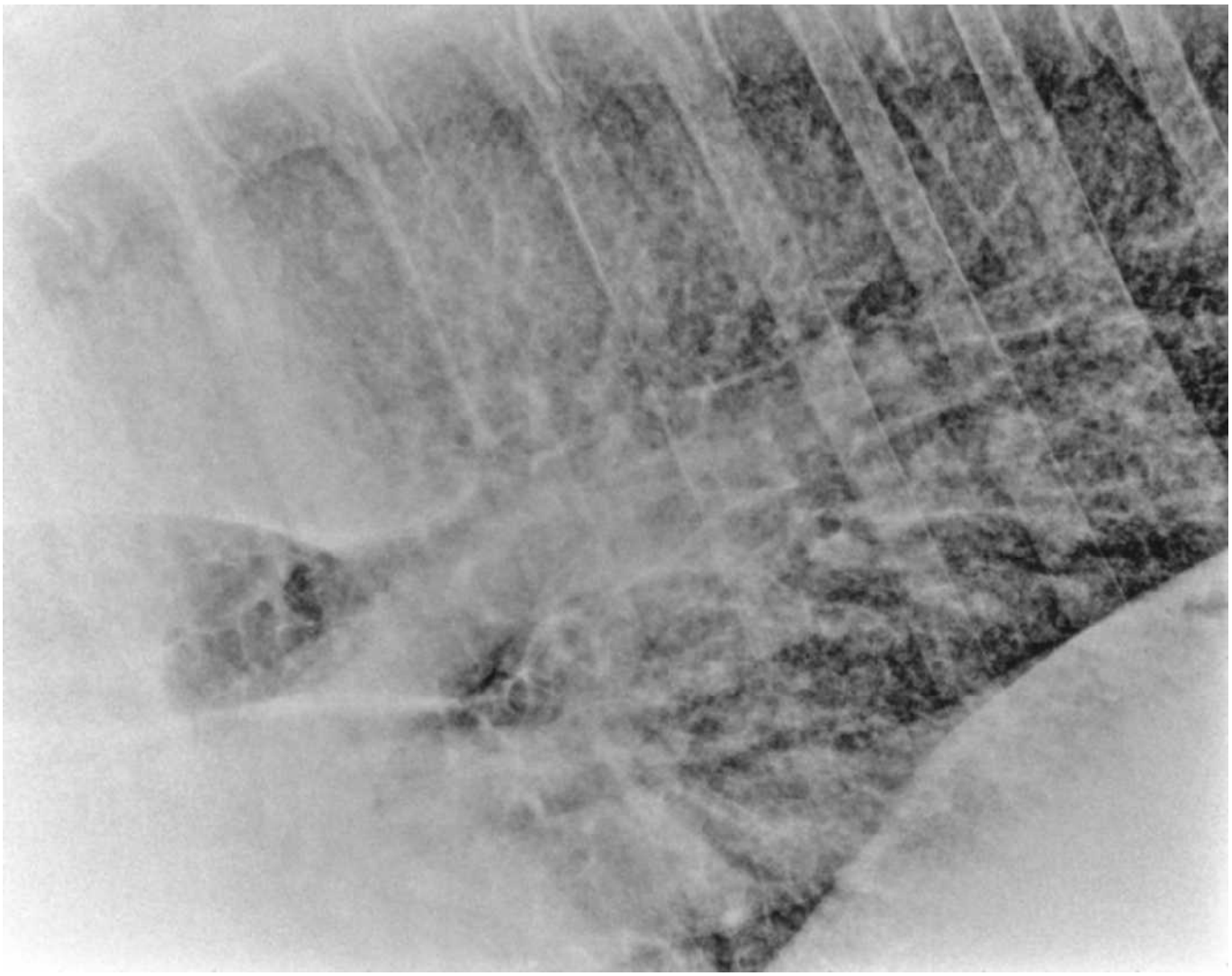


Figure 14.16 Lateral-lateral image of the dorsal caudal aspect of the thorax of a mature horse with poor exercise tolerance. Cranial is to the left. There is diffuse increased opacity throughout the lung fields, a diffuse miliary interstitial pattern. These abnormalities are consistent with eosinophilic pneumonia.

septicaemia, the distribution is most often ventral and bilateral. Haematogenous bacterial infections can be disseminated or patchy throughout the lung. The findings range from an unstructured interstitial pattern to pulmonary consolidation with air bronchogram formation (see Figures 14.7 and 14.20). Care should be taken to inspect the lung of the ventral aspect of the thorax, overlying the cardiac silhouette, because this is a frequent site of early pneumonia that can be difficult to detect. Although most bacterial pneumonias cannot be differentiated on the basis of radiographic signs, when nodular, mass or 'cottonball' lesions are present, particularly with cavitation, chronic *Rhodococcus* pneumonia should be considered (Figure 14.17). *Rhodococcus* pneumonia can have a highly variable radiographic appearance with all types of pulmonary patterns (bronchial, interstitial and alveolar). Nodule, mass (Figure 14.24) or cavitary lung lesion (Figures 14.4a and 14.4b) formation have also been described. Often the nodular or mass lesions have irregular and poorly defined borders, or are associated with surrounding interstitial infiltrates. With abscess

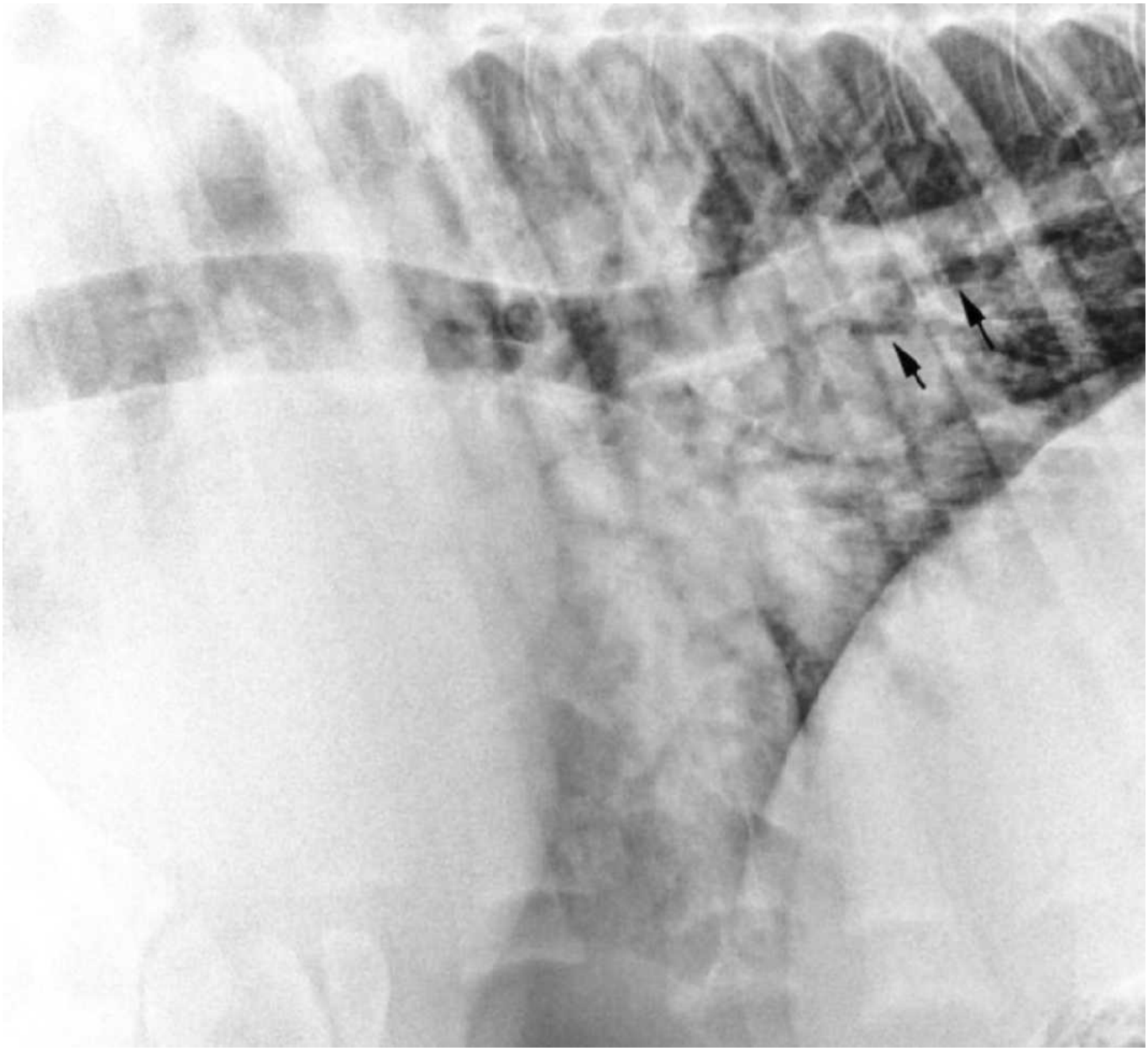


Figure 14.17 Lateral-lateral image of the thorax of a foal. Cranial is to the left. There are multiple large circular opacities. Cavitatory abscesses with a fluid line (arrows) can be identified. The caudal vena cava is partially obscured by 'cottonball' opacities. This is typical of the radiographic appearance of *Rhodococcus equi* pneumonia.

formation there is often cavitation (see 'Cavitary pulmonary lesions', above) and evidence of an air–fluid interface with a 'fluid line' in the cavity. With thick material in the abscess the dorsal margins may curve upwards, forming a meniscus.

In adult horses, bacterial pneumonia is occasionally associated with pleural effusion (pleuropneumonia). Ultrasonography plays a critical role in the evaluation of both the effusion and the underlying lung pathology (see 'Pleural effusion', above) (Figures 14.9 and14w.10b). Regions of consolidation, abscess formation or atelectasis are best identified using ultrasonography in conjunction with thoracic radiography. Chronic pleuropneumonia results in thickening of the pleura, with rounding of the lung margins. Horses

with pneumonia, with or without pleuropneumonia, can develop cavitary lung lesions or abscesses with anaerobic bacteria. Identification of cavitary lung lesions on radiographs is important, because this finding is associated with a poorer prognosis. Immunocompromised horses (e.g. those with pituitary pars intermedia dysfunction; PPID) can develop bacterial pneumonia that is variable in distribution, but characterised by patchy interstitial infiltrates in regions of alveolar consolidation. Rare cases of necrotising and infarctive bacterial pneumonia in adult horses have been associated with specific pathogens (*Klebsiella* sp. pneumonia) (Figure 14.18).

Bronchointerstitial pneumonia of foals/acute respiratory distress syndrome/ acute lung injury

It is currently unclear whether bronchointerstitial pneumonia of foals, acute respiratory distress syndrome (ARDS) and acute lung injury (ALI) are identical; however, the reported clinical and radiographic findings of these

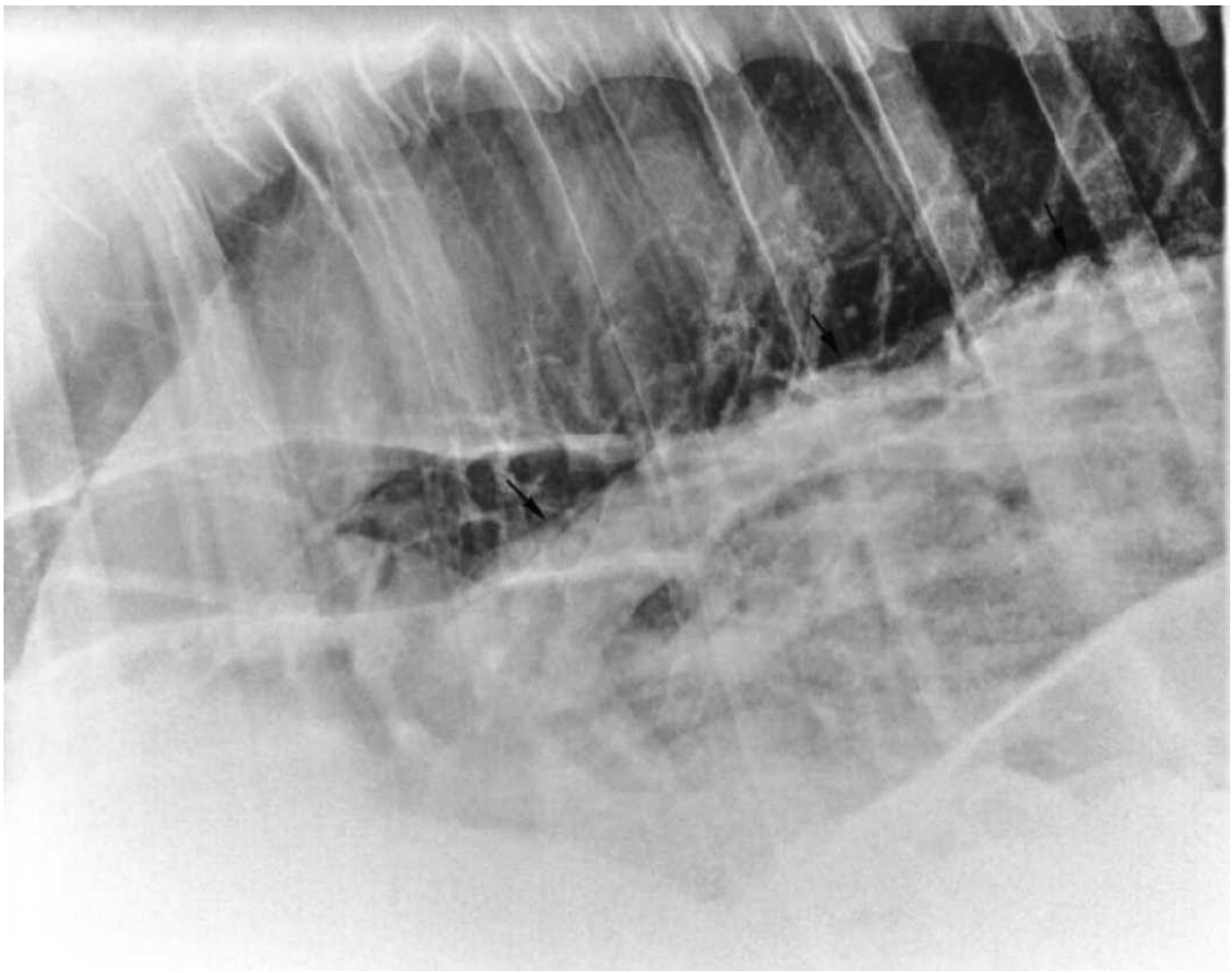


Figure 14.18 Lateral-lateral image of the dorsal aspect of the thorax of a mature horse with dyspnoea and pyrexia. Cranial is to the left. There is a region of diffuse increased opacity of the lung (arrows) with alveolar consolidation. This was associated with *Klebsiella* species pneumonia.

potentially serious syndromes are very similar. These conditions are seen in foals and weanlings and are generally associated with respiratory distress, increased respiratory rate and effort, and tachycardia. The radiographic findings are highly variable, but commonly include a diffuse, moderate to severe interstitial or bronchointerstitial pattern that can coalesce into irregularly margined, poorly defined nodular opacities (Figure 14.19). In severe cases, an alveolar pattern develops throughout the lung that is characterised by widespread opacity of the lung and occasional air bronchograms.

Fungal pneumonia

Fungal pneumonia is uncommon, but does occur in some geographical areas. In the southwest of the USA coccidiomycosis is associated with a variety of different systemic manifestations, but can present with a miliary to nodular pulmonary pattern, often with visible lymphadenomegaly.

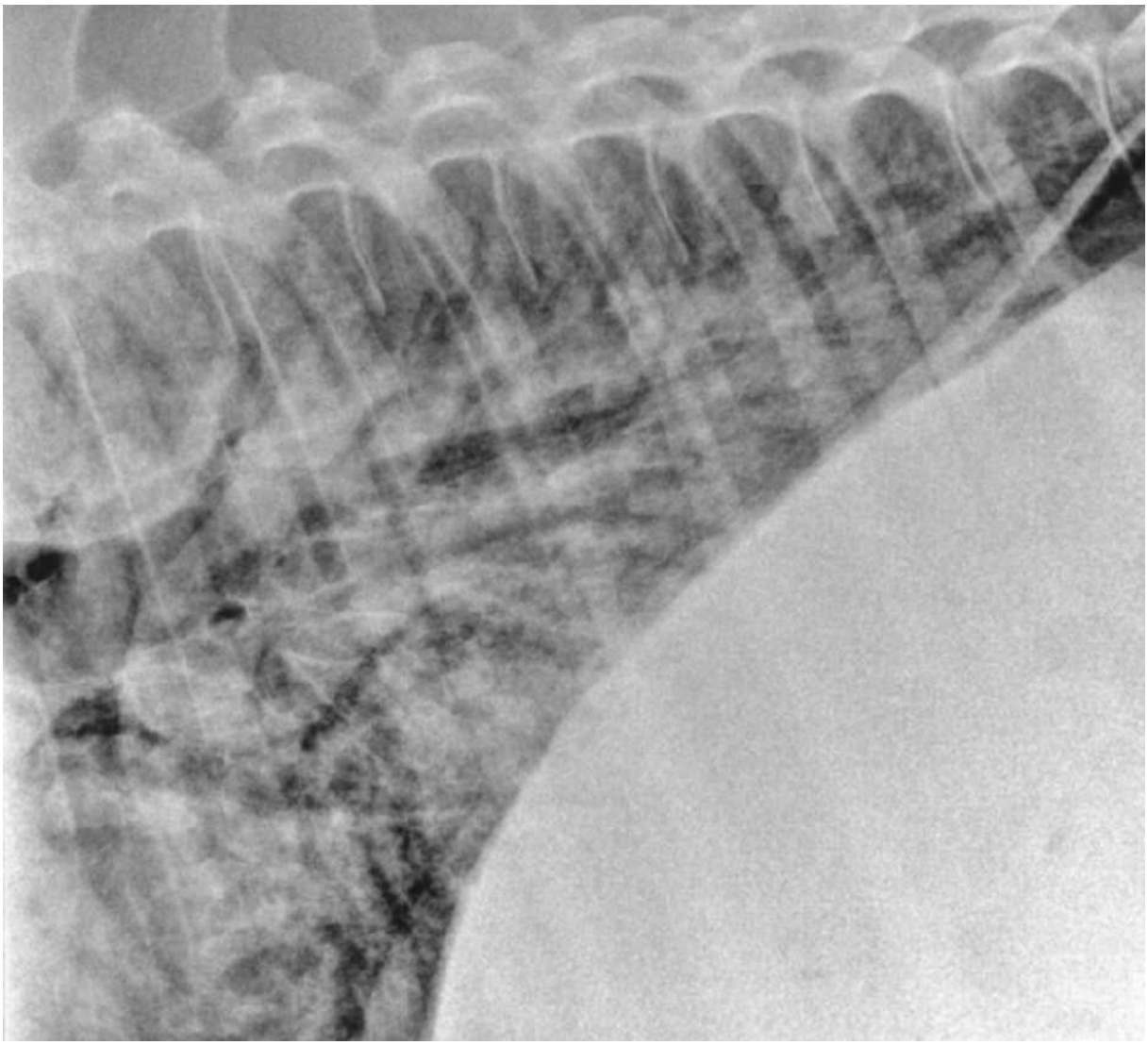


Figure 14.19 Lateral-lateral image of the thorax of a foal with dyspnoea. Cranial is to the left. There is a diffuse, severe interstitial and bronchointerstitial pattern. There are also some discrete rounded opacities. This is consistent with severe bronchointerstitial pneumonia, typical of acute respiratory distress syndrome.

Aspiration pneumonia

Aspiration pneumonia is almost always ventral in distribution, due to the aspiration of particulate matter, and is often associated with severe consolidation. It results in a generalised increase in lung opacity and loss of all lung detail except for air bronchogram formation (Figure 14.20; see also Figure 14.7). If aspiration occurs when the patient is in dorsal or lateral recumbency the distribution will be in the dependent portion of the lung at the time of aspiration. In these cases, determination of the cause of aspiration may help treatment.

Inhalation pneumonia

Inhalation pneumonia usually has a more dorsocaudal distribution compared with aspiration pneumonia, due to the non-particulate nature of the inhalant. In general, inhalation pneumonia is less consolidative than aspiration pneumonia and results in a more generalised interstitial pattern. If the inhalant is very irritating (smoke or toxic fumes), the lining of the air spaces may become so damaged that it results in oedema and alveolar flooding. Air bronchograms may then be seen in the consolidated lung.

Cavitary pulmonary lesions

A cavitary pulmonary lesion (CPL) is a term used to describe a cavity that occurs in the lung. In the horse the most common form is the result of abscess formation, liquefaction and loss of the fluid centre through a communicating bronchus (Figure 14w.21; see also Figures 14.4a and 14.4b). Cavitary pulmonary lesions are usually seen in young horses and have a thick opaque wall. Other abscesses or granulomata may also be seen. An air–fluid interface is often present. The lesions usually resolve with the associated pneumonia, but may be the last radiographic sign to disappear. The effect of geometric distortion is substantial and therefore positioning, phase of respiration and change due to growth of the patient must be taken into consideration when evaluating the size, progression and resolution of a CPL.

Other forms of CPL exist, but are rare in the horse. They include neoplastic, traumatic and congenital cavitary lesions or bullae (Figures 14.22 and 14.23). Neoplastic cavitary lesions have not been described in the horse, but might be difficult to distinguish from infective CPLs because both infectious and neoplastic CPLs have thick walls. Traumatic cavitary lesions (in other species) have walls that vary in thickness and usually resolve spontaneously. They may remain as thin-walled ring shadows, which in the horse might be hard to distinguish from an end-on bronchus, without a history of known thoracic trauma. Congenital CPLs in other species are usually thin walled and may contain some fluid. Any cavitary lesion may rupture and result in pneumothorax (see 'Pneumothorax', above), pneumomediastinum (see 'Pneumomediastinum', above), or other complications, depending on their content.

Pulmonary masses

Abscesses

In the horse the most common form of pulmonary masses are abscesses, which appear as opaque masses with or without a lucent gas cap dorsally (see Figure 14.4). Solitary abscesses may be quite large (Figure 14.24) and if

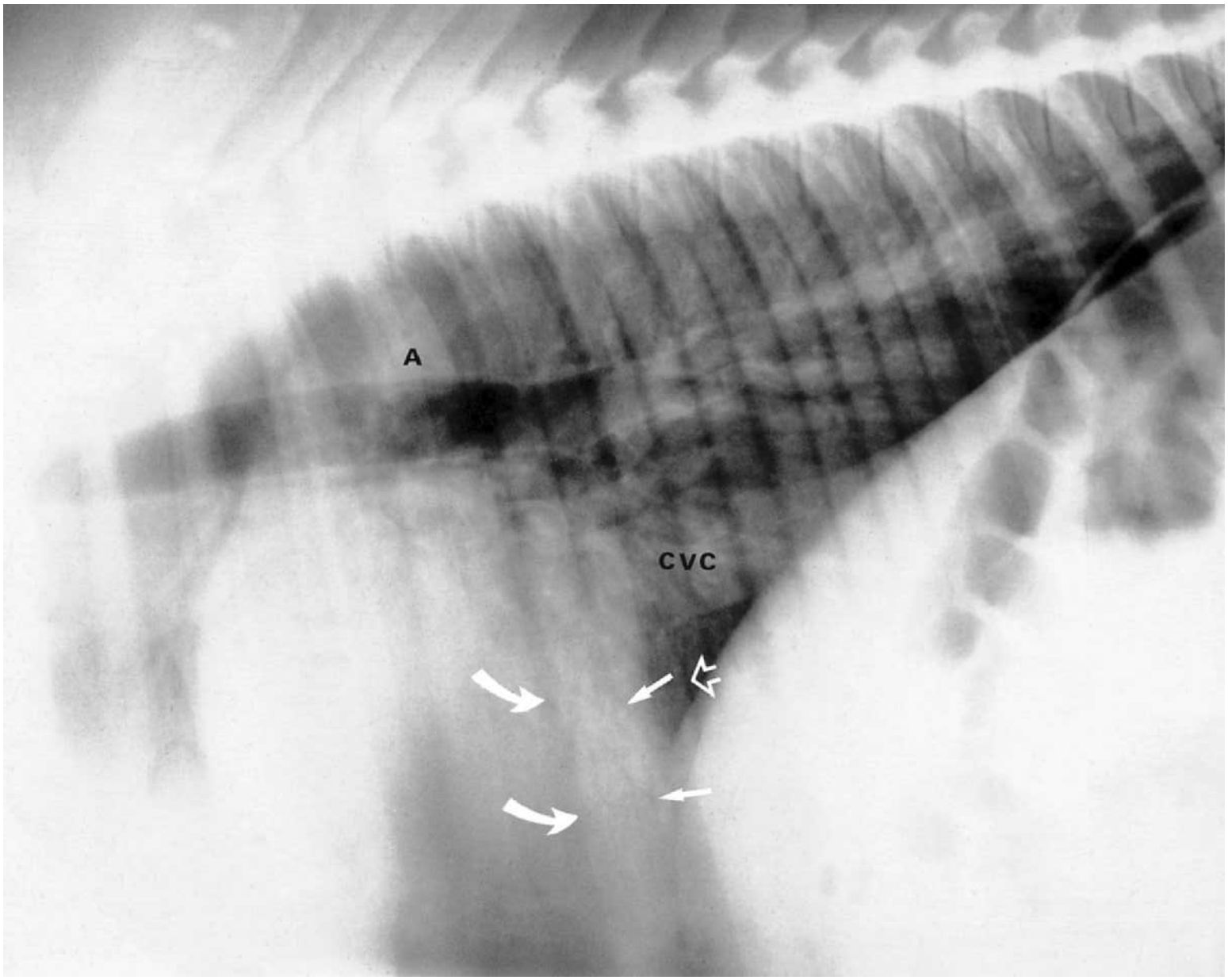


Figure 14.20 Right lateral-lateral recumbent image of the thorax of a newborn foal. Cranial is to the left. There is an interstitial pattern in all lung lobes and an alveolar pattern over the cardiac silhouette extending from the curved white arrows to the caudal aspect of the heart (open arrow), below the caudal vena cava (CVC). Straight white arrows demonstrate air bronchograms. The interstitial pattern obscures the aortic root (A). The bowel pattern is normal. Because of the ventral distribution and the air bronchogram formation, both aspiration and bacterial pneumonia should be considered.

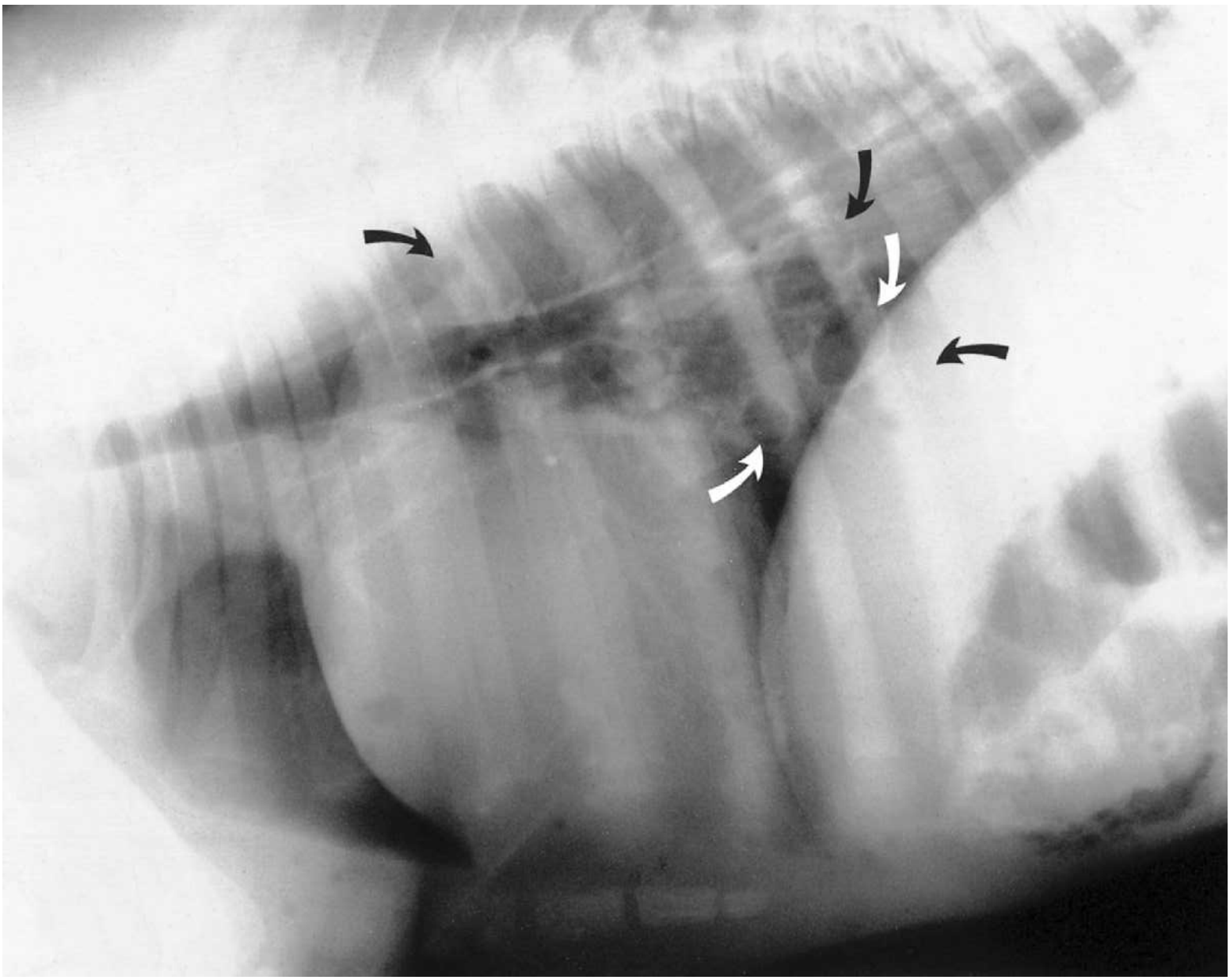
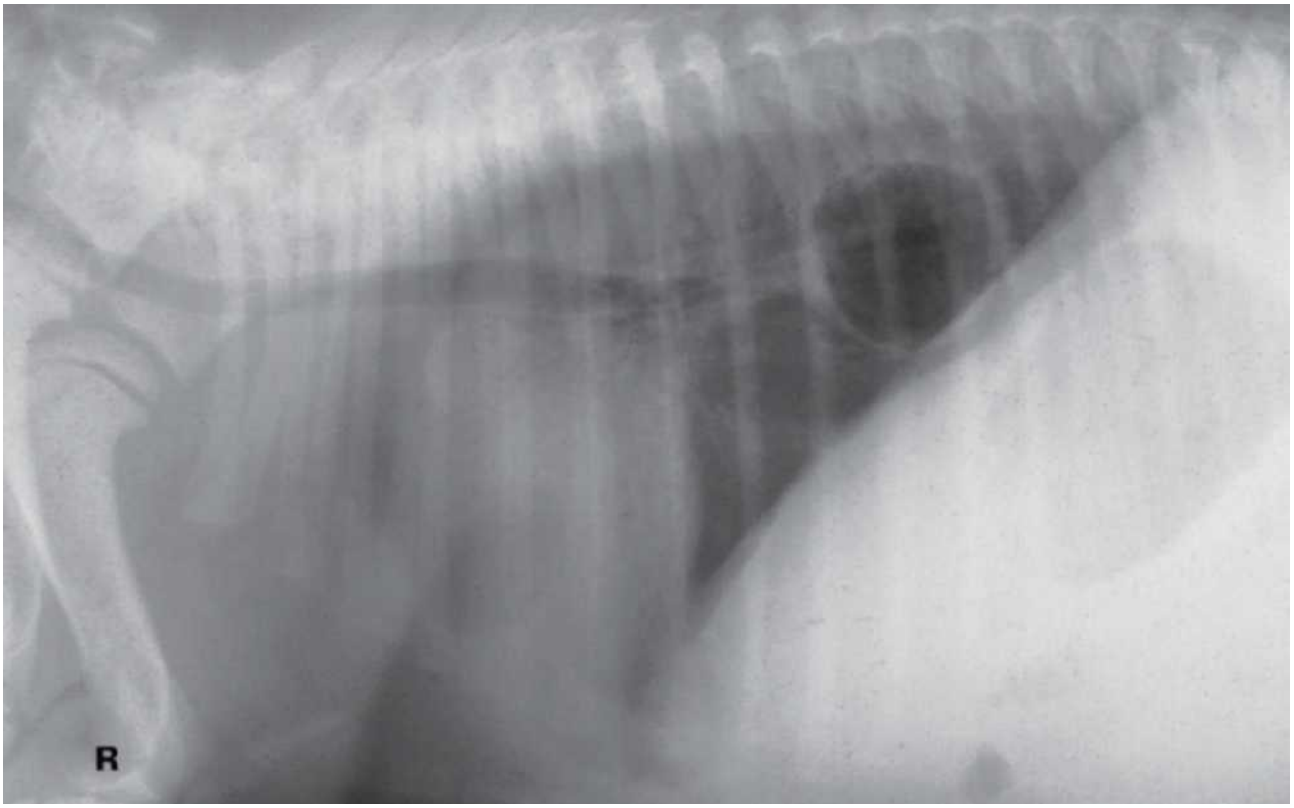
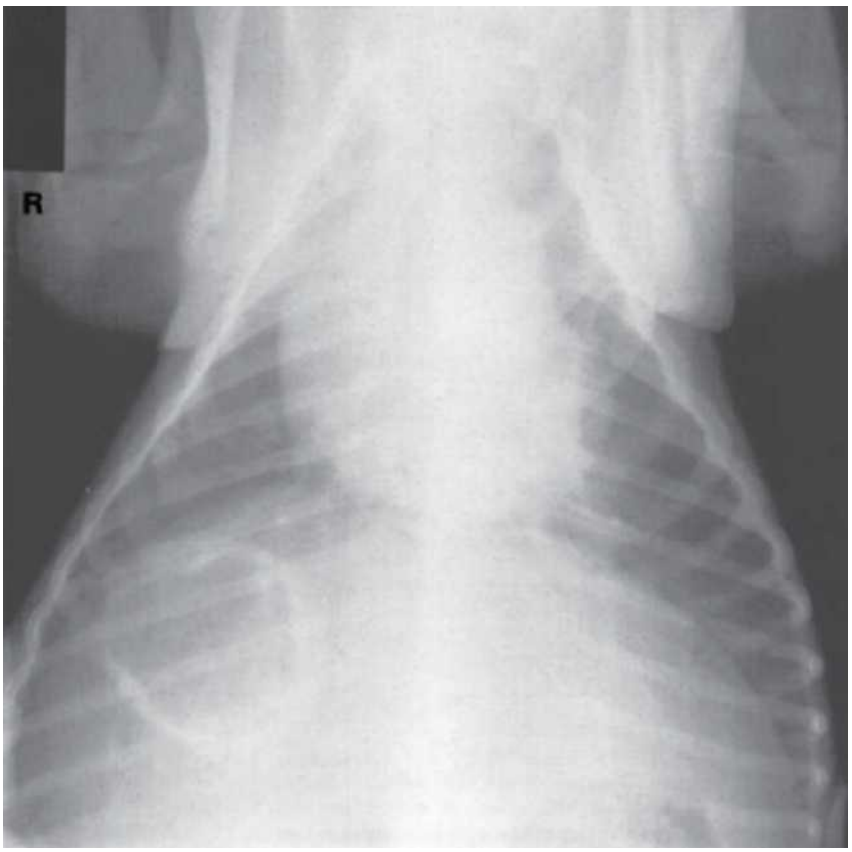


Figure 14.22 A foal born 2 weeks prematurely, with a profuse watery diarrhoea. Lateral-lateral image of the thorax; cranial is to the left. There are multiple, various-sized, thin-walled cavitary pulmonary lesions (white and black arrows). The cranial lung lobes are normal. The caudal lung lobes have an increase in both interstitial and bronchial markings, which are likely to be age-related, reflecting incomplete inflation. Diagnosis: multiple cavitary pulmonary lesions. The cavitary pulmonary lesions may represent a congenital cyst, resolving haematomas from a difficult parturition or, less likely, abscessation. Compare with Figures 14.2, 14.20 and 14.23.



(a)



(b)

Figure 14.23 Six-day-old miniature horse born prematurely, with *Salmonella* diarrhoea, but no clinical signs of respiratory disease. A lateral-lateral radiograph (cranial to the left) (a) shows a large, thick-walled air-filled bulla which can be seen in the caudal right lung lobe. The inner wall of the bulla is irregular. The remainder of the thorax is normal. A dorsoventral radiograph (right is to the left) (b) also demonstrates the lesion. Differential diagnosis should include a congenital bulla, or a pneumatocoele secondary to a haematoma, or an infarct. Abscessation is considered to be less likely, because of the lack of associated pulmonary disease. Compare this case with Figures 14.4a, 14.4b, 14.21 and 14.22. Diagnosis: congenital cavitary pulmonary lesion.

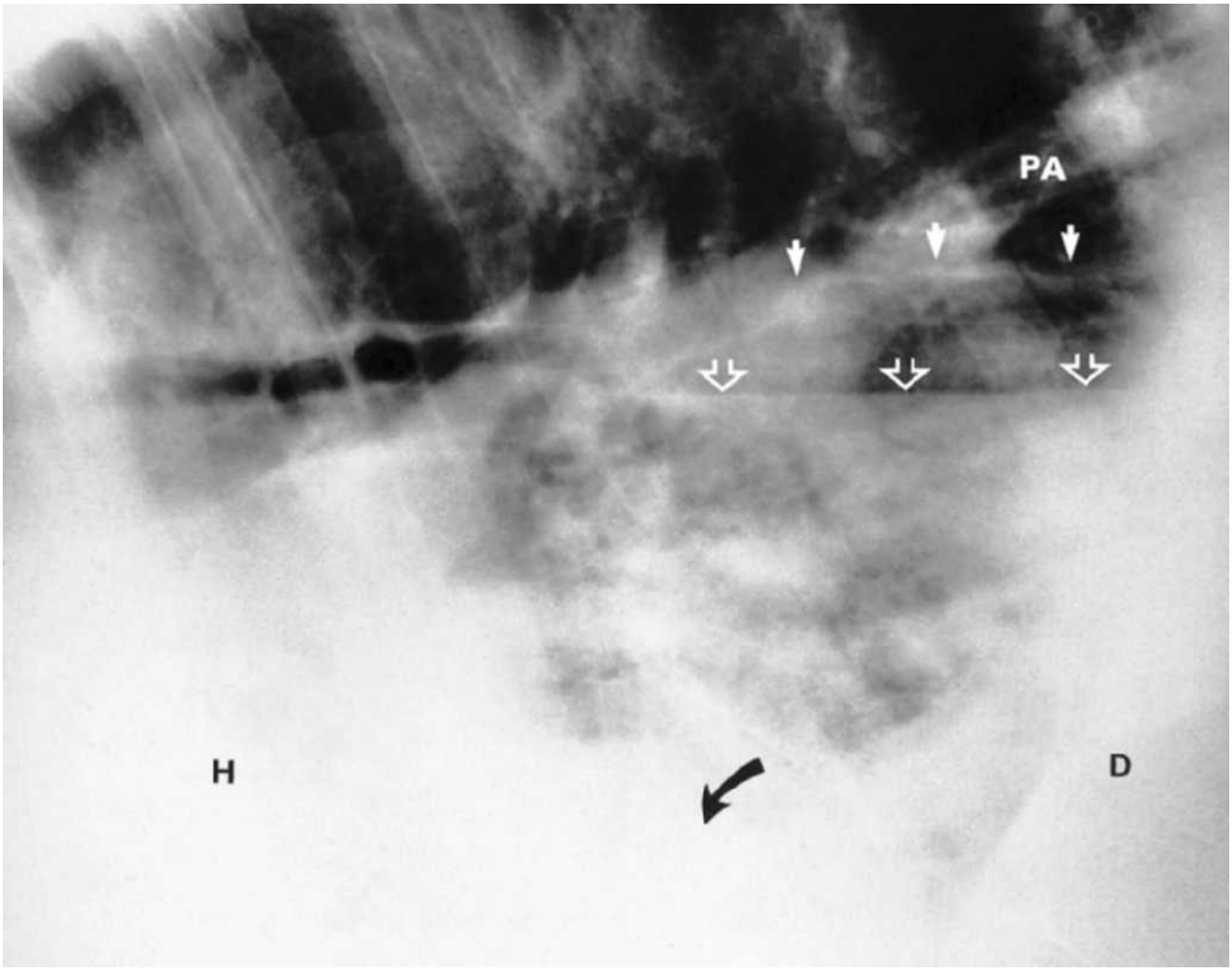


Figure 14.24 Two-year-old Thoroughbred stallion with a 3-week history of pleuropneumonia. Lateral-lateral image of the thorax; cranial is to the left. Twenty-two litres of fluid were drained from the left hemithorax the day before these radiographs were obtained. There is a large pulmonary abscess in the caudal ventral aspect of the thorax between the heart (H) and the diaphragm (D), ventral to the solid white arrows. There is a fluid line below the open arrows and an air space between the open arrows and the wall of the abscess (solid white arrows). The pulmonary arteries (PA) are marked. There is a generalised interstitial and bronchial pattern in the remainder of the thorax. Other smaller and less well-defined abscesses can be seen above the heart. They are poorly defined because they are in the right hemithorax and this radiograph is a right to left lateral-lateral projection in order to demonstrate the size and character of the larger abscess. A chest tube is in place in the thoracic cavity: the curved black arrow denotes the position of a metallic marker on the chest drain. Diagnosis: multiple pulmonary abscesses with a large cavitating abscess in the left hemithorax; hydrothorax.

cavitated may be confused with a hollow viscus from a diaphragmatic hernia (see Figure 14.26). Abscesses are always associated with other signs of infection including interstitial and usually alveolar infiltrates. In general they have irregular indistinct margins and may form CPLs (see 'Cavitary pulmonary lesions', above).

GRANULOMATA

Like abscesses, granulomata may be associated with other intrapulmonary disease, but may also be the only remnants of a previous more active disease. Granulomata are opaque and their margins may be more distinct than abscesses.

INFARCTS AND EMBOLISM

Infarcts and emboli occur occasionally, especially in the caudal dorsal lung lobes. They usually present as interstitial opacities with a somewhat triangular shape, with a sharply defined cranial margin and an indistinct periphery (Figure 14.25). Infarcts and exercise-induced pulmonary haemorrhage (EIPH) appear similar radiographically, but may be differentiated by obtaining serial radiographs. Infarcts persist, whereas increased opacity associated with EIPH resolves rapidly, unless EIPH is chronically recurrent.

METASTATIC LUNG DISEASE

Metastatic lung disease is occasionally seen as multiple circular opacities that vary in size and in the sharpness of their margins. The appearance of the metastatic lesion depends on the cell type of the original tumour, the

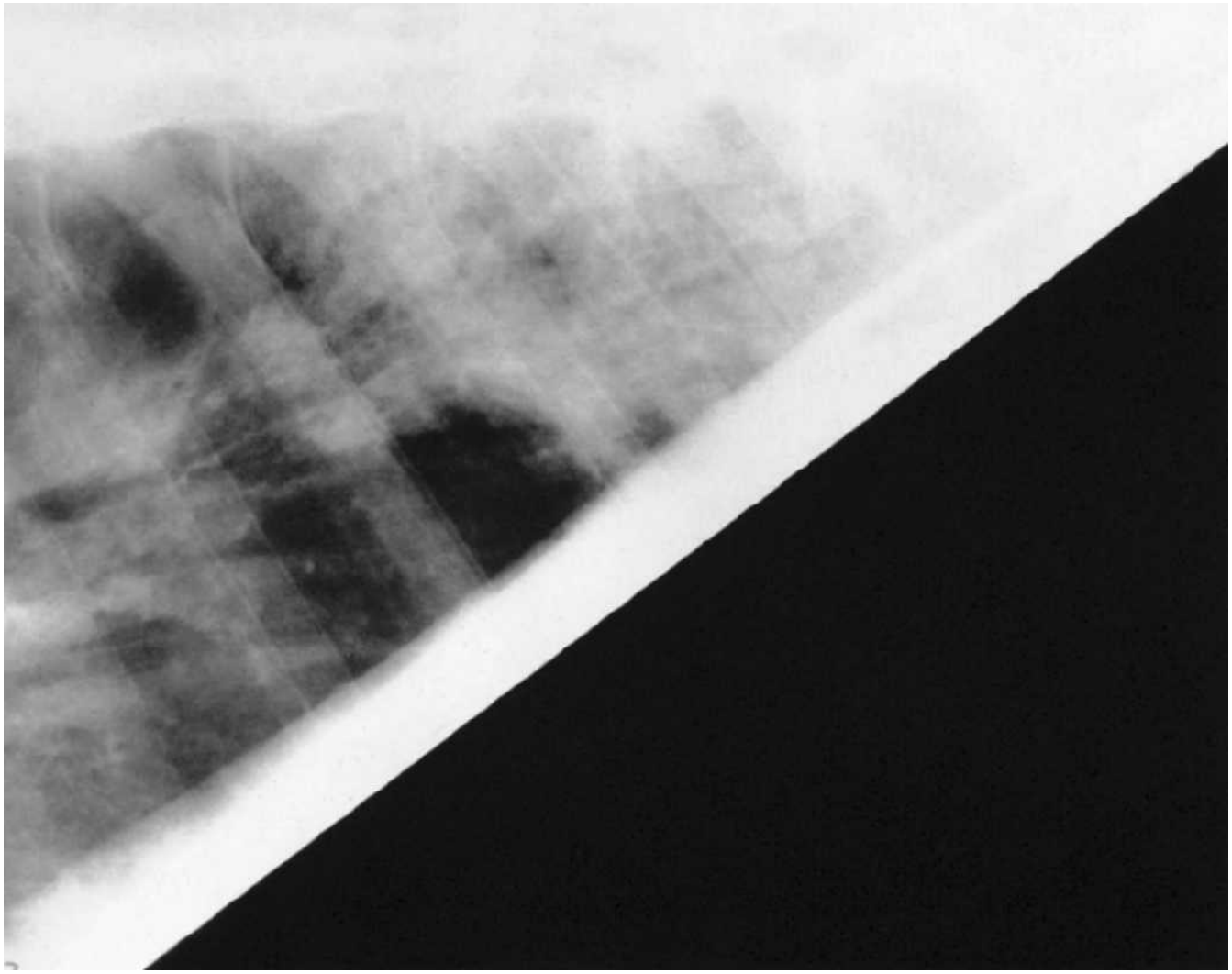


Figure 14.25 Three-year-old Thoroughbred filly with a history of chronic pleuritis and weight loss. Lateral-lateral image of the thorax; cranial is to the left. There is a caudodorsal lung mass of mixed interstitial and alveolar infiltrates. The cranial margins of the mass are well-circumscribed. The findings are suggestive of infarct or pulmonary haemorrhage. The possibility of bacterial pneumonia cannot be ruled out. The smooth margins cranially, the triangular shape and less distinct peripheral margins are more characteristic of infarct. Diagnosis: caudal thoracic mass, probably an infarct.

tumour-doubling time, the location of the nodule in the lung and whether there have been single or multiple showers of neoplastic cells. Solitary masses of 0.5 cm or less in diameter are usually missed, and masses as large as 2 cm in diameter may be overlooked. However, superimposition of multiple nodules of 1 cm or larger can usually be identified with careful examination.

PRIMARY LUNG TUMOURS

Primary lung tumours are rare but, when they occur, tend to be well-circumscribed and solitary. The most common lung tumour in the horse is adenocarcinoma. When present a tumour usually appears as a singular mass; these vary in size depending on the tumour-doubling rate and the length of time that they have been present. The tumour is usually quite large when found and may be seen as an incidental finding when examining the lung for other diseases. Tumours should be differentiated from abscesses, granulomata and resolving EIPH.

Exercise-induced pulmonary haemorrhage

The diagnosis of exercise-induced pulmonary haemorrhage (EIPH) is usually based on the presence of haemorrhage from the nostrils and in the bronchi on endoscopic examination immediately following strenuous exercise. Radiographic findings when present are limited to the caudodorsal aspect of the lungs and consist of interstitial opacities with a wispy appearance that often obliterate the thoraco-phrenic angle and summate with the diaphragmatic shadow. The opacities are usually more circumscribed toward the hilus and less well-defined toward the periphery. Resolution of haemorrhage is expected to occur rapidly, within approximately 7–10 days. Horses with chronic, repeated EIPH develop interstitial opacity that can persist over a much longer period and which may last for several months, with a gradual decrease in size and opacity.

Diaphragmatic hernia

Diaphragmatic hernias may be either congenital or acquired. Congenital diaphragmatic hernias may occur dorsally, in the mid-diaphragm on the left side, or ventrally, where they are usually larger. Although congenital hernias are reported to have smooth, well-rounded margins, this change is not seen radiographically. Large defects have been reported in foals with arthrogryphosis and scoliosis.

Acquired diaphragmatic hernias are usually associated with trauma or violent exercise (jumping) or increased intra-abdominal pressure (parturition, a fall, or colic). When signs of trauma are absent, consideration must be given to the existence of a congenital defect that has been exacerbated by exercise or increased intra-abdominal pressure.

There may be no clinical signs that relate to the diaphragmatic rupture immediately after the initial trauma. However, acute signs of abdominal distress (colic) or respiratory distress may be noted later.

The diagnosis of diaphragmatic hernia is made through the identification of displaced abdominal viscera within the thoracic cavity. This can include gas-capped fluid levels and bowel patterns in the ventral aspect of the thorax,

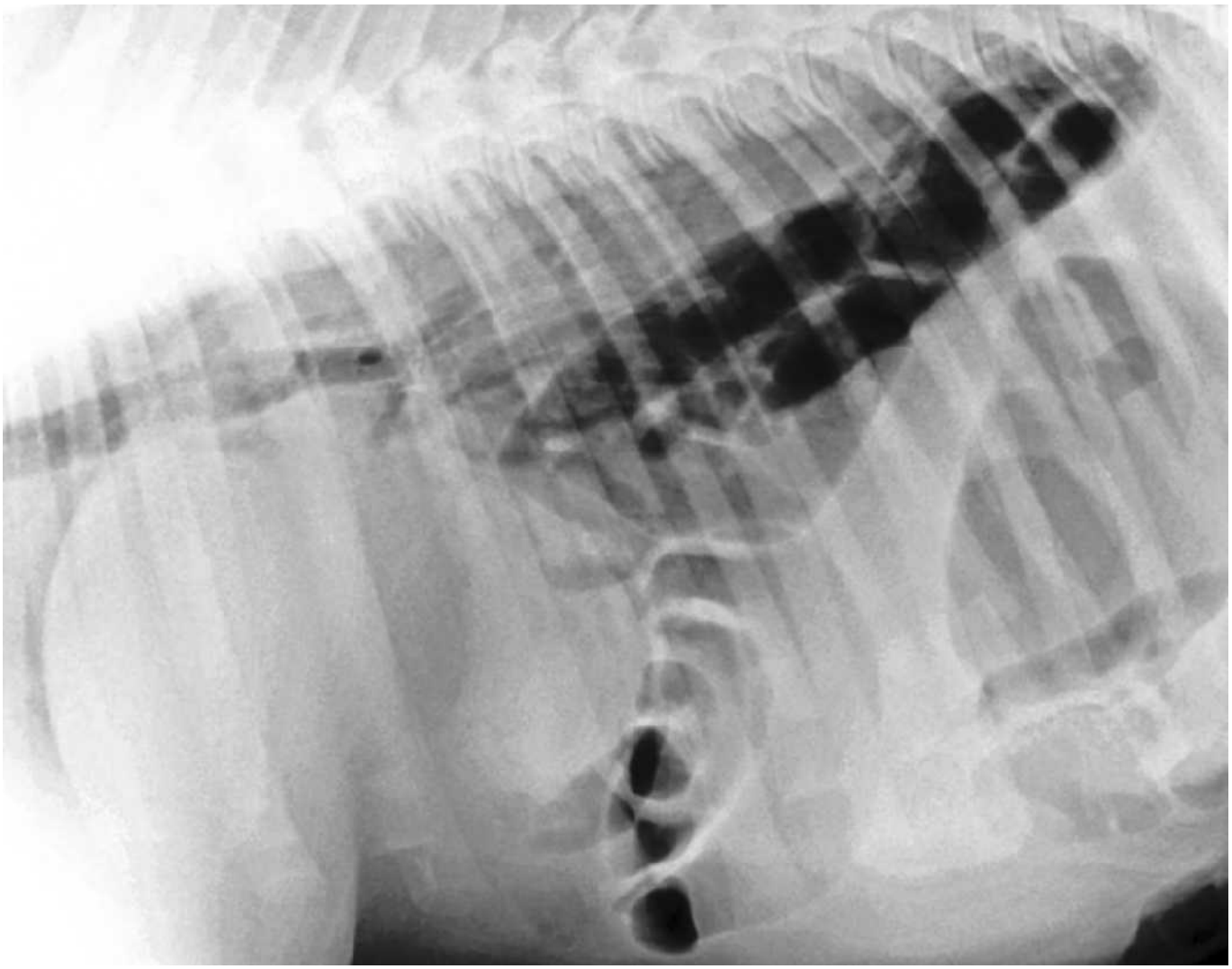


Figure 14.26 Lateral-lateral image of a thorax; cranial is to the left. Radiographic abnormalities characteristic of a diaphragmatic hernia in a foal. The caudal half of the thorax is occupied by gas-filled and fluid-filled loops of intestine. The lungs appear abnormally opaque dorsally due to compression and atelectasis.The caudal margin of the heart is obscured by superimposition of abdominal viscera. Source: Reproduced with permission of R. J. Hepburn.

with or without free fluid (Figure 14.26). Fluid opacities may be present when liver, spleen or omentum are in the thoracic cavity without accompanying bowel structures. Striations or crescent-shaped lines through gas-containing structures may indicate haustra of the large bowel. Normal structures such as the pulmonary vessels and the heart may be displaced by the presence of abdominal viscera in the thoracic cavity.

Laterality of the hernia may be determined by obtaining both right to left and left to right lateral-lateral projections of the thorax and comparing the image sharpness and magnification. Lesions or structures will be on the side in which they appear smaller and more sharply delineated. If laterality cannot be determined by this method, the defect may be near the midline.

Ultrasonographic evaluation can aid in differentiating diaphragmatic hernias from other disease, as well as defining the structures that have been displaced.

Cardiac diseases

In general, cardiac disease in the large equine patient does not lend itself to radiographic diagnosis, and diagnostic ultrasonography is usually much more valuable. Congenital cardiac disease may occasionally be diagnosed in the foal (Figure 14.27). Left-sided heart dysfunction leads to over-perfusion of the pulmonary vasculature, culminating in cardiogenic pulmonary oedema. Radiographically, enlarged pulmonary vasculature with patchy moderate interstitial infiltrates to patchy alveolar pattern can be seen. The pulmonary infiltrates may be more pronounced toward the hilus. Right-sided heart dysfunction, including that caused by pericardial disease, results in systemic vascular congestion (jugular/vena cava distension/liver congestion), that is unlikely to be identified on thoracic radiographs. Chronic pulmonary disease is associated with pulmonary hypertension that can result in enlarged and tortuous pulmonary vasculature. This is also a rare radiographic diagnosis. Congenital cardiac disease may occasionally be diagnosed in a foal using radiographs (Figure 14.27), but more frequently diagnosis is by ultrasonography. Valvular, myocardial and pericardial disease, congenital septal defects and complex cardiac anomalies can be characterised using cardiac ultrasonography. Radiography is dependent on the identification of secondary signs, such as changes in size of the cardiac silhouette, pulmonary vascular size, or pulmonary oedema. Cardiac silhouette enlargement may also be inferred by identification of displacement of adjacent intra-thoracic structures, such as the trachea, carina and great vessels.

Thoracic wall or rib lesions

TRAUMA OR RIB FRACTURES

The identification of rib fractures on radiographs is difficult. In horses with known thoracic trauma, radiographs can be centred over the region of interest and the generator settings adjusted to a higher mAs setting to allow for greater contrast. Similarly, if the site of trauma is known, ultrasonography can be used to make the diagnosis. Radiographic signs of rib fractures include rib incongruency, malalignment or, in more chronic cases, findings of rib thickening or callus/periosteal proliferation.

Ultrasonography provides a detailed evaluation of the external surface of the rib that is disrupted with a fracture. When there is no known history of thoracic wall trauma, rib fractures are more difficult to detect, and nuclear scintigraphy can be useful.

Cranial rib fractures may also manifest as abnormal behaviour when being tacked up or mounted, ipsilateral forelimb lameness, abduction of the limb during protraction, or muscle atrophy. Caudal rib fractures may manifest as respiratory pain or performance problems.

With recent fractures it is important to consider whether other lesions may be present, such as haemothorax, pneumothorax, pulmonary contusion, or even myocardial contusion.

Fractures may persist as chronic non-union fractures due to motion. The ends of the opposing ribs may appear slightly flared adjacent to the lucent fibrous union. A report detailing 25 rib lesions identified using scintigraphy showed that just over one half were present in the first rib. Images of the first

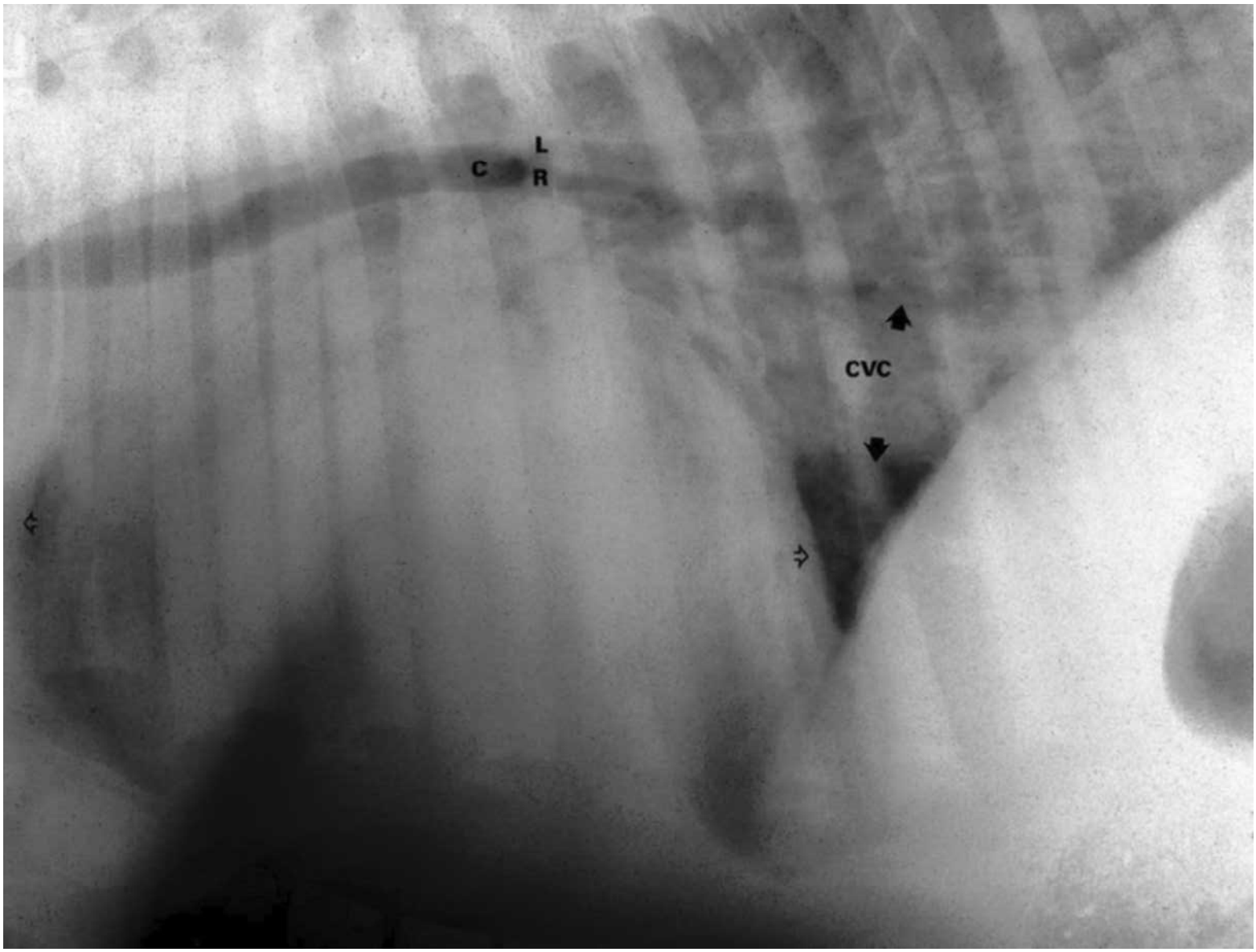


Figure 14.27 A 45-day-old Thoroughbred colt with harsh lung sounds and poor growth. Lateral-lateral image of the thorax; cranial is to the left. There is cardiac enlargement with dorsal displacement of the trachea just cranial to the carina (C). The left mainstem bronchus (L) is slightly elevated over the right (R). The caudal vena cava (CVC) is markedly dilated (solid arrows). There is a generalised increase in pulmonary interstitial infiltrates in all lung lobes. This results in an overall opacification of the lungs. The cranial and caudal margins of the cardiac silhouette are marked with an open arrow. Diagnosis: congenital right and left heart enlargement with congestive heart failure.

rib may best be acquired by using the technique described for radiography of the shoulder (see Chapter 8, 'Scapulohumeral (shoulder) joint and humerus – Radiographic technique').

Rib fractures also occur in foals, usually as a complication of parturition. The most common location is near to, or at, the costochondral junction. In a comparative study, ultrasonography was more sensitive than radiographs for their identification. Dorsoventral or ventrodorsal radiographic projections are more sensitive than lateral-lateral projections for detection of rib fractures.

OSTEOMYELITIS

Rib osteomyelitis can occur as a result of haematogenous bacterial or fungal infection, or it can be associated with thoracic wall trauma. Lesions are often lytic with poor lesion margination. Ultrasonography is also useful for diagnosis.

CONGENITAL MALFORMATION OF RIBS

Occasionally congenital malformation of one or more ribs is identified. These are usually characterised by smoothly marginated abnormal shape and are often asymptomatic unless associated soft-tissue abnormalities involve the brachial plexus.

TUMOURS

When productive lesions are noted on the ribs or when a pleural mass appears to be associated with a rib, chondrosarcoma should be considered. These tumours may simply appear as a mass, and it may be difficult to define either bone destruction or production, although both components are usually present.

MULTIPLE OSTEOCHONDROMATA

Multiple hereditary osteochondromatosis has been reported in the horse and should be suspected when smoothly marginated bone protrusions are noted on flat bones. Other osteochondromata may be found on long bones (see Chapter 7, 'New bone formation' and Chapter 8, 'Osteochondroma of the distal aspect of the radius'). Osteochondromata are not usually of any clinical significance, but they may be considered to be potentially pre-cancerous growths.

Also see 'Hypertrophic osteopathy' in Chapter 1.

Sternum

Lateral-lateral views of the sternum can be obtained using portable x-ray equipment. Digital systems are recommended, but adequate images may be obtained using rare earth screens and appropriate film. The sternum is best radiographed with one forelimb protracted to minimise the amount of soft tissues that the x-ray beam has to penetrate. The x-ray beam is centered caudal to the elbow approximately 10cm proximal to the ventral aspect of the thorax.

At birth the sternum consists of seven bony segments, sternebrae, which are united by intersternebral cartilages. The two most caudal sternebrae fuse

by approximately 3 months of age, but the remainder only partially fuse. Only the caudal one-third to one-half of the sternum can be easily seen radiographically because the structures of the forelimb overlie it cranially. The sternum inclines ventrally from cranial to caudal (Figure 14.28a). The dorsal border is straight, whereas the ventral border is smoothly curved with indentations at the site of the intersternebral articulations. The most caudal aspect of the sternum is rather variable in shape among horses, being pointed, or slightly rounded. The so-called costal cartilages are mineralised and are seen radiographically. They articulate with the ribs dorsally.

Radiographic abnormalities of the sternum, costal cartilages or ribs are not common, but have been identified in horses demonstrating abnormal behaviour when tacked up or mounted. Abnormalities include a fracture of a costal cartilage, fragmentation of the most caudal aspect of the sternum (Figure 14.28b) and irregular intersternebral articulations.

Additional figures

The book companion website at www.clinical-radiology-horse.com includes additional figures that are not included in the printed book or e-book formats. Please see '**About the Companion Website**' at the start of the book for details on how to access the website. These figures are prefixed with the letter 'w' in the printed book, e.g. Figures 1w.4c–f.

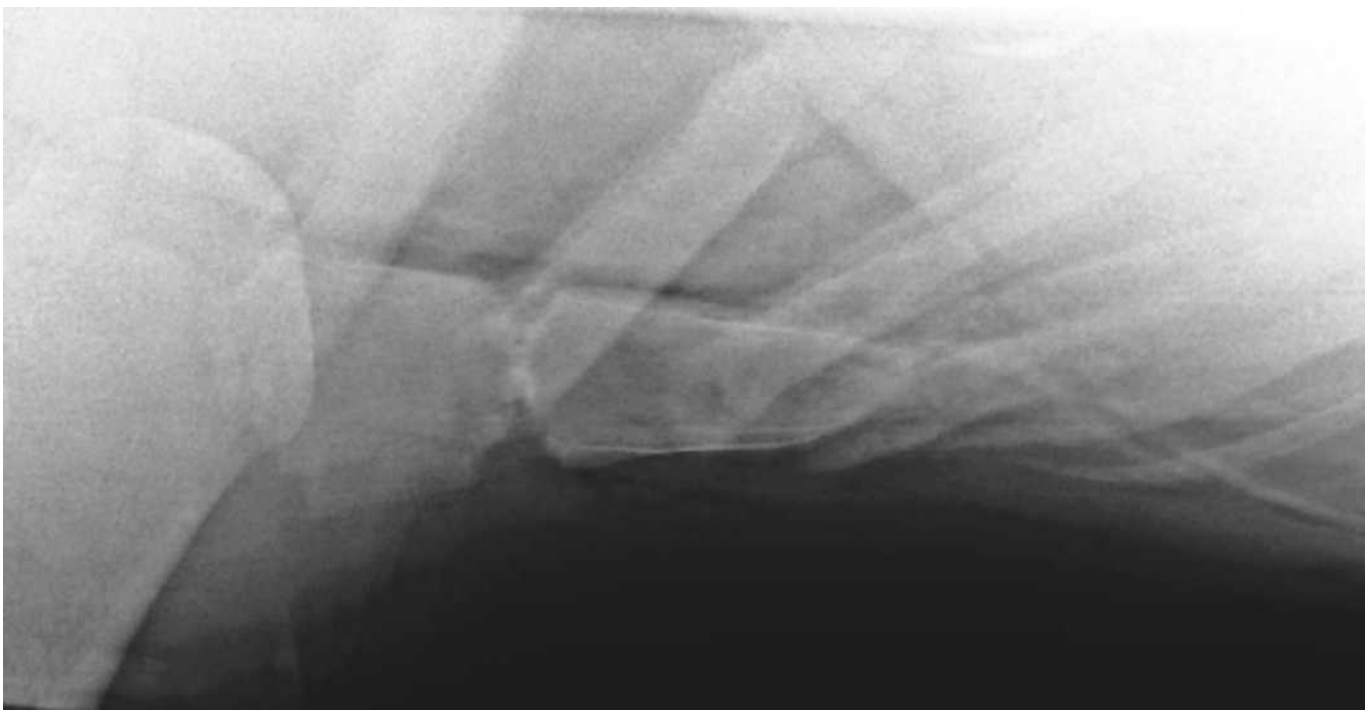


Figure 14.28(a) Lateral-lateral image of the caudal one-third of the sternum and the costal cartilages of a normal adult horse. Cranial is to the left. Note the indentations ventrally at the intersternebral articulations.



Figure 14.28(b) Lateral-lateral image of the caudal aspect of the sternum of a mature polo pony. Cranial is to the left. There is fragmentation at the most caudal aspect of the sternum (compare with Figure 14.28a). The pony had shown a sudden onset of violent bucking behaviour when tacked-up or when mounted. When re-examined 6 weeks later, the sternum had modelled considerably; the pony resumed full work without recurrence of abnormal behaviour.

FURTHER READING

Ainsworth, D., Eicker, S., Yeagar, A., et al. (1998) Associations between physical examination, laboratory and radiographic findings and outcome and subsequent racing performance of foals with *Rhodococcus equi* infection: 115 cases (1984–1992). *J. Am. Vet. Med. Ass.* **213**, 510–515

Ainsworth, D., Erb, H., Eicker, S., et al. (2000) Effects of pulmonary abscesses on racing performance of horses treated at referral veterinary medical teaching hospitals: 45 cases (1985–1997). *J. Am. Vet. Med. Ass.* **216**, 1282–1287

Boy, M., Sweeney, C. (2000) Pneumothorax in 40 cases (1980–1997). *J. Am. Vet. Med. Ass.* **216**, 1965–1967

Back, H., Kendall, A., Grandon, R., et al. (2012) Equine multinodular pulmonary fibrosis in association with asinine herpesvirus type 5 and equine herpesvirus type 5: a case report. *Acta Vet. Scand.* **54**, 57

Bell, S., Drew, C., Wilson, D., Pusterla, N. (2008) Idiopathic chronic eosinophilic pneumonia in 7 horses. *J Vet. Intern. Med.* **22**, 648–653

Buergelt, C.D., Hines, S.A., Cantor, G., Stirk, A., Wilson, J.H. (1986) A retrospective study of proliferative interstitial lung disease of horses in Florida. *Vet. Pathol.* **23**, 750–756

Carlsten, J. (1986) Imaging of the equine heart. An angiographic and echocardiographic investigation. Thesis, Uppsala, Sweden, Merkantil-Tryckeriet AB, Uppsala

Carlsten, J., Kvart, C., Jeffcott, L.B. (1984) Method of selective and non-selective angiocardiography for the horse. *Equine Vet. J.* **12**, 47–52

Carr, E., Carlsen, G., Wilson, D., Reed, D. (1997) Acute haemorrhagic pulmonary infarction and necrotizing pneumonia in horses: 21 cases (1967–1993). *J. Am. Vet. Med. Ass.* **210**, 1774–1778

Cook, G., Divers, T., Rowland, P. (1995) Hypercalcaemia and erythrocytosis in a mare with associated metastatic carcinoma. *Equine Vet. J.* **27**, 316–318

Farrow, C.S. (1981a) Equine thoracic radiology. *J. Am. Vet. Med. Ass.* **179**, 776–781

Couetil, L., Hodgson, J., Buechner-Maxell, V., Viel, L., Wood, J., Lavoie, J.-P. (2007) ACVIM Consensus Statement: Inflammatory Airway Disease of Horses. *J. Vet. Intern. Med.* **21**, 356–361

Dahlberg, J., Ross, M., Martin, B., Davidson, E., Leitch, M. (2011) Clinical relevance of abnormal scintigraphic findings of adult equine ribs. *Vet. Radiol. Ultrasound* **52**, 573–579

Dunkel, B., Dolente, B., Boston, R. (2005) Acute lung injury/acute respiratory distress syndrome in 15 foals. *Equine Vet. J.* **37**, 435–440

Farrow, C.S. (1981b) Radiography of the equine thorax: anatomy and technique. *Vet. Radiol.* **22**, 62–78

Farrow, C.S. (1981) Radiographic aspects of inflammatory lung disease in the horse. *Vet. Radiol.* **22**, 107–114

Farrow, C.S. (1976) Pneumomediastinum in the horse: a complication of transtracheal aspiration. *Vet. Radiol.* **17**, 192–195

Farrow, C.S. (1982) Inhalation pneumonia in a horse. *Can. Vet. J.* **23**, 340–341

Gehlen, H., Stadler, P., Ohnesorge, B. (2005) Tracheal obstruction in a horse with oesophageal stenosis and diverticulum. *Equine Vet. Educ.*, **17**, 132–134

Gronvold, A., Ihler, C., Hanche-Olsen, S. (2005) Conservative treatment of tracheal perforation in a 13 year old hunter stallion. *Equine Vet. Educ.* **17**, 142–145

Hillidge, C.J. (1986) Review of *Corynebacterium* (*Rhodococcus*) *equi* lung abscess in foals: pathogenesis, diagnosis and treatment. *Vet. Rec.* **119**, 261–264

Jean, D., Lavoie, J.-P., Nunez, L., Lagace, A. (1994) Cutaneous haemangiosarcoma with pulmonary metastasis in a horse. *J. Am. Vet. Med. Ass.* **204**, 776–778

Jean, D., Picandet, V., Macieira, S., Beauregard, G., D'Anjou, M., Beauchamp, G. (2007) Detection of rib trauma in newborn foals in an equine critical care unit: a comparison of ultrasonography, radiography and physical examination. *Equine Vet. J.* **39**, 158–163

Jorgensen, J., Geoly, F., Berry, C., Breuhaus, B. (1992) Lameness and pleural effusion associated with an aggressive fibrosarcoma in a horse. *J. Am. Vet. Med. Ass.* **210**, 1328–1331

Kangstrom, L.E. (1968) The radiological diagnosis of equine pneumonia. *Vet. Radiol.* **9**, 80–88

Kohn, C.W. (1981) Recognition and management of equine viral respiratory disease. *Compend. Contin. Educ.* **3**(3), 73–81

Kosch, P.C., Koterba, A.M., Coons, T.J., Webb, A.I. (1984) Developments in management of the newborn foal in respiratory distress 1: Evaluation. *Equine Vet. J.* **16**, 312–318

Koterba, A.M., Brewer, B.D., Tarplee, F.A. (1984) Clinical and clinicopathological characteristics of the septicaemic neonatal foal: review of 38 cases. *Equine Vet. J.* **16**, 376–383

Kvart, C., Carlsten, J., Jeffcott, L.B., Nilsfors, L. (1985) Diagnostic value of contrast echocardiography in the horse. *Equine Vet. J.* **17**, 357–360

Lakritz, J., Wilson, W., Berry, C., Schrenzel, M., Carlson, G., Madigan, J. (1993) Bronchointerstitial pneumonia and respiratory distress in young horses: clinical, clinicopathologic, radiographic, and pathological findings in 23 cases (1984–1989). *J. Vet. Intern. Med.* **7**, 277–288

Lamb, C.R., O'Callaghan, M.W., Pradis, M.R. (1990) Thoracic radiography in the neonatal foal: a preliminary report. *Vet. Radiol.* **31**, 11–16

Lavoie, J., Fiset, L., Laverty, S. (1994) Review of 40 cases of lung abscesses in foals and adult horses. *Equine Vet. J.* **26**, 348–352

Mair, T. (1991) Treatment and complications of pleuropneumonia. *Equine Vet. J.* **23**, 5

Mair, T., Hillyer, M., Brown, P. (1992) Mesothelioma of the pleural cavity in a horse. *Equine Vet. Educ.* **4**, 59–61

Mair, T., Rush, B., Tucker, R. (2004) Clinical and diagnostic features of thoracic neoplasia in the horse. *Equine Vet. Educ.* **16**, 30–36

Marenzoni, M., Passamonti, F., Lepri, E., et al. (2011) Quantification of Equid herpesvirus 5 DNA in clinical and necropsy specimens collected from a horse with equine multinodular pulmonary fibrosis. *J. Vet. Diagn. Invest.* **23**, 802–806

Martens, R.J., Martens, J.G., Fiske, R.A. (1989) *Rhodococcus equi* foal pneumonia: pathogenesis and immunoprophylaxis. *Proc. Am. Ass. Equine Prac.* **35**, 199–213

Martens, R.J., Renshaw, H.W. (1982) Foal pneumonia. A practical approach to diagnosis and therapy. *Compend. Contin. Educ.* **4**(9), 217–228

Mazan, M., Vin, R., Hoffman, A. (2005) Radiographic scoring lacks predictive value in inflammatory airway disease. *Equine Vet. J.* **37**, 541–545

Morris, D.D., Beech, J. (1983) Disseminated intravascular coagulation in six horses. *J. Am. Vet. Med. Ass.* **183**, 1067–1072

Neil, K., Charman, R., Vasey, J. (2010) Rib osteomyelitis in three foals. *Aust. Vet. J.* **88**, 96–100

Niedermaier, G., Poth, T., Gehlen, H. (2010) Clinical aspects of multinodular pulmonary fibrosis in two warmblood horses. *Vet. Rec.* **166**, 426–430

Nout, Y., Hinchcliffe, K., Smaii, V., et al. (2002) Chronic pulmonary disease with radiographic interstitial opacity (interstitial pneumonia) in foals. *Equine Vet. J.* **34**, 542–549

O'Callaghan, M.W., Seehermans, H.J. (1989) New ways of looking at lung disease in the horse using radiography and scintigraphy. *Proc. Am. Ass. Equine Prac.* **35**, 221–232

Pascoe, J.R., O'Brien, T.R., Wheat, J.D., Meagher, D.M. (1983) Radiographic aspects of exercise-induced pulmonary hemorrhage in racing horses. *Vet. Radiol.* **24**, 85–92

Prescott, J., Wilcock, B., Carman, P., Hoffman, A. (1991) Sporadic, severe bronchointerstitial pneumonia of foals. *Can. Vet. J.* **32**, 421–425

Pusterla, N., Pesavento, P., Leutenegger, C., et al. (2002) Disseminated pulmonary adiaspiromycosis caused by *Emmonscia crescens* in a horse. *Equine Vet. J.* **34**, 749–752

Rantanen, N.W. (1986) Diagnostic ultrasound. *Vet. Clin. N. Amer.: Equine Prac.* 2, No. 1, W.B. Saunders, Philadelphia

Rantanen N., McKinnon, A. (1998) Equine Diagnostic Ultrasonography, 1st edn, Williams and Wilkins, Baltimore

Reef, V. (1998) Equine Diagnostic Ultrasound, 1st edn, W.B. Saunders, Philadelphia

Robinson, N. (2001). International Workshop on Equine Chronic Airway Disease. *Equine Vet. J.* **33**, 5–19

Rossdale, P., Greet, T., McGladdery, A., Ricketts, S., Aqel, N. (2004) Pulmonary leiomyosarcoma in a 13 year old Thoroughbred stallion presenting as a differential diagnosis to recurrent airway obstruction. *Equine Vet. Educ.* **16**, 21–28

Schwarzwald, C., Stewart, A., Morrison, C., Bonagura, J. (2006) Cor pulmonale in a horse with granulomatous pneumonia. *Equine Vet. Educ.* **18**, 182–187

Seltzer, K., Byars, T.D. (1996) Prognosis for return to racing after recovery from pleuropneumonia in Thoroughbred racehorses: 70 cases (1984–1989). *J. Am. Vet. Med. Ass.* **208**, 1300–1301

Shively, J.F., Dellers, R.W., Buergelt, C.D., et al. (1973) *Pneumocystis carinii* pneumonia in two foals. *J. Am. Vet. Med. Ass.* **162**, 648–652

Silverman, S., Poulos, P.W., Suter, P.F. (1976) Cavitary pulmonary lesions in animals. *J. Am. Vet. Radiol. Soc.* **17**, 134–146

Soare, T., Leeming, G., Morgan, R., et al. (2011) Equine multinodular pulmonary fibrosis in horses in the UK. *Vet. Rec.* **169**, 313

Sweeney, C., Gillette, D. (1989) Thoracic neoplasia in equids: 35 cases (1967–1987). *J. Am. Vet. Med. Ass.* **195**, 374–377

Toal, R.L., Cudd, T. (1986) Equine neonatal thoracic radiography: a radiographic-pathologic correlation. *Proc. Am. Ass. Equine Pract.* **32**, 117–128

Uhlorn, M., Hurst, M., Demmers, S. (2006) Disseminated eosinophilic pulmonary granulomas in a pony. *Equine Vet. Educ.* **18**, 178–181

Verschooten, F., Oyaert, W., Muylle, E., DeMoor, A., Steenhaut, M., Moens, Y. (1977) Diaphragmatic hernia in the horse: four case reports. *J. Vet. Radiol.* **18**(2), 45–50

Walker, M., Goble, D. (1980) Barium sulphate bronchography in horses. *Vet. Radiol.* **21**, 85–90

Williams, K., Maes, R., Del Piero, F., et al. (2007) Equine multinodular pulmonary fibrosis: a newly recognized herpesvirus-associated fibrotic lung disease. *Vet. Pathol.* **44**, 849–862

Wisner, E., O'Brien, T., Lakritz, J., et al. (1993) Radiographic and microscopic correlation of diffuse interstitial and broncho-interstitial pulmonary patterns in the caudodorsal lung of adult Thoroughbred horses in race training. *Equine Vet. J.* **25**, 293–298

Wong, D., Belgrave, R., Williams, K., et al. (2008) Multinodular pulmonary fibrosis in five horses. *J. Am. Vet. Med. Assoc.* **232**, 898–905

Chapter 15
The alimentary and urinary systems

Although the oesophagus could be discussed in a regional manner, we have chosen to include it in its entirety with the alimentary system. Diseases of the diaphragm are discussed with the thorax (see Chapter 14, 'Diaphragmatic hernia'). The large size of the adult horse and the difficulty of obtaining any abdominal views other than lateral-lateral images reduce the clinical value of abdominal radiography because only limited information can be obtained. Ultrasonography should always be considered in horses and foals with clinical signs referable to the abdominal viscera or peritoneum. Ultrasonography provides more information regarding structural abnormalities within the soft tissues, including the viscera, gastrointestinal tract, lymph system and peritoneum. Emphasis has therefore been placed on those conditions in which abdominal radiography is of particular value.

RADIOGRAPHIC TECHNIQUE

Equipment

With the exception of the cervical oesophagus, radiographic evaluation of the alimentary system of adult horses cannot be accomplished with portable equipment. High-output portable units can be used in small horses and foals, and small-animal x-ray units can be used for young foals and miniature horses. Radiography of the abdomen of adult horses is of little value except for the diagnosis of enterolithiasis, diaphragmatic hernia (see Chapter 14, 'Diaphragmatic hernia'), bowel obstruction, sand impaction in the large colon and urinary calculi. Abdominal radiography in adult horses can only be performed with large stationary equipment and exposures in the range 90–120 kVp and 180–600 mAs. It is difficult, if not impossible, to obtain diagnostic radiographs from horses with an abdominal width greater than 70 cm. Although digital systems have largely replaced conventional radiography, the use of fast rare earth screens and a focused grid can enable film images to be obtained. While grids are mandatory with film–screen systems, they may not always be needed for digital systems.

A grid with a 140 cm focus, 103 lines per cm and a 10:1 ratio is recommended for use with film. For digital systems the grid must be chosen by trial and error, to avoid the production of moiré lines.

Abdominal radiography in an adult horse is usually performed standing, using four lateral-lateral images with overlapping fields: (a) cranioventral,

Clinical Radiology of the Horse, Fourth Edition. Janet A. Butler, Christopher M. Colles, Sue J. Dyson, Svend E. Kold and Paul W. Poulos.
© 2017 John Wiley & Sons, Ltd. Published 2017 by John Wiley & Sons, Ltd.
Companion website: www.clinical-radiology-horse.com

(b) mid-ventral, (c) mid-dorsal and (d) dorsocaudal. In young foals and miniature horses one or two views are usually sufficient to evaluate the entire abdomen (Figures 15.1, 15.2a and 15.2b). Recumbent radiographs may be obtained, but standing lateral-lateral images are preferred (Figures 15.3a and 15.3b). The radiographs should be obtained with the side with the area of interest next to the cassette or imaging plate. Regardless of positioning for the initial radiograph, a second one should be obtained in the opposite lateral-lateral direction, centred over the area of concern. Evaluation of the stomach should always be performed with the left side against the cassette or imaging plate. In a recumbent foal both lateral-lateral and ventrodorsal views are recommended, especially when contrast medium is used.

Positioning

The oesophagus

Examination of the oesophagus of adult horses should be performed with the patient standing with its left side next to the cassette or imaging plate. If recumbent radiographs are obtained, the patient should be in left lateral recumbency. If contrast medium is to be used in a conscious recumbent animal, it should be limited to barium paste which is easier to swallow and less likely to be aspirated than barium suspension.

The abdomen

Abdominal radiography in young and adult horses is always performed in the standing position, whereas abdominal radiography of the neonatal equine patient or a miniature horse may be carried out either standing or in lateral recumbency (when the cassette or imaging plate is placed on the floor or using a standard x-ray table). Standing and recumbent abdominal radiographs differ in the distribution of gas and fluid. Gas-capped fluid levels can only be evaluated on radiographs obtained in the upright (standing) position (Figure 15.3b). Ventrodorsal radiographs of adult horses are seldom used because of the need for general anaesthesia and the paucity of information gained; however, they can be obtained in neonates and miniature horses using minimal chemical restraint.

Contrast examinations

Contrast examinations are covered in detail with each specific area to be examined, but the clinician must be aware of the basic principle that proper evaluation of a hollow viscus requires that the viscus must be distended. The distension can be obtained with a positive contrast medium (barium- or iodine-containing compounds), a negative contrast medium (air), or a combination of the two. In general, micropulverised barium sulphate should be administered as a 30% (weight per volume) suspension. In foals and young horses, a dosage of 5 ml/kg body weight may be used, whereas in adult horses a dosage of 3 ml/kg body weight is recommended. When barium paste is used the dosage is quite variable, depending on the tolerance of the patient. The paste is placed in the mouth and the patient is allowed to



Figure 15.1 Lateral-lateral radiograph (cranial is to the left) of a normal abdomen of a 6-day-old Thoroughbred filly, obtained with the foal recumbent. There is gas, fluid and food material within the stomach. The lack of abdominal visceral detail is due to the age of the patient. There is gas in the large and small intestines.

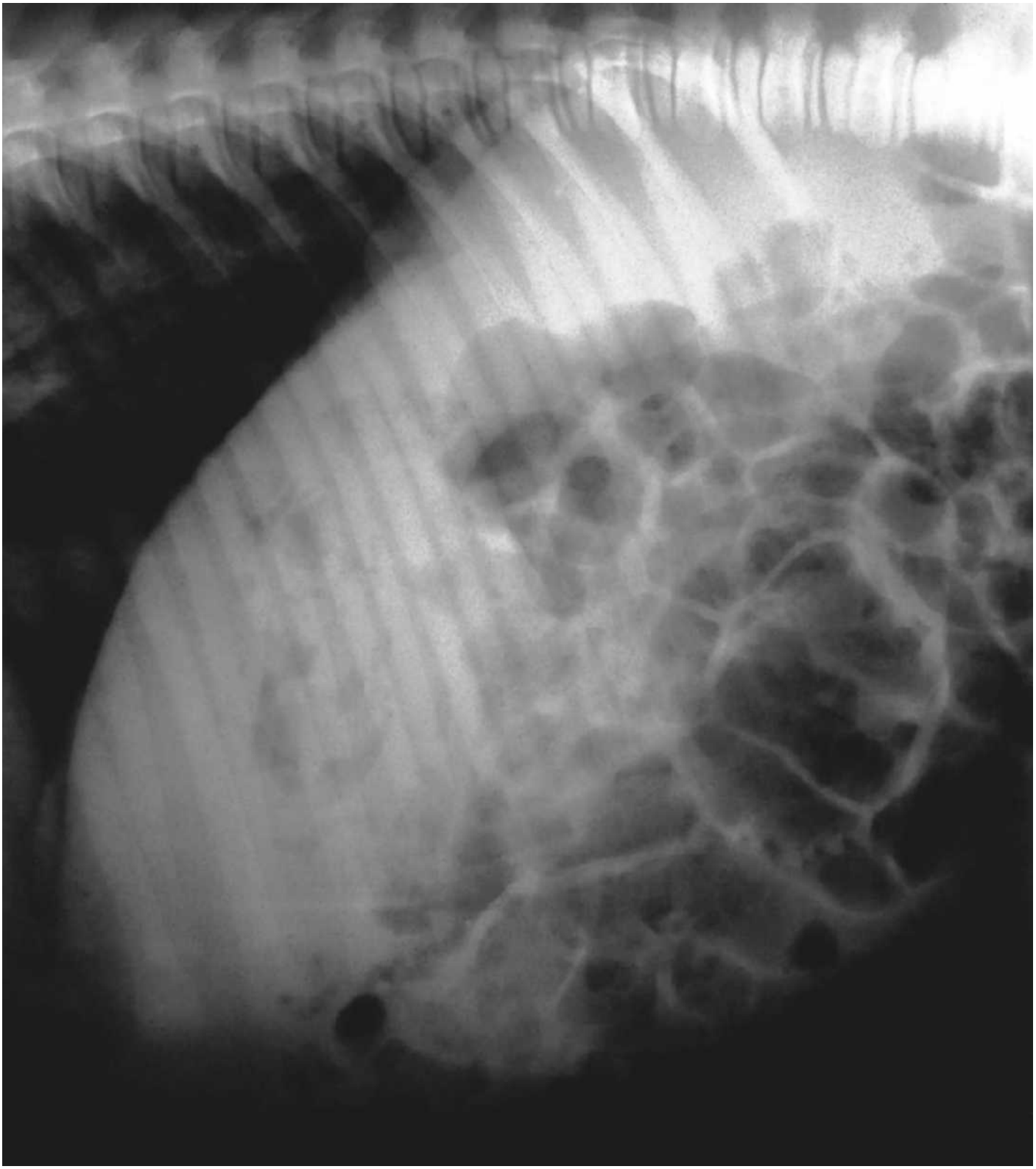


Figure 15.2(a) Lateral-lateral recumbent radiograph of the normal cranial aspect of the abdomen of a 3-day-old foal. Cranial is to the left. There is food and gas within the stomach. The large and small intestines are mostly gas-filled loops without evidence of over-distension.

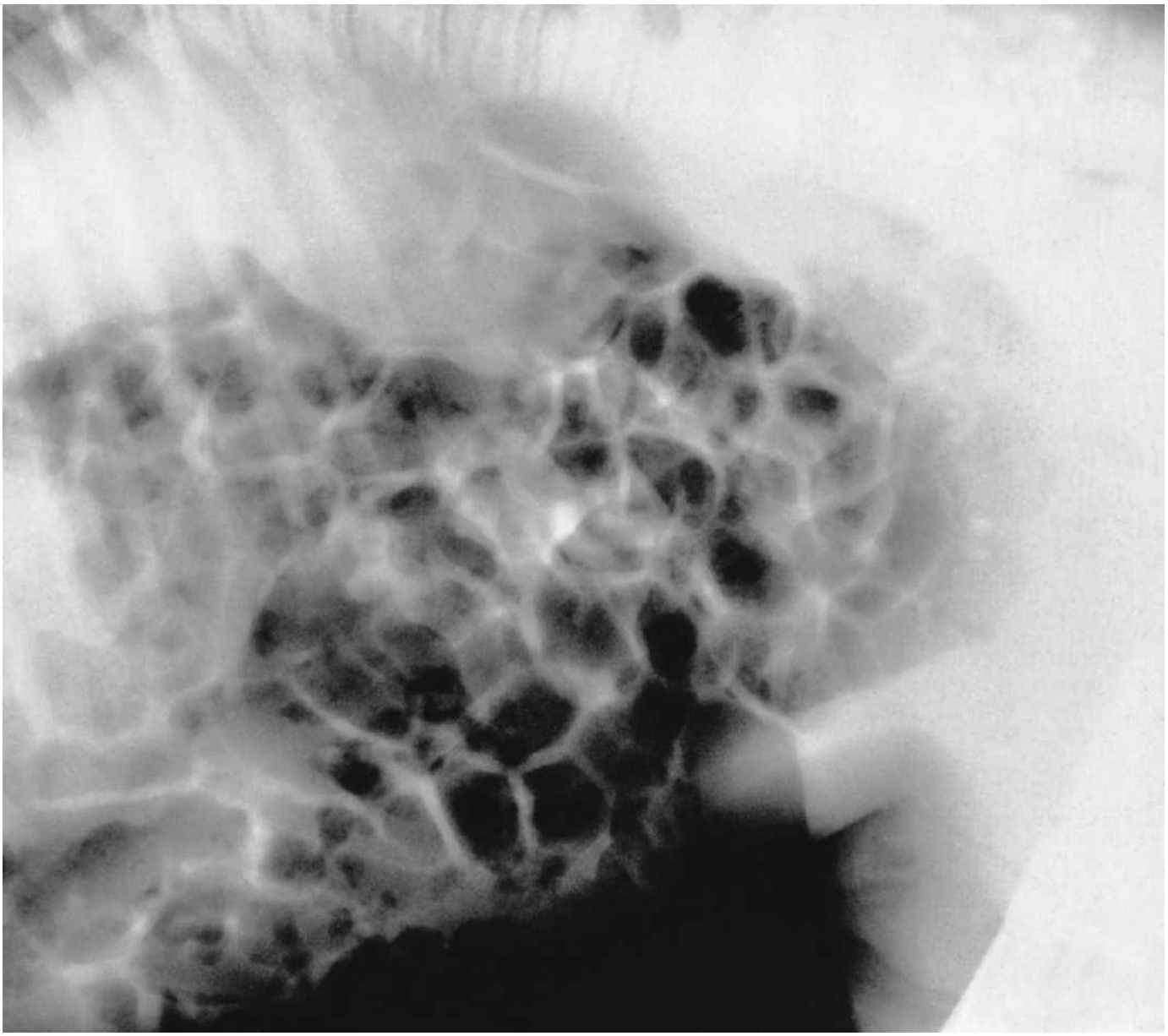
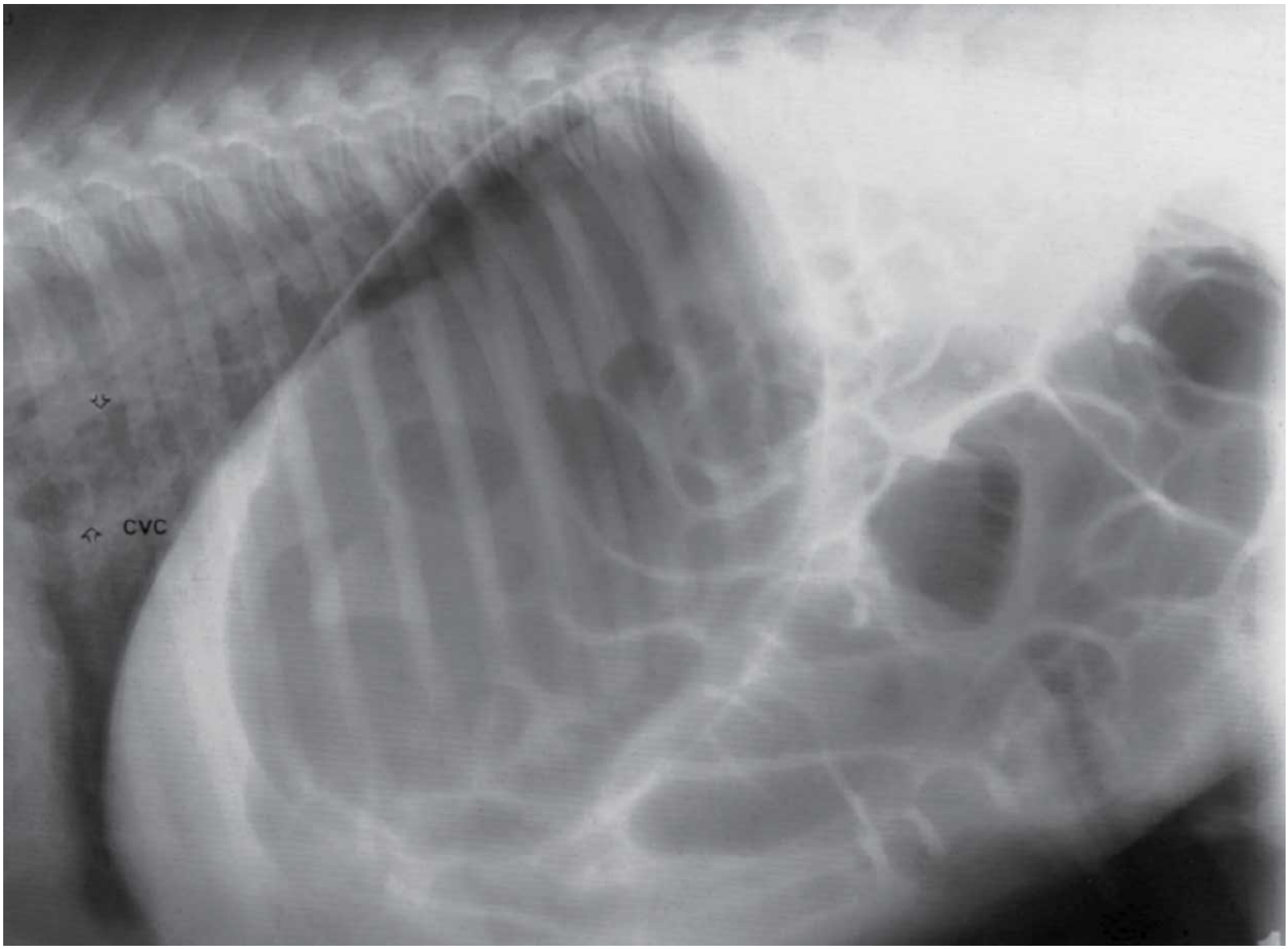


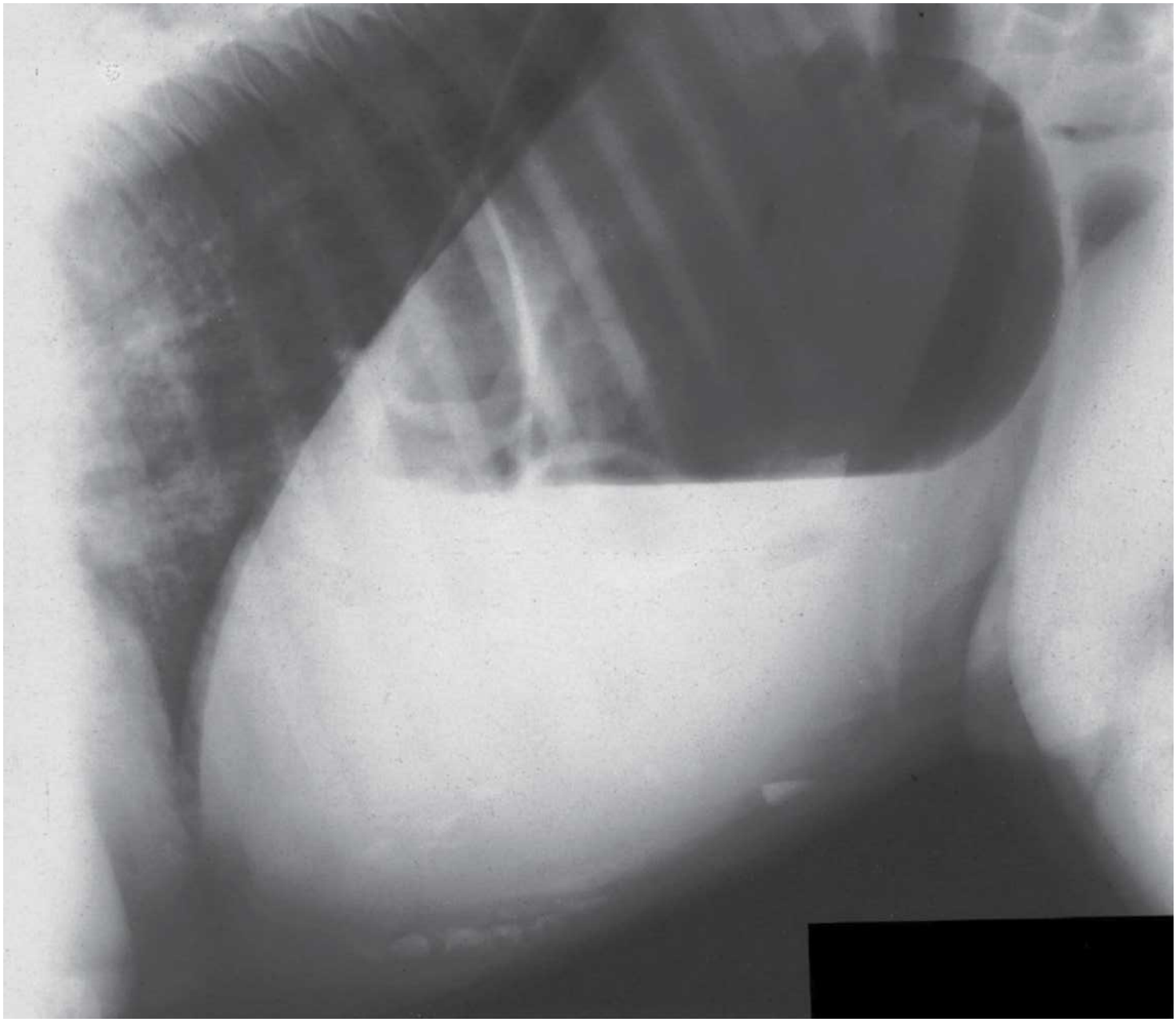
Figure 15.2(b) Lateral-lateral recumbent radiograph (cranial to the left) of the normal caudal abdomen of a 3-day-old foal, demonstrating gas- and fluid-filled large and small intestine loops. The urinary bladder can be seen adjacent to the caudoventral abdominal wall.

swallow in a normal manner. For contrast studies of the abdomen the patient should be starved for 12 hours prior to the examination to enhance detail. Depending on the area of interest (i.e. if the oesophagus is not to be assessed) barium sulphate suspension may be administered via nasogastric tube. Occasionally, administration of barium paste is not tolerated by the patient and in order to perform an oesophagram, barium suspension must be administered via naso-oesophageal tube into the proximal aspect of the oesophagus.



(a)

Figure 15.3 Recumbent lateral-lateral (a) and standing lateral-lateral (b) images of a normal abdomen of a 3-day-old Thoroughbred colt. Cranial is to the left. (a) There is a well-circumscribed gas lucency noted in the caudal aspect of the oesophagus (arrows) overlying the caudal vena cava (CVC). There is gas and fluid distension of the stomach. The large and small intestines contain both gas and fluid, but there is no indication of over-distension or obstruction. There is a generalised increase in interstitial markings in the portions of the lung that are visible. This is probably due to age and pressure from the distended stomach, preventing complete inflation.



(b)

Figure 15.3 *Cont'd* (b) This standing lateral-lateral image of the abdomen was obtained several hours after (a). Note that the gas and fluid now form a fluid line. The caudal aspect of the abdomen cannot be as well assessed in the standing lateral-lateral image because of the position of the limbs which cover the caudal aspect of the abdomen. Gas and fluid can be seen in both the large and small intestines. Opaque material in the ventral colon is sand.

Oesophagus

RADIOGRAPHIC TECHNIQUE

The general principles of appropriate technique and for contrast studies are discussed above. Detail of positioning for the cervical oesophagus is similar to that for the cervical vertebrae (see Chapter 12, 'Cervical vertebrae – Radiographic technique').

NORMAL ANATOMY AND ACTION OF THE OESOPHAGUS

In a normal horse there is no air in the oesophagus. As the oesophagus passes through the thoracic inlet it may drape over, and partially obscure, the dorsum of the trachea. The oesophagus then elevates slightly as it passes over the heart and caudally through the cardia into the stomach. The oesophagus is not normally visible on thoracic radiographs.

When eating, a bolus of food (or contrast medium) gradually collects rostral to the epiglottis at the base of the tongue. When the horse swallows, the bolus passes into the retropharyngeal area and on into the oesophagus. It is carried rapidly down the oesophagus by the stripping motion of the oesophageal contractions. The passage of a bolus takes between 4 and 10 seconds. Occasionally, a food bolus is not completely stripped from the oesophagus and a secondary peristaltic wave will pass through, removing residual material from the lumen. Although the act of deglutition can only be followed with fluoroscopy, the results can often be noted on serial radiographs obtained after the administration of contrast medium.

Contrast examination of the oesophagus

When there is a history of dysphagia, oesophageal obstruction or recurrent oesophageal disease, and survey radiographs are normal, a contrast examination of the oesophagus should be performed. Barium paste is used to evaluate the oesophageal mucosa. The paste coats the mucosa and has the advantage of outlining structures for several minutes. In a normal oesophagus the contrast medium is seen as fine radiopaque linear streaking outlining the longitudinal oesophageal mucosal folds after the passage of the bolus. A bolus may be seen on a single radiograph, but will normally pass on gradually, or be carried away with the next bolus. The bolus should not be in the same location in subsequent radiographs.

Barium suspension is the contrast medium of choice when diverticuli or mega-oesophagus are suspected, because of the greater volume of contrast medium required to demonstrate such changes. Liquid barium given per os or by stomach tube into the cranial aspect of the oesophagus is passed in a similar manner to barium paste, but does not coat the oesophageal mucosa as well. Occasionally a small amount of contrast medium is held momentarily at the thoracic inlet or just cranial to the cardiac silhouette. Contrast medium may also remain momentarily at the cardia, but passes gradually into the stomach. Barium-coated food such as pellets or hay can also be used to demonstrate strictures which may not be demonstrated by the use of liquid barium alone. If oesophageal rupture is suspected, caution is urged in the selection of contrast medium. Barium products are associated with mediastinitis. In cases where rupture is suspected, non-ionic, iodine contrast media should be used.

Delayed oesophageal emptying and distension with air and contrast medium have been reported as a sequel to recent passage of a nasogastric tube and have also been associated with the use of tranquillisers.

If liquid barium is administered by mouth, in some cases traces will be seen dorsal to the soft palate, or in the larynx or trachea. This is abnormal and indicative of abnormal pharyngeal function. A clinical evaluation of the nasopharynx and larynx should be performed to differentiate conditions such as cleft palate, a foreign body and Eustachian tube diverticulum mycosis from primary oesophageal diseases.

DISEASES OF THE OESOPHAGUS

Diseases of the oesophagus can be divided into three main categories.

Diseases that decrease the diameter

Stricture from scar tissue

Intramural scar tissue results from damage due to previous trauma such as choke, a foreign body, a penetrating wound, previous surgery or overzealous attempts to relieve a choke. The stricture can usually be demonstrated with barium paste, but may require a mixture of food and barium. The primary finding is a narrowing of the oesophageal lumen, characterised by smooth walls at the point of stricture. Barium and/or food will be retained cranial to the stricture (Figure 15.4). Normal peristalsis can have a similar appearance to a stricture, and so confirmation of this lesion should be obtained through sequential radiographs. A stricture appears the same on consecutive images, whilst peristalsis is seen as a transient narrowing.

Abscessation

Abscessation of the oesophageal wall may result from penetration from inside or outside. Soft-tissue swelling and irregularity of the mucosal surface may be noted when an abscess originates from internal trauma. The mucosal surface may be smooth if the abscessed wall has not yet ruptured into the lumen. Wounds to the oesophagus may result in fistula formation as well as scarring and abscessation (as noted above). Following rupture of the oesophagus, food and gas may be seen in the perioesophageal tissues (Figure 15.5).

Spasm

Spasm is usually a temporary condition and may not be found on subsequent radiographs. The mucosal surface is smooth and a second examination is often necessary to differentiate spasm from stricture.

External masses

Extra-luminal masses such as a tumour, thyroid enlargement or external abscess may cause displacement or compression of the oesophagus, or alteration in shape and size if involving the wall of the oesophagus (Figure 15.6).

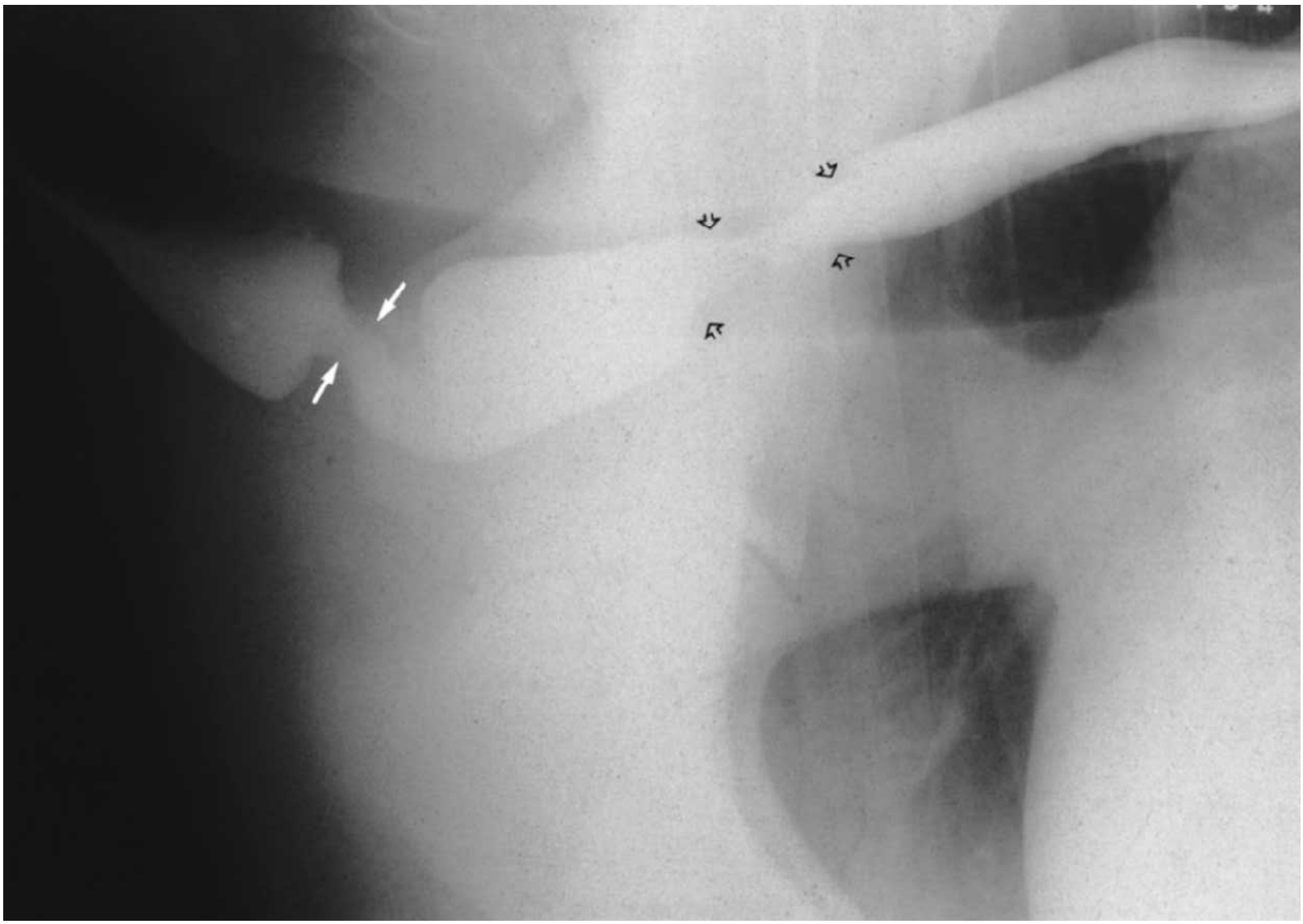


Figure 15.4 Lateral-lateral image of the thoracic inlet; cranial is to the left. This 4-year-old Standardbred filly was presented with a history of choke 28 days previously. The horse is now having difficulty swallowing. Survey radiographs of the cervical oesophagus did not demonstrate any abnormality. Fifty millilitres of micronised barium sulphate diluted in a similar volume of water was administered via stomach tube in the cranial aspect of the oesophagus. There is a stricture of the oesophagus at the thoracic inlet (solid arrows), with pre- and post-stenotic dilatation. A second area of stenosis is noted caudal to the first (open arrows). The remainder of the oesophagus is normal. Diagnosis: oesophageal stricture at two locations.



Figure 15.5 This yearling Thoroughbred filly was presented with a swollen neck. There was no evidence of a skin wound.
A lateral-lateral radiograph of the cervical area (cranial is to the left) demonstrates the soft-tissue swelling which appears to compress the trachea (T) and narrow the tracheal lumen. There is gas in the cranial aspect of the oesophagus (O) and a mottled irregular heterogeneous opacity more caudally apparently overlying the oesophagus and trachea, representing both gas and food material in the soft tissues. Diagnosis: ruptured oesophagus with food and gas in the peri-oesophageal soft tissues.



Figure 15.6 Lateral-lateral image of the cranial cervical region of a mature horse with dysphagia. Cranial is to the left. Barium sulphate paste coats the lining of the oesophagus which is displaced dorsally. There is a multiloculated area (white arrow) representing gas, ventral to which is a radiopaque line (black arrow). There is residual barium in the caudal aspect of the pharynx, some of which has entered the cranial aspect of the trachea. These abnormalities are consistent with a perioesophageal abscess with a wire foreign body.

Depending on the origin of the mass, the oesophagus may be seen to deviate around the mass, particularly if gas or contrast media are present within the oesophageal lumen. Ultrasonographic examination may be helpful, especially if the mass is in the cervical region.

Neoplasia and intramural cysts

Oesophageal neoplasia and intramural cysts (Figure 15w.7) are rare in the horse, but must be considered in cases where there is a mass in the oesophageal wall. Neoplasia should be considered when irregularity of the mucosal surface of the oesophagus is present. The differential diagnosis includes abscessation.

Diseases that increase the diameter

Mega-oesophagus – dilatation of the oesophagus

The affected segment of the oesophagus may be dilated with gas (Figure 15.8), fluid or food, either alone or in combination (Figure 15.9).

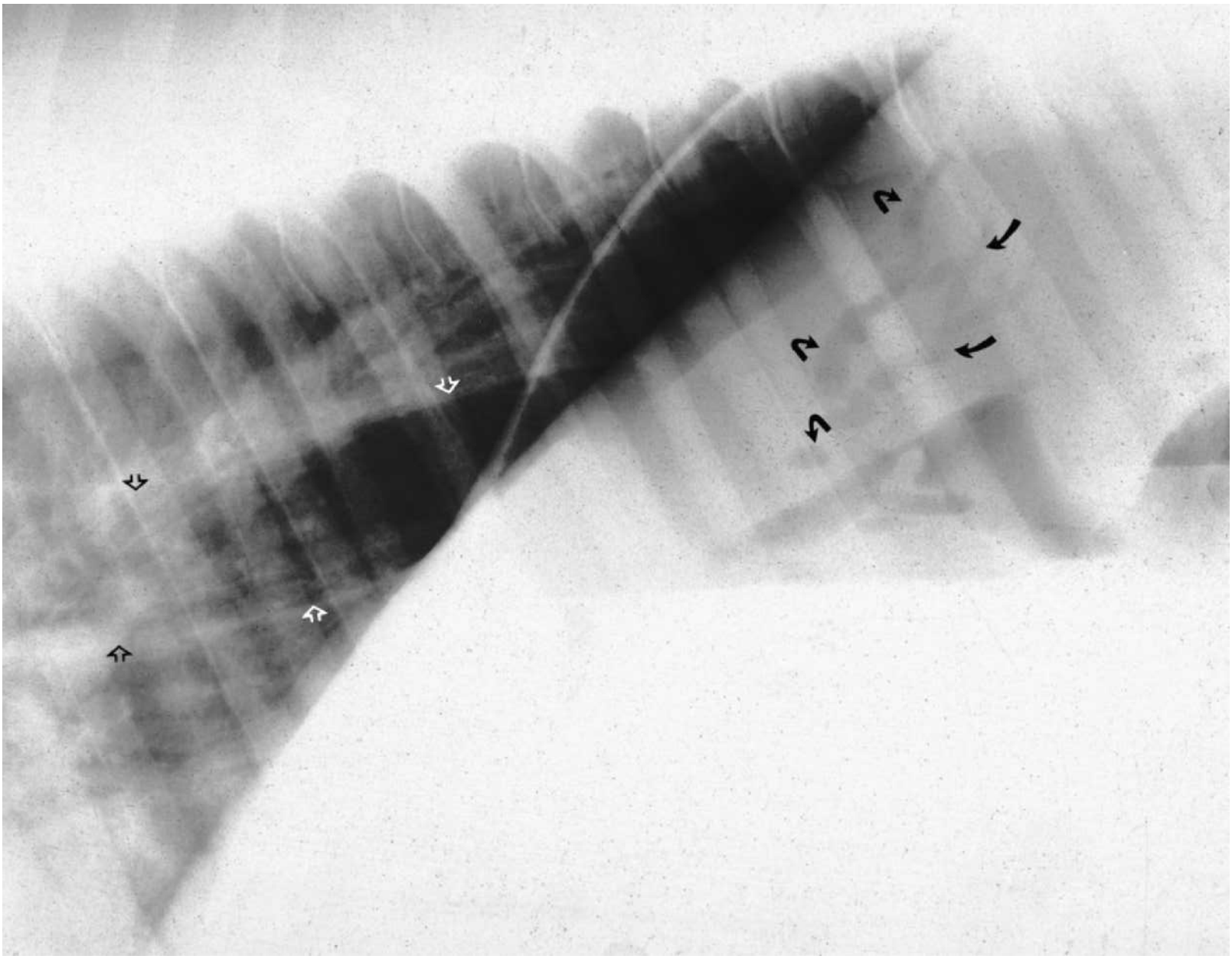


Figure 15.8 Lateral-lateral image of the caudal aspect of the thorax and cranial aspect of the abdomen. Cranial is to the left. This 4-month-old Thoroughbred colt was presented with a history of black tarry diarrhoea. The tentative diagnosis was gastroduodenal ulcer disease. The gas-distended oesophagus is seen in the caudal dorsal aspect of the thorax, between open arrows. The increased opacity in the caudal dorsal lung lobes is due to pulmonary interstitial infiltrates. A fluid line can be seen in the gas- and fluid-distended stomach. Gas is seen in the biliary tree (curved arrows). Radiographic diagnosis: gastric dilatation with air and fluid, mega-oesophagus, pulmonary interstitial infiltrates and gas in the biliary tree. These findings are indicative of gastroduodenal ulcer disease of the foal.

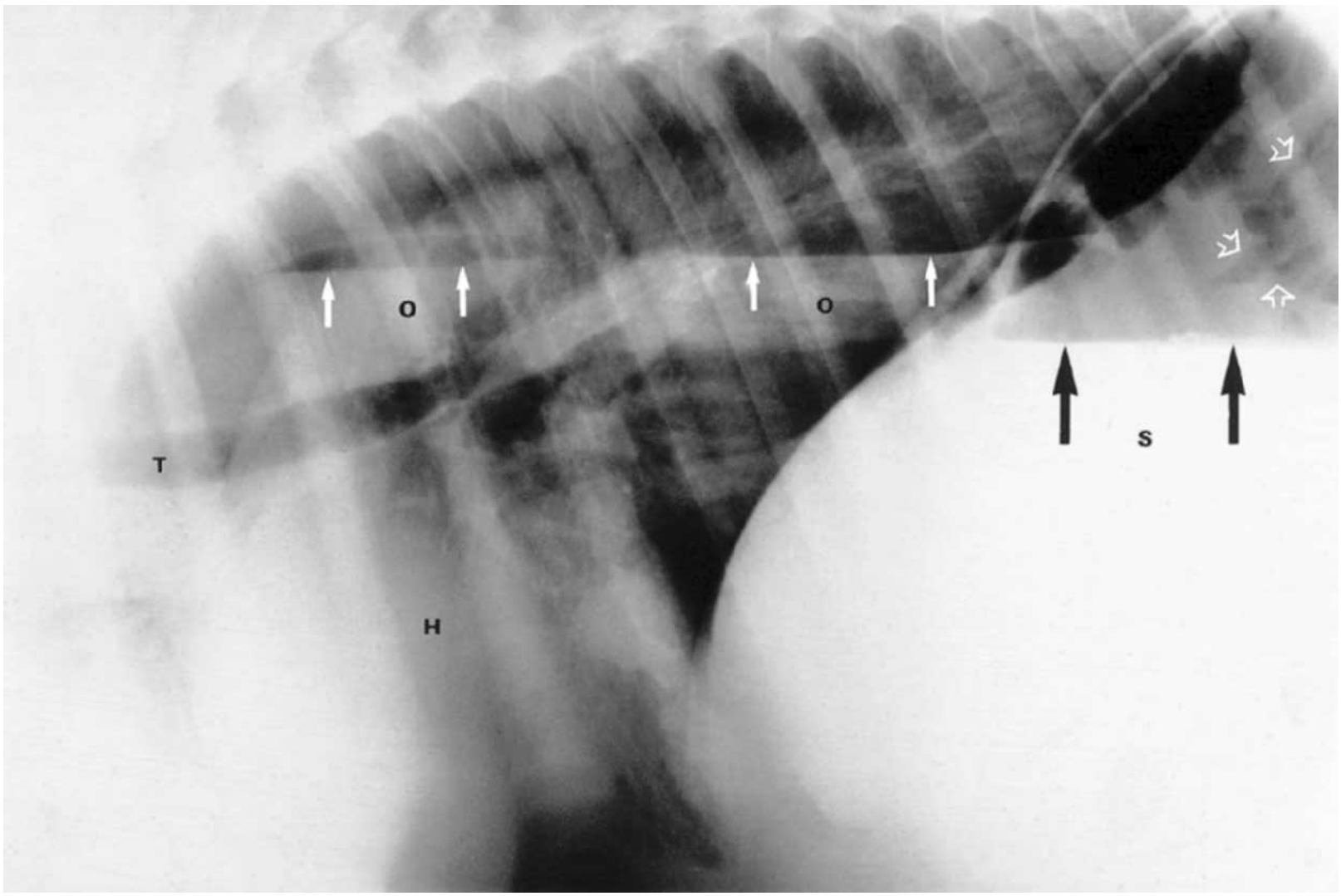


Figure 15.9 This 1-month old Thoroughbred colt was presented depressed and with a painful abdomen, with a 3-week history of signs compatible with gastric ulcer disease. The lateral-lateral radiograph (cranial to the left) demonstrates mega-oesophagus with fluid and air resulting in a gas-capped fluid line (solid white arrows) in the dilated oesophagus (O). The oesophagus is depressing the trachea (T) over the base of the heart (H). There is a mixed alveolar and interstitial pattern in the caudal ventral lungs which is best seen over the caudal margin of the cardiac silhouette. The stomach (S) is distended with fluid and air, resulting in a gas-capped fluid level (large black arrows). Gas can also be seen in the biliary tree as branching lucencies (open white arrows) over the opaque liver. Diagnosis: gastroduodenal ulcer disease with mega-oesophagus, aspiration pneumonia and gas in the biliary tree.

Mega-oesophagus can be the result of mechanical or functional obstructions. Focal mega-oesophagus may result from mural, intraluminal or extraluminal obstructions such as a stricture, a foreign body or an annular ring anomaly. When the entire oesophagus is dilated, a functional problem such as a neuromuscular dysfunction or a distal obstruction such as an abnormality of the cardiac sphincter should be considered as the primary cause. Generalised mega-oesophagus has been reported in chronic grass sickness in the United Kingdom. In foals, generalised mega-oesophagus may be seen in gastroduodenal ulcer disease (Figure 15.9) (see 'Gastroduodenal ulcer disease in foals', below). Focal mega-oesophagus with accumulation of food is usually considered to be the result of oesophageal obstruction (see below). Lack of oesophageal motility can be demonstrated using liquid barium and obtaining several exposures without moving the patient. If oesophageal motility is present, the contrast column or contrast–air interface will change on sequential radiographs. A common sequel to mega-oesophagus is aspiration pneumonia (see 'Aspiration pneumonia' in Chapter 14).

Diverticuli

Horses with a diverticulum of the oesophagus may have a history of spontaneous occurrence or of previous injury or choke. Diverticula may be classified as either pulsion or traction.

A pulsion diverticulum is the result of mucosal herniation through an acquired defect in the muscularis, due to over dilatation at an impaction site which caused separation of the muscularis. These diverticuli may be large. Regardless of size or cause, a diverticulum appears as a rounded out-pouching of the oesophagus rather than the linear appearance of the normal oesophagus cranial and caudal to the diverticulum (Figures 15.10a-c and 15.11a-c). The internal content of the out-pouching is often of heterogeneous radiopacity, including fragmented or mottled gas with soft tissue.

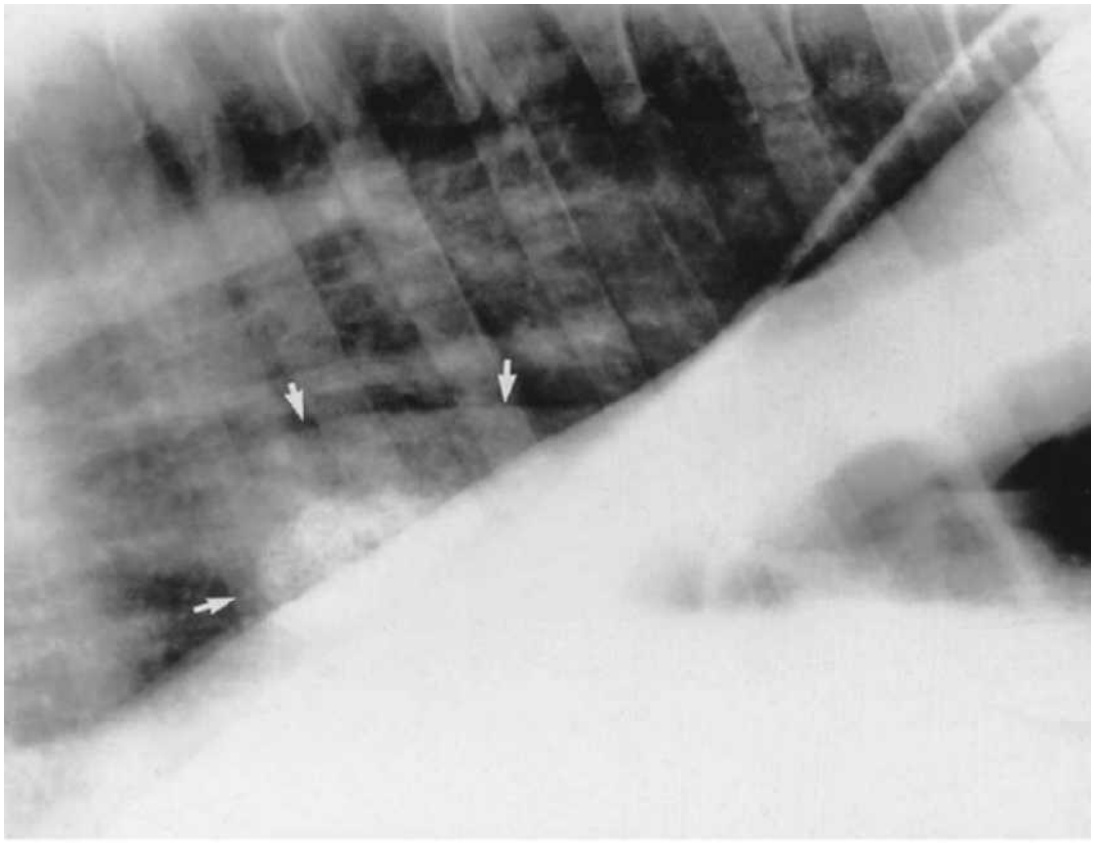
A traction diverticulum is caused by an extra-oesophageal lesion impacting the oesophagus and is usually small and of little significance. It may have a pointed rather than a rounded appearance because it results from perioesophageal scarring which exerts traction on a segment of the wall.

Oesophageal dysfunction and obstruction (choke)

Choke

Although oesophageal obstruction is often related to the rapid ingestion of food, it may also occur secondarily to mechanical obstruction, including scar formation or diverticula (Figures 15.10 and 15.11) within the oesophagus, or as a result of impingement upon the oesophagus from masses or annular ring anomalies, or for no discernible reason.

The radiographic appearance varies depending upon the cause of the obstruction, but most often has a heterogeneous mottled gas and soft-tissue opacity resulting from the mixture of gas and food material (Figures 15.10 and 15.11). The mass is most commonly oval in shape. Air may be seen at one or both ends of the mass and conforms to the shape of the mass and then tapers sharply to a point. The obstruction may occur at any location within the oesophagus, but the thoracic inlet, base of the heart and the cardia are the most common sites when there is no underlying pathology causing the obstruction.



(a)



(b)



(c)

Figure 15.10 This 14-year-old Quarterhorse mare had a history of four episodes of nasal regurgitation in the previous 6 months. Lateral-lateral images of the caudal aspect of the thorax; cranial is to the left. (a) Survey radiograph of the caudal aspect of the thorax demonstrates focal dilatation of the caudal oesophageal hiatus (arrows). There is opaque granular food material within the mass. Tentative diagnosis: oesophageal diverticulum or gastro-oesophageal invagination. (b) Approximately 50 ml of micropulverised barium sulphate was administered via stomach tube and a radiograph of the suspected diverticulum was obtained immediately. Contrast medium is seen in the normal oesophagus to the level of the mass, where it passes over the mass and delineates the dorsal border. Increased interstitial markings in the lungs probably represent chronic fibrosis secondary to regurgitation. (c) Administration of additional barium sulphate and air dilates the oesophagus and demonstrates the extent of the diverticulum (curved white and black arrows). A fluid line can be seen in the oesophagus due to the air–fluid interface. The dorsal oesophageal margins are marked (open white and black arrows). Diagnosis: oesophageal diverticulum and secondary pulmonary fibrosis.

Contrast medium will aid in the definition of the obstruction, but care must be taken that reflux of the contrast medium into the trachea does not occur. Aspiration pneumonia may be seen as a sequel to oesophageal obstruction (see 'Aspiration pneumonia' in Chapter 14). A post-treatment control study, using barium sulphate paste, is helpful in the evaluation of the oesophagus after the obstruction has been relieved (Figure 15.11c).

Grass sickness

In some cases of grass sickness (in the United Kingdom) a bolus of food (or contrast medium) passes down the oesophagus more slowly than normal and may oscillate to and fro, particularly at the thoracic inlet or at the diaphragm. A bolus may remain stationary at the diaphragm for several minutes before passing into the stomach.

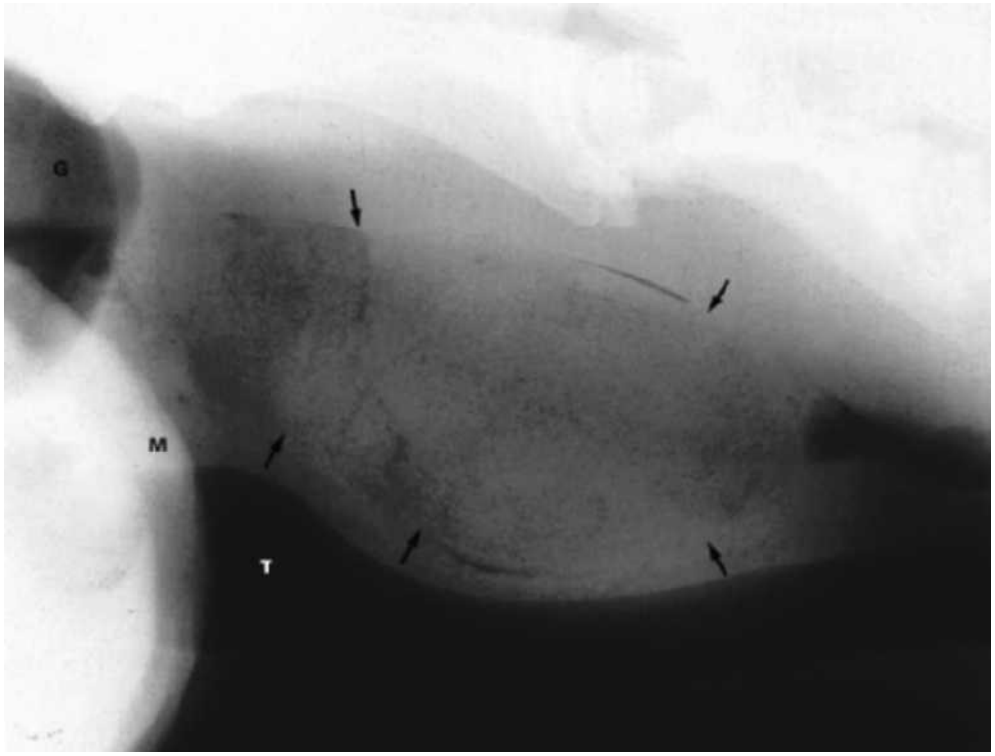


Figure 15.11(a) A lateral-lateral radiograph (cranial to the left) of the cranial cervical oesophagus of an immature horse demonstrating a large granular gas- and fluid-containing mass within the oesophagus (arrows), compressing the trachea ventrally. There is gas caudal to the mass within the oesophageal lumen. The guttural pouches are identified (G). The right and left rami of the mandible (M) can be seen over the guttural pouches, a portion of the oesophagus and the trachea (T). Diagnosis: oesophageal obstruction, 'choke' of the cervical oesophagus.

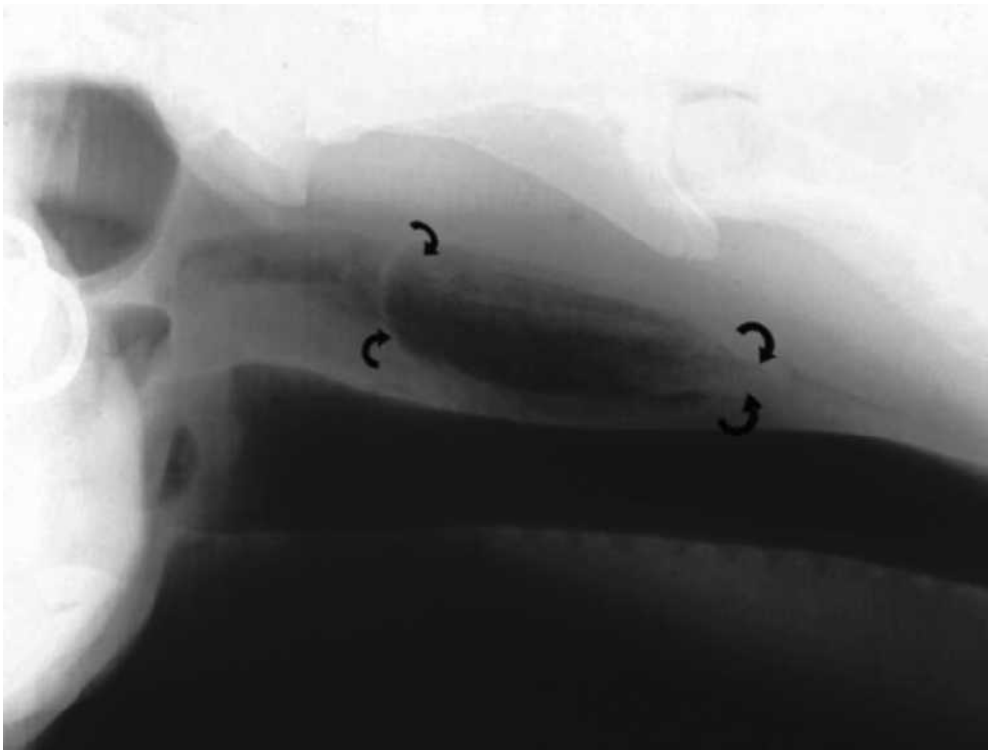


Figure 15.11(b) Lateral-lateral image of the cranial cervical region of the same horse as Figure 15.11a; cranial is to the left. Six days after relief of the 'choke' the oesophagus remains dilated and somewhat irregular. There appears to be mucosal folding at several locations (curved arrows). The trachea remains compressed beneath the gas-containing mass. Gas can also be noted in the lateral ventricle (L).

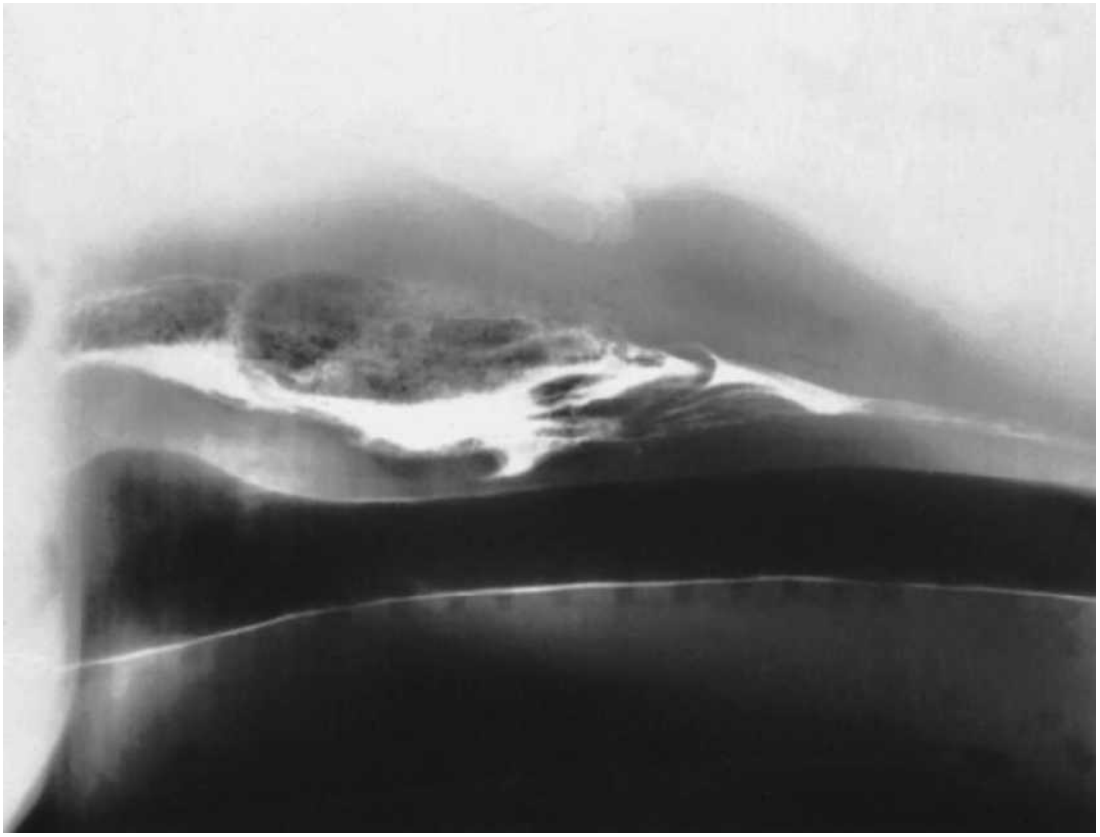


Figure 15.11(c) Lateral-lateral image of the cranial cervical region; cranial is to the left. Barium sulphate paste was administered immediately following the survey radiographs (b) (the same horse as Figure 15.11a). The contrast examination demonstrates mucosal irregularity and contrast material in the wall of the oesophagus. The thickened oesophageal wall can be seen between the contrast medium column and the trachea. The trachea is depressed by the mass. Aspirated contrast medium lines the tracheal wall. The oesophagus is normal beyond the developing diverticulum. Diagnosis: oesophageal obstruction due to chronic oesophageal wall disease and developing diverticulum.

Abdomen and gastrointestinal tract

RADIOGRAPHIC ANATOMY

Foal abdomen

The most common reason for abdominal radiography in a foal is acute abdominal discomfort. In young foals, abdominal structures may be poorly defined due to the lack of abdominal fat that usually helps differentiation of structures (Figure 15.12). A normal standing lateral-lateral abdominal radiograph has the appearance of a mixture of gas, fluid and ingesta, with occasional bowel loops having gas-capped fluid levels. There is often a large amount of gas in the terminal bowel. Distension of small bowel loops is considered to be present when their diameter is greater than the length of the body of the first lumbar vertebra. This measurement can only be made when there is enough gas distension for the small bowel loops to be identified.

Right-left lateral-lateral standing position

The fundus of the stomach is located adjacent to the left crus of the diaphragm, with the body of the stomach inclining slightly forward against the liver. When both air and fluid are present in the stomach, there is a gas cap dorsally in the fundus and against the diaphragm. Fluid and/or food are located ventrally in the pyloric area. Gastric size is considered normal when the height of the stomach is approximately half the length. The duodenum exits the pylorus near the mid to ventral third of the abdomen. The diaphragmatic flexure of the colon is found ventral to the stomach and in contact with the liver. The ventral colon is just caudal to the diaphragmatic flexure against the ventral abdominal wall. Crescent-shaped folds may be identified between the haustra of the ventral colon when the content is more or less dense than soft tissue. The caecum is located in the mid-abdomen and often has a gas cap. The colon lies ventrally with the sternal flexure, beneath the diaphragmatic flexure. The dorsal and ventral flexures of the colon cannot usually be separated. The pelvic flexure is found ventrally adjacent to the urinary bladder. The small colon and rectum are located dorsocaudally. The kidneys are rarely seen radiographically.

Right and left lateral recumbent positions

There is little change in the anatomical location of structures, but they may become more or less visible due to the shifting of air and fluid contents or, in the case of contrast examination, the passage of contrast medium silhouetted against soft tissue or a gas-filled viscus.

Ventrodorsal position

The stomach is located to the left of the midline, with the diaphragmatic flexure of the colon crossing over against the liver and occupying the right side of the cranial aspect of the abdomen. The duodenum exits the pyloric antrum caudal to the main body of the stomach and the sigmoid loop extends approximately two-thirds of the way to the right body wall, just caudal to the ventral colon, before passing caudally as the descending loop. The descending loop passes caudally to about the level of the last rib before changing course medially and cranially to form the caudal flexure. The jejunum is caudal to the stomach and lies mostly on the left side. The base of the caecum is located in the right caudal abdomen, with the apex near the xiphoid cartilage. The small colon is located on the left side. The right and left ventral and dorsal large colon lie on both sides ventrally.

Adult abdomen

The liver lies adjacent to the diaphragm and separates the stomach from the sternum in the cranioventral aspect of the abdomen. The stomach is craniodorsal on the left side, but is not fixed in position.

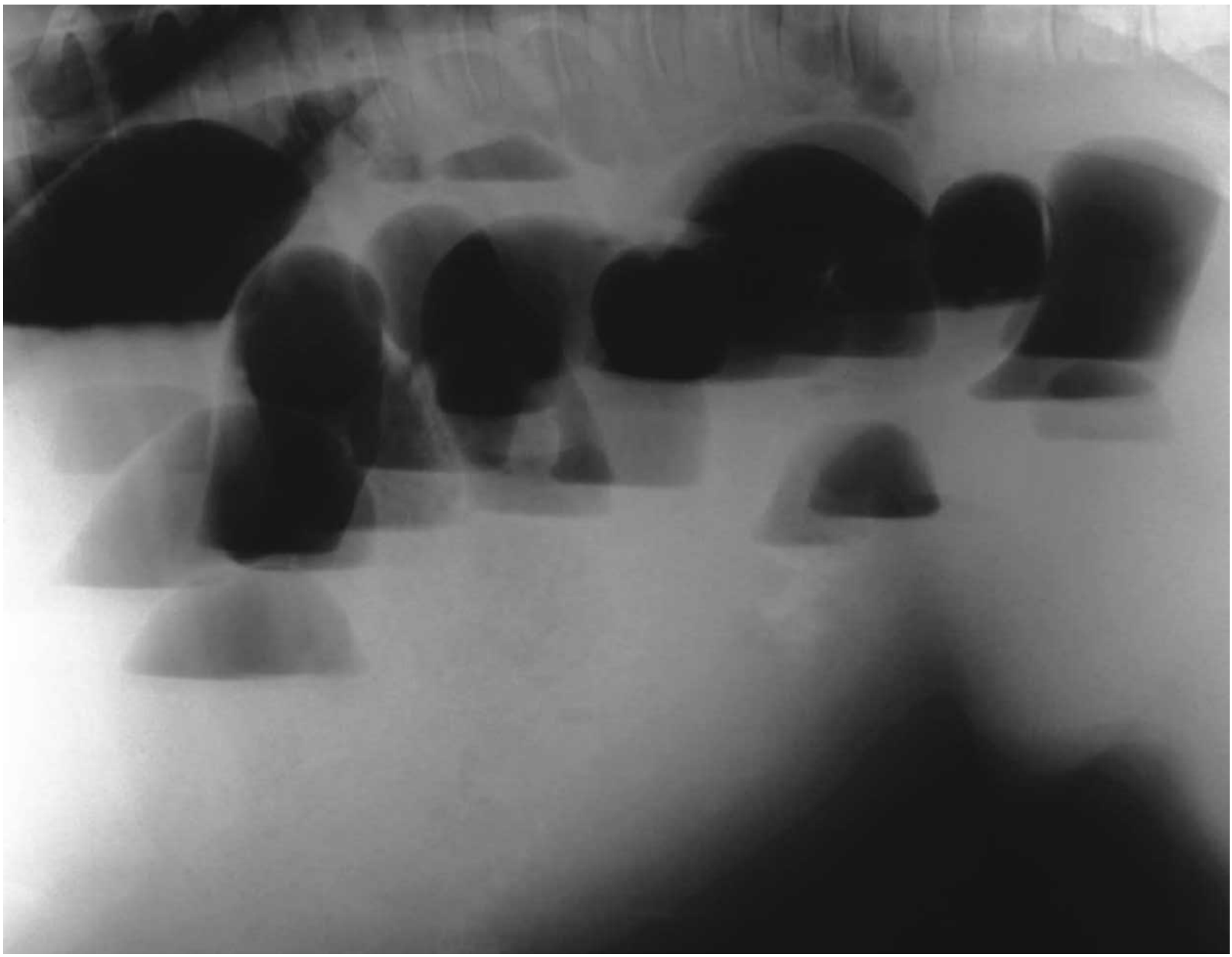


Figure 15.12 A standing lateral-lateral radiograph (cranial is to the left) of a 3-week-old foal demonstrates lack of abdominal visceral detail ventrally with some granular opaque material, sand, which is apparently within the large intestine. The moderately dilated small intestinal loops with unequal fluid levels (inverted Us) are suggestive of mechanical ileus.

ANATOMICAL VARIATIONS

The main difference in the anatomy of a foal and an adult horse is the relative change in size of the stomach, the caecum and large colon. In a foal the stomach is larger in proportion, but this decreases with age as the caecum and colon increase in size.

Contrast studies in the foal

Survey radiographs should always be obtained before the administration of contrast medium in order to have baseline information regarding the size, shape and position of organs prior to contrast medium administration.

A foal cannot be fasted for the same time interval as an adult because fluid and electrolyte balance must be maintained. Therefore, fasting should not be more than 4 hours in foals that are still on fluid diet and 12 hours for foals that are eating solid food. Fasting should be limited to solid matter and not fluids. Contrast medium should be administered by nasogastric tube at the rate of 5 ml of barium sulphate suspension (30% w/v) per kilogram. Radiographs should be obtained immediately and at 30 minutes, 1 hour and then at hourly intervals thereafter until the contrast medium reaches the small colon. Additional radiographs can be obtained as required. When possible, standing right-left lateral-lateral and ventrodorsal radiographs should be obtained. Normal transit time is approximately 8 hours.

The stomach is best evaluated using a double-contrast technique following a 4–12-hour fast (see above). Barium sulphate suspension 30% w/v is then administered via stomach tube at a rate of 5 ml/kg. Normally there is adequate air in the stomach, but if not it should be slightly distended by administration of air. Care must be taken not to over-distend the stomach. The standing patient is placed with the left side to the cassette and radiographed. In a recumbent foal, right and left lateral-lateral recumbent and ventrodorsal radiographs should be obtained immediately following administration of the contrast medium and air. These radiographs should be repeated at 30 minutes, 1 hour and 2 hours post-administration. Contrast medium may begin to exit the stomach as early as 10 minutes after administration, but emptying may vary greatly depending on the gastric content. The pylorus and the duodenum may not be recognised as distinct features, but contrast medium may be defined in the descending duodenum within the first 10 minutes as it exits the pylorus in the mid to lower third of the abdomen and passes over the gas-filled stomach. The remainder of the small bowel then fills and contrast medium usually reaches the caecum in 4–5 hours.

DISEASES OF THE GASTROINTESTINAL TRACT

Small intestinal obstruction

With small intestinal obstruction multiple small intestinal loops are distended with gas and fluid (Figures 15.12, 15.13; see also Figure 15.16a). Hairpin curves are often noted, as well as many gas-capped fluid levels. The stomach may also be gas distended. Mechanical or functional obstruction cannot be differentiated. Distended small intestinal loops can also be identified

by abdominal ultrasonography. Occasionally, the cause of the obstruction such as an intussusception can be detected using ultrasonography. The small bowel can have variable distension.

Large intestinal obstruction

Meconium retention or large intestinal obstruction may be seen on lateral-lateral standing or recumbent radiographs as an ileus (Figures 15.13, 15.14 and 15w.15). Gas-distended bowel may outline the meconium retention. If the meconium is not seen on a survey radiograph, barium or air may be placed in the rectum with the aid of either a stomach tube and gravity flow or a rubber syringe, thus demonstrating the area of blockage. With a barium or air enema, care must be exercised. Stop immediately if pressure is encountered.

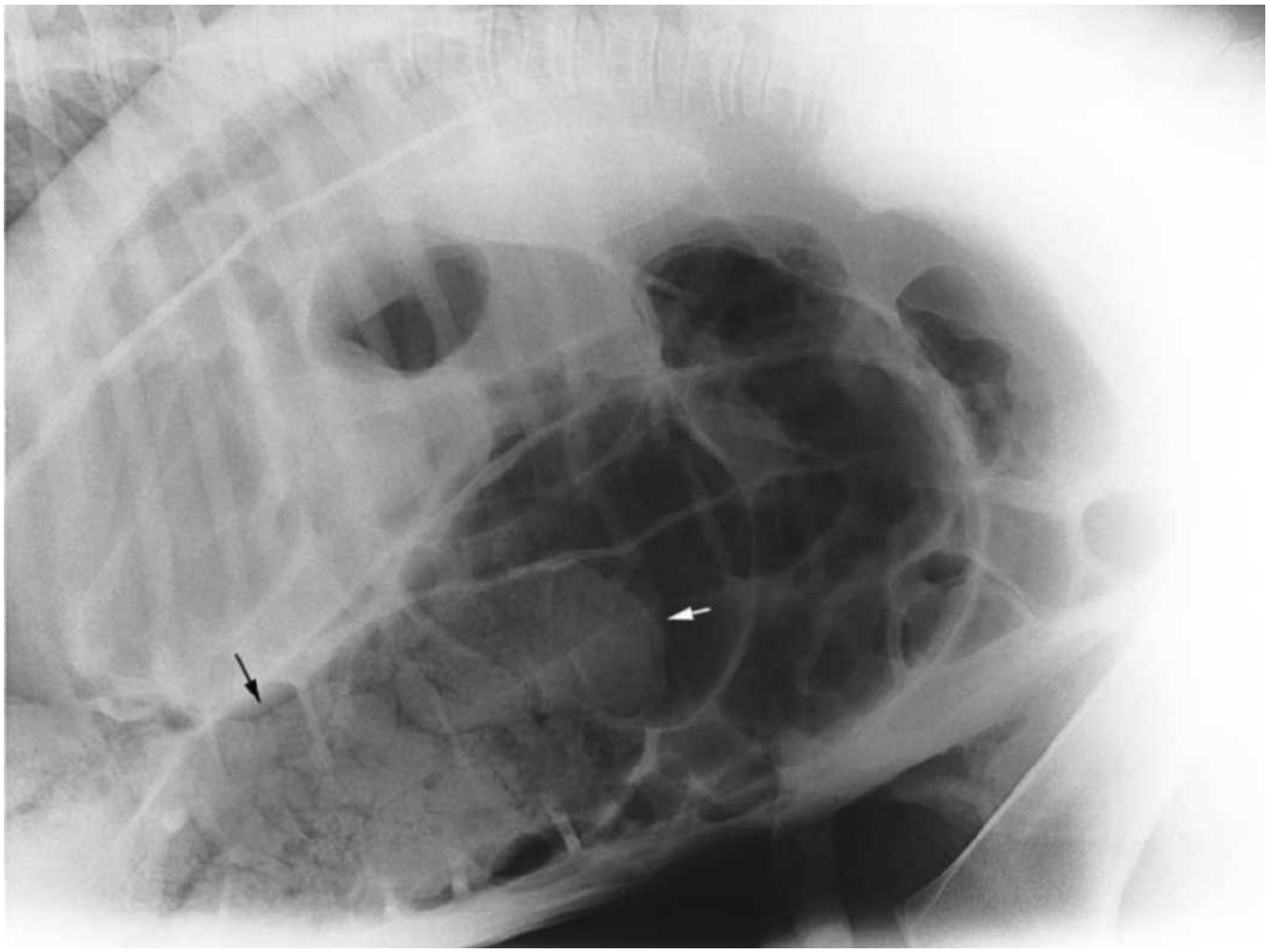


Figure 15.13 Lateral-lateral image of the abdomen of a Thoroughbred foal with suspected meconium impaction. Cranial is to the left. There are gas-distended large and small intestines. Cranioventrally there is opaque granular-appearing material in the large intestine which probably represents retained meconium (arrows). Radiographic diagnosis: obstructive ileus, probably due to meconium in the mid-large bowel.

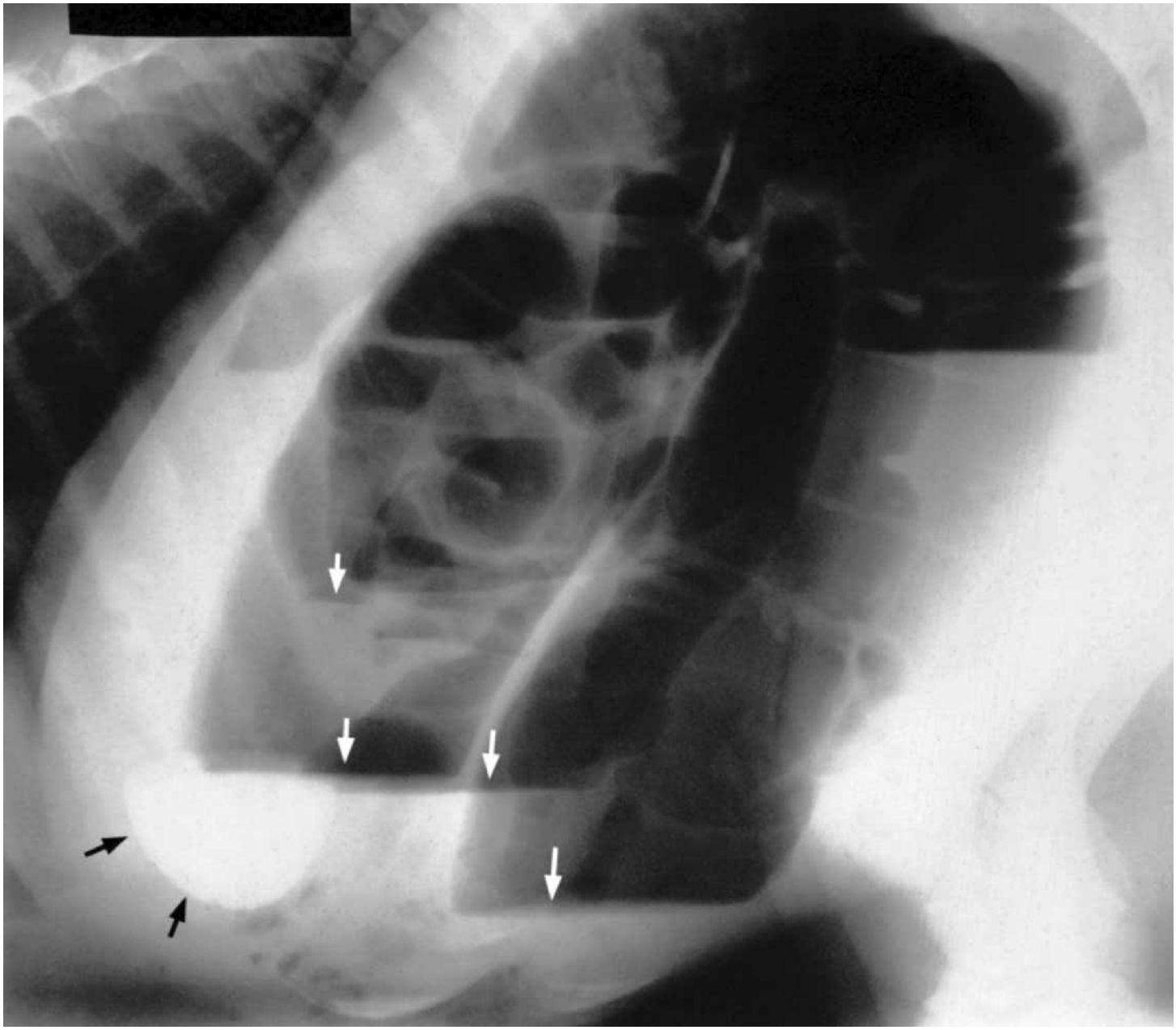


Figure 15.14 Lateral-lateral image of an abdomen; cranial is to the left. This 1-week-old Quarterhorse filly was presented because of recurrent colic. Meconium had passed normally, but there had been no faecal matter noted since then. Radiographs of the abdomen demonstrated markedly dilated large intestine with variable fluid lines (white arrows). The small intestine appears normal. There is sand in the stomach (black arrows). Radiographic diagnosis: large intestine obstruction.

Atresia coli

Atresia coli has been reported in foals and must be differentiated from other causes of ileus and colic. The lesion can be demonstrated by injection of contrast medium into the rectum, showing a lack of communication with the remainder of the large intestine (Figure 15.16a and b).

Ileocolonic aganglionosis

Ileocolonic aganglionosis occurs in white progeny of Overo Spotted Horses: 'lethal white foal'. These foals are normal at birth but do not defaecate. They develop signs of colic in the first day of life and this must be differentiated from meconium retention, atresia coli (which may also occur in these foals) and atresia ani, as well as other causes of colic. Radiographic diagnosis in these cases is based on ruling out other causes of colic and on the presence of distension of the stomach, small intestines and large bowel. A barium enema will not be expelled due to lack of contractility.

Gastroenteritis

With gastroenteritis there is a decrease in the granular appearance of the intestinal content, which appears to be more uniformly fluid-filled than normal. Gas-capped fluid levels may be common, but there is no distension and hairpin loops are seldom seen. The gas caps do not stay in the same location on subsequent images, indicating that there is intestinal motility. Transit time is usually much shorter than the expected 8 hours. Distended bowel loops are also identified on abdominal ultrasonography. Small intestinal distension, wall thickness, wall layering and small intestinal motility can be evaluated with ultrasonography, which provides important clinical information to aid in the differentiation of the cause of colic.

Gastroduodenal ulcer disease in foals

With gastroduodenal ulcer disease in foals standing lateral-lateral radiographs demonstrate gastric distension that does not diminish with fasting. A gas cap is usually noted and air is often seen in the hepatic ducts (see Figures 15.8 and 15.9). Double-contrast gastrography, performed with the foal in right lateral recumbency, demonstrates delayed gastric emptying for up to 4 hours and the contrast fills the pylorus and duodenal ampulla. Ulcers in the non-glandular portion of the stomach may be demonstrated as round to elliptically shaped lucent (black) filling defects with well-marginated walls of increased opacity (white). Ulcers can best be demonstrated by obtaining both right and left lateral-lateral recumbent and ventrodorsal radiographs, which allow for double-contrast coating of the mucosal surfaces. Standing thoracic radiographs may demonstrate mega-oesophagus with fluid and/or air. Contrast studies may demonstrate gastro-oesophageal reflux or retention of contrast medium in the oesophagus. Affected foals often have increased interstitial lung markings which are in part due to an inability to make a maximal inspiratory effort due to the abdominal

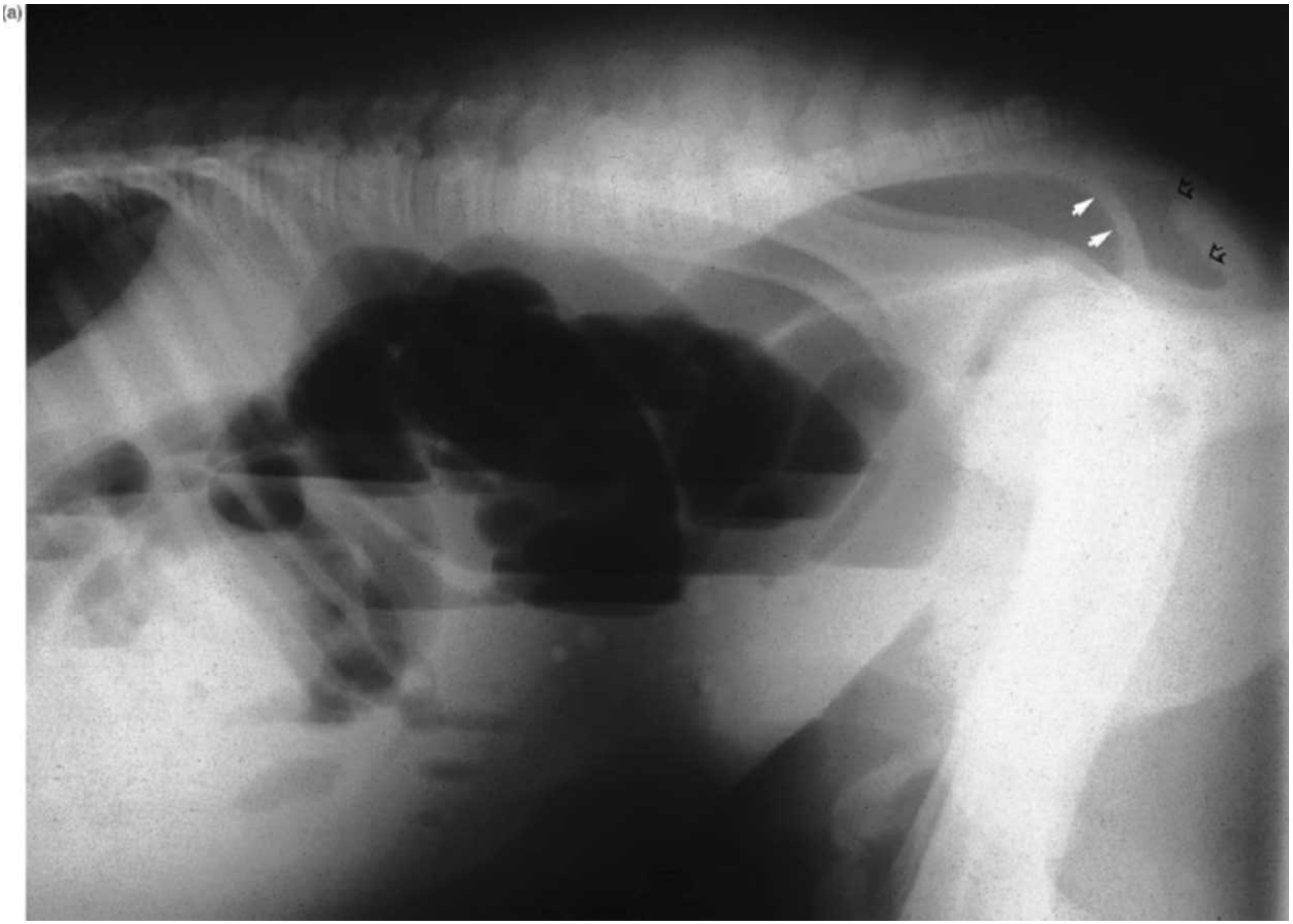


Figure 15.16 This 12-hour-old Arabian foal was born 3 weeks prematurely and had not passed meconium. Lateral-lateral image of the abdomen; cranial is to the left.
(a) A survey radiograph shows fluid- and gas-distended bowel loops with varying fluid levels indicative of obstructive ileus. The large bowel appears to terminate at a soft-tissue wall (solid white arrows). Gas in the rectum (open arrows) does not appear to communicate with the remainder of the bowel.

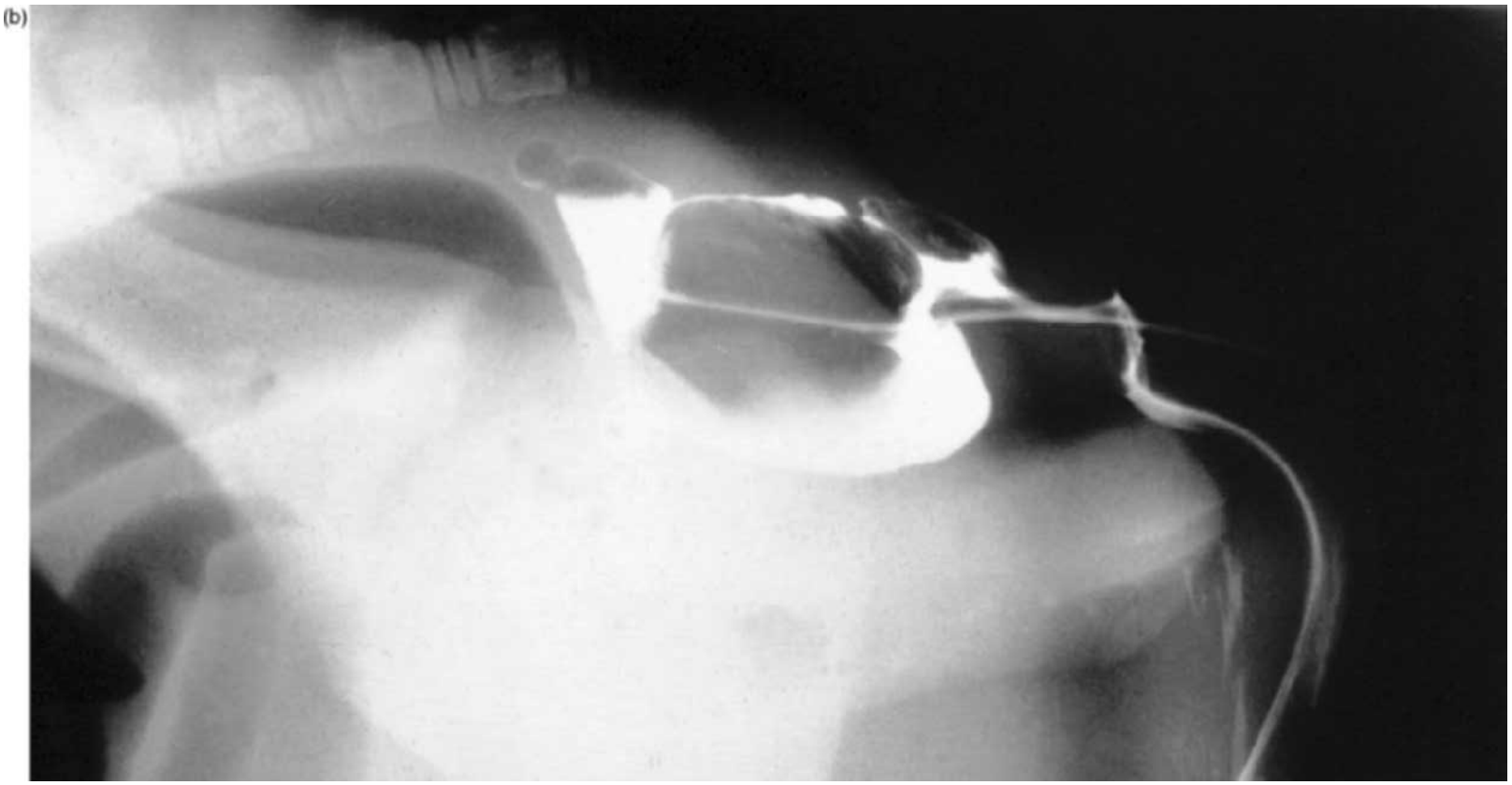


Figure 15.16 *Cont'd* (b) Barium sulphate injected into the rectum does not communicate with the terminal large bowel. The soft-tissue wall is again noted. Radiographic diagnosis: atresia coli.

distension. Inhalation (aspiration) pneumonia may be a complication of this disease (see 'Inhalation pneumonia' in Chapter 14).

Rupture of a hollow viscus

A hallmark of rupture of a hollow viscus is free abdominal gas (Figure 15.17), which highlights the poles of the kidneys and is often seen between the stomach and the diaphragm. Gas-filled intestinal loops appear to be elevated in the abdomen or to float due to free abdominal fluid, which also causes loss of abdominal visceral detail. The abdomen may appear pendulous and there may be a generalised increase in opacity of the abdomen. Ultrasonography is useful to identify free peritoneal fluid and gas.

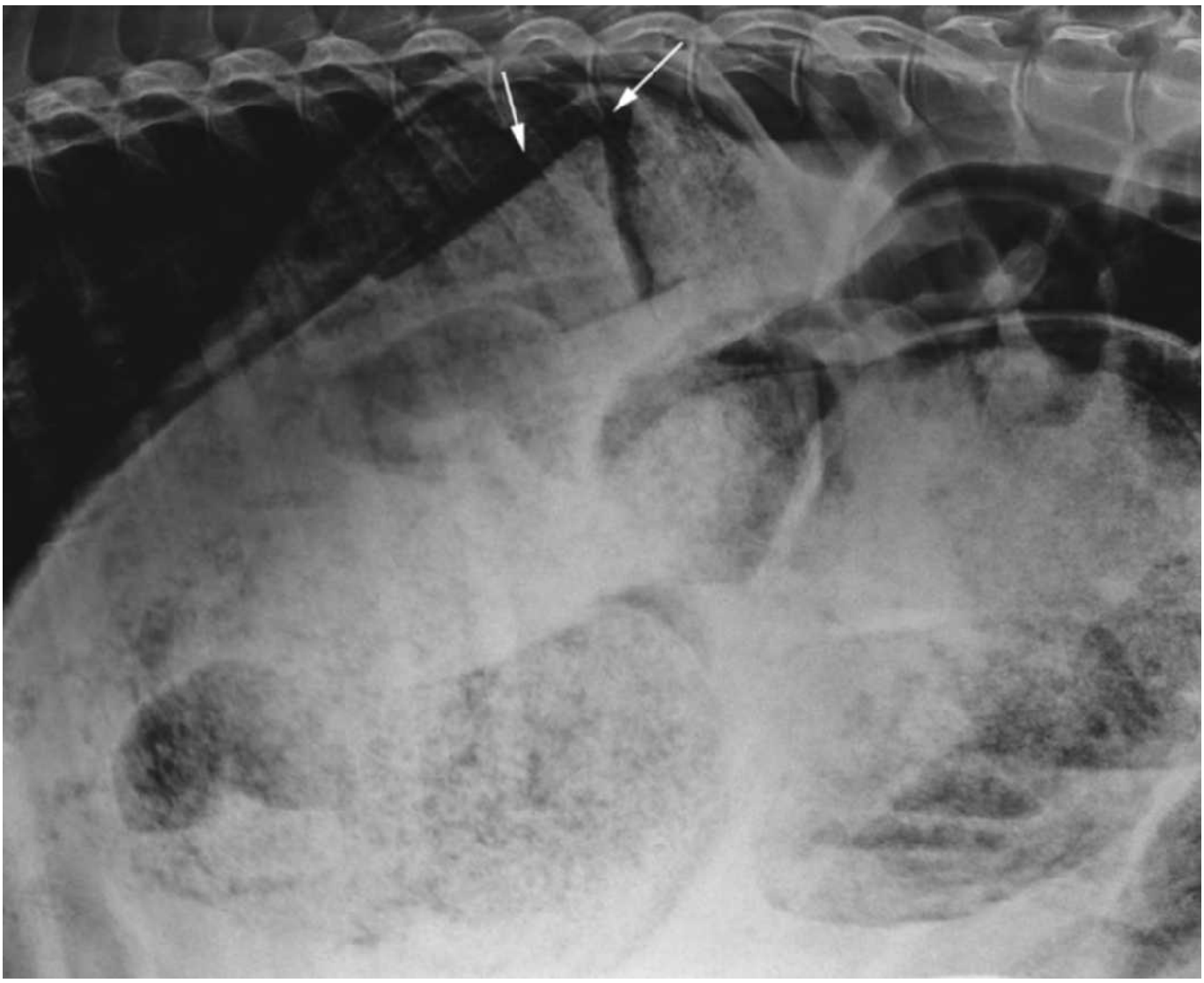


Figure 15.17 Lateral-lateral image of an abdomen of an adult pony. Cranial is to the left. There is free gas in the dorsocranial aspect of the abdomen between the stomach and diaphragm (arrows). There is a widespread heterogeneous increase in radiopacity in the mid and ventral abdominal cavity and lack of visceral detail. Dorsally there are gas-filled loops of intestine. This appearance is indicative of a ruptured hollow viscus.

Enterolithiasis of adult horses

Enterolithiasis is endemic in some geographic areas and should be suspected in patients with moderate, recurrent abdominal pain which is refractory to conservative therapy and when there is evidence of bowel obstruction. Enterolithiasis has been described in both the small intestine and the rectum, but the majority of cases occur in the colon.

When enteroliths are suspected, radiographs should be obtained with the right side of the horse against the cassette or imaging plate. Right to left lateral–lateral radiographs should be obtained if further information is needed. Radiographic diagnosis is made by defining single or multiple mineral opaque enteroliths (Figure 15w.18). Digital radiography has improved the overall sensitivity of radiography for the diagnosis of enterolithiasis compared with film–screen radiography. The diagnosis is sometimes aided by the presence of air adjacent to an enterolith. The sensitivity of radiographs for large colon enteroliths is very high, however, the absence of radiographic findings does not preclude the presence of enteroliths, particularly when an enterolith is present in the transverse or small colon. The identification of an enterolith alone does not always signify the presence of obstructive intestinal disease.

Sand impaction

Abdominal discomfort can be caused by the accumulation of sand within the colon. Sand can result in an impaction or be associated with enteritis and abdominal discomfort. Sand generally accumulates in the ventral colon and is identified on radiographs as a mineral opacity that generally conforms to the lumen of the intestines. When sand fills the haustra of the large intestine, it can create a confusing appearance that can be very similar to enterolithiasis. Sand is generally associated with a flat dorsal margin that expands to the internal diameter of the intestinal wall (Figure 15.19). Radiographs are useful for the identification and monitoring of horses with sand impaction. As the impaction resolves, the amount of sand decreases and thus it becomes less radiopaque and interspersed soft tissue and gas opacities will accumulate; reduction of opacity of the mass can occur prior to reduction in overall size of the sand impaction.

Urinary system

In an adult horse, abdominal radiography for the diagnosis of urinary tract disease is primarily of use for identification of calculi. The use of ultrasonography is generally superior for the evaluation of the kidneys.

CONTRAST EXAMINATION

Intravenous pyelography is of limited value, but can be used to assess the kidneys and ureters (see 'Intravenous pyelography' in Chapter 16). Cystography (positive or double contrast) is useful for evaluating the bladder of a foal (see below and 'Pneumocystography' in Chapter 16).

Positive contrast cystography should be preceded by survey radiography of the caudal aspect of the abdomen to assess bladder size and position. A flexible catheter is then placed in the urinary bladder and urine is withdrawn. This allows

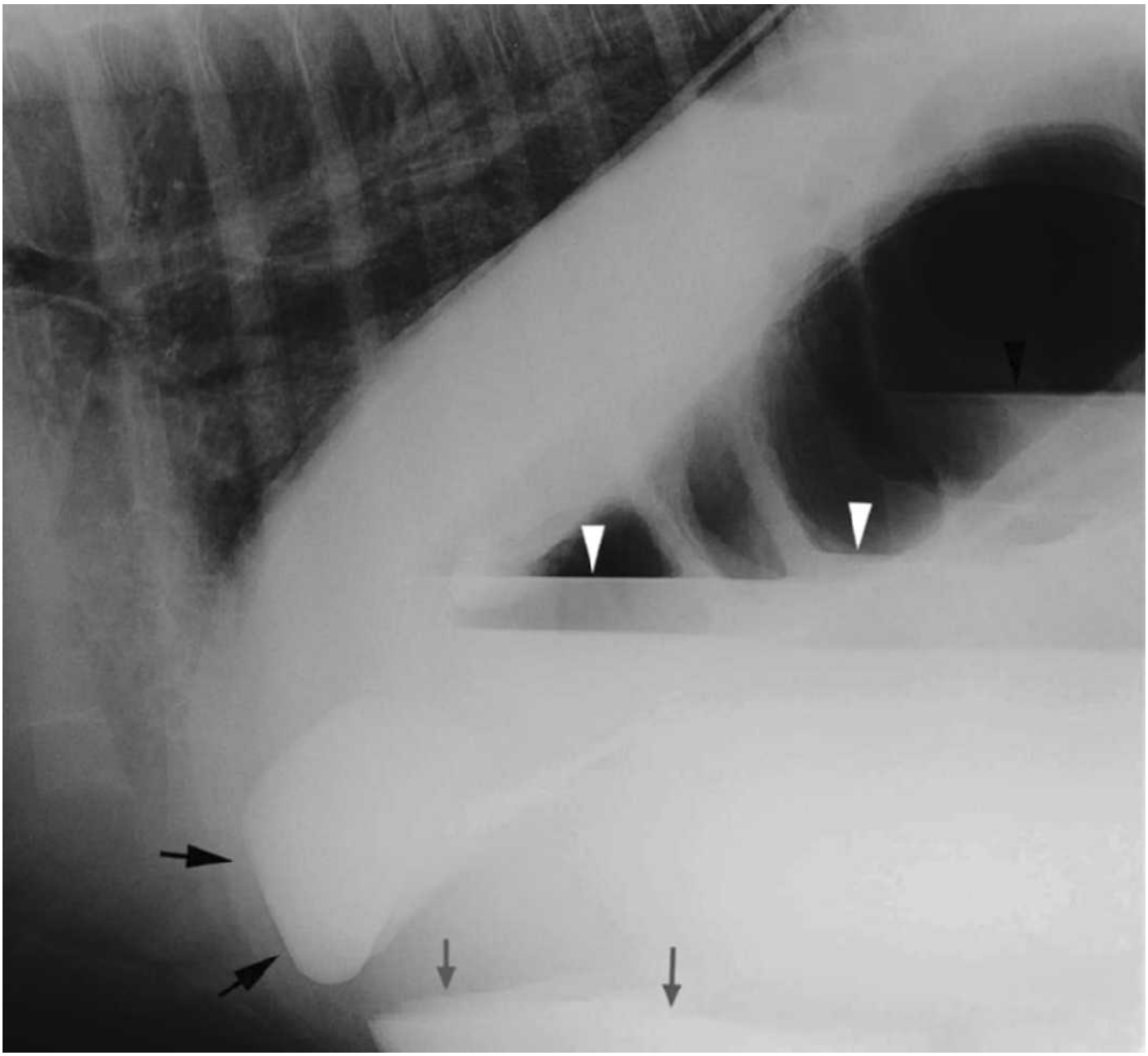


Figure 15.19 Lateral-lateral image of the cranial aspect of the abdomen of an immature horse. Cranial is to the left. There are well-circumscribed opacities in the ventral colon (black arrows). This appearance, and the flat dorsal margin (grey arrows) is typical of sand impaction. There are also multiple fluid lines (arrowheads) with gas caps within distended loops of intestine.

for evaluation of the urine as well as giving some idea of the volume of urine present. Between 2 and 5 ml of local anaesthetic solution is injected through the catheter into the urinary bladder so that the bladder may be distended without causing discomfort. A solution of equal volumes of any water-soluble contrast medium, which is recommended for intravenous use, and sterile saline is then injected. The total volume of contrast mixture required to distend the urinary bladder adequately can be calculated based on 12 ml/kg of body weight.

If no urine is retrieved after catheterisation, half of the calculated amount of contrast medium can be infused and a radiograph obtained to evaluate

the urinary bladder for content and placement. Additional contrast medium, over the amount of urine withdrawn, or 50% of the calculated dose should be given slowly by syringe or by gravity flow. When resistance is noted, the filling should stop. Lateral-lateral and two ventrodorsal oblique radiographs are then obtained. These three images allow for assessment of the entire urinary tract including the bladder wall. The positive contrast medium is then removed and an equal volume of air placed in the urinary bladder and the three radiographic views are repeated.

DISEASES OF THE URINARY BLADDER OF THE FOAL

Patent urachus

Although the diagnosis of congenital patent urachus does not require radiography, cystography or catheterisation of the urachal remnant, these techniques may be of value in assessing the degree of the defect and the condition of the urinary bladder. Ultrasonographic examination of the urachus is often helpful in defining associated abscesses and free fluid and to monitor patency. A patent urachus (Figure 15.20) or urachal remnant (Figure 15.21) often results in cystitis (see below) and may be the nidus for recurrent cystitis as well as for the development of polyarthritis/polyosteomyelitis (see 'Infectious arthritis' in Chapter 1). Patency may be demonstrated radiographically either by placing contrast medium in the urinary bladder or by injection of the urachal remnant. Umbilical cord infection is often present without the presence of a patent urachus. Acquired patent urachus is caused by extension of inflammation and necrosis from the umbilical artery, vein or urachal remnant causing the urachus to reopen.

Cystitis

Cystitis, regardless of cause, is evident radiographically by the appearance of a thickened and irregular bladder wall. The cranial ventral portion of the bladder is often most severely affected. In severe cases the entire bladder wall may be involved. Thickness and irregularity of the bladder wall can only be assessed when the urinary bladder has been adequately distended.

Rupture

Rupture of the urinary bladder is most common in foals. The most consistent radiographic sign is the presence of free abdominal fluid, but an ileus may result and signs of ileus, as well as the presence of fluid, may be noted.

The area of rupture may be demonstrated by cystography, but demonstration may require that radiographs are obtained while contrast medium is being instilled into the urinary bladder. Free contrast medium in the abdominal cavity does not present a problem provided that a sterile solution of water-soluble contrast medium is used and the patient is well hydrated. Barium should never be placed in the urinary bladder.

Ultrasonographic examination can demonstrate free fluid in the abdomen and will often demonstrate a tear.



Figure 15.20 This 1-day-old Thoroughbred colt was presented because of a swollen prepuce and umbilicus. Lateral-lateral image of the abdomen; cranial is to the left. A patent urachus was suspected and a cystogram was performed by the placement of a catheter into the urinary bladder. Distension of the urinary bladder with contrast medium demonstrates a patent urachus in the cranial ventral bladder wall (arrow) and accumulation of contrast medium in the subcutaneous tissues of the abdominal wall (arrowheads).

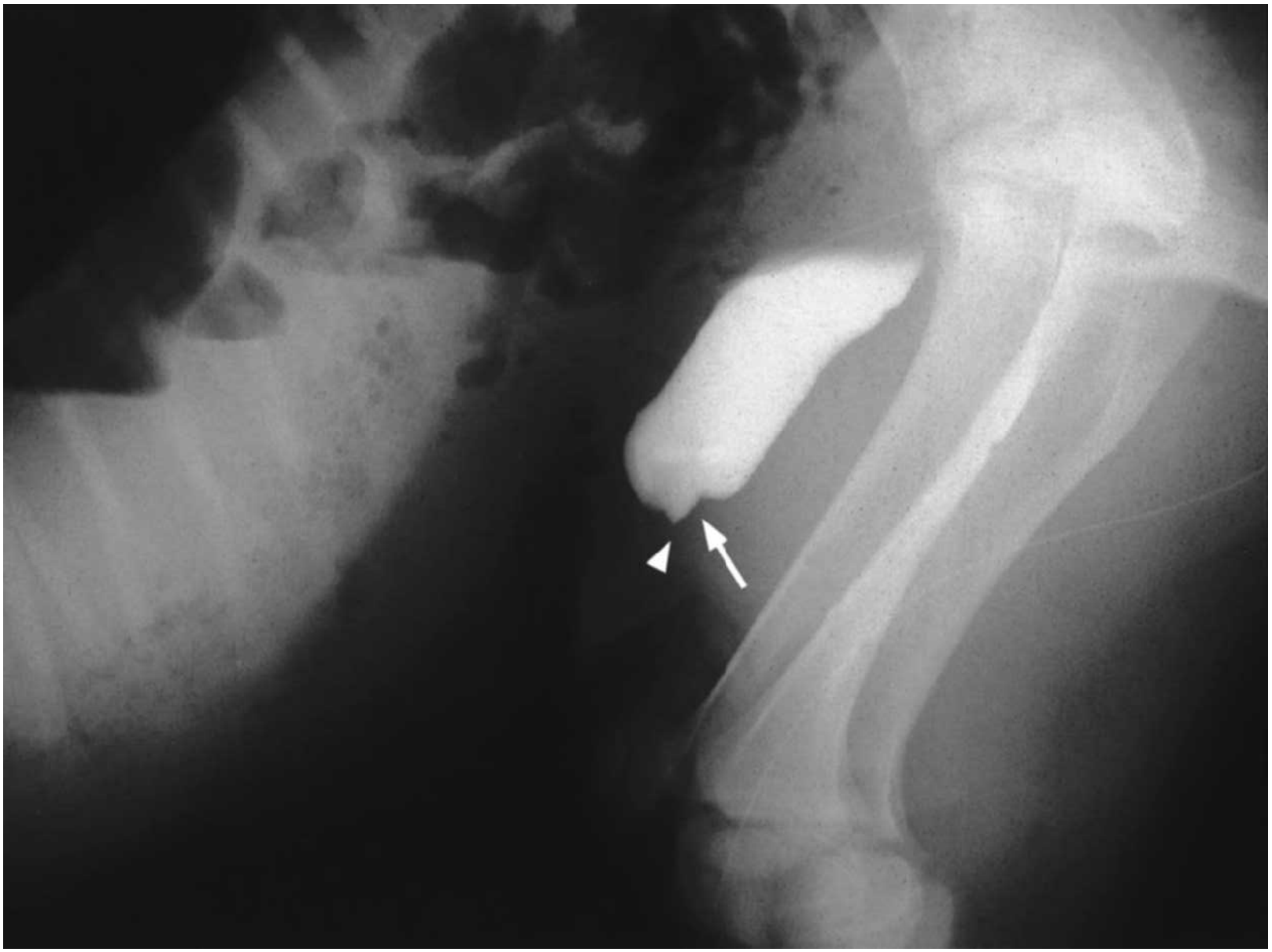


Figure 15.21 This 10-day-old Arabian colt presented because he did not exteriorise his penis and had urine scalds. Cystitis was suspected and a cystogram was performed by injection of contrast medium through a urethral catheter. The standing lateral-lateral radiograph (cranial to the left) demonstrates a normal foal abdomen. The urinary bladder is in a normal position, but there is a urachal remnant noted in the mid-ventral portion of the urinary bladder (arrowhead). The bladder wall is thickened adjacent to the diverticulum (arrow). Radiographic diagnosis: urachal diverticulum with concurrent cystitis.

Additional figures

The book companion website at www.clinical-radiology-horse.com includes additional figures that are not included in the printed book or e-book formats. Please see '**About the Companion Website**' at the start of the book for details on how to access the website. These figures are prefixed with the letter 'w' in the printed book, e.g. Figures 1w.4c–f.

FURTHER READING

Aanes, W.A. (1975) The diagnosis and surgical repair of a diverticulum of the oesophagus. *Proc. Am. Ass. Equine Pract.* **21**, 211–222

Adams, S.B., Fessler, J.F. (1987) Umbilical cord remnant infections in foals: 16 cases (1975–1985). *J. Am. Vet. Med. Ass.* **190**, 316–318

Aronoff, N., Reed, A.L., Aronson, E. (1997) Radiographic diagnosis—gastric tumor in a horse. *Vet. Radiol. Ultrasound* **38**, 185–186

Bowman, K.F., Vaughan, J., Quick, C., et al. (1978) Megaoesophagus in a colt. *J. Am. Vet. Med. Ass.* **172**, 334–337

Campbell, M.L., Ackerman, N., Peyton, L.C. (1984) Radiographic gastrointestinal anatomy of the foal. *Vet. Radiol.* **25**, 194–204

Campbell-Thompson, M.L., Brown, M., Slone, D., Merritt, M., Moll, H., Levy, M. (1986) Gastroenterostomy for treatment of gastroduodenal ulcer disease in 14 foals. *J. Am. Vet. Med. Ass.* **188**, 840–844

Dik, K.J., Kalsbeek, H.C. (1985) Radiography of the equine stomach. *Vet. Radiol.* **26**, 48–52

Fischer, A.T., Kerr, L.Y., O'Brien, T.R. (1987) Radiographic diagnosis of gastrointestinal disorders in the foal. *Vet. Radiol.* **28**, 42–48

Fischer, A., Yarbrough, T. (1995) Retrograde contrast radiography of the distal portions of the intestinal tract in foals. *J. Am. Vet. Med. Ass.* **207**, 734–737

Gehlen, H., Stadler, P., Ohnesorge, B. (2005) Tracheal obstruction in a horse with oesophageal stenosis and diverticulum. *Equine Vet. Educ.* **17**, 132–134

Greet, T.R.C. (1982) Observations on the potential role of oesophageal radiography in the horse. *Equine Vet. J.* **14**, 73–79

Greet, T.R.C., Whitwell, K.E. (1986) Barium swallow as an aid to the diagnosis of grass sickness. *Equine Vet. J.* **18**, 294–297

Hammock, P.D., Freeman, D.E., Baker, G.J. (1998) Failure of psyllium mucilloid to hasten evacuation of sand from the equine large intestine. *Vet. Services* **27**, 547–554

Hultgren, B.D. (1982) Ileocolonic aganglionosis in white progeny of Overo Spotted Horses. *J. Am. Vet. Med. Ass.* **180**, 289–292

Kelleher, M.E., Puchalski, S.M., Drake, C., le Jeune, S.S. (2014) Use of digital abdominal radiography for the diagnosis of enterolithiasis in equids: 238 cases (2008–2011). *J. Am. Vet. Med. Ass.* **245**, 126–129

Kendall, A., Ley, C., Egenvall, A., Brojer, J. (2008) Radiographic parameters for diagnosing sand colic in horses. *Acta Vet. Scand.* **50**, 17–23

Keppie, N.J., Rosenstein, D.S., Holcombie, S.J., Schott, H.C. (2008) Objective radiographic assessment of abdominal sand accumulation in horses. *Vet. Radiol. Ultrasound* **49**, 122–128

Korolainen, R., Ruohoniemi, M. (2002) Reliability of ultrasonography compared to radiography in revealing intestinal sand accumulation in horses. *Equine Vet. J.* **34**, 499–504

Kraus, B.M., Baird, A.N., Baird, D.K. (2002) Vet Med Today: What is your diagnosis? *J. Am. Vet. Med. Ass.* **221**, 1395–1396

Maher, O., Puchalski, S.M., Drake, C., le Jeune, S. (2011) Abnormal computed radiography for the diagnosis of enterolithiasis in horses: 142 cases (2003–2007). *J. Am. Vet. Med. Ass.* **11**, 1483–1485

Merritt, A. M. (1999) Normal equine gastroduodenal secretion and motility. *Equine Vet. J,* **29**, 7–13

Niinisto, K., Hewetson, M., Kaikkonen, R., Sykes, B.W., Raekallio, M. (2014) Comparison of the effects of enteral psyllium, magnesium sulphate and their combination for removal of sand from the large colon of horses. *Vet. J.* **202**, 608–611

Pankowski, R.L., Fubini, S.L. (1987) Urinary bladder rupture in a two-year-old horse: Sequel to a surgically repaired neonatal injury. *J. Am. Vet. Med. Ass.* **191**, 560–562

Pauwels, F.F., Hawkins, J.F., MacHarg, M.A., Rothenbuhler, R.D., Baird, D.K., Moulton, J.S. (2007) Congenital retrosternal (Morgagni) diaphragmatic hernias in three horses. *J. Am. Vet. Med. Ass.* **231**, 427–432

Pearson, H., Pinsent, P.J.N., Polley, L.R., Waterman, A. (1977) Rupture of the diaphragm in the horse. *Equine Vet. J.* **9**, 32–36

Peterson, F.B., Donawick, W., Merritt, A., Raker, C., Reid, C., Rooney, J. (1972) Gastric stenosis in a horse. *J. Am. Vet. Med. Ass.* **160**, 328–332

Rantanen N., McKinnon, A. (1998) Equine Diagnostic Ultrasonography, 1st edn, Williams & Wilkins, Baltimore

Reef, V. (1998) Equine Diagnostic Ultrasound, 1st edn, W.B. Saunders, Philadelphia

Rindermann, G.F., Velde, K., Nagy, A.D. (2007) Vet Med Today: What is your diagnosis? *J. Am. Vet. Med. Ass.* **10**, 1465–1466

Romero, E., Alfredo, A., Rodgerson, H. (2010) Diaphragmatic herniation in the horse: 31 cases from 2001–2006. *Can. J. Vet.* **51**, 1247–1250

Rose, J.A., Rose, E.M., Sande, R.D. (1980) Radiography in the diagnosis of equine enterolithiasis. *Proc. Am. Ass. Equine Pract.* **26**, 211–220

Ruohoniemi, M., Kaikkonen, R., Raekallio, M., Luukkanen, L. (2001) Abdominal radiography in monitoring the resolution of sand accumulation from the large colon of horses treated medically. *Equine Vet. J.* **33**, 59–64

Schleining, J., Voss, E. (2004) Hypertrophic osteopathy secondary to gastric squamous cell carcinoma in a horse. *Equine Vet. Educ.* **16**, 304–307

Schneider, J.E., Leipold, H.W. (1978) Recessive lethal white in two foals. *J. Equine Med. Surg.* **2**, 479–482

Swain, J., McGorum, B., Scudamore, C., Pirie, R. (2004) Persistent oesophageal obstruction (choke) associated with diverticulum of the terminal oesophagus in a pony. *Equine Vet. Educ.* **16**, 195–200

Traub, J.L., Gallina, A., Grant. B., Reed S., Gavin, P., Paulsen, L. (1983) Phenylbutazone toxicosis in the foal. *Am. J. Vet. Res.* **44**, 1410–1418

Verschooten, F., Oyaert, W., Muylle, E., De Moor, A., Steenhaut, M., Moens, Y. (1977) Diaphragmatic hernia in the horse: four case reports. *Vet. Rec.* **18**, 45–50

West, H.J., Kelly, D.F. (1987) Renal carcinomatosis in a horse. *Equine Vet. J.* **19**, 548–551

Wimberly, H.C., Andrews, E.J., Haschek, W.M. (1977) Diaphragmatic hernias in the horse: a review of the literature and analysis of six additional cases. *J. Am. Vet. Med. Ass.* **170**, 1404–1407

Wong, D., Hepworth, K., Yaeger, M., Miles, K., Wilgenbusch, C. (2015) Imaging diagnosis—hypoglycemia associated with cholangiocarcinoma and peritoneal carcinomatosis in a horse. *Vet. Radiol. Ultrasound* **56**, E9–E12

Yarsborough, T., Langer, D., Snyder, J., et al. (1994) Abdominal radiography for diagnosis of enterolithiasis: 141 cases (1990–1992). *J. Am. Vet. Med. Ass.* **205**, 592–595

Chapter 16
Miscellaneous techniques

ARTHROGRAPHY AND BURSOGRAPHY

Arthrography is the technique of introducing a contrast medium into a joint prior to obtaining radiographs. It has been used to aid evaluation of articular cartilage, meniscal damage, subchondral bone and synovial membrane or to determine the presence of communication between adjacent synovial structures (Figure 9.32c). It may be indicated in cases showing chronic joint distension, without apparent radiological abnormality on plain radiographs, radiographic findings incompatible with the clinical signs, or suspected joint capsule or articular cartilage damage. More specific indications include evaluation of a so-called 'articular synovial cyst', joint capsule herniation, rupture or penetration, evaluation of cartilage flaps in osteochondrosis, to look for a cartilaginous joint fragment, and to differentiate between intra-articular and extra-articular bone fragments. It can also be used to determine whether an osseous cyst-like lesion communicates with a joint. Bursography is the technique of introduction of a contrast medium into a bursa. It can be used to assess the integrity of the bursal wall, to identify filling defects due to a space-occupying lesion and, for example, to facilitate identification of a fibrocartilage defect on the palmar aspect of the navicular bone or to identify an adhesion of the deep digital flexor tendon to the navicular bone. Diagnostic ultrasonography can also be useful in assessment of some of these problems. Contraindications for arthrography may include infections of the joint or adjacent tissues, inflammation, and patients known to be allergic to contrast media.

For positive (or radiopaque) contrast studies, any media approved for intravenous use may be used. Concentrated contrast media may obscure the joint surface, and thus obscure the lesions they are intended to outline, so dilution of the contrast medium may be required. Approximately 25% triiodinated water-soluble contrast medium is recommended. Some radiologists recommend the use of negative (or radiolucent) contrast (air, nitrogen or carbon dioxide), or double contrast, i.e. the use of negative and positive media together. Negative-contrast techniques may cause artefacts, due to gas bubbles forming in the synovial fluid during injection, and for this reason negative and double-contrast studies are not often carried out. The formation of bubbles can be reduced by injecting the gas prior to the positive contrast medium, and by using a positive contrast medium with a low viscosity.

Clinical Radiology of the Horse, Fourth Edition. Janet A. Butler, Christopher M. Colles, Sue J. Dyson, Svend E. Kold and Paul W. Poulos.
© 2017 John Wiley & Sons, Ltd. Published 2017 by John Wiley & Sons, Ltd.
Companion website: www.clinical-radiology-horse.com

Technique

The patient may require sedation or general anaesthesia. The skin overlying the joint is prepared aseptically. Plain survey radiographs should be obtained immediately prior to the contrast study in order to re-evaluate the joint, because the contrast agent may remain in the joint or adjacent tissues for some time, making subsequent plain radiography impractical.

A needle is introduced into the joint using aseptic technique. A volume of synovial fluid is then withdrawn and the equivalent volume of contrast medium introduced. The volumes will vary from 2 to 20 ml, depending on the size of the joint concerned. For double-contrast studies, as much fluid as possible is withdrawn initially, and after injection of positive contrast medium as much fluid as possible is again withdrawn. The joint is then distended with gas in order to outline the structures of the joint. (Although this is the normal technique, which first allows acquisition of radiographs with positive contrast medium only if desired, it has been suggested that introduction of the gas first results in fewer artefacts from the formation of bubbles.)

After the injection of contrast medium, the joint should be extended and flexed, in order to spread the contrast medium evenly throughout the joint. The study should be completed as soon as possible, and certainly within 20 minutes, or the contrast medium will begin to be absorbed through the synovial membrane and the sharp appearance of the structures will be lost (see Figure 5.15b and Figure 8.12).

Diagnostic criteria

Positive contrast medium fills the joint, mixing with the synovial fluid. It outlines the joint pouches and lies as a thin layer over the cartilage surfaces. The radiograph should be carefully examined, initially to ensure that areas of contrast medium conform with the normal anatomical shape of the joint. Subsequently the areas of contrast medium should be searched for any lucent areas (filling defects). These may represent radiolucent tissue masses (e.g. in chronic proliferative synovitis, see Figure 5.15b), or simply be areas of the joint to which contrast medium has failed to be dispersed for some other reason. The differentiation between the two may be difficult, but further passive movement of the joint may help ensure even filling. The cartilage surfaces should be carefully examined for irregularity of the contrast medium adjacent to the cartilage surface. This may be particularly useful for detection of cartilage flaps, where contrast medium will be seen between the flap and the underlying bone, resulting in a visible cartilage irregularity and a lucent area in the contrast medium overlying the defect.

Positive contrast arthrography may be used to determine if a wound has penetrated a synovial cavity. The joint capsule must be adequately distended with the contrast medium to determine if there is any leakage.

If double contrast studies are used, care must be taken that bubbles of gas are not misdiagnosed as tissue masses.

TENDONOGRAPHY

The term ‘tendonography’ includes any radiographic study of tendons. However, plain radiography of tendons is generally not very rewarding and so this section only describes studies involving the use of contrast media. The

tendons and ligaments on the palmar and plantar aspects of the third metacarpal and metatarsal bones may be assessed using contrast media. Although diagnostic ultrasonography has largely superseded tendonography for the assessment of tendons and ligaments, it can permit detection of tears of the manica flexoria (Figure 5w.17b) which might otherwise be overlooked and lateral margin tears of the deep digital flexor tendon in the fetlock region (Figure 5w.17c).

Technique and diagnostic criteria

Radiological examination of the tendon sheaths and bursae can be performed in a manner similar to that described above for arthrography, using similar techniques and concentrations of contrast medium. When presented with a horse with distension of the digital flexor tendon sheath, positive contrast medium (5–7ml sodium meglumine diatrozoate) can be injected at the same time as local anaesthetic solution (10ml). Lateromedial images can be acquired before reassessment of lameness. In a normal horse the manica flexoria is outlined by two parallel lines of contrast medium in a lateromedial image. The presence of a tear of the manica flexoria is indicated by the two lines of contrast medium diverging, loss of one of the lines of contrast medium, contrast medium within the manica flexoria or pooling of contrast medium dorsal to the deep digital flexor tendon at the level of the manica flexoria (Figures 5w.17a–c). A tear of the lateral margin of the deep digital flexor tendon is indicated by the presence of contrast medium within the tendon. In a study of 23 horses with lameness associated with distention of a digital flexor tendon sheath, comparison was made between the results of contrast radiography and tenoscopy. Contrast radiography had 90% sensitivity and 81% specificity for identification of manica flexoria tears and 57% sensitivity and 84% specificity for identification of marginal tears of the deep digital flexor tendon.

For evaluation of soft-tissue structures the use of air as the contrast medium may be preferable. Air tendograms can be performed under mild sedation with the horse standing. An area of skin is clipped over the centre of the flexor tendons of the metacarpus/metatarsus, on the palmar or plantar surface. The skin is then prepared aseptically. Local anaesthetic solution is infiltrated at the site where the air is to be injected. A needle is passed through the skin and air injected subcutaneously and between the flexor tendons and ligaments. One hundred millilitres of air is usually sufficient. In order to separate the tendons and peritendonous tissues, considerable pressure may be required. Most of the air will be resorbed in 24 hours, and no adverse reactions have been reported. Standard radiographic views are acquired, using approximately half the mAs normally required.

ANGIOGRAPHY

Angiography is the technique whereby blood vessels are assessed by the injection of a positive-contrast medium at the time of radiography. It is used to gain information about the anatomical position of blood vessels, to gain evidence of vascular disease and, in some circumstances, to study the flow of blood through the vessels. Although it has been largely used for experimental purposes in equine veterinary medicine, it has an important role to

play in the investigation and treatment of certain diseases, such as auditory tube diverticulum mycosis (see 'Eustachian tube diverticulum mycosis' in Chapter 11) and suspected vascular abnormalities. It has also been used extensively in studies of the distal aspect of the limb of the horse.

The technique is normally (but not invariably) carried out under general anaesthesia. For examination of the arteries, a positive contrast medium is injected into a major artery supplying the area. For venous studies, however, contrast may be injected via a major artery, allowing normal flow to carry it into the veins, or it may be injected directly into a suspected venous abnormality. It is also possible to stop venous outflow from an area with a tourniquet, and inject contrast medium into a vein, filling the veins 'against the flow', i.e. a retrograde injection. Although it is advantageous to obtain a series of radiographs after injection in order to assess flow through the blood vessels, it may be adequate for many clinical cases to obtain a single radiograph, the timing depending on the area to be examined, but generally being about 2–5 seconds after the end of the injection.

Technique

The skin over the vessel to be injected is prepared as for surgery. Subcutaneous vessels may be injected directly with a percutaneous injection, but deeper vessels such as the carotid or common digital arteries are best approached surgically. It is important that arteries are handled with care, because trauma may cause spasm and give false results. It is recommended that the Seldinger technique be used to catheterise arteries, as this permits the introduction of a catheter of relatively large diameter with the minimum of trauma. After the study is completed, the catheter may be withdrawn and haemorrhage controlled by applying finger pressure to the vessel for at least 2 minutes. For deeper injection sites, it is recommended that the tissues should be sutured and the incision closed prior to the withdrawal of the catheter, unless the patient is suspected to have clotting defects. Subsequent to withdrawal, pressure applied to the area with fingers or a pressure pad and bandage is normally adequate to stem haemorrhage. If a very large-diameter catheter is used, then a purse-string suture should be placed in the vessel wall prior to removal of the catheter, and pulled tight and tied after catheter withdrawal. Once a catheter has been introduced into a blood vessel, it may be passed on through the vessel, and manipulated to follow branches of the vessel (e.g. the internal carotid artery may be catheterised by passing a catheter with a curved tip along the common carotid artery). When injections of contrast medium are made, the tip of the catheter should be positioned at least 5 cm to the cardiac side of any branches of the vessel that are to be examined as part of the study.

A pressure injector is recommended if flow studies are required, or for adequate assessment of large vessels where a large volume of contrast medium is required. Hand injections are adequate in many practice situations, although they may require the use of a larger-diameter catheter to allow injection of adequate volumes of contrast medium. There are many contrast media available for use in angiography and there are no special requirements for the horse. The volume of contrast medium required should be just sufficient so that when the injection is completed, it fills the arterial vessels only, with no contrast medium evident in the capillary bed or veins.

This varies with the area involved and the size of patient (approximately 5 ml for an injection into the common digital artery or 20 ml for injection into the common carotid artery).

Diagnostic criteria

Figures 16.1, 16.3a and 16.3b show normal angiograms of the head and distal aspect of a limb of a horse. A detailed description is not given, since reference to the figures will give adequate information on the normal appearance. More detailed information on the techniques and results can be obtained from the 'Further reading' list. The information that follows gives a general outline of the changes that can be anticipated to be found on angiograms of any area.

Clinically significant lesions found will vary with the site radiographed, but may include those given below.

Irregular arterial wall

1 There may be an irregular 'roughened' appearance to the arterial wall. There may be little overall change in diameter of the arterial lumen, or there may be obvious narrowing of a section or all of the artery. This may indicate arterial disease, e.g. thrombosis. This is seen in the internal carotid in some cases of auditory tube diverticulum mycosis, where it may indicate the initial stages of thrombosis of the artery. It also occurs in the digital arteries of many normal horses.

2 A condition known as 'beading' may occur, when the arterial wall goes into spasm. This gives regular narrowed bands along the length of the vessel, although the wall appears to have a generally smooth internal surface. This can occur in normal vessels, and is probably triggered by the pressure of the injection. It is most common in vessels that are already sensitive, either from rough handling when being catheterised or if suffering from arterial disease.

Distension of a vessel

1 A vessel may become enlarged because of an increased peripheral resistance or increased flow to an inflamed area, and does not necessarily indicate arterial disease.

2 Out-pouchings of a vessel are abnormal. The most common cause is an aneurysm (Figure 16.2). This results from a weakness of the arterial wall, which allows the arterial lining to be forced through a defect in the wall. They are seen on angiograms as an out-pouching, with a slight narrowing on the cardiac side of the defect. They may be congenital or acquired. Frequently they will give rise to spontaneous haemorrhage.

Narrowing of a vessel and failure to fill

Narrowing of a vessel and failure to fill have many common causes, which must be determined in the light of the available clinical information:

1 Arterial spasm may prevent a vessel filling or may cause partial filling or beading (see above). If serial radiographs are obtained using a rapid automatic serial plate changer, the vessel may be visible for part of the time,

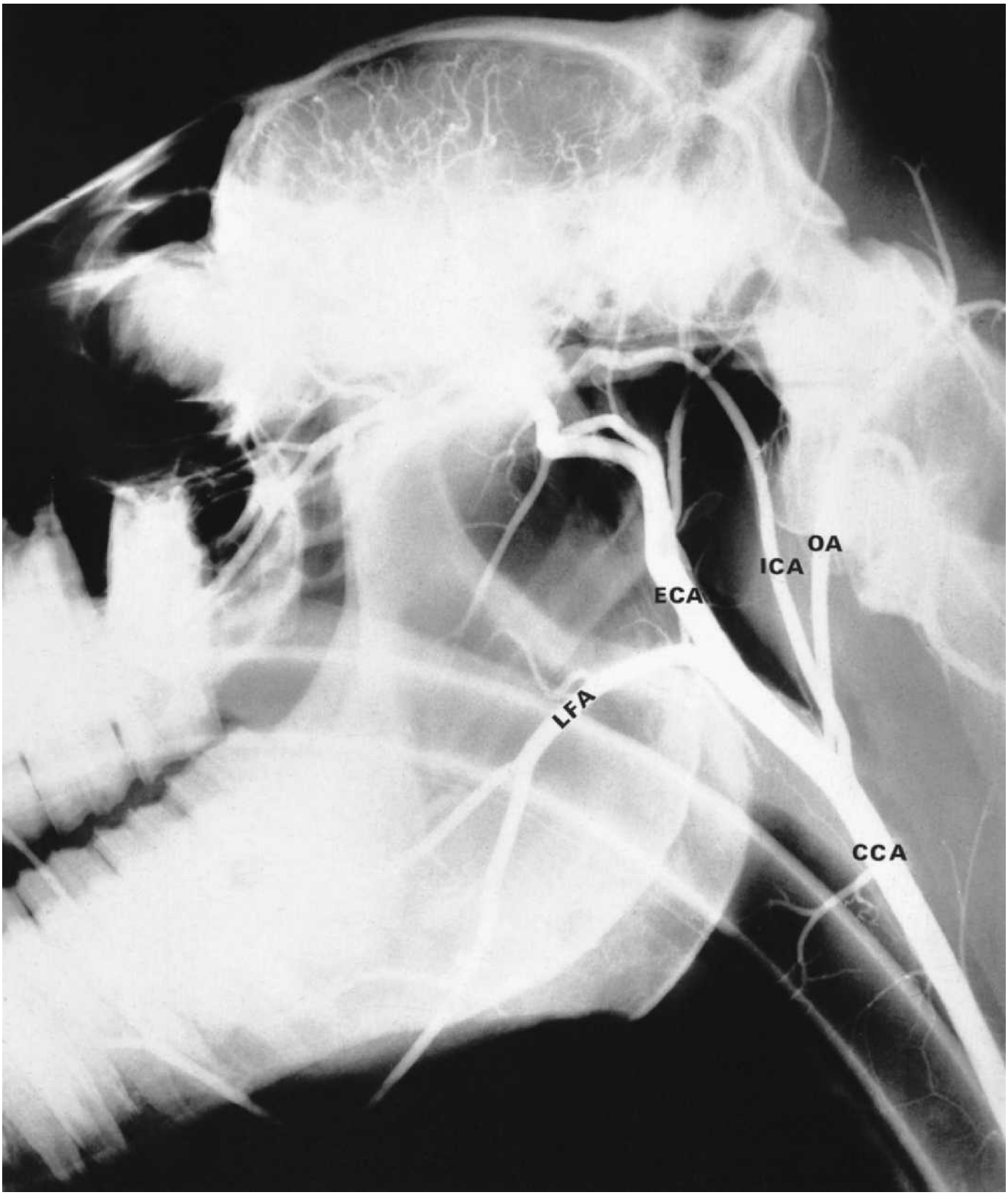


Figure 16.1 Lateral-lateral image of the pharyngeal region to show a normal angiogram of the head. Rostral is to the left. The radiograph was obtained with the horse under general anaesthesia. Note the endotracheal tube, common carotid artery (CCA), occipital artery (OA), internal carotid artery (ICA), external carotid artery (ECA) and linguofacial artery (LFA).

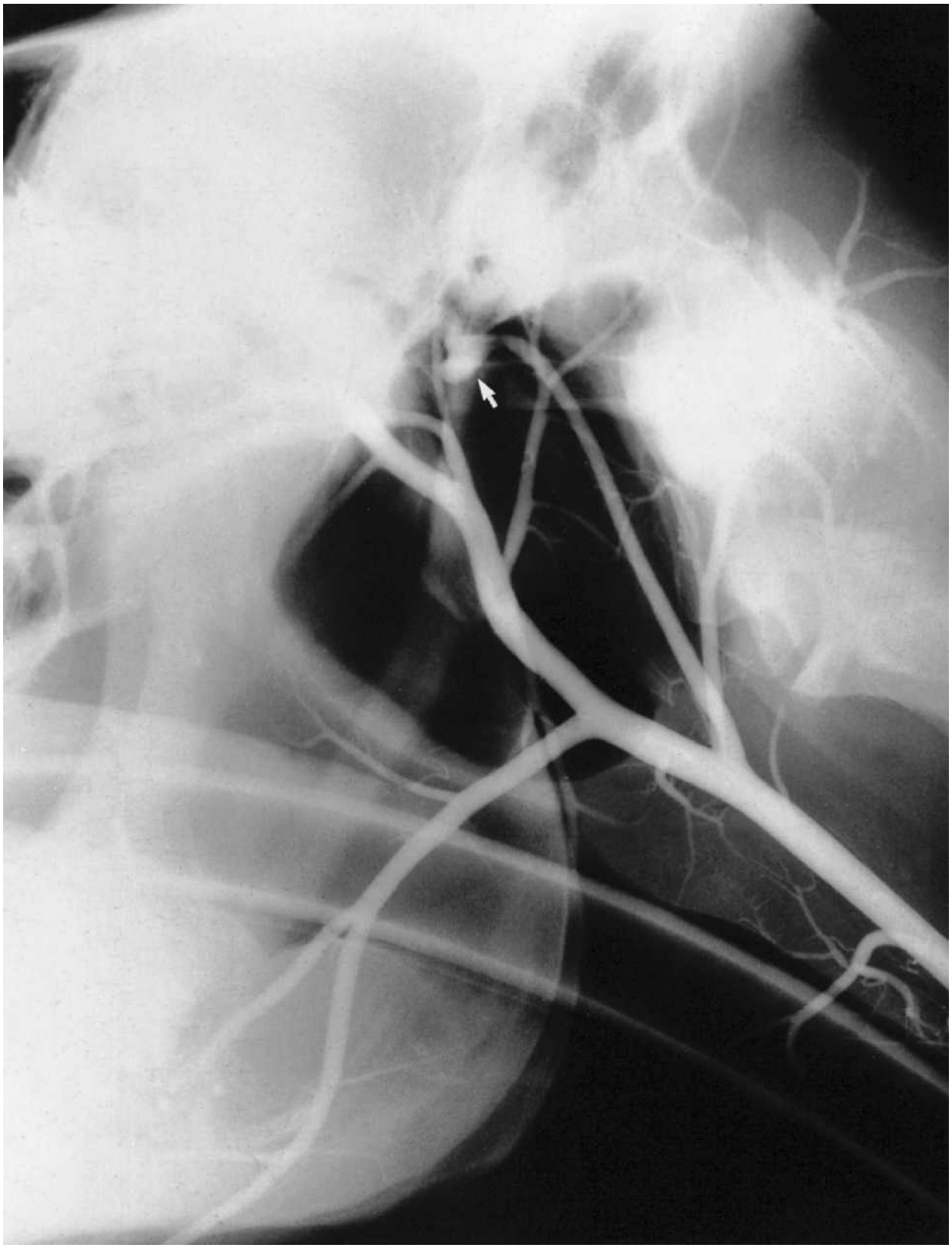


Figure 16.2 Lateral-lateral image of the pharyngeal region of a 7-year-old Thoroughbred with a recent history of epistaxis and dysphagia. Rostral is to the left. Endoscopic examination confirmed the presence of auditory tube diverticulum mycosis. This angiogram demonstrates an aneurysm of the internal carotid artery (arrow).



Figure 16.3(a) Lateromedial image of the foot of a normal pony. This angiogram was obtained 2.5 seconds after injection of the contrast medium into the common digital artery approximately 5 cm distal to the carpus (the pony was under general anaesthesia).

being occluded usually at the start of the injection. Repeat injections may be needed, but may result in repeat occlusion or narrowing of the vessel.

2 Another common cause of failure of an artery to fill is external pressure on the vessel. This may be caused by a haematoma, abscessation, neoplasia or incorrect positioning of the patient.

3 Arterial thrombosis may cause partial or complete occlusion of vessels (see also 'Distension of a vessel', above).

4 Inadequate concentration, volume or rate of injection of contrast medium may result in inadequate contrast medium for assessment of a vessel.

VENOGRAPHY

Digital venograms are used to obtain information about veins which are compressed by dislocated soft and/or osseous tissues. Venograms are acquired with a tourniquet in place, thus the foot circulation is isolated and therefore venograms give no information about digital blood flow. Retrograde venography in the digit has been described, usually in cases of laminitis, but also in horses with chronic foot pain associated with abnormalities of the conformation of the hoof capsule and/or abnormal orientation of the distal phalanx.

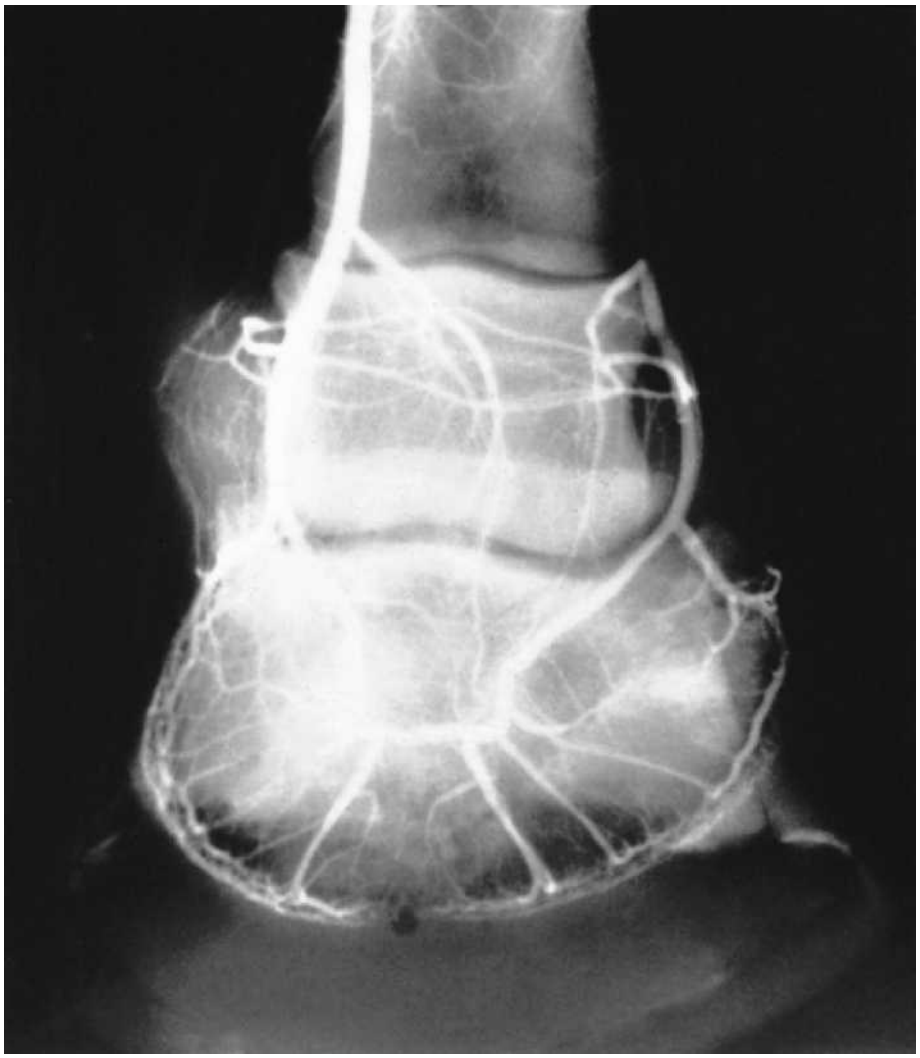


Figure 16.3(b) Dorsoproximal-palmarodistal oblique image of the foot of a normal pony. The angiogram was obtained 2.5 seconds after injection of the contrast medium into the common digital artery approximately 5 cm distal to the carpus (the pony was under general anaesthesia).

Technique and interpretation

The technique can be performed in a standing sedated horse, but requires a team of well-prepared people, each of whom knows exactly what to do (ideally one person to hold the horse, a second person to support and manipulate the limb, a third person to perform the injections and hold the imaging plates and a fourth person to acquire the radiographs). The shoe should be removed so that regions of the sole are not obscured. The pastern region should be clipped in the region of the palmar digital veins. The lateral palmar digital vein is usually injected, but it is useful if the medial palmar digital vein is also prepared in case injection complications arise. Two 10 ml syringes are preloaded with sodium meglumine diatrozoate. Perineural analgesia of the palmar nerves at the level of the proximal sesamoid bones is performed. The horse is positioned with both feet on low wooden blocks. Pre-injection lateromedial and dorsopalmar radiographs are acquired to check positioning; radiographs should be centred at the level of the distal phalanx to avoid distortion of the circumflex vessels. Accurate positioning is key for accurate interpretation. A tourniquet is applied around the fetlock. An assistant positions himself/herself in front

of the limb so that shoulder pressure can be applied against the horse's carpus if it tries to move, and so that the limb can be manipulated after the first injection. After aseptic preparation of the skin in the pastern region, a 21 gauge, 1.9 cm butterfly catheter with 30.5 cm tubing is passed distally into the lateral digital vein in the mid-pastern. Blood should flow freely. A screw-on cap is applied to the end of the tubing. One of the preloaded syringes is attached to the tubing (after removal of the cap) and contrast medium is injected. The tubing is clamped with mosquito forceps and the carpus is flexed and then extended to unload and reload the heel. The second preloaded syringe is attached, the mosquito forceps are released and the contrast medium is injected. When the injection is complete the tubing is clamped using mosquito forceps and both are taped to the limb at the level of the fetlock. Lateromedial and dorsopalmar (and optional dorsoproximal-palmarodistal oblique) views are obtained, followed immediately by second lateromedial and dorsopalmar views. All radiographic images need to be acquired within 45 seconds of injection. The tourniquet is removed, followed by the butterfly catheter. Pressure should be applied immediately over the injection site using a firm bandage.

The lateral and medial digital veins, capillaries and arteries are filled retrograde, permitting assessment of the terminal arch, coronary plexus, dorsal lamellar vessels, circumflex vessels and vessels of the heel region (see Figure 3.57a). The second lateromedial view can demonstrate the contrast medium diffusing into the soft tissues, and may delineate an abnormality. In chronic laminitis, displacement of the distal phalanx, morphological changes in the laminae and compression of vessels can all contribute to alterations of the vasculature, notably in the coronary plexus, dorsal lamellar vessels and circumflex vessels (see Figure 3.57b). Such abnormalities may have some influence on treatment and prognosis.

In a normal horse the contrast medium stays within the vessels and the distal phalanx is proximal to the circumflex vein. In laminitis there may be alteration of the vasculature, notably compression of vessels in the coronary plexus, sublamellar plexus, terminal and solear papillae and the circumflex vein (Figure 3.57b). The position of the toe of the distal phalanx relative to the circumflex vein may be altered. There may be distribution of the contrast medium into the abnormal sublamellar tissues (Figure 3w.57c). There may be distortion of the circumflex vessels dorsally because of inward growth of solear horn (Figure 3w.57d). Venography permits evaluation of the severity of vascular changes and can predict osseous pathology (e.g. distal displacement of the distal phalanx) before it happens. Venography may be repeated every 3 to 7 days to assess both progression of the disease and the response or otherwise to treatment.

The most common problems associated with the technique are due to an inadequate volume of contrast medium being used. This may be the result of failure of the tourniquet, or perivascular injection, often after several venepunctures. The total volume of injected contrast medium for large horses may need to be increased to 25–30 ml. With an inadequate amount of contrast medium the vessels may appear thin and may have a slightly beaded appearance. Failure to unload and reload the heel during injection may result in reduced filling of the vessels in regions under load. Delay in acquisition of the first radiographs may result in the contrast medium diffusing into the soft tissues.

MYELOGRAPHY

Myelography is the technique of introducing contrast medium into the vertebral canal before radiography. It is usually performed to define the site or sites of cervical spinal cord compression in an ataxic horse, when a detailed clinical examination has suggested a lesion involving the cervical spinal cord. It is essential if surgical treatment is being considered. Survey radiographs should be obtained prior to myelography and are often suggestive of the site of a lesion. Recent evidence suggests that the technique can be unreliable and that semiquantitative evaluation of plain radiographs may be more accurate.

Technique

Myelography can be performed in a standing sedated horse, but is best performed under general anaesthesia, because it results in fewer untoward side-effects, and the neck can be examined radiographically in the normal, flexed and extended positions. This is essential for identification of dynamic compressive lesions. It also enables ventrodorsal views to be obtained (see 'Cervical vertebrae – Radiographic technique – The anaesthetised horse' in Chapter 12 for details of the radiographic technique).

At present, the following anaesthetic regimen is recommended for myelography, because it has been associated with minimal side-effects: premedication with acepromazine, detomidine or xylazine, followed by induction of anaesthesia using guianfenesin and thiopentone or ketamine, and maintenance using isoflurane or halothane in oxygen. Pretreatment with phenylbutazone is recommended.

The horse is positioned in lateral recumbency and plain lateral-lateral survey radiographs are obtained. It is important to support the neck with radiolucent cushions in order to obtain true lateral-lateral projections, which are essential for correct interpretation (see 'Cervical vertebrae – Radiographic technique – The anaesthetised horse' in Chapter 12).

The skin over the poll is clipped and prepared aseptically. The head is elevated approximately 30° and positioned so that the long axis of the head is perpendicular to the long axis of the neck. This prevents cranial passage of contrast medium. An 18 gauge 86 mm spinal needle is inserted at the intersection of a line joining the cranial borders of the wings of the atlas and the dorsal midline. It is directed perpendicularly to the skin, aiming for the lower incisor teeth. A change of resistance can usually be appreciated as the needle penetrates the dorsal atlanto-occipital membrane and the cervical dura mater. The needle's stilette is withdrawn, and cerebrospinal fluid (CSF) will appear at the hub if the needle is correctly positioned. It is important not to insert the needle too deeply, since spinal cord puncture may result, with severe adverse consequences. Injection can be performed under ultrasound guidance.

Approximately 40–50 ml of CSF is slowly withdrawn (over approximately 3 minutes) before injecting a similar volume of contrast agent over 3–5 minutes. Once injection is complete the needle is removed. Elevation of the head for 5 minutes after injection may facilitate spread of the contrast medium caudally and minimise the risk of spread cranially.

A superior technique involves the insertion of needles at both the cisterna magna and the lumbosacral subarachnoid cistern. To achieve the latter, a spinal needle is inserted on the dorsal midline approximately level with the

cranial edge of the tubera sacrale and the caudal border of each tuber coxae, between the caudal edge of the spinous process of the sixth lumbar vertebra and the cranial edge of the second sacral spinous process. The latter landmarks can be difficult to palpate in a well-muscled horse. Care should be taken to advance the needle in the sagittal plane. The needle is advanced into the ventral subarachnoid space, through the interarcuate ligament, dorsal dura mater and arachnoid and the conus medullaris. Forty to sixty millilitres of contrast medium are injected slowly via the cisterna magna, and CSF is allowed to flow from the lumbosacral site. The stilette should be replaced in the needle at the lumbosacral site while images are obtained. This method, although technically more difficult, encourages contrast medium to flow in a caudal direction.

Historically metrizamide was used successfully in the horse, although there were a number of side-effects, including delayed recovery from anaesthesia, muscle fasciculations, depression, pyrexia and deterioration of ataxia (it is not clear whether this last is due to the contrast medium or the effects of manipulating the neck during myelography and recovery from anaesthesia). Other, less irritant, non-ionic, water-soluble contrast agents have been introduced, and the use of either iopamidol (370mg iodine/ml) or iohexol (350mg iodine/ml) is strongly recommended. An iodine concentration of 300mg/ml will give an adequate contrast in a small horse, but a higher concentration may be preferable in larger horses, although total volume (50ml) may be more important.

Approximately 5 minutes after completion of the injection (or 1–2 minutes if the double-needle technique is used), the horse's head may be repositioned level with the rest of the body, and radiography can be repeated. Cranial, mid-neck and caudal neck (to include the articulation between the seventh cervical and first thoracic vertebrae) lateral-lateral images should routinely be obtained, with the neck in the neutral position. If a lesion is obvious on an image acquired with the neck in a neutral position it may be prudent not to manipulate the neck to avoid exacerbation of any lesion. In the absence of an obvious lesions, with the neck in flexion, at least cranial and mid-neck lateral-lateral views should be repeated, and with the neck in extension, at least a caudal neck lateral-lateral view should be repeated. Flexion and extension of the neck should be performed carefully to obtain radiographs in these 'stressed' positions, which will help to define any dynamic component to compression. If necessary, the horse may then be positioned in dorsal recumbency in order to obtain ventrodorsal radiographic views and identify sites of lateral compression. These views are difficult to obtain and are limited to the cranial two-thirds of the neck. The myelographic study should be performed quickly, because radiographic contrast may be reduced with time by dilution and resorption of the contrast medium.

Occasionally the contrast medium 'fails to flow' and accumulates in the region of the most cranial cervical vertebrae. It usually does eventually mix with cerebrospinal fluid, although resultant image quality may be poor. This is thought to be characteristic of subdural injection.

Interpretation of the myelogram

The myelogram should be evaluated with the neck in normal, flexed and extended positions in order to identify both static and dynamic lesions. Using 40ml of contrast agent there should be complete filling of the subarachnoid

space to the cervicothoracic junction. With the neck in the neutral position, the dorsal column of contrast medium is usually of more uniform width, and is wider than the ventral column (Figures 16.4a and 16.5). There is slight widening of the dorsal column of contrast medium at the caudal aspect of each vertebral foramen, and slight narrowing at the cranial aspect of each vertebral foramen. The ventral column of contrast medium usually narrows slightly and is slightly elevated at the intervertebral spaces.

If the neck is flexed, the width of the dorsal column of contrast medium remains uniform (Figure 16.4b), whereas the ventral column becomes narrower at the intervertebral spaces due to pressure from the intervertebral disc. This is most marked at the articulations between the third and fourth, and fourth and fifth cervical vertebrae. Extension of the neck results in slight widening of the ventral column in the fifth, sixth and seventh cervical vertebrae, with no change in the dorsal column.

Diagnostic criteria

The aim of these examinations is to determine if there is compression of the spinal cord. Focal narrowing of the dorsal contrast medium column when the neck is extended or flexed (Figures 16.6a, 16.6b and 16.7), together with narrowing of the ventral contrast medium column at similar sites, or occlusion of the passage of contrast medium, may be indicative of a site of spinal cord compression. Several different criteria have been used for determination of spinal cord compression using myelography, including a dorsal contrast medium column of <2 mm, narrowing of the dorsal contrast medium column by more than 50% and reduction of the dural diameter by more than 20%. However, a study that compared subjective assessment of plain radiographs, semi-quantitative scoring of plain radiographs and myelography (positive results defined as ≥50% reduction in dorsal contrast column) in a group of horses with histologically confirmed spinal cord disease due to cervical vertebral malformation has been carried out. This found that the semi-quantitative method of assessment of plain radiographs was most accurate. Semi-quantitative measurements resulted in a higher sensitivity (87%), higher specificity (94%), more powerful positive predictive value (95%) and more powerful negative predictive value (84%) than either of the other techniques when assessing horses with spinal cord compression due to cervical vertebral malformation.

Narrowing of the dorsal column of contrast medium by more than 50% was historically considered to be significant, but should be interpreted with care and in the light of other findings. In a comparative myelographic and post-mortem study, 50% reduction in the dorsal contrast medium column rule had good specificity but inadequate sensitivity in mid-cervical sites in the neutral position. False-positive results can occur. Focal narrowing of the ventral contrast medium column alone, when the neck is in the normal position or flexed, or of the dorsal column of contrast medium alone when the neck is extended, must be interpreted with extreme care, because these are normal findings. If a horse has either a narrow vertebral foramen or a small subarachnoid space, stress radiography is more likely to narrow the dural sac or obliterate the subarachnoid space. Overflexion can result in obliteration of both columns of contrast medium in the mid-neck region, especially in small horses, and may potentially accentuate spinal cord damage. Dorsal displacement of the spinal cord, so-called 'lifting', does



Figure 16.4(a) Lateral-lateral image (cranial is to the left) of the second to fifth cervical vertebrae to show a normal myelogram of a mature Thoroughbred. Note that the dorsal contrast column is much wider than the ventral column. The ventral column of contrast medium narrows slightly at the intervertebral articulations, but the dorsal column of contrast medium remains of uniform width.



Figure 16.4(b) Flexed lateral-lateral view of the third to fifth cervical vertebrae (cranial is to the left) to show a normal myelogram (the same horse as in Figure 16.4a). Narrowing of the ventral contrast medium column is accentuated at the intervertebral articulations, but the dorsal column of contrast medium remains a uniform width.

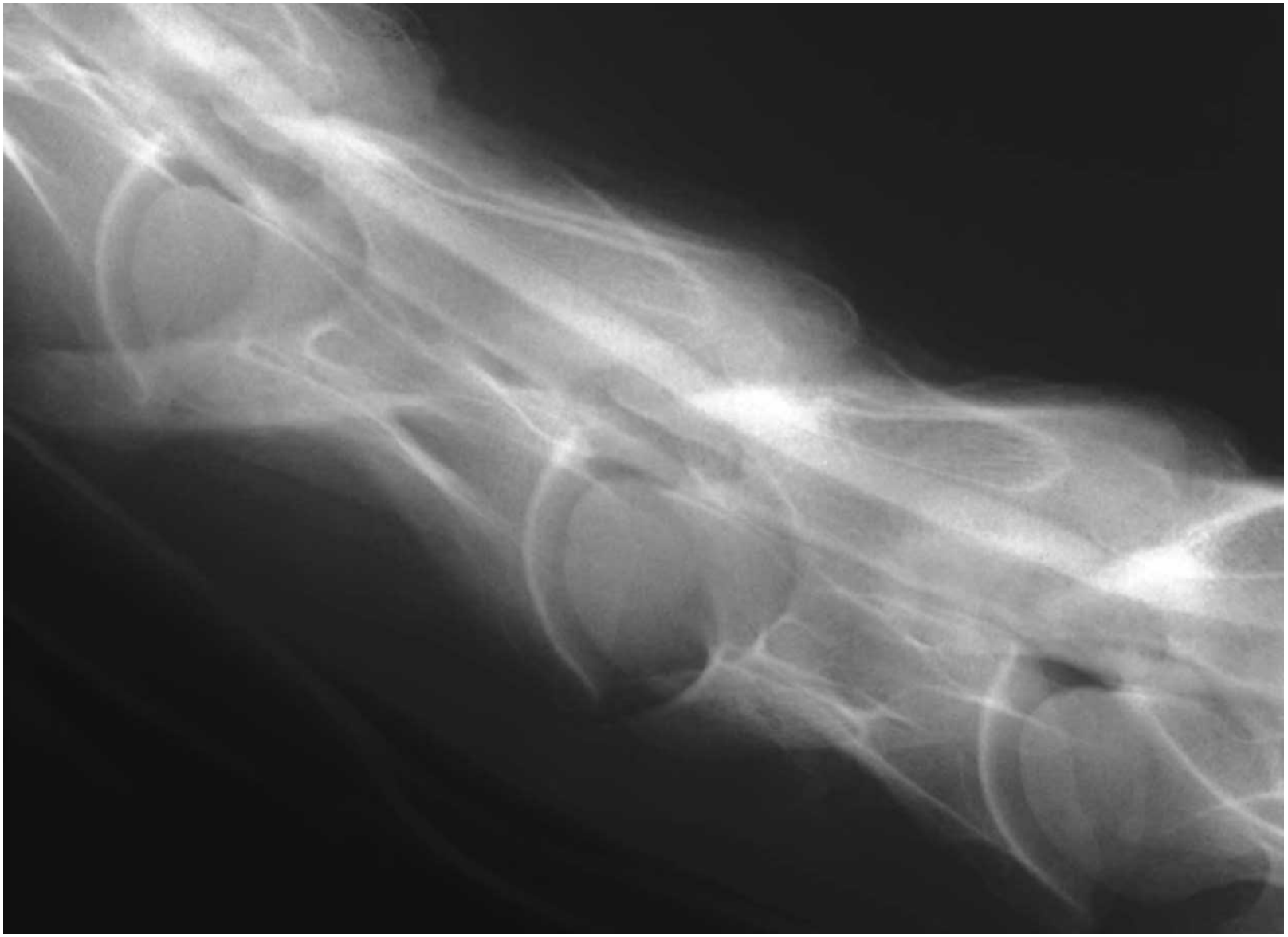


Figure 16.5 Lateral-lateral image (cranial to the left) of the fourth to seventh cervical vertebrae to show a normal myelogram (same horse as in Figures 16.4a and 16.4b).



Figure 16.6(a) Lateral-lateral image of the second to fifth cervical vertebrae (cranial is to the left) of a yearling Thoroughbred colt with mild hindlimb ataxia. Note the slight dorsal deviation of the fourth cervical vertebra, the suggestion of slight stenosis at its cranial orifice and the prominent caudal epiphysis of the third cervical vertebra. The myelogram was obtained with the neck in a normal (neutral) position. There is subtle narrowing of the dorsal contrast medium column at the articulation between the third and fourth cervical vertebrae. The ventral contrast medium column is narrower at each of the intervertebral articulations – a normal feature.



Figure 16.6(b) Flexed lateral-lateral image of the second to fifth cervical vertebrae (the same colt as in Figure 16.6a). Cranial is to the left. Dorsal displacement of the head of the fourth cervical vertebra is accentuated and there is more obvious narrowing of the dorsal contrast medium column at this level, confirming a site of spinal cord compression. This was verified at post-mortem examination.



Figure 16.7 Lateral-lateral image of the fifth to seventh cervical vertebrae of a 3-year-old Thoroughbred filly with severe hindlimb and forelimb ataxia. Cranial is to the left. There is tremendous enlargement of the articular process joints between the fifth and sixth and sixth and seventh cervical vertebrae, with marked irregularity of the joint spaces. These changes are compatible with severe degenerative joint disease. There is marked narrowing of the dorsal and ventral contrast medium columns at the articulations between the fifth and sixth cervical vertebrae and to a lesser extent between the sixth and seventh. This is indicative of two sites of spinal cord compression. The filly was treated by fusion of the fifth, sixth and seventh cervical vertebrae and showed marked clinical improvement associated with some remodelling of the articular process joints.

usually reflect significant vertebral malalignment. The shape and angulation of the spinal cord should be assessed carefully. The myelogram should be carefully inspected for evidence of more than one site of potential narrowing of the vertebral canal, because this will influence surgical treatment and prognosis. In some instances, interpretation of the myelogram by subjective evaluation of the width of the contrast columns is equivocal. In these cases, measurements of the minimum dural sagittal diameter (Figure 16.8) may be useful, provided that a standardised radiographic technique is employed to allow for magnification, and comparison is made with horses of similar size. Alternatively the maximum and minimum dural sagittal diameters can be compared within a horse, with a 20% reduction in dural diameter being considered significant. In the caudal neck region (C6–C7) this technique has high sensitivity and specificity for detection of cervical stenotic myelopathy in both neutral and flexed positions, but in the mid-neck region this test has low sensitivity and high specificity in the neutral position. Flexion of the neck increases the frequency of false-positive diagnoses.

Separation of the dorsal or ventral contrast column of contrast medium from the wall of the vertebral foramen is suggestive of an epidural or

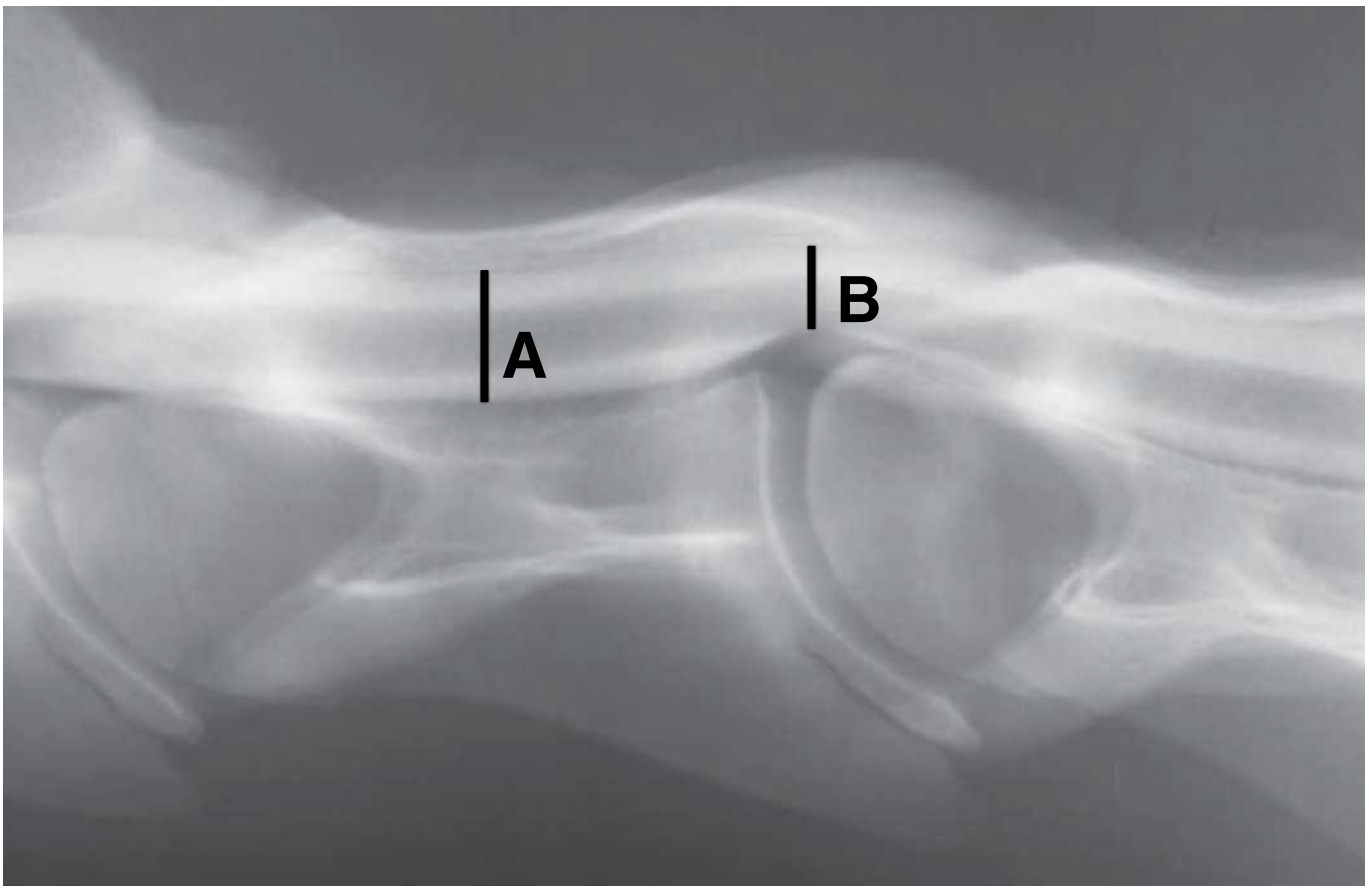


Figure 16.8 Lateral-lateral myelogram of the cranial cervical vertebrae (C_2–C_4). Cranial is to the left. Measurement of the minimum dural sagittal diameter. 'A' denotes the minimum dural sagittal diameter in the middle of C_3; 'B' denotes the minimum dural sagittal diameter at the intervertebral articulation between C_3 and C_4. Note that the ventral contrast medium column is markedly narrowed at this site, but the dorsal contrast medium column is only slightly changed. Note also the 'ski jump' appearance of the proximocaudal aspect of the vertebral body of C_3 and the slight malalignment between C_3 and C_4.

extradural space-occupying lesion, e.g. epidural haemorrhage or a prolapsed intervertebral disc. False-negative results may occur due to failure to identify a laterally compressive lesion. With a laterally compressive lesion associated with cervical vertebral malformation the minimum sagittal diameter of the vertebra is often quite small, resulting in a low minimum sagittal dural diameter but within the normal range. There may be a blanching of the overall contrast medium column, widening of the space occupied by the spinal cord and sometimes two dorsal borders of the contrast column caused by asymmetrical dorsolateral compression (Figure 16w.9). A ventrodorsal myelogram may confirm transverse compression, although diagnostic-quality ventrodorsal radiographs of the caudal cervical vertebrae are difficult to acquire. The value and reliability of oblique radiographic images remains to be determined.

In conclusion, myelograms should be interpreted carefully using a variety of techniques including:

- Minimum sagittal dural diameter (mean minus 2 standard deviations)
- ≥50% decrease in opposing dorsal and ventral contrast medium columns compared to a mid-vertebral site cranial or caudal to the lesion
- Reduction of the dorsal column of contrast medium to a thickness of <2 mm
- Failure of the contrast medium to pass a site.

Interpretation should be performed in conjunction with semi-quantitative assessment of plain lateral-lateral images acquired in a standing horse (see 'Cervical vertebrae – Normal anatomy, variations and incidental findings' in Chapter 12).

PNEUMOCYSTOGRAPHY

'Urinary system – Contrast examination' in Chapter 15 describes the use of positive contrast cystography. Pneumocystography involves the introduction of air into the bladder, prior to radiographs being obtained. This provides negative (radiolucent) contrast within the bladder, allowing radiographic assessment of the internal surface of the bladder wall. While this can be carried out with the horse standing, the bladder can only be seen on lateral-lateral radiographs of small horses. It is therefore normally necessary to carry out the technique under general anaesthesia, so that the bladder can be radiographed using the standard ventrodorsal views used for the pelvis (see 'Pelvis – Radiographic technique – Positioning' in Chapter 13).

Technique

Pneuomocystography can be used in conscious foals or, if necessary, under mild sedation. The horse is positioned in dorsal recumbency as for pelvic radiography (see 'Pelvis – Radiographic technique – Positioning' in Chapter 13). A urinary catheter is then introduced into the bladder (a standard equine urinary catheter of approximately 7 mm diameter is adequate for this purpose in either sex). Any urine present should be withdrawn, and air is then introduced into the bladder and a radiograph obtained. The urethra in mares and geldings is sufficiently narrow for little air to escape around the catheter, but some device must be used to prevent egress of air through the catheter during the exposure. In adult Thoroughbreds, up to 5 litres of air may be used.

Diagnostic criteria

In a normal horse, the bladder is seen as a roughly pear-shaped lucent shadow lying in the abdomen and pelvic canal, the broader part being within the abdomen. It is important to realise that the outline of the cranial portion of the bladder may be modified by pressure on the bladder from the intestines. In some horses, there is a tendency for a mineralised 'sandy' deposit to collect in the bladder. Normally this is voided in part or in total with the urine, but if a portion is left in the bladder, it will be evident on radiographs as a rather amorphous radiopacity lying in the dependent part of the bladder.

Pneuomocystography is particularly useful in foals with suspected rupture of the bladder. It can be carried out in a standing foal. It is important to look for air escaping from the bladder into the abdominal cavity, and not just to assess the outline of the bladder.

Positive (opaque) and double-contrast studies can also be made, either introducing opaque contrast medium into the bladder via a catheter as above, or as a result of intravenous pyelography (see below). Interpretation is similar to that outlined above, but is generally more difficult than with pneumocystography.

INTRAVENOUS PYELOGRAPHY

Intravenous pyelography is of limited value, but can be used to assess the outline of the kidneys, ureters and bladder. It is normally performed under general anaesthesia with the horse in dorsal recumbency. Ventrodorsal views of the pelvic and abdominal areas are required (see Chapters 13 and 15), but lateral-lateral views of the abdominal region may also be helpful in thinner horses. Ultrasonography is often helpful for evaluation of the kidneys.

Technique

There is little information available on the use of this technique in the horse, but it can be successfully performed as follows. The horse is placed in dorsal recumbency, and the bladder catheterised. Any urine present is withdrawn. The jugular vein is catheterised, and 100 ml of sodium meglumine diatrozoate is injected over 30 seconds. Radiographs are acquired at five 5-minute intervals, centering over the kidneys. Good images of the kidneys and ureters can be obtained using ventrodorsal views. The exact entrance of the ureters to the bladder is difficult to see on ventrodorsal or lateral-lateral views, because it tends to be superimposed upon the pelvis or abdominal viscera. This makes this technique of limited value in cases of suspected ectopic ureter. Within 15–20 minutes, the contrast medium collects in the bladder, and good positive-contrast images of the bladder can be obtained.

OTHER TECHNIQUES

Contrast media can be used to outline sinus tracts (so-called *sinography or fistulography*), and to determine whether they extend to other pathological lesions (Figures 16.10a and 16.10b). Contrast medium may also outline

foreign bodies lying within sinuses. The technique varies, depending on the position and size of the sinus. If possible, a Foley catheter should be used, to limit leakage and allow injection under pressure if necessary. In smaller tracts, it may be sufficient to introduce the contrast medium through a flexible catheter of 2–3 mm external diameter, introduced no more than 1 cm into the sinus. In other situations, contrast medium may be introduced by passing a flexible catheter as far into the sinus as possible. Sedation of the patient may be necessary, and the infusion of local anaesthetic solution into the sinus may also be beneficial. Diagnostic ultrasonography may also be useful.



Figure 16.10(a) Craniocaudal radiographic image of the right elbow of an 11-year-old Irish Draught horse that had sustained a kick injury 3 weeks previously. Lateral is to the right. There was soft-tissue swelling and a discharging sinus on the lateral aspect of the elbow. There is diffuse soft-tissue swelling and a small, displaced chip fracture on the distal lateral aspect of the humerus (arrow).



Figure 16.10(b) Craniocaudal radiographic image of the right elbow of the same horse as in Figure 16.10(a). A radiodense contrast medium has been injected into the sinus, which communicates with the site of the chip fracture.

Contrast medium is likely to 'leak' from the sinus during injection, and should be cleaned from the skin surface prior to radiography. As always, more than one view of the area should be obtained. The results should be interpreted with care. Sinuses frequently do not fill fully and artefactual filling defects are quite common.

The nasolacrimal duct can also be assessed using a contrast medium suitable for intravenous injection (*dacryocystorhinography*). The contrast medium is introduced through a flexible catheter most easily via the puncta lacrimalia, but can be retrograde through the nasal ostium. If the duct is blocked, it is important to take care that it is not ruptured, because contrast medium may cause a marked soft-tissue reaction.

The duct commences as two separate branches about 1 cm from the medial canthus of the eye. They join at the medial canthus; the duct then passes forward over the outer wall of the frontal sinus to open at the lower commissure of the nostril. The duct generally has a consistent diameter throughout its length, and runs a relatively straight.

Additional figures

The book companion website at www.clinical-radiology-horse.com includes additional figures that are not included in the printed book or e-book formats. Please see '**About the Companion Website**' at the start of the book for details on how to access the website. These figures are prefixed with the letter 'w' in the printed book, e.g. Figures 1w.4c–f.

FURTHER READING

ARTHROGRAPHY

Arnbjerg, J. (1969) Contrast studies of joints and tendon sheaths in the horse. *Nord. Vet. Med.* **21**, 318

Dik, K.J. (1984) Equine arthrography. *Vet. Radiol.* **25**, 93–96

Kamm, J., Goodrich, L., Werpy, N., McIlwraith, C. (2012) A descriptive study of the equine proximal interphalangeal joint using magnetic resonance imaging, contrast arthrography and arthroscopy. *Vet. Surg.* **41**, 677–684

Lacourt, M., MacDonald, M., Rossier, Y., Laverty, S. (2013) Equine articular synovial cysts: 16 cases. *Vet. Surg.* **42**, 99–106

Marshall, K., Adkins, A. (2014) Synovial herniation as a complication of arthroscopy in a Thoroughbred yearling. *Equine Vet. Educ.* **26**, 288–291

Nichols, F., Sande, R. (1989) Radiographic and arthroscopic findings in the equine stifle. *J. Am. Vet. Med. Ass.* **181**, 918–924

Nixon, A., Spencer, C. (1990) Arthrography of the equine shoulder. *Equine Vet. J.* **22**, 107–113

Swanstorm, O., Lewis, R. (1969) Arthrography of the equine fetlock. *Proc. Am. Ass. Equine Pract.* **15**, 221–225

Turner, T. (2013) How to perform and interpret navicular bursography. *Proc.Am. Ass. Equine Pract*. **59**, 197–202

TENDONOGRAPHY

Fiske-Jackson, A., Barker, W., Eliahsar, E., et al. (2013) The use of intrathecal analgesia and contrast radiography as preoperative diagnostic methods for digital flexor tendon sheath pathology. *Equine Vet. J.* **45**, 36–40

Hago, B.E.D., Vaughan, L.C. (1986) Radiographic anatomy of tendon sheaths and bursae in the horse. *Equine Vet. J.* **18**, 102–106

Verschooten, F., De Moor, A. (1978) Tendinitis in the horse: radiographic diagnosis with air tendograms. *J. Am. Vet. Radiol. Soc.* **19**, 23–30

ANGIOGRAPHY

Benredouane, K., Lepage, O. (2012) Trans-arterial embolization of the internal carotid artery in standing horses. *Vet. Surg.* **41**, 404–409

Colles, C.M., Cook, W.R. (1983) Carotid and cerebral angiography in the horse. *Vet. Rec.* **113**, 483–489

Colles, C.M., Garner, H.E., Coffman, J.R. (1979) The blood supply of the horse's foot. *Proc. 25th Am. Ass. Equine Pract.* pp. 385–398

Herbert, W.W. (1964) Angiographic artefacts which simulate or mask abnormality. *Am. J. Roentgenol.* **92**, 907–917

Hertsh, B-W. (1983) Arteriographische Untersuchungen an den Extremitäten beim Pferd, Habilitationsschrift, Hanover

Lindbom, A. (1957) Arterial spasm caused by puncture and catheterisation. *Acta Radiol.* **47**, 449–459

Seldinger, S.I. (1953) Catheter replacement of the needle in percutaneous arteriography. *Acta Radiol.* **39**, 368

Wickbom, I., Bartley, O. (1957) Arterial spasm in peripheral arteriography. *Acta Radiol.* **47**, 433–448

VENOGRAPHY

Collins, S.N., van Eps, A.W., Pollitt, C.C., Kuwano, A. (2010) The lamellar wedge. *Vet. Clin. N. Am.: Equine Pract*. **26**, 179–195.

D'Arpe, L., Bernardini, D. (2010) Digital venography in horses and its clinical application in Europe. *Vet. Clin. N. Am.: Equine Pract*. **26**, 339–359

Eustace, R. (2010) Clinical presentation, diagnosis and prognosis of chronic laminitis in Europe. *Vet. Clin. N. Am.: Equine Pract*. **26**, 391–403

Redden, R. (2001) A technique for performing digital venography in the standing horse. *Equine Vet. Educ.* **5**, 172–178

Rucker, A., Redden, R., Arthur, E. et al. (2006) How to perform the digital venogram. *Proc. Am. Ass. Equine Pract.* **52**, 526–530

Rucker, A. (2010) Clinical applications of digital venography. *J. Equine Vet. Sci.* **30**, 491–503

Rucker, A. (2010) Equine venography and its clinical application in North America. *Vet. Clin. N. Am.: Equine Pract*. **26**, 167–177

MYELOGRAPHY

Audigie, F., Tapprest, J., Didierlaurent, D., Denoix, J.-M. (2004) Utrasound-guided atlanto-occipital puncture for myelography in the horse. *Vet. Radiol. Ultrasound* **45**, 340–344

Beech, J. (1979) Metrizamide myelography in the horse. *J. Am. Vet. Radiol. Soc.* **20**, 22–31

Burbidge, H., Kannegieter, N., Dickson, L., Goulden, B. (1988) Iohexol myelography in the horse. *Equine Vet. J.* **21**, 347–350

Conrad, R. (1984) Metrizamide myelography of the equine cervical spine: 14 case histories. *J. Am. Vet. Radiol. Soc.* **25**, 73–77

Foley, J., Gatlin, S., Selcer, B. (1986) Standing myelography in 6 adult horses. *J. Am. Vet. Radiol. Soc.* **27**, 54–57

Hubbell, J., Reed, S., Myer, C., Muir, W. (1988) Sequelae of myelography in the horse. *Equine Vet. J.* **20**, 438–440

Hudson, N., Mayhew, I. (2005) Radiographic and myelographic assessment of the equine cervical vertebral column and spinal cord. *Equine Vet. Educ.* **17**, 34–38

May, S., Wyn-Jones, G., Church, S., Brouwer, G., Jones, R. (1986) Iopamidol myelography in the horse. *Equine Vet. J.* **18**, 199–202

Nyland, T., Blythe, L., Pool, R., Helphrey, M., O'Brien, T. (1980) Metrizamide myelography in the horse: clinical, radiographic and pathological changes. *Am. J. Vet. Res.* **41**, 204–211

Papageorges, M., Gavin, P., Sande, R., Barbee, D., Grant, B. (1987) Radiographic and myelographic examination of the cervical vertebral column in 306 ataxic horses. *Vet. Radiol.* **28**, 53–59

Rantanen, N., Gavin, P., Barbee, D., Sande, R. (1981) Ataxia and paresis in horses, part ii: radiographic and myelographic examination of the cervical vertebral column. *Comp. Cont. Educ.* **4**, 161–171

Rose, P., Abutarbush, S., Duckett, W. (2007) Standing myelography in the horse using a nonionic contrast agent. *Vet. Radiol. Ultrasound* **48**, 535–538

Schwarz, T., Edwards, G., Sullivan, M. (2002) Subdural injection of myelographic contrast in two horses. *Equine Vet. Educ.* **14**, 179–181

Van Biervliet, J., Scrivani, P., Divers, T., Erb, H., de la Hunta, A., Nixon, A. (2004) Evaluation of decision criteria for detection of spinal cord compression based on cervical myelography. *Equine Vet. J.* **35**, 14–20

Widmer, W., Blevins, W., Jakovljevic, S., et al. (1998) A prospective clinical trial comparing metrizamide and iohexol for equine myelography. *Vet. Radiol. Ultrasound* **39**, 106–109

OTHER TECHNIQUES

Crispin, S. (1988) Nasolacrimal duct cannulation in the horse. *In Practice* **10**, 154–156

Lundin, C., Clem, M., DeBowes, R., Bertone, A. (1988) Diagnostic fistulography in horses. *Comp. Cont. Educ.* **10**, 639–645

Appendix A
Fusion times of physes and suture lines

HEAD AND VERTEBRAL COLUMN

Area	Centres	Notes	Closure	
HEAD				
Occipital	Squamous		Lateral-basilar	By 4 months
	Lateral		Squamous to lateral-basilar	12–24 months
	Basilar		Parieto-occipital	5 years*
			Spheno-occipital	5 years*
			Occipitomastoid	Aged*
Sphenoid	Pre-sphenoid			Uncertain, but in first year
	Post-sphenoid		Spheno-occipital	5 years*
Ethmoid	Perpendicular			Uncertain, but soon after birth
	Cribriform			
Parietal	One centre		Parietal suture	4 years*
			Parieto-occipital	5 years*
Premaxilla	One centre		Left and right	During 4th year*
Nasal	One centre		Left and right	Do not fuse
			Naso-frontal	1 year*
Mandible	Two halves		Left and right	3 months*
CERVICAL SPINE				
Atlas	Two halves	Faint longitudinal line evident in ventrodorsal view in neonate		
Axis	Dens, head, body, caudal epiphysis		Dens to head	About 7 months
			Caudal epiphysis	Complete 4–5 years
C3–C7	Cranial vertebral physis			Complete by 2 years
	Caudal vertebral physis			Complete by 4–5 years
THORACOLUMBAR SPINE				
T1–L6	Cranial vertebral physis			6–12 months
	Caudal vertebral physis			2–4 years
T2–T8	Separate centres of ossification in cartilaginous summits	Develop at about 12 months Gradual ossification		Remain separate throughout life

* Obliteration of suture; all others are fusion of suture.

Clinical Radiology of the Horse, Fourth Edition. Janet A. Butler, Christopher M. Colles, Sue J. Dyson, Svend E. Kold and Paul W. Poulos.
© 2017 John Wiley & Sons, Ltd. Published 2017 by John Wiley & Sons, Ltd.
Companion website: www.clinical-radiology-horse.com

Area	Centres	Notes	Closure	
SCAPULA	Scapular cartilage Body of scapula Cranial glenoid cavity of scapula	Cranial glenoid cavity of scapula and supraglenoid tubercle incompletely ossified at birth	Cranial glenoid cavity with body	About 5 months
	Supraglenoid tubercle		Supraglenoid tubercle	By 12–24 months
HUMERUS				
Proximal	Diaphysis Humeral head Greater tubercle	Lesser tubercle develops from same ossification centre as humeral head – incompletely ossified at birth	Centres of proximal epiphysis Proximal physis	Merge about 3–4 months 24–36 months
Distal	Diaphysis Distal epiphysis Epiphysis of medial epicondyle			11–24 months
RADIUS				
Proximal	Single epiphysis			11–24 months
Distal	Diaphysis Epiphysis Lateral styloid process		Lateral styloid process with epiphysis Physis	Within 1 year 20–24 months
ULNA	Single proximal epiphysis	Incompletely ossified at birth Occasionally a separate centre for anconeal process	Physis	24–36 months
METACARPUS				
Third metacarpus	Proximal physis Distal physis		Physis Physis	Fused at birth About 6 months
Second and fourth		Distal epiphysis cartilaginous at birth, gradually ossifies	Fuses with shaft	1–9 months
PROXIMAL PHALANX	Proximal epiphysis Diaphysis		Proximal physis	About 1 year
	Distal epiphysis		Distal physis	Fused at birth
MIDDLE PHALANX	Proximal epiphysis Diaphysis		Proximal physis	8–12 months
	Distal epiphysis		Distal physis	Fused at birth
DISTAL PHALANX	Single centre	Models until about 18 months Palmar processes model over 12 months		–
NAVICULAR BONE	Single centre	Models until about 18 months		–
PROXIMAL SESAMOID BONES	Single centre	Outline complete about 3–4 months Enlarge until 18 months		–
CARPAL BONES	Single centre each	Fully developed about 18 months		–

Area	Centres	Notes	Closure	
PELVIS	Ilium – iliac crest and tuber coxae		Iliac crest and tuber coxae	About 10 months
	Pubis	Symphyseal branches of pubis and ischium fused at birth	Pubic symphysis	Remains open
	Ischium		Caudal portion of bone and tuber ischii	About 10–12 months
			Articular portions of pubis, ilium and ischium to form acetabulum	About 1 year
FEMUR				
Proximal	Femoral head		Femoral head	24–36 months
	Trochanter major		Trochanter major to femoral shaft	18–30 months
	Trochanter minor		Trochanter minor	About 2 years
Distal	Epiphysis	Trochlear ridges develop over about 5 months	Physis	24–30 months
	Diaphysis	Medial trochlear ridge becomes more prominent at about 2 months		
TIBIA				
Proximal	Epiphysis		Apophysis-epiphysis	9–12 months
	Metaphysis		Epiphysis-metaphysis	24–30 months
	Tibial tuberosity (apophysis)		Apophysis-metaphysis	30–36 months
Distal	Lateral malleolus	(distal epiphysis of fibula)	Fuses to epiphysis	By 3 months
	Epiphysis		Epiphysis-metaphysis	17–24 months
TUBER CALCANEI		May be absent at birth, gradually ossified	Fuses to calcaneus	By 16–24 months
FIRST AND SECOND TARSAL BONES				Usually fused at birth
PATELLA	Single centre	Incompletely ossified at birth		
		Fully modelled about 4 months		
FIBULA		Little ossification until 2 months		
DISTAL TO TARSUS: Same as thoracic limb				

Appendix B
Exposure guide, image quality and film processing faults

EXPOSURE GUIDE

Altering the table factors

The exposures below are based on a 500 kg horse of Thoroughbred type. As an approximate guide the kV should be increased by 5% for limb radiography of heavier horses, and reduced for neonatal foals both by 5 kV and halving the mAs. Focal film distance (source image distance) factors must be considered when converting the above exposure guide. If using film the relative speed rating of the film screen system must also be considered. More efficient imaging plates with advances in digital technology allow reduced exposures; guidance should be sought from the supplier.

Film/screen exposure guide

Area/view	RS	FFD (cm)	AWF	Grid	kV	mAs
Head						
Cranium, lateral	600	150	—	CH	65	40
Cranium (under GA)	600	150	—	CH	75/80	64
Sinus, lateral	600	150	—	—	55	12
Pharynx	600	150	—	CH	65	35
Rostral, lateral	600	150	—	CH	60	18
Cervical spine						
Cranial	600	150	—	CH	68	45
Mid	600	150	—	CH	70	50
Caudal	600	150	—	CH	75	64
Caudal/T1	600	150	—	CH	90	90
Thoracolumbar spine						
Withers (SP's)	600	150	yes	CH	65	50
Mid thoracic (SP's)	600	150	yes	CH	65	50
Caudal thoracic (SP's)	600	150	yes	CH	75	64
Cranial lumbar (SP's)	600	150	yes	CH	85	80
Mid thoracic APJ's/vertebrae	600	150	—	CH	100	160/180
Cranial lumbar APJ's/vertebrae	600	150	—	CH	125	200
Sacrum (cranial)	600	150	yes	CH	110	80
Sacrum (caudal)	600	150	yes	CH	70	63
Cranial coccygeal	600	150	—	CH	70	40/50

Clinical Radiology of the Horse, Fourth Edition. Janet A. Butler, Christopher M. Colles, Sue J. Dyson, Svend E. Kold and Paul W. Poulos.
© 2017 John Wiley & Sons, Ltd. Published 2017 by John Wiley & Sons, Ltd.
Companion website: www.clinical-radiology-horse.com

APPENDIX B

Exposure guide, image quality and film processing faults

Area/view	RS	FFD (cm)	AWF	Grid	kV	mAs
Scapulohumeral joint						
ML, standing	600	150	yes	CH	100/105	100/130
CrM-CdLO, standing	600	120	yes	—	80	25
ML, under GA (cassette tunnel)	600	130	yes	CH	100/105	130/160
Elbow						
ML, standing	600	150	yes	CH	70	20
CrCd, standing	600	120	—	—	66	13
Carpus						
LM and obliques	150	100	—	—	63	10
DPa	150	100	—	—	65	12
DPr-DDiO	150	100	—	—	65	10
Metacarpus/tarsus						
LM and obliques	150	100	—	—	62	9
DPa	150	100	—	—	66	12
MC/MT II/IV	150	100	—	—	57	10
Metacarpo/tarsophalangeal joint						
LM and obliques	150	100	—	—	62	9
DPa/DPl	150	100	—	—	65	12
L45°Pr-MDiO	150	105	—	—	60	10
Pastern						
Flexed oblique	150	100	—	—	62	10
Feet						
Lateral	150	100	—	8 : 1	70	22
Lateral	150	100	—	—	62	16
DPr-PaDiO, distal phalanx	150	100	yes	8 : 1	60	9
DPr-PaDiO, navicular	150	100	—	8 : 1	73	25
PaPr-PaDiO, navicular	150	100	—	—	66	14
DPa, weight-bearing	150	100	—	8 : 1	70	22
Pelvis						
Ischium	600	130	—	2	120	160
Pelvic canal	600	130	—	2	130	250
Coxofemoral joint	600	130	—	2	135	220
Sacroiliac joint	600	130	—	2	135/140	320
Ilial wing	600	130	—	2	135	220
Stifle						
LM, Cd60°L-CrMO, standing	600	120	yes	—	57	13
CdCr, standing	600	120	yes	—	75	20
LM, under GA	600	120	yes	CH	65	40
CdCr, under GA	600	120	yes	CH	80	64
Patella, CrPr-CrDiO	600	120	yes	—	65	13
Tarsus						
LM, Obliques	150	100	—	—	60	13
DPl	150	100	—	—	70	13
DPl, flexed	150	100	—	—	70	15

Area/view	RS	FFD (cm)	AWF	Grid	kV	mAs
Thorax						
Caudodorsal (diaphragm)	600	150	—	CH	80	36
Craniodorsal (aortic arch)	600	150	—	CH	90	36
Caudoventral (caudal heart)	600	150	—	CH	90	36
Cranioventral (cranial heart)	600	150	—	CH	110	40
Sternum, lateral	600	150	yes	CH	85	100
Abdomen						
Lateral, standing (7 day foal)	600	150	—	CH	70	63

Notes:
RS: Relative speed rating of screens.
FFD: Focus/film distance.
AWF: Aluminium wedge filter.
Grids:
CH – Cross-hatch parallel 12 : 1 ratio grid.
2 – Two crossed 12 : 1 ratio focused grids.
8 : 1 – 8 : 1 ratio focused grid, 47 lines/cm.

Digital exposure guide

Area/view	SID (cm)	Grid	kV	mAs
Head				
Cranium, lateral	100	No	75	10
Cranium, DV	100	No	85	10
Sinus, lateral	100	No	70	5
Teeth, oblique	100	No	75	8
Pharynx/larynx/ETD's/Rostral, lateral	100	No	75	5
Cervical spine				
Cranial, lateral	150	Yes	85	20
Mid, lateral	150	Yes	90	25
Caudal, lateral	150	Yes	95	40
C7/T1, lateral	150	Yes	110	80
Oblique	150	No	75	30
Thoracolumbar spine				
Withers/mid thoracic (SP's)	150	Yes	95	36
Caudal thoracic (SP's)	150	Yes	105	45
Cranial lumbar (SP's)	150	Yes	110	63
Mid/caudal thoracic APJ's, oblique	150	Yes	90	56
Caudal thoracic/cranial lumbar APJ's, lateral	150	Yes	110	100
Sacrum (cranial)	150	Yes	115	100
Sacrum (caudal/coccygeal)	150	Yes	110	50
Withers/mid thoracic (SP's)	150	No (air gap)	90	20
Caudal thoracic (SP's)	150	No (air gap)	96	32
Cranial lumbar (SP's)	150	No (air gap)	105	45
Shoulder				
Mediolateral	150	Yes	110	90
CrM-CdLO	150	No	80	32
CrPr-CrDiO	100	No	80	14

APPENDIX B
Exposure guide, image quality and film processing faults

Area/view	SID (cm)	Grid	kV	mAs
Elbow				
Mediolateral	150	No	75	5
CrCd	100	No	75	5
Carpus				
LM and Obliques	80	No	70	2
DPa	80	No	75	2
DPr-PaDiO	80	No	75	3.6
Metacarpus/Tarsus, Fetlock, Pastern				
LM and Obliques	80	No	70	2
DPa/DPl	80	No	75	2
Foot				
Lateral	80	No	70	2.5
DPr-PaDiO - distal phalanx	80	No	60	2
DPr-PaDiO - navicular	80	No	60	4
PaPr-PaDiO	70	No	60	6.4
DPa/DPl - weight-bearing	80	No	70	3
Obliques	80	No	60	2
Pelvis				
Ischium, VD	130	Yes	120	80
Pelvic canal, VD	130	Yes	130	125
Sacroiliac, VD	130	Yes	140	160
Ilial wing, VD	130	Yes	140	125
Coxofemoral joint, VD	130	Yes	140	125
Lateral-lateral oblique, standing	130	No	100	80
Stifle				
LM and Obliques	100	No	75	6.3
CdCr	100	No	80	14
CrPr-CrDiO Patella	100	No	85	10
Tarsus				
LM and Obliques	80	No	70	2.1
DPl	80	No	70	2.1
DPl flexed	80	No	70	2.8
Thorax				
Dorsocaudal	150	Yes	105	20
Dorsocranial	150	Yes	120	36
Ventrocaudal	150	Yes	125	40
Ventrocranial	150	Yes	130	63
Sternum				
Lateral	150	Yes	85	63
Foals				
Distal limb (1month old)	80	No	66	1.4
Stifle (1month old), lateral	80	No	66	1.4
Stifle (1 month old), CdCr	80	No	70	1.4
Thorax (1 week old)	100	No	80	1.8
Abdomen (1 week old)	100	No	80	4.5

Relative speed (RS) of film/screen combinations

Speed classification of film/screen combinations in terms of relative speed enables comparison of systems among manufacturers. Although the exposures required will be the same to produce images of similar opacity, the detail and resolution may vary. Some manufacturers use 100, 200, etc., some may use 2, 4, 8, etc., but the interrelationship is the same. Speed 8 requires half the exposure (mA s) needed for speed 4; speed 200 requires double the exposure (mA s) of speed 400 screens, etc. Generally speaking, if using only one screen from a pair (i.e. when used with single emulsion film) the speed of the system will halve, e.g. one screen from a pair rated 400 will give a speed of 200.

Distance

The distance between the source (focus) and the cassette (film) affects the radiopacity of the image produced. When the focus–film distance (FFD) is altered, the total amount of x-rays (mA s) must be increased or decreased to make a comparable exposure. The equation to calculate the exposure for a change in distance is:

$$\text{Old mAs} \times \frac{(\text{new FFD})^2}{(\text{old FFD})^2} = \text{New mAs}$$

i.e. The mA s decreases as the square of the distance.

FACTORS AFFECTING IMAGE QUALITY

There are many factors which have an effect on contrast, sharpness, resolution and opacity of the radiographic image. Screen, film and controlling scatter are major factors and need to be carefully considered. Individual films have inherent contrast and latitude values. Digital processing will have an effect on opacity according to the algorithms applied to the acquired image. The final choice of factors will be a compromise for any given area radiographed.

Film

Rare earth vs. calcium tungstate screens

Rare earth screens are more efficient and require less exposure than calcium tungstate, the light conversion of rare earth phosphors being approximately four times greater. As a general rule rare earth screens produce better detail than calcium tungstate screens. Faster film–screen combinations require less exposure, giving shorter exposure times which reduces the risk of movement blur, but as speed increases image detail (sharpness) decreases.

Spectral sensitivity of screens and films

Screens emit light in a specific part of the spectrum. It is therefore important to match the spectral output of the screen to the spectral sensitivity of the film. Failure to do so, in general, will result in loss of system speed and loss

of information transfer. Calcium tungstate phosphors are blue emitting; rare earth phosphors may be blue, green or ultraviolet. Ensure the darkroom light filtration is correct for the type of film in use.

Single vs. double emulsion film

Single-emulsion films, so-called mammography films, offer greater detail than conventional double-emulsion films, and are used with a single screen. They do not suffer from parallax unsharpness, which is evident with double-emulsion films. They are, however, much slower and are not practical when using low-output portable machines as exposure times are too long, increasing the risk of movement. They can be used in conjunction with medium-speed screens, as opposed to specific mammography screens, to increase the speed of the system without sacrificing too much detail.

Scatter

Scattered radiation has a significant effect on image contrast. There are three factors that affect the amount of scattered radiation produced. Increased kVp, increased area of interaction with the primary x-ray beam, and increased depth of tissue being imaged will all increase the amount of scatter.

Collimation

Good collimation will effectively reduce the amount of scatter produced. It will also have an effect on how digital systems assess information within the image during processing.

Grids

Grids can be used to control scattered radiation to improve contrast. However, they increase the exposure required, resulting in longer exposure times and increasing the risk of movement blur. Focused grids need careful positioning to avoid grid cut-off and must be used at the correct distance for optimum results. Parallel grids have slightly more latitude when using FFDs greater than 120 cm. Whether focused or parallel grids are used they must be aligned perpendicular to the primary x-ray beam. The higher both the grid ratio and lines per centimetre, the more effective the grid is in reducing scatter, but the higher the grid factor. The grid factor denotes how much an exposure needs to be increased to give comparable opacity to a film obtained without a grid, e.g. grid factor 2 – double the mAs. If a grid is unavailable, an air gap between the object and the cassette helps to attenuate scattered radiation. An air gap will, however, increase magnification and geometric unsharpness. See Chapter 2 for guidance on grids for use with digital systems.

Air-gap technique

A gap of 20–30 cm between the subject and cassette or imaging plate will reduced the amount of scatter reaching the image. It will, however, increase magnification and there will be a small increase in geometric unsharpness.

Unsharpness

Movement is a common cause of unsharpness of the radiographic image. This can be reduced by the use of short exposure times as well as sedation of the patient. The former can be achieved by using a shorter focus–film distance, but the shorter FFD increases geometric unsharpness (penumbra).

Penumbra is the result of the focal spot in the tube not being a point source. The amount of unsharpness increases with an increase in focal spot size. It is also increased with reduced focal–film distance and increased object–film distance.

Poor screen–film contact is another cause of image blur and usually results in only part of the radiograph appearing unsharp. This can be checked by placing a thin wire mesh on top of the cassette and making an exposure using a large FFD. Areas of poor contact will result in blurring of the image.

Focal spot size

With high-output stationary x-ray machines there is usually a facility to select different-sized focal spots. A smaller focal spot (e.g. 0.6 mm) usually results in better resolution, but an increased exposure time is required to achieve the same mAs output. When movement is likely to be a problem, e.g. in most proximal limb examinations, a larger focal spot (e.g. 1.5–2.0 mm) should be used to reduce exposure times to a minimum. In portable x-ray machines the focal spot is fixed.

FILM PROCESSING FAULTS

Automatic processor faults	Longitudinal scratches	Usually caused by the film guides on the racks
	Tacky films	Usually a fixer problem rather than the dryer
High-density marks	Black splashes	Developer or water splashed on film before development
	Black crescent-shaped marks	Poor handling after exposure
	Black fingerprints	Developer or water on hands when handling film before processing
	Static	Can be the result of formica workbench, dry darkroom atmosphere, man-made fabrics or loading/unloading the cassette
	Black marks around edge of film	Localised fogging due to light leakage in a cassette or the film box has been opened in white light

Overall high density	Over-development	Developer too hot, development time too long or developer too strong
	Heat	20 °C is maximum temperature for 3 months' storage
	Time	Film has a limited 'shelf life'. Fogging increases with age
	Safe light	Bulb too strong, close to working surface, incorrect filter, crack in filter
	Background radiation	Higher than recommended level of background radiation
Low-density marks	White splashes	Fixer, grease or oil on film before processing
	White crescent-shaped marks	Poor handling before exposure
	White fingerprints	Fixer, grease or oil on fingers when handling film before processing
	Sharply defined marks	Usually inside cassette on screen
Overall low density	Under-development	Developer too cold, development time too short or developer too weak or exhausted
Other processing faults	Very patchy image with no contrast over entire film	Developer contaminated with fixer
	Milky white stain or image	Image not cleared due to insufficient fixing
	Brown stain after period of storage	Inadequate washing

DIGITAL FILM FAULTS

See Chapter 2.

DEFINITIONS (ALSO SEE GLOSSARY, APPENDIX C)

Resolution objective measurement of how much detail can be provided by a film–screen combination, measured in line pairs per millimetre. Indicates size of the smallest object that the system will record, i.e. the smallest distance that must exist between two objects before they can be seen as two separate entities.

Definition subjective impression of the amount of detail that is seen in a radiograph. This is difficult to quantify.

Appendix C
Glossary

This glossary is not meant to be comprehensive, but provides brief definitions of some colloquial terms which may differ in usage in different countries, some anatomical terms which have recently been changed or adopted, a few radiological or radiographic terms, and other words not easily found in a dictionary or standard radiology text. Explanations of many technical terms may be found in the text by reference to the Index. Some radiological terms are discussed in greater detail in Chapter 1. Some words have different meanings when used in different circumstances, but only the definition relevant to the context of this book is included.

air gap space (occupied by air) between the object being radiographed and the cassette or imaging plate; the air gap will attenuate scattered radiation, thus a grid is not required.

antebrachiocarpal joint formerly called the radiocarpal joint.

antebrachium the forearm.

apophysis bony outgrowth with a separate centre of ossification, such as a tuberosity or process, under tensile forces from, e.g., a ligament.

arthropathy colloquial non-specific term to describe pathological changes within a joint (e.g. steroid arthropathy).

backscatter deflection or production of radiation back towards the source from the object being radiographed, or any object behind this point; its effect on the film can be minimised by placing a sheet of lead behind the cassette; radiographers should be aware of the radiation hazard caused by backscatter.

Birkeland fracture articular fracture of the proximal palmar or, more commonly, plantar aspect of the proximal phalanx; the term has been used to encompass fragments from a number of different locations; some of these fragments may be developmental in origin.

bucked shins colloquial term used to describe periosteal and endosteal modelling on the dorsal aspect of the third metacarpal (metatarsal) bone resulting in an acquired convex contour to the bone; it is usually preceded by obvious soreness to palpation of the metacarpus (metatarsus). Also commonly referred to as 'Sore shins'.

callus, external new bone formation in response to a fracture on the external side of the bone (periosteal new bone).

callus, internal new bone formation in response to a fracture on the internal side of the cortex (endosteal new bone).

carpitis colloquial term used to describe inflammation of the antebrachiocarpal and/or middle carpal joints. Synovitis may or may not be accompanied by detectable radiographic abnormalities.

centrodistal joint formerly called the distal intertarsal joint (of the tarsus or hock).

chondroid inspissated pus (found in a paranasal sinus or guttural pouch) appearing radiographically as a radiopaque mass.

chondroma tumour composed of cells closely resembling those of normal cartilage, usually appearing radiographically as a space-occupying mass with some mineralisation.

Clinical Radiology of the Horse, Fourth Edition. Janet A. Butler, Christopher M. Colles, Sue J. Dyson, Svend E. Kold and Paul W. Poulos.
© 2017 John Wiley & Sons, Ltd. Published 2017 by John Wiley & Sons, Ltd.
Companion website: www.clinical-radiology-horse.com

Codman's triangle triangular area of new bone adjacent to the cortex which develops as a result of elevation of the periosteum associated with neoplasia, inflammation, infection or trauma.

collimator device for restricting the field covered by the primary x-ray beam.

cone method of collimating the x-ray beam.

contrast degree of definition on an x-ray between adjacent structures of differing radiopacities.

contrast medium substance used to delineate a structure or structures; a positive contrast medium (agent) is radiopaque; a negative contrast medium (gas) is radiolucent.

cross-hatch grid grid composed of two sets of parallel lead lines perpendicular to each other.

CT compute(rise)d tomography.

definition clarity or distinctness with which radiographic image detail is seen.

delayed union failure of a fractured bone to unite within the expected period; if the cause is corrected healing should occur eventually.

density (radiographic) degree to which a tissue absorbs incident x-rays.

density (tissue) weight per unit volume.

dental sac developing tooth.

dentigerous cyst cyst containing all or part of a tooth (or teeth); also called a temporal teratoma. All dentigerous cysts are temporal teratomata although not all temporal teratomata contain dentigerous material.

desmitis inflammation of a ligament.

desmopathy injury of a ligament.

detail degree of sharpness with which individual shadows appear on the radiograph.

diaphysis shaft of a long bone.

distal interphalangeal joint formerly called the coffin, pedal or coronopedal joint.

distal intertarsal joint now called the centrodistal joint.

dorsal conchus formerly called the dorsal turbinate.

double contrast use of both positive and negative contrast media (agents), e.g. barium and air.

dystrophic mineralisation mineralisation in soft tissues (possibly due to abnormal nutrition of the tissue). Occurs in areas of cell necrosis.

edge effect or edge enhancement term synonymous with a Mach line or band; a radiolucent line which may be created by one bone edge superimposed on another.

entheseophyte new bone formation at the site of insertion of a tendon, ligament or joint capsule.

epiphysis separate centre of ossification at each end of a long bone.

epiphysitis colloquial term used incorrectly to describe inflammation in the region of a physis or growth plate, most commonly the distal radial physis.

exposure latitude degree of overexposure or underexposure that can be tolerated in a correctly developed film and still produce an image of acceptable radiographic quality.

fatigue fracture synonymous with a stress fracture: an incomplete fracture, the result of repetitive overload and microfractures.

flatness lack of contrast on a radiograph.

fluid line horizontal interface separating a radiopaque area (fluid) from a more lucent area (often air).

fluoroscopy production of a visual image on a fluorescent screen for diagnosis.

focal distance (of grid) perpendicular distance from a focused grid to the place in space where the planes that pass through the grid would converge.

focal–film/imaging plate distance distance between the x-ray tube focal spot and the plane of the radiographic film or imaging plate.

focused grid grid with lead strips slightly angled so that if they continued they would meet at some line in space, the focal point.

graininess lack of homogeneity in a radiographic image due to a clumping together of silver particles when using conventional film–screen radiography. When using digital imaging part of the image may look grainy because of juxtaposition of tissues of greatly different densities. Also an appearance of underexposure with digital images.

grid thin plate consisting of alternating strips of radiolucent and radiopaque (lead) materials used to attenuate scattered radiation.

grid cut-off absorption of excessive amounts of primary radiation by the grid (and thus underexposure of part of the film) commonly due to an incorrect angle between the primary x-ray beam and the grid (when a parallel grid is used); when a focused grid is used, the x-ray beam must be perpendicular to the grid and centred on the centre of the grid and with the focal spot of the x-ray tube at the proper focus distance to avoid grid cut-off. Also seen if a focused grid is used back to front.

grid ratio ratio between the height of the lead strips and the distance between them in a grid.

hairline fracture incomplete non-displaced fracture, sometimes used incorrectly as synonymous with a fatigue or stress fracture.

intercarpal joint now called the middle carpal joint.

involucrum a rim of opaque bone surrounding a sequestrum.

joint mouse small bony or mineralised fragment within a joint, usually mobile.

kV kilovoltage.

kVp kilovoltage peak (generally synonymous with kV).

kyphosis abnormal flexion of the thoracolumbar vertebrae in the sagittal plane so that the dorsum appears abnormally convex; may be congenital or acquired.

light beam diaphragm method of collimating the primary x-ray beam by use of adjustable lead sheets incorporating a light beam to indicate the surface area to be exposed.

linear grid grid in which the lead strips are parallel to each other.

lordosis abnormal extension of the thoracolumbar vertebrae in the sagittal plane so that the dorsum appears abnormally concave; may be congenital or acquired.

luxation complete dislocation or displacement of a joint.

Mach line or band synonymous with edge enhancement; a radiolucent line which may be created by one bone edge superimposed on another.

mA milliamperage – number of x-rays produced during an exposure.

margination definition of a bone contour, i.e. well or poorly marginated.

mA s milliamperage-seconds – exposure magnitude expressed as the product of milliamperage and time in seconds.

metaphysis wider part at the end of the diaphysis (shaft) of a long bone, adjacent to the physis.

middle carpal joint formerly called the intercarpal joint.

modelling there is confusion between the histological and radiographic use of the terms 'modelling' and 'remodelling'. Histologically, modelling refers to resorption and formation of bone which is not coupled and occurs at anatomically different sites (bone drift). It is a continuous process which regulates the macroscopic structure according to Wolff's law. Radiographically, modelling has been used to describe the formation of bone relevant to the cartilage model which is being replaced, i.e. the normal formation of bone. Thus the two definitions do not agree, so to avoid confusion, strictly speaking the term 'modelling' should be used to describe the macroscopic changes in the shape of a bone as it adapts to the stresses applied to it (see also 'remodelling').

Moiré lines interference pattern seen primarily in digital radiography, caused usually by grid lines interfering with other linear patterns in the system. Literally, appearance of shot silk.

MRI magnetic resonance imaging.

non-focused grid grid in which the lead strips are parallel, perpendicular to the surface of the grid.

non-screen film high-definition x-ray film designed for exposure without intensifying screens; much higher exposure factors are required than if screens are used.

non-union cessation of fracture healing without bony union; may be classified radiographically as an atrophic non-union or a hypertrophic non-union.

odontoma tumour arising in tissues which normally produce teeth, usually solid and radiopaque.

opacity literally the state of being opaque. Seen in an image as the degree of whiteness of the object being radiographed.

osselet colloquial term used to describe enlargement on the dorsal aspect of a metacarpophalangeal joint which may be associated with thickening of the joint capsule and/or synovial proliferation, degenerative joint disease or an articular chip fracture. There may be mineralised tissue within the abnormal synovial tissue.

osseous metaplasia formation of bone in a non-bony structure.

osteitis inflammation of bone.
osteoarthritis synonymous with degenerative joint disease.
osteochondroma (a) benign tumour of projecting adult bone capped by cartilage undergoing endochondral ossification; (b) radiopaque body of mineralised cartilage which may be free floating or attached to synovial tissue (synovial osteochondroma).
osteolysis bone destruction and resorption seen more easily in cortical bone than cancellous bone because of greater contrast. There is a delay of at least 10 days between histologic and radiographic evidence of lysis.
osteoma solid, radiopaque tumour of bone, usually well marginated.
osteomalacia decreased bone density due to insufficient or abnormal mineralisation of osteoid.
osteomyelitis inflammation of the bone marrow due to infection.
osteopenia decrease in the radiopacity of bone due to osteoporosis or to osteomalacia.
osteophyte spur of new bone.
osteophyte, marginal or articular spur of new bone at the chondro-synovial junction of an articular margin.
osteoporosis loss of bone density due to imbalance between bone resorption and formation.
parallel grid grid in which the lead strips are parallel to each other.
pastern joint correctly called the proximal interphalangeal joint.
periosteal new bone new bone production, the result of inflammation of the periosteum, or elevation of the periosteum from the cortex; there is usually a lag of at least 14 days between the initial stimulus and the radiographic detection of new bone.
physeal dysplasia abnormality of development of the physis; in some cases this may be a more appropriate term than physitis for a physeal abnormality.
physis growth plate of a long bone.
physitis inflammation of the physis often incorrectly called 'epiphysitis', characterised radiographically by irregular width of the physis with or without modelling of the adjacent metaphysis. Remnant cartilage cones may be seen as triangular radiolucent areas in the metaphysis.
primary cut-off absorption by a grid of the primary beam (also called grid cut-off).
podotrochlear apparatus the navicular bone, distal sesamoidean impar ligament and collateral sesamoidean ligament.
podotrochleitis inflammation of the navicular bone (and/or navicular bursa).
primary radiation, primary beam radiation from the x-ray tube which is incident on the subject matter or which continues unaltered in photon energy after passing through it.
proximal interphalangeal joint formerly the pastern joint.
proximal intertarsal joint now called the talocalcaneal-centroquartal joint.
radiocarpal joint now called the antebrachiocarpal joint.
radiography practice of obtaining radiographs.
radiology study of radiographs; the science and application of ionising radiation.
radiolucency degree of blackness of the object being radiographed.
radiopacity degree of whiteness of the object being radiographed.
rare earth screens intensifying screens that use rare earth phosphors; reduced exposure factors can be used in comparison to calcium tungstate screens.
remodelling there is confusion between the histological and radiographic usage of the terms 'remodelling' and 'modelling'. Histologically, remodelling refers to resorption and formation of bone which is coupled and occurs in basic multicellular units. This regulates the microstructure of bone without altering its shape and is a continuous process, replacing damaged bone with new bone. Thus it cannot be seen macroscopically or appreciated radiographically. The term has been used radiographically to describe the reshaping of bone to match form and function (e.g. after fracture repair), but strictly speaking the term 'modelling' should be used (see also 'modelling').
resolution objective measurement of how much detail can be provided by a film–screen combination, measured in line pairs per millimetre. Indicates the size of the smallest object that the system will record, i.e. the smallest distance that must exist between two objects before they can be seen as two separate entities.
ringbone colloquial term used to describe new bone formation in the pastern region, which may encircle the parent bone. It is a non-specific term and its use is discouraged

because of confusion caused by the prefixes high and low, true and false, articular and non-articular.

scatter radiation multidirectional radiation resulting from the interaction of the primary x-ray beam and an object; it causes loss of contrast between parts of the image on the radiograph, and is a significant cause of radiation hazard to those obtaining radiographs.

scintigraphy production of two-dimensional images of the distribution of radioactivity in tissues after systemic administration of a radioisotope attached to an appropriate tissue-targeting substance.

sclerosis a term colloquially used to describe increased opacity of bone. Strictly speaking it refers to increased hardness of bone, which cannot be determined from radiographs.

scoliosis curvature of the thoracolumbar vertebrae from side to side; usually congenital.

secondary radiation particles (such as electrons) or photons (such as x-rays) produced by the interaction of the primary x-ray beam with matter.

seedy toe term with different usage in the USA and the UK. In the UK it describes separation at the white line, the space filled with crumbly dry material. It is often of uncertain aetiology. It is not generally associated with rotation of the distal phalanx. Unless white line separation is extensive there is usually no associated lameness. In the USA the term is used to describe separation at the white line seen secondary to chronic laminitis and rotation of the distal phalanx.

sequestrum necrotic fragment of bone; a sequestrum usually is a sharply demarcated sclerotic fragment separated from the parent bone by a zone of radiolucency and an outer rim of sclerotic bone (the involucrum).

silhouette sign effect produced when two fluid opacities are contiguous and the clear outline of one is lost; the two fluid opacities thus merge into one; often used in thoracic radiology.

soft x-ray beam low-energy, low-penetrating x-ray beam made at low kVp settings.

sore shins see 'bucked shins'.

splint colloquial term used to describe (a) active or inactive periosteal new bone on a second or fourth metacarpal (metatarsal) bone; (b) inflammation of the interosseous ligament.

splint bones second and fourth metacarpal (metatarsal) bones.

standing lateral positioning technique for a lateral-lateral (the trunk) or lateromedial (limb) projection using a horizontal x-ray beam, vertically positioned cassette and standing patient. (A standing lateral image of the limb implies the patient is weight bearing on that limb.)

stress fracture synonymous with a fatigue fracture.

stressed radiographs radiographs of a joint obtained with the joint manipulated to aid assessment of joint integrity, and to detect subluxation or luxation.

subluxation partial dislocation (displacement) of a joint.

summation radiopacity created by superimposition of more than one structure.

survey radiograph (a) radiographic study of a large area; (b) plain radiograph obtained prior to performing a contrast study.

talocalcaneal-centroquartal joint formerly called proximal intertarsal joint.

tarsocrural joint formerly called the tibiotarsal joint.

temporal teratoma neoplasm in the temple region comprising a number of different types of tissue, none of which is native to the area in which it occurs.

tibiotarsal joint currently called tarsocrural joint.

turbinate bone now called conchus.

ultrasonography imaging of soft tissues using the principle of echography: the variable transmission or reflection of ultrasound waves by tissues of differing densities.

valgus bent outwards: a deformity in which the angulation of the part is away from the midline of the body. Usage is confusing when terms such as carpal valgus are employed since, although the limb distal to the carpus is angled outwards, the carpus often appears 'knock-kneed', i.e. deviates inwards.

varus bent inwards: a deformity in which the angulation of the part is toward the midline of the body. Usage is confusing when terms such as fetlock varus is used: the distal limb is angled inward, but the fetlock appears to deviate outward.

weight-bearing radiograph radiograph of part of a limb obtained with the horse bearing some weight on the limb, ideally with the foot flat.

Wolff's law modelling of bone according to the stresses placed on it, to be functionally competent while using the minimum amount of bone tissue.

xeroradiography dry radiographic process in which the sensitive material consists of a plate carrying an electrical charge on the surface; when radiation interacts with the surface the charge is released; the plate is dusted with a special powder and an image is formed by the powder being attracted and retained in the charged area. Definition is high, but the technique is now seldom used.

Index

Page numbers in *italics* denote figures, those in **bold** denote tables.

abdomen
  anatomy 705–7
  foal *689*, *690*, *691*, 705–7, *707*
  positioning for radiography 688
  see also gastrointestinal tract; urinary system
abscess
  oesophageal 695, *697*
  pulmonary 671, 675, *675*
acetabulum 613, 614, 616, 622, *623*, 624, *625*
  fractures 628, 630
  osseous cyst-like lesions 626
  osteochondrosis 626
  modelling 626
active-matrix liquid crystal displays (AMLCDs) 46
acute respiratory distress syndrome (ARDS) 669–70, *670*
adamantinoma *see* ameloblastoma
additional images 9–10, *10–12*
adenocarcinoma
  lung 677
  paranasal sinuses 479
ageing *see* older horses
air bronchogram *656*, 657, 667, 670, 671, *672*
air tendogram 725
air-gap technique 45, 758
alimentary system *see* gastrointestinal system
aluminium wedge filter 8, *8*
alveolar lung disease 655–7, *656*
ameloblastic odontoma 478–9, *481*
ameloblastoma 478–9, *479–81*, 493
aneurysm of internal carotid artery 520, *729*
aneurysmal bone cyst 346, 527
angiography 725–30
  diagnostic criteria 728–32, *728–31*
    beading of arterial wall 727
    vessel distension 727, *729*
    vessel narrowing and failure to fill 727, 730
  technique 726–7
ankylosis 284, 382, 595
  carpometacarpal joint 282
  centrodistal joint 362
  proximal interphalangeal joint 161
  tarsometatarsal joint 362
antebrachiocarpal joint *3*, 262, *263–5*, 266, *267–9*
  degenerative changes 278–9, 281–2, *281*, *283*
  osteophytes 275, 279
  soft-tissue swelling 277–8
antebrachium
  kick injuries 278
  radiographic technique 261–2
  see also carpal bones/carpus
aorta *643*, *645–8*, 650, *661*
aortic arch 651
aortic silhouette 650
apophysis **751**
  calcaneal *391*
  humeral 343
  tibial 403, *404*, *419*, *444*
  ulnar 331, *332*, *333*
artefacts 47–9
  imaging plate 47
  operator-induced 49
  plate reader 47–9, *48*, *49*
arterial wall, irregular 727
arteries
  distension 727
  narrowing 727, 730

Clinical Radiology of the Horse, Fourth Edition. Janet A. Butler, Christopher M. Colles, Sue J. Dyson, Svend E. Kold and Paul W. Poulos.

© 2017 John Wiley & Sons, Ltd. Published 2017 by John Wiley & Sons, Ltd.

Companion website: www.clinical-radiology-horse.com

arthritis
infectious 35–6
pelvis 624
tarsus 389–90, *391*
infectious polyarthritis in foals 35
osteoarthritis *23*, 37
distal interphalangeal joint 96
foot 90
scapulohumeral joint 321–2
thoracolumbar vertebrae *585*, *586*
see also degenerative joint disease
arthrography 723–4
scapulohumeral joint 305, 312–13, *315*
arthropathy
articular process 558
steroid 282
temporohyoid osteoarthropathy 457, *460*, *461*
arytenoid chondritis 523, 525, *525*
aspiration pneumonia 671, *672*
ataxia 531, 532, 540, 549, 552
hindlimb *548*
sedation 532
atlantoaxial joint subluxation 560–1, *562*
atlas *515*, 516, 519, *542, 550, 562*, 733, **749**
atresia ani 711
atresia coli 711, *713*
automatic processing 7–8
avulsion fractures
distal interphalangeal joint, collateral ligament insertion 97
fibularis tertius *435*, 439
nuchal crest 465
rectus capitis ventralis major 465
suspensory ligament origin 247–8, *248*
third metacarpal bone *33*
tibial malleoli 385
axis 541, *541–3*, *550*, *562*
fractures 567

backscatter 47
bacterial pneumonia 666–9, *668*, *669*
barium suspension
contrast examination of abdomen 688
contrast examination of oesophagus 688, 694–5, *696*, *698*
foals 708
basioccipito-basisphenoid suture separation 465
biceps brachii
entheseous new bone at insertion 337, *339*
tendon mineralisation 320, *322*
bicipital apparatus *see* humerus, tubercles
Birkeland fracture 153, 171, 198
bladder rupture 717
bog spavin 356
bone
changes 20–4
circumscribed opacities 26–7
cortical thickening 22, 240
cysts 346, 527
demineralisation 20–2, *21*, *22*
endochondral ossification 36, 37, 262, 285, 391, 421
see also osteochondrosis
enostosis-like lesions 26, *27*, 242, 326, 346, 442, 634
fractures *see* fractures
fragility syndrome 329
fusion times, cranium **453**, **749**
heterotopic ossification 27–8
increased production 22–4, *23*
lesions 24–32
hypertrophic osteopathy 25–6
neoplasia *see* neoplasia
osteitis/osteomyelitis 25
physitis *see* physitis
mineralisation *see* mineralisation
modelling *see* modelling
neoplasia *see* tumours
periosteal new bone formation
metacarpal 238, *238*
tarsus 383–5, *385*, *386*
resorption 81, *83*, 104, 166, 168, 440
sclerosis 24, 285–7, *285–6*
spur formation 279, *281*
stress-related injury 19, 20, 23, 24, 31
metacarpals 204–5, *205*
metatarsals 204–5, *205*
see also fatigue (stress) fractures
trauma *see* fractures
brachygnathia 489
bronchial disease 655
bronchiectasis 663, *665*
bronchiolitis 662
bronchitis 662
bronchointerstitial pneumonia of foals 669–70, *670*
bucked shins 230
bursography 723–4

calcaneus
apophysis *391*
entheseophytes 358, *358*
sustentaculum tali *352*, *355*, *366*, *367*
tuber calcanei *368*
calcification 38

calcinosis circumscripta
carpus 285
stifle 435, *436*
calcium tungstate screens 757
callus 24, 27, 29, *30*, *87*, 169, 235, *247*, *254*, *345*, *441*
endosteal 29, 328, 344
periosteal 29, *30*, 237, 245, 247, 327, 328
calculus, urinary 587
canine teeth (tushes) 480, *483*, **483**, 488
cardiac disease 679, *680*
cardiac notch *646*
cardiac silhouette *642*, *644*, *646*, 650, 651, *656*, *658*, *659, 663*, 667, *672*, 679, *680*, 694, *700*
carina 650, 651, *656*
carpal angular limb deformities 289–91, *290*
carpal bones *see* carpus/carpal bones
carpal sheath distension 278, 284, *284*
carpal valgus deformity 289, *290*
carpal varus deformity 289
carpi radialis, extensor, tendon sheath distension 278
carpometacarpal joint
ankylosis 282
degenerative changes 278–9, 281–2, *281*, *283*
new bone formation 279*, 280*, 282
osteophytes 279, *280*
carpus/carpal bones 259–99
accessory carpal bone *297*
calcinosis circumscripta 285
degenerative joint disease 278–9, 281–2, *281*, *283*, 294
desmitis 278
dorsolateral-palmaromedial views *19*, *281*, *297*
dorsomedial-palmarolateral views *273*, *275–7*, *279*
dorsopalmar view 260, 266, *281*, *288*
dorsoproximal-dorsodistal views 260–1, *261*, 271, *272*, *285–6*, *295*, *296*
entheseophytes *280*, 282
exostosis 284
fifth carpal bone 274
first carpal bone 274, *279*
fourth carpal bone *273*, 275
fractures 297
radiopacity 286
fractures 286, 293–8
accessory carpal bone 296–7, *297*
chip 293–4, *293*, *295*
complex 298
parasagittal 296, *296*
second/fourth carpal bones 297
slab 294–6, *295*
hygroma 277
incidental findings 271, 274–5, *275–9*
incomplete ossification 291, *292*
lateromedial view 260, *260*, 262, 266, *270*, 271, *274*, *283*, *284*, *288*, *295*
limb deformities 289–91, *290*
new bone formation 282–5, *283*, *284*
normal anatomy 262–7
adult 262–7, *273–7*
immature horse 262, *263*, *264*
osseous cyst-like lesions 287–8, *288*
osteochondroma 291
osteomyelitis 287, *288*
osteophytes 275, 279, *280*, 282
physis fusion times **750**
physitis 288–9, *289*
polydactyly 288
positioning for radiography
antebrachium 261–2
carpus 259–61
radial carpal bone
osteophytes *280*
radiolucency *283*
remodelling *280*, *281*, 282
radiographic technique 259–62
radiolucency 266, *275*, *282*, *285*
radiopacity 271, 274–5, *279*, 282, *286*
second carpal bone 226, 271, *273*, 274, *280*
fractures 297
significant findings 275, 277–98
soft-tissue swelling 275, 277–8
spur formation 279, *281*
subluxation 293
synoviocoele 277
third carpal bone 226, 274, *280*
radiolucency *288*
remodelling 282
sclerosis 285–7, *285–6*
ulnar carpal bone 271
cassette holders 12
cathode ray tubes (CRTs) 46
caudal vena cava *642*, 651
cavitary pulmonary lesions (CPL) 657, 671, *673*, *674*
centrodistal joint *355*
degenerative changes 10, *363*, 375 *378–80*, *598*
lucency *360*
osteophytes *376*

cervical vertebral column 531–68
anatomical variations 534–48
angulation 553–4, *554*, *555*
articular process joint 532, 533, 534, *534*, 535, *535*, 536, *537*, *538*, 543, *544*, 545, *546*, 547, *547*, *548*, 549, 550, 555–60, *555–60*
caudal epiphyseal enlargement *551*, 552
characteristics 541–5, *541–5*
congenital abnormalities 549
degenerative changes 562, *563*
developmental abnormalities 549–50, *551*, **551**, **552**
discospondylitis 563–4, *565*
dorsal lamina *537*, 554, 560
epiphysis 541, 550, 554
fractures 567–9, *567*, *568*
fusion 549
hyperflexion 534, 555
incidental findings 534–48
intercentral articulations, degenerative changes 562, *563*
instability 553–4, *554*, *555*
intervertebral sagittal ratio 539, *539*, *540*, **552**
intravertebral sagittal ratio 537, 539, *539*, **540**, **552**
lateral-lateral view 534–40, *535–40*, **537**, *541*
lateroventral-laterodorsal view 545–8, *545–8*
minimum sagittal diameter (MSD) 536, **537**, *538*, **540**
corrected 540, **540**
modelling *554–61*, 555–60
neurofibromatosis 565
nuchal ligament insertion, entheseophytes *463*, 561–2
occipito-atlanto-axial malformation 549, *550*
osseous cyst-like lesions 564
ossification centres 541, *541*, 545, *547*, 550, *553*, *557*
osteomyelitis 563, *564*
pedicle *537*, 556, *561*, 567
physis 539, *539*, 554
physis/suture lines, fusion times **749**
radiographic technique 531–4
anaesthetised horse 533–4
equipment 531–2
standing horse 532–3, *534*
scoliosis 567
significant findings 549–68
'ski jumps' 550, *551*, 552, *554*
soft-tissue lesions 566
spinous processes *537*, *544*, 545
spondylitic spurs 545
spondylosis 566
stenosis 536, 552, *553*
subluxations 553–4, *554*, *555*
atlantoaxial joint 560–1, *562*
C5, C6 and C7 561
tumours 565, *566*
vertebral body 535, *535*, *537*, *538*, 539
see also intervertebral sagittal ratio, intravertebral sagittal ratio, above
vertebral canal
caudal extension 554
narrowing *554*
vertebral fusion 549
zig-zag orientation 553, *554*
charge-coupled device (CCD) 43
cheek teeth 484–7, *485–7*
chestnut *see* toreus carpeus; torus tarseus
chip fractures 34
carpus 293–4, *293*, *295*
deltoid tuberosity 328
proximal phalanx 206
choanal restriction/atresia 456–7
choke 695, *696*, 701, *702–5*, 703
chondritis, arytenoid 523, 525, *525*
chondroid 133, 518, *518*
chondroma rodens 527
chondromalacia, patella 437
chondrosis, Eustachian tube diverticulum 518, *518*
chronic obstructive pulmonary disease *see* recurrent airway obstruction
cleft palate 526
coccygeal vertebrae 602–3, *602*, *603*
coffin joint *see* distal interphalangeal joint
collateral desmitis 191, *192*
collateral ligament injury *21*, 88, 97, 163, 166, 191, 198, 251, 427, 430
collateral sesamoidean ligament 114, 126, 127, 129, 137, *137*, *138*, 140
collimation 12, 46, 758
colon, enterolithiasis 715
comminuted fractures 466
computed radiography *see* digital imaging
computed tomography (CT)
thorax 644
tooth root infection 499
metacarpal condylar fractures 177, 218, 243, *244, 245*

computerised radiography 41–3
  imaging plate reading 42–3
conchal sinus 467, *469*
  dystrophic mineralisation *478*
congenital abnormalities
  agenesis of distal phalanx 92
  cervical vertebrae 550
    occipito-atlanto-axial malformation 549, *550*
    vertebral fusion 549
  dysgenesis of distal phalanx 92, 128
  humeral tubercles 321
  navicular bone 128
  ribs 681
  sustentaculum tali 368, *369*
congestive heart failure 679, *680*
contrast of image 4
contrast studies
  angiography 725–30
  arthrography 305, 312–13, *315*, 723–4
  cystography 715–16
  double contrast 278, 708, 715, 723, 724, 744
  fistulography 744
  gastrointestinal tract 688, 691, 708
  intravenous pyelography 744–6, *745*
  myelography 733–43
  negative contrast 688, 723
  oesophagus 694–5
  pneumocystography 743–4
  positive contrast 135, 191, 195, 526, 599, 688, 715, 744
  sinography 744
  tendonography 724–5
  urinary system 715–17
  venography 108, *109*, 730–2
cortical thickening 22–3, 240
costal cartilages 682, *682*
'cottonball' lesions 667
coxofemoral joint *618*, *621*, *623*
  degenerative changes 624–6, *625*
  fractures 630, *631*
  luxation 624
  osteochondrosis 626
  osteophytes 624, *625*, 626
  radiographic technique 609, 611, *612*, 613, *613*, 622
  subluxation 622, 624
cranial tibial tendon, dystrophic mineralisation *359*
craniomandibular osteopathy 505
cranium 451–66
  bone fusion times **453**
  choanal restriction/atresia 456–7
  dentigerous cysts 456, *460*
  entheseophytes 461–2, *463*
  fractures 463–6, *464*
  hydrocephalus 461
  lateral-lateral view 452, *454*
  nasal polyps 461, *462*
  nasal septum abnormalities 457
  normal variations/incidental findings 452–6
    adult 452–6, *454–6*, *458–9*
    immature horse 452, *453*
  oblique views 452
  radiographic technique 452
  significant findings 456–66
  temporohyoid osteoarthropathy 457, *460*, *461*
  ventrodorsal view 452, *458*
  see also head
crena solearis 66, *72*
cross-hatch grid 613
cruciate ligaments
  rupture 431
  sprain 432, *432*
crush fractures of humerus 328
curve of Spee 487
cystitis 717, *719*
cystography, contrast 715–16
cysts
  aneurysmal bone cyst 346, 527
  dentigerous 456, *460*
  mandible 504
  maxilla 474
  maxillary sinus 472, 474, *475*
  oesophagus 698
  sub-epiglottic 523, *524*
  subchondral bone cyst 36–7, 420–4, *422*, *423*
  submucosal 472
  see also osseous cyst-like lesions

dacryocystorhinography 746
darkroom
  lighting 758
  procedures 6
deep digital flexor tendon *see* digital flexor tendon, deep
definition 760
degenerative joint disease 37–8
  antebrachiocarpal joint 278–9, 281–2, *281*, *283*
  articular process joint
    cervical 562, *563*
    thoracolumbar 594–6, *595*, *596*
  carpus 278–9, 281–2, *281*, *283*, 294
  centrodistal joint 375, *375–80*
  cervical spine 562, *563*

degenerative joint disease (*cont'd*)
coxofemoral joint *609*, 614–16, *625*
distal interphalangeal joint 88–91, *89–91*
elbow joint 337, *338*
femorotibial joint 427–9, *427–8*
meniscal instability/tears 431
metacarpophalangeal joint 193–6, *194*, *195*
metatarsophalangeal joint *21*, *193*, *194*, *198*, *203*
middle carpal joint 279, *279*
navicular bone 128–39, *130–8*
osteophytes *see* osteophytes
pelvis 614–16, *625*
proximal interphalangeal joint 161–2, *162*
scapulohumeral joint 319–20, *321*
stifle 427–9, *427*, *428*
talocalcaneal-centroquartal joint 375, 383, *384*
tarsocrural joint 383, *384*
tarsometatarsal joint 375, *376*, *377*, *380*
tarsus 375–83, *375–81, 384*
temporomandibular joint 506, 508
thoracolumbar spine 594–6, *595*, *596*
delayed union 31–2, *522*
demineralisation 20–2, *21*, *22*
focal 21–2, *22*
generalised 20, *21*
localised 21, *21*
density (radiographic) 44
density (tissue) 644, 645
dental sac *494*
dentigerous cysts 456, *460*
desmitis
collateral 191, *192*
intercarpal ligament 278
distal sesamoidean impar ligament 162, *163*
oblique sesamoidean ligament 162, *163*, 165
patellar ligament 434
straight sesamoidean ligament 162, *163*
suspensory ligament *201*, 202, 219, *236*, 237, 248, 249, 252, *254*
desmopathy of suspensory ligament 235, *236–7*
detail, film 5, 7
detomidine 449
developer chemicals 6, **759–60**
developmental abnormalities
cervical vertebrae 549–50, *551*, **551**, **552**
metacarpophalangeal joint 196–9, *197*, *198*
diaphragm 577
hernia 677, *678*
silhouette 651
diaphragm, collimator *8*, 12
diaphysis 634, **750**
diastema 501, 503, *504*
DICOM (Digital Imaging and Communications in Medicine) 41
file transmission 53
image compression 53
monitors 46–7
servers 53
digital exposure guide **755–6**
digital annular ligament
distal 153, *159*, *162*, 163, 165, 167
proximal 153, 165, *165*
digital extensor tendon, common 74
digital flexor tendon, deep 63, *64*, 102, 112, 118–19, 129
avulsion 340, *341*
adhesion 133, *133*
disruption 91
mineralisation 139, *139*
osseous changes 88, *89*
radiographic outline 121
trauma 140, *140*, 284
digital flexor tendon, superficial 204, 262, 271
periostitis 341
digital flexor tendon sheath, distension 192–3, 203
digital images 41–54
advantages 53–4
archiving and transmission 52–3
artefacts 47–9, *48*, *49*
computerised radiography 41–3
direct digital radiography 43
exposure factors 44–6, *46*
exposure index 45
image reading 50–2, *50–2*
image resolution 43–4
image retrieval 52
labelling 14–15
manipulation 50–1
monitors 46–7
operator induced artefacts 49
direct digital radiography 43
discospondylitis
cervical vertebrae 563–4, *565*
thoracolumbar vertebrae 599
dislocation *see* luxation
distal digital annular ligament 153, *159*, *162*, 163, 165, 167

distal interphalangeal joint 66, *72*, *75*, *122*
collateral ligaments 66, 68, *69*, *73*, 81, *82*, *84*, 88, 98
degenerative joint disease 88–91, *89–91*
distal phalanx fractures 92–7, *92–4*, *96*, *97*
osseous cyst-like lesions 81, *82*
osteoarthritis 96
osteophytes 90
subluxation 91–2
synovial invaginations 121, *122*
distal intertarsal joint, see centrodistal joint
distal phalanx, see phalanx, distal
distal sesamoid bone see navicular bone
distal sesamoidean impar ligament 114
attachment *120*, 122, *122*
disruption of 141
dystrophic mineralisation 126, 171
origins 122, 126
osseous changes 88, *89*
double contrast 278, 708, 715, 723, 724, 744
dural sagittal diameter 742, *742*
dysplasia of proximal interphalangeal joint 158
dystrophic mineralisation
conchal sinus *478*
cranial tibial tendon *359*
distal sesamoidean impar ligament 126, 171
metacarpophalangeal joint 193, *193*
navicular bursa 139
nuchal ligament insertion 566
tendon of fibularis tertius 358, *360*

edge effect 68, *222*, *309*
effusion
femoropatellar joint *420*
pleural 657–62, *658*, *659*
elbow joint 330–46
craniocaudal views 331, 335, *335*, *338*
craniomedial-caudolateral oblique view *336*
degenerative joint disease 337, *338*
entheseophytes 339, *339*, *340*
fractures 343–6, *343–5*
hereditary multiple exostosis 342
infection 342
luxation 341
mediolateral view 330–1, 333, *333*, *334*
new bone formation 337, 339, *339*, *340*
normal variations/incidental findings 331–7
adult 331–7, *334–6*
immature horse 331, *332*, *333*
oblique views 331
osseous cyst-like lesions 337
osteochondrosis 337
osteophytes *338*
radiographic anatomy 331–7
radiographic technique 330–1
significant findings 337–46
emboli 676, *676*
emphysema 663, *665*
empyema, Eustachian tube diverticulum 516–17, *517*
enamel organ tumours 478
endochondral ossification 36, 37, 262, 285, 391, 421
see also osteochondrosis
endosteal callus 29, 328, 344
enostosis 26, *27*
femur 634
radius 346
scapulohumeral joint 326
tibia *27*, 442–3
enterolithiasis 715
entheseophytes 23, 60, 88, *88*
calcaneus 358, *358*
carpus *280*, 282, *283*
cervical spine 561–2
distal phalanx 60
elbow joint *339*, *340*
femorotibial joint 430
foot 60, 88, *88*
interspinous ligament 587, *588–9*
metatarsal bone 221, *359*
middle phalanx 153, 157, *159*, 163, 165, 194
navicular bone 129, 130, 137
nuchal ligament insertion *463*, 561–2
occiput 461–2, *463*
proximal phalanx 153, 157, *159*, 163, 165, 194
proximal sesamoid bones 189
suspensory ligament origin 219, 235–7
suspensory ligament branch insertion 202
third metatarsal bone 221, *359*
see also new bone formation
enthesopathy
insertional of biceps brachii tendon 337, *339*
insertional of semitendinosus 434
palmar annular ligament 202, *202*
proximal interphalangeal joint *162*
supraspinous 576
thoracolumbar spine interspinous ligament 587, *595*, 596, *596*

eosinophilic pneumonia 666, *667*
epidural space-occupying lesion 742–3
epiglottis 516
  entrapment 521, *523*
  shortening 522–3
  sub-epiglottic cysts 523, *524*
epiphysitis 24
  metacarpophalangeal joint 199
  radius 24
  see also physitis
epistaxis 520, *729*
equine multinodular pulmonary fibrosis 663, 666, *666*
equine odontoclastic tooth resorption and hypercementosis (EOTRH) 493, 495, *498*
ethmoid haematoma 474, *476*, *477*
ethmoid turbinates 456
Eustachian tube diverticula 456, 512–27
  chondrosis 518, *518*
  empyema 516–17, *517*
  infection 516
  masses 520, *521*
  mycosis 520
  normal anatomy *514*, *515*, 516
  radiographic technique 512–13
  tympany 518–20, *519*
examination for purchase 13–14
exercise-induced pulmonary haemorrhage (EIPH) 676, 677
exostosis
  carpus 284
  elbow joint 342
  metacarpal bone *228*, *231*, 239
  metatarsal bone 226, *229*
exposure chart 8
exposure factors 4–5, 44–6, *46*
  algorithms 45–6
  overexposure 44
  underexposure 45
exposure guide 753–7, **753–6**
exposure latitude 5
extradural space-occupying lesion 743

fabellae 153, 407, 439
facia flexoria 63
facial bone deformity 472, *473*
facial nerve paralysis 457, *460*
fatigue (stress) fractures 27, 28
  humerus 328, *330*
  ilial wing 630
  ilial shaft 630
  metacarpal bone 237
    third 204
  proximal phalanx 170
  radius 344
  lumbar articular process 596
  tibia 443–4, *444*
femoral condyles
  adult 407, 408, 411
  caudal lateral-craniomedial oblique views 406–7
  caudal proximal-craniodistal oblique view 408
  fractures *429*, 439
  immature horse 403
  infection 429
  lateral *409*, 411, *412*, 421
  medial *52*, 400, 408, *409*, 421
    immature horse 403
    osseous cyst-like lesions 36–7, *423*, 424, 426, 431, *431*
  necrosis 426, *428*
femoral epicondyles 430
  lateral 408
femoral head 613
  deformation 622
  displacement 624
  flattening 624
  infection 624
  ossification centres 614
  physis *615*
femoral physis 403, 439, *615*
  fusion times **751**
  immature horse 403
femoropatellar joint
  attachments *416*
  bone fragments in 437
  effusion *419*, *420*
  instability 435
  osteophytes 427, *427*, 429
  radiopaque fragments 415
  septic arthritis *430*
femorotibial joint 403, *413*
  collateral ligament injury 166, 191, 430
  cruciate ligaments
    rupture 431
    sprain 432, *432*
  entheseophytes 430
  meniscal damage 431, *431*
  osteophytes *431*, *433*
femur 632–5
  enostosis-like lesions 634
  fractures 439, 634–5, *635*
    diaphyseal 634
    greater trochanter 630, 634
    third trochanter 634–5, *635*
  greater trochanter 613, *613*, 622, *623*, 630, 634
  ossification centres 614

physis fusion times **751**
radiographic anatomy 633–4
radiographic technique 632–3
suture lines **751**
third trochanter 633, 634–5, *635*
trochlear groove *409*, 412, 414
trochlear ridges
adult 406, *408*, *409*, *414*
immature horse 403
osteochondrosis 415, *418*, *419*
see also entries under femoral
fetlock *see* metacarpophalangeal joint; metatarsophalangeal joint
fibroplasia 663
non-neoplastic focal 83
fibrosarcoma *83*
fibula
fractures 440, *441*
immature horse 405
ossification 405, *406*, *407*
physis fusion times **751**
fibularis tertius, avulsion fracture *435*, 439
films 5–6
development 6, **759–60**
double emulsion 758
exposure guide 753–5, **753–5**
fogging 6
image quality 757–8
labelling 14–15
low-density **760**
processing 6–8
faults **759–60**
relative speed 757
single emulsion 758
spectral sensitivity 757–8
film badges 13
film-screen radiography 41, 42, 44–5
filters 6, *8*
aluminium wedge *8*
Kodak GS1 6
Wratten Series 6B 6
Firth's classification
infectious polyarthritis of foals 35–6
osteomyelitis 25
fistulography 112, 744, *745*
penetrating injury of foot 112
fistulous withers 599
fixer 6
fluid line
head 464, *464*, 470, 472, *472*, 516, *517*, 520
thorax *649*, 657, *668*, *675*
fluoroscopy 694
foal
abdomen *689–91*, 705–7, *707*
alimentary system 705–7, *707*
atresia coli 711, *713*
atresia ani 711
avulsion fractures 198, *435*
bladder rupture 717
carpal incomplete ossification *292*
carpal valgus deformity *290*
carpus *263*, *264*, *288*
cavitatory pulmonary lesions *668*, *673*
cervical vertebrae *541*
coccygeal vertebrae *573*
congenital abnormalities 679
contrast studies 688, 708–9, *709*, 715
craniocaudal dimension, cardiac 650
cystitis 717, *719*
dentigerous cyst *460*
diaphragmatic hernia *678*
distal phalanx fracture *94*
elbow *332*
femoral condyles, necrosis 426
femoropatellar joint, septic arthritis *430*
foot *63*
gastroduodenal ulcer disease *699*, 711, 714
hock *353*, *354*, 369, *369*, *371*, *390*
ileocolonic aganglionosis 711
incomplete ossification
carpal bones *292*
tarsal bones *370*
infectious polyarthritis 35–6
joint infection 35
mega-oesophagus 698–701, *699*, *700*
metacarpal region *224*
metacarpophalangeal joint *183*, *209*
obstructive ileus *712*
osteomyelitis 25, *288*, *563*
patent urachus 717
pelvis *615*
pneumocystography 743, 744
pneumonia 644, *670*, *672*
proximal sesamoid bones, fracture 208, *209*
restraint 303
sacral vertebrae *573*, *615*
scapulohumeral joint *306*, *327*
thoracolumbar vertebrae *573*, *615*
absence of mineralisation *572*
stifle *404*, *405*, *419*, *426*, *429*, *430*
tarsal bones, incomplete ossification *370*
third metacarpal bone, fracture 242
third metatarsal bone, fracture 242
see also immature horse

focal distance (of grid) 640, 757
focal impact fractures 196
focal spot 3
  size 759
focal-film/imaging plate distance 757
focus-film distance (FFD) 4, 8
focused grid 758
fogging of X-ray films 6
foot 55–147
  angiogram *730*
  bursography 723–4
  coffin bone *see* distal phalanx
  collateral ligaments of distal interphalangeal joint 66, 68, *69*, *73*, 81, *82*, *84*, 88, 98
  collateral sesamoidean ligament 114, 126, 127, 129, 137, *137*, *138*, 140
  conformation 77, 95, 98, 99, 100–2, *101*
  deep digital flexor tendon 88, *89*
  degenerative joint disease 88–91, *89–91*
  distal phalanx *see* phalanx, distal (pedal bone)
  distal interphalangeal joint 63, *65*, 66, *67*, *72*, *73*, *75*
    collateral ligament injury 88
    degenerative joint disease 81, 88–91, *89*, *90*
    osseous cyst-like lesions 81, *82*
    subluxation 90–1
  distal sesamoidean impar ligament 114
    attachment *120*, 122, *122*
    disruption of 141
    dystrophic mineralisation 126, 171
    origins 122, 126
    osseous changes 88, *89*
  dorsolateral-palmaromedial oblique views *13*, 68, *69–71*, *74*, *87*
  dorsomedial-palmarolateral oblique views 68, *69–71*, *79*
  dorsopalmar view 66, *67*, *74*
  dorsoproximal-palmarodistal oblique views *12*, *56*, *63*, 64–6, *65*
  dystrophic mineralisation 74, 127, 137, *137*, *138*
  entheseophytes 23, 60, 88, *88*
  extensor process of distal phalanx *61*, *64*, 66
    anatomical variations 62, *63*, *73*
    contour 68, *71*
    fragments 75, *75*
    remodelling 56
  foreign bodies 112, 142
    fistulography 112
    foot infection 111
    sinography 744
  fractures 92–7, *92–7*
  hoof *see* hoof
  hoof wall separation 56, 112, *113*
  imbalance
    dorsopalmar 100
    mediolateral 66, 87, 90
  incidental findings 70–6, *72–5*
  infectious osteitis 79–80
  keratoma 81–2, *83*
  laminitis 77, 102–8, *103–7*
  lateromedial view 62–4, *63*, *64*, *72*, *82*
  long-toe low-heel syndrome 108, 110, *110*
  middle phalanx *see* phalanx, middle
  navicular bone *see* navicular bone
  navicular bursa *130*, 139–40
  navicular disease 128–35, *130–6*
  normal anatomy 62–70
    adult 62–70, *63–5*, *67–70*
    immature horse 62, *63*
  osseous changes, facia flexoria 88, *89*
  osseous cyst-like lesions 80–1, *82*
  ossification centres 74, 75, *86*, *87*, 95
  packing artefacts 55
  palmaroproximal-palmarodistal oblique view 66, 68, *68*
  pedal bone, see phalanx, distal (pedal bone)
  pedal osteitis 76–9, *77–9*
  penetrating injuries 112
  radiographic technique
    distal phalanx (pedal bone) 55–62
    hoof 97–100
    navicular bone 113–19
  seedy toe 139–40
  solear margin fracture 95
  synovial invaginations 121, *122*
  significant findings 76–97
  tumours 83, *83*
  ungular cartilage (sidebone) ossification 83–8, *84–8*
  venography 108, *109*
foreign bodies, foot 112, 142
  fistulography 112
  foot infection 111
  sinography 744
fossa 121
  see also navicular bone
fovea capitis 616
fractures 28–32
  acetabulum 628, 630
  avulsion *see* avulsion fractures
  Birkeland 153, 171, 198
  carpus 286, 293–8
  cervical spine 567–9, *567*, *568*

chip *see* chip fractures
classification 28, *29*
comminuted 466
cranium 463–6, *464*
crush 328, *330*
elbow joint 343–6, *343–5*
fatigue (stress) *see* fatigue (stress) fractures
femur 439, 634–5, *635*
fibrous union 29
focal impact 196
hairline 600
healing 29–30
humerus 326–9, *327–30*
hyoid apparatus 520, *522*
ilium 629–30, *629*
internal fixation 170, 207, 242, 243, 246, 294, 296–7
intra-articular 34
ischium 630, 632, *632*, *633*
mandible 466, 508, *509–11*
metacarpal region *30*, 242–55, *244–50*, 251–2, *252–5*
metatarsal region 250, *250*, 251–2, *251*, *253*, *255*
navicular bone 140–2, *140–2*
nasofrontal suture *464*
  non-union 632, 679
nuclear scintigraphy
  metacarpal region 218
  metatarsal region 218, 249
  phalangeal 168
parasagittal 286
palmar cortical incomplete of third metacarpal bone *249*
patellar *31*, 437–9, *437*, *438*
pelvis 628–32, *628*
phalanges
  distal 92–7, *92–6*
  middle 167–71, *168–72*
  proximal 167–71, *168–72*, 206–7, *207*
proximal sesamoid bones 207–8, *208*, *209*
radius *30*, *295*, 297, 343–4, 345, *345*
ribs 679, 681
Salter-Harris classification 28, *29*
'saucer' 243
simple 466
slab 34, 286, 294–6, *295*, *296*
stifle 437–40, *437*, *438*, *440*, *441*
stylohyoid bone 457, *460*
tarsus 392–5, *393*, *394*
teeth 495, 499
thoracolumbar vertebrae 600, *601*
  tibia 439–40, *440*, 443–4, *444*
  ulna 343, *344*
frontal bone, fractures 463–4
frontal sinus 746
  adenocarcinoma 479
  normal anatomy *455*, 467, *469*
  sinusitis 467
fungal pneumonia 670

gas cap *641*, 671, 677, 688, *700*
gas shadows *16*
gastrocnemius, muscle injury 434, 439
gastrocnemius tendon, avulsion of origin 439
gastroduodenal ulcer disease in foals 711, 713
gastroenteritis 711
gastrography, double-contrast 711
gastrointestinal tract 687–715, *689–93*, 704–15
  anatomy 705–7
    adult 708
    immature horse 705–6, *707*
    variations 708
  diseases of 709–15
    atresia ani 711
    atresia coli 711, *713*
    enterolithiasis of adult horses 715
    gastroduodenal ulcer disease in foals 711, 713
    gastroenteritis 711
    ileocolonic aganglionosis 711
    large intestinal obstruction 709, *709*, *710*
    ruptured hollow viscus 714, *714*
    sand impaction 715, *716*
    small intestinal obstruction *707*, 709, *709*, *712*
  positioning for radiography 688, *689–93*
    right and left lateral recumbent positions 706
    right-left lateral-lateral standing position 706
    ventrodorsal position 706
  radiographic technique 687–93, *689–93*
    contrast examination 688, 691
    equipment 687–8
  see also oesophagus
graininess of films 45
granulomata 675
grass sickness 703–4
greater trochanter of femur 613, *613*, 622, *623*, 630, 634

greater tubercle of humerus 302, 303, 306, *307*, *308*, *310*, *311*, 327, **750**
grids 8–9, 215, 758
  cross-hatched 613
  focused 758
  parallel 56
grid cut-off 758
grid ratio 117, 758
guttural pouches *see* Eustachian tube diverticula

hairline fractures 600
head 449–530
  angiography *728–9*
  arytenoid chondritis 523, 525, *525*
  choanal restriction 456–7
  cleft palate 526
  craniomandibular osteoarthropathy 505
  curve of Spee 487
  dentigerous cyst 456, *460*
  diastema 501, 503, *504*, *505*
  dorsoventral/ventrodorsal views, technique 450–1, *451*
  epiglottis 516
    entrapment 521, *523*
    shortening 522–3
    sub-epiglottic cysts 523, *524*
  ethmoid haematoma 474, *476*, *477*
  Eustachian tube diverticula *515*, 516
    chondrosis 518, *518*
    empyema 516–17, *517*
    infection 516
    masses 520, *521*
    mycosis 520
    normal anatomy *514*, *515*, 516
    radiographic technique 512–13
    tympany 518–20, *519*
  fluid line 464, *464*, 470, 472, *472*, 516, *517*, 520
  frontal bone, depression fracture 463–4
  guttural pouch *see* Eustachian tube diverticula
  hydrocephalus 461
  interdental space
    infectious osteitis 510
    sequestrum 510, *512*
  larynx 512–27
  lateral-lateral view, technique 450
  mandible
    fractures 466, 508, *509–11*
    infectious osteitis 510
  maxillary sinus cyst 472, 474, *475*
  nasal polyps 461, *462*
  nasal septum 457
  nasofrontal suture exostosis 464–5, *464*
  oblique views 451
  otitis media 457, *460*
    paranasal sinuses 466–80
  pharynx, larynx and Eustachian tube diverticulum 512–27
  physis fusion times **749**
  radiographic technique 449–52
  teeth and mandible 480–512
  sinus
    chonchal 467, *469*, *478*
    cyst, submucosal 472
    frontal *see* frontal sinus
    maxillary *see* maxillary sinus
  soft palate 516
    dorsal displacement 525–6, *526*
  stylohyoid bone, fractures 457, *460*
  submucosal sinus cyst 472
  temporohyoid joint, osteoarthropathy 457, *460*, *461*
  temporomandibular joint (TMJ)
    degenerative joint disease 506, 508
    luxation 508
    radiographic technique 482, 484, *484*
  teeth *see* teeth
  tumours
    dental origin 493
    mandibular 505–6, *506*, *507*, *508*
    paranasal sinuses 478–9, *479–81*
  see also cranium; frontal sinus; mandible; maxilla; maxillary sinus; teeth
heaves 662–3, *665*
hereditary multiple exostosis 342
heterotopic ossification 27–8
  scapulohumeral joint 322
high-definition screens 5
hip dysplasia 622
hock *see* tarsus
hoof *74*, 97–112
  balance 98–9, 100–2, *101*, 102
  dorsopalmar view 98, 100, *101*, *107*, *111*, *115*
  dorsoproximal-palmarodistal oblique view *105*
  hind feet 98
  incidental findings 99–100
  infection 111–12
  laminitis 102–8, *103–7*
  lateromedial view 98, 101, *103*, *104*, *106*, *107*, *110*, *113*

long-toe low-heel syndrome 108, 110, *110*
mediolateral foot imbalance 110, 111, *111*, *115*
normal anatomy 98–9, *99*, *101*
palmaroproximal-palmarodistal oblique view *110*
penetrating injuries 112
radiographic technique 97–8, 100–1, *101*, *103–7*, *110*, *111*, *115*
significant findings 102–13
sole thickness variation 99
see also foot
hoof wall
keratoma 81–2
orientation 63
radiolucent 'halo' 63, 68
separation 56, 112, *113*
Horner's syndrome 520
humeroradial joint *see* elbow joint
humeroulnar joint *see* elbow joint
humerus 301–30
apophysis 343
arthrography 305, 312–13, *315*
caudolateral-craniomedial oblique view 303
cranial medial-caudolateral oblique view 303, *304*, 307, *311–15*
cranioproximal-craniodistal oblique view 304–5, *305*, 312, *314*, *325*
degenerative joint disease 319–20, *321*
deltoid tuberosity *311*, *312*
fractures 328
fractures *330*, 343
greater tubercle *see under* tubercles, below
humeral head 307
immature horse 306, 331
infection 323, 325
lesser tubercle *see under* tubercles, below
luxation 325–6, *325*
mediolateral view 301–3, *302*, 306–7, *308–10*
normal variations/incidental findings 305–10
adult 306–10, *307–17*
immature horse 305–6, *306–7*
osseous cyst-like lesions 315–16, *316–19*, 319
ossification centres 306, *307*, *327*, 332
osteochondrosis 313–14, *316*, *317*, *318*, *321*
physis 343
fusion times **750**
radiographic technique 301–5
septic physitis 325
significant findings 313–29
subchondral bone 307
opacity 314
radiolucency *309*, 314
tubercles *314*
congenital abnormalities 321
greater 302, 303, 306, *307*, *308*, *310*, *311*, 327, **750**
lesions of 321
lesser 304, 306, *306*, 307, *307*, *308*, *310*, *311*, 321, **750**
tumours 346
see also scapulohumeral joint
hydrocephalus 461
hydrothorax *675*
hygroma of carpus 277
hyoid apparatus, fractures 520, *522*
hyperparathyroidism, secondary nutritional 20
hypertrophic osteopathy 25–6, *26*
metacarpal/metatarsal region 242
radius 342

ileocolonic aganglionosis 711
ileus
mechanical *707*
obstructive *709*, *712*
ilium 615, *615*, *619*
fractures 629–30, *629*
image intensifying screens 5–6
images
additional 9–10, *10–12*
archiving, digital 52–3
intensification 5–6
interpretation *see* radiology
manipulation, digital 50–2, *50–2*
production 4
quality 757–9
record keeping 14–15
resolution, digital 43–4
transmission, digital 52–3
see also digital images
imaging plates
artefacts 47
backscatter 47
cleaning 48–9
cracking 47
erasing 47
flexible 47
horizontal lines 48
reader artefacts 47–8

immature horse
bronchointerstitial pneumonia 669–70, *670*
carpus 262, *263*
cranium 452, *453*
elbow joint 331, *332*, *333*
fibula 405, *406*
fibularis tertius, avulsion of origin *435*, 439
foot 62, *63*
gastrointestinal tract 705–6, *707*
contrast studies 708
gastroduodenal ulcer disease 711, 713
humerus 306, 331
ileocolonic aganglionosis 711
infectious polyarthritis 35–6
lethal white foal 711
mandibular cysts 504
mega-oesophagus 698–701, *699*, *700*
metacarpal region *224*
fractures 242
metacarpophalangeal joint 181–2, *183*
metatarsal region, fractures 242
navicular bone 119
patella 403, *404*, *405*
pelvis 613–14, *615*
phalanges
middle 150
proximal 150
scapula 305, *306–7*
pharynx *513*
stifle 403, *404*, 405, *405*
infection 429–30, *429*, *430*
tarsal bone collapse 369–70, *370*, *371*
tarsus 352, *353*, *354*
thoracolumbar spine 571, *572–4*
thorax 647, 650
ulna 331, *332*
urinary tract disease 717–19
bladder rupture 717
cystitis 717, *719*
patent urachus 717, *718*
see also foal
incisive bone (premaxilla), cyst-like lesions 480, *482*, *483*
incisors **483**
radiographic technique 487–8
infection
bone 25
elbow joint 342
Eustachian tube diverticula 520
femoral condyles 429
femoral head 624
hoof 111–12
humerus 325
mycosis 520
navicular bone 139–40
scapulohumeral joint *324*, 325
stifle 429–30, *429*, *430*
tooth root 499–501, *500–3*
umbilical cord 717
see also foreign bodies, foot; osteomyelitis; pneumonia; osteitis, infectious
infectious arthritis 35–6
tarsus 389–90, *391*
infectious osteitis *see* osteitis, infectious
infectious osteomyelitis *see* osteomyelitis
infectious polyarthritis in foals 35–6
inflammatory airway disease 662
infarcts 676, *676*
inhalation pneumonia 671
intercarpal joint *see* middle carpal joint
intercarpal ligament, desmitis 278
interdental space, sequestrum 510, *512*
internal carotid artery *728*
aneurysm 520, *729*
catheterisation 726
internal fixation
carpal bone fractures 294, 296–7
metacarpal bone fractures 242, 243, 246
middle phalanx fractures 170
proximal phalanx fractures 170
proximal sesamoid fractures 207
interosseous ligaments, mineralisation 226
interphalangeal joints *see* distal interphalangeal joint; proximal interphalangeal joint
intersesamoidean ligament 239
desmitis 203
interspinous ligament 576
enthesopathy 587, *588–9*
intervertebral sagittal ratio 539, *539*, *540*, **552**
corrected 540
intra-articular fractures 34
intra-articular swelling 32
intravenous pyelography 744–6, *745*
intravertebral sagittal ratio 537, 539, *539*, **540**, **552**
involucrum 239, *241*
ischium 613, *615*, *623*
fractures 630, 632, *632*, *633*

joints 32–8
arthrography *191*, 305, 312–13, *315*, 723–4
bursography 723–4
calcification 38
degenerative disease *see* degenerative joint disease
immune-mediated disease 32, 38
intra-articular swelling 32, 34
lucent zone 307, *309*, 314
luxation *see* luxation
mineralisation *see* mineralisation
osseous cyst-like lesions 36–7
metacarpophalangeal joint 199–202, *200*
scapulohumeral joint 315–16, *316–19*, 319
osteochondrosis 37
osteoarthritis *see* degenerative joint disease
periarticular swelling 32
subchondral bone cyst 421–424, *422, 423*
subluxation *see* subluxation
swelling 32
see also individual joints

keratoma, distal phalanx 81–2, *83*
kick injuries
antebrachium 278
tibia 443
kidneys, intravenous pyelography 744–6, *745*
kilovoltage (kV) in X-rays 4–5
Kodak GS1 filter 6
kyphosis 594

labelling of films 14–15
laminitis 77, 102–8, *103–7*
distal phalanx rotation 95
hoof distal phalanx distance 99, *99*
sinker syndrome 105, *106*
venography 108, *109*, 730–2
large intestinal obstruction 709, *709*, *710*
laryngeal cartilages, chondritis 523, 525, *525*
larynx 512–27
incidental findings 513–16, *514*, *515*
lateral-lateral view 512
normal variations 513–16, *514*, *515*
radiographic technique 512–13
significant findings 516–27, *517–19*, *521–6*
arytenoid chondritis 523, 525, *525*
cleft palate 526
dorsal displacement of soft palate 525–6, *526*
epiglottic entrapment 521, *523*
epiglottic shortening 522–3
Eustachian tube diverticula *see* Eustachian tube diverticula
hyoid fracture 520, *522*
multilobular osteoma (chondroma rodens) 527
pharyngeal lymphoid hyperplasia 520
subepiglottic cysts 523–5, *524*, *525*
ventrodorsal view 513
lead protective clothing 12
lesion progression 10, *12–13*
lesser tubercle of humerus 304, 306, *306*, 307, *307*, *308*, *310*, *311*, 321, **750**
lethal white foal 711
ligaments
collateral *21*, 88, 97, 163, 166, 191, 198, 251, 427, 430
collateral sesamoidean, navicular 114, 126, 127, 129, 137, *137*, *138*, 140
cruciate 431, 432, *432*
distal digital annular 153, *159*, *162*, 163, 165, 167
distal sesamoidean impar *see* distal sesamoidean impar ligament
intercarpal 278
interosseous 226
intersesamoidean 203, 239
interspinous 576, 587
long plantar *358*
meniscal 431, *431*
nuchal 452, 455, *463*, 561–2, 566
oblique sesamoidean *159*, 162, *163*, 165
palmar annular 202, *202*
palmar intercarpal 278, 294
proximal digital annular 153, *165*, 165
round (teres) 616, *618*, 622, 624
straight sesamoidean 162, *163*, 166
supraspinous 586, *587*
suspensory *see* suspensory ligament
light beam diaphragm *8*, 12
limb deformities
carpus 289–91, *290*
metacarpal/metatarsal bone 239–40
long-toe low-heel syndrome 108, 110, *110*
long plantar ligament *358*
lordosis 594
lucency *see* radiolucency

lumbar vertebrae
  degenerative joint disease of articular process joints 594–6, *595*, *596*
  impinging spinous processes *559*, 587
  number 571
  stress fractures 600
  subluxation 600
  transverse process 616
  see also sacral vertebrae; thoracolumbar vertebral column
lung(s) 662–77
  abscess 671, 675, *675*
  acute injury 669–70, *670*
  cavitation 667, 668, *673*, *674*
  collapse 662, *663*
  embolism 676, *676*
  fluid line *649*, 657, *668*, *675*
  granulomata 675
  infarcts 676, *676*
  masses 657, 671, 675–7, *675*, *676*
lung disease
  acute respiratory distress syndrome 669–70, *670*
  alveolar 655–7, *656*
  bronchial 655
  equine multinodular pulmonary fibrosis 663, 666, *666*
  exercise-induced pulmonary haemorrhage 676, 677
  inflammatory airway disease 662
  interstitial 652–5, *653*, *654*
  monitoring 644
  patterns of 652–7
  pneumonia *see* pneumonia
  recurrent airway obstruction/ heaves 662–3, *665*
  vascular 655
luxation *33*, 34
  atlantoaxial joint 560–1, *562*
  carpal joints 293
  coxofemoral joint 624
  distal interphalangeal joint 91–2
  elbow joint 341
  femorotibial joint 430
  humerus 325–6, *325*
  metacarpophalangeal joint 204
  patella 435–6, *436*
  proximal interphalangeal joint 160, *160*
  scapulohumeral joint 325–6, *325*
  talus 387, *388*
  tarsocrural joint 387
  tarsus 387
  temporomandibular joint 508
  thoracolumbar vertebrae 600
  see also subluxation
Mach line/band 28, 221, *223*
magnetic resonance imaging (MRI) 18
  carpal bones 287
  fat-suppressed images 88
  femur 426
  metacarpal/metatarsal region 218–19
  keratoma 82
  metacarpal bones 196, 234, 236–7, 243
  nasal septum 457
  navicular disease 128–9, 131, 133
  osseous cyst-like lesions 76, 142, 161
  soft-tissue lesions 219
  proximal phalanx 166–7
  pedal osteitis complex 79
  talus 394
  tarsal bones 383
mandible
  aneurysmal bone cyst 527
  craniomandibular osteopathy 505
  cysts 504
  fractures 466, 508, *509–11*
  interdental space sequestrum 510, *512*
  normal anatomy 488–9
  osteomyelitis 504, *506*
  periostitis 503
  radiographic technique 482
  significant findings 489–512, *490–8*, *500–12*
  tooth development **496**
  tooth infections 499–501, *500–3*
  tumours 505–6, *506*, *507*, *508*
mandibular condyle 489, 506
mandibular symphysis 488, *491*
manica flexoria tears 192, 725
Marie's disease *see* hypertrophic osteopathy
mastocytosis 242, 395
maxilla
  cysts 474
  normal variations/incidental findings 467
  radiographic technique 466–7, *468–9*, *470–1*
  significant findings 467–80
  tooth infections 499–501, *500–3*
maxillary sinus 467
  cyst 472, 474, *475*
  normal variations/incidental findings 467
  radiographic technique 466–7, *468–9*, *470–1*
  radiolucency 479
  radiopacity 474, 478–9, *478*
  significant findings 467–80

sinusitis 467, 470–2, *472*
tooth root infection 499–501, *500–3*
mechanical ileus *707*
meconium impaction 709, *709*, *710*, 711, *712*
medial palmar process *110*
mediastinum
disease 657–62, *658–61*
free air 661, *661*
masses 662
mediolateral foot imbalance 111, *111*, *115*
mega-oesophagus 698–701, *699*, *700*
meniscal ligament
damage 431, *431*
tears 431
metacarpal bone
contour 226
fourth *225*
exostosis 229, *231*
fracture 251–2, *251*
periosteal new bone 238, *238*
periostitis 229
lucent lines *231*, 239
lucent space 226
modelling 238
nutrient foramen 221, *223*, 226
periostitis 229–32, *230*, *231*
micro-fractures 230, 232, *233*, *234*
trauma 229–30, *231*
physis fusion times **750**
second 226
exostosis 226, *228*
fracture *253*, *254*
periosteal new bone 238, *238*
periostitis 229
radiolucency *223*
syndesmopathy 232–5
third 226
angular limb deformities 239–40
exostosis 239
fractures *33*, 237, 242–50, *244–50*
infectious osteitis 239, *240*
nutrient foramen 221, 226
osteomyelitis 239, *240*
physitis 199, 241
radiolucency *223*, 226
spur formation 237
stress-related injury 204–5, *205*
trauma 196
metacarpal physis 221, **750**
metacarpal region 215–57
angular limb deformities 239–40
dorsodistal-palmaroproximal oblique view *219*
dorsolateral-palmaromedial oblique view 221, 223, *225*, 226, *227–9*, *233*, *238*, *246*, *247*
dorsomedial-palmarolateral oblique 221, 223, *225*, 226, *227–31*, *254*
dorsopalmar view 221, *222–4*, *248*, *249*, *250*
dorsoproximal-palmarodistal oblique view 217–18, *217*, *218*
enostosis-like lesions 242
entheseophytes in suspensory ligament attachment area 235–7, *236*, *237*
exostoses 226, *228*, *229*, *231*, *233*, 235
fractures *30, 234*, 242–55, *253–5*
hypertrophic osteopathy 242
immature horse *224*
interosseous ligament mineralisation 226
lateromedial view 215, *216*, 219–21, *220*, *224*, *233*
MRI 218–19
normal variations/incidental findings 219–29, *220*, *222–5*, *227–9*
nuclear scintigraphy 218
panosteitis 242
radiographic technique 215–19
radiolucency *222*
significant findings 229–57
soft tissue mineralisation 242
splints 232–235
suspensory desmitis 219, 237, 248, 249, 252, *254*
syndesmosis 232
syndesmopathy 232–5
tumours 252
see also metacarpal bone
metacarpophalangeal joint 175–213
bone trauma 196
degenerative joint disease 193–6, *194*, *195*
developmental orthopaedic disease 196–9, *197*, *198*
dorsodistal-palmaroproximal oblique view *245*
dorsolateral-palmaromedial oblique view *16*, *26*, *159*, 175–6, *194*, *198*, *201*, *208*
dorsomedial-palmarolateral oblique view 175–6, *17, 170*, *201*
dorsopalmar view *11*, *183*, *185, 244*
dorsoproximal-dorsodistal view 180, *181*

metacarpophalangeal joint (*cont'd*)
dorsoproximal-palmarodistal oblique view *33*, 175–6, *195*
dystrophic mineralisation *193*
fractures 205–8, *206*
hypertrophic osteopathy *26*
incidental findings 187–9, *188*
lateromedial view 176, *183*, *184*, *187*, *188*, *192*, *194*, *197*, *207*, *209*
luxation *33,* 204
new bone formation 187, *188*
normal anatomy 181–7
adult 182–7, *184–7*
immature horse 181–2, *183*
osseous cyst-like lesions 199–202, *200*, 204
osteochondral fragments 196–9, *197*, *198*
osteochondrosis 196–9, *197*, *198*
osteophytes 193, 194–5
physitis 199
proximal phalanx *see* phalanx, proximal
proximal sesamoid bones *see* sesamoid bones, proximal
radiographic technique 175–81
radiolucency 186, 189
sesamoiditis 199–202, *201*, *202*
significant findings 189–209
soft-tissue swelling 189–93, *190–3*
soft tissue attachments *154–57*
special oblique view 176–7, *177–9*
supracondylar lysis 191, *192*
synovitis 190–1, *190*, *191*
tangential dorsopalmar view 177, 180, *180*
third metacarpal bone *see* metacarpal bone, third
metaphysis 24
metastases
lung 676–7
spine 599
metastatic mineralisation 38
metatarsal bones
exostoses 226, *229*
fourth *354*, *355*, *361*, 361, *365*, *367*
fractures 251–2, *251*, *253*
nutrient foramen *227*
radiolucency *227*
radiopacity *222*
second *216*, 226, *227*, *251*, *355*, *361*, *365*, *367*
fractures 251–2, *251*, *253*
third
angular limb deformities 239–40
entheseophytes 221, *359*
exostosis 226, *229*
fracture 250, *250*
modelling *356*
osteophytes 221, *236*, 358, *359*, *375*
radiopacity *223*
spur formation 358, *359*, *375*, 381
stress-related injury 204–5, *205*
metatarsal region 215–57
angular limb deformities 239–40
dorsolateral-plantaromedial oblique view 226, *227*, *251*, *253*
dorsomedial-plantarolateral oblique view 226, *228*
dorsoplantar view *223*, *229*, *237*
fractures 250–2, *250*, *251*, *253*, *255*
hypertrophic osteopathy 242
lateral plantar-dorsomedial oblique view *216*, *250*
lateromedial view 215, *216*, 219–21, *220*, *236*
MRI 218–19
new bone formation *236*
normal variations/incidental findings 219–29, *220*, *222–5*, *227–9*
nuclear scintigraphy 218
panosteitis 242
radiographic technique 215–19
significant findings 229–57
soft tissue mineralisation 242
tumours 252
see also metatarsal bone
metatarsophalangeal joint
infectious osteitis 203, *203*
lateromedial view *51*
osteophytes *193*
stress-related injury 204–5, *205*
see also metacarpophalangeal joint
micro-fractures of metacarpal bone 230, 232, *233*, *234*
middle phalanx, see phalanx, middle
middle carpal joint, degenerative changes 279, *279*
mineralisation 38
biceps brachii tendon 320, *322*
cranial tibial tendon *359*
deep digital flexor tendon 139, *139*
distal sesamoidean ligaments 171
interosseous ligaments 226
metacarpophalangeal joint 193, *193*
metastatic 38
nuchal ligament insertion 566
soft tissue 242

tarsal bones 383
see also dystrophic mineralisation
Miniature Horses, scapulohumeral joint abnormalities 322–3, *324*
minimum sagittal diameter (MSD), cervical vertebrae 536, **537**, *538*, **540**
modelling 19, 20, 24, 37, 56, 60, 76
cervical articular process joints *554–61*, 555–60
metacarpal bone 238
proximal interphalangeal joint 162–3
proximal phalanx 187
scapula 314, 316
sustentaculum tali *389*
tarsal bones *371*, *379*
moiré lines 45, *46*
molars **483**, 484, 488
monitors 46–7
movement artefacts 759
multilobular osteoma 527
multiple hereditary osteochondromatosis 681
mycosis of Eustachian tube diverticulum 520
myelography 733–43
diagnostic criteria 735, *739–42*, 742–3
interpretation 734–5, *736–8*
technique 733–4
myositis ossificans *see* heterotopic ossification

nasal polyps 461, *462*
nasal septum, abnormalities 457
nasofrontal suture separation 464–5, *464*
nasolacrimal duct imaging 746
navicular block 116, *116*
navicular bone 66, *72*, 113–42
artefacts 127–8
bipartite 92
congenital abnormalities 128
deep digital flexor tendon mineralisation 139, *139*
disease 128–35, *130–6*
distal border fragments 114, 115, 116, 131, *133,* 135
dorsopalmar view 119, 126–7
dorsoplantar view 119
dorsoproximal-palmarodistal oblique view 115–17, *116*, 122–3, *122*, *123*, 131–3, *132*, *133*, *140–2*
entheseophytes 129, 130, 137
fractures 140–2, *140–2*
incidental findings 126–7
infection 139–40
lateromedial view 113–14, *114*, 119–21, *119–21*, 126, 128–9, *129*, *138*, *139*
lucent areas 119–20, 122, 124, *124*, 125, 126, 128, 129–30, *130*, 133, *133*
new bone formation 135, 137–9, *138*, *139*
normal anatomy 119–26
adult 119–26, *120–5*
immature horse 119
nuclear scintigraphy 141
nutrient foramen *122*
osseous lesions 142
osteophytes *97*, 130, 137–8, *138*
palmar compact bone *120*, *124*, 134
thickening *136*
palmaroproximal-palmarodistal oblique view 117–19, *118*, 124–5, *124*, *125*, 127, 134–6, *135*, *136*
physis fusion times **750**
proximal displacement 141–2
radiographic technique 113–19
radiopacity 133, *133*, 138, *139*
reinforcement line 125
significant findings 127–42
spongiosa 113, 114, 117, 121, 124, *124*, *125*, 126, 127, 129, *130*, *132*, 133, 134, *134*, 135, *135*
synovial invaginations 121, *122*
tripartite 128
see also sesamoid bones
navicular bursa
dystrophic mineralisation 139
infection 139–40
intrathecal analgesia *130*
penetrating injuries *131*, 139–40
positive contrast studies 135
negative contrast 688, 723
neoplasia *see* tumours
neurofibromatosis, cervical spine 565
new bone formation 20, 23–4
carpus 282–5, *283*, *284*
elbow joint 337, 339, *339*, *340*
metacarpal bone 238, *238*
metacarpophalangeal joint 187, *188*
metatarsal region *236*
middle/proximal phalanx 162–5, *163–5*
navicular bone 135, 137–9, *138*, *139*
radius 284, *284*
non-union of fractures 29, 31–2, 632, 679
nuchal crest 454
avulsion fracture 465
nuchal ligament insertion
dystrophic mineralisation 566
entheseophytes *463,* 561–2

nuclear scintigraphy 169
fractures 28
metacarpal region 218
metatarsal region 218, 249
phalangeal 168
navicular bone 141
pedal osteitis complex 76–7
pelvic degenerative joint disease 624
sacroiliac joint 626
thorax 641
nutrient foramen
metacarpal bone 221, *223*, 226
middle/proximal phalanx 150, 156
navicular bone *122*
tibia *442*

oblique sesamoidean ligament *159*, 162, *163*, 165
obstructive ileus 709, *709*, *712*
obturator foramina 614, *618*
occipito-atlanto-axial malformation 549, *550*
odontoma *506*
ameloblastic 478–9, 493
oesophagus 694–704
abscessation 695, *697*
choke 695, *696*, 701, *702–5*, 703
contrast examination 694–5
diverticuli 701, *702–5*
external masses 695, 698, *698*
grass sickness 703–4
intramural cysts 698
mega-oesophagus (dilatation) 698–701, *699*, *700*
neoplasia 698
normal anatomy 694–5
positioning for radiography 688
radiographic technique 694
rupture 694
spasm 695
stricture 695, *696*
olecranon 330, *334*, *336*
fractures 343, *344*
oligodontia 489
opacity 4
see also radiopacity
orbital fractures 465–6
osseous cyst-like lesions (OCLLs) 36–7
acetabulum 626
carpal bones 287–8, *288*
cervical vertebrae 564
cruciate ligament 432
distal phalanx 76
elbow joint 337
foot 80–1, *82*
medial femoral condyles 36–7, *423*, 424
metacarpophalangeal joint 199–202, *200*
middle/proximal phalanx 160–1
pelvis 626
proximal sesamoid bones 204
radius 287–8
scapulohumeral joint 315–16, *316–19*, 319
stifle 421–6
tarsus 380–1, *392*
see also cysts; degenerative joint disease
osseous metaplasia 190
ossification centres
carpus 262, 271
cervical vertebrae 541, *541*, 545, *547*, 550, *553*, *557*
cranium **453**
foot 74, 75, *86*, *87*, 95
metacarpal/metatarsal bone 182
radius 262
scapulohumeral joint 306, *307*, *327*, 331
stifle *419*
tarsus 352, *353*
thoracolumbar vertebrae 571, *572*, *574*, 576, 577
ossification of ungular cartilage 75, 83–8, *84–8*
ossifying spondylosis 597–9, *597–8*
osteitis 25
pedal 76–9, *77–9*
osteitis, infectious 25, 79–80, *80*
metacarpal bone 239, *240*
patella 436
proximal sesamoid bones 203
axial aspect 203–4, *203*
palmar/abaxial aspect 203
thoracolumbar vertebrae 599
osteoarthritis *23*, 37
articular process joints 590, 593
distal interphalangeal joint 96
foot 90
scapulohumeral joint 321–2
spinous process 590, 593
thoracolumbar vertebrae *585*, *586*
see also degenerative joint disease
osteoarthropathy, temporohyoid 457, *460*, *461*
osteoarthrosis 37
see also degenerative joint disease
osteochondral fragments
metacarpophalangeal joint 196–9, *197*, *198*
tarsus 370–74, *372–3*
stifle 414–20, *419–20*
osteochondroma 285, 291, *292*

pubis 628
radius 291, *292*, 342
osteochondromatosis
ribs 681
synovial 36, 285
osteochondrosis 22, 36, 37
acetabulum 626
cervical spine 549
elbow joint 337
femoropatellar joint *418*
metacarpophalangeal joint 196–9, *197*, *198*
metatarsophalangeal joint *198*
patella 435, 437, *438*
pelvis 626
scapulohumeral joint 313–14, *316*, *317*, *318*, *321*
stifle 414–17, 419–20, *419–21*
tarsocrural joint *372*, *373*
tarsus 356, 370–3, *372*, *373*
osteoclasis 28
osteolysis 20, 25, 495, *566*, 595
osteoma
multilobular 527
paranasal sinuses 479
osteomalacia 565
osteomyelitis 25, 35–6
carpus 287, *288*
cervical spine 563, *564*
femorotibial joint 429
Firth's classification 25
mandible 504, *506*
medial trochlear ridge *430*
metacarpal bone 239, *240*
pelvis 624
radius 342
ribs 681
scapulohumeral joint 323, *324*, 325
stifle 429–30, *429*, *430*
tarsus 369, 389–90, *391*
type E 35, 287, *288*, 429, *429*
type P 35, 429
type S 35, 429
type T 35–6
ulna 342
osteopathy *see* hypertrophic osteopathy
osteopenia 21, *21*
osteophytes 23, *23*, 60
antebrachiocarpal joint 275, 279
carpus 275, 279, *280*, 282
carpometacarpal joint 279, *280*
centrodistal joint *376*
coxofemoral joint 624, *625*, 626
distal interphalangeal joint 90
elbow joint *338*
femoropatellar joint 427, *427*, 429
femorotibial joint *431*, *433*
metacarpophalangeal joint 193, 194–5
metatarsophalangeal joint *193*
middle carpal joint 275
middle/proximal phalanx 154, 157, *158*, *159*, 193, 194
navicular bone *97*, 130, 137–8, *138*
periarticular 279–80
periosteal 282
proximal interphalangeal joint 161
proximal sesamoid bones 189, *194*, 195, 202
radius *281*
scapulohumeral joint 320
tarsal bones *371*, *377*, *379*, *384*
tarsometatarsal joint *376*
third metatarsal bone 221, *236*, 358, *359, 375*
see also degenerative joint disease
osteoporosis 20–2, *21*, *22*
osteosarcoma 171
tarsus 395
otitis media 457, *460*
overexposure of films 44

packing artefact 55, *56, 65*
PACS (Picture Archiving and Communication System) 41
palmar annular ligament 202, *202*
palmar intercarpal ligament 278, 294
palmar process of distal phalanx
fractures 60, 92–5, *94*
radiolucency *12*, 56
visualisation of 57, 59, *61*
see also pedal osteitis complex
panosteitis 442
metacarpal/metatarsal region 242
parallel grid 117
paranasal sinuses 466–80
conchae 467, *469*, *478*
ethmoid haematoma 474, *476*, *477*
frontal 467
sinusitis 467, 470–2, *472*
maxillary 467
cyst 472, 474, *475*
radiolucency 479
radiopacity 474, 478–9, *478*
sinusitis 467, 470–2, *472*
normal variations/incidental findings 467
radiographic technique 466–7, *468–9*, *470–1*
significant findings 467–80
submucosal cyst 472, *473*
tumours 478–9, *479–81*

pastern
  dorsolateral-palmaromedial oblique views *69*, *70*
  dorsomedial-palmarolateral oblique view *89*
  dorsoproximal-palmarodistal oblique view 116
  lateromedial view 56
  see also phalanx, middle; phalanx, proximal; proximal interphalangeal joint
patella
  adult 407, *410*, *414*
  apical modelling 435
  chondromalacia 437
  fractures *31*, 437–9, *437*, *438*
  immature horse 403, *404*, *405*
  infectious osteitis 436
  luxation 435–6, *436*
  osseous cyst-like lesions 426, *426*
  osteochondrosis 415–16, *420*
  physis fusion times **751**
patellar ligament 407, *409*, 429
  injuries 433
  opacity 432
patent urachus 717, *718*
pedal bone *see* phalanx, distal (pedal bone)
pedal osteitis complex 76–9, *77–9*
pelvis 609–32
  coxofemoral joint luxation 624
  cranioventral-dorsocaudal view 613, *614*
  degenerative joint disease 624–6, *625*
  fractures 628–32, *628*
    coxofemoral joint 630, *631*
    ilium 629–30, *629*
    ischium 630, 632, *632*, *633*
  hip dysplasia 622
  infectious arthritis/osteomyelitis 624
  lateral dorsal-lateroventral oblique view 613–14, *614*, 622, *623*
  normal variations/incidental findings 613–22
    adult 614–22, *616–21*, *622*
    immature horse 613–14, *615*
  osseous cyst-like lesions 626
  osteochondroma of pubis 628
  osteochondrosis 626
  osteomyelitis 624
  physis fusion times **751**
  radiographic technique 609–13
    equipment 609–10, *610*
  sacroiliac joint disease 626, *627*
  significant findings 612–32
  tuber ischium *617*
  tuber sacrale 613, *613*, 615, *619*, 626, *627*, 734
  ventrodorsal view 611, *612*
penetrating injuries
  hoof 112
  navicular bursa *131*, 139–40
penumbra 759
periarticular swelling 32
periodontal disease 501
  see also teeth
periosteal callus 29, *30*, 237, 245, 247, 327, 328
periosteal new bone
  metacarpals 238, *238*
  tarsus 383–5, *385*, *386*
periostitis
  mandible 503
  metacarpal bone 229–31, *230*, *231*
  radius 341
phalanx, distal (pedal bone) 55–62
  agenesis 92
  articular surfaces 63–4
  bony fragment 74
  demineralisation 76, *77*
  dorsomedial-palmarolateral view *78*
  dorsopalmar view 58–9, *59*
  dorsoproximal-palmarodistal oblique view 57–8, *57*, *58*, *73*, *82*
  entheseophytes 60
  extensor process *61*, *64*, 66
    anatomical variations 62, *63*, *73*
    contour 68, *71*
    fragments 75, *75*
    remodelling 56
  fractures 92–7, *92–4*, *96*, *97*
  halo effect 63
  high coronary technique 64
  hypoplasia 92
  infection 25, 79–80, *80*
  inflammation 76–9, *77–9*
  inspissated pus 79, *80*
  keratoma 81–2, *83*
  lateral palmar process *71*
  lateromedial view 56–7, *72*, *78*, *164*
  oblique view 60–2, *61*, *62*
  osseous cyst-like lesions 75
  osteitis
    infectious 25, 79–80, *80*
    pedal 76–9
  palmar processes 56, 57, 59, 60, *61*, *62*, 62, *64*, *65*, 66, *68*, *69*, 70, *71*, 75, *78*, 81, 83, *86*
    bony fragments 74
    centres of ossification 74, *75*
    cyst-like lesions 81

fractures 92–5, *93*, *94*
radiolucencies *12*, 56, 77
palmaroproximal-palmarodistal oblique view 59, *59*, *110*
parietal sulci 76
physis fusion times **750**
radiographic technique 55–62
radiopacity 74, *75*, *91*, *94*, 96
solear canal 63, *64*, *65*, 66, *67*
solear margin *65*
tumours 83
ungular cartilage (sidebone) 75, 83–8, *84–8*
phalanx, middle 153
articular surfaces 63–4
dorsal medial-plantarolateral view *172*
dorsopalmar view *152*
entheseophytes 153, 157, 163
fractures 167–71, *168–72*
lateromedial view *151*, *155*, *159*
mineralisation 153
new bone formation 162–5, *163–5*
normal anatomy 150–3
adult 150–3, *151*, *152*
immature horse 150
normal variations/incidental findings 153–7, *154–7*
nutrient foramen 150, 156
osseous cyst-like lesions 160–1
osteophytes 154, 157, *158*
physis fusion times **750**
radiographic technique 149–50
radiolucency 150
'scalping' injury 166
significant findings 157–72
soft tissue attachments *154–7*
spur formation 156, *159*
subchondral bone trauma 167
tumours 171
phalanx, proximal 153
dorsolateral-palmaromedial oblique view *159*, *165*
dorsopalmar view *152*, *164*, *168*, *169*
entheseophytes 153, 157, *159*, 165, 194
fractures 167–71, *168–72*, 206–7, *207*
lateromedial view *151*, *155*, *164*, *168*
mineralisation 153
modelling 187
new bone formation 162–5, *163–5*
normal anatomy 150–3
adult 150–3, *151*, *152*
immature horse 150
normal variations/incidental findings 153–7, *154–7*
nutrient foramen 150, 156
osseous cyst-like lesions 160–1
osteophytes 154, 157, *158*, *159*, 193, 194
physis fusion times **252**
proximal subchondral bone plate 184–5, *185*
radiographic technique 149–50
radiolucency 150
'scalping' injury 166
significant findings 157–72
soft tissue attachments *154–7*
subchondral bone trauma 166, 196
tumours 171
see also digital annular ligament; oblique sesamoidean ligament; straight sesamoidean ligament
pharynx 512–27
lymphoid hyperplasia 520
normal variations/incidental findings 513–16, *514*, *515*
radiographic technique 512–13
significant findings 516–23, *517–19*, *521–6*
photons 4
photostimulable phosphors 42, 757–8
physeal dysplasia 24
tarsus 374
physeal scar 182, *265*, *267*, *268*, 342
physis
distal metacarpal 221
distal radial 288
femoral 403, 439
fusion times **749–51**
proximal metacarpal 221
physitis 24, 35
carpus 288–9, *289*
humerus 325
scapulohumeral joint 325
stifle 427
tarsus 374
third metacarpal bone 199, 241
pituitary pars intermedia dysfunction 669
pleural effusion 657–9, *658*, *659*
pleural fluid, free 657, *658*
pleuropneumonia *659,* 668
pneumocystography 743–4
pneumomediastinum 661, *661*
pneumonia *664*
aspiration 671, *672*
mega-oesophagus 698–701, *699*, *700*
oesophageal obstruction *700*
bacterial 666–9, *668*, *669*
bronchointerstititial of foals 669–70, *670*

pneumonia (*cont'd*)
'cottonball' lesions 667
eosinophilic 666, *667*
fungal 670
granulomatous 655
inhalation 671
pneumothorax 659–61, *660*
rib fractures 679, 681
podotrochlear apparatus 101
polyarthritis, infectious, in foals 35–6
polydactyly 288
polydontia 489
polyps, nasal 461, *462*
positive contrast 135, 191, 195, 526, 599, 688, 715, 744
pre-purchase radiographs 13–14
premaxilla (incisive bone) 480, *482*, *483*
premolars **483**, 488
preparation/positioning for imaging 9
see also specific anatomical areas
primary beam cut-off 758
primary radiation 12–13
processing of X-ray films 6–8
automatic 7–8
prognathia 489
protective clothing 12–13
proximal digital annular ligament 616, *618*, 622, 624
proximal interphalangeal joint
ankylosis 161
collateral ligament injury 166
degenerative joint disease 161–2, *162*
dorsolateral-palmaromedial oblique view *163*
dorsoplantar view *162*
dysplasia 158
lateromedial view *160*
modelling 162–3
osteophytes 161
subchondral bone trauma 166–7
subluxation 160, *160*
proximal intertarsal joint *see* talocalcaneal-centroquartal joint
proximal phalanx see phalanx, proximal
proximal sesamoid bones *see* sesamoid bones, proximal
proximal suspensory desmopathy 235, *237*
pubic symphysis 614
pubis, osteochondroma 628
pulmonary disease *see* lung disease
pulmonary abscess 671, 675, *675*
pulmonary lesions, cavitary 657, 671, *673*, *674*
pulmonary masses 657, 671, 675–7
granulomata 675
infarcts and embolism 676, *676*
metastatic lung disease 676–7
primary lung tumours 677
purchase, examination for 13–14
pyelography, intravenous 744–6, *745*

radiation safety 12–13
radiocarpal joint *see* antebrachiocarpal joint
radiographic imaging *see* digital images; images
radiographs
calcium tungstate screens 757
focal spot size 759
image quality 757–9
labelling 14–15
rare earth screens 757
spectral sensitivity 757–8
stressed 33
survey 149, 549, 694, *696*
radiology 15–19, *16*, *17*, *19*
bone changes 20–4, *21–3*
bone lesions 24–32
joint lesions 32–8
radiolucency
carpus 266, *275*, *282*, 283, *285*
distal phalanx, palmar process *12*, 56, 77
hoof wall, 'halo' 63, 68
humerus *309*, 314
maxillary sinus 479
metacarpal bone *222*, *223*, 226
metacarpophalangeal joint 186, 189
metatarsal bone *227*
middle/proximal phalanx 150
navicular bone 119–20, 122, 124, *124*, 126, 127, 129–30, *130*, 133, *133*
proximal sesamoid bones *201*, 202, *202*, 203–4, *203*
radial carpal bone *283*
scapula 307, *309*
talus *364*
third carpal bone *288*
radiopacity
carpus 271, 274–5, *279*, 282, *286*, 287
distal phalanx 74, *75*, *91*, *94*, 96
maxillary sinus 474, 478–9, *478*
metatarsal bone *222*, *223*
navicular bone 133, *133*, 138, *139*
scapula 307
stifle 407, 415, *420*
tarsal bones *380*
radioulnar joint *see* elbow joint

radius *263*, 330–46
angular limb deformities 289–91, *289*, *290*
bone spikes 278
craniocaudal view *30*
dorsopalmar view 266, *267*
dorsoproximal-dorsodistal oblique view 271, *272*
enostosis-like lesions 346
exostosis 284, *284*
fractures *30*, *295*, 297, 343–4, 345, *345*
hypertrophic osteopathy 342
lateromedial view 262, 266, *270*, 271
new bone formation 284, *284*
normal variations/incidental findings 271, 273–5, *281*
osseous cyst-like lesions 287–8
ossification centres 262
osteochondroma 291, *292*, 342
osteophytes *281*
periostitis 341
physis fusion times **750**
physitis 24
radiographic technique 261–2, 330–1
stress fracture 344
torus carpeus (chestnut) 334
transverse crest 334
tumours 346
see also carpal bones/carpus; elbow joint
rare earth screens 757
record keeping 14–15
rectus capitis ventralis major, avulsion fracture 465
recurrent airway obstruction 662–3, *665*
resolution 760
resorption of bone 81, *83*, 104, 166, 168, 440
restraint of horses 12
Rhodococcus pneumonia 667, *668*
ribs
congenital malformation 681
fractures 679, 681
osteochondromatosis 681
osteomyelitis 681
tumours 681
ringbone 162
round (teres) ligament 616, *618*, 622, 624
ruptured hollow viscus 714, *714*

sacral vertebrae 616
number 571
transverse process 616
see also thoracolumbar vertebral column
sacroiliac joint 616, *619*
disease 626, *627*
nuclear scintigraphy 626
sacrum 602–3, *602*, *603*
spinous processes *618*
safety
protective clothing 12–13
radiation 12–13
sagittal ratios
intervertebral 539, *539*, *540*, **552**
intravertebral 537, 539, *539*, **540**, **552**
Salter-Harris classification 28, *29*
sand impaction 715, *716*
'saucer' fractures 243
saucer-shaped lesions 424
'scalping' injury of proximal/middle phalanx 166
scapula 306
fractures 326–9, *327–30*
glenoid cavity 306–7, *309*
fractures 326
glenoid notch 307
immature horse 305, *306*
modelling 314, 316
physis fusion times **750**
radiolucency 307, *309*
radiopacity 307
supraglenoid tubercle
fractures 326, *327*, *328*
physis fusion times 305
see also scapulohumeral joint
scapulohumeral joint 301–29
abnormalities in Shetland Ponies and Miniature Horses 322–3, *324*
arthrography 305, 312–13, *315*
biceps brachii tendon mineralisation 320, *322*
bone fragility syndrome 329
caudolateral-craniomedial oblique view 303
congenital abnormalities of bicipital apparatus 321–2
cranial medial-caudolateral oblique view 303, *304*, 307, *311–15*
cranioproximal-craniodistal oblique view 304–5, *305*, 312, *314*, *325*
degenerative joint disease 319–20, *321*
deltoid tuberosity 307, *311*, *312*
fractures 327, 328
dissecting cartilage flaps 305
enostosis-like lesions 326
heterotopic ossification 322
infection 323, *324*, 325
intertubercular bursa 313, 319, 322
luxation 325–6, *325*

scapulohumeral joint (*cont'd*)
mediolateral view 301–3, *302*, 306–7, *308–10*
normal variations/incidental findings 305–10
adult 306–10, *307–17*
immature horse 305–6, *306–7*
osseous cyst-like lesions 315–16, *316–19*, 319
ossification centres 306, *307*, *327*, 331
osteoarthritis 321–2
osteochondrosis 313–14, *316*, *317*, *321*
osteophytes 320
osteomyelitis 323, *324*, 325
radiographic technique 301–5
septic arthritis 323, *324*, 325
significant findings 313–29
subluxation 323
scar tissue, oesophageal strictures 695, *696*
scatter radiation 8, 758
scintigraphy *see* nuclear scintigraphy
sclerosis 24, 26
third carpal bone 285–7, *285–6*
scoliosis
cervical vertebrae 567
thoracolumbar vertebrae 594
screens (imaging intensifying)
exposure guide 753–5, **753–5**
rare earth vs. calcium tungstate 757
relative speed 757
spectral sensitivity 757–8
sedation 9, 119, 259, 302, 303, 330, 349, 399, 449, 450, 451, 466, 484, 485–7, 513, 532, 591, 613, 724
ataxic horse 532
and altered pharyngeal function 513, 516
seedy toe 112, *113*
semitendinosus, insertional enthesopathy 434
septic arthritis
scapulohumeral joint 323, *324*, 325
stifle 429–30, *429*, *430*
septic physitis of humerus 325
sequestrum 239, *241*
sesamoid bones
navicular bone *see* navicular bone
physis fusion times **750**
see also patella; sesamoid bones, proximal; stifle
sesamoid bones, proximal 187, 221
abnormal position 204
bone necrosis 205
dorsolateral-palmaromedial oblique view *186*
entheseophytes 189
fractures 207–8, *208*, *209*
infectious osteitis
axial aspect 203–4, *203*
palmar/abaxial aspect 203
lateromedial view *187*
normal variations/incidental findings 189
osseous cyst-like lesions 204
osteophytes 189, *194*, 195, 202
palmaroproximal-palmarodistal oblique view 181, *182*
physis fusion times **750**
radiolucency *201*, 202, *202*, 203–4, *203*
soft tissue attachments 155–57
sesamoidean desmitis, 162, *163*, 165
sesamoidean ligament
desmitis *163*
dystrophic mineralisation 171
new bone formation 165
rupture 166
sesamoiditis
metacarpophalangeal joint 199–202, *201*, *202*
proximal sesamoid bones 208
Shetland Ponies, scapulohumeral joint abnormalities 322–3, *324*
shoeing
imbalances 77
solear margin fracture of distal phalanx 95
supportive 79
shoes, removal of 9
shoulder *see* scapulohumeral joint
sidebone *see* ungular cartilage
simple fractures 466
single emulsion films 758
sinker syndrome 105, *106*
sinography 112, 389, 744
sinusitis 467, 470–2, *472*
'ski jumps' 550, *551*, 552, *554*
skull *see* cranium
slab fractures 34
carpus 286, 294–6, *295*, *296*
tarsus 392, *393*
small intestine
enterolithiasis 715
obstruction *707*, 709, *709*, *712*
soft palate 516
cleft palate 526
dorsal displacement 525–6, *526*
soft-tissue lesions 32
carpus 275, 277–8
cervical spine 566

metacarpophalangeal joint 189–93, *190–3*
stifle 430–4, *431–4*
solear canal of distal phalanx 63, *64*, *65*, 66, *67*
sore shins *see* bucked shins
source-image distance (SID) 4
spectral sensitivity 757–8
spinal cord
compression 534, 540, 549, 550, 733, 735, *740*
disease, sagittal ratios **552**
injury 28, 322
'lifting' 735
puncture, myelography 733
spine *see* vertebrae; vertebral column
spinous processes
cervical *537*, *544*, 545
sacral *618*
thoracolumbar *22*, *49*, 342, *559*, 577, *603*
splints (syndesmopathy of metacarpal bone) 232–5
see also exostosis
spondylitic spurs 545
spondylosis
cervical vertebrae 566
thoracolumbar vertebrae 597–9, *597–8*
spondylosis deformans 597–9, *597–8*
sprains 32, *33*, **33**
spur formation
carpus 279, *281*
metacarpal bones 237
metacarpophalangeal joint 193
metatarsal bones 358, *359*, *375*
middle phalanx 156, *159*
stepmouth 503
sternum 681–2, *682*, *683*
steroid arthropathy 284
stifle 399–440
apophyseal-metaphyseal physis 403
bone trauma 426
calcinosis circumscripta 435, *436*
caudocranial view *11*, *62*, 408, 411, *417*, *422*, *423*, *427–8*
caudocranial/caudal proximal-craniodistal oblique view 401, *401*, 408, 411
caudolateral-craniomedial oblique view 400, *401*, 406, *408–11*, *415*
craniolateral-caudomedial oblique/caudomedial-craniolateral oblique view 402, 411–12
cranioproximal-craniodistal oblique view 402, *403*, 412, *414*
degenerative joint disease 427–9, *427*, *428*
fractures 437–40, *437*, *438*, *440*, *441*
immature horse 403, *404*, 405, *405*
infection 429–30, *429*, *430*
joint capsule attachments *415–7*, **418**
lateromedial view *31*, *50*, 400, 405, *407*, *408*, *410*, *418*, *420*
ligament attachments *415–7*, **418**
normal variations/incidental findings 403–14
adult 405–14, *406–17*, **418**
immature horse 403, *404*, 405, *405*
osseous cyst-like lesions 421–6
osteochondrosis 414–17, 419–20, *419–21*
osteomyelitis 429–30, *429*, *430*
physitis 427
radiographic technique 399, 400–2
radiopacity 407, 415, *420*
septic arthritis 429–30, *429*, *430*
significant findings 414–40
soft-tissue injuries 430–4, *431–4*
subchondral bone cysts 421–4, *422*, *423*
tendon attachments *415–7*, **418**
storage phosphors 42
straight sesamoidean ligament 162, *163*
rupture 166
Streptococcus equi 516, 518
stress
bone injury 204–5, *205*
fractures *see* fatigue (stress) fractures
stressed radiographs 33
stylohyoid bone, fractures 457, *460*
sub-epiglottic cysts 523, *524*
subchondral bone cysts 36–7
stifle 420–4, *422*, *423*
subchondral bone trauma 196
subluxation 34
atlantoaxial joint 560–1, *562*
carpus 293
cervical vertebrae 553–4, *554*, *555*, 561
coxofemoral joints 622, 624
distal interphalangeal joint 91–2
proximal interphalangeal joint 160, *160*
scapulohumeral joint 323
tarsometatarsal joint *388*
see also luxation
submucosal cysts, facial deformity 472
summation 134
superficial digital flexor tendon *see* digital flexor tendon, superficial

supracondylar lysis, metacarpophalangeal joint 191, *192*, 195
supraglenoid tubercle
  fractures 326, *327*, *328*
  physis fusion times 305
supraspinous ligament sprain 586, *587*
survey radiograph 149, 549, 694, *696*
suspensory ligament
  desmitis *201*, *236*
  endosteal reaction 235–7, *236*, *237*
  origin, avulsion fractures 247–8, *248*
  sesamoiditis 200
  fracture of proximal sesamoid bone 207–8, *208*, *209*
sustentaculum tali *352*, *355*
sutures/suture lines
  basioccipito-basisphenoid suture separation 465
  fusion times **749–51**
  nasofrontal suture separation 464–5, *464*
symphysis pubis 614, *616*
syndesmopathy of metacarpal bone (splints) 232–5
syndesmosis 232
synostosis 232, 234
synovial invaginations 121, *122*
  see also navicular bone, disease
synovial osteochondromatosis 36, 285
synoviocoele
  carpus 277
  tarsus 387–9, *389*
synovitis
  metacarpophalangeal joint 190–1, *190*, *191*
  villonodular hypertrophic 190

talocalcaneal-centroquartal joint *10*, *368*
  degenerative changes 382, *383*, *384*
talus
  intertrochlear groove *364*
  luxation 387, *388*
  proximal tubercle, fragmentation 386, *387*
  radiolucency *364*
  sustentaculum tali *366*, *367*
    congenital abnormalities 368, *369*
    modelling *389*
  trochlea tali 350, 352, *354*, *355*
    lateral 356, *357*, *365*, *366*
    medial 356, *357*, *359*, 363, 364, *366*
  fracture 394
tarsal bones *see* tarsus/tarsal bones
tarsal groove *368*
tarsal sheath distension 387–9, *389*
tarsocrural joint *10*
  degenerative joint disease 383, *384*
  luxation 387
  osteochondrosis *372*, *373*
  infectious arthritis 389
  see also tarsus/tarsal bones
tarsometatarsal joint *10*
  ankylosis 362
  degenerative joint disease 375, *376*, *377*, *380*
  osteophytes *376*
  subluxation *388*
  see also tarsus/tarsal bones
tarsus/tarsal bones 349–98
  bone trauma 383
  central tarsal bone *353–5*, 358, *361*
    fracture 392
    mineralisation 383
    modelling *371*, *379*
    osteomyelitis 369
    osteophytes *377*, *379*, *384*
    radiopacity *380*
  collapse 369–70, *370*, *371*
  congenital abnormalities 368, *369*
  degenerative joint disease 375–83, *375–81*, *384*
  dorsolateral-plantaromedial oblique view 363–7, *363–5*
  dorsomedial-plantarolateral oblique view 366–8, *366–7*
  dorsoplantar views 350–2, *351*, *360–2*, 361–3, 368, *368*
  first tarsal bone 226, 358
  fourth tarsal bone *353 –6*, 358, *361*, 361, *365*, *367*
  fractures 392–5, *393*, *394*
  infectious arthritis 389–90, *391*
  lateromedial view *10*, 349–50, *355*, 356, *356–9*
  luxation 387
  normal variations/incidental findings 352–68
    adult 353–68, *355–68*
    immature horse 352, *353*, *354*
  osseous cyst-like lesions 380–1, *392*
  ossification centres 352, *353*
  osteochondrosis 356, 370–3, *372*, *373*
  osteomyelitis 389–90, *391*
  periosteal proliferative reactions 383–5, *385*, *386*
  physeal dysplasia 374
  physis fusion times **751**
  physitis 374
  radiographic technique 349–52
  second tarsal bone 226, 358

significant findings 368–95
subluxation *388*
synoviocoele 387–9, *389*
third tarsal bone *353*, 358
deformation *371*
fracture *393*
mineralisation 383
modelling *379*
osteomyelitis 369
osteophytes *371*
radiopacity *380*
trochlear ridges *see* trochlea tali
tumours 395
teeth 480–512
brachygnathia/prognathia 489
canine 480, *483*, **483**
cheek, radiographic technique 484–7, *485–7*
dental tumours 493
development **496**
diastema 501, 503, *504*, *505*
enamel 488
equine odontoclastic tooth resorption and hypercementosis 493, 495, *498*
erupted crown disorders 501–2
extractions 489
fractures 495, 499
incisors **483**
radiographic technique 487–8
molars **483**, 484, 488
normal variations/incidental findings 488–9, *490–7*
oligodontia 489
periodontal disease 501
polydontia 489
premolars **483**, 488
root infection 499–501, *500–3*
significant findings 489–512
Triadan numbering system 480, 482, **483**
wolf teeth 489
teleradiology 53
temporal teratoma 456, *460*
temporohyoid osteoarthropathy 457, *460*, *461*
temporomandibular joint (TMJ)
degenerative joint disease 506, 508
luxation 508
radiographic technique 482, 484, *484*
tendonography 724–5
tendons
biceps brachii 320, *322*, 337
cranial tibial *359*
common digital extensor 74
deep digital flexor *see* digital flexor tendon, deep
of fibularis tertius 358, *360*
of gastrocnemius 439
superficial digital flexor 204, 262, 271
terminology 2, *3*
third trochanter, femur 633, 634
fracture 634–5, *635*
thoracic vertebrae 302, 303, 326, 531, 532, 533, *555, 559*, *565*
intravertebral foramina *546*
spinous process 545, *545*
demineralisation *22*
subluxation 561
see also thoracolumbar vertebral column
thoracolumbar vertebral column 569–601, *619*
articular process joints 570, *570*, *576*, 594
new bone formation *596*
stress fractures 600
degenerative joint disease 594–6, *595*, *596*
discospondylitis 599
facet joints *see* articular process joints
fractures 600, *601*
fusion 593
infectious osteitis 599
interspinous ligament, enthesopathy 587
kyphosis 594
lordosis 594
luxation 600
normal variations/incidental findings 571–85
adult 571–85, *575–86*
immature horse 571, *572–4*
ossification centres 571, *572*, *574*, 576, 577
ossifying spondylosis 597–9, *597–8*
osteoarthritis *585*, *586*
physis fusion times **751**
positioning for radiography 570–1, *570*
radiographic technique 569–71
equipment 569
scoliosis 594
significant findings 586–601
spinous processes *22*, *49*, 342, *537*, *544*, 576–7, *580–6*, *603*
impingement/overriding 587–93, *588–92*
bone bridging *586*, *598*
congenital fusion 593
entheseophytes 576
new bone formation 577
spondylosis deformans 597–9, *597–8*
supraspinous ligament, sprain 586, *587*

thorax 639–85
cardiac disease 679, *680*
computed tomography 643–4
diaphragmatic hernia 677, *678*
disease monitoring 644–5, *648*, *649*
dorsocaudal lung field 650–1
dorsocranial lung field 651
incidental findings 651–2
lung disease 652–7, 662–77
mediastinal masses 662
normal anatomy 645–51, *646*, *647*
adult *640–7*, 650–1
immature horse 647, 650
nuclear scintigraphy 641
pleural effusion 657–9, *658*, *659*
pneumomediastinum 661, *661*
pneumonia *see* pneumonia
pneumothorax 659–61, *660*
positioning for radiography 639–40, *640–7*
radiographic technique 639–45
equipment 639
factors influencing interpretation 651–2
rib lesions 679, 681
significant findings 652–83
sternum 681–2, *682*, *683*
tracheal collapse/stenosis 662, *663*, *664*
ultrasonography 641–3
ventrocaudal lung field 651
ventrocranial lung field 651
see also diaphragm; lung disease; lungs; and entries under pulmonary
thoroughpin 387–9, *389*
tibia 440–4
apophysis 403, *404*, 407, 411, *419*, *444*
craniolateral-caudomedial oblique view *27*
enostosis-like lesions *27*, 442–3
fractures 439–40, *440*, 443–4, *444*
distal intermediate ridge, osteochondrosis *373,* 374
intercondylar eminence 400, 403, 407, 408, *409*
lateral condyle 411
malleoli
avulsion fracture 385
osteochondrosis 371, *373*
medial intercondylar eminence 411, *412*, *413*
osteophytes *433*
normal variations/incidental findings 441, *442*
nutrient foramen *442*
osseous cyst-like lesions 424, *425*, *433*
osseous fragments *434*
physis fusion times **751**
radiographic technique 440–1
significant findings 442–4, *444*
tibial crest 407, 411
tibial condyles 403, *404*
modelling *433*
osteophytes 427
tibial tuberosity *409*, 411
fractures 439
tibiotarsal joint *see* tarsocrural joint
torus carpeus *275*, 334
torus tarseus *355*, 361, *389*
trabecular bone trauma 196
trachea
collapse/stenosis 662, *663*, *664*
rings 516
masses 662
tranquillisers 449
see also sedation
transcuneal ultrasonography 88, 135
trauma
cavitary lung lesions 667, 671, *673*, *674*
collateral ligament 166, 191, 430
diaphragmatic hernia 677, *678*
dystrophic mineralisation *see* dystrophic mineralisation
deep digital flexor tendon 140, *140*, 284
mandibular periostitis 503
metacarpal bone 229–30, *231*
middle phalanx 167
osseous cyst-like lesions *see* osseous cyst-like lesions
periostitis, metacarpal region 229–31, *230*, *231*
proximal interphalangeal joint 166–7
proximal phalanx 166, 196
stifle 426
tarsus 383
trabecular bone 196
see also fractures; luxation
trochlea tali 350, 352, *354*, *355*
lateral 356, *357*, *365*, *366*
medial 356, *357*, *359*, 363, 364, *366*
tuber calcanei *368*
physis fusion times **751**
tuber ischium *617*
tuber sacrale 613, *613*, 615, *619*
tuberculosis, infectious osteitis of spine 599
tumoral calcinosis 435
tumours

bone 24–5
cervical spine 565, *566*
dental 478, 493
distal phalanx (pedal bone) 83
foot 83, *83*
humerus 346
lung 677
mandible 505–6, *506*, *507*, *508*
metacarpal/metatarsal region 252
middle phalanx 171
oesophagus 698
paranasal sinuses 478–9, *479–81*
proximal phalanx 171
radius 346
ribs 681
tarsus 395
see also specific types
tushes (canine teeth) 480, *483*, **483**, 488
tympany of Eustachian tube diverticulum 518–20, *519*

ulcers, gastroduodenal 711, 713
ulna 331
apophysis *332*, *333*
fractures 343, *344*
immature horse 331, *332*
physis fusion times **750**
trochlear notch *334*
see also elbow joint
ulnar carpal bone *19*, *263*, *273*
chip fractures 297
osseous cyst-like lesions 287
palmar aspect 271
see also carpus
ulnaris lateralis, avulsion of origin 340
ultrasonography 18
carpus 278, 284, *284*
cervical articular process joints 559
congenital abnormalities of humeral tubercles 321
coxofemoral joint 624, 626
diagnostic 20, 29, 34
diaphragmatic hernia 677, *678*
metacarpal/metatarsal region 218, 234, 236, 248, 251
oesophageal external masses 695, 698, *698*
pastern 165
pelvis 609, 612, 628
ilial wing fracture 629
osteomyelitis in internal fixation 29
penetrating injuries of foot 112
pleural effusion 657
rib fractures 679, 681
thorax 641–3
transcuneal 88, 135
umbilical cord infection 717
underexposure, digital 45
ungular cartilage, ossification 75, 83–8, *84–8*
unsharpness of image 759
urachal remnant 717
urachus, patent 717, *718*
urinary system 715–19
bladder rupture 717
calculi 587
contrast studies 715–17
disease 717–19
cystitis 717, *719*
patent urachus 717, *718*
intravenous pyelography 744–6, *745*

valgus 289, *290*
see also carpus/carpal bones; metacarpophalangeal joint; tarsus/tarsal bones
varus 289
see also carpus/carpal bones; metacarpophalangeal joint; tarsus/tarsal bones
vascular channels 199
see also navicular bone; proximal sesamoid bones
vena cava, caudal *642, 645*, 650
venography 730–2
laminitis 108, *109*
vertebrae
cervical *see* cervical vertebral column
coccygeal 602–3, *602*, *603*
sacral 616
thoracic *see* thoracic vertebrae
thoracolumbar *see* thoracolumbar vertebral column
vertebral canal, caudal extension of arch 554
vertebral column 531–607
cervical 531–68
physis fusion times **749**
sacrum and coccygeal vertebrae 602–3, *602*, *603*
thoracolumbar 569–601
vestibular disease, peripheral 457
villonodular hypertrophic synovitis 190, *190–1*

wavemouth 503, *505*
weight-bearing radiograph
distal phalanx (pedal bone) 58–9, *59*
foot 66, *67*, *74*

wolf teeth 489
  false (canine teeth, tushes) 480, *483*, **483**, 488
Wolff's law 20, 125
Wratten Series 6B filter 6

X-rays
  attenuation 5
  collimation 12, 46, 758
  exposure factors 4–5
  film 5–6
  production of 3–4
  scatter 8, 758
xeroradiography

zig-zag orientation of cervical vertebrae 553, *554*

WILEY END USER LICENSE AGREEMENT

Go to www.wiley.com/go/eula to access Wiley’s ebook EULA.